DEVELOPMENT OF AROMATIC AND ALIPHATIC C–H FUNCTIONALIZATIONS VIA PHOTOREDOX CATALYSIS

Kaila Ashley Margrey

A dissertation submitted to the faculty of The University of North Carolina at Chapel Hill in partial fulfillment of the requirements for the degree of Doctor of Philosophy in the Department of Chemistry.

Chapel Hill
2018

Approved by:

David Nicewicz

Erik Alexanian

Simon Meek

Michel Gagné

Frank Leibfarth

ABSTRACT

Kaila Ashley Margrey: Development of Aromatic and Aliphatic C–H Functionalizations via Photoredox Catalysis
(Under the direction of David A. Nicewicz)

Carbon–hydrogen (C–H) bonds are ubiquitous in organic compounds, and the ability to functionalize C–H bonds selectively is a powerful strategy for late-stage derivatizations. The direct C–H functionalization of electron-rich arenes with azole coupling partners was demonstrated using an acridinium photoredox catalyst and a nitroxyl radical cocatalyst under an aerobic atmosphere, occurring via the intermediacy of an arene cation radical. High levels of site selectivity were observed with this methodology, and it proved applicable to a wide variety of arene and azole coupling partners, including complex bioactive molecules. Anilines could be constructed using ammonium carbamate as the nucleophilic coupling partner.

The ability to predict the site of C–H functionalization on complex arenes is nontrivial, and for this reason, a predictive model was developed. This enabled the extension of our aryl amination to a wide variety of heterocyclic arenes that are common motifs in pharmaceuticals. Using electron density calculations, we could predict the major site of functionalization for over 60 arene substrates.

We sought to extend this arene functionalization methodology toward aliphatic amine coupling partners. We demonstrated this capability with a wide variety of amino acid and primary amine coupling partners with arene substrates. Site selectivity was dependent on sterics of the arene, unlike our previous work with azoles. We also disclose the

functionalization of arenes that cannot be oxidized by the acridinium catalyst, such as benzene and toluene, supporting a reactive amine cation radical intermediate.

A modular functionalization of unactivated aliphatic C–H bonds was developed utilizing an acridinium photoredox catalyst, phosphate base, and several diverse radical traps. The development of a C–H azidation reaction highlighted good site selectivity on alkanes for tertiary functionalization exclusively. Through modifications of this system, a C–H diversification allowed for the formation of C–F, C–Br, C–Cl, C–SCF_3, and C–C bonds.

To my parents

Keith and Debra Margrey

I will never be able to thank you enough

for all your support.

ACKNOWLEDGEMENTS

I am very fortunate that I had the opportunity to study at UNC Chapel Hill. I sincerely want to thank Dave Nicewicz for being my mentor for the last five years. You have allowed me to have the scientific independence I needed to find out what truly interests me and how to become a better scientist. I also must thank the members of my committee: Erik Alexanian, for providing constant support and always being willing to give advice, and also allowing me to develop a collaborative project with his lab; Simon Meek, for insightful questions and comments on research; Frank Leibfarth, for enthusiasm and eagerness to integrate photochemistry with polymers and encouraging me to venture into another field of chemistry; Michel Gagne, for his cheerful demeanor and always meeting me with a smile in the hallway. I would also like to thank Jillian Dempsey for serving on my preliminary oral defense committee and for really sparking my interest in inorganic chemistry and spectroscopy.

I would be remiss if I didn't thank all of the Nicewicz group members I have had the chance to work with, both past and present. You all have taught me patience, perspective, and what it truly takes to be a member of a larger team.

I must also thank the people who first piqued my interest in chemistry. My high school chemistry teacher, Michelle Karpovich, has an infectious love for science, and without her, I would not be here. At William & Mary, I had several mentors who inspired me to pursue chemistry further. Specifically, Elizabeth Harbron encouraged me to join a research lab and was one of the most amazing professors I ever had the opportunity to take a class

with. Carey Bagdassarian taught me to think outside of the box, and with that perspective, I have been able to approach science more creatively than I previously did. Jonathan Scheerer mentored me in his research lab at William & Mary and taught me how to become a synthetic chemist, which helped me tremendously through graduate school.

While I have had the most amazing teachers to inspire me and keep me motivated throughout all of my schooling, I would not be here without my two supportive and loving parents, Keith and Debbie Margrey. You both have always been encouraging and have never told me I couldn't do something, which gives me strength. My brother, Chris Margrey, is always willing to challenge me and make me look at situations in different ways, even if we don't see eye to eye. To my aunt and uncle, DeeDee and JR Lyons, you both are incredibly supportive, and I am so lucky to have you both in my life. Furthermore, I have to thank my grandmother, Betty Frazee, who shows me what strength truly looks like and has always been an incredible support system for me.

Finally, I have to thank my friends that have been through everything with me in this program including the ups, the downs, and everything in between. Addie Merians, you are the most amazing person I have ever met, and I am so fortunate to have you in my life. Valerie Tripp, I know we are miles apart, but I am so excited to finally be in the same state as you, and I'm glad we have stayed so close through grad school. And Will Czaplyski, you tolerate my frustration on the bad days and celebrate the good days with me, for which I will always be thankful. I can't wait to see where this leads, but I'm so fortunate to have you all with me as you have been before.

TABLE OF CONTENTS

LIST OF FIGURES

LIST OF TABLES

LIST OF ABBREVIATIONS AND SYMBOLS

^{13}C NMR	Carbon-13 nuclear magnetic resonance
^{1}H NMR	Proton magnetic resonance
Å	Angstrom
ABNO	9-Azabicyclo[3.3.1]nonane *N*-oxyl
Ac	Acetyl
acac	Acetylacetonate
BDE	Bond dissociation enthalpy
BDFE	Bond dissociation free energy
BET	Back electron transfer
BHT	3,5-Di-*tert*-butylhydroxytoluene
BLED	Blue light emitting diode
Boc	*tert*-butyloxycarbonyl
bpy	2,2'-bipyridyl
BQ	Benzoquinone
Bz	Benzoate
CuAAC	Copper (I)-catalyzed azide alkyne cycloaddition
CV	Cyclic voltammetry
dba	dibenzylideneacetone
DCE	1,2-Dichloroethane
DCM	Dichloromethane
DDQ	2,3-Dichloro-5,6-dicyano-1,4-benzoquinone
DFT	Density functional theory

Dfs	2,6-Difluorophenylsulfonate
DMF	*N,N*-Dimethylformamide
Dppbz	1,2-Bis(diphenylphosphino)benzene
e^-	Electron
E^*	Excited state redox potential
$E_{1/2}$	Half-wave potential
$E_{p/2}$	Half-peak potential
E_AS	Electrophilic aromatic substitution
ESI	Electrospray ionization
ET	Electron Transfer
Et_2O	Diethyl ether
EtOH	Ethanol
eV	Electronvolt
GC	Gas Chromatography
G or ΔG	Gibbs free energy or change in Gibbs free energy
GPC	Gel permeation chromatography
H or ΔH	Enthalpy or change in enthalpy
HBPE	Hyperbranched polyethylene
Hex	Hexyl
HFIP	1,1,1,3,3,3-Hexafluoroisopropanol
HOMO	Highest occupied molecular orbital
HPLC	High performance liquid chromatography
HRMS	High resolution mass spectrometry

$h\upsilon$	Photon or energy of a photon
i-PP	Isotactic polypropylene
IR	Infrared
K	General symbol for equilibrium constant
k	General symbol for rate constant
LED	Light emitting diode
LFP	Laser flash photolysis
LUMO	Lowest unoccupied molecular orbital
M	Molar or mol L^{-1}
M_N	Number average molar mass
m/z	Mass per change
MeCN	Acetonitrile
Mes	Mesityl
MOM	Methoxymethyl
MS	Mass spectrometry
mV	Millivolt
MVK	Methyl vinyl ketone
NBO	Natural bond order
NCS	*N*-chlorosuccinimide
NFSI	*N*-fluorobenzenesulfonimide
NMO	*N*-methylmorpholine-*N*-oxide
NMP	*N*-methylpyrrolidinone
NMR	Nuclear magnetic resonance

NPA	Natural population analysis
nm	Nanometer
ns	Nanosecond
O_2•–	Superoxide
PDA	Photodiode array
PDI	Polydispersity index
PEE	Poly(ethylethylene)
PEP	Polyethylene-*alt*-propylene
PET	Photoinduced Electron Transfer
PhME	Toluene
Piv	Pivalate
SCE	Saturated calomel electrode
SET	Single electron transfer
SHE	Standard hydrogen electrode
S_n	Singlet state (ground state: n=0; excited state n>1)
S_NAr	Nucleophilic aromatic substitution
T	Temperature
TBA	Tetra *n*-butylammonium
TBAF	Tetrabutylammonium fluoride
TBS	*tert*-Butyl dimethylsilyl
t-Bu	*tert*-Butyl
TCSPC	Time correlated single photon counting
TEMPO or TEMPO•	(2,2,6,6-Tetramethylpiperdin-1-yl)oxyl

$TEMPO^+$ and TEMPOnium	2,2,6,6-Tetramethyl-1-oxopiperdin-1-ium
TEMPO–H	2,2,6,6-Tetramethylpiperdin-1-ol
TFA	Trifluoroacetic acid
TFE	2,2,2-Trifluoroethanol
THF	Tetrahydrofuran
T_n	Triplet state
Ts	*p*-Toluenesulfonyl
Trit	Triphenylmethyl
UV-Vis	Ultraviolet-visible absorption spectroscopy
V	Volt
Xyl	Xylyl or 2,6-dimethylphenyl
Φ_F	Quantum yield of fluorescence
Φ_R	Photochemical quantum yield of reaction
τ_F	Lifetime of fluorescence
λ	Wavelength

CHAPTER 1: DEVELOPMENT OF ARYL C–H FUNCTIONALIZATION REACTIONS

1.1 Introduction

Aromatic rings are ubiquitous in chemistry, present in natural products, pharmaceuticals, materials, and even perfumes. The ability to construct substituted arenes is critical to facilitate access to many valuable products within these fields. Traditional electrophilic aromatic substitution (EAS) reactions have allowed for the installation of aryl nitrates, sulfonates, halides, and ketones, among other functionality.[1] However, this strategy exhibits limited functional group compatibility due to the necessity of strongly Brønsted or Lewis acidic conditions. The complementary strategy of nucleophilic aromatic substitution (S_NAr) enables the synthesis of a variety of substituted arenes but is limited in application to electron-poor systems.

More recently, the general tactic of cross-coupling reactions has been developed and exploited in a wide variety of contexts.[2] In this mode of reactivity as originally developed, a prefunctionalized aryl halide or triflate undergoes a transition metal-catalyzed coupling with an alkene or organometallic nucleophile, which allows for the net construction of carbon-carbon (C–C) bonds. This strategy has been extended to a variety of coupling partners, enabling the formation of carbon–nitrogen (C–N), carbon–oxygen (C–O), and carbon–sulfur (C–S) bonds.

1.2 Aryl Amines

1.2.1 Importance and Traditional Synthesis

The development of novel methods for the synthesis of aryl amines is of significant interest due to the ubiquity of aryl C–N bonds in pharmaceuticals, natural products, pigments, agrochemicals, and optoelectronic materials.[3] For instance, 84% of FDA approved drugs in 1994 contained at least one nitrogen atom, underscoring their importance. Several representative aryl amine compounds are shown in **Figure 1.1**. Traditionally, arene nitration followed by hydrogenation or other reductive conditions has been used to furnish anilines directly. Nitration reactions, however, require strongly oxidizing and acidic conditions, which can limit their applicability due to problems with functional group tolerance. Additionally, selective nitro group reduction in the presence of other sensitive functionality can be problematic.

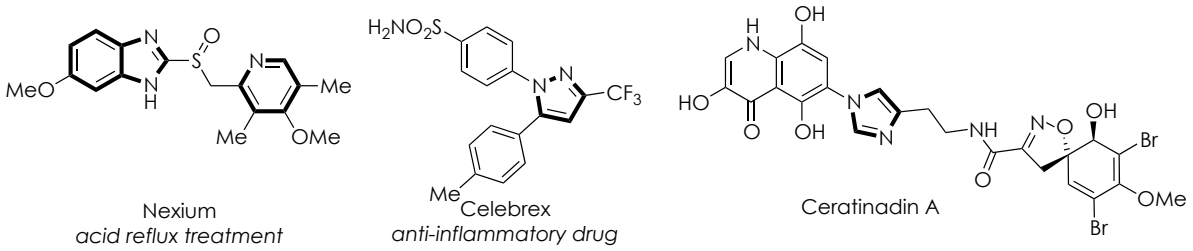

Figure 1.1 Pharmaceuticals and natural products containing nitrogen heterocycles.

1.2.2 Cross-Coupling Strategies for the Synthesis of Aryl Amines

To overcome the limitations of earlier methods for synthesizing aryl amines, several cross-coupling reactions using transition metal catalysts have been developed, particularly the Buchwald-Hartwig[4,5] and Chan-Lam aminations (**Figure 1.2**).[6,7] These reactions are currently the most widely used strategies for the synthesis of aryl amines and generally rely on a palladium or copper-based catalyst system to facilitate the coupling of amines with aryl halides, triflates, or boronic acids.

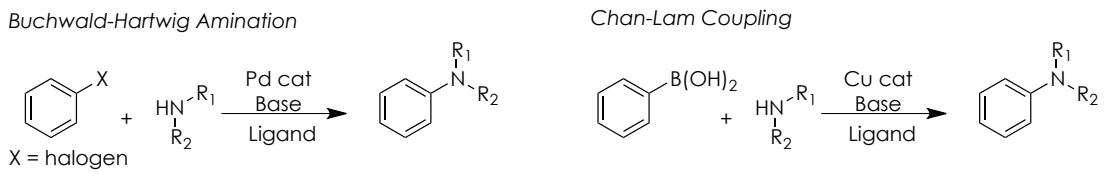

Figure 1.2 General Buchwald-Hartwig amination and Chan-Lam coupling reactions.

While many advances have been made in ligand design and expanding the amine nucleophile scope for Buchwald-Hartwig aminations, several limitations still exist with such systems. Rigorously inert, anhydrous conditions are generally required to prevent catalyst decomposition. Additionally, arenes used in this cross-coupling require prefunctionalization as the halide or triflate, lengthening the synthesis towards aryl amines. In the case of the Chan-Lam reaction, arylboronic acids or esters are required, which are themselves often prepared from the corresponding aryl halide, adding another synthetic step. Furthermore, cross-coupling approaches are generally limited by steric hindrance such that amination *ortho* to another functional group can be very challenging, resulting in diminished yields, as in the *ortho*-methoxy derivative (**Figure 1.3**).[8]

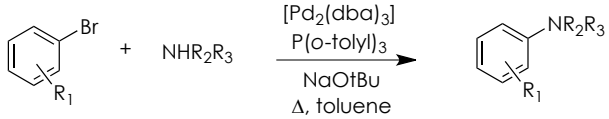

R_1	R_2	R_3	Yield %
3,5-bis-Me	*n*-hexyl	H	88
4-CN	*n*-hexyl	H	97
2-OMe	Ph	Me	66
3-CO_2*t*Bu	$PhCH_2$	H	71

Figure 1.3 Examples of Buchwald-Hartwig aminations with substituted arenes.

1.2.3 Aryl Amine Construction via C–H Functionalization

The ability to convert aryl C–H bonds into C–N bonds directly bears the prospect of streamlining the synthesis of valuable aryl amines. This strategy requires only one synthetic step instead of the minimum of two required for the analogous prefunctionalization/cross-coupling sequence.[9,10] Additionally, this benefit is magnified when applied to the context of late-stage functionalization of pharmaceuticals or other bioactive targets, potentially granting

access to libraries of compounds diversified from a single precursor. While minimizing the number of synthetic steps is a significant advantage of C–H amination reactions, regioselectivity of such transformations can be challenging to control (**Figure 1.4**). An inherent regiochemical bias is required to achieve good site selectivity due to the usual presence of several aryl C–H bonds in a substrate. This results in selectivities that are highly mechanism dependent and dictated by the electronics of a given arene.

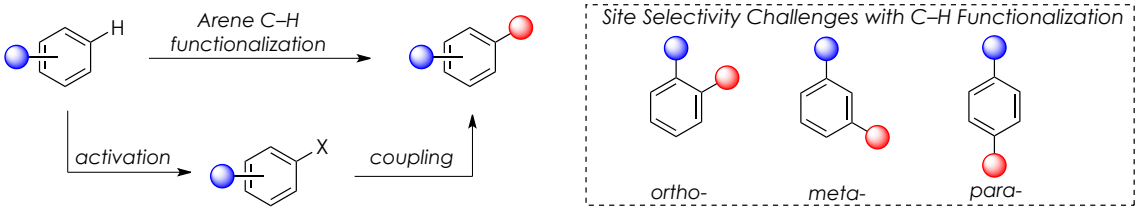

Figure 1.4 Streamlining syntheses through arene C–H functionalization compared to cross coupling reactions.

The regiochemical outcome of transition metal-catalyzed arene C–H functionalization reactions is generally dictated by the presence of a preinstalled Lewis basic directing group, which results in predominantly *ortho*-selectivity with respect to that functionality. Buchwald, in 2005, developed an intramolecular arene C–H amination strategy to form carbazoles from 2-acetaminobiphenyl derivatives (**Figure 1.5**).[11] A palladium catalyst was used along with a stoichiometric amount of copper as a cooxidant under aerobic conditions. The amide directed *ortho*-palladation would form the metallocycle **1.1,** poised to undergo reductive elimination to afford the desired carbazole.

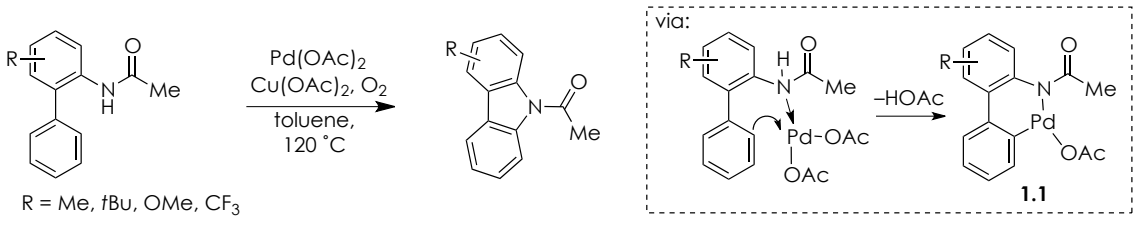

Figure 1.5 Intramolecular C–H amination to construct carbazoles.

Analogous intermolecular arene C–H amination reactions have also been developed, relying on Lewis basic directing groups to form *ortho*-substituted products selectively. In 2010, Shen developed an aerobic copper-mediated aryl amination reaction, in which use of a pyridine or pyrimidine directing group facilitated the addition of a phthalimide nucleophile to arenes using oxygen as a terminal oxidant (**Figure 1.6**).[12] Daugulis also reported a copper-catalyzed *ortho*-selective C–H amination using an 8-aminoquinoline directing group that proceeded through a putative copper (III) intermediate.[13] Additionally, Nakamura has disclosed a method for iron-catalyzed amination with *N*-chloroamines using the quinolin-8-yl moiety as the Lewis basic directing group.[14]

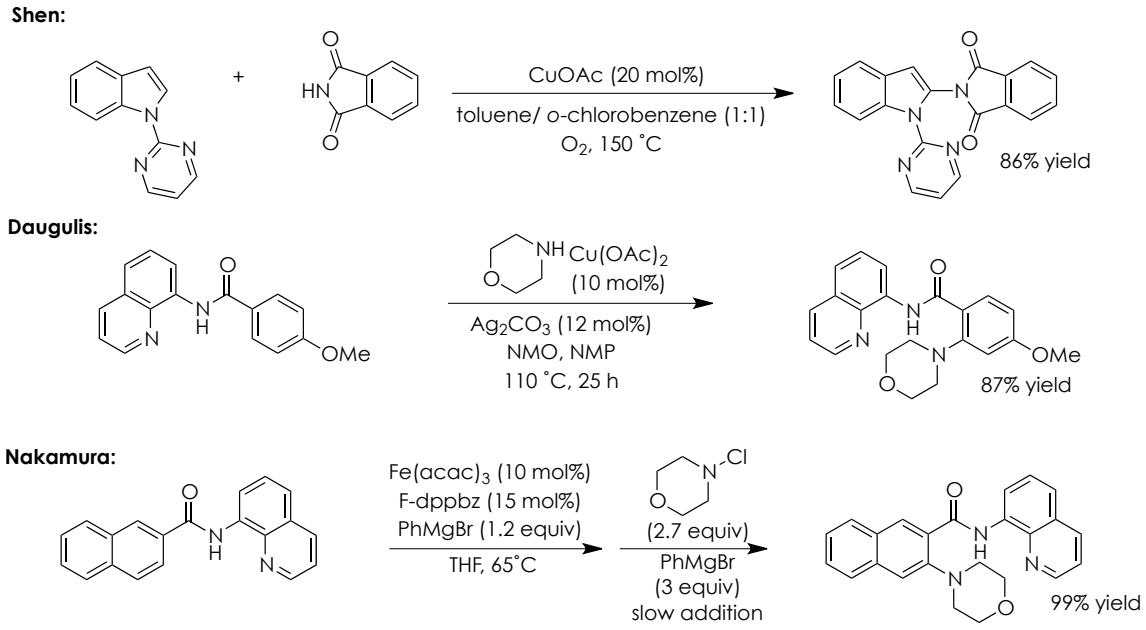

Figure 1.6 Directing group-mediated aryl C–H aminations.

While *ortho* selectivity is most common in directing group-mediated strategies, several examples of *meta*-selective arene amination reactions have also been reported. Hartwig has demonstrated a sterically controlled intermolecular arene amination using phthalimide as the nucleophile with diacetoxyiodobenzene as a superstoichiometric terminal oxidant (**Figure 1.7**).[15] While many reactions favored *meta*-functionalization instead of

ortho- reactivity, selectivity over *para*-functionalization was generally low. These reactions also required that the arene coupling partner be used as the solvent to obtain synthetically useful yields.

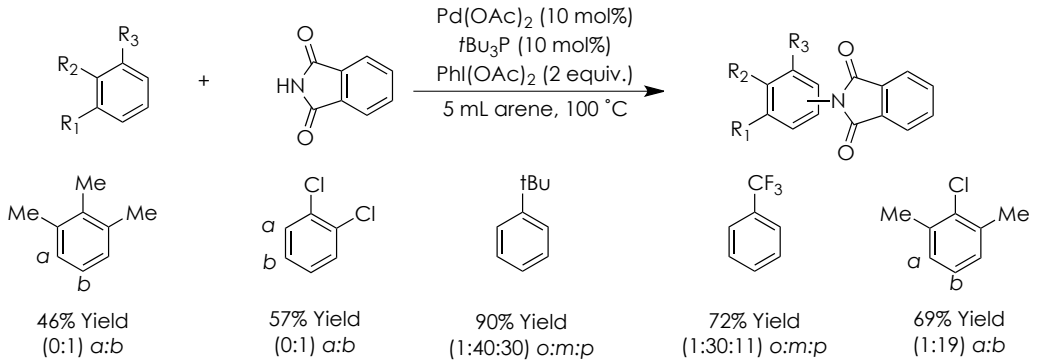

Figure 1.7 *Meta*-selective palladium-catalyzed aryl amination.

DeBoef reported a metal-free intermolecular oxidative dual C–H and N–H bond functionalization reaction (**Figure 1.8**).[16] In the presence of diacetoxyiodobenzene and microwave irradiation, the authors proposed that an arene substrate could be oxidized to the aryl cation radical. This intermediate, most electrophilic at the *ortho*- and *para*- positions, was susceptible to nucleophilic addition by amide derivatives and subsequent oxidation by superstoichiometric diacetoxyiodobenzene to form the aminated products at the *ortho*- and *para*- positions in roughly 1:1 ratios. Minor amounts of *meta*-functionalized product were observed, but never as the major regioisomer. The utility of this method was limited by the necessity of a significant excess of the arene, in some cases even as the reaction solvent, to attain synthetically useful yields. DeBoef continued this work more recently, reporting that the use of a gold catalyst with diacetoxyiodobenzene as the oxidant could selectively form *para*-functionalized products.[17] While this system improved upon previous regioselectivity, it required the arene to be used as the solvent, limiting potential applicability. In a related work, Cho and Chang reported the amination of arenes using imide nucleophiles under the action of

superstoichiometric diacetoxyiodobenzene.[18] Unlike the aryl cation radical postulated by DeBoef, however, Cho and Chang proposed that an *N*-(phenylacetoxyiodo)imido species detected by ESI-MS can undergo direct reaction with the arene, furnishing functionalization products as a mixture of regioisomers.

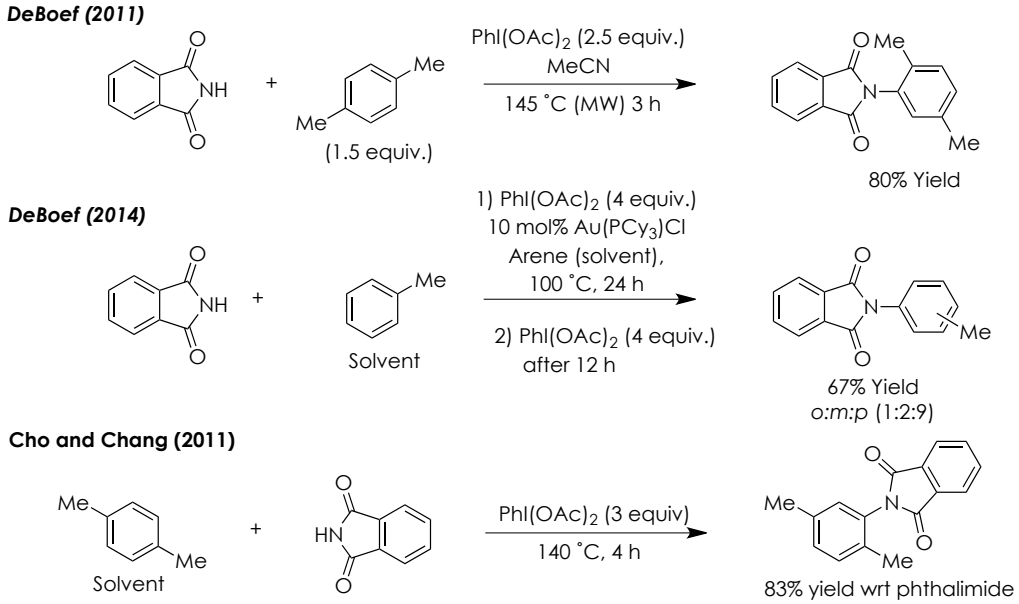

Figure 1.8 Aryl amination mediated by diacetoxyiodobenzene.

The addition of discretely formed nitrogen-centered radicals to arenes has proven to be an effective strategy for the synthesis of aryl amines. Baran developed *N*-succinimidyl perester **1.2** as a progenitor to the nitrogen-centered succinimidyl radical mediated by Cp_2Fe (**Figure 1.9**).[19] In this system, C–H imidation of arenes and heteroarenes was possible, generally affording the products as mixtures of regioisomers. Itami also disclosed a strategy for aryl and heteroaryl C–H imidation using *N*-fluorobenzenesulfonimide (NFSI) under copper catalysis via a putative imidyl radical.[20] In this work, single regioisomers were generally formed due to the use of substrates that possessed high levels of symmetry or several preexisting substituents. In both of these examples, however, the addition of only one nitrogen nucleophile is demonstrated.

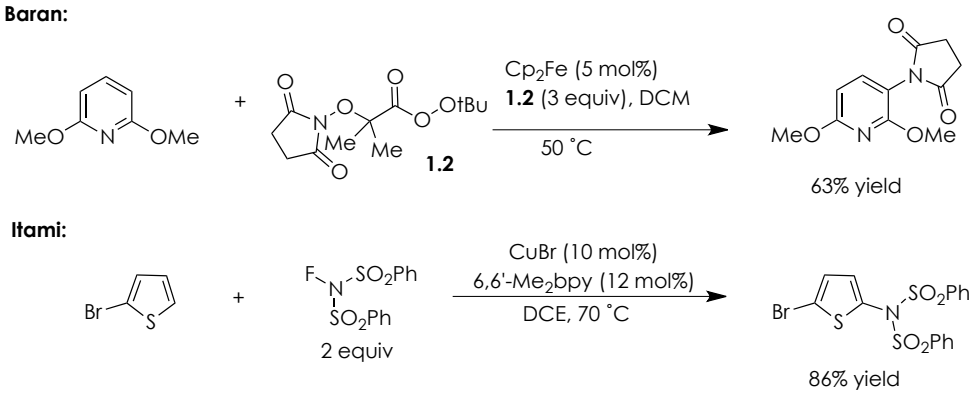

Figure 1.9 Applications of nitrogen-centered radicals in aryl amination.

Recently, Ritter explored the use of charge-transfer complexes to facilitate *para* selective functionalization of arenes using dicationic palladium catalyst **1.3** (**Figure 1.10**).[21] A dicationic radical generated by single electron reduction of Selectfluor could add to arenes, forming predominantly the *para* adduct **1.4** in the case of monosubstituted substrates. When disubstituted benzenoids or heteroarenes were used, the strongest directing substituent dictated regiochemistry, and deprotection afforded piperazine-functionalized arenes in good yields and regioselectivities. Fukui indices were used to explain the regiochemistry observed based on electron density.

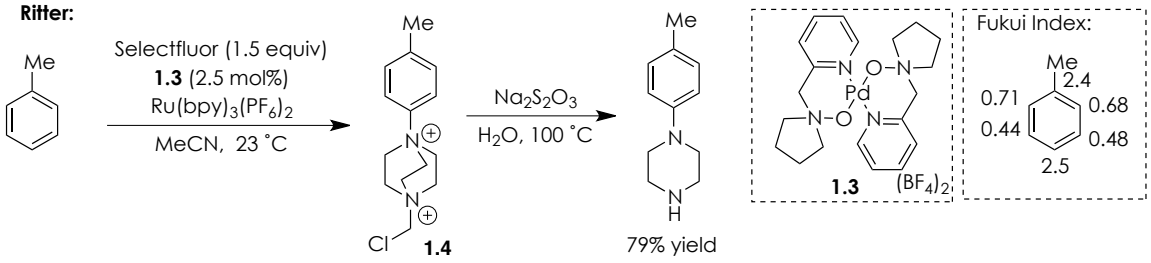

Figure 1.10 *Para*-selective aryl amination via a charge-transfer mechanism.

Photoredox catalysis has also been used to generate nitrogen-centered radicals for arene addition. In 2014, Sanford disclosed a visible light photocatalyzed, $Ir(ppy)_3$-mediated system in which *N*-acyloxyphthalimide **1.5** could be reduced to the radical anion with subsequent fragmentation to form the trifluoroacetate anion and the nitrogen-centered

phthalimidyl radical (**Figure 1.11**).[22] Addition of this species to arenes and heteroarenes, present in significant excess of 10 – 20 equivalents, followed by rearomatization produced aryl amine adducts. Due to the use of a prefunctionalized phthalimide derivative, no external oxidant was required for the system. Many of the substrates underwent functionalization at the *ortho* position, but *meta* selectivity was observed with pyridines. A related work was disclosed by Lee, in which *N*-chlorophthalimide served as a precursor to the phthalimidyl radical under photoredox catalysis with $Ir(dFppy)_3$.[23] More recently, Itami used photoredox catalysis to facilitate the C–H imidation of arenes and heteroarenes with diphenylsulfonimide as the nucleophile.[24]

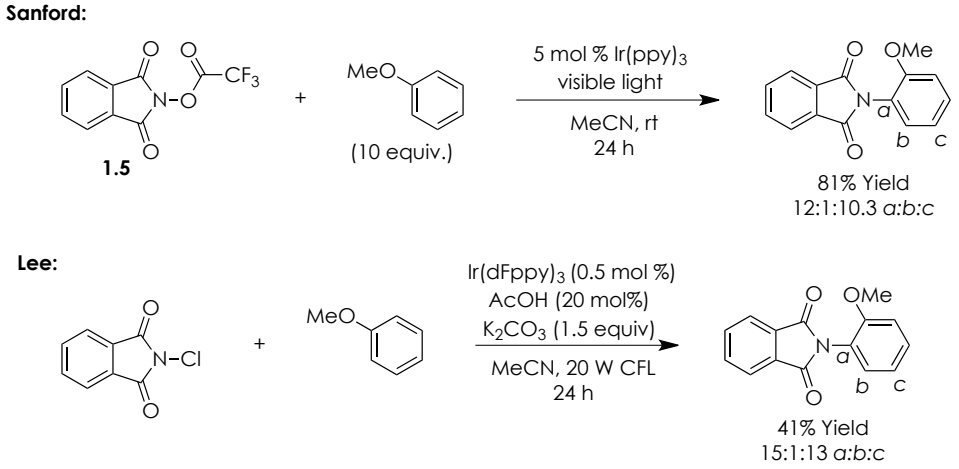

Figure 1.11 Photoredox-catalyzed generation of nitrogen-centered radicals for aryl amination.

1.3 Photoredox Catalysis

1.3.1 Underlying Photophysical Processes

Radical chemistry has garnered much attention in recent years due to the complementary reactivity of radical (single electron) and polar (two electron) chemistry. The ability to harness an open shell pathway with unpaired electrons can allow for the development of mild methods that unlock unique chemical reactivity. This interest has also

sparked a focus on photochemical methods of radical generation and, more specifically, photoredox catalysis. The ability of a chromophore to absorb light and access an excited state can be described based on its photophysical properties.[25]

A general representation of possible photophysical processes for an organic molecule is depicted in a Jablonski diagram (**Figure 1.12**). When a closed shell compound absorbs a photon of light of a suitable wavelength (A), it can undergo transition from the ground singlet state S_0 to the first electronically excited singlet state S_1 with no change in electron spin. By the Franck-Condon principle, electronic excitation is nearly instantaneous with respect to nuclear motion, so the geometry of the molecule in the S_1 state is similar to that from which it originated in the S_0 state. As a result, excitation tends to promote a compound to a higher vibrational level within the S_1 state instead of to the vibrational ground state. The process of vibrational relaxation (B) causes rapid relaxation to the lowest vibrational state within S_1.

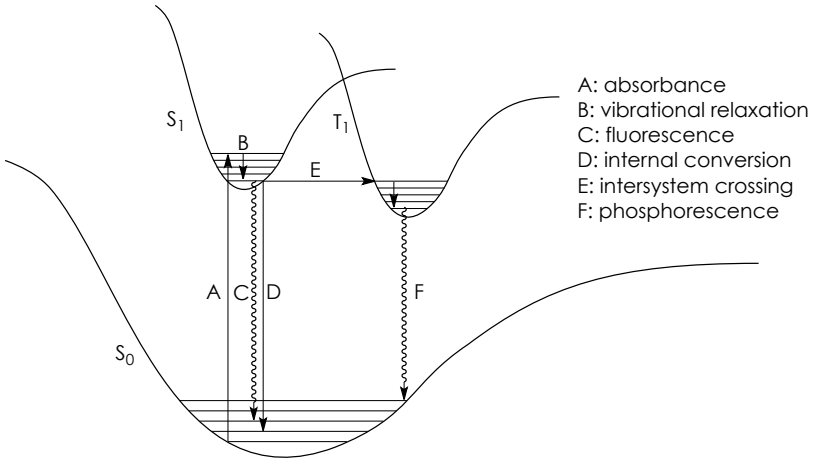

Figure 1.12 Jablonski diagram.

At this point, there are several possible fates of the excited state. Fluorescence (C), the emission of a photon with energy corresponding to a transition between the S_1 and S_0 states, can occur, reverting the molecule back to the ground state. The exact energy of the photon can vary, resulting in a vibrationally excited compound within the S_0 state; however,

the energy of a photon emitted via fluorescence is less than that of the photon initially absorbed, corresponding to a Stokes shift of the fluorescence spectrum when compared to the absorption spectrum. The excited state can also undergo internal conversion (D), a non-radiative decay in which the additional energy that had been absorbed is lost to the surroundings in the form of heat. Additionally, intersystem crossing (E) to a triplet excited state T_1, through which the electron changes spin multiplicity, can occur. By electronic selection rules, this transition is forbidden, but it can occur via spin-orbit coupling, which is more likely for molecules containing heavy atoms such as bromine or iodine. Once in T_1, the molecule can undergo phosphorescence (F), the radiative process through which the molecule is converted to the S_0 state.

1.3.2 Excited State Electron Transfer

In an electronically excited singlet or triplet state, electron transfer processes can occur and are critical for the activity of photoredox catalysts. In a general sense, such a catalyst can serve as either the excited state acceptor or donor for electron transfer. Considering a donor D and acceptor A, electron transfer from D to A is not thermodynamically feasible since the LUMO of A is significantly higher than the HOMO of D (**Figure 1.13**). If A is excited with light, an electron can be promoted from the molecular HOMO to the LUMO, forming the excited state A*. Since there is now an electron deficiency in the HOMO of A and the HOMOs of D and A are close in energy, electron transfer can occur from the HOMO of D to A, formally oxidizing D to the cation radical and reducing A to the anion radical. From this point, D can undergo further reactivity with additional compounds in solution. Alternately, back electron transfer from the anion radical of A to the unfilled orbital of cation radical D can occur.

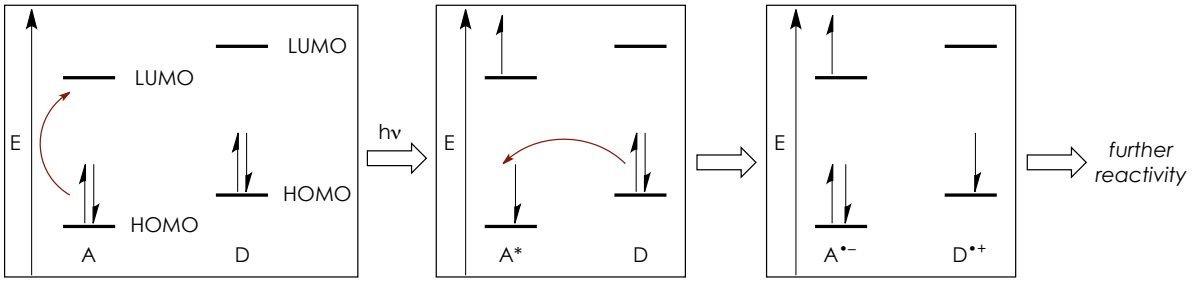

Figure 1.13 Electron transfer depiction. D (Donor) and A (acceptor)

The Gibbs energy of photoinduced electron transfer can be determined to help inform whether a given SET process is favorable. Assuming that the electrostatic work, related to the Coulombic effect of charge separation, is negligible, the Gibbs energy for a photoredox catalyst **cat** acting as an excited state reductant toward substrate **sub** can be formulated as:

$$\Delta G_{PET} = -\mathcal{F}(E^{*}_{\mathrm{red}}(\mathbf{cat}^{*}/\mathbf{cat}^{\bullet-}) - E_{\mathrm{ox}}(\mathbf{sub}^{\bullet+}/\mathbf{sub}))$$

where $\mathcal{F}$ is the Faraday constant, E^{*}_{red} is the excited state reduction potential of **cat**, and E_{ox} is the oxidation potential of **sub**. E^{*}_{red} is calculated by:

$$E^{*}_{\mathrm{red}}(\mathbf{cat}^{*}/\mathbf{cat}^{\bullet-}) = E_{\mathrm{red}}(\mathbf{cat}/\mathbf{cat}^{\bullet-}) + E_{0,0}$$

where $E_{0,0}$ is the excited state energy of the catalyst.

Previous work in the Nicewicz lab has demonstrated the hydrofunctionalization of alkenes, representing a net reductive pathway (**Figure 1.14**).[26] Through a chlorolactonization methodology, our lab has also demonstrated a difunctionalization reaction of alkenes in 2016.[27] The ability to functionalize an alkene or arene in a net sp^2 C–H functionalization would represent a net oxidative pathway that is viable through photoredox catalysis.

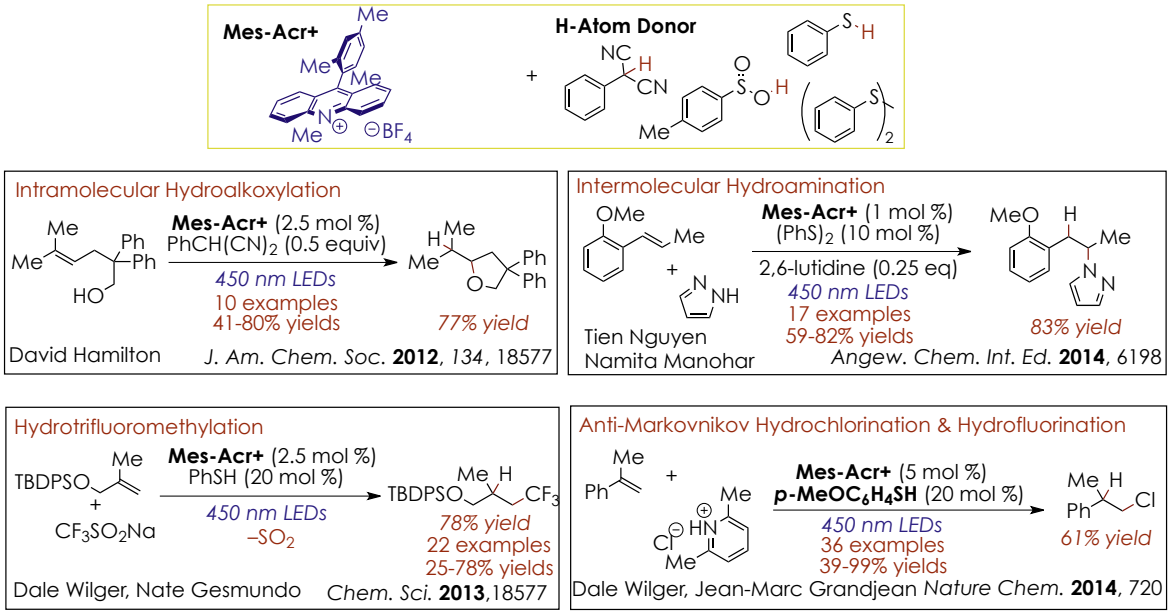

Figure 1.14 Nicewicz lab hydrofunctionalization methodologies.

1.3.3 Arene C–H Functionalization via Cation Radical Intermediates

Recently, synthetic electrochemistry has garnered increased attention as a method for facilitating the donation or removal of an electron from a given substrate, with commercial setups now readily available. Yoshida reported an electrooxidative method for aryl C–H amination in 2014 using anodic oxidation (**Figure 1.15**).[28] In this transformation, single electron oxidation of an aromatic substrate formed an arene cation radical, which was susceptible to nucleophilic addition of nitrogen heterocycles, generating cationic intermediate **1.6**, for example, that was resistant to further oxidation and could be deprotected to afford a net amination product. The intermediacy of an arene cation radical allows for a transient electrophilic coupling partner to be generated *in situ* in a controlled manner. This methodology highlighted excellent site selectivity, affording single regioisomers in most cases. A similar approach enabled access to a variety of aniline derivatives.[29] Using DFT calculations, Yoshida proposed that the amine nucleophile added to the carbon bearing the hydrogen with the largest coefficient of the LUMO of the cation radical.

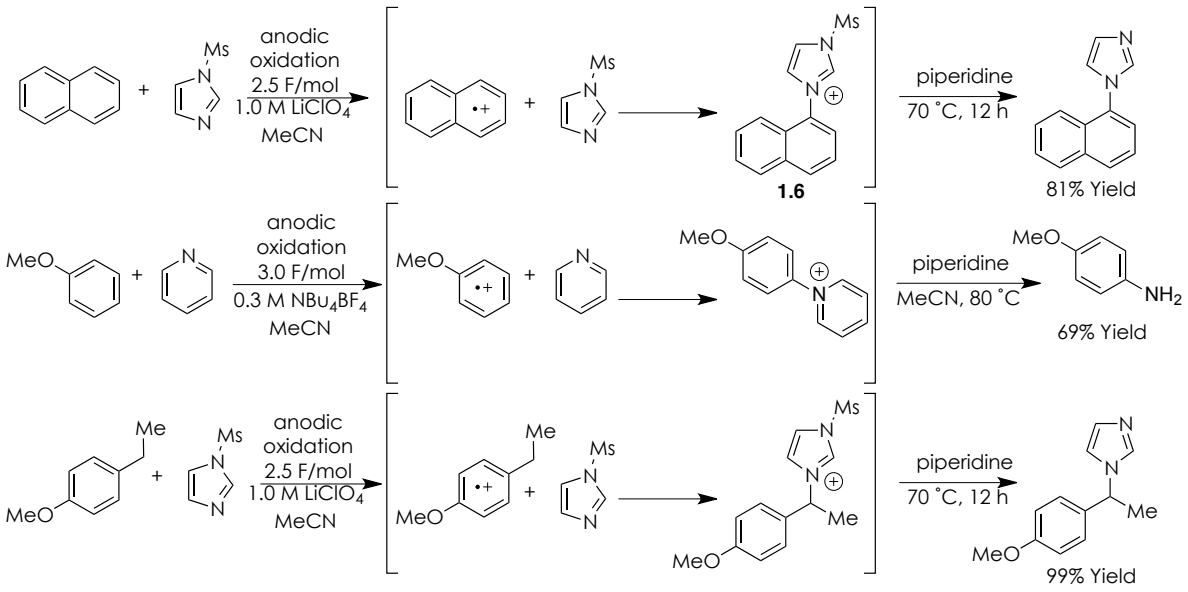

Figure 1.15 Electrooxidative aryl and benzylic functionalization methodologies.

Complimentary to the aryl amination methodologies, Yoshida used alkyl-substituted arenes and modified reaction conditions to favor benzylic amination over aryl amination.[28] Upon formation of a similar arene cation radical via electrooxidation, deprotonation of the benzylic C–H bond, with a calculated pKa of –20, is thermodynamically favorable and leads to formation of the benzylamine.[30]

The ability to generate arene cation radicals has been applied to other arene functionalization reactions. Fukuzumi has demonstrated the use of an acridinium photoredox catalyst, **Mes-Acr-MeClO$_4$**, to mediate C–H bromination[31] and chlorination[32] reactions of electron-rich arenes using hydrobromic or hydrochloric acid, respectively, and dioxygen (O_2) as a stoichiometric oxidant (**Figure 1.16**). Although the reactions could produce some haloarenes in quantitative yield, the products obtained were often those that could be accessed through traditional EAS methods. Mediated by visible light irradiation, it was proposed that catalyst **Mes-Acr+** could be excited and undergo single electron transfer (SET) from the arene to produce the arene cation radical **1.7**. This transient intermediate could

undergo nucleophilic halide addition to form the cyclohexadienyl radical **1.8**, which could be rearomatized to afford the halogenated product **1.9**. Based on the detection of hydrogen peroxide in the crude reaction mixtures, it was believed that O_2 was capable of oxidizing the acridine radical **Mes-Acr•** to reenter the catalytic cycle, with the resultant hydroperoxy radical being involved with product rearomatization. Subsequent reports of aryl functionalization from Fukuzumi include C–H hydroxylation mediated by DDQ.[33]

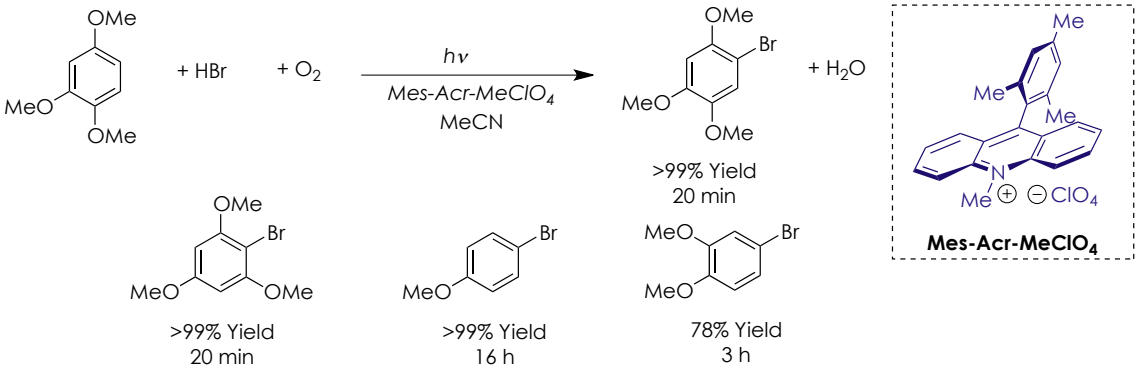

Figure 1.16 Acridinium-catalyzed aryl bromination.

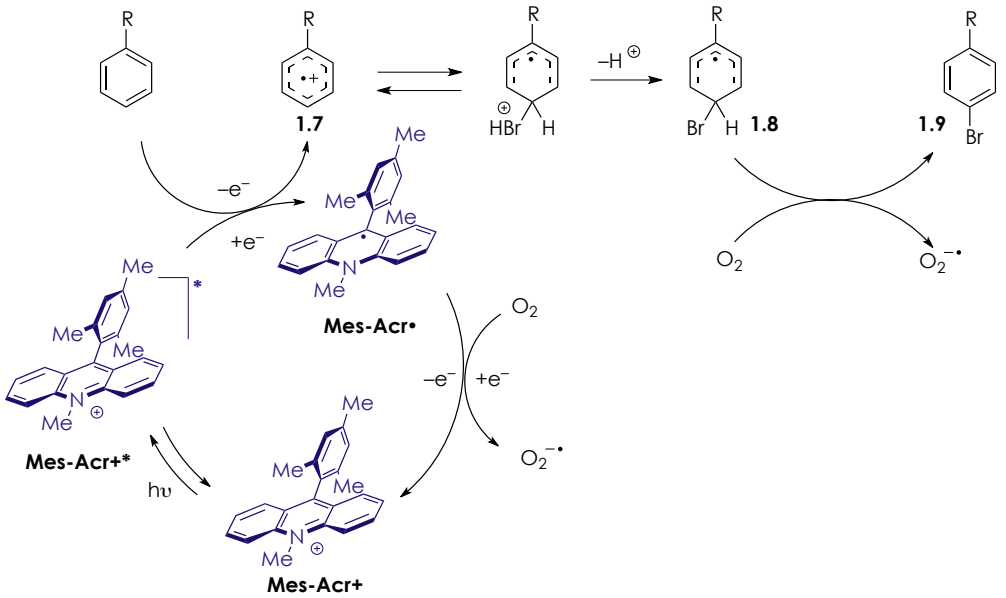

Figure 1.17 Proposed mechanism for acridinium-catalyzed aryl bromination.

Fukuzumi further examined the selectivity of the transformations by using computational predictions of where bromination would occur. Through DFT calculations at the B3LYP/6-31+G(d,p) level of theory, Fukuzumi showed that the position of the largest positive charge density through natural population analysis (NPA) values in the neutral aromatic compound was the same as in the cation radical for 1,2,3-trimethoxybenzene and 1,2,4-trimethoxybenzene.[31] It was proposed that this similarity accounts for why the selectivity of cation radical-based bromination is the same as that for electrophilic bromination. Further explanations of reactivity were highlighted by examining differences in energy between brominated radical **1.8** and the arene cation radical **1.7**. When the brominated radical intermediate was more stable than the cation radical, the reaction times were significantly shorter, although both reactions proceeded in nearly quantitative yields if run for a sufficient length of time. As demonstrated with both Yoshida's and Fukuzumi's work, DFT calculations can be used to account for the regioselectivity of arene C–H functionalization reactions in a facile and practical manner.

1.3.4 Considerations for Arene C–H Functionalization via Photoredox Catalysis

As highlighted in Fukuzumi's aryl functionalizations, photoredox catalysts can be used to generate reactive intermediates efficiently, particularly arene cation radicals. However, for productive reactivity to ensue, careful considerations of both the catalyst and the substrate must be made. To remove an electron from an arene substrate, reduction potentials of the photoredox catalyst excited state must be understood. For this reason, redox potentials are critical to define the thermodynamic feasibility of SET. Common metal-based photoredox catalysts, including those that are ruthenium- or iridium-based, are not as oxidizing compared to an acridinium catalyst. $Ru(bpy)_3$ and $Ir(ppy)_3$ do not possess high

enough excited state reduction potentials to ($E_{1/2}^{red*}$ = +0.77 V vs. SCE and +0.31V vs SCE) remove an electron from any but the most electron-rich arenes. However, acridinium catalysts are powerful enough oxidants to remove an electron based on redox potentials alone ($E_{1/2}^{red*}$ = + 2.0 V vs. SCE). For this reason, using acridinium-based catalysis for arene functionalization can be rationalized due the thermodynamic favorability of electron transfer.

Work disclosed by the Nicewicz lab thoroughly examined the oxidation and reduction potentials of a large group of commercial reagents via cyclic voltammetry (CV), and this compilation is an important tool for understanding whether a given substrate can undergo SET with a particular catalyst.[34] As shown in **Figure 1.18**, groupings were made based on functional group to highlight redox potentials. Furthermore, this study also disclosed a computational predictive model for calculating oxidation and reduction potentials, which is particularly valuable if access to a potentiostat is problematic. This model was verified by the correlation of over 180 experimental values with the predicted values, generally in high agreement.

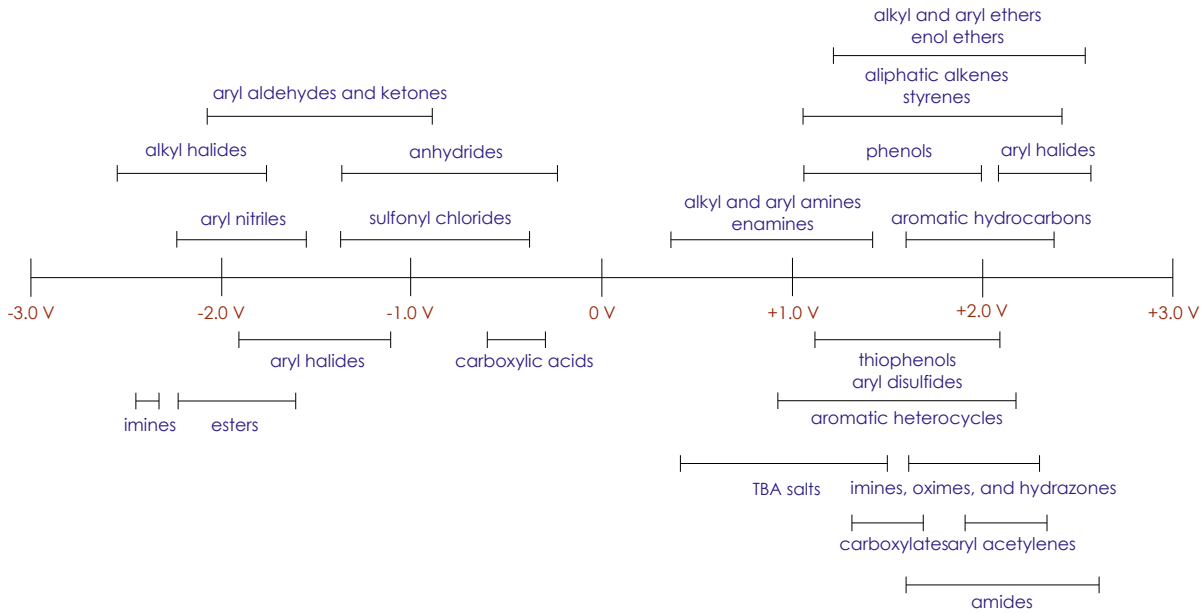

Figure 1.18 Common functional group redox potentials in V vs SCE in MeCN.

REFERENCES

(1) Taylor, R. J. Wiley: Electrophilic Aromatic Substitution Chichester, West Sussex, England ; New York, 1990.

(2) Johansson Seechurn, C. C. C.; Kitching, M. O.; Colacot, T. J.; Snieckus, V. *Angew. Chem. Int. Ed.* **2012**, *51*, 5062–5085.

(3) Vitaku, E.; Smith, D. T.; Njardarson, J. T. *J. Med. Chem.* **2014**, *57*, 10257–10274.

(4) Wolfe, J. P.; Wagaw, S.; Marcoux, J.-F.; Buchwald, S. L. *Acc. Chem. Res.* **1998**, *31*, 805–818.

(5) Hartwig, J. F. *Acc. Chem. Res.* **1998**, *31*, 852–860.

(6) Lam, P. Y. S.; Vincent, G.; Clark, C. G.; Deudon, S.; Jadhav, P. K. *Tetrahedron Lett.* **2001**, *42*, 3415–3418.

(7) Sanjeeva Rao, K.; Wu, T.-S. *Tetrahedron* **2012**, *68*, 7735–7754.

(8) Surry, D. S.; Buchwald, S. L. *Chem Sci* **2011**, *2*, 27–50.

(9) Neufeldt, S. R.; Sanford, M. S. *Acc. Chem. Res.* **2012**, *45*, 936–946.

(10) Shul'Pin, G. B. In *Transition Metals for Organic Synthesis*; Beller, M.; Bolm, C., Eds.; Wiley-VCH Verlag GmbH, 2004; pp. 215–241.

(11) Tsang, W. C. P.; Zheng, N.; Buchwald, S. L. *J. Am. Chem. Soc.* **2005**, *127*, 14560–14561.

(12) Xu, H.; Qiao, X.; Yang, S.; Shen, Z. *J. Org. Chem.* **2014**, *79*, 4414–4422.

(13) Tran, L. D.; Roane, J.; Daugulis, O. *Angew. Chem. Int. Ed.* **2013**, *52*, 6043–6046.

(14) Matsubara, T.; Asako, S.; Ilies, L.; Nakamura, E. *J. Am. Chem. Soc.* **2014**, *136*, 646–649.

(15) Shrestha, R.; Mukherjee, P.; Tan, Y.; Litman, Z. C.; Hartwig, J. F. *J. Am. Chem. Soc.* **2013**, *135*, 8480–8483.

(16) Kantak, A. A.; Potavathri, S.; Barham, R. A.; Romano, K. M.; DeBoef, B. *J. Am. Chem. Soc.* **2011**, *133*, 19960–19965.

(17) Marchetti, L.; Kantak, A.; Davis, R.; DeBoef, B. *Org. Lett.* **2015**, *17*, 358–361.

(18) Kim, H. J.; Kim, J.; Cho, S. H.; Chang, S. *J. Am. Chem. Soc.* **2011**, *133*, 16382–16385.

(19) Foo, K.; Sella, E.; Thomé, I.; Eastgate, M. D.; Baran, P. S. *J. Am. Chem. Soc.* **2014**, *136*, 5279–5282.

(20) Kawakami, T.; Murakami, K.; Itami, K. *J. Am. Chem. Soc.* **2015**, *137*, 2460–2463.

(21) Boursalian, G. B.; Ham, W. S.; Mazzotti, A. R.; Ritter, T. *Nat. Chem.* **2016**, *8*, 810–815.

(22) Allen, L. J.; Cabrera, P. J.; Lee, M.; Sanford, M. S. *J. Am. Chem. Soc.* **2014**, *136*, 5607–5610.

(23) Kim, H.; Kim, T.; Lee, D. G.; Roh, S. W.; Lee, C. *Chem Commun* **2014**, *50*, 9273–9276.

(24) Ito, E.; Fukushima, T.; Kawakami, T.; Murakami, K.; Itami, K. *Chem* **2017**, *2*, 383–392.

(25) Romero, N. A.; Nicewicz, D. A. *Chem. Rev.* **2016**.

(26) Margrey, K. A.; Nicewicz, D. A. *Acc. Chem. Res.* **2016**, *49*, 1997–2006.

(27) Griffin, J. D.; Cavanaugh, C. L.; Nicewicz, D. A. *Angew. Chem. Int. Ed Engl.* **2017**, *56*, 2097–2100.

(28) Morofuji, T.; Shimizu, A.; Yoshida, J. *J. Am. Chem. Soc.* **2014**, *136*, 4496–4499.

(29) Morofuji, T.; Shimizu, A.; Yoshida, J. *J. Am. Chem. Soc.* **2013**, *135*, 5000–5003.

(30) Bordwell, F. G.; Cheng, J. P. *J. Am. Chem. Soc.* **1989**, *111*, 1792–1795.

(31) Ohkubo, K.; Mizushima, K.; Iwata, R.; Fukuzumi, S. *Chem. Sci.* **2011**, *2*, 715.

(32) Ohkubo, K.; Mizushima, K.; Fukuzumi, S. *Res. Chem. Intermed.* **2012**, *39*, 205–220.

(33) Ohkubo, K.; Hirose, K.; Fukuzumi, S. *Chem. - Eur. J.* **2015**, *21*, 2855–2861.

(34) Roth, H.; Romero, N.; Nicewicz, D. *Synlett* **2016**, *27*, 714–723.

CHAPTER 2: ARYL C–H AMINATION VIA ORGANIC PHOTOREDOX CATALYSIS

Adapted from Romero, N. A.; Margrey, K. A.; Tay, N. E.; Nicewicz, D. A. *Science* **2015**, *349*, (6254), 1326–1330.

2.1 Introduction

This chapter will detail our efforts in developing an aryl C–H amination reaction. The ability to form aryl C–N bonds is important in natural product synthesis as well as pharmaceutical development due to the prevalence of nitrogen atoms in biologically active compounds. While this bond construction is often accomplished through methods such as cross-couplings that rely on prefunctionalized aromatic systems, the direct formation of aryl C–N bonds from aryl C–H bonds would streamline the preparation of valuable molecules.[1,2,3,4] Through this work, we developed reaction conditions to facilitate the aryl C–H amination of a wide variety of arenes with azole coupling partners. This strategy was applied to several complex molecules to highlight its utility in late stage functionalization, and an extension toward direct aniline synthesis using ammonium carbamate was also detailed.[5]

2.2 Reaction Development

Based on prior knowledge of Fukuzumi's aryl bromination work that highlighted the ability of an acridinium photoredox catalyst to generate arene cation radicals via single electron transfer (SET)[6] (see **Chapter 1.3.3**), we wondered if other nucleophiles, such as

amines, could be employed (**Figure 2.1**). For such a transformation to be synthetically useful, the arene undergoing functionalization would be the limiting reagent and could react with a wide variety of nitrogenous coupling partners. The reaction would also need to exhibit high levels of site selectivity and, ideally, be easily tunable. We envisioned reactivity similar to that reported by Fukuzumi, in which single electron oxidation of an arene would be followed by nucleophilic addition and deprotonation to form a cyclohexadienyl radical. Under aerobic conditions, this species would undergo rearomatization to afford the C–H functionalization product.

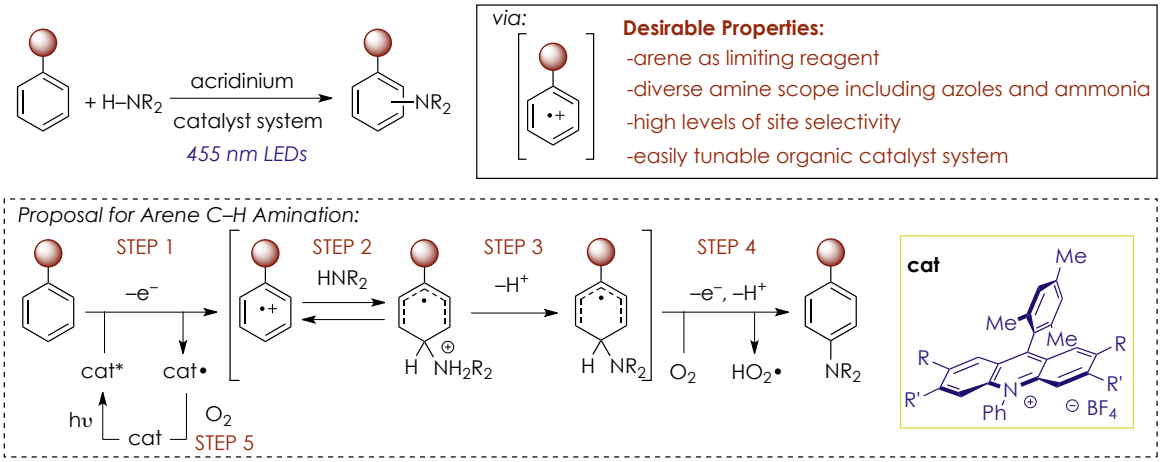

Figure 2.1 Reaction blueprint for site-selective C–H amination of arenes.

2.2.1 Initial Optimization

Beginning with a simple system consisting of anisole and pyrazole as the arene and azole coupling partners, respectively, in DCE under a balloon of oxygen with BLED irradiation, we observed initial reactivity of 47% yield of **2.1a** and **2.1b** with 6.7:1 *para:ortho* regioselectivity (**Table 2.1, entry 1**). As proposed by Fukuzumi, oxygen was used for catalyst turnover from the acridine intermediate to re-enter the catalytic cycle as well as product aromatization.[7] The importance of oxygen was verified by the control reaction without an oxygen atmosphere or sparge, in which only trace amounts (<5 % yield) of the

amination products were observed (**Table 2.1, entry 2**). DCE was the superior solvent for the reaction (**Table 2.1, entries 3 – 5**), with other solvents used in prior acridinium-catalyzed systems affording only trace amounts of product. Dimethyl-substituted acridinium, catalyst **B**, shown to be more robust in prior work involving alkene hydrohalogenation,[8] was slightly less effective than unsubstituted acridinium, catalyst **A** (**Table 2.1, entry 6**). Additionally, through the testing of other terminal oxidants such as hypervalent iodine, benzoquinone, and persulfates (**Table 2.1, entries 7 – 9**), we determined that other common oxidants were inferior to a simple oxygen atmosphere.

Table 2.1 Initial optimization of aryl amination.

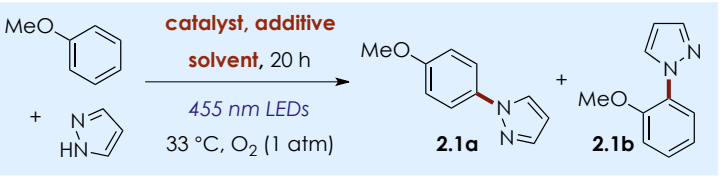

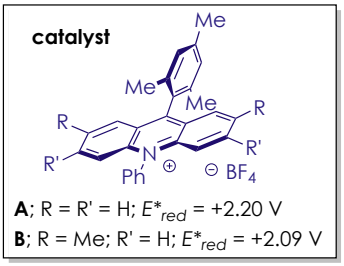

entry	additive	catalyst	solvent [M]	yield	*p:o*
1	none	A	DCE [0.25]	47%	6.7:1
2	no O_2	A	DCM [0.25]	2%	–
3	none	A	MeCN [0.25]	6%	2.0:1
4	none	A	MeOH [0.25]	4%	1:2.9
5	none	A	TFE[0.25]	9%	1:25
6	none	B	DCE [0.25]	37%	3.6:1
7	$PhI(OAc)_2$ (1.0 eq.)	B	DCE [0.25]	20%	4.1:1
8	Benzoquinone (1.0 eq.)	B	DCE [0.25]	18%	6.9:1
9	$K_2S_2O_8$ (1.0 eq.)	B	DCE [0.25]	14%	1.8:1

2.2.2 Product Stability Studies and Byproduct Formation

Since the reaction yields could not be easily improved, at this stage we decided to examine product stability during the course of the reaction. When products **2.2** and **2.3** were resubmitted to the reaction conditions, either no product was observed or only 23% yield of returned product, respectively (**Figure 2.2**). This demonstrated that there was a very

significant problem with product degradation during the course of the reaction. Accordingly, we determined the oxidation potentials of the starting arene, anisole, to be +1.87 V vs SCE and that of product **2.3** to be +1.50V vs SCE. Because aryl amine **2.3** is more electron rich than anisole, its oxidation potential is lower, indicating that it is more readily oxidized by the acridinium than anisole is.

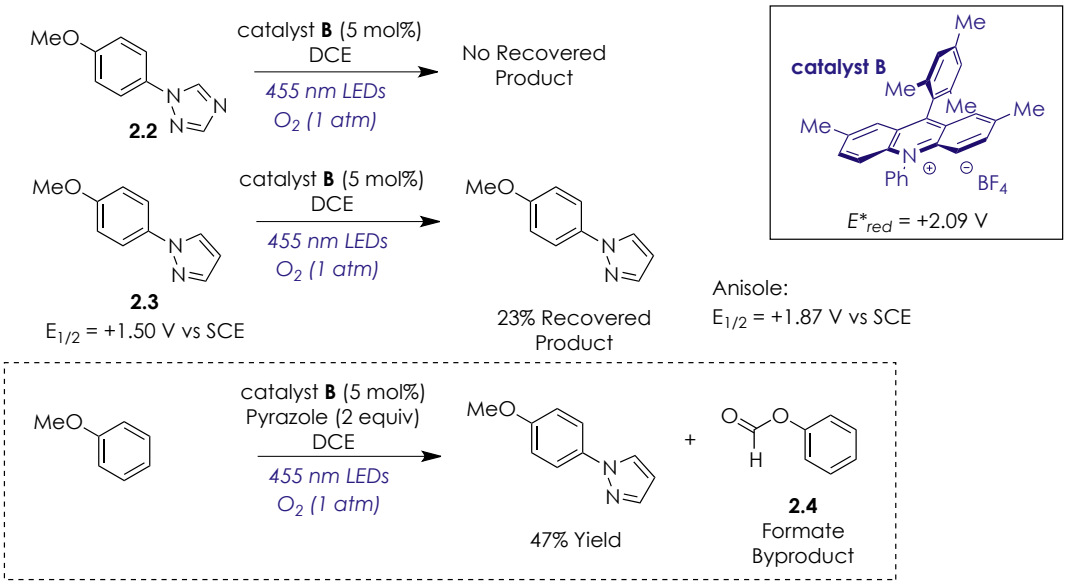

Figure 2.2 Product stability studies and byproduct formation.

We also investigated the byproducts formed during the reaction via ^{1}H NMR and GC-MS analysis and determined that **2.4** was produced in significant amounts, presumably through the oxidation of the alkoxy substituent on the arene. Fukuzumi has previously disclosed that hydrogen peroxide can be formed using an acridinium catalyst under aerobic reaction conditions via a hydroperoxy radical intermediate.[6] Due to this precedent, we believe that a hydroperoxy radical is most likely formed *in situ* and is responsible for the formation of **2.4** via C–H abstraction from the methoxy group and subsequent oxidation.

2.2.3 Additional Optimization

Knowing that product stability was problematic and that byproducts arising from radical side reactions were present, we screened additives that could serve to mitigate these processes that are detrimental to overall yield. Several additives were screened in catalytic amounts (**Table 2.2, entries 1 – 5**), including TEMPO, ABNO, and BHT. Cocatalytic TEMPO showed significantly increased yields and maintained the high levels of *para* to *ortho* selectivity. Increased amounts of TEMPO hindered the reaction, and the highest yields were observed with 20 mol % TEMPO (**Table 2.2, entry 2**). Replacing TEMPO with the TEMPOniumBF$_4$ salt led to similar reaction efficiency (**Table 2.2, entry 6**), suggesting that it can produce TEMPO under the reaction conditions. Lowering the concentration of the reaction led to slight increases in yield (**Table 2.2, entry 8**).

Over the course of a reaction, the solution would begin yellow in color and eventually become a very deep red color, sometimes even brown. We wondered if catalyst degradation could be problematic, especially with a potent nucleophile such as the azole in solution, since previous work by Nathan Romero demonstrated that thiols can add to an undecorated acridinium at the 3-position.[9] The use of 3,6-di-*tert*-butyl-*N*-phenyl-mesityl acridinium tetrafluoroborate **C** ($E^*_{1/2}$ = +2.15 V vs SCE),[10] a small amount of which was provided by Merck, afforded the amination products in 88% yield with excellent *para* to *ortho* selectivity (**Table 2.2, entry 9**). It is postulated that the enhanced yield is due to improved catalyst stability, since the most electrophilic positions of the acridinium are shielded by the *tert*-butyl substituents. This more hindered catalyst is therefore more robust under the reaction

Table 2.2 Optimization with nitroxyl radicals for aryl amination.

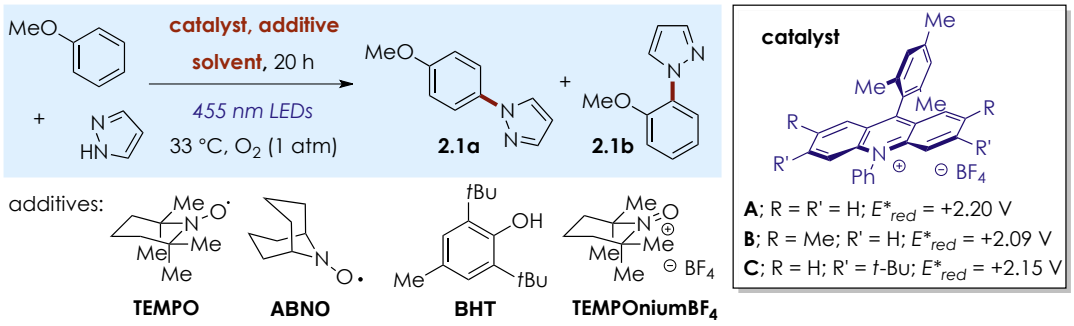

entry	additive	catalyst	solvent [M]	yield	*p*:*o*
1	**TEMPO** (0.1 eq.)	B	DCM[0.25]	65%	6.7:1
2	**TEMPO** (0.2 eq.)	B	DCM[0.25]	74%	6.2:1
3	**TEMPO** (0.5 eq.)	B	DCM[0.25]	45%	6.3:1
4	**ABNO** (0.2 eq.)	B	DCM[0.25]	60%	7.7:1
5	**BHT** (0.5 eq.)	B	DCM[0.25]	42%	6.4:1
6	**TEMPOniumBF$_4$** (0.2 eq.)	B	DCM[0.25]	69%	6.5:1
7	**TEMPO** (0.2 eq.)	A	DCM[0.1]	61%	6.8:1
8	**TEMPO** (0.2 eq.)	B	DCM[0.1]	79%	6.7:1
9	**TEMPO** (0.2 eq.)	C	DCM[0.1]	88%	6.9:1
10	**TEMPO** (0.2 eq.) (air)*	C	DCM[0.1]	97%	7.5:1
11	polymer-**TEMPO** (0.2 eq.)	C	DCM[0.1]	65%	6.7:1

(*) Reaction run for 3 days.

conditions, leading to higher yields. Using catalyst **C** under air instead of an oxygen atmosphere provided the final product in nearly quantitative yields (**Table 2.2, entry 10**), although longer reaction times of three days instead of 20 hours were required. Polymer-bound TEMPO was also effective as an additive, affording the desired product in 65% yield (**Table 2.2, entry 11**). Additionally, the polymer-bound TEMPO could be recovered via filtration and reused in the reaction, albeit in lower yields.

The synthesis of catalyst **C** provided by Merck was then optimized so that we could access this catalyst on a useful scale for reaction screening and product isolation (**Figure 2.3**). Previously, the Merck route took seven steps and required the use of nitromethane and several chromatography steps. Through optimization of this route, we could use 4-*tert*-

butyltoluene as the starting material for the synthesis and construct the catalyst in six steps with only one chromatographic separation.

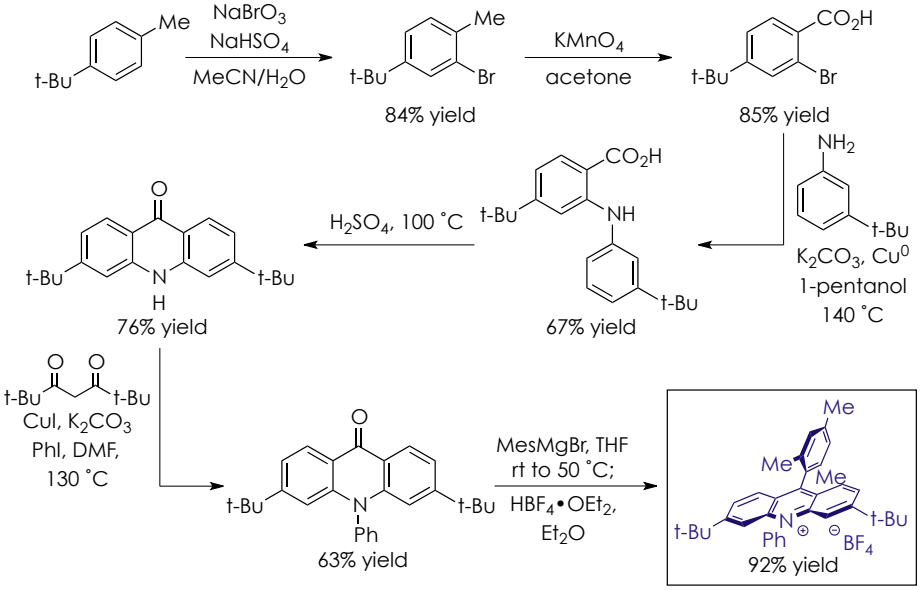

Figure 2.3 Modified synthetic route to *tert*-butyl substituted acridinium catalyst (catalyst **C**).

2.2.4 Arene Scope for Aryl Amination

With the optimized conditions, we screened a diverse range of arenes to determine the scope of this reaction (**Figure 2.4**). A variety of mono-substituted phenolic ethers participated in the reaction, affording the amination products **2.1, 2.5** – **2.8** in modest to good yields, in all cases favoring formation of the *para* isomer over the *ortho* isomer. The use of biphenyl provided **2.9** in good yield and similar *para* to *ortho* selectivity. Arenes disubstituted with a methoxy group and a halogen substituent were competent in the reaction, delivering **2.10** and **2.11**, respectively, as single regioisomers. Additionally, high levels of selectivity were observed with a biaryl substrate containing two electronically distinct arenes, affording **2.12** in good yield as a single regioisomer.

While the ability to functionalize various benzenoid derivatives is important for highlighting functional group tolerance and site selectivity, we also sought to extend the

substrate scope to heterocyclic compounds. Several types of heterocycles participated in the reaction in good yields with good regioselectivity, including a pyridine, quinoline, quinazolinedione, indazole, and dihydrocoumarin (**2.15** – **2.19**).

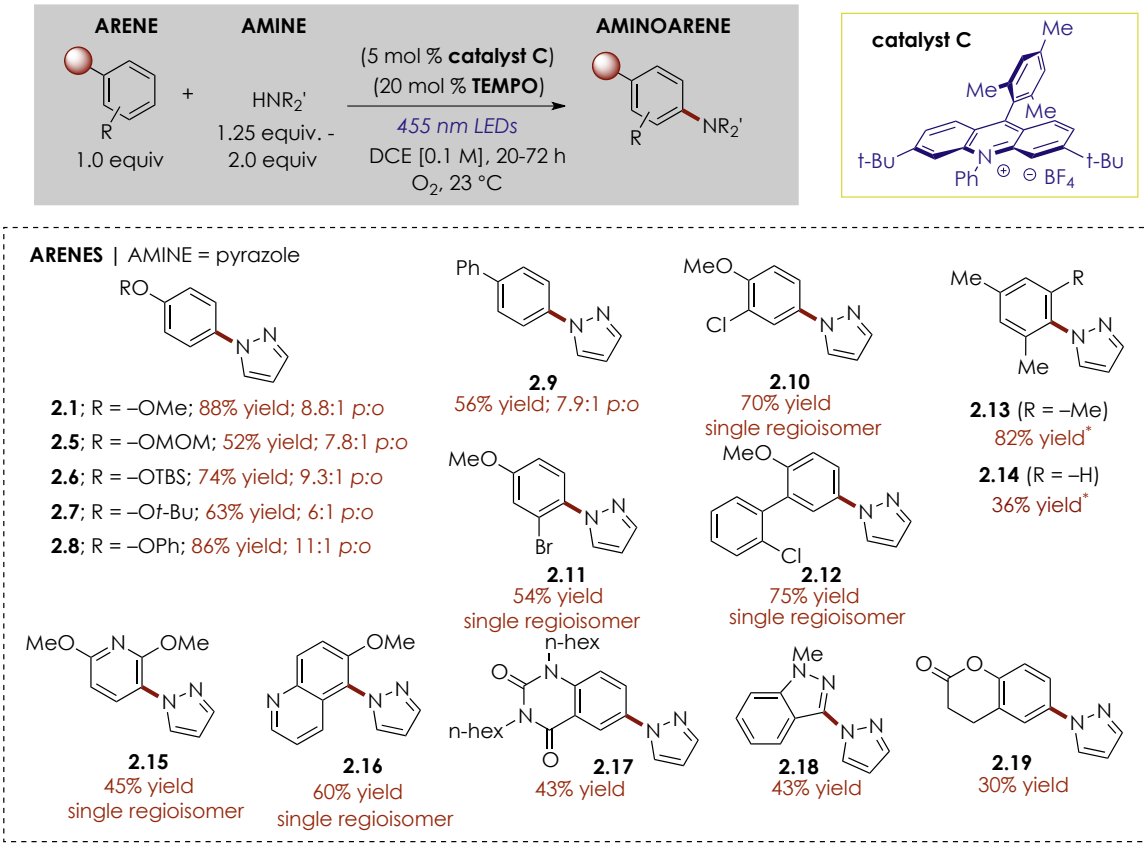

Figure 2.4 Arene scope for aryl amination methodology. Reactions were run in 1,2-dichloroethane (DCE) at 0.1 M concentration with respect to the arene limiting reagent. (*) indicates a reaction run with 2.0 equivalents of arene, 1.0 equivalent of amine, and 1.0 equivalent of TEMPO under an N_2 atmosphere for 44 hours. Hex, hexyl group.

2.2.5 Development of Conditions for Alkyl-Substituted Arenes

While a variety of benzenoids and heterocycles worked in these reaction conditions, when we tried any alkyl-substituted arenes such as mesitylene or *meta*-xylenes, the reactions to produce **2.13** and **2.14** were not as clean as with other substrates. When previously optimized conditions were used with mesitylene, we observed the desired aryl amination product, a difunctionalization product, **2.20**, and oxidized byproduct **2.21** (**Table 2.3, entries**

1 and 2). Bordwell predicts that the pKa of a benzylic C–H bond of an arene cation radical is roughly –20.[11]

Table 2.3 Alkyl-substituted arene optimization.

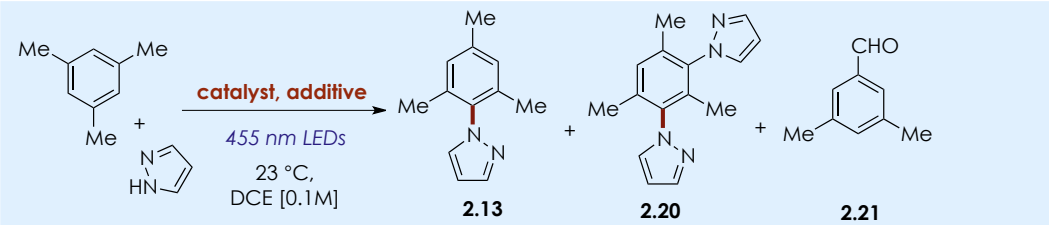

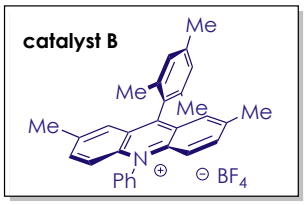

additives:

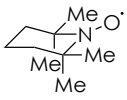

TEMPO

entry	Atmosphere	Arene:Amine	TEMPO	Time	Yield **2.13**	Yield **2.20**	Yield **2.21**
1	O_2	1:2	None	24 hours	39%	16%	10%
2	O_2	1:2	0.2 equiv.	24 hours	40%	49%	5%
3	O_2	2:1	0.2 equiv.	24 hours	78%	12%	20%
4	O_2	2:1	0.2 equiv.	48 hours	80%	11%	22%
5	N_2	1:2	0.2 equiv.	24 hours	20%	3%	0%
6	N_2	1:2	1.0 equiv.	24 hours	52%	3%	0%
7	N_2	2:1	1.0 equiv.	24 hours	70%	2%	0%
8	N_2	2:1	1.0 equiv.	48 hours	86%	3%	0%
9	N_2	1:2	None	24 hours	11%	1%	0%

Previous groups, including Yoshida and Fukuzumi, have used this to their advantage by demonstrating benzylic amination and oxidation, respectively, via deprotonation of the arene cation radical.[12,7] In fact, the aldehyde byproduct **2.21** we observed was one of the desired oxidation products in Fukuzumi's work (**Figure 2.5**), leading us to conclude that further optimization for alkyl-substituted arenes would be required. To limit the amount of difunctionalization, we inverted the stoichiometry of the arene and amine coupling partners and, in fact, observed diminished difunctionalization product (**Table 2.3, entries 3 and 4**). However, this also increased the amount of oxidation byproduct observed, which proved challenging to remove via column chromatography.

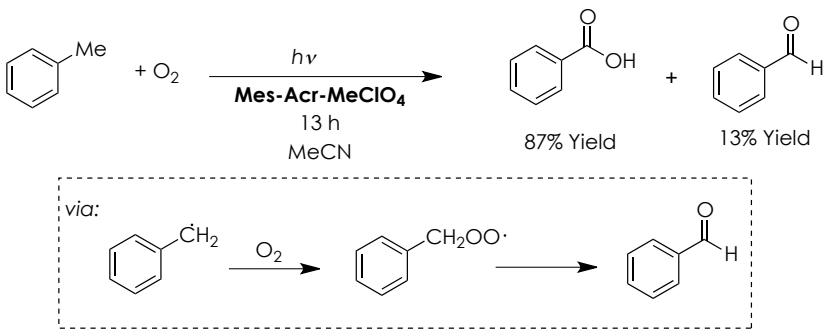

Figure 2.5 Benzylic oxidation via photoredox catalysis.

To completely retard the oxidation pathway, we examined what happened in the reaction without a balloon of oxygen and instead a nitrogen sparge and atmosphere. Interestingly, we observed roughly 20% yield of the desired aryl amine when excluding the terminal oxidant, oxygen (**Table 2.3, entry 5**). We hypothesized that TEMPO could instead act as a terminal oxidant which resulted in the 20% yield of product observed. After further optimization, it was determined that with a stoichiometric amount of TEMPO along with two days of irradiation, the aryl amination could be improved to 86% yield of the mono-aminated product (**Table 2.3, entry 8**). The exclusion of TEMPO and oxygen provided product in only 11% yield, highlighting the necessity of an oxidant for the desired reactivity. Overall, we were able to demonstrate this aryl amination methodology with 16 different simple arene coupling partners with yields ranging from 30 to 88% yield.

2.2.6 Arene Scope – Unsuccessful Substrates

While these previous arenes all participated in the aryl amination reaction, there were several types of compounds that we could not functionalize (**Figure 2.6**). While some arenes gave trace amounts of products, yields could not be improved to be synthetically viable. The use of several anilines as the starting arene was pursued; however, in most cases, little to no product was observed even though the arene oxidation potentials lied within the range of the catalyst redox potential. We believe that lack of functionalization under our conditions is a

result of the aniline being so electron-rich that it is in the Marcus Inverted region, where desired electron transfer is less favorable.[13] Carbamate-protected phenols also did not facilitate productive amination chemistry. The use of 2-iodoanisole prevented product formation, which we hypothesize is due to the heavy atom effect.[14] The use of 3-fluoroanisole lead to *ipso* functionalization at the site of the fluorine but no desired C–H functionalization. Naphthalene and 1-methoxynaphthalene also did not provide the desired amination product. Tetrahydronaphthalene was not capable of forming the desired product due to the highly oxidation prone benzylic positions, and the use of anaerobic conditions did provide the desired adduct in low yield that could not be improved to synthetically viable values. 3-Bromotoluene was not electron rich enough to be oxidized by the acridinium catalyst. Protected indoles were used but never provided the desired adduct regardless of the protecting group used. Heterocycles such as 2-methoxypyrimidine were also used but were insufficiently electron rich to undergo SET with the catalyst.

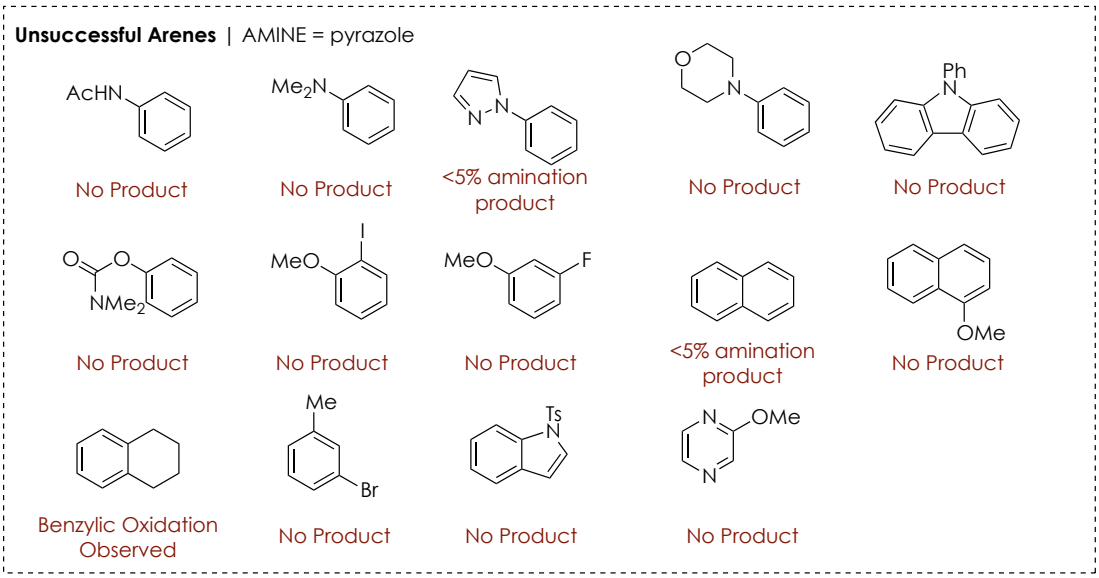

Figure 2.6 Unsuccessful arene substrates for aryl amination.

2.2.7 Amine Scope for Aryl Amination

With an arene scope in hand, we also explored the types of azole coupling partners we could use in this reaction methodology (**Figure 2.7**). Several methyl-substituted pyrazoles could be used in this reaction, providing product in good yields and regioselectivities (**2.22** – **2.24**). 1,2,3- and 1,2,4-triazole were also shown as coupling partners, producing adducts **2.25** and **2.26** with more modest regioselectivity. Additional five-membered nitrogen-containing heterocycles were competent in the reaction as nucleophiles (**2.27** – **2.31**). Interestingly, more biologically relevant nitrogen nucleophiles could be used, forming products **2.32** and **2.33**. This ability to use histidine and adenine derivatives highlights the power of this system, in that more complex nucleophilic coupling partners can be used to construct C–N bonds rapidly, in good yield, and with relatively good regioselectivity.

2.2.8 Application to Late-Stage Functionalization

Having shown that a variety of arenes and azoles could be coupled using this methodology, we applied it to late-stage functionalization of complex molecules (**Figure 2.8**). A derivative of capsaicin underwent amination with pyrazole as the nucleophile in 66% yield to afford **2.34** despite the presence of a disubstituted olefin in the substrate, which could be problematic for other C–H functionalization strategies. Naproxen methyl ester provided **2.35** in low yield, and the trifluoroacetate salt of a quinine derivative delivered **2.36** in 53% yield. In each case, single regioisomers were isolated, highlighting the excellent site selectivity of this methodology. The ability to utilize this chemistry to functionalize complex, bioactive targets in a site selective manner highlights that this strategy for C–H amination is amenable to a wide variety of arenes and is highly regioselective.

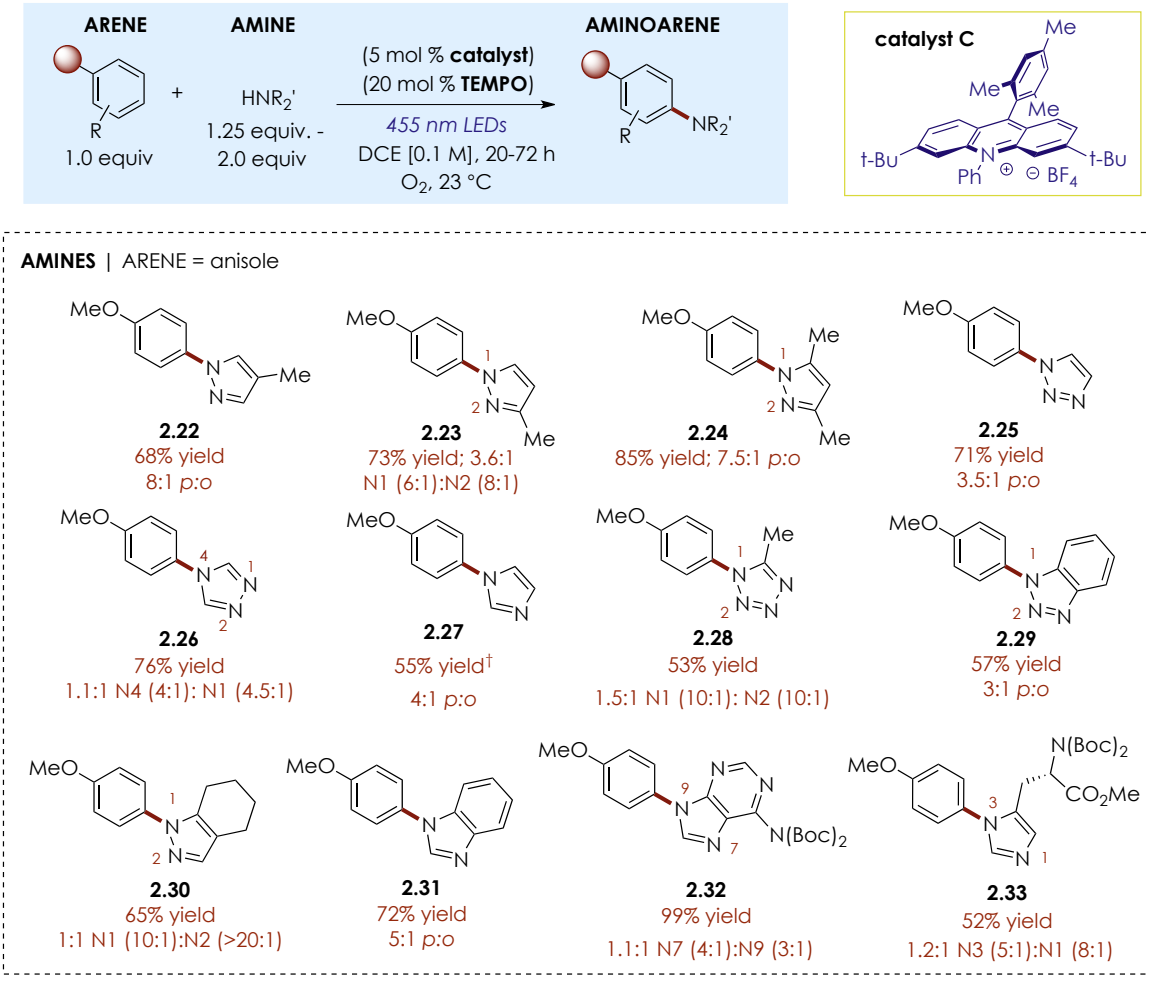

Figure 2.7 Amine scope for aryl amination methodology. Parenthetical ratios refer to *para*:*ortho* (*p*:*o*) selectivity for a given *N*-isomer. Reactions were run in 1,2-dichloroethane (DCE) at 0.1 M concentration with respect to the arene limiting reagent. (†) indicates a reaction run under N_2 with 1.0 equivalent of TEMPO.

2.2.9 Aniline Construction for Aryl Amination

Traditionally, the construction of anilines occurs through arene nitration, requiring highly oxidizing and acidic conditions, followed by hydrogenation.[15,16] Through the screening of several ammonium salts, it was found that ammonium carbamate was optimal as a nucleophile to directly access anilines via an arene cation radical intermediate (**Table 2.4**). This solid is less expensive than liquid ammonia per mole of reagent. Direct construction of

eight different anilines (**2.37** – **2.44**) was demonstrated with modest regioselectivities and yields (**Figure 2.9**).

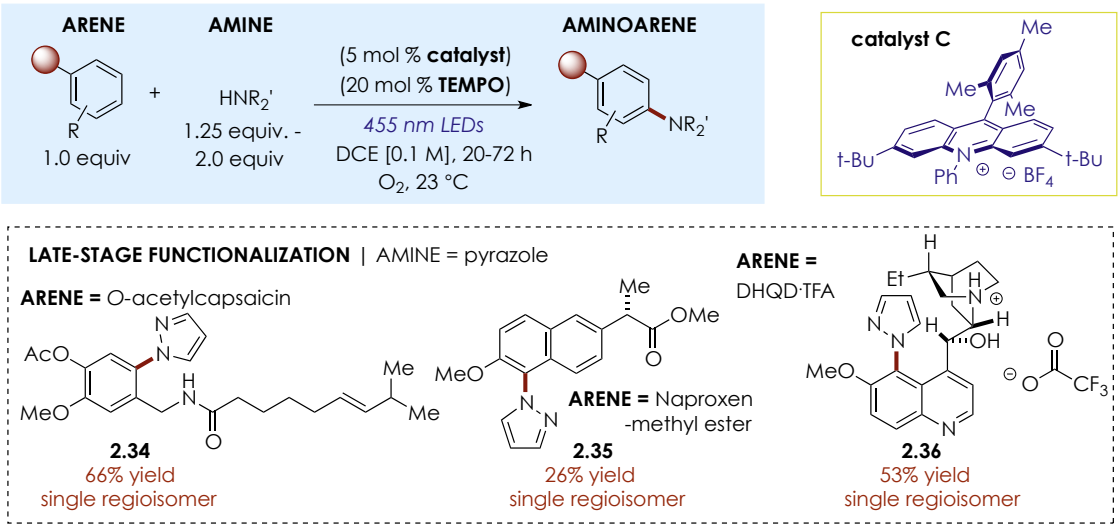

Figure 2.8 Complex derivatives for late-stage functionalization. Reactions were run in 1,2-dichloroethane (DCE) at 0.1 M concentration with respect to the arene limiting reagent.

Table 2.4 Optimization for aniline formation.

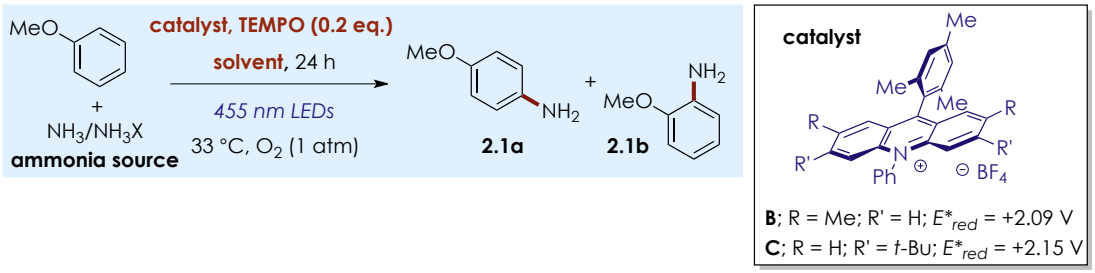

entry	ammonia source	catalyst	solvent [M]	yield	*p*:*o*
1	**NH_4OAc** (2.0 eq.)	B	DCE [0.10]	15%	1:1
2	**NH_4HCO_3** (2.0 eq.)	B	DCE [0.10]	24%	1:1.5
3	**$(NH_4)_2CO_3$** (2.0 eq.)	B	DCE [0.10]	35%	1:1
4	**$(NH_4)_2CO_3$** (2.0 eq.)	B	MeCN [0.10]	24%	2:1
5	**$(NH_4)_2SO_3$** (2.0 eq.)	B	DCE [0.10]	0%	NA
6	**$(NH_4)_2CO_3$** (2.0 eq.)	B	DCE:H_2O [0.10]*	43%	1.6:1
7	**$(NH_4)_2CO_3$** (4.0 eq.)	C	DCE:H_2O [0.10]*	40%	1.2:1
8	**$NH_4O_2CNH_2$** (4.0 eq.)	C	DCE:H_2O [0.10]*	58%	1.4:1
9	**$NH_4O_2CNH_2$** (2.0 eq.)	C	DCE:H_2O [0.10]*	45%	1.5:1
10	**$NH_4O_2CNH_2$** (4.0 eq.)	B	DCE:H_2O [0.10]*	47%	1.4:1
11	**$NH_4O_2CNH_2$** (4.0 eq.)	C	TFE [0.10]	7%	NA
12	**$NH_4O_2CNH_2$** (4.0 eq.)	C	DCE:TFE [0.10]*	25%	1:1

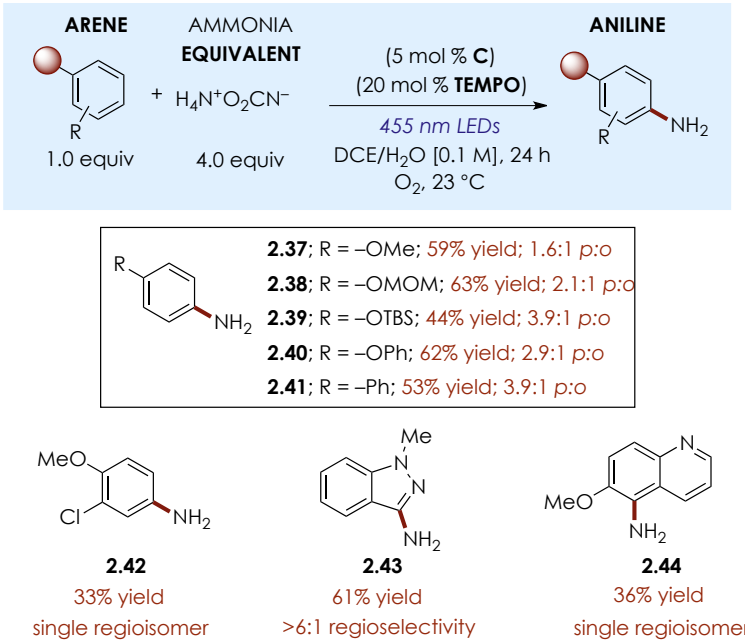

Figure 2.9 Aniline substrate scope.

2.2.10 Proposed Mechanism for Aryl Amination

Based on previous work by Fukuzumi,[6] we propose that the acridinium photoredox catalyst is excited using 455 nm BLEDs (**Figure 2.10**). This excited state photocatalyst is capable of undergoing SET from the arene to generate the arene cation radical **2.45**. Nucleophilic addition of the azole coupling partner followed by deprotonation affords cyclohexadienyl radical intermediate **2.47**, which can then be rearomatized to afford the aryl amine **2.48**. Based on Fukuzumi's mechanistic work for his aryl bromination methodology, we believe that oxygen can oxidize acridine radical intermediate **Mes-Acr•**, allowing it to renter the catalytic cycle. Oxygen is also important for the rearomatization to afford the final product. While TEMPO was important to achieve optimal yields in our system, at this point we believe that the main role of TEMPO is to act as a radical scavenger, inhibiting deleterious side reactions. TEMPO could also assist with the cyclohexadienyl radical

rearomatization step; however, due to the yields achieved without TEMPO, the aerobic reaction conditions are sufficient for this step to occur.

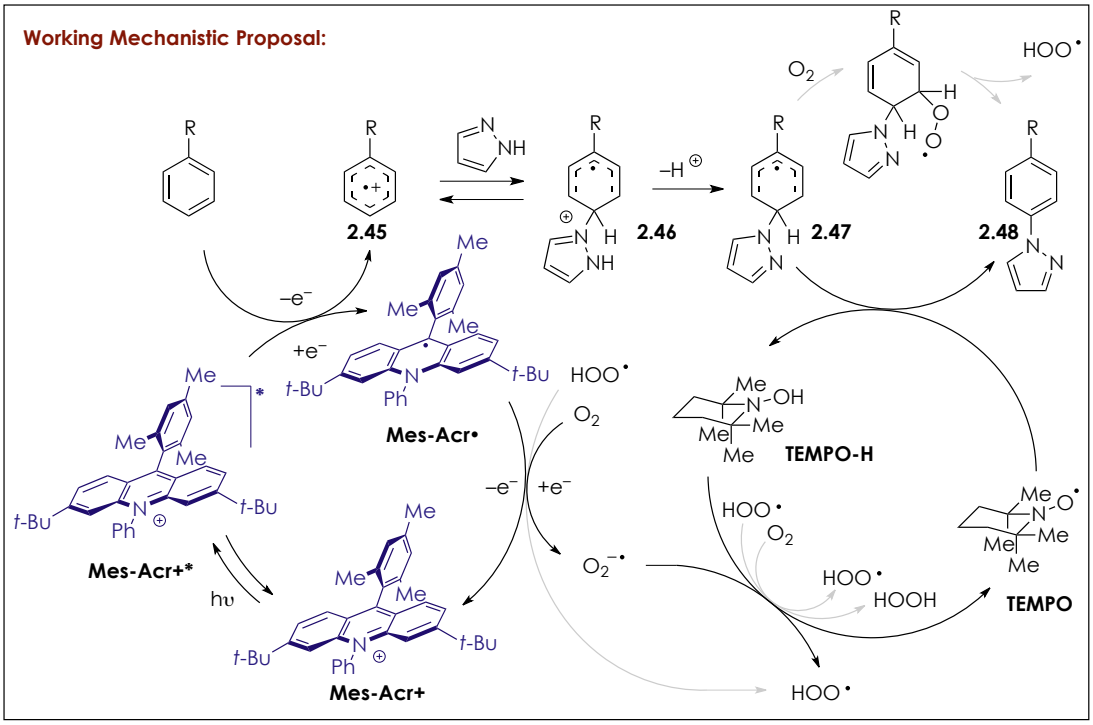

Figure 2.10 Proposed mechanism for aryl amination.

Since the various azole coupling partners delivered products with differing *para* to *ortho* selectivities, we further examined what could cause this deviation and observed a strong correlation between pKa and selectivity (**Figure 2.11**). We believe that this supports that the deprotonation of intermediate **2.46** is the regioselectivity-determining step of the reaction. If the heterocycle is more basic, the *para* isomer is favored more strongly. Cole Cruz in the Nicewicz lab has investigated this further and has shown that the addition of acid can erode regioselectivity to a nearly 1:1 mixture of *para* and *ortho* isomers. Further efforts to determine the importance of TEMPO lend credence to it acting as an *in situ* radical inhibitor.

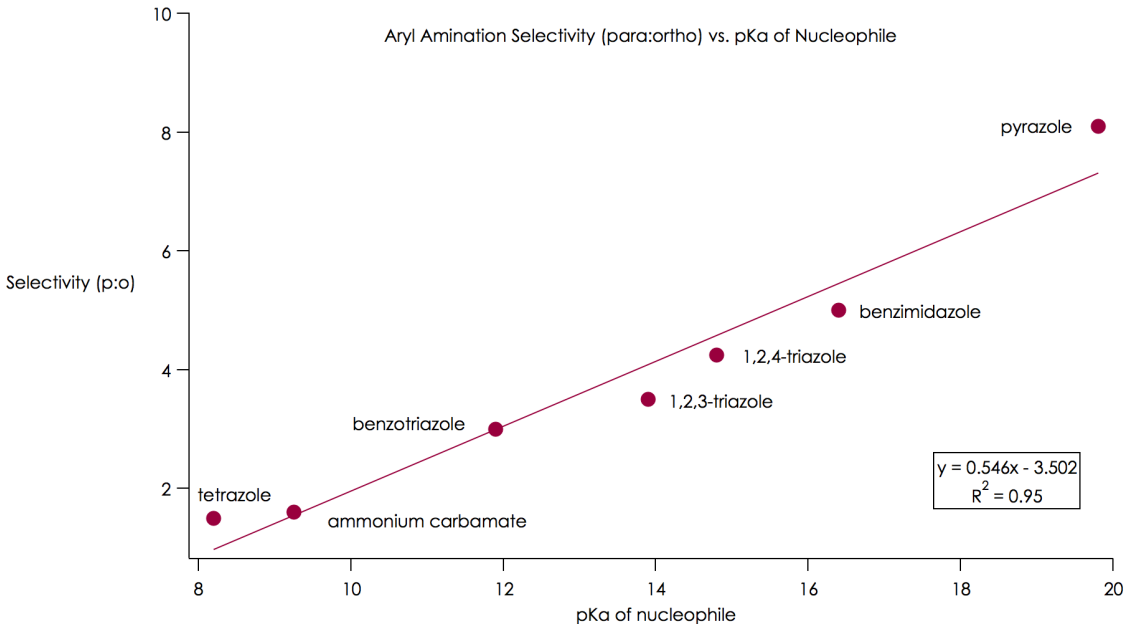

Figure 2.11 Aryl amination selectivity and basicity of nucleophile. Reactions were run in 1,2-dichloroethane (DCE) at 0.1 M concentration with respect to the arene limiting reagent. Selectivity was determined by ^{1}H NMR ratios of regioisomers.

REFERENCES

(1) Lyons, T. W.; Sanford, M. S. *Chem. Rev.* **2010**, *110*, 1147–1169.

(2) Tran, L. D.; Roane, J.; Daugulis, O. *Angew. Chem. Int. Ed.* **2013**, *52*, 6043–6046.

(3) Xu, H.; Qiao, X.; Yang, S.; Shen, Z. *J. Org. Chem.* **2014**, *79*, 4414–4422.

(4) Allen, L. J.; Cabrera, P. J.; Lee, M.; Sanford, M. S. *J. Am. Chem. Soc.* **2014**, *136*, 5607–5610.

(5) Romero, N. A.; Margrey, K. A.; Tay, N. E.; Nicewicz, D. A. *Science* **2015**, *349*, 1326–1330.

(6) Ohkubo, K.; Mizushima, K.; Iwata, R.; Fukuzumi, S. *Chem. Sci.* **2011**, *2*, 715.

(7) Fukuzumi, S.; Ohkubo, K. *Org. Biomol. Chem.* **2014**, *12*, 6059–6071.

(8) Wilger, D. J.; Grandjean, J.-M. M.; Lammert, T. R.; Nicewicz, D. A. *Nat. Chem.* **2014**, *6*, 720–726.

(9) Romero, N. A.; Nicewicz, D. A. *J. Am. Chem. Soc.* **2014**, 10.1021/ja506228u.

(10) Joshi-Pangu, A.; Lévesque, F.; Roth, H. G.; Oliver, S. F.; Campeau, L.-C.; Nicewicz, D.; DiRocco, D. A. *J. Org. Chem.* **2016**, *81*, 7244–7249.

(11) Bordwell, F. G.; Cheng, J. P. *J. Am. Chem. Soc.* **1989**, *111*, 1792–1795.

(12) Morofuji, T.; Shimizu, A.; Yoshida, J. *J. Am. Chem. Soc.* **2014**, *136*, 4496–4499.

(13) Marcus, R. A. *Rev. Mod. Phys.* **1993**, *65*, 599–610.

(14) Koziar, J. C.; Cowan, D. O. *Acc. Chem. Res.* **1978**, *11*, 334–341.

(15) Del Pesco, T. W. 4001260.

(16) DelPesco, T. W. 4031106.

CHAPTER 3: PREDICTIVE MODEL FOR SITE-SELECTIVE ARYL C–H FUNCTIONALIZATION REACTIONS

Adapted from Margrey, K. A.; McManus, J. B.; Bonazzi, S.; Zerci, F.; Nicewicz, D. A. *J. Am. Chem. Soc.* **2017**, *139* (32), 11288–11299.

3.1 Introduction

The development of novel synthetic methodologies is at the forefront of research in organic chemistry, facilitating new routes to construct novel bonds or undergo a desired transformation more effectively. While this capability is required for research to advance, the ability to predict the outcome of a given reaction instills a deeper understanding of the reaction mechanism and provides insight to those wanting to apply the methodology. For this reason, we believed that a computational predictive model for our aryl C–H amination chemistry would greatly expand the scope of arenes we could functionalize and be useful as a tool for those wanting to apply the chemistry to substrates not disclosed in the original publication.[1]

3.2 Previous Predictive Models

Predictive models for reactions such as site-selective C–H functionalizations can be important tools for synthetic chemists, giving them the greatest insight into where reactivity is most likely to occur. To this end, several other groups have developed predictive models to better understand the selectivity exhibited by a given reagent or catalyst. White and co-workers have developed a catalyst-controlled aliphatic C–H oxidation methodology

incorporating a predictive model that correlates the physical properties of a given substrate with the experimental observations of oxidation site selectivity.[2] Baran and Blackmond demonstrated a radical-based C–H functionalization of electron-deficient heteroarenes and systematically investigated a number of parameters that influenced regioselectivity, highlighting general trends as their model.[3] Sigman and Davies developed a computational model for their rhodium-catalyzed C–H insertion chemistry based on predicted infrared vibrations of a diazo ester starting material and natural bond order (NBO) point charges of the substrate.[4] These types of predictive models are important when applying the corresponding reactions to a broader class of substrates, when site selectivity can be more challenging to predict.

3.3 Reaction Design

We sought to construct a predictive model for our aryl C–H amination methodology with azole coupling partners. This reaction, occurring via an arene cation radical intermediate, strongly favors functionalization at the *para* position of monosubstituted benzenoids; however, predicting site selectivity for heteroarenes and more complex derivatives was not as straightforward. In collaboration with Novartis Biomedical Institute of Research in Cambridge, MA, we were able to examine a wider variety of heterocycles to determine which scaffolds could be reactive under our conditions. At Novartis, we were given access to a 24 well plate with bottom irradiation (450 nm BLEDs), in which 1-dram vials were able to fit. Reactions were set up analogously to how we set up reactions at UNC; however, due to safety reasons, it was preferred that oxygen balloons were not used and instead air was used as a terminal oxidant. With this parameter being changed we knew that yields might not be as high as they would be with oxygen, but reactivity could still be

determined. Automated data processing was used so that samples could be analyzed quickly using an LCMS and then promising reactions were purified by prep HPLC. Arenes that provided the desired products were then run in setups at UNC to determine if oxygen could improve yields, and the specific conditions for each arene are listed in each table.

At the onset of this work, we wondered if precedented aromatic substitution reactivity patterns would accurately describe the electrophilic arene cation radical generated from electron rich arenes in our reactions.[5] While electrophilic aromatic substitution does generally afford *ortho* and *para* functionalized products from electron rich arenes, the mechanistic pathway involves the arene as a nucleophile and not an electrophile. Conversely, nucleophilic aromatic substitution describes a nucleophile adding to an electron poor arene, usually displacing a nucleofuge such as a halogen.[6] For this reason, we thought that neither model would be appropriate for predicting site selectivities and believed that computational insight regarding regioselectivity would be necessary.[7]

3.3.1 Factors Influencing Site Selectivity

It was determined that several factors would influence the predictive model and required consideration, including: 1) the oxidation potential of each arene of interest, 2) the electrophilicity of the corresponding arene cation radical, 3) whether the intermediate after SET would best be described as a delocalized or localized arene cation radical, 4) if sufficient change in electron density between the neutral and cation radical of an arene existed, and 5) the impact of substituents and the electronic nature of the arene.

Previous work in our group by Hudson Roth and Nathan Romero detailed a computational method for the prediction of redox potentials (see **Chapter 1.3.4**).[8] This method was used in the development of our computational model as well. Knowledge of

whether a given arene was electron-rich enough to undergo the desired SET process was critical. Several types of heterocycles, including pyrimidines, pyridazines, pyrazines, purines, and nucleobases, as well as unsubstituted quinoline and pyridine, were not sufficiently electron-rich to undergo SET with an acridinium catalyst. These data are useful for explaining why certain heterocycles are unreactive without needing to obtain experimental CV data for each compound.

Previous work by Yoshida and Fukuzumi used computational data to describe the reactivity of arene cation radicals (see **Chapter 1.3.3**).[9,10] Based on this precedent, we decided to use a similar strategy to predict the electron density of a given arene cation radical intermediate. For each compound, the geometries for the neutral and cation radical of the arene in 1,2-dichloroethane (DCE) were optimized at the B3LYP/6-31G+(d,p) level of theory, and the natural population analysis (NPA)[11] values could then be determined (**Figure 3.1**). Furthermore, we looked at the difference between the cation radical and neutral values for each arene.

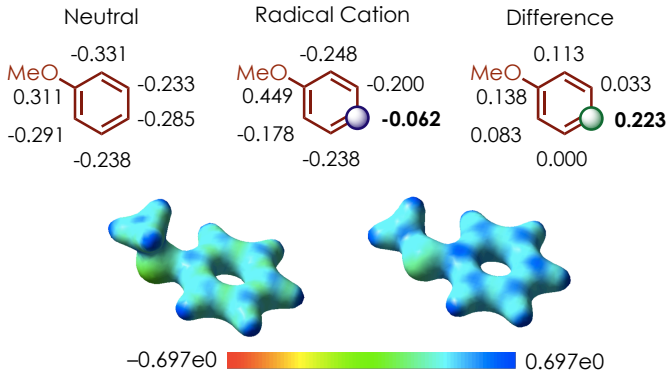

Figure 3.1 Natural population analysis and electrostatic potential maps of anisole.

Generally, arene cation radicals are understood as delocalized with respect to both charge and spin density. The determination of spin density distribution yields insight into where radical character is predominantly located in the arene cation radical. For arenes such

as indole, the cation radical spin density exists primarily at the 3-position, and the positive charge is predominantly at the adjacent carbon atom at the 2-position.[12] Based on these results, it can be understood that a localized iminium radical intermediate is produced by single electron transfer from the indole core (**Figure 3.2**). A careful understanding of what happens for a given arene after SET is critical for determining whether the system is best described as delocalized or localized.

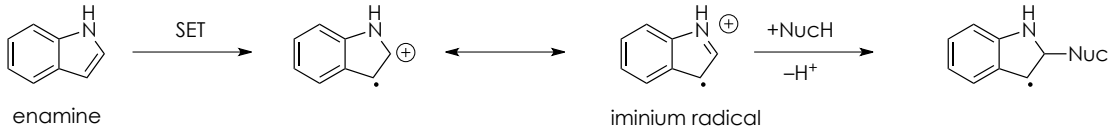

Figure 3.2 Iminium radical reactivity of indole.

3.3.2 Aromatic Classes

Expanding on our prior work (see Chapter 2), we aimed to determine what other types of aromatic cores commonly used in pharmaceuticals could be functionalized. The aromatic cores could generally be grouped into two categories 1) six-membered aromatics and 2) aromatics with at least one five-membered heteroaromatic ring. The classes that comprise the first category that we investigated are benzenoids, pyridines, and quinolines. Benzenoids are ubiquitous in natural products and pharmaceuticals and are widespread in the development of new drugs. Pyridines and quinolines are among the most prevalent aromatic ring and nitrogen-containing heterocycles found in the U.S. FDA approved pharmaceuticals, and the latter are also present in several natural products, including the cinchona alkaloids.[13,14] The second class includes pyrazoles, indazoles, bridging nitrogen polyaromatics, benzofurans, indoles, and benzazoles.[15–17] Pyrazoles are found in a wide range of pharmaceuticals displaying antimicrobial, anti-cancer, and anti-inflammatory properties. [18,19] While indazoles are not highly prevalent in natural products, they have found

utility in antifungal, antiarrhythmic, and analgesic applications.[20] Imidazo[1,2-*b*]pyridazines, imidazo[1,2-*a*]pyrimidines, pyrazolo[1,5-*a*]pyrimidines, and imidazo[1,2-*a*]pyridines are common bridging nitrogen polyaromatic heterocycles present in compounds displaying a wide range of biological properties including anticancer, antimalarial, antidiabetic, anti-inflammatory, antibacterial, sedative, and anxiolytic.[21–29] Benzofurans have a variety of biological activities including antiviral, antioxidant, and antifungal properties; additionally, some amino-substituted benzofurans exhibit antiarrhythmic activity.[30] Indoles are found in numerous natural products and even in amino acids (tryptophan).[31] In many pharmaceuticals, indole derivatives are substituted at the 3- and 5-positions and can exhibit anticancer, antiproliferative, antibacterial, antidiabetic, antioxidant, anti-inflammatory, and antiviral activities.[31–33]

3.3.2.1 Six-Membered Aromatics

To explore the reactivity of benzenoids in our aryl C–H amination reaction, we examined a sterically and electronically diverse group of benzene derivatives that were sufficiently electron-rich to undergo functionalization. For each mono-substituted benzene, we observed that the *para* isomer was favored with minor amounts of the *ortho* isomer formed (**Figure 3.3**). As determined by the differences between the neutral and cation radical computational NPA values, the *para* position was predicted to be the most electrophilic site in all cases. Phenolic ether substrates and biphenyl underwent functionalization favoring the *para* position to afford **3.2a** – **3.2f**, respectively, as the model suggested. Furthermore, for all of the disubstituted arenes explored, the site predicted to undergo functionalization by the NPA values did, in fact, match the site of experimental amination (**3.2g** – **3.2i**). While modified reaction conditions are required for alkyl-substituted arenes (see **Chapter 2.2.5**),

the computational predictions can still be used to predict the major isomer. Quinazolinedione and dihydrocoumarin substrates underwent amination *para* to the heteroatom to provide **3.2l** and **3.2m**, matching the site of the largest NPA difference value.

Other arenes not previously reported in our original paper were also highlighted in this predictive model. Additional functionality, including esters, *O*-benzyl phenols, and allyl substituents were tolerated in a variety of substrates under aerobic conditions to provide **3.2n – 3.2p**. 1,3-Dimethoxybenzene and *O*-tosyl guaiacol also underwent amination in high yield to afford **3.2q** and **3.2r** as single regioisomers. Trisubstituted arenes were also competent in the C–H amination, providing **3.2s** in 31% yield as a single regioisomer. For all benzenoid substrates studied, the experimental site of functionalization matched the predicted site of the largest NPA value difference.

The functionalization of heterocycles such as pyridine is desirable due to their prevalence in pharmaceuticals, yet unsubstituted pyridine is not sufficiently electron-rich to be oxidized by the acridinium catalyst ($E_{calc,ox}$ (pyridine$^{\bullet+}$/pyridine) = +2.64 V vs SCE).[8] The addition of electron-donating groups lowers the oxidation potential enough that SET can occur with the acridinium catalyst. The previously reported substrate 2,6-dimethoxypyridine underwent functionalization at the 3-position, matching the site of largest NPA value difference (**Figure 3.4**).[1] A similar trend was observed with 3,5-dimethoxypyridine, in which the computational model accurately predicts the site of functionalization. Interestingly, the site of the largest NPA value difference for 2,4-dimethoxypyridine did not match the experimental site of functionalization. We propose that this is due to the steric repulsion caused by the methoxy substituents, hindering functionalization at the 3-position and leading to predominant amination at the 5-position. Additionally, methyl-substituted pyridines

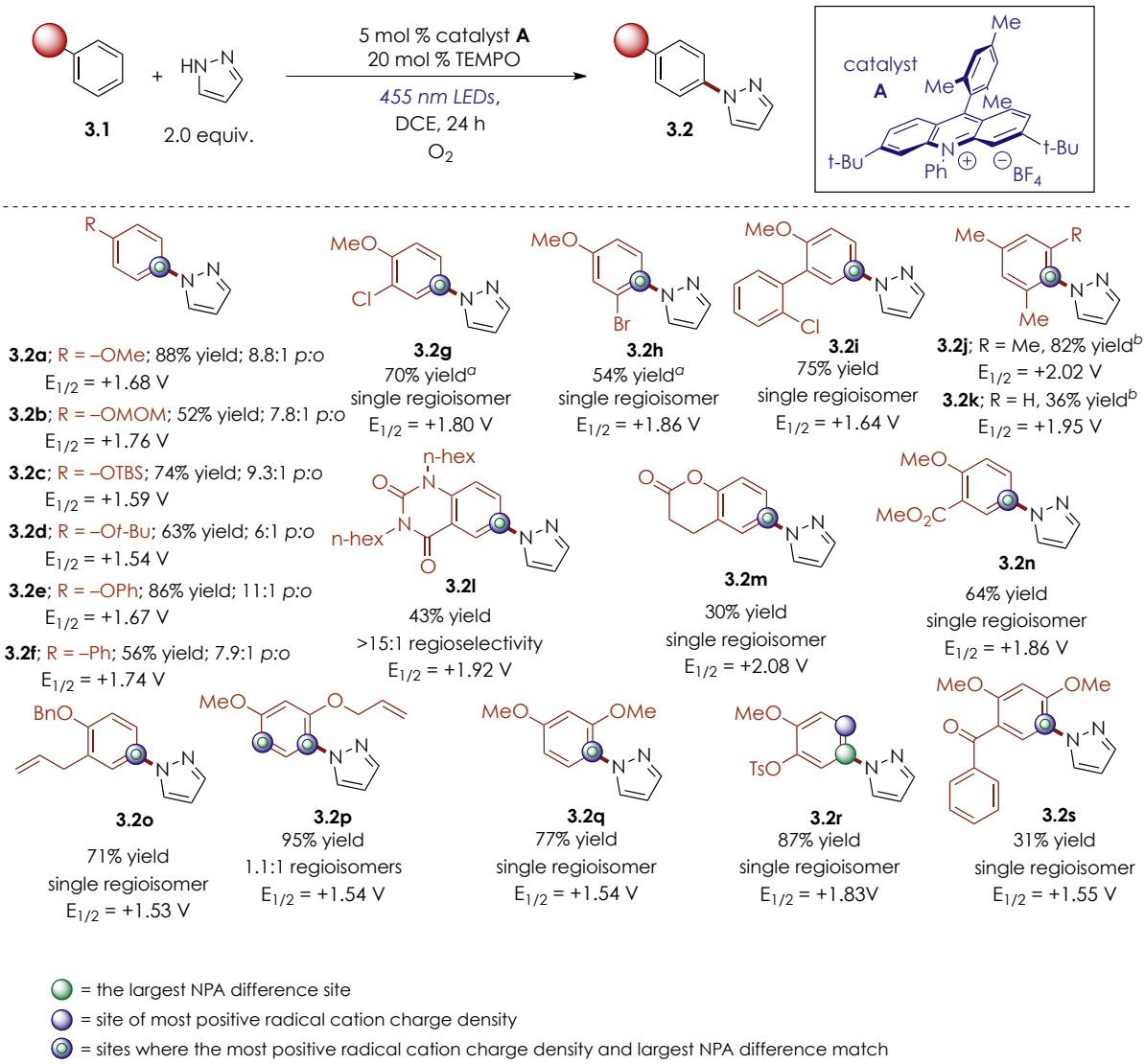

Figure 3.3 Benzenoid scope with predictions of site selectivity. Ratios refer to *para*:*ortho* (*p*:*o*) selectivity for the given isomer. Reactions were run in 1,2-dichloroethane (DCE) at 0.1 M concentration with respect to the arene limiting reagent. Computational results are highlight using the circles indicated in the figure. All of the redox potentials were computationally determined and were calculated vs SCE in MeCN. ([a]) The reaction was run for 48 h. ([b]) The reaction was run under N_2 with 1 equiv of TEMPO.

could be functionalized, albeit in a 1:1 mixture of regioisomers (**3.4e**:**3.4f**). Overall, pyridines generally undergo amination at the computationally predicted site of functionalization; however, steric parameters could be considered for a more detailed predictive model.

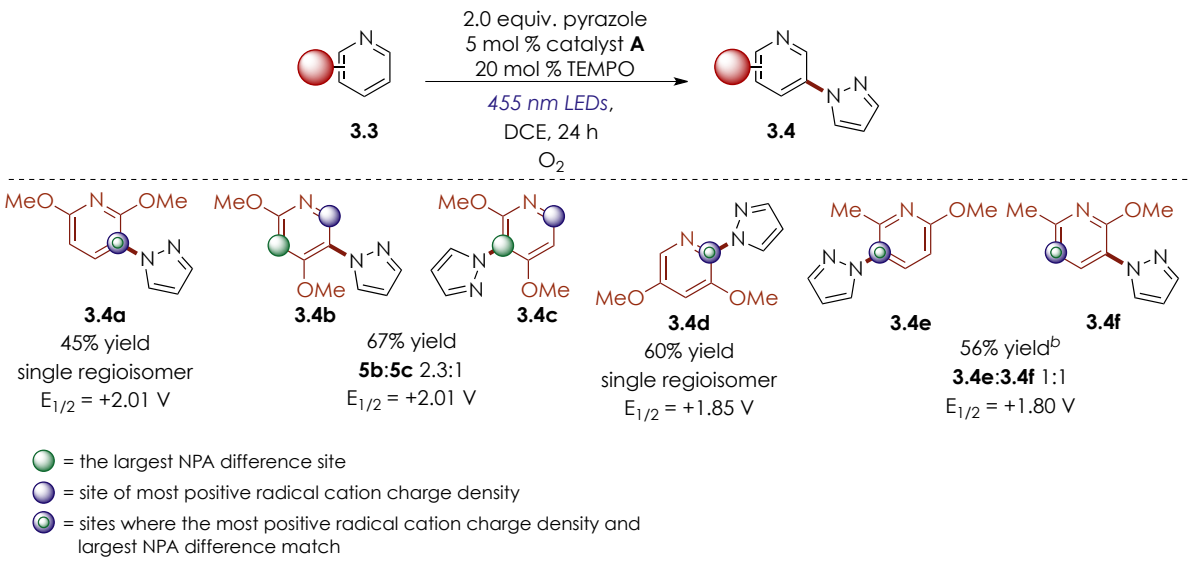

Figure 3.4 Pyridine scope with predictions of site selectivity. Reactions were run in 1,2-dichloroethane (DCE) at 0.1 M concentration with respect to the arene limiting reagent. Computational results are highlight using the circles indicated in the figure. All of the redox potentials were computationally determined and were calculated vs SCE in MeCN. ([a]) The reaction was run under air instead of O_2, ([b]) The reaction was run under N_2 with 1.0 equiv of TEMPO.

The last six-membered heterocycle class probed was quinolines (**Figure 3.5**). For several quinoline substrates, the site of functionalization could be predicted using the largest NPA value difference (**3.6a** – **3.6d**). For 4-bromo-7-methoxyquinoline (**3.5e**), no amination product was formed. For this substrate, there was no significant difference in the NPA values computationally, highlighting that a sufficient change in NPA values must be achieved for functionalization to occur. In general, when a sufficient difference is observed between NPA values, good yields and single regioisomers are observed. The site of functionalization on the quinoline core is dependent on the position of the electron-donating substituents and for some quinolines such as **3.6d**, *ipso* substitution at the methoxy group was observed as a minor product. When large differences in NPA values are observed, quinolines generally can undergo the desired transformation with good site selectivity.

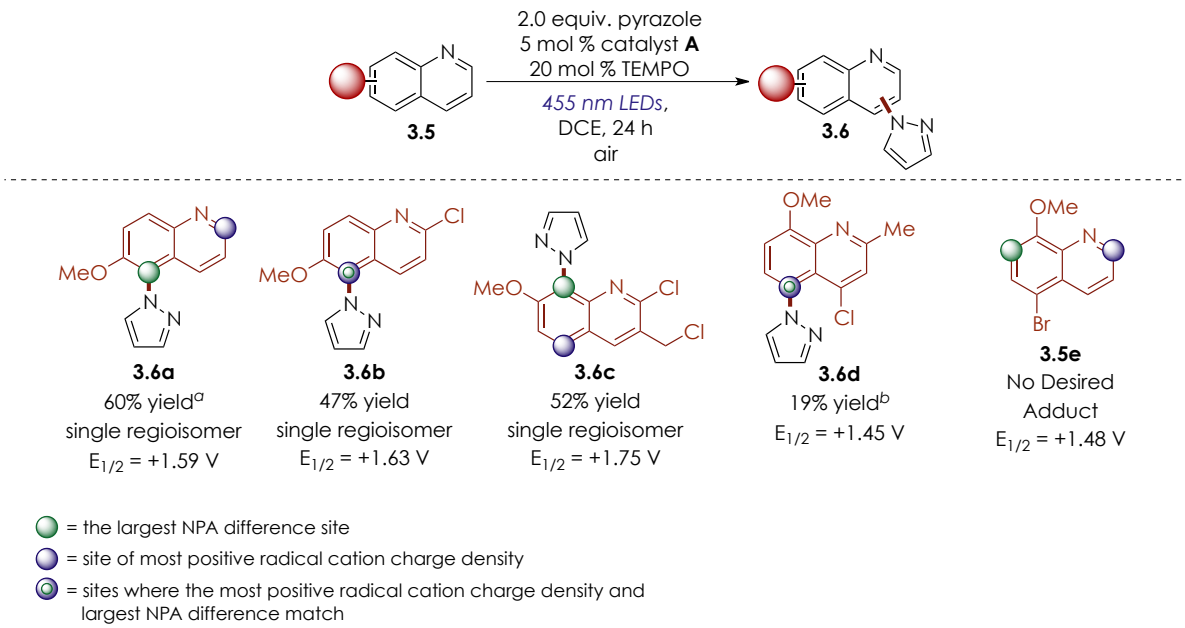

Figure 3.5 Quinoline scope with predictions of site selectivity. Reactions were run in 1,2-dichloroethane (DCE) at 0.1 M concentration with respect to the arene limiting reagent. Computational results are highlight using the circles indicated in the figure. All of the redox potentials were computationally determined and were calculated vs SCE in MeCN. ([a]) The reaction was run under O_2 instead of air, ([b]) Ipso substitution of the methoxy group was also observed.

For six-membered aromatic compounds, selectivity can generally be predicted based on rules for electrophilic aromatic substitution, despite the differences between the two mechanisms.[5] The theoretical basis of understanding for the predictive model is critical for understanding site selectivity, but it is also convenient to note that E_AS selectivity rules can predict regioselectivity for benzenoids, pyridines, and quinolines.

3.3.2.2 Aromatics Containing at Least One Five-Membered Ring

We predicted that aromatic systems with at least one five-membered ring would react differently than those with six membered rings only. Pyrazoles and indoles possess enamine character, which dictates the site of nucleophilicity in E_AS reactions. Enamine nucleophilicity is not observed in five-membered heterocycles such as indazoles or benzoxazoles, which are incapable of adopting enamine-like resonance structures. Based on this prior knowledge of

five-membered heterocyclic reactivity, we wondered whether these compounds would undergo functionalization at a position similar to that observed during E_AS reactions or if their reactivity would be akin to that of a distonic iminium radical (**Figure 3.3**). When enamines undergo SET, iminium radical intermediates are formed, rendering the iminium carbon poised for nucleophilic addition. Discerning if this type of mechanism is operative is critical for understanding how heterocycles with enamine character react in our system.

N-methylpyrazole is not sufficiently electron-rich to be oxidized by the acridinium photocatalyst used in the reaction (**Figure 3.6**). The addition of a methyl substituent lowered the oxidation potential sufficiently to render the compounds able to undergo SET with the acridinium. For both 1,3- and 1,4-dimethylpyrazole, functionalization at the 5-position was observed to provide **3.8b** and **3.8c**, matching the most electrophilic site predicted by the model. However, 1,5-dimethylpyrazole did not undergo amination under the reaction conditions. From these data, aryl functionalization of *N*-substituted pyrazoles occurs at the 5-position, unless this site is blocked by a substituent, in which case no functionalization ensues. If pyrazoles reacted similarly to six-membered heterocycles with E_AS selectivity, functionalization at the 4-position would be predicted.[34,35] However, *N*-substituted pyrazoles deviate from this trend and instead react at the most electrophilic position of the iminium radical generated via SET.

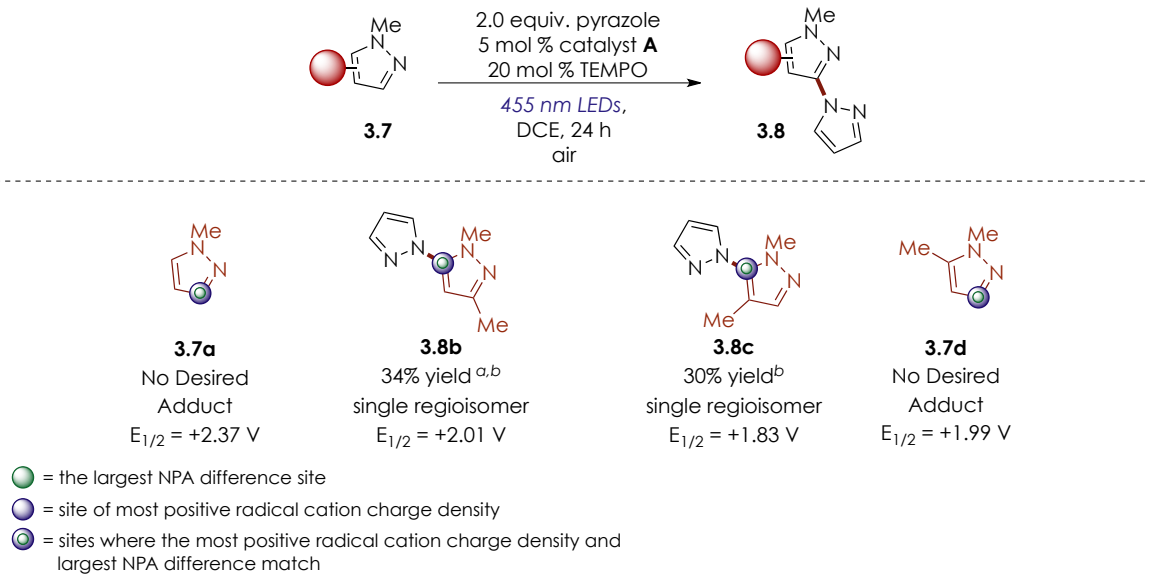

Figure 3.6 *N*-methylpyrazole scope with predictions of site selectivity. Reactions were run in 1,2-dichloroethane (DCE) at 0.1 M concentration with respect to the arene limiting reagent. Computational results are highlight using the circles indicated in the figure. All of the redox potentials were computationally determined and were calculated vs SCE in MeCN. ([a]) The reaction was run under O_2 instead of air, ([b]) ^{1}H NMR yield with hexamethyldisiloxane as an internal standard.

In our prior work, we disclosed that *N*-methylindazole underwent amination at the 3-position to afford **3.10a**, matching the predicted site of functionalization based on the largest NPA value difference (**Figure 3.7**). Indazoles are not able to adopt any enamine character as observed with pyrazoles and for that reason it is not a viable way to predict site selectivity. Functionalization at the 3-position also occurred with 7-bromo-*N*-methylindazole (**3.10b**) with a minor regioisomer formed at the 4-position (**3.10c**). This also corresponds to the predicted site of functionalization; however, the NPA differences between the 3- and 4-positions were not significant, highlighting that this model could predict the minor regioisomer. 3-Substituted indazoles, such as 3-bromo-*N*-methylindazole (**3.9d**), did not produce any aryl functionalization products, potentially due to steric hindrance at the 4- and 7-positions with the bulky pyrazole nucleophile. These few examples of indazole

functionalization can be described as functionalization at the same site that E_AS reactivity predicts, which matches the site predicted by the largest NPA value difference of the model.

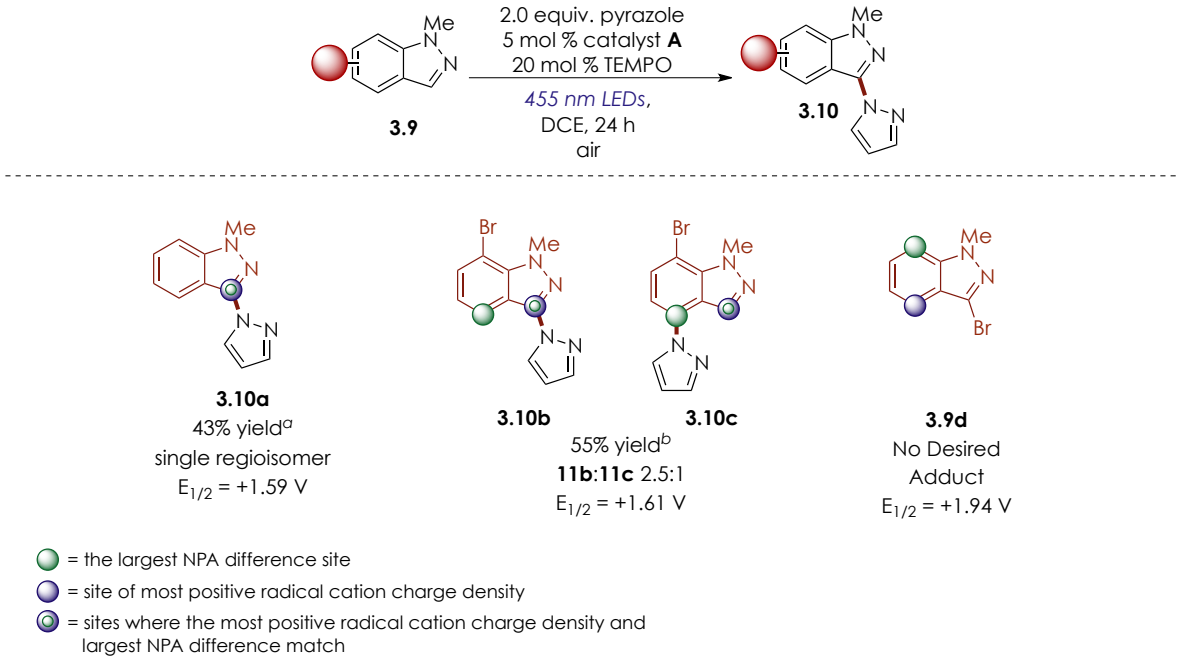

Figure 3.7 *N*-methylindazole scope with predictions of site selectivity. Reactions were run in 1,2-dichloroethane (DCE) at 0.1 M concentration with respect to the arene limiting reagent. Computational results are highlight using the circles indicated in the figure. All of the redox potentials were computationally determined and were calculated vs SCE in MeCN. ([a]) The reaction was run under O_2 instead of air, ([b]) ^{1}H NMR yield with hexamethyldisiloxane as an internal standard.

Imidazopyrimidines, imidazopyridazines, and pyrazolopyrimidines are all heterocycles that are sufficiently electron-rich to undergo SET with an acridinium catalyst (**Figure 3.8**). In all cases shown, functionalization occurs selectively at one site of the polyaromatic core. Imidazo[1,2-*b*]pyridazines afforded products with functionalization at the 3-position regardless of substitution (**3.12a** – **3.12d**). Halogenated imidazo[1,2-*b*]pyridazine **3.11d**, which is more electron-poor, showed a decrease in yield, but functionalization still occurred at the 3-position. For imidazo[1,2-*a*]pyrimidine, only one regioisomer was formed in good yield at the 3-position (**3.12e**), matching the predicted site of functionalization. For imidazo[1,2-*b*]pyridazines and imidazo[1,2-*a*]pyrimidines, enamine character is present in

the ring system. As observed with *N*-methylpyrazoles, reactivity in these cases occurs at the iminium carbon of the iminium radical intermediate. Pyrazolo[1,5-*a*]pyrimidine produced adduct **3.12f** in 42% yield, also undergoing functionalization at the 3-position. For this type of heterocycle, an iminium radical cannot be formed that is unsubstituted at the most electrophilic site. Substrate classes such as this highlight the necessity of a computational predictive model to anticipate the observed regioselectivity.

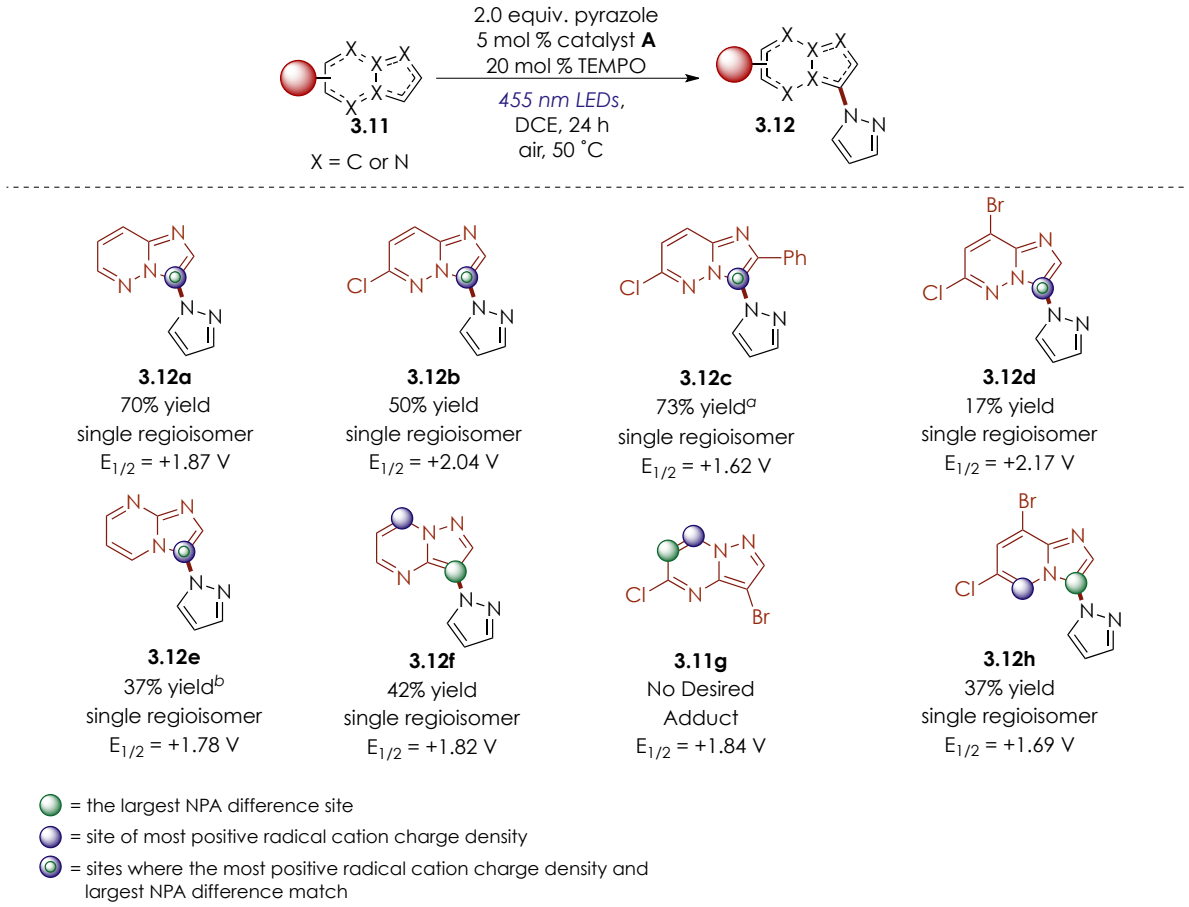

Figure 3.8 Bridging nitrogen polyaromatic scope with predictions of site selectivity. Reactions were run in 1,2-dichloroethane (DCE) at 0.1 M concentration with respect to the arene limiting reagent. Computational results are highlight using the circles indicated in the figure. All of the redox potentials were computationally determined and were calculated vs SCE in MeCN. ([a]) The reaction was run under O_2 instead of air, ([b]) ^{1}H NMR yield with hexamethyldisiloxane as an internal standard.

Similarly to what we observed with 3-bromo-*N*-methylindazole, for **3.11g**, a significant difference in NPA values between the neutral and cation radical did not occur and, accordingly, no amination product was formed. Halogen substituents were tolerated on the imidazo[1,2-*a*]pyridine core, affording adducts such as **3.12h** in 37% yield, matching the site of greatest NPA difference. This regioselectivity for functionalization correlates to the site of highest electrophilicity in the iminium radical generated by SET. For most bridging nitrogen polyaromatic systems, enamine character dictates site selectivity, which correlates to the computational predictions for the most electrophilic position. However, when enamine character is not present, the experimental functionalization does still match that of the predictive model.

Undecorated benzofuran was an incompetent substrate under the reaction conditions, never affording the desired amination product (**Figure 3.9**). The inclusion of a methoxy substituent on the benzofuran core at the 5- or 7-position produced aryl amination products **3.14b**, **3.14c** and **3.14d,** respectively. For 5-methoxybenzofuran, functionalization afforded **3.14b** and **3.14c** in a 29% combined yield and 1.2:1 ratio. Interestingly, when a 2-substituted benzofuran was used, such as **3.13e**, only difunctionalization occurred. Unlike other classes of heterocycles, all benzofurans underwent functionalization at the 2-position, matching the site of the largest NPA value of the cation radical instead of the site of largest difference. The 2-position does correlate to the position of a distonic oxocarbenium radical, generated by SET from the cyclic enol ether, to which nucleophilic addition would occur. We propose that following nucleophilic addition to the oxocarbenium radical, the benzylic radical intermediate can be oxidized to the carbocation, which is susceptible to addition by a second equivalent of nucleophile to form **3.14c** and **3.14e**. While benzofurans do not match the

predictive model in terms of functionalization at the site of the largest NPA difference, this class does undergo amination at the most electrophilic site of the oxocarbenium radical that has the largest NPA value.

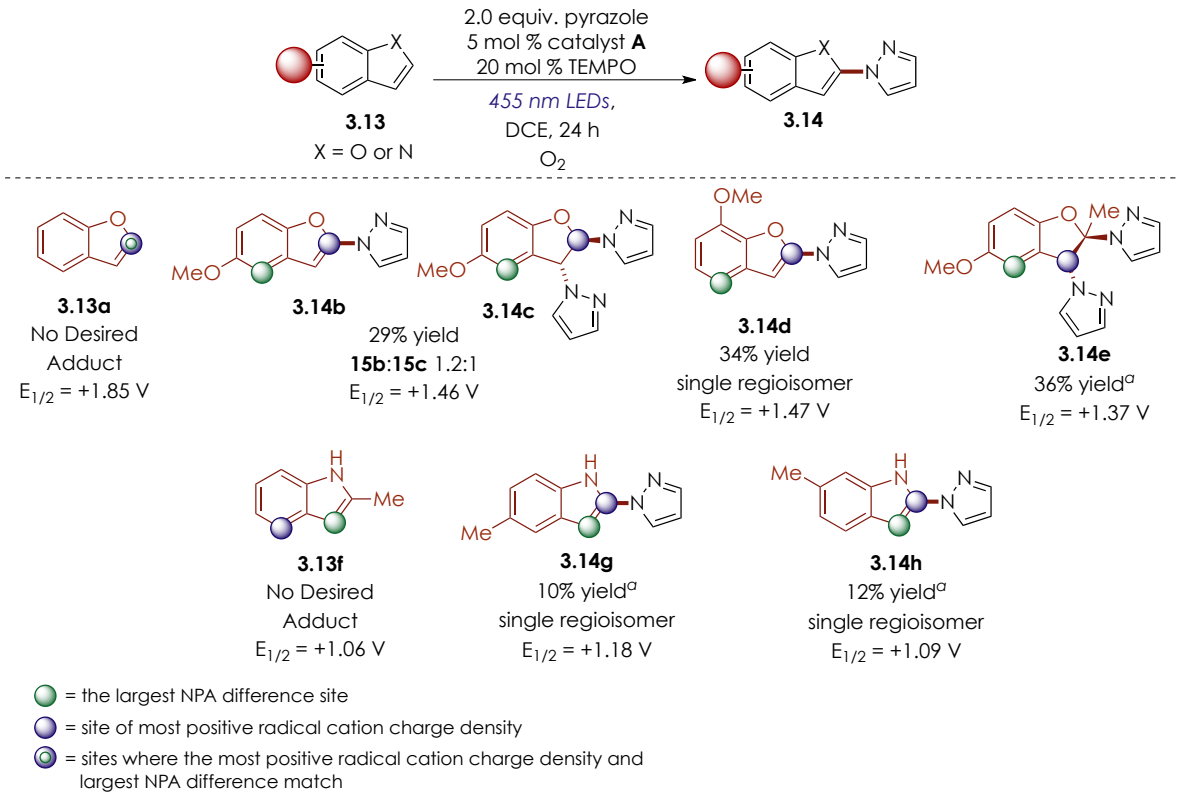

Figure 3.9 Benzofuran and indole scope with predictions of site selectivity. Reactions were run in 1,2-dichloroethane (DCE) at 0.1 M concentration with respect to the arene limiting reagent. Computational results are highlight using the circles indicated in the figure. All of the redox potentials were computationally determined and were calculated vs SCE in MeCN. ([a]) The reaction was run under air.

Similarly to benzofuran, undecorated indole did not provide any amination product (**Figure 3.9**). When a methyl group was installed at the 2-position, no functionalization was observed (**3.14f**). If the methyl group was instead located at the 5- or 6-position, amination did occur, albeit in very low yields. Further optimization of indole substrates would be required for application to a greater number of compounds. Similarly to benzofurans, indoles preferentially undergo functionalization at the 2-position (**3.14g** and **3.14h**), matching the

largest NPA value of the cation radical and the most electrophilic position of the iminium radical. Nucleophilic addition to the iminium, resulting in the formation of a more stable benzylic radical, leads to the observed regioselectivity.

Overall, benzofurans and indoles possess less aromatic character compared to other heterocycles discussed previously.[36,37] For this reason, we propose that they should not be treated as aromatic compounds for the purpose of the predictive model and that they instead should be viewed as cyclic styrenes, in which regioselectivity is dictated by the iminium or oxocarbenium radical intermediate. If these compounds exhibited significant aromatic character, rearomatization from the benzylic radical would outcompete the oxidation that gives rise to the difunctionalized product. Accordingly, benzofurans and indoles should be treated as distonic alkene cation radicals instead of delocalized arene cation radicals.

Several types of benzazoles were also shown as competent substrates in this methodology (**Figure 3.10**). 2-Methylbenzoxazole formed **3.16a** as the major product, matching the site of largest NPA difference value. Benzothiazoles were also reactive, forming **3.16b** and **3.16c** in modest yields but greater than 10:1 regioselectivity, again corresponding to the site of the largest NPA difference. The model also accurately predicted the major product for 2-chloro-*N*-methylbenzimidazole, which formed **3.16d** and **3.16e** in a 3:1 ratio and 42% yield. The site of functionalization for these benzazoles matches the site predicted using E_AS selectivity rules, as seen previously with six-membered heterocycles.[38,39] Although the computational model was necessary for developing a theoretical underpinning of site selectivity, E_AS regioselectivity can be used as a strategy to predict selectivity without requiring computational effort.

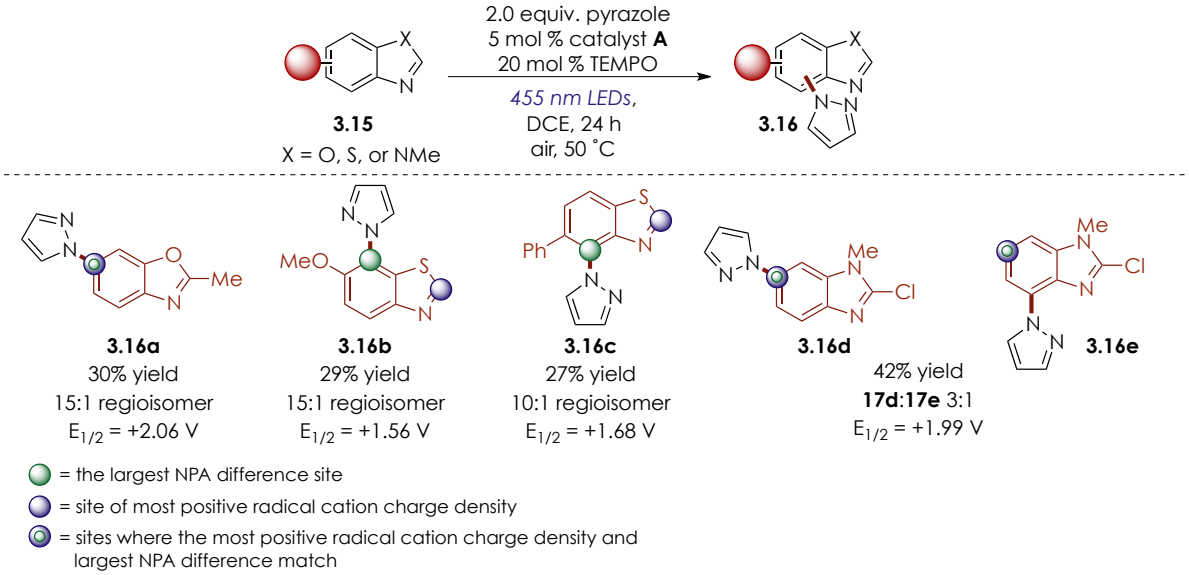

Figure 3.10 Benzazole scope with predictions of site selectivity. Reactions were run in 1,2-dichloroethane (DCE) at 0.1 M concentration with respect to the arene limiting reagent. Computational results are highlight using the circles indicated in the figure. All of the redox potentials were computationally determined and were calculated vs SCE in MeCN.

3.3.3 Nucleophile Scope and Complex Derivatives

To this point, only pyrazole had been used as the nucleophilic coupling partner. Demonstration of other nucleophiles in this work and determining whether the resultant products still matched the predicted site of functionalization would be critical to understand the generalizability of the model. The use of ammonium carbamate as the nucleophile (see **Chapter 2.8**) afforded aniline products **3.17a** and **3.17b** that matched the computational predictions for the site of functionalization. Other nitrogen heterocycles were also shown as competent nucleophiles experimentally, with the products arising from amination at the site with the largest NPA difference value (**3.17c** – **3.17g**). In 2017, the Nicewicz lab also demonstrated the C–H cyanation of electron-rich arenes using a similar photoredox catalyzed approach and TMSCN as the nucleophile.[40] For **3.17h** and **3.17i**, the cyanation site selectivity matched the position with the largest NPA difference value, as predicted by the model.

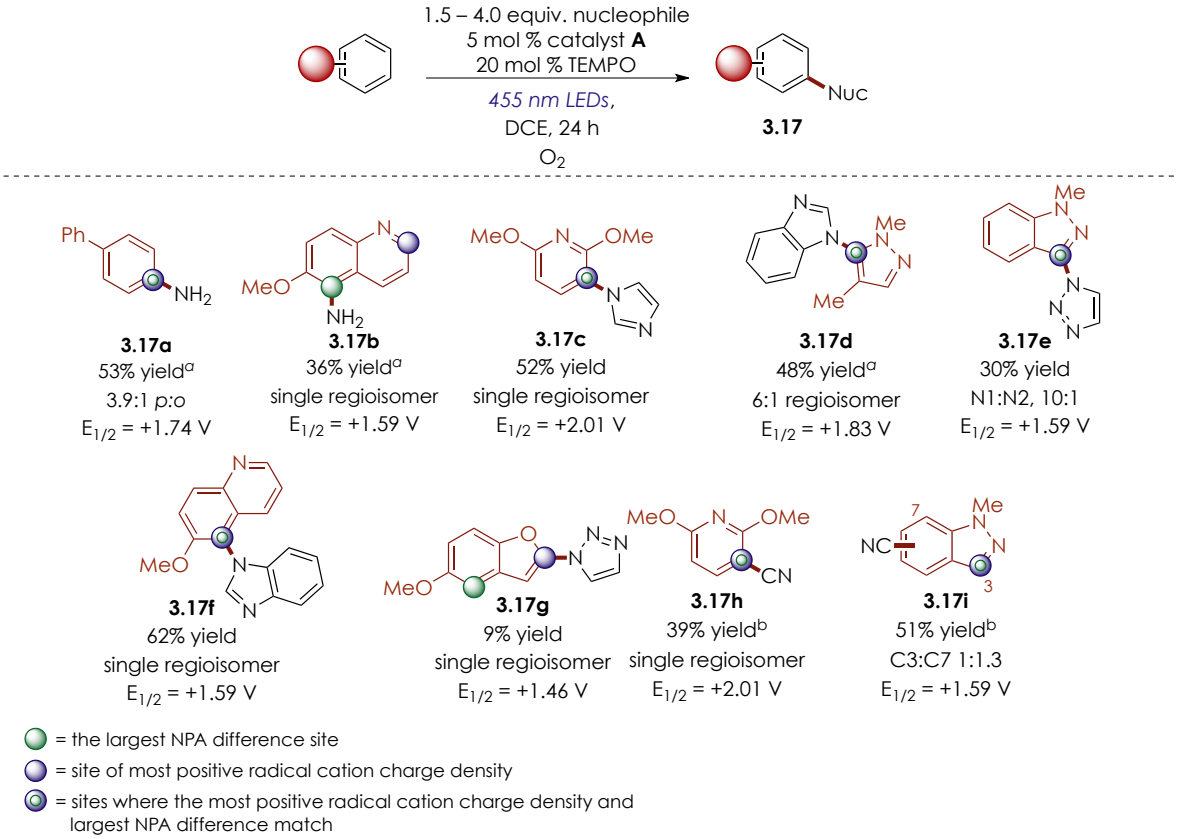

Figure 3.11 Nucleophile scope with predictions of site selectivity. Reactions were run in 1,2-dichloroethane (DCE) at 0.1 M concentration with respect to the arene limiting reagent. Computational results are highlight using the circles indicated in the figure. All of the redox potentials were computationally determined and were calculated vs SCE in MeCN. ([a]) $NH_4CO_2NH_2$ (4.0 equiv), 5 mol % catalyst **1**, 20 mol % TEMPO, 10:1 DCE/H_2O, O_2, 24 h, ([b]) TMSCN (1.5 equiv), 5 mol % catalyst **1**, 10:1 MeCN/pH 9 Buffer, O_2, 24 h.

The ability to utilize this C–H functionalization for late stage derivatization was important for the broader application of the methodology (see **Chapter 2.2.7**). Using more complex arene substrates in this chemistry, we could predict the site of functionalization based on which position possessed the largest difference in NPA values between the neutral and cation radical. This correlation held for several different complex substrates with pyrazole as the nitrogenous coupling partner (**Figure 3.12**). Additionally, using either pyrazole or TMSCN as the nucleophile afforded the same, predicted regioisomer for the

cholesterol-lowering agent gemfibrozil methyl ester as well as Boc-protected melatonin (**3.18e** – **3.18f**).

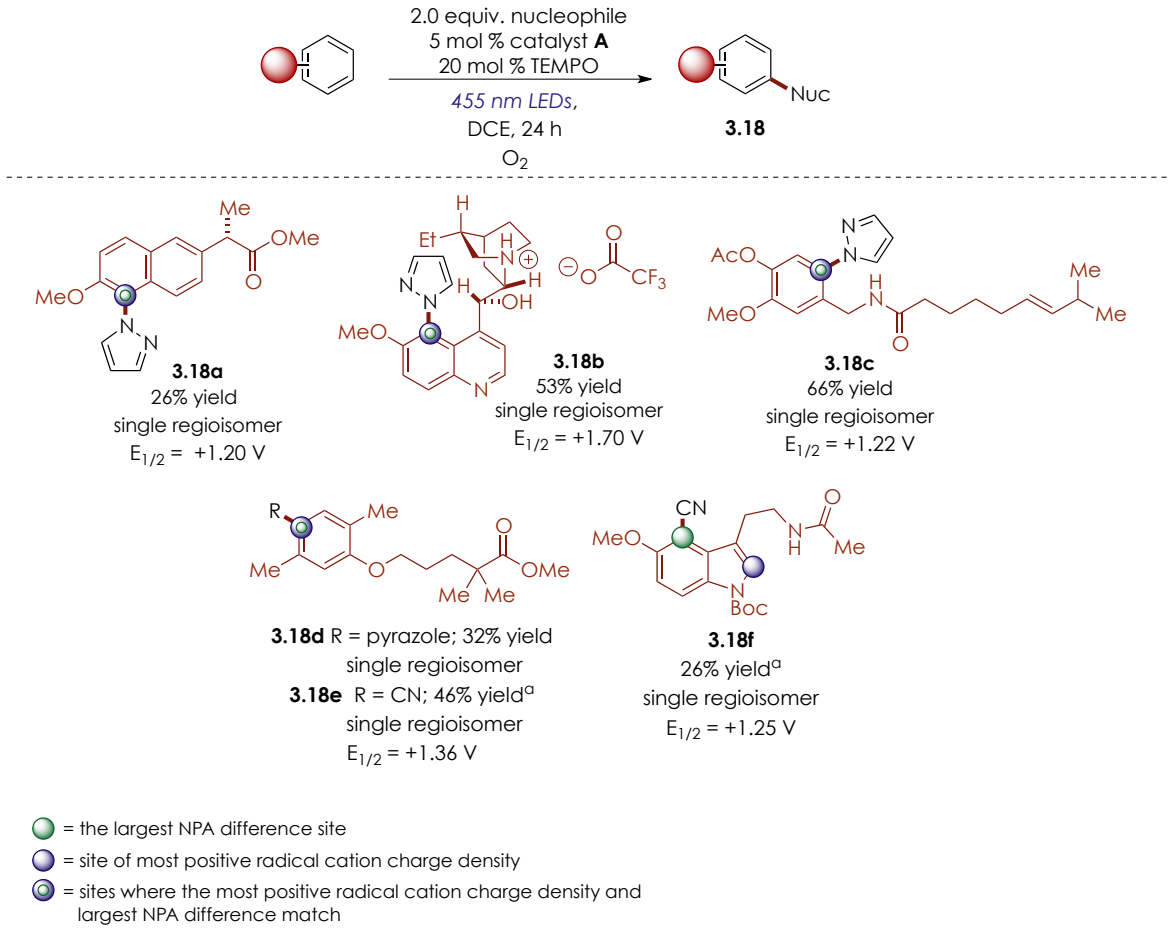

Figure 3.12 Complex molecule scope with predictions of site selectivity. Reactions were run in 1,2-dichloroethane (DCE) at 0.1 M concentration with respect to the arene limiting reagent. Computational results are highlight using the circles indicated in the figure. All of the redox potentials were computationally determined and were calculated vs SCE in MeCN. ([a]) TMSCN (1.5 equiv), 5 mol % catalyst **1**, 10:1 MeCN/pH 9 Buffer, O_2, 24 h.

Several other complex derivatives were used as substrates during the high-throughput screening at Novartis; however, in many instances, only starting material was recovered, likely due to the substrates not being oxidizable by the acridinium catalyst. Derivatives of both histidine and tryptophan were screened in the reaction with pyrazole as a nucleophile (**Figure 3.13**). Histidine methyl ester did couple to give product **3.20a** as determined by LCMS and ^{1}H NMR after isolation, but the yield was very poor and could not be improved.

Tryptophan did undergo the desired nucleophilic addition, but instead of undergoing rearomatization, the resultant benzylic radical was trapped by oxygen to form amino alcohol **3.20d** in 17% yield.

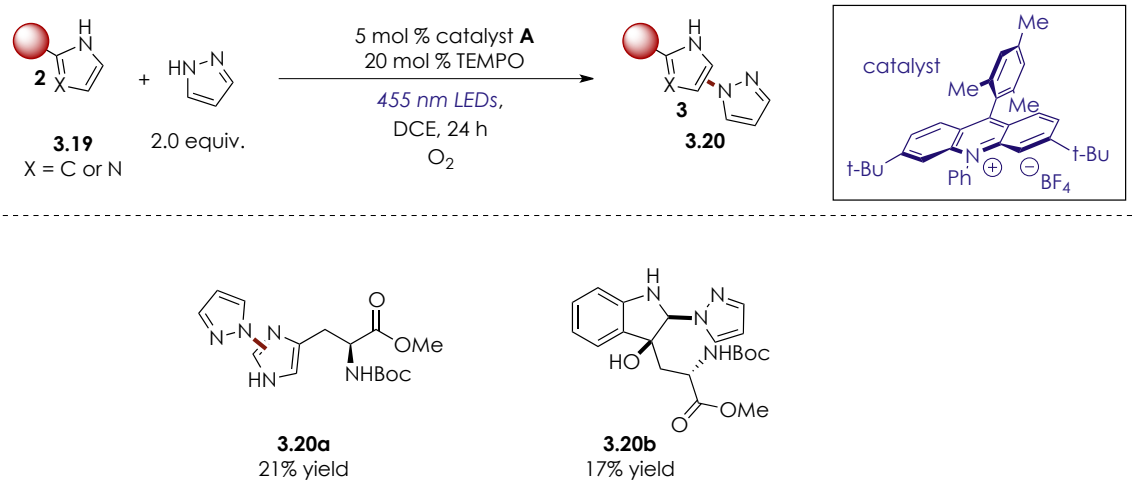

Figure 3.13 Amino acid arene scope with predictions of site selectivity. Reactions were run in 1,2-dichloroethane (DCE) at 0.1 M concentration with respect to the arene limiting reagent.

Overall, several heterocyclic classes can be functionalized using this photoredox-catalyzed aryl C–H functionalization strategy. A simple computational predictive model was constructed that relied on 1) the oxidation potential of the arene, 2) the most electrophilic site of the arene cation radical, and 3) whether sufficient change in electron density between the cation radical and neutral arene existed. All heterocycles explored could be grouped into one of two categories: i) heterocycles that follow E_AS selectivity (**Figure 3.14, Part A**) and ii) heterocycles that possess enamine or enol character and react through iminium or oxocarbenium radical intermediates, respectively (**Figure 3.14, Part B**). Benzenoids, pyridines, quinolines, indazoles, and benzazoles constitute the first category, and pyrazoles, bridging nitrogen polyaromatics, benzofurans, and indoles comprise the second category. A flowchart for predicting site selectivity is shown in **Figure 3.15**.

3.3.4 Unsuccessful Arene Substrates

While the heterocycle classes detailed so far generally exhibit good reactivity, several explored groups were not sufficiently electron rich to undergo SET to the acridinium catalyst, including pyrimidines, pyridazines, pyrazines, purines, and nucleobases (**Figure 3.14, Part C**). A more specific list of arenes that were tried in the high-throughput experimentation at Novartis is disclosed in **Figures 3.16** and **3.17**. Some of these substrates gave slight conversion to the desired amination adduct but could not be optimized or quantified at Novartis, and many formed no product under the reaction conditions used. Due to experimental limitations with the available HTE setup, air was used instead of oxygen, so the use of an oxygen atmosphere could prove useful for further optimization. With the knowledge that certain heterocycles are not reactive with this methodology, the ability to functionalize electron-rich arenes over electron-poor arenes selectively becomes available and can be broadly useful in the context of late stage complex molecule functionalization.

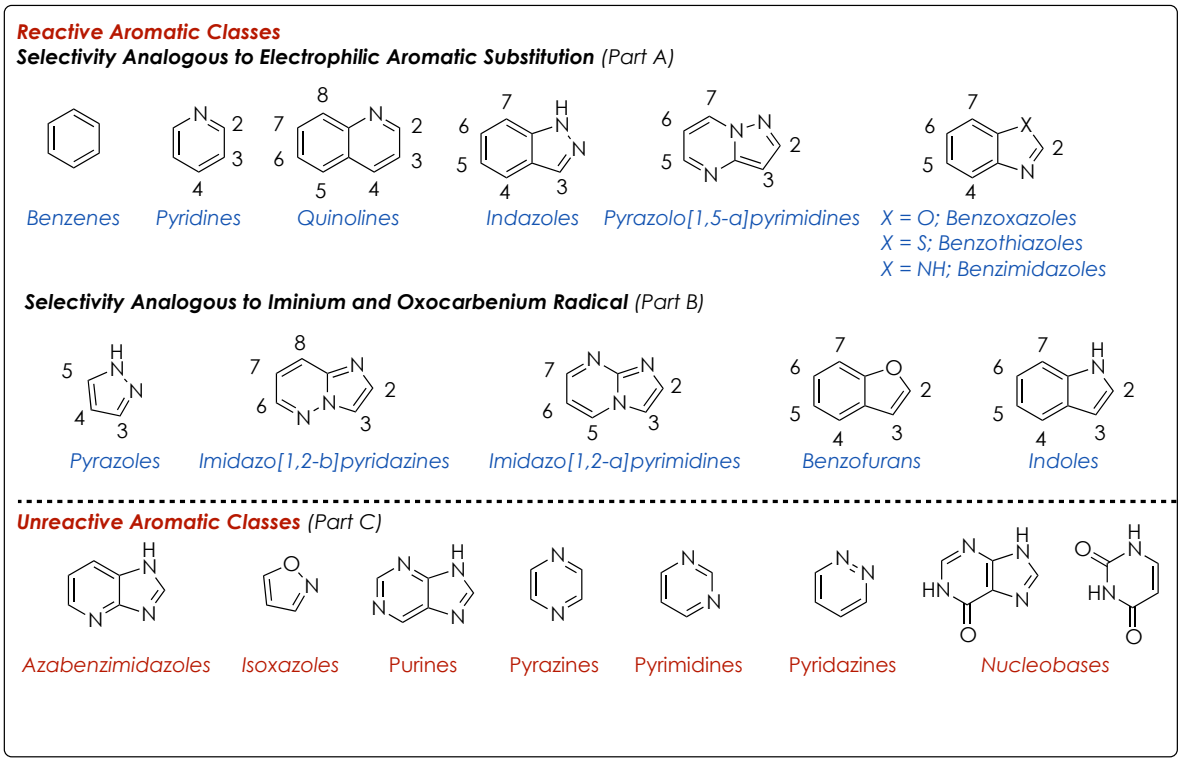

Figure 3.14 Summary of reactivity patterns for heterocycle classes

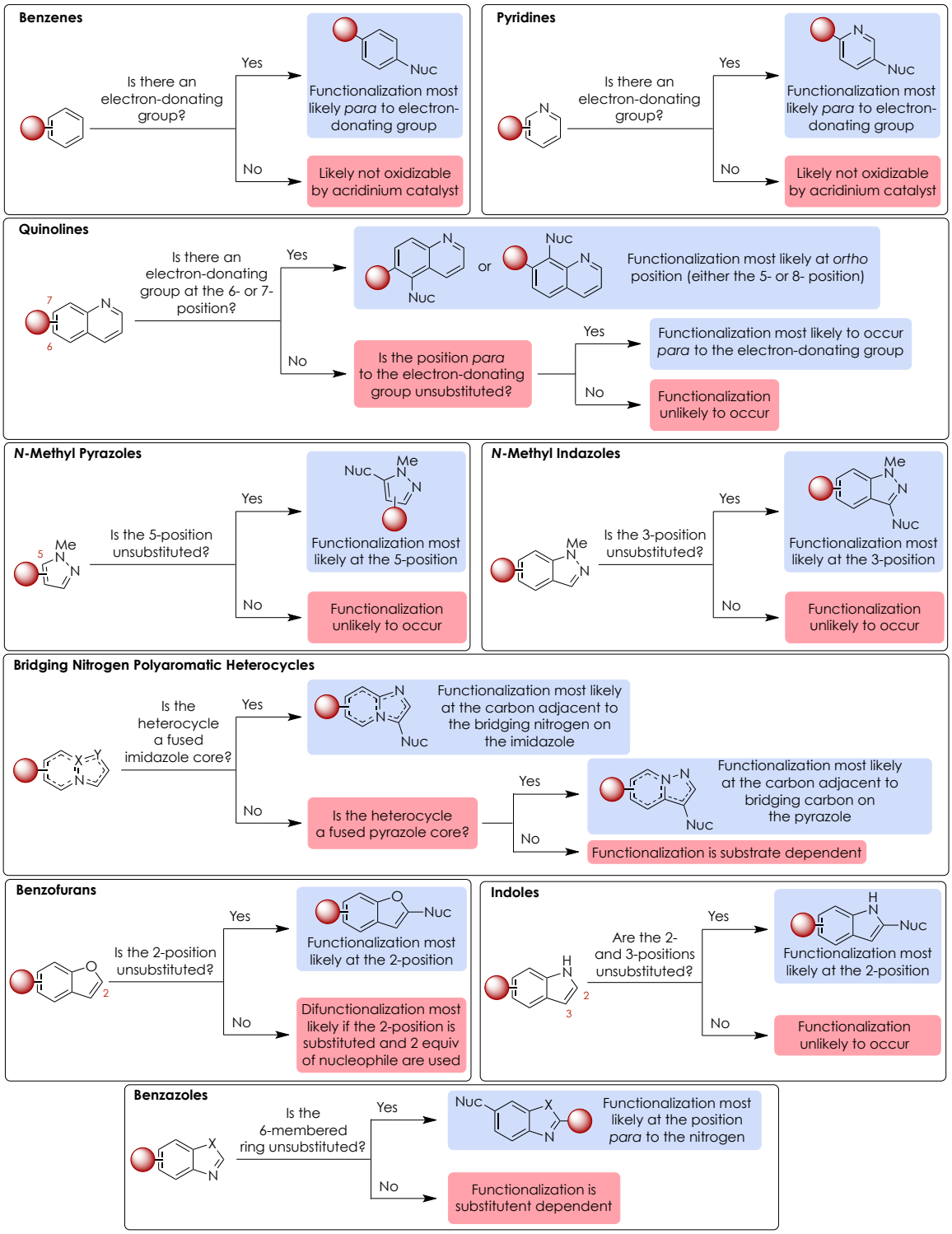

Figure 3.15 Flowchart describing general selectivities for heterocycles grouped by class

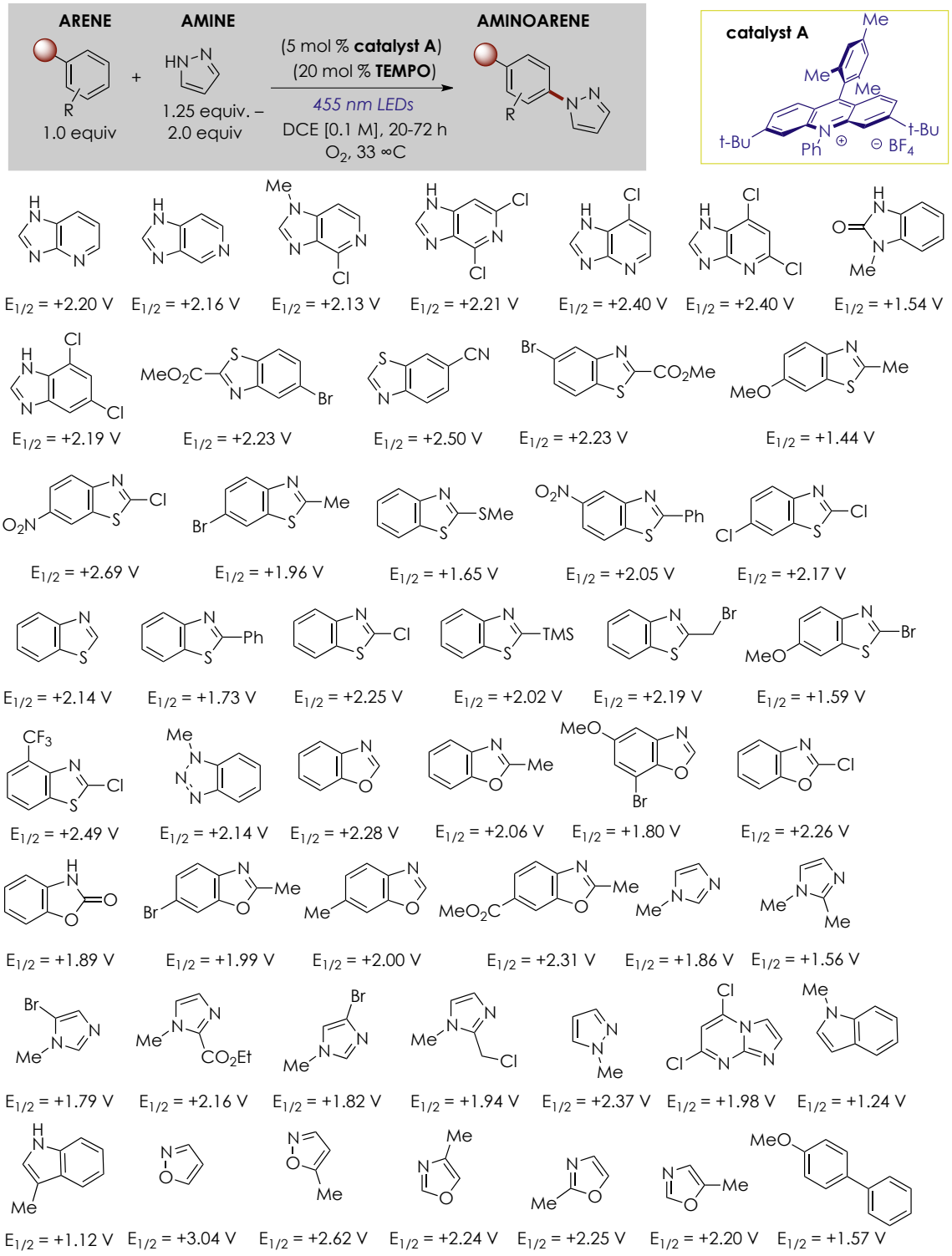

Figure 3.16 Unsuccessful arenes from Novartis high-throughput screen with redox potentials. All measurements were computationally determined in V vs SCE in MeCN.

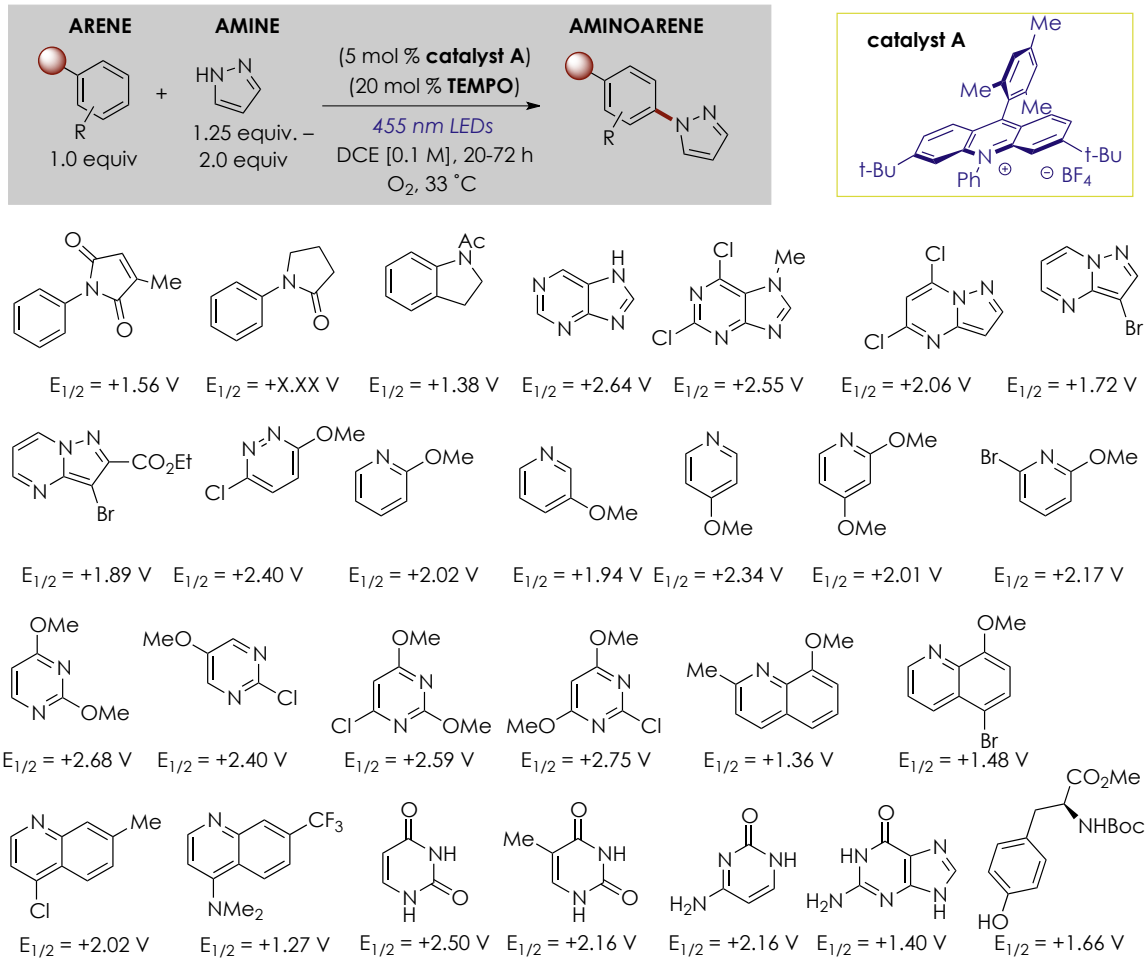

Figure 3.17 Unsuccessful arenes from Novartis high-throughput screen with redox potentials (continued). All measurements were computationally determined in V vs SCE in MeCN.

REFERENCES

(1) Romero, N. A.; Margrey, K. A.; Tay, N. E.; Nicewicz, D. A. *Science* **2015**, *349*, 1326–1330.

(2) Gormisky, P. E.; White, M. C. *J. Am. Chem. Soc.* **2013**, *135*, 14052–14055.

(3) O'Hara, F.; Blackmond, D. G.; Baran, P. S. *J. Am. Chem. Soc.* **2013**, *135*, 12122–12134.

(4) Bess, E. N.; Guptill, D. M.; Davies, H. M. L.; Sigman, M. S. *Chem Sci* **2015**, *6*, 3057–3062.

(5) Taylor, R. J. Wiley: Electrophilic Aromatic Substitution Chichester, West Sussex, England ; New York, 1990.

(6) Bunnett, J. F.; Zahler, R. E. *Chem. Rev.* **1951**, *49*, 273–412.

(7) Schmittel, M.; Burghart, A. *Angew. Chem. Int. Ed. Engl.* **1997**, *36*, 2550–2589.

(8) Roth, H.; Romero, N.; Nicewicz, D. *Synlett* **2015**.

(9) Ohkubo, K.; Mizushima, K.; Fukuzumi, S. *Res. Chem. Intermed.* **2013**, *39*, 205–220.

(10) Morofuji, T.; Shimizu, A.; Yoshida, J. *J. Am. Chem. Soc.* **2014**, *136*, 4496–4499.

(11) Reed, A. E.; Weinstock, R. B.; Weinhold, F. *J. Chem. Phys.* **1985**, *83*, 735–746.

(12) Walden, S. E.; Wheeler, R. A. *J. Phys. Chem.* **1996**, *100*, 1530–1535.

(13) Vitaku, E.; Smith, D. T.; Njardarson, J. T. *J. Med. Chem.* **2014**, *57*, 10257–10274.

(14) Prajapati, S. M.; Patel, K. D.; Vekariya, R. H.; Panchal, S. N.; Patel, H. D. *RSC Adv.* **2014**, *4*, 24463.

(15) Demmer, C. S.; Bunch, L. *Eur. J. Med. Chem.* **2015**, *97*, 778–785.

(16) Prajapati, N. P.; Vekariya, R. H.; Borad, M. A.; Patel, H. D. *RSC Adv* **2014**, *4*, 60176–60208.

(17) Bansal, Y.; Silakari, O. *Bioorg. Med. Chem.* **2012**, *20*, 6208–6236.

(18) Song, S.; Sun, X.; Li, X.; Yuan, Y.; Jiao, N. *Org. Lett.* **2015**, *17*, 2886–2889.

(19) Khan, M. F.; Alam, M. M.; Verma, G.; Akhtar, W.; Akhter, M.; Shaquiquzzaman, M. *Eur. J. Med. Chem.* **2016**, *120*, 170–201.

(20) Wada, Y.; Shirahashi, H.; Iwanami, T.; Ogawa, M.; Nakano, S.; Morimoto, A.; Kasahara, K.; Tanaka, E.; Takada, Y.; Ohashi, S.; *et al. J. Med. Chem.* **2015**, *58*, 6048–6057.

(21) Byth, K. F.; Cooper, N.; Culshaw, J. D.; Heaton, D. W.; Oakes, S. E.; Minshull, C. A.; Norman, R. A.; Pauptit, R. A.; Tucker, J. A.; Breed, J.; *et al. Bioorg. Med. Chem. Lett.* **2004**, *14*, 2249–2252.

(22) Choi, H.-S.; Rucker, P. V.; Wang, Z.; Fan, Y.; Albaugh, P.; Chopiuk, G.; Gessier, F.; Sun, F.; Adrian, F.; Liu, G.; *et al. ACS Med. Chem. Lett.* **2015**, *6*, 562–567.

(23) Chen, X.; Xu, W.; Wang, K.; Mo, M.; Zhang, W.; Du, L.; Yuan, X.; Xu, Y.; Wang, Y.; Shen, J. *J. Med. Chem.* **2015**, *58*, 8529–8541.

(24) O'Connor, S. P.; Wang, Y.; Simpkins, L. M.; Brigance, R. P.; Meng, W.; Wang, A.; Kirby, M. S.; Weigelt, C. A.; Hamann, L. G. *Bioorg. Med. Chem. Lett.* **2010**, *20*, 6273–6276.

(25) Venkatesan, A. M.; Dehnhardt, C. M.; Chen, Z.; Santos, E. D.; Dos Santos, O.; Bursavich, M.; Gilbert, A. M.; Ellingboe, J. W.; Ayral-Kaloustian, S.; Khafizova, G.; *et al. Bioorg. Med. Chem. Lett.* **2010**, *20*, 653–656.

(26) Elie, R.; Rüther, E.; Farr, I.; Emilien, G.; Salinas, E. *J. Clin. Psychiatry* **1999**, *60*, 536–544.

(27) Xu, Y.; Brenning, B. G.; Kultgen, S. G.; Foulks, J. M.; Clifford, A.; Lai, S.; Chan, A.; Merx, S.; McCullar, M. V.; Kanner, S. B.; *et al. ACS Med. Chem. Lett.* **2015**, *6*, 63–67.

(28) Enguehard-Gueiffier, C.; Gueiffier, A. *Mini-Rev. Med. Chem.* **2007**, *7*, 888–899.

(29) Cheng, Y.; Moraski, G. C.; Cramer, J.; Miller, M. J.; Schorey, J. S. *PLoS ONE* **2014**, *9*, e87483.

(30) Asif, M. *J. Anal. Pharm. Res.* **2016**, *3*.

(31) Ishikura, M.; Abe, T.; Choshi, T.; Hibino, S. *Nat. Prod. Rep.* **2013**, *30*, 694.

(32) de Sa Alves, F.; Barreiro, E.; Manssour Fraga, C. *Mini-Rev. Med. Chem.* **2009**, *9*, 782–793.

(33) Sravanthi, T. V.; Manju, S. L. *Eur. J. Pharm. Sci.* **2016**, *91*, 1–10.

(34) Zhao, Z.; Wang, Z. *Synth. Commun.* **2007**, *37*, 137–147.

(35) Rodriguez, R. A.; Pan, C.-M.; Yabe, Y.; Kawamata, Y.; Eastgate, M. D.; Baran, P. S. *J. Am. Chem. Soc.* **2014**, *136*, 6908–6911.

(36) Balaban, A. T.; Oniciu, D. C.; Katritzky, A. R. *Chem. Rev.* **2004**, *104*, 2777–2812.

(37) Palmer, M. H.; Kennedy, S. M. F. *J. Chem. Soc. Perkin Trans. 2* **1974**, 1893.

(38) Kihel, A. E.; Benchidmi, M.; Essassi, E. M.; Danion-Bougot, R. *Synth. Commun.* **1999**, *29*, 387–397.

(39) Ward, E. R.; Poesche, W. H. *J. Chem. Soc. Resumed* **1961**, 2825.

(40) McManus, J. B.; Nicewicz, D. A. *J. Am. Chem. Soc.* **2017**.

CHAPTER 4: DIRECT ARYL C–H AMINATION WITH PRIMARY AMINES USING ORGANIC PHOTOREDOX CATALYSIS

Adapted from Margrey, K. A.; Levens, A.; Nicewicz, D. A. *Angew. Chem. Int. Ed.*, **2017**, *56*, 15644–15648.

4.1 Introduction

Arene C–H functionalization methodologies have been developed by our lab using nitrogen heterocycles,[1] ammonia surrogates, cyanide,[2] and, in select cases, fluorine as coupling partners. This reactivity hinges on the use of electron-rich arenes that can undergo SET with an acridinium catalyst to afford an electrophilic arene cation radical, which is susceptible to addition by the nucleophilic partner. Several other photoredox-catalyzed systems have been used to generate electrophilic coupling partners different from the alkene and arene cation radicals commonly utilized by our lab.[3] The ability to generate additional types of electrophilic cation radical coupling partners via an acridinium catalyst would facilitate the development of novel bond constructions and reactivity (**Figure 4.1**).

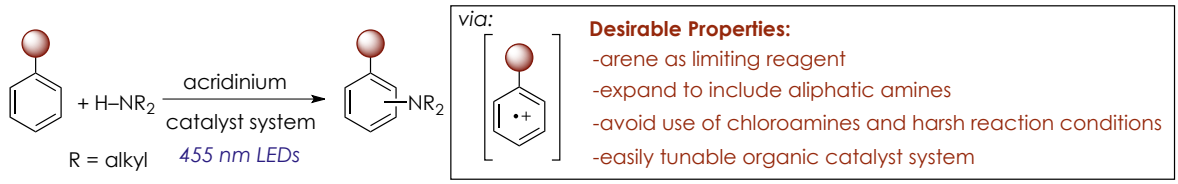

Figure 4.1 General template for aliphatic aryl amination.

4.2 Arene Functionalization with Aliphatic Amines

Prior work focused on the use of azoles as coupling partners for aryl C–H amination (see Chapter 2) and the development of a predictive model for the site selectivity of the transformation (see Chapter 3). At the onset of this project, we wondered whether additional nitrogen coupling partners, namely aliphatic amines, could be used for a similar C–H amination strategy. Due to the relatively low oxidation potentials associated with such amines (+0.40 to +1.90 V vs SCE), it was not clear if the amine or arene would be more likely to undergo SET with the acridinium catalyst and whether subsequent productive coupling could occur.[4]

In 1973, Minisci reported that by exposing *N*-chloroamines to iron (II) sulfate in strongly acidic media, amine cation radicals could be generated and undergo addition to arenes to form substituted aniline derivatives (**Figure 4.2**).[5,6] Minisci demonstrated that this was a viable mechanism mostly for secondary amines, but in some cases, primary amines could also be used. Anisole reacted with *N*-chloropiperidine, affording only *para* and *ortho* isomers, while toluene reacted with *N*-chloromethylamine to produce all regioisomers in a 2:1:1 *para*:*meta*:*ortho* ratio. However, chloroamines are only stable for storage at low temperatures and can undergo N–Cl bond homolysis upon exposure to visible light, rendering them quite unstable and challenging to use. Furthermore, the necessity of strongly acidic conditions limits the available functional group compatibility in this type of reaction.

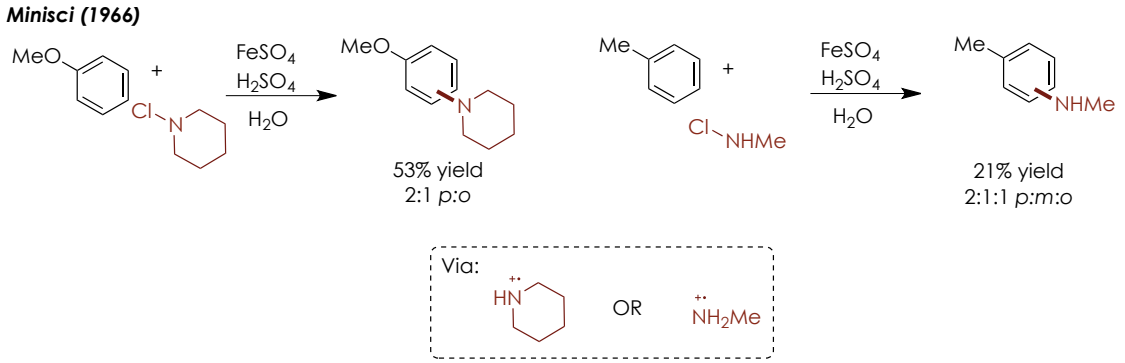

Figure 4.2 Aryl amination using *N*-chloroamines.

4.3 Photoredox-Mediated Functionalization of Aliphatic Amines

Inspired by this precedent for arene amination with aliphatic chloroamines, we investigated other strategies to generate amine cation radicals that avoided the use of prefunctionalization, including through electrochemistry, chemical oxidants, UV light-mediated photochemistry, and visible light-mediated photochemistry. Specifically, in the context of visible light-mediated reactivity, photoredox catalyst excited states can often be quenched by amines through SET to generate the amine cation radical. Due to their particularly low oxidation potentials (<+1.0 V vs SCE), tertiary aliphatic amines were frequently used in these earlier works and have also been used more recently by Rueping, Stephenson, and Rovis, among others, to harness this process to generate synthetically useful intermediates.[7,8,9] Amine cation radicals can generally undergo either H atom abstraction at the weakened C–H bond adjacent to nitrogen or deprotonation to generate an iminium or radical adjacent to nitrogen, respectively (**Figure 4.3**). Both of these intermediates have been exploited to functionalize alkyl amines.

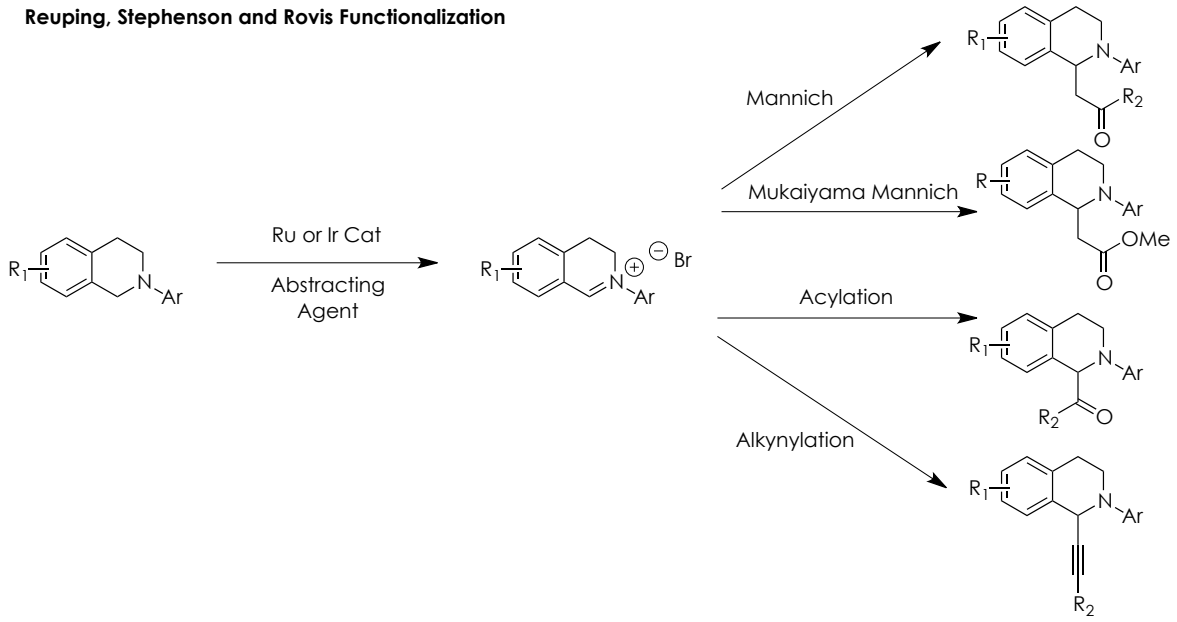

Figure 4.3 Previous photoredox-mediated functionalization of aliphatic amines.

One example of iminium generation by the Stephenson group used $BrCCl_3$ as a stoichiometric oxidant to facilitate H atom abstraction adjacent to nitrogen.[8] Several different sp^3 and sp^2 carbon nucleophiles were able to add into the iminium intermediate. To enable this type of reactivity, the amine generally must be tertiary and is often derived from aniline. This allows for the amine to be electron-rich enough to undergo SET with the ruthenium or iridium-based photoredox catalysts ($E^*_{1/2} \approx +0.7$ to $+1.2$ V vs SCE).

Primary and secondary amines have been underutilized in photoredox processes to this point. While these general motifs are not as electron-rich as tertiary amines, they generally are still sufficiently electron-rich to undergo SET with photocatalysts such as an acridinium (see Appendix C). We hoped to utilize an acridinium catalyst to undergo SET with an alkyl amine and generate a reactive electrophilic intermediate. Since aliphatic amines are very prevalent in synthesis and biological systems such as amino acids, we felt that the ability to generate reactive species from these abundant starting materials would be important.

Recently, the Knowles group demonstrated that an iridium-based photocatalyst could be used to generate a secondary amine cation radical, which underwent anti-Markovnikov addition to unactivated alkenes.[10] Primary amines could not be used in this reaction, but there was a wide scope of secondary amines and alkene coupling partners. We felt that utilizing an amine cation radical intermediate could be useful in arylation chemistry, accessing aniline derivatives from non-oxidizable arenes using an acridinium photocatalyst.

4.4 Primary Amine Aryl Functionalization via Photoredox Catalysis

The ability to construct aryl C–N bonds is particularly important due to the prevalence of aryl amines in natural products, pharmaceuticals, and materials. This type of reaction mode allows for rapid functionalization and derivatization of arenes, streamlining synthetic routes and avoiding the preoxidation step that is required to install halides or other cross-coupling functional handles. Most previously developed C–H amination strategies relied on using electron-poor nitrogen coupling partners such as amides and imides (see **Chapter 1**). Subsequently, we developed a photoredox catalyzed strategy for C–H amination using nitrogen heterocycles and ammonia surrogates with a predictive model for site selectivity (see **Chapters 2 and 3**) (**Figure 4.4**). While these nitrogen nucleophiles were more electron-rich than most amides or imides, they, in most cases, were not sufficiently electron-rich to undergo SET with an acridinium catalyst. The cyanation chemistry developed in our lab uses TMSCN as a nucleophile, which is not capable of being oxidized by the catalyst ($E_{p/2} \geq +3.0$ V vs SCE).[2] With the knowledge that most nucleophiles that could participate in our lab's aryl C–H functionalization methodologies were not oxidizable, we wondered whether aryl functionalization could still occur when using electron-rich amines, such as primary amines, as the coupling partner.

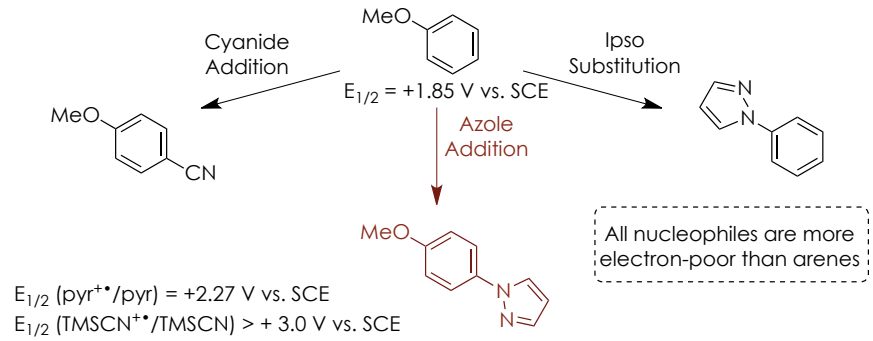

Figure 4.4 Previous aryl functionalizations demonstrated by the Nicewicz lab. Redox potentials were determined experimentally in MeCN.

4.4.1 Initial Reactivity and Optimization

We hoped to extend our aryl amination chemistry beyond just nitrogen heterocycles and study amine coupling partners that can be oxidized by the acridinium photocatalyst. With commercial valine methyl ester hydrochloride as a non-volatile and inexpensive primary amine source, we began by screening solvents with anisole as the coupling partner. Initially, we found that the desired adduct was formed in 29% yield under aerobic conditions with slight excess of the amine and using DCE and 4M pH 8 phosphate buffer as the solvent, favoring formation of the *ortho* product (**Table 4.1, entry 1**). Replacing the pH 8 buffer with saturated aqueous sodium bicarbonate provided 39% yield of the desired product (**Table 4.1, entry 2**). The basic aqueous cosolvent proved necessary to deprotonate the HCl salt of the amine, and due to concerns with reaction reproducibility, the phosphate buffer was used for further optimization. Increasing the amount of amine in the reaction produced yields of up to 55% when using three equivalents (**Table 4.1, entries 3 – 4**), and inversion of the stoichiometry proved to be inferior (**Table 4.1, entry 5**). An oxygen atmosphere was necessary for reactivity to occur, with only 2% yield of the desired adduct produced when the reaction was only sparged with oxygen and not run under an aerobic atmosphere (**Table 4.1, entry 6**).

The yield of the reaction could not be increased further at this point, so we considered whether this was due to product instability under the reaction conditions, especially since the products of C–H amination are more prone to oxidation ($E_{1/2}$(**4.3**/**4.3**+•) = +0.74 V vs SCE than the starting arenes. Unlike with azole coupling partners, the addition of TEMPO did not increase the yield of the reaction (**Table 4.1, entry 7**). However, decreasing the reaction time to four hours, the point at which full consumption of the starting arene was observed, increased the yield to 67% (**Table 4.1, entry 8**). Using a slightly less oxidizing catalyst **B** with the shortened reaction time provided the product in 80% yield (**Table 4.1, entry 9**). Using an additional lamp, catalyst **A**, or more dilute reaction concentrations significantly decreased the yield of the desired product (**Table 4.1, entries 10 – 12**). The free base of valine could also be used in the reaction with only slightly lower yields, so owing to commercial availability, the HCl salts of amino acids were used.

Compared to the aryl C–H functionalization with azoles detailed in **Chapter 2**, this aryl C–H amination deviated significantly with respect to the regioselectivity. As seen in **Figure 4.4**, prior art from our lab was highly *para* selective for anisole functionalization; however, with valine methyl ester as the coupling partner, a statistical mixture of *ortho* and *para* isomers is produced. When we used TBS phenyl ether as a substrate with primary amines as the coupling partner, we observed that the *para* isomer was favored, yet never to the extent that we saw with azoles.

Table 4.1 Initial optimization for aryl amination with primary amines.

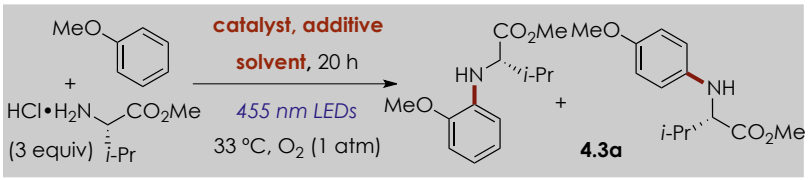

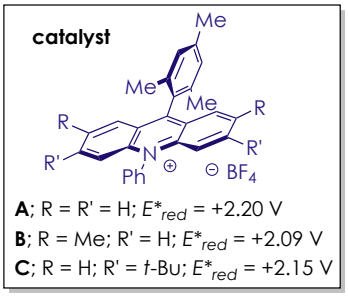

additives:

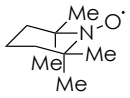

TEMPO

entry	deviation from above	catalyst	solvent [M]	yield	o:p
1	1.5 equiv amine	**C**	4:1 DCE:pH 8 Buffer [0.1]	29%	5.3:1
2	1.5 equiv amine	**C**	4:1 DCE: sat. Bicarb. [0.1]	39%	2.3:1
3	2 equiv amine	**C**	4:1 DCE:pH 8 Buffer [0.1]	39%	4.1:1
4	none	**C**	4:1 DCE:pH 8 Buffer [0.1]	55%	2.3:1
5	3 equiv arene and 1 equiv amine	**C**	4:1 DCE:pH 8 Buffer [0.1]	25%	7.3:1
6	No O_2, only sparge	**C**	4:1 DCE:pH 8 Buffer [0.1]	2%	-
7	20 mol% **TEMPO**	**C**	4:1 DCE:pH 8 Buffer [0.1]	45%	2.0:1
8	4 hours of irradition	**C**	4:1 DCE:pH 8 Buffer [0.1]	67%	1.9:1
9	**4 hours of irradiation**	**B**	**4:1 DCE:pH 8 Buffer [0.1]**	**80%**	**2.2:1**
10	2 Lamps	**B**	4:1 DCE:pH 8 Buffer [0.1]	25%	4.0:1
11	none	**A**	4:1 DCE:pH 8 Buffer [0.1]	32%	2.0:1
12	none	**B**	4:1 DCE:pH 8 Buffer [0.05]	50%	3.2:1

4.4.2 Amine Scope for Primary Amine Functionalization

Based on the divergent regioselectivity observed between anisole and TBS phenyl ether, we examined whether this trend would hold for a number of amine coupling partners (**Figure 4.5**). For a range of amino acids, the aryl amination favored formation of the *ortho* isomer with anisole and *para* isomer with TBS phenyl ether (**4.1** – **4.14**). Protected serine and threonine, *N*-Boc lysine, and glutamic and aspartic acid esters all reacted smoothly, affording **4.10** – **4.14** in good yields for both arene coupling partners. Amination adducts formed when using isoleucine (**4.6**) and threonine (**4.11**) showed only one diastereomer by ^{1}H NMR analysis, demonstrating that the stereocenter did not epimerize during the reaction. Overall,

14 different amino acid esters were shown as competent coupling partners in this reaction, with generally good yields.

Commercially available primary amines such isopropylamine and *n*-propylamine also served as effective coupling partners to produce **4.15** and **4.16**, even though they are more prone to oxidative degradation under an aerobic atmosphere than amino acids are. When using such amine free bases instead of HCl salts, the pH 8 buffer could be omitted with no change in yield. Halogenated amines afforded the desired aryl amine (**4.17**), albeit in lower yields. Allyl- and benzylamines also provided the desired adducts (**4.18** and **4.19)** in moderate to high yields.

Interestingly, (*S*)-methylbenzylamine worked well with both anisole and TBS phenyl ether (**4.20**). HPLC analysis of the amination products revealed that, despite the presence of a benzylic C–H bond weakened by hyperconjugation from nitrogen, the chiral center did not epimerize over the course of the reaction. This coupling with anisole was amenable to scale-up by 25-fold using a flow apparatus and short retention time in the flow cell. When this retention time was too long (i.e. 89 min), yields were very low; however, when retention times were fast (i.e. 1 min with continuous loop), the desired product could be formed in 61% yield. Finally, *tert*-butylamine also participated as a coupling partner with anisole, although in low yield (**4.21**).

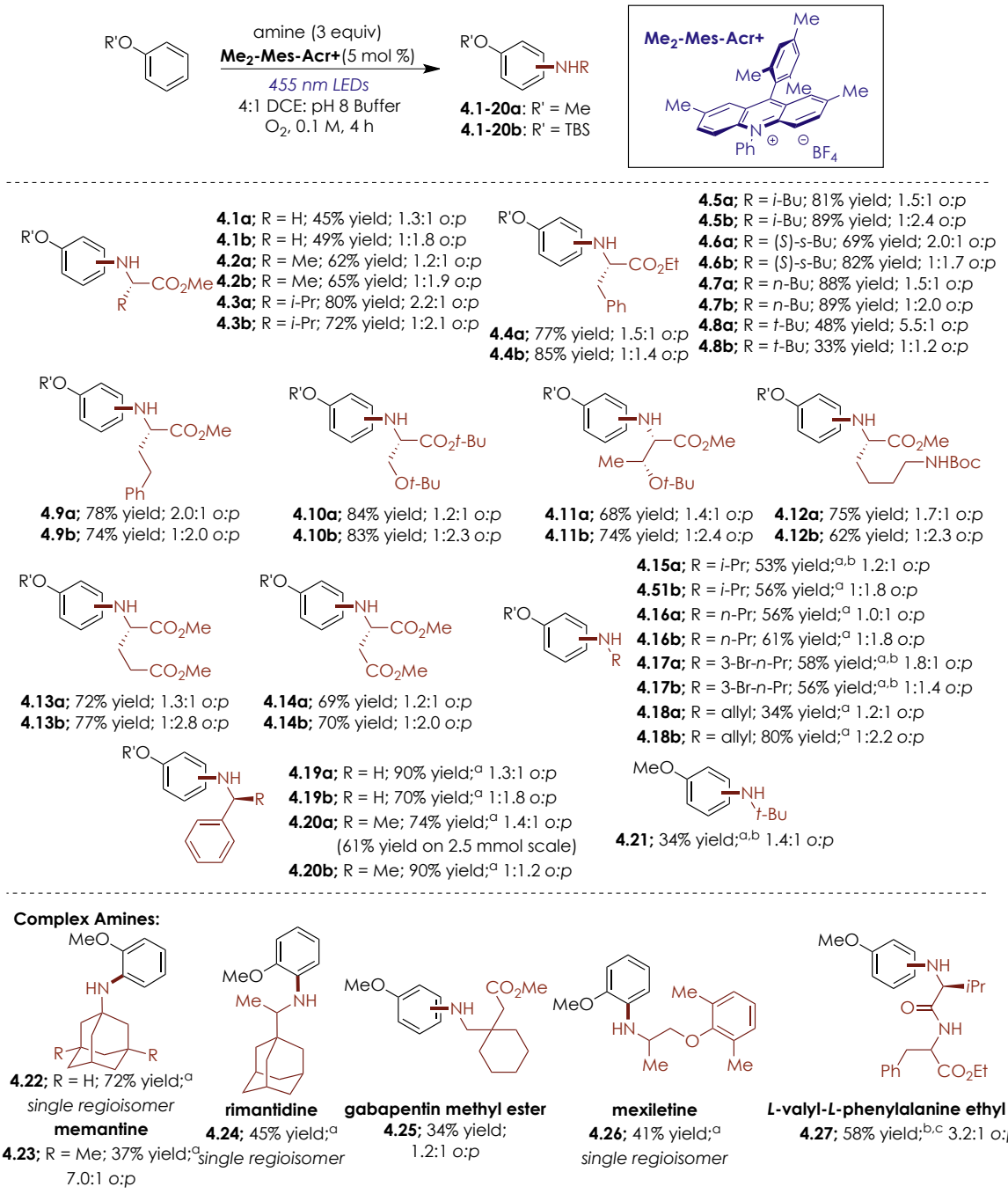

Figure 4.5 Primary amine substrate scope. Ratios refer to *ortho*:*para* (*o*:*p*) selectivity for the given adduct. Reactions were run in 4:1 DCE/pH8 phosphate buffer at 0.1 M concentration with respect to the arene limiting reagent. ([a]) Reaction run in DCE in 0.1 M concentration with respect to the arene limiting reagent. ([b]) Yield of adduct determined by ^{1}H NMR spectroscopy. ([c]) Reaction run in DCE at 0.1 M concentration, with respect to the arene limiting reagent, for 14 h.

To highlight the utility of this C–H amination method for complex applications, we demonstrated its utility with several bioactive amines. Adamantylamine and memantine, anti-Parkinson and anti-Alzheimer pharmaceuticals, respectively, provided **4.22** and **4.23** in modest to good yield.[11] Rimantidine, an anti-viral agent,[12] also generated the amination product in moderate yield (**4.24**). Interestingly, the three adamantyl-containing amines all gave excellent regioselectivity favoring the *ortho* isomer. Gabapentin methyl ester, a medication used to treat seizures,[13] participated as the amine coupling partner to form **4.25**, while anti-arrhythmic pharmaceutical, mexiletine,[14] provided **4.26** in 41% yield. Additionally, the use of *L*-valyl-*L*-phenylalanine ethyl ester to functionalize anisole afforded **4.27** in 58% yield and highlights the applicability of this strategy to dipeptides. Overall, a wide variety of amines, including amino acids and biologically active amines, could be shown as competent coupling partners in this methodology.

Several amines, however, did not participate in this reaction (**Figure 4.6**). Whereas amino acid esters worked well under the reaction conditions, no desired amination was observed with amino acids, likely due to competitive decarboxylative processes. Secondary amines were also problematic due to oxidation adjacent to nitrogen, forming amides and imides instead of the desired adducts. Aniline did not work as either the arene or amine component, similarly to our prior work (see **Chapter 2.2.5**). Methylamine HCl did provide trace quantities of amination product that could not be greatly improved through optimization, possibly owing to the volatility of the free base. Amines containing unprotected alcohols, such as serine methyl ester, or protected thiols, including trityl-protected cysteine, also did not participate in the reaction.

O-Benzyl tyrosine also did not produce any amination product under the reaction conditions. Ornithine methyl ester, containing two different amines, also did not provide the desired adduct, and returned starting material was observed. Trityl-protected histidine methyl ester provided 25% yield of the aryl amine, but this could not be improved further. α–Acetyl-lysine methyl ester was able to serve as the amine coupling partner at the ε nitrogen in 30% yield under the previously optimized conditions, which might be further modified to improve the yields for both histidine and lysine derivatives. The ability to functionalize lysine at the ε nitrogen could lead to applications in the selective arylation of lysine in proteins.

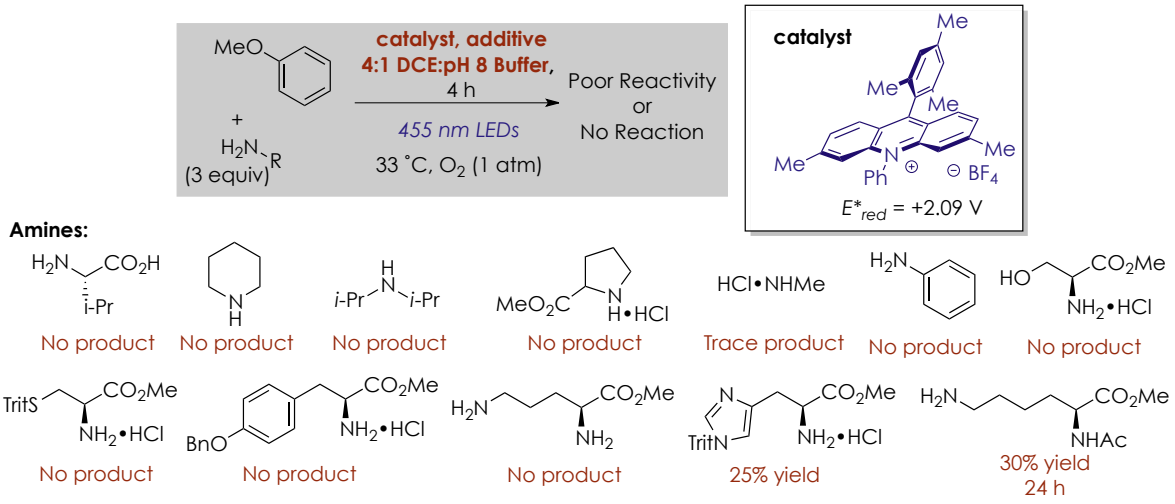

Figure 4.6 Unsuccessful aliphatic amine coupling partners. Reactions were run in 4:1 DCE/pH8 phosphate buffer at 0.1 M concentration with respect to the arene limiting reagent.

4.4.3 Arene Scope for Primary Amine Functionalization

Having shown that a variety of primary amines participated in this reaction, we also sought to demonstrate that a range of arenes could undergo C–H functionalization under these conditions (**Figure 4.7**). A series of monosubstituted arenes underwent amination with valine methyl ester HCl to afford **4.3** and **4.28** – **4.34** in good yield. Regioselectivity could be altered based on the sterics of the substituent on the arene such that bulkier phenolic ethers led to increased formation of the *para* isomer.

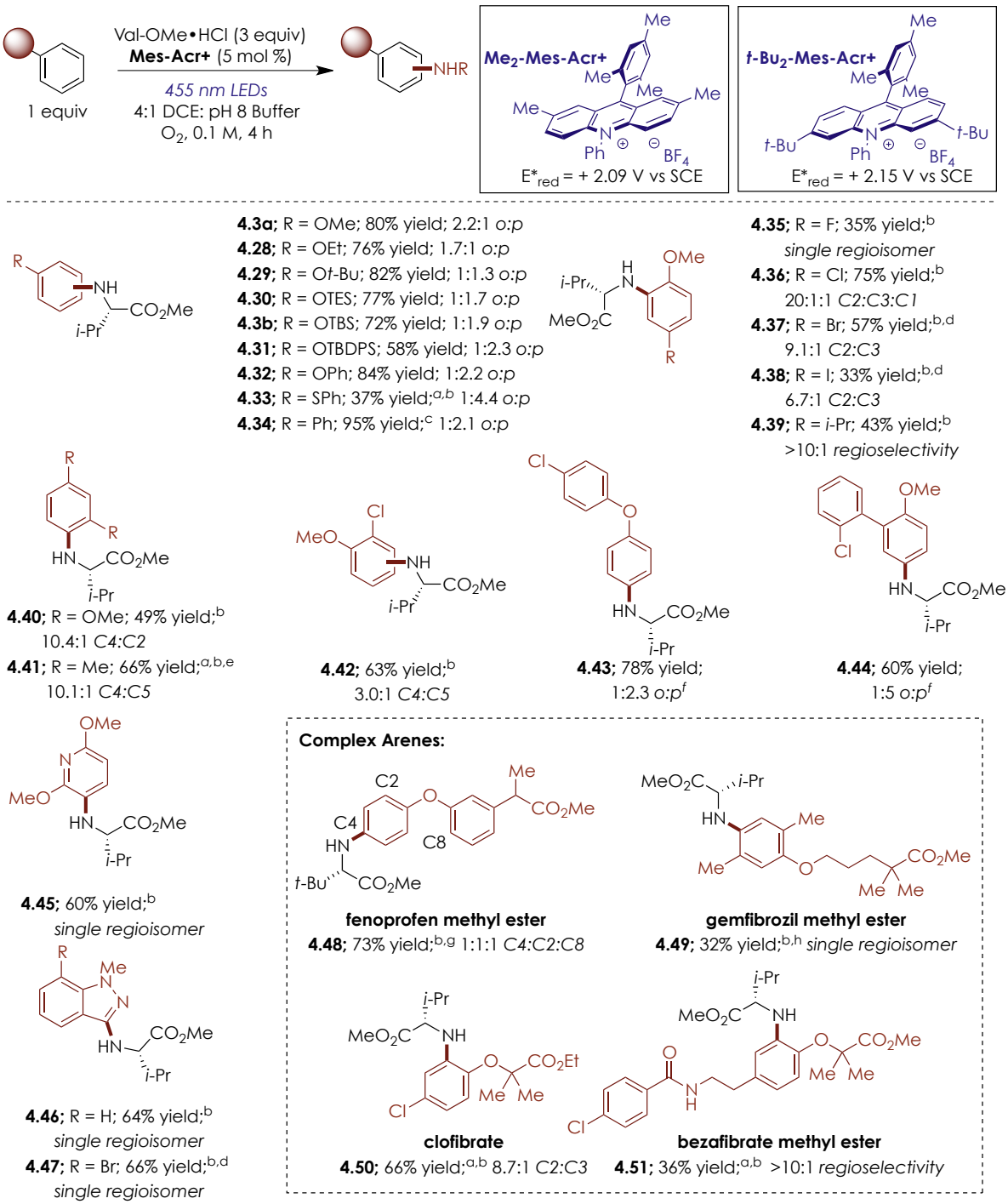

Figure 4.7 Arene substrate scope. Ratios refer to *ortho*:*para* (*o*:*p*) selectivity for the given isomer unless otherwise specified. Reactions were run using Me_2-Mes-Acr+ in 4:1 DCE/pH 8 phosphate buffer at 0.1 M concentration with respect to the arene limiting reagent. ([a]) Yield of adduct as determined by ^{1}H NMR, ([b]) Reactions run with 40 mol % TEMPO and 5 mol % tBu$_2$-Mes-Acr+ for 15–26 h, ([c]) Reaction run for 13 h, ([d]) Reactions were run in 4:1 trifluorotoluene/pH 8 phosphate buffer, ([e]) 10 equiv of *meta*-xylene was used with the limiting amine, ([f]) The *o*:*p* ratio determined after isolation, ([g]) Reaction was run with 3 equiv of *tert*-leucine methyl ester hydrochlroide, ([h]) 5 equiv of amine used.

As previously discussed, optimized conditions for anisole and TBS phenyl ether required that the reaction only be run for 4 hours without TEMPO. When attempting to expand the arene scope to 1,4-disubstituted arenes, these reaction conditions were no longer sufficient (**Table 4.2**). The addition of a cocatalytic amount of TEMPO improved the reactivity for disubstituted arenes; however, too much TEMPO proved to be deleterious to the yields. Finally, the use of catalyst **B** gave an increased yield, affording the aniline with functionalization predominantly *ortho* to the methoxy substituent.

Table 4.2 Optimization of 1,4-disubstitued arene substrate.

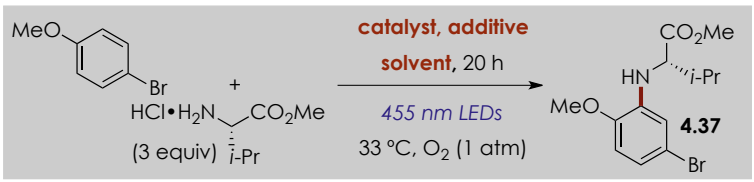

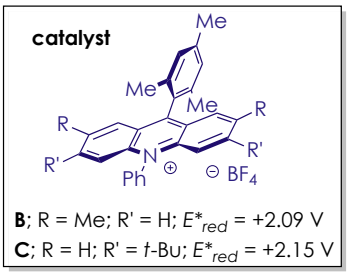

additives:

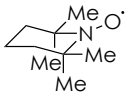

TEMPO

entry	additive	catalyst	solvent [M]	yield
1	none	**C**	4:1 DCE:pH 8 Buffer [0.1]	28%
2	TEMPO (0.2 eq.)	**C**	4:1 DCE:pH 8 Buffer [0.1]	60%
3	TEMPO (0.2 eq.)	**B**	4:1 DCE:pH 8 Buffer [0.1]	52%
4	TEMPO (0.8 eq.)	**C**	4:1 DCE:pH 8 Buffer [0.1]	31%
5	TEMPO (0.4 eq.)	**C**	4:1 DCE:pH 8 Buffer [0.1]	57%

With these modified reaction conditions, functionalization of halogenated anisoles could be demonstrated (**Figure 4.7**), favoring the isomer with amination *ortho* to the methoxy group (**4.35** – **4.38**). 4-Alkyl substituted anisole derivatives also worked with TEMPO as an additive, allowing access to **4.39** in 43% yield with excellent regioselectivity. 1,3-Disubstituted benzenoids underwent amination, forming both **4.40** and **4.41** in good yield and regioselectivity. 2-Chloroanisole was competent as well, affording **4.42** in 63% yield. The ability to functionalize disubstituted benzenoids of any substitution pattern greatly

expands the arene scope for the transformation. Substrates with more than one arene also underwent amination to form **4.43** and **4.44**, favoring reactivity at the more electron-rich ring in both examples. Further, heterocycles such as pyridines and *N*-methyl indazoles formed adducts **4.45** – **4.47** as single regioisomers in good yield, highlighting applicability to pharmaceutically relevant scaffolds.

Similarly to the amine scope, we applied our C–H amination strategy to complex, bioactive arenes (**Figure 4.7**). Coupling *tert*-leucine methyl ester with fenoprofen methyl ester, an anti-inflammatory drug, afforded the aniline **4.48** in 73% yield favoring reactivity on the more electron-rich ring. Members of the fibrate family, a class of cholesterol lowering drugs, including gemfibrozil methyl ester, clofibrate, and bezafibrate,[15,16] underwent C–H amination with valine methyl ester HCl in moderate to good yields (**4.49** – **4.51**), even observing a single regioisomer in the case of **4.51**. These examples highlight the ability to utilize primary amine coupling partners in late stage C–H functionalization reactions with complex substrates.

4.4.4 Unsuccessful Arene Substrates

Several other arenes were used as substrates but did not provide the desired product, or the yields could not be improved to achieve synthetic utility (**Figure 4.8**). 1,2- and 1,4-disubstituted arenes with two electron-donating groups were never viable substrates; however 1,3-dimethoxybenzene did work in the reaction. Trisubstituted arenes did not work, and we hypothesize that this is due to steric hindrance. Naphthalene did not provide any product, and aniline derivatives gave low yields of the desired product and could not be improved. We propose that SET with these arenes is very rapid compared to the amine coupling partner, and back electron transfer for these substrates is very facile (see **Chapter 2.2.5** 3-Fluoroanisole

did not provide any desired product, and, instead, *ipso* substitution at the 3-position was observed. 4-Methoxyacetophenone provided the desired product, albeit in only 25% yield, and that value could not be improved by modifying the reaction conditions. Heterocycles that previously worked for the azole aryl amination chemistry (see **Chapter 2**) did not work for this reaction. Additionally, trifluorotoluene did not undergo functionalization even when used as the reaction solvent, since the arene is insufficiently nucleophilic and not electron-rich enough to be oxidized.

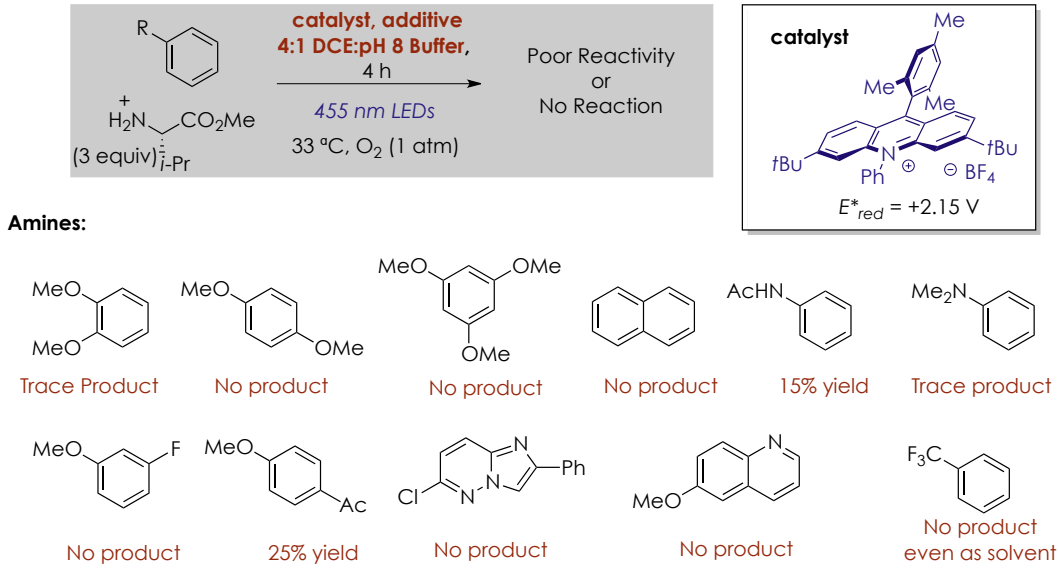

Figure 4.8 Arenes that could not be functionalized with aliphatic amines. Reactions were run in 4:1 DCE/pH8 phosphate buffer at 0.1 M concentration with respect to the arene limiting reagent.

4.4.5 Amine Cation Radical Mechanism

Previously, we highlighted that an electrophilic arene cation radical could be generated via SET from an arene to an acridinium catalyst. Since the present system has two reagents that could be oxidized, the arene and the amine, we wanted to understand whether the amine cation radical was a pathway that would lead toward productive reactivity. To answer this question, we examined arenes that are not sufficiently electron-rich to undergo

SET with the acridinium (redox potential above +2.15 V vs. SCE). With modified reaction conditions that used solvent-level substrate, we observed that benzene and toluene could both undergo amination (**Figure 4.9**), even though SET from the arene is not plausible. The ratio of *ortho*, *meta*, and *para* products afforded when using toluene as the substrate closely resembles the ratio observed by Minisci (**Figure 4.2**).[6] This lends further credence to the intermediacy of an amine cation radical for the functionalization of these substrates.

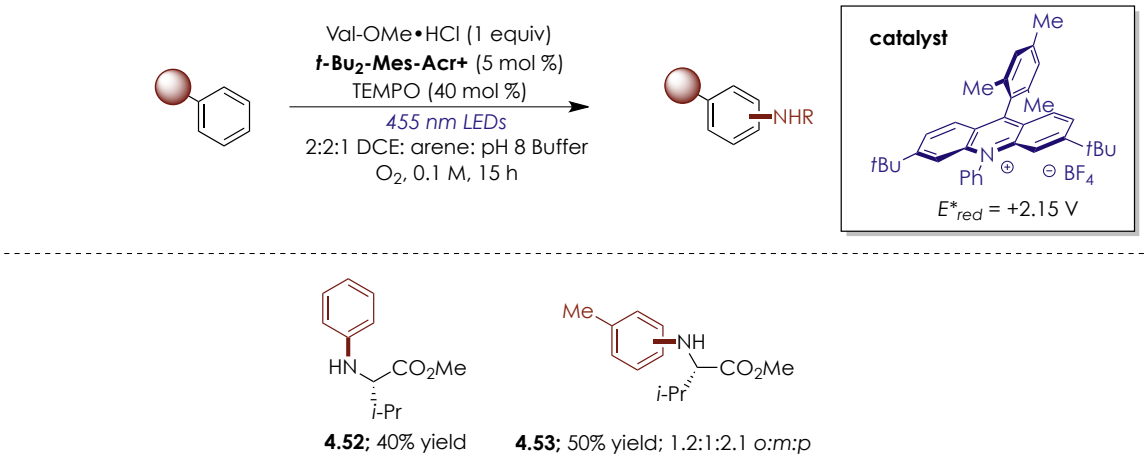

4.52; 40% yield **4.53;** 50% yield; 1.2:1:2.1 *o:m:p*

Figure 4.9 Amination of benzene and toluene. Reactions were run in 4:1:1 DCE/pH8 phosphate buffer/arene at 0.1 M concentration with respect to the amine limiting reagent.

Based on Stern-Volmer fluorescence quenching studies in DCE, both the amine and electron-rich arenes can quench the excited state of the catalyst (**Figure 4.10**). Normalization of the ensuing fluorescence quenching constants to account for the stoichiometry used in the reaction leads to the quenching rates being nearly identical for the arene and the amine. Arenes such as toluene do not quench the excited state of the catalyst, as expected from the high oxidation potential.

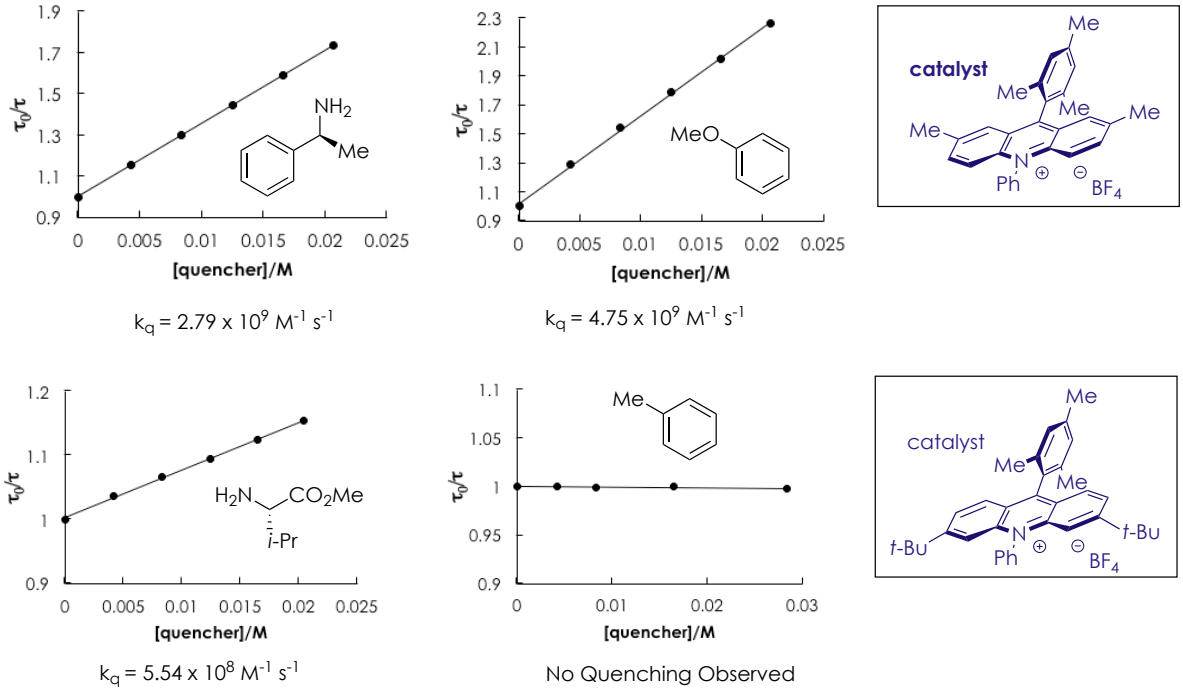

Figure 4.10 Stern-Volmer quenching studies for aliphatic amines and arenes. Quenching data were determined in DCE.

Based on these results, we propose that the reaction begins with the excitation of **Mes-Acr+** with 455 nm LEDs to **Mes-Acr+*** (**Figure 4.11**). The excited state of the catalyst can then remove an electron from the primary amine, generating the amine cation radical, **4.54**. Nucleophilic addition of the arene substrate followed by deprotonation affords the cyclohexadienyl radical, **4.55**. Oxygen then facilitates the rearomatization step,[17] furnishing the final aniline **4.56**. Similarly to our prior work and consistent with precedent from Fukuzumi, oxygen also assists in the oxidization of the acridine radical to the acridinium to regenerate the active catalyst. While this is the mechanism most likely to be operative for the amination of insufficiently electron-rich arenes such as benzene and toluene, an arene cation radical mechanism cannot be excluded for more electron rich arenes (**Figure 4.12**, see **Chapter 2.2.9** for further details).

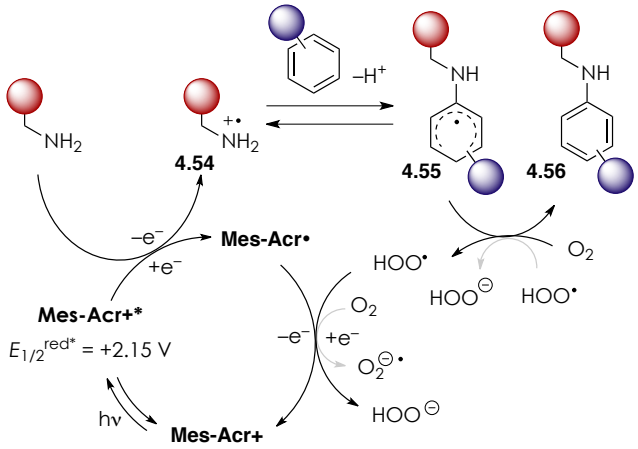

Figure 4.11 Proposed amine cation radical-mediated mechanism.

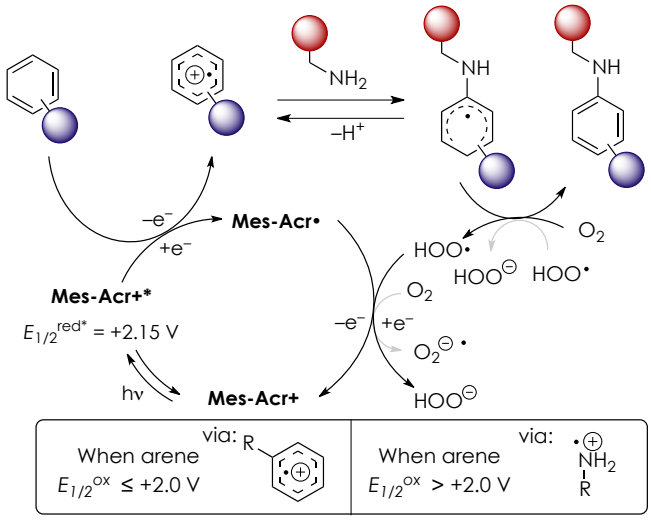

Figure 4.12 Proposed arene cation radical-mediated mechanism.

We have developed a direct aryl C–H amination reaction using primary amines via photoredox catalysis. This reactivity occurs under mild conditions and is compatible with a variety of functional groups. Extending this work to secondary amines would further expand the scope of anilines that can be accessed through this strategy. Furthermore, this methodology exhibits the ability to functionalize non-oxidizable arenes due to a reactive amine cation radical intermediate, extending the substrate scope beyond that established in **Chapter 2**.

REFERENCES

(1) Romero, N. A.; Margrey, K. A.; Tay, N. E.; Nicewicz, D. A. *Science* **2015**, *349*, 1326–1330.

(2) McManus, J. B.; Nicewicz, D. A. *J. Am. Chem. Soc.* **2017**.

(3) Margrey, K. A.; Nicewicz, D. A. *Acc. Chem. Res.* **2016**, *49*, 1997–2006.

(4) Roth, H.; Romero, N.; Nicewicz, D. *Synlett* **2015**.

(5) Chow, Y. L.; Danen, W. C.; Nelsen, S. F.; Rosenblatt, D. H. *Chem. Rev.* **1978**, *78*, 243–274.

(6) Minisci, F. *Synthesis* **1973**, *1973*, 1–24.

(7) Rueping, M.; Vila, C.; Koenigs, R. M.; Poscharny, K.; Fabry, D. C. *Chem Commun* **2011**, *47*, 2360–2362.

(8) Freeman, D. B.; Furst, L.; Condie, A. G.; Stephenson, C. R. J. *Org. Lett.* **2012**, *14*, 94–97.

(9) DiRocco, D. A.; Rovis, T. *J. Am. Chem. Soc.* **2012**, *134*, 8094–8097.

(10) Musacchio, A. J.; Nguyen, L. Q.; Beard, G. H.; Knowles, R. R. *J. Am. Chem. Soc.* **2014**, *136*, 12217–12220.

(11) Brown, P. D.; Pugh, S.; Laack, N. N.; Wefel, J. S.; Khuntia, D.; Meyers, C.; Choucair, A.; Fox, S.; Suh, J. H.; Roberge, D.; *et al. Neuro-Oncol.* **2013**, *15*, 1429–1437.

(12) Donath, E.; Herrmann, A.; Coakley, W. T.; Groth, T.; Egger, M.; Taeger, M. *Biochem. Pharmacol.* **1987**, *36*, 481–487.

(13) Traa, B. S.; Mulholland, J. D.; Kadam, S. D.; Johnston, M. V.; Comi, A. M. *Pediatr. Res.* **2008**, *64*, 81–85.

(14) Logigian, E. L.; Martens, W. B.; Moxley, R. T.; McDermott, M. P.; Dilek, N.; Wiegner, A. W.; Pearson, A. T.; Barbieri, C. A.; Annis, C. L.; Thornton, C. A.; *et al. Neurology* **2010**, *74*, 1441–1448.

(15) Corbett, G. T.; Roy, A.; Pahan, K. *J. Immunol.* **2012**, *189*, 1002–1013.

(16) Beggs, P. W.; Clark, D. W. J.; Williams, S. M.; Coulter, D. M. *Br. J. Clin. Pharmacol.* **2001**, *47*, 99–104.

(17) Ohkubo, K.; Mizushima, K.; Fukuzumi, S. *Res. Chem. Intermed.* **2013**, *39*, 205–220.

CHAPTER 5: A GENERAL STRATEGY FOR ALIPHATIC C–H FUNCTIONALIZATION ENABLED BY ORGANIC PHOTOREDOX CATALYSIS

Adapted from Margrey, K. A.; Czaplyski, W. L.; Nicewicz, D. A.; Alexanian, E. J. *J. Am. Chem. Soc.* **2018**, *140* (12), 4213–4217.

5.1 Introduction

Aliphatic C–H bonds are ubiquitous in organic molecules, including natural products, pharmaceuticals, and materials.[1–3] The ability to functionalize a particular C–H bond selectively in these types of complex molecules can lead to powerful tools for chemical synthesis, specifically in the context of late stage derivatization.[4] A significant amount of attention has been focused on this field in recent years due to the potential impact of transformations accessible using bonds previously regarded as "inert." Intramolecular, or substrate-directed, methods are commonly used to this end and offer opportunities in accessing high levels of site selectivity; however, the requirement of specific moieties to act as directing groups restricts the substrates that can undergo functionalization using this strategy. Instead, intermolecular variations that could be applied to a wider range of substrates are more desirable. In many instances, however, excess amounts of the alkane substrate are required to achieve synthetically useful yields, limiting the applicability to valuable complex molecules.

5.2 Aliphatic C–H Functionalization

5.2.1 Unactivated Aliphatic C–H Oxidation

Several groups have developed intermolecular C–H functionalization methodologies to allow access to C–H oxidation, azidation, and halogenation transformations in a site-selective manner. In 1989, Curci developed a C–H oxidation using a strained dioxirane reagent (**Figure 5.1**).[5] A moderate amount of functional groups were compatible with the transformation, and selectivity for monofunctionalization at tertiary C–H bonds distal from electron-withdrawing groups was generally observed. While the products accessed are synthetically valuable, the dioxirane reagents are unstable at temperatures above –20 ˚C and to visible light, hindering their broad application. In a related transformation disclosed in 2009, DuBois utilized a benzoxathiazine catalyst, aqueous hydrogen peroxide, and acetic acid to perform a tertiary-selective C–H oxidation.[6] The putative mechanism for this reaction involves the intermediacy of an oxaziridine that is capable of C–H hydroxylation, similarly to dioxiranes.

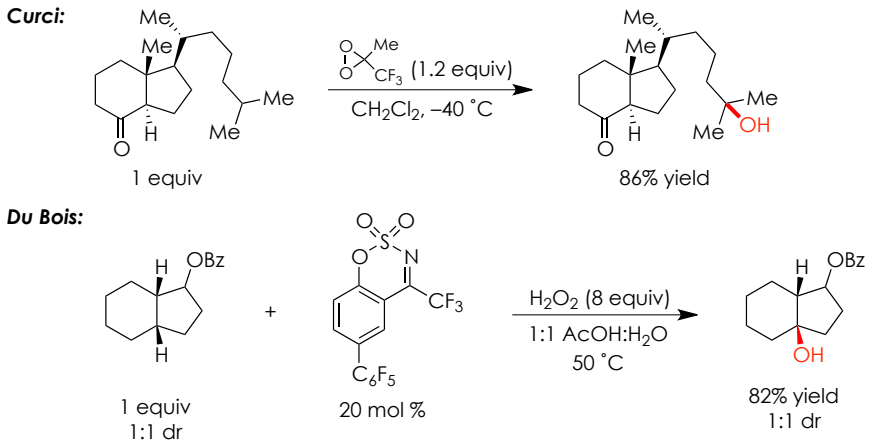

Figure 5.1 Aliphatic C–H oxidation via strained heterocycles.

White developed an aliphatic biomimetic C–H oxidation that also favored tertiary functionalization using an iron (II) catalyst, acetic acid, and hydrogen peroxide (**Figure**

5.2).[7,8] A variety of functional groups were compatible with this system, but electron-rich arenes and compounds containing basic nitrogen functionality were not demonstrated with the metal-oxo catalyst. Recent modifications have enabled the oxidation of basic nitrogen-containing compounds.[9] In many cases, however, the chromatographic recycling of starting material was required to access synthetically useful yields. Further work by White demonstrated that oxidation site selectivity could be altered based on the catalyst used and could be controlled by non-bonding interactions instead of innate stereoelectronic factors.[10]

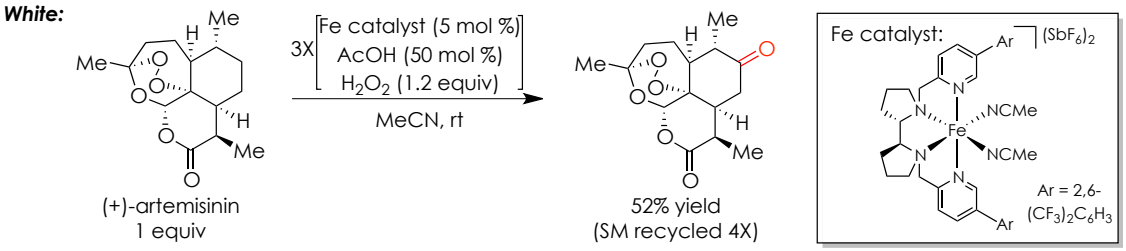

Figure 5.2 Iron-catalyzed aliphatic C–H oxidation.

5.2.2 Unactivated Aliphatic C–H Amination

The site selective installation of nitrogen-containing groups via C–H functionalization has also been pursued by several groups. Baran reported a Ritter-type C–H amidation strategy using a copper catalyst and acetonitrile as the nitrogen source, favoring reactivity at tertiary sites (**Figure 5.3**).[11] Additionally, Du Bois has used rhodium catalysis to generate nitrenoids capable of C–H insertion from aryloxysulfonamide precursors.[12] Reactivity at both tertiary and benzylic sites was observed, and a collaboration with the Sigman group provided a predictive model for determining the site selectivity of functionalization.[13]

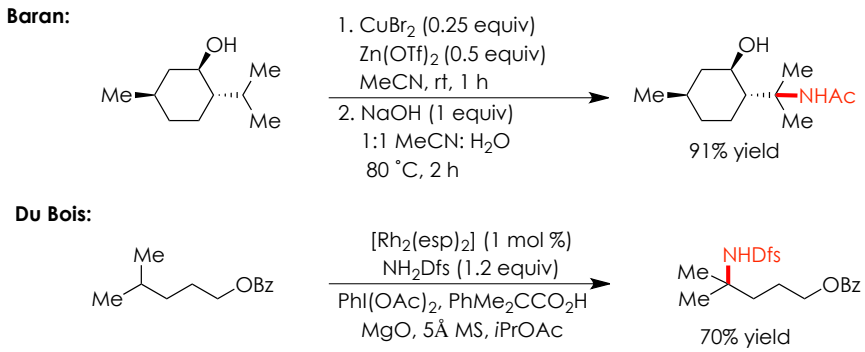

Figure 5.3 Transition metal-catalyzed aliphatic C–H amination.

In 2015, Hartwig disclosed a tertiary selective aliphatic C–H azidation reaction using an iron (II) catalyst and azidoiodinane reagent (**Figure 5.4**).[14] In this system, the substrates could be used as the limiting reagent and generally underwent functionalization in modest yields. Further extensions of this methodology to complex molecule azidation were reported in the following year.[15] Tang also reported a metal-free tertiary-selective azidation using potassium persulfate as the C–H abstracting agent.[16] Secondary-selective C–H azidation is also possible and has been reported by Groves using a manganese porphyrin catalyst.[17,18]

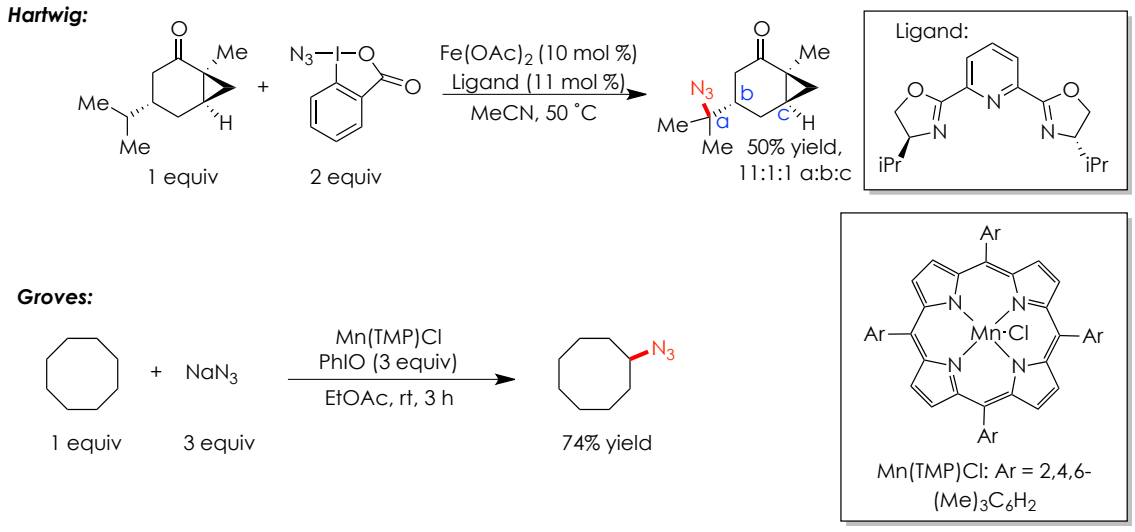

Figure 5.4 Transition metal-catalyzed aliphatic C–H azidation.

5.2.3 Unactivated Aliphatic C–H Halogenation and Xanthylation

Intermolecular C–H halogenation reactions have also been developed to allow direct synthesis of alkyl halides from unactivated alkanes. Groves has reported chlorination of alkanes using a manganese porphyrin system, tetrabutylammonium chloride, and sodium hypochlorite (**Figure 5.5**).[19] Excess substrate was required to achieve synthetically useful yields, and functionalization occurred at the most sterically accessible secondary C–H bonds. A similar system was used for the C–H fluorination of alkanes, again showing site selectivity for secondary positions.[20] Several other strategies for aliphatic fluorination have been developed, generally involving ultraviolet irradiation or transition metal catalysis.[21–24]

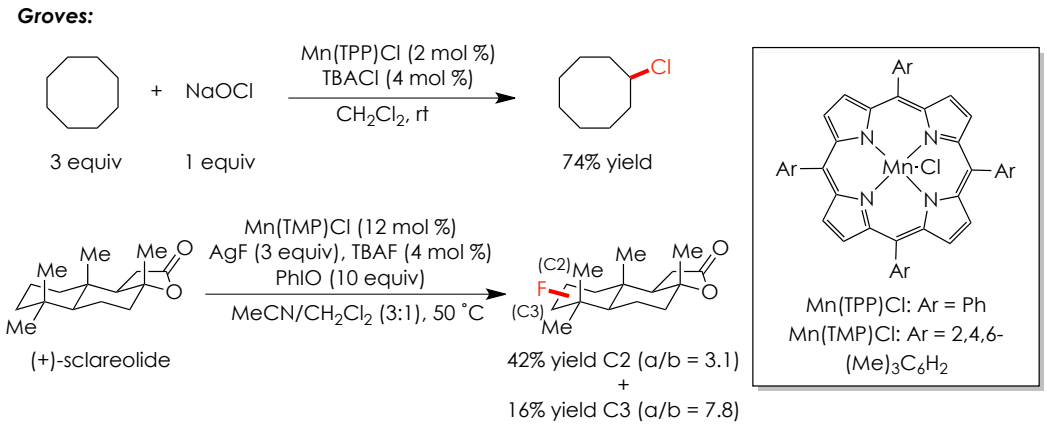

Figure 5.5 Manganese porphyrin-catalyzed aliphatic C–H halogenation.

Recently, the Alexanian group demonstrated the C–H bromination and chlorination of unactivated alkanes (**Figure 5.6**).[25,26] Both systems relied on *N*-haloamide reagents, in which light-mediated N–X homolysis forms an amidyl radical capable of abstracting a hydrogen atom from an alkane substrate with subsequent trapping to form the alkyl halide products. Selectivity for electron-rich secondary C–H bonds is observed, largely due to the electron-poor nature of the amidyl radical and the steric hindrance of the *N*-*t*Bu substituent.

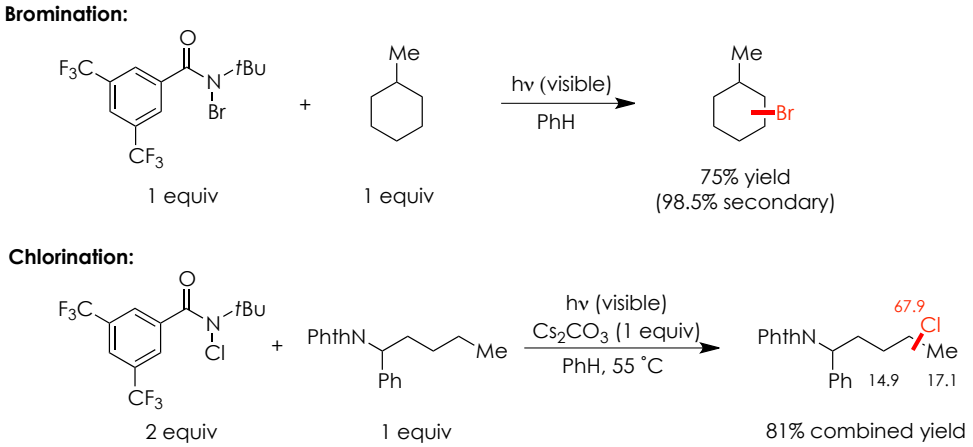

Figure 5.6 Aliphatic C–H halogenation via *N*-haloamides.

This work was extended to an intermolecular C–H xanthylation (dithiocarbonation) using *N*-xanthylamide **5.1** (**Figure 5.7**).[27] Similar selectivities to the halogenation reactions were observed owing to the intermediacy of the same amidyl radical, and the alkyl xanthate products were highly versatile, allowing the net conversion of C–H to C–C, C–N, C–D, C–O, and C–S bonds.

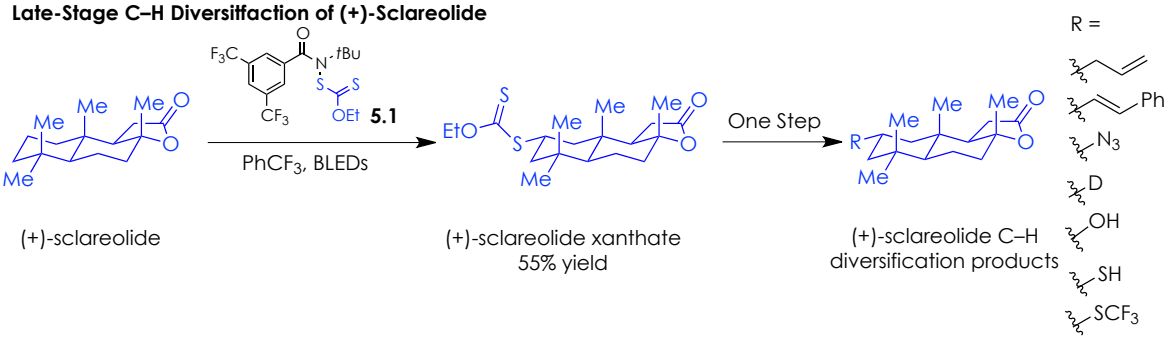

Figure 5.7 Aliphatic C–H diversification via C–H xanthylation.

5.2.4 Photoredox-Catalyzed Aliphatic C–H Bond Functionalization

C–H bonds at positions activated by hyperconjugation, including those adjacent to π systems or heteroatoms, are particularly poised for functionalization due to their lowered BDEs.[28] MacMillan has demonstrated the utility of photoredox catalysis for functionalizing

such bonds, achieving C–H alkylation and arylation at C–H bonds adjacent to heteroatoms (**Figure 5.8**).[29–35]

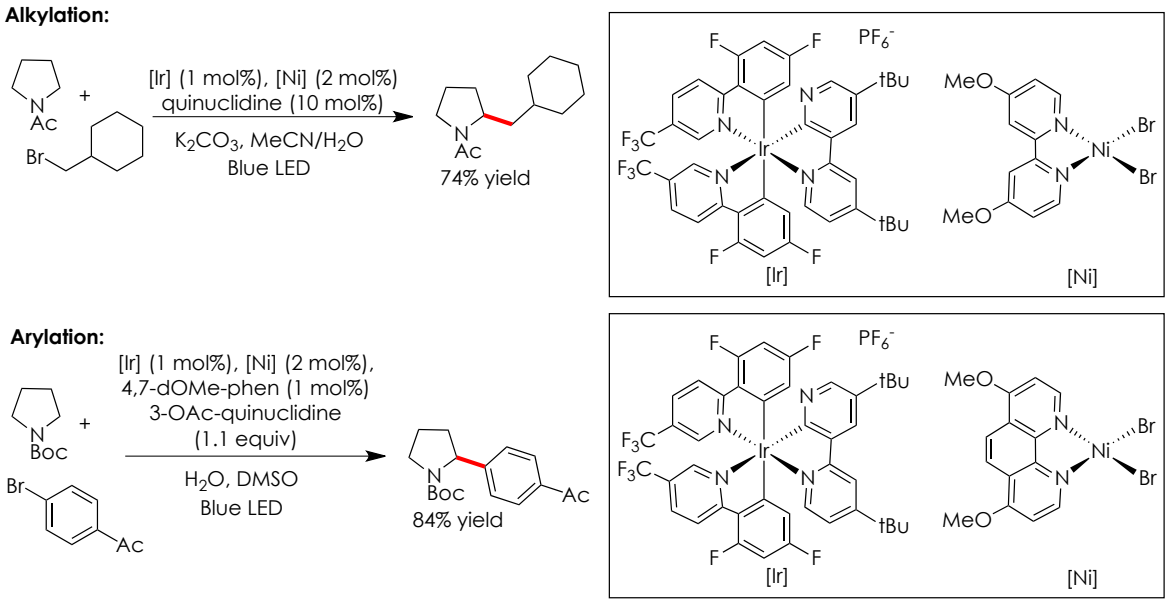

Figure 5.8 Photoredox-catalyzed C–H alkylation and arylation of aliphatic amines.

While the functionalization of activated aliphatic C–H bonds via photoredox catalysis has been well-documented, there are few reports detailing similar reactivity of unactivated aliphatic C–H bonds. Glorius reported that an iridium-based photoredox catalyst could oxidatively generate benzoate radicals capable of C–H abstraction,[36] and this was leveraged in a strategy for C–H trifluoromethylthiolation (**Figure 5.9**). The development of further strategies for unactivated C–H bond functionalization via photoredox catalysis would offer new opportunities for complex molecule functionalization.

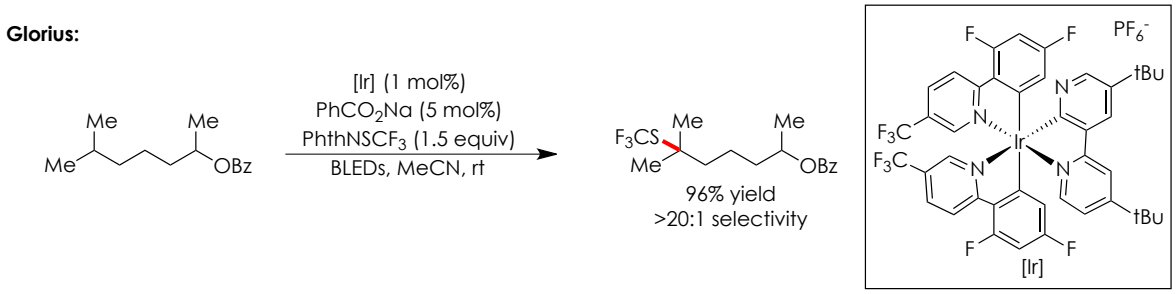

Figure 5.9 Aliphatic C–H trifluoromethylthiolation via photoredox catalysis.

5.3 Reaction Development

Previously reported intermolecular C–H functionalization strategies are inherently limited due to the inability to access a variety of transformations using a single catalyst or reagent. Rather, to achieve each desired C–H functionalization, a new reaction system must be developed. The ability to access a variety of products from a single alkane substrate with common site selectivity would provide the opportunity for a C–H diversification strategy. While the C–H xanthylation reported by the Alexanian group accomplishes this in two synthetic steps, a more ideal approach would allow for single step strategy to access a variety of products.

Direct aryl C–H functionalization has been demonstrated in the Nicewicz lab with nitrogen, carbon, and fluorine coupling partners (see **Chapters 2 – 4**). In collaboration with the Alexanian group, we wanted to develop a photoredox-catalyzed method for unactivated aliphatic sp^3 C–H functionalization. Whereas electron-rich arenes are poised to undergo functionalization via direct SET to an acridinium photoredox catalyst, unactivated alkanes do not possess such an ability. Inspired by Glorius' C–H trifluoromethylthiolation strategy, we sought to use an acridinium catalyst to generate a reactive intermediate capable of intermolecular C–H bond abstraction. This would decouple the abstraction and radical trapping steps, raising the possibility of a modular C–H functionalization system.

5.3.1 Reaction Optimization

We postulated that a highly oxidizing acridinium photoredox catalyst **A** (**$E_{1/2}$**(cat*/cat•) = +2.08 V vs SCE)[37] would be capable of oxidatively generating heteroatom-centered radicals capable of abstracting unactivated aliphatic C–H bonds. We initially found that blue LED irradiation of cyclooctane in the presence of catalyst **A** and sulfonyl azide trap

5.2 in a DCE/pH 8 phosphate buffer solvent system produced cyclooctyl azide in 24% yield (**Table 5.1, entry 1**). The use of tribasic potassium phosphate (K_3PO_4) led to 30% yield of the product, but increasing the amount of K_3PO_4 led to a slight decrease in yield (**Table 5.1, entries 2 – 3**). Changing the solvent from DCE to a 1:1 mixture of DCE/TFE provided the azide in 40% yield (**Table 5.1, entry 4**), and using TFE as the sole solvent increased the yield further, to 50% (**Table 5.1, entry 5**). Replacing TFE with HFIP led to a further increase in yield to 70% (**Table 5.1, entry 6**), and the reaction concentration was optimal at 0.1 M (**Table 5.1, entries 6 – 8**). The pH 8 buffer proved less effective in this reaction than K_3PO_4 with HFIP as the solvent, providing the azide in 60% yield (**Table 5.1, entry 9**). The same yield was observed when sulfonyl azide **5.2** was replaced with the more electron deficient **5.3** (**Table 5.1, entry 10**); since this increase was more pronounced in the azidation of other substrates, we elected to study the substrate scope with sulfonyl azide **5.3**.

Table 5.1 Initial optimization of C–H azidation.

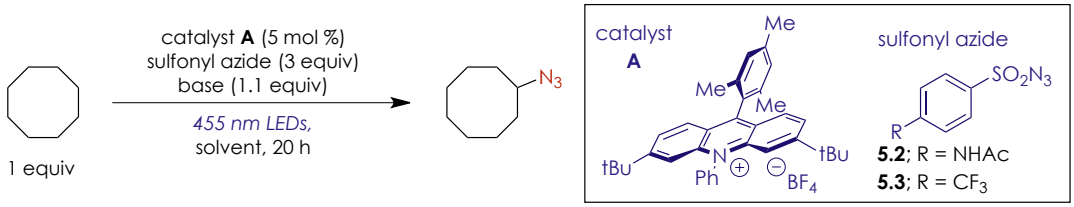

Entry	Sulfonyl Azide	Solvent (concentration)	Base	^{1}H NMR Yield
1	**5.2**	DCE/pH 8 phosphate buffer (4:1, 0.1 M)	–	32%
2	**5.2**	DCE (0.1 M)	K_3PO_4	30%
3	**5.2**	DCE (0.1 M)	K_3PO_4 (3 equiv)	23%
4	**5.2**	DCE/TFE (1:1, 0.1 M)	K_3PO_4	40%
5	**5.2**	TFE (0.1 M)	K_3PO_4	50%
6	**5.2**	HFIP (0.1 M)	K_3PO_4	70%
7	**5.2**	HFIP (0.05 M)	K_3PO_4	53%
8	**5.2**	HFIP (0.2 M)	K_3PO_4	65%
9	**5.2**	HFIP/pH 8 phosphate buffer (4:1, 0.1 M)	–	60%
10	**5.3**	HFIP (0.1 M)	K_3PO_4	71%

To probe the site selectivity of the C–H azidation, we subjected methyl 6-methylheptanoate to the previously optimized conditions and found that azidation occurred exclusively at the tertiary position in 71% yield with good mass balance (**Table 5.2, entry 1**).

Table 5.2 Base optimization of C–H azidation.

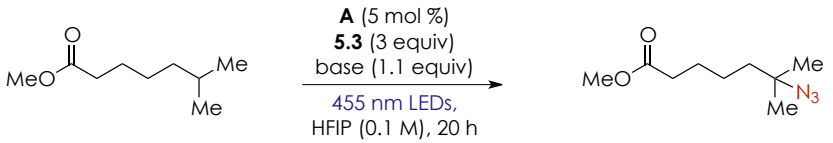

Entry	Base	^{1}H NMR Yield	Remaining Substrate
1	K_3PO_4	71%	28%
2	K_2HPO_4	52%	48%
3	KH_2PO_4	9%	71%
4	KOBz	39%	60%
5	$(NBu_4)OBz$	32%	68%
6	$NaHCO_3$	36%	56%
7	Na_2CO_3	61%	15%
8	Cs_2CO_3	33%	16%
9	$NiPr_2Et$	3%	95%

Wondering how critical the identity of the base was for reactivity, we varied this component of the reaction. Dibasic potassium phosphate provided the azide in 52% yield (**Table 5.2, entry 2**), and the monobasic version produced only 9% of the desired product (**Table 5.2, entry 3**). Due to the ability of benzoate salts to readily undergo single electron oxidation as reported by Glorius, we also explored their utility in our azidation. Both potassium and tetrabutylammonium benzoate afforded the tertiary azidation product, albeit in diminished yields (**Table 5.2, entries 4 – 5**), and similar results were observed for sodium bicarbonate (**Table 5.2, entry 6**). Use of sodium carbonate produced 61% yield of the tertiary azide but led to poor mass balance relative to the other bases (**Table 5.2, entry 7**), possibly due to deleterious polar processes. Changing the cation and using cesium carbonate led to 33% yield of the tertiary azide with similarly poor mass balance (**Table 5.2, entry 8**). Use of Hünig's

base produced only trace azidation (**Table 5.2, entry 9**), suggesting that the anionic character of the base is important for reactivity. For all bases, azidation occurred exclusively at the tertiary site, with no secondary products detected by ^{1}H NMR analysis, consistent with a common mechanistic role of the base.

5.3.2 C–H Azidation Substrate Scope

With optimized conditions in hand, we explored the substrate scope for this direct alkane C–H azidation (**Figure 5.10**). Cyclic hydrocarbons provided azides **5.4** – **5.6** in good yields. *Trans*-decalin afforded only secondary azides **5.7** in 57% combined yield, and adamantane could also be functionalized exclusively at the tertiary C–H bond to give **5.8** in 75% yield. Benzylic positions could also undergo azidation, as exemplified by propylbenzene producing **5.9** in modest yield. *Tert*-butylcyclohexane reacted at the tertiary position to provide azide **5.10**, and c*is*-4-methylcyclohexyl pivalate produced azide **5.12** in 52% yield. Additionally, isobutylbenzene underwent azidation favoring the tertiary position to give **5.11** in modest yield, serving as a precursor to the psychostimulant pharmaceutical, phentermine.

In these simple systems, we observed preferential tertiary functionalization over secondary or primary functionalization when multiple types of C–H bonds were present in a compound. Accordingly, we studied the site selectivity of this system further. As discussed above, methyl-6-methylheptanoate produced tertiary azide **5.13** in 71% yield as a single regioisomer. Methyl hexanoate, which contains several electronically deactivated secondary C–H bonds and no tertiary sites, did not undergo functionalization with this system, suggesting a strong sensitivity to the BDEs of the C–H bonds in the substrate. In order to examine the electronic site selectivity of the C–H azidation further, several dihydrocitronellol

derivatives were next examined, each containing two tertiary C–H bonds. In all substrates, azidation was favored at the tertiary site distal to the other functionality present. Acetate and benzoate esters delivered **5.14** and **5.15** in 73% and 91% yield, respectively, with good levels of regioselectivity. Derivatives with protected primary amines or halide functionality also worked in this reaction, affording **5.16** and **5.17** in good yield. Dihydrocitronellol itself was a competent substrate, providing **5.18** in 63% yield with no observed oxidation of the free alcohol, highlighting the mild nature of the system.

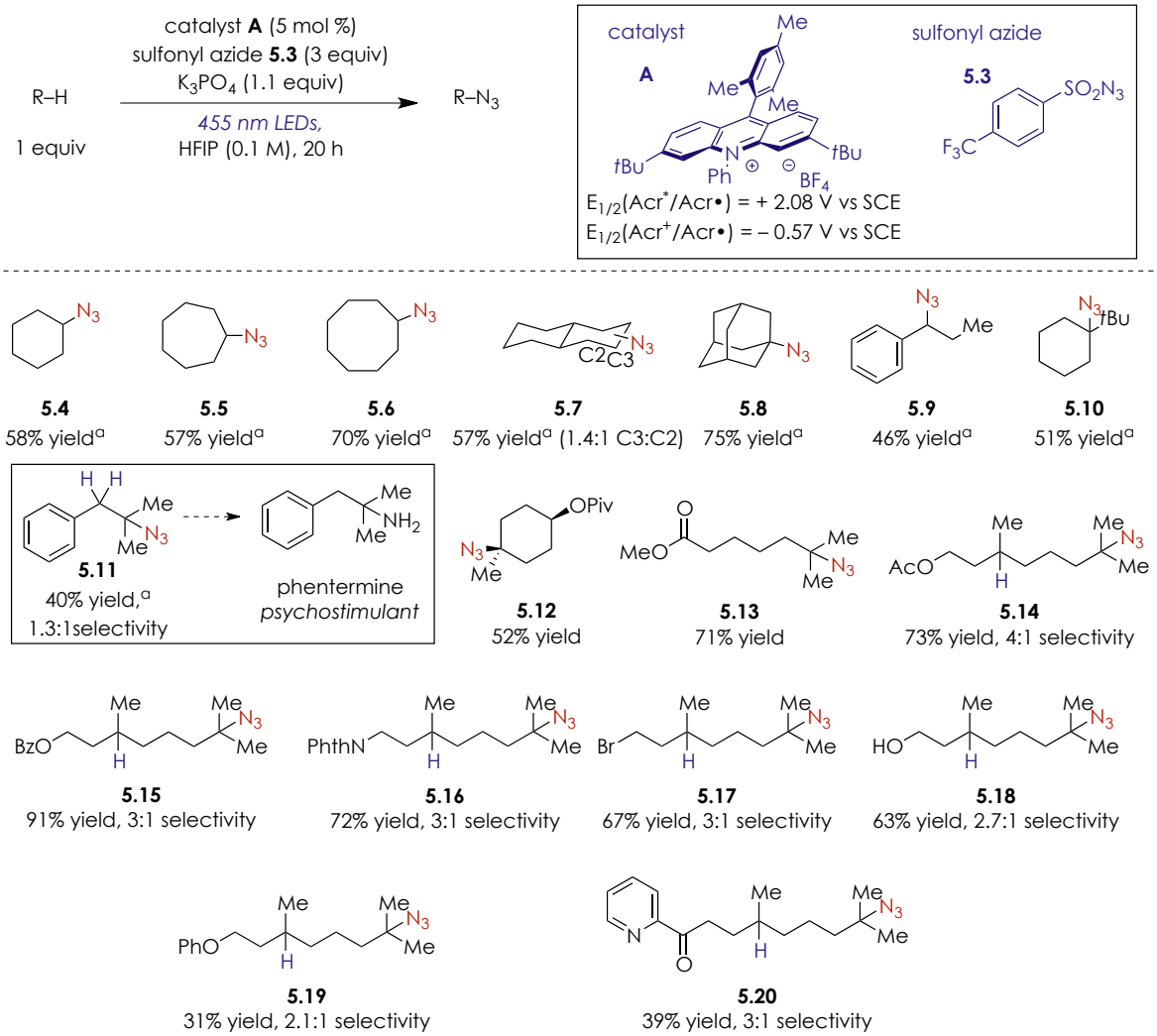

Figure 5.10 C–H azidation substrate scope. Yields refer to isolated yields. [a]NMR yield with hexamethyldisiloxane (HMDS) as an internal standard.

A phenyl ether was tolerated to deliver **5.19** in low yield and regioselectivity, even though oxidation of the arene is possible using the acridinium catalyst. Heterocyclic nitrogen functionality, commonly problematic for metal-oxo catalyzed reactions but important in the application to late stage functionalization of pharmaceuticals, could be tolerated in this system. Azidation of a pyridyl ketone substrate provided **5.20** in modest yield.

5.3.3 Development of Modular C–H Transformations

With azidation conditions optimized, we sought to expand our work toward developing a strategy for a modular C–H functionalization. Using cyclooctane as the substrate and limiting reagent, we examined a variety of radical traps (**Figure 5.11**). To facilitate the solubility of all reagents, we chose to use DCE as the solvent with a pH 8 phosphate buffer instead of exogenous K_3PO_4 as the base. Changing the sulfonyl azide trap for *N*-fluorobenzenesulfonimide (NFSI) delivered fluorocyclooctane in moderate yield. Other halogens could also be installed through this strategy. Using diethyl bromomalonate as the radical trap afforded bromocyclooctane in good yield, and *N*-chlorosuccinimide functioned as a chlorine atom source to access chlorocyclooctane in 32% yield. We pursued the installation of the trifluoromethylthiol group, based on its proven use in medicinal chemistry due to the beneficial effects imparted upon polarity and lipophilicity.[38] Using the reagent **5.21** developed by Shen as a radical trifluoromethylthiol source,[39] we accessed trifluoromethylthiocyclooctane, albeit in low yields owing to product instability over long reaction times. In all of these transformations, we could access a variety of products simply by switching the radical trap. No additional optimization parameters were explored for these reactions, so further effort to improve each reaction would be desirable. Nevertheless, this

highlights that a simple modification of a single reaction parameter can produce a variety of C–H functionalization products in a single step.

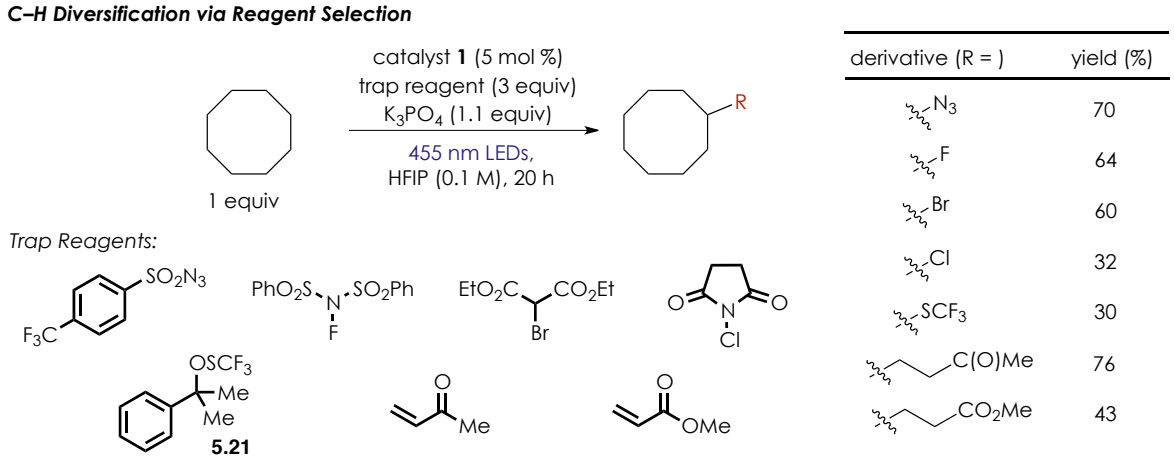

Figure 5.11 Modular C–H functionalization of cyclooctane.

We next sought to develop a related intermolecular C–C bond formation from unactivated aliphatic C–H bonds. Knowles and Rovis have previously reported the use of iridium photoredox catalysts to generate amidyl radicals that can undergo 1,5-hydrogen atom abstraction on a tethered alkane, generating a carbon-centered radical.[40–42] The resultant radical is trapped by an electron-poor alkene for a net C–H alkylation.

We began related studies by examining the electron-poor methyl acrylate in our system. A mixture of DCE and 2,2,2-trifluoroethanol (TFE) as the solvent with 4M pH 8 phosphate buffer as the base provided 10% yield of the desired C–C adduct (**Table 5.3, entry 1**). Due to the reduction potential of the radical produced after addition to the olefin,[43] we used a more reducing acridinium catalyst **B** that increased the yield to 23% (**Table 5.3, entry 2**). TFE was essential for the desired reactivity (**Table 5.3, entry 3**), but TFE alone as solvent proved inferior (**Table 5.3, entry 4**). Considering whether a more basic buffer could be employed to increase yield, we examined the reactions with pH 9 and 10 buffers and found them to be inferior to pH 8 (**Table 5.3, entries 5 – 6**). The use of a less concentrated 2M pH

8 buffer provided the adduct in the same yield as the 4M buffer (**Table 5.3, entry 7**). Doubling the amount of 4M pH 8 buffer but keeping the amount of organic solvent constant led to 43% yield of the desired adduct (**Table 5.3, entry 8**), but a further increase in the amount of buffer lead to no increase in yield (**Table 5.3, entry 9**). Similar conditions to those optimized for methyl acrylate facilitated the use of methyl vinyl ketone (MVK) as the radical trap, affording the adduct in 76% yield. To our knowledge, this is the first report of a visible light-mediated unactivated C–H bond alkylation using the substrate as the limiting reagent.[44]

Table 5.3 Optimization of C–H alkylation

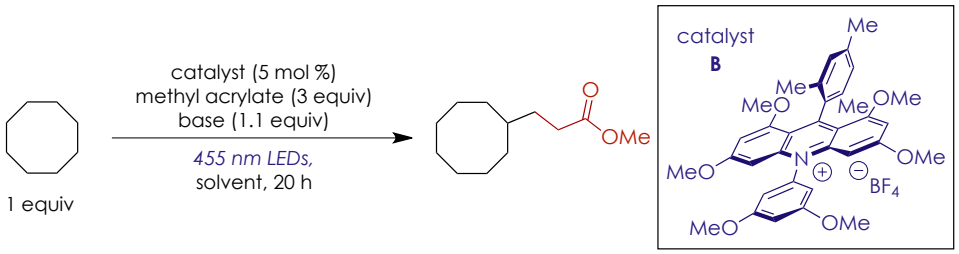

Entry	Catalyst	Solvent (concentration)	^{1}H NMR Yield
1	**A**	DCE/TFE/4M pH 8 phosphate buffer (7:1:2, 0.1 M)	10%
2	**B**	DCE/TFE/4M pH 8 phosphate buffer (7:1:2, 0.1 M)	23%
3	**B**	DCE/4M pH 8 phosphate buffer (4:1, 0.1 M)	0%
4	**B**	TFE/4M pH 8 phosphate buffer (4:1, 0.1 M)	5%
5	**B**	DCE/TFE/4M pH 9 phosphate buffer (7:1:2, 0.1 M)	12%
6	**B**	DCE/TFE/4M pH 10 phosphate buffer (7:1:2, 0.1 M)	2%
7	**B**	DCE/TFE/2M pH 8 phosphate buffer (7:1:2, 0.1 M)	23%
8	**B**	DCE/TFE/4M pH 8 phosphate buffer (7:1:4, 0.08 M)	**43%**
9	**B**	DCE/TFE/4M pH 8 phosphate buffer (7:1:8, 0.06 M)	23%

5.3.4 C–H Functionalization of Complex Targets

We next explored the application of this modular C–H functionalization system to bioactive molecules possessing multiple potentially reactive sites (**Figure 5.12**). Benzoate protected (–)-menthol afforded azide **5.22** in 54% yield, favoring functionalization at the most electron-rich tertiary position. Since adamantyl derivatives are present in several pharmaceutical compounds, we sought to subject these compounds to several

transformations. The azidation of *N*-phthalimide protected memantine, an NMDA receptor antagonist used in the treatment Alzheimer's disease, exclusively produced the tertiary product **5.23** in 55% yield. The same substrate could also be fluorinated providing **5.24** in 86% yield with NFSI as the trap with the same tertiary selectivity. A precursor to differin, a topical retinoid, afforded tertiary azide **5.25** in modest yield, even in the presence of an oxidizable aromatic ring, highlighting the mild nature of our system. This substrate also underwent intermolecular alkylation using methyl vinyl ketone, forming adduct **5.26** in 45% yield. Ibuprofen methyl ester, possessing both tertiary and benzylic positions, underwent azidation that slightly favored the benzylic product **5.27** in a combined 57% yield.

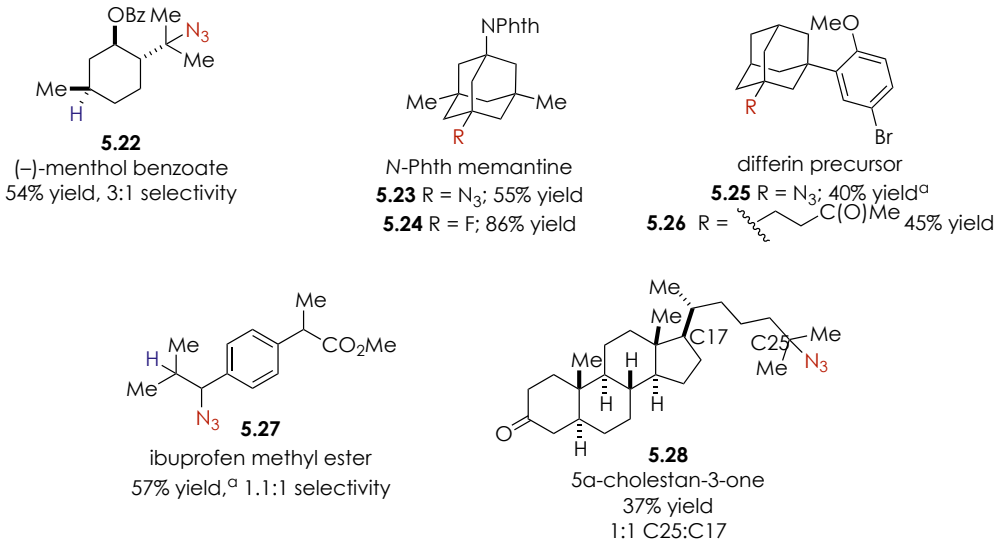

Figure 5.12 Modular functionalization of complex derivatives. For reaction details see the Supporting Information. Yields refer to NMR yields with hexamethyldisiloxane (HMDS) or fluorobenzene as an internal standard.

Previous reports of the azidation of this substrate could produce only the benzylic azide, demonstrating that our system enables access to novel derivatives of common pharmaceuticals. Steroid 5α–cholestan-3-one, possessing 46 aliphatic C–H bonds, could be

functionalized at the C17 and C25 positions in a combined 39% yield of **5.28**, similar to the selectivity observed in Curci's hydroxylation using dioxiranes.[45]

Having installed an azide directly from a C–H bond, we also wanted to highlight the utility of this functionalization via copper-catalyzed azide-alkyne cycloaddition (CuAAC). By coupling memantine azide **5.23** and ethynylestradiol, we could isolate the cycloadduct **5.29** in 61% yield, highlighting the importance of this application in bioconjugation and late-stage diversification (**Figure 5.13**).

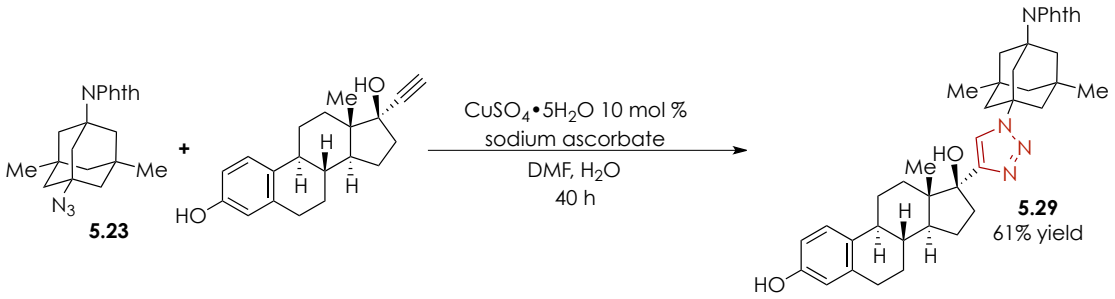

Figure 5.13 Click reaction with C–H azidation product.

5.3.5 Mechanistic Experiments

Despite the success of this system in functionalizing a variety of substrates, the active C–H bond abstracting species remained unclear. To this end, we sought to clarify the role of each component of the reaction, focusing primarily on the azidation. Stern-Volmer analysis determined that sulfonyl azide **5.3** did not quench the acridinium fluorescence (**Figure 5.14**). Owing to the presence of K_3PO_4 (pKa = 12.32 in H_2O) and HFIP (pKa = 9.3 in H_2O) in the optimized conditions, deprotonation of HFIP is thermodynamically favorable, and we wondered whether the resultant alkoxide could be oxidized by the acridinium catalyst to produce an oxygen-centered radical. Stern-Volmer with sodium 1,1,1,3,3,3-hexafluoroisopropoxide in HFIP indicated no quenching of the acridinium fluorescence,

suggesting that oxidation of this species to the corresponding oxygen-centered radical does not occur.

We next turned our attention toward the base used in the reactions. While K_3PO_4 or the pH 8 phosphate buffer were used in the reactions, we could not obtain reliable Stern-Volmer quenching with them due to insolubility or immiscibility regardless of what solvent was used. To circumvent this issue, we synthesized a soluble dibasic phosphate salt **5.30** from the corresponding phosphoric acid **5.31**. We found that **5.30** could, in fact, quench the excited state of the acridinium but the protonated acid did not, highlighting the necessity of the anionic phosphate (**Figure 5.14**).

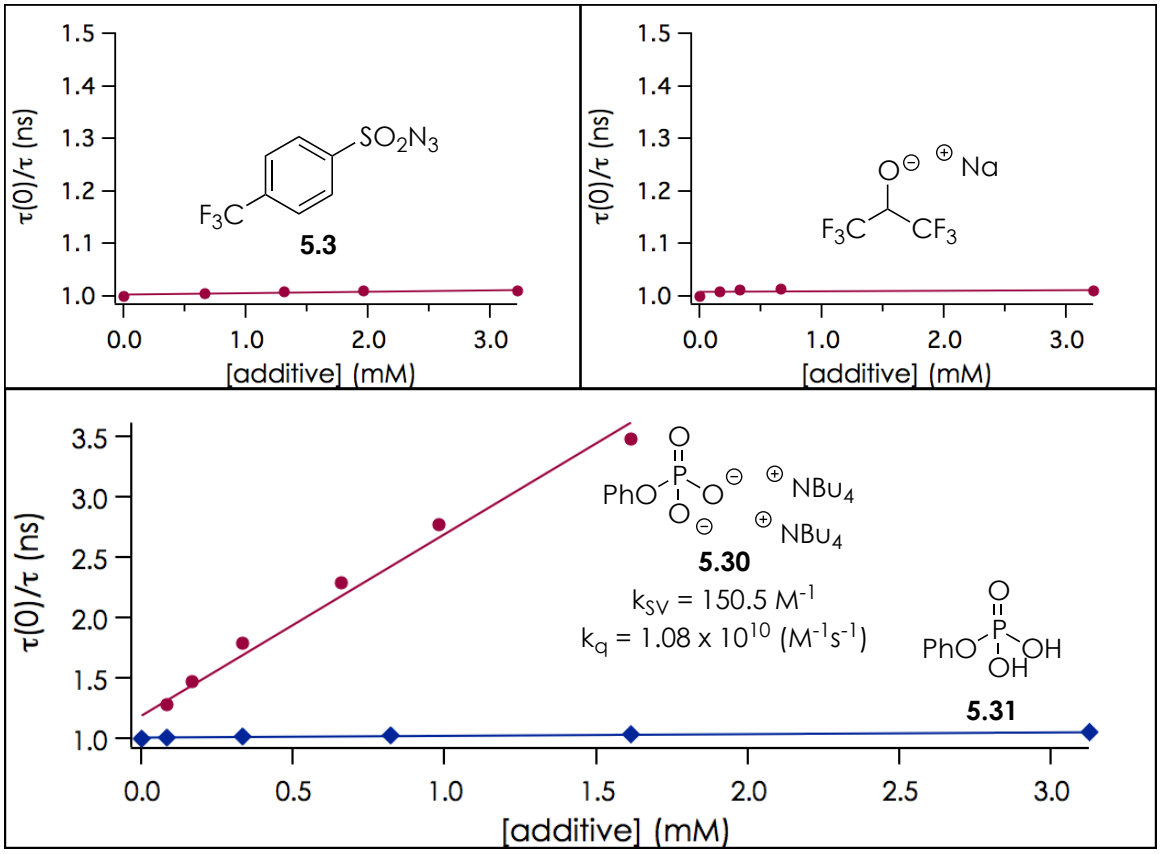

Figure 5.14 Stern-Volmer quenching of acridinium catalyst. Quenching data were determined in DCE with compounds **5.3**, **5.30**, and **5.31** and in HFIP for sodium 1,1,1,3,3,3-hexafluoroisopropoxide.

Addition of **5.30** also led to shifts in the ^{1}H NMR of the catalyst **A** in $CDCl_3$ (**Figure 5.15**), suggesting a possible complex between the catalyst and salt in solution.

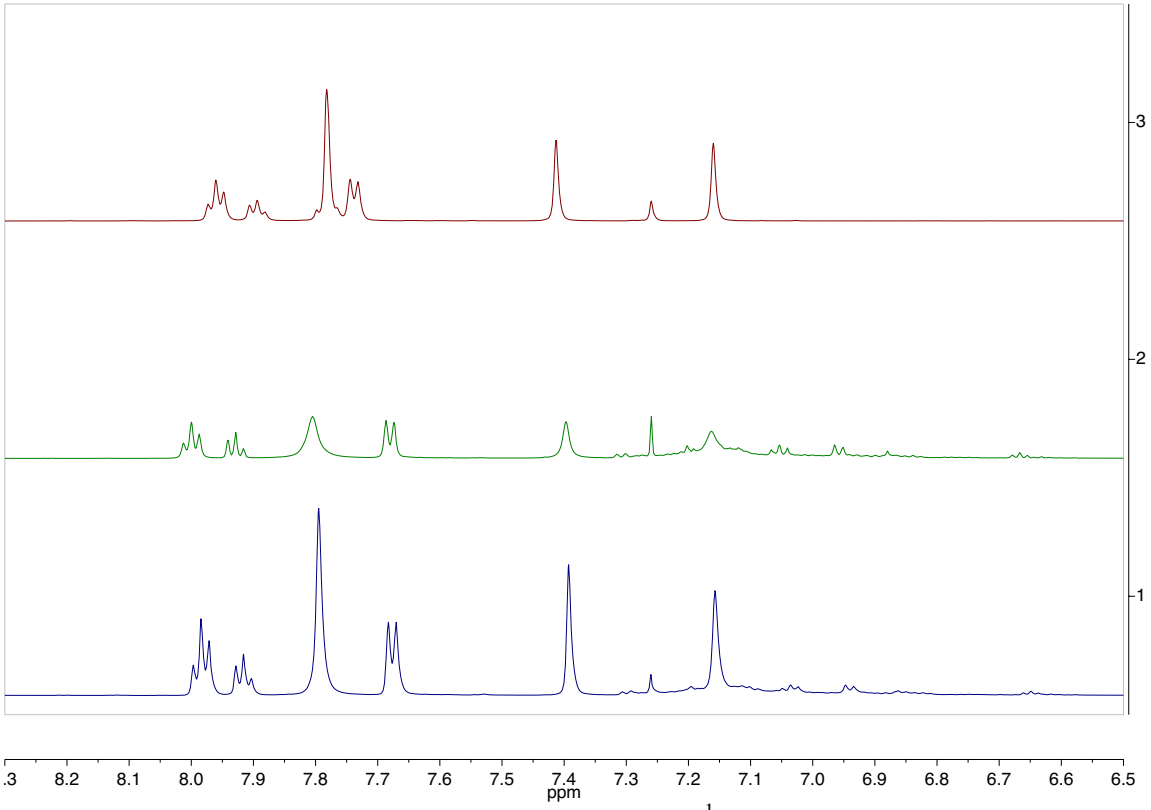

Figure 5.15 Addition of **5.30** to acridinium catalyst **A** ^{1}H NMR. Top: only catalyst **A**, Middle: 1 equiv of catalyst **A** and 1 equiv of **5.30**, Bottom: 2 equiv of catalyst **A** and 1 equiv of **5.30**.

We also examined the reactivity of dibasic phosphate **5.30** under the azidation conditions with cyclooctane as the substrate (**Figure 5.16, eq 1**). The use of substoichiometric **5.30** (5 or 20 mol %) produced up to 48% yield of azide **5.6**, consistent with catalytic activity of the base. However, employing stoichiometric **5.30** led to a diminished yield of 17%. Using methyl 6-methylheptanoate as the substrate with 20 mol % **5.30** produced azide **5.13** in 20% yield (**Figure 5.16, eq 2**). Importantly, only functionalization at the tertiary C–H bond occurred, suggesting that **5.30** and K_3PO_4 serve the same role in the transformation.

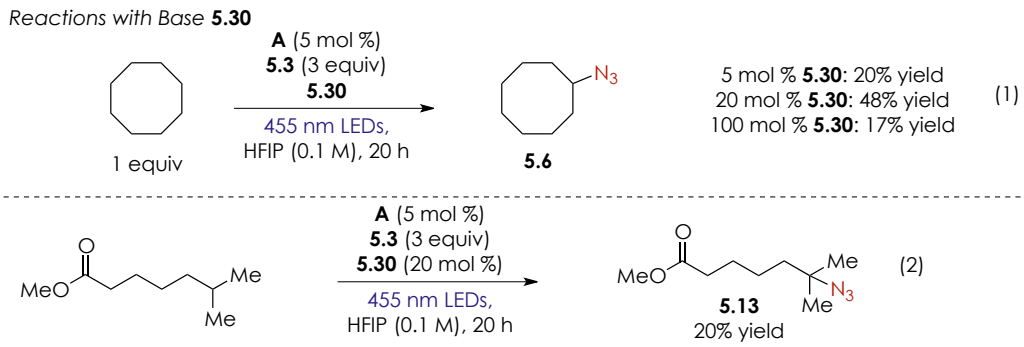

Figure 5.16 Reactions with dibasic phosphate **5.30**.

5.3.6 Proposed Mechanism

Based on these mechanistic data, we propose an operative mechanism for the C–H azidation system (**Figure 5.17**). Using 455 nm LEDs, the acridinium photoredox catalyst is excited and undergoes SET from the phosphate salt, generating oxygen centered radical **5.32**. Abstraction of the most electron-rich C–H bond generates carbon-centered radical **5.33**, which is subsequently trapped by the sulfonyl azide **5.3** to afford the desired product and a sulfonyl radical. Based on previous work in our lab, we believe that this radical is capable of oxidizing the acridine radical, regenerating the acridinium catalyst.[46]

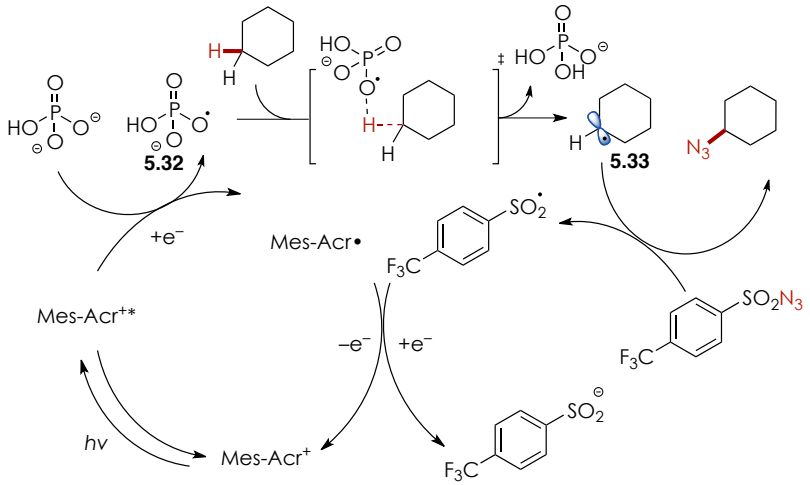

Figure 5.17 Proposed mechanism for C–H azidation.

5.4 Initial Studies in Polyolefin Functionalization

5.4.1 Background

Polyolefins are widely prevalent in consumer products and have a range of uses, including plastics for automobile parts, agriculture, and food products.[47] These polymers possess a variety of useful properties, including high tensile strength, processibility, resistance to chemical degradation, and low density. Traditionally, these compounds are synthesized via the polymerization of α-olefin monomers, particularly through transition metal-catalyzed chain-growth polymerizations. These processes, developed initially by Ziegler and Natta, give good control of the properties of the resultant materials. However, owing to their lack of additional functional groups, polyolefins do not interface well with other materials, rendering applications in which a combination of properties is desirable challenging.

Additional functionality can be incorporated into polyolefins through the copolymerization of the desired α-olefin with another monomer containing the preferred polar moiety.[48] However, most polar monomers contain Lewis basic heteroatoms that can complex to oxophilic transition metal catalysts, inhibiting the polymerization and changing the properties of the resultant materials.[49] An alternate strategy to accomplish the same goal is to perform a copolymerization of the α-olefin with a monomer containing a masked functionality that can be converted, following polymerization, into the desired functionality.[50] The groups compatible with this strategy tend to be limited and include divinylbenzene, boranes, and *p*-methylstyrene, and the inclusion of the alternate monomer can impact the material properties of the final polyolefin material.

An alternate strategy that avoids the need for copolymerization and can use existing polyolefins as feedstocks is post-polymerization modification (PPM), in which C–H functionalization can be used to install desired groups directly. This strategy has traditionally been used to functionalize tertiary C–H bonds of polyolefins with maleic anhydride through techniques such as reactive extrusion or high temperature radical initiation.[51] Due to the vigorous conditions required for such reactivity to occur, tertiary radicals that form along the polymer backbone are prone to chain coupling or scission processes, both of which degrade the desirable physical properties of the starting material.

Recently, several groups have developed new C–H functionalization strategies for the functionalization of polyolefins. Liu and Bielawski reported the azidation of isotactic polypropylene (*i*-PP) using an azidoiodinane at elevated temperatures without an external radical initiator,[52] presumably via an iodanyl radical as the C–H abstracting agent (**Figure 5.18**). Up to 3.5% azidation could be accomplished with this system, but the material in all cases exhibited a significant decrease in M_n, indicative of polyolefin chain cleavage, and in increase in the dispersity (Đ). Hillmyer reported the C–H oxidation of polyethylene-*alt*-propylene (PEP) using a manganese porphyrin catalyst with aqueous Oxone as the terminal oxidant and benzyldimethyltetradecylammonium chloride (BDTAC) as a phase transfer agent.[53] Ketones and tertiary alcohols were detected via IR and ^{1}H NMR analyses, with up to 1.4% hydroxylation observed. Hartwig and Hillmyer collaborated to study the rhodium-catalyzed primary-selective borylation of poly(ethylethylene) (PEE);[54] after basic hydrogen peroxide workup, the resultant alkylboronate esters could be oxidized to afford primary alcohol substituents on the polyolefin. Up to 19 mol % functionalization occurred, but the reactions required elevated temperatures (150 – 200 ˚C). Hartwig and Lee more recently

disclosed the nickel-catalyzed C–H oxidation of polyethylenes with *m*CPBA as the oxidant.[55] Mixtures of hydroxyl, ketone, and chloride functionality were installed with up to 88% selectivity for hydroxylation. Alexanian and Leibfarth have also demonstrated the secondary selective C–H xanthylation of several polyolefins, observing up to 18 mol % xanthylation.[56] Little chain scission is observed in the radical-mediated process, and the resultant xanthate products could be converted into a variety of functionalized polyolefin materials.

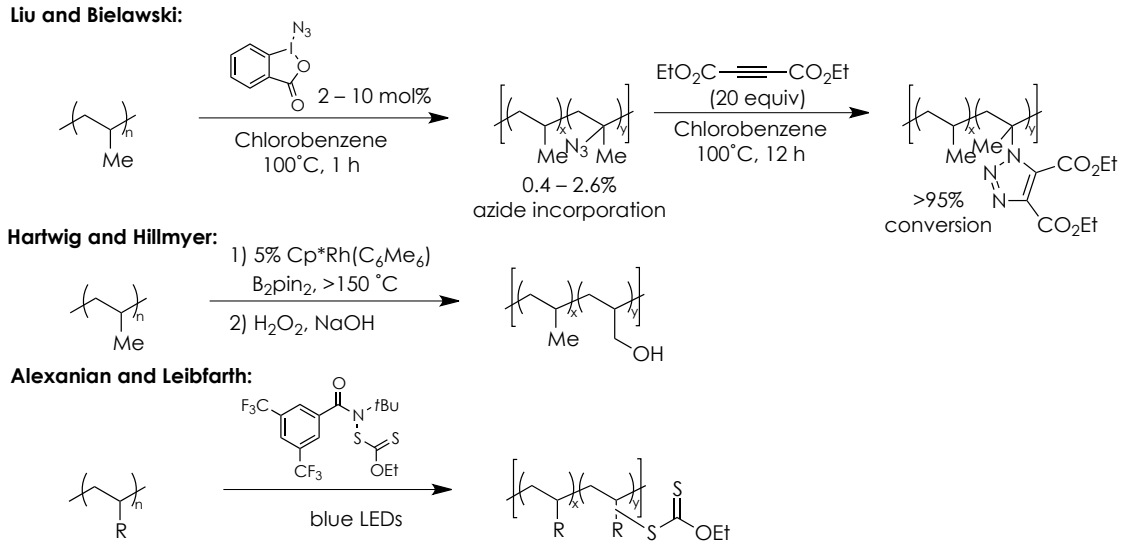

Figure 5.18 Recent methods for polyolefin C–H functionalization

5.4.2 Photoredox-Catalyzed C–H Azidation of Polyolefins

Using our photoredox-catalyzed alkane functionalization strategy, we turned our attention toward the functionalization of polyolefins. When applying tertiary selective radical-mediated C–H functionalizations to polyolefin substrates, a major challenge is preventing chain coupling or scission of the polymer due to the usually harsh reaction conditions. Due to the lowered reaction temperatures associated with our system and the generation of a C–H abstracting species in catalytic quantities, we wondered whether we could apply our conditions to enable tertiary azidation of polymers without concomitant chain scission.

In collaboration with the Alexanian and Leibfarth groups, using poly(ethylethylene) (PEE) as an initial substrate, we sought to determine whether the photoredox-catalyzed system was competent for polyolefin azidation. We applied the conditions previously optimized for azidation and observed no azide stretch by IR spectroscopy and no secondary azidation by ^{1}H NMR (**Figure 5.19**). To confirm the lack of C–H azidation, we subjected the isolated polyolefin to CuAAC conditions with *p*-tolylacetylene and detected no cycloadduct formation. Reasoning that the absence of azidation might be due to immiscibility of the polymer with HFIP, we switched to DCE as the solvent (**Figure 5.20**). IR spectroscopy revealed a characteristic azide peak at 2098 cm^{-1} (**Figure 5.21**), and ^{1}H NMR analysis did not show the presence of primary or secondary alkyl azides, suggesting exclusively tertiary functionalization. CuAAC was successful in forming a triazole-functionalized polymer, and by ^{1}H NMR analysis, up to 4 mol % triazole was incorporated into the polyolefin. Gel permeation chromatography (GPC) indicated a slight decrease in the M_n of the polymer and a negligible increase in the Đ. A new absorbance peak was observed at 252 nm by photodiode array (PDA) detection (**Figure 5.22**), indicating that the reaction sequence had, in fact, installed aromatic functionality onto the polyolefin.

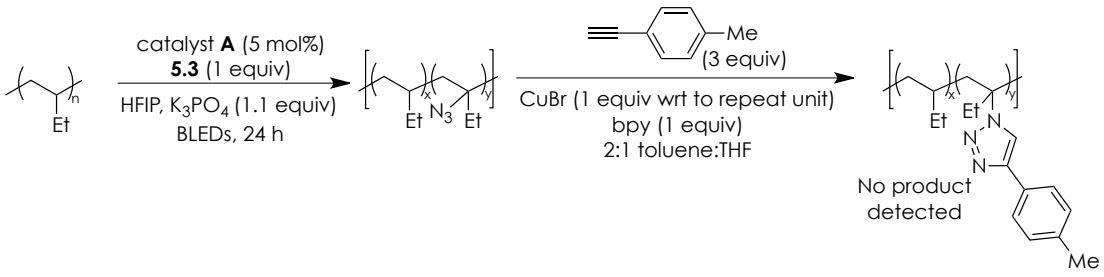

Figure 5.19 Initial azidation attempt with PEE.

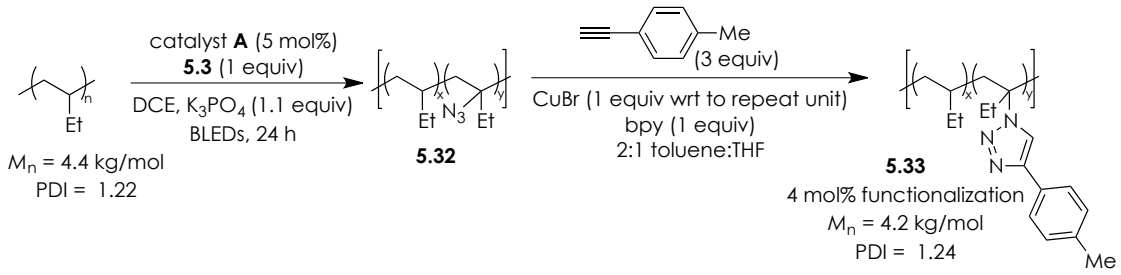

Figure 5.20 C–H azidation and CuAAC of PEE.

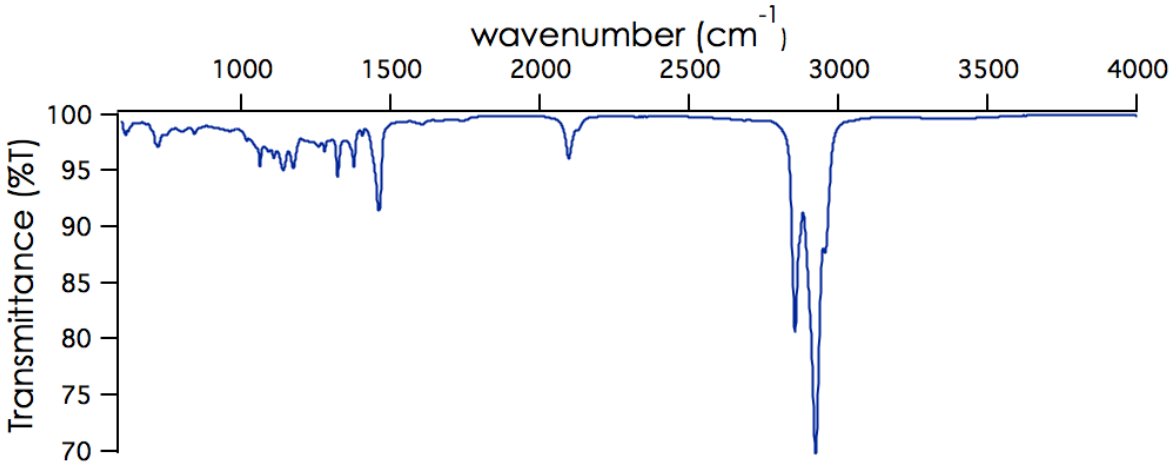

Figure 5.21 Infrared spectrum of **5.32**, with azide stretch at 2100 cm^{-1}.

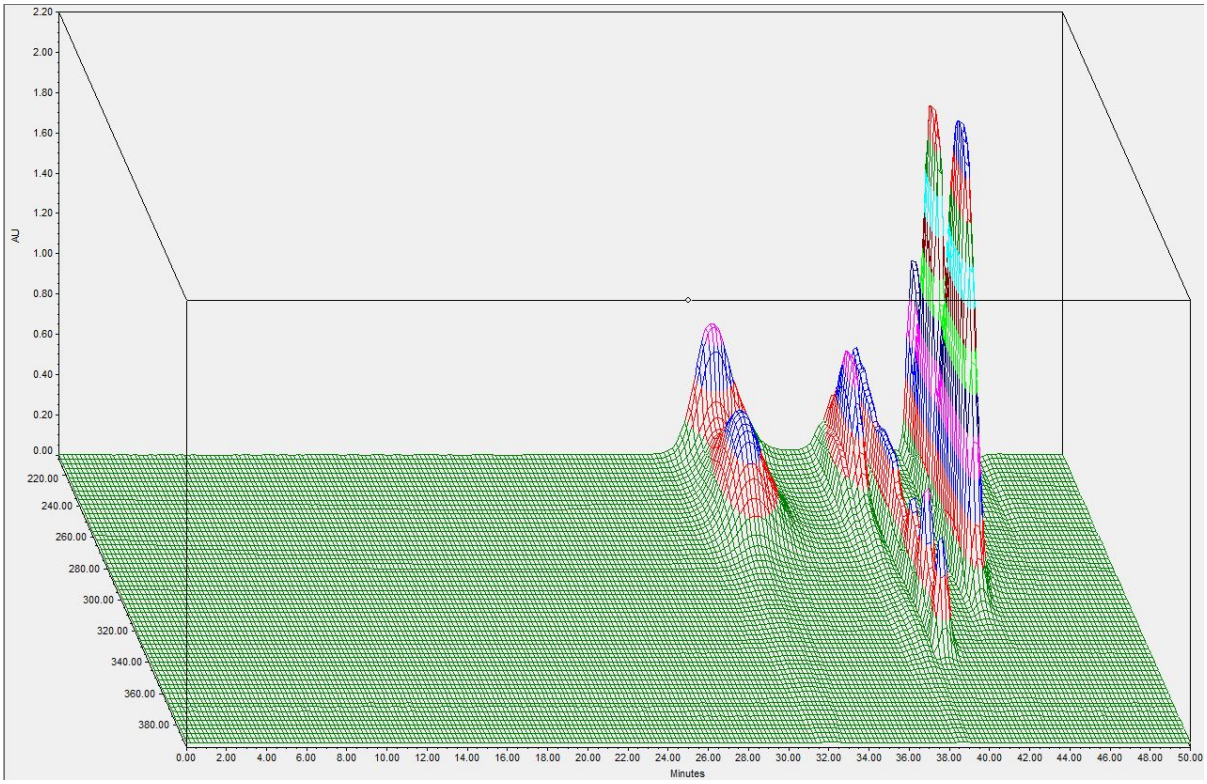

Figure 5.22 Gel permeation chromatogram of **5.33**.

Having observed productive azidation with PEE as the substrate, we sought to use a higher molecular weight polymer, hyperbranched polyethylene (HBPE),[57] that would be useful as a larger molecular weight material. Azidation in DCE was unsuccessful, presumably due to immiscibility of the polymer with the solvent. Switching to a mixture of chlorobenzene and DCE led to effective azidation as determined by IR spectroscopy (**Figure 5.23**). Based on ^{1}H NMR analysis, no secondary or primary azidation occurred, suggestive of only tertiary functionalization, and GPC analysis indicated that no polymer degradation had occurred. CuAAC led to triazole formation, with 0.5 mol % functionalization detected. Correcting for the fact that the polymer possesses branching and therefore tertiary sites on only 13% of the monomer units, functionalization occurred on 3.8 mol % of the branch sites, a similar efficiency to the azidation of PEE. Further work will aim to control the amount of C–H azidation, and the reaction could be extended to additional polyolefin substrates to access a variety of useful materials.

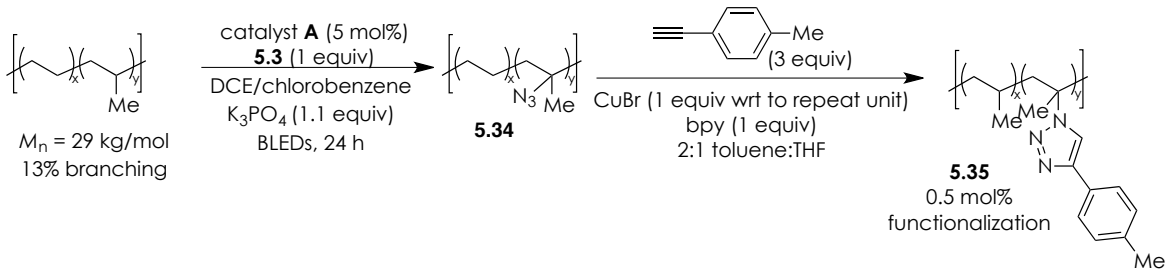

Figure 5.23 C–H azidation and CuAAC of HBPE.

Through this work, we have developed a mild and modular functionalization of unactivated alkanes using a completely organic photoredox catalytic system. The ability to accomplish this with a number of substrates and wide variety of traps unlocks a strategy for the late stage derivatization of complex small molecules. Furthermore, initial results toward the C–H azidation of polyolefins suggest utility in the arena of post-polymerization modification to access functionalized materials under mild conditions.

REFERENCES

(1) Yamaguchi, J.; Yamaguchi, A. D.; Itami, K. *Angew. Chem. Int. Ed.* **2012**, *51*, 8960–9009.

(2) Newhouse, T.; Baran, P. S. *Angew. Chem. Int. Ed.* **2011**, *50*, 3362–3374.

(3) White, M. C. *Science* **2012**, *335*, 807–809.

(4) Cernak, T.; Dykstra, K. D.; Tyagarajan, S.; Vachal, P.; Krska, S. W. *Chem Soc Rev* **2016**, *45*, 546–576.

(5) Mello, R.; Fiorentino, M.; Fusco, C.; Curci, R. *J. Am. Chem. Soc.* **1989**, *111*, 6749–6757.

(6) Brodsky, B. H.; Du Bois, J. *J. Am. Chem. Soc.* **2005**, *127*, 15391–15393.

(7) Chen, M. S.; White, M. C. *Science* **2007**, *318*, 783–787.

(8) Chen, M. S.; White, M. C. *Science* **2010**, *327*, 566–571.

(9) Howell, J. M.; Feng, K.; Clark, J. R.; Trzepkowski, L. J.; White, M. C. *J. Am. Chem. Soc.* **2015**, *137*, 14590–14593.

(10) Gormisky, P. E.; White, M. C. *J. Am. Chem. Soc.* **2013**, *135*, 14052–14055.

(11) Michaudel, Q.; Thevenet, D.; Baran, P. S. *J. Am. Chem. Soc.* **2012**, *134*, 2547–2550.

(12) Roizen, J. L.; Zalatan, D. N.; Du Bois, J. *Angew. Chem. Int. Ed.* **2013**, *52*, 11343–11346.

(13) Bess, E. N.; DeLuca, R. J.; Tindall, D. J.; Oderinde, M. S.; Roizen, J. L.; Du Bois, J.; Sigman, M. S. *J. Am. Chem. Soc.* **2014**, *136*, 5783–5789.

(14) Sharma, A.; Hartwig, J. F. *Nature* **2015**, *517*, 600–604.

(15) Karimov, R. R.; Sharma, A.; Hartwig, J. F. *ACS Cent. Sci.* **2016**, *2*, 715–724.

(16) Tang, R.-Y.; Li, G.; Yu, J.-Q. *Nature* **2014**, *507*, 215–220.

(17) Huang, X.; Bergsten, T. M.; Groves, J. T. *J. Am. Chem. Soc.* **2015**, *137*, 5300–5303.

(18) Huang, X.; Groves, J. T. *ACS Catal.* **2016**, *6*, 751–759.

(19) Liu, W.; Groves, J. T. *J. Am. Chem. Soc.* **2010**, *132*, 12847–12849.

(20) Liu, W.; Huang, X.; Cheng, M.-J.; Nielsen, R. J.; Goddard, W. A.; Groves, J. T. *Science* **2012**, *337*, 1322–1325.

(21) Bloom, S.; Pitts, C. R.; Miller, D. C.; Haselton, N.; Holl, M. G.; Urheim, E.; Lectka, T. *Angew. Chem. Int. Ed.* **2012**, *51*, 10580–10583.

(22) Halperin, S. D.; Fan, H.; Chang, S.; Martin, R. E.; Britton, R. *Angew. Chem. Int. Ed.* **2014**, *53*, 4690–4693.

(23) Bloom, S.; Knippel, J. L.; Lectka, T. *Chem Sci* **2014**, *5*, 1175–1178.

(24) Kee, C. W.; Chin, K. F.; Wong, M. W.; Tan, C.-H. *Chem Commun* **2014**, *50*, 8211–8214.

(25) Schmidt, V. A.; Quinn, R. K.; Brusoe, A. T.; Alexanian, E. J. *J. Am. Chem. Soc.* **2014**, *136*, 14389–14392.

(26) Quinn, R. K.; Könst, Z. A.; Michalak, S. E.; Schmidt, Y.; Szklarski, A. R.; Flores, A. R.; Nam, S.; Horne, D. A.; Vanderwal, C. D.; Alexanian, E. J. *J. Am. Chem. Soc.* **2016**, *138*, 696–702.

(27) Czaplyski, W. L.; Na, C. G.; Alexanian, E. J. *J. Am. Chem. Soc.* **2016**, *138*, 13854–13857.

(28) Mendes, J.; Zhou, C.-W.; Curran, H. J. *J. Phys. Chem. A* **2014**, *118*, 1300–1308.

(29) Hager, D.; MacMillan, D. W. C. *J. Am. Chem. Soc.* **2014**, *136*, 16986–16989.

(30) Jeffrey, J. L.; Terrett, J. A.; MacMillan, D. W. C. *Science* **2015**, *349*, 1532–1536.

(31) Le, C.; Liang, Y.; Evans, R. W.; Li, X.; MacMillan, D. W. C. *Nature* **2017**, *547*, 79–83.

(32) Qvortrup, K.; Rankic, D. A.; MacMillan, D. W. C. *J. Am. Chem. Soc.* **2014**, *136*, 626–629.

(33) Cuthbertson, J. D.; MacMillan, D. W. C. *Nature* **2015**, *519*, 74–77.

(34) Jin, J.; MacMillan, D. W. C. *Angew. Chem. Int. Ed.* **2015**, *54*, 1565–1569.

(35) Shaw, M. H.; Shurtleff, V. W.; Terrett, J. A.; Cuthbertson, J. D.; MacMillan, D. W. C. *Science* **2016**, *352*, 1304–1308.

(36) Mukherjee, S.; Maji, B.; Tlahuext-Aca, A.; Glorius, F. *J. Am. Chem. Soc.* **2016**, *138*, 16200–16203.

(37) Joshi-Pangu, A.; Lévesque, F.; Roth, H. G.; Oliver, S. F.; Campeau, L.-C.; Nicewicz, D.; DiRocco, D. A. *J. Org. Chem.* **2016**, *81*, 7244–7249.

(38) Landelle, G.; Panossian, A.; Leroux, F. *Curr. Top. Med. Chem.* **2014**, *14*, 941–951.

(39) Shao, X.; Xu, C.; Lu, L.; Shen, Q. *Acc. Chem. Res.* **2015**, *48*, 1227–1236.

(40) Choi, G. J.; Zhu, Q.; Miller, D. C.; Gu, C. J.; Knowles, R. R. *Nature* **2016**, *539*, 268–271.

(41) Chu, J. C. K.; Rovis, T. *Nature* **2016**, *539*, 272–275.

(42) Chen, D.-F.; Chu, J. C. K.; Rovis, T. *J. Am. Chem. Soc.* **2017**, *139*, 14897–14900.

(43) Bortolamei, N.; Isse, A. A.; Gennaro, A. *Electrochimica Acta* **2010**, *55*, 8312–8318.

(44) Kamijo, S.; Takao, G.; Kamijo, K.; Tsuno, T.; Ishiguro, K.; Murafuji, T. *Org. Lett.* **2016**, *18*, 4912–4915.

(45) Bovicelli, P.; Lupattelli, P.; Mincione, E.; Prencipe, T.; Curci, R. *J. Org. Chem.* **1992**, *57*, 5052–5054.

(46) Perkowski, A. J.; Nicewicz, D. A. *J. Am. Chem. Soc.* **2013**, *135*, 10334–10337.

(47) Liu, P.; Liu, W.; Wang, W.-J.; Li, B.-G.; Zhu, S. *Macromol. React. Eng.* **2016**, *10*, 156–179.

(48) Boaen, N. K.; Hillmyer, M. A. *Chem. Soc. Rev.* **2005**, *34*, 267.

(49) Johnson, L. K.; Mecking, S.; Brookhart, M. *J. Am. Chem. Soc.* **1996**, *118*, 267–268.

(50) Chung, T. C.; Lu, H. L.; Li, C. L. *Polym. Int.* **1995**, *37*, 197–205.

(51) Moad, G. *Prog. Polym. Sci.* **1999**, *24*, 81–142.

(52) Liu, D.; Bielawski, C. W. *Polym. Int.* **2017**, *66*, 70–76.

(53) Boaen, N. K.; Hillmyer, M. A. *Macromolecules* **2003**, *36*, 7027–7034.

(54) Kondo, Y.; García-Cuadrado, D.; Hartwig, J. F.; Boaen, N. K.; Wagner, N. L.; Hillmyer, M. A. *J. Am. Chem. Soc.* **2002**, *124*, 1164–1165.

(55) Bunescu, A.; Lee, S.; Li, Q.; Hartwig, J. F. *ACS Cent. Sci.* **2017**, *3*, 895–903.

(56) Private communication

(57) Bézier, D.; Daugulis, O.; Brookhart, M. *Organometallics* **2017**, *36*, 443–447.

APPENDIX A: SUPPORTING INFORMATION FOR CHAPTER 2

Materials:

Commercially available reagents were purchased from Sigma-Aldrich, Acros, Alfa Aesar, or TCI, Matrix Scientific, Chem Impex International, and Fisher Scientific and were used as received unless otherwise noted. Diethyl ether (Et_2O), dichloromethane (DCM), tetrahydrofuran (THF), toluene, and dimethylformamide (DMF) were dried by passing through activated alumina under nitrogen prior to use. Other common solvents and chemical reagents were purified by standard published methods as noted. The following compounds employed as reagents in the *C-H* amination reactions were obtained from commercial vendors and used as received: 2,2,6,6- Tetramethyl-1-piperidinyloxy (TEMPO), polystyrene-divinylbenzene-bound TEMPO, diacetoxyiodobenzene, potassium persulfate, benzoquinone, (diacetoxyiodo)benzene, anisole, diphenyl ether, biphenyl, 2-chloroanisole, 3-bromoanisole, mesitylene, *m*-xylene, 2,6- dimethoxypyridine, 6-methoxyquinoline, 3,4-dihydrocoumarin, 4-methyl pyrazole, 3-methyl pyrazole, 1,2,3-triazole, 5-methyltetrazole, 1,2,4-triazole, 1,2,3-benzotriazole, 4,5,6,7-tetrahydro- 1*H*-indazole, benzimidazole, and imidazole.

General Methods:

Proton, carbon, and fluorine nuclear magnetic resonance spectra (^{1}H NMR, ^{13}C NMR, ^{19}F NMR) were recorded on a Bruker Avance 400 (^{1}H NMR at 400 MHz, ^{13}C NMR at 100 MHz, and ^{19}F NMR at 376 MHz) or a Bruker Avance III 600 (^{1}H NMR at 600 MHz and ^{13}C NMR at 151 MHz) spectrometer. Chemical shifts for protons are reported in parts per million downfield from tetramethylsilane and are referenced to residual protium in the solvent (^{1}H NMR: $CHCl_3$ at 7.26 ppm). Chemical shifts for carbon signals are reported in parts per million downfield from tetramethylsilane and are referenced to the carbon resonances of the

solvent peak (^{13}C NMR: $CDCl_3$ at 77.16 ppm). Fluorine chemical shifts are referenced to trichlorofluoromethane as an external standard at 0 ppm. ^{1}H NMR data are reported as follows: chemical shift, multiplicity (s = singlet, d = doublet, t = triplet, q = quartet, hept = heptet, dd = doublet of doublets, ddd = doublet of doublet of doublets, m = multiplet, br s = broad singlet, app = apparent), coupling constants (Hz), and integration. Infrared (IR) spectra were obtained using a Jasco 260 Plus Fourier transform infrared spectrometer. High Resolution Mass Spectra (HRMS) were obtained using a Thermo LTqFT mass spectrometer with electrospray ionization in positive mode. Thin layer chromatography (TLC) was performed on SiliaPlate 250 μm thick silica gel plates provided by Silicycle. Visualization was accomplished with short wave UV light (254 nm), or development with iodine, ninhydrin stain, cerium ammonium molybdate or potassium permanganate solution followed by heating. Column chromatography was performed using SiliaFlash P60 silica gel (40- 63 μm) purchased from Silicycle. Unless noted all reactions were run under an atmosphere of oxygen in flame-dried glassware with magnetic stirring. Irradiation of photochemical reactions was carried out using a PAR38 Royal Blue aquarium LED lamp (Model #6851) fabricated with high-power Cree XR-E LEDs as purchased from Ecoxotic (www.ecoxotic.com) with standard borosilicate glass vials purchased from Fischer Scientific. For all photolyses, reactions were stirred using a PTFE coated magnetic stir bar on a magnetic stir plate. Gas chromatography (GC) was performed on an Agilent 6850 series instrument equipped with a split- mode capillary injection system and Agilent 5973 network mass spec detector (MSD). Yield refers to isolated yield of analytically pure material unless otherwise noted. NMR yields were determined using hexamethyldisiloxane as an internal standard. All other reagents were obtained from commercial sources and used without further

purification unless otherwise noted.

Photoreactor Configuration.

Reactions were irradiated using a simple photoreactor consisting of two Par38 Royal Blue Aquarium LED lamps (Model #6851) is shown in which four reactions (2 dram vials) are irradiated simultaneously with a foil barrier preventing irradiation by two lamps. In order to ensure that the reactions are run near room temperature, a simple cooling fan was installed above the reactor to aid in dissipating the heat generated from both nonradiative decay pathways of the excited state catalysts and the heat generated from high power LEDs. An equilibrium temperature of 33 ˚C was measured with a standard alcohol thermometer. While a number of other blue LED sources are effective, we have found that LED emitters with high luminous flux and narrow viewing angle give the best results.

Preparation of Acridinium Photocatalysts

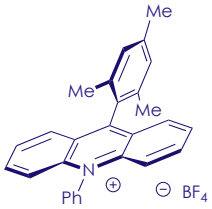

9-Mesityl-10-phenyl acridinium tetrafluoroborate (Catalyst A).

The title compound was prepared as previously reported by our lab.[1] The spectral data matched the values reported in the literature.

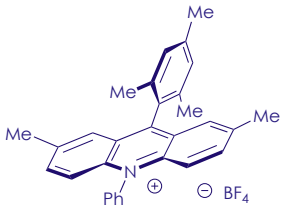

9-Mesityl-2,7-dimethyl-10-phenylacridinium tetrafluoroborate (Catalyst B).

The title compound was prepared as previously reported by our lab.[1] The spectral data matched the values reported in the literature.

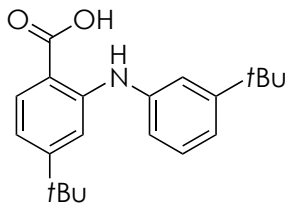

4-(*tert*-butyl)-2-((3-(*tert*-butyl)phenyl)amino)benzoic acid. To a flame dried 2-neck round bottom flask equipped with a condenser was added potassium carbonate (9.0 g, 65.3 mmol, 1.4 equiv.), copper (594 mg, 9.34 mmol, 0.2 equiv.) and 2-bromo-4-(*tert*-butyl)benzoic acid (12 g, 46.7 mmol, 1.0 equiv.). The setup was evacuated and back filled with nitrogen gas three times for 15 minutes each cycle. *m-Tert*-butyl aniline (10.3 mL, 65.3 mmol, 1.4 equiv.) and 1-pentanol (72 mL) were both sparged with nitrogen for 15 minutes. Pentanol was added to the reaction flask followed by the aniline. The solution was heated to 140 ˚C for 16 hours. The solution was cooled to room temperature and diluted with water (100 mL), washed with 3M HCl (100 mL) and extracted with dichloromethane (3x 100 mL). The organic layer was washed with ammonium chloride (100 mL), brine (100 mL) and dried over sodium sulfate. The organic solution was concentrated to afford a brown solid. The crude product was recrystallized from methanol to afford the desired aryl amine (10.1 g, 67% yield). **^{1}H NMR** (600 MHz, $CDCl_3$): δ 11.74 (br s, 1H), 9.32 (s, 1H), 8.00 (d, J = 9 Hz, 1H), 7.36-7.35 (m, 2H), 7.32 (t, J = 7.8 Hz, 1H), 7.16 (d, J = 8.4 Hz, 1H), 7.07 (dd, J = 7.8 Hz, J = 0.6 Hz, 1H), 6.83 (dd, J = 8.4 Hz, J = 1.2 Hz, 1H), 1.35 (s, 9H), 1.27 (s, 9H); **^{13}C NMR** ($CDCl_3$, 151 MHz): δ 173.4, 159.0, 152.5, 148.6, 140.3, 132.3, 129.0, 120.6, 119.6, 119.5, 115.1, 111.0, 108.0, 35.3, 34.8, 31.4, 30.8. **IR** (thin film): 3340.10, 2963.09, 2569.68, 2360.44, 1659.45,

1565.92, 1416.46, 1242.90, 963.27, 700.99.; **HRMS** (ESI): Calculated for [M+H_2O]= 348.1940; found 348.1932.

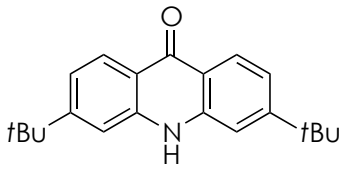

3,6-di-*tert*-butylacridin-9(10*H*)-one. To an Erlenmeyer flask equipped with a stir bar was added sulfuric acid (38 mL), which was heated to 100 ˚C. 4-(*tert*-butyl)-2-((3-(*tert*-butyl)phenyl)amino)benzoic acid (5.1 g, 15.7 mmol) was added to the sulfuric acid in portions and stirred for 3 hours at 100 ˚C. The solution was cooled to room temperature and the acidic solution was then poured into water at 0 ˚C, forming a yellow precipitate. Ammonium hydroxide was added until an alkaline pH persisted. The yellow solid was then filtered over a medium fritted funnel to afford the desired product along with the undesired regioisomer in an 8:1 mixture. Hot filtration from methanol removed insoluble salts, followed by a recrystallization from methanol and dichloromethane to afford the desired acridone (3.6 g, 76% yield). **^{1}H NMR** (400 MHz, 3:1 $CDCl_3$:MeOD) δ 8.12 (d, *J* = 8.9 Hz, 2H), 7.26 (d, *J* = 1.8 Hz, 2H), 7.29-7.18 (m, 2H), 3.15 (br. s, 1H), 1.16 (d, *J* = 2.5 Hz, 18H).; **^{13}C NMR** (151 MHz, $CDCl_3$) δ 178.26, 157.33, 141.19, 125.73, 119.82, 118.44, 112.70, 48.73, 35.02, 30.51.; **IR** (thin film): 3087.48, 2962.13, 2321.87, 1632.45, 1594.84, 1552.42, 1368.25, 1235.18, 1094.40 765.60.; **HRMS** (ESI): Calculated for [M+H_2O]= 308.2014; found 308.2004.

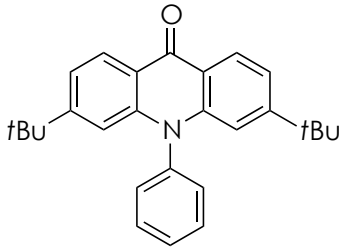

3,6-di-*tert*-butyl-10-phenylacridin-9(10*H*)-one. To a flame-dried round bottom flask was added 3,6-di-*tert*-butylacridin-9(10*H*)-one (3.75 g, 12.2 mmol, 1 equiv.), copper (I) iodide (232 mg, 1.22 mmol, 0.1 equiv.) and potassium carbonate (3.37 g, 24.4 mmol, 2.0 equiv.). Iodobenzene (1.48 mL, 13.3 mmol, 1.1 equiv.) and 2,2,6,6-tetramethylheptane-3,5-dione (0.51 mL, 2.44 mmol, 0.2 equiv.) were added in a nitrogen-filled glovebox along with dimethylformamide (62 mL). The solution was heated to 130 ˚C for 48 hours. The solution was then cooled to room temperature and quenched with 3M HCl (50 mL). The aqueous solution was extracted with dichloromethane (3x 100 mL). The combined organic layers were washed with sodium bicarbonate (150 ml), ammonium chloride (150 mL), brine, dried over sodium sulfate and then concentrated. The final pale yellow solid (2.95 g, 63% yield) was obtained after flash chromatography (20% EtOAc/Hexanes). **^{1}H NMR** (400 MHz, $CDCl_3$) δ 8.50 (d, *J* = 8.5 Hz, 2H), 7.72 (t, *J* = 7.5 Hz, 2H), 7.66 (d, *J* = 7.3 Hz, 1H), 7.40-7.37 (m, 2H), 7.33 (dd, *J* = 8.5, 1.6 Hz, 2H), 6.71 (d, *J* = 1.6 Hz, 2H), 1.20 (s, 18H).; **^{13}C NMR** (151 MHz, $CDCl_3$) δ 177.73, 156.93, 143.38, 139.30, 131.01, 130.21, 129.59, 126.98, 119.94, 119.77, 113.03, 35.46, 31.01.; **IR** (thin film): 3049.87, 2964.05, 2868.59, 1606.41, 1452.14, 1307.50, 1197.58, 997.02, 867.81, 682.68; **HRMS** (ESI): Calculated for [M+H_2O]= 384.2327; found 384.2319.

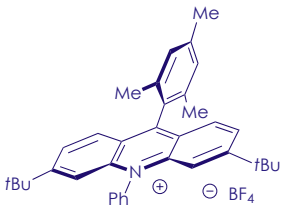

9-Mesityl-3,6-di-*tert*-butyl-10-phenylacridinium tetrafluoroborate (Catalyst C). To a flame dried round bottom flask equipped with a stir bar was added 3,6-di-*tert*-butyl-10-phenylacridin-9(10*H*)-one (1.5 g, 3.91 mmol, 1.0 equiv.). The acridone was dissolved in dry THF (112 mL). Mesityl magnesium bromide (9.8 mL, 9.8 mmol, 1 M in Et_2O, 2.5 equiv.) was added dropwise and the solution was stirred at room temperature for 24 hours. The solution was then heated to 50 ˚C for 72 hours. The red solution was cooled and quenched with sodium bicarbonate (100 mL). The aqueous layer was extracted with DCM (3x 100 mL) followed by a brine wash, drying over sodium sulfate and concentration to afford a red oil. The oil was dried on high vacuum for 4 hours. The oil was then dissolved in ether (67 mL) and tetrafluoroboric acid diethyl ether complex (0.65 mL, 4.7 mmol, 1.2 equiv.) in ether (12.5 mL) was added dropwise and the solution was stirred for 1 hour, during which a precipitate quickly appeared with the addition of acid. The yellow solid that precipitated out was then filtered and washed with ether (200 mL) to afford the final 3,6-di-*tert*-butyl-9-mesityl-10-phenylacridin-10-ium tetrafluoroborate (2.05 g, 92% yield).**^{1}H NMR** (400 MHz, $CDCl_3$) δ 7.99-7.93 (m, 2H), 7.93-7.89 (m, 1H), 7.78 (q, *J* = 1.6 Hz, 3H), 7.77-7.70 (m, 2H), 7.41 (d, *J* = 3.2 Hz, 2H), 7.26 (s, 1H), 7.16 (d, *J* = 2.7 Hz, 2H), 2.48 (s, 3H), 1.86 (d, *J* = 3.5 Hz, 6H), 1.29 (d, *J* = 3.5 Hz, 9H).; **^{13}C NMR** (151 MHz, $CDCl_3$) δ 163.72, 162.44, 142.25, 140.31, 136.95, 136.25, 131.96, 131.75, 129.40, 129.07, 128.41, 128.12, 127.60, 124.16, 115.19, 36.80, 30.34, 21.42, 20.36.; **IR** (thin film): 2965.02, 2863.77, 1615.09, 1540.85,

1436.71, 1252.54, 1055.84, 915.06, 780.06, 728.96; **HRMS** (ESI): Calculated for [M+H_2O]= 486.3161; found 486.3158.

Preparation of Arene Substrates

Anisole, diphenyl ether, biphenyl, 2-chloroanisole, 3-bromoanisole, mesitylene, *m*-xylene, 2,6-dimethoxypyridine, 6-methoxy quinoline, 3,4-dihydrocoumarin, 4-methyl pyrazole, 3-methyl pyrazole, 1,2,3-triazole, 5-methyl tetrazole, 1,2,4-triazole, 1,2,3-benzotriazole, 4,5,6,7-tetrahydro-1*H*-indazole, benzimidazole, and imidazole were purchased commercial sources and used without further purification unless otherwise noted.

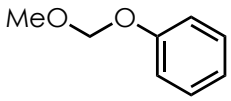

(methoxymethoxy)benzene. Prepared according to a published procedure; spectral data were in agreement with literature values. [2]

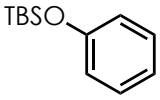

***tert*-butyldimethyl(phenoxy)silane.** Prepared according to a published procedure; spectral data were in agreement with literature values. [3]

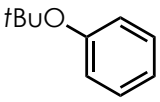

***tert*-butoxybenzene.** Prepared according to a published procedure; spectral data were in agreement with literature values.[4]

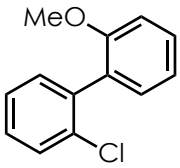

2-chloro-2'-methoxy-1,1'-biphenyl. Under an inert atmosphere, 173 mg

Tetrakis(triphenylphosphine)palladium(0) (0.15 mmol, 0.03 equiv.) was added to a flame-dried round bottom flask containing a magnetic stir bar, along with 938 mg (2-chlorophenyl)boronic acid (6.0 mmol, 1.2 equiv.) and 1.38 g K_2CO_3 (10. mmol, 2.0 eq.). Separately, a 9:1 (v/v) mixture of THF/H_2O was sparged with nitrogen, then added to the flask containing palladium, boronic acid, and carbonate. The mixture was warmed to 50 ˚C for 10 minutes while 2-bromoanisole was sparged with nitrogen in a separate vial. 2-Bromoanisole was added, and the reaction was heated at reflux for 26 hours. After cooling to room temperature, 20 mL H_2O was added, along with 10 mL saturated aqueous NH_4Cl. The layers were separated, and the aqueous phase was extracted twice with diethyl ether. The combined extracts were washed with brine and dried with $MgSO_4$. After filtration and concentration in vacuo, the crude oil was dissolved in pentanes and crystallization occurred when cooled in a –20 ˚C freezer. The white crystals were collected by vacuum filtration, washed with cold pentanes, and dried in vacuo to give 930 mg pure material. The spectral data were in agreement with literature values.

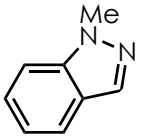

1-methyl-1*H*-indazole. The title compound was prepared by the published procedure. The material was recrystallized from a mixture of ethyl acetate and hexanes and dried in vacuo. The ^1H NMR spectrum matches the reported data.

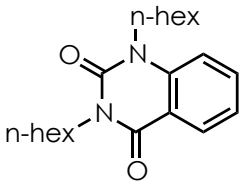

1,3-dihexylquinazoline-2,4(1*H*,3*H*)-dione. Benzoyleneurea (1 g, 6.2 mmol, 1.0 equiv.) was dissolved in dry DMF and potassium carbonate was added (2.8 g, 20.1 mmol, 3.3 equiv.). Hexyl bromide (3.5 mL, 24.7 mmol, 4.0 equiv.) was added dropwise and the solution was stirred for 84 hours. The solution was concentrated and then diluted with dichloromethane. The organic solution was washed with water (50 mL), and the aqueous layer was extracted with CH_2Cl_2 (3x 50 mL). The combined organic layers were washed with brine, dried over sodium sulfate and concentrated to give a pale yellow solid. The crude product was purified by flash chromatography (0-20% EtOAc/Hex) to afford the desired pale yellow oil (1.1 g, 54% yield). **^{1}HNMR** (600 MHz, $CDCl_3$) δ 8.24 (dd, *J* = 7.9, 1.7 Hz, 1H), 7.66 (ddd, *J* = 8.7, 7.2, 1.7 Hz, 1H), 7.33-7.12 (m, 2H), 4.17-4.04 (m, 4H), 1.77-1.61 (m, 4H), 1.42-1.23 (m, 11H), 0.95-0.79 (m, 7H).; **^{13}C NMR** (151 MHz, $CDCl_3$) δ 161.79, 150.80, 139.89, 134.94, 129.19, 122.68, 115.88, 113.57, 43.84, 42.05, 31.63, 31.63, 31.58, 27.88, 27.37, 26.78, 26.59, 22.69, 22.67, 14.15, 14.11; **IR** (thin film): 2956.34, 2930.31, 2857.99, 2357.55, 1704.76, 1660.41, 1608.34, 1483.96, 1352.82, 757.89. **HRMS** (ESI): Calculated for [M+H_2O]= 331.2385; found 331.2379.

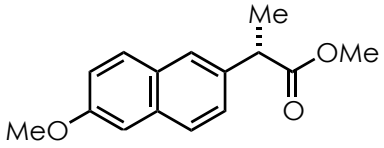

(*S*)-methyl 2-(6-methoxynaphthalen-2-yl)propanoate. Prepared according to a published procedure; spectral data were in agreement with literature values. [5]

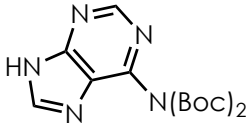

Bis-Boc-adenine. Prepared according to a published procedure; spectral data were in agreement with literature values. [6]

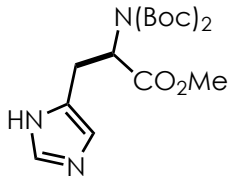

methyl (*tert*-butoxycarbonyl)-*L*-histidinate. The title compound was prepared by the published procedure. The material was recrystallized from a mixture of ethyl acetate and hexanes and dried in vacuo. The ^{1}H NMR spectrum matches the reported data.

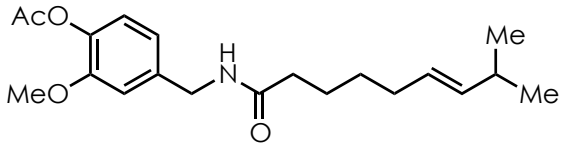

(*E*)-2-methoxy-4-((8-methylnon-6-enamido)methyl)phenyl acetate. The title compound was synthesized from capsaicin, which was obtained from Sigma-Aldrich as a 2:1 mixture of capsaicin ((*E*)-*N*-(4-hydroxy-3-methoxybenzyl)-8-methylnon-6-enamide) and dihydrocapsaicin (*N*-(4-hydroxy-3-methoxybenzyl)-8-methylnonanamide). The capsaicin was used as received and acylated by the following procedure: 750 mg capsaicin (2.5 mmol, 1.0 equiv.) was cooled to 0 ˚C in 11 mL DCM, and 262 μL acetyl chloride was added (3.7 mmol, 1.5 equiv.), followed by 693 μL trimethylamine. The mixture was stirred for 1 hour at 0 ˚C, then at ambient temperature for an additional 1 hour. The mixture was diluted with 25 mL DCM and washed with brine, dilute HCl, then saturated aqueous $NaHCO_3$. The organic phase was again washed with brine and dried with $MgSO_4$. After concentrating in vacuo, the crude tan solid was recrystallized from a mixture of EtOAc and hexanes, and collected by vacuum filtration, yielding 813 mg of a white solid. The proton NMR spectra indicates that the ratio between *O*-acetyl capsaicin and *O*-acetyl dihydrocapsaicin is identical to the starting material. Note: the indicated proton resonances refer to the title compound; see the included ^{1}HNMR spectrum below

for the resonances of the saturated compound. The carbon resonances listed include the resonances for both the unsaturated and saturated compounds in the mixture. **^{1}HNMR** (600 MHz, $CDCl_3$) δ 6.98 (d, *J* = 8.0 Hz, 1H), 6.90 (s, 1H), 6.84 (d, *J* = 8.0 Hz, 1H), 5.68 (s, 1H), 5.41 – 5.28 (m, 2H), 4.42 (d, *J* = 5.7 Hz, 2H), 3.82 (s, 3H), 2.31 (s, 3H), 2.21 (t, *J* = 7.4 Hz, 2H), 1.99 (q, *J* = 7.0 Hz, 2H), 1.67 – 1.63 (m, 2H), 1.51 (hept, *J* = 6.7 Hz, 1H), 1.39 (p, *J* = 7.6 Hz, 2H), 0.95 (d, *J* = 6.7 Hz, 6H). ; **^{13}C NMR** (151 MHz, $CDCl_3$) δ 172.96, 169.29, 151.35, 139.21, 138.25, 137.53, 126.60, 123.01, 120.19, 112.29, 100.12, 56.04, 43.60, 39.10, 37.00, 36.84, 32.38, 31.12, 29.45, 28.09, 27.39, 25.93, 25.40, 22.80, 20.82. **IR** (thin film): 3287.07, 2928.38, 2359.48, 1766.48, 1642.09, 1511.92, 1388.25, 1272.79, 1195.54, 1035.59. **HRMS**: Calculated for $(M+Na)^+$: 370.1995 and 372.2151; found: 370.1987 and 370.2141.

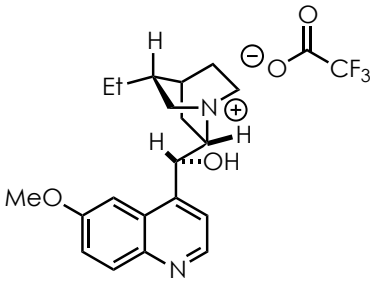

(9*S*)-10,11-dihydro-6'-methoxycinchonan-9-ol·2,2,2-trifluoroacetic acid. The title compound was prepared by stirring 1.0 g dihydroquinidine (3.1 mmol, 1.0 equiv.) in a 15:1 (v/v) mixture of Et_2O/MeOH at 0 ˚C and adding 237 μL trifluoroacetic acid (3.1 mmol, 1.0 equiv.) slowly. The mixture was stirred for 2 hours and concentrated in vacuo. The crude white foam was recrystallized by dissolving in hot toluene and cooling. The tan solid was collected by vacuum filtration and washed with toluene. The solid was dried in vacuo to give quantitative yield of the salt. **^{1}HNMR** (600 MHz, $CDCl_3$) δ 12.34 (s, 1H), 8.69 (d, *J* = 4.5 Hz, 1H), 7.86 (d, *J* = 9.3 Hz, 1H), 7.62 (d, *J* = 4.4 Hz, 1H), 7.18

(s, 1H), 6.98 (s, 1H), 6.37 (s, 1H), 5.66 (s, 1H), 4.16 – 3.91 (m, 1H), 3.83 (s, 3H), 3.54 – 3.22 (m, 3H), 3.18 (s, 1H), 2.39 – 2.24 (m, 1H), 1.95 (s, 1H), 1.86 – 1.51 (m, 5H), 1.02 – 0.88 (m, 4H). **^{13}C NMR** (151 MHz, $CDCl_3$) δ 162.93 (q, J = 34.9 Hz), 158.20, 146.85, 144.30, 143.27, 131.19, 125.16, 122.30, 118.36, 116.71 (q, J = 292.7 Hz), 99.36, 66.40, 60.23, 55.79, 50.03, 49.38, 35.26, 25.16, 24.30, 23.93, 17.68, 11.50. **^{19}F NMR** (376 MHz, CDCl3) δ –75.34. **IR** (thin film): 3249.47 (br), 2964.05, 2556.18, 2360.44, 1672.95, 1509.99, 1433.82, 1242.90, 1199.51, 834.06. **HRMS**: Calculated for $(M-C_2O_2F_3)^+$: 327.2072; found: 327.2067.

Procedures for the Photoredox-Catalyzed Synthesis of Aryl Amines

Notes: All isolated yields and regioisomeric ratios reported are the average of duplicate experiments. For inseparable mixtures of regioisomers, analytical data was collected for the sample as isolated from chromatography, which, in most cases, is a mixture of *para*- and *ortho*- isomers.

General Method A: Synthesis of 2.1, 2.5–2.19, 2.22–2.26, 2.28–2.32, 2.34–2.36 The synthesis of aryl pyrazoles **2.1a** and **2.1b** from anisole and pyrazole is representative of the following general procedure:

To a 2 dram vial containing a Teflon-coated magnetic stir bar was added 25 μmol of Catalyst **C** (0.05 equiv.), 68 mg of pyrazole (1.0 mmol, 2 equiv.), and 16 mg of (2,2,6,6-tetramethylpiperidin-1-yl)oxyl (0.1 mmol, 0.2 equiv.). Dichloromethane or 1,2-Dichloroethane was added (5.0 mL), followed by the arene (0.5 mmol, 1.0 equiv.). The vial was sealed with a Teflon-lined septum screw cap. The septum was pierced with a disposable steel needle connected to an oxygen-filled balloon. A vent needle was inserted and the reaction medium was sparged for 5 minutes by bubbling oxygen through the

mixture. The vent needle was removed, and the oxygen balloon was maintained, providing approximately 1 atm of oxygen to the vial headspace for the course of the reaction. The vial was positioned on a stir plate approximately 10 cm from a Par38 LED lamp supplying blue light (λ = 440 – 460 nm). After irradiation for 20 hours, the reaction mixture was analyzed by GC-MS or concentrated in vacuo and purified by column chromatography on silica gel with hexanes/ethyl acetate (or with the eluent noted for each substrate). For reaction optimization as shown in **Table 2.1** and **Table 2.2**, crude reaction mixtures were analyzed by GC-MS by the following modification to General Procedure A: reactions were run under concentrations given in **Table 2.1** and **Table 2.2** relative to anisole on a 0.5 mmol scale. Following irradiation for 20 hours, 33 μL 1,3-dimethoxybenzene (0.25 mmol, 0.5 equiv.) was added to the reaction mixture, which was passed through a short pad of silica gel and rinsed with an equal volume of dichloromethane. Samples were analyzed using an Agilent 5973 GC-MS system, wherein product yields and anisole conversions were calculated relative to the internal standard according to the instrument response factors, which were determined separately by construction of calibration curves.

General Method B: Synthesis of Alkyl-Substituted Arenes.

The synthesis of aryl pyrazole **2.12** from mesitylene and pyrazole is representative of the following general procedure:

To a 2 dram vial containing a Teflon-coated magnetic stir bar was added 25 μmol of Catalyst **C** (0.05 equiv.), 34 mg of pyrazole (0.5 mmol, 1 equiv.), and 16 mg of (2,2,6,6-tetramethylpiperidin-1-yl)oxyl (0.1 mmol, 0.2 equiv.). Dichloromethane or 1,2-Dichloroethane was added (5.0 mL), followed by addition of alkyl arene (1.0 mmol, 2

equiv.). The vial was sealed with a Teflon-lined septum screw cap. The septum was pierced with a disposable steel needle connected to a nitrogen-filled balloon. A vent needle was inserted and the reaction medium was sparged for 5 minutes by bubbling nitrogen through the mixture. The vent needle was removed, and the nitrogen line was maintained, providing approximately 1 atm of nitrogen to the vial headspace for the course of the reaction. The vial was irradiated as described in **General Procedure A** for 44 hours, and the reaction mixture was analyzed by GC-MS or concentrated in vacuo and purified by column chromatography on silica gel with the eluent noted for each substrate.

General Method C: Synthesis of Anilines 42-49

To a vial containing a Teflon-coated magnetic stir bar was added Catalyst **B** or **C** (0.05 equiv.), ammonium carbamate (4.0 equiv.), and TEMPO (0.2 equiv.). A 10:1 solvent mixture of 1,2- dichloroethane/water was added (0.1M), followed by the arene (1.0 equiv.). The vial was sealed with a Teflon-lined septum screw cap, and the reaction mixture was sparged with O_2 and irradiated in the same fashion as **General Method A**.

Characterization for Aryl Amination Products.

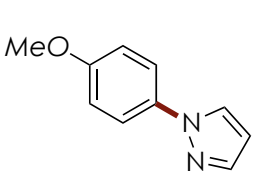

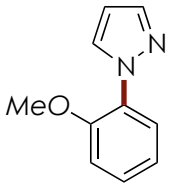

1-(4-methoxyphenyl)-1*H*-pyrazole, 1-(2-methoxyphenyl)-1*H*-pyrazole. The title compounds were prepared using **General Method A** with an irradiation time of 20 hours. The average *para*:*ortho* ratio of the inseparable mixture was 8.8:1 as determined by ^{1}H NMR of the isolated product. The title compound was purified by column

chromatography on silica gel (10% to 20% EtOAc/Hexanes) to yield a pale yellow solid in 88%. Spectral data were in agreement with literature values. [7,8]

2.1a. ^{1}**H NMR** (400 MHz, $CDCl_3$) δ 7.82 (s, 1H), 7.69 (s, 1H), 7.59 (d, *J* = 8.9 Hz, 2H), 6.97 (d, *J* = 8.9 Hz, 2H), 6.43 (s, 1H), 3.84 (s, 3H).; ^{13}**C NMR** (100 MHz, $CDCl_3$) δ 158.25, 140.64, 134.06, 126.85, 120.91, 114.54, 107.21, 55.60.

2.1b. ^{1}**H NMR** (400 MHz, $CDCl_3$) δ 8.03 (s, 1H), 7.72 (m, 1H), 7.69 (m, 2H), 7.30 (m, 1H), 7.06 (m, 1H), 6.43 (s, 1H), 3.87 (s, 3H).; ^{13}**C NMR** (100 MHz, $CDCl_3$) δ 151.36, 140.10, 131.59, 128.05, 125.31, 121.19, 112.29, 106.20, 55.97.

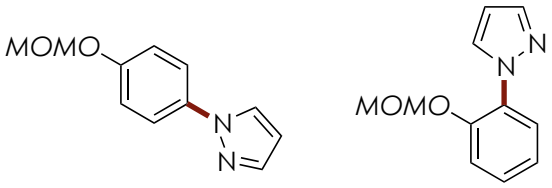

1-(4-(methoxymethoxy)phenyl)-1*H*-pyrazole and 1-(2-(methoxymethoxy)phenyl)-1*H*-pyrazole. The title compounds were prepared using **General Method A** with an irradiation time of 20 hours. The average *para*:*ortho* ratio of the inseparable mixture was 7.8:1 as determined by ^{1}H NMR of the isolated product. The title compound was purified by column chromatography on silica gel (10% to 20% EtOAc/Hexanes) to yield a pale yellow solid in 52%.

2.5a. ^{1}**H NMR** (600 MHz, $CDCl_3$) δ 7.83 (d, *J* = 2.4 Hz, 1H), 7.69 (d, *J* = 1.7 Hz, 1H), 7.59 (d, *J* = 9.0 Hz, 2H), 7.11 (d, *J* = 9.0 Hz, 2H), 6.43 (d, *J* = 2.2 Hz, 1H), 5.19 (s, 2H), 3.49 (s, 3H).; ^{13}**C NMR** (151 MHz, $CDCl_3$) δ 155.91, 140.80, 135.03, 126.88, 120.84, 117.08, 107.35, 94.75, 56.15.

2.5b. ^{1}**H NMR** (600 MHz, $CDCl_3$) δ 8.03 (dd, *J* = 2.4, 0.8 Hz, 1H), 7.74-7.70 (m, 2H), 7.28-7.25 (m, 3H), 6.43 (d, *J* = 2.2 Hz, 1H), 5.19 (s, 2H), 3.42 (s, 3H).; ^{13}**C NMR** (151

MHz, $CDCl_3$) δ 149.10, 140.24, 135.03, 131.58, 128.16, 125.55, 116.41, 106.38, 95.44, 56.43.

IR (thin film): 3452.67, 3124.12, 2955.38, 1597.73, 1523.49, 1396.21, 1311.36, 1237.11, 1079.94, 997.98, 752.10; **HRMS** (ESI): Calculated for [M+H_2O]= 205.0977; found 205.0970.

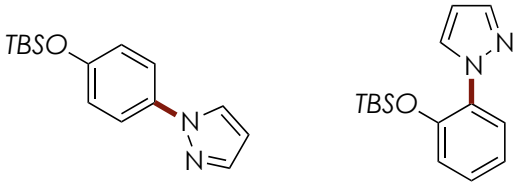

1-(4-((*tert*-butyldimethylsilyl)oxy)phenyl)-1*H*-pyrazole and 1-(2-((*tert*-butyldimethylsilyl) oxy)phenyl)-1*H*-pyrazole. The title compounds were prepared using **General Method A** with an irradiation time of 20 hours. The average *para*:*ortho* ratio of the inseparable mixture was 9.3:1 as determined by ^{1}H NMR of the isolated product. The title compound was purified by column chromatography on silica gel (10% to 20% EtOAc/Hexanes) to yield a pale yellow oil in 74%.

2.6a. ^{1}H NMR (600 MHz, $CDCl_3$) δ 7.83 (s, 1H), 7.70 (s, 1H), 7.56-7.54 (d, *J* = 8.1 Hz, 2H), 6.93-6.92 (d, *J* = 8.1 Hz, 2H), 6.44 (d, *J* = 2.1 Hz, 1H), 1.02 (s, 9H), 0.24 (s, 6H).; **^{13}C NMR** (151 MHz, $CDCl_3$) δ154.11, 140.37, 134.26, 126.57, 120.56, 120.51, 106.93, 25.45, 18.00, -4.65.

2.6b. ^{1}H NMR (600 MHz, $CDCl_3$) δ 7.93 (d, *J* = 2.0 Hz, 1H), 7.70 (s, 1H), 7.63 (d, *J* = 7.9 Hz, 1H), 7.25-7.19 (m, 1H), 7.10-7.05 (m, 1H), 6.99 (dt, *J* = 8.1, 1.3 Hz, 1H), 6.43 (s, 1H), 0.90 (s, 9H), 0.05 (s, 6H).; **^{13}C NMR** (151 MHz, $CDCl_3$) δ 147.58, 139.79, 132.08, 131.30, 127.79, 125.88, 121.81, 120.86, 105.79, 25.38, 17.91, -5.02.

IR (thin film): 2956.34, 2930.31, 2857.99, 1596.77, 1521.56, 1471.42, 1395.25, 1266.04, 913.13, 839.84, 781.99, 747.28; **HRMS** (ESI): Calculated for [M+H_2O]= 275.1580; found 275.1575.

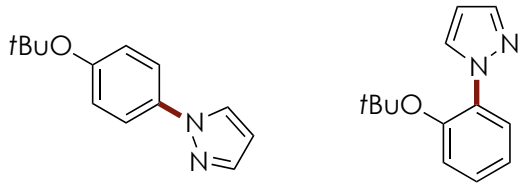

1-(4-(*tert*-butoxy)phenyl)-1*H*-pyrazole and 1-(2-(*tert*-butoxy)phenyl)-1*H*-pyrazole. The title compounds were prepared using **General Method A** with an irradiation time of 20 hours. The average *para*:*ortho* ratio of the inseparable mixture was 6:1 as determined by ^{1}H NMR of the isolated product. The title compound was purified by column chromatography on silica gel (10% to 20% EtOAc/Hexanes) to yield a pale yellow solid in 63%.

2.7a. ^{1}H NMR (400 MHz, $CDCl_3$) δ 7.90 (s, 1H), 7.74 (s, 1H), 7.62 (d, *J* = 8.4 Hz, 2H), 7.11 (d, *J* = 8.4 Hz, 2H), 6.48 (s, 1H), 1.41 (s, 9H).; **^{13}C NMR** (151 MHz, $CDCl_3$) δ 153.49, 140.43, 135.70, 126.47, 124.62, 119.65, 106.97, 78.58, 28.42.

2.7b. ^{1}H NMR (400 MHz, $CDCl_3$) δ 8.12 (s, 1H), 7.74 (s, 1H), 7.25 (d, *J* = 7.8 Hz, 2H), 7.22-7.19 (m, 2H), 6.46 (s, 1H), 1.17 (s, 9H).; **^{13}C NMR** (151 MHz, $CDCl_3$) δ 146.78, 139.72, 135.32, 131.47, 126.86, 125.03, 124.00, 105.73, 80.56, 27.82.

IR (thin film): 3122.19, 2976.59, 2933.20, 2360.44, 1521.56, 1394.28, 1240.00, 1161.90, 1046.19, 892.88, 750.17; **HRMS** (ESI): Calculated for [M+H_2O]= 239.1160; found 239.1152.

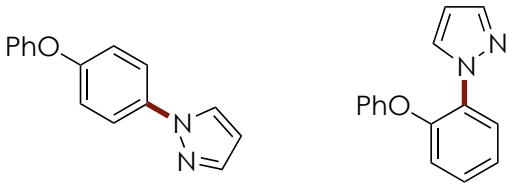

1-(4-phenoxyphenyl)-1*H*-pyrazole and 1-(2-phenoxyphenyl)-1*H*-pyrazole. The title compounds were prepared using **General Method A** with an irradiation time of 20 hours. The average *para*:*ortho* ratio of the inseparable mixture was 11:1 as determined by ^{1}H NMR of the isolated product. The title compound was purified by column chromatography on silica gel (10% to 20% EtOAc/Hexanes) to yield a pale yellow solid in 86%.

2.8a. ^{1}H NMR (600 MHz, $CDCl_3$) δ 7.88 (d, *J* = 2.4 Hz, 1H), 7.73 (d, *J* = 1.8 Hz, 1H), 7.66 (d, *J* = 8.9 Hz, 2H), 7.37 (dd, *J* = 8.5, 7.3 Hz, 2H), 7.14 (td, *J* = 7.4, 1.1 Hz, 1H), 7.11 (d, *J* = 8.8 Hz, 2H), 7.07-7.03 (m, 2H), 6.47 (t, *J* = 2.1 Hz, 1H).; **^{13}C NMR** (151 MHz, $CDCl_3$) δ 157.18, 155.80, 141.03, 136.0, 129.96, 126.92, 123.61, 120.98, 119.74, 118.92, 107.60.

2.8b. ^{1}H NMR (600 MHz, $CDCl_3$) δ 8.10 (d, *J* = 2.3 Hz, 1H), 7.94-7.90 (m, 1H), 7.70 (d, *J* = 1.7 Hz, 1H), 7.32 (dd, *J* = 8.5, 7.3 Hz, 2H), 7.27 (d, *J* = 3.7 Hz, 2H), 7.14 (td, *J* = 7.4, 1.1 Hz, 1H), 7.11 (d, *J* = 8.8 Hz, 1H), 6.98 (dd, *J* = 7.6, 1.1 Hz, 2H), 6.38 (d, *J* = 2.1 Hz, 1H).; **^{13}C NMR** (151 MHz, $CDCl_3$) δ 156.73, 147.88, 140.55, 132.36, 131.26, 129.61, 127.91, 125.39, 124.60, 120.98, 118.24, 115.54, 106.92.

IR (thin film): 3056.62, 2359.48, 1589.06, 1521.56, 1488.78, 1395.25, 1236.15, 1046.19, 936.27, 841.78; **HRMS** (ESI): Calculated for [M+H_2O]= 237.1028; found 237.1020.

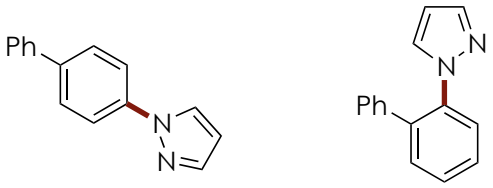

1-([1,1'-biphenyl]-4-yl)-1*H*-pyrazole and 1-([1,1'-biphenyl]-2-yl)-1*H*-pyrazole. The title compounds were prepared using **General Method A** with an irradiation time of 20 hours. The average *para*:*ortho* ratio of the inseparable mixture was 7.9:1 as determined by ^{1}H NMR of the isolated product. The title compound was purified by column chromatography on silica gel (10% to 20% EtOAc/Hexanes) to yield a pale yellow solid in 56%.

2.9a. ^{1}H NMR (600 MHz, $CDCl_3$) δ 7.97 (s, 1H), 7.79-7.76 (m, 3H), 7.69 (dd, *J* = 8.7, 1.9 Hz, 2H), 7.64-7.62 (m, 2H), 7.48-7.45 (m, 2H), 7.39-7.36 (m, 1H), 6.50 (s, 1H).; **^{13}C NMR** (151 MHz, $CDCl_3$) δ 141.29, 140.22, 139.49, 139.44, 128.99, 128.17, 127.61, 127.08, 126.81, 119.5, 107.83.

2.9b. ^{1}H NMR (600 MHz, $CDCl_3$) δ 7.65-7.60 (m, 1H), 7.50-7.44 (m, 2H), 7.32-7.28 (m, 3H), 7.26 (m, 2H), 7.13-7.12 (dd, *J* = 6.7, 2.7 Hz, 2H), 7.08 (m, 1H), 6.20 (q, *J* = 1.9 Hz, 1H).; **^{13}C NMR** (151 MHz, $CDCl_3$) δ 140.36, 138.68, 136.78, 131.43, 131.13, 128.64, 128.55, 128.47, 128.35, 127.53, 126.67, 106.48.

IR (thin film): 3130.87, 3107.72, 2358.52, 1607.38, 1530.24, 1486.85, 1394.28, 1050.05, 836.96, 743.42; **HRMS** (ESI): Calculated for [M+H_2O]= 221.1079; found 221.1072.

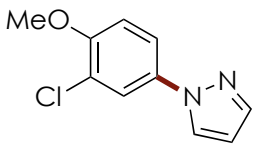

1-(3-chloro-4-methoxyphenyl)-1*H*-pyrazole (2.10). The title compound was prepared using **General Method A** with an irradiation time of 44 hours. The title compound was

purified by column chromatography on silica gel (10% to 20% EtOAc/Hexanes) to yield a pale yellow solid in 70%. **^{1}H NMR** (600 MHz, $CDCl_3$) δ 7.80 (d, *J* = 2.4 Hz, 1H), 7.73 (d, *J* = 2.6 Hz, 1H), 7.68 (d, *J* = 1.8 Hz, 1H), 7.53 (dd, *J* = 9.0, 2.6 Hz, 1H), 6.96 (d, *J* = 8.8 Hz, 1H), 6.43 (s, 1H), 3.91 (s, 3H).; **^{13}C NMR** (151 MHz, $CDCl_3$) δ 153.67, 141.07, 134.17, 126.84, 123.20, 121.73, 118.59, 112.40, 107.71, 56.51; **IR** (thin film): 3124.12, 2965.02, 2839.67, 2359.48, 1585.20, 1504.20, 1397.17, 1278.57, 1062.59, 750.17; **HRMS** (ESI): Calculated for [M+H_2O]= 231.0301; found 231.0294.

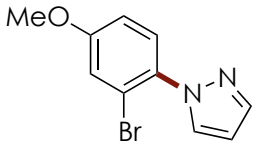

1-(2-bromo-4-methoxyphenyl)-1*H*-pyrazole (2.11). The title compound was prepared using **General Method A** with an irradiation time of 44 hours. The title compound was purified by column chromatography on silica gel (10% to 20% EtOAc/Hexanes) to yield a white solid in 54% (two trials). **^{1}H NMR** (600 MHz, $CDCl_3$) δ 7.71 (dd, *J* = 11.3, 2.1 Hz, 2H), 7.39 (d, *J* = 8.9 Hz, 1H), 7.20 (d, *J* = 2.5 Hz, 1H), 6.93 (dd, *J* = 8.7, 2.5 Hz, 1H), 6.43 (t, *J* = 2.3 Hz, 1H), 3.83 (s, 3H).; **^{13}C NMR** (151 MHz, $CDCl_3$) δ 153.71, 141.10, 134.21, 126.85, 123.24, 121.77, 118.62, 112.43, 107.73, 56.55.; **IR** (thin film): 3101.94, 2965.02, 2837.74, 1602.56, 1521.56, 1396.21, 1293.04, 1232.29, 1034.62, 850.45, 753.07; **HRMS** (ESI): Calculated for [M+H_2O]= 252.9976; found 252.9971.

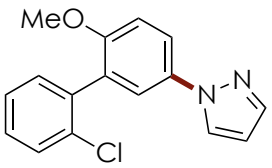

1-(2'-chloro-6-methoxy-[1,1'-biphenyl]-3-yl)-1*H*-pyrazole (2.12). The title compound was prepared using **General Method A** with an irradiation time of 20 hours. The title

compound was purified by column chromatography on silica gel (5% to 10% EtOAc/Hexanes) to yield the desire product in 75%. **^{1}H NMR** (600 MHz, $CDCl_3$) δ 7.86 (d, *J* = 2.4 Hz, 1H), 7.72 – 7.68 (m, 1H), 7.68 (d, *J* = 2.8 Hz, 1H), 7.52 (d, *J* = 2.8 Hz, 1H), 7.49 – 7.44 (m, 1H), 7.37 – 7.29 (m, 3H), 7.05 (d, *J* = 8.9 Hz, 1H), 6.45 (t, *J* = 2.0 Hz, 1H), 3.83 (s, 3H);; **^{13}C NMR** (151 MHz, $CDCl_3$) δ 155.51, 140.85, 136.88, 133.95, 133.70, 131.69, 129.51, 129.43, 129.09, 126.97, 126.69, 122.54, 120.44, 111.64, 107.41, 56.17. **IR** (thin film): 3055.66, 2934.16, 2835.81, 1593.88, 1518.67, 1400.07, 1253.50, 1141.65, 1046.19, 750.17; **HRMS** (ESI): Calculated for [M+H_2O]= 307.0614; found 307.0606.

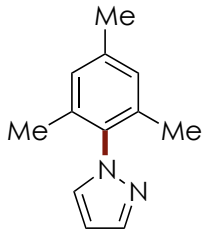

1-mesityl-1*H*-pyrazole (2.13). The title compound was prepared using **General Method B** with an irradiation time of 44 hours. The title compound was purified by column chromatography on silica gel (5% to 10% EtOAc/Hexanes) to yield a yellow oil in 82%. **^{1}H NMR** (400 MHz, $CDCl_3$) δ 8.17 (s, 1H), 7.86 (d, *J* = 2.3 Hz, 1H), 7.40 (s, 2H), 6.88 (s, 1H), 2.79 (s, 3H), 2.43 (s, 6H).; **^{13}C NMR** (151 MHz, $CDCl_3$) δ 140.07, 138.82, 137.05, 135.97, 130.93, 128.85, 105.83, 21.19, 17.30.; **IR** (thin film): 3103.87, 2921.63, 2358.52, 1594.84, 1516.74, 1393.32, 1190.83, 1044.26, 852.38, 751.14; **HRMS** (ESI): Calculated for [M+H_2O]=187.1235; found 187.1228.

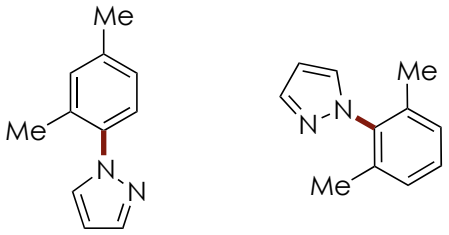

1-(2,4-dimethylphenyl)-1*H*-pyrazole and1-(2,6-dimethylphenyl)-1*H*-pyrazole. The title compounds were prepared using **General Method B** with an irradiation time of 44 hours. The average ratio of the inseparable mixture was >15:1 as determined by ^{1}H NMR of the isolated product. The title compound was purified by column chromatography on silica gel (5% to 10% EtOAc/Hexanes) to yield a yellow oil in 36%.

2.14a. ^{1}H NMR (400 MHz, $CDCl_3$) δ 8.00 (s, 1H), 7.85 (s, 1H), 7.51 (d, *J* = 7.4 Hz, 1H), 7.42 (s, 1H), 7.37 (d, *J* = 7.4 Hz, 1H), 6.72 (s, 1H), 2.68 (s, 3H), 2.50 (s, 3H).; **^{13}C NMR** (151 MHz, $CDCl_3$) δ 136.07, 134.08, 133.47, 129.32, 127.74, 126.68, 123.05, 121.93, 102.03, 17.13, 13.90.

2.14b. ^{1}H NMR (400 MHz, $CDCl_3$) δ 8.04 (s, 1H), 7.74 (s, 1H), 7.25 (s, 3H), 6.75 (s, 1H), 2.31 (s, 6H).; **^{13}C NMR** (151 MHz, $CDCl_3$) δ 136.03, 135.21, 132.07, 126.81, 124.91, 124.07, 101.89, 13.28.

IR (thin film): 3103.94, 2972.73, 2936.09, 287052, 1670.05, 1507.10, 1464.67, 1395.25, 1241.93, 1043.30; **HRMS** (ESI): Calculated for [M+H_2O]= 195.0898; found 195.0891.

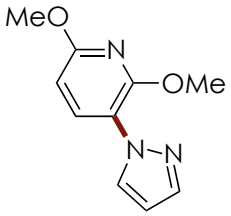

2,6-dimethoxy-3-(1*H*-pyrazol-1-yl)pyridine (2.15). The title compound was prepared using **General Method A** with an irradiation time of 20 hours. The title compound was

purified by column chromatography on silica gel (0% to 10% EtOAc/Hexanes) to yield the desired product in 45%. **^{1}H NMR** (600 MHz, $CDCl_3$) δ 7.98 (d, *J* = 2.4 Hz, 1H), 7.93 (d, *J* = 8.4 Hz, 1H), 7.68 (d, *J* = 1.6 Hz, 1H), 6.45 – 6.37 (m, 2H), 4.02 (s, 3H), 3.96 (s, 3H). **^{13}C NMR** (151 MHz, $CDCl_3$) δ 161.15, 154.17, 140.22, 136.29, 131.06, 117.65, 106.33, 101.58, 54.02, 53.95. **IR** (thin film): 3103.87, 2949.59, 1592.91, 1591.63, 1486.85, 1392.35, 1230.36, 1021.12, 812.85, 753.07; **HRMS** (ESI): Calculated for [M+H_2O]= 228.0749; found 228.0741.

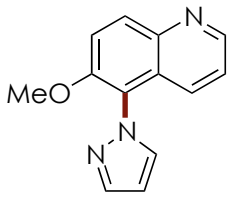

6-methoxy-5-(1*H*-pyrazol-1-yl)quinoline (2.16). The title compound was prepared using **General Method A** with an irradiation time of 20 hours. The title compound was purified by column chromatography on silica gel (50% to 100% EtOAc/Hexanes) to yield a yellow oil in 60%. **^{1}H NMR** (600 MHz, $CDCl_3$) δ 8.79 (dt, *J* = 4.1, 2.1 Hz, 1H), 8.21 (d, *J* = 9.4 Hz, 1H), 7.85 (t, *J* = 2.1 Hz, 1H), 7.72-7.62 (m, 2H), 7.58 (d, *J* = 9.4 Hz, 1H), 7.33 (m, 1H), 6.54 (m, 1H), 3.89 (s, 3H).; **^{13}C NMR** (151 MHz, $CDCl_3$) δ 152.42, 148.91, 143.37, 140.87, 133.16, 132.07, 131.01, 127.29, 116.62, 106.30, 56.92.; **IR** (thin film): 311640, 2941.88, 1618.95, 1506.13, 1398.14, 1325.82, 1267.97, 1091.51, 908.31, 827.31; **HRMS** (ESI): Calculated for [M+H_2O]= 226.0980; found 226.0974.

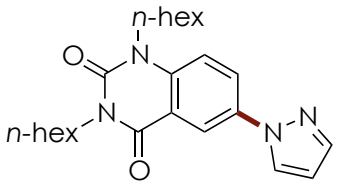

1,3-dihexyl-6-(1*H*-pyrazol-1-yl)quinazoline-2,4(1*H*,3*H*)-dione (2.17). The title compound was prepared using **General Method A** with an irradiation time of 20 hours. The average *para*:*ortho* ratio of the inseparable mixture was >15:1 as determined by ^{1}H NMR of the isolated product. The title compound was purified by column chromatography on silica gel (10% to 20% EtOAc/Hexanes) to yield a yellow oil in 43%. **^{1}H NMR** (600 MHz, $CDCl_3$) δ 8.36 (d, *J* = 3.0 Hz, 1H), 8.18-8.17 (m, 1H), 8.00 (d, *J* = 2.9 Hz, 1H), 7.73 (s, 1H), 7.27-7.26 (m, 1H), 6.49 (s, 1H), 4.14-4.07 (m, 4H), 1.73-1.68 (m, 4H), 1.44-1.32 (m, 12H), 0.97-0.84 (m, 6H).; **^{13}C NMR** (151 MHz, $CDCl_3$) δ 161.22, 150.43, 141.43, 137.96, 135.49, 126.77, 126.43, 117.76, 116.27, 115.05, 108.17, 44.04, 42.19, 31.54, 31.49, 27.78, 27.36, 26.68, 26.49, 22.60, 14.09, 14.04.; **IR** (thin film): 3122.19, 2930.31, 2857.99, 1703.80, 1659.45, 1524.45, 1480.10, 1394.28, 1045.23, 752.10; **HRMS** (ESI): Calculated for [M+H_2O]= 419.2423; found 419.2416.

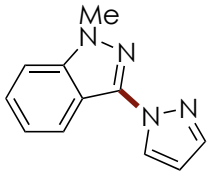

1-methyl-3-(1*H*-pyrazol-1-yl)-1*H*-indazole (2.18). The title compound was prepared using **General Method A** with an irradiation time of 20 hours. The title compound was purified by column chromatography on silica gel (0% to 20% EtOAc/Hexanes) to yield the desired product in 43%. **^{1}H NMR** (600 MHz, $CDCl_3$) δ 8.32 (dt, *J* = 8.3, 1.0 Hz, 1H), 8.25 (d, *J* = 2.5 Hz, 1H), 7.81 (d, *J* = 2.0 Hz, 1H), 7.45 (ddd, *J* = 8.3, 6.8, 1.1 Hz, 1H), 7.36 (d, *J* = 8.6 Hz, 1H), 7.24-7.16 (m, 1H), 6.49 (t, *J* = 2.1 Hz, 1H), 4.05 (s, 3H).; **^{13}C NMR** (151 MHz, $CDCl_3$) δ 141.68, 141.42, 127.84, 127.58, 122.63, 121.37, 115.20, 109.01, 107.01, 35.65.; **IR** (thin film): 3124.12, 3063.37, 2936.09, 1617.98, 1549.52,

1397.17, 1256.40, 1043.30, 919.88, 743.43; **HRMS** (ESI): Calculated for [M+H_2O]= 221.0803; found 221.0796.

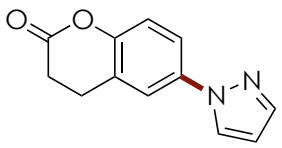

6-(1*H*-pyrazol-1-yl)chroman-2-one (2.19). The title compound was prepared using a modified **General Method A** procedure. The reaction was run with 2 equivalences of 3,4-dihydrocoumarin and 1 equivalent of pyrazole (2:1 ratio of arene: amine) without a cooling fan and with an irradiation time of 44 hours. The title compound was purified by column chromatography on silica gel (25% to 50% EtOAc/Hexanes) to yield a yellow solid in 30%. **^{1}H NMR** (600 MHz, $CDCl_3$) δ 7.87 (d, *J* = 2.5 Hz, 1H), 7.71 (d, *J* = 1.7 Hz, 1H), 7.60 (d, *J* = 2.6 Hz, 1H), 7.51 (dd, *J* = 8.7, 2.6 Hz, 1H), 7.11 (d, *J* = 8.7 Hz, 1H), 6.47 (t, *J* = 2.2 Hz, 1H), 3.06 (dd, *J* = 8.3, 6.3 Hz, 2H), 2.81 (dd, *J* = 8.3, 6.2 Hz, 2H).; **^{13}C NMR** (151 MHz, $CDCl_3$) δ168.06, 150.33, 141.28, 136.73, 126.86, 123.94, 119.25, 118.90, 117.85, 107.90,, 29.03, 23.93.; **IR** (thin film): 3127.01, 2918.73, 1769.37, 1600.63, 1502.28, 1395.25, 1343.18, 1217.83, 1144.55, 899.63; **HRMS** (ESI): Calculated for [M+H_2O]= 215.0820; found 201.0813.

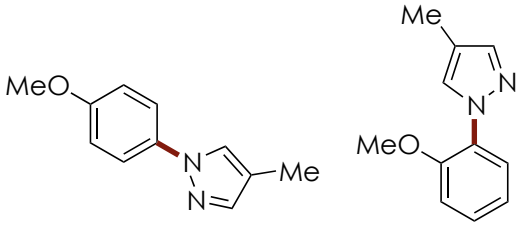

1-(4-methoxyphenyl)-4-methyl-1*H*-pyrazole, 1-(2-methoxyphenyl)-4-methyl-1*H*-pyrazole. The title compounds were prepared using **General Method A** with an irradiation time of 20 hours. The average *para*:*ortho* ratio of the inseparable mixture was

8:1 as determined by ^{1}H NMR of the isolated product. The title compound was purified by column chromatography on silica gel (20% EtOAc/Hexanes) to yield the desired product in 68%.

2.22a. ^{1}H NMR (600 MHz, $CDCl_3$) δ 7.59 (s, 1H), 7.54 (d, *J* = 9.0 Hz, 2H), 7.49 (s, 1H), 6.94 (d, *J* = 9.0 Hz, 2H), 3.82 (s, 3H), 2.14 (s, 3H).; **^{13}C NMR** (151 MHz, $CDCl_3$) δ 157.96, 141.30, 134.23, 125.55, 120.44, 117.84, 114.52, 55.61, 9.03.

2.22b. ^{1}H NMR (600 MHz, $CDCl_3$) δ = 7.80 (s, 1H), 7.68 (dd, *J* = 7.9, 1.5 Hz, 1H), 7.51 (s, 1H), 7.27 – 7.24 (m, 1H), 7.06 – 7.00 (m, 2H), 3.86 (s, 3H), 2.16 (s, 3H).; **^{13}C NMR** (151 MHz, $CDCl_3$) δ = 151.21, 140.89, 130.24, 130.00, 127.70, 125.05, 121.21, 116.69, 112.27, 77.16, 55.97, 9.08.

IR (thin film): 2966.95, 2839.67, 1519.63, 1455.03, 1261.22, 1181.19, 1041.37, 953.63, 829.24, 610.36; **HRMS** (ESI): Calculated for [M+H_2O]= 211.0847; found 211.0842.

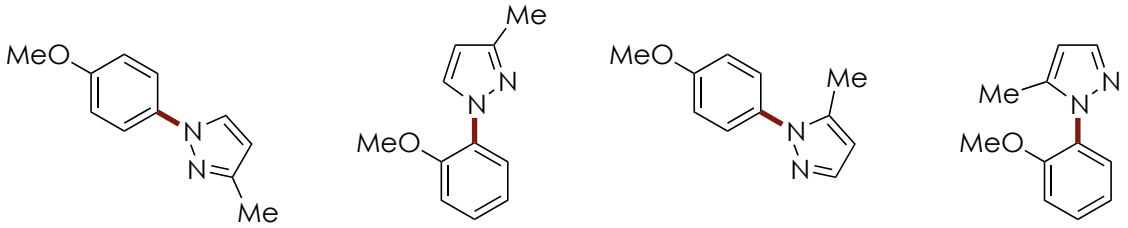

1-(4-methoxyphenyl)-3-methyl-1*H*-pyrazole, 1-(2-methoxyphenyl)-3-methyl-1*H*-pyrazole[9], 1-(4-methoxyphenyl)-5-methyl-1*H*-pyrazole[10], 1-(2-methoxyphenyl)-5-methyl-1*H*-pyrazole[9]

The title compounds were prepared using **General Method A** with an irradiation time of 20 hours. The average *para*:*ortho* ratio of the inseparable mixture was 3.6:1 N1 (6:1): N2 (8:1) as determined by ^{1}H NMR of the isolated product. The title compound was purified by column chromatography on silica gel (5% to 50% EtOAc/Hexanes) to yield the desired product in 73%.

2.23a. **^{1}H NMR** (600 MHz, $CDCl_3$) δ 7.70 (s, 1H), 7.54 (d, *J* = 8.9 Hz, 2H), 6.94 (d, *J* = 8.9 Hz, 2H), 6.20 (s, 1H), 3.82 (s, 3H), 2.37 (s, 3H).; **13C NMR** (151 MHz, CDCl3) δ 157.86, 150.00, 134.09, 127.43, 120.53, 114.43, 106.99, 55.53, 13.72.;

2.23b. **^{1}H NMR** (600 MHz, $CDCl_3$) δ 7.92 (d, *J* = 2.2 Hz, 1H), 7.72 – 7.69 (m, 1H), 7.26 – 7.22 (m, 1H), 7.07 – 6.99 (m, 2H), 6.21 – 6.20 (m, 1H), 3.85 (s, 3H), 2.38 (s, 3H).; **^{13}C NMR** (151 MHz, $CDCl_3$) δ 151.16, 149.33, 132.31, 129.79, 127.54, 125.07, 121.13, 112.16, 106.14, 55.89, 13.67.

IR (thin film): 3459.67, 2932.23, 1646.91, 1515.77, 1456.96, 1363.43, 1247.72, 1181.19,1045.23, 830.21 **HRMS** (ESI): Calculated for [M+H_2O]= 211.0847; found 211.0841.

2.23c. **^{1}H NMR** (600 MHz, $CDCl_3$) δ 7.54 (d, *J* = 1.6 Hz, 1H), 7.34 (d, *J* = 8.9 Hz, 2H), 6.97 (d, *J* = 8.9 Hz, 2H), 6.17 (d, *J* = 1.3 Hz, 1H), 3.85 (s, 3H), 2.29 (s, 3H).; **^{13}C NMR** (151 MHz, $CDCl_3$) δ 159.09, 139.59, 138.82, 133.17, 126.53, 114.27, 106.42, 55.66, 12.34.

2.23d. **^{1}H NMR** (600 MHz, $CDCl_3$) δ 7.59 (d, *J* = 1.6 Hz, 1H), 7.43 – 7.39 (m, 1H), 7.33 – 7.31 (m, 1H), 7.07 – 7.01 (m, 2H), 6.17 – 6.16 (m, 1H), 3.79 (s, 3H), 2.15 (s, 3H).; **^{13}C NMR** (151 MHz, $CDCl_3$) δ 154.81, 140.75, 140.00, 130.26, 129.24,120.92, 112.12, 105.30, 55.93, 11.41.

HRMS (ESI): Calculated for [M+H_2O]= 211.0847; found 211.0841.

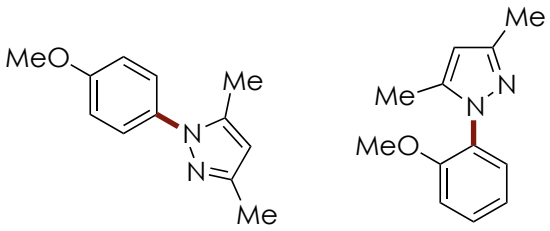

1-(4-methoxyphenyl)-3,5-dimethyl-1*H*-pyrazole[11]**, 1-(2-methoxyphenyl)-3,5-dimethyl-1*H*- pyrazole**[12]

The title compounds were prepared using Method A with an irradiation time of 20 hours. The average *para*:*ortho* ratio of the inseparable mixture was 7.5:1 as determined by ^{1}H NMR of the isolated product. The title compound was purified by column chromatography on silica gel (0% to 20% EtOAc/Hexanes) to yield the desired product in 85% (two trials).

2.24a. ^{1}H NMR (600 MHz, $CDCl_3$) δ 7.32 (d, *J* = 8.9 Hz, 2H), 6.95 (d, *J* = 8.9 Hz, 2H), 5.96 (s, 1H), 3.84 (s, 3H), 2.29 (s, 3H), 2.24 (s, 3H).; **^{13}C NMR** (151 MHz, $CDCl_3$) δ 158.87, 148.63, 139.57, 133.22, 126.49, 114.21, 106.35, 55.64, 13.64, 12.28.

2.24b. ^{1}H NMR (600 MHz, $CDCl_3$) δ 7.38 (td, *J* = 8.0, 1.7 Hz, 1H), 7.33 – 7.32 (m, 1H), 7.04 – 6.99 (m, 2H), 5.96 (s, 1H), 3.79 (s, 3H), 2.30 (s, 3H), 2.09 (s, 3H).; **^{13}C NMR** (151 MHz, $CDCl_3$) δ 154.77, 149.03, 141.56, 130.00, 129.37, 128.79, 120.90, 111.97, 105.27, 55.88, 13.80, 11.39.

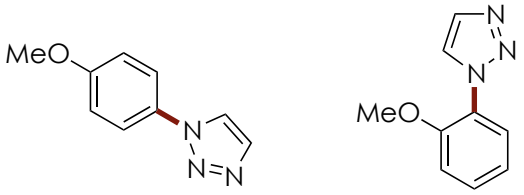

1-(4-methoxyphenyl)-1*H*-1,2,3-triazole[13]**, 1-(2-methoxyphenyl)-1*H*-1,2,3-triazole**[13]

The title compounds were prepared using **General Method A** with an irradiation time of 20 hours. The average *para*:*ortho* ratio of the inseparable mixture was 3.5:1 as determined by ^{1}H NMR of the isolated product. The title compound was purified by column chromatography on silica gel (0% to 20% EtOAc/Hexanes) to yield the desired products in 71%.

2.25a. **^{1}H NMR** (600 MHz, $CDCl_3$) δ 7.91 (s, 1H), 7.83 (s, 1H), 7.64 (d, *J* = 8.8 Hz, 2H), 7.03 (d, *J* = 8.8 Hz, 2H), 3.88 (s, 3H).; **^{13}C NMR** (151 MHz, $CDCl_3$) δ 159.95, 134.42, 122.46, 121.98, 114.91, 112.38, 55.77.

2.25b. **^{1}H NMR** (600 MHz, $CDCl_3$) δ 8.12 (s, 1H), 7.81 (s, 1H), 7.78 (d, *J* = 7.9 Hz, 1H), 7.43 (t, *J* = 7.9 Hz, 1H), 7.14 – 7.05 (m, 2H), 3.89 (s, 3H).; **^{13}C NMR** (151 MHz, $CDCl_3$) δ 151.31, 141.52, 133.39, 131.66, 130.64, 130.20, 125.74, 121.37, 56.11.

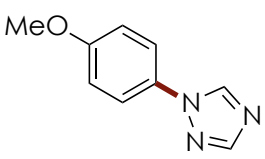

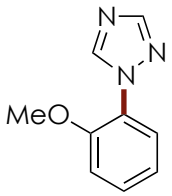

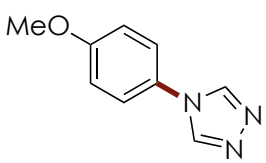

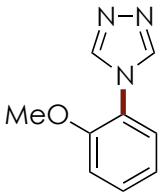

1-(4-methoxyphenyl)-1*H*-1,2,4-triazole[14], **1-(2-methoxyphenyl)-1*H*-1,2,4-triazole**[14], **4-(4-methoxyphenyl)-4*H*-1,2,4-triazole**[15], **4-(2-methoxyphenyl)-4*H*-1,2,4-triazole**

The title compounds were prepared from anisole and 1,2,4-triazole according to **General Method A** with an irradiation time of 20 hours. The crude residue was purified by column chromatography on silica gel with an eluent of 50% EtOAc/hexanes to 5% MeOH/EtOAc from which were isolated two sets of fractions. The first contained a mixture of *N*1 isomers **2.26a** and **2.26b** in 36% yield and a 4.5:1 ratio, but which was separable by additional chromatography. The second contained an inseparable mixture of *N*4 isomers **2.26c** and **2.26.d** in 40% yield and a 4:1 ratio. The spectral data for the known compounds **2.26a**(*58*) and **2.26b**(*58*) are consistent with the literature reports. Although **2.26c** was reportedly synthesized (*59*), the analytical data provided by the authors appeared identical to those reported for compound **2.26a**. We provide a correct assignment for **2.26c** with the corresponding spectral data.

2.26a. **^{1}H NMR** (600 MHz, CDCl3) δ 8.44 (s, 1H), 8.07 (s, 1H), 7.56 (d, *J* = 8.9 Hz, 2H),

7.00 (d, J = 8.9 Hz, 2H), 3.85 (s, 3H). **^{13}C NMR** (151 MHz, CDCl3) δ 159.56, 152.48, 140.90, 130.56, 121.98, 114.92, 55.74.

2.26b . ^{1}H NMR (600 MHz, CDCl3) δ 8.74 (s, 1H), 8.07 (s, 1H), 7.77 (dd, J = 7.9, 1.3 Hz, 1H), 7.39 – 7.32 (m, 1H), 7.10 – 7.07 (m, 2H), 3.92 (s, 3H). **^{13}C NMR** (151 MHz, CDCl3) δ 151.40, 151.04, 144.71, 129.21, 126.44, 124.66, 121.45, 112.31, 56.11.

2.26c. ^{1}H NMR (600 MHz, CDCl3) δ 8.38 (s, 2H), 7.29 (d, J = 8.9 Hz, 2H), 7.01 (d, J = 8.9 Hz, 2H), 3.85 (s, 3H). **^{13}C NMR** (151 MHz, CDCl3) δ 160.20, 142.01, 126.78, 124.15, 115.41, 55.82.

2.26d. ^{1}H NMR (600 MHz, CDCl3) δ 8.40 (s, 2H), 7.44 – 7.41 (m, 1H), 7.28 – 7.27 (m, 1H), 7.09 – 7.05 (m, 2H), 3.85 (s, 3H). **^{13}C NMR** (151 MHz, CDCl3) δ 152.42, 143.02, 130.55, 125.26, 121.35, 112.58, 56.04.

IR (thin film): 3438.46, 3139.54, 1536.99, 2836.77, 1457.92, 1269.90, 1256.40, 1097.30, 1032.69, 831.17; **HRMS**: Calculated for $(M+H)^{+}$: 176.0824; found: 176.0817.

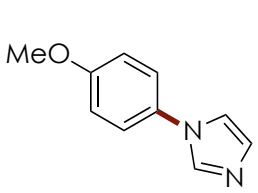

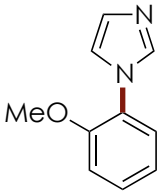

1-(4-methoxyphenyl)-1*H*-imidazole, 1-(2-methoxyphenyl)-1*H*-imidazole. The title compounds were prepared using **General Method B** with the following modifications: 1.0 equiv. anisole and 2.0 equiv. imidazole were irradiated for 20 hours without nitrogen sparging or a balloon of nitrogen over the course of the reaction. Note: **General Method A** was incompatible with imidazole as a substrate, leading to complete suppression of product under the aerobic conditions. The crude residue was purified by column chromatography on silica gel with an eluent of 75% EtOAc/hexanes to EtOAc to 5%

MeOH/EtOAc giving an inseparable mixture of **2.27a** and **2.27b** in a ratio of 4:1 in 55% yield, along with the product of *ipso*-substitution, **2.27c** in 7% yield. The spectral data match the literature report for compounds **2.27a, 2.27b,** and **2.27c** (*63*)**.**

2.27a. ^{1}H NMR (600 MHz, CDCl3) δ 7.76 (s, 1H), 7.30 (d, *J* = 8.9 Hz, 2H), 7.20 (s, 1H), 7.18 (s, 1H), 6.98 (d, *J* = 8.8 Hz, 2H), 3.85 (s, 3H).

2.27b . ^{1}H NMR (600 MHz, CDCl3) δ 7.78 (s, 1H), 7.37 – 7.34 (m, 1H), 7.29 – 7.28 (m, 1H), 7.21 (s, 1H), 7.16 (s, 1H), 7.07 – 7.02 (m, 2H), 3.85 (s, 3H).

2.27c . ^{1}H NMR (600 MHz, CDCl3) δ7.86 (s, 1H), 7.48 (t, *J* = 7.8 Hz, 2H), 7.41 – 7.36 (m, 3H), 7.27 (s, 1H), 7.21 (s, 1H).

^{13}**C NMR** (151 MHz, CDCl3) δ 158.92, 152.58, 137.81, 137.35, 135.86, 135.58, 130.69, 130.40, 130.03, 129.89, 128.96, 128.79, 127.49, 126.50, 125.53, 123.20, 121.47, 121.00, 120.28, 118.77, 118.25, 114.89, 112.34, 55.82, 55.61.

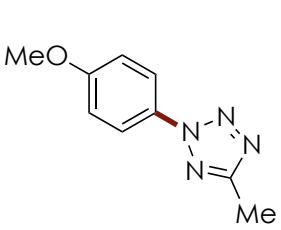

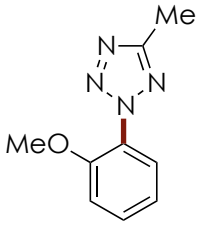

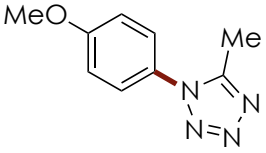

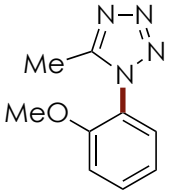

2-(4-methoxyphenyl)-5-methyl-2*H*-tetrazole[16]**, 2-(2-methoxyphenyl)-5-methyl-2*H*-tetrazole, 1-(4-methoxyphenyl)-5-methyl-1*H*-tetrazole**[17]**, 1-(2-methoxyphenyl)-5-methyl-1*H*-tetrazole**[17]

The title compounds were prepared using **General Method A** with an irradiation time of 20 hours. The average *para*:*ortho* ratio of the inseparable mixture was 1.5:1 N1 (10:1): N2 (10:1) as determined by ^{1}H NMR of the isolated product. The title compound was purified by column chromatography on silica gel (0% to 20% EtOAc/Hexanes) to yield a white solid in 53%.

2.28a. **^{1}H NMR** (600 MHz, $CDCl_3$) δ 8.00 (d, *J* = 9.1 Hz, 2H), 7.03 (d, *J* = 9.1 Hz, 2H), 3.88 (s, 3H), 2.62 (s, 3H).; **^{13}C NMR** (151 MHz, $CDCl_3$) δ 163.11, 160.48, 130.61, 121.40, 114.77, 77.16, 55.79, 11.13.

2.28b . **^{1}H NMR** (600 MHz, $CDCl_3$) δ 7.58 – 7.46 (m, 2H), 7.18 – 7.06 (m, 2H), 3.87 (s, 3H), 2.66 (s, 3H).; **^{13}C NMR** (151 MHz, $CDCl_3$) δ 162.96, 153.55, 132.00, 127.12, 126.51, 120.84, 112.80, 77.16, 56.38, 11.16.

IR (thin film): 2943.80, 2840.63, 1732.73, 1646.91, 1507.10, 1456.96, 1418.39, 1254.47, 1023.05, 837.92; **HRMS** (ESI): Calculated for [M+H_2O]= 191.0933; found 191.0927.

2.28c. **^{1}H NMR** (600 MHz, $CDCl_3$) δ 7.35 (d, *J* = 7.4 Hz, 2H), 7.05 (d, *J* = 7.3 Hz, 2H), 3.87 (s, 3H), 2.55 (s, 3H).; **^{13}C NMR** (151 MHz, $CDCl_3$) δ 160.93, 151.78, 126.54, 126.16, 115.07, 55.80, 9.71.

2.28d. **^{1}H NMR** (600 MHz, $CDCl_3$) δ 7.54 (t, *J* = 8.0 Hz, 1H), 7.35 – 7.32 (m, 1H), 7.12 – 7.09 (m, 2H), 3.81 (s, 3H), 2.42 (s, 3H).; **^{13}C NMR** (151 MHz, $CDCl_3$) δ 153.72, 153.41, 132.44, 128.09, 122.38, 121.23, 112.43, 55.99, 9.12.

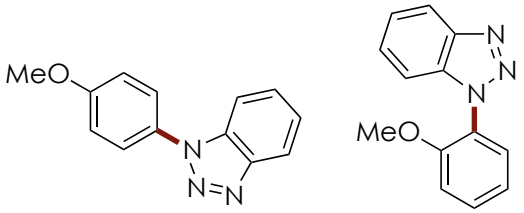

1-(4-methoxyphenyl)-1*H*-benzo[*d*][1,2,3]triazole[18]**, 1-(2-methoxyphenyl)-1*H*-benzo[*d*][1,2,3]triazole**

The title compounds were prepared using **General Method A** with an irradiation time of 20 hours. The average *para*:*ortho* ratio of the inseparable mixture was 3:1 as determined by ^{1}H NMR of the isolated product. The title compound was purified by column

chromatography on silica gel (5% to 10% EtOAc/Hexanes) to yield the desired product in 57%.

2.29a. **^{1}H NMR** (600 MHz, $CDCl_3$) δ 8.14 (d, *J* = 8.4 Hz, 1H), 7.68 (app d, *J* = 8.9 Hz, 3H), 7.54 (t, *J* = 8.0 Hz, 1H), 7.43 (t, *J* = 7.6 Hz, 1H), 7.12 (d, *J* = 8.9 Hz, 2H), 3.92 (s, 3H).; **^{13}C NMR** (151 MHz, $CDCl_3$) δ 159.88, 146.36, 132.70, 130.04, 128.10, 124.67, 124.32, 120.25, 115.04, 110.33, 55.75.

2.29b . **^{1}H NMR** (600 MHz, $CDCl_3$) δ 8.12 (d, *J* = 8.2 Hz, 1H), 7.55 – 7.49 (m, 2H), 7.49 – 7.44 (m, 1H), 7.37 (app t, *J* = 7.4 Hz, 2H), 7.17 – 7.12 (m, 2H), 3.79 (s, 3H).; **^{13}C NMR** (151 MHz, $CDCl_3$) δ 153.75, 145.74, 134.14, 131.11, 128.19, 127.62, 125.35, 123.92, 121.16, 119.91, 112.43, 111.27, 55.88.

IR (thin film): 3064.33, 2934.16, 2358.52, 1613.16, 1517.70, 1454.06, 1253.50, 1067.41, 833.41, 746.32; **HRMS** (ESI): Calculated for [M+H_2O]= 226.0980; found 226.0975.

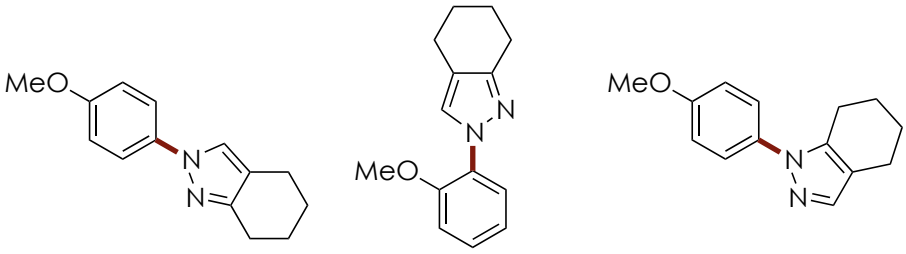

2-(4-methoxyphenyl)-4,5,6,7-tetrahydro-2*H*-indazole, 2-(2-methoxyphenyl)-4,5,6,7-tetrahydro-2*H*-indazole, 1-(4-methoxyphenyl)-4,5,6,7-tetrahydro-1*H*-indazole[19]

The title compounds were prepared using **General Method A** with an irradiation time of 20 hours. The average *para*:*ortho* ratio of the inseparable mixture was 1:1 N1(10:1): N2 (>20:1) as determined by ^{1}H NMR of the isolated product. The title compound was purified by column chromatography on silica gel (0% to 20% EtOAc/Hexanes) to yield the desired product in 65%.

2.30a. **^{1}H NMR** (600 MHz, $CDCl_3$) δ 7.54 – 7.49 (m, 3H), 6.93 (d, *J* = 9.0 Hz, 2H), 3.82 (s, 3H), 2.77 (t, *J* = 6.3 Hz, 2H), 2.61 (t, *J* = 6.2 Hz, 2H), 1.93 – 1.81 (m, 2H), 1.81 – 1.72 (m, 2H).; **^{13}C NMR** (151 MHz, $CDCl_3$) δ 157.72, 150.82, 134.46, 123.93, 120.37, 117.84, 114.50, 77.16, 55.64, 23.63, 23.61, 20.80.

2.30b. **^{1}H NMR** (600 MHz, $CDCl_3$) δ 7.72 (s, 1H), 7.68 (dd, *J* = 7.9, 1.6 Hz, 1H), 7.25 – 7.21 (m, 1H), 7.04 – 6.99 (m, 2H), 3.87 (s, 2H), 2.80 – 2.74 (m, 2H), 2.64 – 2.58 (m, 2H), 1.87 – 1.83 (m, 2H), 1.79 – 1.75 (m, 2H).; **^{13}C NMR** (151 MHz, $CDCl_3$) δ 151.09, 150.18, 130.19, 128.64, 127.27, 125.02, 121.23, 116.86, 112.15, 77.16, 55.98, 23.66, 23.58, 20.85.

IR (thin film): 2932.23, 2853.17, 1517.70, 1456.96, 1377.89, 1254.47, 1023.05, 837.92; **HRMS** (ESI): Calculated for [M+H_2O]= 251.1160; found 251.1154.

2.30c. **^{1}H NMR** (600 MHz, $CDCl_3$) δ 7.43 (s, 1H), 7.38 (d, *J* = 8.9 Hz, 2H), 6.95 (d, *J* = 8.9 Hz, 2H), 3.84 (s, 3H), 2.66 (t, *J* = 5.8 Hz, 2H), 2.58 (t, *J* = 5.7 Hz, 2H), 1.82 – 1.75 (m, 4H).; **^{13}C NMR** (151 MHz, $CDCl_3$) δ 158.46, 138.40, 138.29, 133.56, 124.84, 117.34, 114.29, 77.16, 55.67, 23.47, 23.27, 23.03, 20.88.

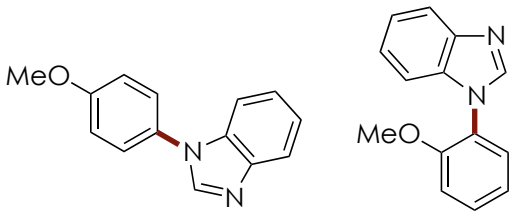

1-(4-methoxyphenyl)-1*H*-benzo[*d*]imidazole[20], 1-(2-methoxyphenyl)-1*H*-benzo[*d*]imidazole[21]

The title compounds were prepared using Method A with an irradiation time of 20 hours. The average *para*:*ortho* ratio of the inseparable mixture was 5:1 as determined by ^{1}H

NMR of the isolated product. The title compound was purified by column chromatography on silica gel (1.5% MeOH/DCM) to yield the desired product in 72%.

2.31a. **^{1}H NMR** (600 MHz, $CDCl_3$) δ 8.04 (s, 1H), 7.88 – 7.86 (m, 1H), 7.45 – 7.44 (m, 1H), 7.40 (d, *J* = 8.9 Hz, 2H), 7.28 – 7.33 (m, 2H), 7.06 (d, *J* = 8.9 Hz, 2H), 3.87 (s, 3H).; **^{13}C NMR** (151 MHz, $CDCl_3$) δ 159.37, 143.90, 142.62, 134.29, 129.20, 125.77, 123.57, 122.63, 120.55, 115.17, 110.40, 55.71.

2.31b. **^{1}H NMR** (600 MHz, $CDCl_3$) δ 8.07 (s, 1H), 7.88 – 7.86 (m, 1H), 7.45 – 7.42 (m, 1H), 7.41 – 7.39 (m, 1H), 7.33 – 7.27 (m, 3H), 7.13 – 7.08 (m, 2H), 3.78 (s, 3H).; **^{13}C NMR** (151 MHz, $CDCl_3$) δ 154.00, 143.39, 134.50, 129.78, 127.31, 124.84, 123.29, 122.37, 121.07, 120.30, 112.50, 110.81, 55.79.

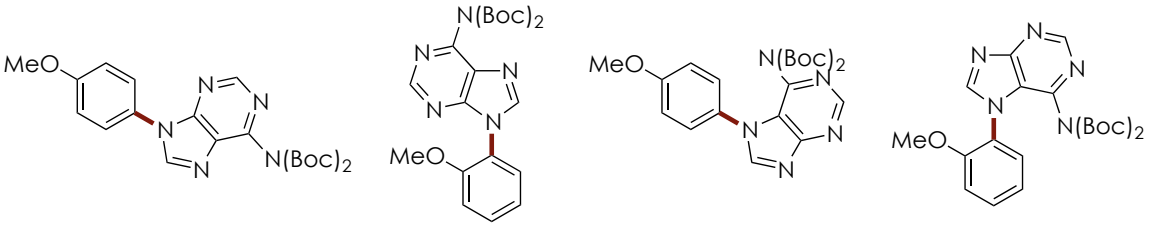

9-(4-methoxyphenyl)-*N6,N6*-bis(*tert*-butoxycarbonyl)-9*H*-purin-6-amine, 9-(2-methoxyphenyl)-*N6,N6*-bis(*tert*-butoxycarbonyl)-9*H*-purin-6-amine, 7-(4-methoxyphenyl)-*N6,N6*-bis(*tert*-butoxycarbonyl)-7*H*-purin-6-amine, 7-(2-methoxyphenyl)-*N6,N6*-bis(*tert*-butoxycarbonyl)-7*H*-purin-6-amine. The title compounds were prepared from anisole and Boc2-adenine **S10** according to **General Method A** with an irradiation time of 20 hours and the modification that 1.25 equiv. The crude residue was purified by column chromatography on silica gel with an eluent of hexanes to 50% EtOAc/hexanes to EtOAc from which were isolated two sets of fractions. The first contained an inseparable mixture of *N*9 isomers **2.32a** and **2.32b** in 47% yield and a 3:1 ratio. The second contained an inseparable mixture of *N*7 isomers **2.32c** and

2.32d in 52% yield and 4:1 ratio.

2.32a. **^{1}H NMR** (600 MHz, $CDCl_3$) δ 8.91 (s, 1H), 8.28 (s, 1H), 7.59 (d, *J* = 8.9 Hz, 2H), 7.10 (d, *J* = 8.9 Hz, 2H), 3.89 (s, 3H), 1.49 (s, 18H). **^{13}C NMR** (151 MHz, $CDCl_3$) δ 159.66, 153.69, 153.49, 153.10, 152.61, 152.45, 150.64, 150.49, 150.33, 143.94, 130.52, 129.01, 128.41, 127.47, 126.86, 125.18, 122.29, 121.08, 115.06, 112.33, 83.79, 83.68, 55.61, 27.75, 27.74.

2.32b. **^{1}H NMR** (600 MHz, $CDCl_3$) δ 8.87 (s, 1H), 8.28 (s, 1H), 7.57 (d, *J* = 5.9 Hz, 1H), 7.48 (t, *J* = 7.9 Hz, 1H), 7.18 – 7.11 (m, 2H), 3.80 (s, 3H), 1.48 (s, 18H). **^{13}C NMR** (151 MHz, $CDCl_3$) δ 153.69, 153.49, 152.45, 150.33, 145.86, 130.52, 128.41, 126.86, 125.12, 122.29, 121.08, 112.33, 83.68, 55.80, 27.74.

IR (thin film): 2979.48, 2935.13, 1790.58, 1758.76, 1595.81, 1519.63, 1455.99, 1340.28, 1140.69; **HRMS**: Calculated for $(M+H)^+$: 442.2090; found: 442.2087.

2.32c. **^{1}H NMR** (600 MHz, $CDCl_3$) δ 9.08 (s, 1H), 8.28 (s, 1H), 7.33 (d, *J* = 8.8 Hz, 2H), 6.99 (d, *J* = 8.8 Hz, 2H), 3.87 (s, 3H), 1.30 (s, 18H). **^{13}C NMR** (151 MHz, $CDCl_3$) δ 163.68, 160.48, 153.06, 149.84, 148.71, 144.26, 127.70, 126.88, 121.51, 115.00, 84.15, 55.83, 27.93.

2.32d . **^{1}H NMR** (600 MHz, $CDCl_3$) δ 9.06 (s, 1H), 8.33 (s, 1H), 7.48 (t, *J* = 8.0 Hz, 1H), 7.36 – 7.33 (m, 1H), 7.10 – 7.04 (m, 2H), 3.79 (s, 3H), 1.30 (s, 18H). **^{13}C NMR** (151 MHz, $CDCl_3$) δ163.49, 153.79, 152.77, 150.13, 144.08, 131.04, 127.65, 125.32, 123.49, 121.34, 121.03, 112.41, 83.94, 55.92, 27.85.

IR (thin film): 3077.83, 2980.45, 2935.13, 2237.99, 1739.48, 1768.40, 1613.16, 1515.77, 1369.21, 1252.54; **HRMS**: Calculated for $(M+Na)^+$: 464.1910; found: 464.1910.

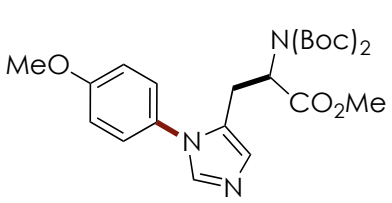

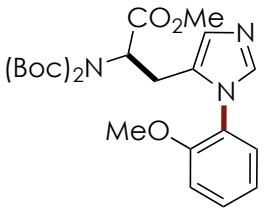

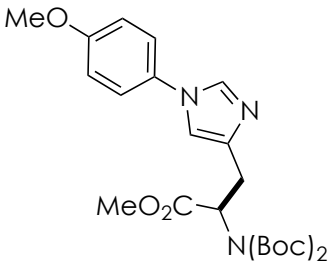

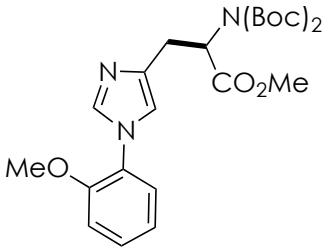

methyl N^{α}-(*tert*-butoxycarbonyl)-N^{τ}-(4-methoxyphenyl)-*L*-histidinate, methyl N^{α}-(*tert*- butoxycarbonyl)-N^{τ}-(2-methoxyphenyl)-*L*-histidinate, methyl N^{α}-(*tert*-butoxycarbonyl)-N^{π}-(4-methoxyphenyl)-*L*-histidinate, methyl N^{α}-(*tert*-butoxycarbonyl)-N^{π}-(2-methoxyphenyl)-*L*-histidinate. The title compounds were prepared using **General Method B** with the following modifications: 1.0 equiv. anisole and 2.0 equiv. of histidine nucleophile were irradiated for 20 hours without nitrogen sparging or a balloon of nitrogen over the course of the reaction. Note: **General Method A** was incompatible with imidazole as a substrate, leading to complete suppression of product under the aerobic conditions. The crude residue was purified by column chromatography on silica gel with an eluent of 75% EtOAc/hexanes to EtOAc to 5% MeOH/EtOAc, from which were isolated 2 sets of fractions. The first set contained **2.33a** and **2.33b** in 24% yield and 8:1 ratio. The second set contained **2.33c** and **2.33d** in 24% yield and 5:1 ratio.

2.33a. ^{1}**H NMR** (600 MHz, $CDCl_3$) δ 7.66 (s, 1H), 7.25 (d, J = 8.9 Hz, 2H), 6.96 (d, J = 9.0 Hz, 3H), 5.90 (d, J = 8.1 Hz, 1H), 4.65 – 4.53 (m, 1H), 3.84 (s, 3H), 3.72 (s, 3H),

3.15 (dd, J = 14.8, 5.6 Hz, 1H), 3.08 (dd, J = 14.7, 4.8 Hz, 1H), 1.43 (s, 9H). **^{13}C NMR** (151 MHz, $CDCl_3$) δ 172.73, 159.00, 155.75, 138.41, 135.62, 130.64, 123.07, 116.42, 115.01, 79.80, 55.73, 53.64, 52.39, 30.43, 28.48.

2.33b. ^{1}H NMR (600 MHz, $CDCl_3$) δ 7.69 (s, 1H), 7.35 – 7.32 (m, 1H), 7.25 – 7.22 (m, 1H), 7.05 – 7.00 (m, 2H), 6.97 (s, 1H), 5.56 (d, J = 8.2 Hz, 1H), 4.61 – 4.57 (m, 1H), 3.83 (s, 3H), 3.72 (s, 3H), 3.02 (dd, J = 15.0, 5.0 Hz, 1H), 2.90 (dd, J = 15.7, 4.4 Hz, 1H), 1.44 (s, 9H). ; **^{13}C NMR** (151 MHz, $CDCl_3$) δ 171.59, 152.52, 137.66, 130.01, 129.00, 127.57, 126.46, 125.41, 121.14, 117.98, 112.46, 80.52, 55.92, 53.74, 52.32, 30.39, 28.40.

IR (thin film): 3369.07, 2976.59, 2841.60, 1746.23, 1705.73, 1517.70, 1366.32, 1251.58, 1166.72, 1021.12; **HRMS**: Calculated for $(M+H)^+$:376.1872; found: 376.1863.

2.33c. ^{1}H NMR (600 MHz, $CDCl_3$) δ 7.51 (s, 1H), 7.20 (d, J = 8.8 Hz, 2H), 6.99 (d, J = 8.8 Hz, 2H), 6.92 (s, 1H), 4.95 (d, J = 7.9 Hz, 1H), 4.39 – 4.34 (m, 1H), 3.86 (s, 3H), 3.62 (s, 3H), 3.06 (dd, J = 15.4, 5.2 Hz, 1H), 2.97 (dd, J = 15.5, 6.7 Hz, 1H), 1.39 (s, 9H). 13**C NMR** (151 MHz, $CDCl_3$) δ 171.98, 159.89, 155.04, 138.59, 129.01, 128.50, 127.73, 121.10, 114.88, 80.21, 55.71, 52.72, 52.57, 28.39, 27.14.

2.33d. ^{1}H NMR (600 MHz, $CDCl_3$) δ 7.46 – 7.42 (m, 2H), 7.22 – 7.18 (m, 1H), 7.07 – 7.04 (m, 2H), 6.93 (s, 1H), 5.00 (d, J = 7.6 Hz, 1H), 4.41 – 4.33 (m, 1H), 3.81 (s, 3H), 3.63 (s, 3H), 2.94 – 2.90 (m, 2H), 1.39 (s, 9H). **^{13}C NMR** (151 MHz, $CDCl_3$) δ 172.13, 160.77, 154.66, 153.68, 138.73, 130.78, 128.86, 128.08, 127.76, 127.41, 112.25, 80.11, 55.87, 52.89, 52.50, 28.42, 26.83.

IR (thin film): 3421.10, 2976.59, 1732.73, 1683.55, 1652.70, 1518.67, 1363.43, 1249.65, 1166.72, 1024.98; **HRMS**: Calculated for $(M+H)^+$:376.1872; found: 376.1863.

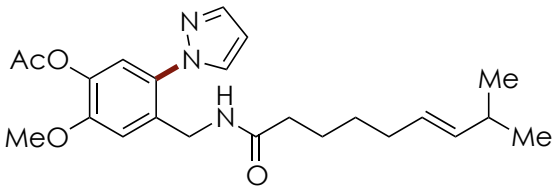

(*E*)-2-methoxy-4-((8-methylnon-6-enamido)methyl)-5-(1*H*-pyrazol-1-yl)phenyl acetate. The title compounds were prepared from anisole and *O*-acetylcapsaicin according to **General Method A** with the modification that 1.25 equiv were employed for an irradiation time of 40 hours. The crude residue was purified by column chromatography on silica gel with an eluent of hexanes to 75% EtOAc/hexanes giving a white solid in 66% yield. Note: The product contains the same ratio of unsaturated to saturated capsaicin analogues as the starting material (~3:2)**.** The provided proton NMR peak list below refers only to the unsaturated product **2.34**; see spectrum for peaks corresponding to saturated product **2.34'**.

^{1}**H NMR** (600 MHz, $CDCl_3$) δ 7.70 (s, 1H), 7.64 (d, *J* = 2.3 Hz, 1H), 7.19 (d, *J* = 1.9 Hz, 1H), 7.01 (s, 1H), 6.92 (t, *J* = 6.0 Hz, 1H), 6.45 (t, *J* = 2.1 Hz, 1H), 5.38 – 5.28 (m, 2H), 4.23 (d, *J* = 6.3 Hz, 2H), 3.87 (s, 3H), 2.32 (s, 3H), 2.20 – 2.14 (m, 2H), 1.97 (q, *J* = 7.0 Hz, 2H), 1.62 – 1.58 (m, 2H), 1.50 (hept, *J*=6.7Hz, 1H), 1.36 (p, *J* = 7.6 Hz, 2H), 0.94 (d, *J* = 6.7 Hz, 6H). ^{13}**C NMR** (151 MHz, $CDCl_3$) δ 172.95, 172.83, 168.87, 151.09, 140.87, 138.84, 138.08, 133.08, 132.50, 130.75, 126.75, 119.88, 115.31, 107.11, 100.12, 56.47, 40.00, 39.10, 37.10, 36.96, 32.41, 31.11, 29.77, 29.46, 29.42, 28.09, 27.39, 25.76, 25.27, 22.80, 22.78, 20.75.

IR (thin film): 3288.04. 2928.38, 2865.70, 1768.40, 1649.80, 1521.56, 1368.25, 1206.26, 1039.44, 755.00; **HRMS**: Calculated for $(M+Na)^+$: 436.2213 and 438.2369; found: 436.2200 and 438.2363.

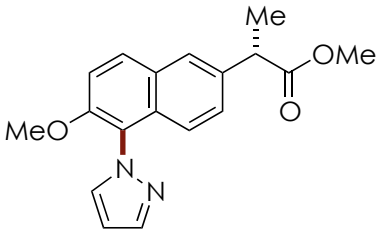

(*S*)-methyl 2-(6-methoxy-5-(1*H*-pyrazol-1-yl)naphthalen-2-yl)propanoate (2.35). The title compound was prepared using a modified **General Method A** procedure. The reaction was run with 1 equivalent of naproxen methyl ester and 4 equivalences of pyrazole (1:4 arene: amine) with an irradiation time of 20 hours. The title compound was purified by column chromatography on silica gel (25% to 50% EtOAc/Hexanes) to yield a yellow solid in 26%. **^{1}H NMR** (600 MHz, $CDCl_3$) δ 7.92 (d, *J* = 9.1 Hz, 1H), 7.86 (d, *J* = 2.0 Hz, 1H), 7.72 (d, *J* = 2.0 Hz, 2H), 7.65 (d, *J* = 2.3 Hz, 1H), 7.40-7.34 (m, 2H), 7.22 (d, *J* = 8.9 Hz, 1H), 6.54 (d, *J* = 2.3 Hz, 1H), 3.87 (s, 3H), 3.65 (s, 3H), 1.56 (d, *J* = 7.3, 3H).; **^{13}C NMR** (151 MHz, $CDCl_3$) δ 174.98, 152.61, 140.70, 136.66, 133.06, 131.47, 130.65, 128.97, 127.94, 125.97, 123.24, 122.83, 113.97, 106.10, 57.00, 52.24, 45.39, 18.57.; **IR** (thin film): 2949.59, 2844.49, 1732, 1606.41, 1455.99, 1341.25, 1278.57, 1196.61, 1071.26, 755.96; **HRMS** (ESI): Calculated for [M+H_2O]= 333.1216; found 333.1207.

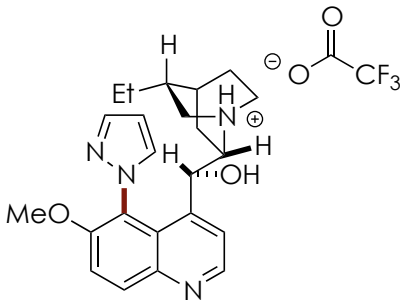

(9*S*)-10,11-dihydro- 6'-methoxy-5'-(1*H*-pyrazol-1-yl)cinchonan-9-ol · 2,2,2-trifluoroacetic acid (2.36)

The title compound was prepared using **General Method A** with an irradiation time of 20 hours. The title compound was purified by column chromatography on silica gel (0% to 5% MeOH/DCM to 5% MeOH/DCM/0.05% TFA) to yield the desired product in 53%.

^{1}H NMR (600 MHz, $CDCl_3$) δ 10.85 (br s, 1H), 8.83 (d, *J* = 4.5 Hz, 1H), 8.34 (d, *J* = 9.4 Hz, 1H), 7.97 (d, *J* = 4.5 Hz, 1H), 7.94 (d, *J* = 1.8 Hz, 1H), 7.58 (d, *J* = 9.4 Hz, 1H), 7.38 (d, *J* = 2.2 Hz, 1H), 6.89 (br s, 1H), 6.52 (t, *J* = 2.0 Hz, 1H), 4.36 (s, 1H), 3.87 (s, 3H), 3.81 (t, *J* = 10.5 Hz, 2H), 3.68 (t, *J* = 9.8 Hz, 1H), 3.16 – 3.09 (m, 1H), 2.99 (q, *J* = 9.3 Hz, 1H), 1.81 – 1.59 (m, 5H), 1.52 – 1.36 (m, 2H), 0.85 (t, *J* = 7.4 Hz, 3H), 0.41 (dt, *J* = 13.7, 7.7 Hz, 1H).; **^{13}C NMR** (151 MHz, $CDCl_3$) δ 162.54 (q, *J* = 35.2 Hz), 156.32, 148.37, 143.69, 143.37, 142.21, 134.37, 134.30, 123.76, 122.24, 121.13, 116.76 (q, *J* = 292.3 Hz), 115.56, 108.15, 66.00, 60.59, 57.02, 51.03, 48.45, 35.46, 25.68, 24.20, 23.68, 18.68, 11.56.

IR (thin film): 3213.79, 2963.09, 2241.84, 1671.02, 1508.06, 1464.67, 1268.93, 1201.43, 1136.83, 725.10; **HRMS** (ESI): Calculated for [M+H_2O]= 393.2290; found 393.2282.

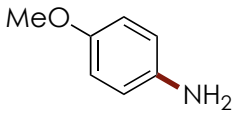

***p*-anisidine (2.37a)**. The title compound was prepared using Method C with an irradiation time of 24 hours. The reaction was run through a plug of silica, concentrated and the reaction was purified by column chromatography on silica gel (20% EtOAc/Hexanes) to afford a dark-purple solid in 36% yield. The spectral data were in agreement with previously reported literature values. [22] **^{1}H NMR** (600 MHz, $CDCl_3$) δ

6.76 (d, J = 8.8 Hz, 1H), 6.66 (d, J = 8.8 Hz, 1H), 3.76 (s, 3H), 3.44 (br s, 2H); **^{13}C NMR** (151 MHz, $CDCl_3$) δ 152.95, 140.03, 116.56, 114.94, 55.88.

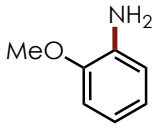

***o*-anisidine (2.37b).** The title compound was prepared using Method C with an irradiation time of 24 hours. The reaction was run through a plug of silica, concentrated and the reaction was purified by column chromatography on silica gel (20% EtOAc/Hexanes) to afford a dark brown liquid in 22% yield. The spectral data were in agreement with previously reported literature values. [22] **^{1}H NMR** (600 MHz, $CDCl_3$) δ 6.85 - 6.78 (m, 2H), 6.78 - 6.70 (m, 2H), 3.86 (s, 3H), 3.80 (br s, 2H); **^{13}C NMR** (151 MHz, $CDCl_3$) δ 147.45, 136.26, 121.20, 118.62, 115.16, 110.56, 55.56.

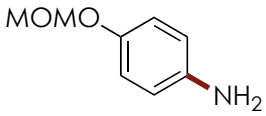

4-(methoxymethyl)aniline (2.38a). The title compound was prepared using Method C with an irradiation time of 24 hours. The reaction was run through a plug of silica, concentrated and the reaction was purified by column chromatography on silica gel (20% to 50% EtOAc/Hexanes) to afford a brown oil in 43% yield. The spectral data were in agreement with previously reported literature values. [23] **^{1}H NMR** (600 MHz, $CDCl_3$) δ 6.87 (d, J = 8.8 Hz, 2H), 6.63 (d, J = 8.8 Hz, 2H), 5.08 (s, 3H), 3.47 (s, 5H); **^{13}C NMR** (151 MHz, $CDCl_3$) δ 150.32, 141.33, 117.98, 116.32, 95.62, 55.93.

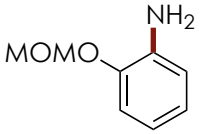

2-(methoxymethyl)aniline (2.38b). The title compound was prepared using Method C with an irradiation time of 24 hours. The reaction was run through a plug of silica, concentrated and the reaction was purified by column chromatography on silica gel (20% to 50% EtOAc/Hexanes) to afford a yellow oil in 21% yield. The spectral data were in agreement with previously reported literature values. [24] **^{1}H NMR** (600 MHz, $CDCl_3$) δ 7.03 (dd, *J* = 8.1, 1.3 Hz, 1H), 6.85 (td, *J* = 7.6, 1.3 Hz, 1H), 6.77 – 6.67 (m, 2H), 5.20 (s, 2H), 3.82 (br s, 2H), 3.51 (s, 3H); **^{13}C NMR** (151 MHz, $CDCl_3$) δ 144.93, 136.88, 122.61, 118.65, 115.60, 114.89, 95.21, 56.20.

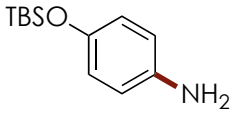

4-((*tert*-butyldimethylsilyl)oxy)aniline (2.39a). The title compound was prepared using Method C with an irradiation time of 24 hours. The reaction was run through a plug of silica, concentrated and the reaction was purified by column chromatography on silica gel (10 to 20% EtOAc/Hexanes) to afford a yellow in 35% yield. The spectral data were in agreement with previously reported literature values. [25] **^{1}H NMR** (600 MHz, $CDCl_3$) δ 6.67 (m, 2H), 6.59 (m, 2H), 3.41 (br s, 2H), 0.98 (s, 9H), 0.16 (s, 6H); **^{13}C NMR** (151 MHz, $CDCl_3$) δ 148.34, 140.39, 120.80, 116.43, 29.85, 25.89, 18.33, -4.35.

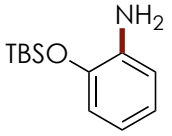

2-((*tert*-butyldimethylsilyl)oxy)aniline (2.39b). The title compound was prepared using Method C with an irradiation time of 24 hours. The reaction was run through a plug of silica, concentrated and the reaction was purified by column chromatography on silica gel (10 to 20% EtOAc/Hexanes) to afford a yellow in 9% yield. The spectral data were in

agreement with previously reported literature values. [26] **^{1}H NMR** (600 MHz, $CDCl_3$) δ 6.79 (td, *J* = 7.5, 1.4 Hz, 1H), 6.76 – 6.71 (m, 2H), 6.63 (ddd, *J* = 7.9, 7.3, 1.7 Hz, 1H), 3.70 (br s, 2H), 1.03 (s, 9H), 0.25 (s, 6H); **^{13}C NMR** (151 MHz, $CDCl_3$) δ 143.05, 138.27, 121.95, 118.61, 118.53, 115.78, 25.97, 18.38, -4.10. **IR** (thin film): 3445.17, 2955.38, 2929.34, 2857.02, 1646.91, 1519.63, 1275.68, 1226.50, 923.74, 832.13.

HRMS: Calculated for $(M+H)^+$: 224.1470; found: 224.1464.

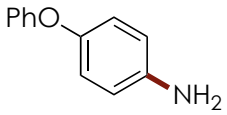

4-phenoxyaniline (2.40a). The title compound was prepared using Method C with an irradiation time of 24 hours. The reaction was run through a plug of silica, concentrated and the reaction was purified by column chromatography on silica gel (20% EtOAc/Hexanes) to afford a light brown solid in 46% yield. The spectral data were in agreement with previously reported literature values. [27] **^{1}H NMR** (600 MHz, $CDCl_3$) δ 7.32 - 7.26 (m, 2H), 7.05 - 6.99 (m, 1H), 6.97 - 6.92 (m, 2H), 6.92 - 6.85 (m, 2H), 6.72 - 6.67 (m, 2H), 3.59 (br s, 2H); **^{13}C NMR** (151 MHz, $CDCl_3$) δ 159.02, 148.72, 142.80, 129.65, 122.19, 121.27, 117.34, 116.37.

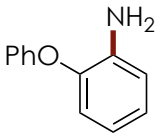

2-phenoxyaniline (2.40b). The title compound was prepared using Method C with an irradiation time of 24 hours. The reaction was run through a plug of silica, concentrated and the reaction was purified by column chromatography on silica gel (20% EtOAc/Hexanes) to afford a yellow in 16% yield. The spectral data were in agreement with previously reported literature values. [28] **^{1}H NMR** (600 MHz, $CDCl_3$) δ 7.34 – 7.28

(m, 2H), 7.06 (tt, J = 7.3, 1.1 Hz, 1H), 7.01 – 6.95 (m, 3H), 6.88 (dd, J = 8.0, 1.4 Hz, 1H), 6.83 (dd, J = 7.9, 1.6 Hz, 1H), 6.72 (td, J = 7.7, 1.6 Hz, 1H), 3.80 (br s, 2H); **^{13}C NMR** (151 MHz, $CDCl_3$) δ 157.61, 143.19, 138.86, 129.84, 125.03, 122.76, 120.40, 118.92, 117.23, 116.61.

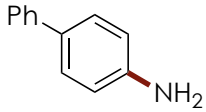

[1,1'-biphenyl]-4-amine (2.41a). The title compound was prepared using Method C with an irradiation time of 24 hours. The reaction was run through a plug of silica, concentrated and the reaction was purified by column chromatography on silica gel (20% EtOAc/Hexanes) to afford a brown crystalline solid in 42% yield. [22] **^{1}H NMR** (600 MHz, $CDCl_3$) δ 7.56 (d, J = 7.8 Hz, 2H), 7.48 - 7.35 (m, 4H), 7.33 - 7.24 (m, 1H), 6.78 (d, J = 8.4 Hz, 2H), 3.74 (br s, 2H); **^{13}C NMR** (151 MHz, $CDCl_3$) δ 145.93, 141.26, 131.68, 128.76, 128.12, 126.51, 126.36, 115.49.

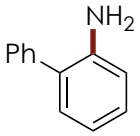

[1,1'-biphenyl]-2-amine (2.41b): The title compound was prepared using Method C with an irradiation time of 24 hours. The reaction was run through a plug of silica, concentrated and the reaction was purified by column chromatography on silica gel (20% EtOAc/Hexanes) to afford a brown crystalline solid in 11% yield. The spectral data were in agreement with previously reported literature values. [22] **^{1}H NMR** (600 MHz, $CDCl_3$) δ 7.49 – 7.42 (m, 4H), 7.38 – 7.33 (m, 1H), 7.20 – 7.12 (m, 2H), 6.84 (td, J = 7.4, 1.2 Hz, 1H), 6.78 (dd, J = 8.0, 1.1 Hz, 1H), 3.76 (br s, 2H). **^{13}C NMR** (151 MHz, $CDCl_3$) δ 143.62, 139.64, 130.59, 129.22, 128.94, 128.62, 127.77, 127.29, 118.78, 115.72.

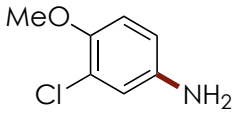

3-chloro-4-methoxyaniline (2.42). The title compound was prepared using Method C with an irradiation time of 48 hours. The reaction was run through a plug of silica, concentrated and the reaction was purified by column chromatography on silica gel (50% EtOAc/Hexanes) to afford a yellow oil in 33% yield. **^{1}H NMR** (600 MHz, CDCl3) δ 6.78 (d, *J* = 8.7 Hz, 1H), 6.76 (d, *J* = 2.8 Hz, 1H), 6.56 (dd, *J* = 8.7, 2.8 Hz, 1H), 3.83 (s, 3H), 3.47 (br s, 2H); **^{13}C NMR** (151 MHz, $CDCl_3$) δ 148.31, 140.86, 123.32, 117.53, 114.39, 114.15, 57.06. **IR** (thin film): 3421.10, 3361.32, 3219.58, 2931.27, 2835.81, 1634.38, 1505.17, 1439.60, 1272.79, 1229.40. **HRMS**: Calculated for $(M+H)^+$: 158.0373; found: 158.0366.

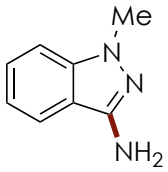

1-methyl-1*H*-indazol-3-amine (2.43). The title compound was prepared using Method C with an irradiation time of 24 hours. The reaction was run through a plug of silica, concentrated and the reaction was purified by column chromatography on silica gel (50% to 70% EtOAc/Hexanes) to afford a pink-red crystalline solid in 33% yield. The spectral data were in agreement with previously reported literature values. [29] **^{1}H NMR** (600 MHz, $CDCl_3$) δ 7.55 (d, *J* = 8.1 Hz, 1H), 7.36 (dd, *J* = 8.1, 6.9 Hz, 1H), 7.22 (d, *J* = 8.6, 1H), 7.03 (dd, *J* = 7.8, 6.9, 1H), 4.04 (br s, 2H), 3.86 (s, 3H); **^{13}C NMR** (151 MHz, $CDCl_3$) δ 146.99, 141.66, 127.00, 119.62, 118.54, 114.60, 108.79, 34.94.

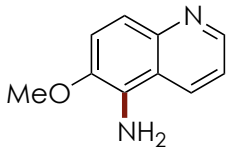

6-methoxy-quinolin-5-amine (2.44). The title compound was prepared using Method C with an irradiation time of 32 hours. The reaction was run through a plug of silica, concentrated and the reaction was purified by column chromatography on silica gel (70% EtOAc/Hexanes) to afford a green solid in 36% yield. The spectral data were in agreement with previously reported literature values. [30] **^{1}H NMR** (600 MHz, $CDCl_3$) δ 8.78 (dd, *J* = 4.1, 1.6 Hz, 1H), 8.14 (d, *J* = 8.6, 1H), 7.61 (d, *J* = 9.1, 1H), 7.45 (d, *J* = 9.1 Hz, 1H), 7.32 (dd, *J* = 8.6, 4.1 Hz, 1H), 4.27 (br s, 2H), 4.00 (s, 3H); **^{13}C NMR** (151 MHz, $CDCl_3$) δ 148.38, 144.17, 142.72, 129.41, 129.11, 119.79, 119.72, 118.89, 116.52, 56.76.

Electrochemical Measurements

Electrochemical half peak redox potentials ($E_{p/2}$) were estimated from cyclic voltammograms obtained by the method described previously (*73*). Measurements were performed in acetonitrile with tetrabutylammonium hexafluorophosphate (0.1 M) as the electrolyte, and the cyclic voltammograms were collected using a glassy carbon working electrode, a platinum wire counter electrode, and a Ag/AgCl reference electrode in saturated NaCl. The observed half peak potential was referenced to SCE by addition of 30 mV to the value obtained vs. Ag/AgCl. For a typical measurement, the potential was increased from an initial potential of 0.5 V to a vertex potential of 2.8 V, then returning to a final potential of 0.5 V. With these parameters, all compounds listed in Table S4 exhibited irreversible oxidation waves. Excited state reduction potentials for Catalysts A-C are estimated as described in the aforementioned reference from the ground state

reduction potentials (Catalyst A: $E_{1/2}$ = -0.47 V vs. SCE, Catalyst B: $E_{1/2}$ = -0.58 V vs. SCE, Catalyst C: $E_{1/2}$ = -0.52 V vs. SCE) and the excited state energy ($E_{0,0}$) of the locally excited singlet state for 9- mesityl-10-methylacridinium tetrafluoroborate. Electrochemical Half Peak Potentials for ($E_{p/2}$) for the arenes and select amine nucleophiles employed

Substrate	$E_{p/2}^{ox}$ (V vs. SCE)	Substrate	$E_{p/2}^{ox}$ (V vs. SCE)
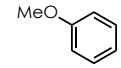	1.87	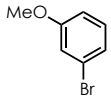	1.96
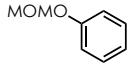	1.89	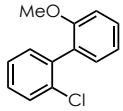	1.86
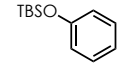	1.89	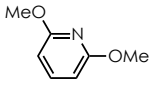	1.59
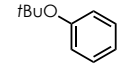	1.74	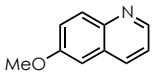	1.66
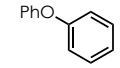	1.97	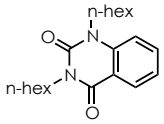	1.92
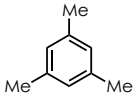	2.13		1.60
	2.28	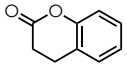	2.19
	1.96	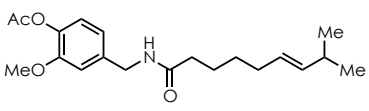	1.74
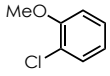	2.00	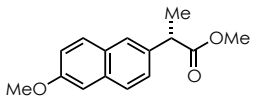	1.43

REFERENCES

(1) Wilger, D. J.; Grandjean, J.-M. M.; Lammert, T. R.; Nicewicz, D. A. *Nat. Chem.* **2014**, *6*, 720–726.

(2) Seganish, W. M.; DeShong, P. *J. Org. Chem.* **2004**, *69*, 6790–6795.

(3) Baker, M. S.; Phillips, S. T. *J. Am. Chem. Soc.* **2011**, *133*, 5170–5173.

(4) Bartoli, G.; Bosco, M.; Locatelli, M.; Marcantoni, E.; Melchiorre, P.; Sambri, L. *Org. Lett.* **2005**, *7*, 427–430.

(5) Bodnar, B. S.; Vogt, P. F. *J. Org. Chem.* **2009**, *74*, 2598–2600.

(6) Dey, S.; Garner, P. *J. Org. Chem.* **2000**, *65*, 7697–7699.

(7) Chevallier, F.; Halauko, Y. S.; Pecceu, C.; Nassar, I. F.; Dam, T. U.; Roisnel, T.; Matulis, V. E.; Ivashkevich, O. A.; Mongin, F. *Org. Biomol. Chem.* **2011**, *9*, 4671.

(8) Teo, Y.-C.; Yong, F.-F.; Poh, C.-Y.; Yan, Y.-K.; Chua, G.-L. *Chem. Commun.* **2009**, 6258.

(9) Furuta, Y.; Komatsu, K.; Kaya, A.; Takahata, S.; Tabata, Y. US2014030209 (A1), January 30, 2014.

(10) Zhu, L.; Li, G.; Luo, L.; Guo, P.; Lan, J.; You, J. *J. Org. Chem.* **2009**, *74*, 2200–2202.

(11) DeAngelis, A.; Wang, D.-H.; Buchwald, S. L. *Angew. Chem. Int. Ed.* **2013**, *52*, 3434–3437.

(12) Schneider, Y.; Prévost, J.; Gobin, M.; Legault, C. Y. *Org. Lett.* **2014**, *16*, 596–599.

(13) Kumar, A. S.; Ghule, V. D.; Subrahmanyam, S.; Sahoo, A. K. *Chem. – Eur. J.* **2013**, *19*, 509–518.

(14) Kommu, N.; Ghule, V. D.; Kumar, A. S.; Sahoo, A. K. *Chem. – Asian J.* **2014**, *9*, 166–178.

(15) Xu, Z.-L.; Li, H.-X.; Ren, Z.-G.; Du, W.-Y.; Xu, W.-C.; Lang, J.-P. *Tetrahedron* **2011**, *67*, 5282–5288.

(16) Onaka, T.; Umemoto, H.; Miki, Y.; Nakamura, A.; Maegawa, T. *J. Org. Chem.* **2014**, *79*, 6703–6707.

(17) Gaydou, M.; Echavarren, A. M. *Angew. Chem. Int. Ed.* **2013**, *52*, 13468–13471.

(18) Gann, A. W.; Amoroso, J. W.; Einck, V. J.; Rice, W. P.; Chambers, J. J.; Schnarr, N. A. *Org. Lett.* **2014**, *16*, 2003–2005.

(19) Cho, C. S.; Patel, D. B. *Tetrahedron* **2006**, *62*, 6388–6391.

(20) Yang, K.; Qiu, Y.; Li, Z.; Wang, Z.; Jiang, S. *J. Org. Chem.* **2011**, *76*, 3151–3159.

(21) Wentzel, M. T.; Hewgley, J. B.; Kamble, R. M.; Wall, P. D.; Kozlowski, M. C. *Adv. Synth. Catal.* **2009**, *351*, 931–937.

(22) Vo, G. D.; Hartwig, J. F. *J. Am. Chem. Soc.* **2009**, *131*, 11049–11061.

(23) Shimizu, Y.; Morimoto, H.; Zhang, M.; Ohshima, T. *Angew. Chem. Int. Ed.* **2012**, *51*, 8564–8567.

(24) Nojiri, A.; Kumagai, N.; Shibasaki, M. *Angew. Chem. Int. Ed.* **2012**, *51*, 2137–2141.

(25) Rahaim, R. J.; Maleczka, R. E. *Org. Lett.* **2005**, *7*, 5087–5090.

(26) Macías, F. A.; Marín, D.; Oliveros-Bastidas, A.; Chinchilla, D.; Simonet, A. M.; Molinillo, J. M. G. *J. Agric. Food Chem.* **2006**, *54*, 991–1000.

(27) Maiti, D.; Buchwald, S. L. *J. Am. Chem. Soc.* **2009**, *131*, 17423–17429.

(28) Yao, L.; Zhou, Q.; Han, W.; Wei, S. *Eur. J. Org. Chem.* **2012**, *2012*, 6856–6860.

(29) Liu, H.-J.; Hung, S.-F.; Chen, C.-L.; Lin, M.-H. *Tetrahedron* **2013**, *69*, 3907–3912.

(30) Fryatt, T.; Pettersson, H. I.; Gardipee, W. T.; Bray, K. C.; Green, S. J.; Slawin, A. M.; Beall, H. D.; Moody, C. J. *Bioorg. Med. Chem.* **2004**, *12*, 1667–1687.

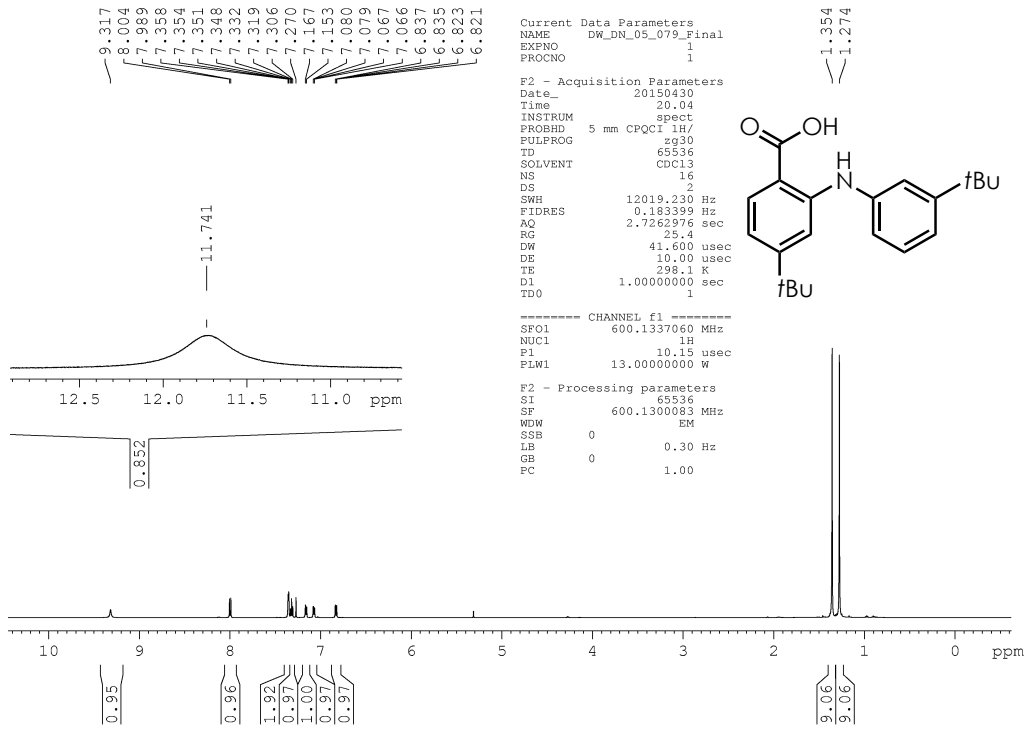
9.317
8.004
7.989
7.358
7.354
7.351
7.348
7.332
7.319
7.306
7.270
7.167
7.153
7.080
7.079
7.067
7.066
6.837
6.835
6.823
6.821
1.354
1.274
11.741
12.5
12.0
11.5
11.0
ppm
0.852
Current Data Parameters
NAME DW_DN_05_079_Final
EXPNO 1
PROCNO 1
F2 - Acquisition Parameters
Date_ 20150430
Time 20.04
INSTRUM spect
PROBHD 5 mm CPQCI 1H/
PULPROG zg30
TD 65536
SOLVENT CDCl3
NS 16
DS 2
SWH 12019.230 Hz
FIDRES 0.183399 Hz
AQ 2.7262976 sec
RG 25.4
DW 41.600 usec
DE 10.00 usec
TE 298.1 K
D1 1.00000000 sec
TD0 1
======== CHANNEL f1 ========
SFO1 600.1337060 MHz
NUC1 1H
P1 10.15 usec
PLW1 13.00000000 W
F2 - Processing parameters
SI 65536
SF 600.1300083 MHz
WDW EM
SSB 0
LB 0.30 Hz
GB 0
PC 1.00
OH
H
N
tBu
tBu
10
9
8
7
6
5
4
3
2
1
0
ppm
0.95
0.96
1.92
0.97
1.00
0.97
0.97
9.06
9.06

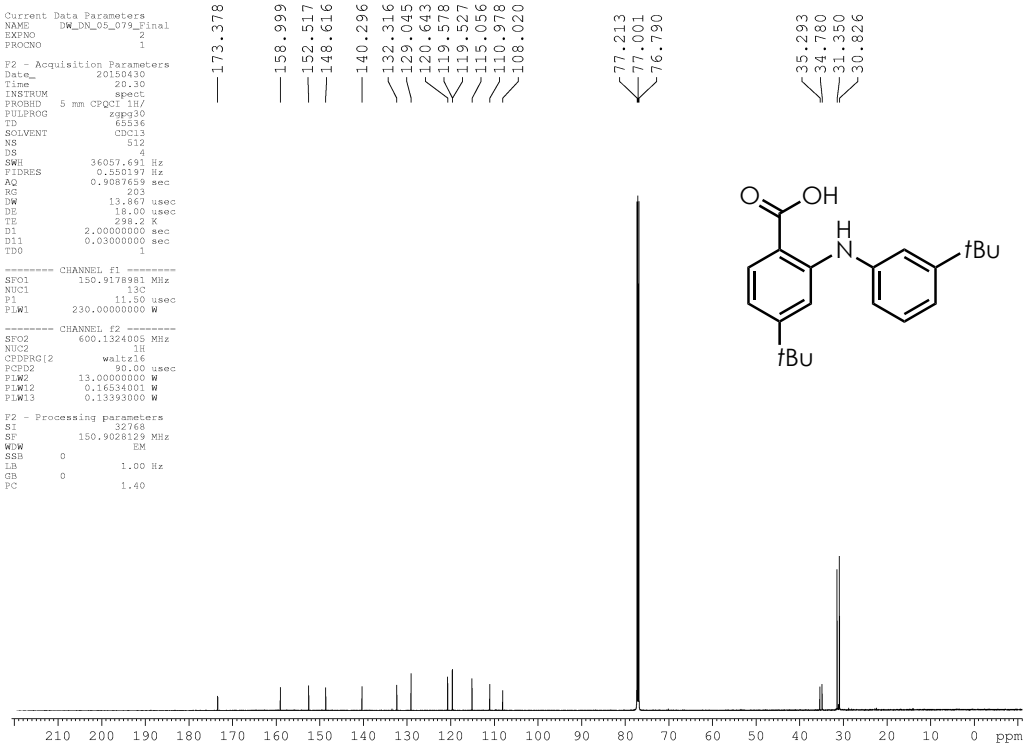
Current Data Parameters
NAME DW_DN_05_079_Final
EXPNO 2
PROCNO 1
F2 - Acquisition Parameters
Date_ 20150430
Time 20.30
INSTRUM spect
PROBHD 5 mm CPQCI 1H/
PULPROG zgpg30
TD 65536
SOLVENT CDCl3
NS 512
DS 4
SWH 36057.691 Hz
FIDRES 0.550197 Hz
AQ 0.9087659 sec
RG 203
DW 13.867 usec
DE 18.00 usec
TE 298.2 K
D1 2.00000000 sec
D11 0.03000000 sec
TD0 1
======== CHANNEL f1 ========
SFO1 150.9178981 MHz
NUC1 13C
P1 11.50 usec
PLW1 230.00000000 W
======== CHANNEL f2 ========
SFO2 600.1324005 MHz
NUC2 1H
CPDPRG[2 waltz16
PCPD2 90.00 usec
PLW2 13.00000000 W
PLW12 0.16534001 W
PLW13 0.13393000 W
F2 - Processing parameters
SI 32768
SF 150.9028129 MHz
WDW EM
SSB 0
LB 1.00 Hz
GB 0
PC 1.40
173.378
158.999
152.517
148.616
140.296
132.316
129.045
120.643
119.578
119.527
115.056
110.978
108.020
77.213
77.001
76.790
35.293
34.780
31.350
30.826
OH
H
N
tBu
tBu
210
200
190
180
170
160
150
140
130
120
110
100
90
80
70
60
50
40
30
20
10
0
ppm

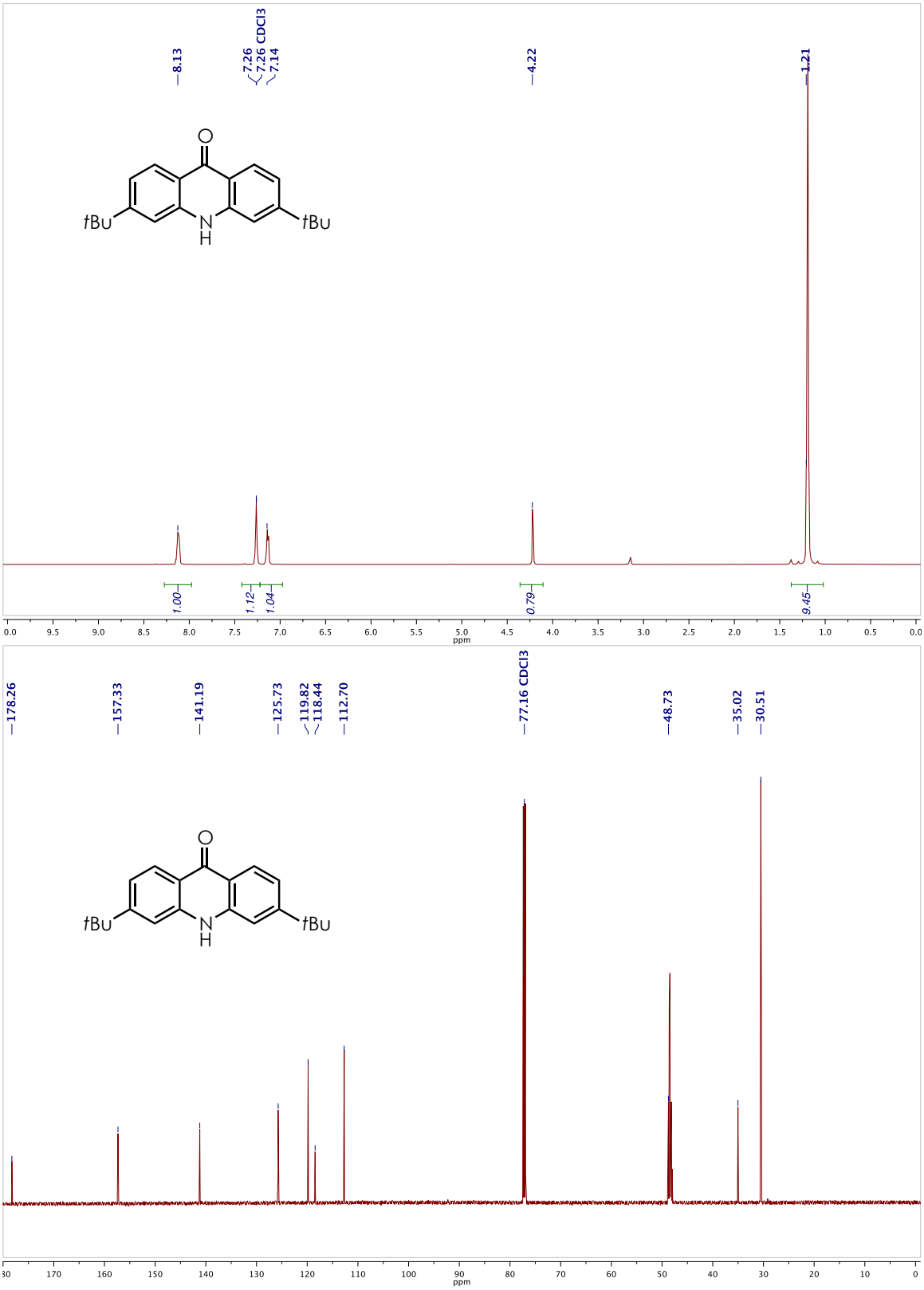
8.13
7.26
7.26 CDCl3
7.14
4.22
1.21
tBu
tBu
N
H
1.00
1.12
1.04
0.79
9.45
ppm
178.26
157.33
141.19
125.73
119.82
118.44
112.70
77.16 CDCl3
48.73
35.02
30.51
tBu
tBu
N
H
ppm

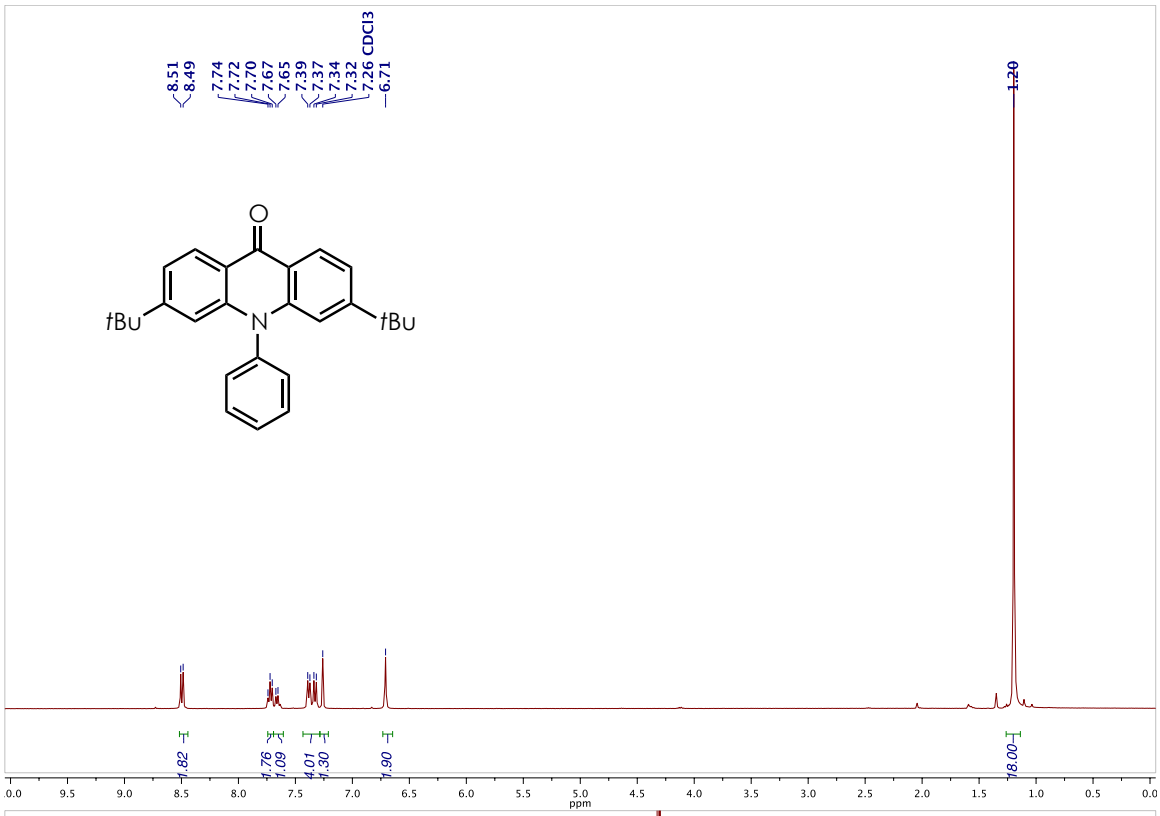
8.51
8.49
7.74
7.72
7.70
7.67
7.65
7.39
7.37
7.34
7.32
7.26 CDCl3
6.71
1.20
tBu
tBu
N
O
1.82
1.76
1.09
4.01
1.30
1.90
18.00
ppm

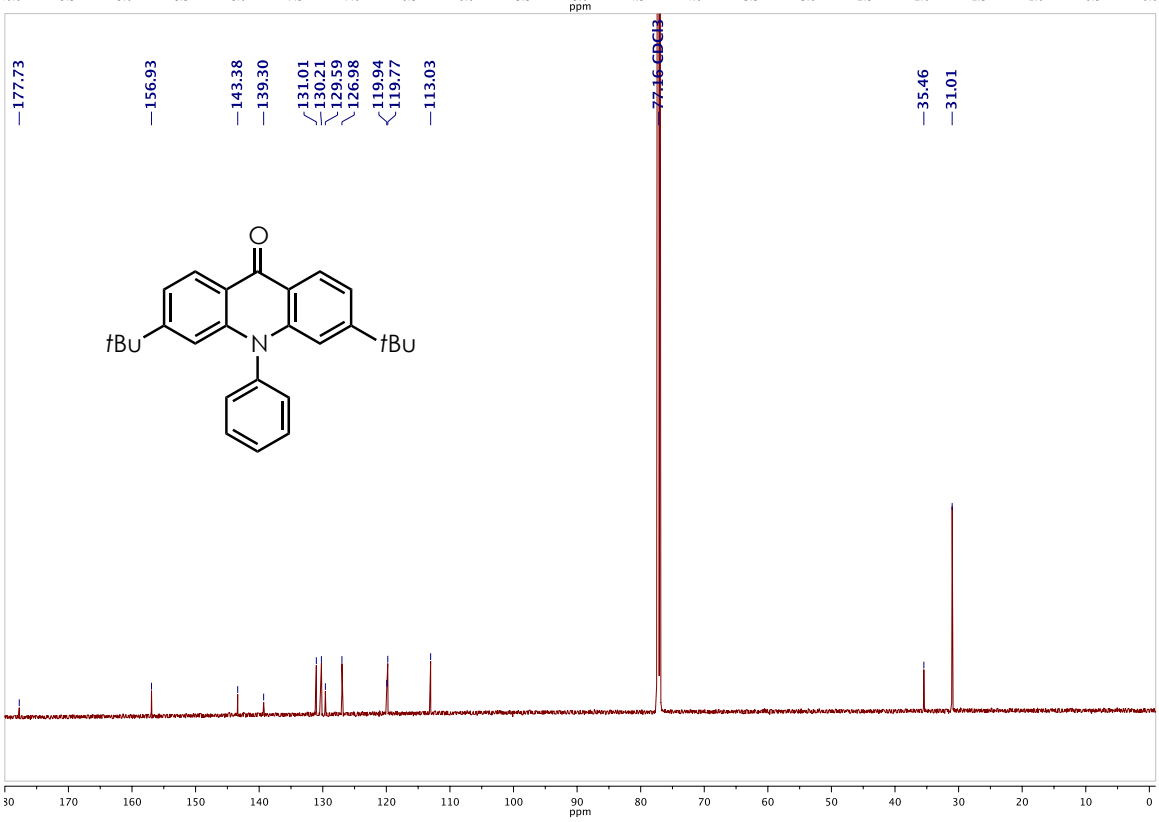
177.73
156.93
143.38
139.30
131.01
130.21
129.59
126.98
119.94
119.77
113.03
77.16 CDCl3
35.46
31.01
tBu
tBu
N
O
ppm

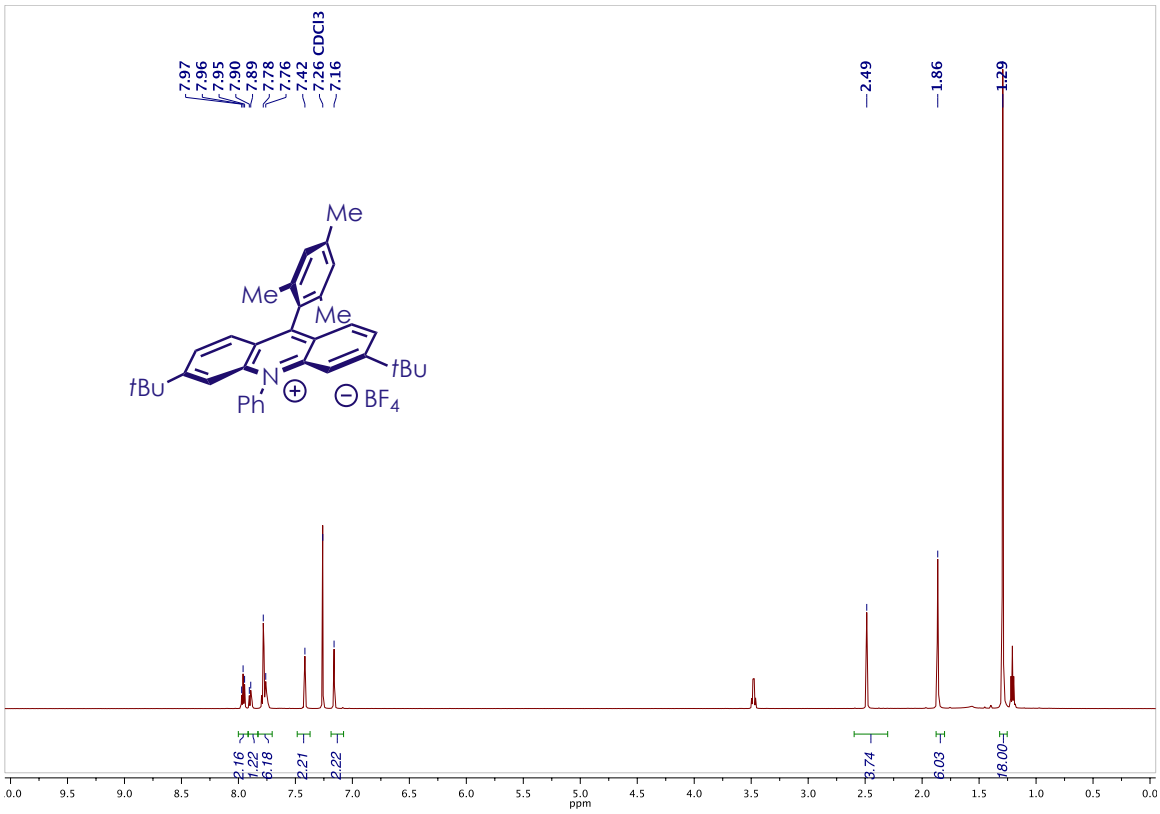
7.97
7.96
7.95
7.90
7.89
7.78
7.76
7.42
7.26 CDCl3
7.16
2.49
1.86
1.29
Me
Me
Me
tBu
tBu
N
Ph
BF4
2.16
1.22
6.18
2.21
2.22
3.74
6.03
18.00
ppm

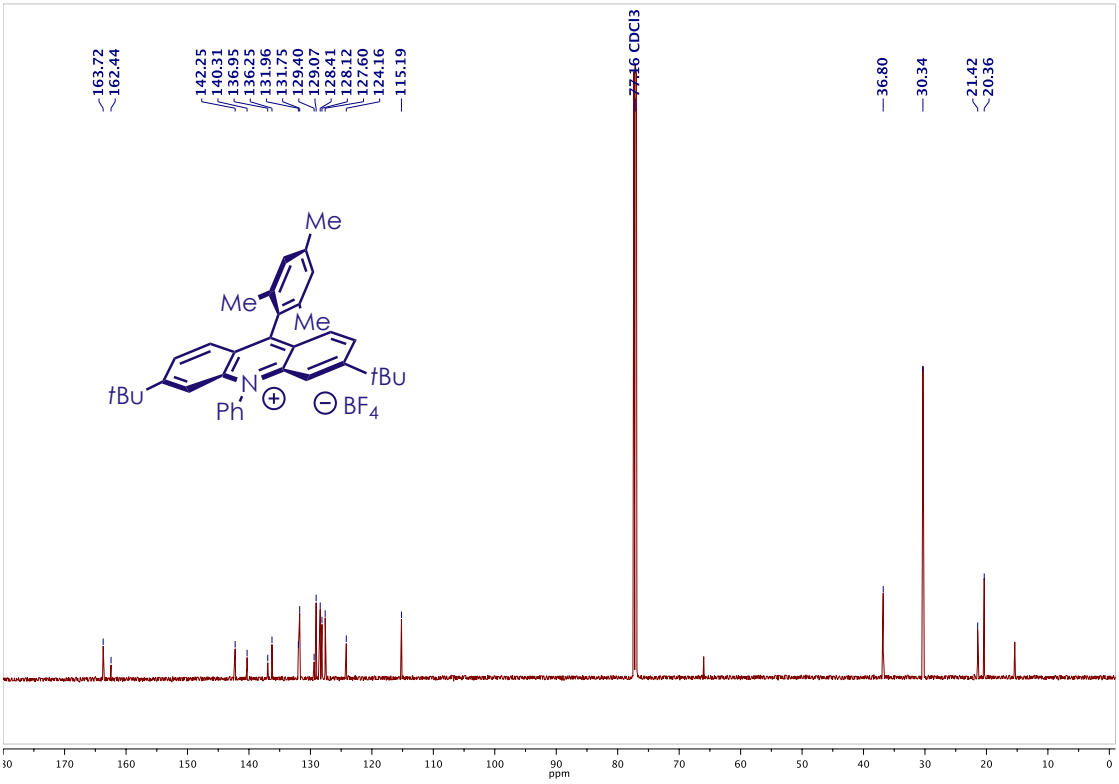
163.72
162.44
142.25
140.31
136.95
136.25
131.96
131.75
129.40
129.07
128.41
128.12
127.60
124.16
115.19
77.16 CDCl3
36.80
30.34
21.42
20.36
Me
Me
Me
tBu
tBu
N
Ph
BF4
ppm

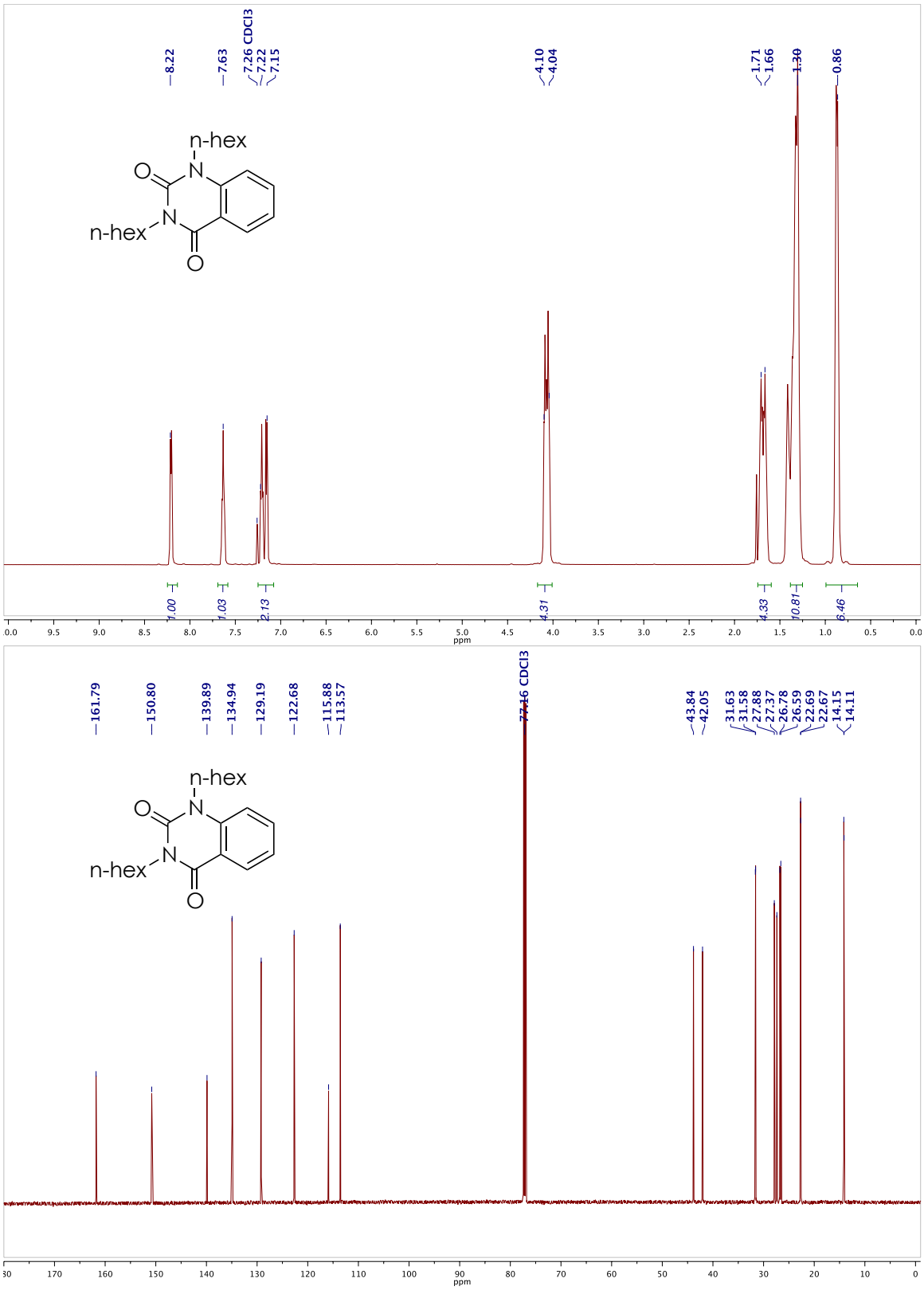
8.22
7.63
7.26 CDCl3
7.22
7.15
4.10
4.04
1.71
1.66
1.30
0.86
n-hex
n-hex
1.00
1.03
2.13
4.31
4.33
10.81
6.46
ppm
161.79
150.80
139.89
134.94
129.19
122.68
115.88
113.57
77.16 CDCl3
43.84
42.05
31.63
31.58
27.88
27.37
26.78
26.59
22.69
22.67
14.15
14.11
n-hex
n-hex
ppm

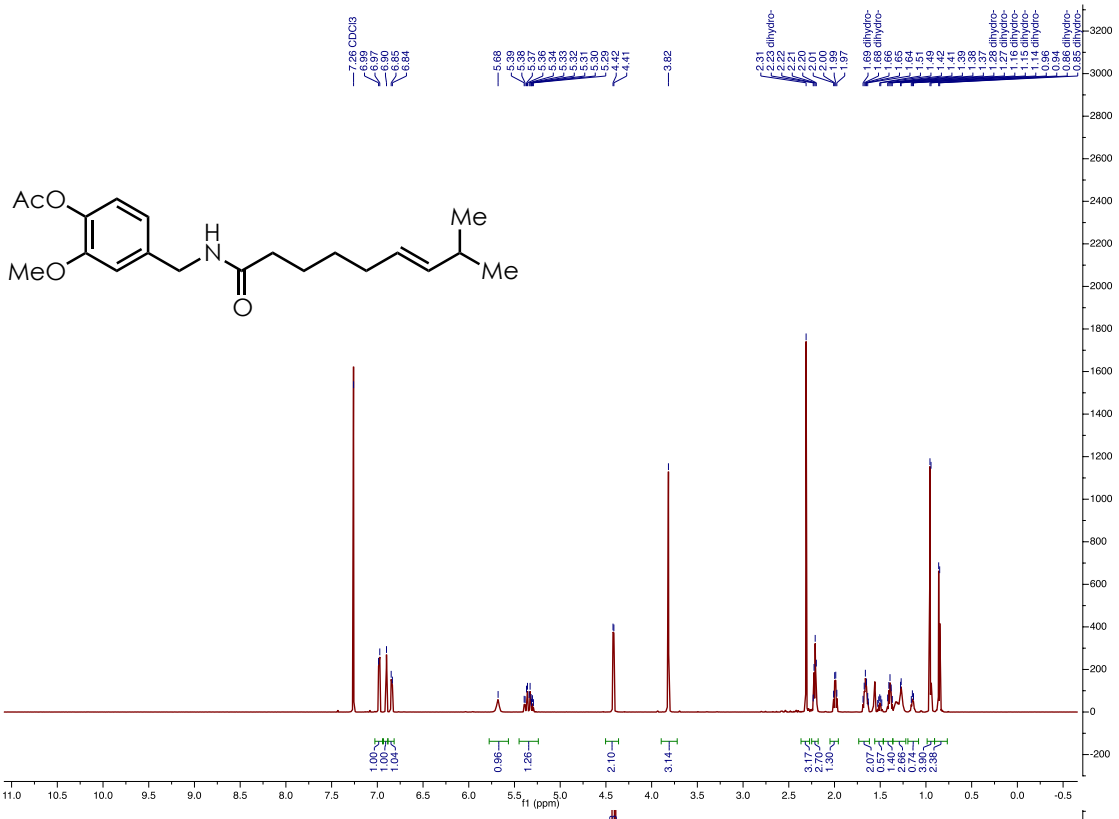
AcO
MeO
H
N
O
Me
Me

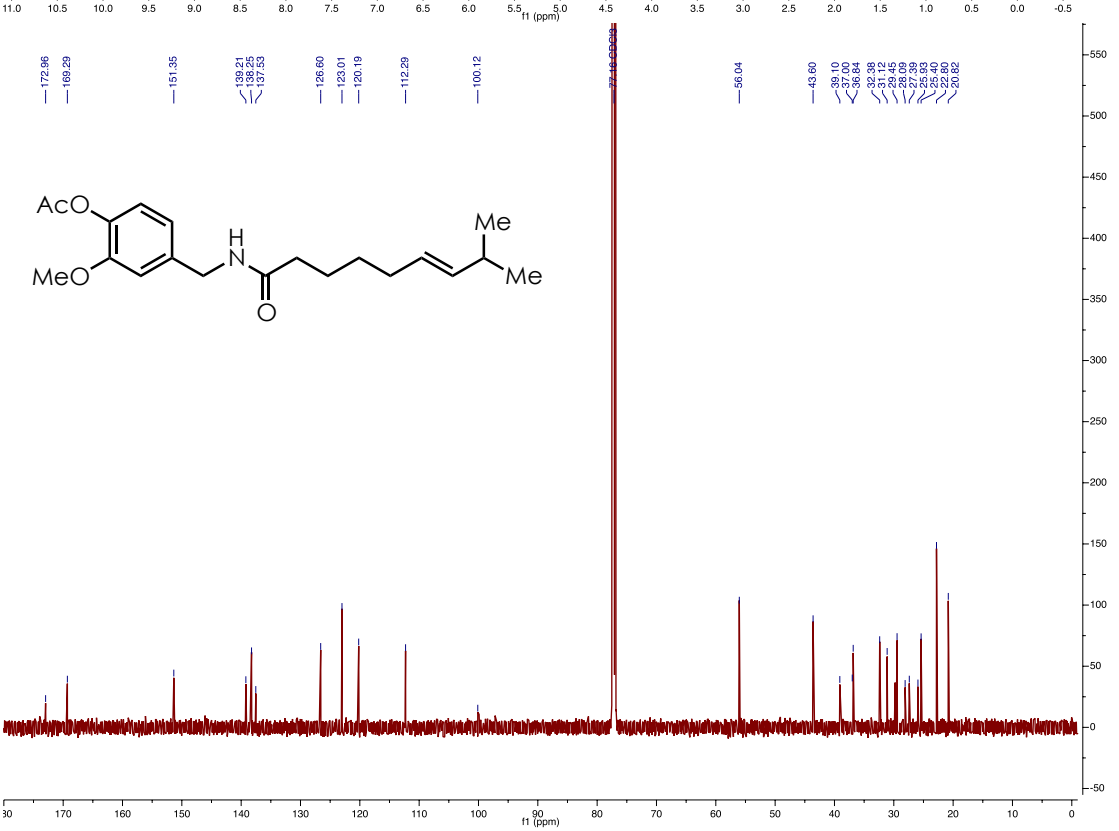
AcO
MeO
H
N
O
Me
Me

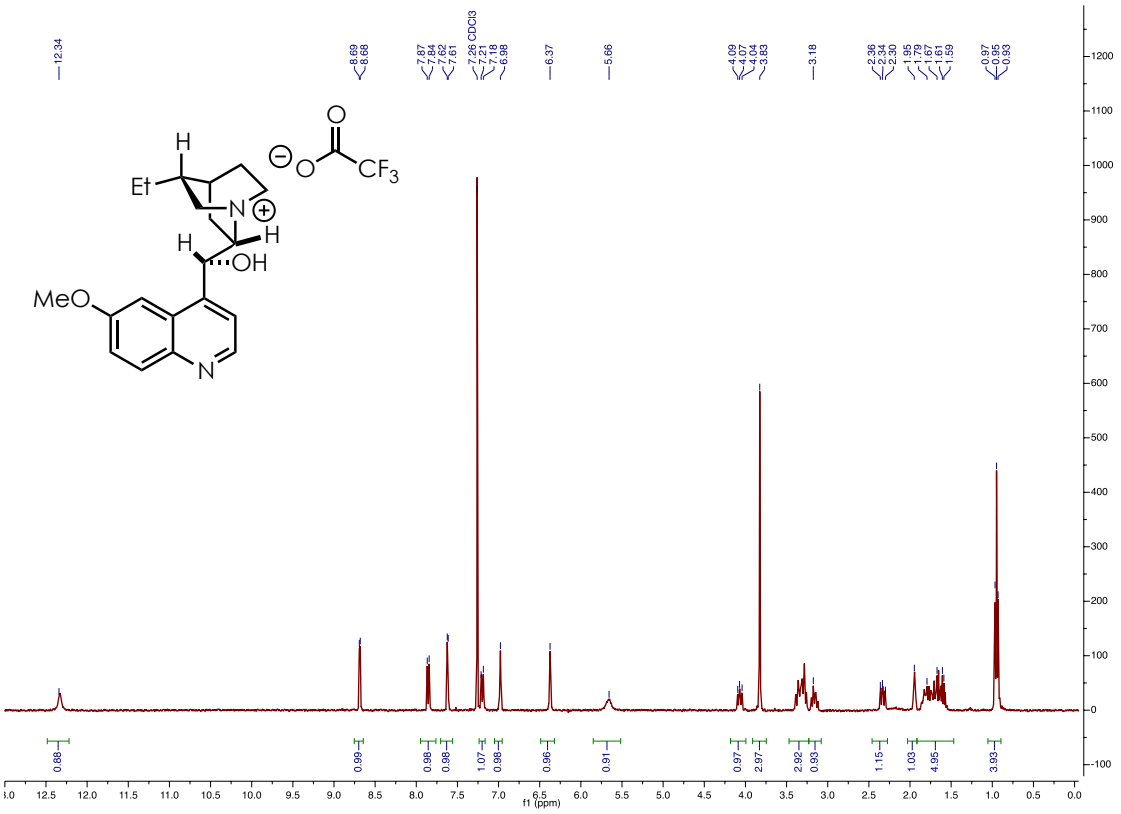
12.34
8.89
8.88
7.87
7.84
7.62
7.61
7.26 CDCl3
7.21
7.18
6.98
6.37
5.66
4.09
4.07
4.04
3.83
3.18
2.36
2.34
2.30
1.95
1.79
1.67
1.61
1.59
0.97
0.95
0.93
0.88
0.99
0.98
0.98
1.07
0.98
0.96
0.91
0.97
2.97
2.92
0.93
1.15
1.03
4.95
3.93
f1 (ppm)
Et
H
N
H
OH
MeO
N
O
O
CF3

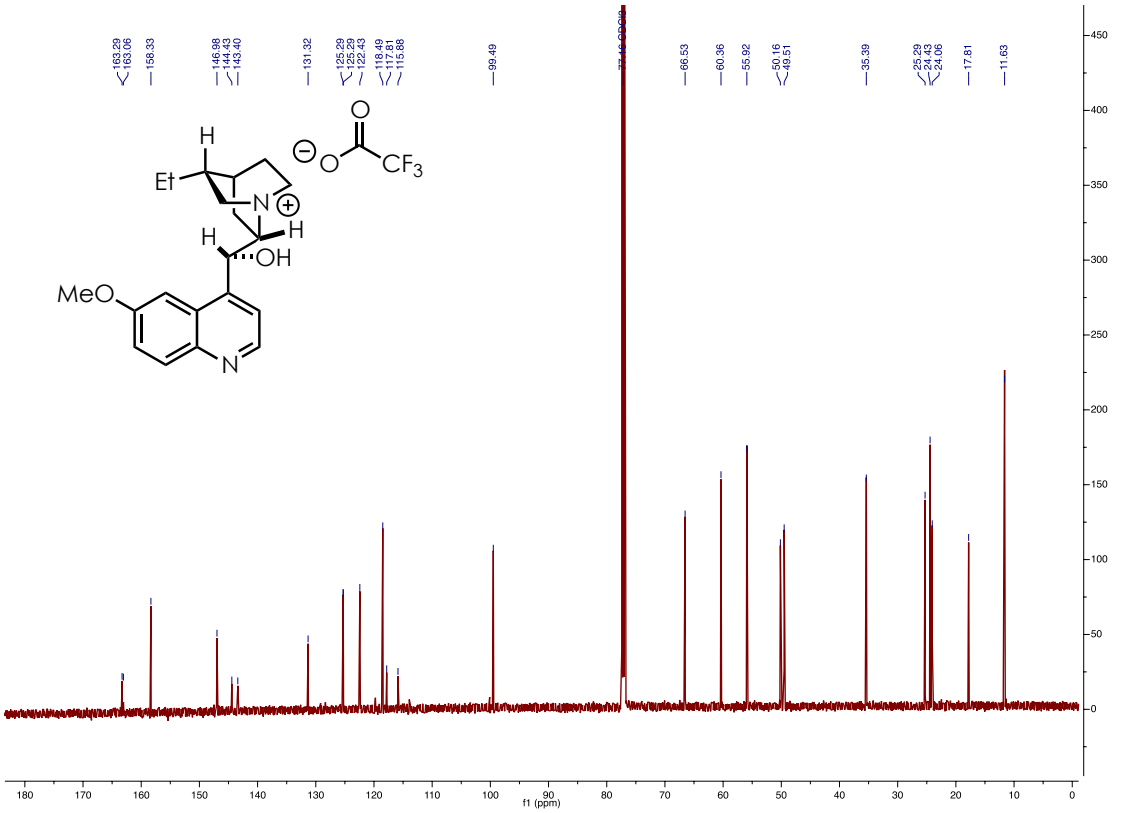
163.29
163.06
158.33
146.98
144.43
143.40
131.32
125.29
125.23
122.43
119.49
117.81
115.88
99.49
77.45 CDCl3
66.53
60.36
55.92
50.16
49.51
35.39
25.29
24.43
24.06
17.81
11.63
f1 (ppm)
Et
H
N
H
OH
MeO
N
O
O
CF3

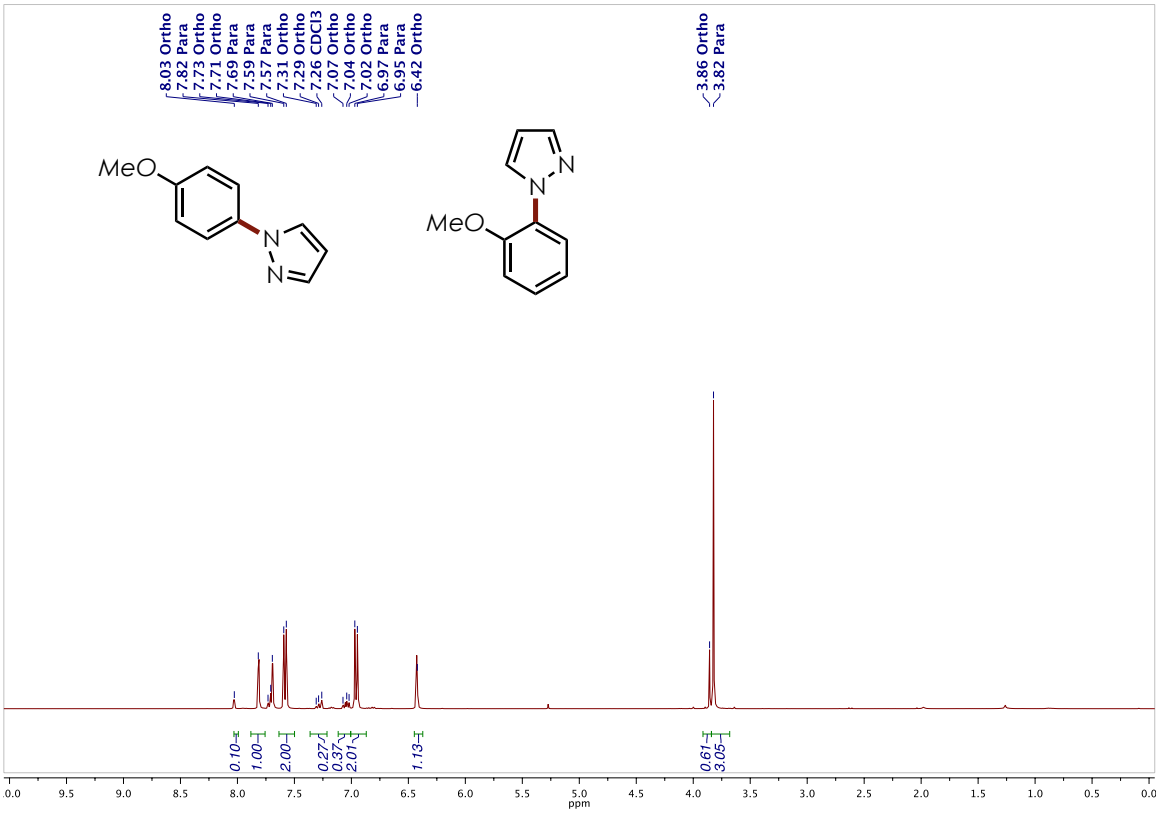
8.03 Ortho
7.82 Para
7.73 Ortho
7.71 Ortho
7.69 Para
7.59 Para
7.57 Para
7.31 Ortho
7.29 Ortho
7.26 CDCl3
7.07 Ortho
7.04 Ortho
7.02 Ortho
6.97 Para
6.95 Para
6.42 Ortho
3.86 Ortho
3.82 Para
MeO
MeO
0.10
1.00
2.00
0.27
0.37
2.01
1.13
0.61
3.05
ppm

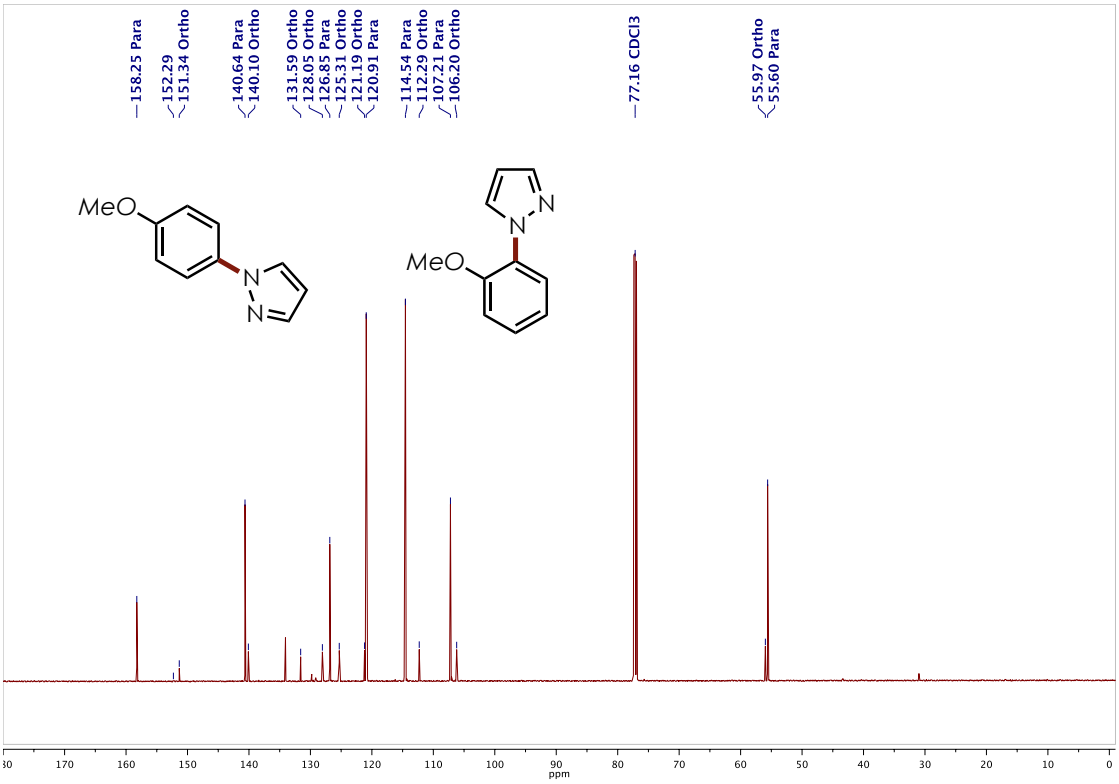
158.25 Para
152.29
151.34 Ortho
140.64 Para
140.10 Ortho
131.59 Ortho
128.05 Ortho
126.85 Para
125.31 Ortho
121.19 Ortho
120.91 Para
114.54 Para
112.29 Ortho
107.21 Para
106.20 Ortho
77.16 CDCl3
55.97 Ortho
55.60 Para
MeO
MeO
ppm

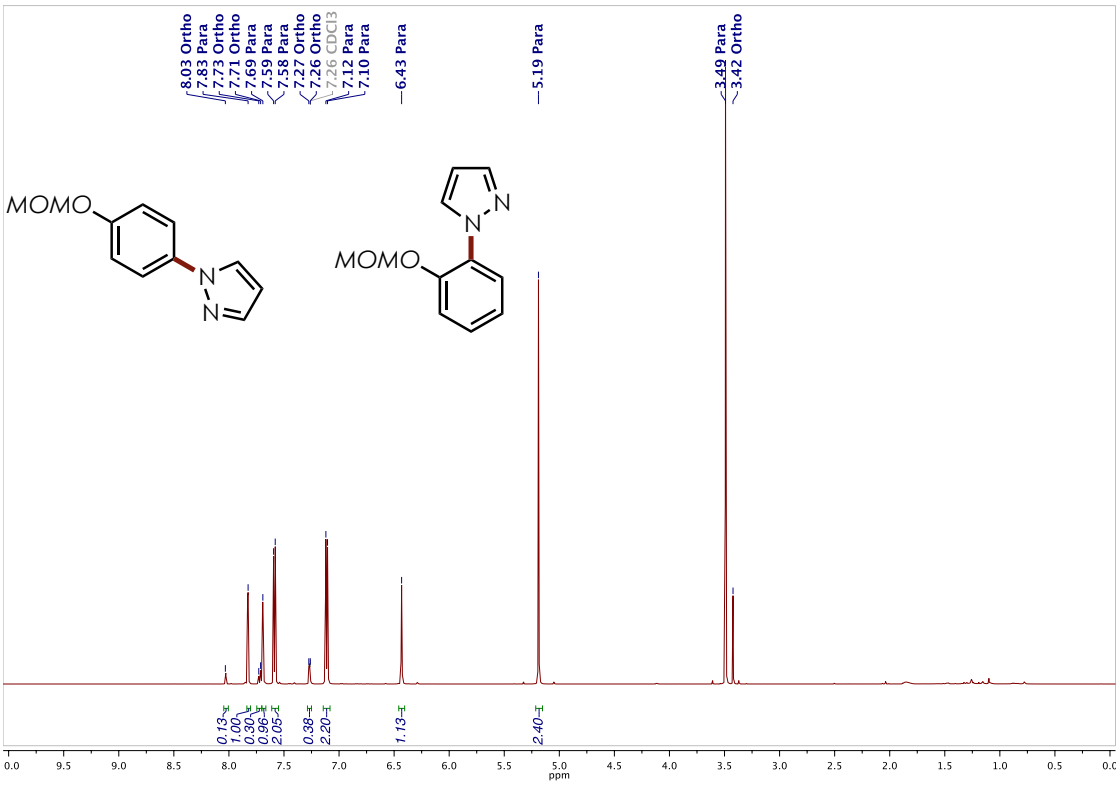
8.03 Ortho
7.83 Para
7.73 Ortho
7.71 Ortho
7.69 Para
7.59 Para
7.58 Para
7.27 Ortho
7.26 Ortho
7.26 CDCl3
7.12 Para
7.10 Para
6.43 Para
5.19 Para
3.49 Para
3.42 Ortho
MOMO
MOMO
0.13
1.00
0.30
0.96
2.05
0.38
2.20
1.13
2.40
ppm

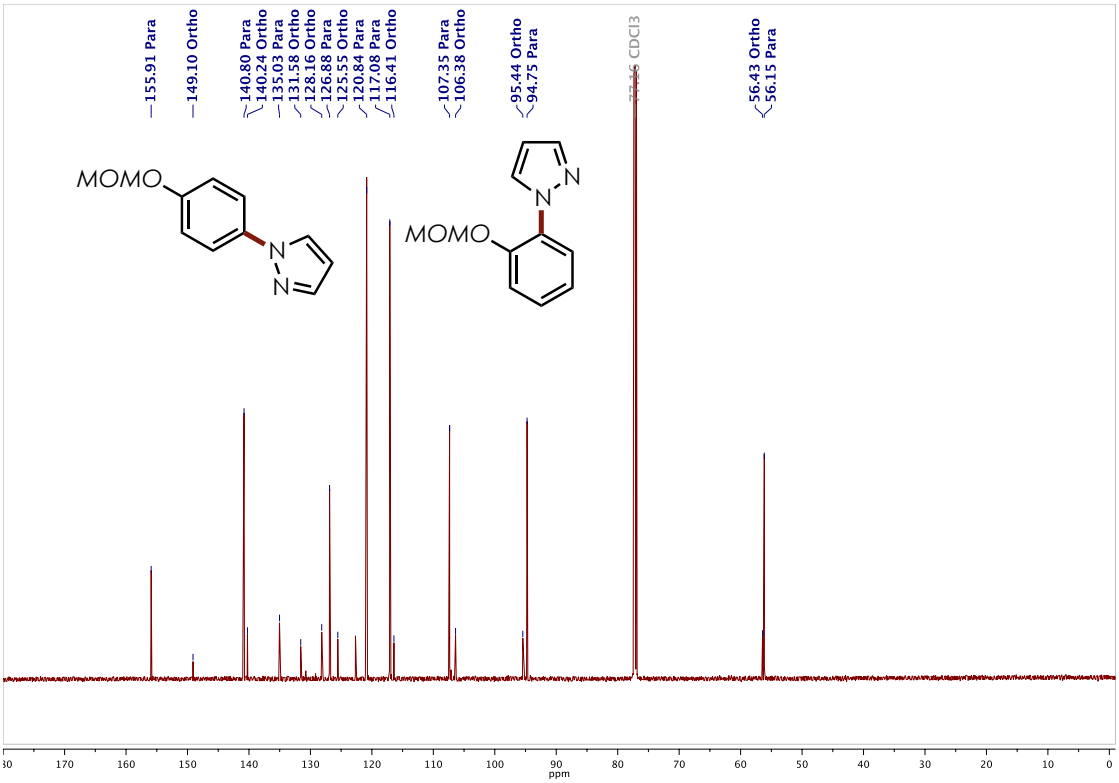
155.91 Para
149.10 Ortho
140.80 Para
140.24 Ortho
135.03 Para
131.58 Ortho
128.16 Ortho
126.88 Para
125.55 Ortho
120.84 Para
117.08 Para
116.41 Ortho
107.35 Para
106.38 Ortho
95.44 Ortho
94.75 Para
77.16 CDCl3
56.43 Ortho
56.15 Para
MOMO
MOMO
ppm

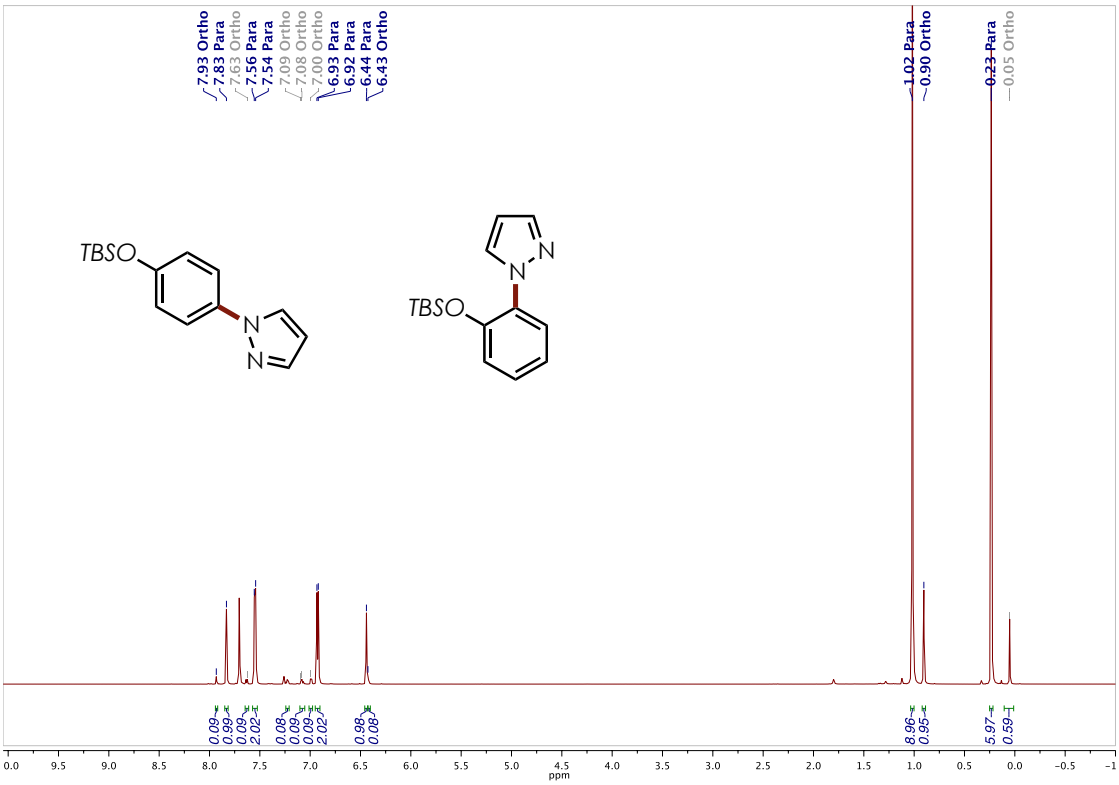
7.93 Ortho
7.83 Para
7.63 Ortho
7.56 Para
7.54 Para
7.09 Ortho
7.08 Ortho
7.00 Ortho
6.93 Para
6.92 Para
6.44 Para
6.43 Ortho
1.02 Para
0.90 Ortho
0.23 Para
0.05 Ortho
TBSO
TBSO
ppm

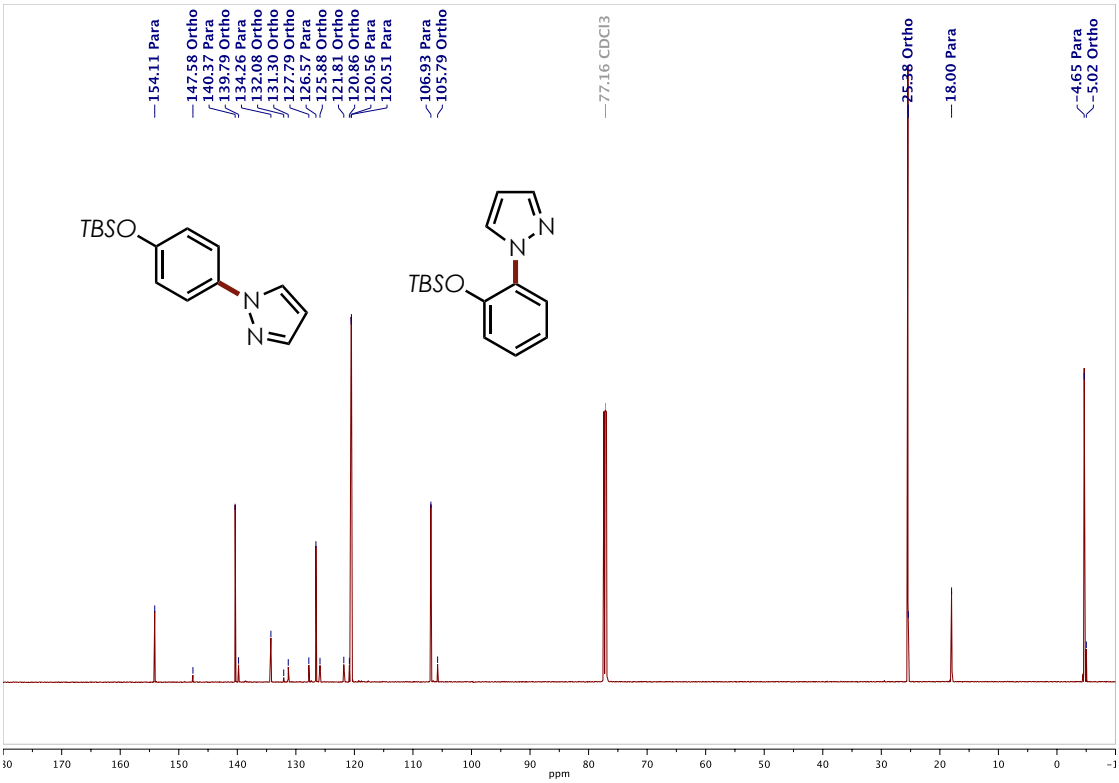
154.11 Para
147.58 Ortho
140.37 Para
139.79 Ortho
134.26 Para
132.08 Ortho
131.30 Ortho
127.79 Ortho
126.57 Para
125.88 Ortho
121.81 Ortho
120.86 Ortho
120.56 Para
120.51 Para
106.93 Para
105.79 Ortho
77.16 CDCl3
25.38 Ortho
18.00 Para
4.65 Para
5.02 Ortho
TBSO
TBSO
ppm

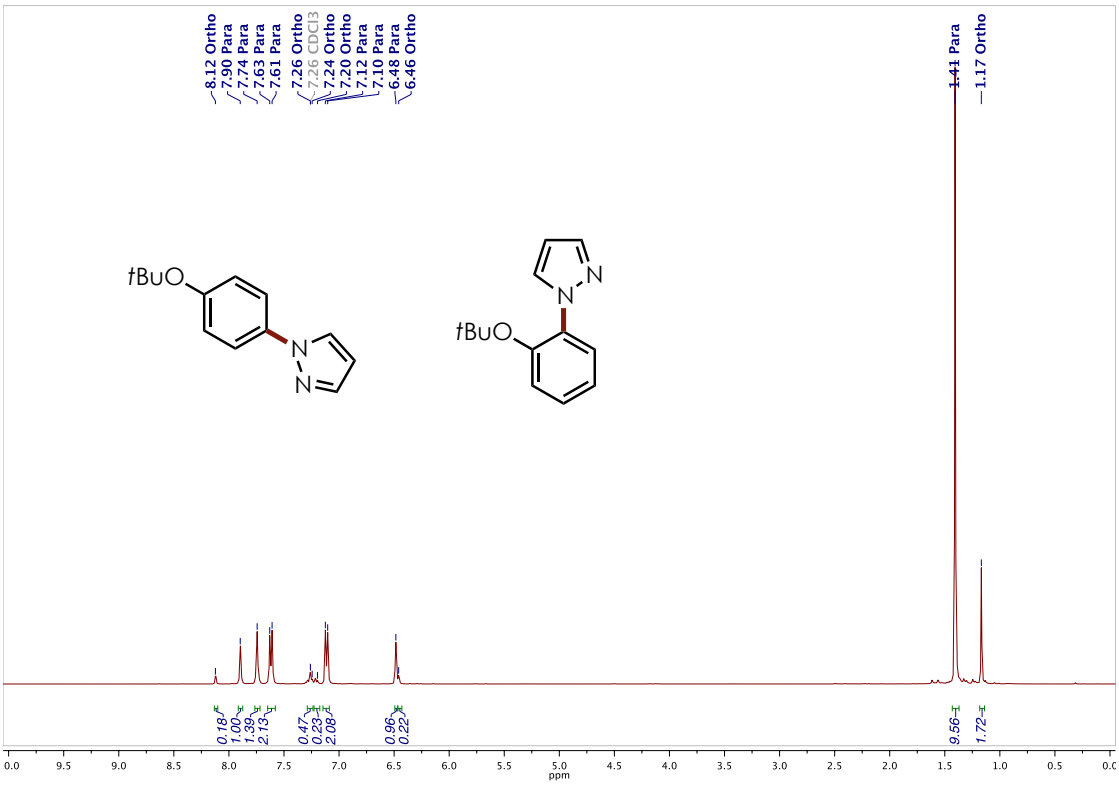
8.12 Ortho
7.90 Para
7.74 Para
7.63 Para
7.61 Para
7.26 Ortho
7.26 CDCl3
7.24 Ortho
7.20 Ortho
7.12 Para
7.10 Para
6.48 Para
6.46 Ortho
1.41 Para
1.17 Ortho
tBuO
tBuO
0.18
1.00
1.39
2.13
0.47
0.23
2.08
0.96
0.22
9.56
1.72
ppm

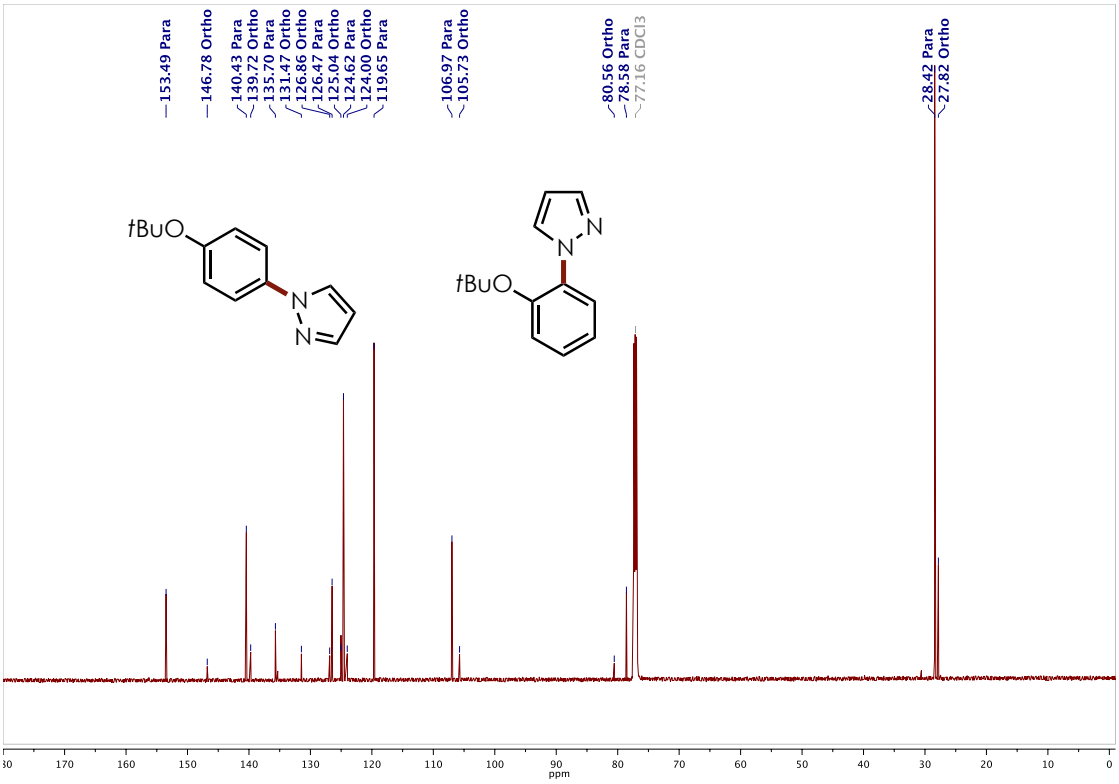
153.49 Para
146.78 Ortho
140.43 Para
139.72 Ortho
135.70 Para
131.47 Ortho
126.86 Ortho
126.47 Para
125.04 Ortho
124.62 Para
124.00 Ortho
119.65 Para
106.97 Para
105.73 Ortho
80.56 Ortho
78.58 Para
77.16 CDCl3
28.42 Para
27.82 Ortho
tBuO
tBuO
ppm

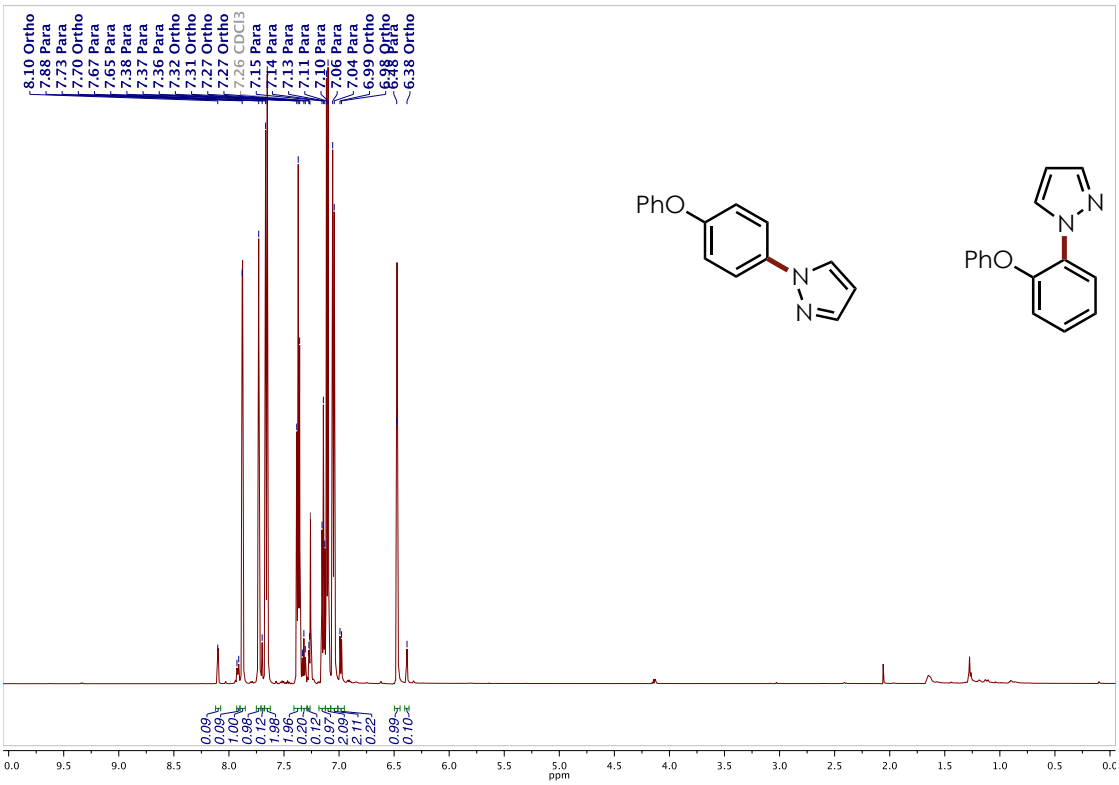
8.10 Ortho
7.88 Para
7.73 Para
7.70 Ortho
7.67 Para
7.65 Para
7.38 Para
7.37 Para
7.36 Para
7.32 Ortho
7.31 Ortho
7.27 Ortho
7.26 CDCl3
7.15 Para
7.14 Para
7.13 Para
7.11 Para
7.10 Para
7.06 Para
7.04 Para
6.99 Ortho
6.98 Para
6.38 Ortho
PhO
N
N
PhO
N
N
ppm

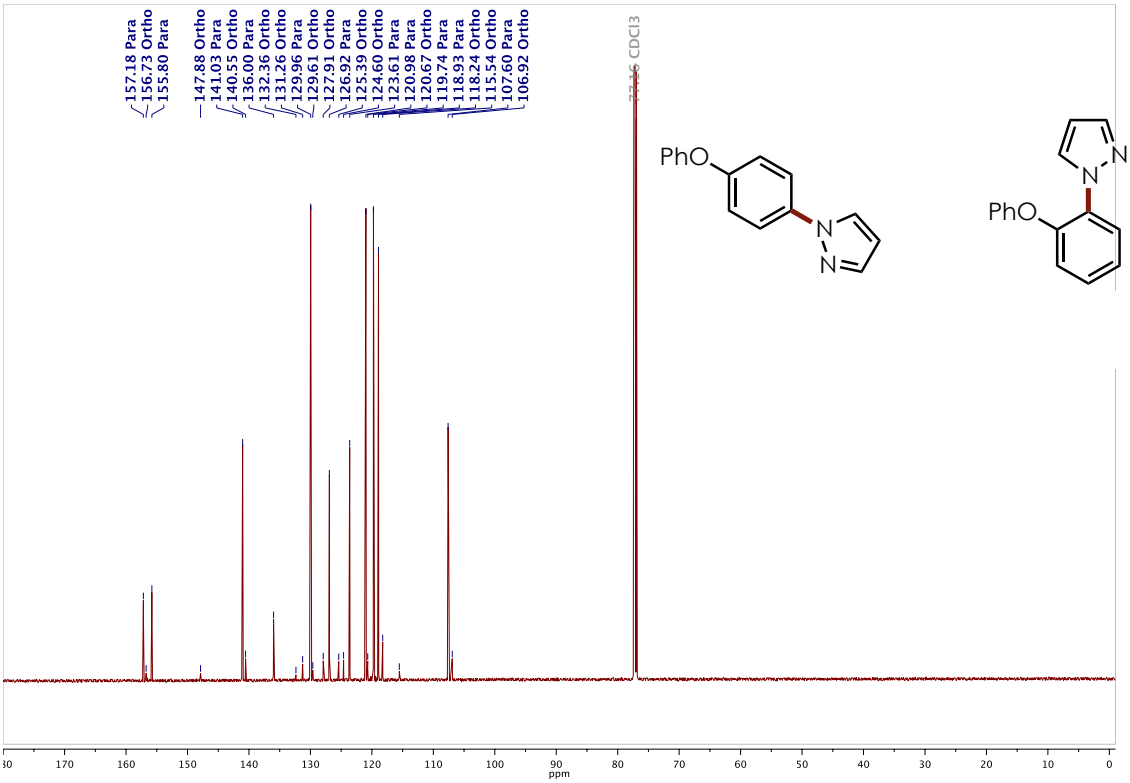
157.18 Para
156.73 Ortho
155.80 Para
147.88 Ortho
141.03 Para
140.55 Ortho
136.00 Para
132.36 Ortho
131.26 Ortho
129.96 Para
129.61 Ortho
127.91 Ortho
126.92 Para
125.39 Ortho
124.60 Ortho
123.61 Para
120.98 Para
120.67 Ortho
119.74 Para
118.93 Para
118.24 Ortho
115.54 Ortho
107.60 Para
106.92 Ortho
77.16 CDCl3
PhO
N
N
PhO
N
N
ppm

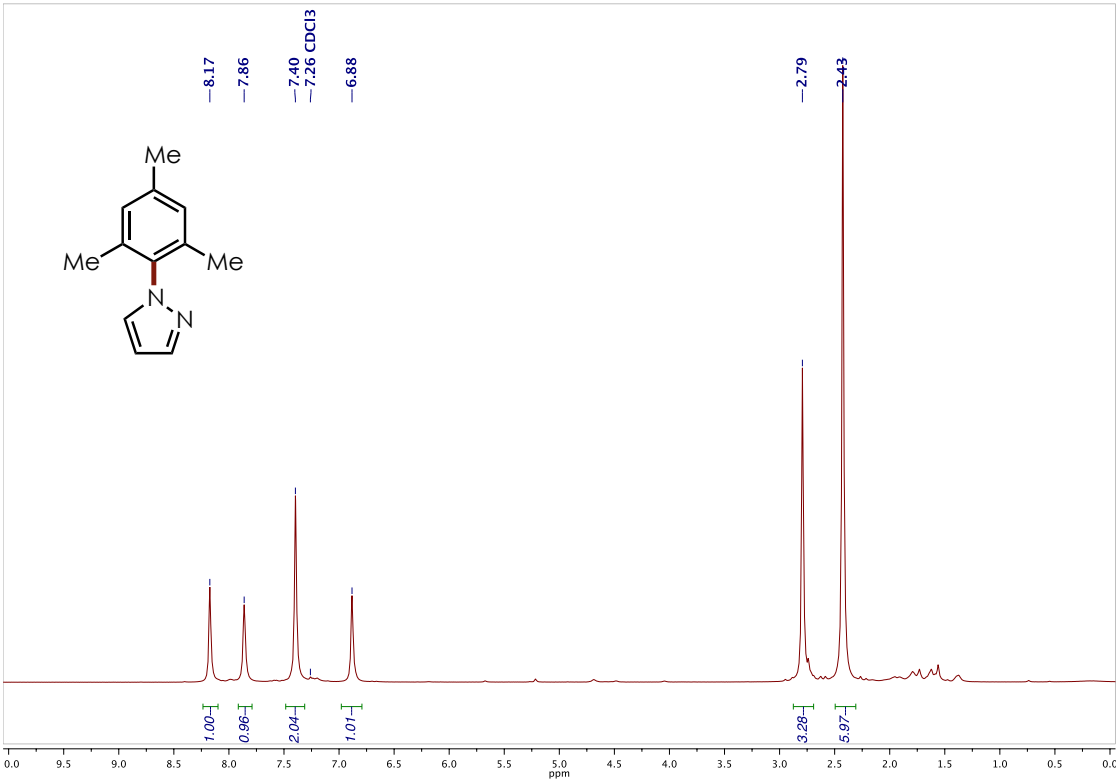
8.17
7.86
7.40
7.26 CDCl3
6.88
2.79
2.43
Me
Me
Me
N
N
1.00
0.96
2.04
1.01
3.28
5.97
ppm

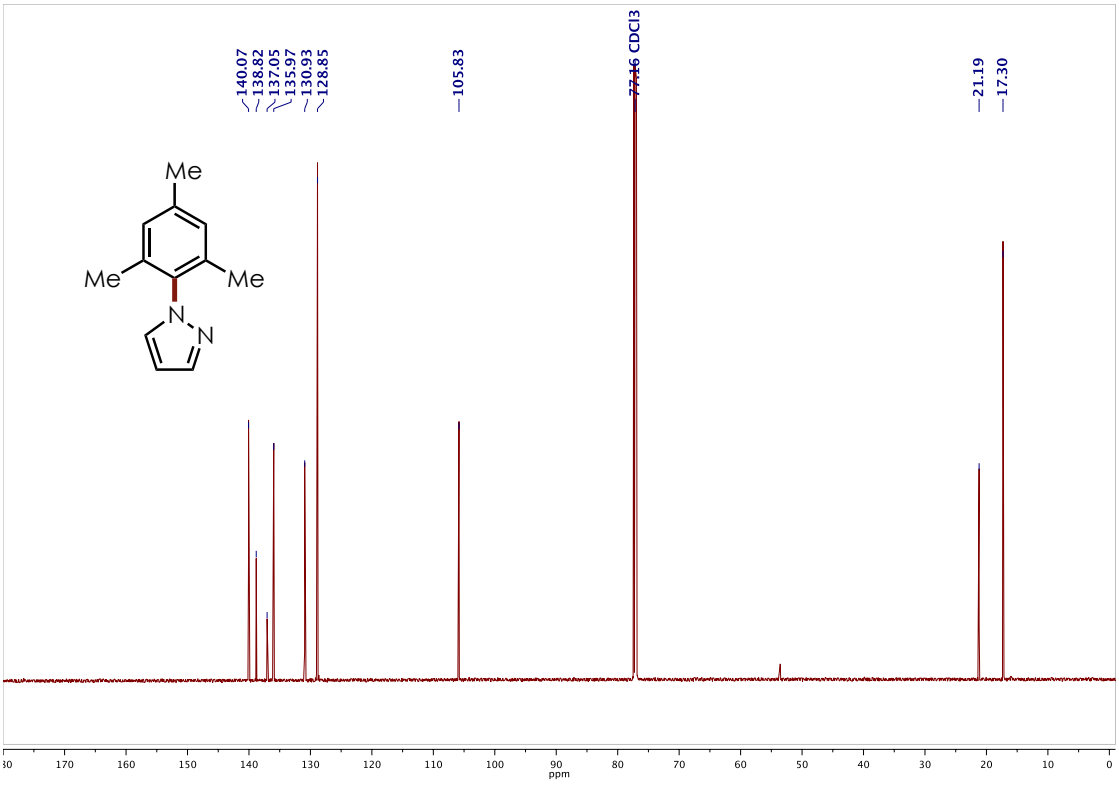
140.07
138.82
137.05
135.97
130.93
128.85
105.83
77.16 CDCl3
21.19
17.30
Me
Me
Me
N
N
ppm

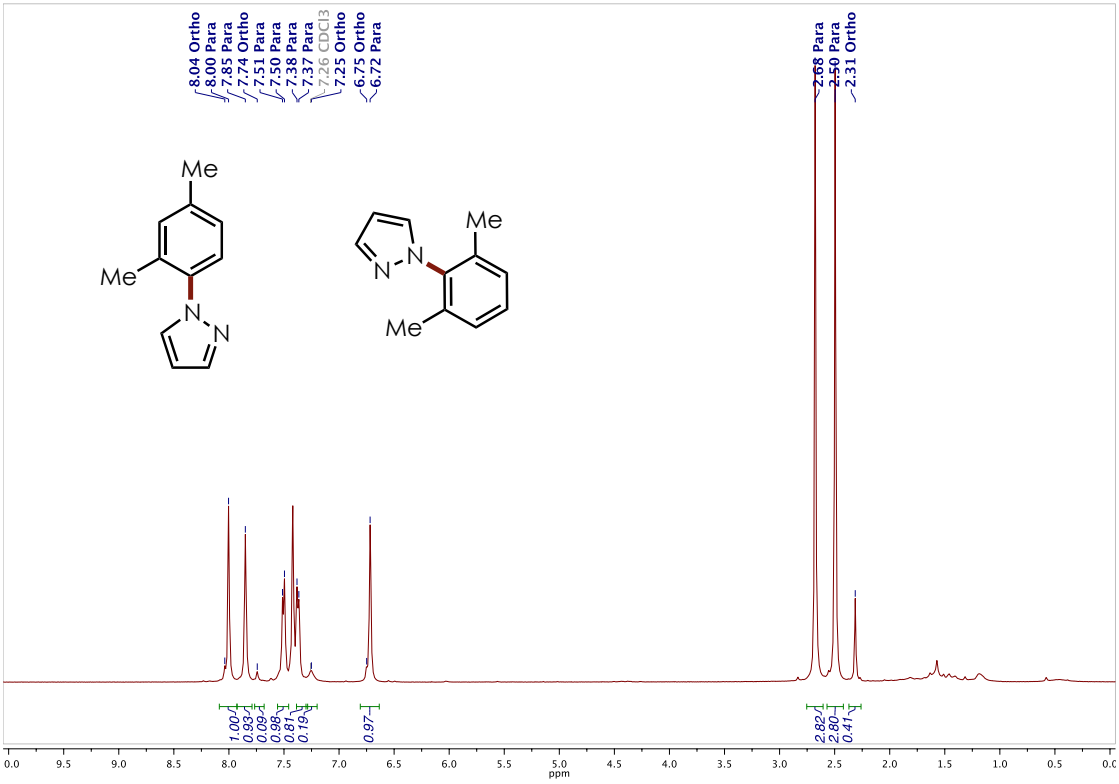
8.04 Ortho
8.00 Para
7.85 Para
7.74 Ortho
7.51 Para
7.50 Para
7.38 Para
7.37 Para
7.26 CDCl3
7.25 Ortho
6.75 Ortho
6.72 Para
2.68 Para
2.50 Para
2.31 Ortho
Me
Me
N
N
Me
N
N
Me
1.00
0.93
0.09
0.98
0.81
0.19
0.97
2.82
2.80
0.41
ppm

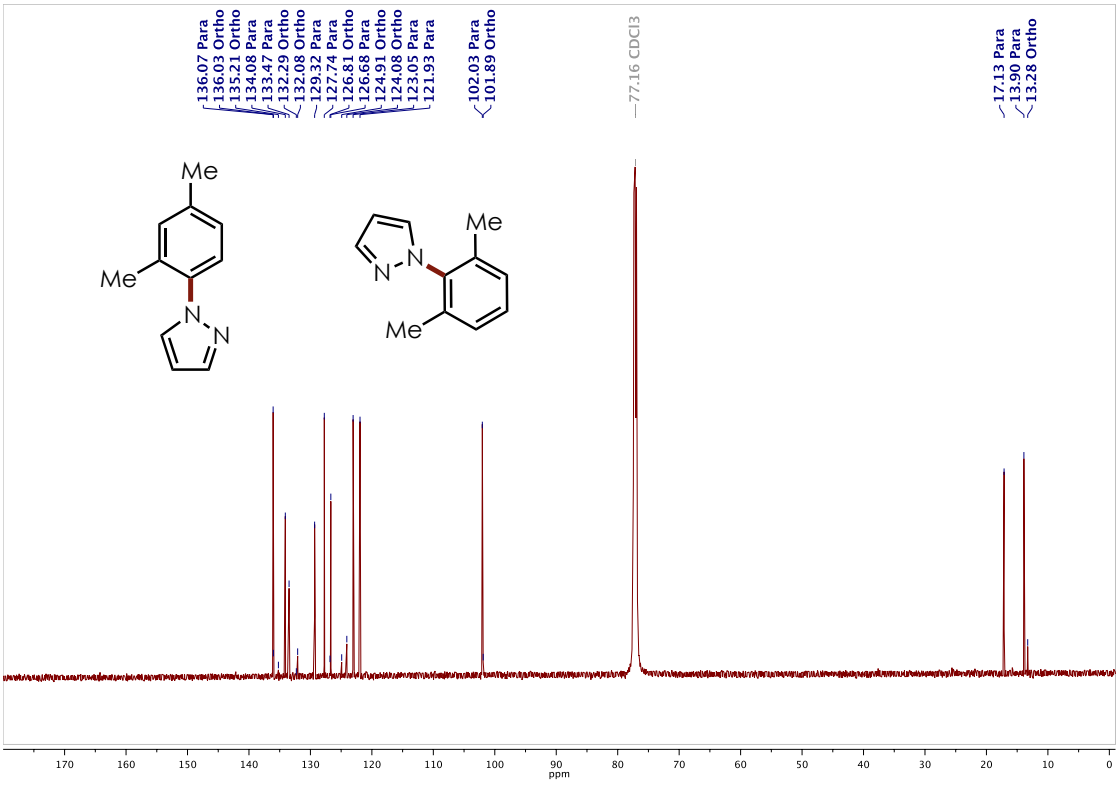
136.07 Para
136.03 Ortho
135.21 Ortho
134.08 Para
133.47 Para
132.29 Ortho
132.08 Ortho
129.32 Para
127.74 Para
126.81 Ortho
126.68 Para
124.91 Ortho
124.08 Ortho
123.05 Para
121.93 Para
102.03 Para
101.89 Ortho
77.16 CDCl3
17.13 Para
13.90 Para
13.28 Ortho
Me
Me
N
N
Me
N
N
Me
ppm

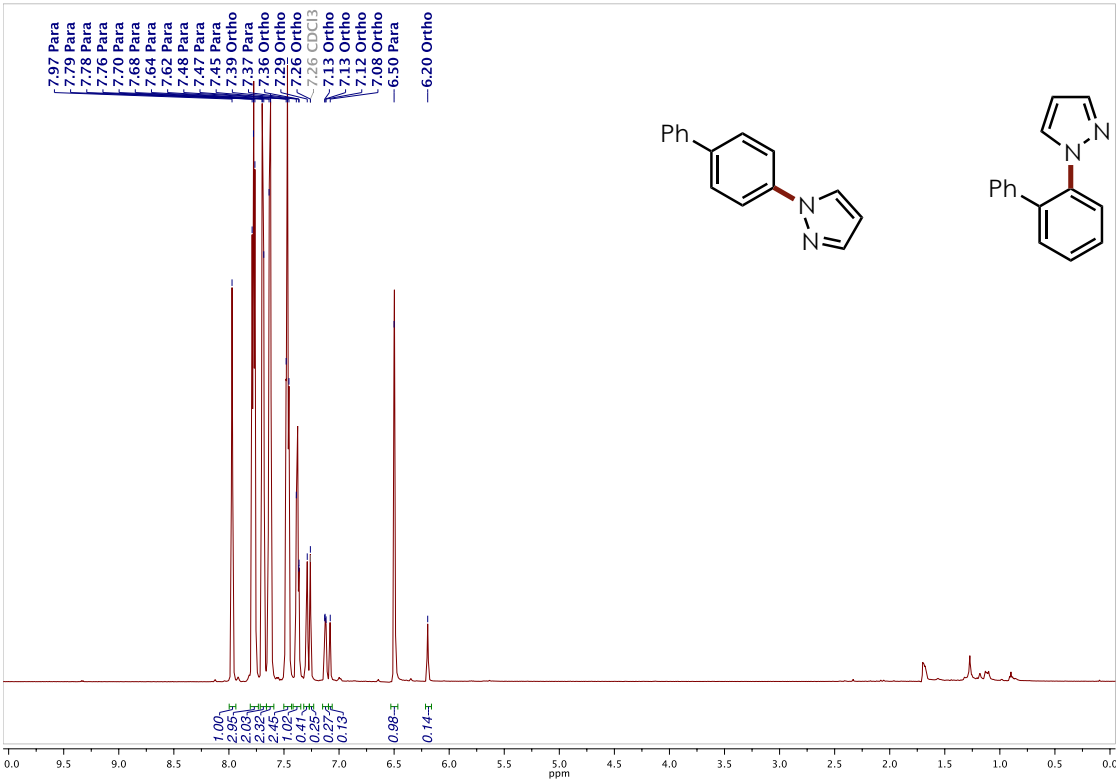
7.97 Para
7.79 Para
7.78 Para
7.76 Para
7.70 Para
7.68 Para
7.64 Para
7.62 Para
7.48 Para
7.47 Para
7.45 Para
7.39 Ortho
7.37 Para
7.36 Ortho
7.29 Ortho
7.26 Ortho
7.26 CDCl3
7.13 Ortho
7.13 Ortho
7.12 Ortho
7.08 Ortho
6.50 Para
6.20 Ortho
1.00
2.95
2.03
2.32
2.45
1.02
0.41
0.27
0.13
0.98
0.14
Ph
N
N
Ph
N
N
ppm

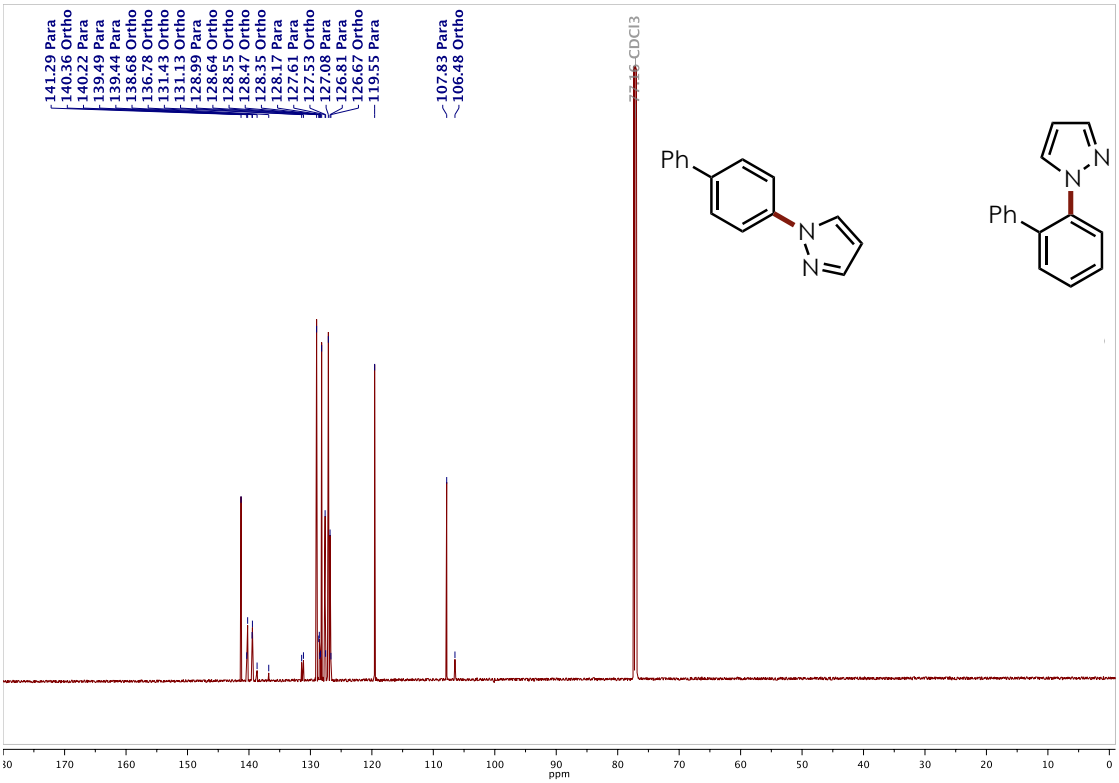
141.29 Para
140.36 Ortho
140.22 Para
139.49 Para
139.44 Para
138.68 Ortho
136.78 Ortho
131.43 Ortho
131.13 Ortho
128.99 Para
128.64 Ortho
128.55 Ortho
128.47 Ortho
128.35 Ortho
128.17 Para
127.61 Para
127.53 Ortho
127.08 Para
126.81 Para
126.67 Ortho
119.55 Para
107.83 Para
106.48 Ortho
77.16 CDCl3
Ph
N
N
Ph
N
N
ppm

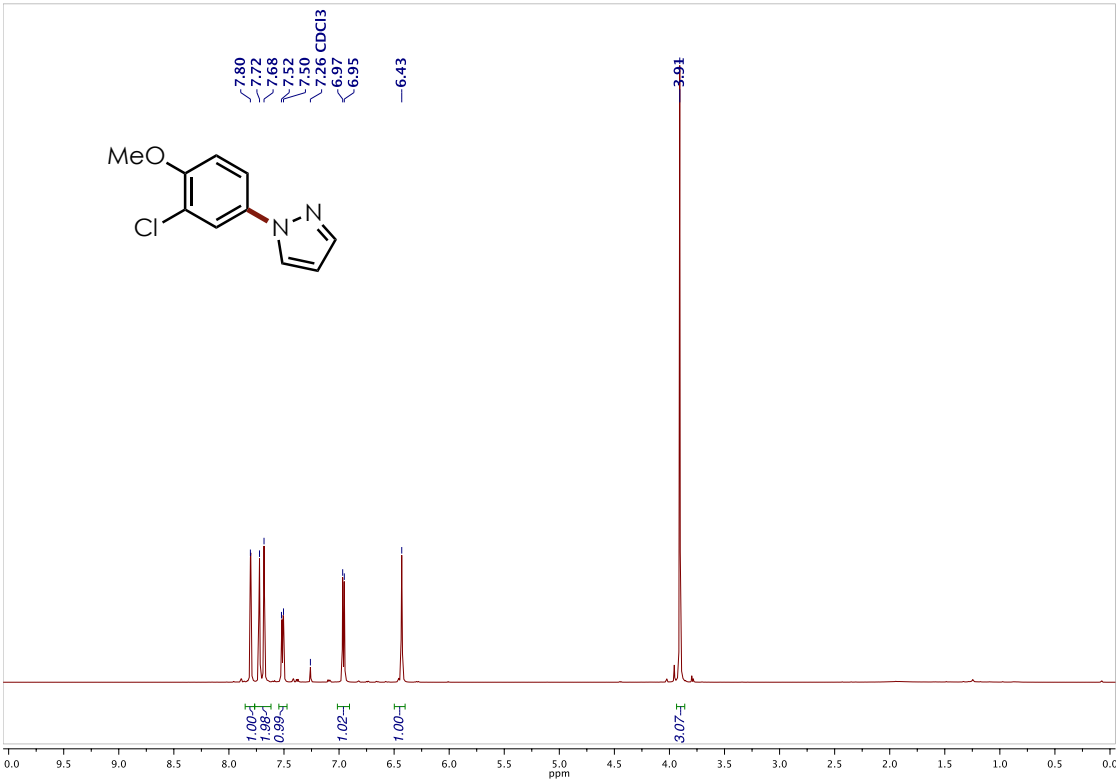
7.80
7.72
7.68
7.52
7.50
7.26 CDCl3
6.97
6.95
6.43
3.91
MeO
Cl
N
N
1.00
1.98
0.99
1.02
1.00
3.07
ppm

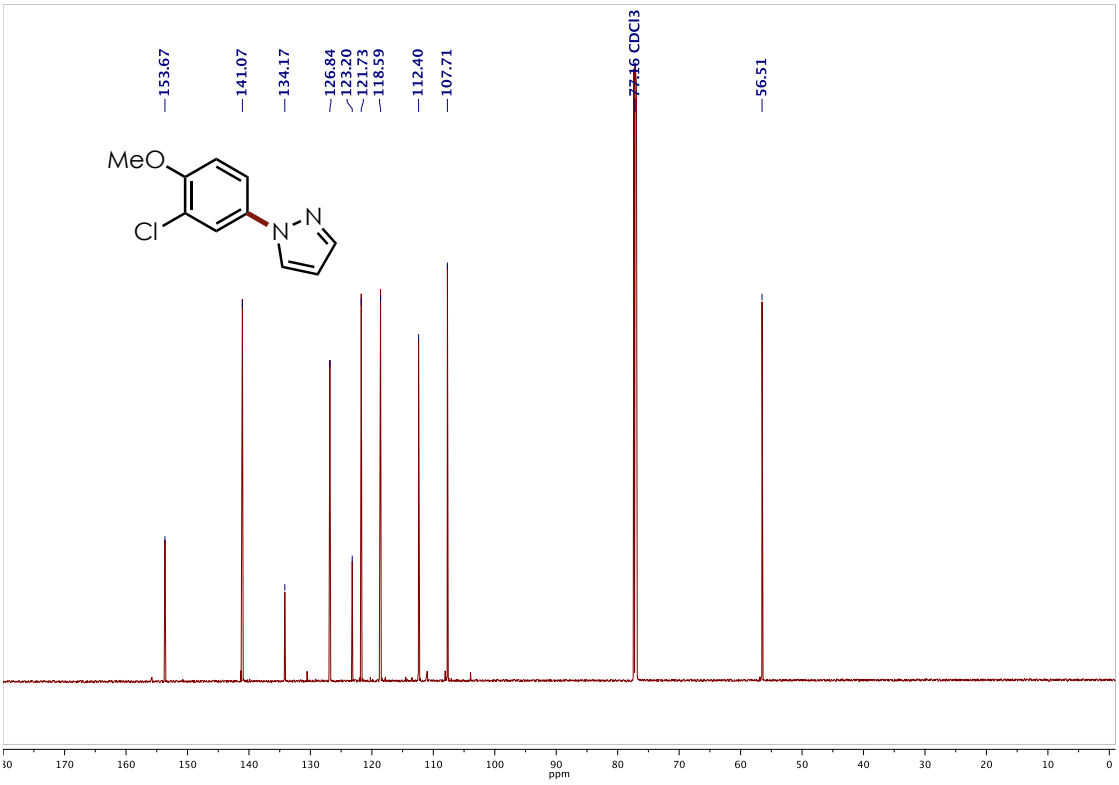
153.67
141.07
134.17
126.84
123.20
121.73
118.59
112.40
107.71
77.16 CDCl3
56.51
MeO
Cl
N
N
ppm

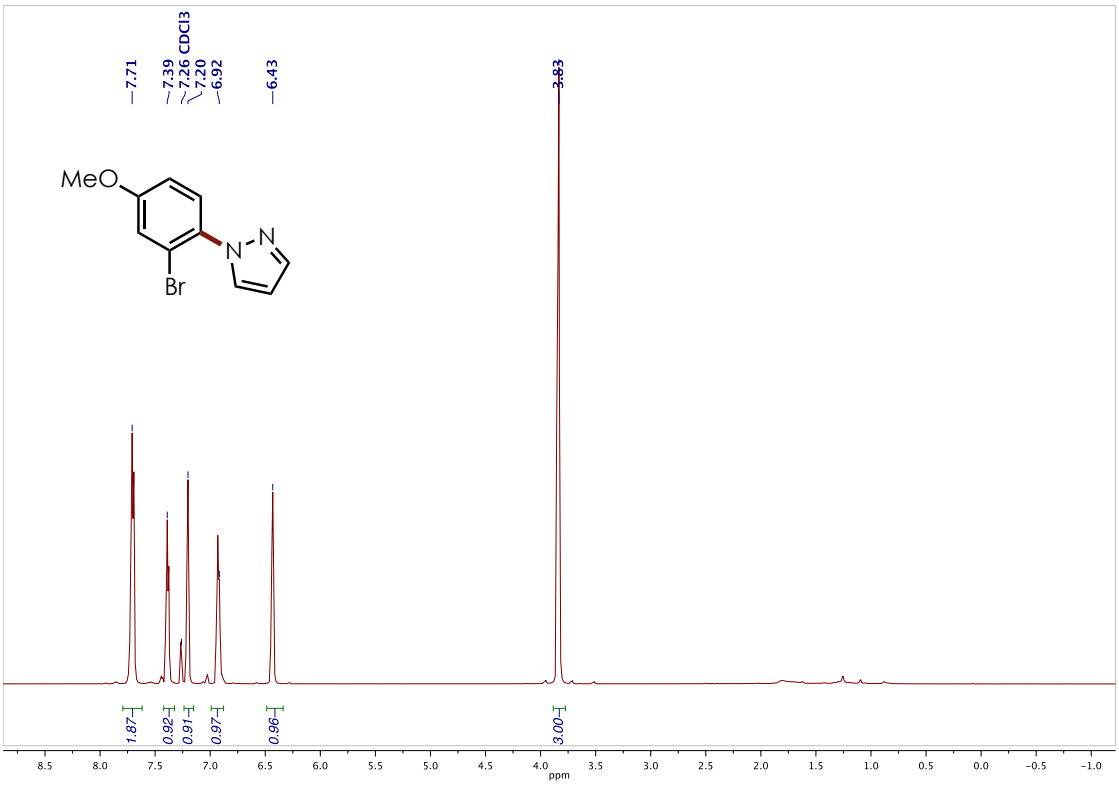
7.71
7.39
7.26 CDCl3
7.20
6.92
6.43
3.83
MeO
N
N
Br
1.87
0.92
0.91
0.97
0.96
3.00
ppm

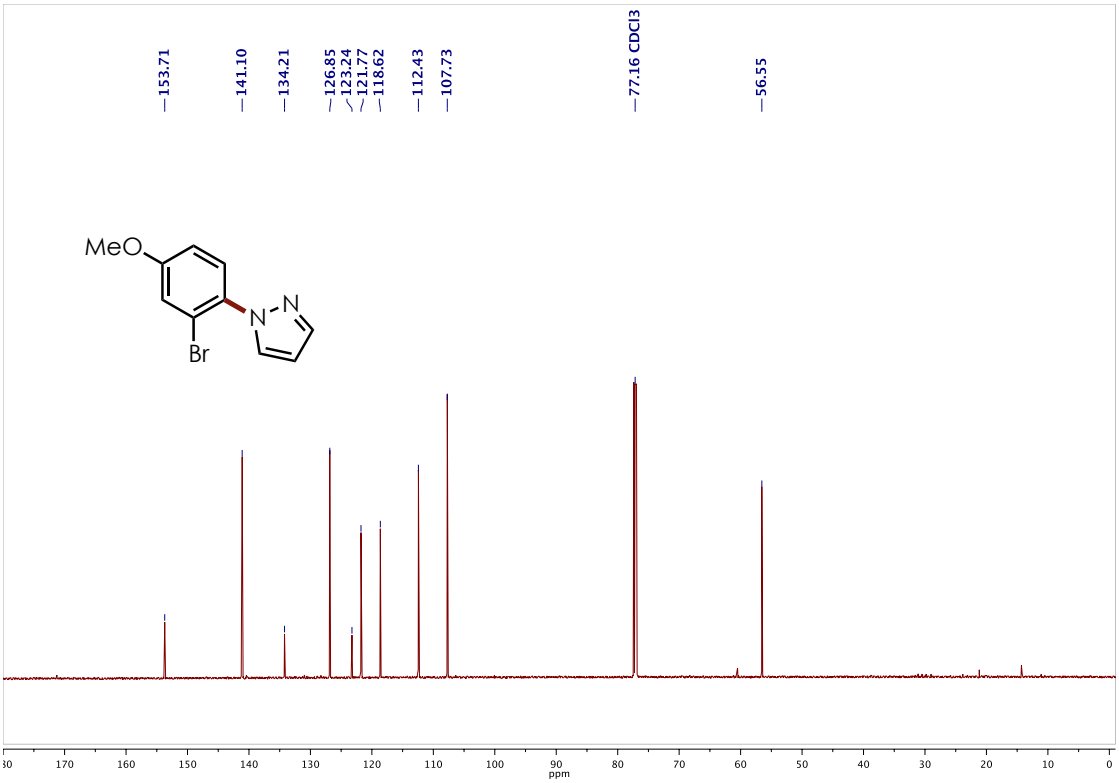
153.71
141.10
134.21
126.85
123.24
121.77
118.62
112.43
107.73
77.16 CDCl3
56.55
MeO
N
N
Br
ppm

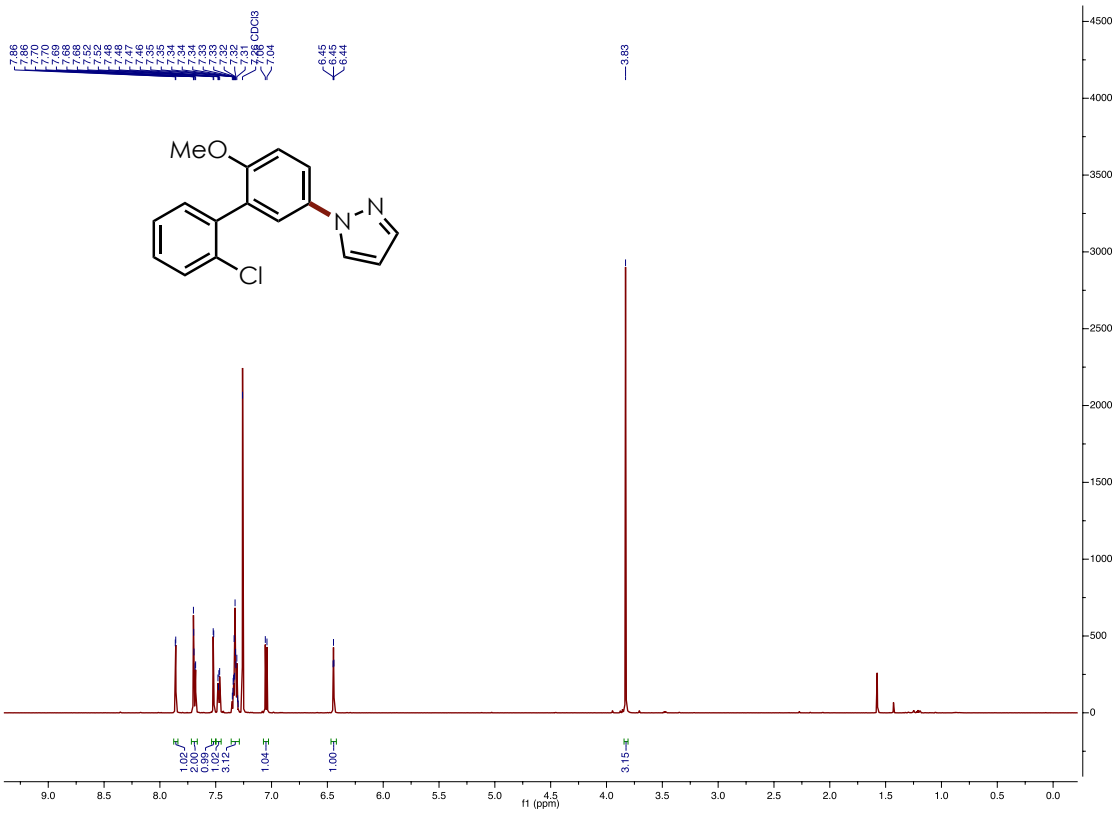
7.88
7.86
7.70
7.70
7.69
7.69
7.68
7.52
7.52
7.48
7.48
7.47
7.46
7.35
7.35
7.34
7.34
7.33
7.33
7.32
7.31
7.26 CDCl3
7.04
6.45
6.45
6.44
3.83
MeO
N
N
Cl
1.02
2.00
0.99
1.02
3.12
1.04
1.00
3.15
f1 (ppm)

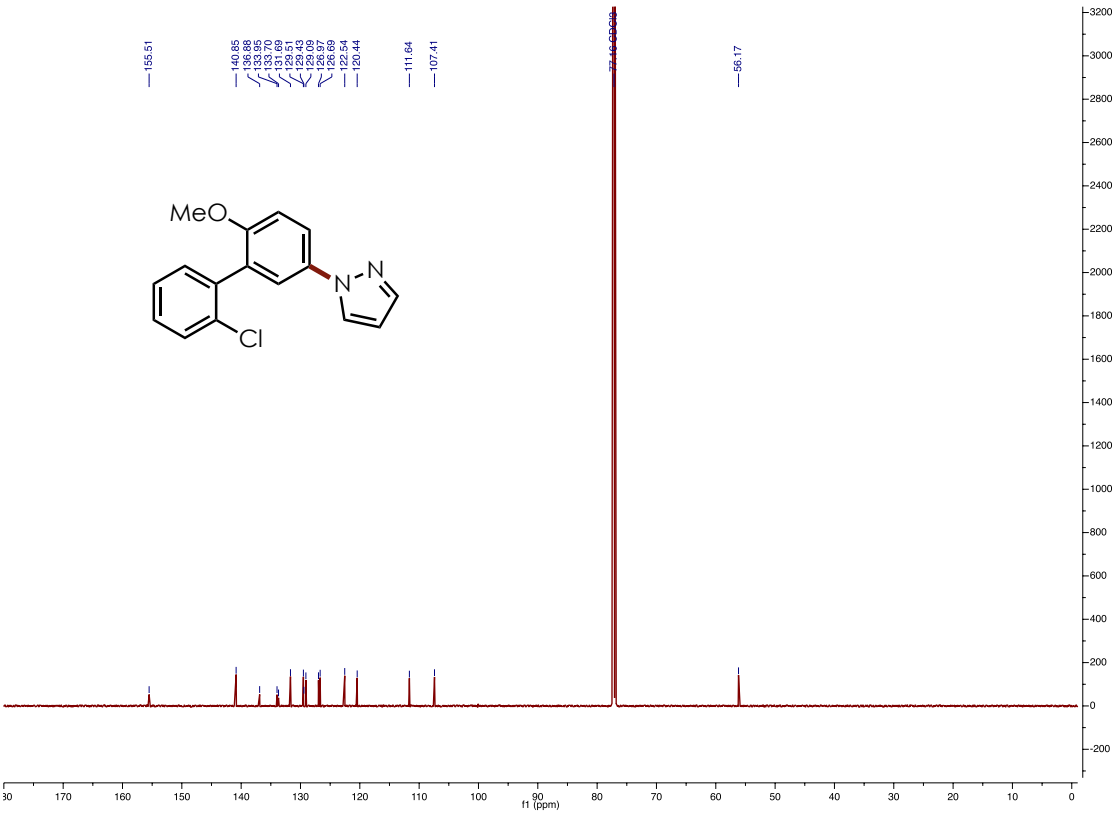
155.51
140.85
136.88
133.95
133.70
131.69
129.51
129.43
129.09
128.97
126.69
122.54
120.44
111.64
107.41
77.16 CDCl3
56.17
MeO
N
N
Cl
f1 (ppm)

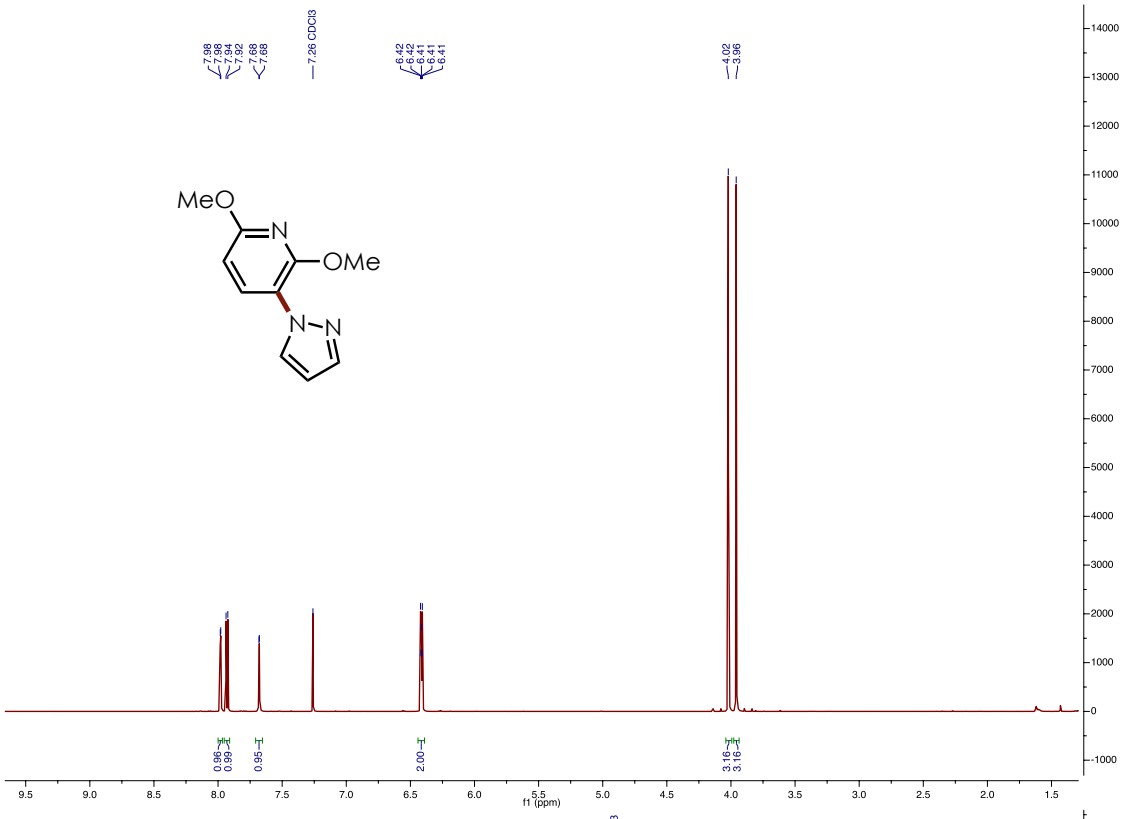
7.98
7.98
7.94
7.92
7.88
7.88
7.26 CDCl3
6.42
6.42
6.41
6.41
6.41
4.02
3.96
MeO
N
OMe
N
N
0.96
0.99
0.95
2.00
3.16
3.16
f1 (ppm)

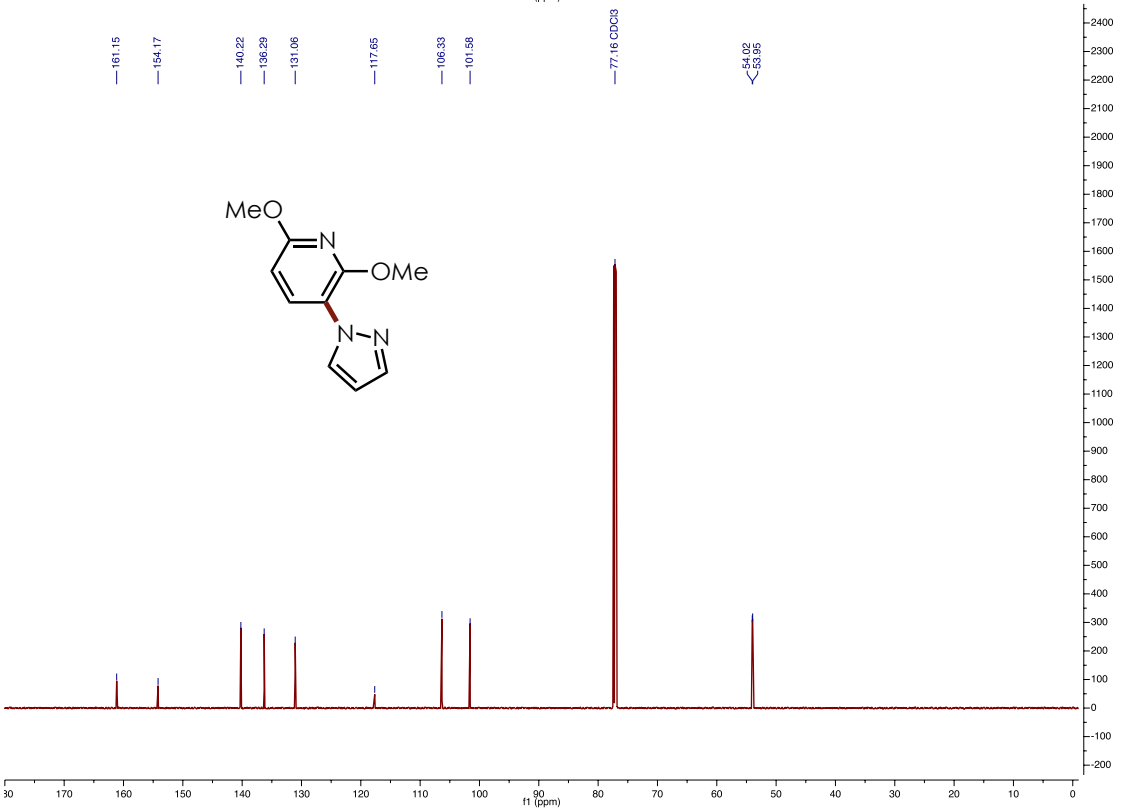
161.15
154.17
140.22
136.29
131.06
117.65
106.33
101.58
77.16 CDCl3
54.02
53.95
MeO
N
OMe
N
N
f1 (ppm)

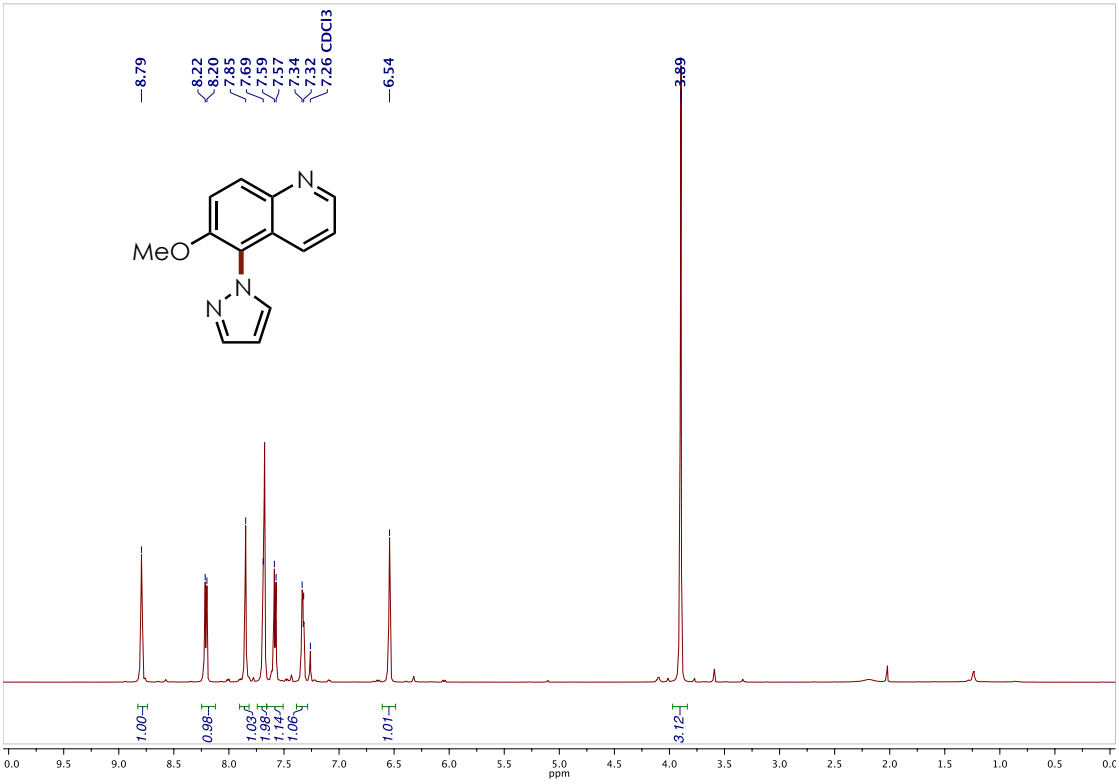
8.79
8.22
8.20
7.85
7.69
7.59
7.57
7.34
7.32
7.26 CDCl3
6.54
3.89
MeO
N
N
N
1.00
0.98
1.03
1.98
1.14
1.06
1.01
3.12
ppm

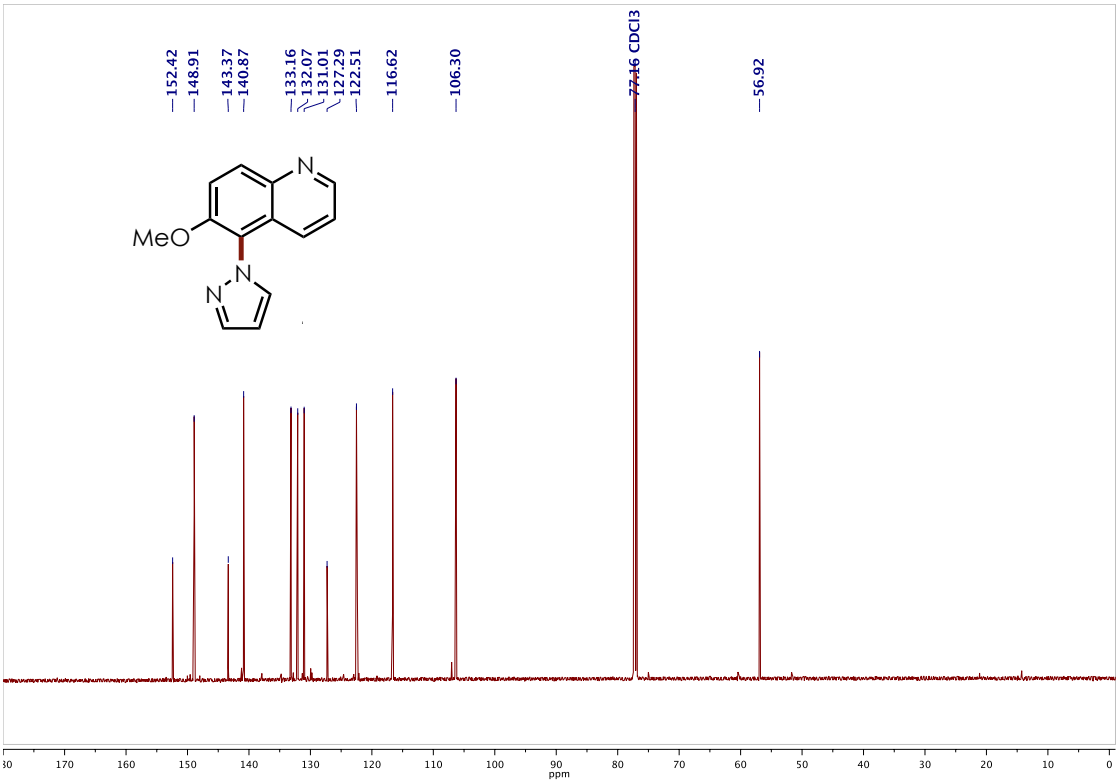
152.42
148.91
143.37
140.87
133.16
132.07
131.01
127.29
122.51
116.62
106.30
77.16 CDCl3
56.92
MeO
N
N
N
ppm

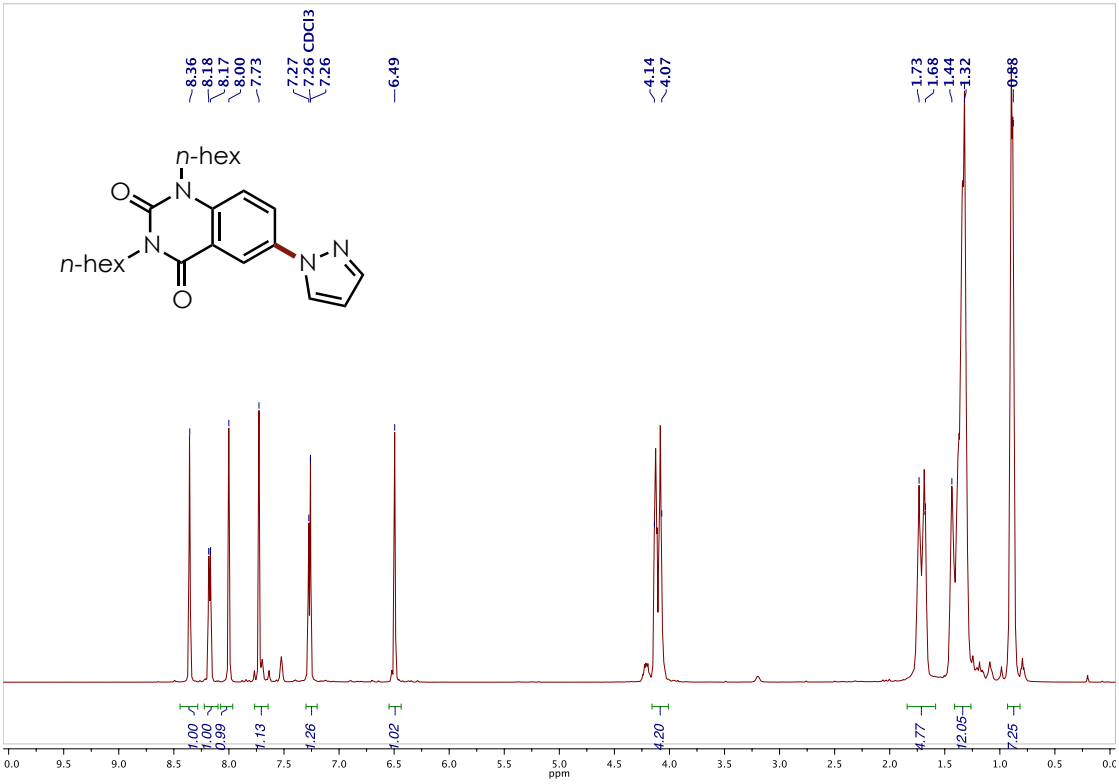
8.36
8.18
8.17
8.00
7.73
7.27
7.26 CDCl3
7.26
6.49
4.14
4.07
1.73
1.68
1.44
1.32
0.88
n-hex
n-hex
1.00
1.00
0.99
1.13
1.26
1.02
4.20
4.77
12.05
7.25
ppm

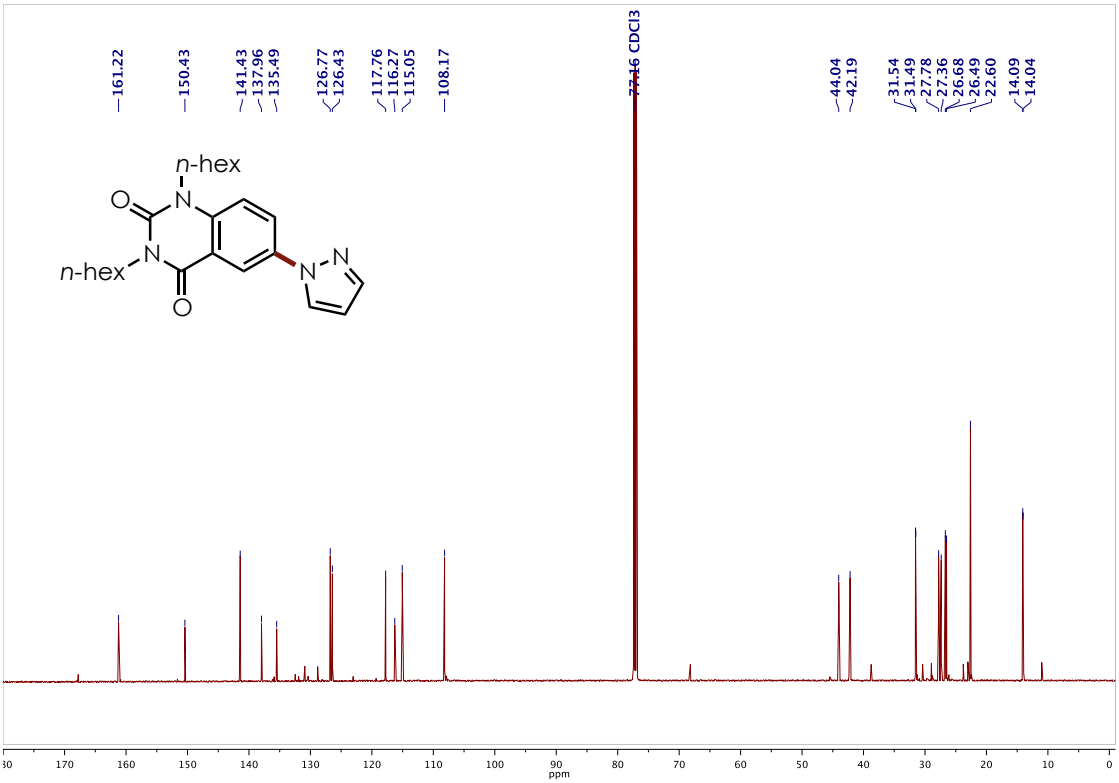
161.22
150.43
141.43
137.96
135.49
126.77
126.43
117.76
116.27
115.05
108.17
77.16 CDCl3
44.04
42.19
31.54
31.49
27.78
27.36
26.68
26.49
22.60
14.09
14.04
n-hex
n-hex
ppm

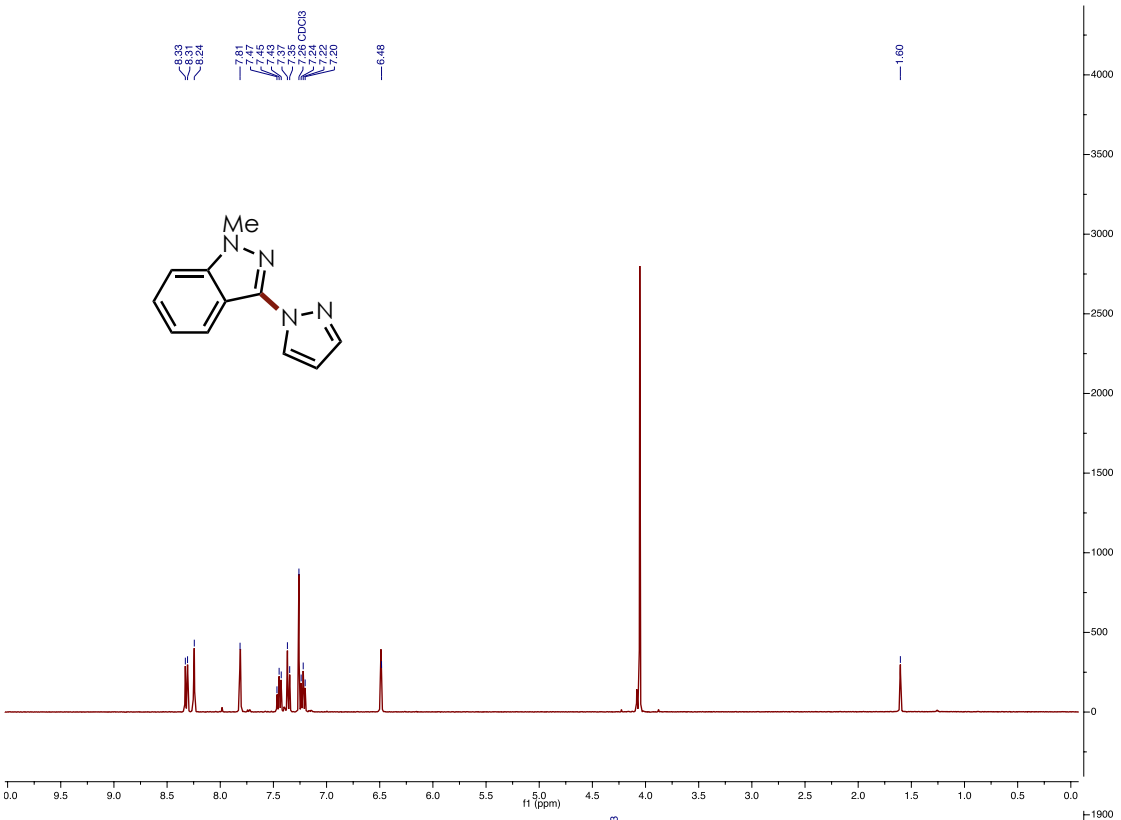
8.33
8.31
8.24
7.61
7.47
7.45
7.43
7.37
7.35
7.26 CDCl3
7.24
7.22
7.20
6.48
1.60
Me
N
N
N
N
f1 (ppm)

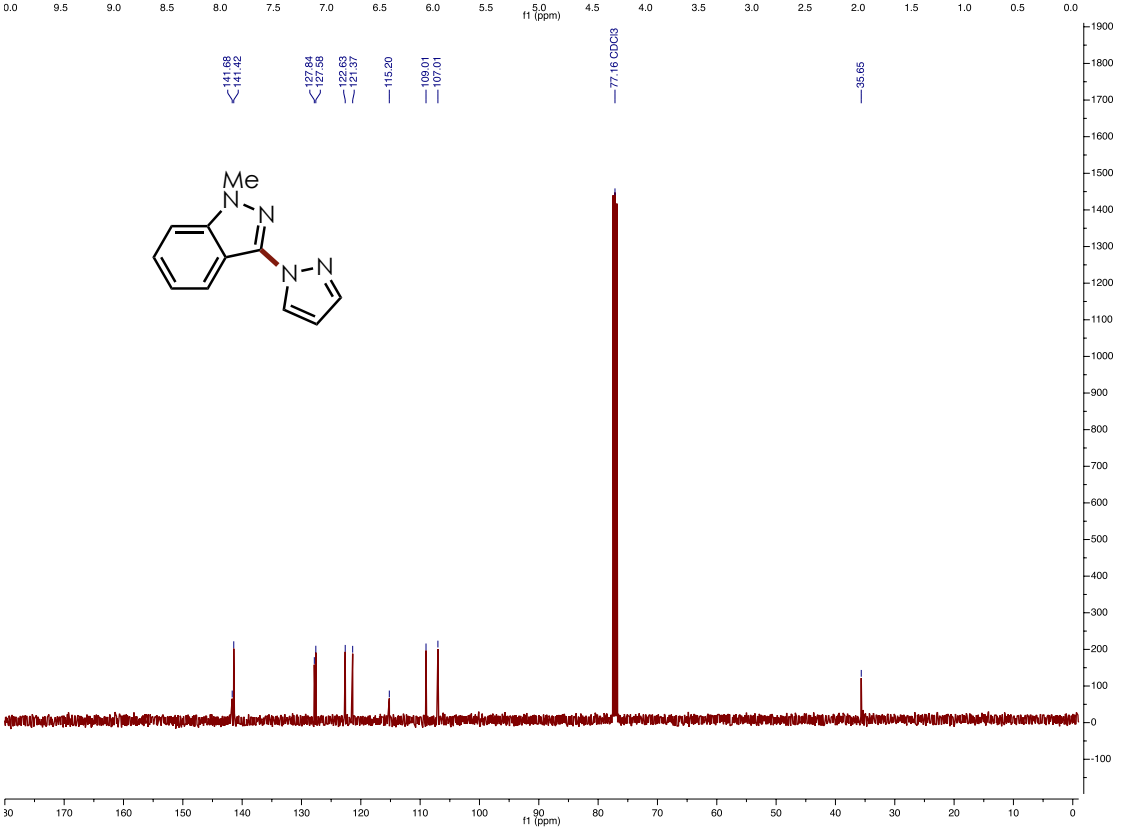
141.68
141.42
127.84
127.58
122.63
121.37
115.20
109.01
107.01
77.16 CDCl3
35.65
Me
N
N
N
N
f1 (ppm)

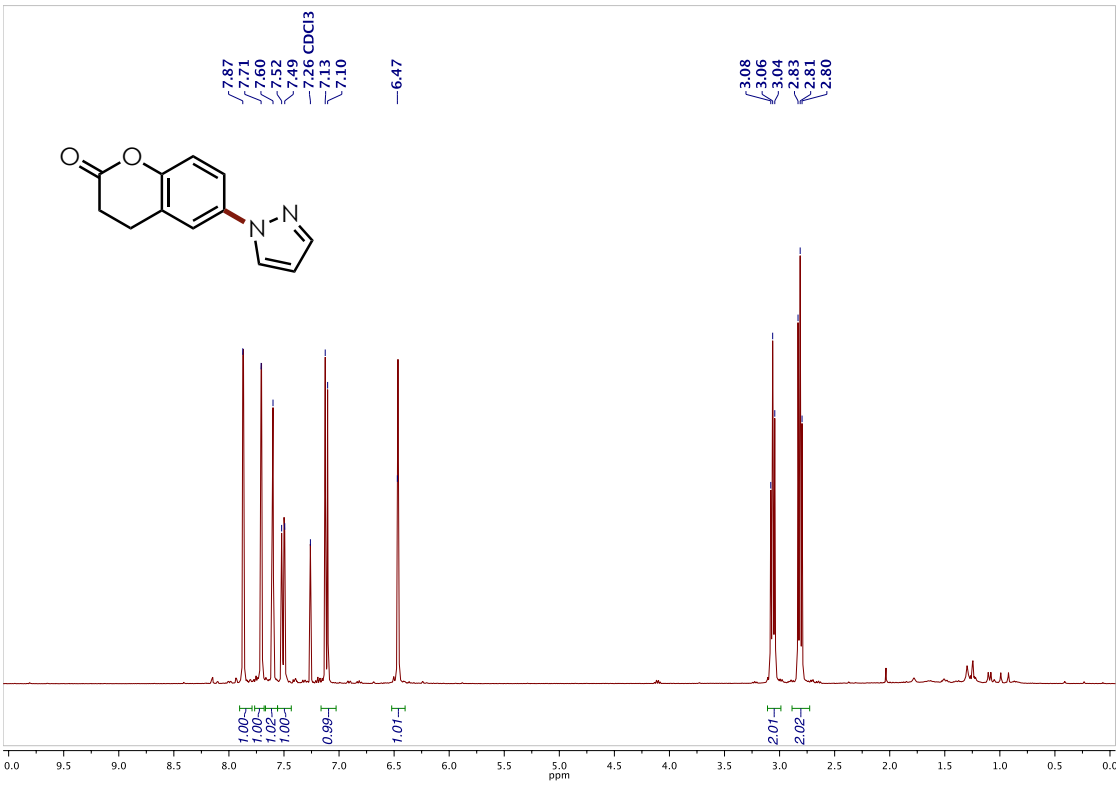
7.87
7.71
7.60
7.52
7.49
7.26 CDCl3
7.13
7.10
6.47
3.08
3.06
3.04
2.83
2.81
2.80
1.00
1.00
1.02
1.00
0.99
1.01
2.01
2.02
ppm

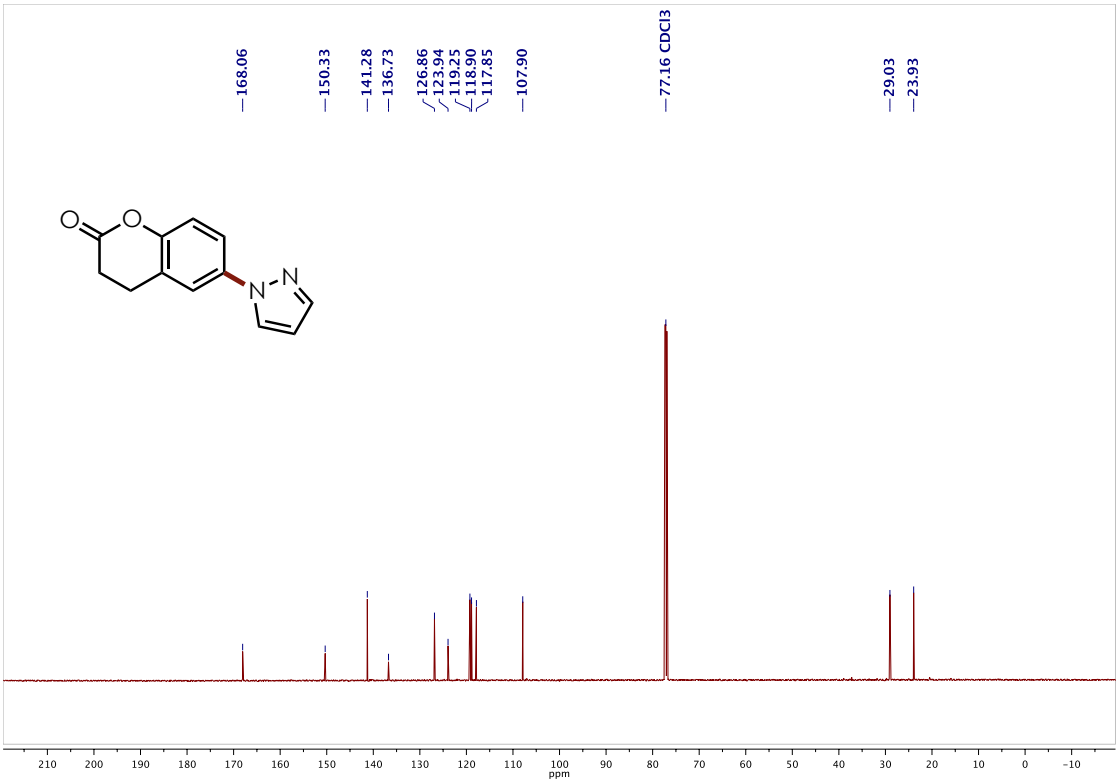
168.06
150.33
141.28
136.73
126.86
123.94
119.25
118.90
117.85
107.90
77.16 CDCl3
29.03
23.93
ppm

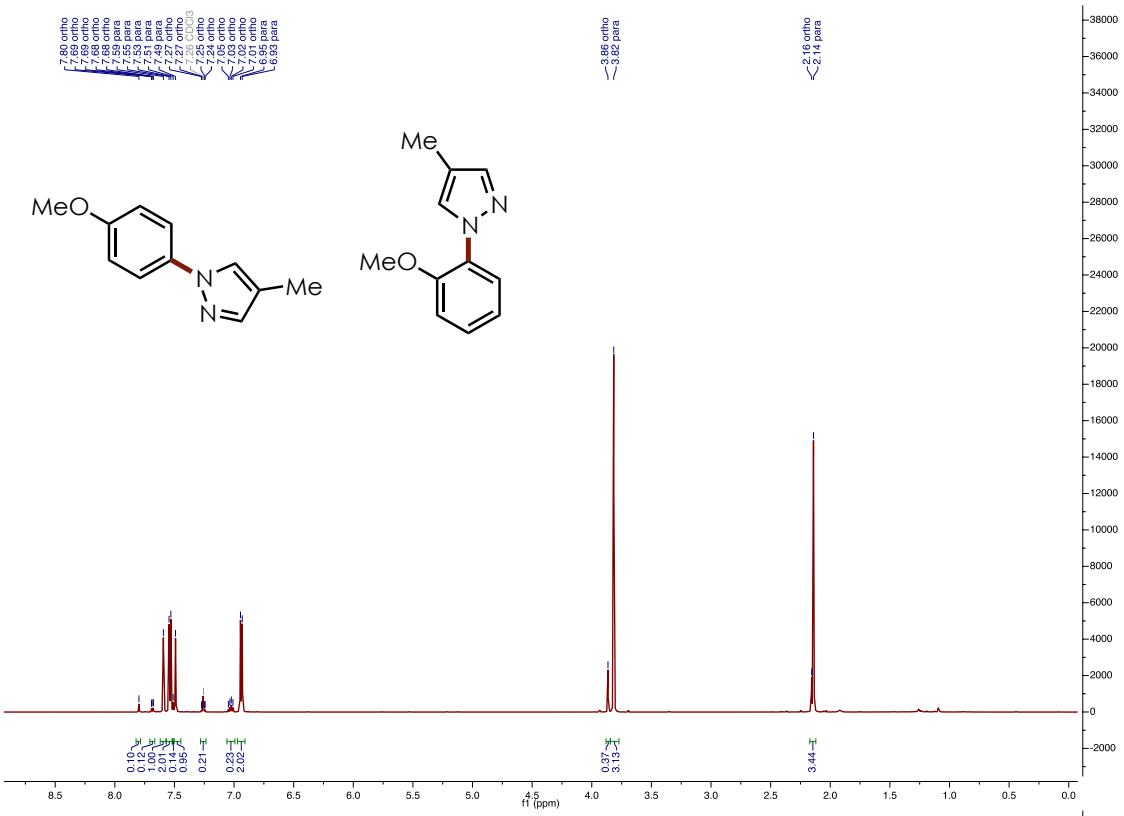
7.80 ortho
7.69 ortho
7.68 ortho
7.68 ortho
7.68 ortho
7.59 para
7.55 para
7.51 para
7.49 para
7.27 ortho
7.26 ortho
7.26 CDCl3
7.25 ortho
7.24 ortho
7.04 ortho
7.03 ortho
7.02 ortho
6.91 ortho
6.91 para
6.93 para
3.86 ortho
3.82 para
2.16 ortho
2.14 para
MeO
N
N
Me
Me
N
N
MeO
0.10
0.12
1.00
2.01
0.14
0.95
0.21
0.23
2.02
0.37
3.13
3.44
f1 (ppm)

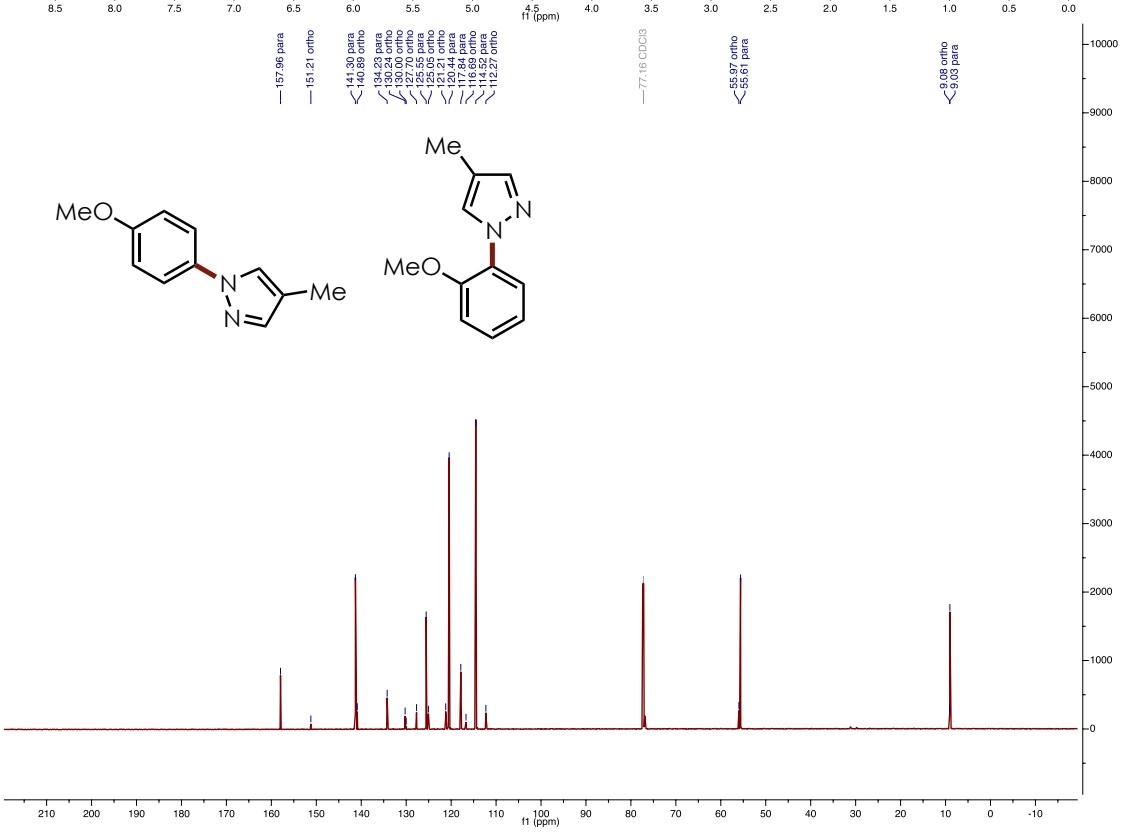
157.96 para
151.21 ortho
141.30 para
140.88 ortho
134.23 para
130.24 ortho
130.00 ortho
127.70 ortho
125.55 para
125.00 ortho
121.21 ortho
120.44 para
117.84 para
116.68 ortho
114.52 para
112.27 ortho
77.16 CDCl3
55.97 ortho
55.61 para
9.08 ortho
9.03 para
MeO
N
N
Me
Me
N
N
MeO
f1 (ppm)

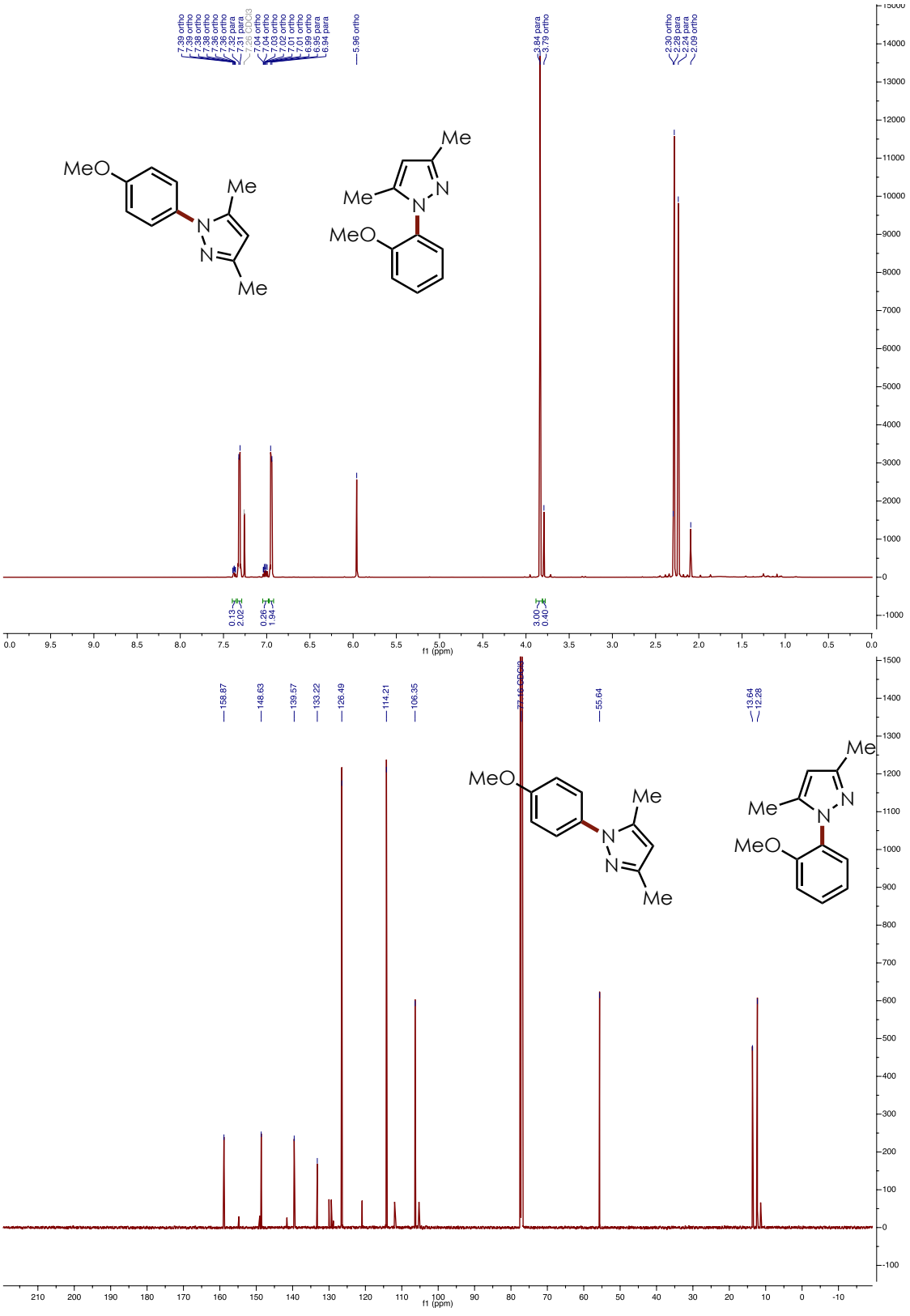
MeO
Me
N
N
Me
Me
N
N
MeO
Me
7.39 ortho
7.39 ortho
7.38 ortho
7.38 ortho
7.38 ortho
7.38 ortho
7.32 para
7.31 para
7.04 ortho
7.04 ortho
7.03 ortho
7.03 ortho
7.01 ortho
7.01 ortho
6.99 ortho
6.98 para
6.94 para
5.96 ortho
3.84 para
3.79 ortho
2.30 ortho
2.28 ortho
2.24 para
2.09 ortho
0.13
2.02
0.26
1.94
3.00
0.40
f1 (ppm)
158.87
148.63
139.57
133.22
126.49
114.21
106.35
77.16 CDCl3
55.64
13.64
12.28
f1 (ppm)

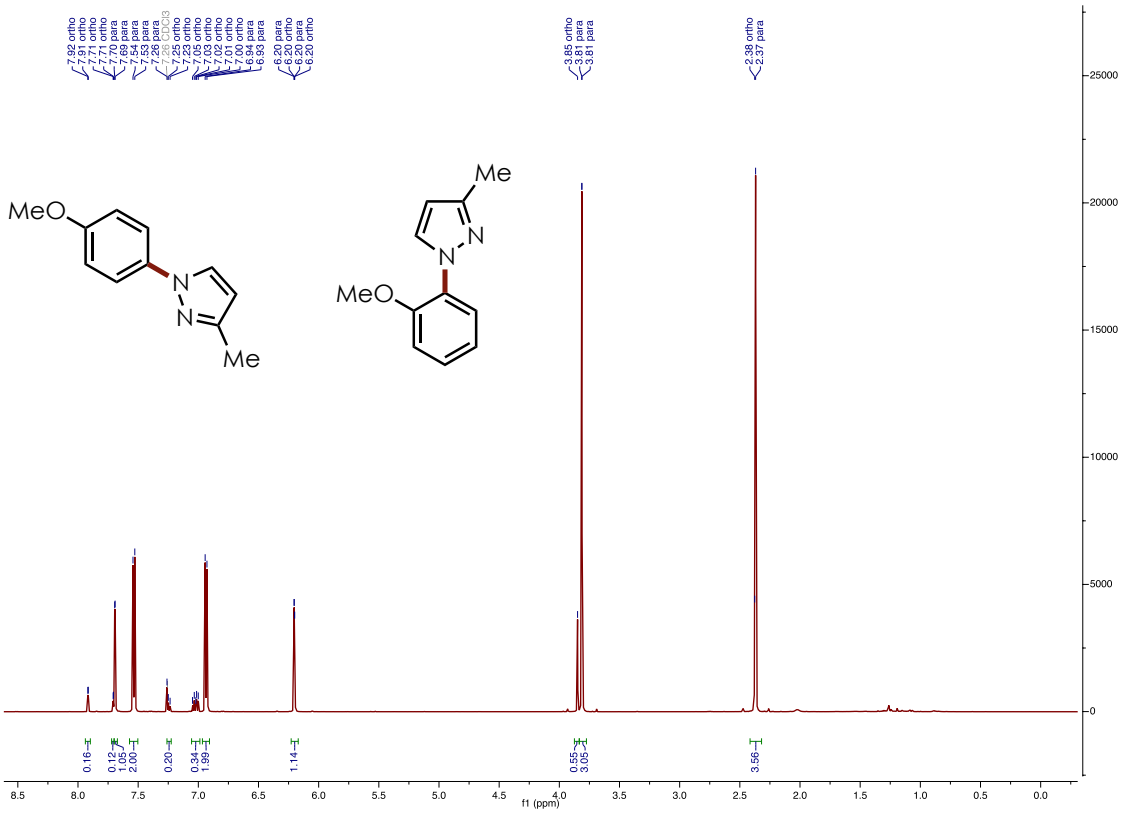
7.92 ortho
7.91 ortho
7.71 ortho
7.71 ortho
7.70 para
7.69 para
7.54 para
7.53 para
7.28 para
7.25 CDCl3
7.25 ortho
7.23 ortho
7.05 ortho
7.03 ortho
7.02 ortho
7.01 ortho
7.00 ortho
6.94 para
6.93 para
6.20 para
6.20 ortho
6.20 para
6.20 ortho
3.85 ortho
3.81 para
3.81 para
2.38 ortho
2.37 para
MeO
N
N
Me
Me
N
N
MeO
0.16
0.12
1.05
2.00
0.20
0.34
1.99
1.14
0.55
3.05
3.56
f1 (ppm)

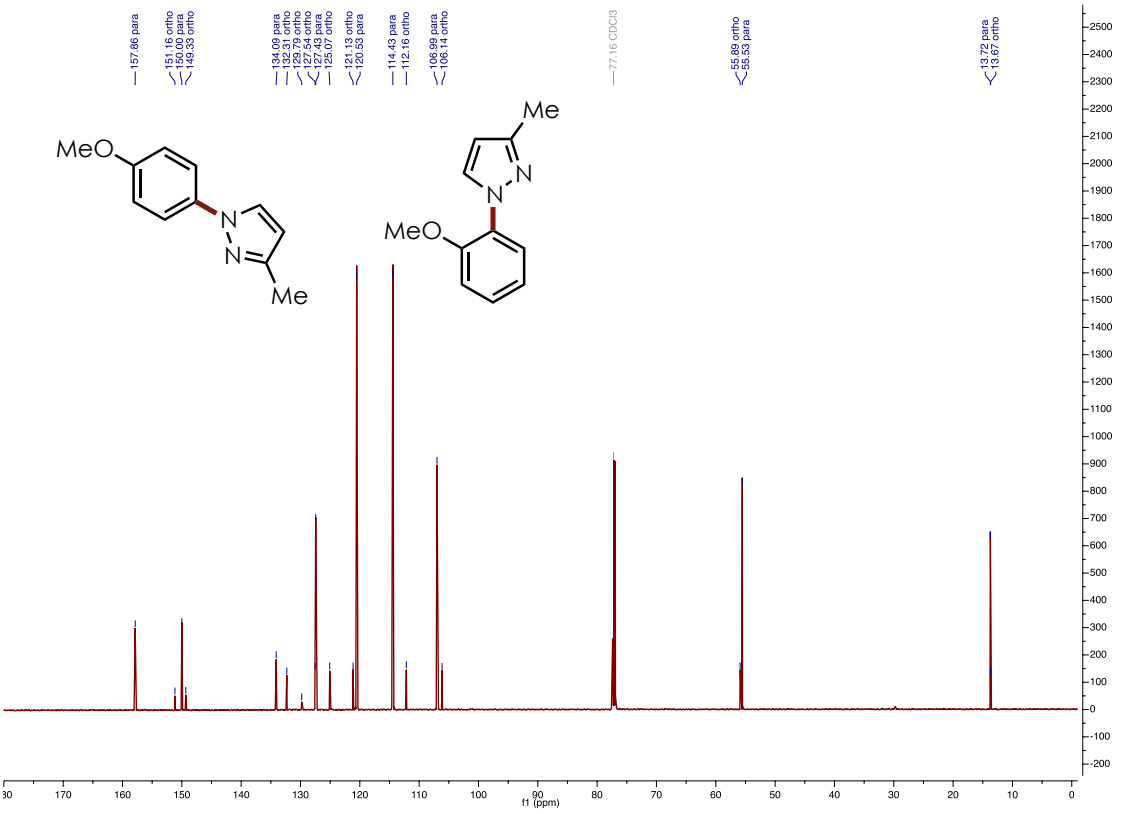
157.86 para
151.16 ortho
150.00 para
149.33 ortho
134.09 para
132.31 ortho
129.79 ortho
127.43 para
125.07 ortho
121.13 ortho
120.53 para
114.43 para
112.16 ortho
106.99 para
106.14 ortho
77.16 CDCl3
55.89 ortho
55.53 para
13.72 para
13.67 ortho
MeO
N
N
Me
Me
N
N
MeO
f1 (ppm)

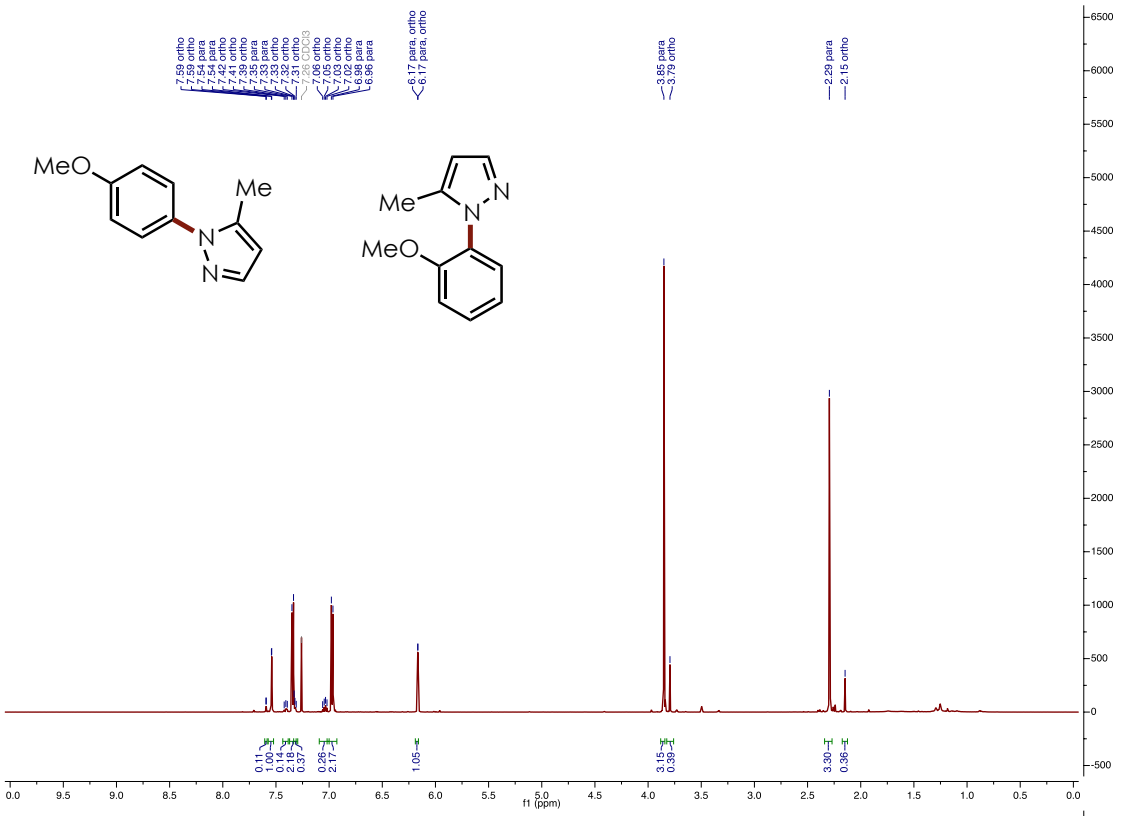
7.59 ortho
7.59 ortho
7.54 para
7.54 para
7.44 ortho
7.41 ortho
7.39 ortho
7.35 para
7.33 para
7.33 ortho
7.32 ortho
7.31 ortho
7.26 CDCl3
7.06 ortho
7.05 ortho
7.03 ortho
7.02 ortho
6.98 para
6.96 para
6.17 para, ortho
6.17 para, ortho
3.85 para
3.79 ortho
2.29 para
2.15 ortho
MeO
Me
N
N
Me
N
MeO
0.11
1.00
0.14
2.18
0.37
0.26
2.17
1.05
3.15
0.39
3.30
0.36
f1 (ppm)

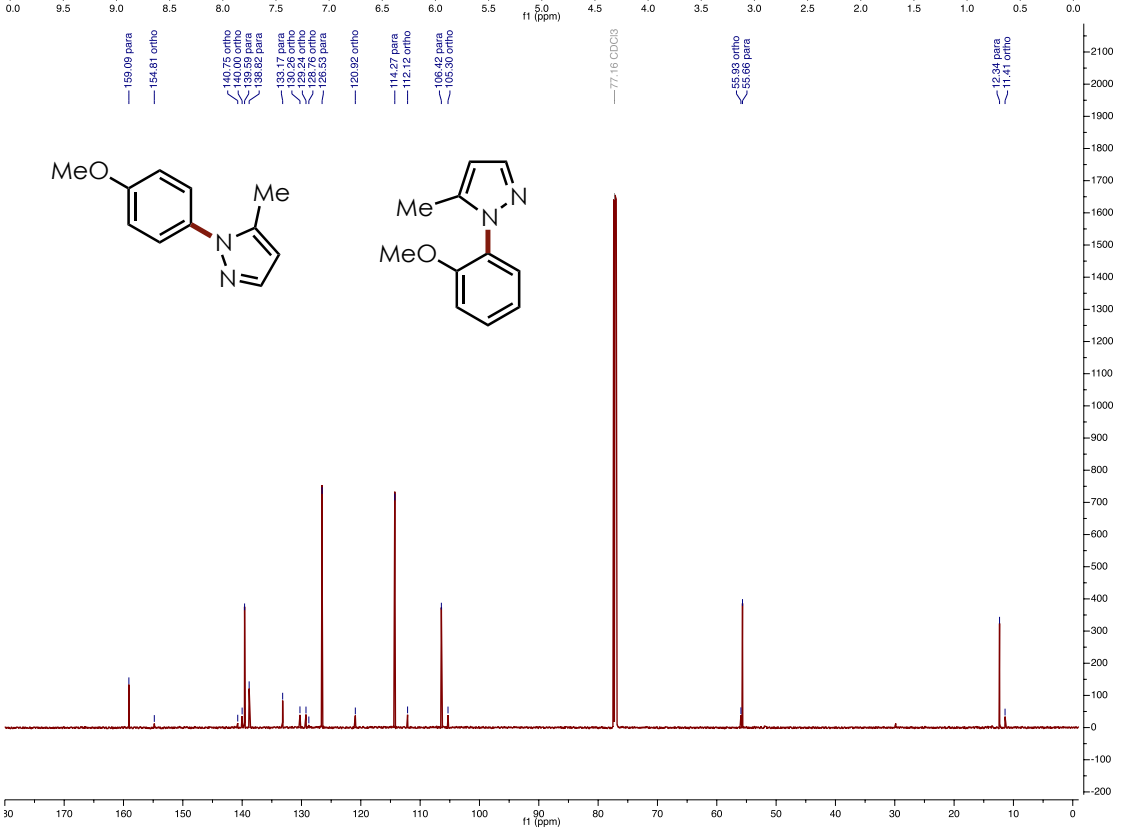
159.09 para
154.81 ortho
140.76 ortho
140.07 ortho
139.59 para
138.82 para
133.17 para
130.26 ortho
129.24 ortho
128.76 ortho
126.53 para
120.92 ortho
114.27 para
112.12 ortho
106.42 para
105.30 ortho
77.16 CDCl3
55.93 ortho
55.66 para
12.34 para
11.41 ortho
MeO
Me
N
N
Me
N
MeO
f1 (ppm)

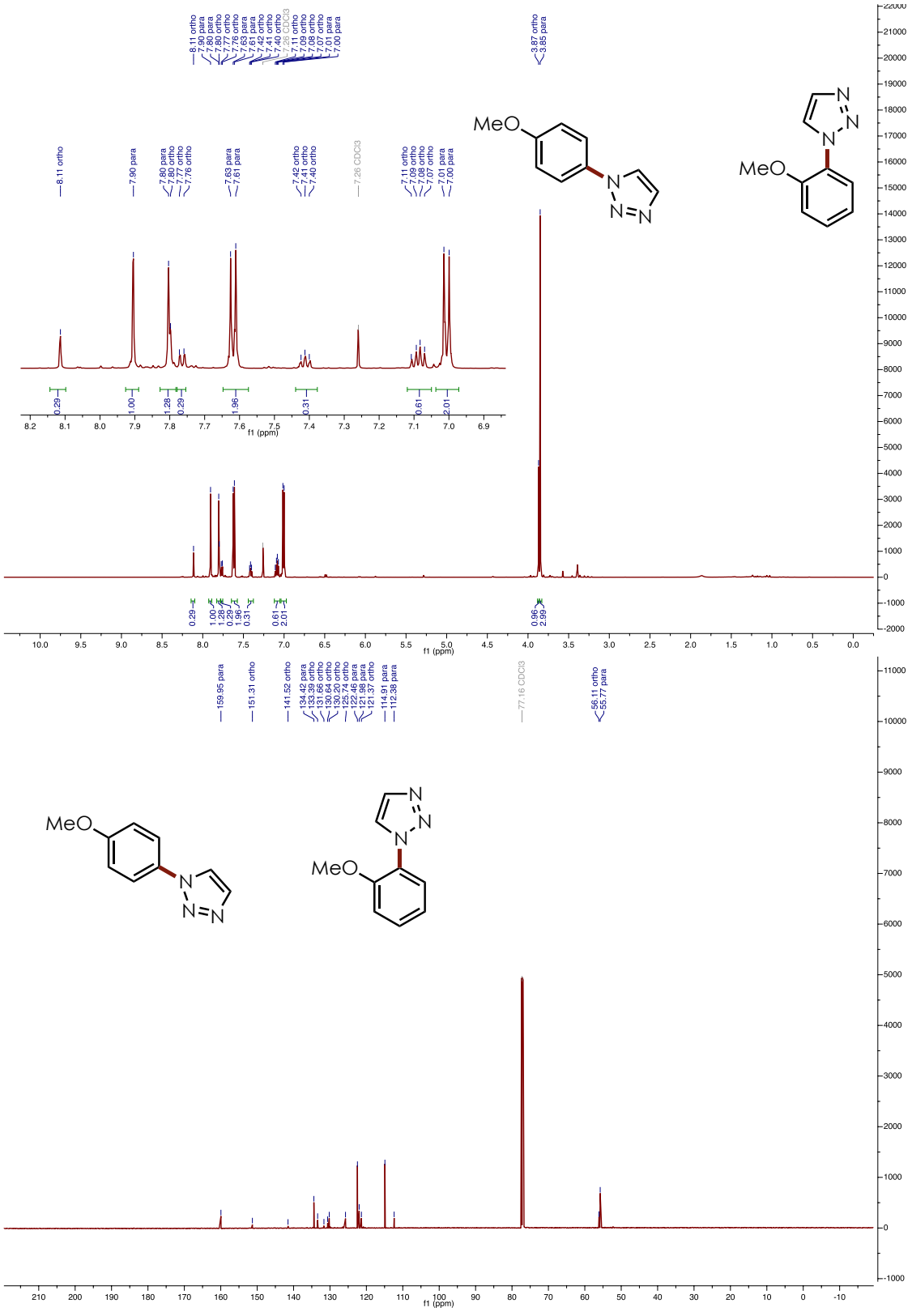
8.11 ortho
7.90 para
7.80 para
7.80 ortho
7.77 ortho
7.76 ortho
7.63 para
7.61 para
7.42 ortho
7.41 ortho
7.40 ortho
7.26 CDCl3
7.11 ortho
7.09 ortho
7.08 ortho
7.07 ortho
7.01 para
7.00 para
3.87 ortho
3.86 para
MeO
f1 (ppm)
159.95 para
151.31 ortho
141.52 ortho
134.42 para
133.39 ortho
131.66 ortho
130.84 ortho
130.20 ortho
125.74 ortho
122.46 para
121.89 para
121.37 ortho
114.91 para
112.38 para
77.16 CDCl3
56.11 ortho
55.77 para

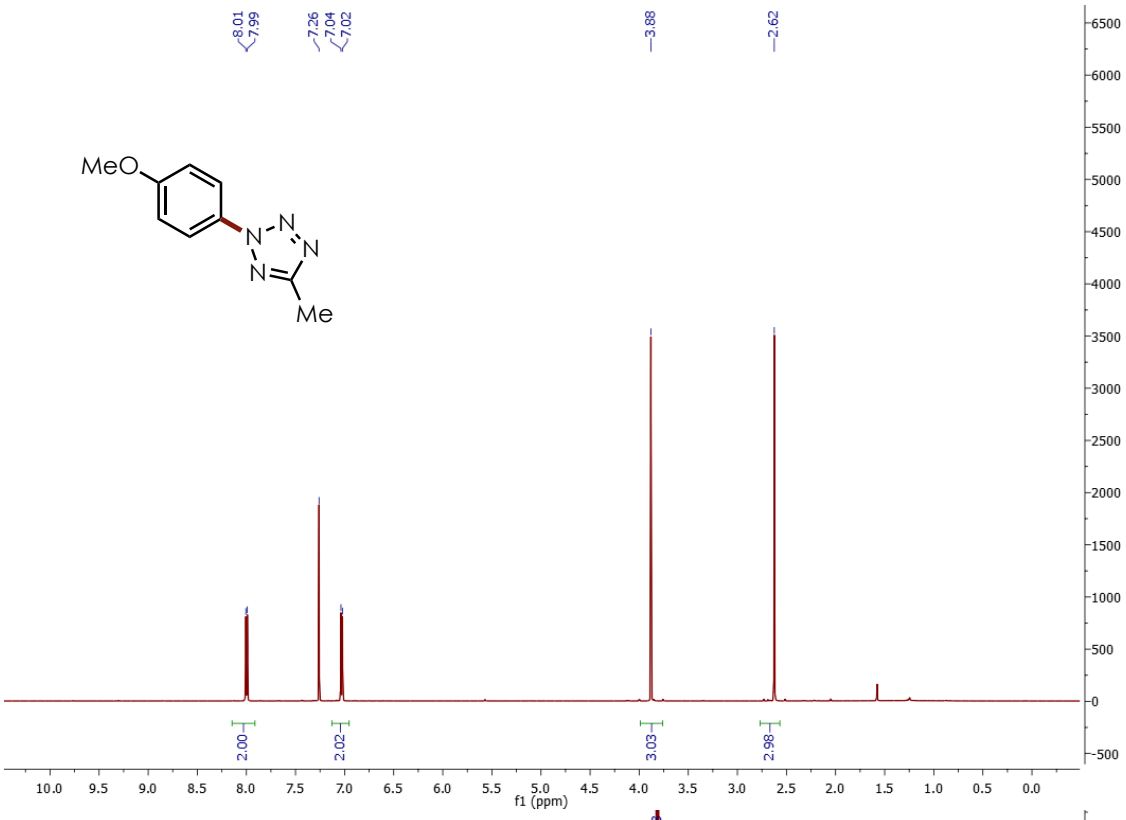
8.01
7.99
7.26
7.04
7.02
3.88
2.62
MeO
N
N
N
N
Me
2.00
2.02
3.03
2.98
f1 (ppm)

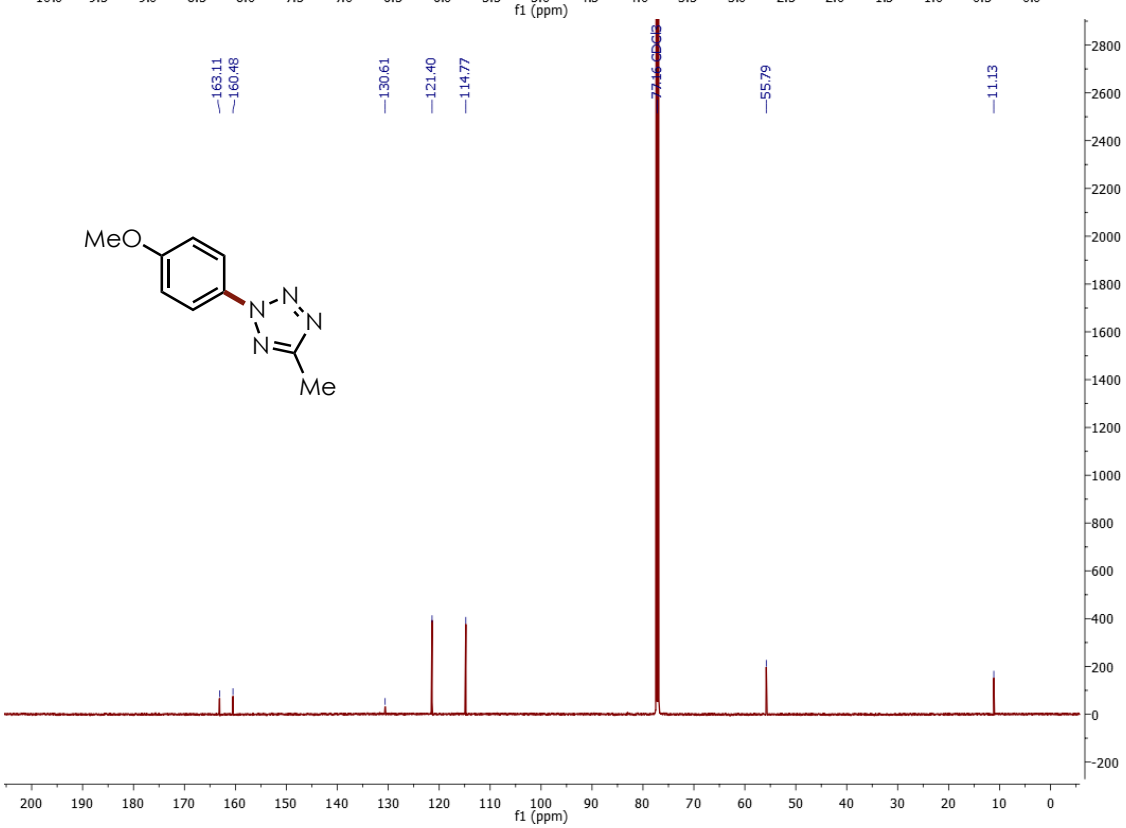
163.11
160.48
130.61
121.40
114.77
55.79
11.13
MeO
N
N
N
N
Me
f1 (ppm)

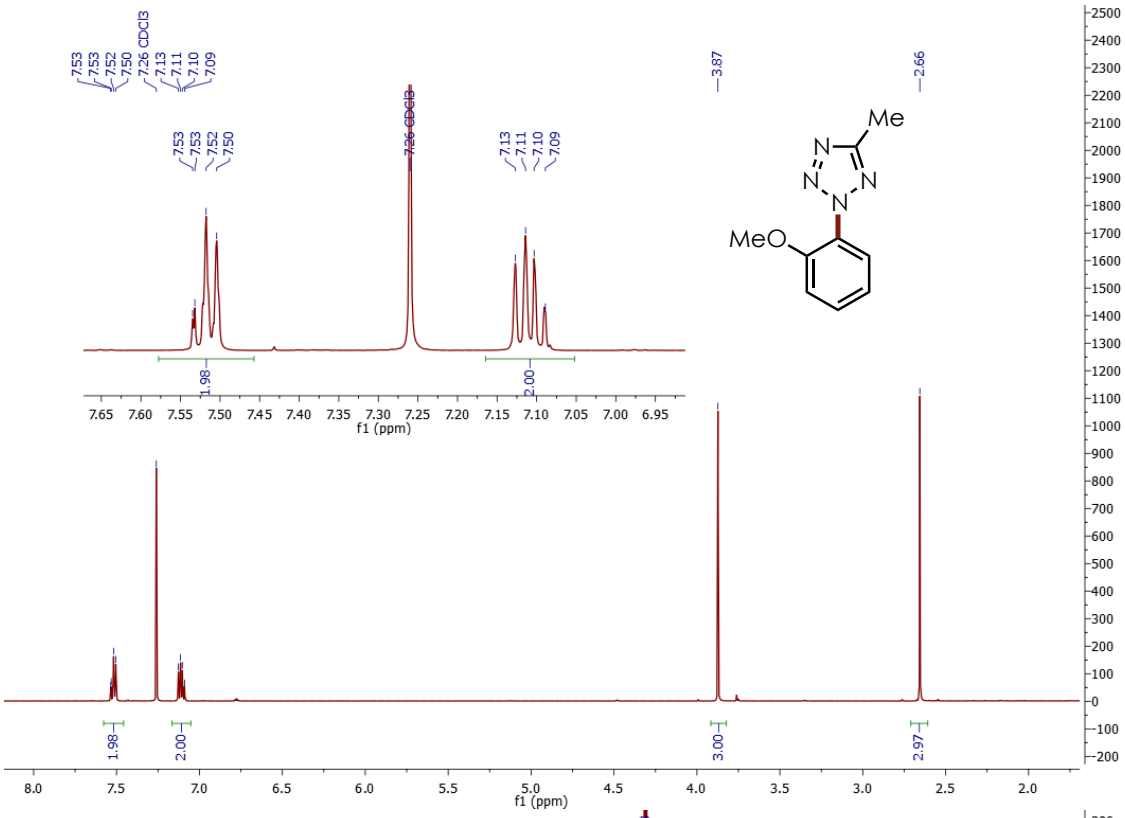
7.53
7.53
7.52
7.50
7.26 CDCl3
7.13
7.11
7.10
7.09
3.87
2.66
Me
N
N
N
N
MeO
1.98
2.00
3.00
2.97
f1 (ppm)

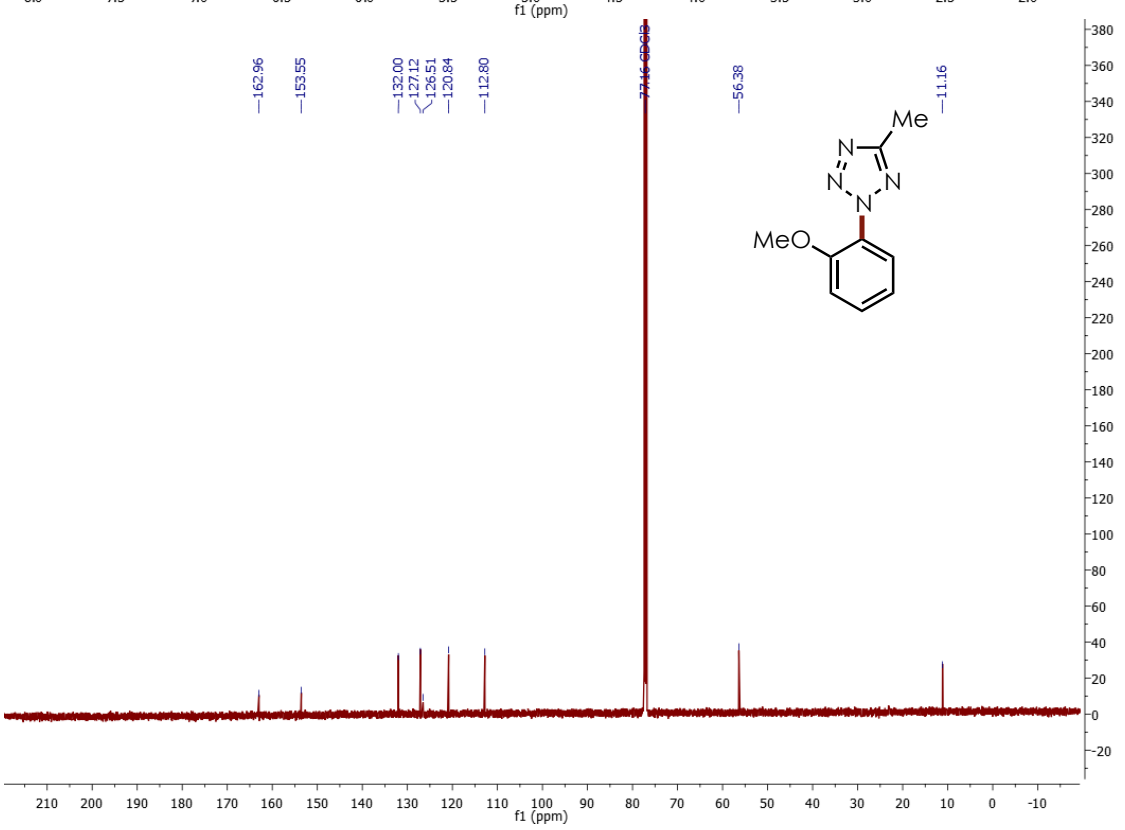
162.96
153.55
132.00
127.12
126.51
120.84
112.80
77.16 CDCl3
56.38
11.16
Me
N
N
N
N
MeO
f1 (ppm)

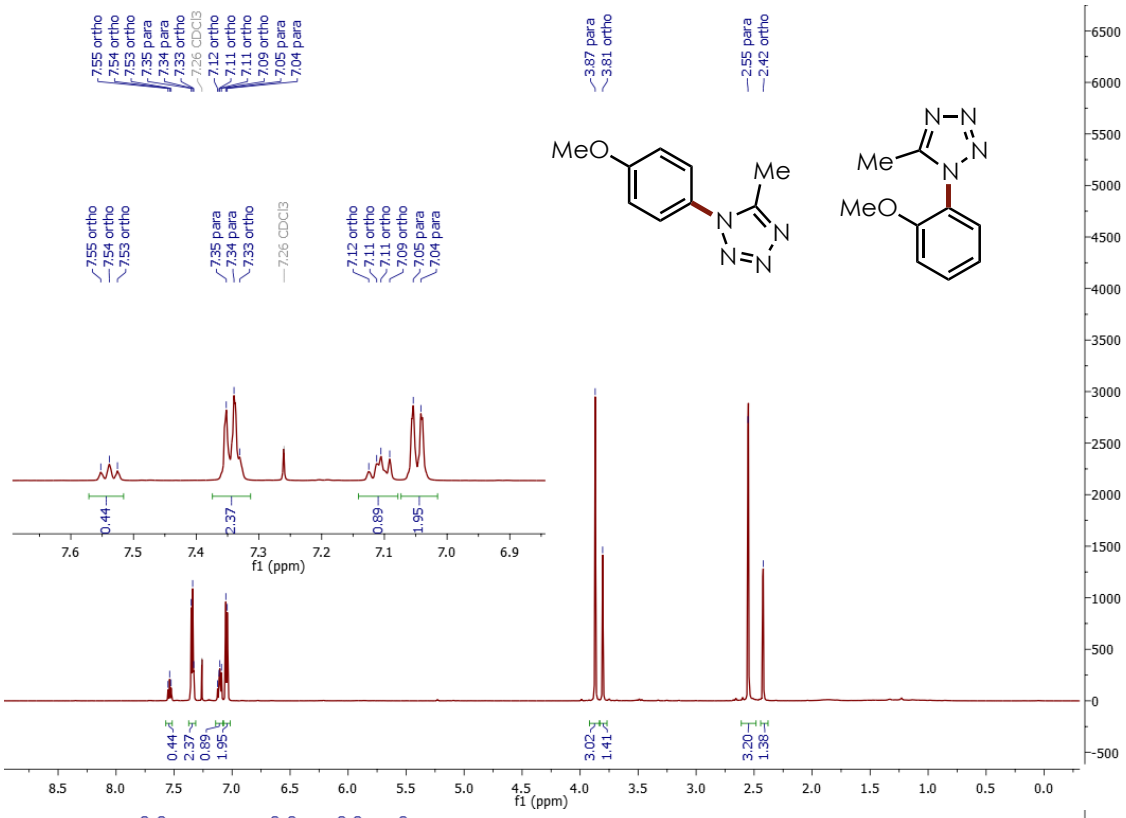
7.55 ortho
7.54 ortho
7.53 ortho
7.35 para
7.34 para
7.33 ortho
7.26 CDCl3
7.12 ortho
7.11 ortho
7.11 ortho
7.09 ortho
7.05 para
7.04 para
3.87 para
3.81 ortho
2.55 para
2.42 ortho
MeO
Me
N
N
N
N
Me
N
N
MeO
0.44
2.37
0.89
1.95
3.02
1.41
3.20
1.38
f1 (ppm)

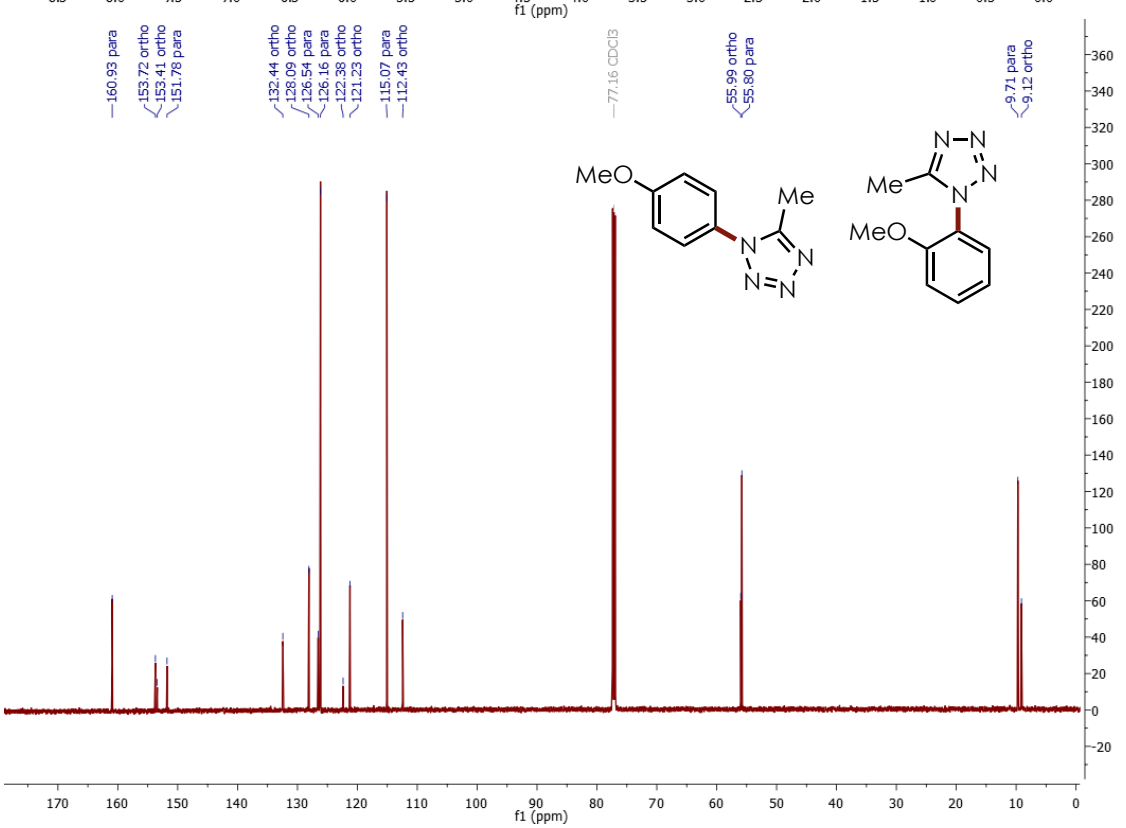
160.93 para
153.72 ortho
153.41 ortho
151.78 para
132.44 ortho
128.09 ortho
126.54 para
126.16 para
122.38 ortho
121.23 ortho
115.07 para
112.43 ortho
77.16 CDCl3
55.99 ortho
55.80 para
9.71 para
9.12 ortho
MeO
Me
N
N
N
N
Me
N
N
MeO
f1 (ppm)

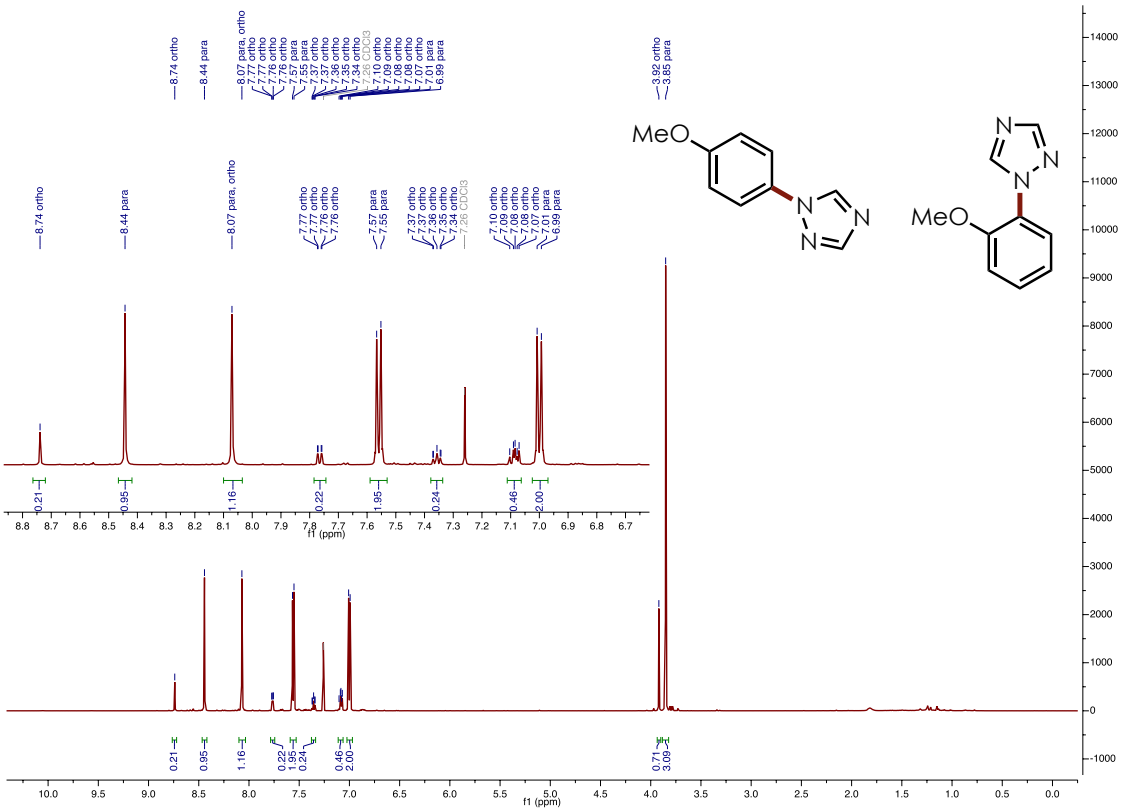
8.74 ortho
8.44 para
8.07 para, ortho
7.77 ortho
7.76 ortho
7.57 para
7.55 para
7.37 ortho
7.36 ortho
7.35 ortho
7.34 ortho
7.26 CDCl3
7.10 ortho
7.09 ortho
7.08 ortho
7.07 ortho
7.01 para
6.99 para
3.92 ortho
3.85 para
MeO
f1 (ppm)

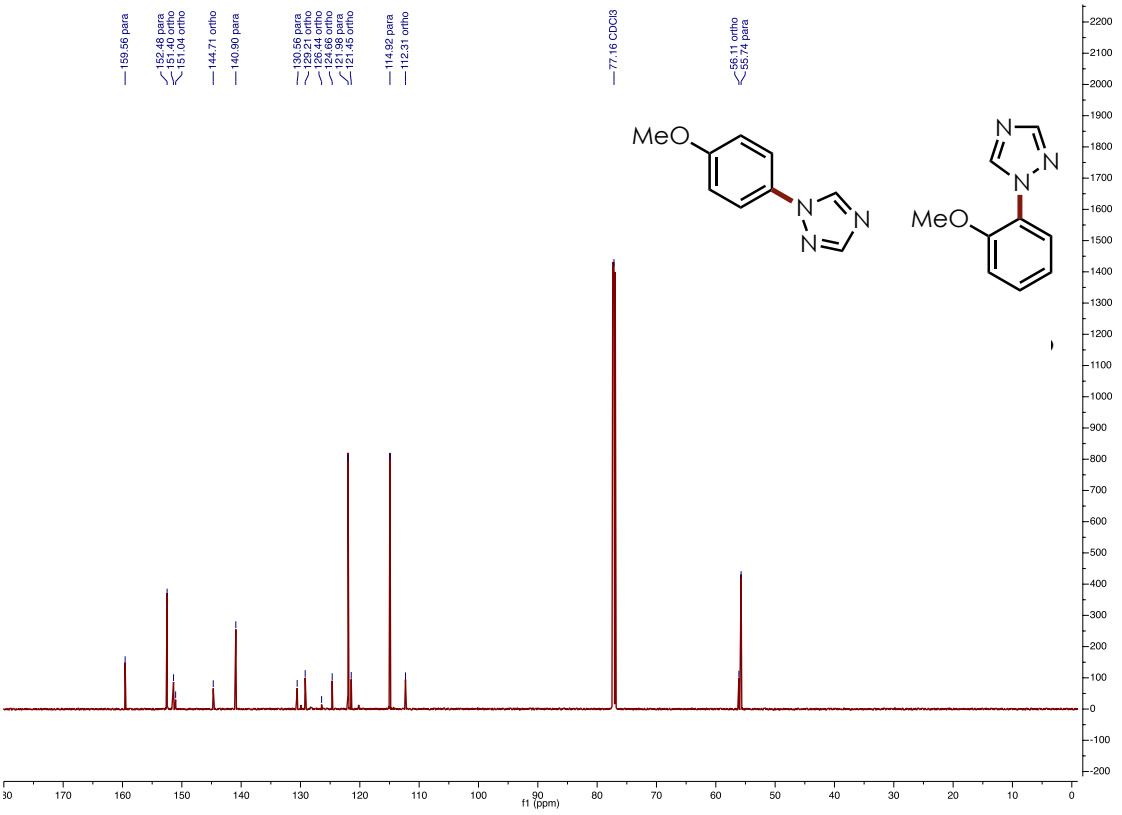
159.56 para
152.48 para
151.40 ortho
151.04 ortho
144.71 ortho
140.90 para
130.56 para
129.41 ortho
128.44 ortho
124.66 ortho
121.98 para
121.45 ortho
114.92 para
112.31 ortho
77.16 CDCl3
56.11 ortho
55.74 para
MeO
f1 (ppm)

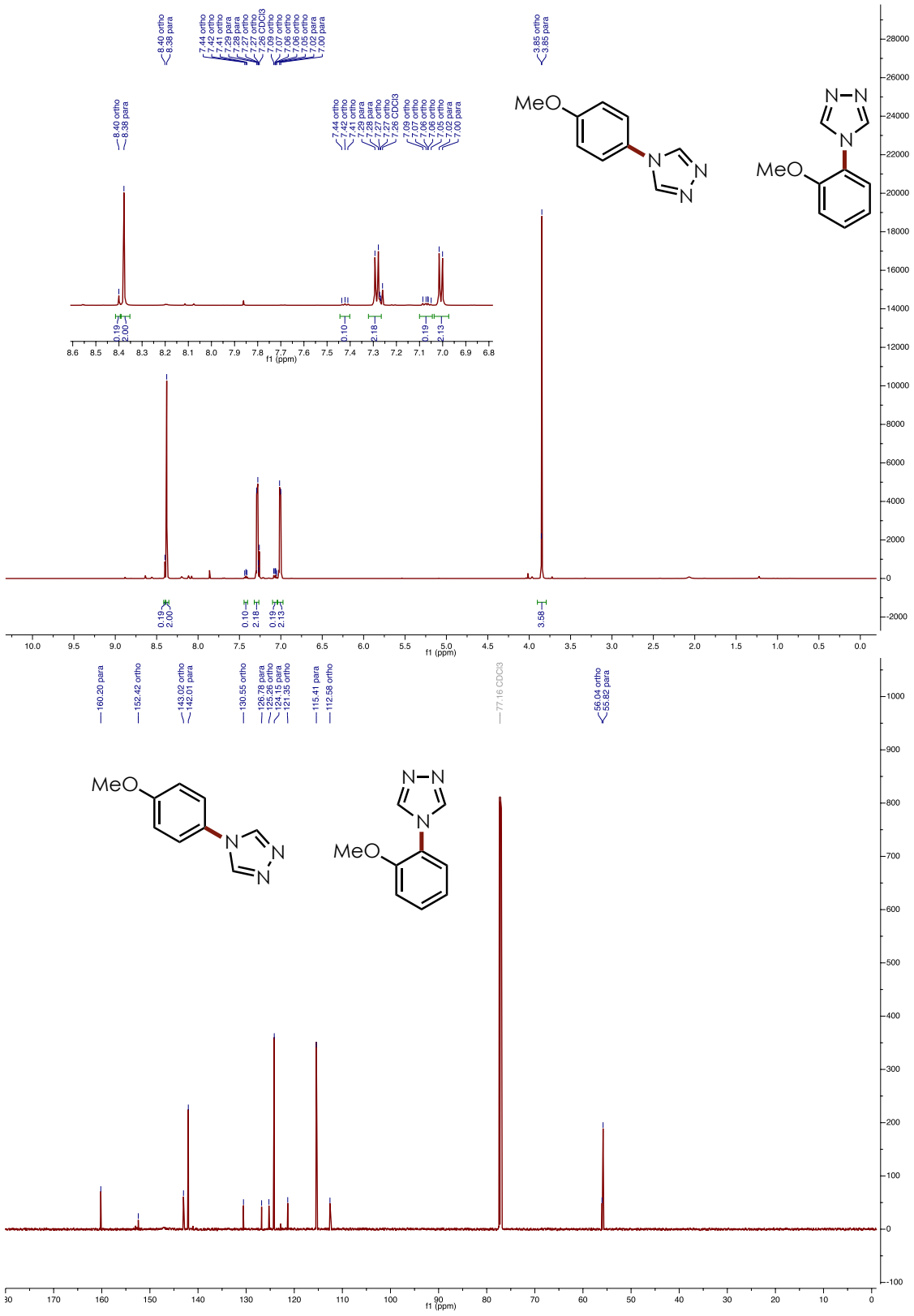
8.40 ortho
8.38 para
7.44 ortho
7.42 ortho
7.41 ortho
7.29 para
7.28 para
7.27 ortho
7.27 ortho
7.26 CDCl3
7.09 ortho
7.07 ortho
7.06 ortho
7.06 ortho
7.05 ortho
7.02 para
7.00 para
3.85 ortho
3.85 para
MeO
N
N
N
MeO
N
N
N
f1 (ppm)
160.20 para
152.42 ortho
143.02 ortho
142.01 para
130.55 ortho
126.78 para
125.26 ortho
124.15 para
121.35 ortho
115.41 para
112.58 ortho
77.16 CDCl3
56.04 ortho
55.82 para
MeO
N
N
N
MeO
N
N
N
f1 (ppm)

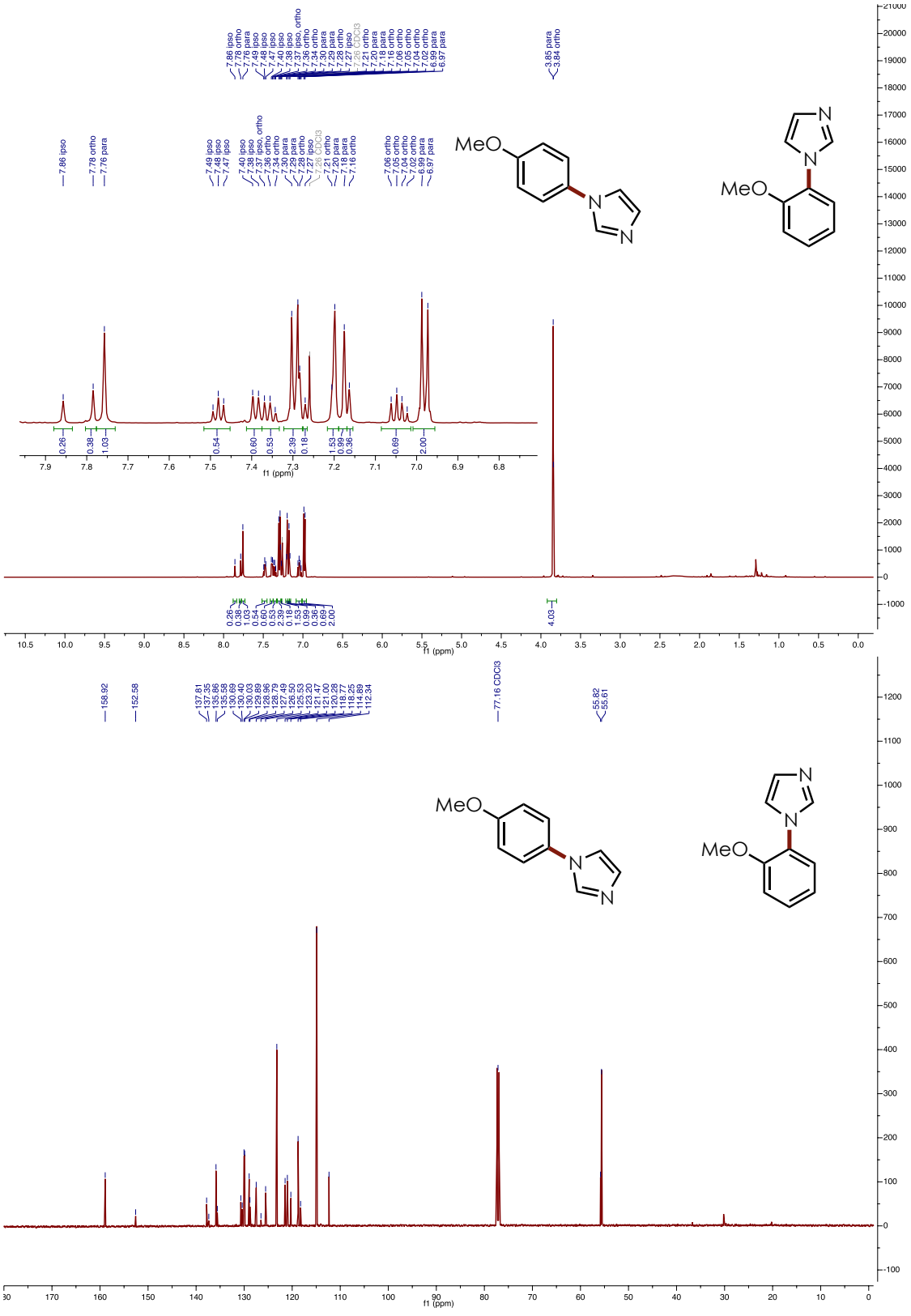
7.86 ipso
7.78 ortho
7.76 para
7.49 ipso
7.48 ipso
7.47 ipso
7.40 ipso
7.38 ipso, ortho
7.37 ipso, ortho
7.36 ortho
7.34 ortho
7.30 para
7.28 ortho
7.27 ipso
7.26 CDCl3
7.21 ortho
7.20 para
7.18 para
7.16 ortho
7.06 ortho
7.05 ortho
7.04 ortho
7.02 ortho
6.99 para
6.97 para
3.85 para
3.84 ortho
MeO
MeO
f1 (ppm)
158.92
152.58
137.81
137.35
135.68
135.58
130.69
130.40
130.03
129.89
128.96
128.79
127.44
126.50
125.53
123.20
123.47
121.00
120.28
118.77
118.25
114.89
112.34
77.16 CDCl3
55.82
55.61
MeO
MeO
f1 (ppm)

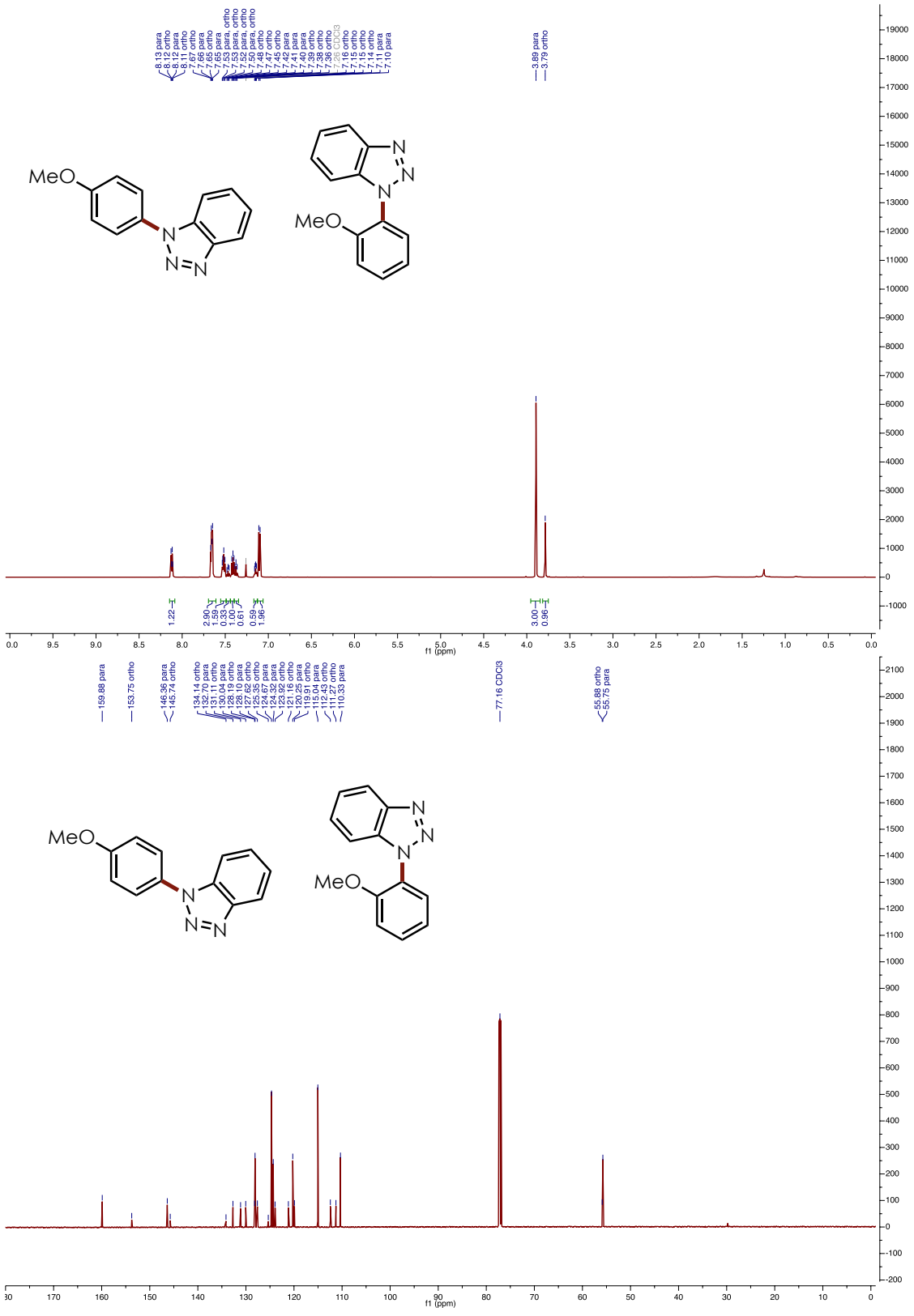
8.13 para
8.12 ortho
8.12 para
8.11 ortho
8.07 ortho
7.66 para
7.65 ortho
7.65 para
7.53 para, ortho
7.53 para, ortho
7.52 para, ortho
7.50 para, ortho
7.48 ortho
7.47 ortho
7.45 ortho
7.42 para
7.41 para
7.40 para
7.39 ortho
7.38 ortho
7.36 ortho
7.26 CDCl3
7.16 ortho
7.15 ortho
7.14 ortho
7.11 para
7.10 para
3.89 para
3.79 ortho
MeO
N
N
N
MeO
1.22
2.90
1.89
0.33
1.00
0.61
0.59
1.98
3.00
0.96
f1 (ppm)
159.88 para
153.75 ortho
146.36 para
145.74 ortho
134.14 ortho
132.70 para
131.11 ortho
130.04 para
128.19 ortho
128.10 para
127.62 ortho
125.35 ortho
124.67 para
124.32 para
123.92 ortho
121.16 ortho
120.25 para
119.84 ortho
115.04 para
112.43 ortho
111.27 ortho
110.38 para
77.16 CDCl3
55.88 ortho
55.75 para
MeO
N
N
N
MeO
f1 (ppm)

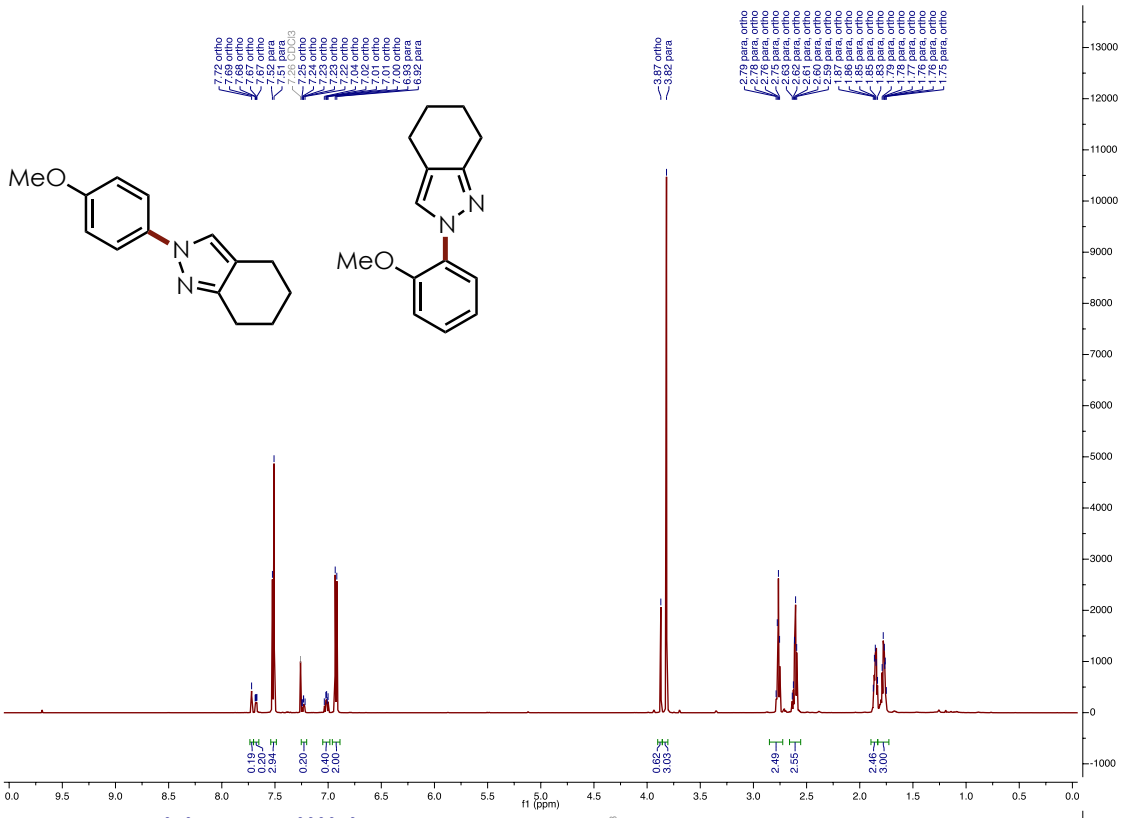
MeO
N
N
MeO
N
N
7.72 ortho
7.69 ortho
7.68 ortho
7.67 ortho
7.67 ortho
7.52 para
7.51 para
7.25 ortho
7.24 ortho
7.23 ortho
7.23 ortho
7.22 ortho
7.04 ortho
7.02 ortho
7.01 ortho
7.00 ortho
6.93 para
6.92 para
3.87 ortho
3.82 para
2.79 para, ortho
2.78 para, ortho
2.76 para, ortho
2.75 para, ortho
2.63 para, ortho
2.62 para, ortho
2.61 para, ortho
2.60 para, ortho
2.59 para, ortho
1.87 para, ortho
1.86 para, ortho
1.85 para, ortho
1.83 para, ortho
1.79 para, ortho
1.78 para, ortho
1.77 para, ortho
1.76 para, ortho
1.75 para, ortho
0.19
0.20
2.94
0.20
0.40
2.00
0.62
3.03
2.49
2.55
2.46
3.00
f1 (ppm)

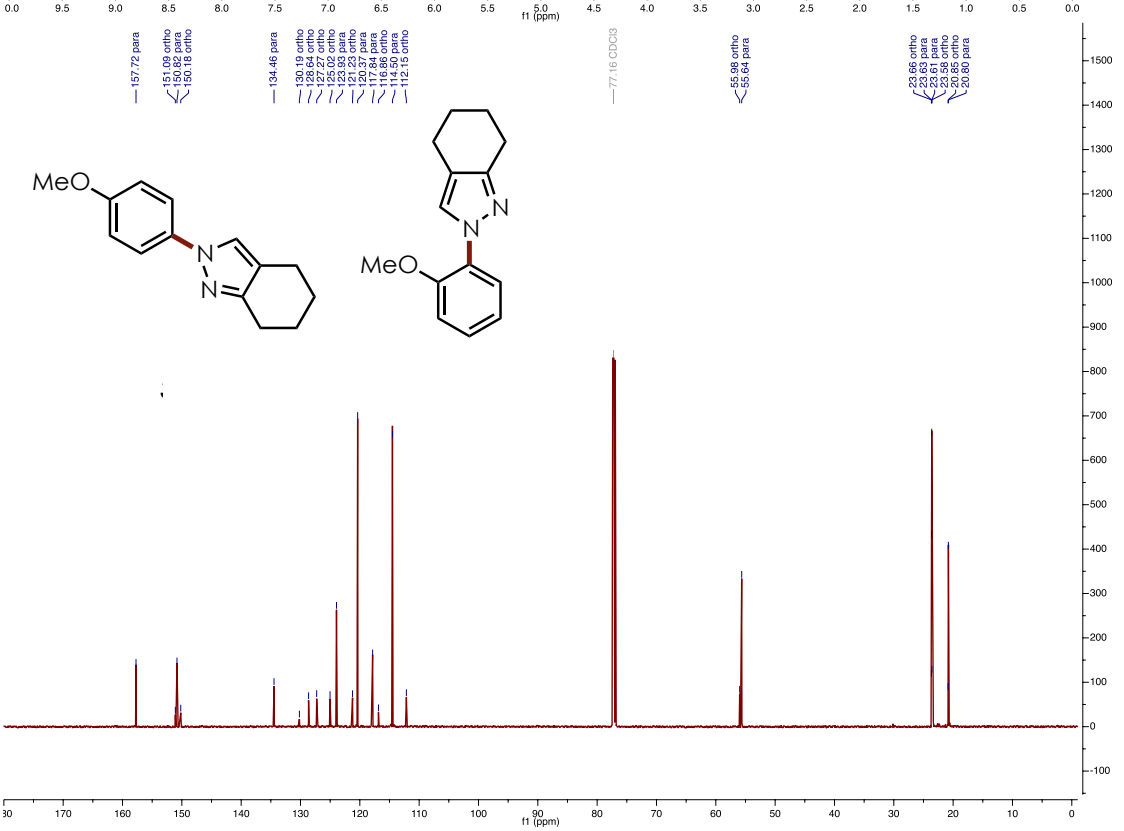
MeO
N
N
MeO
N
N
157.72 para
151.09 ortho
150.82 para
150.18 ortho
134.46 para
130.19 ortho
128.64 ortho
127.27 ortho
125.02 ortho
123.93 para
121.23 ortho
120.24 para
117.84 para
116.86 ortho
114.50 para
112.15 ortho
77.16 CDCl3
55.98 ortho
55.64 para
23.66 ortho
23.61 para
23.61 para
23.58 ortho
20.85 ortho
20.80 para
f1 (ppm)

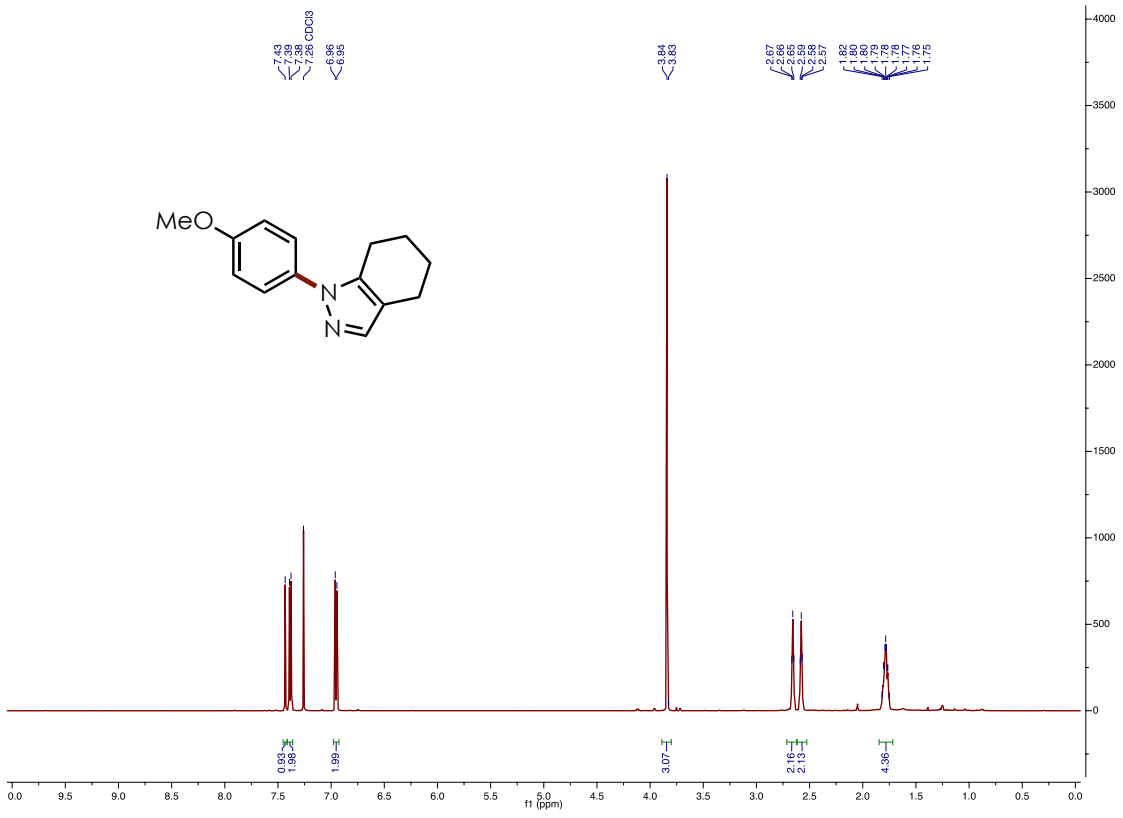
7.43
7.39
7.38
7.26 CDCl3
6.96
6.95
3.84
3.83
2.67
2.66
2.65
2.59
2.58
2.57
1.82
1.80
1.80
1.79
1.78
1.78
1.77
1.76
1.75
MeO
N
N
0.93
1.98
1.99
3.07
2.16
2.13
4.96
f1 (ppm)

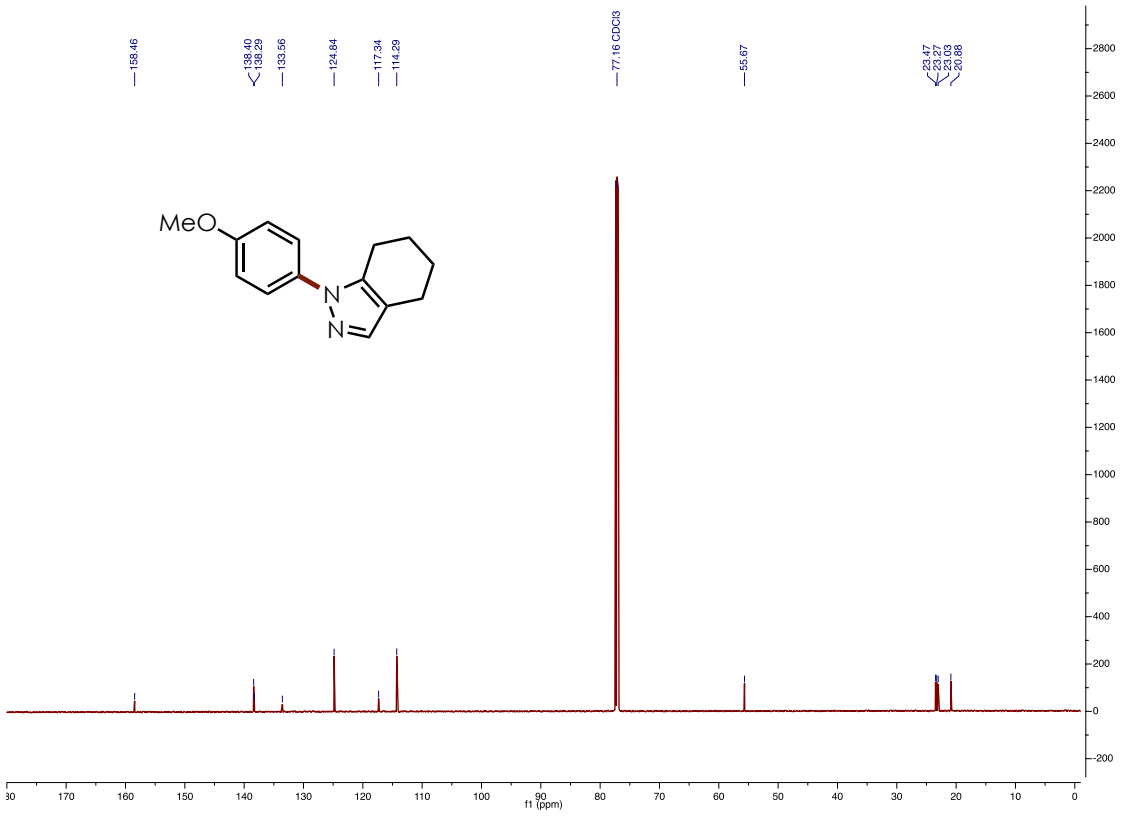
158.46
138.40
138.29
133.56
124.84
117.34
114.29
77.16 CDCl3
55.67
23.47
23.27
23.03
20.88
MeO
N
N
f1 (ppm)

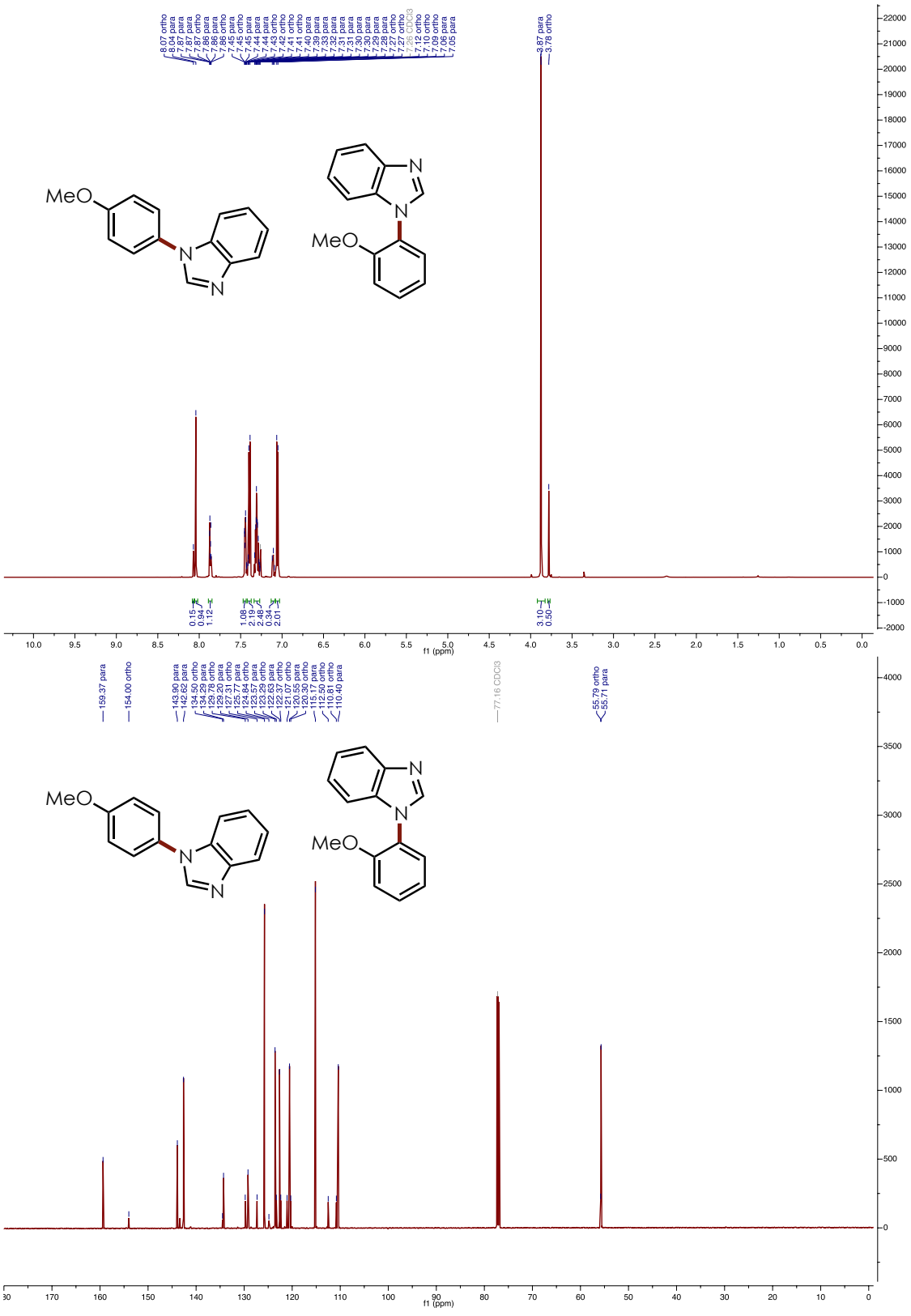
8.07 ortho
8.04 para
7.87 para
7.87 ortho
7.86 para
7.86 ortho
7.45 para
7.45 ortho
7.44 para
7.44 para
7.43 ortho
7.43 ortho
7.41 ortho
7.41 ortho
7.40 para
7.40 para
7.33 para
7.32 para
7.31 para
7.31 para
7.30 para
7.30 para
7.28 para
7.27 para
7.27 ortho
7.26 CDCl3
7.10 ortho
7.10 ortho
7.09 ortho
7.08 para
7.08 para
7.05 para
3.87 para
3.78 ortho
MeO
N
N
MeO
0.15
0.94
1.12
1.08
2.19
2.48
0.94
2.01
3.10
0.50
f1 (ppm)
159.37 para
154.00 ortho
143.90 para
142.62 para
134.50 ortho
134.20 para
129.78 ortho
129.20 para
127.31 ortho
127.17 para
124.84 ortho
123.57 para
123.28 ortho
123.08 para
122.37 ortho
121.07 ortho
120.55 para
120.39 ortho
115.17 para
112.50 ortho
110.81 ortho
110.40 para
77.16 CDCl3
55.79 ortho
55.71 para
MeO
N
N
MeO
f1 (ppm)

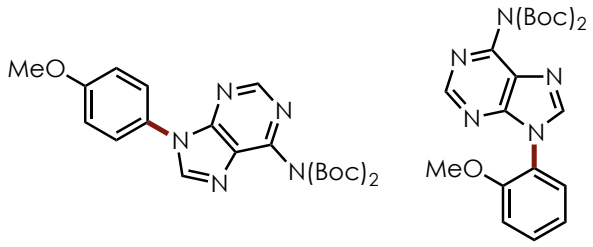
MeO
N(Boc)2
N(Boc)2
MeO

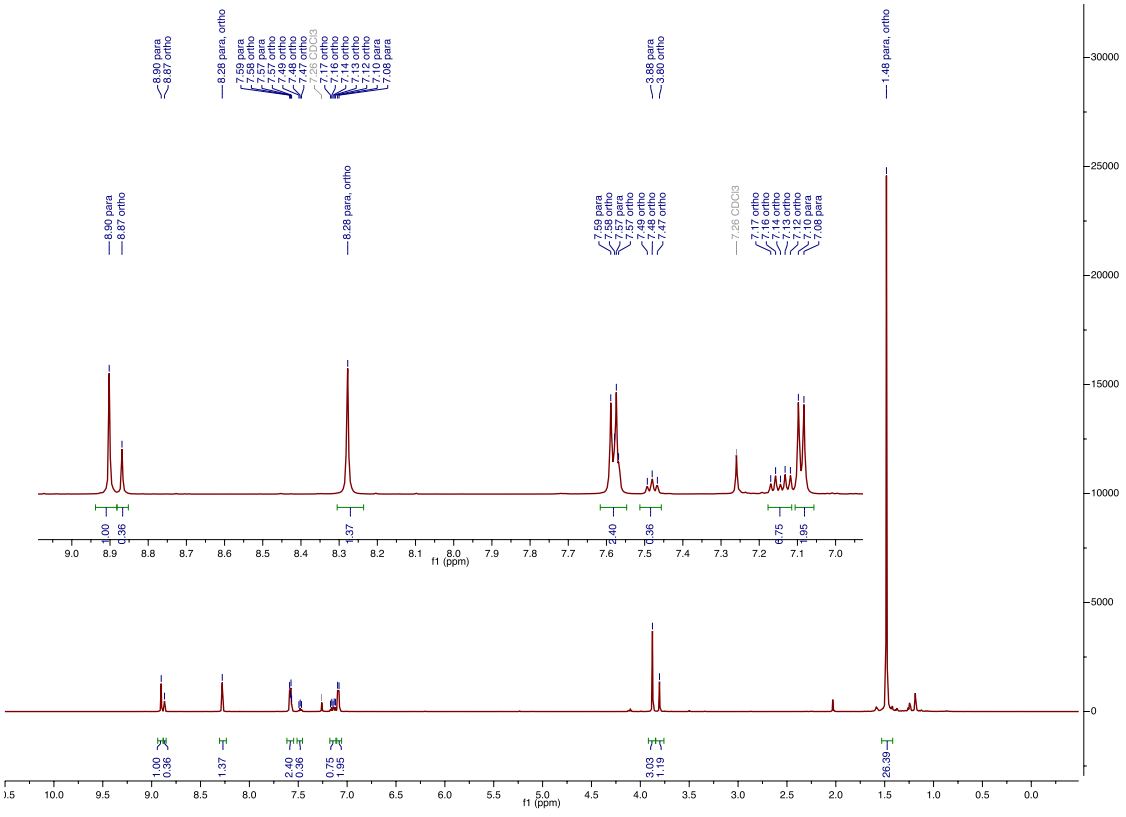
8.90 para
8.87 ortho
8.28 para, ortho
7.59 para
7.58 ortho
7.57 para
7.57 ortho
7.49 ortho
7.48 ortho
7.47 ortho
7.26 CDCl3
7.17 ortho
7.16 ortho
7.14 ortho
7.13 ortho
7.12 ortho
7.10 para
7.08 para
3.88 para
3.80 ortho
1.48 para, ortho
f1 (ppm)

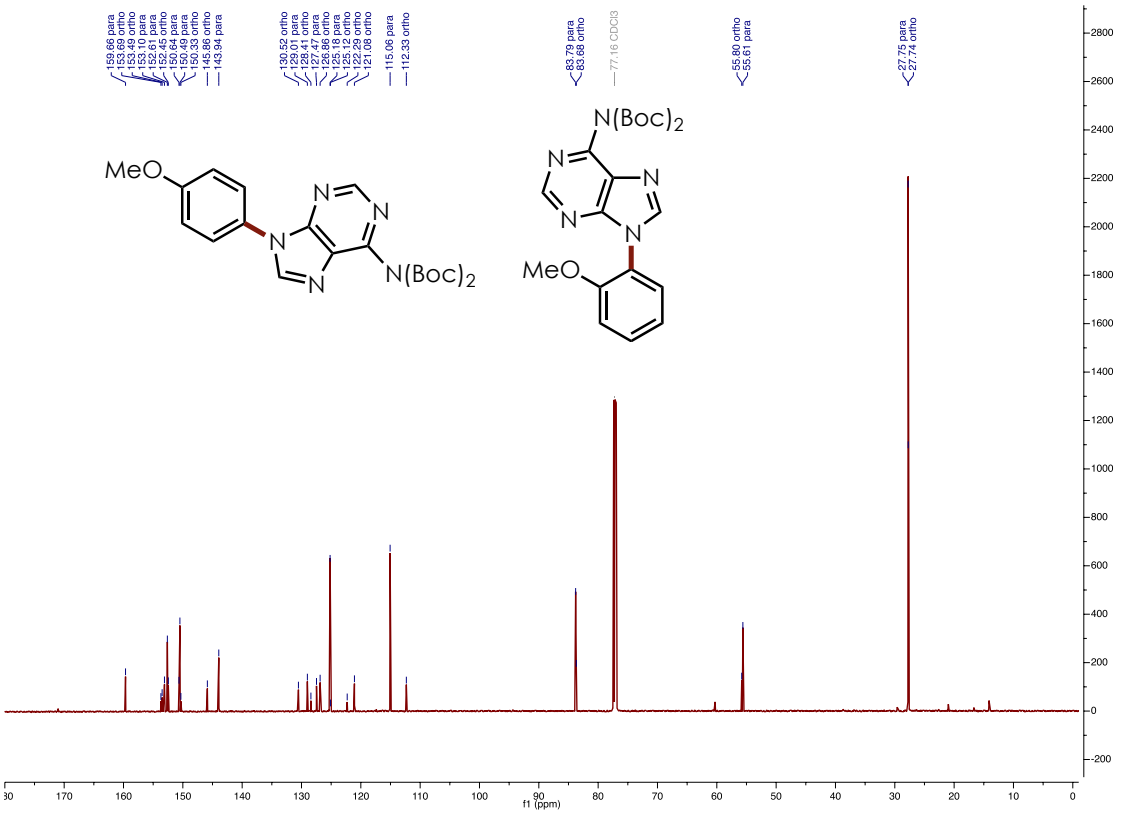
159.66 para
153.69 ortho
153.49 ortho
153.10 para
152.67 para
152.45 ortho
150.64 para
150.49 para
150.33 ortho
145.86 ortho
143.94 para
130.52 ortho
130.01 para
128.41 ortho
127.47 para
126.86 ortho
125.18 para
125.12 ortho
122.29 ortho
121.08 ortho
115.06 para
112.33 ortho
83.79 para
83.68 ortho
77.16 CDCl3
55.80 ortho
55.61 para
27.75 para
27.74 ortho
MeO
N(Boc)2
f1 (ppm)

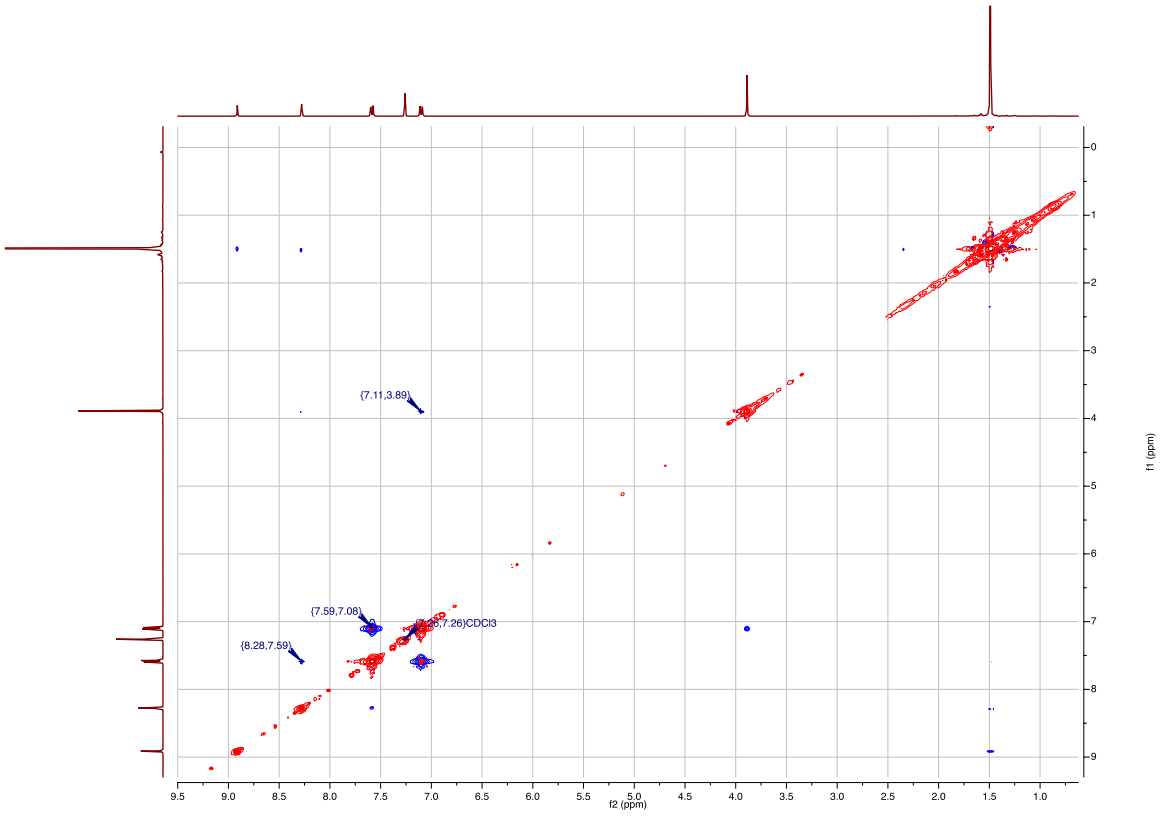
{7.11,3.89}
{7.59,7.08}
{8.28,7.59}
{7.26,7.26}CDCl3
f2 (ppm)
f1 (ppm)

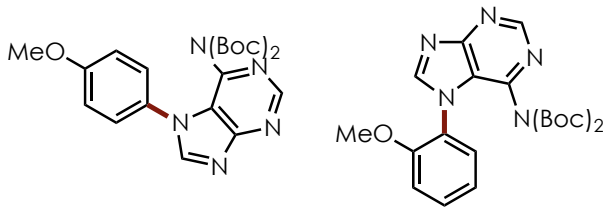
MeO
N(Boc)2
N
N
N
N
MeO
N(Boc)2
N
N
N
N

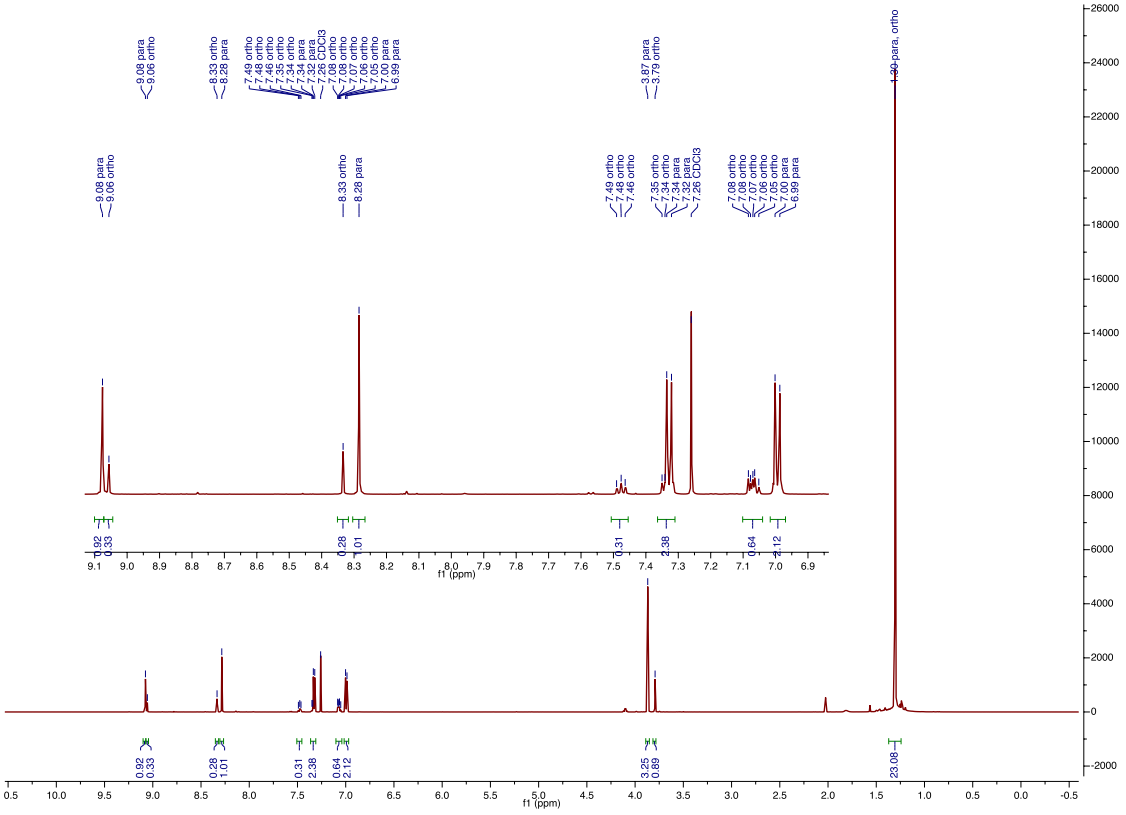
9.08 para
9.06 ortho
8.33 ortho
8.28 para
7.49 ortho
7.48 ortho
7.46 ortho
7.35 ortho
7.34 ortho
7.34 para
7.32 para
7.26 CDCl3
7.08 ortho
7.07 ortho
7.06 ortho
7.05 ortho
7.00 para
6.99 para
3.87 para
3.79 ortho
1.30 para, ortho
f1 (ppm)

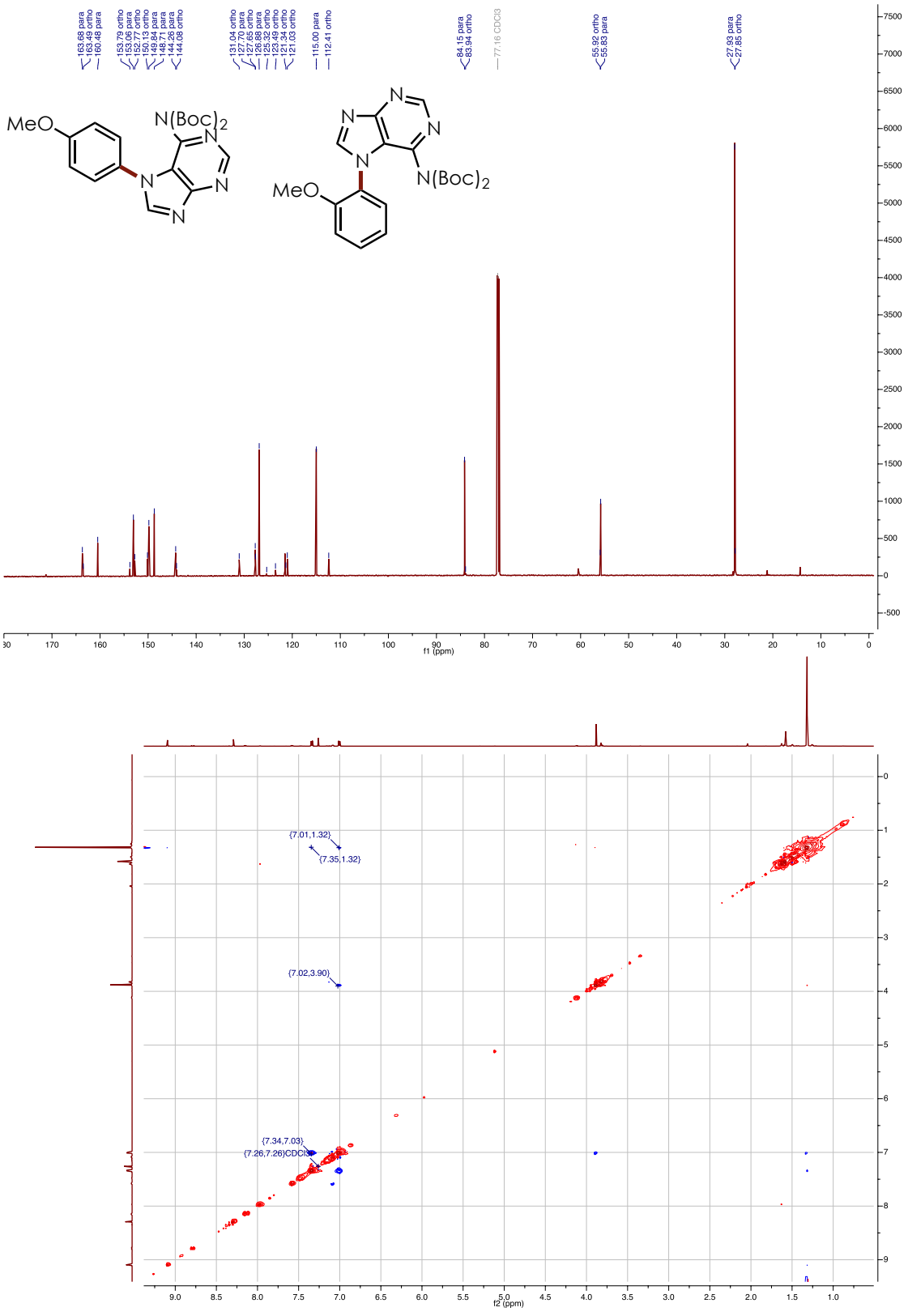
163.68 para
163.49 ortho
160.48 para
153.79 ortho
153.06 para
152.77 ortho
150.13 ortho
149.84 para
148.71 para
144.28 para
144.08 ortho
131.04 ortho
127.70 para
127.65 ortho
126.88 para
125.32 ortho
123.49 ortho
121.34 ortho
121.03 ortho
115.00 para
112.41 ortho
84.15 para
83.94 ortho
77.16 CDCl3
55.92 ortho
55.83 para
27.93 para
27.85 ortho
MeO
N(Boc)2
f1 (ppm)
{7.01,1.32}
{7.35,1.32}
{7.02,3.90}
{7.34,7.03}
{7.26,7.26}CDCl3
f2 (ppm)
f1 (ppm)

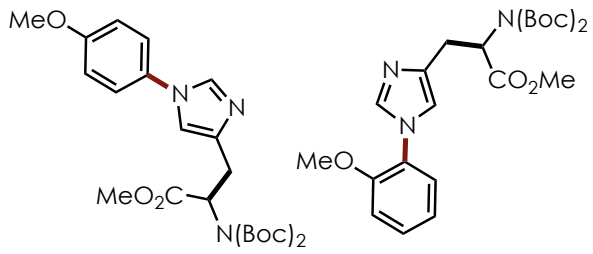
MeO
N
N
MeO2C
N(Boc)2
N(Boc)2
CO2Me
N
N
MeO

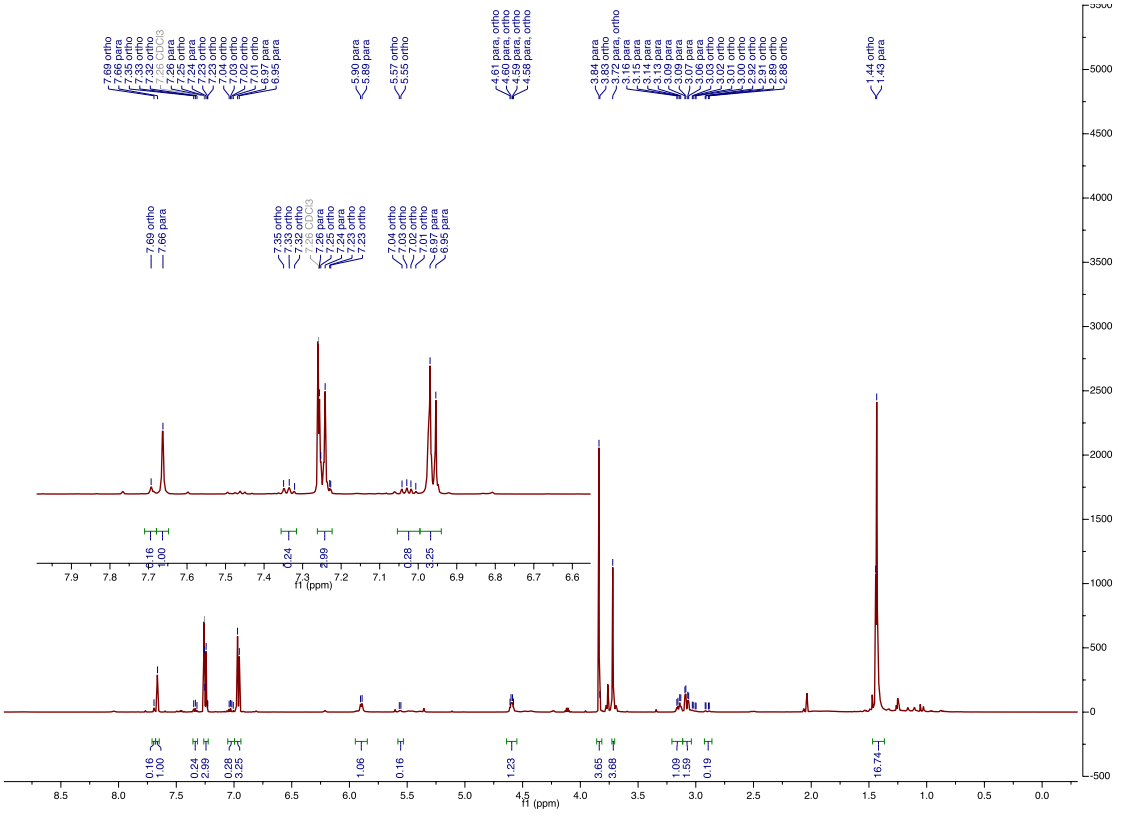
7.69 ortho
7.66 para
7.35 ortho
7.33 ortho
7.32 ortho
7.26 CDCl3
7.26 para
7.25 ortho
7.24 para
7.23 ortho
7.04 ortho
7.03 ortho
7.02 ortho
7.01 ortho
6.97 para
6.95 para
5.90 para
5.89 para
5.57 ortho
5.55 ortho
4.61 para, ortho
4.60 para, ortho
4.59 para, ortho
4.58 para, ortho
3.84 para
3.83 ortho
3.76 para, ortho
3.16 para
3.15 para
3.14 para
3.13 para
3.09 para
3.07 para
3.05 ortho
3.03 ortho
3.02 ortho
3.01 ortho
2.93 ortho
2.92 ortho
2.91 ortho
2.89 ortho
2.88 ortho
1.44 ortho
1.43 para
f1 (ppm)
f1 (ppm)

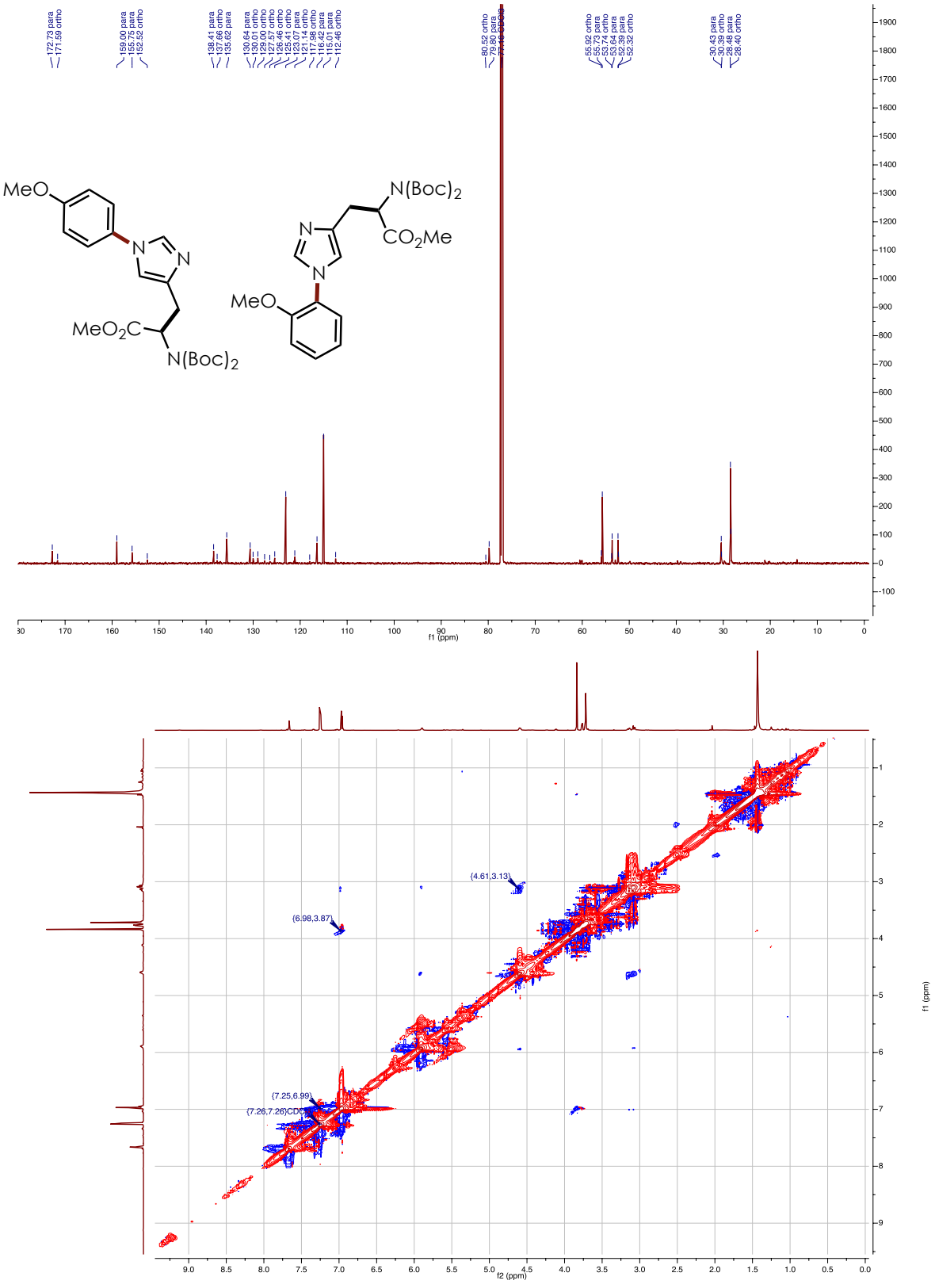
MeO
N
N
MeO2C
N(Boc)2
N(Boc)2
N
N
CO2Me
MeO
172.73 para
171.59 ortho
159.00 para
155.75 para
152.52 ortho
138.41 para
137.66 ortho
135.62 para
130.64 para
130.01 ortho
129.00 ortho
127.57 ortho
126.46 ortho
125.41 ortho
123.07 para
121.14 ortho
117.98 ortho
116.42 para
115.01 para
112.46 ortho
80.52 ortho
79.80 para
55.92 ortho
55.73 para
53.74 ortho
53.48 para
52.93 para
52.32 ortho
30.43 para
30.39 ortho
28.48 para
28.40 ortho
f1 (ppm)
f2 (ppm)
f1 (ppm)
{4.61,3.13}
{6.98,3.87}
{7.25,6.99}
{7.26,7.26}CDCl3

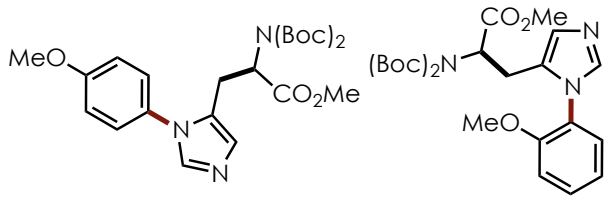
MeO
N(Boc)2
CO2Me
N
N
(Boc)2N
CO2Me
N
N
MeO

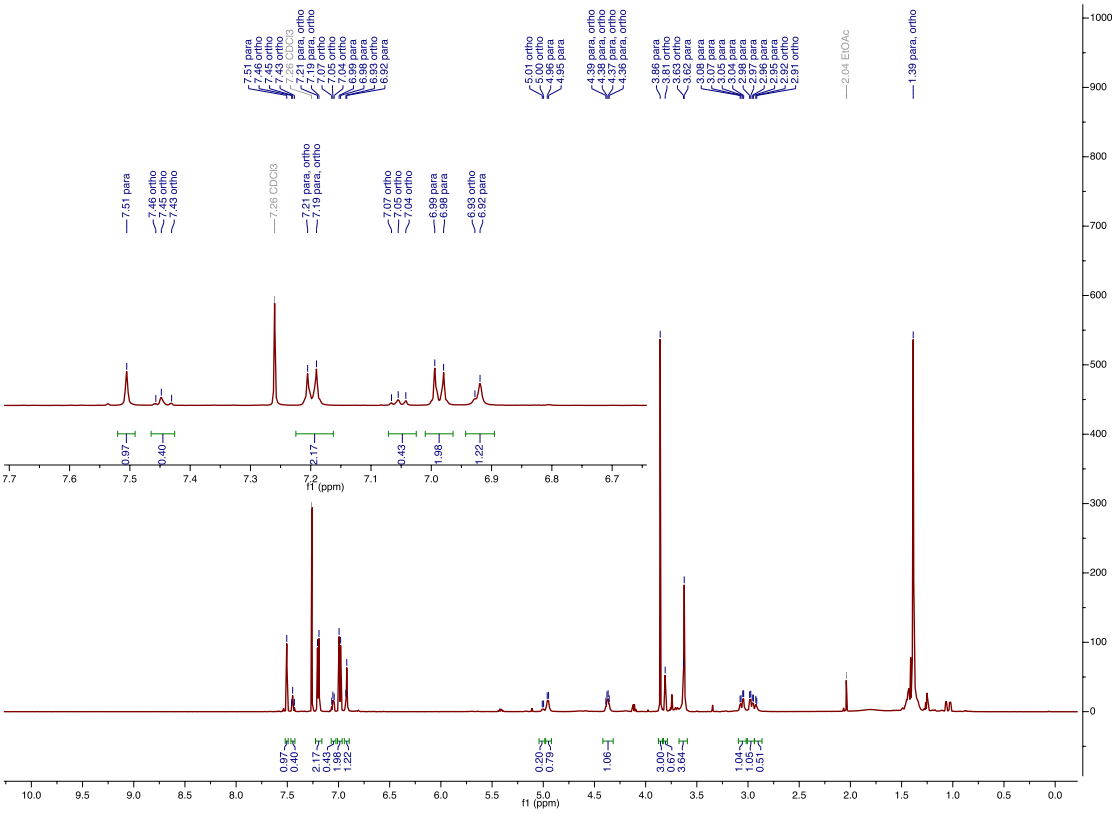
7.51 para
7.46 ortho
7.45 ortho
7.43 ortho
7.26 CDCl3
7.21 para, ortho
7.19 para, ortho
7.07 ortho
7.05 ortho
7.04 ortho
6.99 para
6.98 para
6.93 ortho
6.92 para
5.01 ortho
5.00 ortho
4.96 para
4.95 para
4.39 para, ortho
4.38 para, ortho
4.37 para, ortho
4.36 para, ortho
3.86 para
3.81 ortho
3.63 ortho
3.62 para
3.09 para
3.07 para
3.05 para
3.04 para
2.99 para
2.97 para
2.96 para
2.95 para
2.92 ortho
2.91 ortho
2.04 EtOAc
1.39 para, ortho
0.97
0.40
2.17
0.43
1.98
1.22
0.20
0.79
1.06
3.00
0.72
3.64
1.04
1.05
0.51
f1 (ppm)

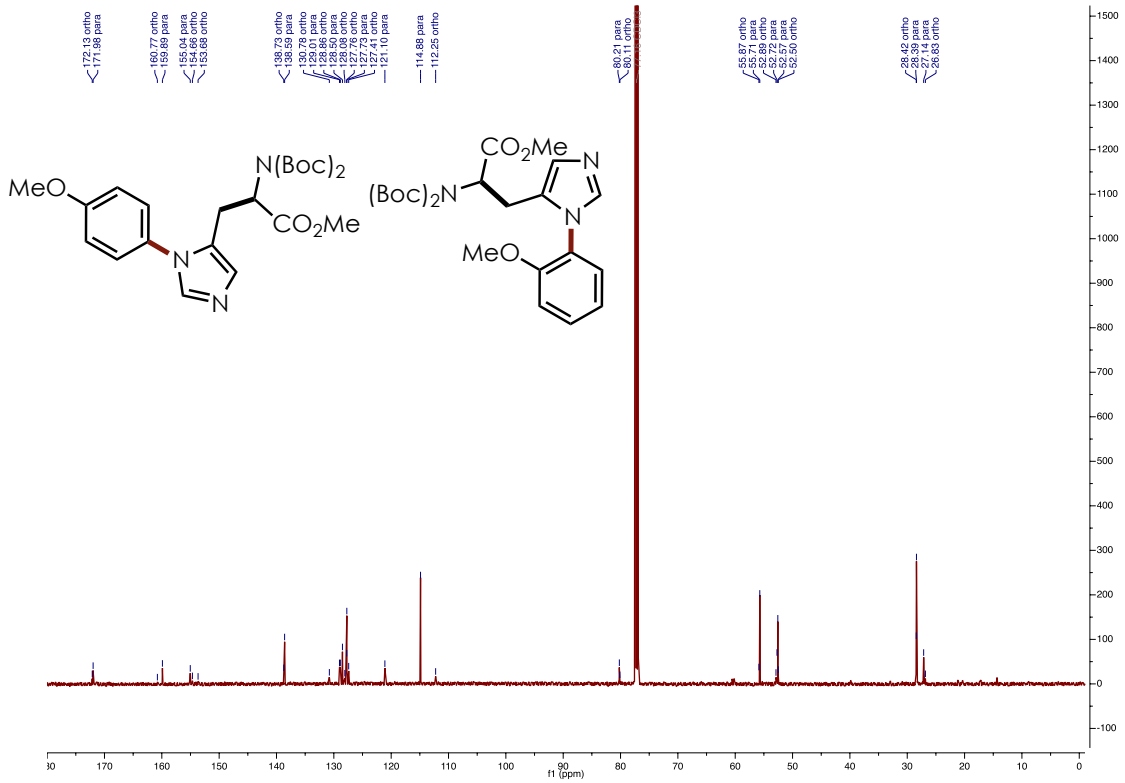
172.13 ortho
171.88 para
160.77 ortho
159.89 para
155.04 para
154.68 ortho
153.88 ortho
138.73 ortho
138.59 para
130.78 ortho
129.01 para
128.86 ortho
128.50 para
128.09 ortho
127.76 ortho
127.73 para
127.41 ortho
121.10 para
114.88 para
112.25 ortho
80.21 para
80.11 ortho
55.87 ortho
55.71 para
55.69 ortho
52.72 para
52.57 para
52.50 ortho
28.42 ortho
28.39 para
27.14 para
26.83 ortho
MeO
N(Boc)2
CO2Me
(Boc)2N
CO2Me
MeO
f1 (ppm)

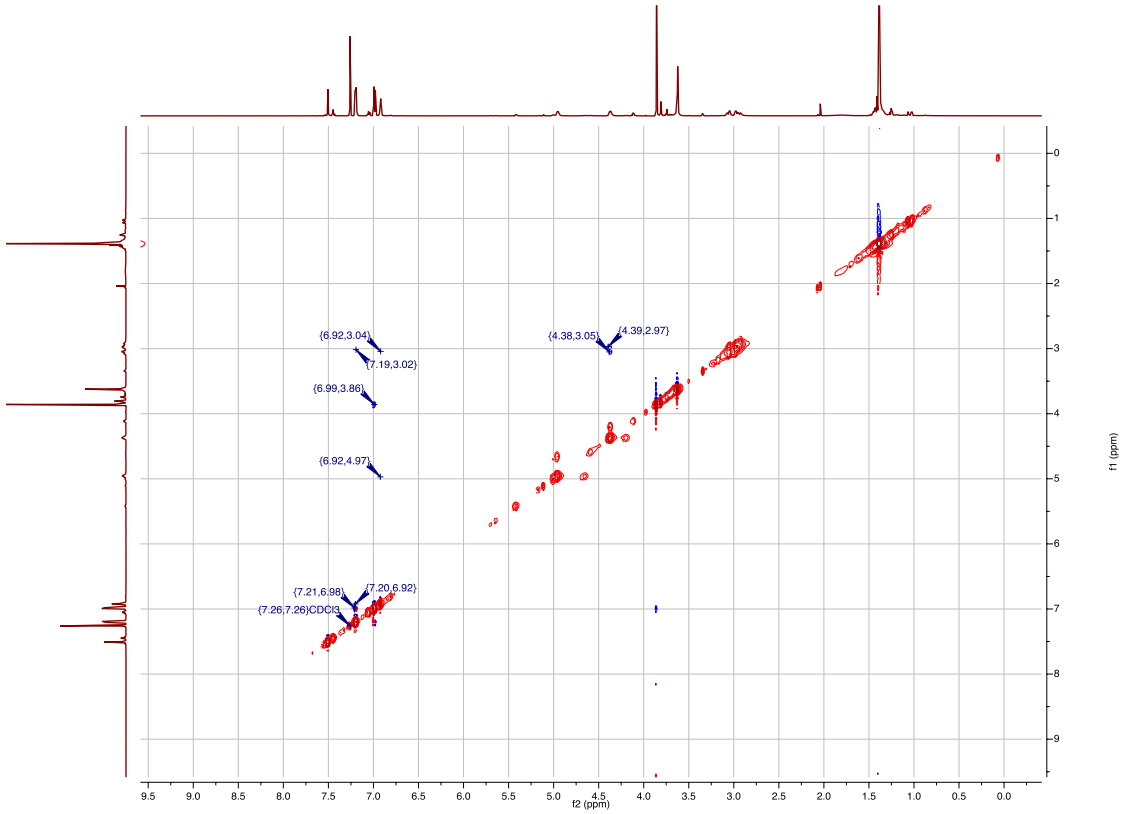
{6.92,3.04}
{7.19,3.02}
{6.99,3.86}
{6.92,4.97}
{4.38,3.05}
{4.39,2.97}
{7.21,6.98}
{7.20,6.92}
{7.26,7.26}CDCl3
f2 (ppm)
f1 (ppm)

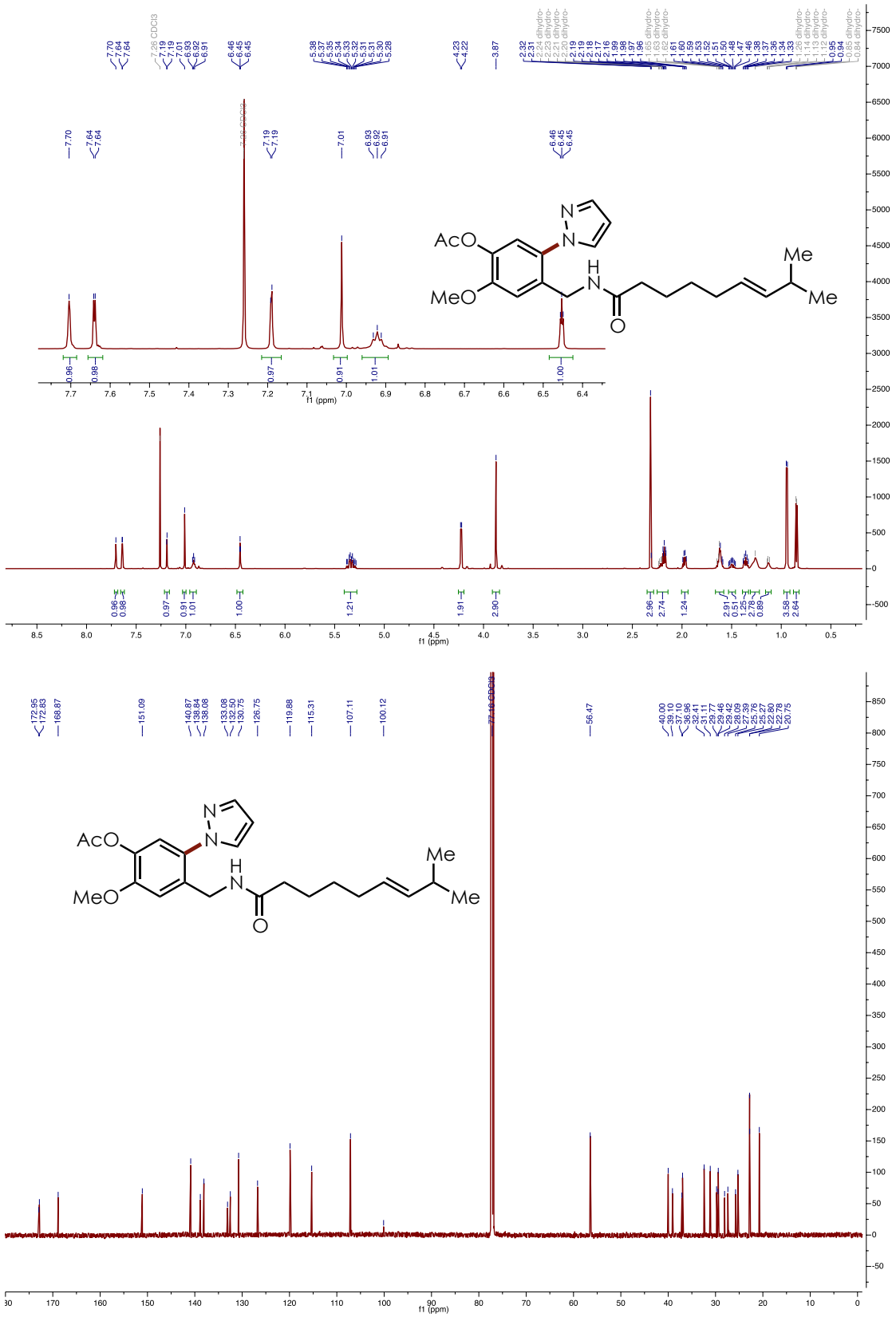
AcO
MeO
N
N
H
N
O
Me
Me
f1 (ppm)

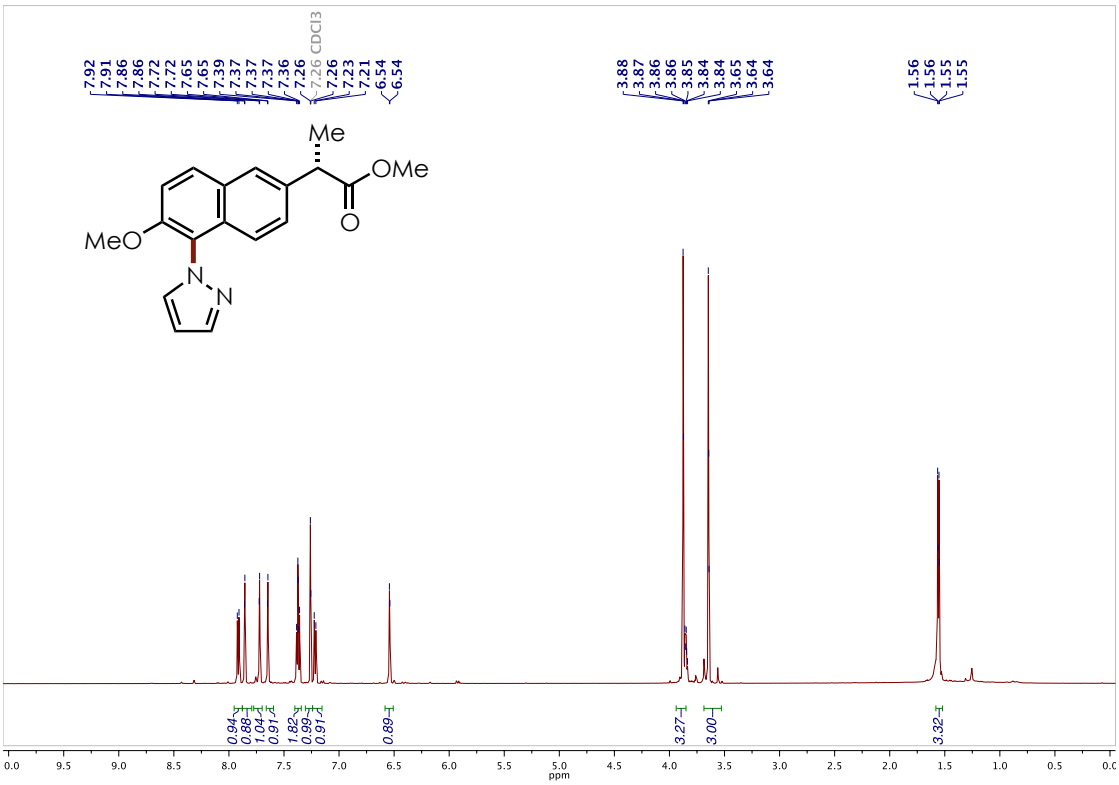
7.92
7.91
7.86
7.86
7.72
7.72
7.65
7.65
7.39
7.37
7.37
7.37
7.36
7.26
7.26 CDCl3
7.23
7.21
6.54
6.54
3.88
3.87
3.86
3.86
3.85
3.84
3.84
3.65
3.64
3.64
1.56
1.56
1.55
1.55
Me
OMe
O
MeO
N
N
0.94
0.88
1.04
0.91
1.82
0.99
0.91
0.89
3.27
3.00
3.32
ppm

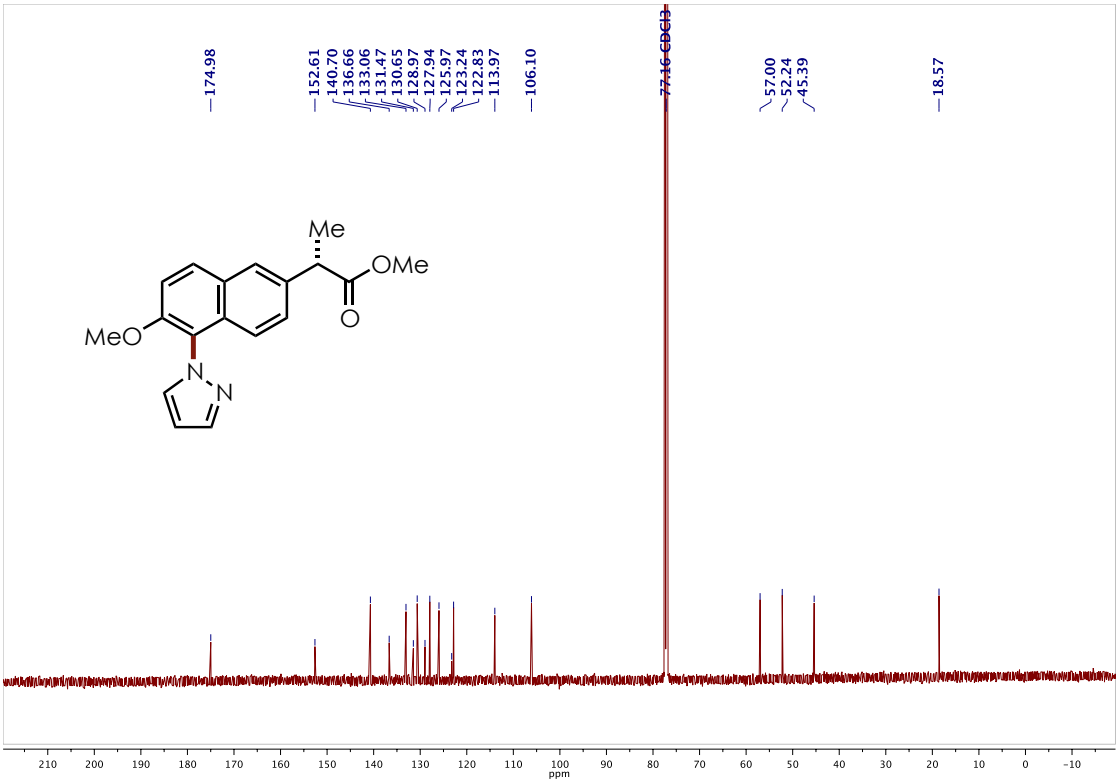
174.98
152.61
140.70
136.66
133.06
131.47
130.65
128.97
127.94
125.97
123.24
122.83
113.97
106.10
77.16 CDCl3
57.00
52.24
45.39
18.57
Me
OMe
O
MeO
N
N
ppm

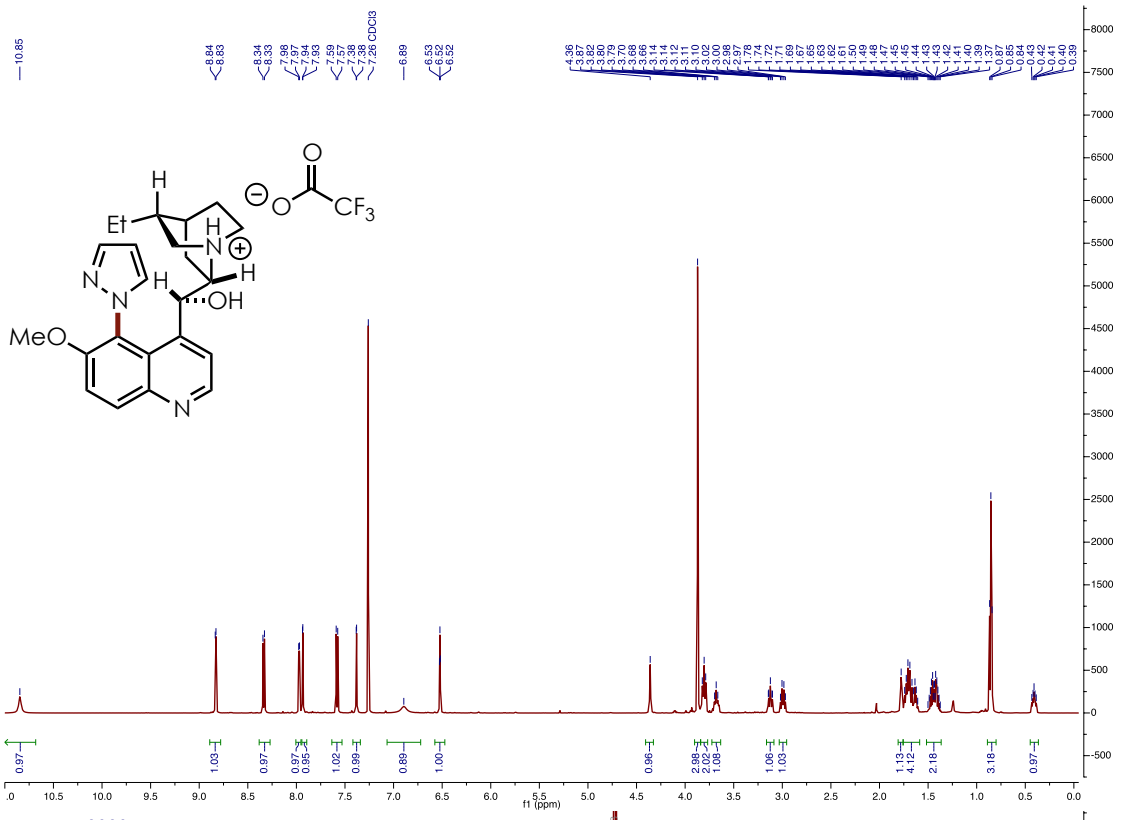
10.85
8.84
8.83
8.34
8.33
7.98
7.97
7.94
7.93
7.59
7.57
7.38
7.36
7.26 CDCl3
6.89
6.53
6.52
6.52
4.36
3.87
3.82
3.80
3.79
3.70
3.68
3.66
3.14
3.12
3.11
3.10
3.02
3.00
2.98
2.97
1.78
1.74
1.72
1.71
1.69
1.67
1.65
1.63
1.62
1.61
1.50
1.49
1.48
1.47
1.45
1.45
1.44
1.43
1.42
1.41
1.40
1.39
1.37
0.87
0.85
0.84
0.43
0.42
0.41
0.40
0.39
Et
H
N
H
N
H
OH
MeO
N
O
O
CF3
0.97
1.03
0.97
0.97
0.95
1.02
0.99
0.89
1.00
0.96
2.98
2.02
1.08
1.06
1.03
1.13
4.12
2.18
3.18
0.97
f1 (ppm)

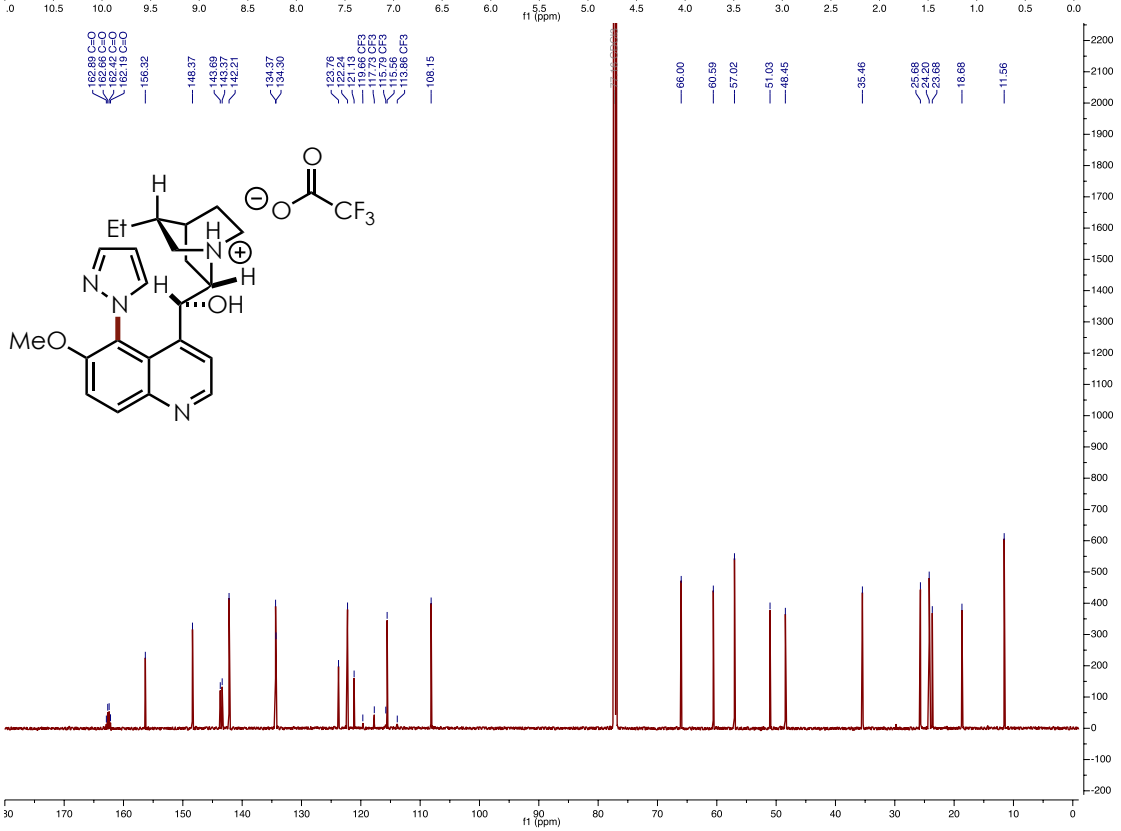
162.89 C=O
162.66 C=O
162.42 C=O
162.19 C=O
156.32
148.37
143.69
143.27
142.21
134.37
134.30
123.76
122.24
121.11
119.18 CF3
117.73 CF3
115.79 CF3
113.86 CF3
108.15
66.00
60.59
57.02
51.03
48.45
35.46
25.68
24.20
23.88
18.68
11.56
Et
H
N
H
N
H
OH
MeO
N
O
O
CF3
f1 (ppm)

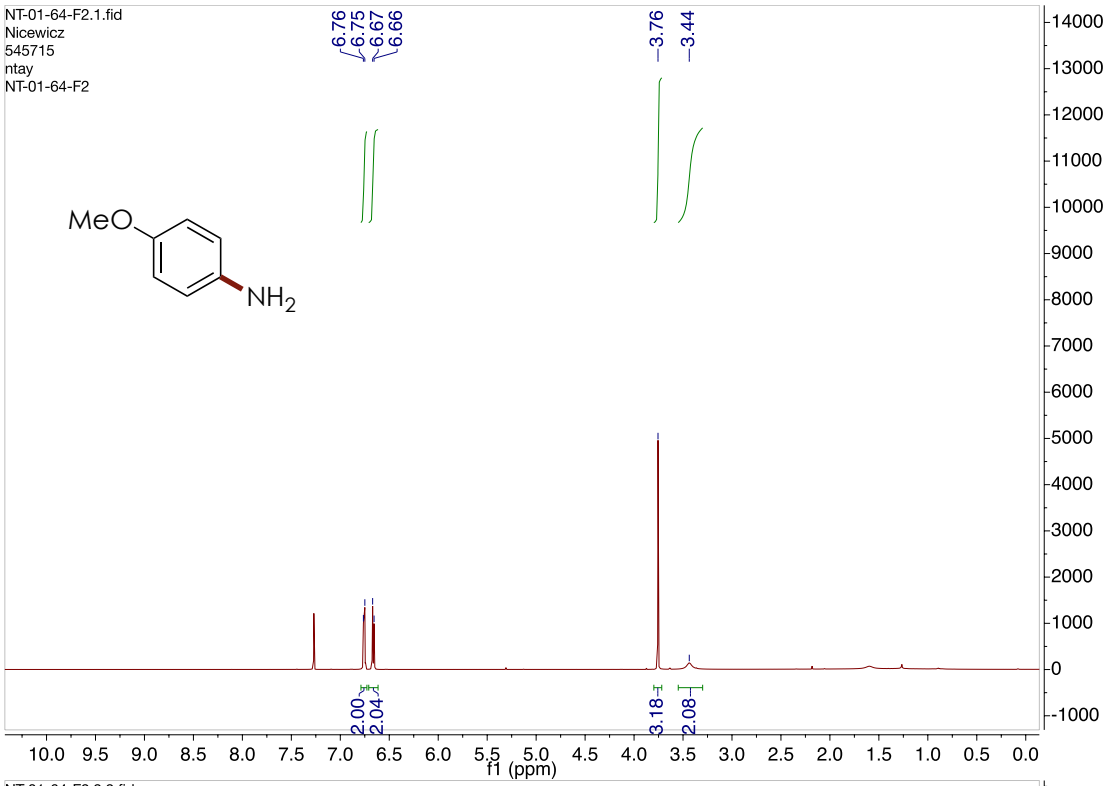
NT-01-64-F2.1.fid
Nicewicz
545715
ntay
NT-01-64-F2
6.76
6.75
6.67
6.66
3.76
3.44
MeO
NH2
2.00
2.04
3.18
2.08
f1 (ppm)

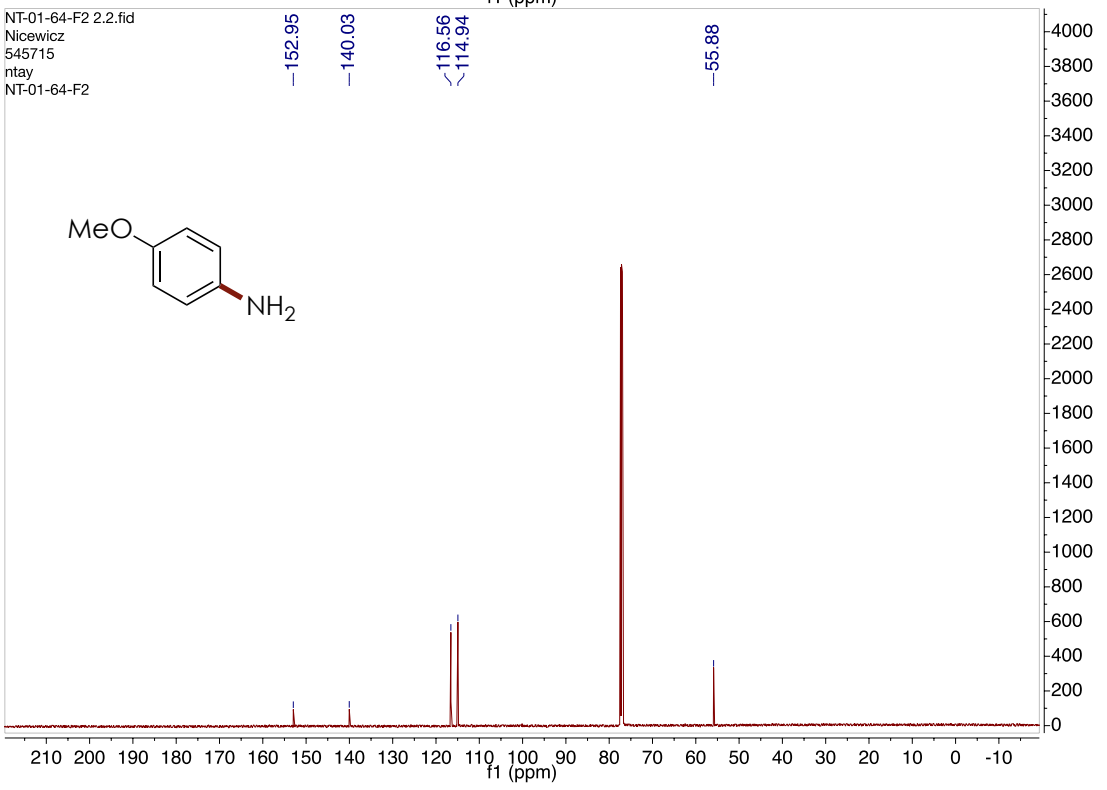
NT-01-64-F2 2.2.fid
Nicewicz
545715
ntay
NT-01-64-F2
152.95
140.03
116.56
114.94
55.88
MeO
NH2
f1 (ppm)

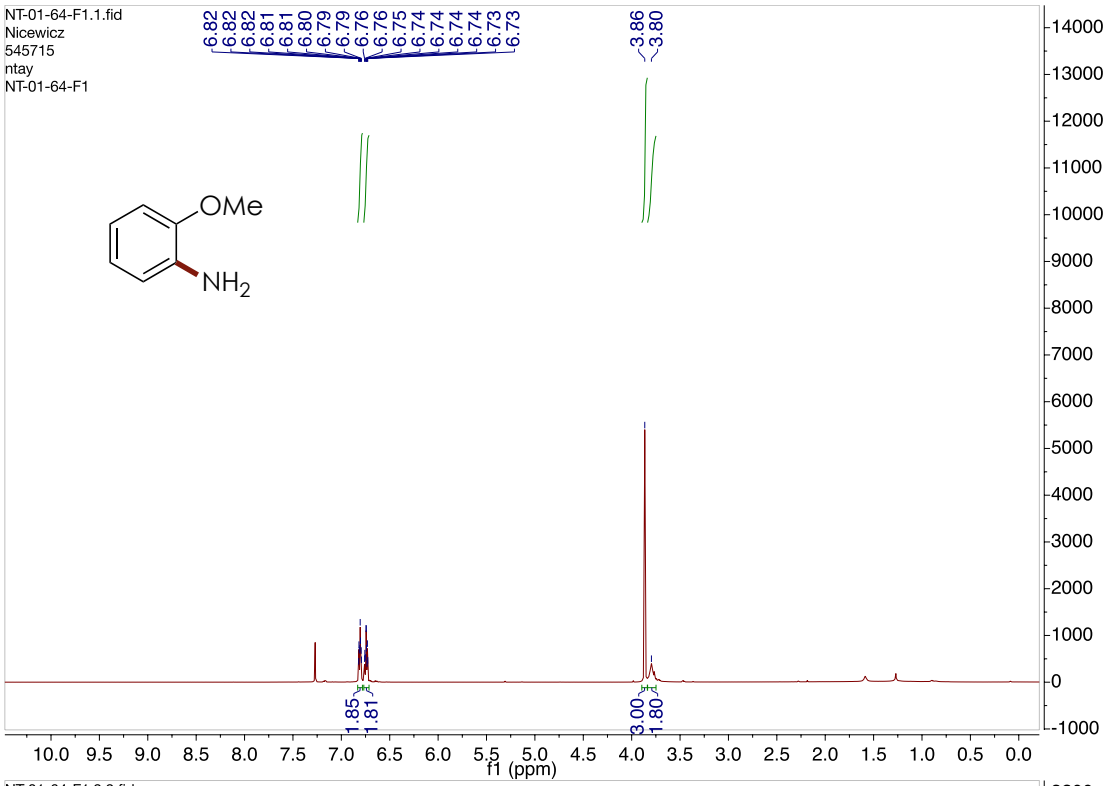
NT-01-64-F1.1.fid
Nicewicz
545715
ntay
NT-01-64-F1
6.82
6.82
6.82
6.81
6.81
6.80
6.79
6.79
6.76
6.76
6.75
6.74
6.74
6.74
6.73
3.86
3.80
OMe
NH2
1.85
1.81
3.00
1.80
f1 (ppm)

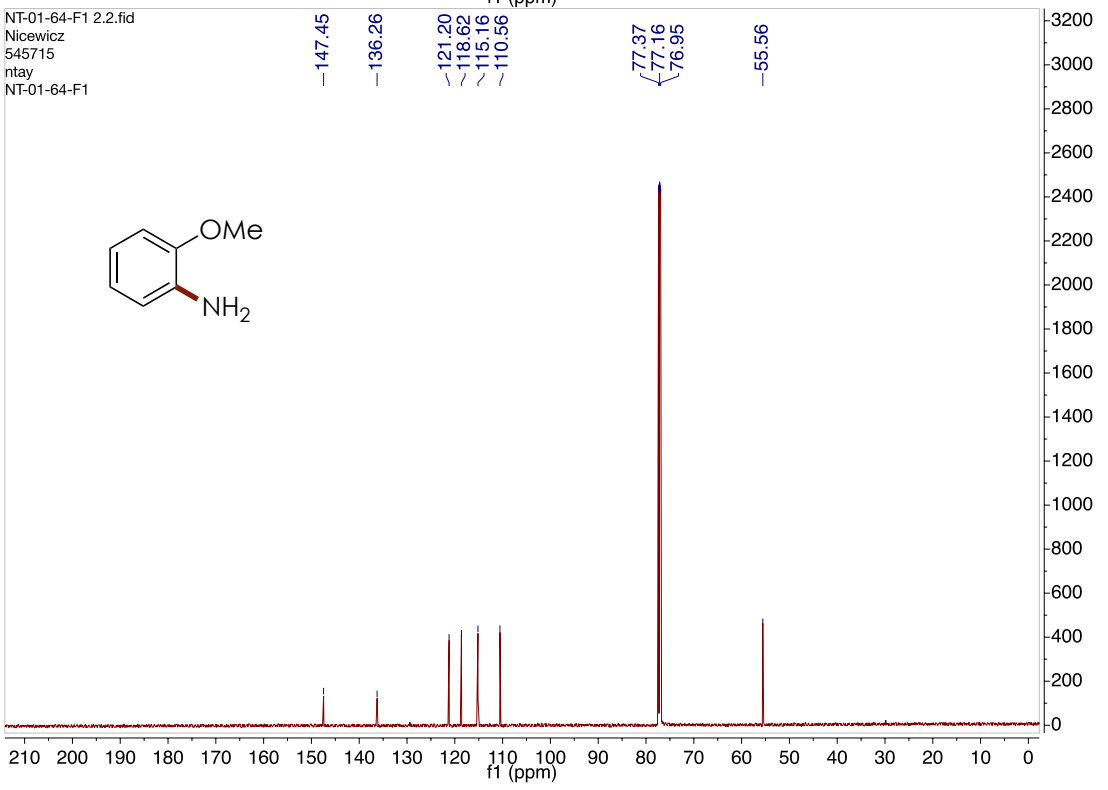
NT-01-64-F1 2.2.fid
Nicewicz
545715
ntay
NT-01-64-F1
147.45
136.26
121.20
118.62
115.16
110.56
77.37
77.16
76.95
55.56
OMe
NH2
f1 (ppm)

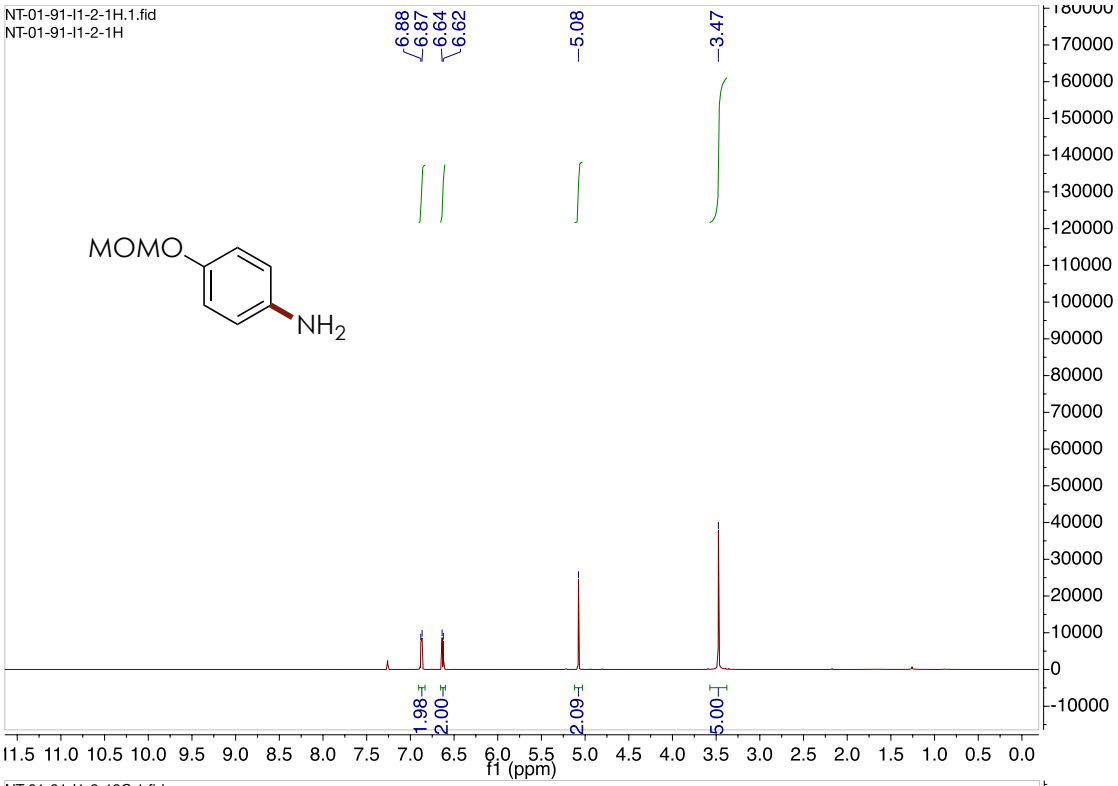
NT-01-91-I1-2-1H.1.fid
NT-01-91-I1-2-1H
6.88
6.87
6.64
6.62
5.08
3.47
MOMO
NH2
1.98
2.00
2.09
5.00
f1 (ppm)

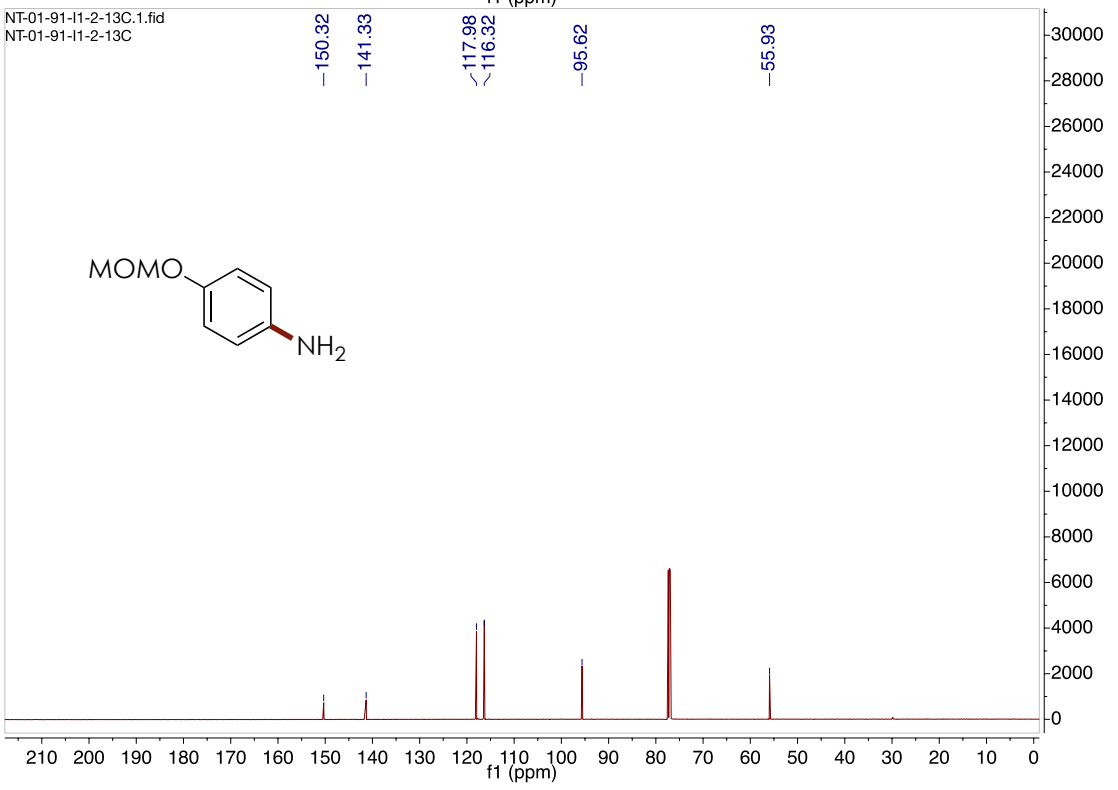
NT-01-91-I1-2-13C.1.fid
NT-01-91-I1-2-13C
150.32
141.33
117.98
116.32
95.62
55.93
MOMO
NH2
f1 (ppm)

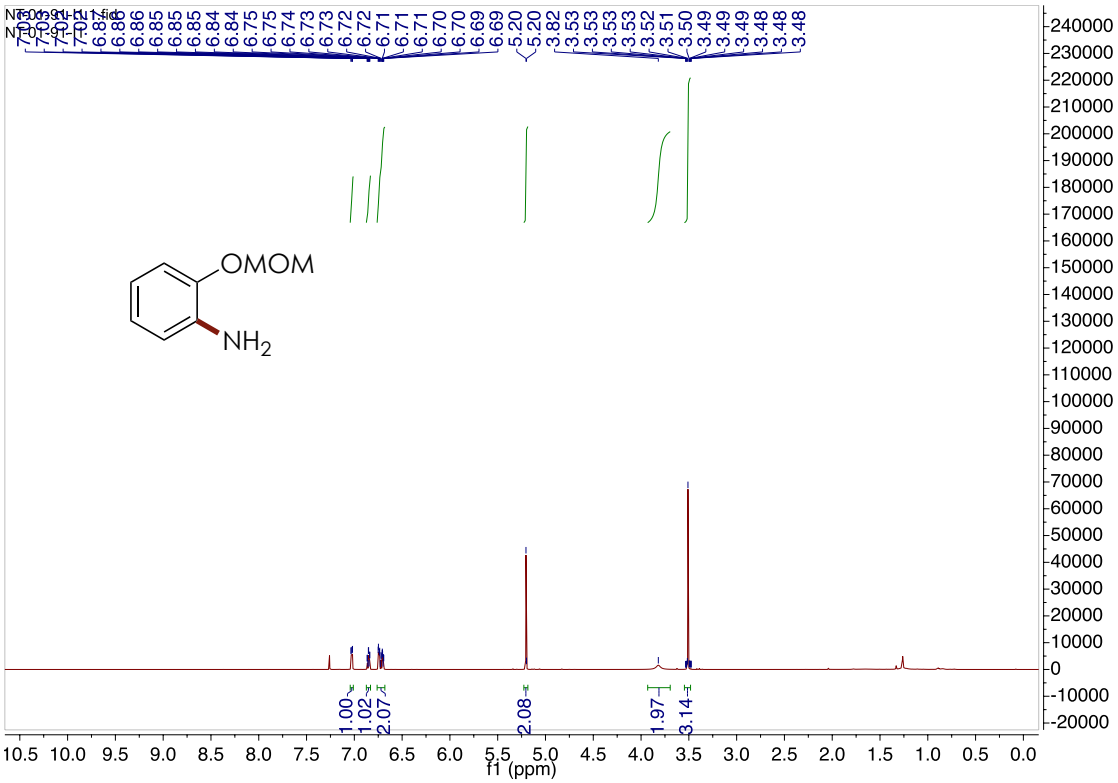
NT-01-91-I1.1.fid
NT-01-91-I1
OMOM
NH2
1.00
1.02
2.07
2.08
1.97
3.14
f1 (ppm)

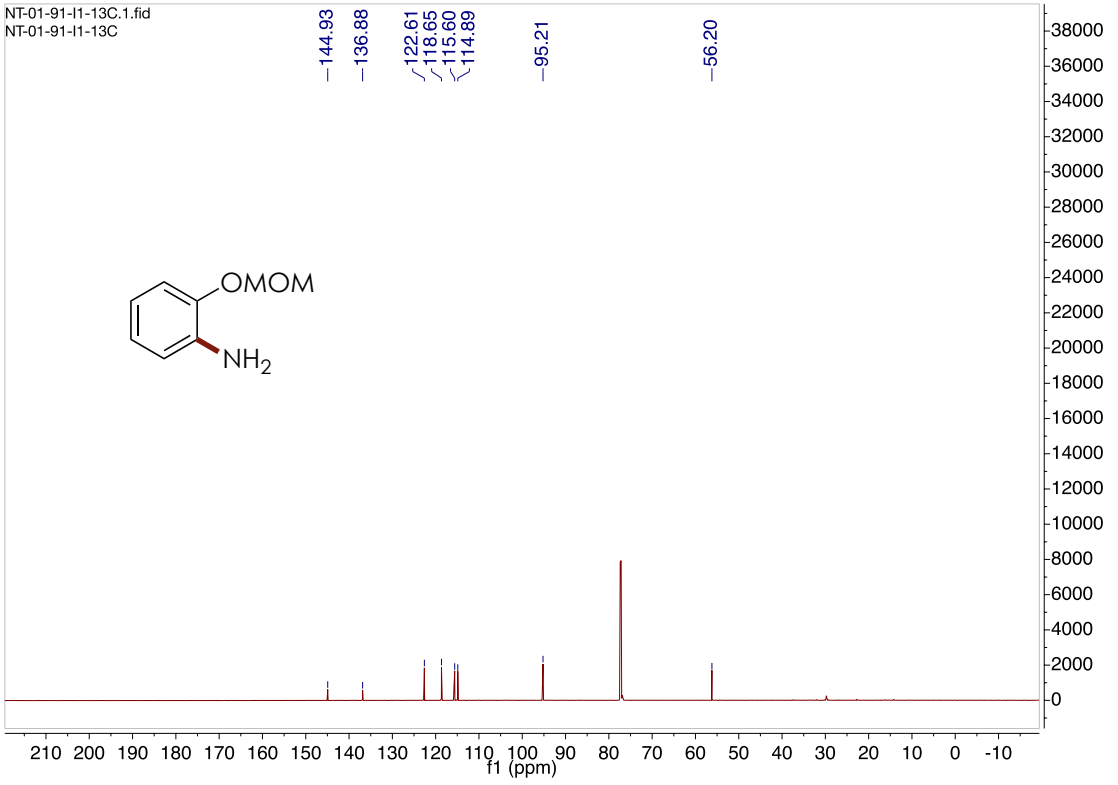
NT-01-91-I1-13C.1.fid
NT-01-91-I1-13C
144.93
136.88
122.61
118.65
115.60
114.89
95.21
56.20
OMOM
NH2
f1 (ppm)

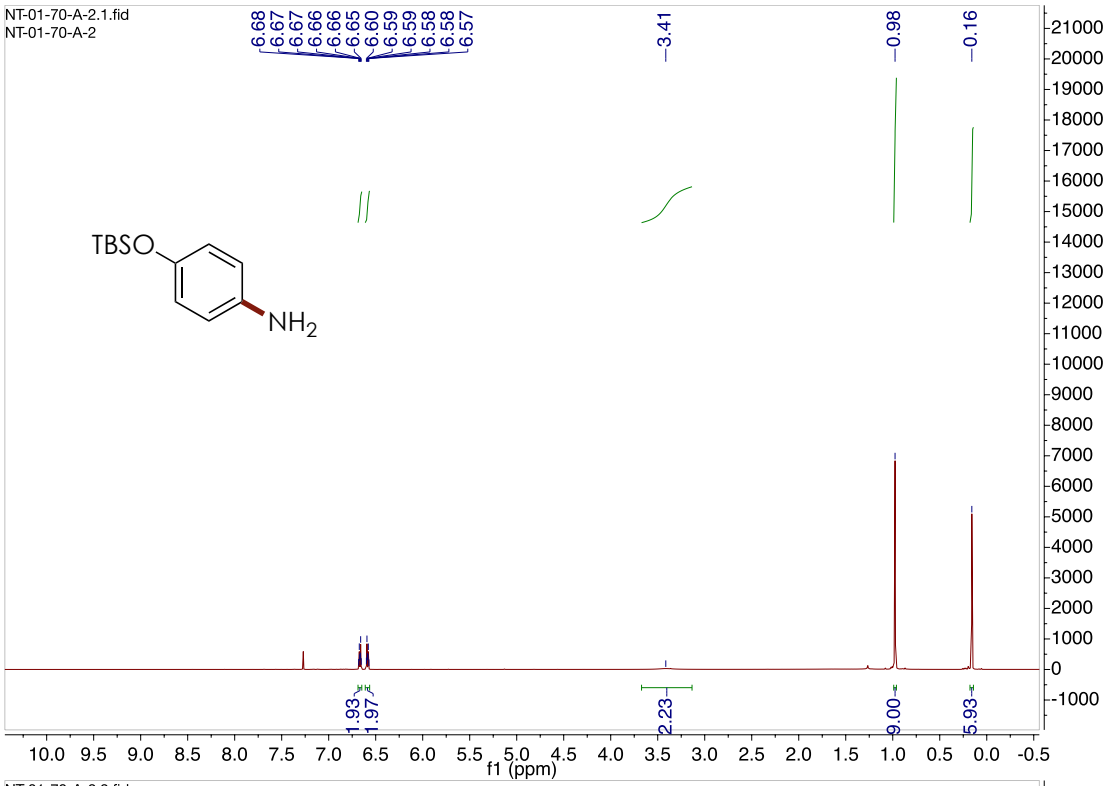
NT-01-70-A-2.1.fid
NT-01-70-A-2
6.68
6.67
6.67
6.66
6.66
6.65
6.60
6.59
6.59
6.58
6.58
6.57
3.41
0.98
0.16
TBSO
NH2
1.93
1.97
2.23
9.00
5.93
f1 (ppm)

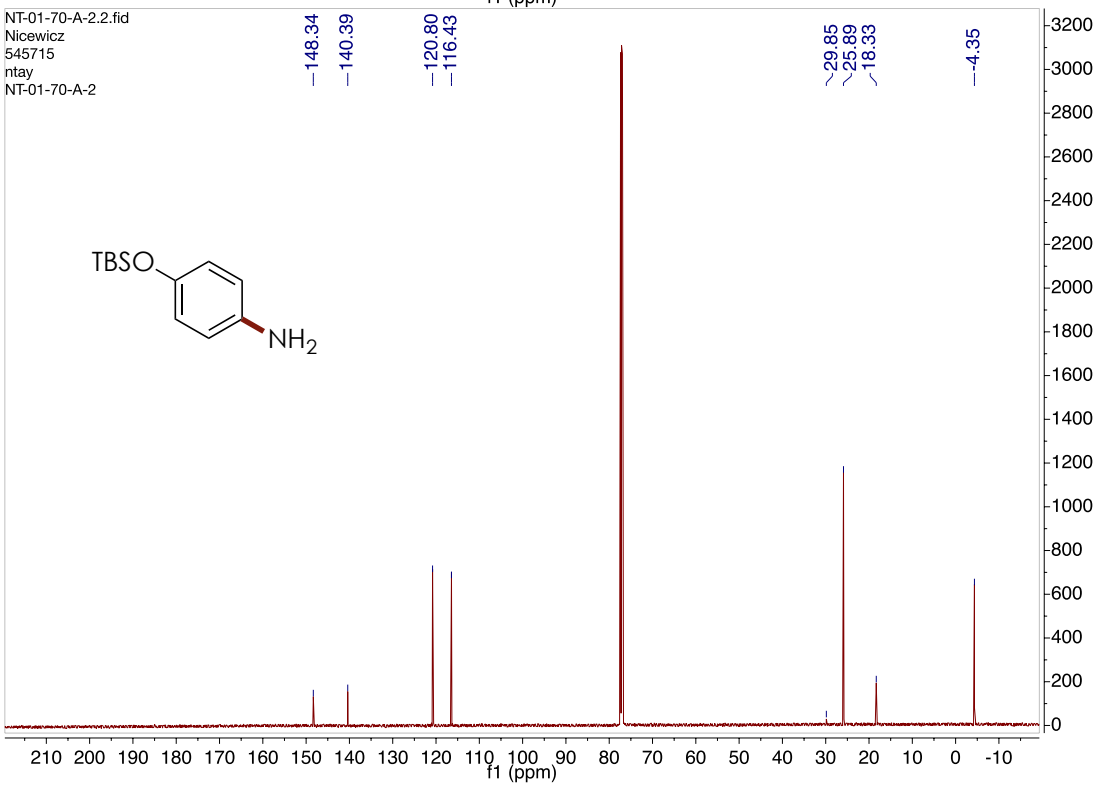
NT-01-70-A-2.2.fid
Nicewicz
545715
ntay
NT-01-70-A-2
148.34
140.39
120.80
116.43
29.85
25.89
18.33
-4.35
TBSO
NH2
f1 (ppm)

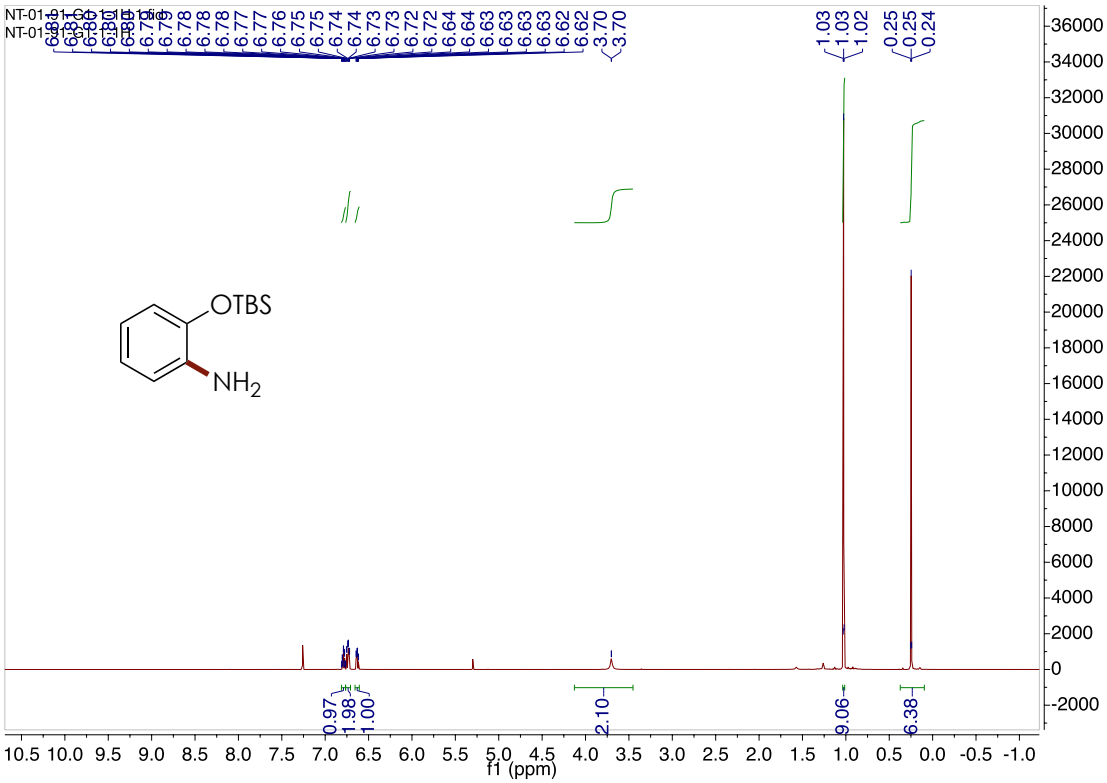
NT-01-91-G1-1-1H.1.fid
NT-01-91-G1-1-1H
6.83
6.81
6.80
6.79
6.78
6.77
6.76
6.75
6.74
6.73
6.72
6.64
6.63
6.62
3.70
1.03
1.02
0.25
0.24
OTBS
NH2
0.97
1.98
1.00
2.10
9.06
6.38
f1 (ppm)

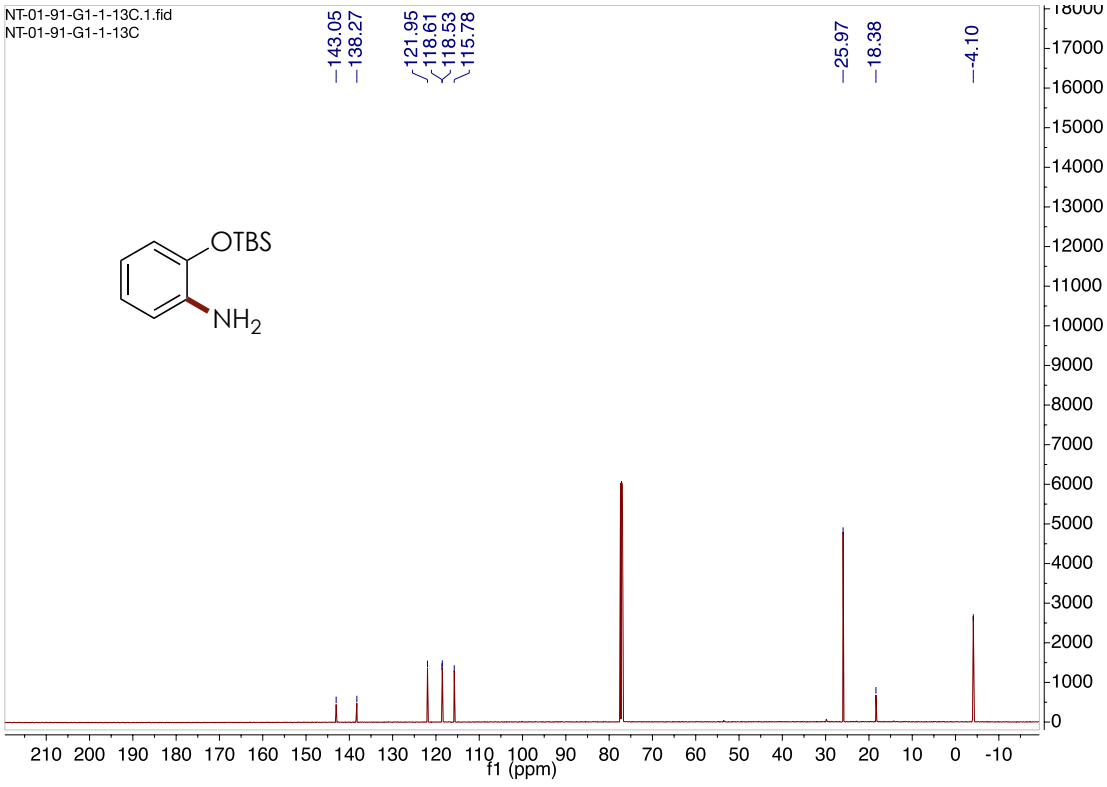
NT-01-91-G1-1-13C.1.fid
NT-01-91-G1-1-13C
143.05
138.27
121.95
118.61
118.53
115.78
25.97
18.38
4.10
OTBS
NH2
f1 (ppm)

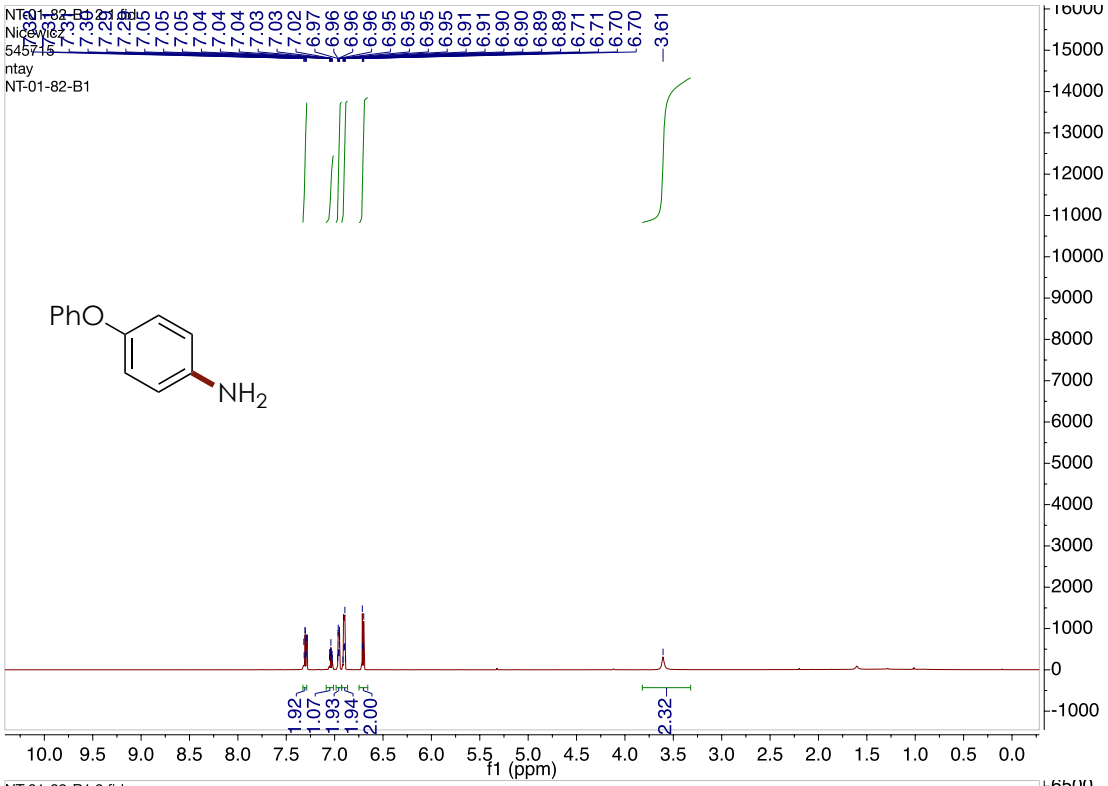
NT-01-82-B1.1.fid
Nicewicz
545715
ntay
NT-01-82-B1
7.33
7.25
7.05
7.04
7.03
7.02
6.97
6.96
6.95
6.91
6.90
6.89
6.71
6.70
3.61
PhO
NH2
1.92
1.07
1.93
1.94
2.00
2.32
f1 (ppm)

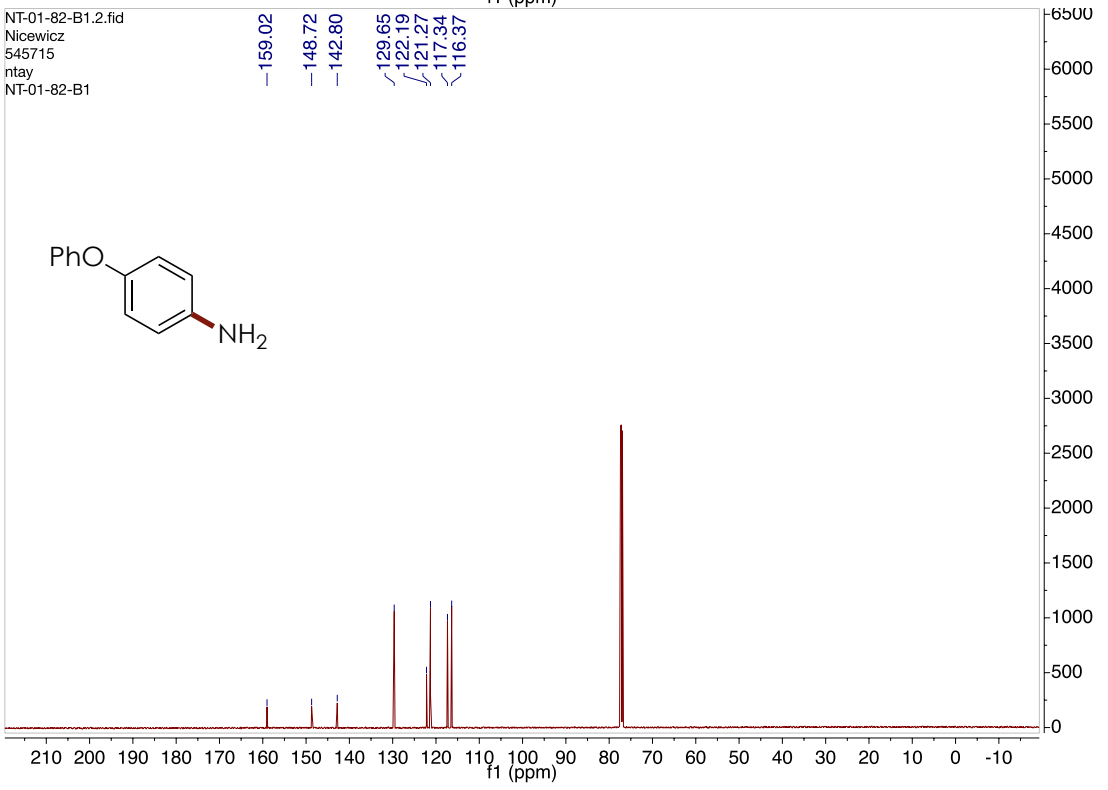
NT-01-82-B1.2.fid
Nicewicz
545715
ntay
NT-01-82-B1
159.02
148.72
142.80
129.65
122.19
121.27
117.34
116.37
PhO
NH2
f1 (ppm)

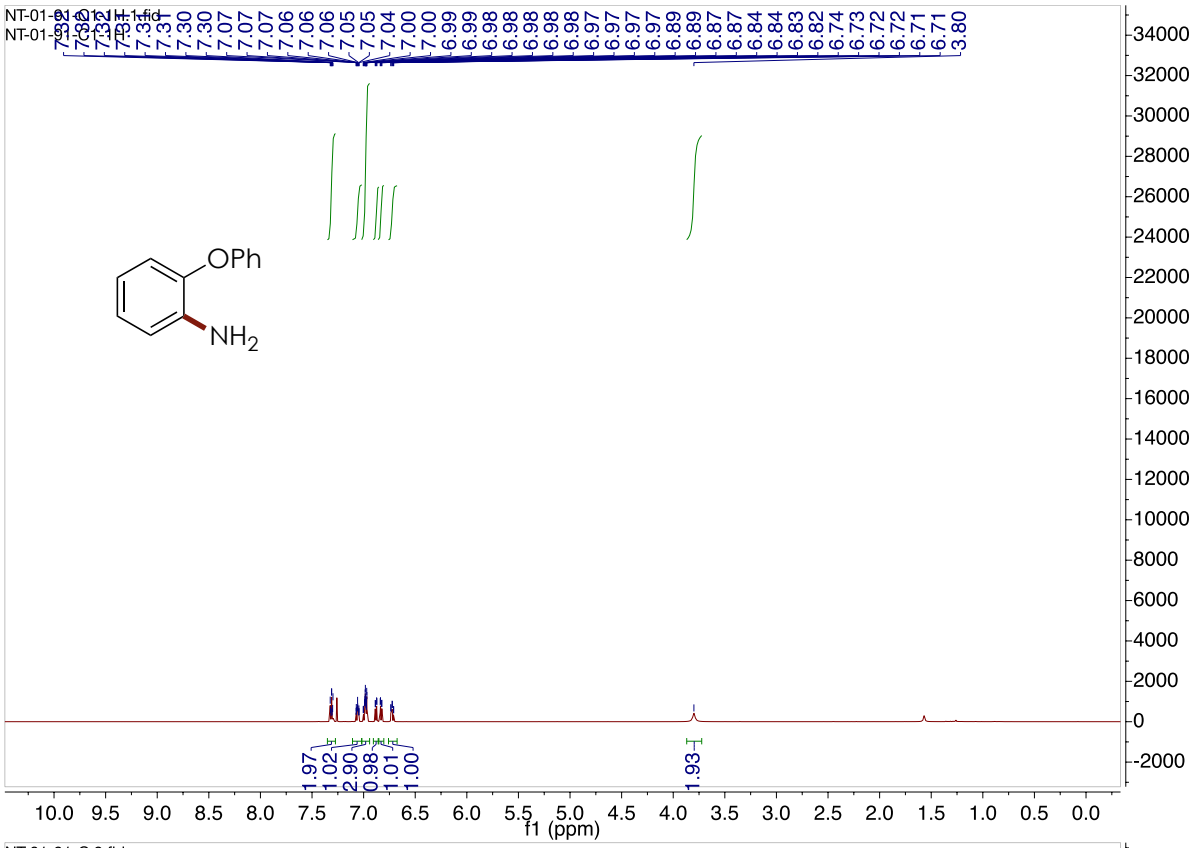
NT-01-91-H.1.fid
7.32
7.31
7.30
7.07
7.06
7.05
7.04
7.00
6.99
6.98
6.89
6.87
6.84
6.83
6.82
6.74
6.73
6.72
6.71
3.80
OPh
NH2
1.97
1.02
2.90
0.98
1.01
1.00
1.93
f1 (ppm)

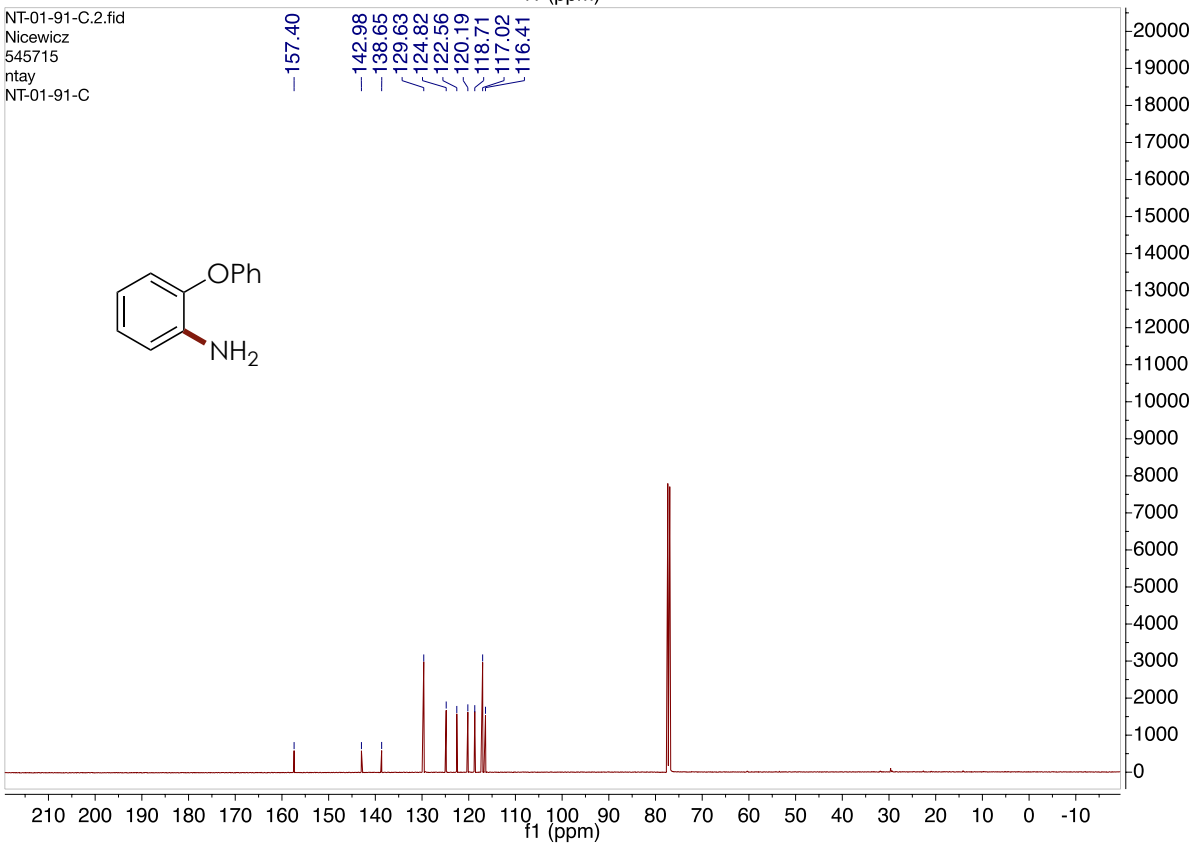
NT-01-91-C.2.fid
Nicewicz
545715
ntay
NT-01-91-C
157.40
142.98
138.65
129.63
124.82
122.56
120.19
118.71
117.02
116.41
OPh
NH2
f1 (ppm)

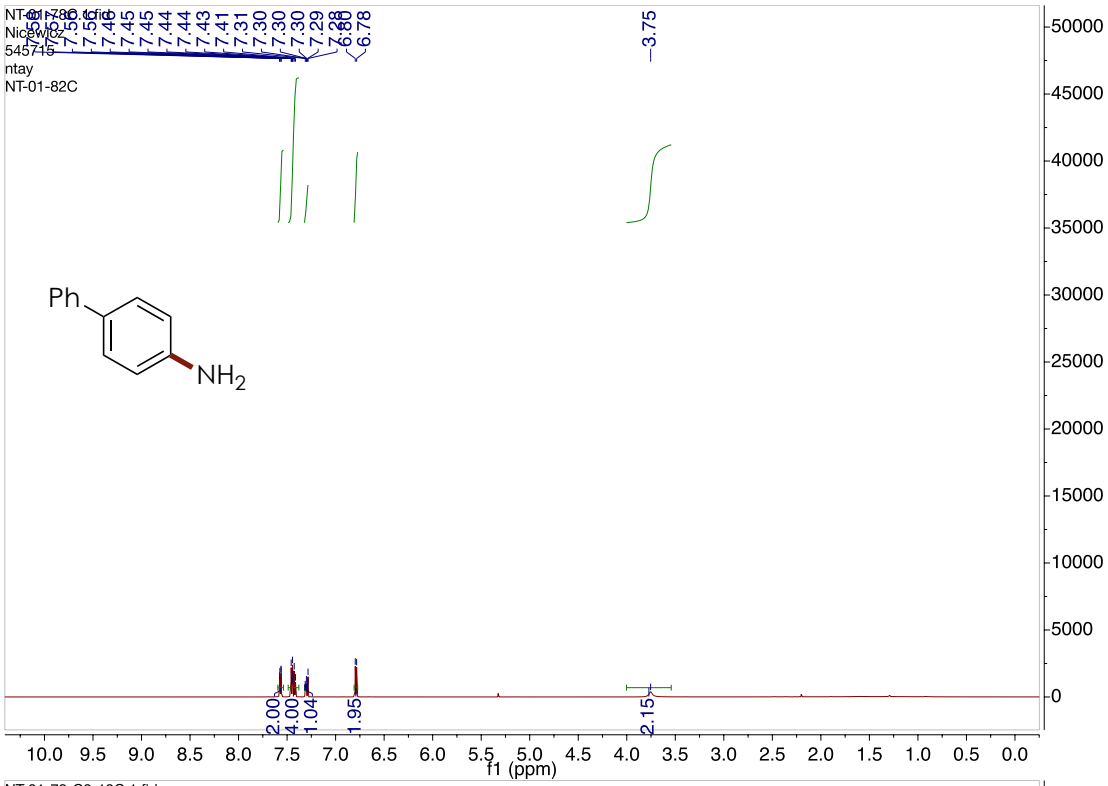
NT-01-78C.1.fid
Nicewicz
545715
ntay
NT-01-82C
7.56
7.55
7.46
7.45
7.45
7.44
7.44
7.43
7.41
7.31
7.30
7.30
7.29
7.28
6.80
6.78
3.75
Ph
NH2
2.00
4.00
1.04
1.95
2.15
f1 (ppm)

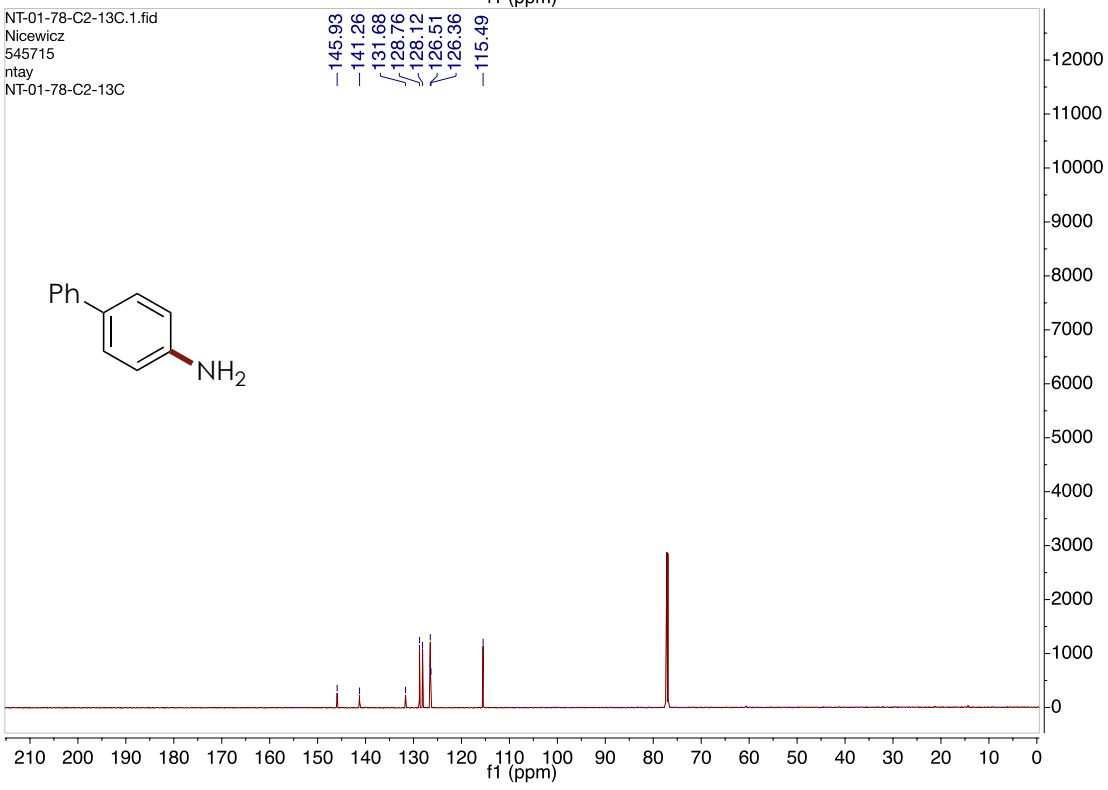
NT-01-78-C2-13C.1.fid
Nicewicz
545715
ntay
NT-01-78-C2-13C
145.93
141.26
131.68
128.76
128.12
126.51
126.36
115.49
Ph
NH2
f1 (ppm)

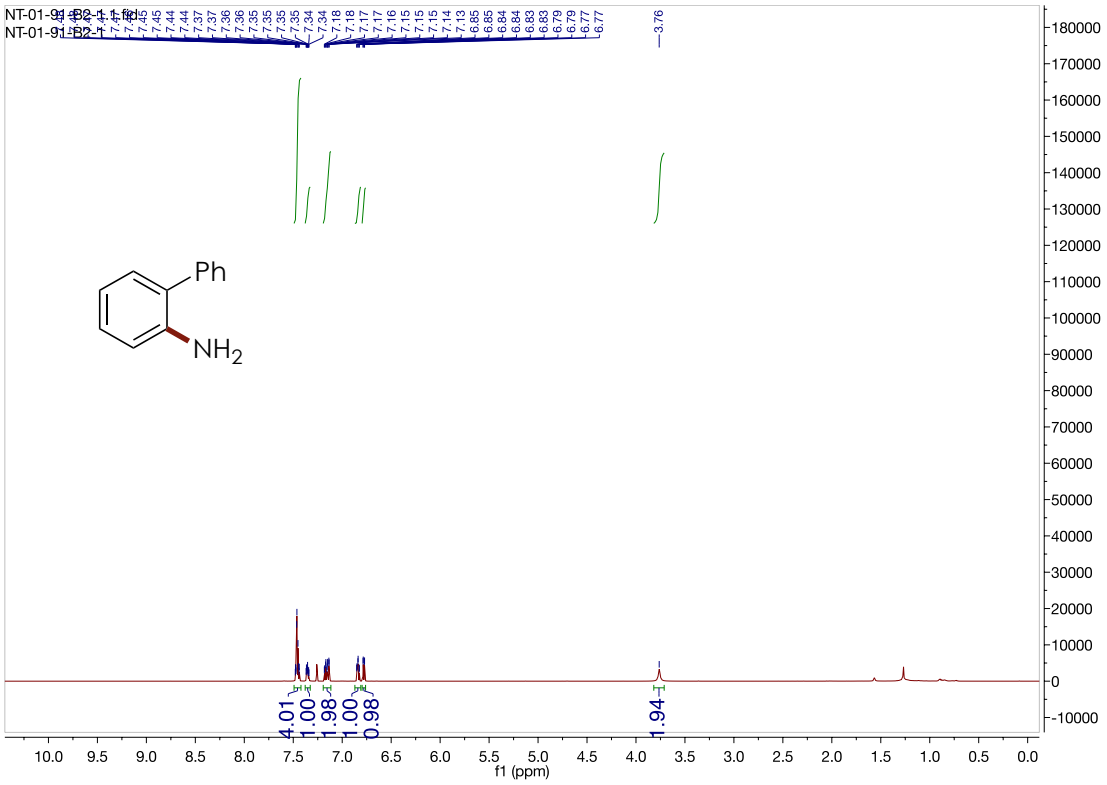
NT-01-91-B2-1-1.fid
NT-01-91-B2-1
7.45
7.44
7.37
7.36
7.35
7.34
7.18
7.17
7.16
7.15
7.14
7.13
6.85
6.84
6.83
6.79
6.77
3.76
Ph
NH2
4.01
1.00
1.98
1.00
0.98
1.94
f1 (ppm)

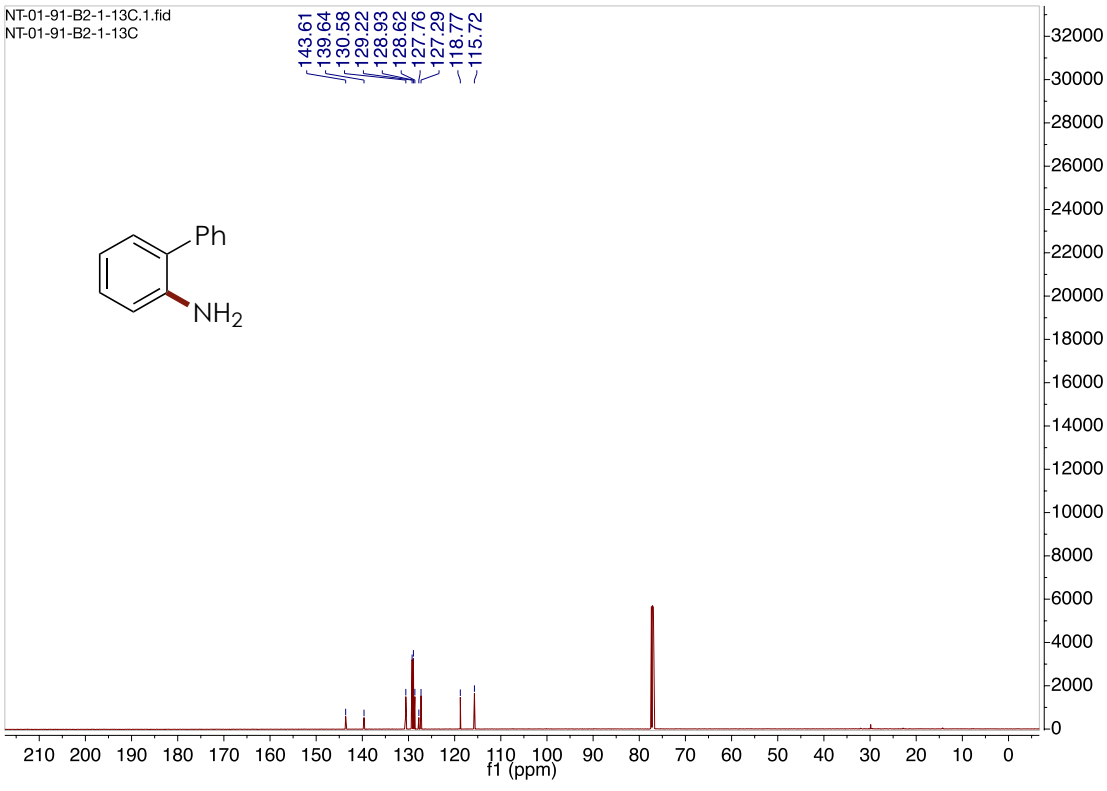
NT-01-91-B2-1-13C.1.fid
NT-01-91-B2-1-13C
143.61
139.64
130.58
129.22
128.93
128.62
127.76
127.29
118.77
115.72
Ph
NH2
f1 (ppm)

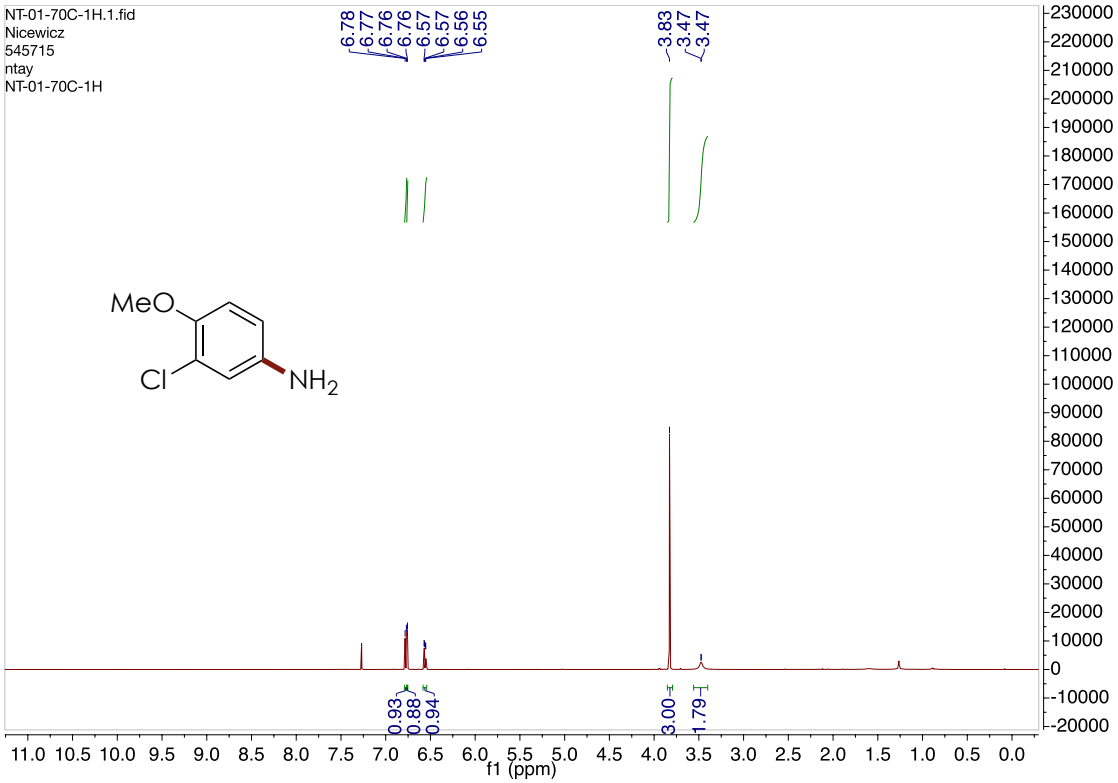
NT-01-70C-1H.1.fid
Nicewicz
545715
ntay
NT-01-70C-1H
6.78
6.77
6.76
6.76
6.57
6.57
6.56
6.55
3.83
3.47
3.47
MeO
Cl
NH2
0.93
0.88
0.94
3.00
1.79
f1 (ppm)

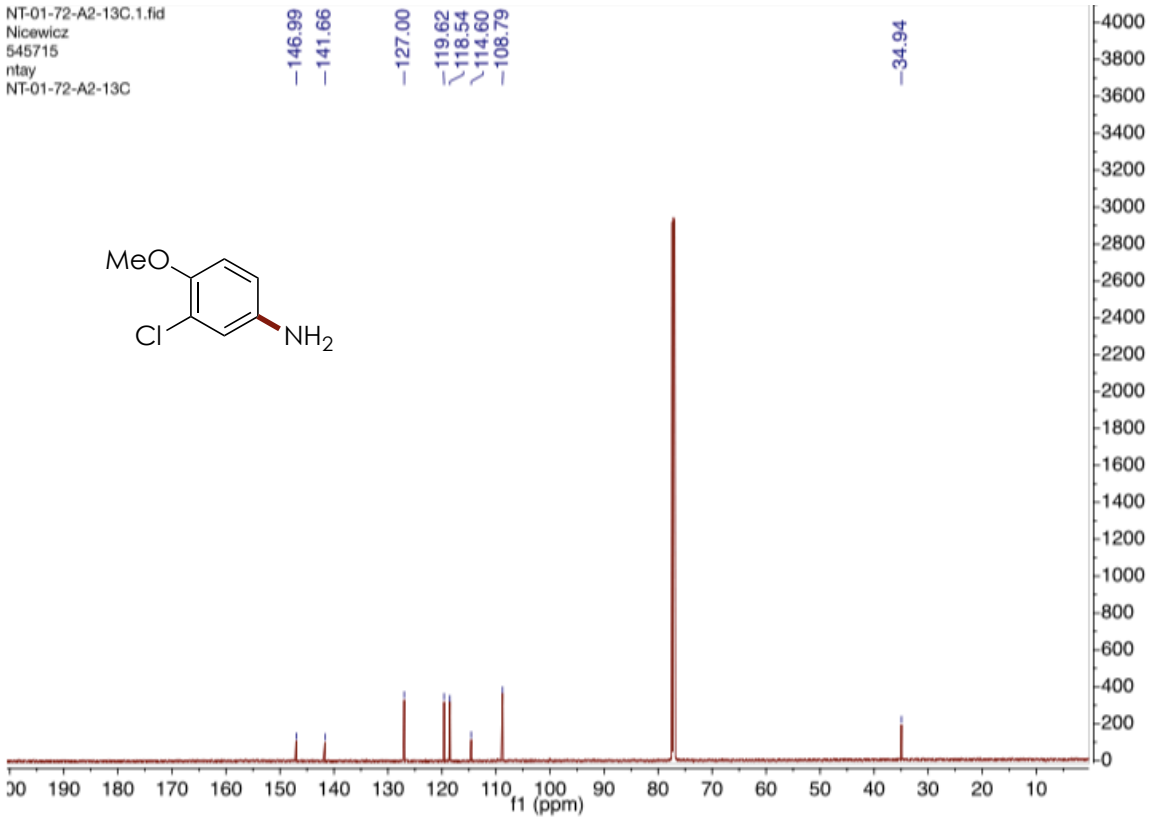
NT-01-72-A2-13C.1.fid
Nicewicz
545715
ntay
NT-01-72-A2-13C
146.99
141.66
127.00
119.62
118.54
114.60
108.79
34.94
MeO
Cl
NH2
f1 (ppm)

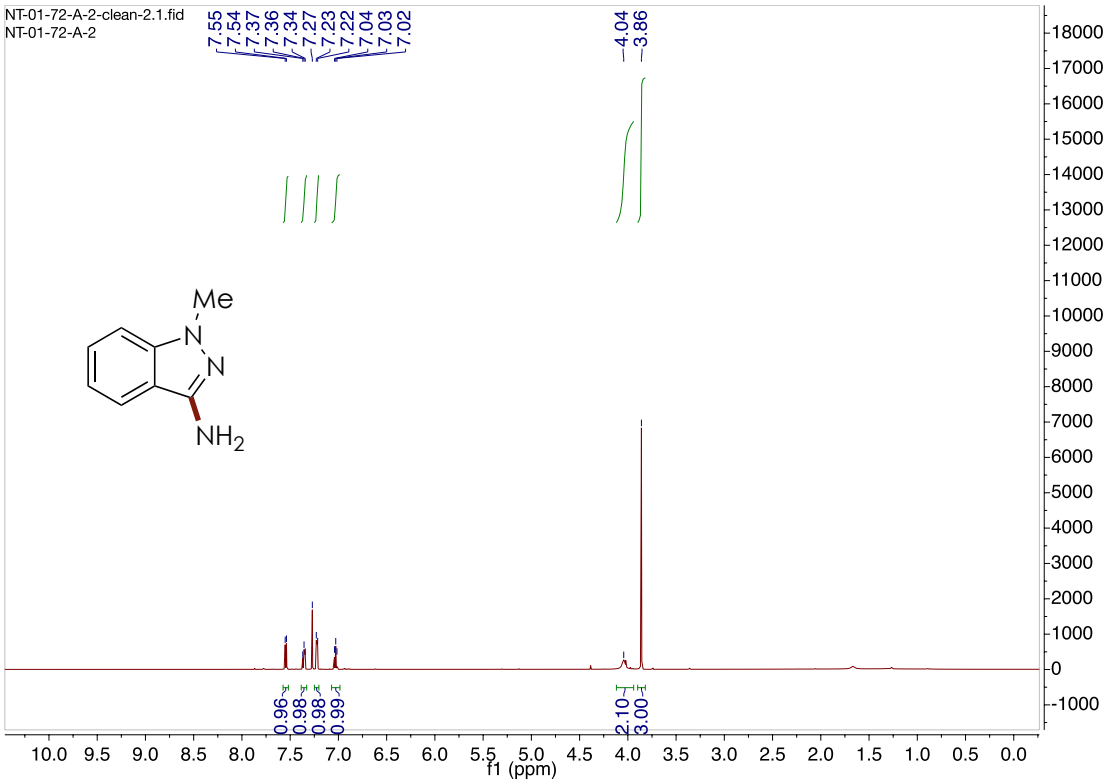
NT-01-72-A-2-clean-2.1.fid
NT-01-72-A-2
7.55
7.54
7.37
7.36
7.34
7.27
7.23
7.22
7.04
7.03
7.02
4.04
3.86
Me
N
N
NH2
0.96
0.98
0.98
0.99
2.10
3.00
f1 (ppm)

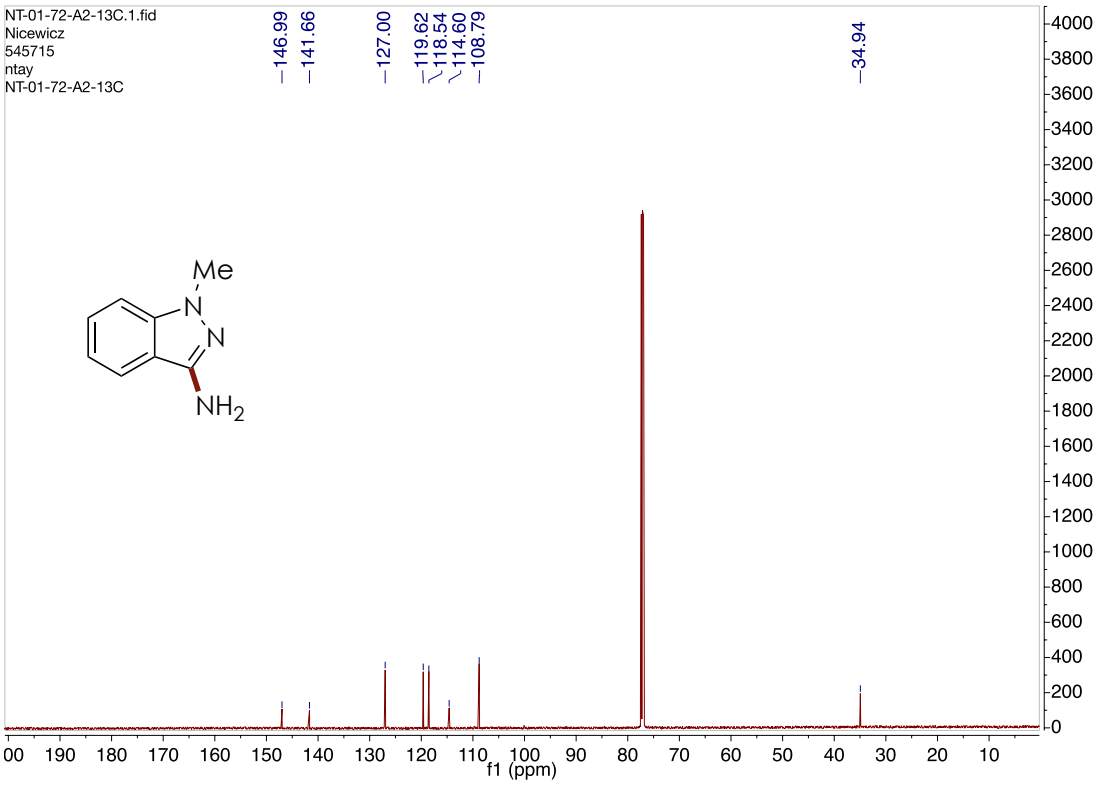
NT-01-72-A2-13C.1.fid
Nicewicz
545715
ntay
NT-01-72-A2-13C
146.99
141.66
127.00
119.62
118.54
114.60
108.79
34.94
Me
N
N
NH2
f1 (ppm)

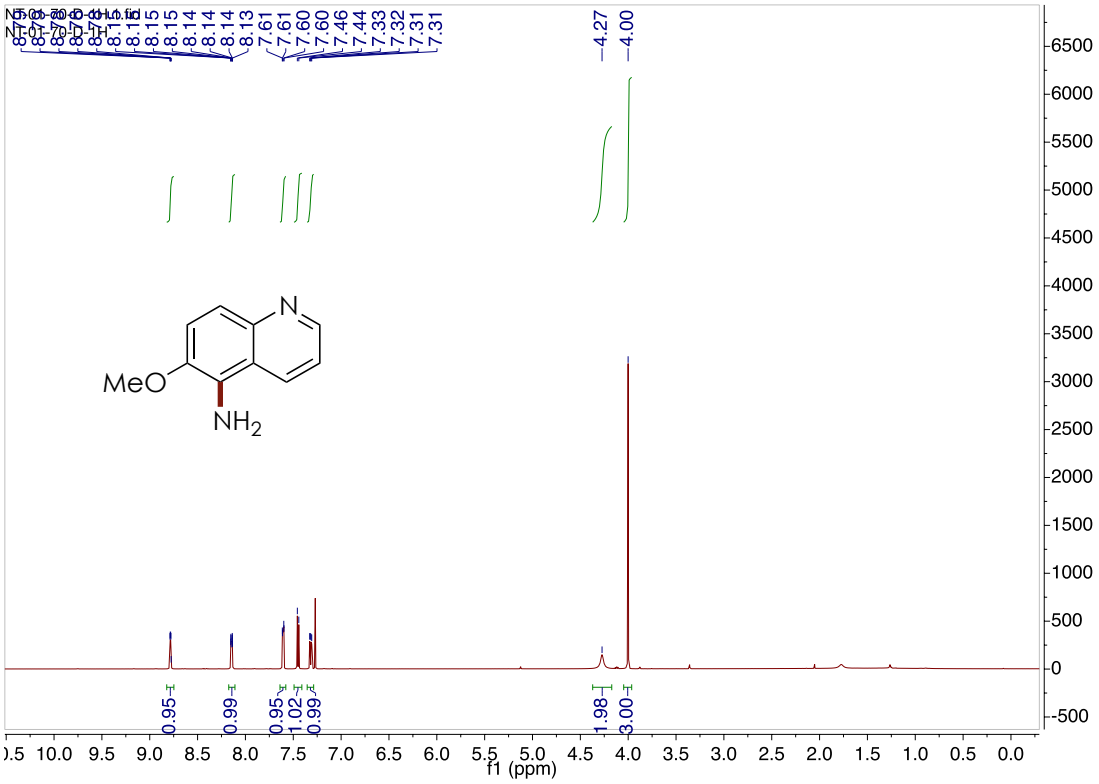
NT-01-70-D-1H
8.15
8.14
8.13
7.61
7.60
7.46
7.44
7.33
7.32
7.31
4.27
4.00
N
MeO
NH2
0.95
0.99
0.95
1.02
0.99
1.98
3.00
f1 (ppm)

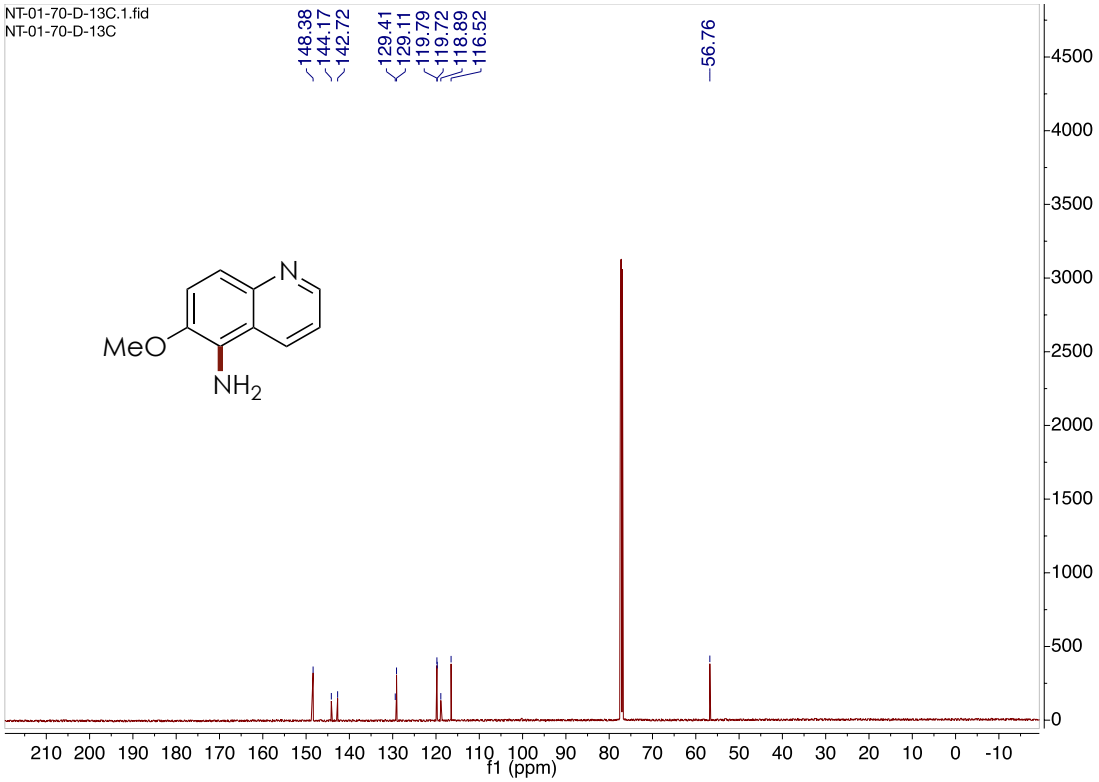
NT-01-70-D-13C.1.fid
NT-01-70-D-13C
148.38
144.17
142.72
129.41
129.11
119.79
119.72
118.89
116.52
56.76
N
MeO
NH2
f1 (ppm)

APPENDIX B: SUPPORTING INFORMATION FOR CHAPTER 3

General Methods:

Proton and carbon magnetic resonance spectra (^{1}H NMR and ^{13}C NMR) were recorded on a Bruker model DRX 400 (^{1}H NMR at 400 MHz and 600 MHz and ^{13}C NMR at 100 and 151 MHz) spectrometer. Chemical shifts for protons are reported in parts per million downfield from tetramethylsilane and are referenced to residual protium in the solvent (^{1}H NMR: $CHCl_3$ at 7.27 ppm). Chemical shifts for carbons are reported in parts per million downfield from tetramethylsilane and are referenced to the carbon resonances of the solvent peak (^{13}C NMR: $CDCl_3$ at 77.16 ppm). ^{1}H NMR data are reported as follows: chemical shift, multiplicity (s = singlet, d = doublet, t = triplet, dd = doublet of doublets, ddt = doublet of doublet of triplets, ddd = doublet of doublet of doublets, dddd = doublet of doublet of doublet of doublets m = multiplet, brs = broad singlet), coupling constants (Hz), and integration. Infrared (IR) spectra were obtained using a Jasco 260 Plus Fourier transform infrared spectrometer. High resolution mass spectra (HRMS) were obtained using a Thermo LTqFT mass spectrometer with electrospray ionization in positive mode. Thin layer chromatography (TLC) was performed on SiliaPlate 250 μm thick silica gel plates provided by Silicycle. Visualization was accomplished with short wave UV light (254 nm), cerium ammonium molybdate or potassium permanganate solution followed by heating. Flash chromatography was performed using SiliaFlash P60 silica gel (40-63 μm) purchased from Silicycle. Unless noted all reactions were run under an atmosphere of oxygen in flame-dried glassware with magnetic stirring. Irradiation of photochemical reactions was carried out using a PAR38 blue aquarium LED lamp (Model #6851) fabricated with high-power Cree LEDs as purchased from Ecoxotic (www.ecoxotic.com)

with standard borosilicate glass vials purchased from Fischer Scientific. For all photolyses, reactions were stirred using a PTFE coated magnetic stir bar on a magnetic stir plate. Gas chromatography (GC) was performed on an Agilent 6850 series instrument equipped with a split- mode capillary injection system and Agilent 5973 network mass spec detector (MSD). Yield refers to isolated yield of analytically pure material unless otherwise noted. NMR yields were determined using hexamethyldisiloxane as an internal standard. All other reagents were obtained from commercial sources and used without further purification unless otherwise noted.

Photoreactor Configuration. Reactions were irradiated using a simple photoreactor consisting of two Par38 Royal Blue Aquarium LED lamps (Model #6851) is shown in which reations (1 dram vials) are irradiated simultaneously. In order to ensure that the reactions are run near room temperature, a simple cooling fan was installed above the reactor to aid in dissipating the heat generated from high power LEDs. While a number of other blue LED sources are effective, we have found that LED emitters with high luminous flux and narrow viewing angles give the best results.

Preparation of Acridinium Photocatalysts

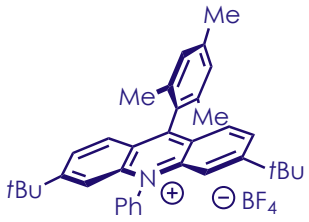

9-Mesityl-3,6-di-*tert*-butyl-10-phenylacridinium tetrafluoroborate (Catalyst A).

The title compound was prepared as previously reported by our lab. The spectral data matched the values reported in the literature.[1]

Preparation of Arene Substrates

Arene substrates were purchased from commercial sources and used without further purification unless otherwise noted.

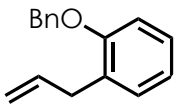

1-allyl-2-(benzyloxy)benzene was prepared according to a published procedure; spectral data were in agreement with literature values.[2]

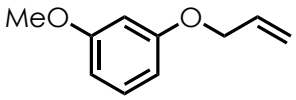

1-(allyloxy)-3-methoxybenzene was prepared according to a published procedure; spectral data were in agreement with literature values.[3]

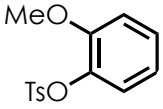

2-methoxyphenyl 4-methylbenzenesulfonate was prepared according to a published procedure; spectral data were in agreement with literature values.[2]

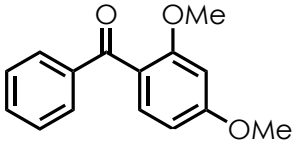

(2,4-dimethoxyphenyl)(phenyl)methanone was prepared according to a published procedure; spectral data were in agreement with literature values.[4]

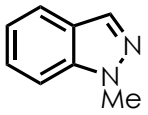

1-methyl-1*H*-indazole was prepared according to a published procedure; spectral data were in agreement with literature values.[1]

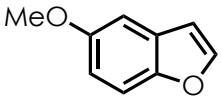

5-methoxybenzofuran was prepared according to a published procedure; spectral data were in agreement with literature values**.**[5]

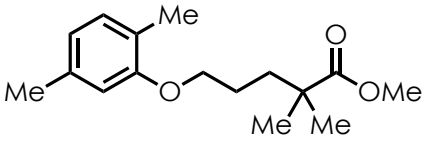

Methyl 5-(2,5-dimethylphenoxy)-2,2-dimethylpentanoate (gemfibrozil methyl ester) was prepared according to a published procedure; spectral data were in agreement with literature values.[2]

Previously Synthesized Aryl Amination Products

Arene products **3.2a**-**3.2m**, **3.4a**, **3.6a**, **3.10a**, **3.18a**, **3.18b**, **3.18h**, **3.18i** and **3.19a**–**19c** were previously reported by our lab.[1]

General Procedure (Method A) for C–H amination (Air Conditions)

To a 1 dram vial containing a Teflon-coated magnetic stir bar was added the arene (0.15 mmol, 1 equiv.), 4.3 mg of acridinium tetrafluoroborate (0.0075 mmol, 0.05 equiv.), 20.4 mg of pyrazole (0.3 mmol, 2 equiv.), and 4.7 mg of (2,2,6,6-tetramethylpiperidin-1-yl)oxyl (0.03 mmol, 0.2 eq.). The solids were dissolved in 1,2-Dichloroethane (1.5 mL). The vial was sealed with a Teflon-lined septum screw cap. The vial was positioned on a stir plate approximately 10 cm from a Par38 LED lamp supplying blue light (λ = 440-460 nm). After irradiation for 20 hours, the reaction mixture was concentrated in vacuo and purified by column chromatography on silica gel with hexanes/ethyl acetate with the eluent noted for each substrate.

General Procedure (Method B) for C–H amination (Aerobic Conditions)

To a 1 dram vial containing a Teflon-coated magnetic stir bar was added the arene (0.15 mmol, 1 equiv.), 4.3 mg of acridinium tetrafluoroborate (0.0075 mmol, 0.05 equiv.), 20.4 mg of pyrazole (0.3 mmol, 2 equiv.), and 4.7 mg of (2,2,6,6-tetramethylpiperidin-1-yl)oxyl (0.03 mmol, 0.2 eq.). The solids were dissolved in 1,2-Dichloroethane (1.5 mL). The vial was sealed with a Teflon-lined septum screw cap. The septum was pierced with a disposable steel needle connected to an oxygen-filled balloon. A vent needle was inserted and the reaction medium was sparged for 5 minutes by bubbling oxygen through the mixture. The vent needle was removed, and the oxygen balloon was maintained, providing approximately 1 atm of oxygen to the vial headspace for the course of the reaction. The vial was positioned on a stir plate approximately 10 cm from a Par38 LED lamp supplying blue light (λ = 440-460 nm). After irradiation for 20 hours, the reaction

mixture was concentrated in vacuo and purified by column chromatography on silica gel with hexanes/ethyl acetate with the eluent noted for each substrate.

General Procedure (Method C) for C–H amination (Anaerobic Conditions)

To a 1 dram vial containing a Teflon-coated magnetic stir bar was added the arene (0.15 mmol, 1 equiv.), 4.3 mg of acridinium tetrafluoroborate (0.0075 mmol, 0.05 equiv.), 20.4 mg of pyrazole (0.3 mmol, 2 equiv.), and 23.4 mg of (2,2,6,6-tetramethylpiperidin-1-yl)oxyl (0.15 mmol, 1.0 equiv.). The solids were dissolve in 1,2-Dichloroethane (1.5 mL). The vial was sealed with a Teflon-lined septum screw cap. The septum was pierced with a disposable steel needle connected to a nitrogen line. A vent needle was inserted and the reaction medium was sparged for 5 minutes by bubbling nitrogen through the mixture. The vent needle was removed, and the nitrogen line was maintained, providing approximately 1 atm of nitrogen to the vial headspace for the course of the reaction. The vial was positioned on a stir plate approximately 10 cm from a Par38 LED lamp supplying blue light (λ = 440-460 nm). After irradiation for 20 hours, the reaction mixture was concentrated in vacuo and purified by column chromatography on silica gel with the eluent noted for each substrate.

General Procedure (Method D) for C–H amination with heating

To a 1 dram vial containing a Teflon-coated magnetic stir bar was added the arene (0.15 mmol, 1 equiv.), 4.3 mg of acridinium tetrafluoroborate (0.0075 mmol, 0.05 equiv.), 20.4 mg of pyrazole (0.3 mmol, 2 equiv.), and 4.7 mg of (2,2,6,6-tetramethylpiperidin-1-yl)oxyl (0.03 mmol, 0.2 eq.). The solids were dissolved in 1,2-Dichloroethane (1.5 mL). The vial was sealed with a Teflon-lined septum screw cap and placed on a hot plate set to

50 ˚C. The vial was positioned on a stir plate approximately 10 cm from a Par38 LED lamp supplying blue light (λ = 440-460 nm). After irradiation for 20 hours, the reaction mixture was concentrated in vacuo and purified by column chromatography on silica gel with hexanes/ethyl acetate with the eluent noted for each substrate.

Characterization for Aryl Amination Products.

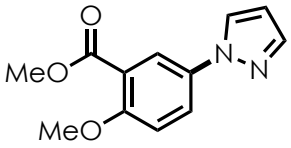

Methyl 2-methoxy-5-(1*H*-pyrazol-1-yl)benzoate (3.1n). The title compound was prepared using Method B with an irradiation time of 20 hours. The title compound was purified by column chromatography on silica gel (10% to 60% EtOAc/Hexanes) to give an orange solid in 64% yield.

3.1n. ^{1}H NMR (600 MHz, Chloroform-*d*) δ 8.10 (d, *J* = 2.9 Hz, 1H), 7.88 (d, *J* = 2.5 Hz, 1H), 7.81 (dd, *J* = 9.0, 2.9 Hz, 1H), 7.70 (d, *J* = 1.8 Hz, 1H), 7.05 (d, *J* = 9.0 Hz, 1H), 6.45 (t, *J* = 2.2 Hz, 1H), 3.93 (s, 3H), 3.91 (s, 3H). **^{13}C NMR** (151 MHz, $CDCl_3$) δ 165.76, 157.60, 140.97, 133.27, 126.77, 124.43, 122.51, 120.34, 112.93, 107.61, 56.40, 52.28.

IR (thin film): 3442.31, 3144.37, 2951.52, 2840.63, 1729.83, 1591.95; **HRMS** (ESI): calculated for $C_{12}H_{13}N_2O_3$ $[M+H]^+$= 233.0921; found 233.0919.

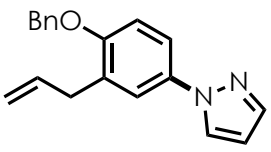

1-(3-allyl-4-(benzyloxy)phenyl)-1*H*-pyrazole (3.1o). The title compound was prepared using Method B with an irradiation time of 20 hours. The title compound was purified by column chromatography on silica gel (3% to 12% EtOAc/Hexanes) to give an orange oil in 71% yield.

3.1o. ^{1}H NMR (600 MHz, Chloroform-*d*) δ 7.86 (d, *J* = 2.4 Hz, 1H), 7.74 (d, *J* = 1.8 Hz, 1H), 7.56 (d, *J* = 2.7 Hz, 1H), 7.51 – 7.47 (m, 3H), 7.44 (t, *J* = 7.6 Hz, 2H), 7.38 (t, *J* = 7.3 Hz, 1H), 6.99 (d, *J* = 8.7 Hz, 1H), 6.47 (t, *J* = 2.1 Hz, 1H), 6.08 (ddt, *J* = 16.8, 10.0, 6.7 Hz, 1H), 5.18 – 5.11 (m, 4H), 3.55 (d, *J* = 6.6 Hz, 2H). **^{13}C NMR** (151 MHz, $CDCl_3$) δ 154.98, 140.61, 137.00, 136.20, 133.99, 130.28, 128.61, 127.96, 127.19, 126.89, 121.55, 118.33, 116.33, 112.20, 107.16, 70.31, 34.53.

IR (thin film): 3659.27, 3142.44, 2912.95, 2867.63, 2518.58, 2303.55, 1713.44; **HRMS** (ESI): Calculated for $C_{19}H_{19}N_2O$ $[M+H]^+$= 291.1492 found 291.1487.

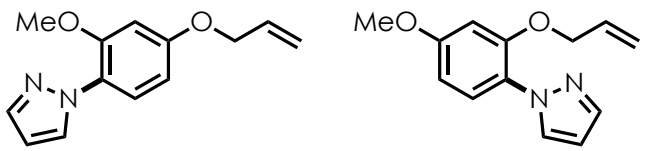

1-(4-(allyloxy)-2-methoxyphenyl)-1*H*-pyrazole (3.1pi) and 1-(2-(allyloxy)-4-methoxyphenyl)-1*H*-pyrazole (3.1pii). The title compound was prepared using Method B with an irradiation time of 20 hours. The title compound was purified by column chromatography on silica gel (3% to 12% EtOAc/Hexanes) to give an inseparable mixture as an orange oil in 95% yield (1.1:1; **3.1pi:3.1pii**).

3.1pi and 3.1pii. ^{1}H NMR (600 MHz, Chloroform-*d*) δ 7.96 (d, *J* = 2.4 Hz, 1H), 7.89 (d, *J* = 2.4 Hz, 1H), 7.70 (d, *J* = 2.1 Hz, 1H), 7.63 – 7.60 (m, 1H), 7.55 (d, *J* = 8.7 Hz, 1H), 6.66 – 6.56 (m, 4H), 6.42 (s, 1H), 6.13 – 6.05 (m, 1H), 6.00 (ddt, *J* = 17.2, 10.3, 5.0 Hz,

1H), 5.49 – 5.44 (m, 1H), 5.39 – 5.32 (m, 2H), 5.28 (dd, *J* = 10.6, 1.8 Hz, 1H), 4.59 (dd, *J* = 5.0, 1.6 Hz, 2H), 4.57 (d, *J* = 5.1 Hz, 2H), 3.85 (s, 6H). **^{13}C NMR** (151 MHz, $CDCl_3$) δ 159.49, 158.71, 152.84, 151.56, 139.78, 139.69, 132.88, 132.48, 131.44, 131.39, 126.35, 126.29, 123.94, 123.66, 118.06, 117.75, 105.86, 105.33, 105.03, 100.93, 100.30, 77.30, 77.09, 76.88, 69.61, 69.13, 55.91, 55.60.

IR (thin film): 3666.02, 3413.39, 3051.80, 2305.48, 2055.75, 1867.72, 1716.34; **HRMS** (ESI): Calculated for $C_{13}H_{15}N_2O_2$ $[M+H]^+$= 231.1128 found 231.1126.

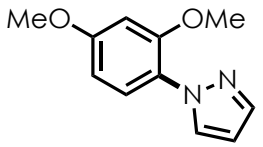

1-(2,4-dimethoxyphenyl)-1*H*-pyrazole (3.1q). The title compound was prepared using Method B with an irradiation time of 20 hours. The title compound was purified by column chromatography on silica gel (10% to 40% EtOAc/Hexanes) to give an orange oil in 77% yield.

3.1q. ^{1}H NMR (600 MHz, Chloroform-*d*) δ 7.89 (d, *J* = 2.4 Hz, 1H), 7.70 (d, *J* = 1.8 Hz, 1H), 7.56 (d, *J* = 8.6 Hz, 1H), 6.62 – 6.56 (m, 2H), 6.43 (t, *J* = 2.1 Hz, 1H), 3.86 (s, 3H), 3.85 (s, 3H). **^{13}C NMR** (151 MHz, $CDCl_3$) δ 159.77, 152.89, 139.78, 131.42, 126.43, 123.57, 105.86, 104.47, 55.92, 55.63.

IR (thin film): 3396.03, 2951.52, 1610.27, 1590.99, 1503.24, 1397.17; **HRMS** (ESI): Calculated for $Na_2C_{11}H_{12}N_2O_2$ $[M+2Na–H]^+$= 249.0611 found 249.0731

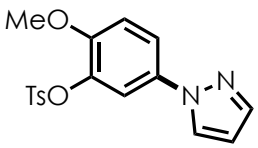

2-methoxy-5-(1*H*-pyrazol-1-yl)phenyl 4-methylbenzenesulfonate (3.1r). The title compound was prepared using Method B with an irradiation time of 20 hours. The title compound was purified by column chromatography on silica gel (25% to 45% EtOAc/Hexanes) to give yellow solid in 87% yield.

3.1r. ^{1}H NMR (600 MHz, Chloroform-*d*) δ 7.81 – 7.75 (m, 3H), 7.68 (d, *J* = 1.8 Hz, 1H), 7.59 – 7.51 (m, 2H), 7.31 (d, *J* = 8.1 Hz, 2H), 6.90 (d, *J* = 8.9 Hz, 1H), 6.44 (t, *J* = 2.1 Hz, 1H), 3.56 (s, 3H), 2.44 (s, 3H). **^{13}C NMR** (151 MHz, $CDCl_3$) δ 150.28, 145.37, 141.03, 138.36, 133.57, 132.84, 129.46, 128.66, 126.79, 118.68, 115.69, 113.07, 107.72, 55.88, 21.71.

IR (thin film): 3136.65, 3053.73, 2850.27, 2305.48, 1927.50, 1595.81; **HRMS** (ESI) Calculated for $C_{17}H_{17}N_2O_4S$ $[M+H]^+$= 345.0904 found 345.0898.

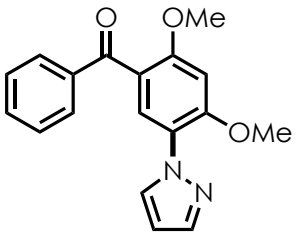

(2,4-dimethoxy-5-(1*H*-pyrazol-1-yl)phenyl)(phenyl)methanone (3.1s). The title compound was prepared using Method B with an irradiation time of 20 hours. The title compound was purified by column chromatography on silica gel (20% to 60% EtOAc/Hexanes) to give a yellow solid in 31% yield.

3.1s. ^{1}H NMR (600 MHz, Chloroform-*d*) δ 7.89 (d, *J* = 2.4 Hz, 1H), 7.82 (dd, *J* = 8.1, 1.4 Hz, 2H), 7.75 (s, 1H), 7.68 (d, *J* = 1.8 Hz, 1H), 7.55 (td, *J* = 7.3, 1.3 Hz, 1H), 7.44 (t, *J* = 7.7 Hz, 2H), 6.65 (s, 1H), 6.42 (t, *J* = 2.1 Hz, 1H), 3.96 (s, 3H), 3.79 (s, 3H). **^{13}C**

NMR (151 MHz, $CDCl_3$) δ 194.62, 158.39, 155.16, 140.10, 138.20, 132.75, 131.45, 129.74, 128.21, 128.04, 122.93, 121.00, 106.20, 96.31, 56.27, 56.13.

IR (thin film): 3054.69, 2976.59, 2847.38, 2304.52, 1961.25, 1788.65, 1723.09, 1645.95, 1265.07. **HRMS** (ESI) Calculated for $C_{18}H_{17}N_2O_3$ $[M+H]^+$= 309.1233; found 309.1230.

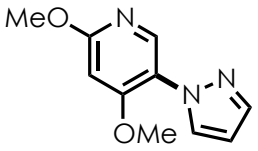

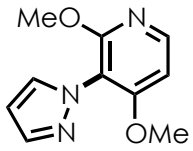

2,4-dimethoxy-5-(1*H*-pyrazol-1-yl)pyridine (3.4b) and 2,4-dimethoxy-3-(1*H*-pyrazol-1-yl)pyridine (3.4c). The title compounds were prepared using Method B with an irradiation time of 20 hours. The title compound was purified by column chromatography on silica gel (20% to 80% EtOAc/Hexanes) to give a yellow oil in a combined 67% yield. The minor regioisomer is contaminated with an inseparable byproduct.

3.4b. ^{1}H NMR (600 MHz, $CDCl_3$) d = 8.27 (d, *J* = 1.4 Hz, 1H), 7.76 (d, *J* = 1.5 Hz, 1H), 7.72 (d, *J* = 1.6 Hz, 1H), 6.44 (d, *J* = 1.9 Hz, 1H), 6.34 (d, *J* = 1.4 Hz, 1H), 4.01–3.96 (m, 3H), 3.93–3.84 (m, 3H).; **^{13}C NMR** (151 MHz, $CDCl_3$) d = 164.92, 160.83, 143.60, 140.64, 131.68, 122.86, 106.58, 93.09, 56.11, 54.03.

IR (thin film): 2943.80, 2854.13, 1614.13, 1540.85, 1397.17, 1209.15, 1046.19; **HRMS** (ESI): Calculated for $C_{10}H_{12}N_3O_2$ $[M+H]^+$= 206.0929; found 206.09255.

3.4c. ^{1}H NMR (600 MHz, $CDCl_3$) d = 8.17–8.08 (m, 1H), 7.78 (dt, *J* = 2.4, 1.5 Hz, 1H), 7.51 (d, *J* = 2.5 Hz, 1H), 6.71–6.59 (m, 1H), 6.48–6.37 (m, 1H), 3.99–3.90 (m, 3H), 3.86–3.81 (m, 3H).; **^{13}C NMR** (151 MHz, $CDCl_3$) d = 162.96, 161.11, 148.16, 140.82, 132.58, 112.65, 106.14, 102.40, 56.59, 54.46.

IR (thin film): 2927.41, 2851.24, 1698.02, 1593.88, 1507.10, 1118.51; **HRMS** (ESI): Calculated for $C_{10}H_{12}N_3O_2$ $[M+H]^+$= 206.0929; found 206.09255.

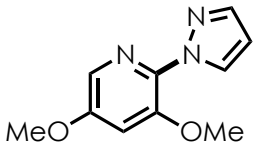

3,5-dimethoxy-2-(1*H*-pyrazol-1-yl)pyridine (3.4d). The title compound was prepared using Method B with an irradiation time of 20 hours. The title compound was purified by column chromatography on silica gel (10% to 40% EtOAc/Hexanes) to give an orange oil in 60% yield.

3.4d. ^{1}H NMR (600 MHz, $CDCl_3$) d = 8.03 (d, *J* = 2.5 Hz, 1H), 7.82 (d, *J* = 2.6 Hz, 1H), 7.76 (d, *J* = 1.9 Hz, 1H), 6.94 (d, *J* = 2.4 Hz, 1H), 6.43 (t, *J* = 2.2 Hz, 1H), 3.92 (s, 3H), 3.89 (s, 3H).; **^{13}C NMR** (151 MHz, $CDCl_3$) d = 156.21, 148.62, 140.94, 135.52, 130.64, 124.92, 108.00, 106.43, 56.37, 56.29.

IR (thin film): 2941.88, 1593.88, 1518.67, 1507.10, 1337.39, 1201.43, 1018.23; **HRMS** (ESI): Calculated for $C_{10}H_{12}N_3O_2$ $[M+H]^+$= 206.0929; found 206.09210.

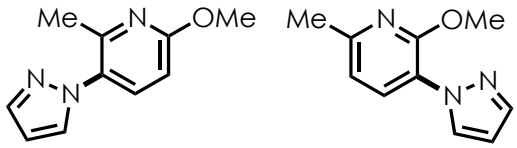

6-methoxy-2-methyl-3-(1*H*-pyrazol-1-yl)pyridine (3.4e) and 2-methoxy-6-methyl-3-(1*H*-pyrazol-1-yl)pyridine (3.4f). The title compounds were prepared using Method A with an irradiation time of 20 hours. The title compound was purified by column chromatography on silica gel (10% to 40% EtOAc/Hexanes) to give a yellow oil in a 56% yield.

3.4e and 3.4f. ^{1}H NMR (600 MHz, $CDCl_3$) d = 8.16 (d, *J* = 2.4 Hz, 1H), 7.96 (d, *J* = 7.8 Hz, 1H), 7.72 (d, *J* = 1.8 Hz, 1H), 7.70 (d, *J* = 1.7 Hz, 1H), 7.55 (d, *J* = 2.3 Hz, 1H), 7.52 (d, *J* = 8.5 Hz, 1H), 6.85 (d, *J* = 7.8 Hz, 1H), 6.65 (d, *J* = 8.5 Hz, 1H), 6.45 (t, *J* = 2.1 Hz,

1H), 6.43 (s, 1H), 4.04 (s, 3H), 3.97 (s, 3H), 2.49 (s, 3H), 2.33 (s, 3H).; **^{13}C NMR** (151 MHz, $CDCl_3$) d = 162.72, 154.06, 153.97, 152.04, 140.57, 140.35, 136.79, 132.22, 131.03, 130.84, 129.97, 122.05, 116.27, 108.11, 106.50, 106.43, 53.75, 53.65, 23.73, 20.64.

IR (thin film): 2948.63, 1592.91, 1540.85, 1483.96, 1307.50, 1036.55, 753.01; **HRMS** (ESI): Calculated for $C_{10}H_{12}N_3O$ $[M+H]^+$= 190.0980; found 190.09731.

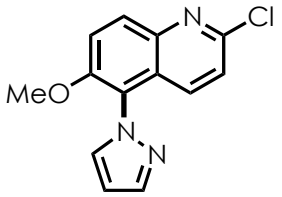

2-chloro-6-methoxy-5-(1*H*-pyrazol-1-yl)quinoline (3.6b). The title compounds were prepared using Method A with an irradiation time of 20 hours. The title compound was purified by column chromatography on silica gel (10% to 40% EtOAc/Hexanes) to give a white solid in 47% yield.

3.6b. ^{1}H NMR (600 MHz, $CDCl_3$) d = 8.14 (dd, *J* = 9.4, 0.8 Hz, 1H), 7.88–7.82 (m, 1H), 7.73–7.68 (m, 2H), 7.60 (s, 1H), 7.33 (s, 1H), 6.56 (s, 1H), 3.93 (s, 3H).; **^{13}C NMR** (151 MHz, $CDCl_3$) d = 152.64, 149.35, 142.84, 141.17, 134.44, 133.28, 131.04, 125.98, 123.85, 122.70, 117.50, 106.61, 57.00.

IR (thin film): 2936.09, 2846.42, 1585.20, 1499.38, 1288.22, 1111.76, 914.09; **HRMS** (ESI): Calculated for $C_{13}H_{11}ClN_3O$ $[M+H]^+$= 260.0591; found 260.05840.

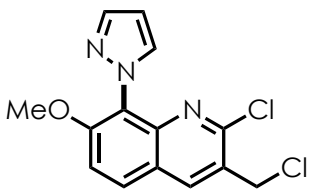

2-chloro-3-(chloromethyl)-7-methoxy-8-(1*H*-pyrazol-1-yl)quinoline (3.6c). The title compounds were prepared using Method A with an irradiation time of 20 hours. The title compound was purified by column chromatography on silica gel (10% to 40% EtOAc/Hexanes) to give a white solid in 52% yield.

3.6c. ^{1}H NMR (600 MHz, $CDCl_3$) d = 8.25 (d, *J* = 2.8 Hz, 1H), 7.93 (d, *J* = 9.1 Hz, 1H), 7.87 (t, *J* = 2.4 Hz, 1H), 7.70 (t, *J* = 2.8 Hz, 1H), 7.48 (d, *J* = 9.1 Hz, 1H), 6.64–6.54 (m, 1H), 4.79 (s, 2H), 3.96 (d, *J* = 2.8 Hz, 3H).; **^{13}C NMR** (151 MHz, $CDCl_3$) d = 156.94, 151.91, 144.72, 140.74, 138.54, 133.42, 129.66, 127.74, 123.50, 122.12, 114.92, 105.99, 57.09, 43.26.

IR (thin film): 2943.80, 1617.02, 1558.20, 1519.63, 1496.49, 1265.07, 1044.26; **HRMS** (ESI): Calculated for $C_{14}H_{12}Cl_2N_3O$ $[M+H]^+$= 308.0357; found 308.03494.

Based on ^{1}H COSY, the peaks at 7.87, 7.70 and 6.64 ppm are correlated and are the protons on the pyrazole ring. The remaining peaks at 8.25, 7.93 and 7.48 ppm are a singlet, and two doublets, respectively, showing that functionalization occurred at the 4- or the 8-position. Based on HSQC, the protons for the benzylic position are at 4.79 ppm and correlate to the carbon at 43 ppm. Based on HMBC, the singlet in the proton at 8.25 ppm correlates to the carbon at 43 ppm demonstrating that the 4-position is unsubstituted. Therefore, functionalization occurred at the 8-position.

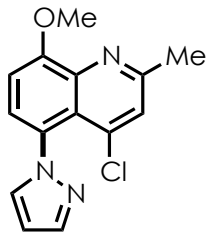

4-chloro-8-methoxy-2-methyl-5-(1*H*-pyrazol-1-yl)quinoline (3.6d). The title compounds were prepared using Method A with an irradiation time of 20 hours. The title compound was purified to give a solid in 19% yield.

3.6d. ^{1}H NMR (400 MHz, DMSO-d6) δ = 7.92 (dd, J = 2.3, 0.6 Hz, 1H), 7.67 (dd, J = 1.9, 0.6 Hz, 1H), 7.66 (s, 1H), 7.53 (d, J = 8.4 Hz, 1H), 7.30 (d, J = 8.4 Hz, 1H), 6.50 – 6.46 (m, 1H), 4.03 (s, 3H), 2.64 (s, 3H).; **^{13}C NMR** (101 MHz, $CDCl_3$) δ = 158.26, 156.30, 141.05, 139.97, 138.85, 134.10, 128.86, 127.89, 126.20, 121.64, 108.32, 106.80, 56.60, 24.66. **HRMS** (ESI): Calculated for $C_{14}H_{13}ClN_3O$ $[M+Na]^+$= 274.014; found 274.20.

Based on ^{1}H NMR, the presence of doublets at 7.53 and 7.30 ppm indicates functionalization occurred at either the 5- or 7-position on the quinoline. Based on NOESY correlations between the peaks at 7.30 and 4.03 ppm, the 7-position is unsubstituted. Therefore, functionalization occurred at the 5-position.

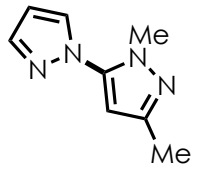

2',5'-dimethyl-2'*H*-1,3'-bipyrazole (3.8b). The title compounds were prepared using Method B with an irradiation time of 20 hours. The title compound was purified by column chromatography on silica gel (10% to 50% EtOAc/Hexanes) to give a tan solid in 34% yield by ^{1}H NMR. The product was contaminated with an inseparable impurity.

3.8b. ^{1}H NMR (600 MHz, $CDCl_3$) d = 7.77 (s, 1H), 7.62 (s, 1H), 6.46 (d, *J* = 2.2 Hz, 1H), 6.08 (s, 1H), 3.79 (s, 3H), 2.29 (s, 3H).; **^{13}C NMR** (151 MHz, $CDCl_3$) d = 142.00, 139.16, 131.45, 107.32, 105.26, 99.90, 36.55, 14.00.

IR (thin film): 2974.66, 1558.20, 1507.10, 1389.46, 1031.73, 931.45, 758.85; **HRMS** (ESI): Calculated for $C_{10}H_{11}N_3O$ $[M+Na]^+$= 185.0803; found 185.07965.

Based on ^{1}H COSY, the peaks at 7.77, 7.62 and 6.46 ppm are correlated and are the pyrazole nucleophile peaks. The peak at 6.08 ppm is the unsubstituted position on the *N*-methyl pyrazole and correlates to the peak at 99.90 ppm based on HSQC. Based on HMBC, the unsubstituted carbon correlates with the 3-methyl group on the pyrazole ring, meaning that the 4-position is unsubstituted. Therefore, functionalization occurred at the 5-position.

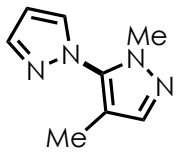

2',4'-dimethyl-2'*H*-1,3'-bipyrazole (3.8c). The title compounds were prepared using Method A with an irradiation time of 20 hours. The title compound was purified by column chromatography on silica gel (10% to 50% EtOAc/Hexanes) to give a tan solid in 30% yield by ^{1}H NMR. The product was contaminated with an inseparable impurity.

3.8c. ^{1}H NMR (600 MHz, $CDCl_3$) d 7.81 (s, 1H), 7.58 (s, 1H), 7.37 (s, 1H), 6.51 (d, *J* = 2.2 Hz, 1H), 3.69 (s, 3H), 1.96 (s, 3H).; **^{13}C NMR** (151 MHz, $CDCl_3$) d = 142.16, 138.72, 136.41, 131.98, 111.23, 107.32, 36.36, 7.97.

IR (thin film): 3196.43, 2973.70, 1539.88, 1396.21, 1030.77, 932.41, 759.82; **HRMS** (ESI): Calculated for $C_8H_{11}N_4$ $[M+H]^+$= 163.0984; found 163.09767.

Based on ^{1}H COSY, the peaks at 7.81, 7.58 and 6.51 ppm are correlated and are the pyrazole nucleophile peaks. Based on HSQC, the peak at 7.37 ppm is the unsubstituted position on the *N*-methyl pyrazole and correlates to the carbon peak at 138.72 ppm. Based on HMBC, the unsubstituted carbon correlates with the 3-methyl group on the

pyrazole ring; however, is not correlated to the *N*-methyl group, meaning that the 3-position is unsubstituted. Therefore, functionalization occurred at the 5-position.

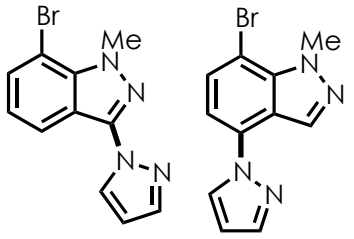

7-bromo-1-methyl-3-(1*H*-pyrazol-1-yl)-1*H*-indazole (3.10b) and 7-bromo-1-methyl-4-(1*H*-pyrazol-1-yl)-1*H*-indazole (3.10c). The title compounds were prepared using Method A with an irradiation time of 20 hours. The title compound was purified by column chromatography to afford the final product in a combined 55% yield by ^{1}H NMR and 2.5:1 mixture of regioisomers, respectively.

3.10b. ^{1}H NMR (400 MHz, DMSO-d_6) d = 8.42 (d, *J* = 2.5 Hz, 1H), 8.27 (dd, *J* = 8.2, 0.8 Hz, 1H), 7.90 (d, J = 1.7 Hz, 1H), 7.75 (dd, J = 7.4, 0.8 Hz, 1H), 7.19–7.11 (m, 1H), 6.74–6.49 (m, 1H), 4.36 (s, 3H).; **^{13}C NMR** (101 MHz, DMSO-d_6) d = 141.64, 139.75, 137.94, 132.05, 128.26, 122.63, 121.64, 116.67, 107.49, 102.39.

3.10c. ^{1}H NMR (400 MHz, DMSO-d_6) d = 8.61 (dd, J = 2.6, 0.5 Hz, 1H), 8.58 (s, 1H), 7.89 (d, J = 1.4 Hz, 1H), 7.72 (d, J = 8.1 Hz, 1H), 7.43 (d, J = 8.1 Hz, 1H), 6.63 (dd, J = 2.5, 1.8 Hz, 1H), 4.39 (s, 3H).; **^{13}C NMR** (151 MHz, $CDCl_3$) d = 141.69, 137.80, 132.65, 132.28, 130.92, 129.25, 117.83, 111.01, 108.06, 99.42.

IR (thin film): 2952.48, 2925.48, 1576.52, 1446.35, 1396.21, 1103.08, 734.74; **HRMS** (ESI): Calculated for $C_{11}H_{10}BrN_4$ $[M+H]^+$= 277.0090; found 277.4.

For **3.10b**, based on ^{1}H NMR and HMBC the peaks at 8.27, 7.75 and 7.15 ppm are all correlated meaning they are unsubstituted. Therefore, functionalization occurred at the 3-position.

For **3.10c**, based on ^{1}H NMR the peaks at 7.72 and 7.43 ppm are doublets, showing that functionalization occurred at the 4- or the 6-position. Based on HMBC, 8.61, 7.89 and 6.63 ppm are correlated and are the pyrazole peaks. Based on NOESY, the peak at 8.61 and 7.43 are correlated, showing that the 5-position at 7.43 ppm is not functionalized. Since a correlation is observed between the pyrazole protons and a proton on the indazole core, the 4-position is functionalized.

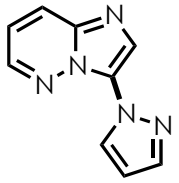

3-(1*H*-pyrazol-1-yl)imidazo[1,2-*b*]pyridazine (3.12a). The title compounds were prepared using Method D with an irradiation time of 20 hours. The title compound was purified by column chromatography on silica gel (20% to 60% EtOAc/Hexanes) to give a light brown solid in 70% yield.

3.12a. ^{1}H NMR (400 MHz, DMSO-d_6) d = 8.62 (dd, *J* = 4.4, 1.5 Hz, 1H), 8.35 (dd, *J* = 2.5, 0.5 Hz, 1H), 8.27 (dd, *J* = 9.3, 1.5 Hz, 1H), 8.06 (s, 1H), 7.87 (d, *J* = 1.4 Hz, 1H), 7.37 (dd, *J* = 9.3, 4.4 Hz, 1H), 6.63 (dd, *J* = 2.4, 1.9 Hz, 1H).; **^{13}C NMR** (101 MHz, DMSO-d_6) d = 144.63, 141.69, 136.91, 132.79, 127.63, 126.46, 126.11, 118.27, 107.29. **IR** (thin film): 3113.51, 2928.38, 1584.24, 1523.49, 1290.14, 1093.44, 758.852; **HRMS** (ESI): Calculated for $C_9H_8N_5$ $[M+H]^+$= 186.0779; found 186.07729.

Functionalization occurred at the 3-position based on carbon chemical shifts matching with predicted values.

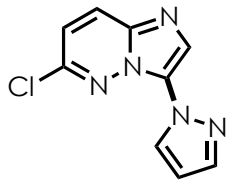

6-chloro-3-(1*H*-pyrazol-1-yl)imidazo[1,2-*b*]pyridazine (3.12b). The title compounds were prepared using Method D with an irradiation time of 20 hours. The title compound was purified by column chromatography on silica gel (20% to 60% EtOAc/Hexanes) to give a yellow solid in 50% yield.

3.12b. ^{1}H NMR (600 MHz, $CDCl_3$) d = 8.31–8.28 (m, 1H), 8.05 (d, *J* = 1.4 Hz, 1H), 7.97 (dd, *J* = 9.5, 1.5 Hz, 1H), 7.84 (d, *J* = 1.6 Hz, 1H), 7.13 (dd, *J* = 9.5, 1.5 Hz, 1H), 6.60–6.55 (m, 1H).; **^{13}C NMR** (151 MHz, $CDCl_3$) d = 148.03, 142.22, 135.68, 130.93, 127.91, 127.55, 127.42, 119.04, 107.75.

IR (thin film): 3100.01, 1698.02, 1575.56, 1519.63, 1304.61, 1113.69; **HRMS** (ESI): Calculated for $C_9H_7ClN_5$ $[M+H]^+$= 220.0390; found 220.03833.

Functionalization occurred at the 3-position based on carbon chemical shifts matching with predicted values.

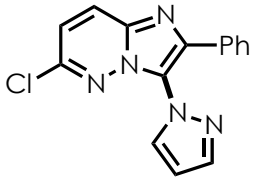

6-chloro-2-phenyl-3-(1*H*-pyrazol-1-yl)imidazo[1,2-*b*]pyridazine (3.12c). The title compounds were prepared using Method B with an irradiation time of 20 hours. The title compound was purified by column chromatography on silica gel (10% to 40% EtOAc/Hexanes) to give a yellow-orange solid in 74% yield.

3.12c. **^{1}H NMR** (400 MHz, DMSO-d_6) d = 8.39 (d, *J* = 9.5 Hz, 1H), 8.18 (dd, *J* = 2.5, 0.5 Hz, 1H), 8.01 (dd, *J* = 1.8, 0.5 Hz, 1H), 7.57 (d, *J* = 9.5 Hz, 1H), 7.48 (dd, *J* = 7.9, 1.9 Hz, 2H), 7.41–7.34 (m, 3H), 6.72 (dd, *J* = 2.4, 1.9 Hz, 1H).; **^{13}C NMR** (101 MHz, $CDCl_3$) d = 147.30, 142.98, 139.64, 135.54, 134.62, 131.34, 129.10, 128.89, 128.12, 126.35, 121.52, 121.24, 108.40.

IR (thin film): 3102.90, 3062.40, 2923.56, 1585.20, 1520.60, 1309.43, 1127.19; **HRMS** (ESI): Calculated for $C_{15}H_{11}ClN_5$ $[M+H]^+$= 296.0703; found 296.06949.

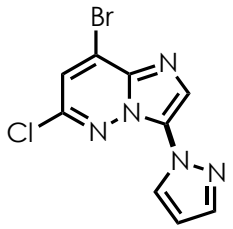

8-bromo-6-chloro-3-(1*H*-pyrazol-1-yl)imidazo[1,2-*b*]pyridazine (3.12d). The title compounds were prepared using Method D with an irradiation time of 20 hours. The title compound was purified by column chromatography on silica gel (20% to 60% EtOAc/Hexanes) to give a yellow solid in 18% yield.

3.12d. **^{1}H NMR** (600 MHz, $CDCl_3$) d = 8.31 (d, *J* = 2.6 Hz, 1H), 8.11 (s, 1H), 7.85 (d, *J* = 1.8 Hz, 1H), 7.45 (s, 1H), 6.59 (t, *J* = 1.3 Hz, 1H).; **^{13}C NMR** (151 MHz, $CDCl_3$) d = 146.99, 142.47, 134.78, 130.86, 128.67, 127.66, 125.10, 121.13, 108.01.

IR (thin film): 2951.52, 1670.05, 1567.84, 1507.10, 1445.70, 1251.58; **HRMS** (ESI): Calculated for $C_9H_5BrClN_5$ $[M+H]^+$= 297.9495; found 297.94890.

Functionalization occurred at the 3-position based on carbon chemical shifts matching with predicted values.

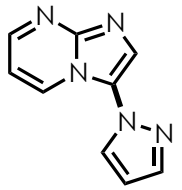

3-(1*H*-pyrazol-1-yl)imidazo[1,2-*a*]pyrimidine (3.12e). The title compounds were prepared using Method D with an irradiation time of 20 hours. The title compound was purified by column chromatography on silica gel to give a pale yellow solid in 37% yield by ^{1}H NMR.

3.12e. ^{1}H NMR (600 MHz, DMSO-d_6) d = 8.77 (dd, *J* = 6.9, 2.0 Hz, 1H), 8.65 (dd, *J* = 4.1, 2.0 Hz, 1H), 8.28 (dd, *J* = 2.5, 0.5 Hz, 1H), 8.00 (s, 1H), 7.97 – 7.89 (m, 1H), 7.16 (dd, *J* = 6.9, 4.1 Hz, 1H), 6.64 (dd, *J* = 2.4, 1.9 Hz, 1H).; **^{13}C NMR** (101 MHz, DMSO-d_6) d = 151.11, 145.47, 142.38, 133.04, 132.56, 126.99, 121.49, 109.79, 107.55.

IR (thin film): 3100.97, 1716.34, 1652.70, 1568.81, 1540.85, 1520.60, 1021.12; **HRMS** (ESI): Calculated for $C_9H_8N_5$ $[M+H]^+$= 186.0779; found 186.07726.

Based on HMBC, the peak at 8.00 ppm is on the 5-membered ring and correlates to carbon peaks at 145.47 and 126.99. If functionalization had occurred at the 2-position the peak at 8.00 ppm would have correlated to the peak at 132.56 ppm. Since this is not observed, functionalization occurred at the 3-position.

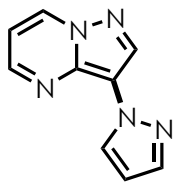

3-(1*H*-pyrazol-1-yl)pyrazolo[1,5-*a*]pyrimidine (3.12f). The title compounds were prepared using Method D with an irradiation time of 20 hours. The title compound was

purified by column chromatography on silica gel (25% to 100% EtOAc/Hexanes) to give a yellow solid in 42% yield.

3.12f. ^{1}**H NMR** (600 MHz, $CDCl_3$) d = 8.67 (dd, *J* = 7.1, 1.7 Hz, 1H), 8.56 (s, 1H), 8.55 (dd, *J* = 4.0, 1.7 Hz, 1H), 8.41 (dd, *J* = 2.4, 0.6 Hz, 1H), 7.75 (d, *J* = 1.8 Hz, 1H), 6.89 (dd, *J* = 7.1, 3.9 Hz, 1H), 6.50 (t, *J* = 2.1 Hz, 1H).; ^{13}**C NMR** (151 MHz, $CDCl_3$) d = 149.55, 140.57, 138.85, 137.27, 135.45, 129.36, 114.78, 108.54, 106.97.

IR (thin film): 3066.26, 1698.02, 1652.70, 1540.85, 1488.78, 775.24; **HRMS** (ESI): Calculated for $C_9H_8N_5$ $[M+H]^+$= 186.0779; found 186.07728.

Functionalization occurred at the 3-position based on carbon chemical shifts matching with predicted values.

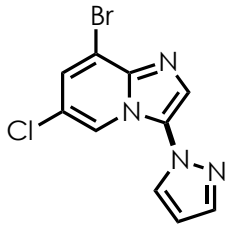

8-bromo-6-chloro-3-(1*H*-pyrazol-1-yl)imidazo[1,2-*a*]pyridine (3.12h). The title compounds were prepared using Method D with an irradiation time of 20 hours. The title compound was purified by column chromatography on silica gel (20% to 50% EtOAc/Hexanes) to give a white solid in 37% yield.

3.12h. ^{1}**H NMR** (600 MHz, $CDCl_3$) d = 8.36 (t, *J* = 1.7 Hz, 1H), 7.94–7.87 (m, 1H), 7.78–7.71 (m, 2H), 7.58–7.50 (m, 1H), 6.60–6.51 (m, 1H).; ^{13}**C NMR** (151 MHz, $CDCl_3$) d = 143.16, 140.25, 132.29, 128.99, 127.48, 124.95, 121.33, 121.17, 112.51, 107.99.

IR (thin film): 3106.97, 1698.02, 1670.05, 1558.20, 1507.10, 1395.25; **HRMS** (ESI): Calculated for $C_{10}H_7BrClN_4$ $[M+H]^+$= 296.9543; found 296.95352.

Based on ^{1}H NMR, no doublet is observed meaning functionalization occurred at either the 2- or 3-position. Functionalization occurred at the 3-position based on carbon chemical shifts matching with predicted values.

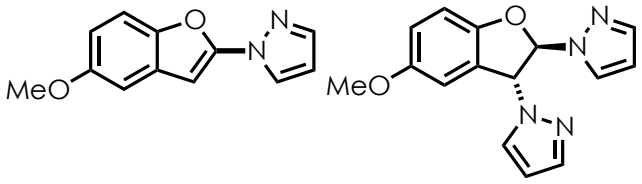

1-(5-methoxybenzofuran-2-yl)-1*H*-pyrazole (3.14b) and 1,1'-((2*R*,3*R*)-5-methoxy-2,3-dihydrobenzofuran-2,3-diyl)bis(1*H*-pyrazole) (3.14c). The title compounds were prepared using Method B with an irradiation time of 20 hours. The title compound was purified by column chromatography on silica gel (10% to 40% EtOAc/Hexanes) to give yellow solids in a combined 29% yield.

3.14b. ^{1}H NMR (400 MHz, DMSO-d_6) d = 8.40 (dd, *J* = 2.6, 0.5 Hz, 1H), 7.90–7.85 (m, 1H), 7.53 (d, *J* = 9.0 Hz, 1H), 7.18 (d, *J* = 2.6 Hz, 1H), 6.90 (dd, *J* = 8.9, 2.7 Hz, 1H), 6.86 (d, *J* = 0.8 Hz, 1H), 6.62 (dd, *J* = 2.6, 1.8 Hz, 1H), 3.80 (s, 3H).; **^{13}C NMR** (101 MHz, DMSO-d_6) d = 156.26, 149.52, 145.78, 142.66, 129.03, 128.88, 112.30, 111.62, 108.29, 103.89, 90.80, 55.58.

IR (thin film): 2924.52, 2850.27, 1634.38, 1507.10, 1418.39, 1197.58, 1030.77; **HRMS** (ESI): Calculated for $C_{12}H_{11}N_2O_2$ $[M+H]^+$= 215.0820; found 215.08136.

Based on NOESY, the peak at 6.86 and 7.18 ppm are correlated and the peak at 3.80 is correlated to both 7.18 and 6.90 ppm. The peak at 7.18 is at the 4-position, and based on correlations the 3-position is unsubstituted. Therefore, functionalization occurred at the 2-position.

3.14c. **^{1}H NMR** (600 MHz, $CDCl_3$) d = 7.64 (d, *J* = 1.9 Hz, 1H), 7.64–7.60 (m, 2H), 7.37 (d, *J* = 2.5 Hz, 1H), 6.91 (t, *J* = 1.9 Hz, 2H), 6.85 (dd, *J* = 2.3, 1.1 Hz, 1H), 6.64 (d, *J* = 3.0 Hz, 1H), 6.51 (d, *J* = 3.0 Hz, 1H), 6.366.34 (m, 1H), 6.30 (t, *J* = 2.2 Hz, 1H), 3.75 (s, 3H).; **^{13}C NMR** (151 MHz, $CDCl_3$) d = 155.49, 153.30, 141.87, 141.27, 129.93, 128.69, 123.51, 117.69, 111.38, 110.33, 107.08, 106.51, 95.74, 68.42, 56.04.

IR (thin film): 2919.70, 1698.02, 1670.05, 1520.60, 1418.39, 1027.87; **HRMS** (ESI): Calculated for $C_{15}H_{15}N_4O_2$ $[M+H]^+$= 283.1195; found 283.11891.

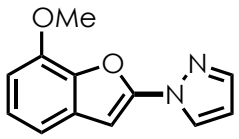

1-(7-methoxybenzofuran-2-yl)-1*H*-pyrazole (3.14d). The title compounds were prepared using Method B with an irradiation time of 20 hours. The title compound was purified by column chromatography on silica gel (10% to 40% EtOAc/Hexanes) to give a yellow oil in 34% yield.

3.14d. **^{1}H NMR** (400 MHz, DMSO-d_6) d = 8.44 (dd, *J* = 2.6, 0.5 Hz, 1H), 7.96–7.88 (m, 1H), 7.27 (d, *J* = 3.3 Hz, 1H), 7.26 (s, 1H), 7.02 (dd, *J* = 6.2, 2.9 Hz, 1H), 6.95 (s, 1H), 6.66 (dd, *J* = 2.6, 1.8 Hz, 1H), 4.01 (s, 3H). **^{13}C NMR** (101 MHz, DMSO-d_6) d = 148.91, 144.69, 142.67, 139.93, 129.64, 129.25, 124.70, 113.17, 108.32, 107.10, 91.13, 55.84.

IR (thin film): 3124.12, 2933.2, 1635.34, 1558.20, 1507.10, 1286.29, 743.42; **HRMS** (ESI): Calculated for $C_{12}H_{11}N_2O_2$ $[M+H]^+$= 215.0820; found 215.08137.

Based on ^{1}H NMR, the peaks at 7.27, 7.26 and 7.02 ppm are correlated and the 6–membered ring of the benzofuran. Based on NOESY, the peak at 7.26 correlates to the 6.95 meaning that the 3-position is unsubstituted. Therefore, functionalization occurs at the 2-position.

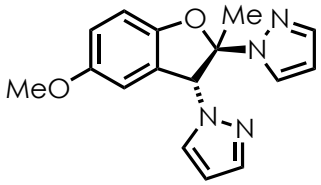

1,1'-((3*R*)-5-methoxy-2-methyl-2,3-dihydrobenzofuran-2,3-diyl)bis(1*H*-pyrazole) (3.14e). The title compounds were prepared using Method A with an irradiation time of 20 hours. The title compound was purified by column chromatography on silica gel (10% to 40% EtOAc/Hexanes) to give a pale yellow solid in 36% yield.

3.14e. ^{1}H NMR (600 MHz, $CDCl_3$) d = 7.71 (dd, *J* = 2.5, 0.7 Hz, 1H), 7.64–7.62 (m, 1H), 7.60 (dd, *J* = 1.7, 0.7 Hz, 1H), 7.31 (d, *J* = 2.4 Hz, 1H), 6.97 (d, *J* = 8.9 Hz, 1H), 6.92 (dd, *J* = 8.9, 2.7 Hz, 1H), 6.82 (d, *J* = 2.6 Hz, 1H), 6.68 (s, 1H), 6.32 (t, *J* = 2.1 Hz, 1H), 6.24 (dd, *J* = 2.5, 1.7 Hz, 1H), 3.72 (s, 3H), 1.45 (s, 3H).; **^{13}C NMR** (151 MHz, $CDCl_3$) d = 155.74, 152.87, 140.78, 140.46, 129.67, 126.83, 124.11, 117.73, 111.32, 111.21, 106.49, 106.03, 102.83, 70.39, 55.98, 21.31.

IR (thin film): 2996.84, 2939.95, 1489.74, 1399.28, 1219.76, 1029.80, 752.10; **HRMS** (ESI): Calculated for $C_{16}H_{17}N_4O_2$ $[M+H]^+$= 297.1351; found 297.13447.

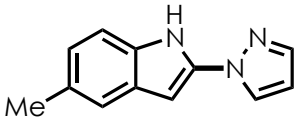

5-methyl-2-(1*H*-pyrazol-1-yl)-1*H*-indole (3.14g). The title compounds were prepared using Method A with an irradiation time of 20 hours. The title compound was purified to give the final product in 10% yield.

3.14g. ^{1}H NMR (400 MHz, DMSO-d_6) d = 11.71 (s, 1H), 8.44 (d, *J* = 2.4 Hz, 1H), 7.81 (d, *J* = 1.4 Hz, 1H), 7.40–7.31 (m, 1H), 7.30 (d, *J* = 8.3 Hz, 1H), 7.03–6.84 (m, 1H), 6.63–6.57 (m, 1H), 6.52 (s, 1H), 2.40 (s, 3H); **^{13}C NMR** (151 MHz, $CDCl_3$) d = 141.21,

136.51, 132.69, 128.91, 128.67, 128.13, 122.99, 119.85, 111.69, 108.16, 87.43, 21.70.

MS (ESI): Calculated for $C_{12}H_{12}N_3$ $[M+H]^+$= 197.10; found 198.20.

Based on NOESY, the peaks at 7.30 and 6.52 are correlated meaning that the 3-position is unsubstituted. Therefore, functionalization occurred at the 2-position.

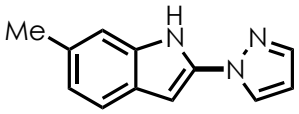

6-methyl-2-(1*H*-pyrazol-1-yl)-1*H*-indole (3.14h). The title compounds were prepared using Method A with an irradiation time of 20 hours. The title compound was purified to give the final product in 12% yield.

3.14h. ^{1}H NMR (400 MHz, DMSO-d_6) d = 11.74 (s, 1H), 8.43 (d, *J* = 2.4 Hz, 1H), 7.82 (d, *J* = 1.5 Hz, 1H), 7.42 (d, *J* = 8.0 Hz, 1H), 7.22 (s, 1H), 6.90 (d, *J* = 8.0 Hz, 1H), 6.65–6.58 (m, 1H), 6.55 (s, 1H), 2.43 (s, 3H); **^{13}C NMR** (151 MHz, $CDCl_3$) d 141.15, 135.79, 134.66, 130.64, 128.95, 125.59, 121.96, 119.96, 111.77, 108.16, 87.77, 21.90. **MS** (ESI): Calculated for $C_{12}H_{12}N_3$ $[M+H]^+$= 197.10; found 198.20.

Based on NOESY, the peaks at 7.42 and 6.55 ppm are correlated meaning that the 3-position is unsubstituted. Therefore, functionalization occurred at the 2-position.

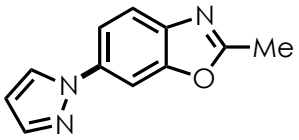

2-methyl-6-(1*H*-pyrazol-1-yl)benzo[*d*]oxazole (3.16a). The title compounds were prepared using Method D with an irradiation time of 20 hours. The title compound was purified by column chromatography on silica gel (20% to 50% EtOAc/Hexanes) to give a yellow solid in 30% yield.

3.16a. ^{1}H NMR (600 MHz, $CDCl_3$) d = 7.95 (d, *J* = 2.8 Hz, 1H), 7.88 (d, *J* = 2.6 Hz, 1H), 7.75 (d, *J* = 2.8 Hz, 1H), 7.68 (s, 1H), 7.65–7.52 (m, 1H), 6.61–6.46 (m, 1H), 2.75–2.50 (m, 3H).; **^{13}C NMR** (151 MHz, $CDCl_3$) d = 165.02, 151.48, 141.41, 140.11, 137.64, 127.38, 119.80, 115.98, 108.02, 102.44, 14.80.

IR (thin film): 2920.66, 2851.24, 1698.02, 1652.70, 1520.60, 1435.74; **HRMS** (ESI): Calculated for $C_{11}H_{10}N_3O$ $[M+H]^+$= 200.0824; found 200.08176.

Functionalization occurred at the 6-position based on carbon chemical shifts matching with predicted values.

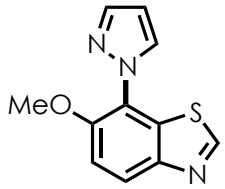

6-methoxy-7-(1*H*-pyrazol-1-yl)benzo[*d*]thiazole (3.16b). The title compounds were prepared using Method X with an irradiation time of 20 hours. The title compound was purified by column chromatography on silica gel (20% to 50% EtOAc/Hexanes) to give a yellow solid in 27% yield.

3.16b. ^{1}H NMR (600 MHz, $CDCl_3$) d = 8.90 (s, 1H), 8.28 (dd, *J* = 2.5, 0.6 Hz, 1H), 8.03 (d, *J* = 8.9 Hz, 1H), 7.84 – 7.78 (m, 1H), 7.32 (d, *J* = 8.9 Hz, 1H), 6.50 (dd, *J* = 2.5, 1.8 Hz, 1H), 4.00 (s, 3H).; **^{13}C NMR** (151 MHz, $CDCl_3$) d = 155.62, 149.16, 148.36, 139.89, 132.25, 129.96, 123.84, 122.06, 112.68, 106.78, 57.20.

IR (thin film): 2929.34, 2842.56, 1683.55, 1520.60, 1473.35, 1270.86, 1041.37; **HRMS** (ESI): Calculated for $C_{11}H_{10}N_3OS$ $[M+H]^+$= 232.0544; found 232.05373.

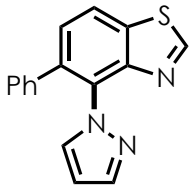

5-phenyl-4-(1*H*-pyrazol-1-yl)benzo[*d*]thiazole (3.16c). The title compounds were prepared using Method D with an irradiation time of 20 hours. The title compound was purified by column chromatography on silica gel (20% to 50% EtOAc/Hexanes) to give a yellow solid in 27% yield. The final product was inseparable from an impurity.

3.16c. ^{1}**H NMR** (600 MHz, $CDCl_3$) d = 9.06 (s, 1H), 8.38 (d, *J* = 1.7 Hz, 1H), 8.04 (d, *J* = 8.3 Hz, 1H), 8.00 (s, 1H), 7.84–7.81 (m, 2H), 7.81–7.76 (m, 3H), 7.73 (dd, *J* = 8.3, 1.8 Hz, 1H), 6.53–6.50 (m, 1H).; ^{13}**C NMR** (151 MHz, $CDCl_3$) d = 154.94, 154.14, 141.40, 139.71, 138.86, 138.76, 132.96, 128.49, 126.84, 124.99, 122.31, 121.84, 119.69, 107.95. **IR** (thin film): 1698.02, 1652.70, 1568.81, 1540.85, 1507.10, 1435.74; **HRMS** (ESI): Calculated for $C_{16}H_{12}N_3S$ $[M+H]^+$= 278.07444; found 278.0752.

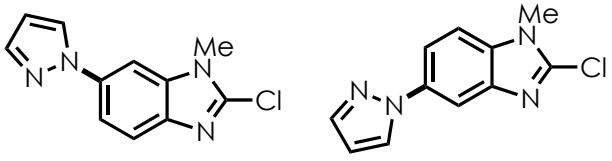

2-chloro-1-methyl-6-(1*H*-pyrazol-1-yl)-1*H*-benzo[*d*]imidazole (3.16d) and 2-chloro-1-methyl-5-(1*H*-pyrazol-1-yl)-1*H*-benzo[*d*]imidazole (3.16e). The title compounds were prepared using Method D with an irradiation time of 20 hours. The title compound was purified by column chromatography on silica gel (20% to 50% EtOAc/Hexanes) to give a pale yellow solid in 42% yield.

3.16d and 3.16e. ^{1}**H NMR** (600 MHz, $CDCl_3$) d = 7.96 (d, *J* = 2.5 Hz, 1H), 7.93 (d, *J* = 2.4 Hz, 0.3H), 7.89 (d, *J* = 2.0 Hz, 0.3H), 7.75 (dd, *J* = 4.6, 1.9 Hz, 2.3H), 7.73 (s, 0.3H),

7.71 (d, J = 8.6 Hz, 1H), 7.50 (dd, J = 8.7, 2.1 Hz, 1H), 7.34 (s, 0.3H), 6.49 (t, J = 2.1 Hz, 1H), 6.48 (s, 0.3H), 3.81 (s, 4H).; **^{13}C NMR** (151 MHz, $CDCl_3$) d = 142.33, 141.94, 141.87, 141.21, 141.08, 140.23, 136.53, 136.47, 136.17, 134.40, 127.45, 127.38, 120.01, 116.24, 114.56, 110.31, 110.00, 107.87, 107.65, 101.30, 30.90, 30.88.

IR (thin film): 3116.40, 2930.31, 1683.55, 1507.10, 1473.35, 1418.39, 751.14; **HRMS** (ESI): Calculated for $C_{11}H_{10}ClN_4$ $[M+H]^+$= 233.0594; found 233.05864.

3.16d. Functionalization occurred at the 6-position based on carbon chemical shifts matching with predicted values.

3.16e. Functionalization occurred at the 5-position based on carbon chemical shifts matching with predicted values.

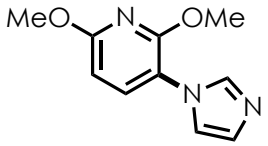

3-(1*H*-imidazol-1-yl)-2,6-dimethoxypyridine (3.17c). The title compound was prepared using Method B with an irradiation time of 20 hours. The title compound was purified by column chromatography on silica gel (20% to 100% EtOAc/Hexanes to 5% MeOH/EtOAc) to give an orange oil in 52% yield. The spectral data matched the values reported in the literature.[6]

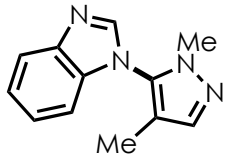

1-(1,4-dimethyl-1*H*-pyrazol-5-yl)-1*H*-benzo[*d*]imidazole (3.17d). The title compounds were prepared using Method A with an irradiation time of 20 hours. The title compound

was purified by column chromatography on silica gel (20% to 50% EtOAc/Hexanes) to give a yellow solid in 48% combined yield and a 6:1 ratio of regioisomers.

3.17d. ^{1}**H NMR** (600 MHz, $CDCl_3$) d = 8.00–7.97 (m, 0.33H), 7.96–7.93 (m, 1H), 7.93–7.88 (m, 1H), 7.83 (dq, *J* = 7.4, 1.6 Hz, 0.33H), 7.51 (d, *J* = 2.8 Hz, 1H), 7.37 (m, 3H), 7.33–7.29 (m, 1H), 7.26 (s, 0.33H), 7.15 (dq, *J* = 7.6, 1.4 Hz, 1H), 4.63–4.41 (s, 1H), 3.94–3.79 (s, 1H), 3.72–3.54 (s, 3H), 2.00–1.77 (s, 3H).; ^{13}**C NMR** (151 MHz, $CDCl_3$) d = 143.86, 143.42, 143.30, 142.82, 140.70, 139.44, 134.42, 133.38, 131.49, 124.68, 123.57, 123.43, 122.93, 122.67, 120.95, 120.75, 113.40, 110.20, 109.25, 46.73, 42.24, 36.02, 7.92.

IR (thin film): 2928.38, 1558.20, 1507.10, 1456.96, 767.53, 745.35; **HRMS** (ESI): Calculated for $C_{12}H_{13}N_4$ $[M+H]^+$= 213.1140; found 213.11328.

Functionalization occurred at the 5-position based on carbon chemical shifts matching with predicted values.

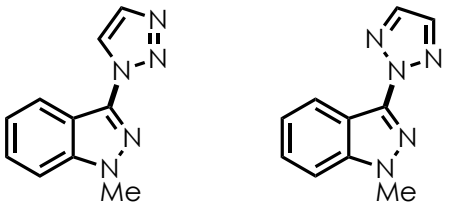

1-methyl-3-(1*H*-1,2,3-triazol-1-yl)-1*H*-indazole (3.17ei) and 1-methyl-3-(2*H*-1,2,3-triazol-2-yl)-1*H*-indazole (3.17eii). The title compound was prepared using Method B with an irradiation time of 20 hours. The title compound was purified by column chromatography on silica gel (5% to 30% EtOAc/Hexanes) to give an inseparable mixture as a pale brown solid in 30% yield (10:1 **3.17ei:3.17eii**).

3.17ei and 3.17eii. **^{1}H NMR** (600 MHz, Chloroform-*d*) δ 8.36 (d, *J* = 1.0 Hz, 1H), 8.34 (d, *J* = 8.3 Hz, 1H), 7.92 (s, 0.2H), 7.87 (d, *J* = 1.0 Hz, 1H), 7.50 – 7.45 (m, 1.1H), 7.39 (d, *J* = 8.6 Hz, 1H), 7.28 (dd, *J* = 9.1, 5.9 Hz, 1.2H), 4.12 (s, 0.3H), 4.07 (s, 3H),. **^{13}C NMR** (151 MHz, $CDCl_3$) δ 141.48, 141.34, 138.03, 135.64, 133.50, 127.91, 127.65, 122.23, 122.07, 121.94, 121.90, 121.61, 114.95, 114.65, 109.20, 109.16, 77.33, 77.11, 76.90, 35.84, 35.76.

IR (thin film): 3429.79, 3144.37, 2951.52, 2840.63, 1729.83, 1591.95. **HRMS** (ESI) Calculated for $C_{10}H_{10}N_5$ $[M+Na]^+$= 222.0800; found 222.0750.

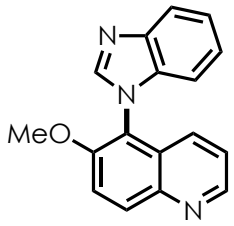

5-(1*H*-benzo[*d*]imidazol-1-yl)-6-methoxyquinoline (3.17f). The title compound was prepared using Method B with an irradiation time of 20 hours. The title compound was purified by column chromatography on silica gel (0% to 100% (5% MeOH DCM)/Hexanes) to give a white solid in 62% yield.

3.17f. **^{1}H NMR** (400 MHz, Chloroform-*d*) δ 8.87 (d, *J* = 4.2 Hz, 1H), 8.35 (d, *J* = 9.3 Hz, 1H), 8.05 (s, 1H), 7.96 (d, *J* = 8.2 Hz, 1H), 7.71 (d, *J* = 9.4 Hz, 1H), 7.58 (d, *J* = 8.6 Hz, 1H), 7.39 – 7.31 (m, 2H), 7.29 – 7.20 (m, 1H), 6.94 (d, *J* = 8.0 Hz, 1H), 3.90 (s, 3H). **^{13}C NMR** (151 MHz, $CDCl_3$) δ 153.39, 149.08, 144.54, 143.44, 143.23, 135.11, 132.53, 130.15, 126.72, 123.62, 122.69, 122.63, 120.44, 116.59, 116.40, 110.57, 56.58.

IR (thin film): 3052.76, 2982.37, 2685.39, 2305.48, 1732.73, 1503.24, 1265.07. **HRMS** (ESI) Calculated for $C_{17}H_{14}N_3O$ $[M+H]^+$= 276.1131 found 276.1131.

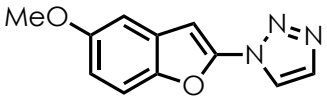

1-(5-methoxybenzofuran-2-yl)-1*H*-1,2,3-triazole (3.17g). The title compound was prepared using Method B with an irradiation time of 20 hours. The title compound was purified by column chromatography on silica gel (10% to 40% EtOAc/Hexanes) to give a white solid in 9% yield.

3.17g. ^{1}H NMR (600 MHz, Chloroform-*d*) δ 8.22 – 8.16 (m, 1H), 7.90 (t, *J* = 0.7 Hz, 1H), 7.69 (d, *J* = 2.2 Hz, 1H), 7.57 (dt, *J* = 9.0, 0.7 Hz, 1H), 7.11 (d, *J* = 9.0 Hz, 1H), 7.01 (dd, *J* = 2.2, 0.9 Hz, 1H), 3.91 (s, 3H). **^{13}C NMR** (151 MHz, $CDCl_3$) δ 150.27, 147.45, 147.20, 133.00, 126.15, 124.70, 118.07, 112.25, 109.78, 106.15, 57.21.

IR (thin film): 3165.58, 3134.72, 3054.69, 2966.95, 2929.34, 2847.38, 1719.23, 1624.73.

HRMS (ESI) Calculated for $C_{11}H_{10}N_3O_2$ $[M+Na]^+$= 238.0600 found 238.05886

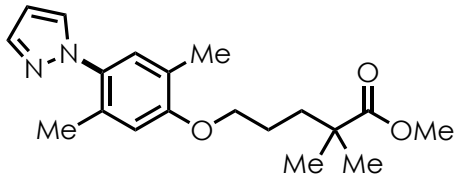

Methyl 5-(2,5-dimethyl-4-(1*H*-pyrazol-1-yl)phenoxy)-2,2-dimethylpentanoate (3.18d). The title compound was prepared using Method B with an irradiation time of 20 hours. The title compound was purified by column chromatography on silica gel (10% to 25% EtOAc/Hexanes) to give a colorless oil in 32% yield.

3.18d. ^{1}H NMR (600 MHz, Chloroform-*d*) δ 7.70 (d, *J* = 2.0 Hz, 1H), 7.55 (d, *J* = 2.4 Hz, 1H), 7.12 (s, 1H), 6.69 (s, 1H), 6.42 (t, *J* = 2.1 Hz, 1H), 3.98 (t, *J* = 5.8 Hz, 2H), 3.70 (s, 3H), 2.22 (s, 3H), 2.17 (s, 3H), 1.81 – 1.72 (m, 4H), 1.25 (s, 6H). ^{13}C NMR (151 MHz, $CDCl_3$) δ 178.30, 156.77, 139.89, 132.48, 132.09, 130.72, 128.41, 124.89, 112.83, 105.77, 68.26, 51.82, 42.11, 37.04, 25.23, 25.12, 17.87, 15.60.

IR (thin film): 3050.83, 2952.48, 2962.45, 2872.45, 1727.91, 1619.91, 1519.63, 1267.00.

HRMS (ESI) Calculated for $C_{19}H_{27}N_2O_3$ $[M+H]^+$= 331.2016 found 331.2015.

Computational Data

All computations were carried out in the Gaussian 09 program suite[7] at the B3LYP/6-31G+(d,p) level of theory. Population analyses (NPA atomic charges and molecular orbital populations) were performed using the NBO formalism.

Redox potentials were calculated as described previously by our lab.[8] All redox potentials were calculated in acetonitrile unless otherwise specified. Energies are listed in Hartrees.

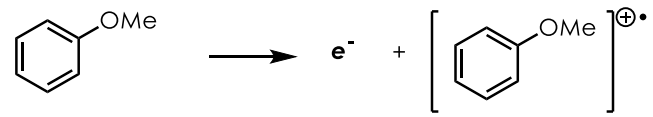

$$\boldsymbol{G_{298}}[\mathbf{neutral}] = -346.6624 \text{ Hartree}$$

$$\boldsymbol{G_{298}}[\mathbf{cation\ radical}] = -346.4380 \text{ Hartree}$$

$$\Delta \boldsymbol{G^{o}_{1/2}} = (\boldsymbol{G_{298}}[\mathbf{neutral}] - \boldsymbol{G_{298}}[\mathbf{cation\ radical}])$$

$$= (-346.6624 - -346.4380 \text{ Hartree})$$

$$\times 627.5 \text{ kcal mol}^{-1}\text{Hartree}^{-1} = -140.8110 \text{ kcal mol}^{-1}$$

$$\boldsymbol{E_{1/2}^{o,calc}} = -\frac{\boldsymbol{\Delta G_{1/2}^{o}}}{n_e \mathcal{F}} - E_{1/2}^{o,SHE} + E_{1/2}^{o,SCE}$$

$$= -\frac{-140.8110 \text{ kcal mol}^{-1}}{23.061 \text{ kcal mol}^{-1}\text{V}^{-1}} - 4.281 \text{ V} - 0.141 \text{ V}$$

$$= \mathbf{1.68 \text{ V vs. SCE}}$$

NPA values were calculated as specified below and were all calculated in DCE. Using gaussview, each compound of interest is drawn in the ground state.

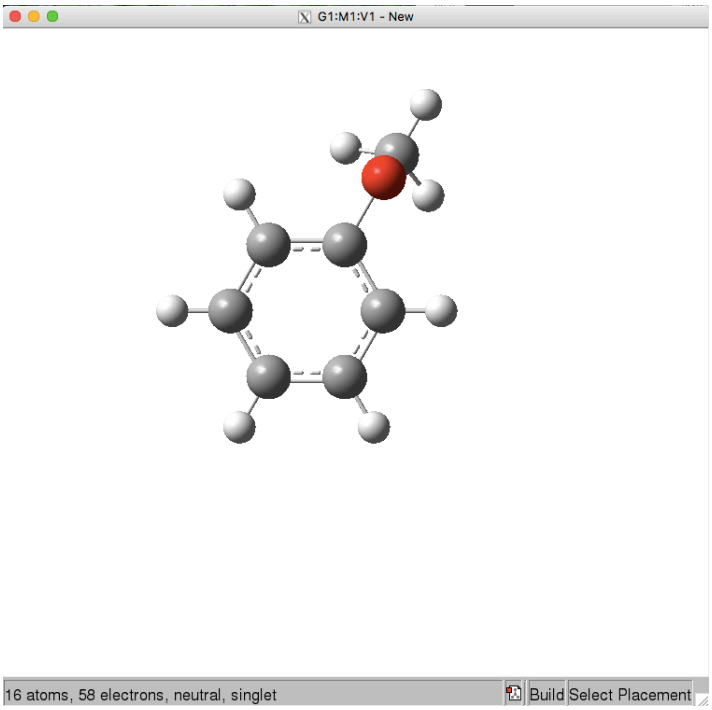

The following basis sets and settings were used in the calculations.

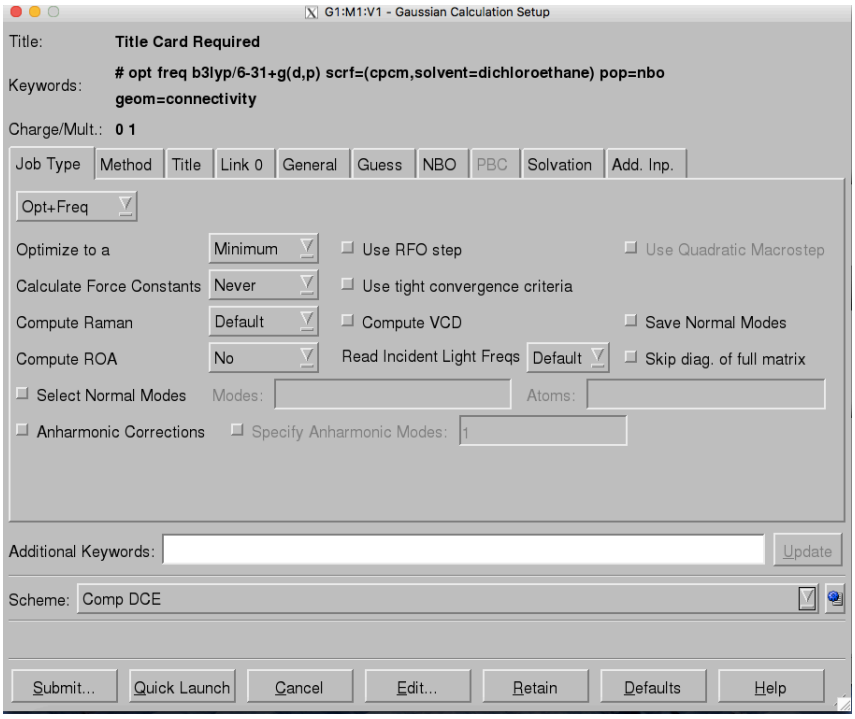
G1:M1:V1 - Gaussian Calculation Setup
Title:
Title Card Required
Keywords:
opt freq b3lyp/6-31+g(d,p) scrf=(cpcm,solvent=dichloroethane) pop=nbo geom=connectivity
Charge/Mult.:
0 1
Job Type
Method
Title
Link 0
General
Guess
NBO
PBC
Solvation
Add. Inp.
Opt+Freq
Optimize to a
Minimum
Use RFO step
Use Quadratic Macrostep
Calculate Force Constants
Never
Use tight convergence criteria
Compute Raman
Default
Compute VCD
Save Normal Modes
Compute ROA
No
Read Incident Light Freqs
Default
Skip diag. of full matrix
Select Normal Modes
Modes:
Atoms:
Anharmonic Corrections
Specify Anharmonic Modes:
1
Additional Keywords:
Update
Scheme:
Comp DCE
Submit...
Quick Launch
Cancel
Edit...
Retain
Defaults
Help

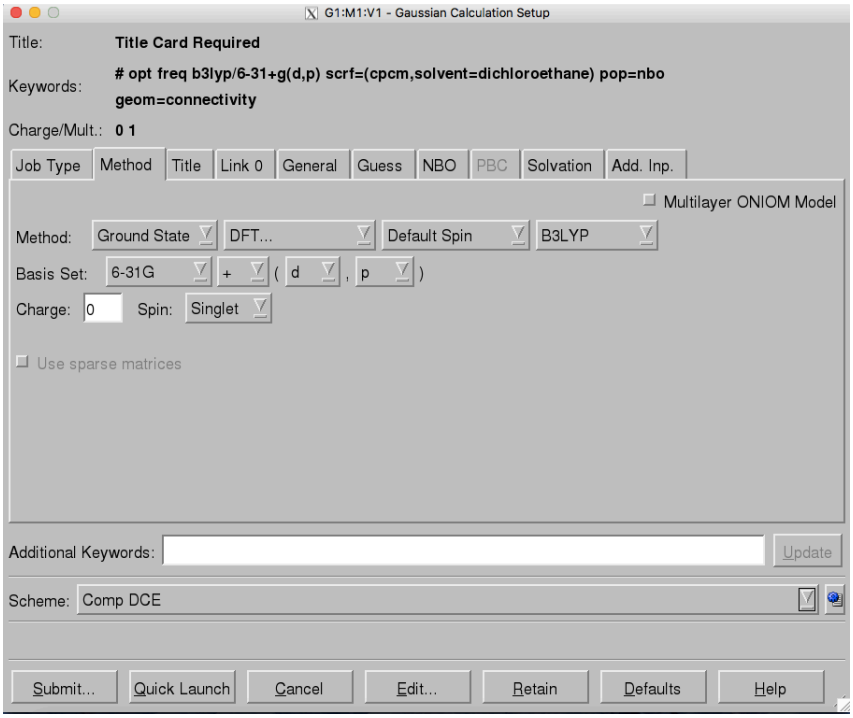
G1:M1:V1 - Gaussian Calculation Setup
Title:
Title Card Required
Keywords:
opt freq b3lyp/6-31+g(d,p) scrf=(cpcm,solvent=dichloroethane) pop=nbo geom=connectivity
Charge/Mult.:
0 1
Job Type
Method
Title
Link 0
General
Guess
NBO
PBC
Solvation
Add. Inp.
Multilayer ONIOM Model
Method:
Ground State
DFT...
Default Spin
B3LYP
Basis Set:
6-31G
+
(
d
,
p
)
Charge:
0
Spin:
Singlet
Use sparse matrices
Additional Keywords:
Update
Scheme:
Comp DCE
Submit...
Quick Launch
Cancel
Edit...
Retain
Defaults
Help

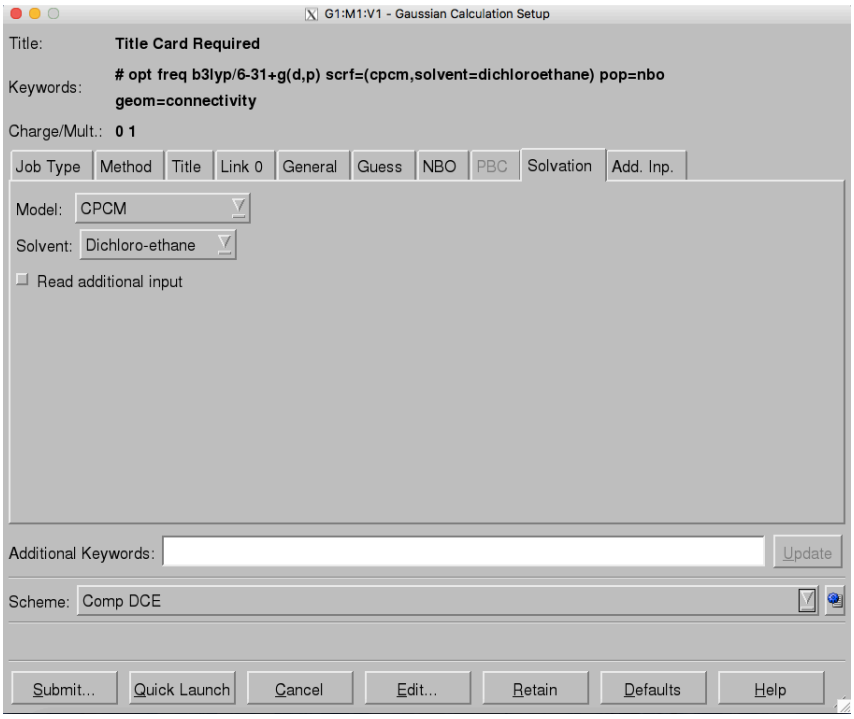

The radical cation was also constructed by changing the charge on the molecule as shown.

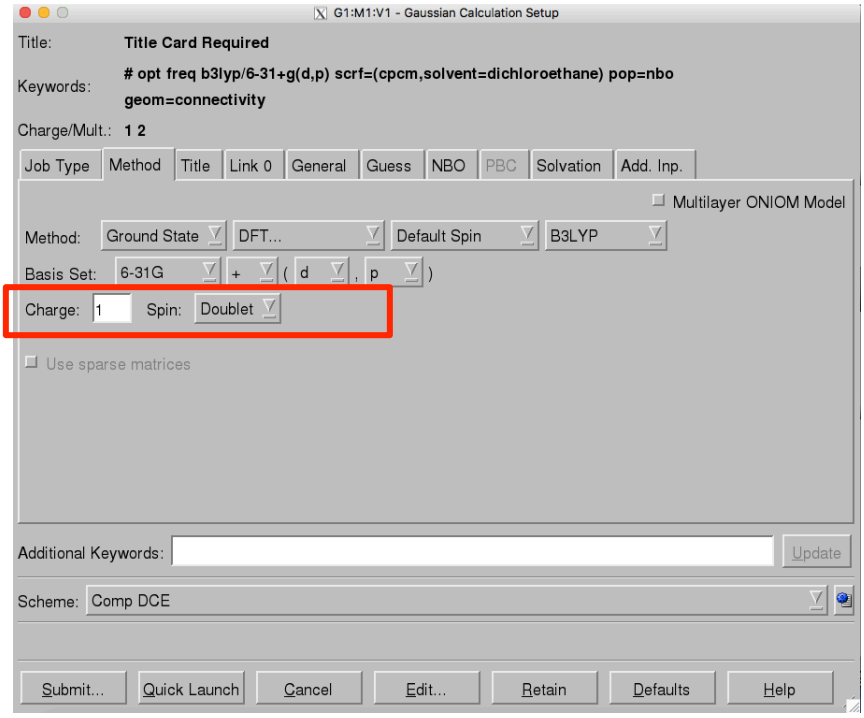

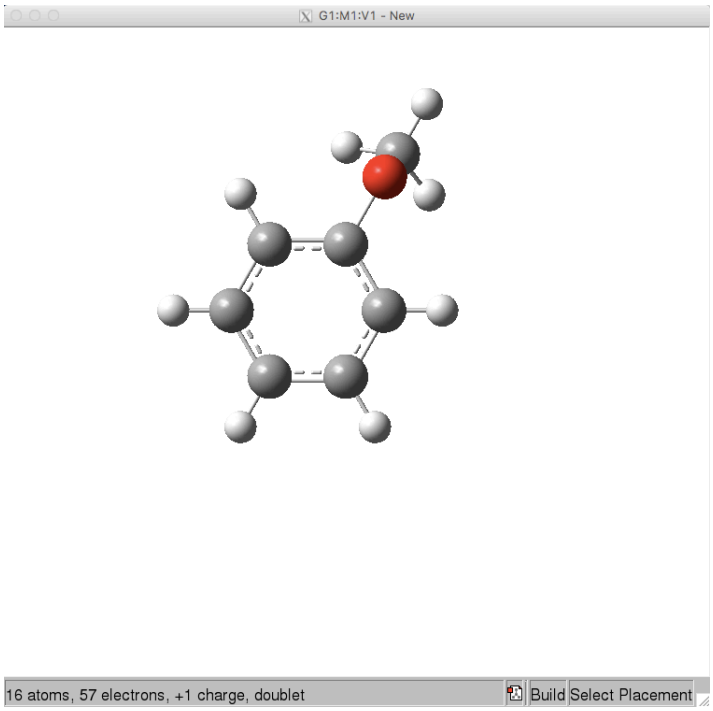

The optimized geometries and frequencies were calculated. Using the gaussview, each structure output was loaded and NPA values were determined using the following sequence of steps.

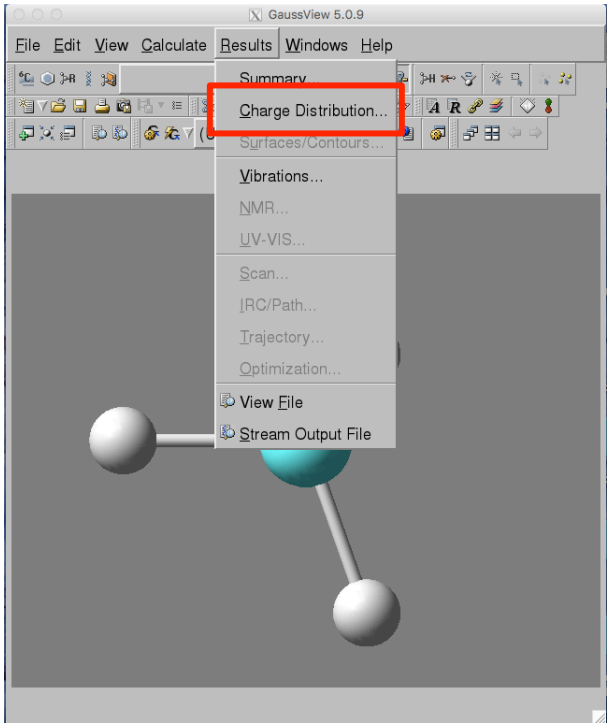

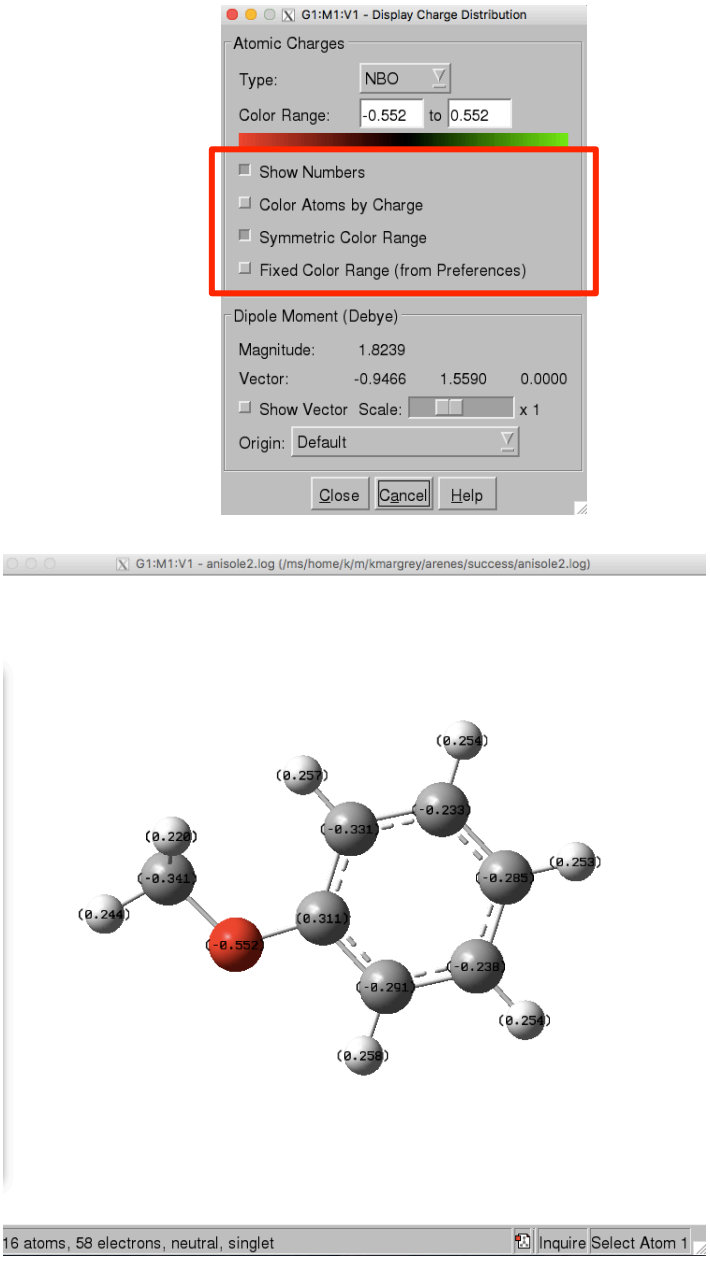

These values are the ground state and radical cation, respectively, and the difference was determined by subtracting the ground state values from the radical cation value. This resulted in values as seen in SI Tables 1–11.

Neutral Arene (DCE)	Radical Cation (DCE)	Difference (DCE)	E^{ox} (V vs SCE) in MeCN
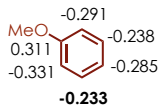	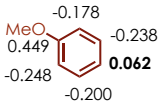	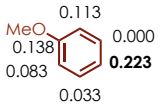	1.68
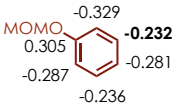	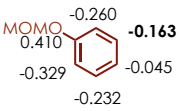	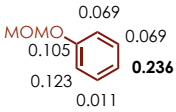	1.76
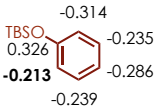	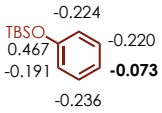	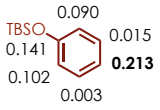	1.59
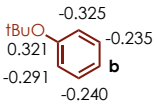	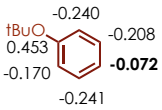	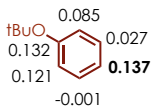	1.54
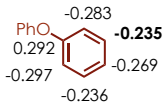	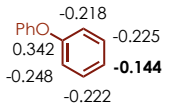	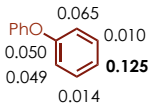	1.67
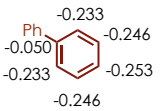	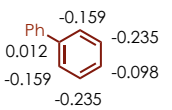	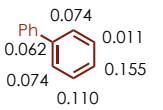	1.74

SI Table 1. Monosubstituted Benzenoids Computations

Neutral Arene (DCE)	Radical Cation (DCE)	Difference (DCE)	E^{ox} (V vs SCE) in MeCN
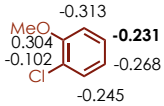	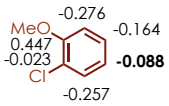	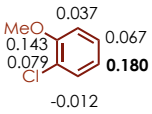	1.80
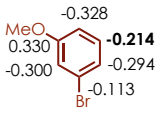	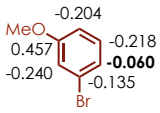	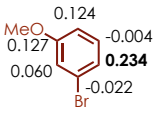	1.86
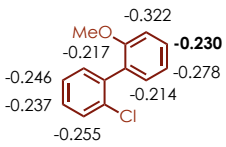	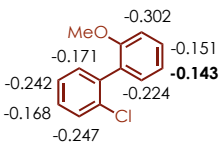	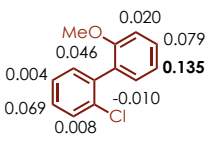	1.64
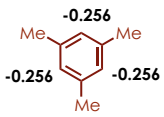	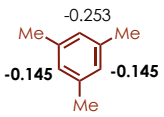	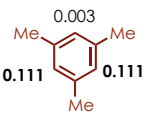	2.02
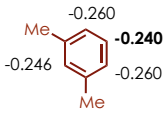	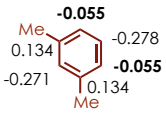	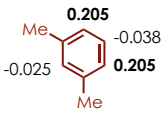	1.95
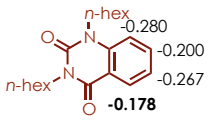	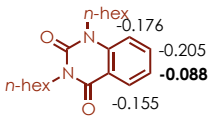	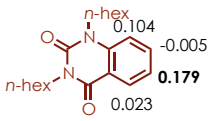	1.92
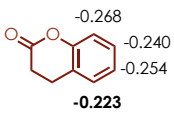	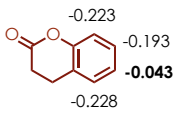	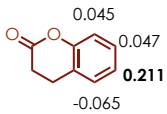	2.08

SI Table 2. Disubstituted Benzenoids Computations

Neutral Arene (DCE)	Radical Cation (DCE)	Difference (DCE)	E^{ox} (V vs SCE) in MeCN
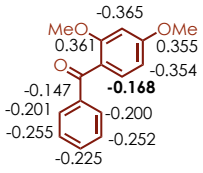	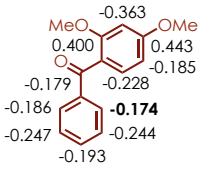	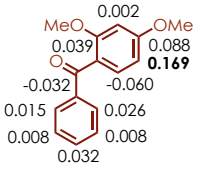	1.55
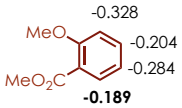	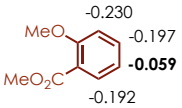	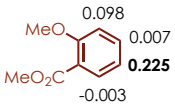	1.86
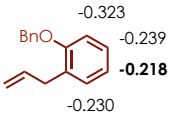	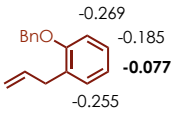	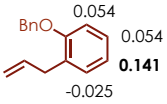	1.53
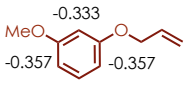	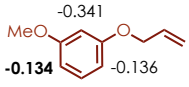	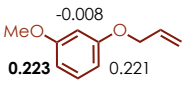	1.54
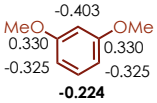	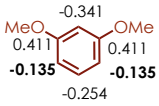	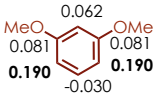	1.54
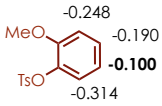	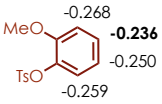	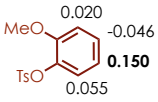	1.83

SI Table 3. New Benzenoid-Containing Compounds Computations

Neutral Arene (DCE)	Radical Cation (DCE)	Difference (DCE)	E^{ox} (V vs SCE) in MeCN
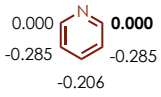	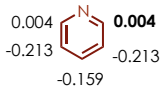	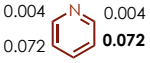	2.64
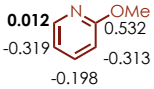	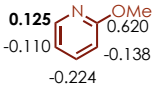	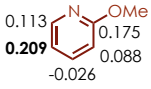	2.02
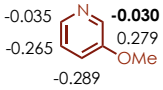	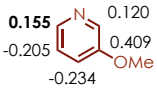	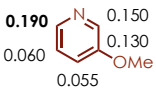	1.94
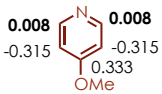	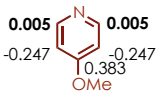	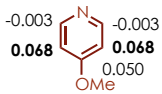	2.34
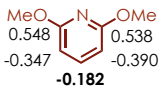	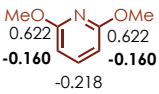	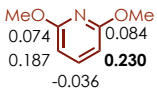	2.01
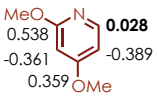	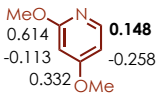	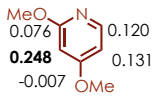	2.01
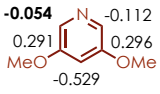	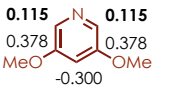	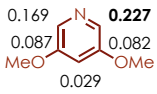	1.85
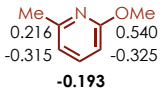	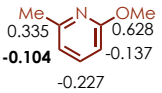	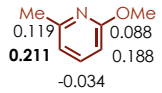	1.80

SI Table 4. Pyridine Computations

Neutral Arene (DCE)	Radical Cation (DCE)	Difference (DCE)	E^{ox} (V vs SCE) in MeCN
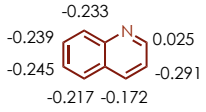	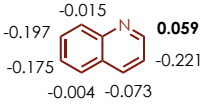	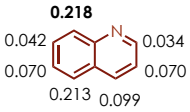	2.01
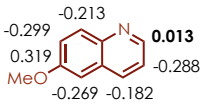	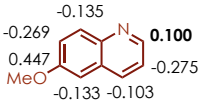	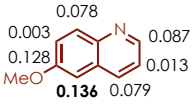	1.59
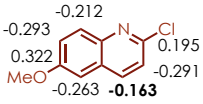	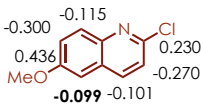	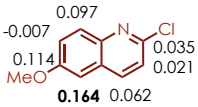	1.63
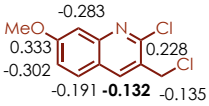	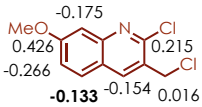	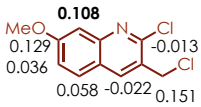	1.75
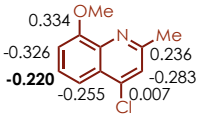	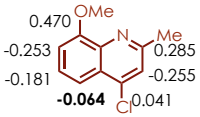	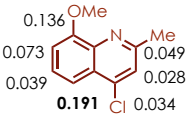	1.45
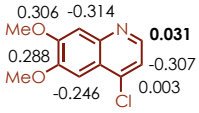	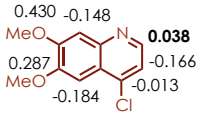	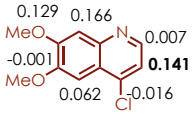	1.54
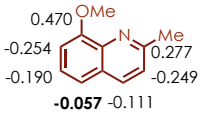	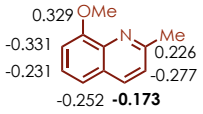	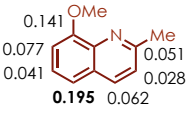	1.36
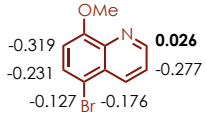	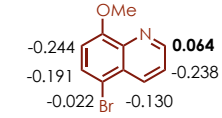	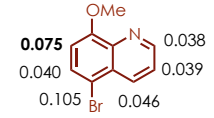	1.48

SI Table 5. Quinoline Computations

Neutral Arene (DCE)	Radical Cation (DCE)	Difference (DCE)	E^{ox} (V vs SCE) in MeCN
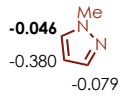	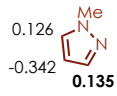	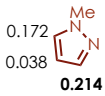	2.37
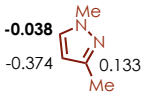	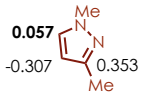	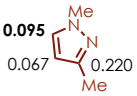	2.01
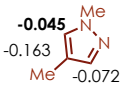	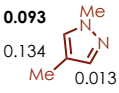	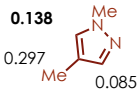	1.83
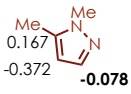	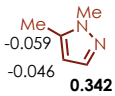	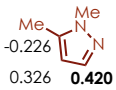	1.99

SI Table 6. Pyrazole Computations

Neutral Arene (DCE)	Radical Cation (DCE)	Difference (DCE)	E^{ox} (V vs SCE) in MeCN
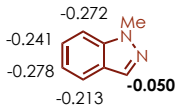	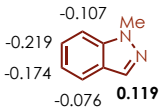	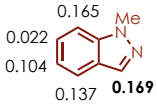	1.59
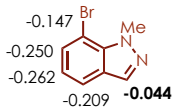	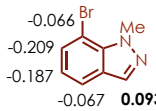	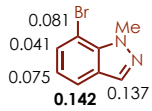	1.61
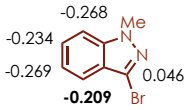	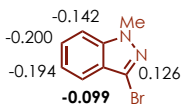	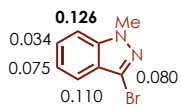	1.94

SI Table 7. Indazole Computations

Neutral Arene (DCE)	Radical Cation (DCE)	Difference (DCE)	E^{ox} (V vs SCE) in MeCN
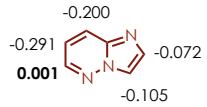	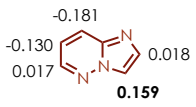	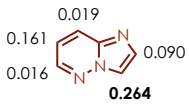	1.87
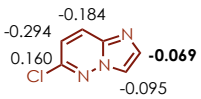	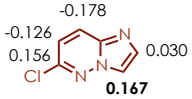	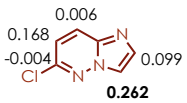	2.04
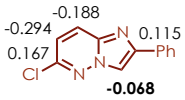	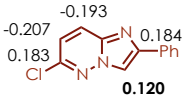	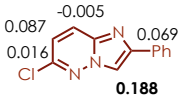	1.62
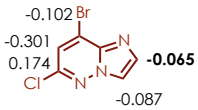	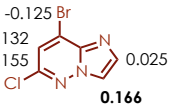	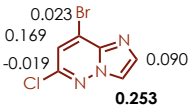	2.17
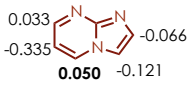	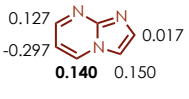	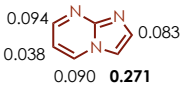	1.78
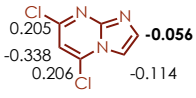	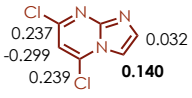	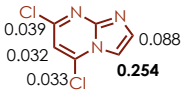	1.98
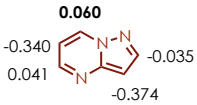	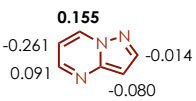	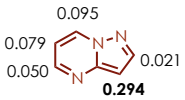	1.82
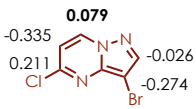	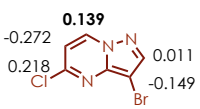	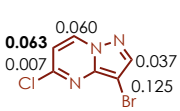	1.84
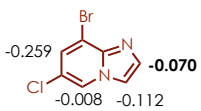	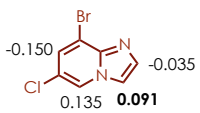	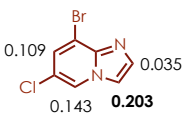	1.69

SI Table 8. Bridging-Nitrogen Polyaromatic Heterocycle Computations

Neutral Arene (DCE)	Radical Cation (DCE)	Difference (DCE)	E^{ox} (V vs SCE) in MeCN
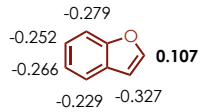	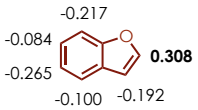	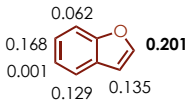	1.85
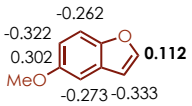	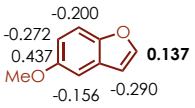	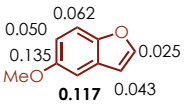	1.46
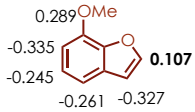	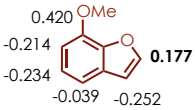	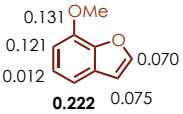	1.47
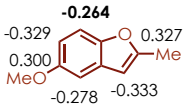	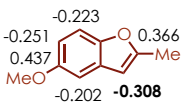	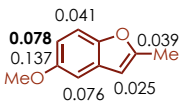	1.37
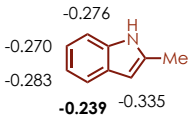	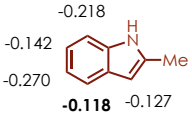	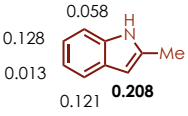	1.06
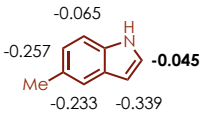	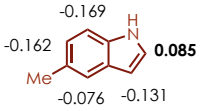	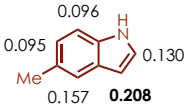	1.18
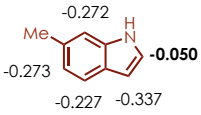	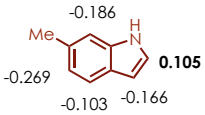	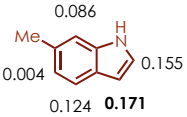	1.09

SI Table 9. Benzofuran and Indole Computations

Neutral Arene (DCE)	Radical Cation (DCE)	Difference (DCE)	E^{ox} (V vs SCE) in MeCN
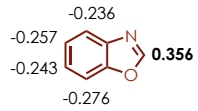	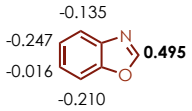	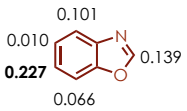	2.28
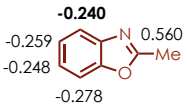	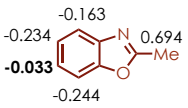	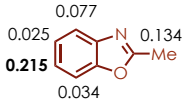	2.06
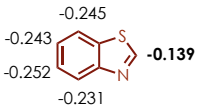	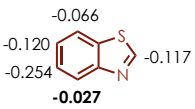	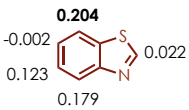	2.14
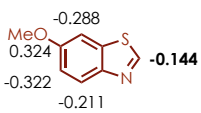	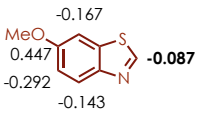	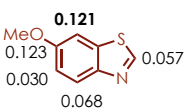	1.56
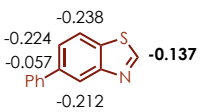	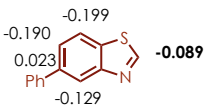	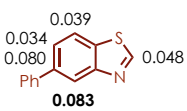	1.68
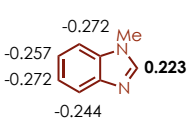	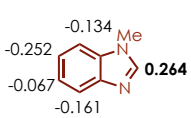	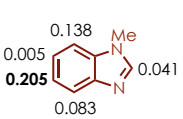	1.82
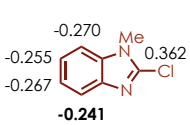	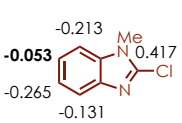	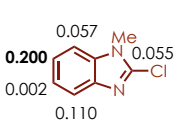	1.99

SI Table 10. Benzazole Computations

Neutral Arene (DCE)	Radical Cation (DCE)	Difference (DCE)
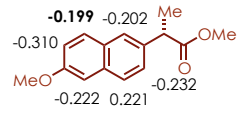	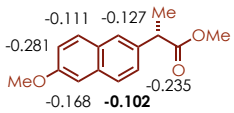	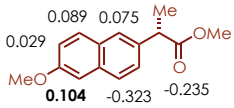
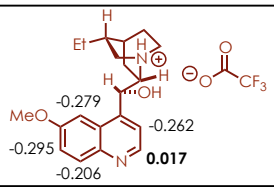	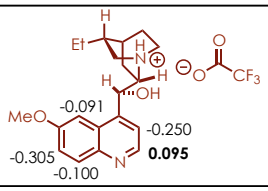	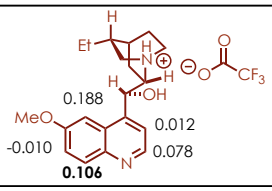
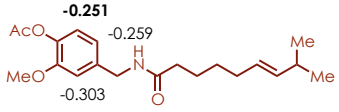	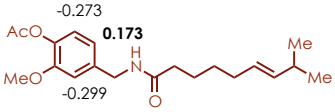	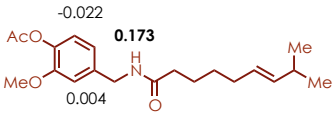
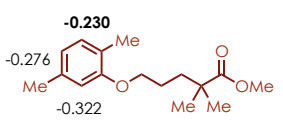	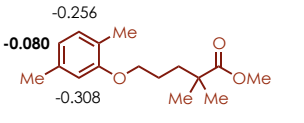	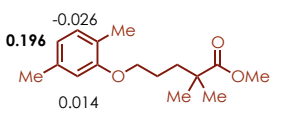
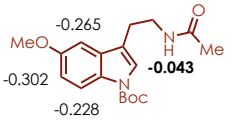	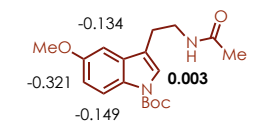	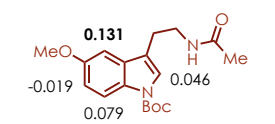

SI Table 11. Complex Molecule Computations

REFERENCES

(1) Romero, N. A.; Margrey, K. A.; Tay, N. E.; Nicewicz, D. A. *Science* **2015**, *349*, 1326–1330.

(2) McManus, J. B.; Nicewicz, D. A. *J. Am. Chem. Soc.* **2017**, *139*, 2880–2883.

(3) Gozzo, F. C.; Fernandes, S. A.; Rodrigues, D. C.; Eberlin, M. N.; Marsaioli, A. J. *J. Org. Chem.* **2003**, *68*, 5493–5499.

(4) Hajipour, A. R.; Zarei, A.; Khazdooz, L.; Ruoho, A. E. *Synth. Commun.* **2009**, *39*, 2702–2722.

(5) Liang, G.-B.; Zhou, C.; Wang, H.; Hou, X. WO 2015/095261.

(6) Aghazada, S.; Huckaba, A. J.; Pertegas, A.; Babaei, A.; Grancini, G.; Zimmermann, I.; Bolink, H.; Nazeeruddin, M. K. *Eur. J. Inorg. Chem.* **2016**, *2016*, 5089–5097.

(7) Gaussian 09, Revision D.01, M. J. Frisch, G. W. Trucks, H. B. Schlegel, G. E. Scuseria, M. A. Robb, J. R. Cheeseman, G. Scalmani, V. Barone, B. Mennucci, G. A. Petersson, H. Nakatsuji, M. Caricato, X. Li, H. P. Hratchian, A. F. Izmaylov, J. Bloino, G. Zheng, J. L. Sonnenberg, M. Hada, M. Ehara, K. Toyota, R. Fukuda, J. Hasegawa, M. Ishida, T. Nakajima, Y. Honda, O. Kitao, H. Nakai, T. Vreven, J. A. Montgomery, Jr., J. E. Peralta, F. Ogliaro, M. Bearpark, J. J. Heyd, E. Brothers, K. N. Kudin, V. N. Staroverov, R. Kobayashi, J. Normand, K. Raghavachari, A. Rendell, J. C. Burant, S. S. Iyengar, J. Tomasi, M. Cossi, N. Rega, J. M. Millam, M. Klene, J. E. Knox, J. B. Cross, V. Bakken, C. Adamo, J. Jaramillo, R. Gomperts, R. E. Stratmann, O. Yazyev, A. J. Austin, R. Cammi, C. Pomelli, J. W. Ochterski, R. L. Martin, K. Morokuma, V. G. Zakrzewski, G. A. Voth, P. Salvador, J. J. Dannenberg, S. Dapprich, A. D. Daniels, Ö. Farkas, J. B. Foresman, J. V. Ortiz, J. Cioslowski, and D. J. Fox, Gaussian, Inc., Wallingford CT, 2009.

(8) Roth, H. G.; Romero, N. A.; Nicewicz, D. A. *Synlett*. **2016**, *27*, 714–723.

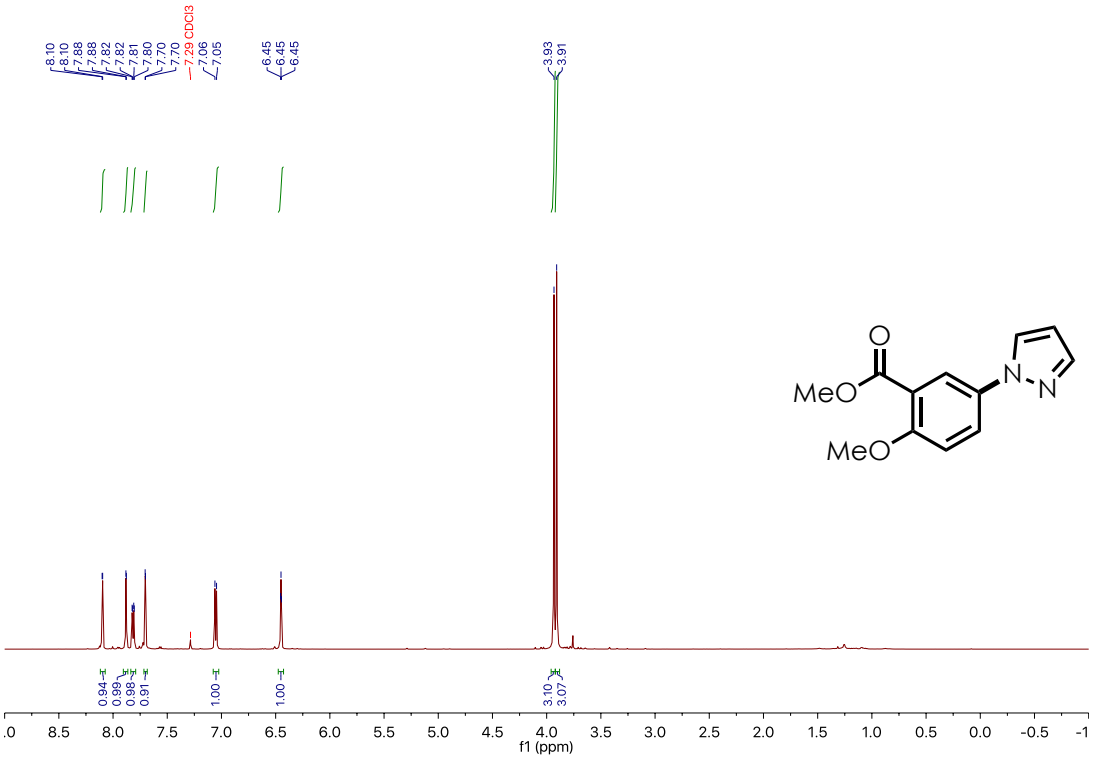
8.10
8.10
7.88
7.88
7.82
7.81
7.80
7.70
7.70
7.29 CDCl3
7.06
7.05
6.45
6.45
6.45
3.93
3.91
MeO
MeO
N
N
0.94
0.99
0.98
0.91
1.00
1.00
3.10
3.07
f1 (ppm)

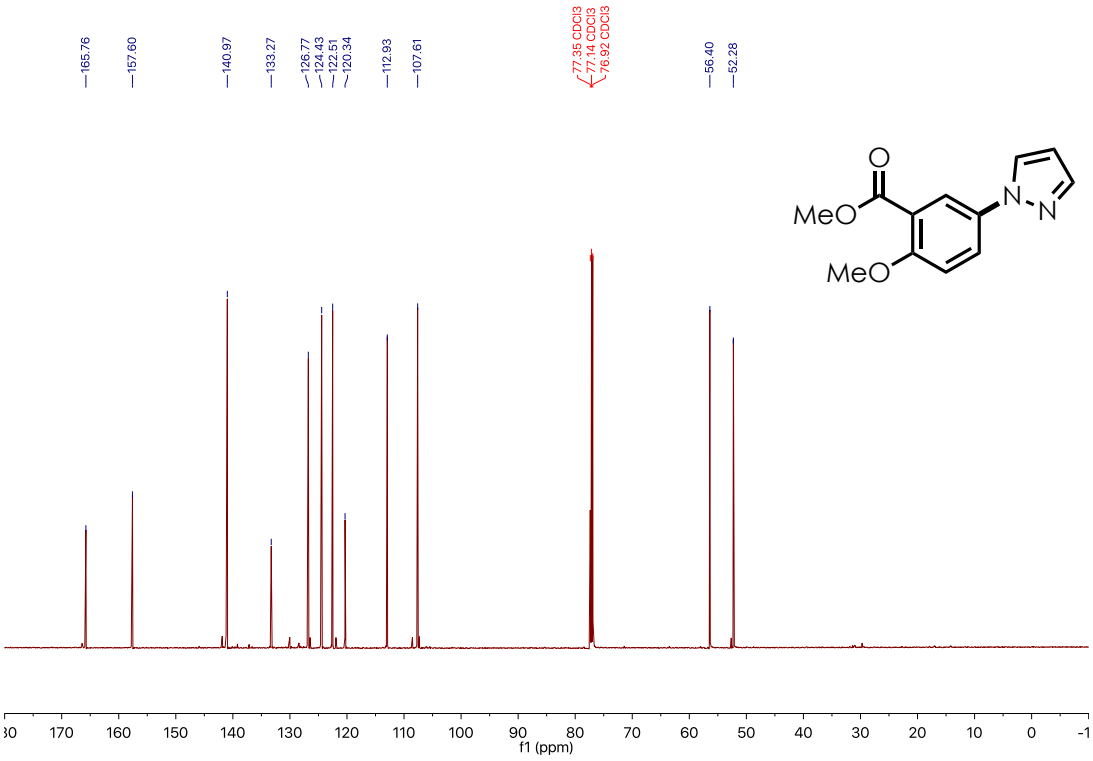
165.76
157.60
140.97
133.27
126.77
124.43
122.51
120.34
112.93
107.61
77.35 CDCl3
77.14 CDCl3
76.92 CDCl3
56.40
52.28
MeO
MeO
N
N
f1 (ppm)

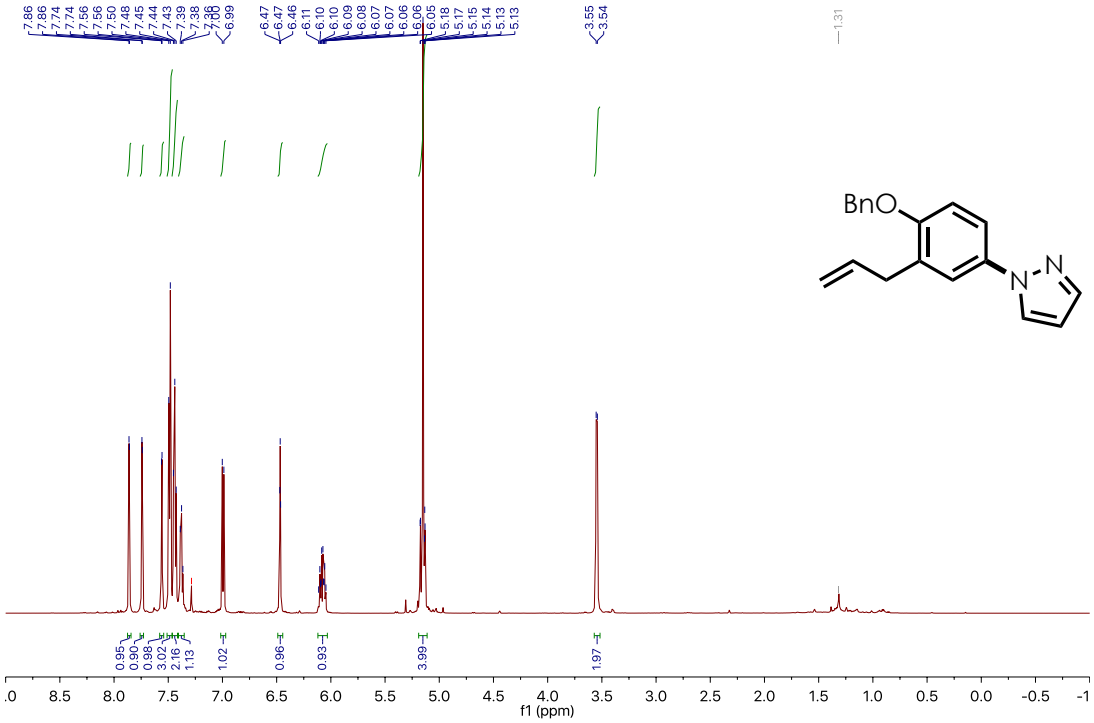
7.86
7.86
7.74
7.74
7.56
7.56
7.50
7.48
7.45
7.44
7.43
7.39
7.38
6.99
6.47
6.47
6.46
6.11
6.10
6.10
6.09
6.08
6.07
6.07
6.06
6.06
6.05
5.18
5.17
5.15
5.14
5.13
5.13
3.55
3.54
1.31
BnO
N
N
0.95
0.90
0.98
3.02
2.16
1.13
1.02
0.96
0.93
3.99
1.97
f1 (ppm)

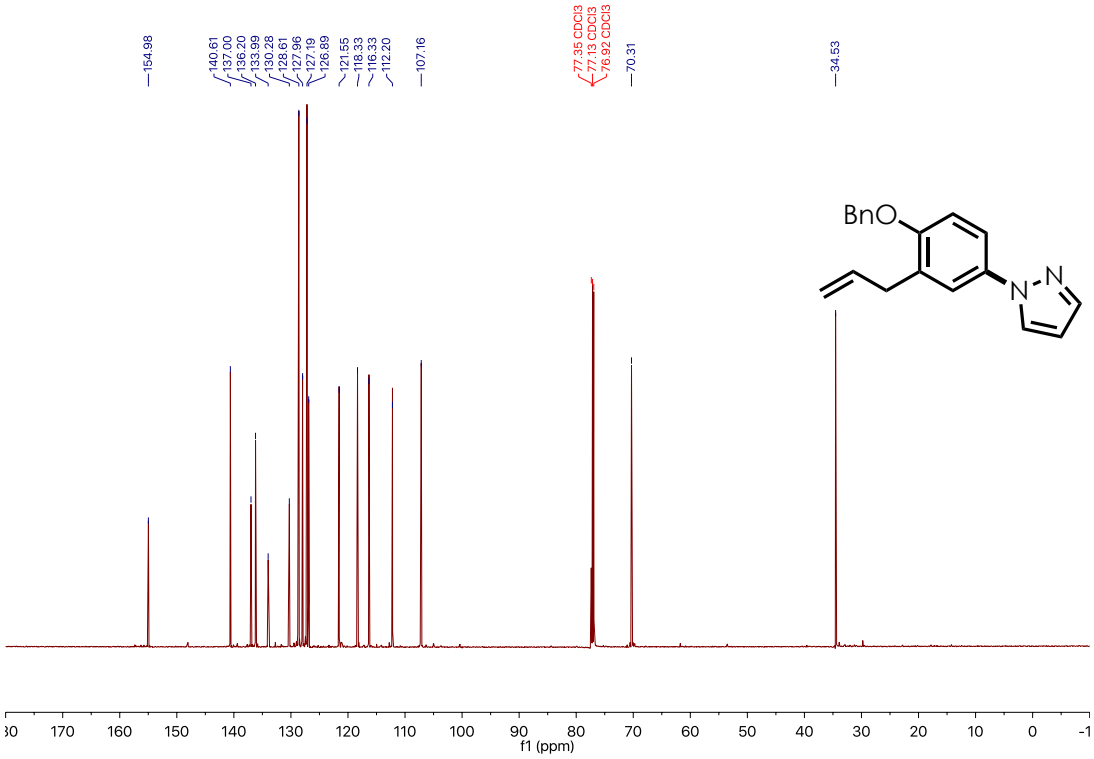
154.98
140.61
137.00
136.20
133.99
130.28
128.61
127.96
127.19
126.89
121.55
118.33
116.33
112.20
107.16
77.35 CDCl3
77.13 CDCl3
76.92 CDCl3
70.31
34.53
BnO
N
N
f1 (ppm)

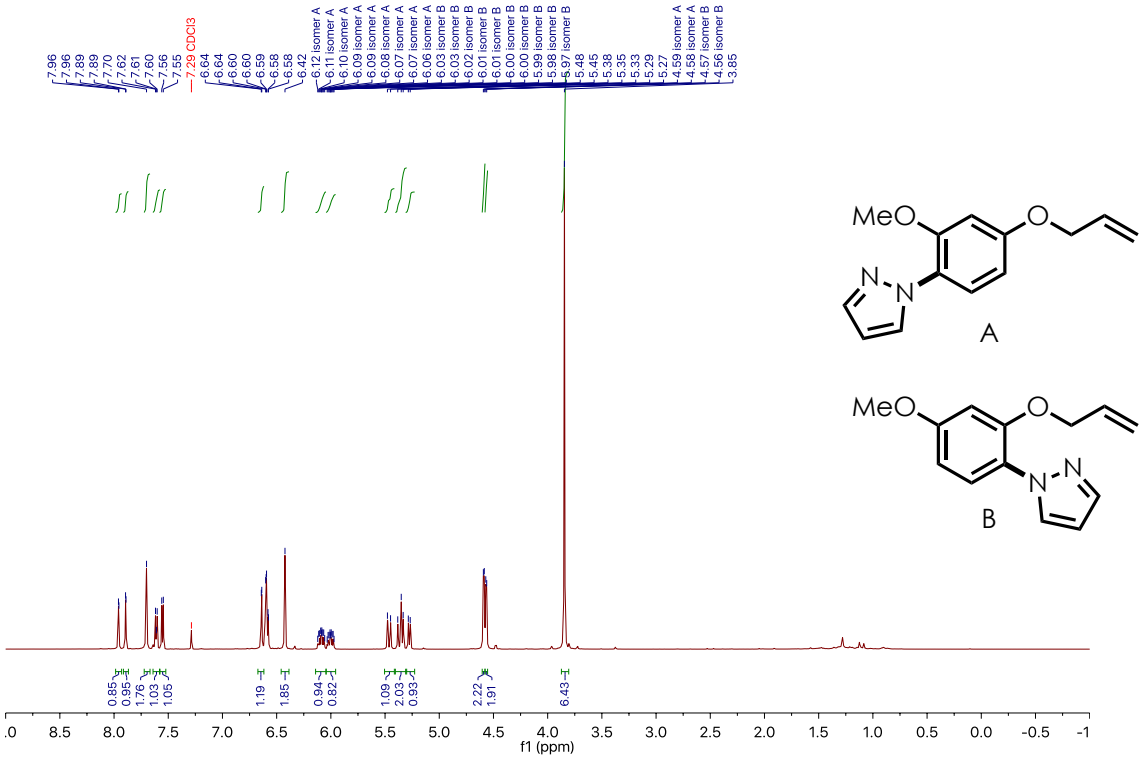
7.96
7.96
7.89
7.89
7.70
7.62
7.61
7.60
7.56
7.55
7.29 CDCl3
6.64
6.64
6.60
6.60
6.59
6.58
6.58
6.42
6.12 isomer A
6.11 isomer A
6.10 isomer A
6.09 isomer A
6.09 isomer A
6.08 isomer A
6.07 isomer A
6.07 isomer A
6.06 isomer A
6.03 isomer B
6.03 isomer B
6.02 isomer B
6.01 isomer B
6.01 isomer B
6.00 isomer B
6.00 isomer B
5.99 isomer B
5.98 isomer B
5.97 isomer B
5.48
5.45
5.38
5.35
5.33
5.29
5.27
4.59 isomer A
4.58 isomer A
4.57 isomer B
4.56 isomer B
3.85
0.85
0.95
1.76
1.03
1.05
1.19
1.85
0.94
0.82
1.09
2.03
0.93
2.22
1.91
6.43
f1 (ppm)

MeO
O
N
N

A

MeO
O
N
N

B

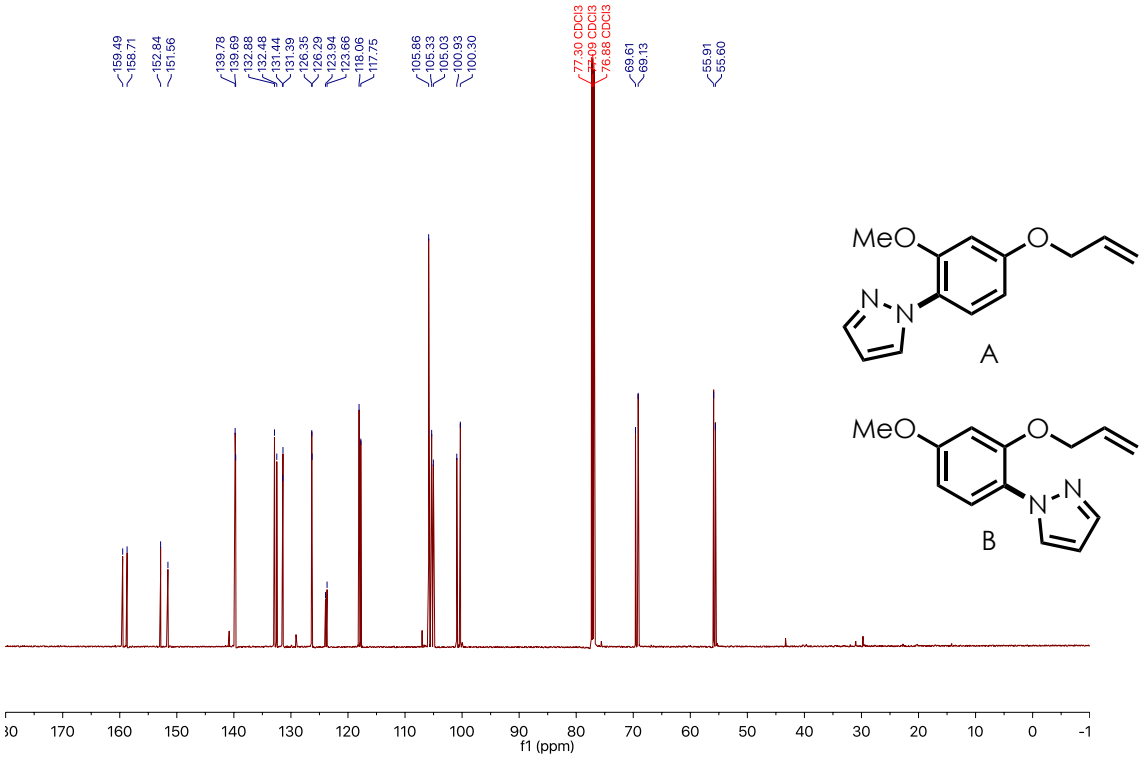
159.49
158.71
152.84
151.56
139.78
139.69
132.88
132.48
131.44
131.39
126.35
126.29
123.84
123.66
118.06
117.75
105.86
105.33
105.03
100.93
100.30
77.30 CDCl3
77.09 CDCl3
76.88 CDCl3
69.61
69.13
55.91
55.60
f1 (ppm)

MeO
O
N
N

A

MeO
O
N
N

B

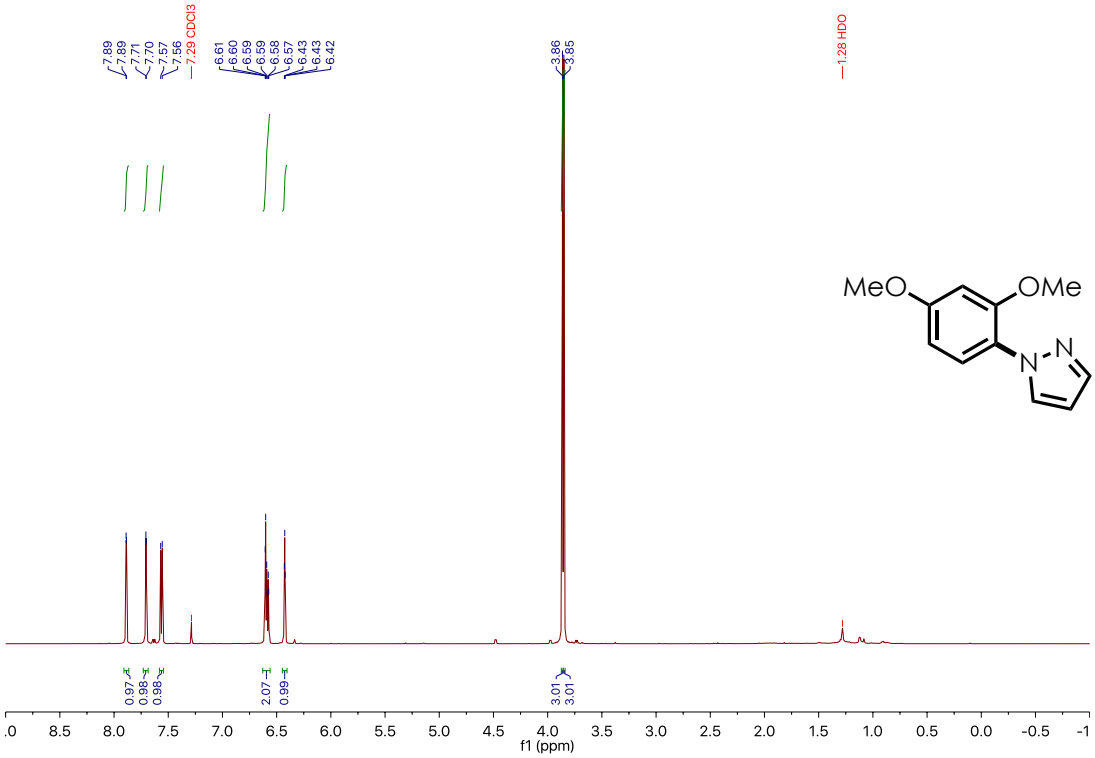
7.99
7.99
7.71
7.70
7.57
7.56
7.29 CDCl3
6.61
6.60
6.59
6.59
6.58
6.57
6.43
6.42
3.86
3.85
1.28 HDO
MeO
OMe
N
N
0.97
0.98
0.98
2.07
0.99
3.01
3.01
f1 (ppm)

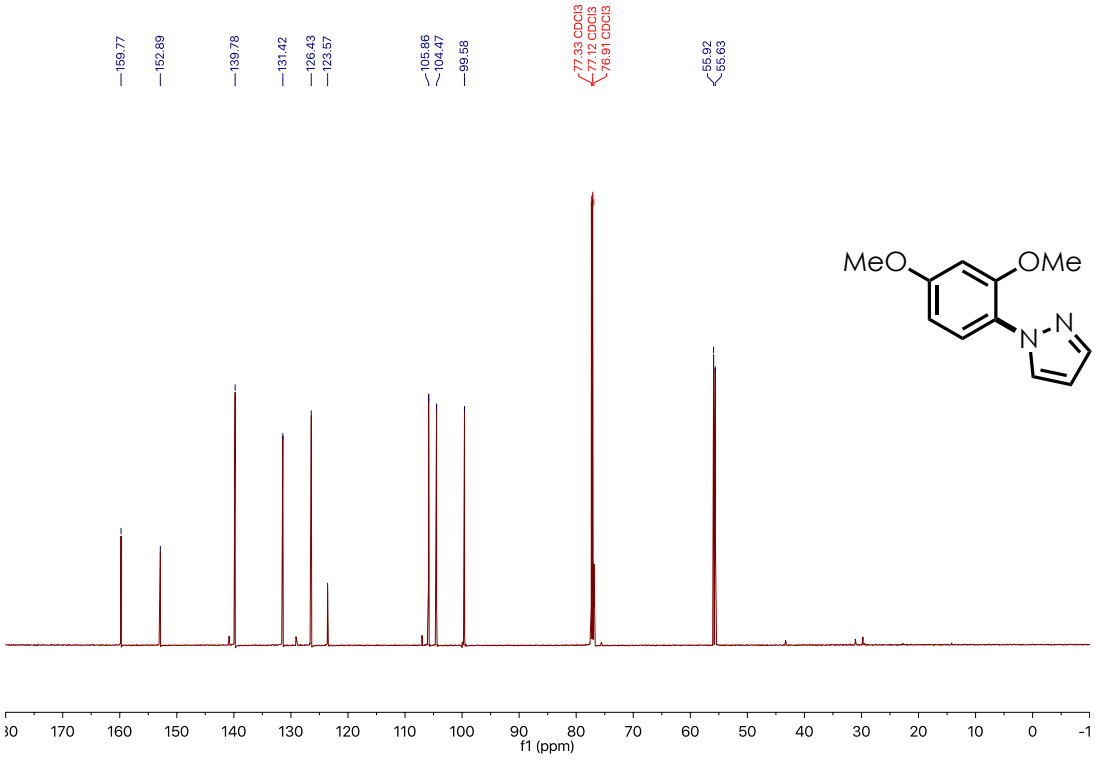
159.77
152.89
139.78
131.42
126.43
123.57
105.86
104.47
99.58
77.33 CDCl3
77.12 CDCl3
76.91 CDCl3
55.92
55.63
MeO
OMe
N
N
f1 (ppm)

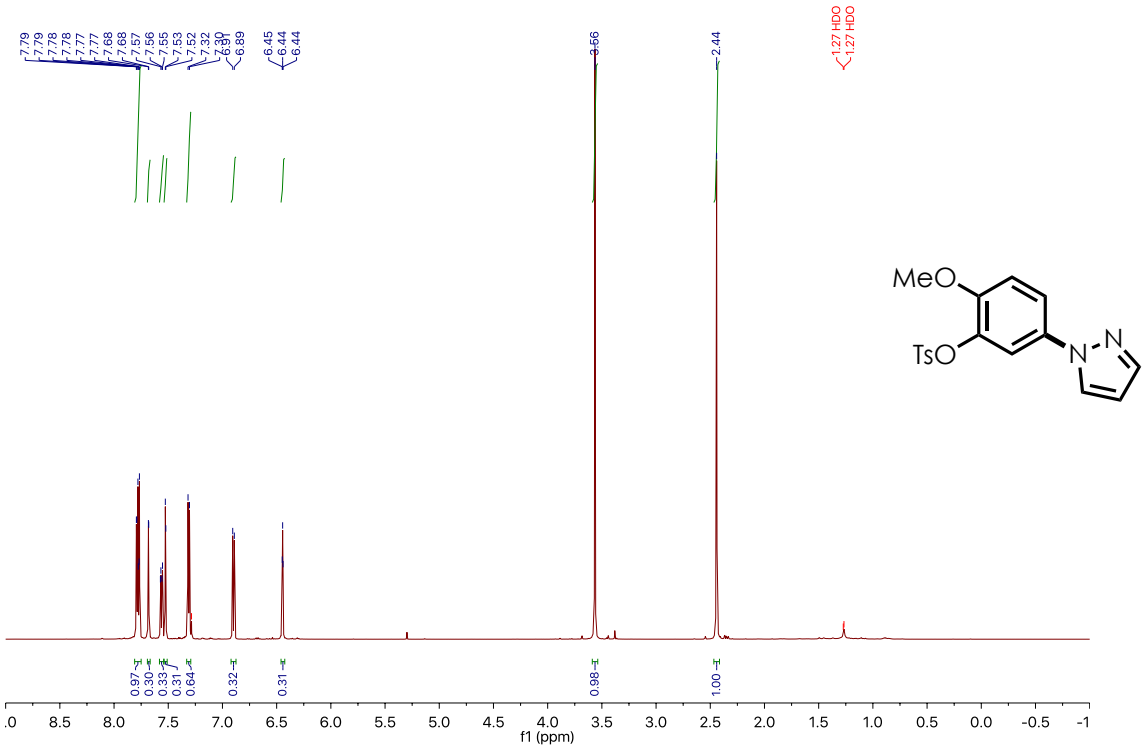
7.79
7.79
7.78
7.78
7.78
7.77
7.77
7.77
7.68
7.67
7.66
7.65
7.63
7.62
7.32
7.30
6.91
6.89
6.45
6.44
6.44
3.66
2.44
1.27 HDO
1.27 HDO
MeO
TsO
N
N
0.97
0.30
0.33
0.31
0.64
0.32
0.31
0.98
1.00
f1 (ppm)

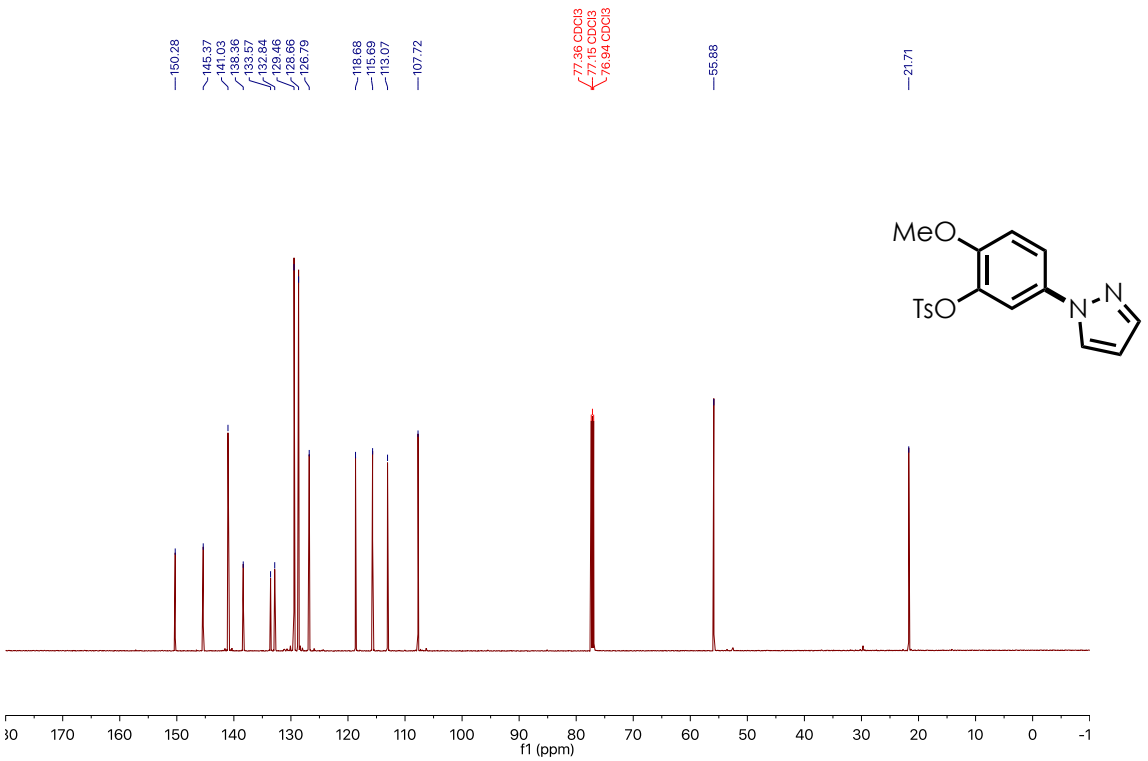
150.28
145.37
141.03
138.36
133.57
132.84
129.46
128.66
126.79
118.68
115.69
113.07
107.72
77.36 CDCl3
77.15 CDCl3
76.94 CDCl3
55.88
21.71
MeO
TsO
N
N
f1 (ppm)

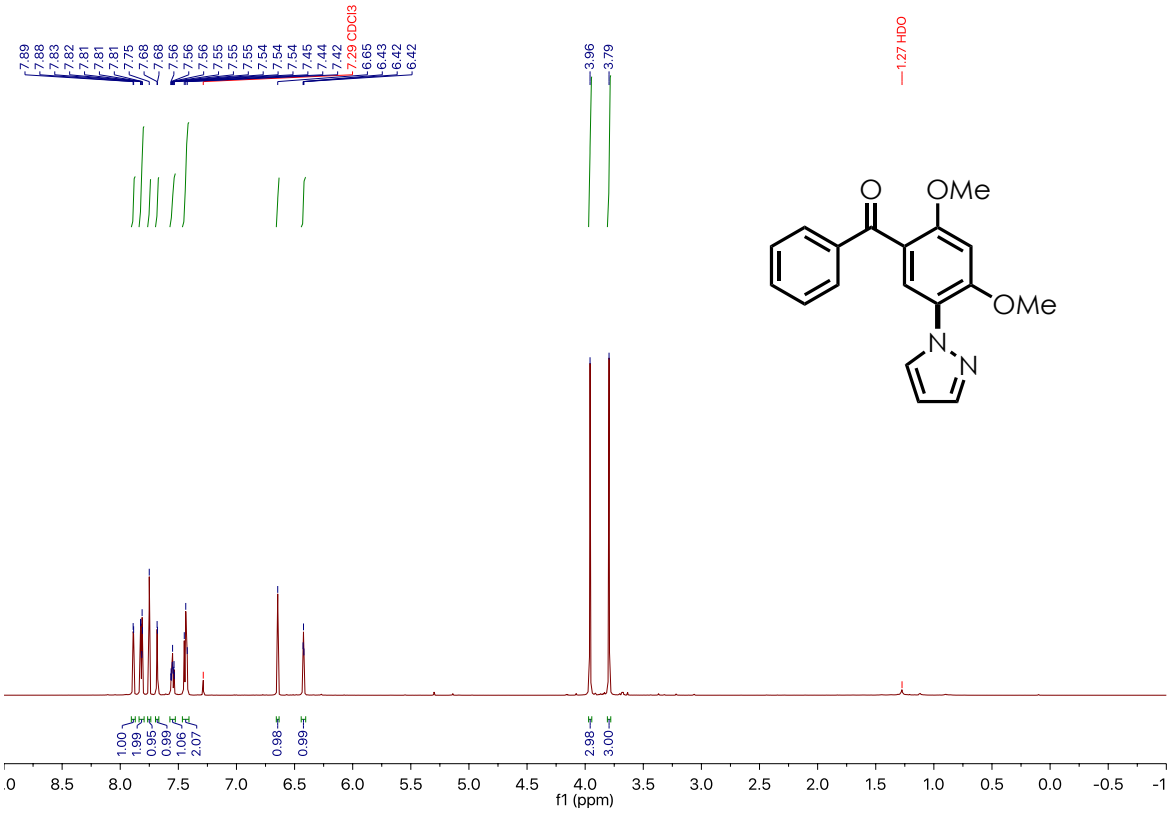
7.89
7.88
7.83
7.82
7.81
7.81
7.81
7.75
7.68
7.68
7.56
7.56
7.56
7.55
7.55
7.55
7.54
7.54
7.54
7.45
7.44
7.42
7.29 CDCl3
6.65
6.43
6.42
6.42
3.96
3.79
1.27 HDO
O
OMe
OMe
N
N
1.00
1.99
0.95
0.99
1.06
2.07
0.98
0.99
2.98
3.00
f1 (ppm)

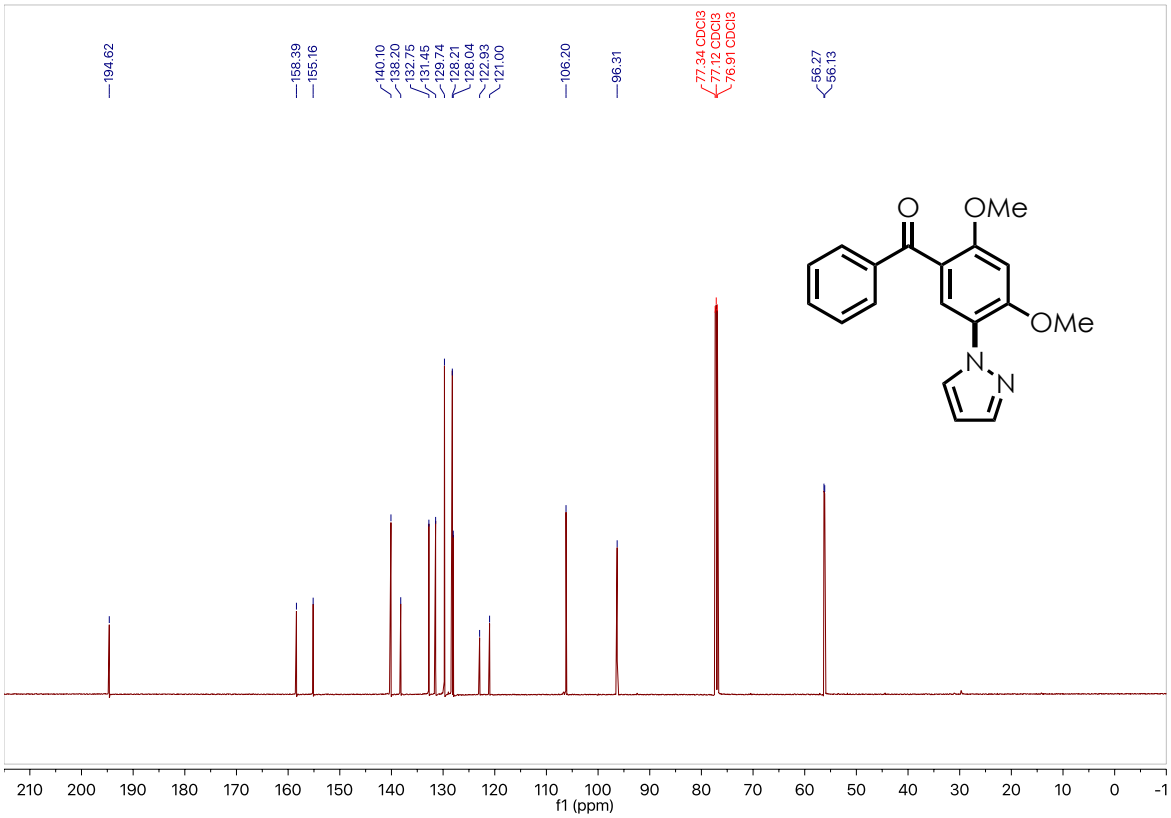
194.62
158.39
155.16
140.10
138.20
132.75
131.45
129.74
128.21
128.04
122.93
121.00
106.20
96.31
77.34 CDCl3
77.12 CDCl3
76.91 CDCl3
56.27
56.13
O
OMe
OMe
N
N
f1 (ppm)

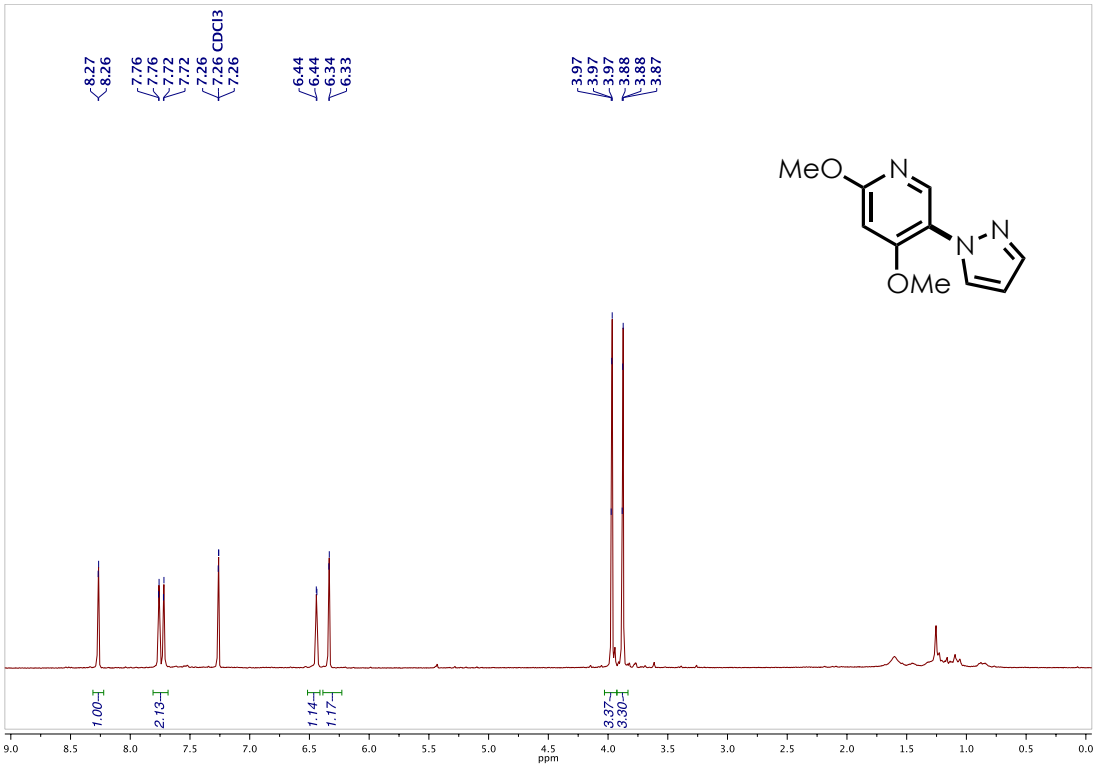
8.27
8.26
7.76
7.76
7.72
7.72
7.26
7.26 CDCl3
7.26
6.44
6.44
6.34
6.33
3.97
3.97
3.97
3.88
3.88
3.87
MeO
N
N
N
OMe
1.00
2.13
1.14
1.17
3.37
3.30
ppm

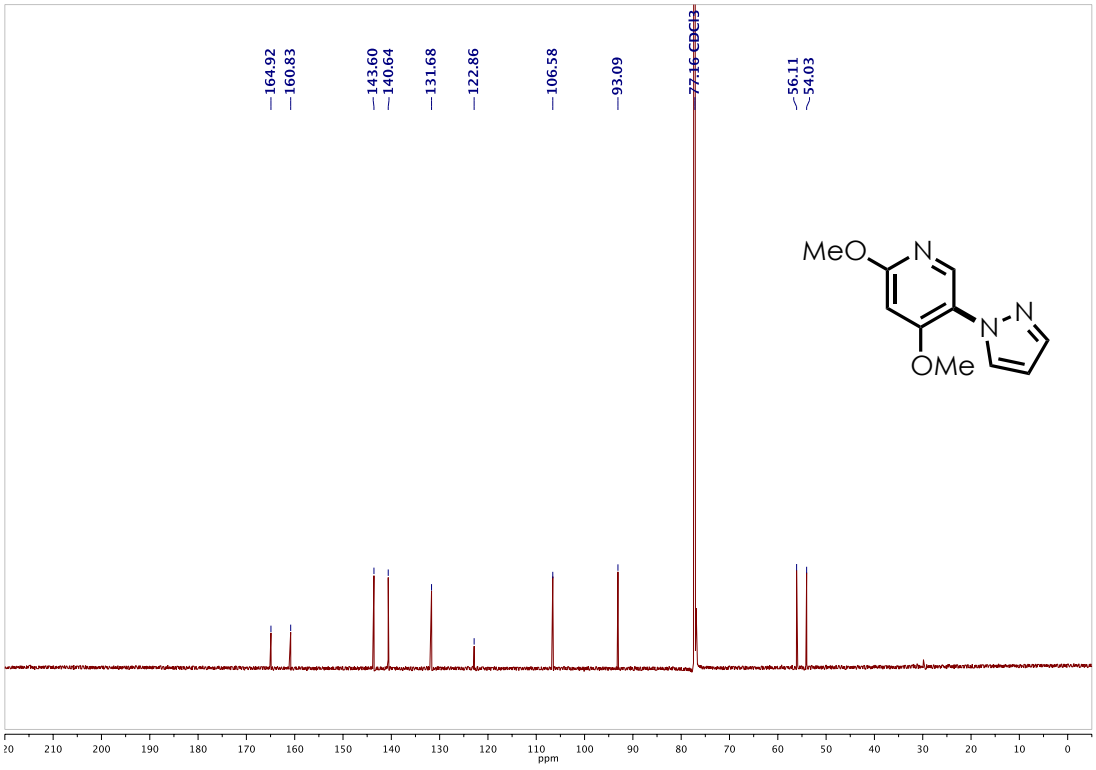
164.92
160.83
143.60
140.64
131.68
122.86
106.58
93.09
77.16 CDCl3
56.11
54.03
MeO
N
N
N
OMe
ppm

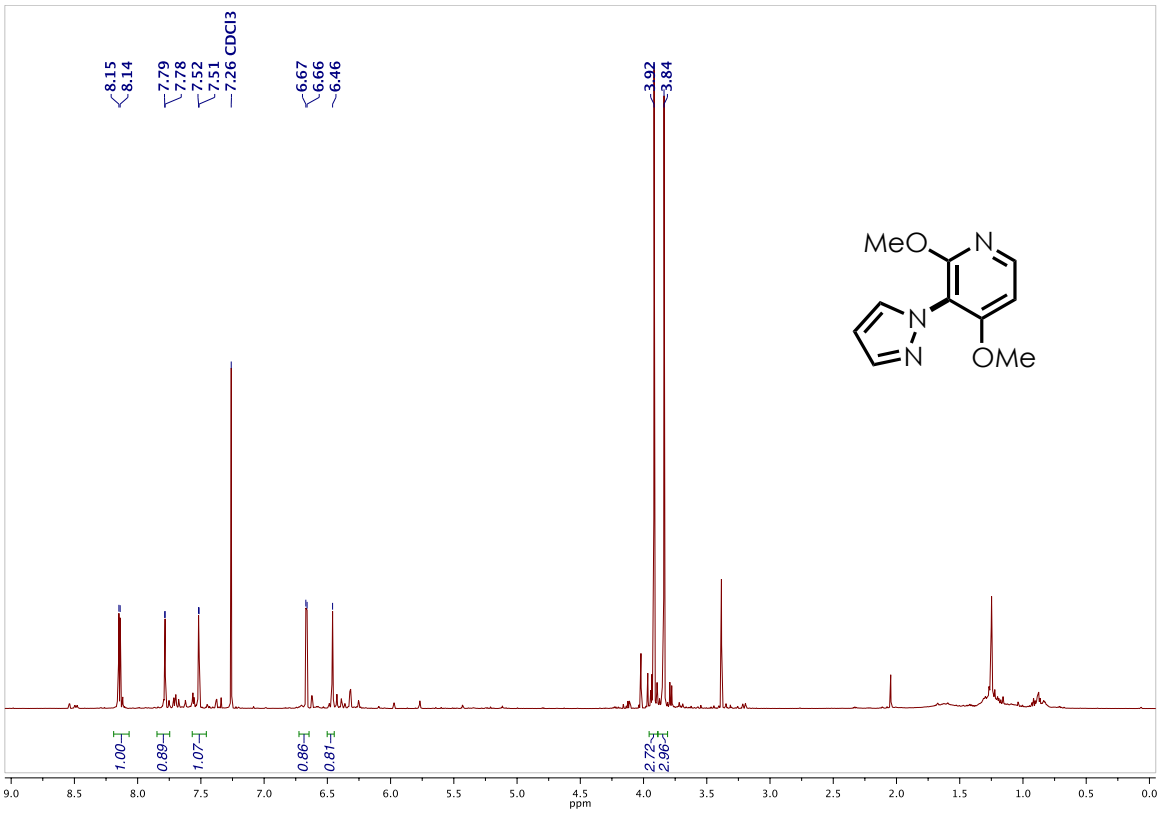
8.15
8.14
7.79
7.78
7.52
7.51
7.26 CDCl3
6.67
6.66
6.46
3.92
3.84
MeO
N
N
N
OMe
1.00
0.89
1.07
0.86
0.81
2.72
2.96
ppm

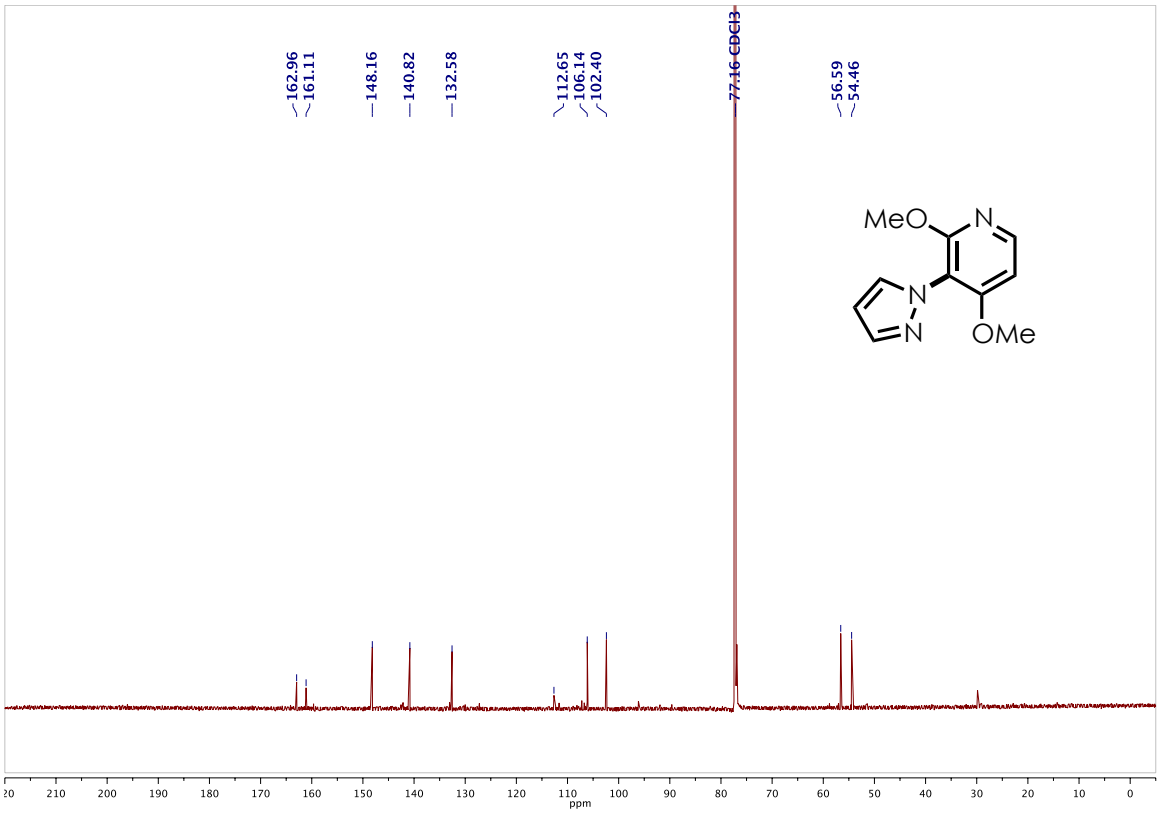
162.96
161.11
148.16
140.82
132.58
112.65
106.14
102.40
77.16 CDCl3
56.59
54.46
MeO
N
N
N
OMe
ppm

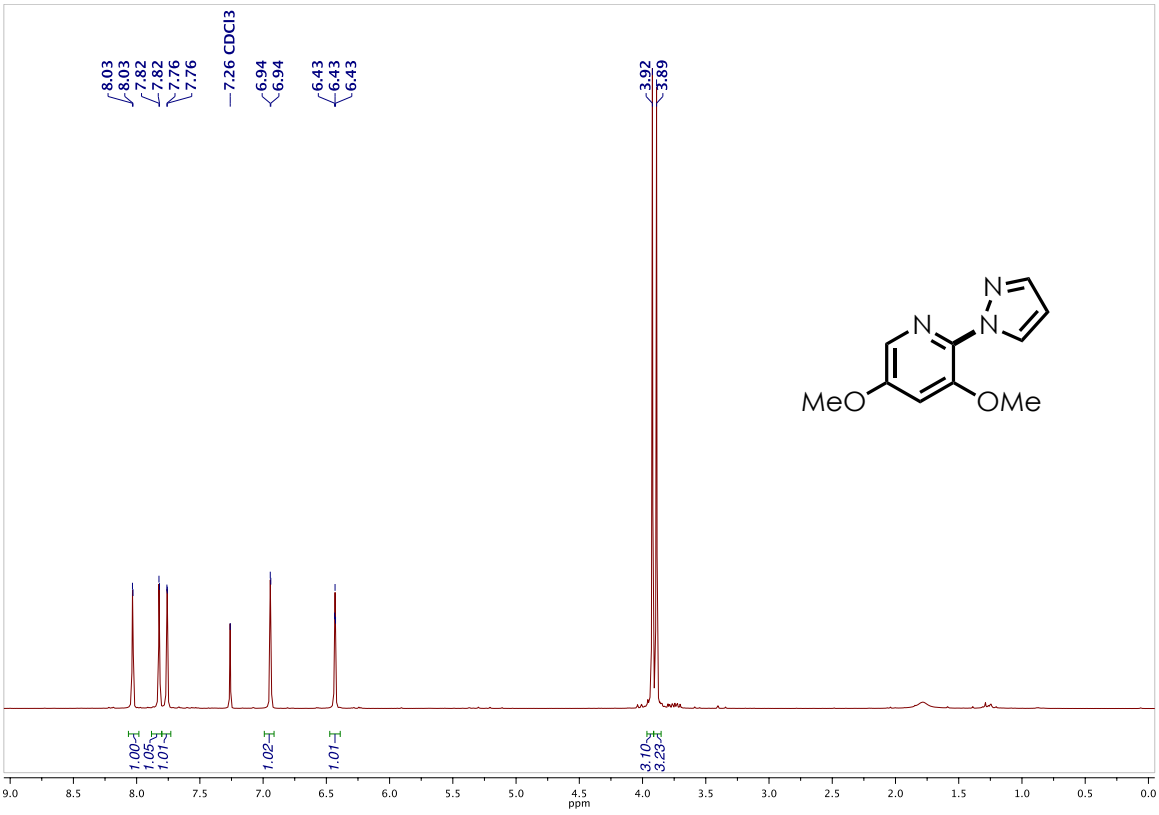
8.03
8.03
7.82
7.82
7.76
7.76
7.26 CDCl3
6.94
6.94
6.43
6.43
6.43
3.92
3.89
1.00
1.05
1.01
1.02
1.01
3.10
3.23
N
N
MeO
OMe
ppm

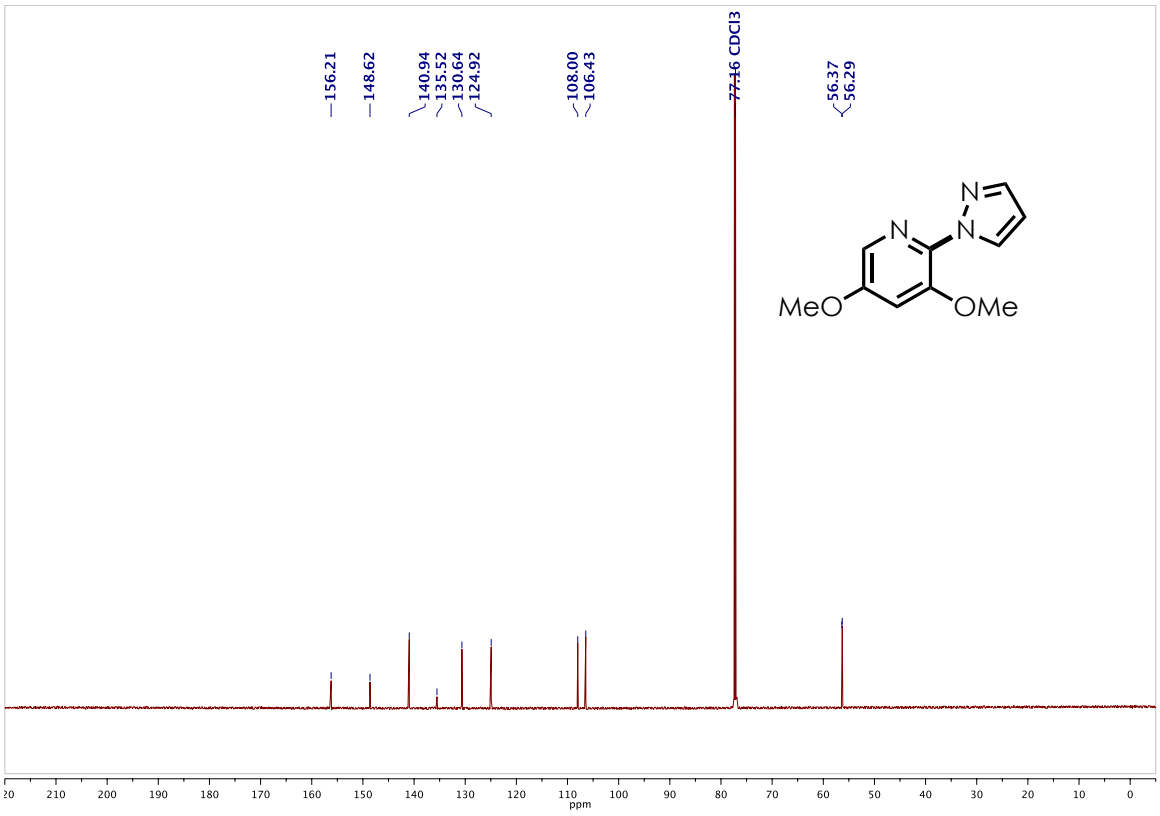
156.21
148.62
140.94
135.52
130.64
124.92
108.00
106.43
77.16 CDCl3
56.37
56.29
N
N
MeO
OMe
ppm

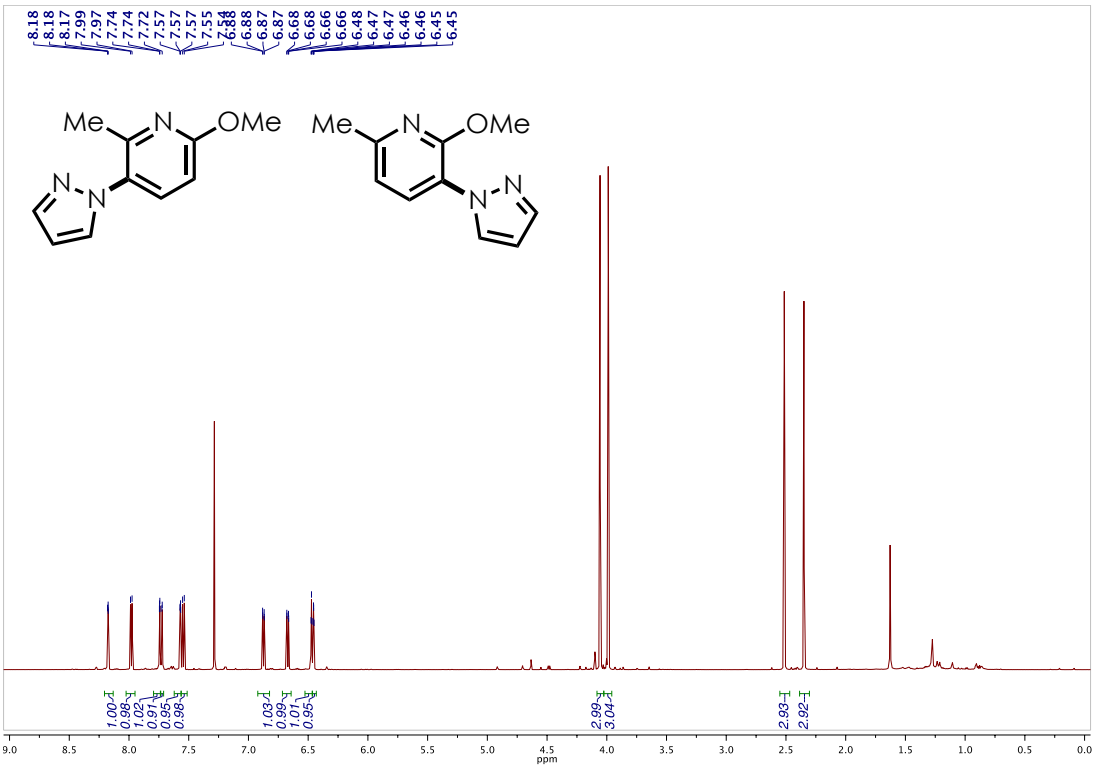
8.18
8.18
8.17
7.99
7.97
7.74
7.74
7.72
7.57
7.57
7.57
7.55
6.88
6.88
6.87
6.87
6.68
6.68
6.66
6.66
6.48
6.47
6.47
6.46
6.46
6.45
6.45
Me
N
OMe
N
N
Me
N
OMe
N
N
1.00
0.98
1.02
0.91
0.95
0.98
1.03
0.99
1.01
0.95
2.99
3.04
2.93
2.92
9.0
8.5
8.0
7.5
7.0
6.5
6.0
5.5
5.0
4.5
4.0
3.5
3.0
2.5
2.0
1.5
1.0
0.5
0.0
ppm

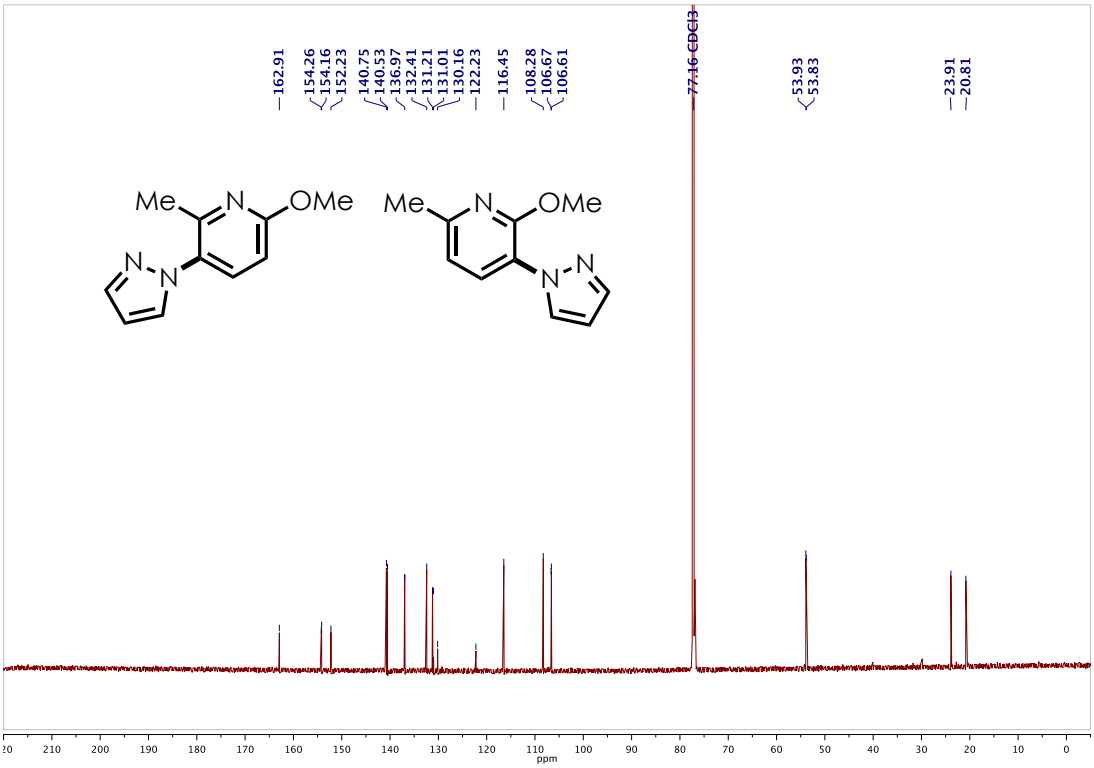
162.91
154.26
154.16
152.23
140.75
140.53
136.97
132.41
131.21
131.01
130.16
122.23
116.45
108.28
106.67
106.61
77.16 CDCl3
53.93
53.83
23.91
20.81
Me
N
OMe
N
N
Me
N
OMe
N
N
210
200
190
180
170
160
150
140
130
120
110
100
90
80
70
60
50
40
30
20
10
0
ppm

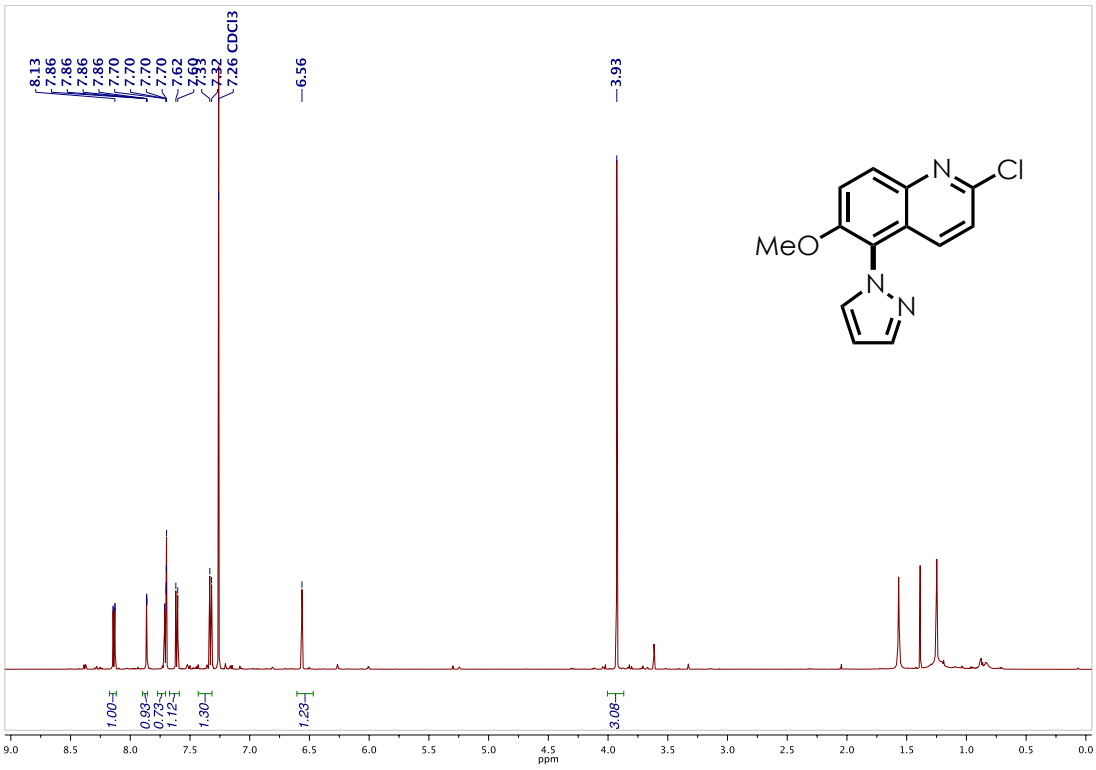
8.13
7.86
7.86
7.86
7.86
7.70
7.70
7.70
7.62
7.60
7.33
7.32
7.26 CDCl3
6.56
3.93
N
Cl
MeO
N
N
1.00
0.93
0.73
1.12
1.30
1.23
3.08
ppm

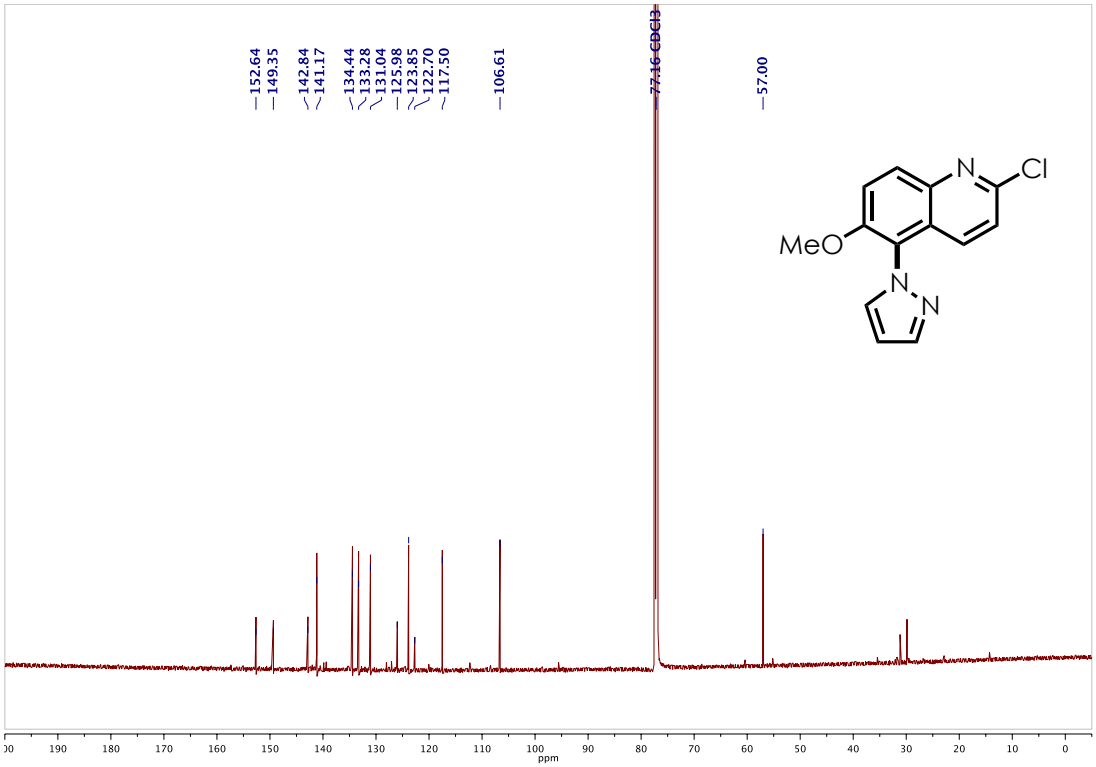
152.64
149.35
142.84
141.17
134.44
133.28
131.04
125.98
123.85
122.70
117.50
106.61
77.16 CDCl3
57.00
N
Cl
MeO
N
N
ppm

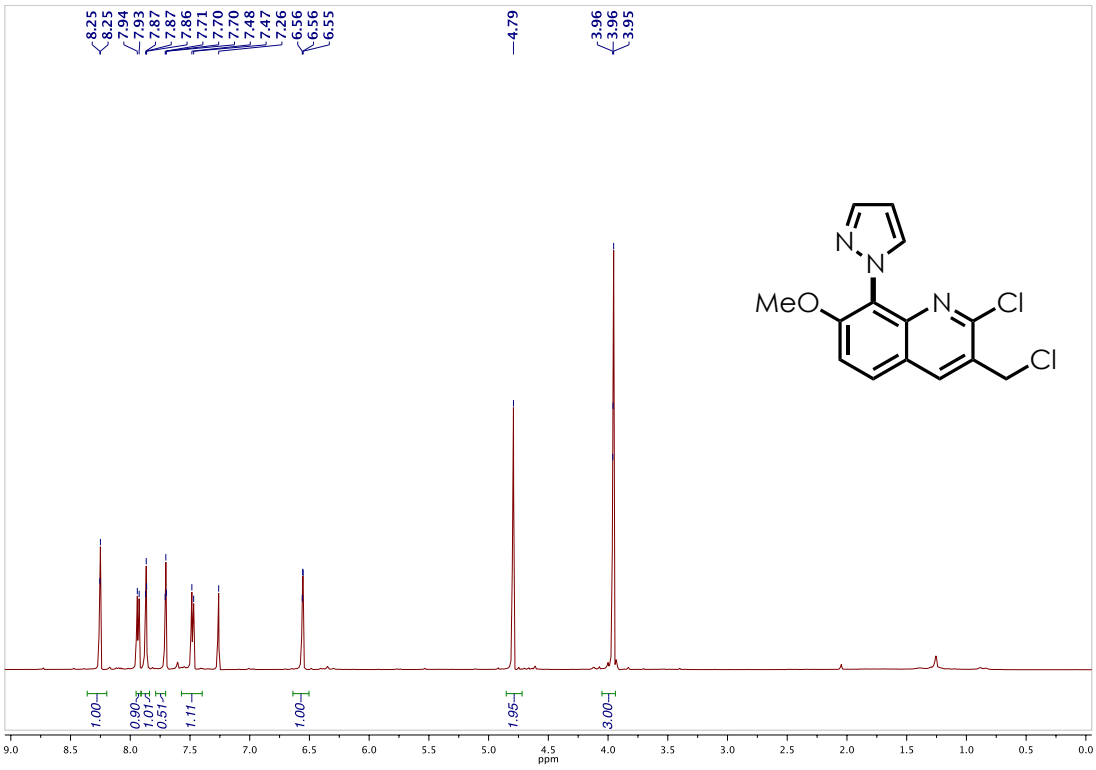
8.25
8.25
7.94
7.93
7.87
7.87
7.86
7.71
7.70
7.70
7.48
7.47
7.26
6.56
6.56
6.55
4.79
3.96
3.96
3.95
1.00
0.90
1.01
0.51
1.11
1.00
1.95
3.00
ppm
MeO
N
Cl
Cl

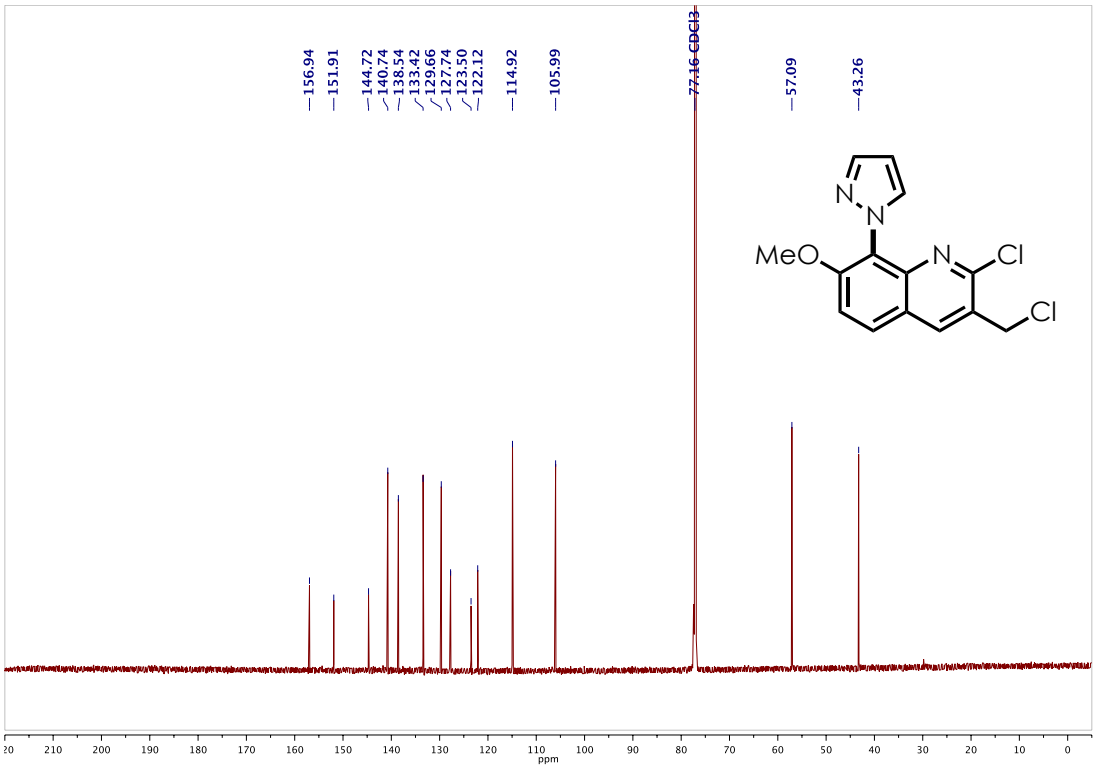
156.94
151.91
144.72
140.74
138.54
133.42
129.66
127.74
123.50
122.12
114.92
105.99
77.16 CDCl3
57.09
43.26
ppm
MeO
N
Cl
Cl

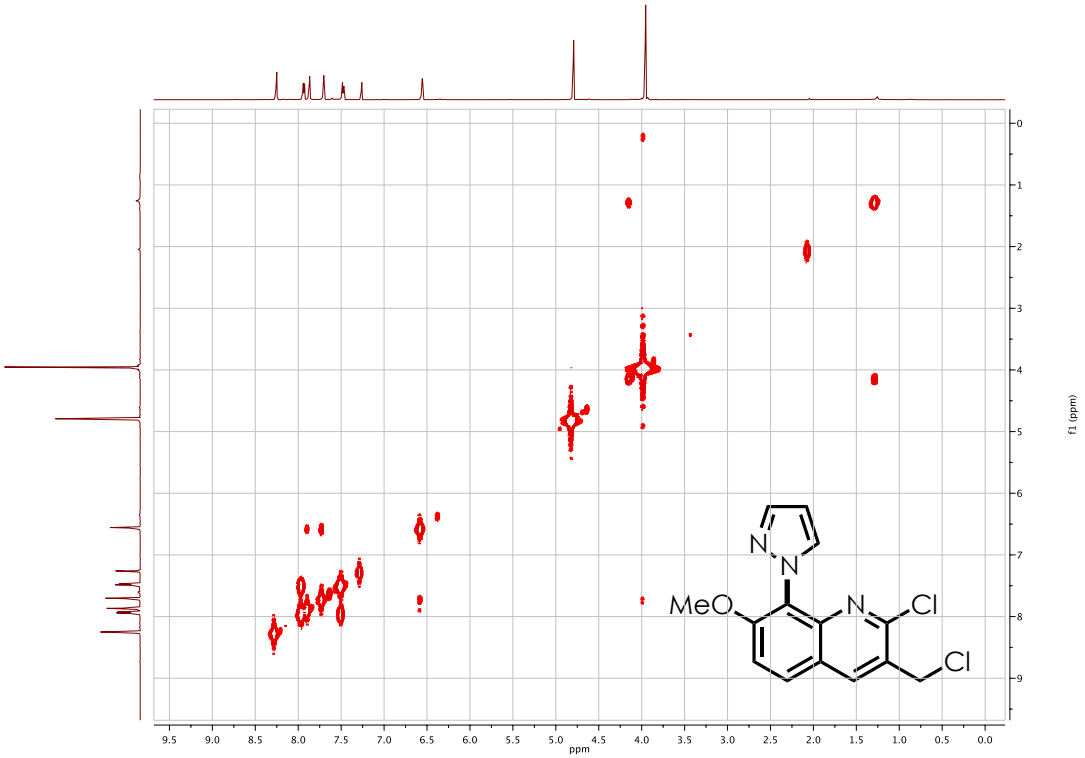
f1 (ppm)
ppm
MeO
N
N
N
Cl
Cl

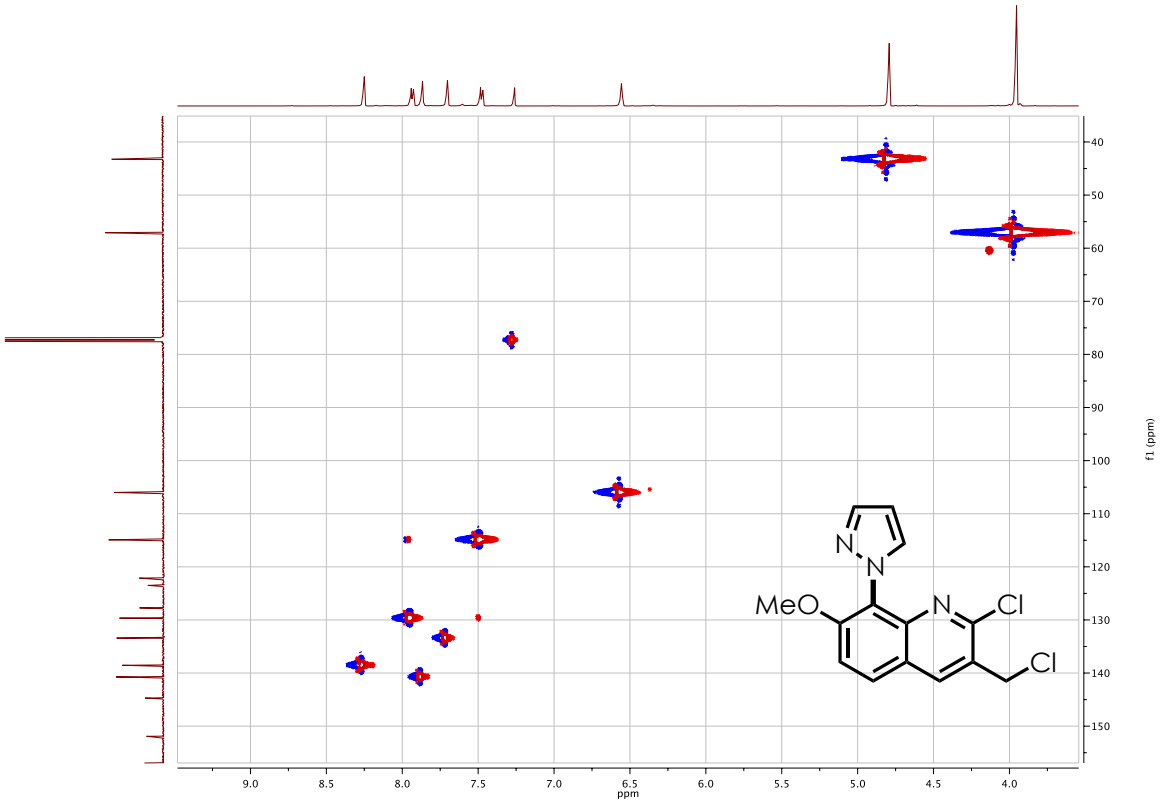
MeO
N
Cl
Cl
ppm
f1 (ppm)

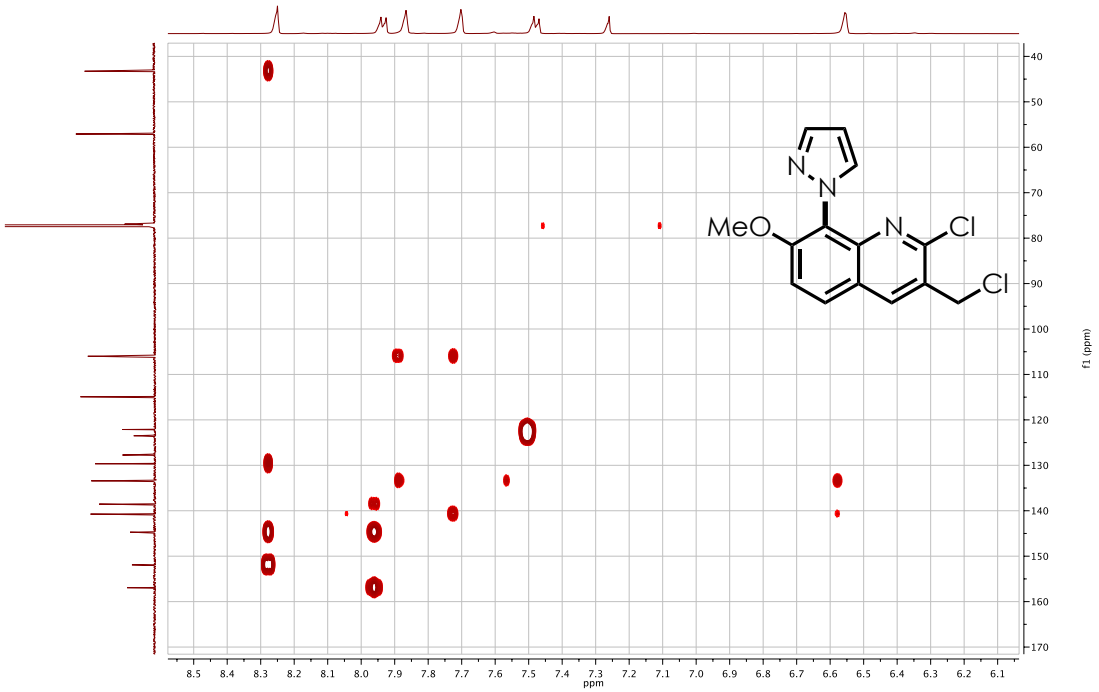
MeO
N
Cl
Cl
ppm
f1 (ppm)

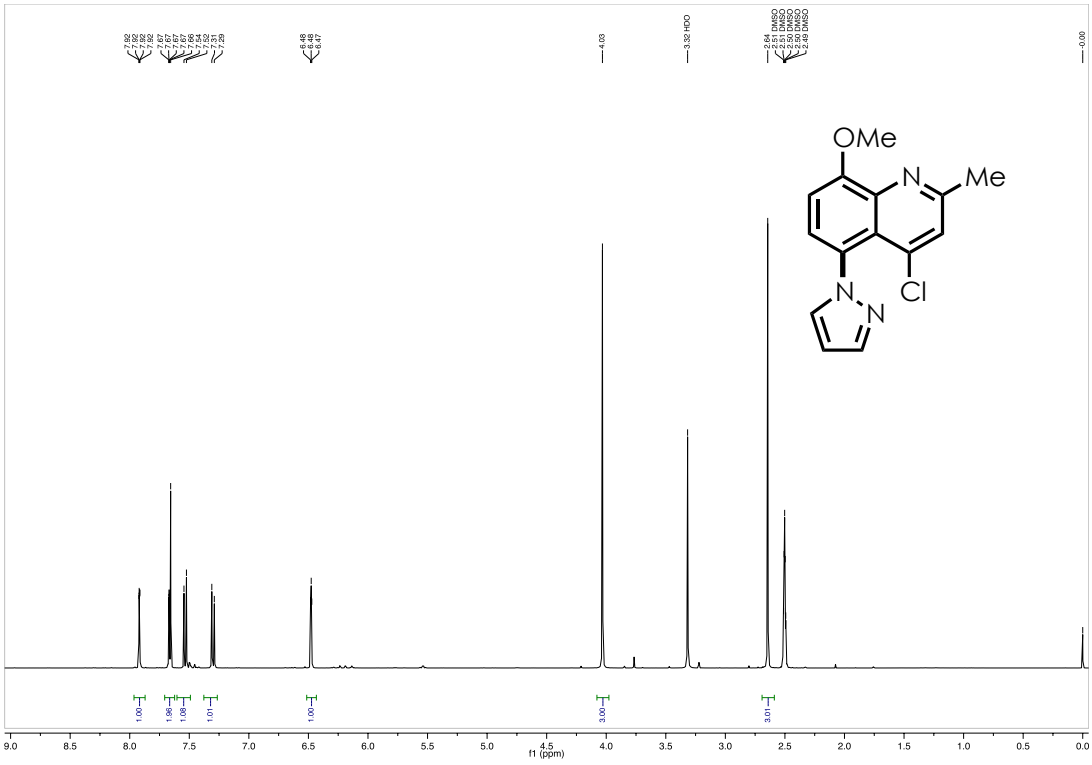
7.92
7.92
7.92
7.92
7.67
7.67
7.67
7.67
7.54
7.54
7.52
7.51
7.29
6.48
6.48
6.47
4.03
3.32 HDO
2.64
2.51 DMSO
2.51 DMSO
2.50 DMSO
2.49 DMSO
0.00
OMe
N
Me
Cl
N
N
1.00
1.96
1.08
1.01
1.00
3.00
3.01
f1 (ppm)

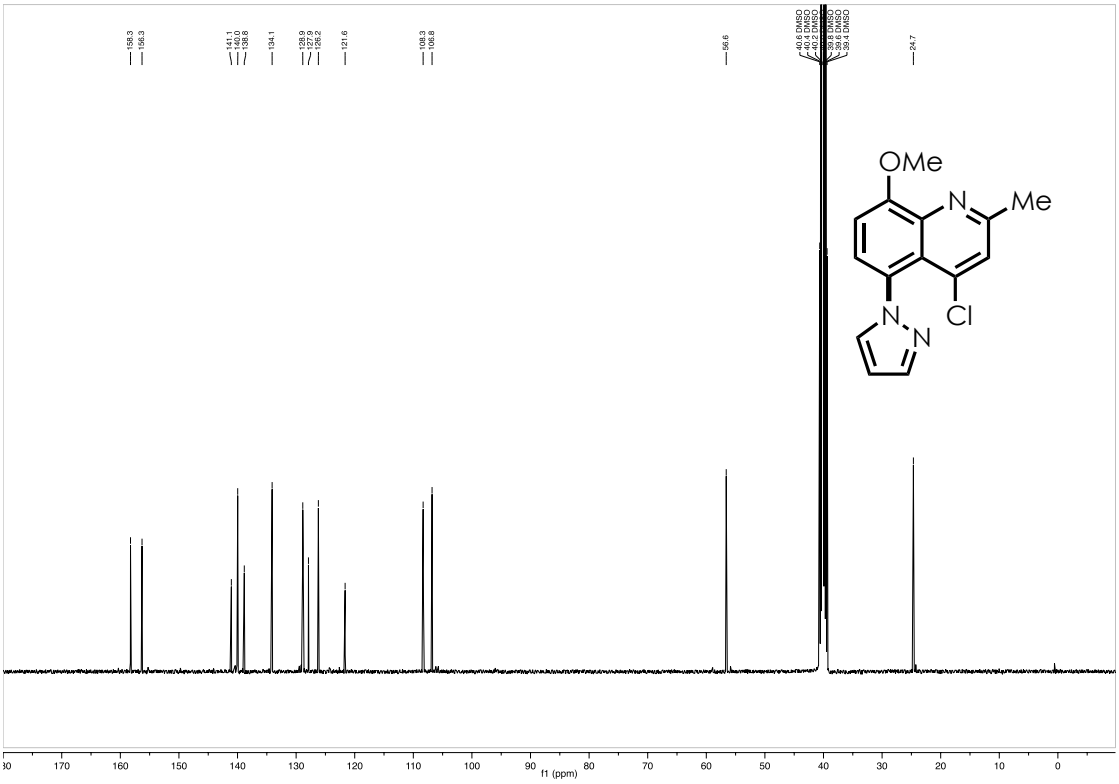
158.3
156.3
141.1
140.0
138.8
134.1
129.9
127.9
126.2
121.6
108.3
106.8
56.6
40.6 DMSO
40.4 DMSO
40.2 DMSO
39.8 DMSO
39.6 DMSO
39.4 DMSO
24.7
OMe
N
Me
Cl
N
N
f1 (ppm)

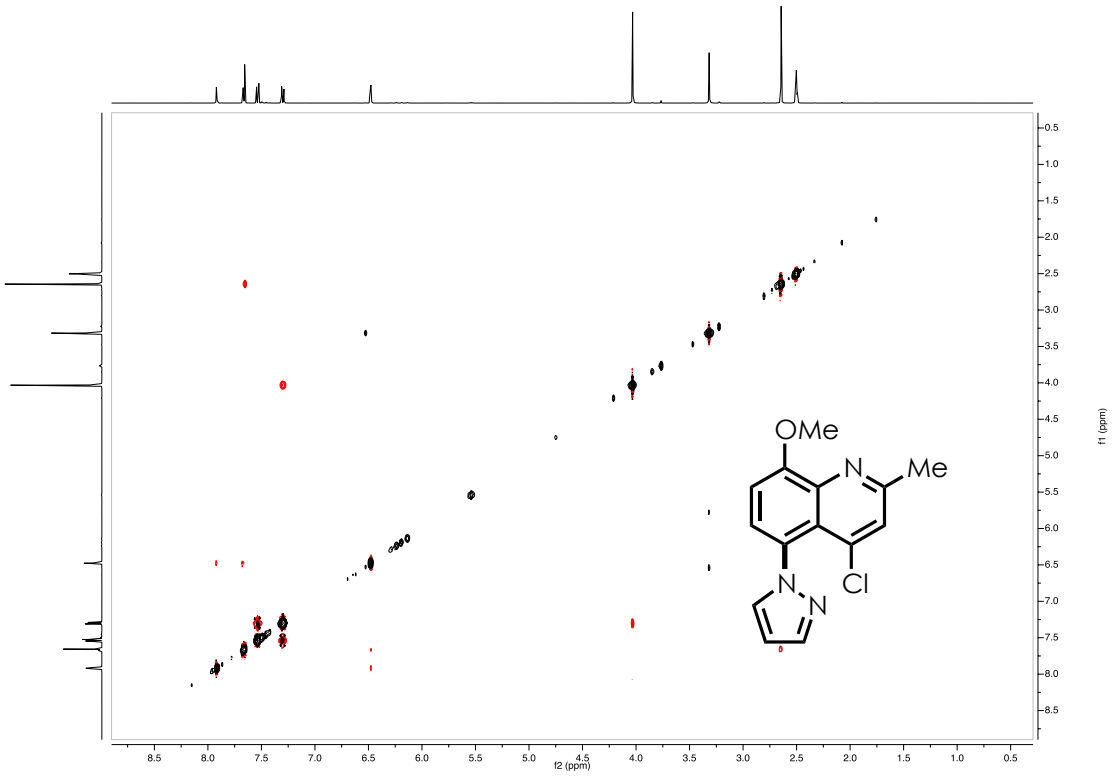
OMe
N
Me
N
N
Cl
f2 (ppm)
f1 (ppm)

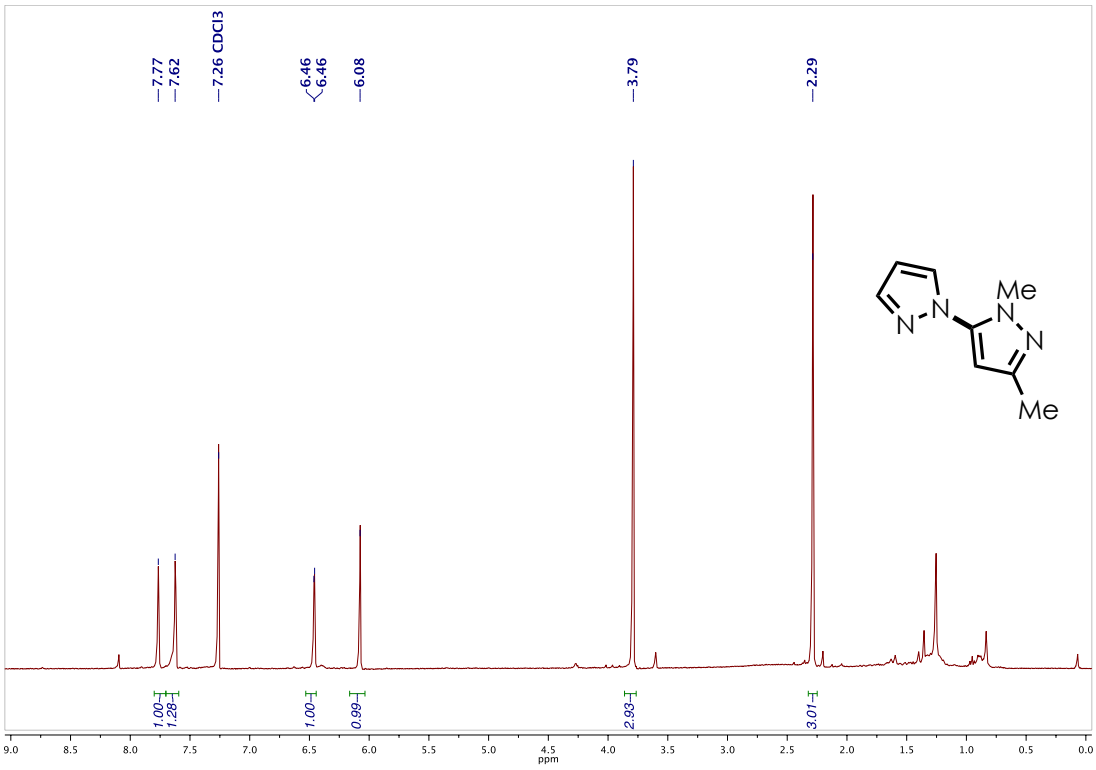
7.77
7.62
7.26 CDCl3
6.46
6.46
6.08
3.79
2.29
Me
N
N
N
Me
1.00
1.28
1.00
0.99
2.93
3.01
ppm

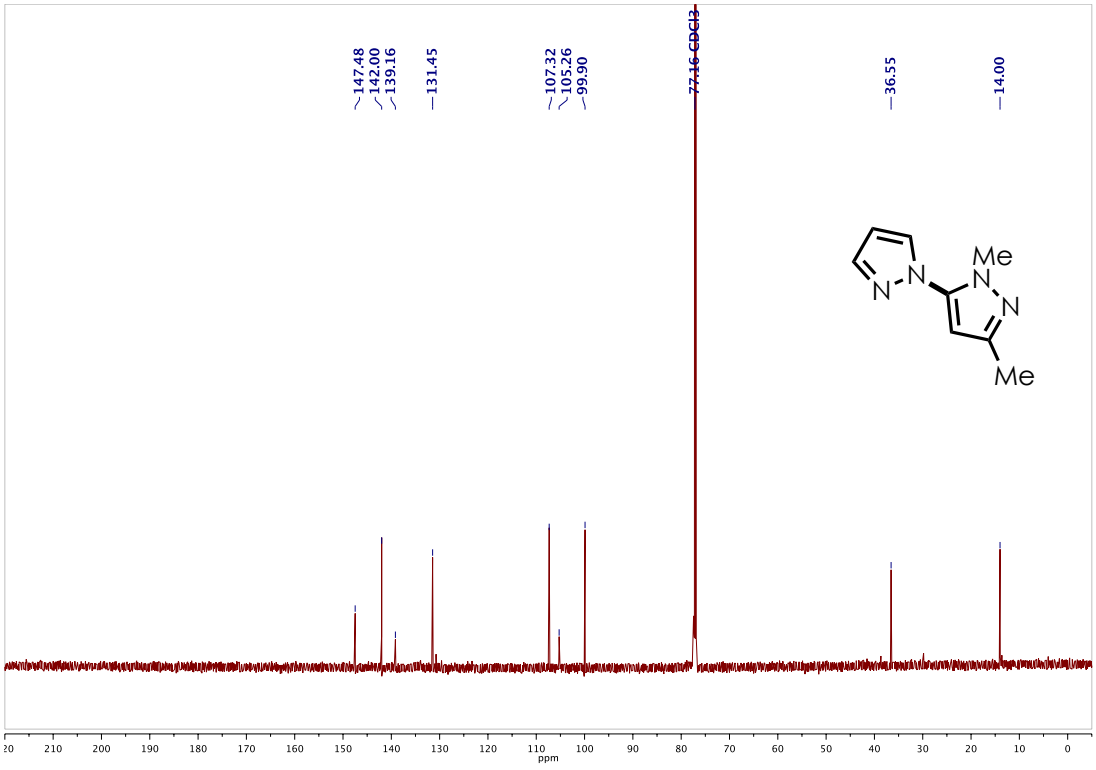
147.48
142.00
139.16
131.45
107.32
105.26
99.90
77.16 CDCl3
36.55
14.00
Me
N
N
N
Me
ppm

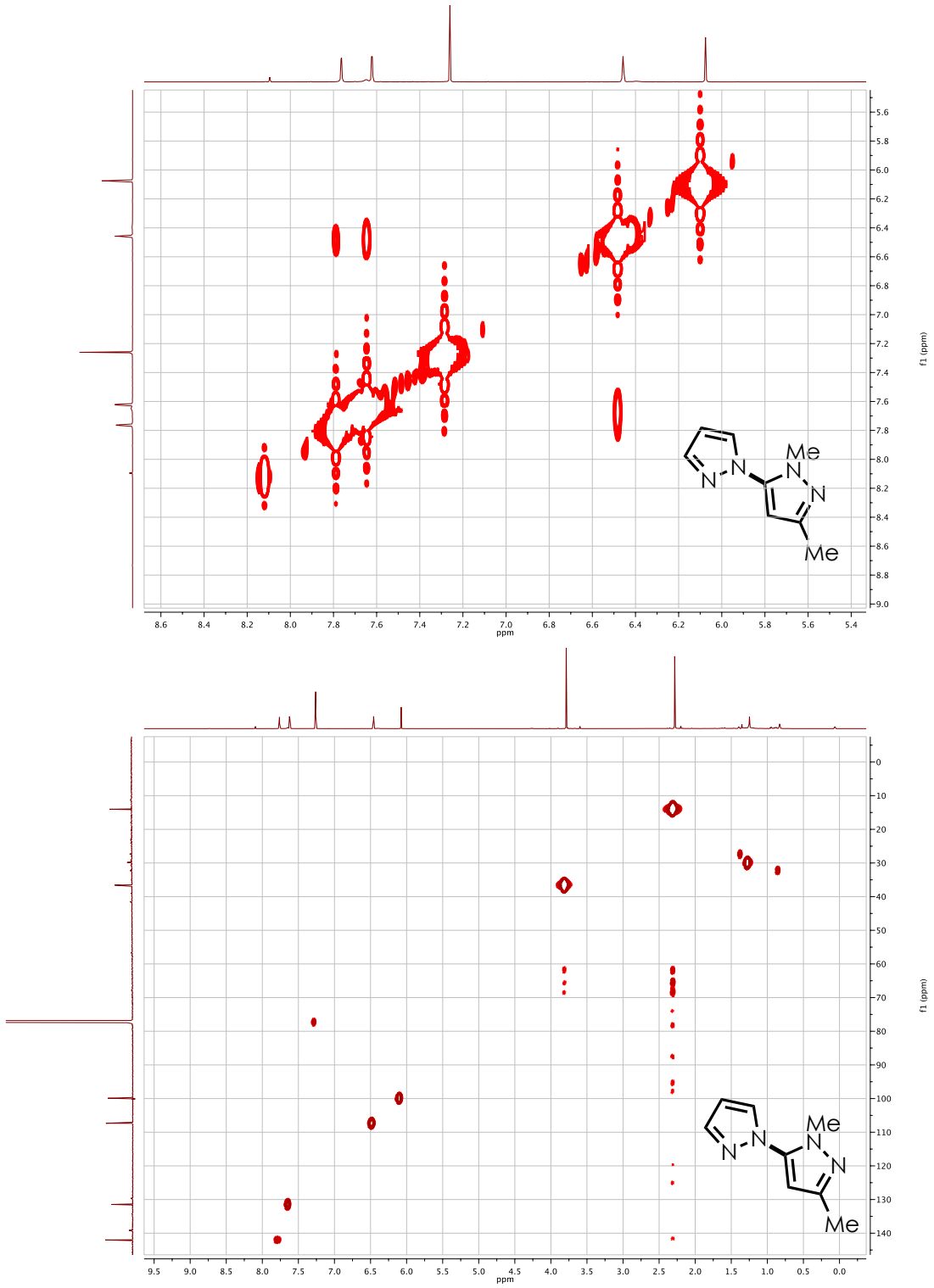
f1 (ppm)
ppm
Me
N
N
N
Me
f1 (ppm)
ppm
Me
N
N
N
Me

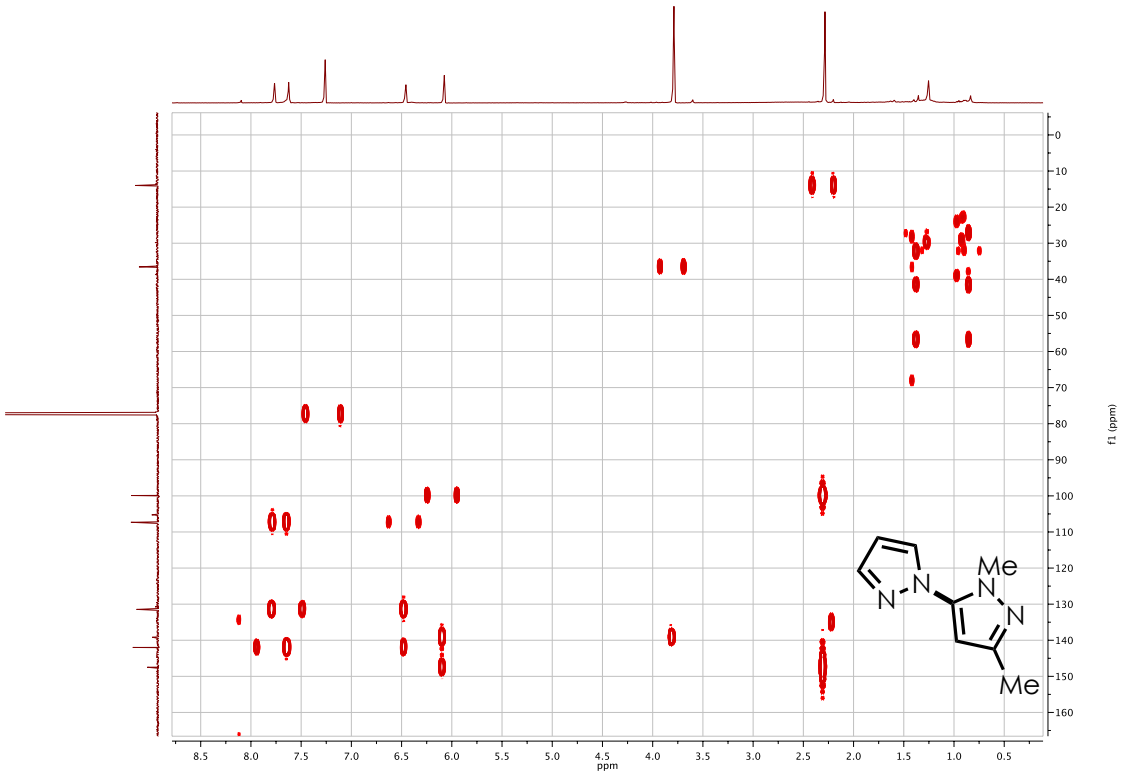
f1 (ppm)
ppm
Me
Me
N
N
N
N

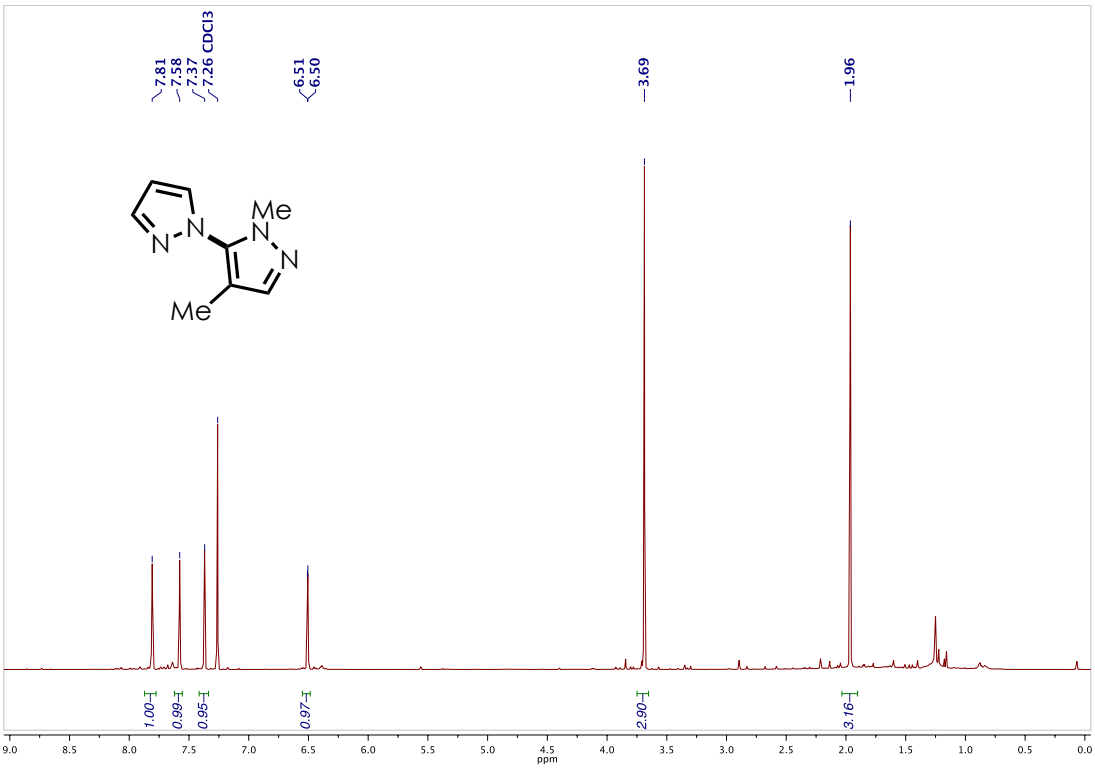
7.81
7.58
7.37
7.26 CDCl3
6.51
6.50
3.69
1.96
Me
N
N
N
Me
1.00
0.99
0.95
0.97
2.90
3.16
ppm

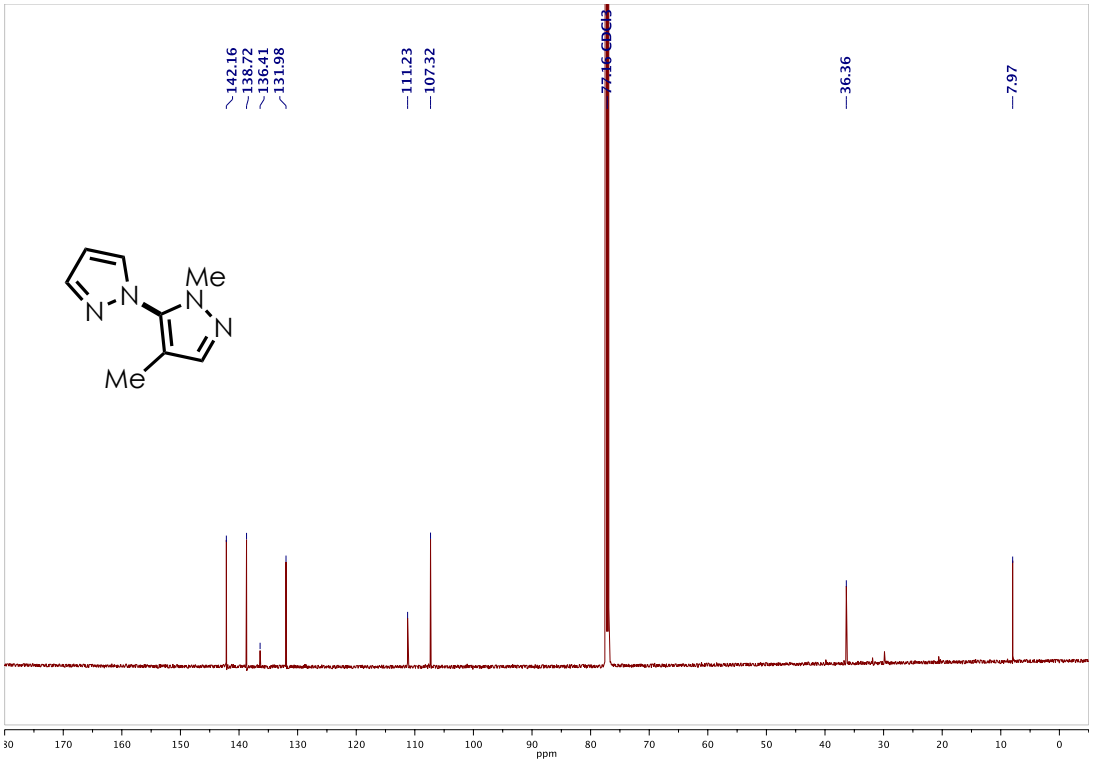
142.16
138.72
136.41
131.98
111.23
107.32
77.16 CDCl3
36.36
7.97
Me
N
N
N
Me
ppm


{7.29,7.26}CDCl3
Me
Me
ppm
f1 (ppm)

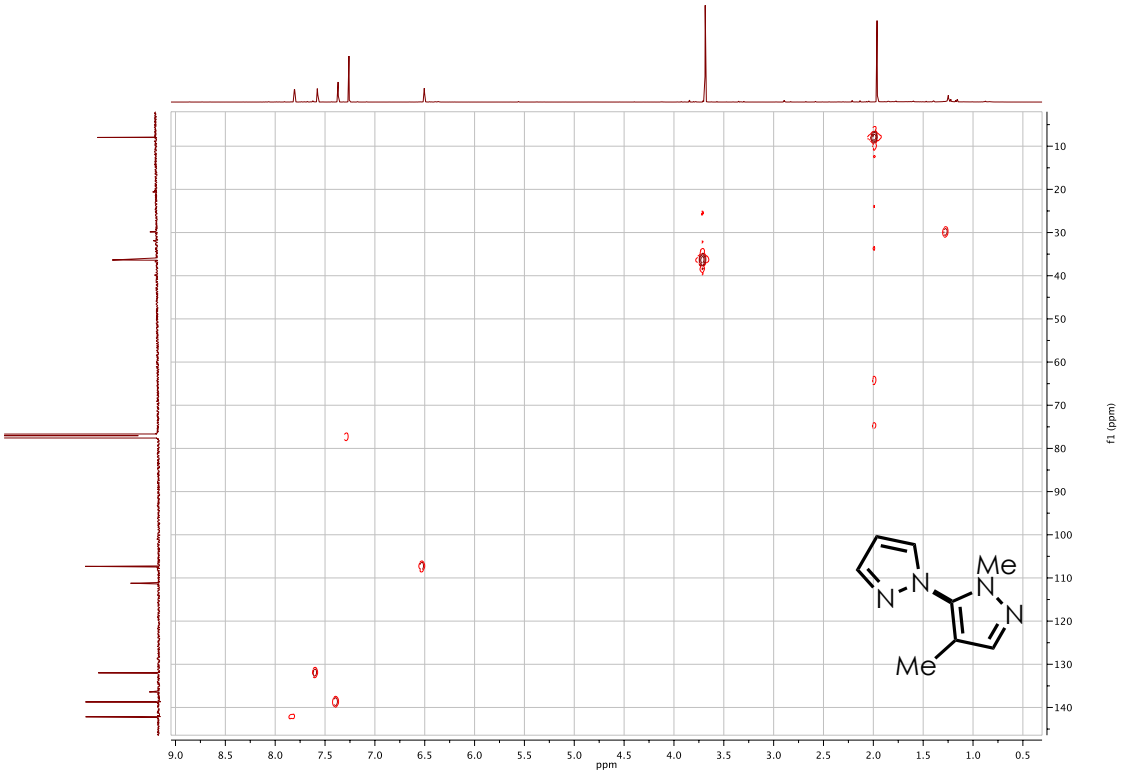
Me
Me
ppm
f1 (ppm)


Me
N
N
N
Me
f1 (ppm)
ppm

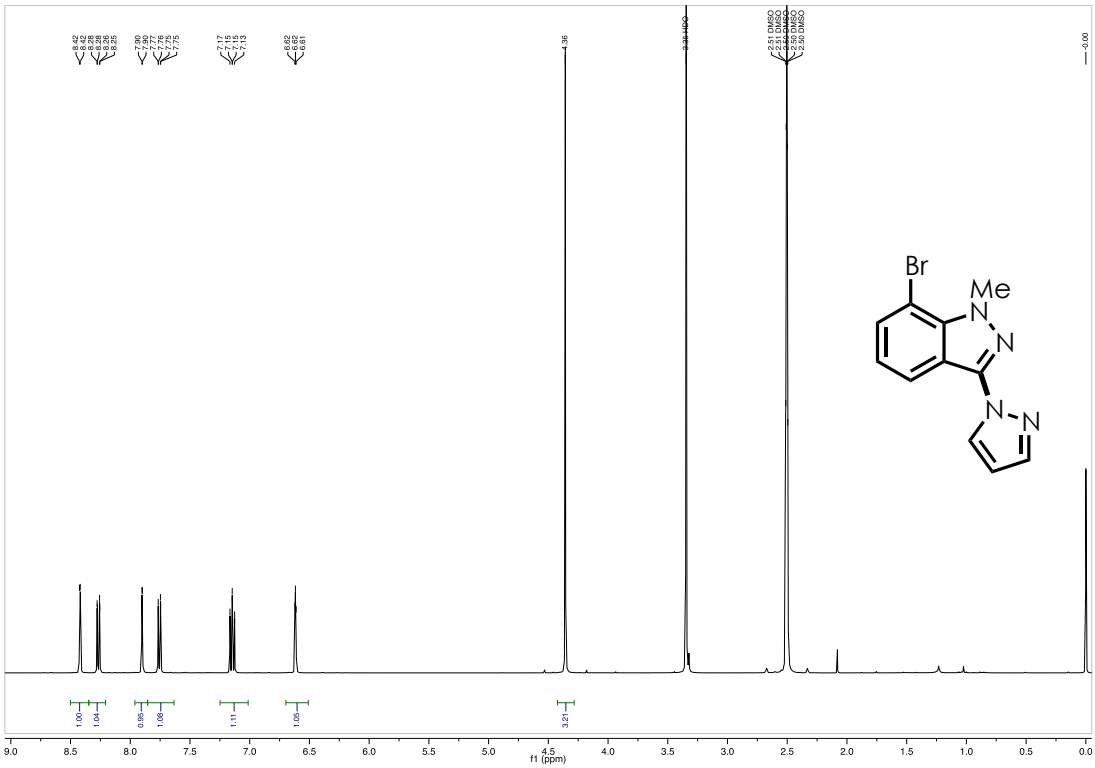
8.42
8.40
8.28
8.26
8.25
7.90
7.77
7.76
7.75
7.17
7.15
7.13
6.82
6.81
4.36
3.31 H2O
2.51 DMSO
2.50 DMSO
0.00
Br
Me
N
N
N
N
1.00
1.04
0.95
1.08
1.11
1.05
3.21
f1 (ppm)

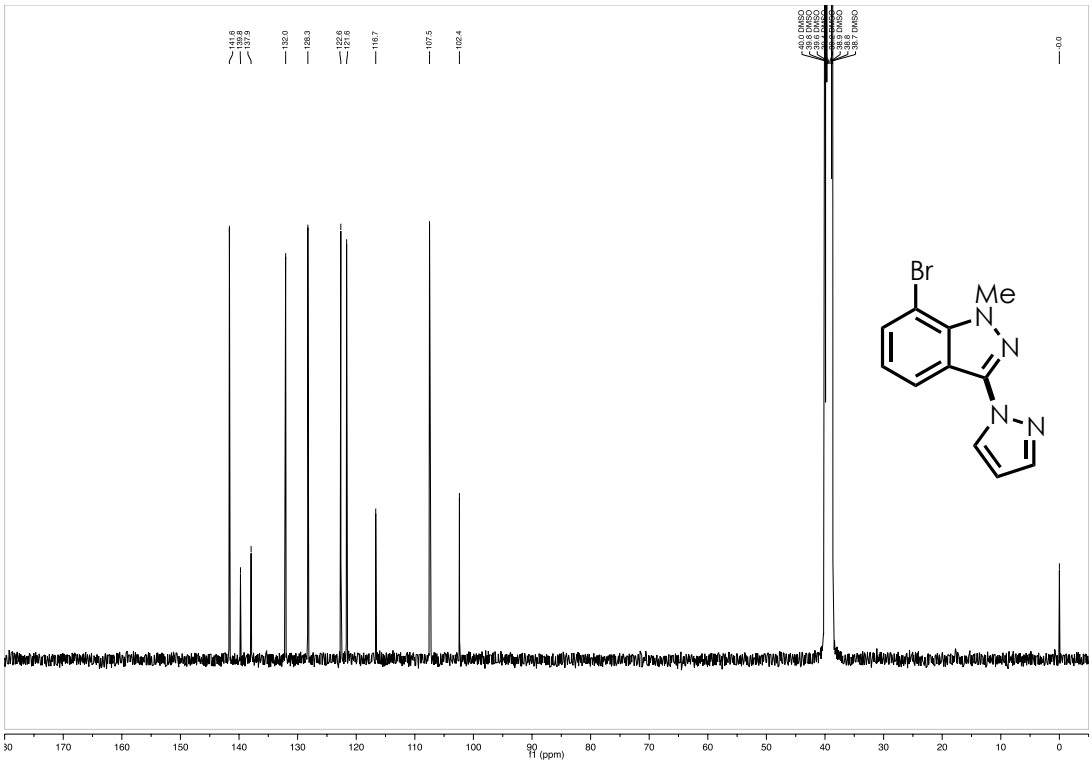
140.8
139.8
137.9
132.0
128.3
122.8
121.6
116.7
107.5
102.4
40.0 DMSO
39.6 DMSO
39.5 DMSO
39.3 DMSO
39.2 DMSO
39.0 DMSO
38.9 DMSO
38.7 DMSO
0.0
Br
Me
N
N
N
N
f1 (ppm)

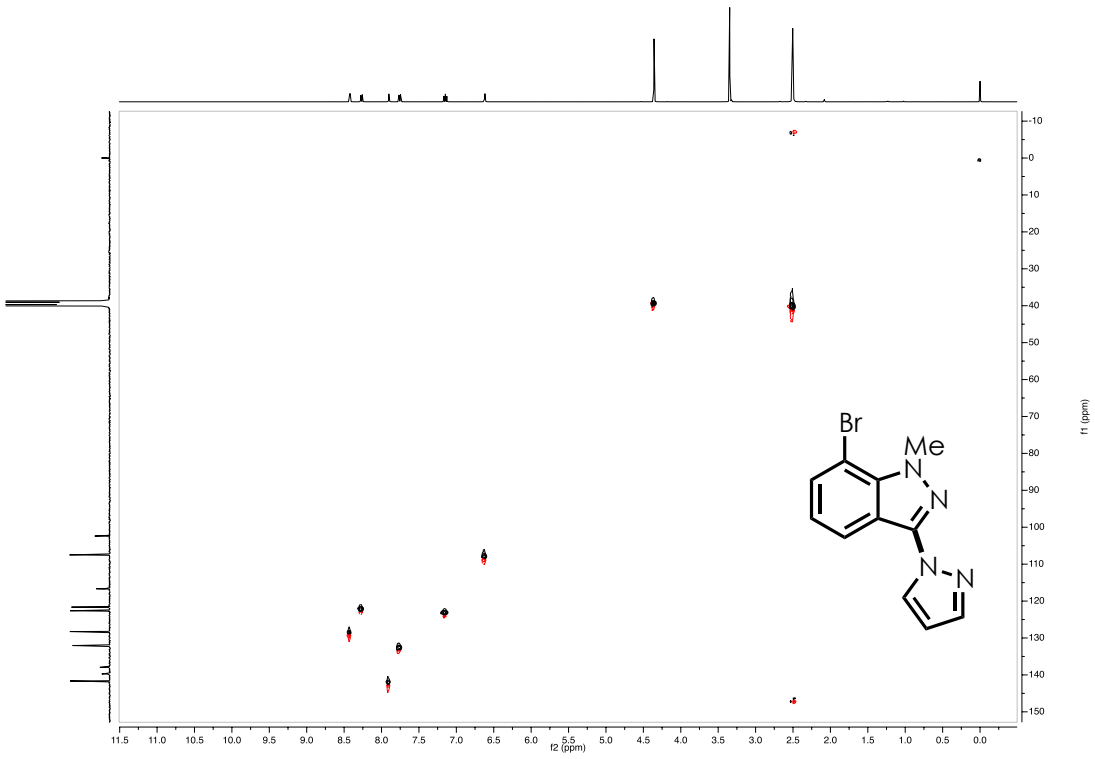
Br
Me
N
N
N
N
f2 (ppm)
f1 (ppm)

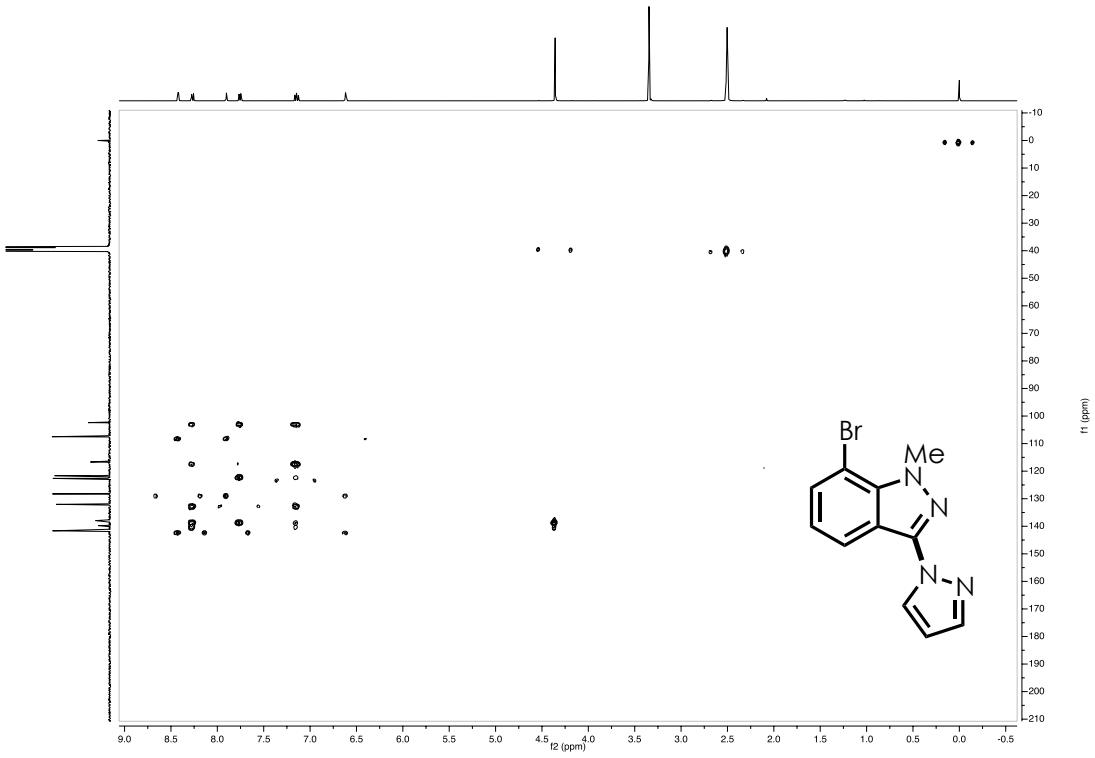
Br
Me
N
N
N
N
f2 (ppm)
f1 (ppm)

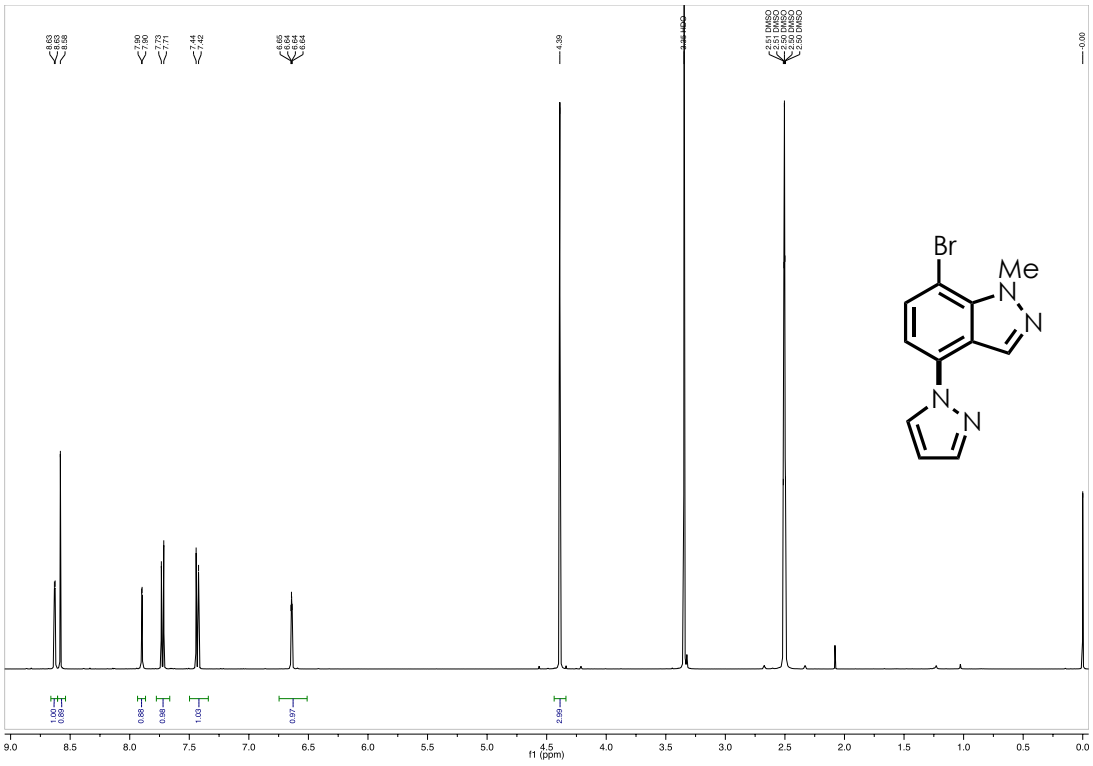
8.63
8.63
8.58
7.90
7.90
7.73
7.71
7.44
7.42
6.65
6.64
6.64
6.64
4.39
3.48 H2O
2.51 DMSO
2.51 DMSO
2.50 DMSO
2.50 DMSO
0.00
1.00
0.88
0.88
0.98
1.03
0.97
2.99
Br
Me
N
N
N
N
f1 (ppm)

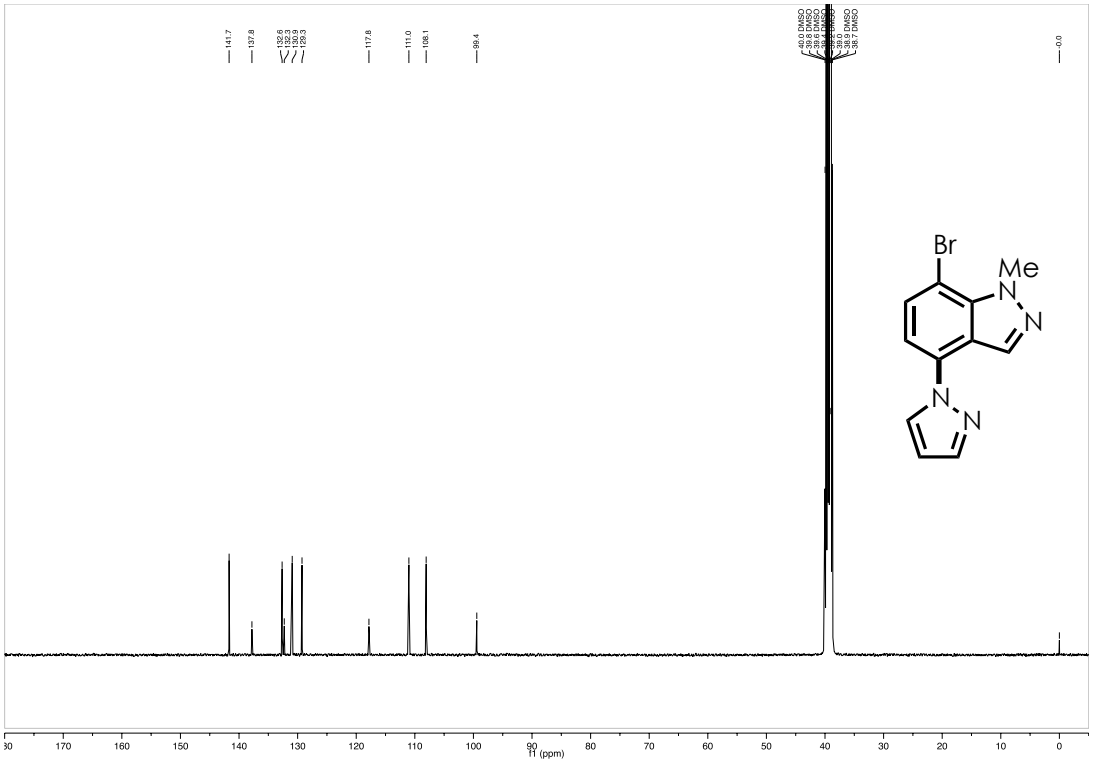
141.7
137.8
132.5
132.1
130.3
129.3
117.8
111.0
108.1
99.4
40.0 DMSO
39.8 DMSO
39.6 DMSO
39.4 DMSO
39.2 DMSO
39.0 DMSO
38.8 DMSO
38.7 DMSO
0.0
Br
Me
N
N
N
N
f1 (ppm)

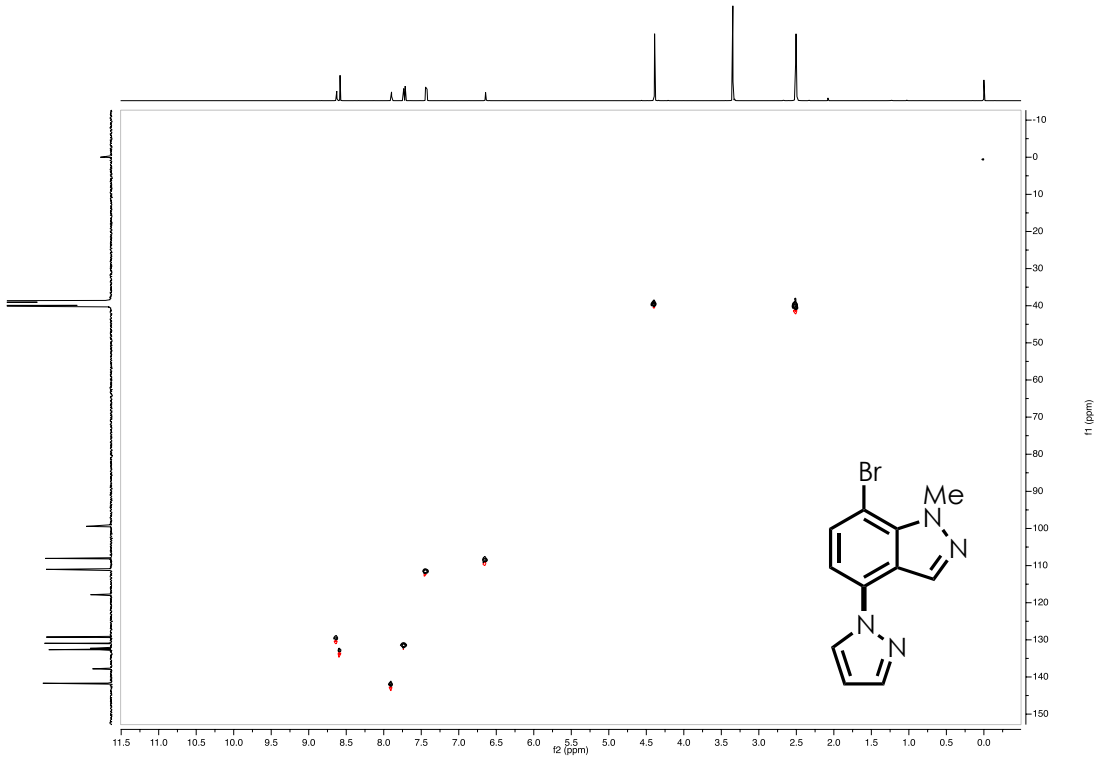
Br
Me
N
N
N
N
f2 (ppm)
f1 (ppm)


Br
Me
N
N
N
N
f2 (ppm)
f1 (ppm)

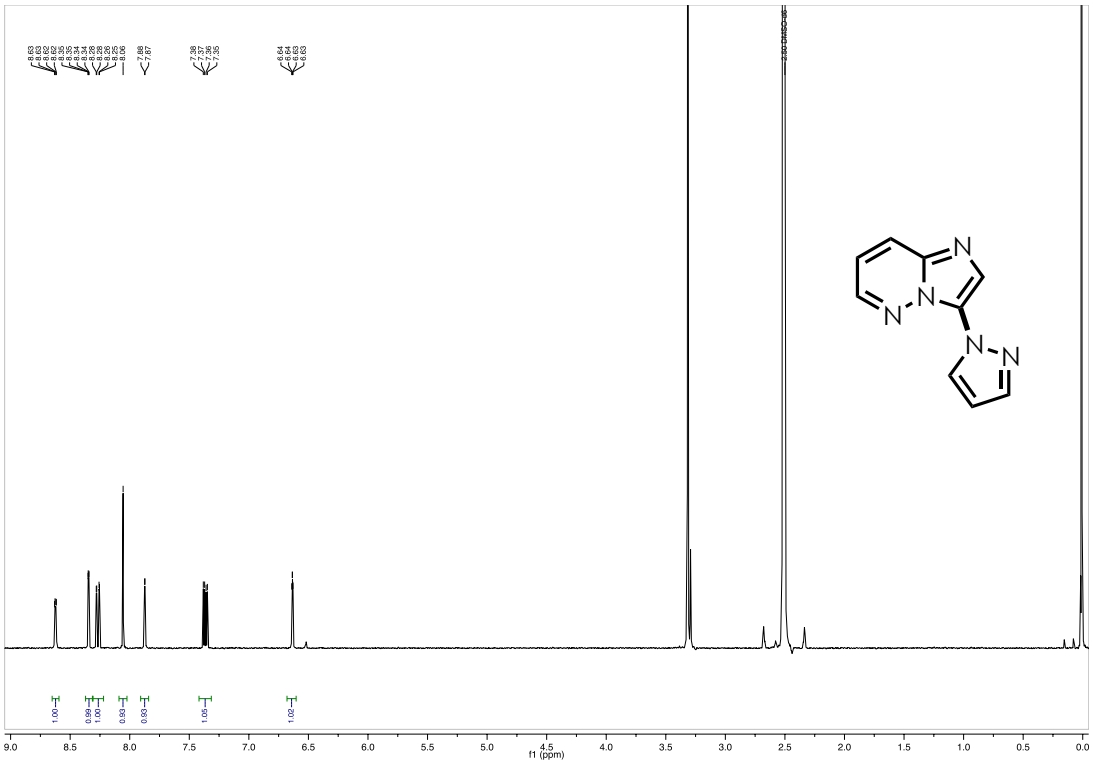
8.63
8.62
8.62
8.52
8.52
8.35
8.34
8.34
8.26
8.26
8.25
8.06
7.88
7.87
7.39
7.39
7.36
7.36
6.64
6.64
6.63
6.63
2.50
1.00
0.99
1.00
0.93
0.93
1.05
1.02
f1 (ppm)

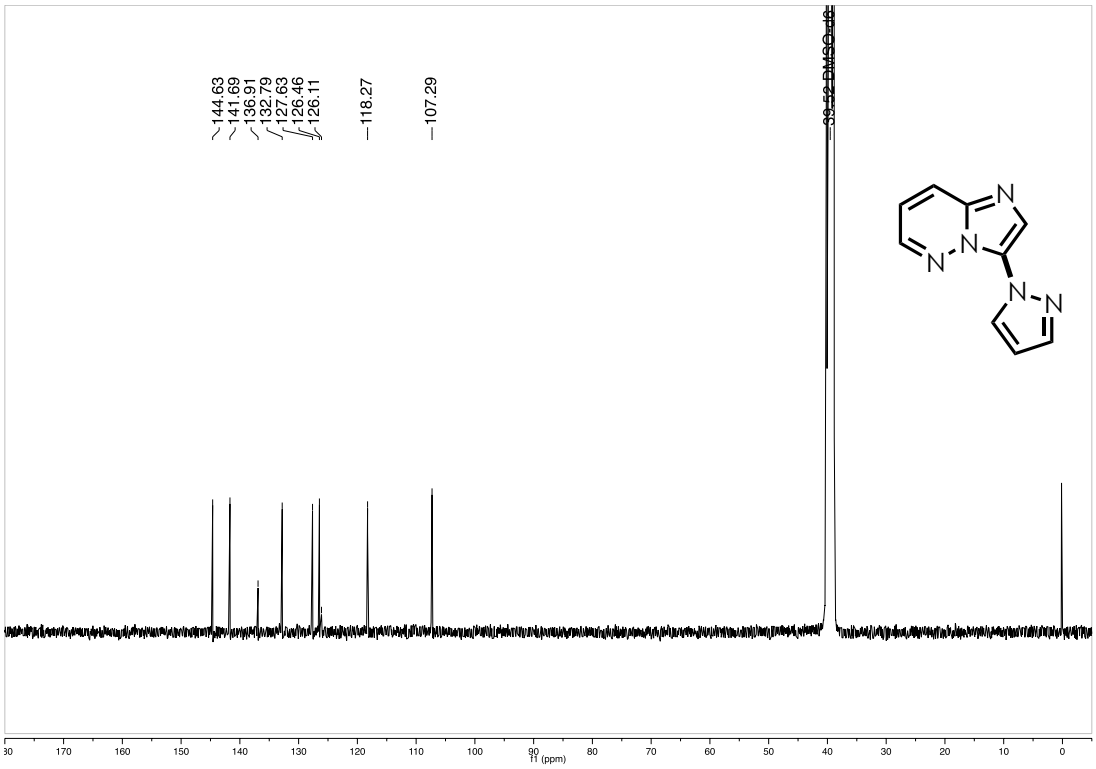
144.63
141.69
136.91
132.79
127.63
126.46
126.11
118.27
107.29
39.52
f1 (ppm)

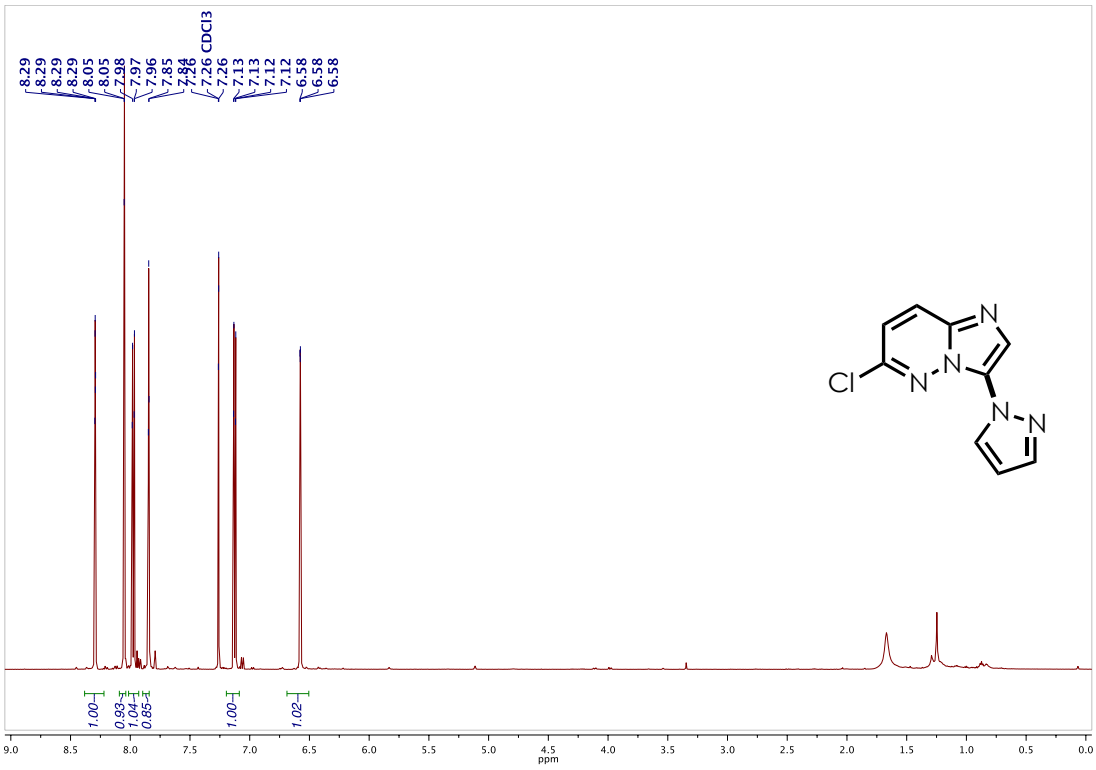
8.29
8.29
8.29
8.29
8.05
8.05
7.98
7.97
7.96
7.85
7.84
7.26 CDCl3
7.26
7.13
7.13
7.12
7.12
6.58
6.58
6.58
1.00
0.93
1.04
0.85
1.00
1.02
ppm
Cl
N
N
N
N
N

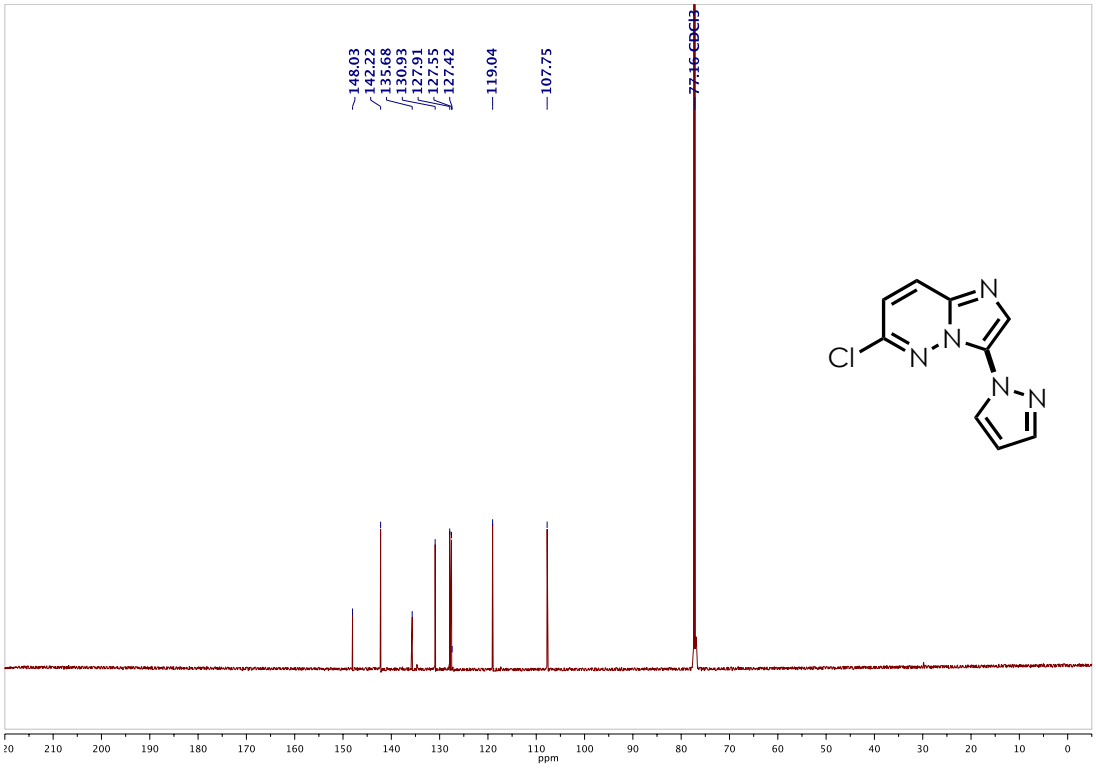
148.03
142.22
135.68
130.93
127.91
127.55
127.42
119.04
107.75
77.16 CDCl3
ppm
Cl
N
N
N
N
N

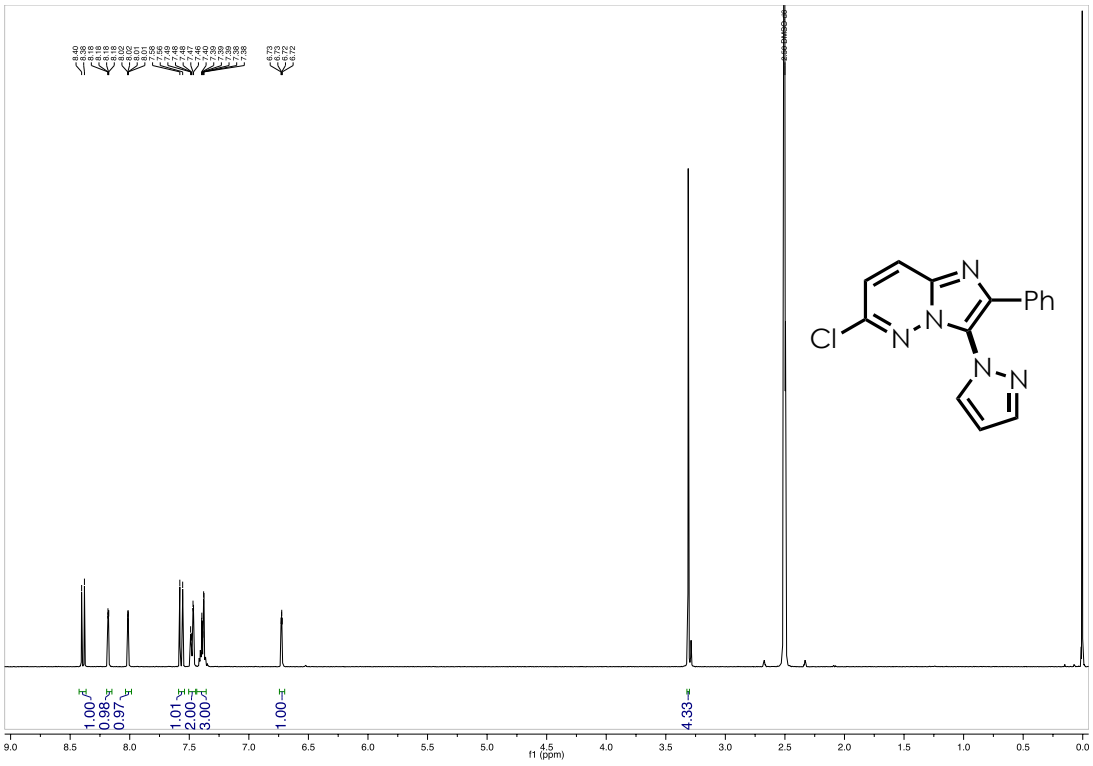
8.40
8.38
8.18
8.16
8.03
8.02
8.01
7.58
7.49
7.48
7.47
7.46
7.40
7.39
7.39
7.38
7.38
6.73
6.72
6.72
6.72
1.00
0.98
0.97
1.01
2.00
3.00
1.00
4.33
f1 (ppm)
N
Ph
Cl
N
N
N

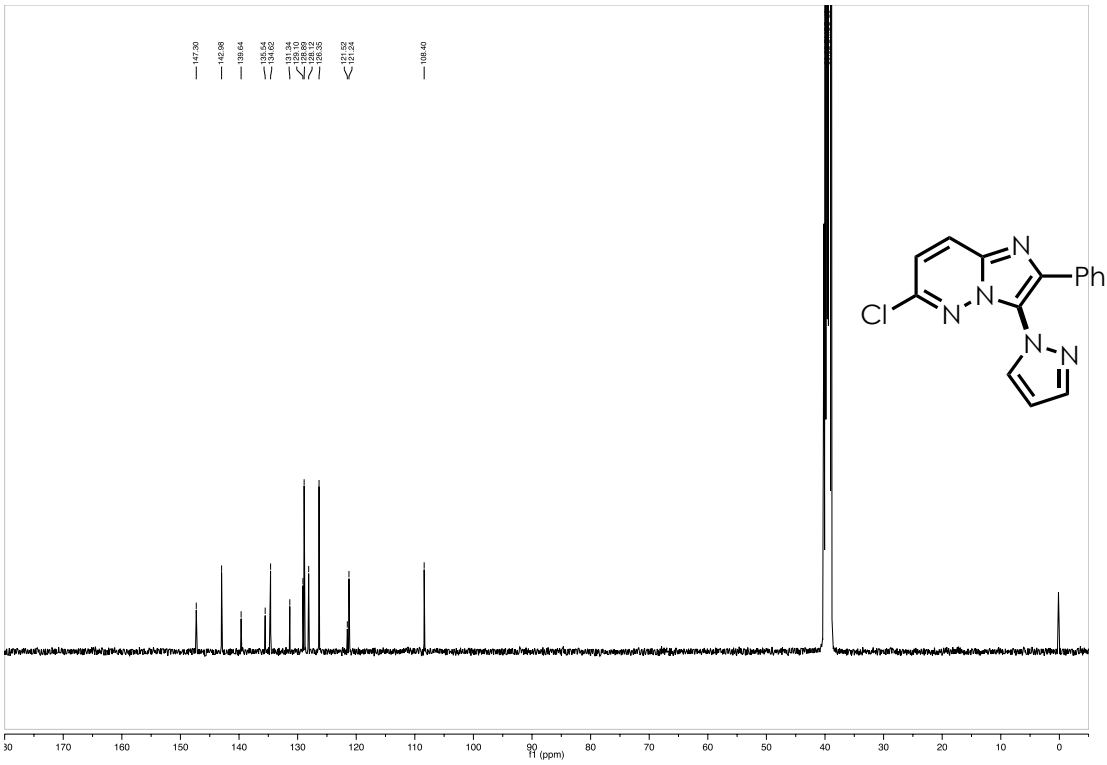
147.30
142.98
139.64
130.64
130.58
131.34
129.10
128.68
128.12
126.35
121.52
121.24
108.40
f1 (ppm)
N
Ph
Cl
N
N
N

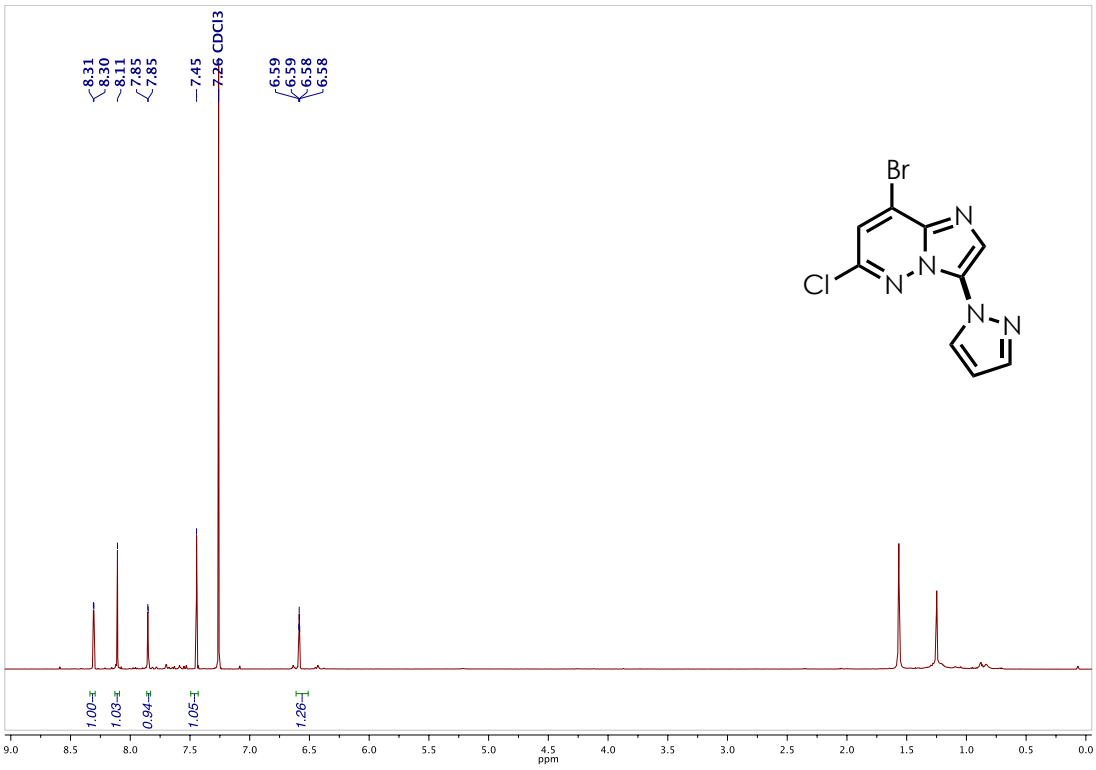
8.31
8.30
8.11
7.85
7.85
7.45
7.26 CDCl3
6.59
6.59
6.58
6.58
1.00
1.03
0.94
1.05
1.26
Br
N
N
Cl
N
N
N
ppm

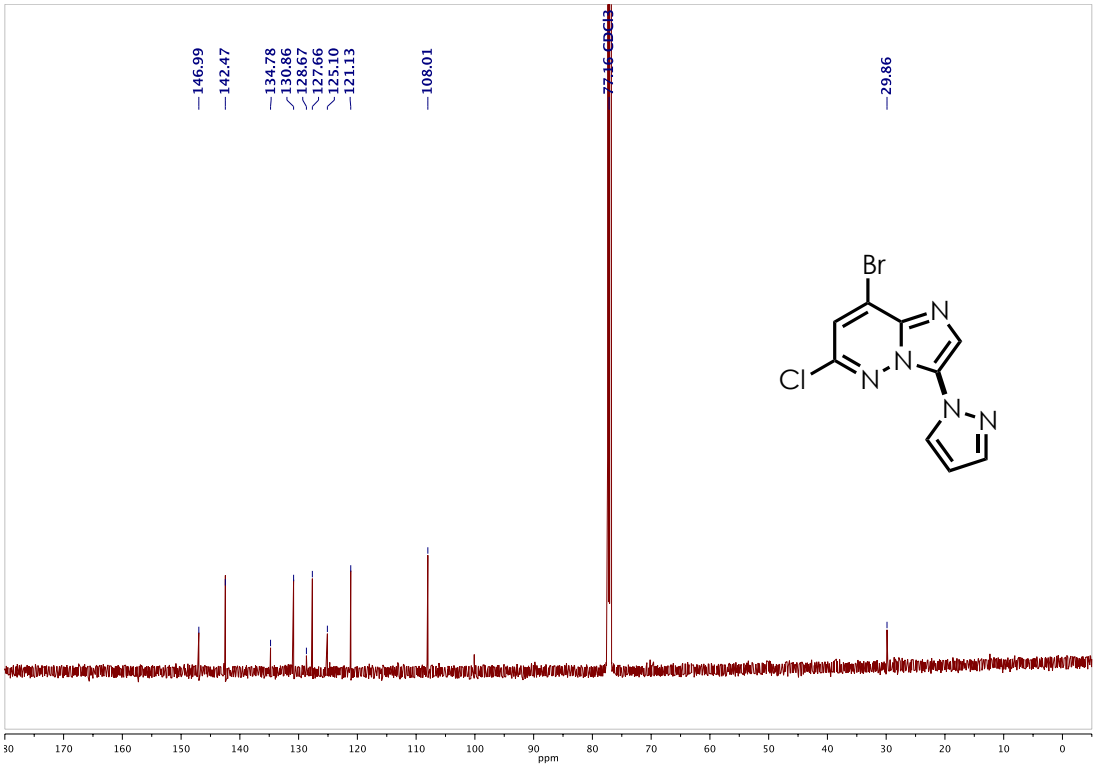
146.99
142.47
134.78
130.86
128.67
127.66
125.10
121.13
108.01
77.16 CDCl3
29.86
Br
N
N
Cl
N
N
N
ppm

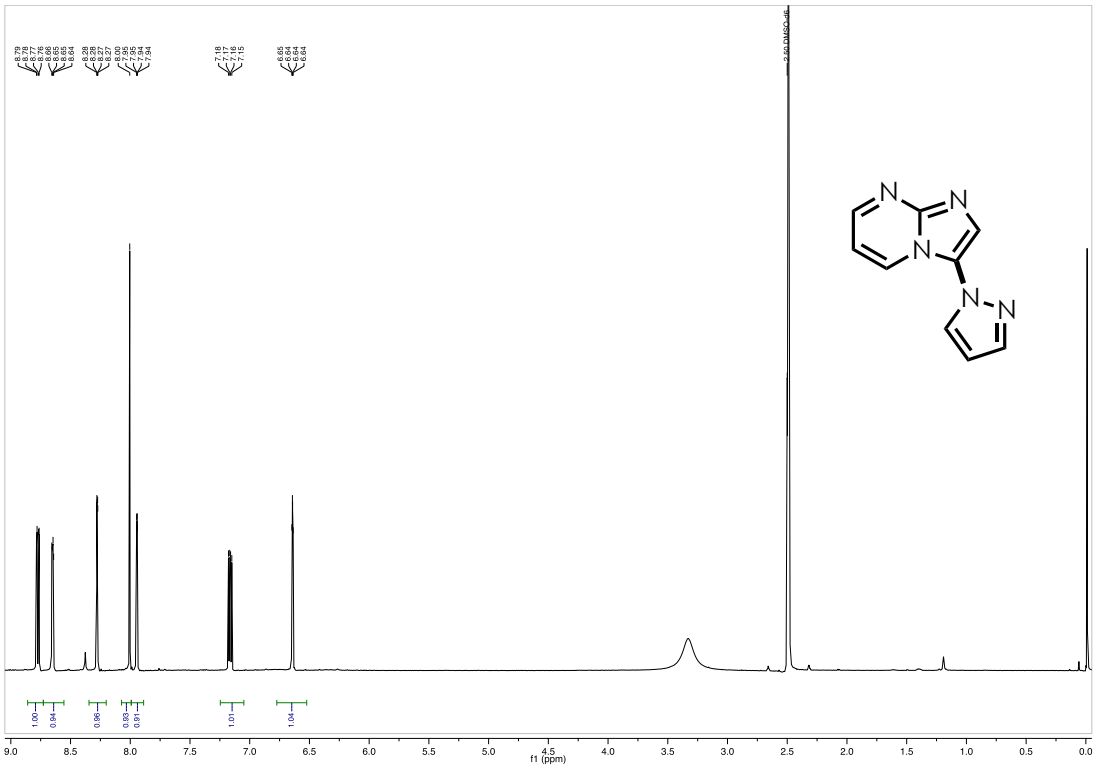
8.79
8.77
8.77
8.66
8.66
8.65
8.65
8.64
8.29
8.28
8.27
8.27
8.00
7.96
7.95
7.94
7.94
7.18
7.17
7.16
7.15
6.66
6.64
6.64
6.64
1.00
0.94
0.96
0.89
0.91
1.01
1.04
9.0
8.5
8.0
7.5
7.0
6.5
6.0
5.5
5.0
4.5
4.0
3.5
3.0
2.5
2.0
1.5
1.0
0.5
0.0
f1 (ppm)

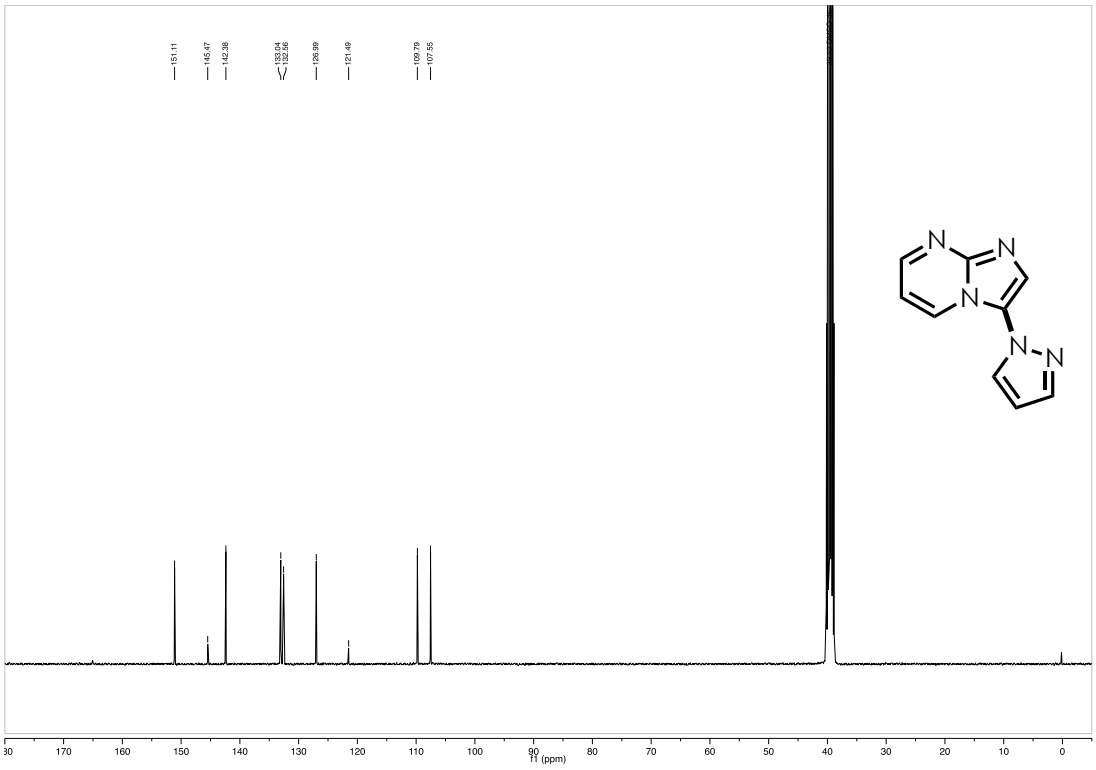
151.11
145.47
142.38
133.04
132.66
126.99
121.49
109.79
107.55
170
160
150
140
130
120
110
100
90
80
70
60
50
40
30
20
10
0
f1 (ppm)

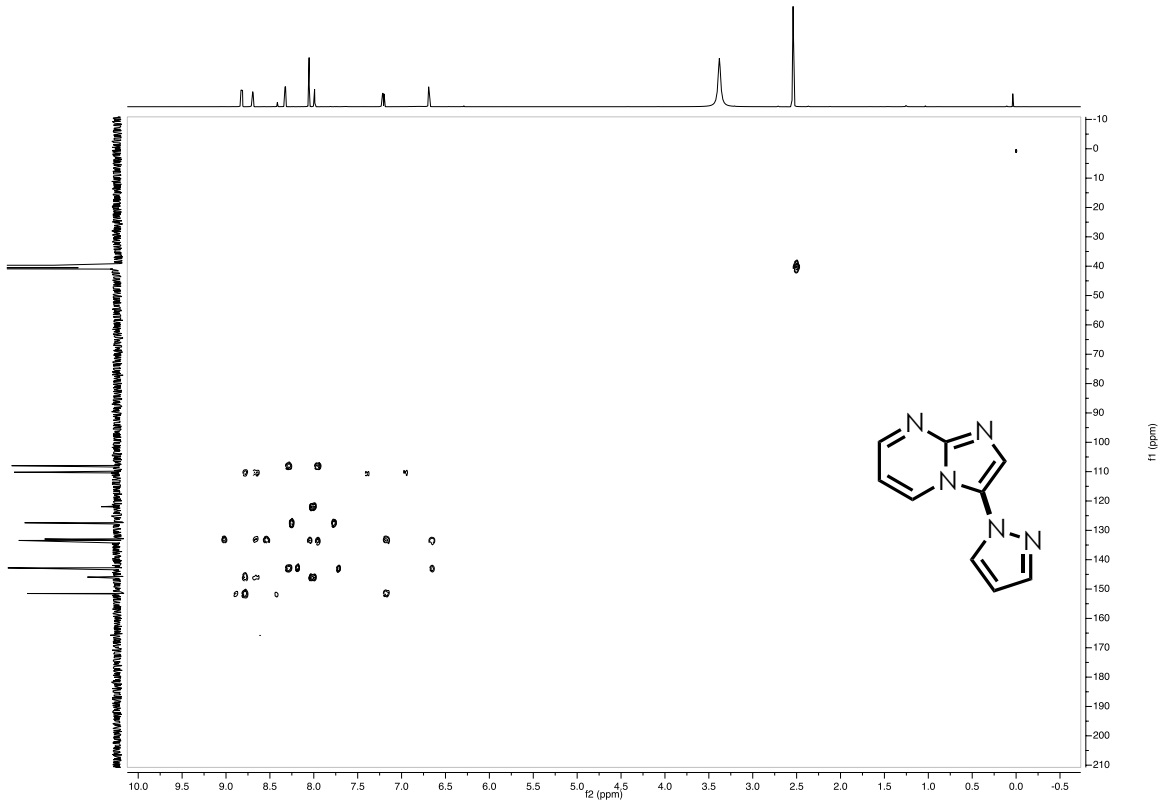
f2 (ppm)
f1 (ppm)

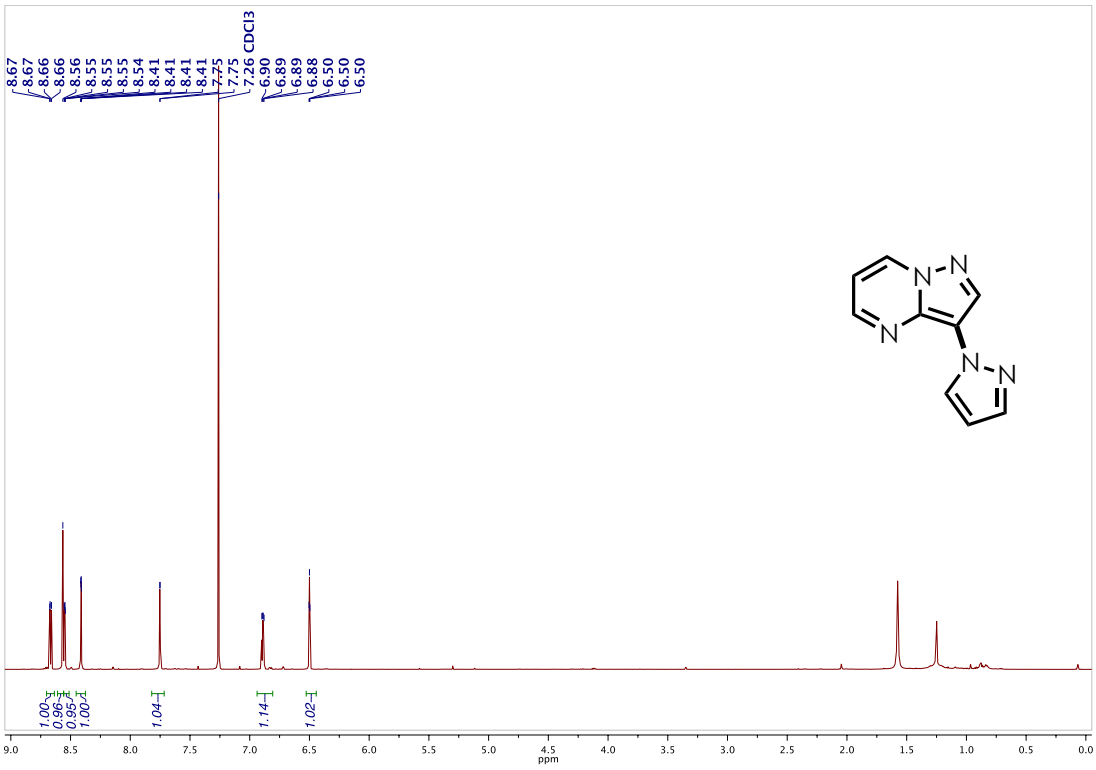
8.67
8.67
8.66
8.66
8.56
8.55
8.55
8.55
8.54
8.41
8.41
8.41
8.41
7.75
7.75
7.26 CDCl3
6.90
6.89
6.89
6.88
6.50
6.50
6.50
1.00
0.96
0.95
1.00
1.04
1.14
1.02
ppm

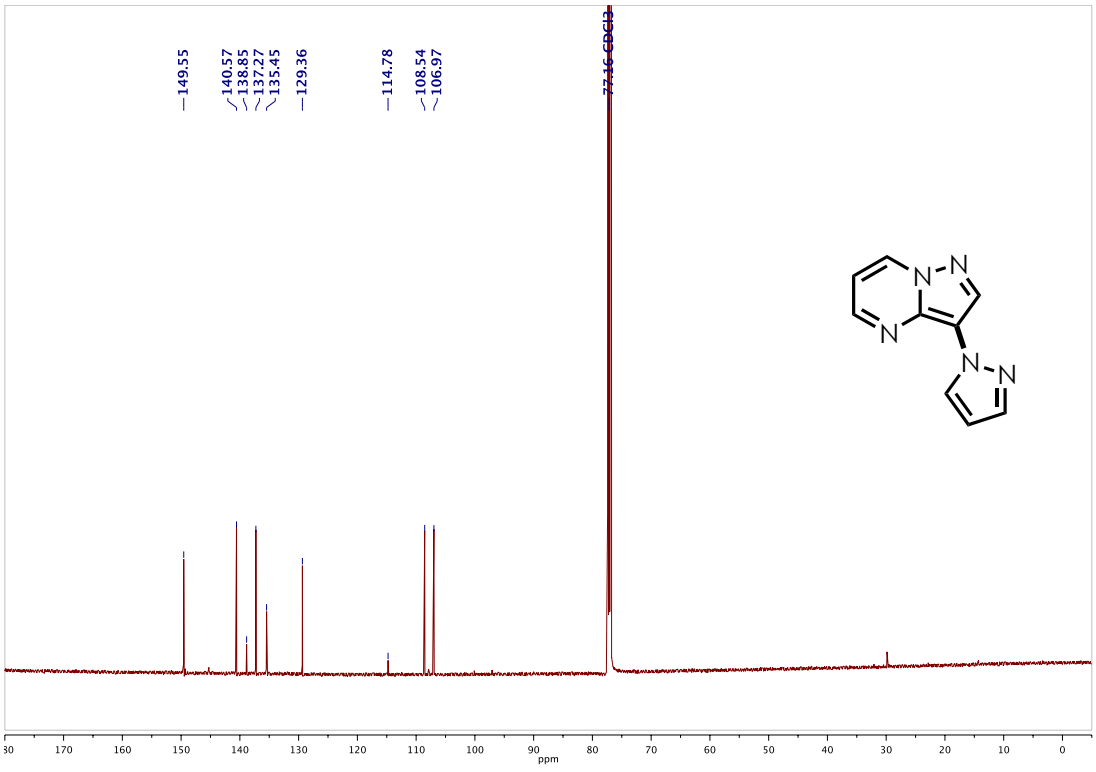
149.55
140.57
138.85
137.27
135.45
129.36
114.78
108.54
106.97
77.16 CDCl3
ppm

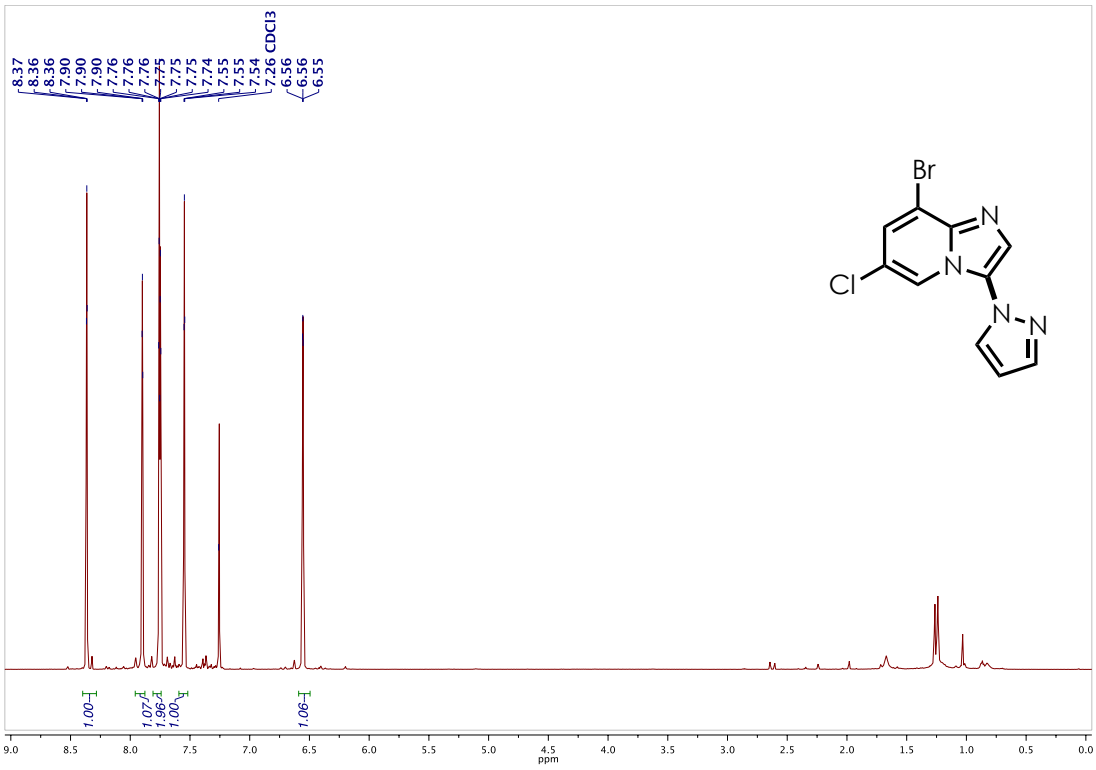
8.37
8.36
8.36
7.90
7.90
7.90
7.76
7.76
7.76
7.75
7.75
7.75
7.74
7.55
7.55
7.54
7.26 CDCl3
6.56
6.56
6.55
1.00
1.07
1.96
1.00
1.06
Br
N
N
Cl
N
N
ppm

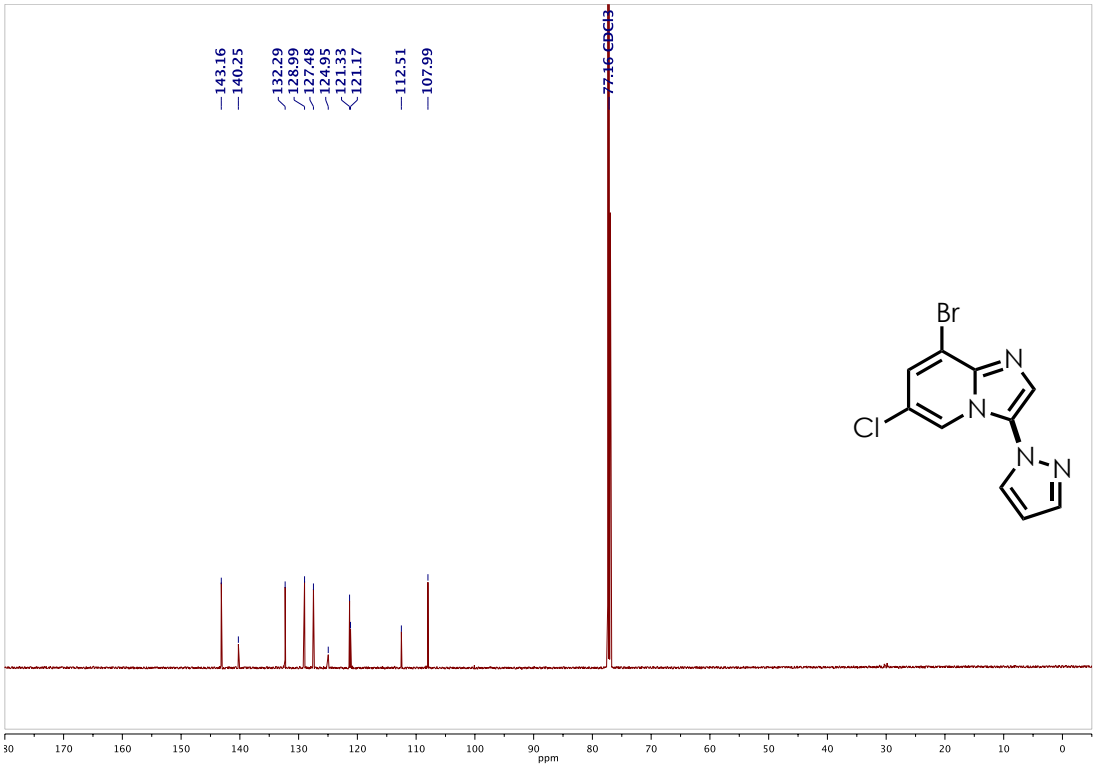
143.16
140.25
132.29
128.99
127.48
124.95
121.33
121.17
112.51
107.99
77.16 CDCl3
Br
N
N
Cl
N
N
ppm

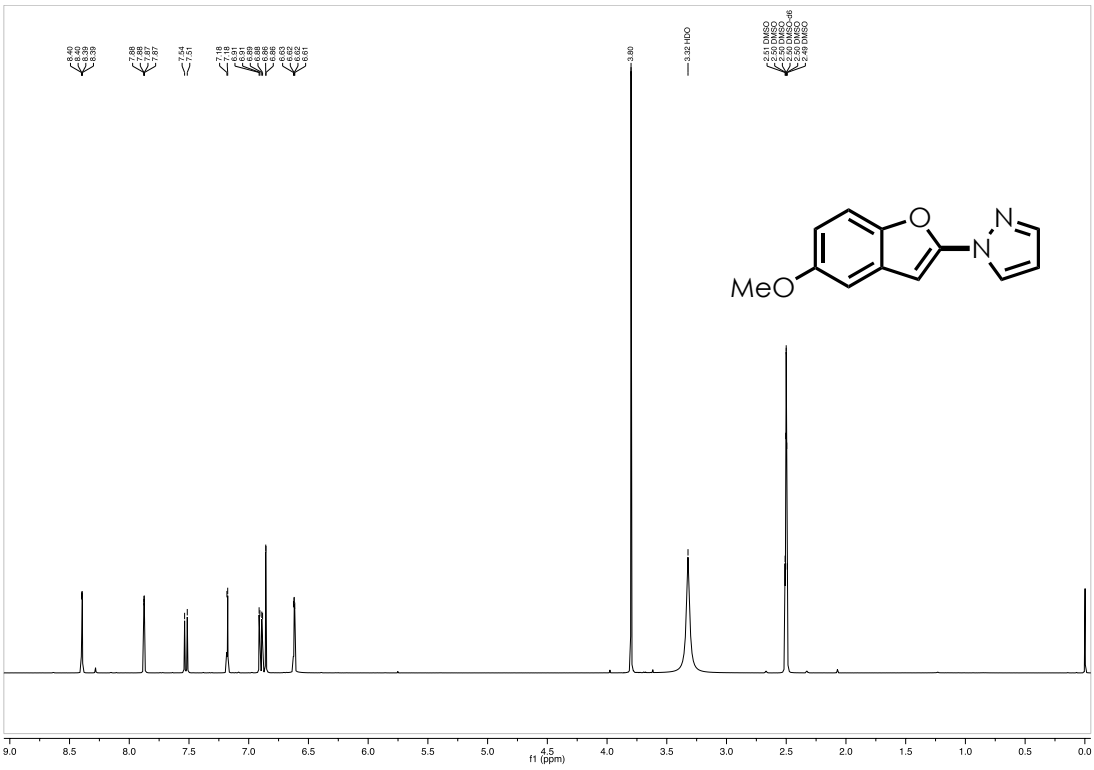
8.40
8.40
8.39
8.39
7.88
7.88
7.87
7.87
7.54
7.51
7.18
7.18
6.91
6.91
6.89
6.88
6.88
6.86
6.63
6.62
6.62
6.61
3.80
3.32 HDO
2.51 DMSO
2.50 DMSO
2.50 DMSO
2.50 DMSO-d6
2.49 DMSO
MeO
O
N
N
f1 (ppm)

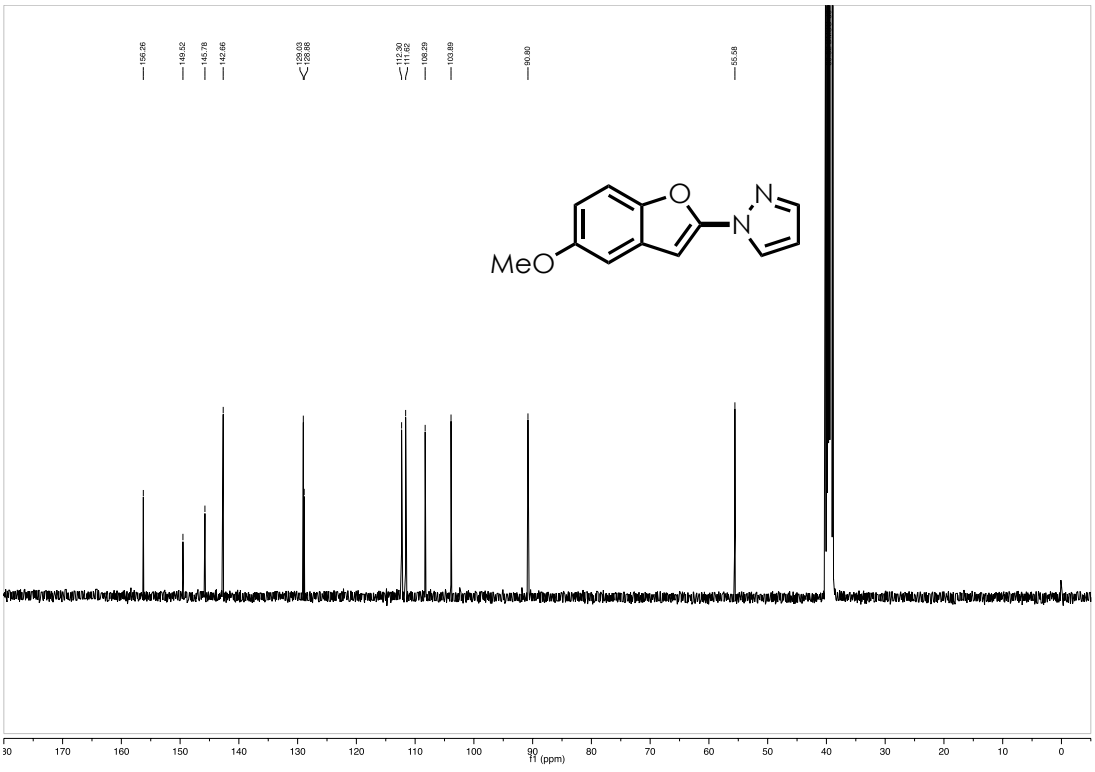
156.26
149.52
145.78
142.66
129.03
128.86
112.30
111.62
108.29
103.89
90.80
55.58
MeO
O
N
N
f1 (ppm)

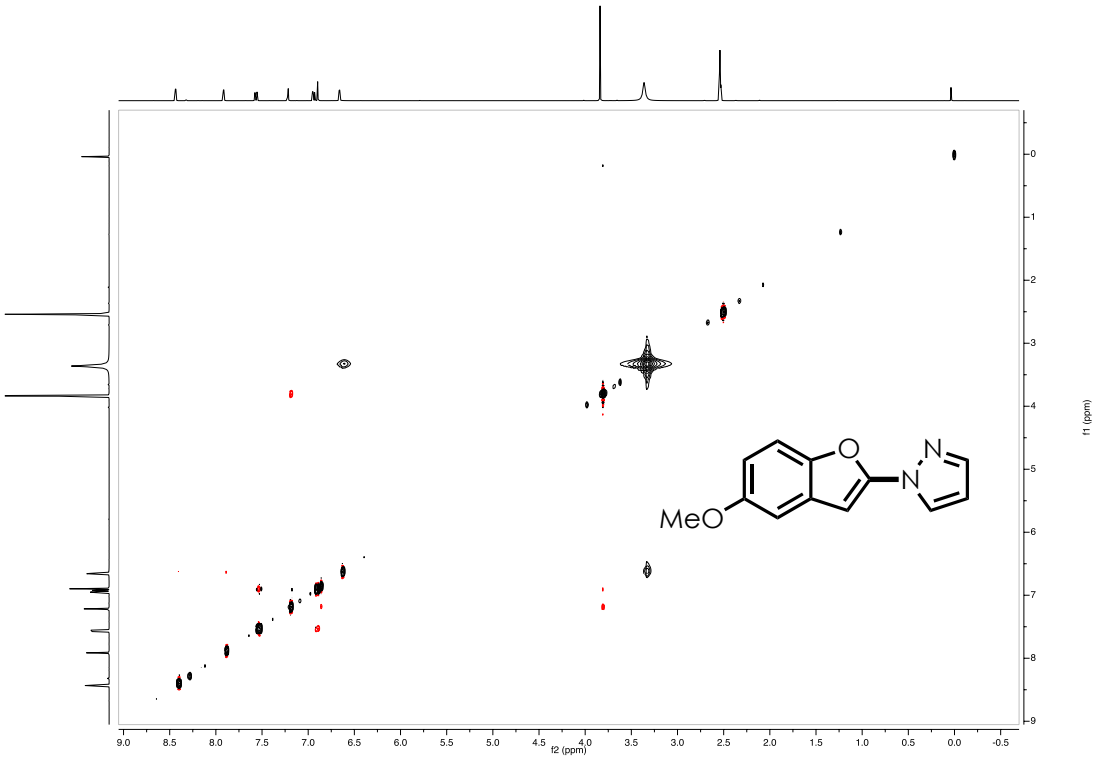
f2 (ppm)
f1 (ppm)
MeO
O
N
N

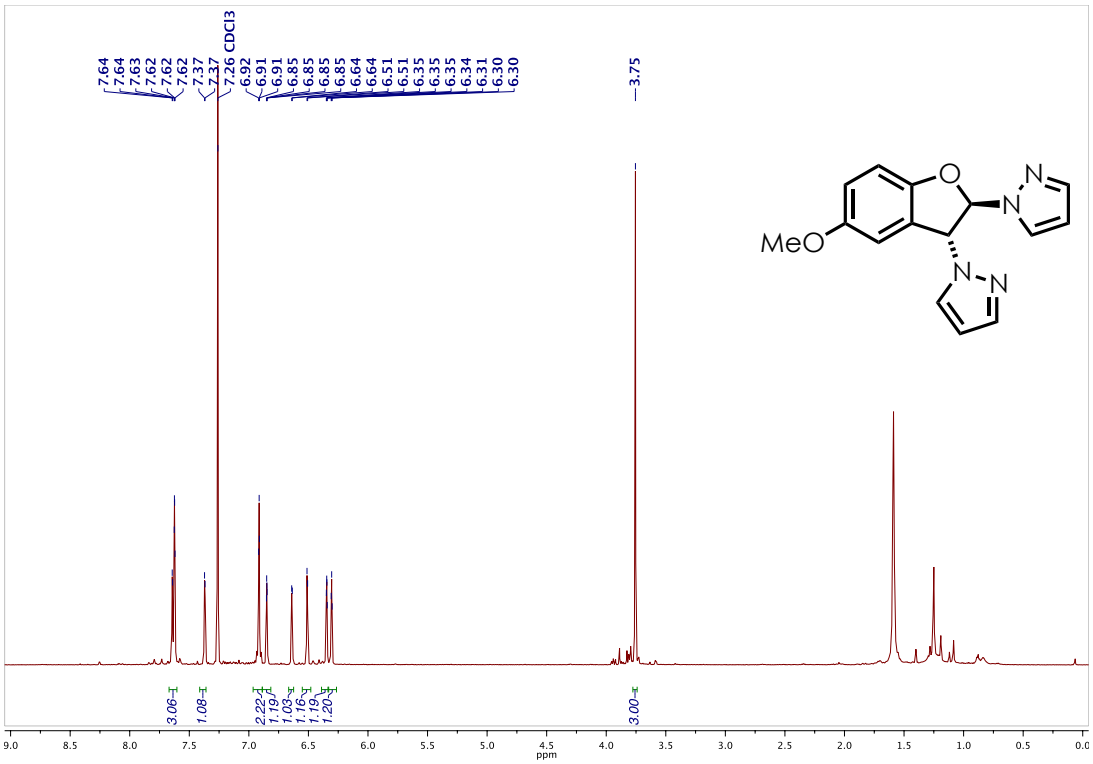
7.64
7.64
7.63
7.62
7.62
7.62
7.37
7.37
7.26 CDCl3
6.92
6.91
6.91
6.85
6.85
6.85
6.85
6.64
6.64
6.51
6.51
6.35
6.35
6.35
6.34
6.31
6.30
6.30
3.75
MeO
3.06
1.08
2.22
1.16
1.03
1.16
1.19
1.20
3.00
ppm

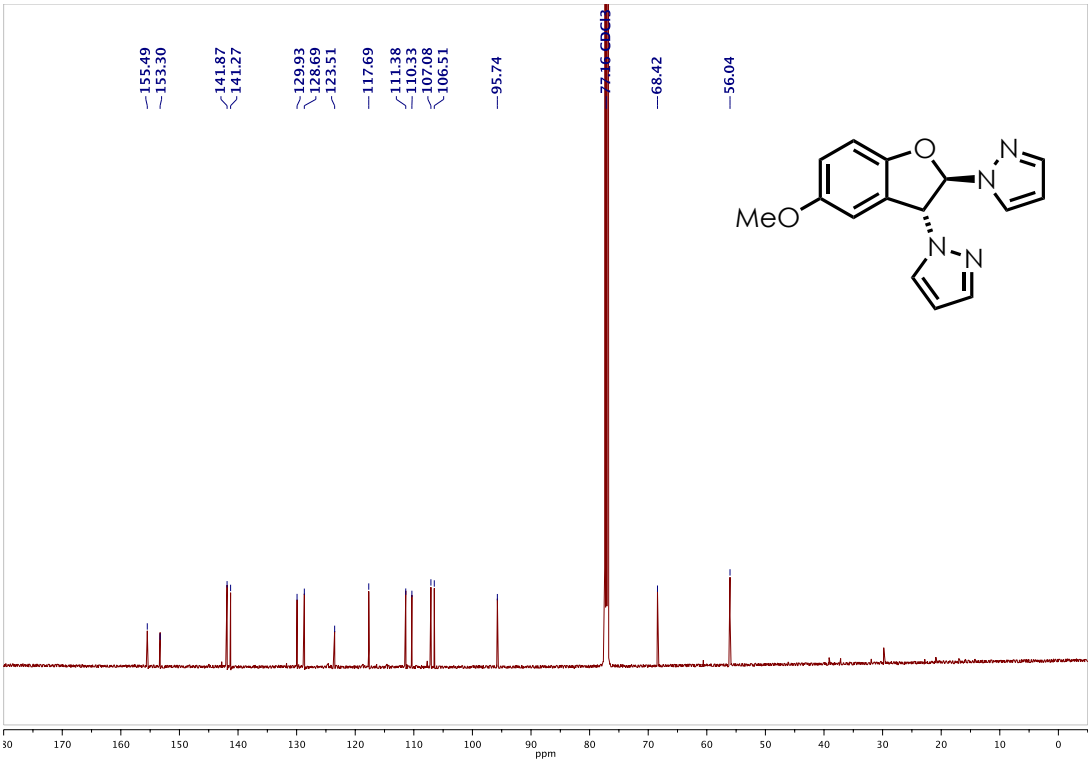
155.49
153.30
141.87
141.27
129.93
128.69
123.51
117.69
111.38
110.33
107.08
106.51
95.74
77.16 CDCl3
68.42
56.04
MeO
ppm

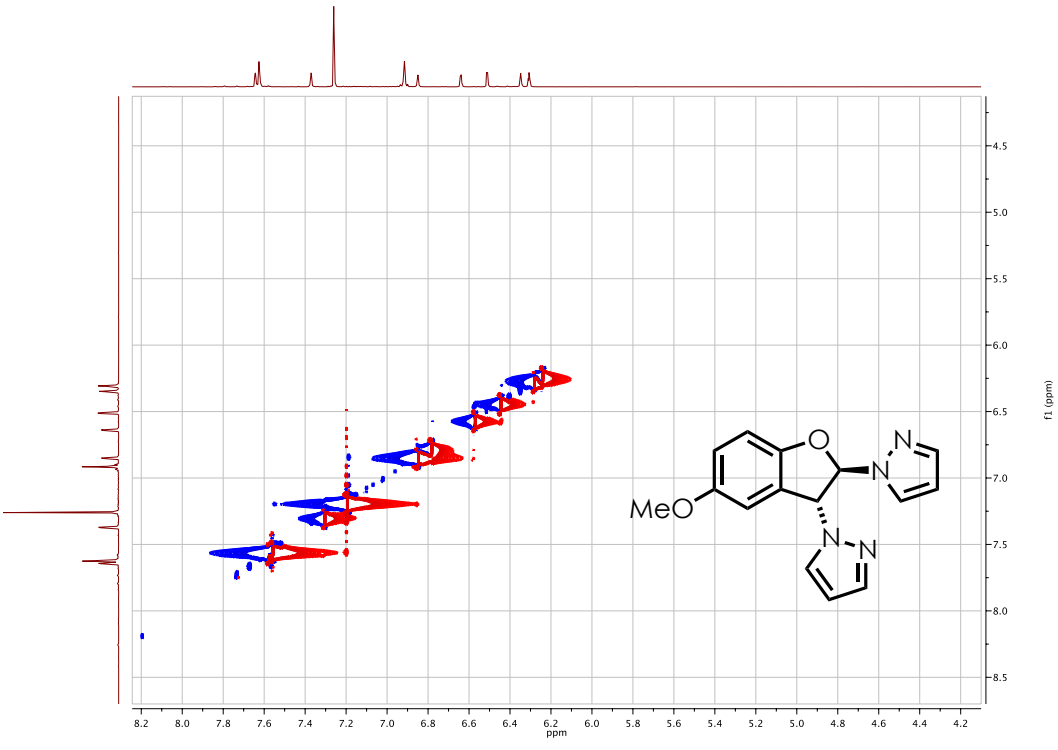
MeO
O
N
N
N
N
8.2
8.0
7.8
7.6
7.4
7.2
7.0
6.8
6.6
6.4
6.2
6.0
5.8
5.6
5.4
5.2
5.0
4.8
4.6
4.4
4.2
ppm
4.5
5.0
5.5
6.0
6.5
7.0
7.5
8.0
8.5
f1 (ppm)

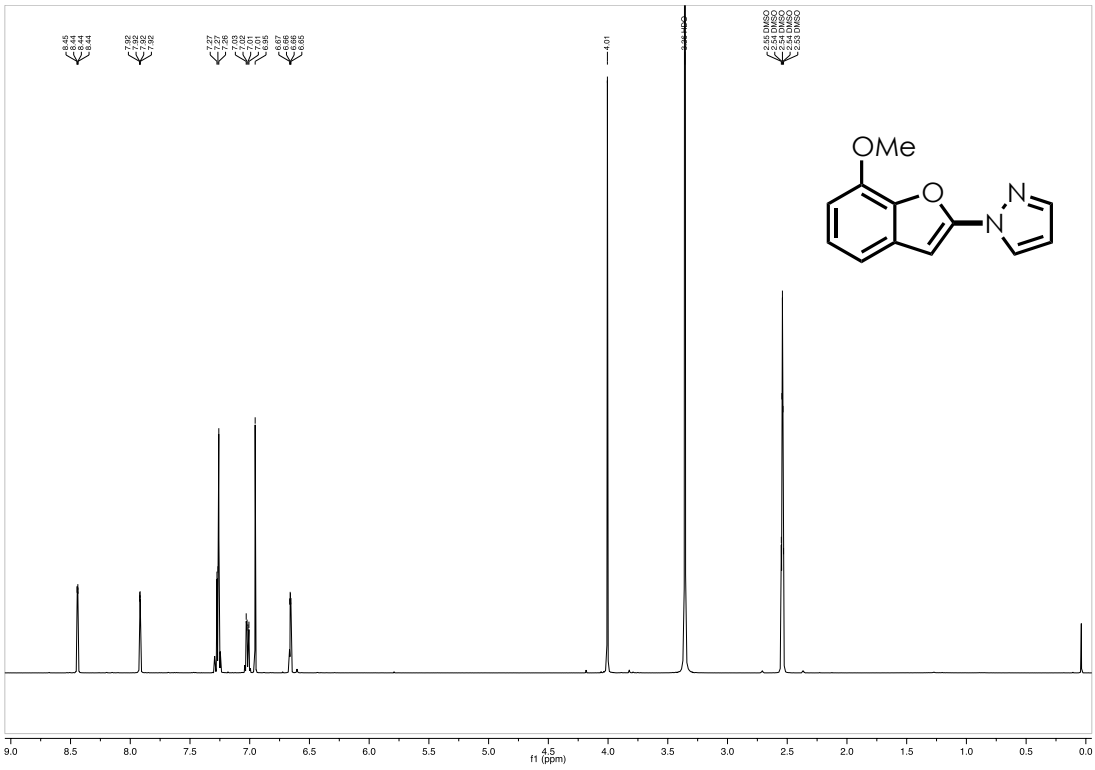
8.45
8.44
8.44
8.44
7.92
7.92
7.92
7.92
7.27
7.27
7.26
7.03
7.02
7.01
7.01
6.66
6.67
6.66
6.66
6.65
4.01
3.34 HDO
2.55 DMSO
2.54 DMSO
2.54 DMSO
2.54 DMSO
2.53 DMSO
OMe
O
N
N
9.0
8.5
8.0
7.5
7.0
6.5
6.0
5.5
5.0
4.5
4.0
3.5
3.0
2.5
2.0
1.5
1.0
0.5
0.0
f1 (ppm)

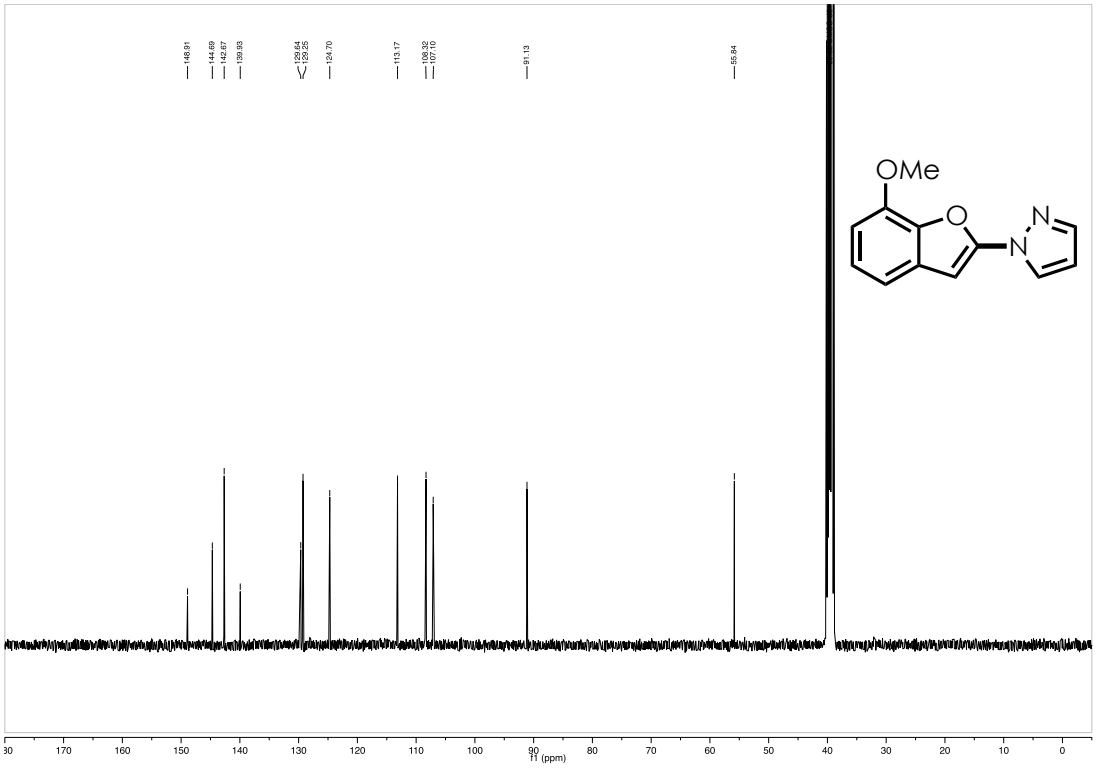
148.91
144.69
142.67
139.93
129.84
129.25
124.70
113.17
108.32
107.10
91.13
55.84
OMe
O
N
N
170
160
150
140
130
120
110
100
90
80
70
60
50
40
30
20
10
0
f1 (ppm)

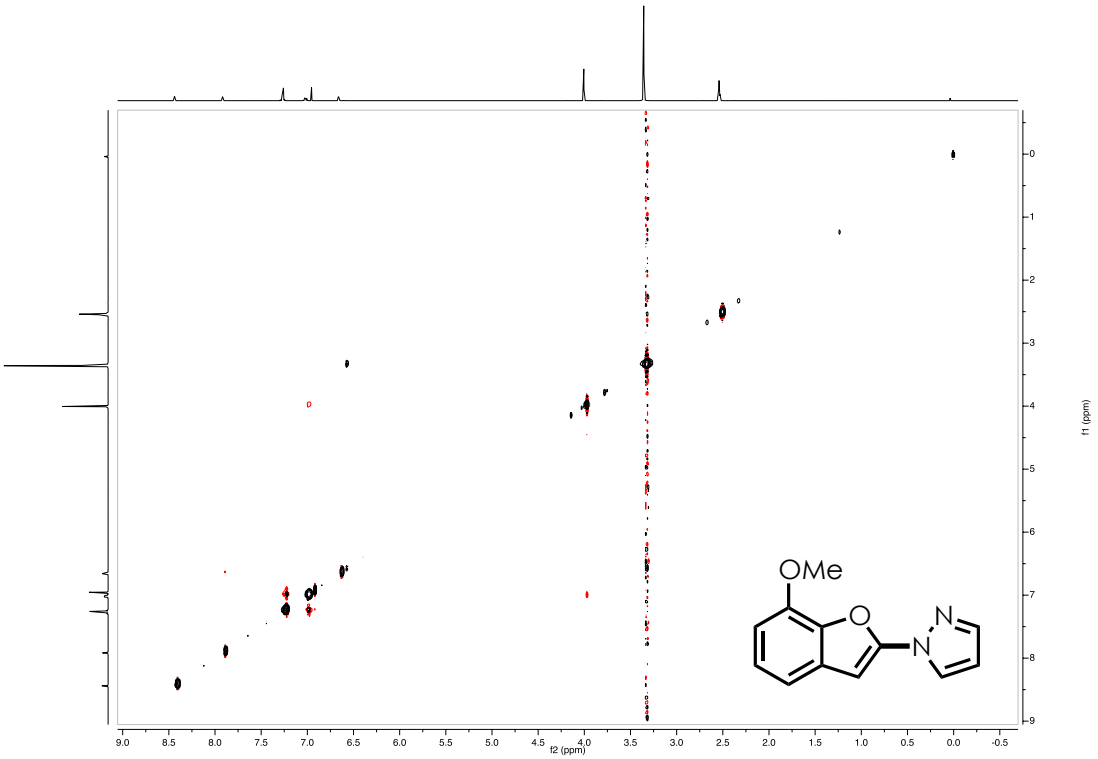
OMe
O
N
N
f2 (ppm)
f1 (ppm)

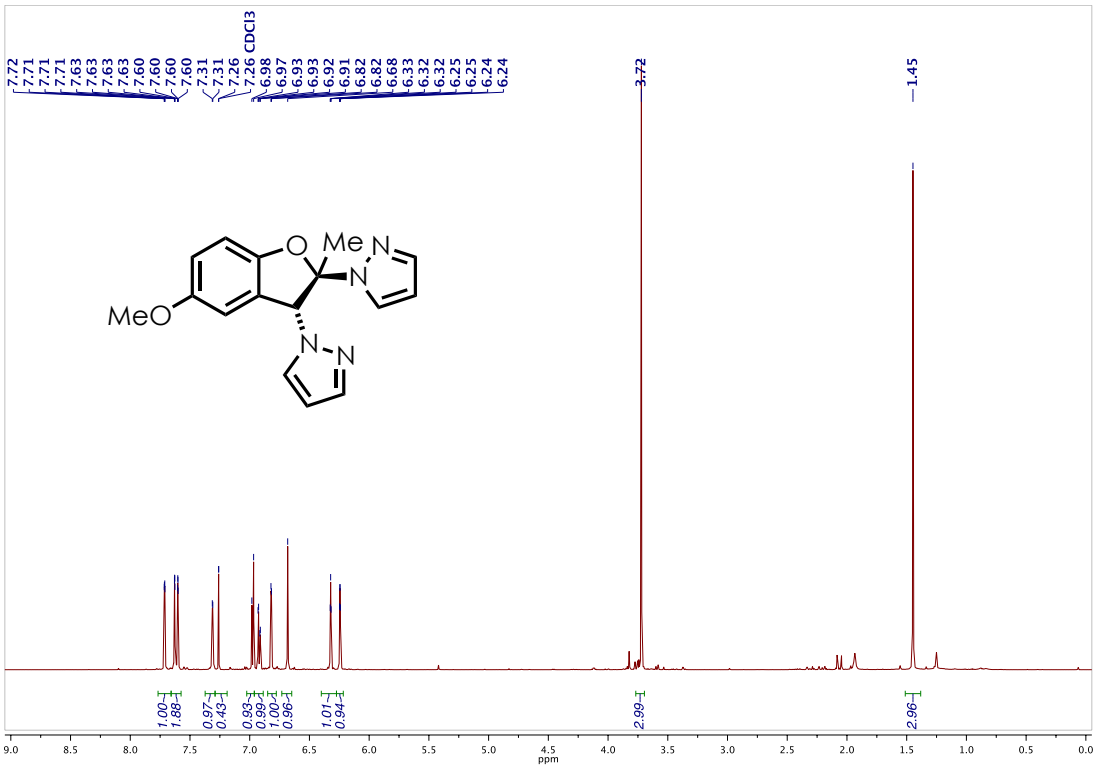
7.72
7.71
7.71
7.71
7.63
7.63
7.63
7.63
7.60
7.60
7.60
7.60
7.31
7.26 CDCl3
6.98
6.97
6.93
6.93
6.92
6.91
6.82
6.82
6.68
6.33
6.32
6.25
6.25
6.24
6.24
3.72
1.45
Me
O
N
N
MeO
N
N
1.00
1.88
0.97
0.43
0.93
0.99
1.00
0.96
1.01
0.94
2.99
2.96
ppm

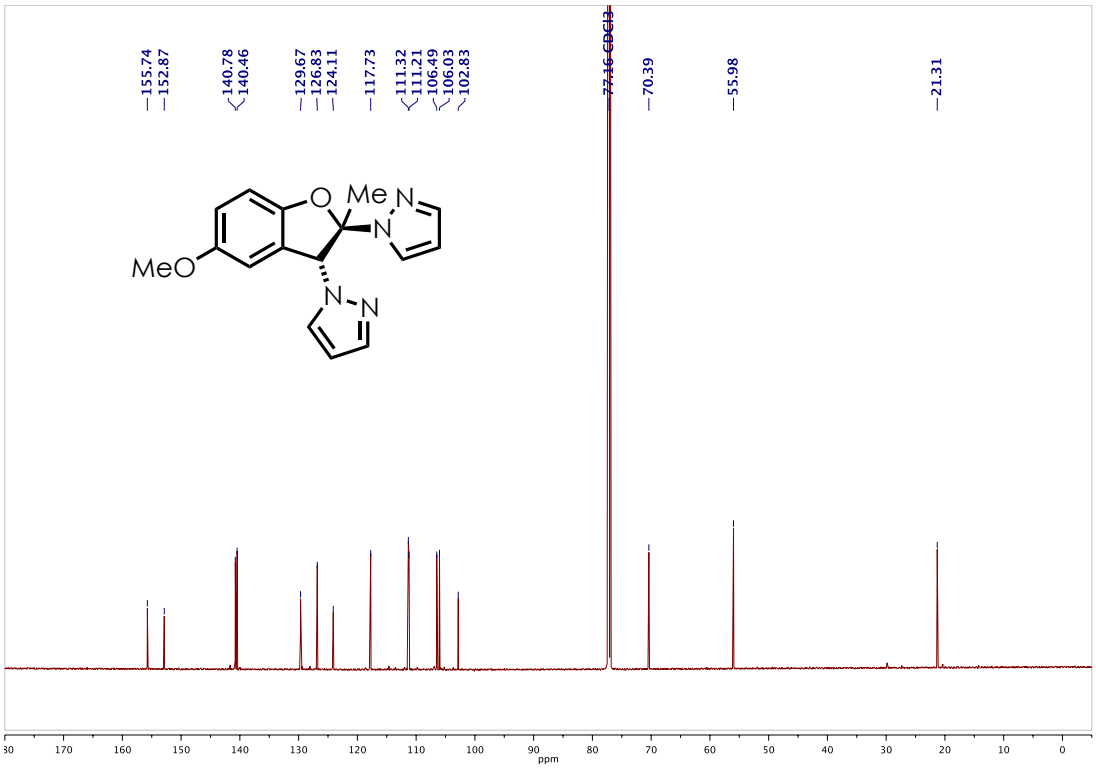
155.74
152.87
140.78
140.46
129.67
126.83
124.11
117.73
111.32
111.21
106.49
106.03
102.83
77.16 CDCl3
70.39
55.98
21.31
Me
O
N
N
MeO
N
N
ppm


8.45
8.44
7.82
7.81
7.32
7.32
7.31
7.31
7.29
6.95
6.95
6.93
6.93
6.60
6.60
6.59
6.59
6.52
3.37 HDO
2.54 DMSO
2.54 DMSO
2.54 DMSO
2.49
H
N
N
N
Me
f1 (ppm)

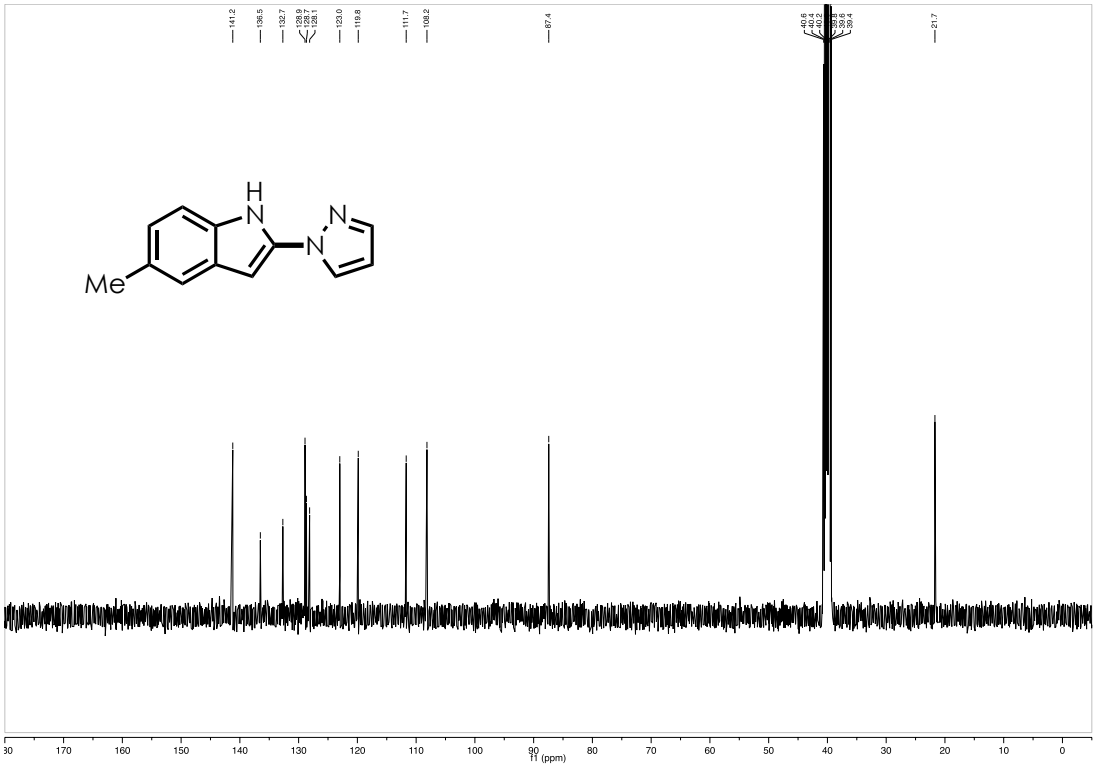
141.2
136.5
132.7
128.9
128.7
128.1
123.0
119.8
111.7
108.2
87.4
40.6
40.4
40.2
39.8
39.6
39.4
21.7
H
N
N
N
Me
f1 (ppm)

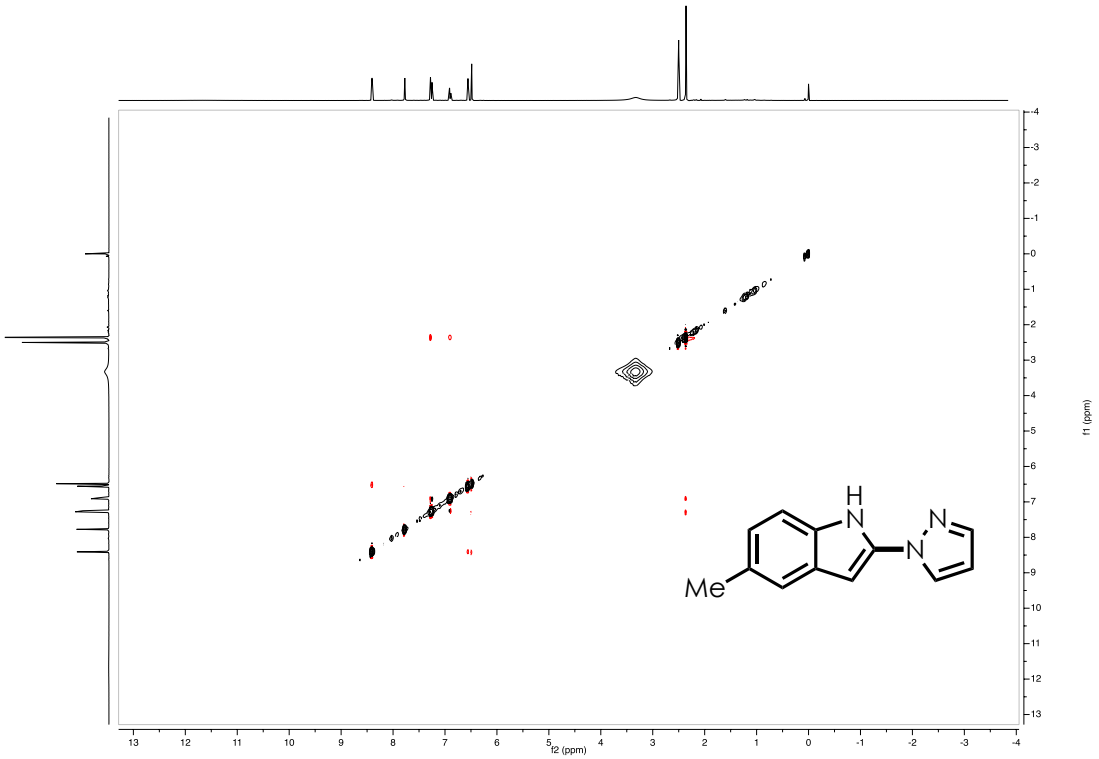
f1 (ppm)
f2 (ppm)
H
N
N
N
Me


8.43
8.43
7.82
7.82
7.43
7.41
7.22
6.91
6.89
6.60
6.59
6.55
3.36 HDO
2.54 DMSO
2.54 DMSO
2.43
2.43
Me
H
N
N
N
f1 (ppm)


141.2
135.9
134.7
130.6
129.0
125.6
122.0
120.0
111.8
108.2
87.8
40.6 DMSO
40.4 DMSO
40.2 DMSO
39.8 DMSO
39.6 DMSO
39.4 DMSO
21.9
Me
H
N
N
N
f1 (ppm)

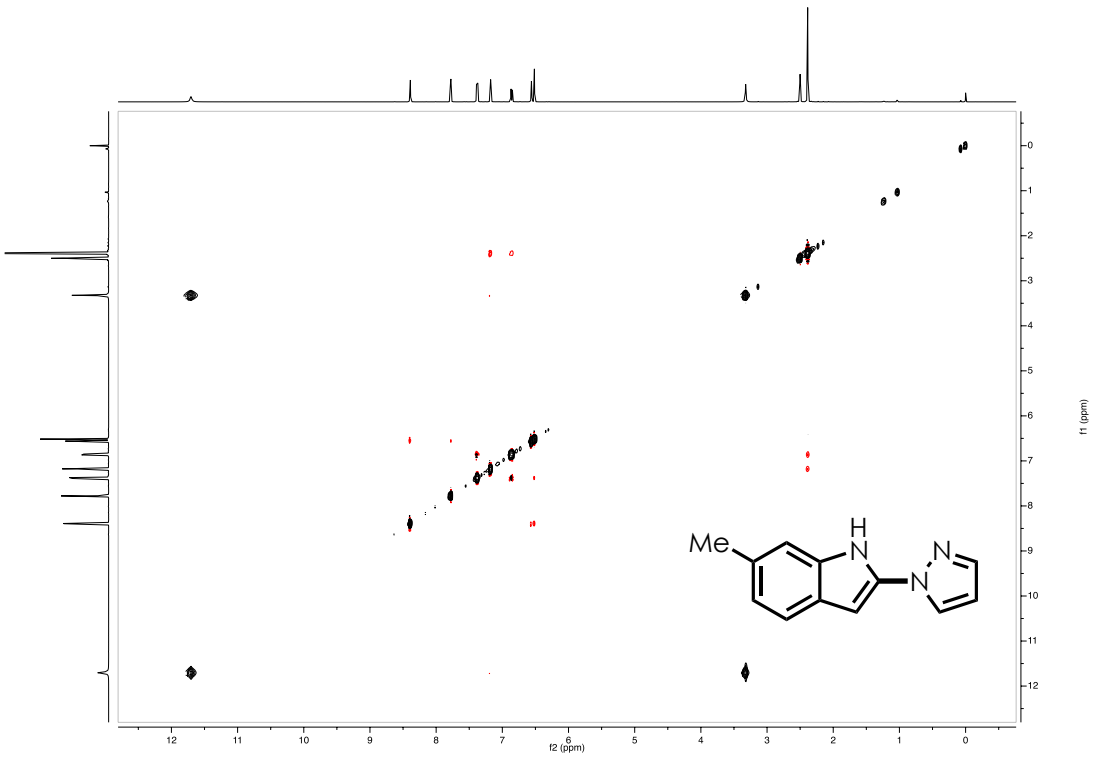
Me
H
N
N
N
f2 (ppm)
f1 (ppm)

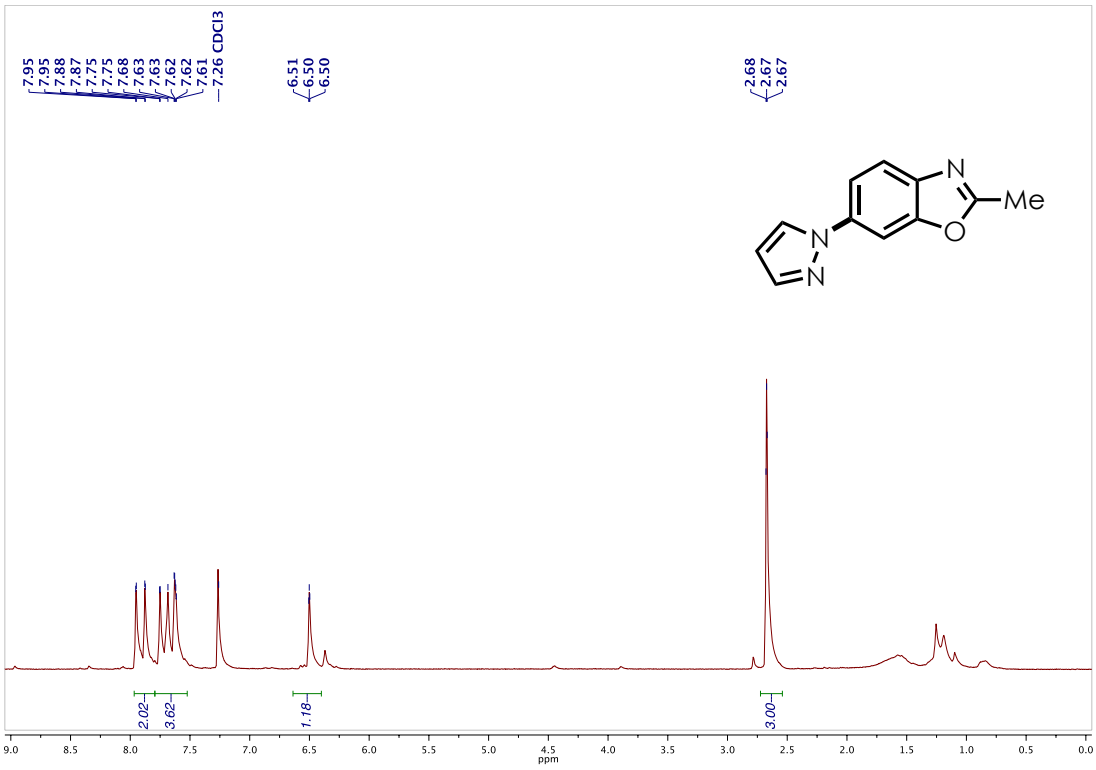
7.95
7.95
7.88
7.87
7.75
7.75
7.68
7.63
7.63
7.62
7.62
7.61
7.26 CDCl3
6.51
6.50
6.50
2.68
2.67
2.67
N
Me
O
N
N
2.02
3.62
1.18
3.00
ppm

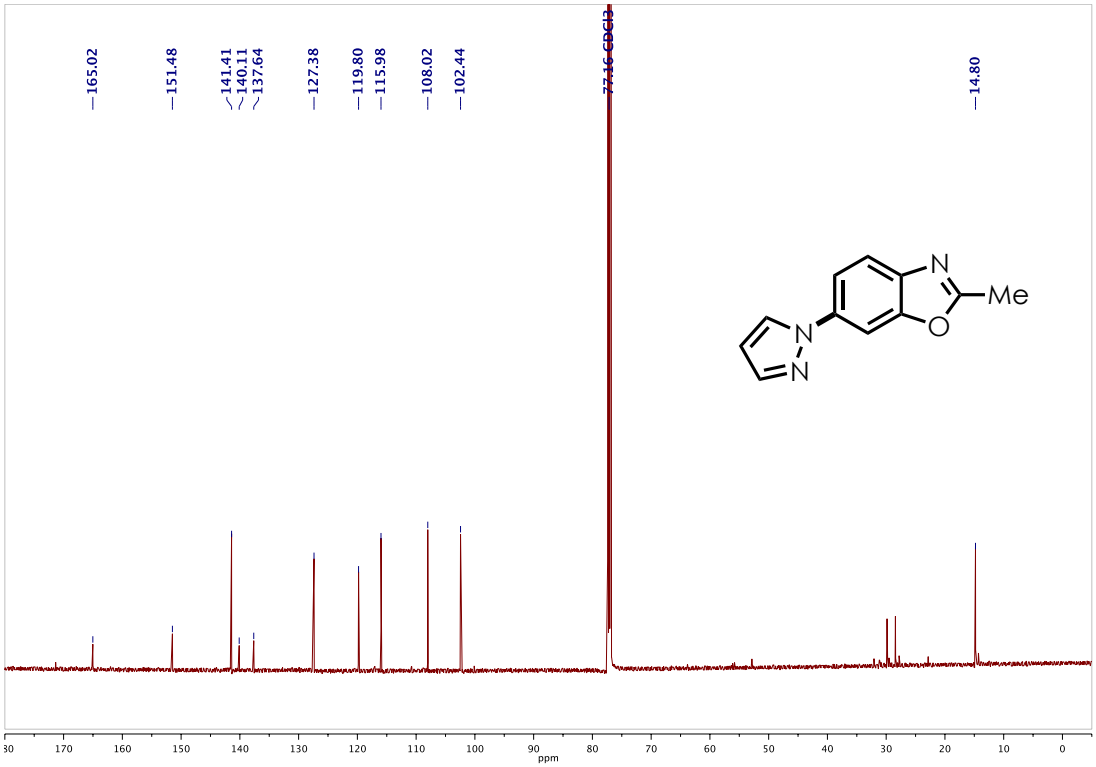
165.02
151.48
141.41
140.11
137.64
127.38
119.80
115.98
108.02
102.44
77.16 CDCl3
14.80
N
Me
O
N
N
ppm

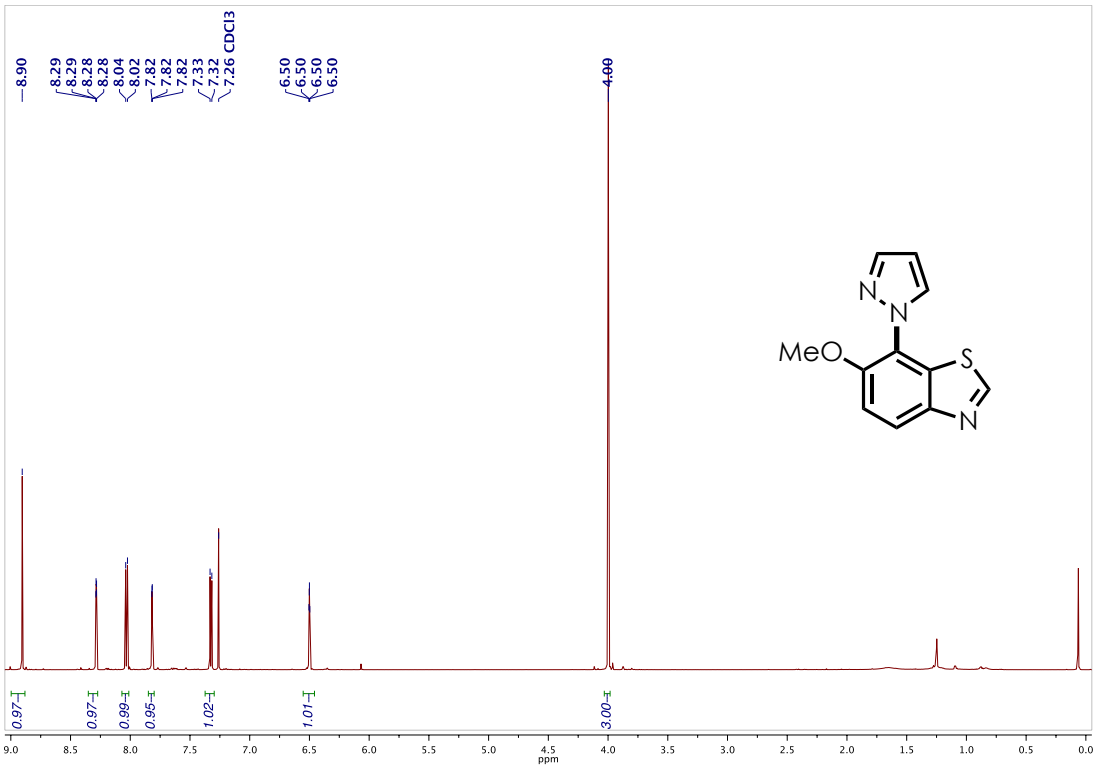
8.90
8.29
8.29
8.28
8.28
8.04
8.02
7.82
7.82
7.82
7.33
7.32
7.26 CDCl3
6.50
6.50
6.50
6.50
4.00
MeO
S
N
N
0.97
0.97
0.99
0.95
1.02
1.01
3.00
ppm

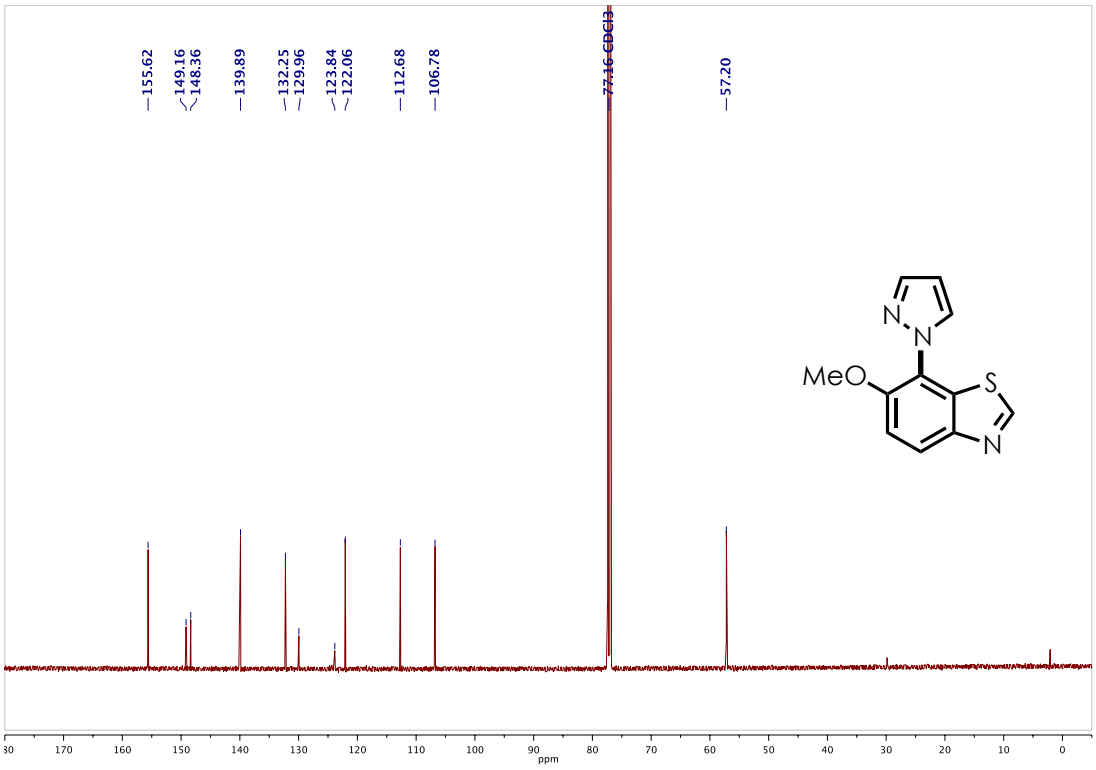
155.62
149.16
148.36
139.89
132.25
129.96
123.84
122.06
112.68
106.78
77.16 CDCl3
57.20
MeO
S
N
N
ppm

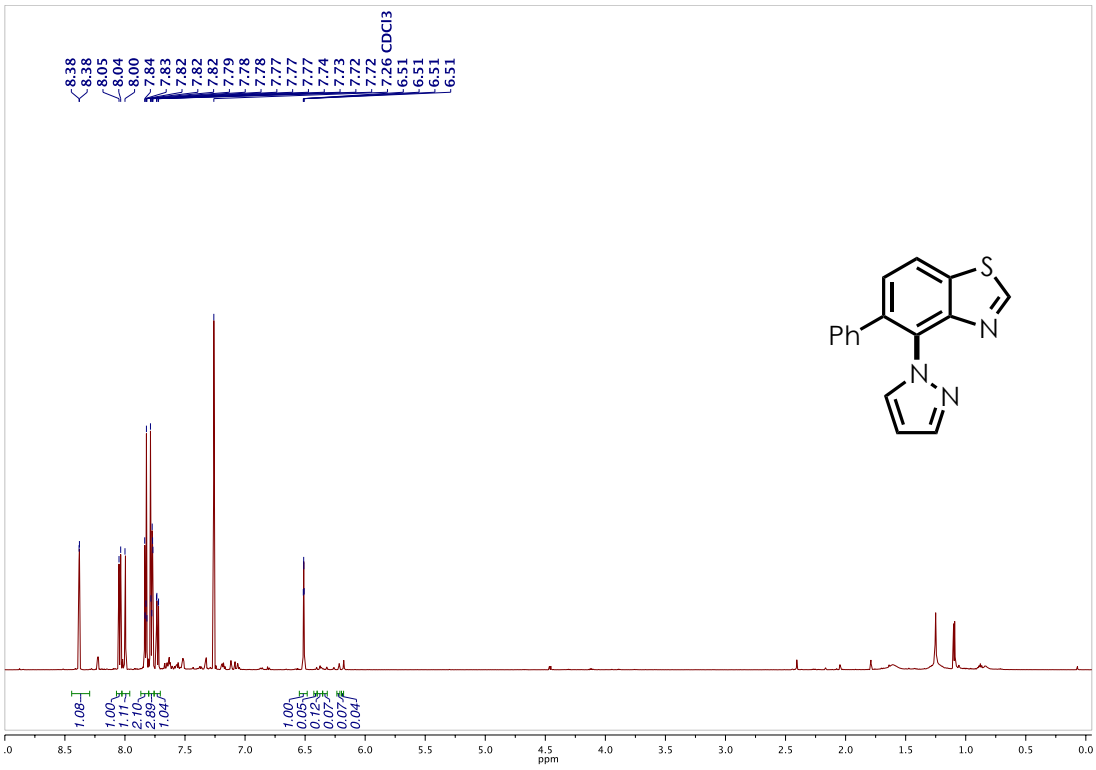
8.38
8.38
8.05
8.04
8.00
7.84
7.83
7.82
7.82
7.82
7.79
7.78
7.78
7.77
7.77
7.77
7.74
7.73
7.72
7.72
7.26 CDCl3
6.51
6.51
6.51
6.51
1.08
1.00
1.11
2.10
2.89
1.04
1.00
0.05
0.12
0.07
0.07
0.04
S
N
Ph
N
N
ppm

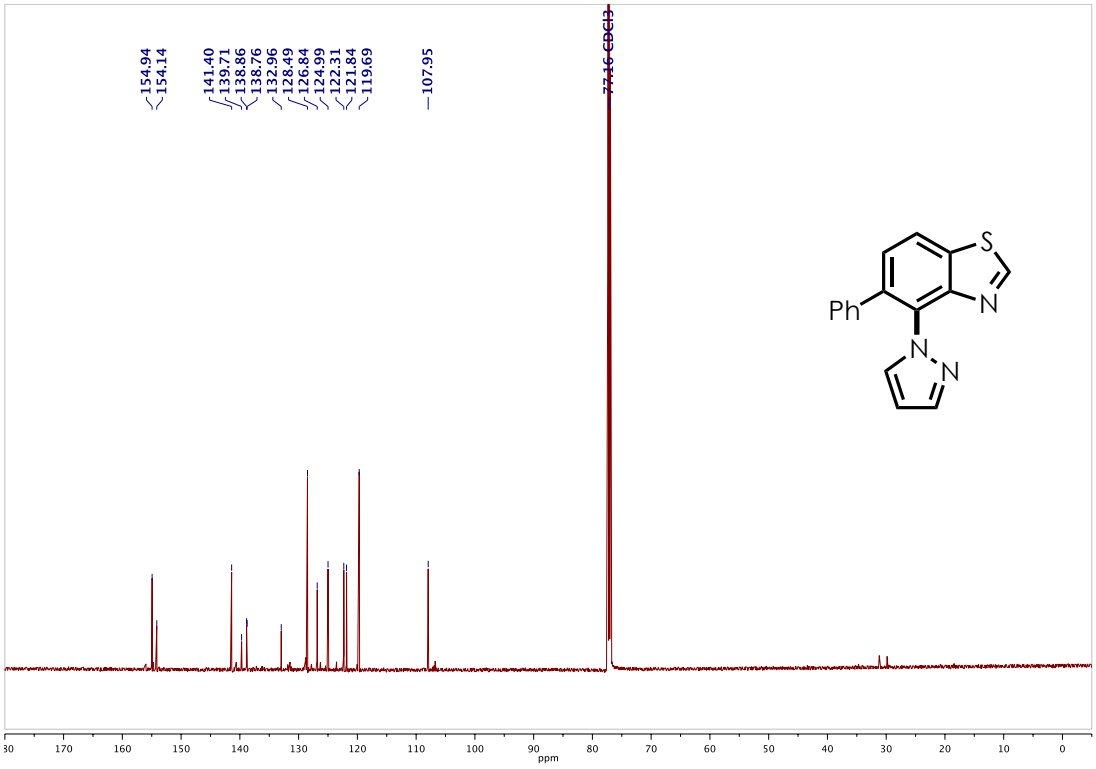
154.94
154.14
141.40
139.71
138.86
138.76
132.96
128.49
126.84
124.99
122.31
121.84
119.69
107.95
77.16 CDCl3
S
N
Ph
N
N
ppm

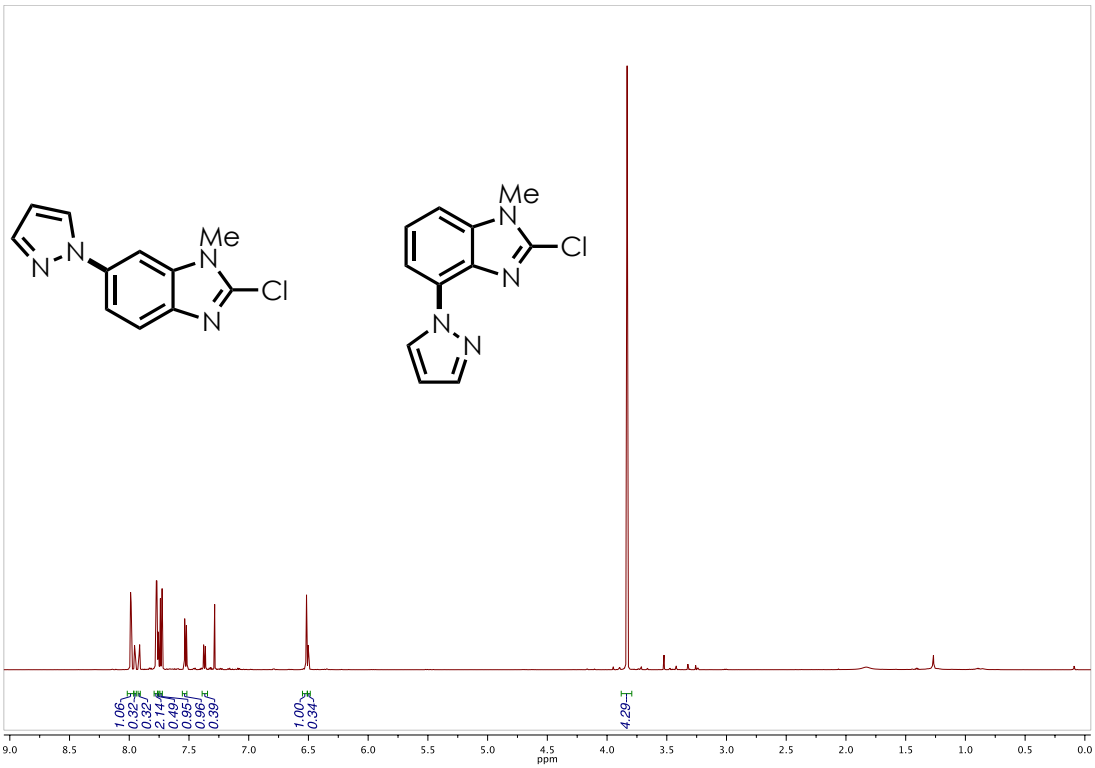
Me
N
Cl
N
N
N
Me
N
Cl
N
N
N
1.06
0.32
0.32
2.14
0.49
0.95
0.96
0.39
1.00
0.34
4.29
9.0
8.5
8.0
7.5
7.0
6.5
6.0
5.5
5.0
4.5
4.0
3.5
3.0
2.5
2.0
1.5
1.0
0.5
0.0
ppm

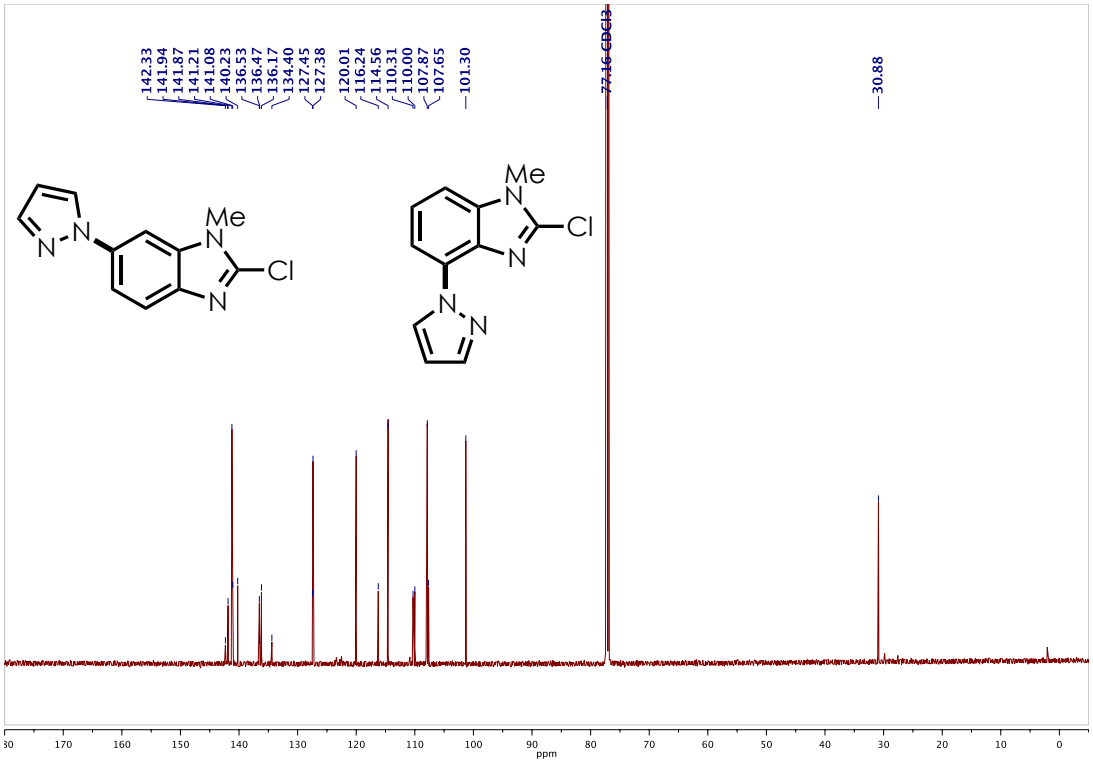
142.33
141.94
141.87
141.21
141.08
140.23
136.53
136.47
136.17
134.40
127.45
127.38
120.01
116.24
114.56
110.31
110.00
107.87
107.65
101.30
77.16 CDCl3
30.88
Me
N
Cl
N
N
N
Me
N
Cl
N
N
N
170
160
150
140
130
120
110
100
90
80
70
60
50
40
30
20
10
0
ppm

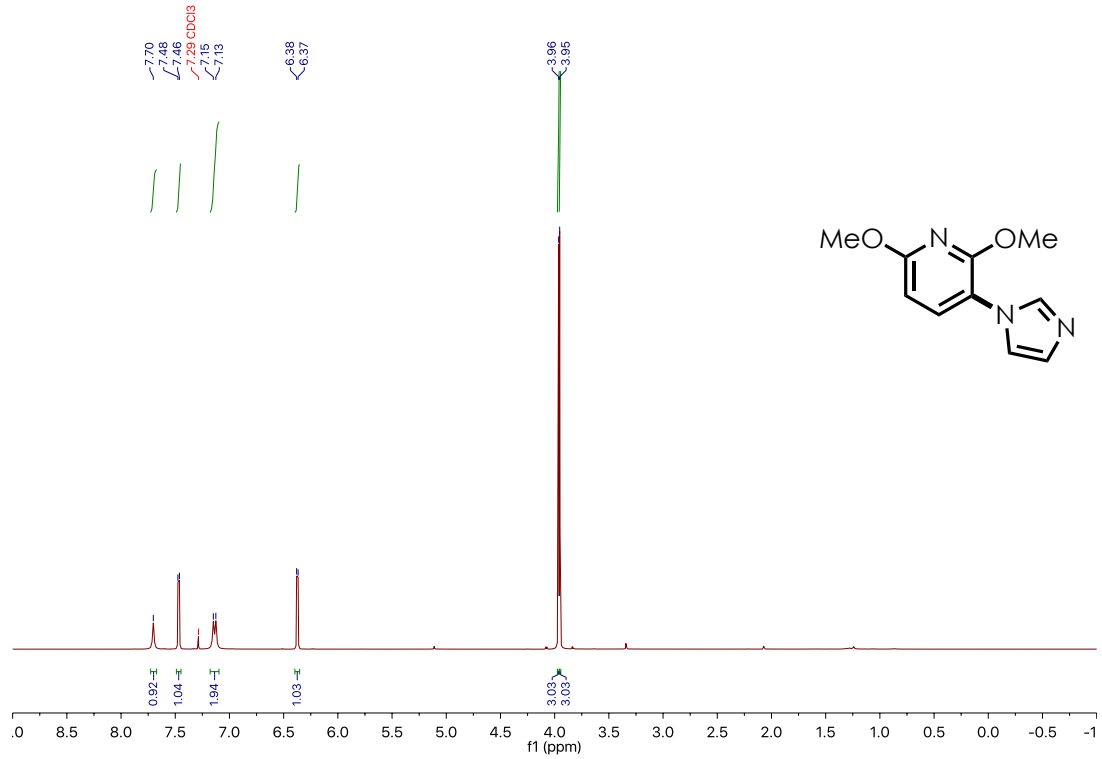
7.70
7.48
7.46
7.29 CDCl3
7.15
7.13
6.38
6.37
3.96
3.95
MeO
N
OMe
N
N
0.92
1.04
1.94
1.03
3.03
3.03
f1 (ppm)

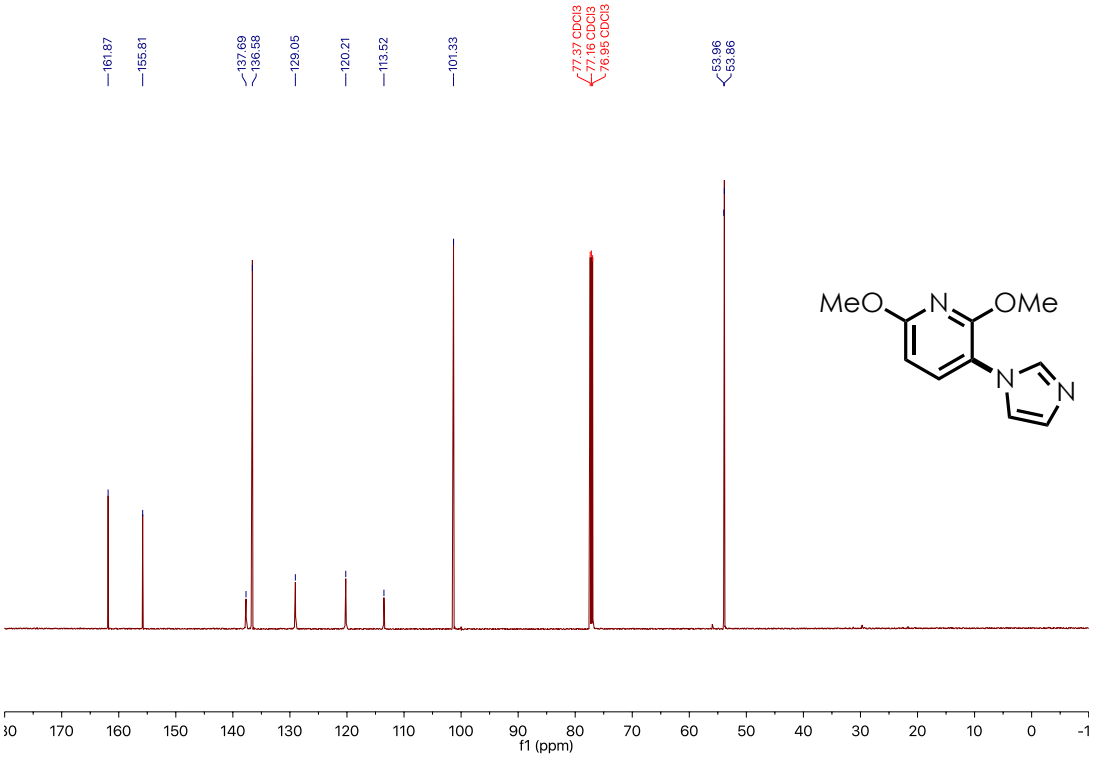
161.87
155.81
137.69
136.58
129.05
120.21
113.52
101.33
77.37 CDCl3
77.16 CDCl3
76.95 CDCl3
53.96
53.86
MeO
N
OMe
N
N
f1 (ppm)

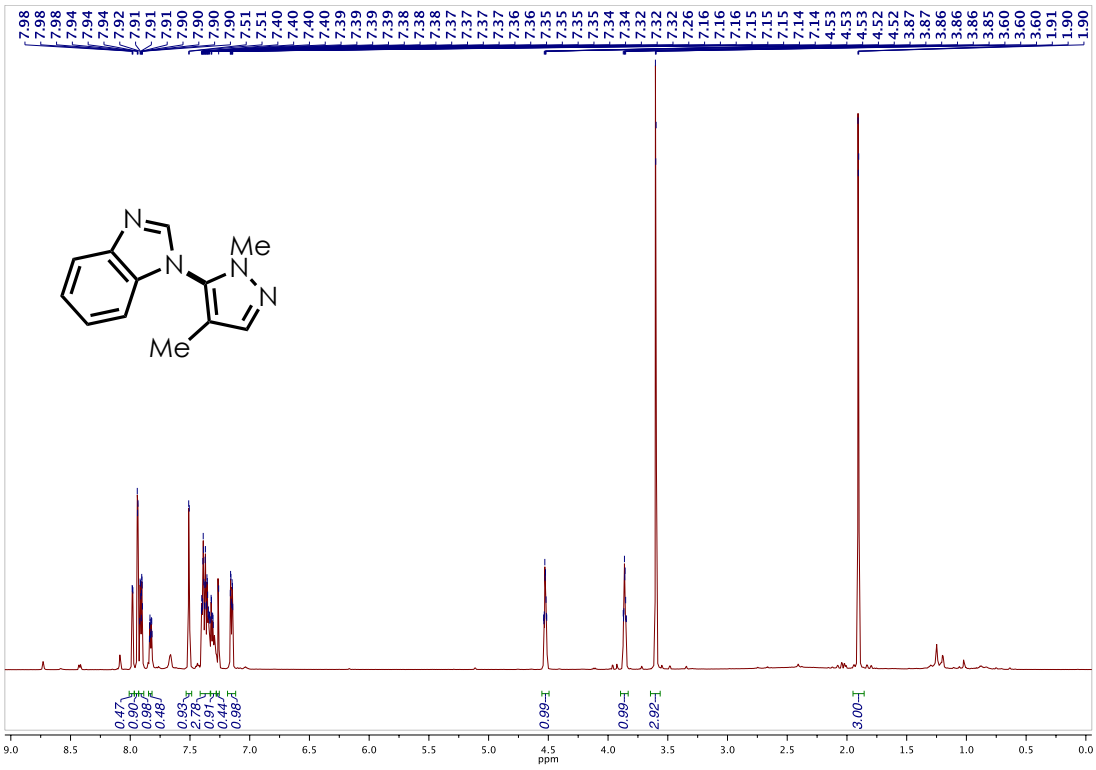
7.98 7.98 7.98 7.94 7.94 7.94 7.92 7.91 7.91 7.91 7.90 7.90 7.90 7.90 7.90 7.51 7.51 7.40 7.40 7.40 7.40 7.39 7.39 7.39 7.39 7.38 7.38 7.38 7.37 7.37 7.37 7.37 7.36 7.36 7.35 7.35 7.35 7.35 7.34 7.34 7.32 7.32 7.32 7.26 7.16 7.16 7.16 7.15 7.15 7.15 7.14 7.14 4.53 4.53 4.52 4.52 3.87 3.87 3.86 3.86 3.86 3.85 3.60 3.60 3.60 1.91 1.90 1.90
N
N
Me
N
N
Me
0.47 0.90 0.98 0.48 0.93 2.78 2.97 0.44 0.98 0.99 0.99 2.92 3.00
9.0 8.5 8.0 7.5 7.0 6.5 6.0 5.5 5.0 4.5 4.0 3.5 3.0 2.5 2.0 1.5 1.0 0.5 0.0
ppm

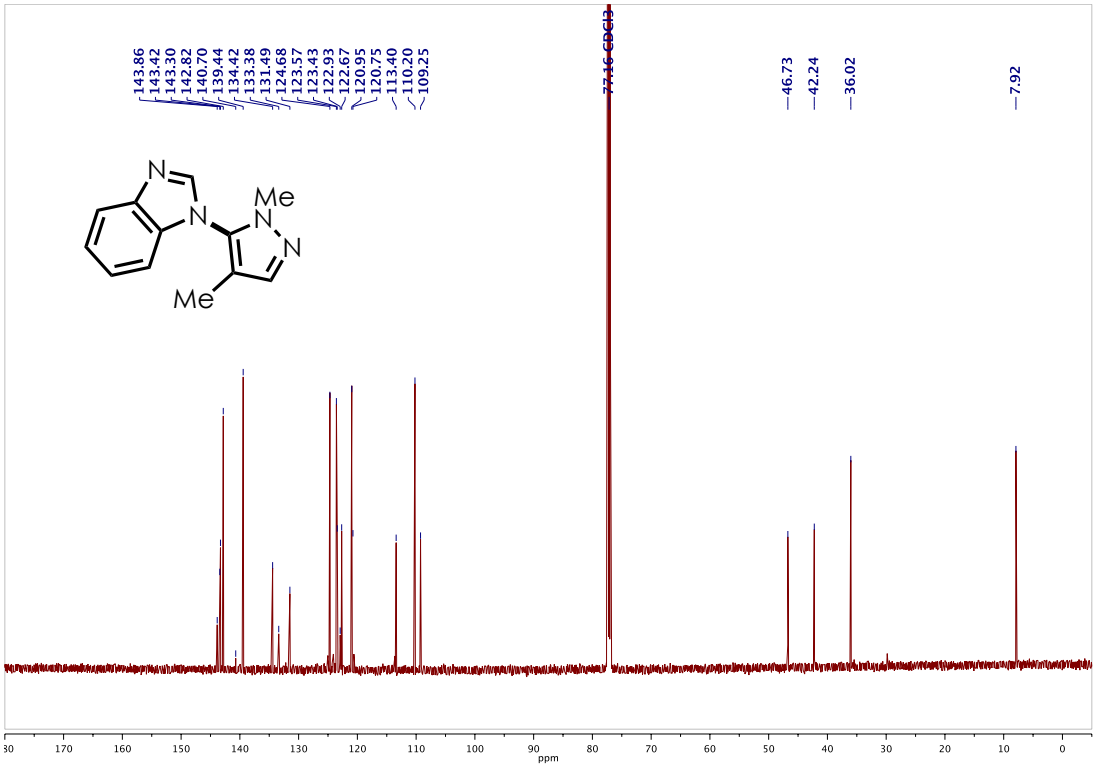
143.86 143.42 143.30 142.82 140.70 139.44 134.42 133.38 131.49 124.68 123.57 123.43 122.93 122.67 120.95 120.75 113.40 110.20 109.25
77.16 CDCl3
46.73 42.24 36.02 7.92
N
N
Me
N
N
Me
30 170 160 150 140 130 120 110 100 90 80 70 60 50 40 30 20 10 0
ppm

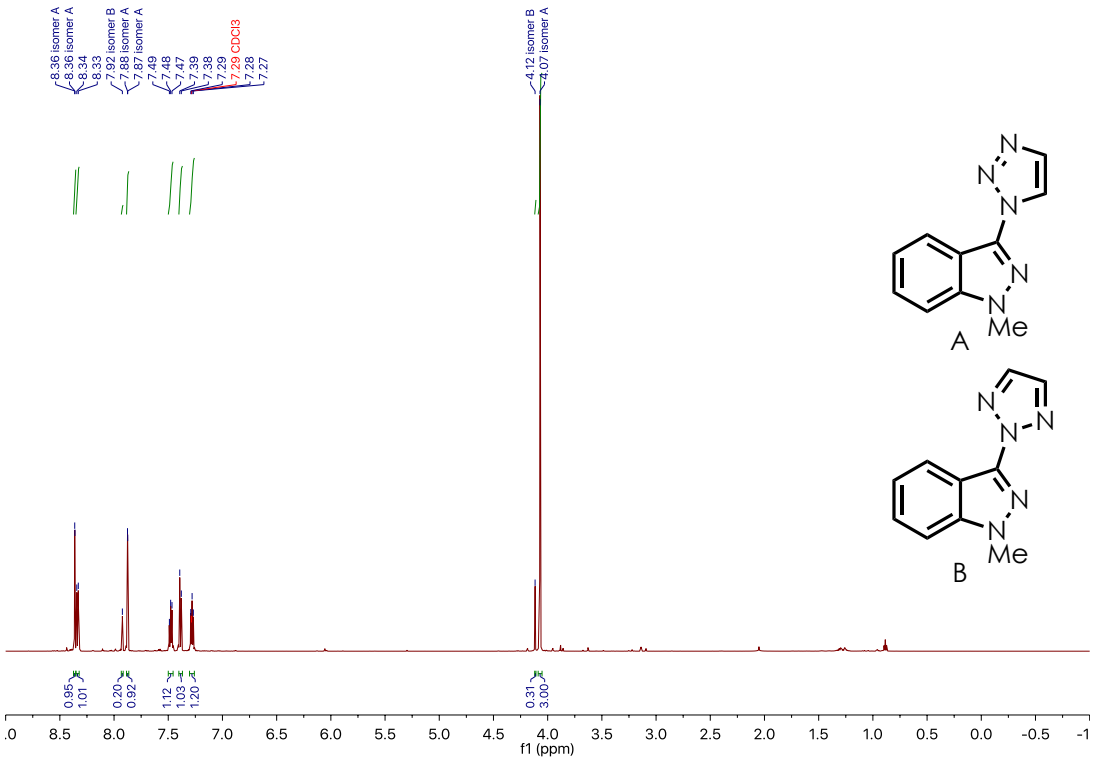
8.36 isomer A
8.36 isomer A
8.34
8.33
7.92 isomer B
7.88 isomer A
7.87 isomer A
7.49
7.48
7.47
7.39
7.38
7.29
7.29 CDCl3
7.28
7.27
4.12 isomer B
4.07 isomer A
N
N
N
N
N
Me
A
N
N
N
N
N
Me
B
0.95
1.01
0.20
0.92
1.12
1.03
1.20
0.31
3.00
.0
8.5
8.0
7.5
7.0
6.5
6.0
5.5
5.0
4.5
4.0
3.5
3.0
2.5
2.0
1.5
1.0
0.5
0.0
-0.5
-1
f1 (ppm)

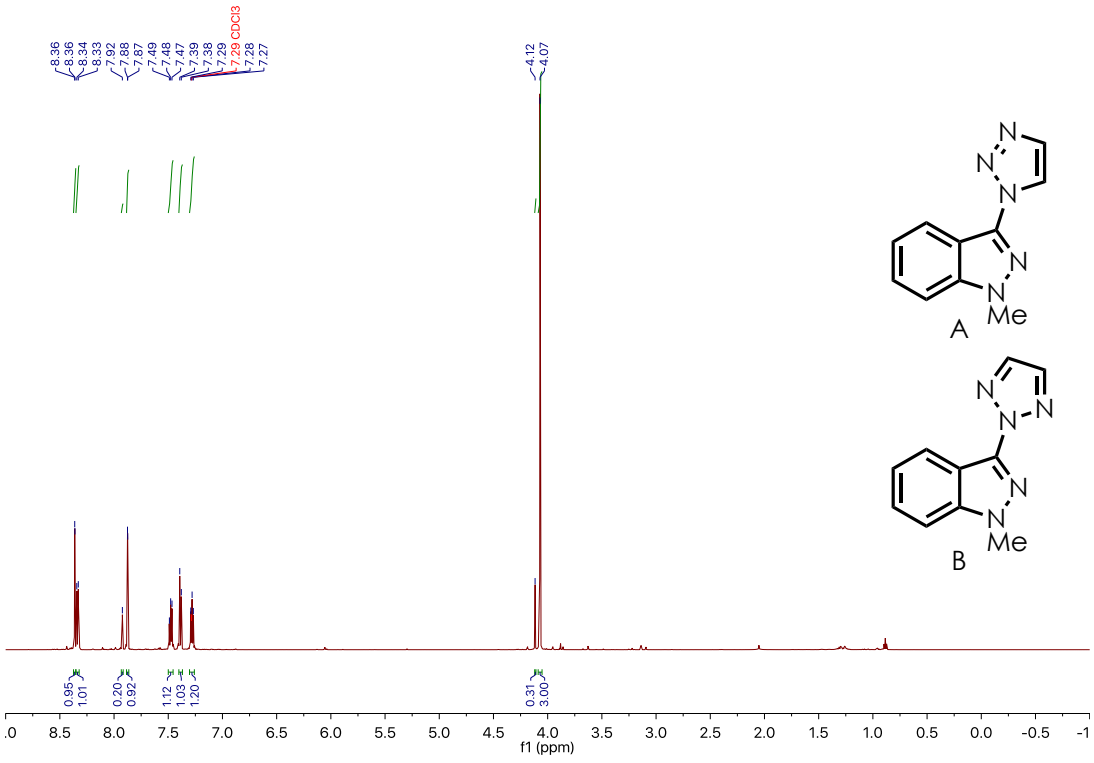
8.36
8.36
8.34
8.33
7.92
7.88
7.87
7.49
7.48
7.47
7.39
7.38
7.29
7.29 CDCl3
7.28
7.27
4.12
4.07
N
N
N
N
N
Me
A
N
N
N
N
N
Me
B
0.95
1.01
0.20
0.92
1.12
1.03
1.20
0.31
3.00
.0
8.5
8.0
7.5
7.0
6.5
6.0
5.5
5.0
4.5
4.0
3.5
3.0
2.5
2.0
1.5
1.0
0.5
0.0
-0.5
-1
f1 (ppm)

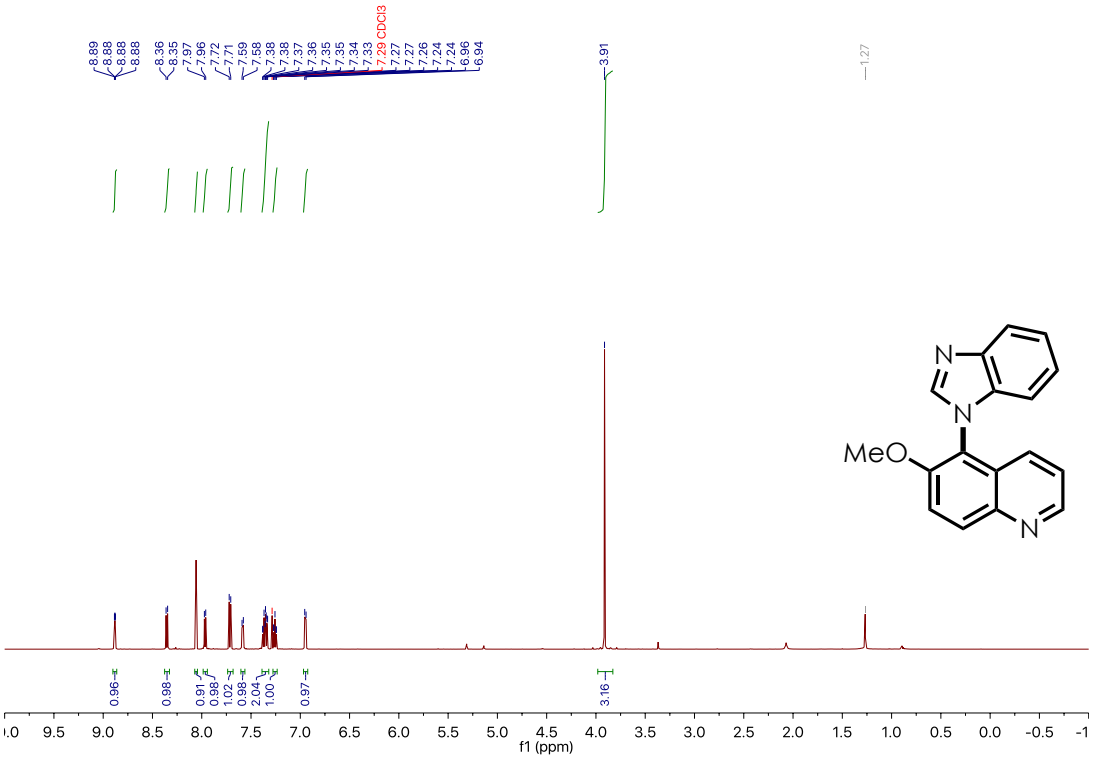
8.89
8.88
8.88
8.88
8.36
8.35
7.97
7.96
7.72
7.71
7.59
7.58
7.38
7.38
7.37
7.36
7.35
7.35
7.34
7.33
7.29 CDCl3
7.27
7.27
7.26
7.24
7.24
6.96
6.94
3.91
1.27
MeO
N
N
N
0.96
0.98
0.91
0.98
1.02
0.98
2.04
1.00
0.97
3.16
f1 (ppm)

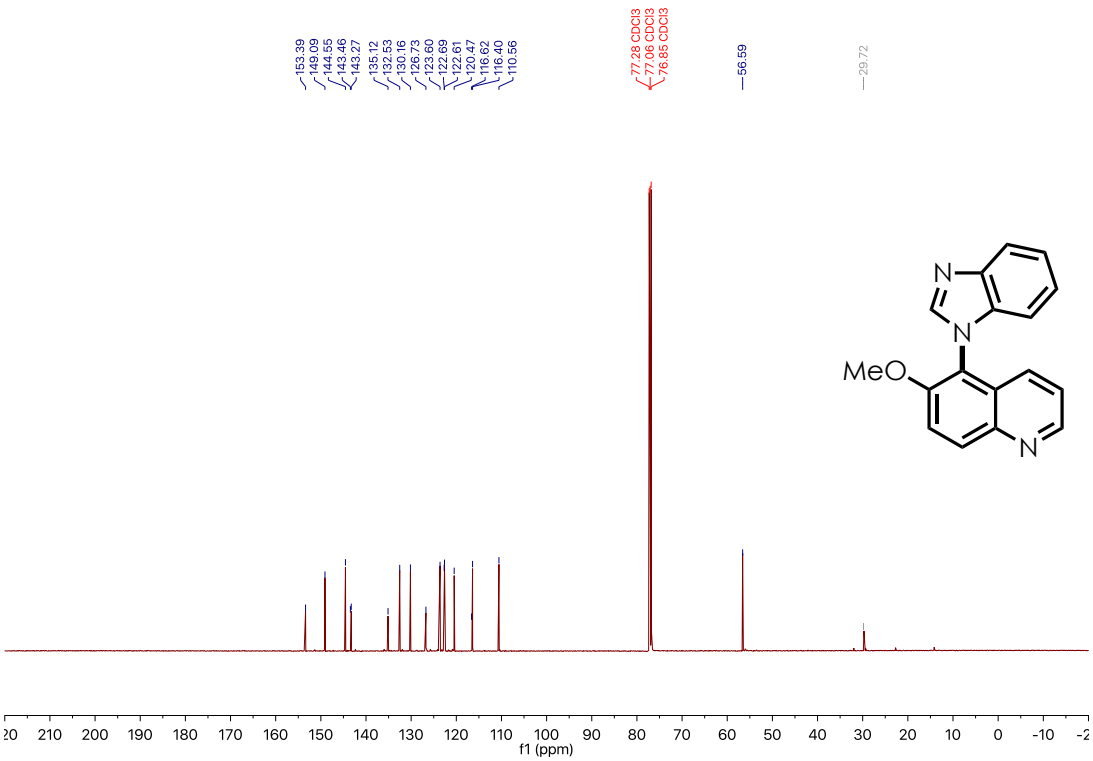
153.39
149.09
144.55
143.46
143.27
135.12
132.53
130.16
126.73
123.60
122.69
122.61
120.47
116.62
116.40
110.56
77.28 CDCl3
77.06 CDCl3
76.85 CDCl3
56.59
29.72
MeO
N
N
N
f1 (ppm)

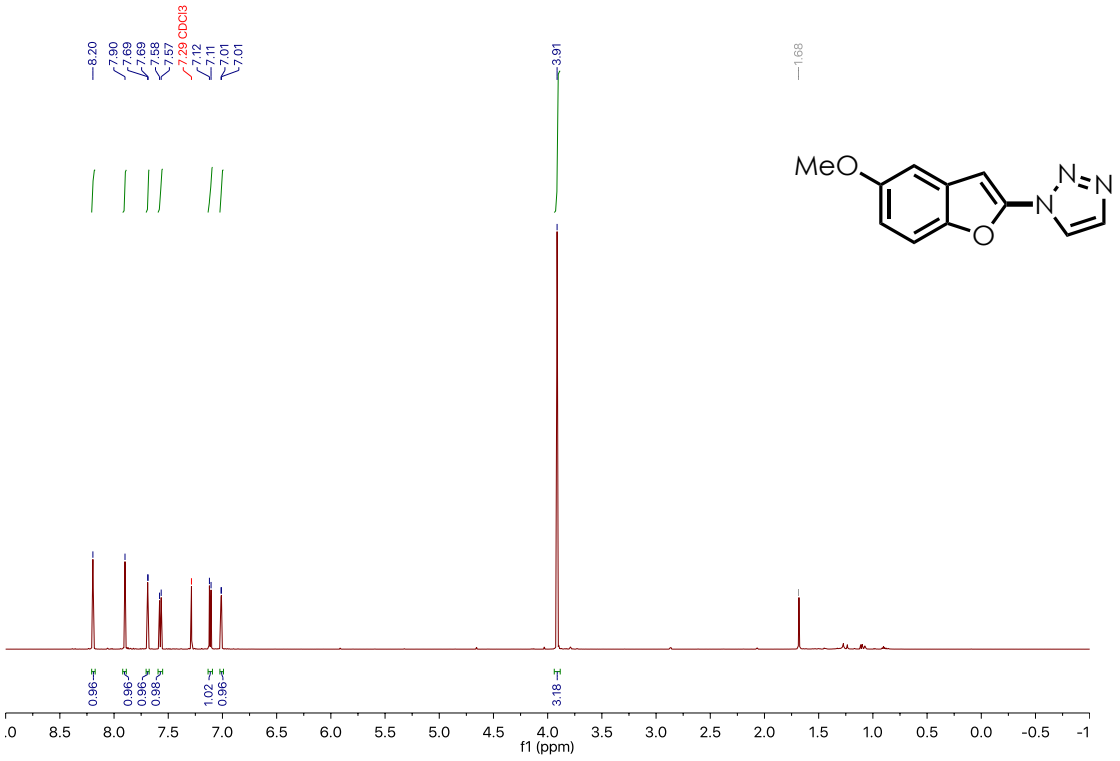
8.20
7.90
7.69
7.69
7.58
7.57
7.29 CDCl3
7.12
7.11
7.01
7.01
3.91
1.68
MeO
N
N
N
O
0.96
0.96
0.96
0.98
1.02
0.96
3.18
f1 (ppm)

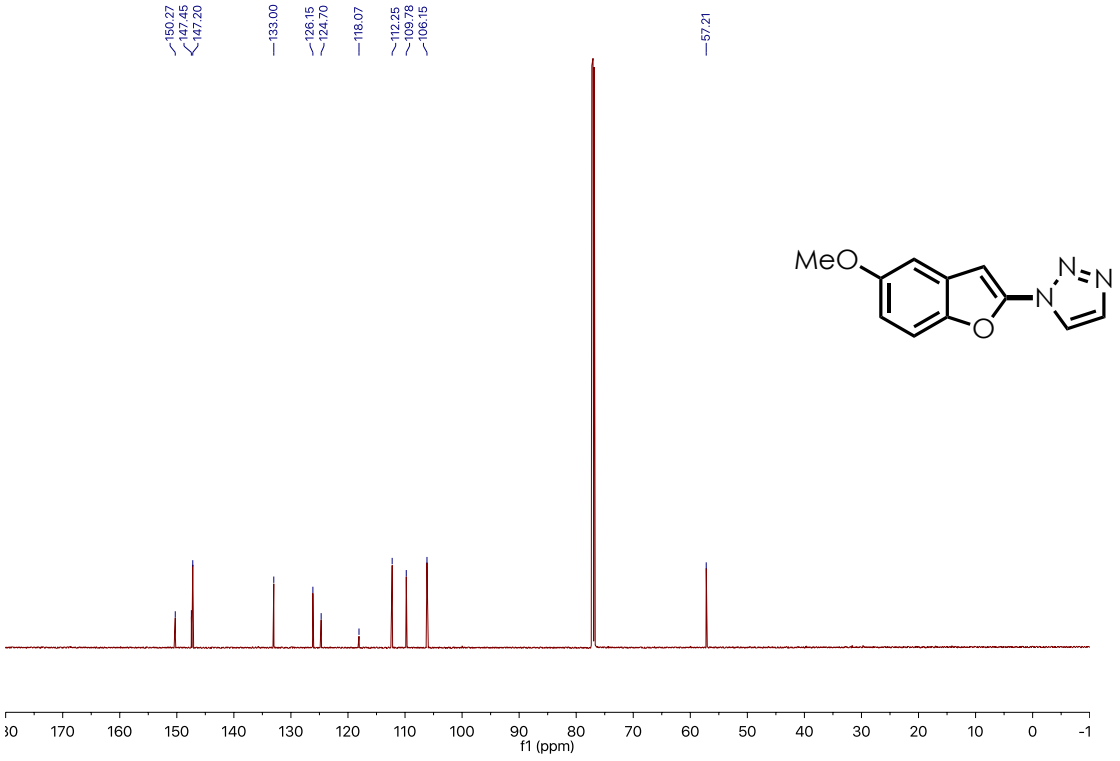
150.27
147.45
147.20
133.00
126.15
124.70
118.07
112.25
109.78
106.15
57.21
MeO
N
N
N
O
f1 (ppm)

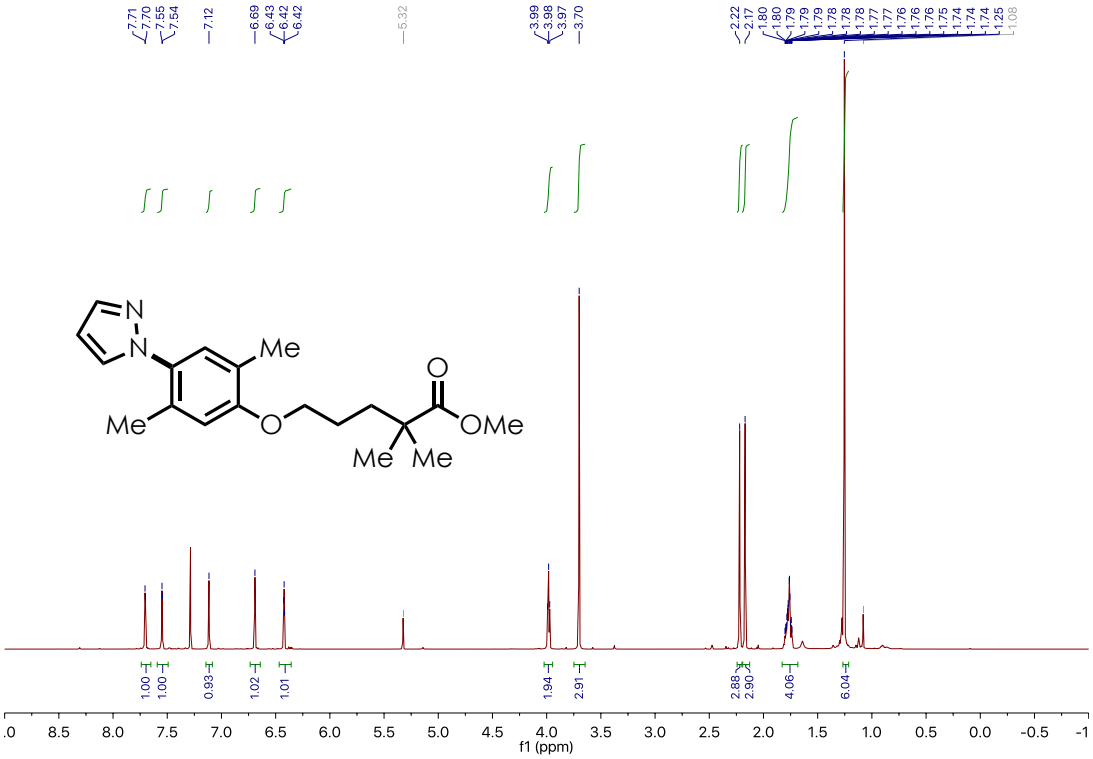
7.71
7.70
7.55
7.54
7.12
6.69
6.43
6.42
6.42
5.32
3.99
3.98
3.97
3.70
2.22
2.17
1.80
1.80
1.79
1.79
1.79
1.78
1.78
1.78
1.77
1.77
1.76
1.76
1.76
1.75
1.74
1.74
1.74
1.25
1.08
N
N
Me
Me
O
O
OMe
Me
Me
1.00
1.00
0.93
1.02
1.01
1.94
2.91
2.88
2.90
4.06
6.04
f1 (ppm)

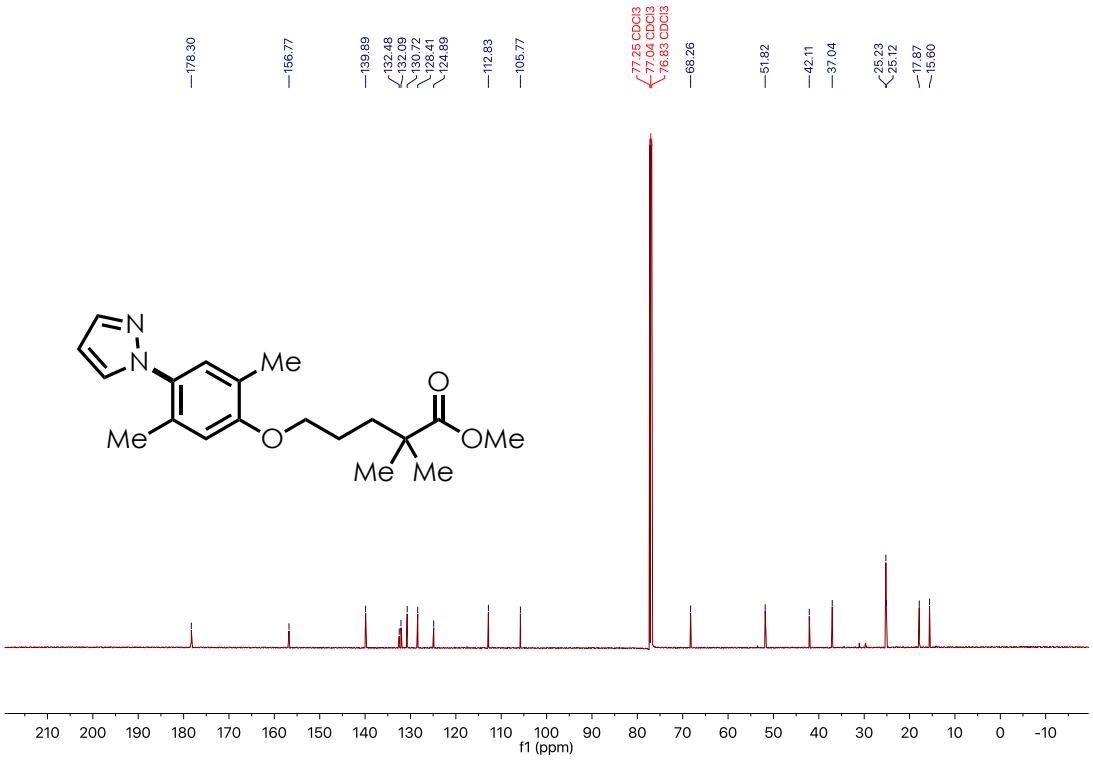
178.30
156.77
139.89
132.48
132.09
130.72
128.41
124.89
112.83
105.77
77.25 CDCl3
77.04 CDCl3
76.83 CDCl3
68.26
51.82
42.11
37.04
25.23
25.12
17.87
15.60
N
N
Me
Me
O
O
OMe
Me
Me
f1 (ppm)

APPENDIX C: SUPPORTING INFORMATION FOR CHAPTER 4

General Methods

Proton and carbon magnetic resonance spectra (^{1}H NMR and ^{13}C NMR) were recorded on a Bruker model DRX 400 or a Bruker Avance III 600 CryoProbe(^{1}H NMR at 400 MHz and 600 MHz and ^{13}C NMR at 100 and 151 MHz) spectrometer. Chemical shifts for protons are reported in parts per million downfield from tetramethylsilane and are referenced to residual protium in the solvent (^{1}H NMR: $CHCl_3$ at 7.26 ppm). Chemical shifts for carbons are reported in parts per million downfield from tetramethylsilane and are referenced to the carbon resonances of the solvent peak (^{13}C NMR: $CDCl_3$ at 77.16 ppm). Chemical shifts for fluorines are referenced to fluorobenzene as an internal standard (^{19}F NMR: C_6H_5F at -113.15 ppm). ^{1}H NMR data are reported as follows: chemical shift, multiplicity (s = singlet, d = doublet, t = triplet, q = quartet, sept = septet, oct = octet, dd = doublet of doublets, ddt = doublet of doublet of triplets, ddd = doublet of doublet of doublets, dddd = doublet of doublet of doublet of doublets, m = multiplet, and prefixed br = broad), coupling constants (Hz), and integration. Infrared (IR) spectra were obtained using a Jasco 260 Plus Fourier transform infrared spectrometer. High resolution mass spectra (HRMS) were obtained using a Thermo LTqFT mass spectrometer with electrospray ionization in positive mode. Thin layer chromatography (TLC) was performed on SiliaPlate 250 μm thick silica gel plates provided by Silicycle. Visualization was accomplished with short wave UV light (254 nm), cerium ammonium molybdate or potassium permanganate solution followed by heating. Flash chromatography was performed using SiliaFlash P60 silica gel (40-63 μm) purchased from Silicycle. Unless noted all reactions were run under an atmosphere of oxygen with magnetic stirring. Irradiation of photochemical reactions was carried out using a PAR38 blue aquarium

LED lamp (Model #6851) fabricated with high-power Cree LEDs as purchased from Ecoxotic (www.ecoxotic.com) with standard borosilicate glass vials purchased from Fischer Scientific. For all photolyses, reactions were stirred using a PTFE coated magnetic stir bar on a magnetic stir plate. Gas chromatography (GC) was performed on an Agilent 6850 series instrument equipped with a split-mode capillary injection system and Agilent 5973 network mass spec detector (MSD). Yield refers to isolated yield of analytically pure material unless otherwise noted. NMR yields were determined using hexamethyldisiloxane as an internal standard. All other reagents were obtained from commercial sources and used without further purification unless otherwise noted.

Photoreactor Configuration. Reactions were irradiated using a simple photoreactor consisting of two Par38 Royal Blue Aquarium LED lamps (Model #6851) in which reactions (1 dram vials) are irradiated simultaneously. In order to ensure that the reactions are run near room temperature, a simple cooling fan was installed above the reactor to aid in dissipating the heat generated from high power LEDs. While a number of other blue LED sources are effective, we have found that LED emitters with high luminous flux and narrow viewing angles give the best results.

Photocatalyst Synthesis

9-Mesityl-2,7-dimethyl-10-phenylacridin-10-ium tetrafluoroborate (Catalyst B).

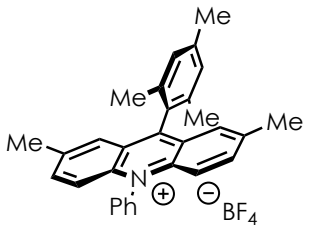

The title compound was prepared as previously reported by our lab. The spectral data matched the values reported in the literature.[1]

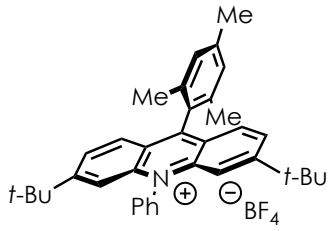

9-Mesityl-3,6-di-*tert*-butyl-10-phenylacridinium tetrafluoroborate (Catalyst C).

The title compound was prepared as previously reported by our lab. The spectral data matched the values reported in the literature.[2]

Preparation of Arene Substrates

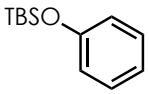

***tert*-Butyldimethyl(phenoxy)silane** was prepared according to a published procedure; spectral data were in agreement with literature values.[3]

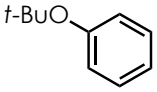

***tert*-Butoxybenzene** was prepared according to a published procedure; spectral data were in agreement with literature values.[4]

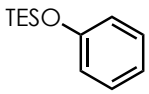

Triethyl(phenoxy)silane was prepared according to a published procedure; spectral data were in agreement with literature values.[5]

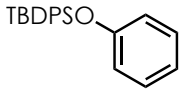

***tert*-Butyl(phenoxy)diphenylsilane** was prepared according to a published procedure; spectral data were in agreement with literature values.[6]

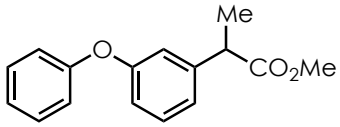

Methyl 2-(3-phenoxyphenyl)propanoate (fenoprofen methyl ester) The title compound was prepared according to a published procedure; spectral data were in agreement with literature values.[6]

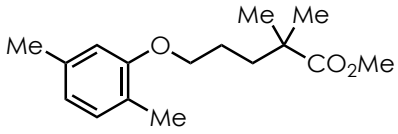

Methyl 5-(2,5-dimethylphenoxy)-2,2-dimethylpentanoate (gemfibrozil methyl ester) The title compound was prepared according to a published procedure; spectral data were in agreement with literature values.[6]

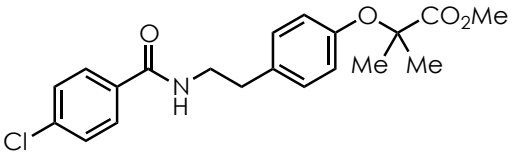

Methyl 2-(4-(2-(4-chlorobenzamido)ethyl)phenoxy)-2-methylpropanoate (bezafibrate methyl ester) To a solution of bezafibrate (0.30 g, 0.8 mmol) in dimethylformamide (5 mL)

at 0 °C was added potassium carbonate (0.57 g, 4.1 mmol). Iodomethane (0.16 mL, 2.5 mmol) was then added slowly and the reaction mixture allowed to warm to room temperature. After 16 hours, the reaction mixture was diluted with ethyl acetate (10 mL), washed with sodium hydrogen carbonate (1 x 15 mL of a saturated aqueous solution), water (2 x 15 mL) and brine (2 x 15 mL) and the organic layer dried ($MgSO_4$) and concentrated in vacuo to give the title compound as a white solid (0.30 g, 96%).

^{1}H NMR (600 MHz, $CDCl_3$) δ 7.61 (AA'BB', *J* = 8.4 Hz, 2H), 7.38 (AA'BB', *J* = 8.4 Hz, 2H), 7.10 (AA'BB', *J* = 8.4 Hz, 2H), 6.80 (AA'BB', *J* = 8.4 Hz, 2H), 6.02 (brt, *J* = 6.6 Hz, 1H), 3.77 (s, 3H), 3.67 (q, *J* = 6.6 Hz, 2H), 2.86 (t, *J* = 6.6 Hz, 2H), 1.59 (s, 6H). **^{13}C NMR** (151 MHz, $CDCl_3$) δ 174.85, 166.51, 153.93, 137.54, 132.99, 132.58, 129.53, 128.73, 128.39, 119.47, 79.12, 52.56, 41.35, 34.73, 25.36.

IR (thin film): 3316.96, 2292.98, 2947.66, 1736.58, 1638.23, 1541.81, 1509.03, 1486.85, 1289.18, 1235.18, 1141.65; **HRMS** (ESI): calculated for $C_{20}H_{22}ClNO_4$ $[M+H]^+$= 376.1310; found 376.1309.

Reaction Conditions and Characterization

General procedure (Method A) for C–H amination (monosubstituted arenes)

To a 1 dram vial containing a Teflon-coated magnetic stir bar was added the arene (0.10 mmol, 1 equiv.), 2.4 mg of **Catalyst B** (0.005 mmol, 0.05 equiv.) and amine coupling partner (0.3 mmol, 3 equiv.). When using amine hydrochloride salts, the reagents were dissolved in 1,2-dichloroethane (0.8 mL) and 4M pH 8 phosphate aqueous buffer solution (0.2 mL). When using free amines, the reagents were dissolved in 1,2-dichloroethane (1.0 mL). The vial was sealed with a Teflon-lined septum screw cap. A vent needle was inserted and the

reaction medium was sparged for 5 minutes by bubbling oxygen through the mixture. The vent needle was removed, and the oxygen balloon was maintained, providing approximately 1 atm of oxygen to the vial headspace for the course of the reaction. The vial was positioned on a stir plate approximately 10 cm from a Par38 LED lamp supplying blue light (λ = 440-460 nm). After irradiation for 4 hours, the reaction mixture was concentrated in vacuo and purified by column chromatography on silica gel with hexanes/ethyl acetate with the eluent noted for each substrate.

General procedure (Method B) for C–H amination (complex arenes)

To a 1 dram vial containing a Teflon-coated magnetic stir bar was added the arene (0.10 mmol, 1 equiv.), 2.9 mg of **Catalyst C** (0.005 mmol, 0.05 equiv.), amine coupling partner (0.3 mmol, 3 equiv.), and 6.3 mg of (2,2,6,6-tetramethylpiperidin-1-yl)oxyl (0.04 mmol, 0.4 eq.). The reagents were dissolved in 1,2-dichloroethane (0.8 mL) and 4M pH 8 phosphate aqueous buffer solution (0.2 mL). The vial was sealed with a Teflon-lined septum screw cap. The septum was pierced with a disposable steel needle connected to an oxygen-filled balloon. A vent needle was inserted and the reaction medium was sparged for 5 minutes by bubbling oxygen through the mixture. The vent needle was removed, and the oxygen balloon was maintained, providing approximately 1 atm of oxygen to the vial headspace for the course of the reaction. The vial was positioned on a stir plate approximately 10 cm from a Par38 LED lamp supplying blue light (λ = 440-460 nm). After irradiation overnight (15–26 hours), the reaction mixture was concentrated in vacuo and purified by column chromatography on silica gel with hexanes/ethyl acetate with the eluent noted for each substrate.

Characterization for aryl amination products

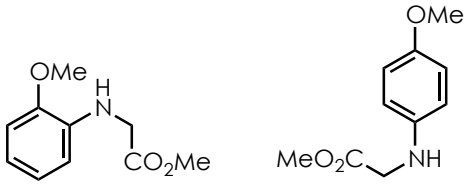

Methyl 2-((2-methoxyphenyl)amino)acetate and methyl 2-((4-methoxyphenyl)amino)acetate (4.1a). The title compound was prepared using Method A with an irradiation time of 4 hours. The title compound was purified by column chromatography on silica gel (10% to 30% EtOAc/Hexanes) to give **4.1a** in 45% yield and a mixture of 1.3:1 *ortho* to *para* regioisomers.

4.1a. ^{1}**H NMR** (600 MHz, $CDCl_3$) δ 6.86 (td, *J* = 7.6, 1.4 Hz, 1H), 6.79 (s, 2.5H), 6.72 (td, *J* = 7.7, 1.5 Hz, 1H), 6.59 (d, *J* = 8.9 Hz, 1.5H), 6.49 (dd, *J* = 7.8, 1.5 Hz, 1H), 4.82 (s, 1H), 4.03 (s, 0.75H), 3.99–3.91 (m, 2H), 3.88 (s, 1.5H), 3.87 (s, 3H), 3.78 (s, 3H), 3.77 (s, 2.25H), 3.75 (s, 2.25). ^{13}**C NMR** (151 MHz, $CDCl_3$) δ 172.03, 171.76, 152.77, 147.18, 141.29, 137.09, 121.26, 117.65, 115.02, 114.50, 110.01, 109.70, 55.87, 55.57, 52.36, 46.78, 45.68. **IR** (thin film): 3420.14, 2952.48, 2836.77, 1748.16, 1508.06, 1249.65, 1225.54; **HRMS** (ESI): calculated for $C_{10}H_{14}NO_3$ $[M+H]^+$= 196.096820; found 196.09713.

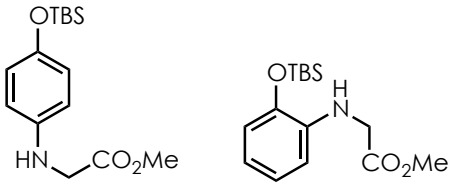

Methyl 2-((2-((*tert*-butyldimethylsilyl)oxy)phenyl)amino)acetate and methyl 2-((4-((*tert*-butyldimethylsilyl)oxy)phenyl)amino)acetate (4.1b). The title compound was prepared using Method A with an irradiation time of 4 hours. The title compound was purified by

column chromatography on silica gel (10% to 30% EtOAc/Hexanes) to give **4.1b** in 49% yield and a mixture of 1.8:1 *para* to *ortho* regioisomers.

4.1b. ^{1}**H NMR** (600 MHz, $CDCl_3$) δ 6.86 (dd, *J* = 7.7, 1.4 Hz, 0.6H), 6.75 (dd, *J* = 7.8, 1.4 Hz, 0.6H), 6.72 – 6.64 (m, 2H), 6.61 (dd, *J* = 7.7, 1.6 Hz, 0.6H), 6.55 – 6.44 (m, 2.6H), 4.76 (s, 0.6H), 4.02 (s, 1H), 3.93 (d, *J* = 5.4 Hz, 1.2H), 3.87 (s, 2H), 3.79 (s, 1.8H), 3.77 (s, 3H), 1.05 (s, 5.4H), 0.96 (s, 9H), 0.25 (s, 3.6H), 0.15 (s, 6H). ^{13}**C NMR** (151 MHz, $CDCl_3$) δ 172.02, 171.59, 148.15, 142.83, 141.59, 139.16, 122.03, 120.88, 117.70, 117.42, 114.28, 110.65, 52.35, 46.71, 45.74, 29.85, 25.94, 25.87, 25.84, 25.77, 18.35, 18.31, -4.17, -4.35.
IR (thin film): 3411.46, 2955.38, 2929.34, 2857.99, 1748.16, 1601.59, 1513.85, 1253.50, 1213.01; **HRMS** (ESI): calculated for $C_{15}H_{26}NO_3Si$ $[M+H]^+$= 296.167651; found 296.16770.

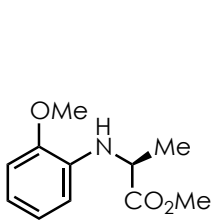

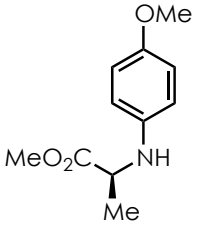

(*S*)-Methyl 2-((2-methoxyphenyl)amino)propanoate and (*S*)-methyl 2-((4-methoxyphenyl)amino)propanoate (4.2a). The title compound was prepared using Method A with an irradiation time of 4 hours. The title compound was purified by column chromatography on silica gel (10% to 30% EtOAc/Hexanes) to give **4.2a** in 62% yield and a mixture of 1.2:1 *ortho* to *para* regioisomers.

4.2a. ^{1}**H NMR** (600 MHz, $CDCl_3$) δ 6.84 (dd, *J* = 7.6, 1.4 Hz, 0.5H), 6.79–6.73 (m, 2.5H), 6.71 (dd, *J* = 7.7, 1.4 Hz, .5H), 6.63–6.53 (m, 2H), 6.51 (dd, *J* = 7.8, 1.4 Hz, .5H), 4.69 (d, *J* = 8.4 Hz, .5H), 4.18–4.13 (m, .5H), 4.08 (s, 1H), 3.86 (d, *J* = 1.3 Hz, 2.5H), 3.80–3.67 (m,

3H), 1.51 (dd, *J* = 7.0, 1.3 Hz, 1.5H), 1.46 (dd, *J* = 7.0, 1.2 Hz, 3H). **^{13}C NMR** (151 MHz, $CDCl_3$) δ 175.56, 175.29, 152.86, 147.09, 140.78, 136.56, 121.25, 117.62, 115.15, 114.99, 110.27, 109.78, 55.81, 55.55, 53.16, 52.36, 52.32, 51.78, 19.23, 19.09.

IR (thin film): 3420.14, 2951.52, 2835.81, 1747.19, 1508.06, 1249.65, 1222.65; **HRMS** (ESI): calculated for $C_{11}H_{16}NO_3$ $[M+H]^+$= 210.112470; found 210.11263.

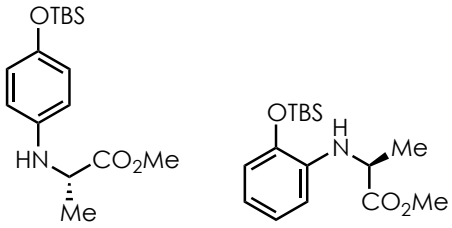

(*S*)-Methyl 2-((2-((*tert*-butyldimethylsilyl)oxy)phenyl)amino)propanoate and (*S*)-methyl 2-((4-((*tert*-butyldimethylsilyl)oxy)phenyl)amino)propanoate (4.2b). The title compound was prepared using Method A with an irradiation time of 4 hours. The title compound was purified by column chromatography on silica gel (10% to 30% EtOAc/Hexanes) to give **4.2b** in 65% yield and a mixture of 1.9:1 *para* to *ortho* regioisomers.

4.2b. ^{1}H NMR (600 MHz, $CDCl_3$) δ 6.83 (td, *J* = 7.7, 1.4 Hz, 0.4H), 6.74 (dd, *J* = 7.8, 1.4 Hz, 0.4H), 6.68 (d, *J* = 8.7 Hz, 2H), 6.60 (dd, *J* = 7.6, 1.5 Hz, 0.4H), 6.54 – 6.47 (m, 2.4H), 4.64 (d, *J* = 8.5 Hz, 0.4H), 4.14 (dd, *J* = 8.4, 6.8 Hz, 0.4H), 4.06 (d, *J* = 7.1 Hz, 1H), 3.87 (s, 1H), 3.72 (s, 1.2H), 3.71 (s, 3H), 1.48 (d, *J* = 6.9 Hz, 1.2H), 1.45 (d, *J* = 6.9 Hz, 3H), 1.04 (s, 3.6H), 0.96 (s, 9H), 0.24 (d, *J* = 5.1 Hz, 2.4H), 0.14 (s, 6H). **^{13}C NMR** (151 MHz, $CDCl_3$) δ 175.56, 175.06, 148.25, 142.80, 141.09, 138.59, 122.05, 120.85, 117.93, 117.35, 114.90, 110.84, 53.09, 52.30, 51.73, 25.95, 25.87, 25.84, 19.26, 19.14, 18.37, 18.30, -4.13, -4.21, -4.35.

IR (thin film): 3393.14, 2955.38, 2930.31, 2857.99, 1743.33, 1511.92, 1253.5, 1211.08, 1160.94; **HRMS** (ESI): calculated for $C_{16}H_{28}NO_3Si$ $[M+H]^+$= 310.183301; found 310.18307.

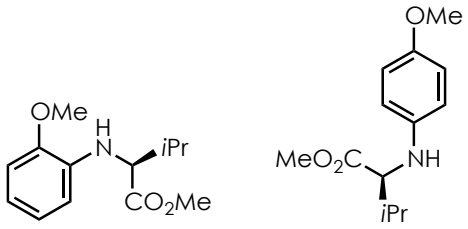

(*S*)-Methyl 2-((2-methoxyphenyl)amino)-3-methylbutanoate and (*S*)-methyl 2-((4-methoxyphenyl)amino)-3-methylbutanoate (4.3a). The title compound was prepared using Method A with an irradiation time of 4 hours. The title compound was purified by column chromatography on silica gel (10% to 30% EtOAc/Hexanes) to give **4.3a** in 80% yield and a mixture of 2.2:1 *ortho* to *para* regioisomers.

4.3a. ^{1}H NMR (600 MHz, $CDCl_3$) δ 6.82 (td, *J* = 7.6, 1.4 Hz, 1H), 6.76 (d, *J* = 8.9 Hz, 2.4H), 6.68 (td, *J* = 7.7, 1.5 Hz, 1H), 6.65–6.58 (m, 1.4H), 6.54 (dd, *J* = 7.8, 1.5 Hz, 1H), 4.73 (d, *J* = 9.2 Hz, 1H), 3.86 (s, 5.1H), 3.78 (s, 1), 3.74 (s, 2.1H), 3.70 (s, 3H), 3.69 (s, 2.1H), 2.16 (dq, *J* = 13.3, 6.7 Hz, 1H), 2.12–2.05 (m, 0.7H), 1.10–0.96 (m, 10.2H). **^{13}C NMR** (151 MHz, $CDCl_3$) δ 174.70, 174.37, 152.78, 147.15, 141.57, 137.26, 121.25, 117.32, 115.31, 114.97, 110.22, 109.85, 63.88, 62.28, 55.84, 55.64, 51.97, 51.95, 31.72, 31.70, 19.32, 19.29, 19.02, 18.85.

IR (thin film): 3393.14, 2957.30, 2930.31, 2857.99, 1740.44, 1509.03, 1253.50; **HRMS** (ESI): calculated for $C_{13}H_{20}NO_3$ $[M+H]^+$= 238.143770; found 238.14400.

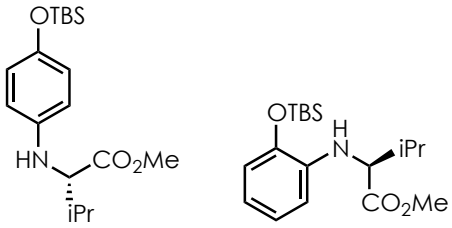

(*S*)-Methyl 2-((2-((*tert*-butyldimethylsilyl)oxy)phenyl)amino)-3-methylbutanoate and (*S*)-methyl 2-((4-((*tert*-butyldimethylsilyl)oxy)phenyl)amino)-3-methylbutanoate (4.3b). The title compound was prepared using Method A with an irradiation time of 4 hours. The title compound was purified by column chromatography on silica gel (10% to 30% EtOAc/Hexanes) to give **4.3b** in 72% yield and a mixture of 2.1:1 *para* to *ortho* regioisomers.

4.3b. ^{1}H NMR (600 MHz, $CDCl_3$) δ 6.82 (d, *J* = 1.4 Hz, 0.6H), 6.74 (dd, *J* = 7.9, 1.4 Hz, 0.6H), 6.67 (d, *J* = 3.4 Hz, 2H), 6.57 (d, *J* = 1.5 Hz, 0.6H), 6.55 – 6.49 (m, 2.6H), 4.68 (dd, *J* = 9.7, 2.9 Hz, 0.6H), 3.89 (dd, *J* = 9.4, 5.6 Hz, 0.6H), 3.86 – 3.81 (m, 1H), 3.77 – 3.72 (m, 1H), 3.69 (d, *J* = 3.7 Hz, 4.8H), 2.17 – 2.11 (m, 0.6H), 2.10 – 2.04 (m, 1H), 1.07 – 1.03 (m, 5.4H), 1.03 – 0.99 (m, 9.6H), 0.96 (d, *J* = 3.3 Hz, 6H), 0.26 (d, *J* = 5.2 Hz, 3.6H), 0.14 (d, *J* = 3.3 Hz, 6H). **^{13}C NMR** (151 MHz, $CDCl_3$) δ 174.70, 174.08, 148.17, 142.81, 141.86, 139.25, 121.98, 120.79, 117.77, 117.10, 115.12, 110.69, 63.85, 61.93, 51.90, 31.75, 31.70, 25.94, 25.87, 19.31, 19.22, 18.87, 18.75, 18.34, 18.29, -4.14, -4.17, -4.35.

IR (thin film): 3392.17, 2957.30, 2930.31, 2857.99, 1740.44, 1509.99, 1471.42, 1253.50; **HRMS** (ESI): calculated for $C_{18}H_{32}NO_3Si$ $[M+H]^+$= 338.214601; found 338.21476.

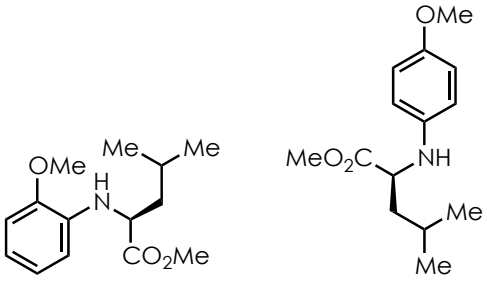

(*S*)-Methyl 2-((2-methoxyphenyl)amino)-4-methylpentanoate and (*S*)-methyl 2-((4-methoxyphenyl)amino)-4-methylpentanoate (4.4a). The title compound was prepared using Method A with an irradiation time of 4 hours. The title compound was purified by column chromatography on silica gel (10% to 30% EtOAc/Hexanes) to give **4.4a** in 81% yield and a mixture of 1.5:1 *ortho* to *para* regioisomers.

4.4a. ^{1}H NMR (600 MHz, $CDCl_3$) δ 6.83 (td, *J* = 7.6, 1.3 Hz, 1H), 6.79–6.75 (m, 1.8H), 6.69 (td, *J* = 7.7, 1.4 Hz, 1H), 6.60 (d, *J* = 8.8 Hz, 0.8H), 6.54 (dd, *J* = 7.9, 1.4 Hz, 1H), 4.56 (d, *J* = 9.1 Hz, 1H), 4.10 (dt, *J* = 9.0, 7.2 Hz, 1H), 4.01 (d, *J* = 7.8 Hz, 0.4H), 3.85 (s, 3H), 3.74 (d, *J* = 7.7 Hz, 1.2H), 3.69 (d, *J* = 5.6 Hz, 4.2H), 1.89–1.75 (m, 1.4H), 1.70 (t, *J* = 7.1 Hz, 2H), 1.67–1.57 (m, 0.8H), 1.04–0.90 (m, 8.4H). **^{13}C NMR** (151 MHz, $CDCl_3$) δ 175.69, 175.40, 152.83, 147.08, 141.18, 136.95, 121.28, 117.50, 115.13, 114.98, 110.17, 109.80, 77.16, 56.38, 55.81, 55.58, 54.84, 52.17, 52.13, 42.62, 42.41, 25.01, 22.93, 22.91, 22.32, 22.30.
IR (thin film): 3394.10, 2955.38, 2870.52, 1747.19, 1515.77, 1456.96, 1245.79, 1227.47; **HRMS** (ESI): calculated for $C_{14}H_{22}NO_3$ $[M+H]^+$= 252.159420; found 252.15946.

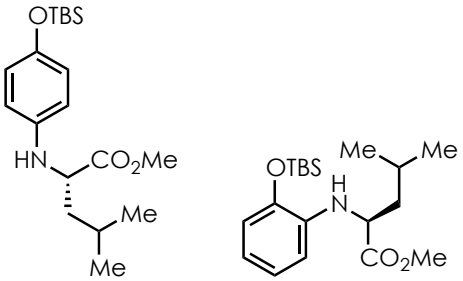

(*S*)-Methyl 2-((2-((*tert*-butyldimethylsilyl)oxy)phenyl)amino)-4-methylpentanoate and (*S*)-methyl 2-((4-((*tert*-butyldimethylsilyl)oxy)phenyl)amino)-4-methylpentanoate (4.4b). The title compound was prepared using Method A with an irradiation time of 4 hours. The title compound was purified by column chromatography on silica gel (10% to 30% EtOAc/Hexanes) to give **4.4b** in 89% yield and a mixture of 2.4:1 *para* to *ortho* regioisomers.

4.4b. ^{1}H NMR (600 MHz, Chloroform-*d*) δ 6.86 – 6.80 (m, 0.5H), 6.74 (dd, *J* = 7.8, 1.4 Hz, 0.5H), 6.68 – 6.63 (m, 2H), 6.58 (td, *J* = 7.7, 1.5 Hz, 0.5H), 6.52 (d, *J* = 8.8 Hz, 2.5H), 4.47 (d, *J* = 9.3 Hz, 0.5H), 4.08 (ddd, *J* = 9.3, 7.8, 6.3 Hz, 0.5H), 4.00 (d, *J* = 7.3 Hz, 1H), 3.74 – 3.69 (m, 1H), 3.68 (d, *J* = 3.6 Hz, 4.2H), 1.83 – 1.74 (m, 1H), 1.67 (dt, *J* = 7.9, 6.4 Hz, 0.5H), 1.62 (td, *J* = 7.1, 1.6 Hz, 2.8H), 1.04 (s, 3.6H), 1.01 – 0.92 (m, 17.4H), 0.24 (d, *J* = 7.4 Hz, 2.4H), 0.14 (s, 6H). **^{13}C NMR** (151 MHz, $CDCl_3$) δ 175.69, 175.15, 148.25, 142.75, 141.48, 138.97, 129.50, 122.07, 120.81, 120.24, 117.88, 117.30, 114.98, 110.71, 56.37, 54.79, 52.10, 52.08, 42.66, 42.56, 25.95, 25.86, 25.82, 25.08, 24.99, 22.91, 22.89, 22.44, 22.37, 18.37, 18.28, -4.14, -4.21, -4.35.

IR (thin film): 3383.50, 2956.34, 2930.31, 2857.99, 1741.41, 1509.99, 1251.58; **HRMS** (ESI): calculated for $C_{19}H_{34}NO_3Si$ $[M+H]^+$= 352.230251; found 352.23103.

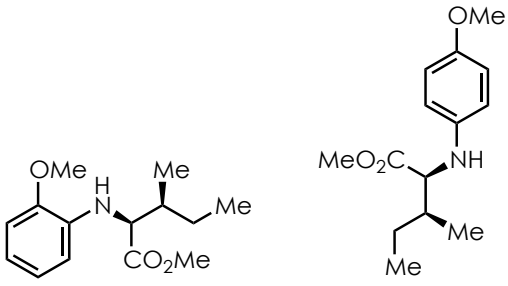

(2*S*,3*S*)-Methyl 2-((2-methoxyphenyl)amino)-3-methylpentanoateand (2*S*,3*S*)-methyl 2-((4-methoxyphenyl)amino)-3-methylpentanoate (4.5a). The title compound was prepared using Method A with an irradiation time of 4 hours. The title compound was purified by column chromatography on silica gel (10% to 30% EtOAc/Hexanes) to give **4.5a** in 69% yield and a mixture of 2.0:1 *ortho* to *para* regioisomers.

4.5a. ^{1}H NMR (600 MHz, $CDCl_3$) δ 6.83 (td, *J* = 7.6, 1.2 Hz, 1H), 6.81–6.72 (m, 2H), 6.73–6.64 (m, 1H), 6.64–6.58 (m, 1H), 6.54 (dd, *J* = 7.8, 1.4 Hz, 1H), 4.74 (d, *J* = 9.2 Hz, 1H), 3.95 (dd, *J* = 9.2, 6.2 Hz, 1H), 3.86 (s, 3H), 3.74 (d, *J* = 0.6 Hz, 1.5H), 3.70 (dd, *J* = 6.6, 0.6 Hz, 3H), 3.69 (s, 3H), 1.91 (dtd, *J* = 8.9, 6.6, 4.4 Hz, 1H), 1.85–1.80 (m, 0.5H), 1.74–1.61 (m, 1.5H), 1.38–1.27 (m, 2H), 1.06 ? 0.88 (m, 12H). **^{13}C NMR** (151 MHz, $CDCl_3$) δ 174.61, 174.28, 152.73, 147.13, 141.42, 137.12, 121.26, 117.26, 115.22, 114.98, 110.14, 109.82, 62.56, 60.91, 55.83, 55.62, 51.92, 51.90, 38.20, 38.10, 25.83, 25.75, 15.68, 11.62.

IR (thin film): 3395.07, 2963.09, 2935.13, 2876.31, 1738.51, 1602.56, 1514.81, 1456.96, 1245.79, 1223.61; **HRMS** (ESI): calculated for $C_{14}H_{22}NO_3$ $[M+H]^+$= 252.159420; found 252.15976.

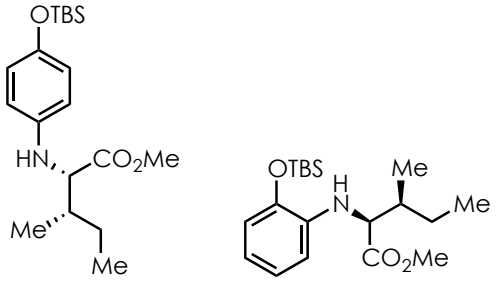

(2*S*,3*S*)-Methyl 2-((2-((*tert*-butyldimethylsilyl)oxy)phenyl)amino)-3-methylpentanoate and (2*S*,3*S*)-methyl 2-((4-((*tert*-butyldimethylsilyl)oxy)phenyl)amino)-3-methylpentanoate (4.5b). The title compound was prepared using Method A with an

irradiation time of 4 hours. The title compound was purified by column chromatography on silica gel (10% to 30% EtOAc/Hexanes) to give **4.5b** in 82% yield and a mixture of 1.7:1 *para* to *ortho* regioisomers.

4.5b. ^{1}**H NMR** (600 MHz, $CDCl_3$) δ 6.82 (td, *J* = 7.7, 1.4 Hz, 0.6H), 6.76 – 6.72 (m, 0.6H), 6.70 – 6.65 (m, 2H), 6.58 (dd, *J* = 7.6, 1.5 Hz, 0.6H), 6.52 (d, *J* = 8.8 Hz, 2.6H), 4.70 (d, *J* = 9.4 Hz, 0.6H), 3.96 (dd, *J* = 9.4, 5.8 Hz, 0.6H), 3.85 (s, 2H), 3.69 (d, *J* = 5.0 Hz, 4.8H), 1.88 (m, 0.6H), 1.84 – 1.79 (m, 1H), 1.67 – 1.58 (m, 2H), 1.36 – 1.22 (m, 2H), 1.05 (s, 5.4H), 0.99 – 0.92 (m, 21H), 0.25 (d, *J* = 6.0 Hz, 3.6H), 0.14 (s, 6H). ^{13}**C NMR** (151 MHz, $CDCl_3$) δ 174.61, 173.97, 148.13, 142.77, 141.73, 139.09, 122.00, 120.80, 117.77, 117.04, 115.04, 110.62, 62.53, 60.70, 51.85, 38.25, 25.93, 25.86, 25.76, 18.29, 15.69, 15.65, 11.77, 11.63, -4.16, -4.18, -4.35, -4.36.

IR (thin film): 3393.14, 2959.23, 2931.27, 2857.99, 1740.44, 1509.99, 1252.54; **HRMS** (ESI): calculated for $C_{19}H_{34}NO_3Si$ $[M+H]^+$= 352.230251; found 352.23054.

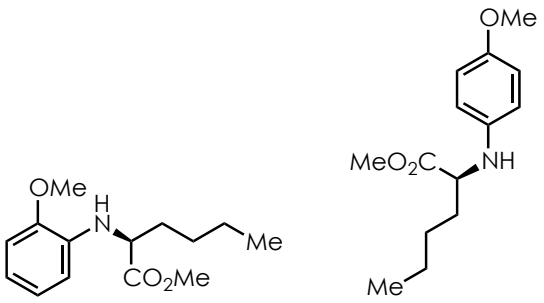

(*S*)-Methyl 2-((2-methoxyphenyl)amino)hexanoate and (*S*)-methyl 2-((4-methoxyphenyl)amino)hexanoate (4.6a). The title compound was prepared using Method A with an irradiation time of 4 hours. The title compound was purified by column chromatography on silica gel (10% to 30% EtOAc/Hexanes) to give **4.6a** in 88% yield and a mixture of 1.5:1 *ortho* to *para* regioisomers.

4.6a. **^{1}H NMR** (600 MHz, $CDCl_3$) δ 6.83 (td, *J* = 7.6, 1.4 Hz, 1H), 6.77 (td, *J* = 7.5, 1.8 Hz, 2.3H), 6.73–6.68 (m, 1H), 6.64–6.58 (m, 1.3H), 6.52 (dd, *J* = 7.8, 1.5 Hz, 1H), 4.67 (d, *J* = 8.7 Hz, 1H), 4.05 (dt, *J* = 8.5, 6.6 Hz, 1H), 3.97 (s, 0.65H), 3.86 (s, 3H), 3.74 (s, 1.95H), 3.71 (s, 3H), 3.70 (s, 1.95H), 1.94–1.84 (m, 0.6H), 1.84–1.78 (m, 1H), 1.38 (m, 0.6H), 1.48–1.30 (m, 4H), 0.91 (t, *J* = 7.2 Hz, 4.95H). **^{13}C NMR** (151 MHz, $CDCl_3$) δ 175.27, 174.99, 152.78, 147.09, 141.13, 136.90, 121.25, 117.43, 115.11, 114.97, 110.19, 109.79, 57.87, 56.42, 55.81, 55.57, 52.18, 52.15, 33.12, 32.97, 27.96, 27.94, 22.59, 14.05.

IR (thin film): 3394.10, 2954.41, 2934.16, 2860.88, 1741.41, 1514.81, 1456.96, 1240.00; **HRMS** (ESI): calculated for $C_{14}H_{22}NO_3$ $[M+H]^+$= 252.159420; found 252.15978.

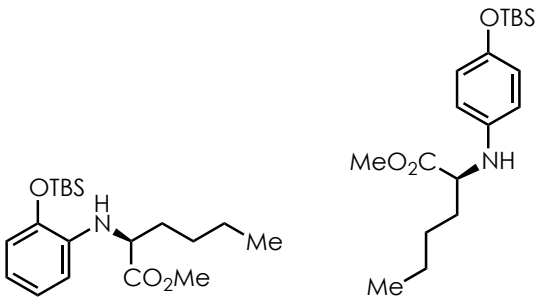

(*S*)-Methyl 2-((2-((*tert*-butyldimethylsilyl)oxy)phenyl)amino)hexanoate and (*S*)-methyl 2-((4-((*tert*-butyldimethylsilyl)oxy)phenyl)amino)hexanoate (4.6b). The title compound was prepared using Method A with an irradiation time of 4 hours. The title compound was purified by column chromatography on silica gel (10% to 30% EtOAc/Hexanes) to give **4.6b** in 89% yield and a mixture of 2.0:1 *para* to *ortho* regioisomers.

4.6b. **^{1}H NMR** (600 MHz, $CDCl_3$) δ 6.82 (td, *J* = 7.7, 1.4 Hz, 0.35H), 6.73 (dd, *J* = 7.9, 1.4 Hz, 0.35H), 6.67 (d, *J* = 8.8 Hz, 2H), 6.58 (td, *J* = 7.7, 1.6 Hz, 0.35H), 6.51 (d, *J* = 8.7 Hz, 2.35H), 4.60 (s, 0.35H), 4.06 (dt, *J* = 8.9, 6.3 Hz, 0.35H), 3.96 (d, *J* = 7.2 Hz, 1H), 3.81 (d, *J* = 8.1 Hz, 1H), 3.70 (d, *J* = 5.0 Hz, 4H), 1.79 (dq, *J* = 9.3, 6.9, 6.3 Hz, 1.6H), 1.75 – 1.67 (m,

1H), 1.43 – 1.31 (m, 5.5H), 1.04 (s, 3H), 0.96 (s, 9H), 0.92 – 0.88 (m, 4H), 0.25 (d, J = 6.2 Hz, 2.1H), 0.14 (s, 6H). **^{13}C NMR** (151 MHz, $CDCl_3$) δ 175.29, 174.73, 148.19, 142.77, 141.45, 138.89, 122.04, 120.83, 117.84, 117.21, 114.94, 110.72, 57.86, 56.24, 52.13, 33.17, 32.90, 27.94, 27.76, 25.95, 25.87, 22.60, 18.37, 18.30, 14.07, -4.14, -4.18, -4.34.

IR (thin film): 3392.17, 2955.38, 2930.31, 2857.99, 1748.16, 1508.06, 1250.61; **HRMS** (ESI): calculated for $C_{19}H_{34}NO_3Si$ $[M+H]^+$= 352.230251; found 352.23075.

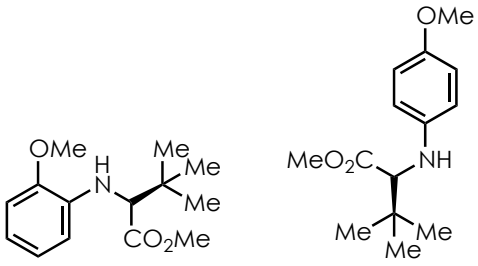

(*S*)-Methyl 2-((2-methoxyphenyl)amino)-3,3-dimethylbutanoate and (S)-methyl 2-((4-methoxyphenyl)amino)-3,3-dimethylbutanoate (4.7a). The title compound was prepared using Method A with an irradiation time of 4 hours. The title compound was purified by column chromatography on silica gel (10% to 30% EtOAc/Hexanes) to give **4.7a** in 48% yield and a mixture of 5.5:1 *ortho* to *para* regioisomers.

4.7a. ^{1}H NMR (600 MHz, $CDCl_3$) δ 6.85 – 6.80 (m, 1H), 6.79 – 6.74 (m, 1.3H), 6.68 (td, J = 7.7, 1.5 Hz, 1H), 6.63 (d, J = 8.9 Hz, 0.3H), 6.57 (dd, J = 7.9, 1.4 Hz, 1H), 4.82 (d, J = 10.1 Hz, 1H), 3.86 (s, 3H), 3.82 (s, 1H), 3.67 (s, 4H), 1.08 (s, 9H), 1.05 (s, 2.7H). **^{13}C NMR** (151 MHz, $CDCl_3$) δ 174.42, 174.10, 152.89, 147.23, 141.82, 137.56, 130.22, 121.26, 117.30, 115.64, 114.94, 110.24, 109.87, 103.70, 67.09, 65.09, 55.83, 55.70, 51.65, 51.61, 34.61, 34.42, 26.92, 26.88, 26.86.

IR (thin film): 3394.10, 2955.38, 2870.52, 1734.66, 1602.56, 1514.81, 1456.96, 1249.65, 1220.72; **HRMS** (ESI): calculated for $C_{14}H_{12}NO_3$ $[M+H]^+$= 252.159420; found 252.15970.

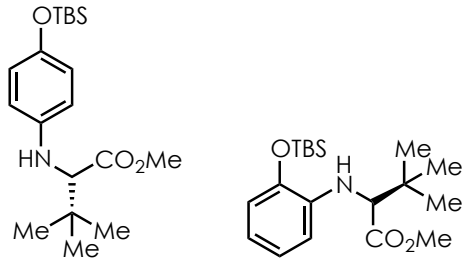

(*S*)-Methyl 2-((2-((*tert*-butyldimethylsilyl)oxy)phenyl)amino)-3,3-dimethylbutanoate and (*S*)-methyl 2-((4-((*tert*-butyldimethylsilyl)oxy)phenyl)amino)-3,3-dimethylbutanoate (4.7b). The title compound was prepared using Method A with an irradiation time of 4 hours. The title compound was purified by column chromatography on silica gel (10% to 30% EtOAc/Hexanes) to give **4.7b** in 33% yield and a mixture of 1.2:1 *para* to *ortho* regioisomers.

4.7b. ^{1}**H NMR** (600 MHz, $CDCl_3$) δ 6.87 – 6.77 (m, 0.9H), 6.77 – 6.69 (m, 0.9H), 6.66 (dd, *J* = 5.5, 3.1 Hz, 2H), 6.59 – 6.51 (m, 3.6H), 4.84 – 4.74 (m, 1H), 3.94 – 3.84 (m, 1H), 3.84 – 3.76 (m, 1H), 3.67 (tq, *J* = 6.2, 3.7, 2.8 Hz, 6.7H), 1.15 – 1.04 (m, 27H), 0.98 – 0.92 (m, 9H), 0.26 (t, *J* = 4.8 Hz, 5.4H), 0.15 (s, 6H). ^{13}**C NMR** (151 MHz, $CDCl_3$) δ 174.42, 173.90, 148.31, 142.89, 142.12, 139.52, 121.96, 120.77, 117.72, 117.11, 115.50, 110.74, 67.09, 65.00, 51.58, 34.61, 34.42, 26.93, 26.89, 26.87, 25.96, 25.87, 25.84, 18.32, 18.29, -4.10, -4.13, -4.35.

IR (thin film): 3393.14, 2955.38, 2931.27, 2858.95, 1735.62, 1509.03, 1239.04; **HRMS** (ESI): calculated for $C_{19}H_{34}NO_3Si$ $[M+H]^+$= 352.230251; found 352.23115.

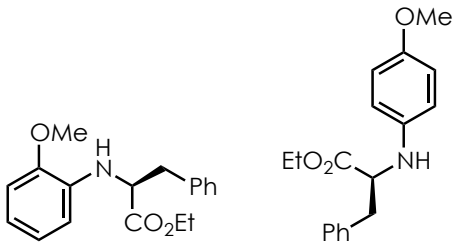

(*S*)-Ethyl 2-((2-methoxyphenyl)amino)-3-phenylpropanoate and (*S*)-ethyl 2-((4-methoxyphenyl)amino)-3-phenylpropanoate (4.8a). The title compound was prepared using Method A with an irradiation time of 4 hours. The title compound was purified by column chromatography on silica gel (10% to 30% EtOAc/Hexanes) to give **4.8a** in 77% yield and a mixture of 1.5:1 *ortho* to *para* regioisomers.

4.8a. ^{1}H NMR (600 MHz, $CDCl_3$) δ 7.31–7.27 (m, 2H), 7.25–7.22 (m, 1H), 7.22–7.18 (m, 2H), 6.82 (td, *J* = 7.6, 1.4 Hz, 1H), 6.77 (dd, *J* = 8.0, 1.4 Hz, 1H), 6.70 (td, *J* = 7.7, 1.5 Hz, 1H), 6.55 (dd, *J* = 7.8, 1.5 Hz, 1H), 4.78 (d, *J* = 8.8 Hz, 1H), 4.32 (dt, *J* = 8.9, 6.6 Hz, 1H), 4.09 (qd, *J* = 7.1, 5.2 Hz, 2H), 3.83 (s, 3H), 3.19–3.11 (m, 2H), 1.14 (t, *J* = 7.1 Hz, 3H). **^{13}C NMR** (151 MHz, $CDCl_3$) 173.41, 147.28, 136.75, 136.51, 129.42, 128.56, 127.00, 121.23, 117.67, 110.60, 109.95, 61.12, 57.94, 55.64, 39.01, 14.24.

IR (thin film): 3395.07, 2934.16, 2834.85, 1732.73, 1518.67, 1508.06, 1456.96; **HRMS** (ESI): calculated for $C_{18}H_{22}NO_3$ $[M+H]^+$= 300.159420; found 300.15964.

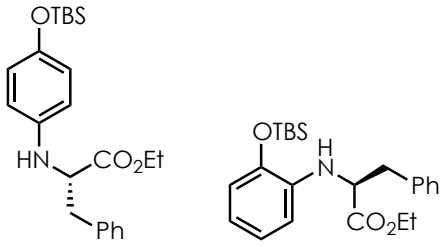

(*S*)-Ethyl 2-((2-((*tert*-butyldimethylsilyl)oxy)phenyl)amino)-3-phenylpropanoate and (*S*)-ethyl 2-((4-((*tert*-butyldimethylsilyl)oxy)phenyl)amino)-3-phenylpropanoate (4.8b). The title compound was prepared using Method A with an irradiation time of 4 hours. The title compound was purified by column chromatography on silica gel (10% to 30% EtOAc/Hexanes) to give **4.8b** in 85% yield and a mixture of 1.4:1 *para* to *ortho* regioisomers.

4.8b. ^{1}H NMR (600 MHz, $CDCl_3$) δ 7.33 – 7.20 (m, 5.1H), 7.18 (ddd, *J* = 18.0, 8.1, 1.4 Hz, 3.4H), 6.84 (td, *J* = 7.7, 1.5 Hz, 0.7H), 6.75 (dd, *J* = 7.8, 1.4 Hz, 0.7H), 6.70 – 6.66 (m, 2H), 6.64 – 6.52 (m, 1.4H), 6.52 (d, *J* = 2.3 Hz, 2H) 4.71 (s, 0.7H), 4.39 (d, *J* = 6.1 Hz, 0.7H), 4.26 (t, *J* = 6.4 Hz, 1H), 4.17 – 4.06 (m, 3.4H), 3.15 (dd, *J* = 6.1, 4.2 Hz, 1.4H), 3.11 (d, *J* = 6.4 Hz, 2H), 1.19 – 1.11 (m, 5.1H), 0.98 (d, *J* = 10.2 Hz, 15.3H), 0.25 – 0.21 (m, 4.2H), 0.15 (s, 6H). **^{13}C NMR** (151 MHz, $CDCl_3$) δ 173.59, 172.96, 148.25, 142.92, 140.95, 138.27, 136.65, 136.52, 129.48, 129.43, 128.58, 128.53, 127.03, 126.94, 121.92, 120.82, 117.77, 117.33, 115.18, 110.95, 61.10, 61.08, 59.03, 57.42, 39.01, 38.59, 25.94, 25.86, 18.31, 18.29, 14.25, -4.13, -4.19, -4.36.

IR (thin film): 3392.17, 3029.62, 2956.34, 2930.31, 2857.02, 1736.58, 1599.66, 1509.99, 1253.50, 1195.65; **HRMS** (ESI): calculated for $C_{23}H_{34}NO_3Si$ $[M+H]^+$= 300.230251; found 400.23047.

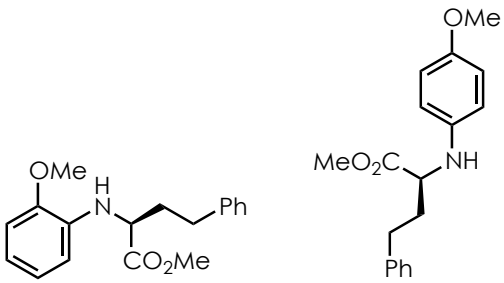

(*S*)-Methyl 2-((2-methoxyphenyl)amino)-4-phenylbutanoate and (*S*)-methyl 2-((4-methoxyphenyl)amino)-4-phenylbutanoate (4.9a). The title compound was prepared using Method A with an irradiation time of 4 hours. The title compound was purified by column chromatography on silica gel (10% to 30% EtOAc/Hexanes) to give **4.9a** in 78% yield and a mixture of 2.0:1 *ortho* to *para* regioisomers.

4.9a. ^{1}H NMR (600 MHz, $CDCl_3$) δ 7.29 (dd, *J* = 8.2, 6.9 Hz, 2H), 7.20 (ddd, *J* = 8.2, 7.1, 1.6 Hz, 3H), 6.84–6.76 (m, 2H), 6.70 (td, *J* = 7.7, 1.5 Hz, 1H), 6.47 (dd, *J* = 7.8, 1.5 Hz, 1H), 4.73 (d, *J* = 9.1 Hz, 1H), 4.09 (ddd, *J* = 9.1, 7.4, 5.7 Hz, 1H), 3.87 (s, 3H), 3.70 (s, 3H), 2.78 (t, *J* = 7.8 Hz, 2H), 2.26–2.17 (m, 1H), 2.16–2.07 (m, 1H). **^{13}C NMR** (151 MHz, $CDCl_3$) δ 174.69, 147.19, 140.99, 136.77, 128.67, 128.59, 126.26, 121.26, 117.62, 110.38, 109.86, 55.79, 55.62, 52.29, 34.72, 31.98.

IR (thin film): 3394.10, 2950.55, 2834,85, 1733.69, 1508.06, 1250.61, 1223.61; **HRMS** (ESI): calculated for $C_{18}H_{22}NO_3$ $[M+H]^+$= 300.159420; found 300.15974.

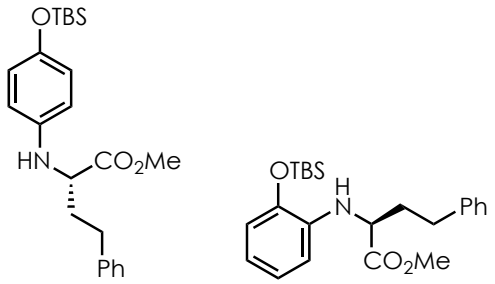

(*S*)-Methyl 2-((2-((*tert*-butyldimethylsilyl)oxy)phenyl)amino)-4-phenylbutanoate and (*S*)-methyl 2-((4-((*tert*-butyldimethylsilyl)oxy)phenyl)amino)-4-phenylbutanoate (4.9b). The title compound was prepared using Method A with an irradiation time of 4 hours. The title compound was purified by column chromatography on silica gel (10% to 30%

EtOAc/Hexanes) to give **4.9b** in 74% yield and a mixture of 2.0:1 *para* to *ortho* regioisomers.

4.9b. ^{1}**H NMR** (600 MHz, $CDCl_3$) δ 7.32 – 7.28 (m, 3H), 7.23 – 7.15 (m, 4.5H), 6.86 – 6.81 (m, .5H), 6.77 (dd, *J* = 7.8, 1.4 Hz, 0.5H), 6.69 – 6.66 (m, 2H), 6.61 (td, *J* = 7.7, 1.6 Hz, 0.5H), 6.51 – 6.46 (m, 2.5H), 4.71 (d, *J* = 9.1 Hz, 0.5H), 4.11 (ddd, *J* = 8.9, 6.9, 5.5 Hz, 0.5H), 4.00 (s, 1H), 3.90 – 3.84 (m, 1H), 3.70 (d, *J* = 2.1 Hz, 4.5H), 2.86 – 2.69 (m, 3H), 2.23 – 2.12 (m, 1.5H), 2.04 (dd, *J* = 7.6, 6.1 Hz, 1.5H), 1.08 (s, 4.5H), 0.97 (s, 9H), 0.32 – 0.26 (m, 3H), 0.16 (s, 6H). ^{13}**C NMR** (151 MHz, $CDCl_3$) δ 174.97, 174.38, 148.30, 142.88, 141.28, 141.02, 138.73, 129.50, 128.64, 128.60, 126.26, 122.05, 120.82, 120.24, 117.91, 117.41, 115.12, 110.86, 57.27, 55.61, 52.23, 52.21, 34.88, 31.96, 31.85, 25.98, 25.86, 18.39, 18.29, -4.09, -4.16, -4.35.

IR (thin film): 3392.17, 3027.69, 2953.45, 2929.34, 2857.02, 1741.41, 1509.03, 1252.54; **HRMS** (ESI): calculated for $C_{23}H_{34}NO_3Si$ $[M+H]^+$= 400.230251; found 400.23108.

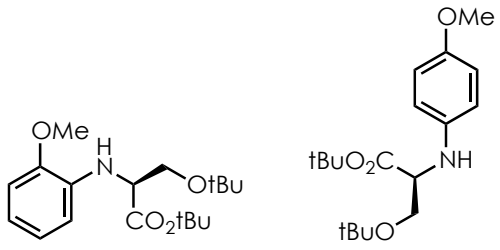

(*S*)-*tert*-Butyl 3-(*tert*-butoxy)-2-((2-methoxyphenyl)amino)propanoate and (*S*)-*tert*-Butyl 3-(*tert*-butoxy)-2-((4-methoxyphenyl)amino)propanoate (4.10a). The title compound was prepared using Method A with an irradiation time of 4 hours. The title compound was purified by column chromatography on silica gel (10% to 30% EtOAc/Hexanes) to give **4.10a** in 84% yield and a mixture of 1.2:1 *ortho* to *para* regioisomers.

4.10a. ^{1}H NMR (600 MHz, $CDCl_3$) δ 6.81 (td, *J* = 7.6, 1.4 Hz, 1H), 6.80–6.73 (m, 2.9), 6.68 (dd, *J* = 7.6, 1.5 Hz, 1H), 6.61 (d, *J* = 8.9 Hz, 1.9H), 6.55 (dd, *J* = 7.9, 1.5 Hz, 1H) 4.09 (d, *J* = 4.6 Hz, 1H), 3.99 (d, *J* = 4.0 Hz, 1H), 3.85 (d, *J* = 2.0 Hz, 3H), 3.74 (d, *J* = 5.9 Hz, 5H), 3.69–3.58 (m, 2H), 1.44 (t, *J* = 5.4 Hz, 18H), 1.17 (t, *J* = 3.0 Hz, 18H).**^{13}C NMR** (151 MHz, $CDCl_3$) δ 171.71, 171.56, 152.61, 147.39, 141.34, 137.10, 121.09, 117.33, 115.37, 114.79, 110.66, 109.82, 73.28, 73.24, 62.81, 62.72, 58.75, 57.45, 55.79, 55.58, 28.16, 27.51, 27.50. **IR** (thin film): 3396.03, 2974.66, 2933.20, 2874.38, 1739.48, 1514.81, 1366.32, 1244.83, 1150.33; **HRMS** (ESI): calculated for $C_{18}H_{30}NO_4$ $[M+H]^+$= 324.216935; found 324.21793.

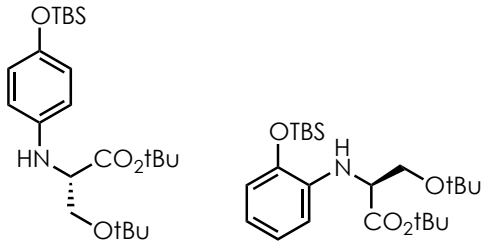

(*S*)-*tert*-Butyl 3-(*tert*-butoxy)-2-((2-((*tert*-butyldimethylsilyl)oxy)phenyl)amino)propanoate and (*S*)-*tert*-butyl 3-(*tert*-butoxy)-2-((4-((*tert*-butyldimethylsilyl)oxy)phenyl)amino)propanoate (4.10b). The title compound was prepared using Method A with an irradiation time of 4 hours. The title compound was purified by column chromatography on silica gel (10% to 30% EtOAc/Hexanes) to give **4.10b** in 83% yield and a mixture of 2.3:1 *para* to *ortho* regioisomers.

4.10b. ^{1}H NMR (600 MHz, $CDCl_3$) δ 6.80 (td, *J* = 7.7, 1.4 Hz, 0.45H), 6.72 (dd, *J* = 7.8, 1.4 Hz, 0.45H), 6.68 – 6.65 (m, 2H), 6.56 (td, *J* = 7.7, 1.5 Hz, 0.45H), 6.53 (d, *J* = 8.8 Hz, 2.45H), 4.94 (d, *J* = 9.8 Hz, 0.45H), 4.19 (s, 1H), 4.05 (dd, *J* = 9.8, 3.9 Hz, 0.45H), 3.98 (t, *J* = 4.0 Hz, 1H), 3.78 (dd, *J* = 8.4, 3.7 Hz, 0.45H), 3.72 (dd, *J* = 8.5, 3.9 Hz, 1H), 3.62 (ddd, *J* = 15.7, 8.4, 4.2 Hz, 1.6H), 1.41 (d, *J* = 5.1 Hz, 13H), 1.16 (s, 13H), 1.04 (s, 4H), 0.95 (s, 9H),

0.25 (d, J = 8.7 Hz, 2.7H), 0.13 (s, 6H). **^{13}C NMR** (151 MHz, $CDCl_3$) δ 171.78, 171.38, 148.00, 142.98, 141.72, 139.18, 121.77, 120.72, 117.74, 116.99, 115.23, 111.02, 81.39, 73.24, 62.72, 62.70, 58.76, 57.38, 28.14, 27.51, 25.89, 18.38, 18.32, -4.10, -4.18, -4.36.

IR (thin film): 3394.10, 2974.66, 2930.31, 2858.95, 1740.44, 1731.76, 1600.63, 1512.88, 1473.35, 1391.39, 1365.35, 1250.61; **HRMS** (ESI): calculated for $C_{23}H_{42}NO_4Si$ $[M+H]^+$= 424.287766; found 424.28807.

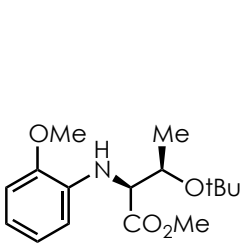

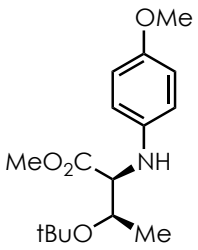

(2*S*,3*R*)-Methyl 3-(*tert*-butoxy)-2-((2-methoxyphenyl)amino)butanoate and (2*S*,3*R*)-methyl 3-(*tert*-butoxy)-2-((4-methoxyphenyl)amino)butanoate (4.11a). The title compound was prepared using Method A with an irradiation time of 4 hours. The title compound was purified by column chromatography on silica gel (10% to 30% EtOAc/Hexanes) to give **4.11a** in 68% yield and a mixture of 1.4:1 *ortho* to *para* regioisomers.

4.11a. ^{1}H NMR (600 MHz, $CDCl_3$) δ 6.84–6.73 (m, 4H), 6.68 (dd, J = 7.7, 1.5 Hz, 1H), 6.63–6.53 (m, 2H), 6.43 (dd, J = 7.8, 1.5 Hz, 1H), 4.24–4.13 (m, 2H), 3.93 (d, J = 3.1 Hz, 1H), 3.90–3.81 (m, 4H), 3.73 (s, 3H), 3.71–3.61 (m, 6H), 1.30 (dd, J = 8.8, 6.2 Hz, 6H), 1.23–1.11 (m, 18H). **^{13}C NMR** (151 MHz, $CDCl_3$) δ 173.69, 173.51, 152.51, 147.40, 141.87, 137.60, 121.12, 117.20, 114.94, 114.92, 109.97, 109.92, 74.20, 74.14, 68.23, 68.20, 63.41, 62.19, 55.84, 55.65, 52.12, 52.05, 28.44, 21.38, 21.16.

IR (thin film): 3395.07, 2975.62, 2951.52, 1749.12, 1732.73, 1515.77, 1242.90; **HRMS** (ESI): calculated for $C_{16}H_{26}NO_4$ $[M+H]^+$= 296.185635; found 296.18627.

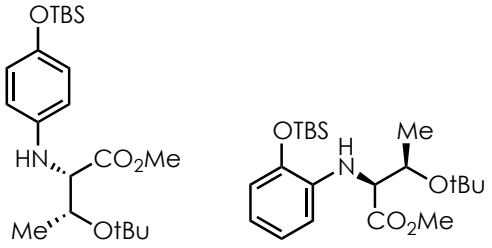

(2*S*,3*R*)-Methyl 3-(*tert*-butoxy)-2-((2-((*tert*-butyldimethylsilyl)oxy)phenyl)amino)butanoate and (2*S*,3*R*)-methyl 3-(*tert*-butoxy)-2-((4-((*tert*-butyldimethylsilyl)oxy)phenyl)amino)butanoate (4.11b). The title compound was prepared using Method A with an irradiation time of 4 hours. The title compound was purified by column chromatography on silica gel (10% to 30% EtOAc/Hexanes) to give **4.11b** in 74% yield and a mixture of 2.4:1 *para* to *ortho* regioisomers.

4.11b. ^{1}H NMR (600 MHz, $CDCl_3$) δ 6.82 – 6.77 (m, 0.4H), 6.74 (dd, *J* = 7.8, 1.4 Hz, 0.4H), 6.66 (d, *J* = 8.7 Hz, 2H), 6.55 (td, *J* = 7.7, 1.5 Hz, 0.4H), 6.49 (d, *J* = 8.8 Hz, 2H), 6.38 (dd, *J* = 7.9, 1.5 Hz, 0.4H), 5.03 (d, *J* = 10.7 Hz, 0.4), 4.27 – 4.22 (m, 1.4H), 4.17 (dd, *J* = 6.2, 2.6 Hz, 1H), 3.93 (dd, *J* = 10.7, 2.1 Hz, 0.4H), 3.82 (dd, *J* = 10.3, 2.6 Hz, 1H), 3.66 (d, *J* = 10.5 Hz, 4.2H), 1.29 (dd, *J* = 8.2, 6.2 Hz, 4.2H), 1.15 (s, 9H), 1.13 (s, 3.6H), 1.05 (s, 3.6H), 0.95 (s, 9H), 0.26 (d, *J* = 14.4 Hz, 2.4H), 0.14 (s, 6H). **^{13}C NMR** (151 MHz, $CDCl_3$) δ 173.76, 173.47, 147.86, 142.93, 142.15, 139.70, 121.88, 120.71, 118.01, 116.74, 114.75, 110.07, 74.13, 68.28, 68.26, 63.39, 61.79, 52.02, 28.50, 28.45, 26.09, 25.88, 21.47, 21.39, 18.29, -4.07, -4.19, -4.34.

IR (thin film): 3395.07, 2974.66, 2955.38, 2930.31, 2857.99, 1749.12, 1732.73, 1509.03, 1252.54; **HRMS** (ESI): calculated for $C_{21}H_{38}NO_4Si$ $[M+H]^+$= 396.256466; found 396.25853.

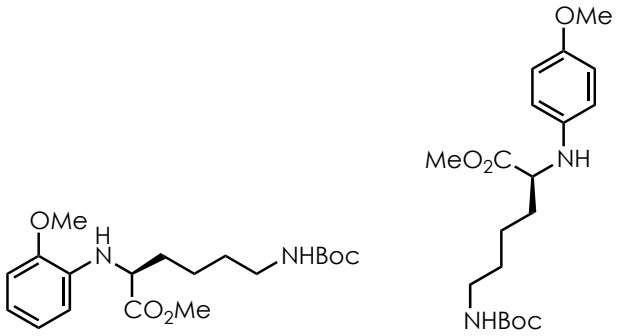

(*S*)-Methyl 6-((*tert*-butoxycarbonyl)amino)-2-((2-methoxyphenyl)amino)hexanoate and (*S*)-methyl 6-((*tert*-butoxycarbonyl)amino)-2-((4-methoxyphenyl)amino)hexanoate (4.12a). The title compound was prepared using Method A with an irradiation time of 4 hours. The title compound was purified by column chromatography on silica gel (10% to 30% EtOAc/Hexanes) to give **4.12a** in 75% yield and a mixture of 1.7:1 *ortho* to *para* regioisomers.

4.12a. ^{1}H NMR (600 MHz, $CDCl_3$) δ 6.82 (td, *J* = 7.6, 1.4 Hz, 1H), 6.80–6.74 (m, 2.6H), 6.70 (dd, *J* = 7.7, 1.5 Hz, 1H), 6.58 (d, *J* = 8.9 Hz, 2.6H), 6.51 (dd, *J* = 7.9, 1.5 Hz, 1H), 4.66 (d, *J* = 8.3 Hz, 0.8H), 4.55 (s, 1H), 4.06 (d, *J* = 6.5 Hz, 1H), 3.99–3.94 (m, 0.8H), 3.85 (d, *J* = 1.8 Hz, 4.2H), 3.73 (d, *J* = 2.0 Hz, 2.6H), 3.70 (d, *J* = 6.9 Hz, 5.4H), 3.17–3.06 (m, 4H), 1.88 (ddd, *J* = 9.2, 4.7, 1.9 Hz, 1.4H), 1.82 (dd, *J* = 4.9, 3.1 Hz, 2H), 1.74 (dt, *J* = 9.2, 3.0 Hz, 1.6H), 1.50 (t, *J* = 6.9 Hz, 4H), 1.47–1.38 (m, 18H). **^{13}C NMR** (151 MHz, $CDCl_3$) δ 175.02, 174.69, 156.07, 152.81, 147.10, 140.99, 136.72, 121.23, 117.57, 115.14, 114.97, 110.21, 109.80, 79.24, 57.75, 56.26, 55.79, 55.55, 52.25, 52.21, 40.41, 40.33, 32.90, 32.78, 29.90, 28.53, 23.06, 23.02.

IR (thin film): 3366.14, 2974.66, 2935.13, 2864.74, 1733.69, 1715.37, 1698.02, 1515.77, 1248.68, 1171.54; **HRMS** (ESI): calculated for $C_{19}H_{31}N_2O_5$ $[M+H]^+$= 367.222749; found 367.22371.

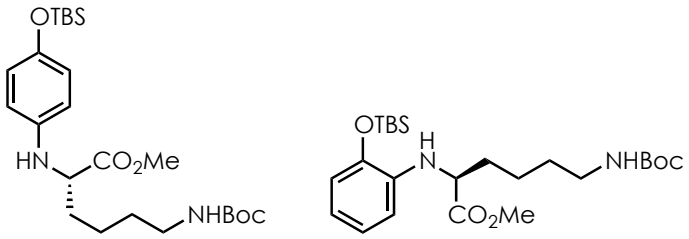

(*S*)-Methyl 6-((*tert*-butoxycarbonyl)amino)-2-((2-((*tert*-butyldimethylsilyl)oxy)phenyl)amino)hexanoate and methyl 6-((*tert*-butoxycarbonyl)amino)-2-((4-((*tert*-butyldimethylsilyl)oxy)phenyl)amino)hexanoate (4.12b). The title compound was prepared using Method A with an irradiation time of 4 hours. The title compound was purified by column chromatography on silica gel (10% to 30% EtOAc/Hexanes) to give **4.12b** in 62% yield and a mixture of 2.3:1 *para* to *ortho* regioisomers.

4.12b. ^{1}H NMR (600 MHz, $CDCl_3$) δ 6.86 – 6.77 (m, 0.3H), 6.73 (dd, *J* = 7.9, 2.3 Hz, 0.3H), 6.70 – 6.62 (m, 2H), 6.61 – 6.56 (m, 0.3H), 6.53 – 6.46 (m, 2.3H), 4.62 (d, *J* = 8.9 Hz, 0.3H), 4.53 (d, *J* = 15.7 Hz, 1H), 4.10 – 4.04 (m, 0.3H), 3.95 (s, 1H), 3.85 (d, *J* = 11.3 Hz, 1H), 3.69 (q, *J* = 3.6, 2.3 Hz, 4H), 3.11 (d, *J* = 7.0 Hz, 2.8H), 1.80 (d, *J* = 7.3 Hz, 1.6H), 1.74 (p, *J* = 7.2 Hz, 1.2H), 1.53 – 1.47 (m, 2.9H), 1.47 – 1.37 (m, 15.8H), 1.04 (t, *J* = 2.3 Hz, 2.7H), 0.95 (t, *J* = 2.3 Hz, 9H), 0.24 (dt, *J* = 4.7, 2.2 Hz, 2.4H), 0.14 (t, *J* = 2.3 Hz, 6H). **^{13}C NMR** (151 MHz, $CDCl_3$) δ 175.03, 174.41, 156.08, 148.24, 142.80, 141.31, 138.70, 122.03, 120.83, 117.87, 117.36, 114.95, 110.76, 79.26, 57.72, 56.09, 52.22, 52.20, 40.35, 32.94, 29.93, 28.54, 25.94, 25.85, 23.01, 22.86, 18.36, 18.28, -4.13, -4.20, -4.36.

IR (thin film): 3366.14, 2952.48, 2930.31, 2857.99, 1733.69, 1716.34, 1698.02, 1509.03, 1250.61; **HRMS** (ESI): calculated for $C_{24}H_{43}N_2O_5Si$ $[M+H]^+$= 467.293580; found 467.29663.

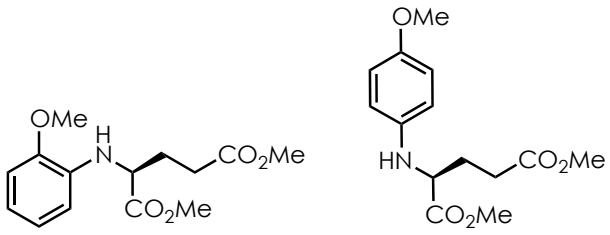

(*S*)-Dimethyl 2-((2-methoxyphenyl)amino)pentanedioate and (S)-dimethyl 2-((4-methoxyphenyl)amino)pentanedioate (4.13a). The title compound was prepared using Method A with an irradiation time of 4 hours. The title compound was purified by column chromatography on silica gel (10% to 30% EtOAc/Hexanes) to give **4.13a** in 72% yield and a mixture of 1.3:1 *ortho* to *para* regioisomers.

4.13a. ^{1}**H NMR** (600 MHz, $CDCl_3$) δ 6.82 (td, *J* = 7.6, 1.4 Hz, 1H), 6.79 – 6.73 (m, 2.8H), 6.73 – 6.67 (m, 1H), 6.61 – 6.56 (m, 1.8H), 6.54 (dd, *J* = 7.9, 1.4 Hz, 1H), 4.71 (d, *J* = 9.1 Hz, 1H), 4.25 – 4.09 (m, 1H), 4.04 (d, *J* = 6.8 Hz, 1H), 3.89 (d, *J* = 6.4 Hz, 1H), 3.85 (s, 3H), 3.75 – 3.70 (m, 8.5H), 3.67 (d, *J* = 1.1 Hz, 5.5H), 2.58 – 2.44 (m, 4H), 2.26 – 2.19 (m, 1H), 2.17 – 2.10 (m, 2H), 2.08 – 1.98 (m, 1H). ^{13}**C NMR** (151 MHz, $CDCl_3$) δ 174.37, 174.01, 173.41, 173.30, 152.88, 147.11, 140.70, 136.45, 121.14, 117.66, 115.26, 114.87, 110.22, 109.78, 57.13, 55.70, 55.48, 55.46, 52.31, 52.28, 51.80, 51.78, 30.22, 30.18, 28.04, 27.90.

IR (thin film): 3383.50, 2999.73, 2952.48, 2835.81, 1735.62, 1602.56, 1515.77, 1456.96, 1436.71, 1240.00; **HRMS** (ESI): calculated for $C_{14}H_{20}NO_5$ $[M+H]^+$= 282.133599; found 282.13389.

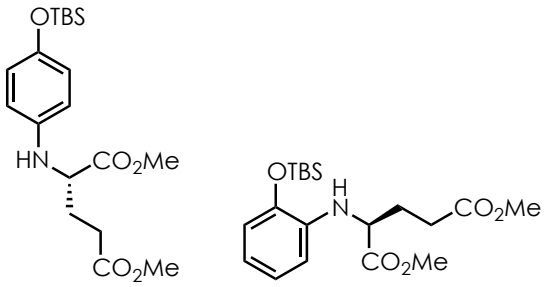

(*S*)-Dimethyl 2-((2-((*tert*-butyldimethylsilyl)oxy)phenyl)amino)pentanedioate and (*S*)-dimethyl 2-((4-((*tert*-butyldimethylsilyl)oxy)phenyl)amino)pentanedioate (4.13b). The title compound was prepared using Method A with an irradiation time of 4 hours. The title compound was purified by column chromatography on silica gel (10% to 30% EtOAc/Hexanes) to give **4.13b** in 77% yield and a mixture of 2.8:1 *para* to *ortho* regioisomers.

4.13b. ^{1}H NMR (600 MHz, $CDCl_3$) δ 6.83 (td, *J* = 7.7, 1.4 Hz, 0.4H), 6.74 (dd, *J* = 7.8, 1.4 Hz, 0.4H), 6.70 – 6.65 (m, 2H), 6.60 (dd, *J* = 7.6, 1.5 Hz, 0.4H), 6.54 (dd, *J* = 8.0, 1.5 Hz, 0.4H), 6.51 (d, *J* = 8.8 Hz, 2H), 4.69 (d, *J* = 8.9 Hz, 0.4H), 4.17 (dt, *J* = 8.9, 6.3 Hz, 0.4H), 4.05 – 4.00 (m, 1H), 3.89 (d, *J* = 8.1 Hz, 1H), 3.71 (d, *J* = 7.7 Hz, 4.2H), 3.67 (d, *J* = 3.0 Hz, 4.2H), 2.55 – 2.40 (m, 2.8H), 2.21 – 2.10 (m, 1.8H), 2.08 – 2.01 (m, 1H), 1.04 (s, 3.6H), 0.95 (s, 9H), 0.25 (d, *J* = 5.5 Hz, 2.4H), 0.14 (s, 6H). **^{13}C NMR** (151 MHz, $CDCl_3$) δ 174.47, 173.81, 173.52, 173.35, 148.40, 142.92, 141.12, 138.49, 122.02, 120.83, 117.89, 117.57, 115.13, 110.89, 57.15, 55.38, 52.38, 52.36, 51.90, 51.87, 30.30, 29.95, 28.17, 28.00, 25.93, 25.85, 25.83, 18.36, 18.28, -4.13, -4.17, -4.36.

IR (thin film): 3392.17, 2954.41, 2930.31, 2857.99, 1741.41, 1509.99, 1252.54; **HRMS** (ESI): calculated for $C_{19}H_{32}NO_3Si$ $[M+H]^+$= 382.204430; found 382.20580.

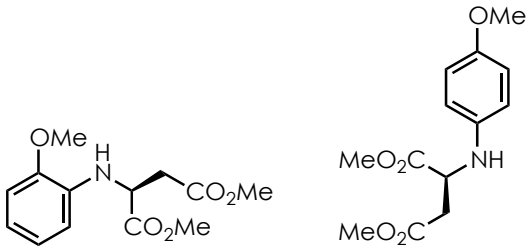

(*S*)-Dimethyl 2-((2-methoxyphenyl)amino)succinate and (*S*)-dimethyl 2-((4-methoxyphenyl)amino)succinate (4.14a). The title compound was prepared using Method A with an irradiation time of 4 hours. The title compound was purified by column chromatography on silica gel (10% to 30% EtOAc/Hexanes) to give **4.14a** in 69% yield and a mixture of 1.2:1 *ortho* to *para* regioisomers.

4.14a. ^{1}H NMR (600 MHz, $CDCl_3$) δ 6.88 (td, *J* = 7.6, 1.4 Hz, 1H), 6.81 – 6.78 (m, 2.6H), 6.76 (dd, *J* = 7.7, 1.5 Hz, 1H), 6.70 – 6.63 (m, 2.6H), 5.00 (d, *J* = 9.1 Hz, 1H), 4.52 (dt, *J* = 9.0, 6.0 Hz, 1H), 4.41 – 4.34 (m, 0.8H), 4.18 (d, *J* = 8.8 Hz, 0.8H), 3.87 (s, 3H), 3.77 (d, *J* = 5.5 Hz, 7.6H), 3.73 (d, *J* = 1.4 Hz, 5.8H), 2.98 – 2.90 (m, 2H), 2.88 (d, *J* = 5.9 Hz, 1.6H). **^{13}C NMR** (151 MHz, $CDCl_3$) δ 173.26, 172.99, 171.21, 171.12, 147.38, 140.38, 136.10, 121.23, 118.09, 115.85, 114.97, 110.59, 110.01, 55.79, 55.63, 54.94, 53.12, 52.74, 52.71, 52.20, 52.18, 37.50, 37.41.

IR (thin film): 3393.14, 3001.66, 2953,45, 2836.77, 1733.69, 1515.77, 1223.61; **HRMS** (ESI): calculated for $C_{13}H_{18}NO_5$ $[M+H]^+$= 268.117949; found 268.11833.

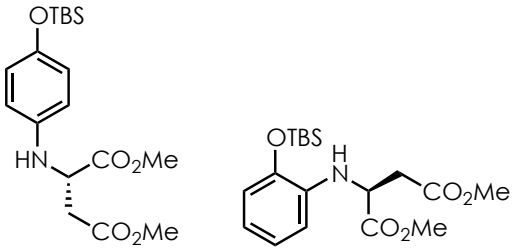

(*S*)-Dimethyl 2-((2-((*tert*-butyldimethylsilyl)oxy)phenyl)amino)succinate and (*S*)-dimethyl 2-((4-((*tert*-butyldimethylsilyl)oxy)phenyl)amino)succinate (4.14b). The title compound was prepared using Method A with an irradiation time of 4 hours. The title compound was purified by column chromatography on silica gel (10% to 30% EtOAc/Hexanes) to give **4.14b** in 70% yield and a mixture of 2.0:1 *para* to *ortho* regioisomers.

4.14b. ^{1}H NMR (600 MHz, $CDCl_3$) δ 6.88 – 6.83 (m, 0.3H), 6.78 – 6.72 (m, 0.3H), 6.69 (dt, *J* = 8.7, 2.3 Hz, 2H), 6.62 (d, *J* = 1.5 Hz, 0.6H), 6.59 – 6.56 (m, 2H), 4.92 (d, *J* = 8.9 Hz, 0.3H), 4.46 (dt, *J* = 5.6, 2.5 Hz, 0.3H), 4.39 – 4.33 (m, 1H), 4.16 (d, *J* = 8.4 Hz, 1H), 3.74 (ddd, *J* = 5.3, 3.3, 1.9 Hz, 3.9H), 3.71 – 3.66 (m, 3.9H), 2.96 – 2.87 (m, 0.6H), 2.85 (dt, *J* = 5.1, 2.3 Hz, 2H), 1.03 (dd, *J* = 3.3, 1.9 Hz, 2.7H), 0.96 (dd, *J* = 3.3, 1.9 Hz, 9H), 0.27 – 0.18 (m, 1.8H), 0.14 (dd, *J* = 3.4, 1.9 Hz, 6H). **^{13}C NMR** (151 MHz, $CDCl_3$) δ 173.27, 172.78, 171.23, 170.98, 148.68, 143.01, 140.69, 138.08, 122.02, 120.87, 118.03, 117.78, 115.56, 110.83, 54.82, 52.69, 52.19, 37.50, 25.90, 25.86, 18.30, -4.35.

IR (thin film): 3392.17, 2954.41, 2930.31, 2857.99, 1742.37, 1509.99, 1253.50; **HRMS** (ESI): calculated for $C_{18}H_{30}NO_5Si$ $[M+H]^+$= 368.188780; found 368.19009.

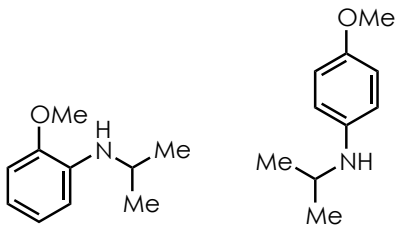

***N*-Isopropyl-2-methoxyaniline and *N*-isopropyl-4-methoxyaniline (4.15a).** The title compound was prepared using Method A with an irradiation time of 4 hours. The title compound was purified by column chromatography on silica gel (10% to 30%

EtOAc/Hexanes) to give **4.15a** in 53% yield by ^{1}H NMR and a mixture of 1.2:1 *ortho* to *para* regioisomers. The spectral data were in agreement with literature values.[7,8]

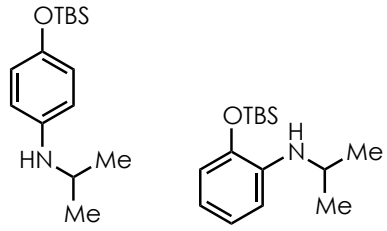

2-((*tert*-Butyldimethylsilyl)oxy)-*N*-isopropylaniline and 4-((*tert*-butyldimethylsilyl)oxy)-*N*-isopropylaniline (4.15b). The title compound was prepared using Method A with an irradiation time of 4 hours. The title compound was purified by column chromatography on silica gel (10% to 30% EtOAc/Hexanes) to give **4.15b** in 56% yield and a mixture of 1.8:1 *para* to *ortho* regioisomers.

4.15b. ^{1}H NMR (600 MHz, $CDCl_3$) δ 6.86 (td, *J* = 7.7, 1.5 Hz, 0.7H), 6.72 (dd, *J* = 7.8, 1.4 Hz, 0.7H), 6.70 – 6.67 (m, 2H), 6.61 (dd, *J* = 7.9, 1.5 Hz, 0.7H), 6.53 (dd, *J* = 7.6, 1.6 Hz, 0.7H), 6.51 – 6.46 (m, 2H), 3.60 (d, *J* = 6.3 Hz, 1H), 3.53 (p, *J* = 6.3 Hz, 1H), 1.21 (d, *J* = 6.3 Hz, 4.2H), 1.18 (d, *J* = 6.3 Hz, 6H), 1.02 (s, 6.3H), 0.97 (s, 9H), 0.22 (s, 4.2H), 0.15 (s, 6H). **^{13}C NMR** (151 MHz, $CDCl_3$) δ 147.30, 142.44, 142.13, 139.58, 129.51, 122.13, 120.80, 117.73, 115.84, 114.76, 111.07, 45.24, 43.98, 25.99, 25.90, 25.83, 23.26, 23.24, 18.39, 18.32, -4.15, -4.34.

IR (thin film): 3395.07, 2958.27, 2929.34, 2857.99, 1508.06, 1254.47, 1239.04; **HRMS** (ESI): calculated for $C_{15}H_{28}NO_3Si$ $[M+H]^+$= 266.193472; found 266.19351.

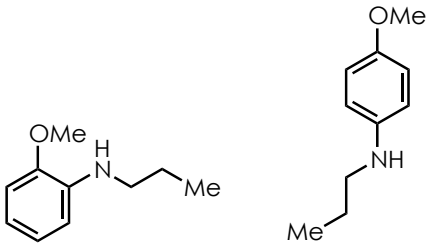

2-Methoxy-*N*-propylaniline and 4-methoxy-*N*-propylaniline (4.16a). The title compound was prepared using Method A with an irradiation time of 4 hours. The title compound was purified by column chromatography on silica gel (10% to 30% EtOAc/Hexanes) to give **4.16a** in 56% yield and a mixture of 1.0:1 *ortho* to *para* regioisomers. The spectral data were in agreement with literature values.[9,10]

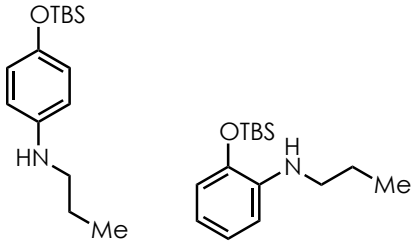

2-((*tert*-Butyldimethylsilyl)oxy)-*N*-propylaniline and 4-((*tert*-butyldimethylsilyl)oxy)-*N*-propylaniline (4.16b). The title compound was prepared using Method A with an irradiation time of 4 hours. The title compound was purified by column chromatography on silica gel (10% to 30% EtOAc/Hexanes) to give **4.16b** in 61% yield and a mixture of 1.8:1 *para* to *ortho* regioisomers.

4.16b. ^{1}H NMR (600 MHz, $CDCl_3$) δ 6.86 (td, *J* = 7.7, 1.4 Hz, 0.7H), 6.72 (dd, *J* = 7.8, 1.4 Hz, 0.7H), 6.69 (d, *J* = 8.8 Hz, 2H), 6.60 (dd, *J* = 7.9, 1.6 Hz, 0.7H), 6.54 (td, *J* = 7.6, 1.6 Hz, 0.7H), 6.51 (d, *J* = 8.8 Hz, 2H), 3.07 (d, *J* = 7.0 Hz, 1.4H), 3.02 (t, *J* = 7.1 Hz, 2H), 1.64 (dq, *J* = 22.8, 7.3 Hz, 3.4H), 1.02 (s, 6.3H), 1.01 – 0.98 (m, 5.1H), 0.97 (s, 9H), 0.24 (s, 4.2H),

0.15 (s, 6H). **^{13}C NMR** (151 MHz, $CDCl_3$) δ 147.34, 143.22, 142.42, 140.64, 129.51, 122.12, 120.79, 120.25, 117.43, 116.09, 113.92, 110.55, 46.88, 45.64, 25.98, 25.91, 25.83, 23.00, 22.90, 18.38, 18.32, 11.86, 11.84, -4.15, -4.28, -4.34.

IR (thin film): 3420.14, 2957.30, 2929.34, 2857.99, 1509.99, 1251.58; **HRMS** (ESI): calculated for $C_{15}H_{28}NOSi$ $[M+H]^+$= 266.193472; found 266.19358.

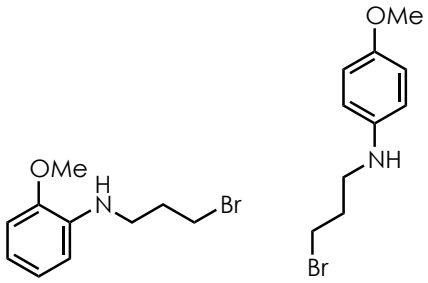

***N*-(3-Bromopropyl)-2-methoxyaniline and *N*-(3-bromopropyl)-4-methoxyaniline (4.17a).** The title compound was prepared using Method A with an irradiation time of 4 hours. The title compound was purified by column chromatography on silica gel (10% to 30% EtOAc/Hexanes) to give **4.17a** in 58% yield by ^{1}H NMR and a mixture of 1.8:1 *ortho* to *para* regioisomers with an inseparable contaminant.

4.17a. ^{1}H NMR (600 MHz, $CDCl_3$) δ 6.90 (ddd, *J* = 9.0, 6.8, 1.5 Hz, 1.5H), 6.87 – 6.82 (m, 1.5H), 6.81 – 6.78 (m, 2H), 6.75 – 6.66 (m, 2H), 3.86 (d, *J* = 8.3 Hz, 3.5H), 3.85 – 3.76 (m, 1.25H), 3.55 (t, *J* = 6.4 Hz, 2.5H), 3.38 (t, *J* = 6.6 Hz, 2.5H), 2.21 (p, *J* = 6.5 Hz, 2.5H). **^{13}C NMR** (151 MHz, $CDCl_3$) δ 147.01, 137.55, 121.39, 121.32, 117.02, 115.66, 115.50, 115.25, 110.20, 109.62, 55.83, 55.54, 41.97, 41.18, 32.14, 31.44, 30.32, 29.84.

IR (thin film): 3394.10, 2931.27, 2849.31, 1615.09, 1507.10, 1261.22; **HRMS** (ESI): calculated for $C_{10}H_{15}NOBr$ $[M+H]^+$= 244.033150; found 244.03383.

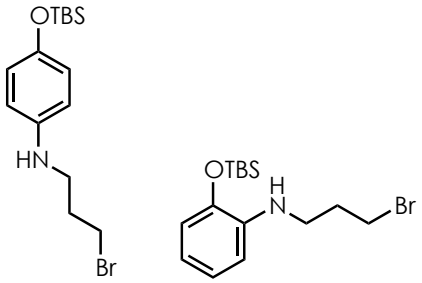

***N*-(3-Bromopropyl)-2-((*tert*-butyldimethylsilyl)oxy)aniline and *N*-(3-bromopropyl)-4-((*tert*-butyldimethylsilyl)oxy)aniline (4.17b).** The title compound was prepared using Method A with an irradiation time of 4 hours. The title compound was purified by column chromatography on silica gel (10% to 30% EtOAc/Hexanes) to give **4.17b** in 56% yield by ^{1}H NMR and a mixture of 1.4:1 *para* to *ortho* regioisomers with an inseparable contaminant.

4.17b. ^{1}H NMR (600 MHz, $CDCl_3$) δ 6.91 – 6.83 (m, 0.8H), 6.73 (dd, *J* = 7.8, 1.5 Hz, 1.1H), 6.69 (s, 0.8H), 6.65 – 6.61 (m, 0.8H), 6.56 (dt, *J* = 6.4, 1.9 Hz, 1.4H), 3.56 – 3.47 (m, 1.8H), 3.46 – 3.37 (m, 1.1H), 3.34 (t, *J* = 6.5 Hz, 2H), 3.28 (t, *J* = 6.6 Hz, 0.7H), 2.20 – 2.12 (m, 2H), 1.01 (d, *J* = 3.7 Hz, 7H), 0.99 – 0.94 (m, 6.3H), 0.23 (d, *J* = 2.5 Hz, 4.8H), 0.19 – 0.16 (m, 2.3H), 0.16 – 0.13 (m, 2H). **^{13}C NMR** (151 MHz, $CDCl_3$) δ 142.61, 139.87, 122.15, 122.12, 120.91, 117.61, 116.68, 114.50, 110.65, 43.39, 41.78, 32.20, 32.14, 31.41, 31.31, 29.85, 26.04, 25.99, 25.88, 25.83, 25.80, 25.77, 18.39, 18.32, -4.11, -4.29, -4.34.

IR (thin film): 3420.14, 2954.41, 2929.34, 2857.99, 1509.03, 1256.40; **HRMS** (ESI): calculated for $C_{15}H_{27}NOBrSi$ $[M+H]^+$= 344.103981; found 344.10511.

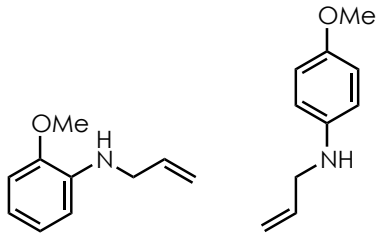

***N*-Allyl-2-methoxyaniline and *N*-allyl-4-methoxyaniline (4.18a).** The title compound was prepared using Method A with an irradiation time of 4 hours. The title compound was purified by column chromatography on silica gel (10% to 30% EtOAc/Hexanes) to give **4.18a** in 34% yield and a mixture of 1.2:1 *ortho* to *para* regioisomers. The spectral data were in agreement with literature values.[11]

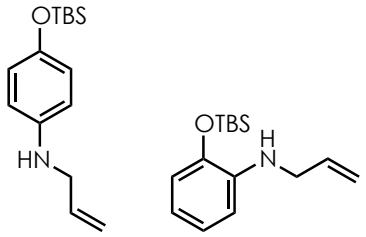

***N*-Allyl-4-((*tert*-butyldimethylsilyl)oxy)aniline and *N*-allyl-2-((*tert*-butyldimethylsilyl)oxy)aniline (4.18b).** The title compound was prepared using Method A with an irradiation time of 4 hours. The title compound was purified by column chromatography on silica gel (10% to 30% EtOAc/Hexanes) to give **4.18b** in 80% yield and a mixture of 2.2:1 *para* to *ortho* regioisomers.

4.18b. ^{1}H NMR (600 MHz, $CDCl_3$) δ 6.90 – 6.82 (m, 0.7H), 6.75 – 6.72 (m, 0.7H), 6.69 (td, *J* = 5.9, 5.4, 2.1 Hz, 2H), 6.64 – 6.55 (m, 1.4H), 6.54 – 6.49 (m, 2H), 5.96 (dddd, *J* = 16.3, 8.2, 4.9, 1.9 Hz, 1.7H), 5.28 (ddt, *J* = 15.5, 3.3, 1.7 Hz, 1.7H), 5.20 – 5.14 (m, 1.7H), 4.20 (s, 0.7H), 3.78 (d, *J* = 5.9 Hz, 1.4H), 3.74 – 3.66 (m, 2.H), 3.49 (s, 0.7H), 1.03 – 0.99 (m, 6.3H), 0.99 – 0.94 (m, 9H), 0.24 (d, *J* = 1.0 Hz, 4.2H), 0.20 – 0.09 (m, 6H). **^{13}C NMR** (151 MHz, $CDCl_3$) δ 147.63, 142.68, 142.61, 140.14, 135.92, 135.68, 122.06, 120.76, 117.56, 116.64, 116.31, 115.94, 114.22, 111.01, 47.64, 46.44, 26.00, 25.90, 18.40, 18.32, -4.10, -4.34.

IR (thin film): 3419.17, 2955.38, 2929.34, 2857.99, 1509.99, 1250.61; **HRMS** (ESI): calculated for $C_{15}H_{26}NOSi$ $[M+H]^+$= 264.177821; found 264.17813.

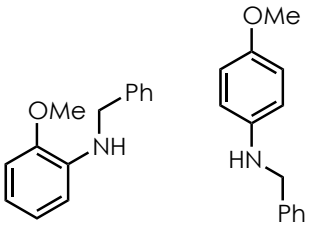

***N*-Benzyl-2-methoxyaniline and *N*-benzyl-4-methoxyaniline (4.19a).** The title compound was prepared using Method A with an irradiation time of 4 hours. The title compound was purified by column chromatography on silica gel (10% to 30% EtOAc/Hexanes) to give **4.19a** in 90% yield and a mixture of 1.3:1 *ortho* to *para* regioisomers. The spectral data were in agreement with literature values.[12]

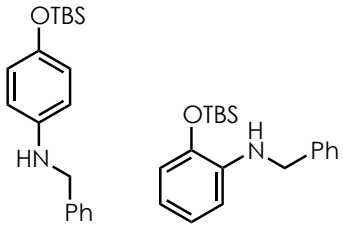

***N*-Benzyl-2-((*tert*-butyldimethylsilyl)oxy)aniline and *N*-benzyl-4-((*tert*-butyldimethylsilyl)oxy)aniline (4.19b).** The title compound was prepared using Method A with an irradiation time of 4 hours. The title compound was purified by column chromatography on silica gel (10% to 30% EtOAc/Hexanes) to give **4.19b** in 70% yield and a mixture of 1.8:1 *para* to *ortho* regioisomers.

4.19b para. ^{1}H NMR (600 MHz, $CDCl_3$) δ 7.40 – 7.36 (m, 2H), 7.34 (ddd, *J* = 7.8, 6.3, 1.8 Hz, 2H), 7.28 (d, *J* = 7.3 Hz, 1H), 6.69 (d, *J* = 8.7 Hz, 2H), 6.54 (d, *J* = 8.8 Hz, 2H), 4.27 (s, 2H), 0.96 (s, 9H), 0.15 (s, 6H). **^{13}C NMR** (151 MHz, $CDCl_3$) δ 147.64, 142.88, 139.79, 128.72, 127.80, 127.33, 120.81, 114.04, 49.40, 25.90, 18.32, -4.33.

4.19b ortho. **^{1}H NMR** (600 MHz, $CDCl_3$) δ 7.44 – 7.35 (m, 4H), 7.31 (m, 1H), 6.87 (s, 1H), 6.79 (d, *J* = 7.8 Hz, 1H), 6.68 – 6.60 (m, 1H), 6.58 (dd, *J* = 8.7, 1.8 Hz, 1H), 4.38 (s, 2H), 0.96 (s, 9H), 0.15 (s, 6H). **^{13}C NMR** (151 MHz, $CDCl_3$) δ 162.14, 142.55, 140.28, 139.80, 128.68, 127.18, 122.13, 117.59, 116.69, 110.92, 48.22, 25.90, 18.32, –4.33.

IR (thin film): 3420.14, 3029.62, 2954.41, 2928.38, 2857.02, 1509.03, 1251.58; **HRMS** (ESI): calculated for $C_{19}H_{28}NOSi$ $[M+H]^+$= 314.193472; found 314.19364.

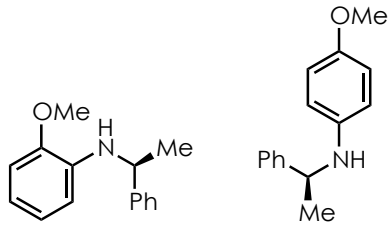

(*S*)-2-Methoxy-*N*-(1-phenylethyl)aniline and (*S*)-4-methoxy-*N*-(1-phenylethyl)aniline (4.20a). The title compound was prepared using Method A with an irradiation time of 4 hours. The title compound was purified by column chromatography on silica gel (10% to 30% EtOAc/Hexanes) to give **4.20a** in 74% yield and a mixture of 1.4:1 *ortho* to *para* regioisomers. The spectral data were in agreement with literature values.[13]

This reaction was conducted on 2.5 mmol scale using a flow apparatus previously described by our laboratory.[14] A 50 mL RBF was charged with **Me_2-Mes-Acr+** (61 mg, 0.13 mmol), anisole (0.27 mL, 2.5 mmol), (*S*)-a-methylbenzylamine (0.97 mL, 7.5 mmol) and 1,2-dichloroethane (25 mL). Oxygen was bubbled through the mixture for 10 minutes, then the vent needle was removed and a balloon of oxygen maintained in the headspace of the flask throughout the course of the reaction. The reaction mixture was stirred vigorously, with the Masterflex L/S Variable-Speed Drive set to 87.5 rpm, then the blue LED floodlamps were switched on. After 6 hours, the reaction was complete, as determined by GCMS. The solvent

was removed under reduced pressure and the crude material purified by column chromatography to give **4.20a** in 61% yield and a mixture of 1.4:1 *ortho* to *para* regioisomers.

The racemic derivative has previously been characterized in the literature.[15,16]

HPLC spectra were obtained using an Aglient 1200 series HPLC with detection at 210, 230, 250 and 254 nm using a Chiralpak IC column using a flow rate of 1 mL per minute. The solvent system used for HPLC resolution of enantiomers was hexanes (A1) and isopropanol (B2). Using a method of 99A1:1B2 for 10 minutes, the racemic standard made through the present methodology was observed at 5.070 min and 5.636 min of equal area. With compound **4.20a**, and the same HPLC conditions, one peak was observed at 5.586 min. No racemization of this product was observed in the reaction.

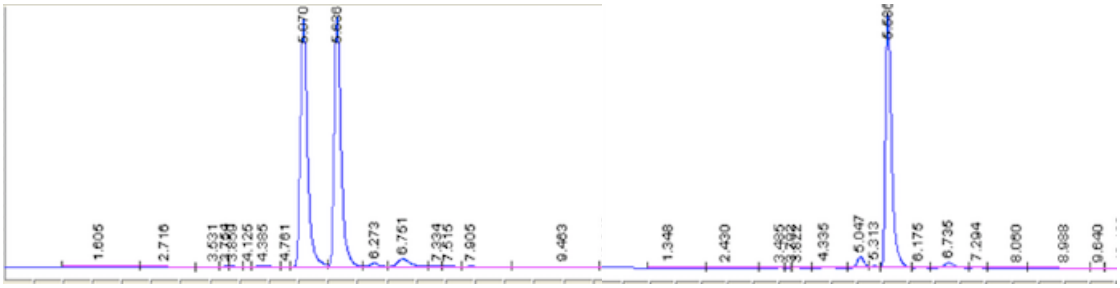

Racemic alpha-methylbenzylamine coupled product trace (S)-alpha-Methylbenzylamine coupled Product trace

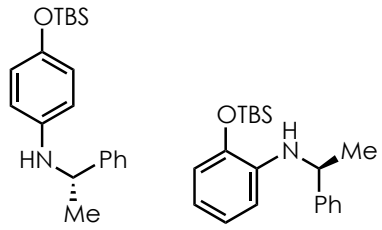

(*S*)-4-((*tert*-Butyldimethylsilyl)oxy)-*N*-(1-phenylethyl)aniline and (*S*)-2-((*tert*-butyldimethylsilyl)oxy)-*N*-(1-phenylethyl)aniline (4.20b). The title compound was

prepared using Method A with an irradiation time of 4 hours. The title compound was purified by column chromatography on silica gel (10% to 30% EtOAc/Hexanes) to give **4.20b** in 90% yield and a mixture of 1.2:1 *para* to *ortho* regioisomers.

4.20b. **^{1}H NMR** (600 MHz, $CDCl_3$) δ 7.39 – 7.34 (m, 3.4H), 7.32 (td, *J* = 7.7, 1.5 Hz, 3.4H), 7.23 (td, *J* = 7.1, 1.7 Hz, 1.7H), 6.73 (dd, *J* = 7.8, 1.4 Hz, 0.7H), 6.70 (td, *J* = 7.7, 1.4 Hz, 0.7H), 6.61 (d, *J* = 8.8 Hz, 2H), 6.51 (td, *J* = 7.7, 1.6 Hz, 0.7H), 6.40 (d, *J* = 8.8 Hz, 2H), 6.33 (dd, *J* = 7.9, 1.5 Hz, 0.7H), 4.53 (d, *J* = 5.1 Hz, 0.7H), 4.45 (dd, *J* = 6.7, 4.6 Hz, 0.7H), 4.41 (q, *J* = 6.7 Hz, 1H), 3.76 (s, 1H), 1.53 (d, *J* = 6.7 Hz, 2.1H), 1.50 (d, *J* = 6.7 Hz, 3H), 1.07 (s, 6.3H), 0.95 (s, 9H), 0.28 (d, *J* = 1.6 Hz, 4.2H), 0.12 (s, 6H). **^{13}C NMR** (151 MHz, $CDCl_3$) δ 147.30, 145.68, 145.60, 142.26, 142.00, 139.43, 128.70, 128.69, 126.91, 126.89, 126.04, 125.89, 122.02, 120.59, 117.46, 116.35, 114.47, 111.72, 54.38, 53.48, 26.01, 25.87, 25.85, 25.45, 25.28, 18.41, 18.27, -4.07, -4.10, -4.36.

IR (thin film): 3419.17, 3026.73, 2956.34, 2929.34, 2857.02, 1509.03, 1255.43; **HRMS** (ESI): calculated for $C_{20}H_{30}NOSi$ $[M+H]^+$= 328.209122; found 328.20957.

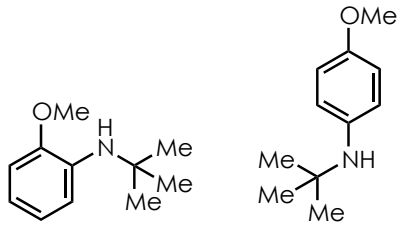

***N*-(*tert*-Butyl)-2-methoxyaniline and *N*-(*tert*-butyl)-4-methoxyaniline (4.21).** The title compound was prepared using Method A with an irradiation time of 4 hours. The title compound was purified by column chromatography on silica gel (10% to 30% EtOAc/Hexanes) to give **4.21** in 34% yield by ^{1}H NMR and a mixture of 1.4:1 *ortho* to *para* regioisomers. The spectral data were in agreement with literature values.[17,18]

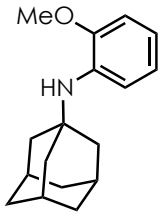

(3*s*,5*s*,7*s*)-*N*-(2-Methoxyphenyl)adamantan-1-amine (4.22). The title compound was prepared using Method A with an irradiation time of 4 hours. The title compound was purified by column chromatography on silica gel (10% to 30% EtOAc/Hexanes) to give **4.22** in 72% yield as a single regioisomer.

4.22. ^{1}H NMR (600 MHz, $CDCl_3$) δ 6.97 (dd, *J* = 7.9, 1.6 Hz, 1H), 6.81 (dd, *J* = 7.6, 1.5 Hz, 1H), 6.80 – 6.75 (m, 1H), 6.70 (td, *J* = 7.7, 1.6 Hz, 1H), 4.14 – 4.07 (m, 1H), 3.83 (d, *J* = 3.0 Hz, 3H), 2.15 – 2.09 (m, 3H), 1.94 (d, *J* = 3.1 Hz, 6H), 1.69 (t, *J* = 3.1 Hz, 6H). **^{13}C NMR** (151 MHz, $CDCl_3$) δ 148.69, 136.04, 120.63, 117.57, 116.48, 109.91, 55.59, 51.89, 43.24, 36.69, 29.88.

IR (thin film): 3410,49, 2904.27, 2848.35, 1599.66, 1508.06, 1455.03, 1237.11; **HRMS** (ESI): calculated for $C_{17}H_{24}NO$ $[M+H]^+$= 258.185241; found 258.18554.

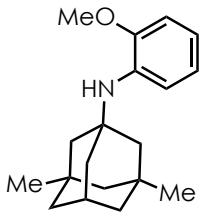

(1*r*,3*R*,5*S*,7*r*)-*N*-(2-Methoxyphenyl)-3,5-dimethyladamantan-1-amine (4.23). The title compound was prepared using Method A with an irradiation time of 4 hours. The title compound was purified by column chromatography on silica gel (10% to 30% EtOAc/Hexanes) to give **4.23** in 37% yield and a mixture of 7:1 *ortho* to *para* regioisomers.

4.23. ^{1}H NMR (600 MHz, $CDCl_3$) δ 6.95 (dd, *J* = 7.9, 1.5 Hz, 1H), 6.86 – 6.79 (m, 1H), 6.77 (dd, *J* = 8.0, 1.5 Hz, 1H), 6.70 (td, *J* = 7.7, 1.5 Hz, 1H), 4.12 (s, 1H), 3.82 (s, 3H), 2.21 – 2.15 (m, 1H), 1.78 (dd, *J* = 3.1, 1.5 Hz, 2H), 1.60 (d, *J* = 11.9 Hz, 2H), 1.56 – 1.50 (m, 2H), 1.39 – 1.35 (m, 2H), 1.31 (dt, *J* = 12.3, 2.6 Hz, 2H), 1.16 (s, 2H), 0.86 (s, 6H). **^{13}C NMR** (151 MHz, $CDCl_3$) δ 148.65, 136.14, 120.65, 117.55, 116.37, 109.93, 55.60, 53.61, 50.95, 49.41, 42.98, 41.74, 32.76, 30.53, 30.43.

IR (thin film): 3335.28, 2942.84, 2899.45, 2840.63, 1519.63, 1508.06, 1233.25; **HRMS** (ESI): calculated for $C_{19}H_{28}NO$ $[M+H]^+$= 286.216541; found 286.21658.

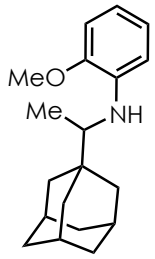

***N*-(1-((3*r*,5*r*,7*r*)-Adamantan-1-yl)ethyl)-2-methoxyaniline (4.24).** The title compound was prepared using Method A with an irradiation time of 4 hours. The title compound was purified by column chromatography on silica gel (10% to 30% EtOAc/Hexanes) to give **4.24** in 45% yield as a single regioisomer.

4.24. ^{1}H NMR (600 MHz, $CDCl_3$) δ 6.95 (dd, *J* = 7.9, 1.6 Hz, 1H), 6.81 (td, *J* = 7.6, 1.5 Hz, 1H), 6.77 (dd, *J* = 8.0, 1.5 Hz, 1H), 6.70 (ddd, *J* = 8.0, 7.4, 1.6 Hz, 1H), 4.12 (s, 1H), 3.82 (s, 3H), 2.17 (p, *J* = 3.2 Hz, 1H), 1.78 (dd, *J* = 3.3, 1.5 Hz, 2H), 1.60 (dt, *J* = 12.0, 1.2 Hz, 2H), 1.55 – 1.51 (m, 2H), 1.39 – 1.34 (m, 2H), 1.33 – 1.27 (m, 2H), 1.16 (q, *J* = 1.2 Hz, 2H), 0.86 (s, 6H). **^{13}C NMR** (151 MHz, $CDCl_3$) δ 148.65, 136.15, 120.65, 117.55, 116.37, 109.94, 55.60, 53.62, 50.96, 49.42, 42.98, 41.74, 32.76, 30.53, 30.43.

IR (thin film): 3420.14, 2942.84, 2898.49, 2839.67, 1519.63, 1508.06, 1455.99, 1233.25; **HRMS** (ESI): calculated for $C_{19}H_{28}NO$ $[M+H]^+$= 286.216541; found 286.21642.

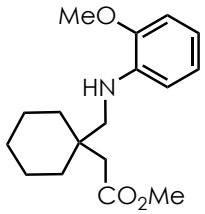

Methyl 2-(1-(((2-methoxyphenyl)amino)methyl)cyclohexyl)acetate (4.25). The title compound was prepared using Method A with an irradiation time of 4 hours. The title compound was purified by column chromatography on silica gel (10% to 30% EtOAc/Hexanes) to give **4.25** in 34% yield and a mixture of 1.2:1 *ortho* to *para* regioisomers.

4.25. ^{1}**H NMR** (600 MHz, $CDCl_3$) δ 6.85 (td, *J* = 7.7, 1.4 Hz, 1H), 6.75 (dd, *J* = 7.9, 1.3 Hz, 1H), 6.69 (dd, *J* = 7.9, 1.5 Hz, 1H), 6.62 (td, *J* = 7.7, 1.5 Hz, 1H), 4.45 (s, 1H), 3.85 (s, 3H), 3.69 – 3.61 (m, 3H), 3.16 (s, 2H), 2.45 (s, 2H), 1.53 (t, *J* = 7.5 Hz, 6H), 1.49 – 1.44 (m, 3H), 1.37 (d, *J* = 8.1 Hz, 1H). ^{13}**C NMR** (151 MHz, $CDCl_3$) δ 173.04, 146.84, 139.14, 121.35, 115.93, 109.91, 109.55, 55.61, 51.45, 37.98, 34.20, 26.18, 21.75.

IR (thin film): 3421.10, 2927.41, 2854.13, 1732.73, 1698.02, 1601.59, 1521.56, 1456.96, 1249.65, 1220.72; **HRMS** (ESI): calculated for $C_{17}H_{25}NO_3$ $[M+H]^+$= 292.190720; found 292.19101.

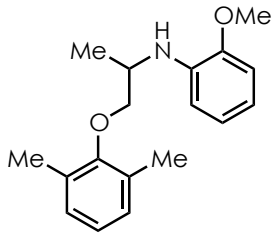

***N*-(1-(2,6-Dimethylphenoxy)propan-2-yl)-2-methoxyaniline (4.26).** The title compound was prepared using Method A with an irradiation time of 4 hours. The title compound was purified by column chromatography on silica gel (10% to 30% EtOAc/Hexanes) to give **4.26** in 41% yield as a single regioisomer.

4.26. ^{1}H NMR (600 MHz, $CDCl_3$) δ 6.99 (d, *J* = 7.4 Hz, 2H), 6.91 (t, *J* = 7.5 Hz, 1H), 6.87 (td, *J* = 7.6, 1.1 Hz, 1H), 6.78 (dd, *J* = 7.9, 1.3 Hz, 1H), 6.74 – 6.61 (m, 1H), 6.67–6.65 (m, 1H), 4.59 (d, *J* = 7.8 Hz, 1H), 3.92 – 3.87 (m, 1H), 3.87 – 3.82 (m, 4H), 3.77 (dd, *J* = 8.8, 5.2 Hz, 1H), 2.26 (s, 6H), 1.50 – 1.43 (m, 3H). **^{13}C NMR** (151 MHz, $CDCl_3$) δ 155.38, 155.32, 152.34, 147.13, 141.42, 137.22, 131.05, 131.01, 129.04, 129.00, 128.36, 124.05, 123.99, 121.34, 116.59, 115.26, 115.03, 110.36, 109.76, 74.36, 55.91, 55.53, 49.87, 48.48, 18.35, 18.26, 16.40, 16.28.

IR (thin film): 3420.14, 2923.56, 2869.56, 1508.06, 1250.61; **HRMS** (ESI): calculated for $C_{18}H_{24}NO_2$ $[M+H]^+$= 286.180155; found 286.18002.

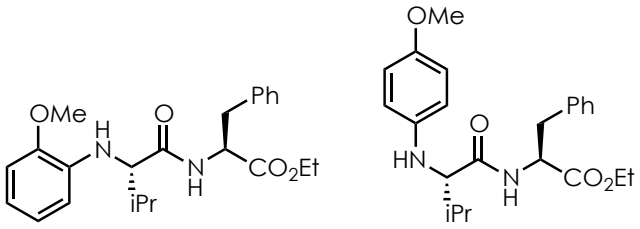

(*S*)-Ethyl 2-((*S*)-2-((2-methoxyphenyl)amino)-3-methylbutanamido)-3-phenylpropanoate and (*S*)-ethyl 2-((*S*)-2-((4-methoxyphenyl)amino)-3-methylbutanamido)-3-phenylpropanoate (4.27). The title compound was prepared using Method A with an irradiation time of 14 hours. The title compound was purified by column chromatography on silica gel (10% to 20% EtOAc/Hexanes) to give a pale yellow oil in 58% yield by ^{1}H NMR and a mixture of 3.2:1 *ortho* to *para* regioisomers. The *para* isomer was

contaminated with an inseparable impurity. The $^{1}H/^{13}C$ NMR peaks corresponding to the para isomer were identified using 2D NMR spectroscopy.

4.27 *ortho* isomer. ^{1}H NMR (600 MHz, $CDCl_3$) δ 7.25 – 7.19 (m, 4H), 7.14 – 7.13 (m, 2H), 6.82 (td, *J* = 7.8, 1.8 Hz, 1H), 6.79 (dd, *J* = 7.8, 1.8 Hz, 1H), 6.74 (td, *J* = 7.8, 1.8 Hz, 1H), 6.51 (dd, *J* = 7.8, 1.8 Hz, 1H), 4.87 (td, *J* = 8.4, 6.0 Hz, 1H), 4.48 (brd, *J* = 4.2 Hz, 1H), 4.06 (q, *J* = 7.2 Hz, 2H), 3.88 (s, 3H), 3.48 (brt, *J* = 4.2 Hz, 1H), 3.17 (dd, *J* = 14.4, 6.0 Hz, 1H), 2.98 (dd, *J* = 14.4, 8.4 Hz, 1H), 2.33 – 2.25 (m, 1H), 1.11 (t, *J* = 7.2 Hz, 3H), 0.93 (d, *J* = 6.6 Hz, 3H), 0.80 (d, *J* = 7.2 Hz, 3H). **^{13}C NMR** (151 MHz, $CDCl_3$) δ 173.12, 171.28, 147.11, 137.48, 136.37, 129.25, 128.62, 127.03, 121.40, 118.45, 112.10, 109.56, 65.49, 61.44, 55.67, 53.12, 38.16, 31.14, 19.80, 17.40, 14.09.

IR (thin film): 3382.53, 3310.21, 2962.13, 2936.09, 1739.48, 1654.62, 1602.56, 1509.03, 1455.99, 1244.83, 1221.68, 1180.22; **HRMS** (ESI): calculated for $C_{23}H_{30}N_2O_4$ $[M+H]^+$= 399.2278; found 399.2281.

4.27 *para* isomer. ^{1}H NMR (600 MHz, $CDCl_3$) δ 7.29 – 7.09 (m, 6H), 6.76 (AA'BB', *J* = 8.4 Hz, 2H), 6.58 (AA'BB', *J* = 8.4 Hz, 2H), 4.86 (td, *J* = 7.8, 6.0 Hz, 1H), 4.09 (q, *J* = 7.2 Hz, 2H), 3.74 (s, 3H), 3.55 (brd, *J* = 4.2 Hz, 1H), 3.42 (brt, *J* = 4.2 Hz, 1H), 3.15 (dd, *J* = 14.4, 6.0 Hz, 1H), 3.00 (dd, *J* = 14.4, 7.8 Hz, 1H), 2.26 – 2.20 (m, 1H), 1.15 (t, *J* = 7.2 Hz, 3H), 0.93 (d, *J* = 7.2 Hz, 3H), 0.79 (d, *J* = 6.6 Hz, 3H). **^{13}C NMR** (151 MHz, $CDCl_3$) δ 173.07, 171.33, 153.26, 141.72, 136.27, 129.26, 128.65, 127.09, 115.54, 114.86, 66.45, 61.51, 55.83, 53.08, 38.14, 31.25, 19.76, 17.52, 14.15.

HRMS (ESI): calculated for $C_{23}H_{30}N_2O_4$ $[M+H]^+$= 399.2278; found 399.2288.

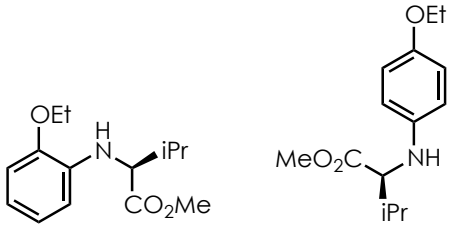

(*S*)-Methyl 2-((2-ethoxyphenyl)amino)-3-methylbutanoate and (*S*)-methyl 2-((4-ethoxyphenyl)amino)-3-methylbutanoate (4.28). The title compound was prepared using Method A with an irradiation time of 4 hours. The title compound was purified by column chromatography on silica gel (5% EtOAc/Hexanes) to give a colorless oil in 76% yield and a mixture of 1.7:1 *ortho* to *para* regioisomers.

4.28 *ortho* isomer. ^{1}H NMR (600 MHz, $CDCl_3$) δ 6.81 (td, *J* = 7.8, 1.8 Hz, 1H), 6.77 (dd, *J* = 7.8, 1.8 Hz, 1H), 6.66 (td, *J* = 7.8, 1.8 Hz, 1H), 6.54 (dd, *J* = 7.8, 1.8 Hz, 1H), 4.77 (brd, *J* = 9.0 Hz, 1H), 4.09 (ABX_3, *J* = 9.0, 7.2 Hz, 1H), 4.06 (ABX_3, *J* = 9.0, 7.2 Hz, 1H), 3.85 (dd, *J* = 9.0, 6.6 Hz, 1H), 3.71 (s, 3H), 2.17 (oct, *J* = 6.6 Hz, 1H), 1.45 (t, *J* = 7.2 Hz, 3H), 1.07 (d, *J* = 6.6 Hz, 3H), 1.02 (d, *J* = 6.6 Hz, 3H). **^{13}C NMR** (151 MHz, $CDCl_3$) δ 174.41, 146.49, 137.49, 121.22, 117.33, 111.10, 110.39, 64.10, 62.40, 51.95, 31.69, 19.29, 18.98, 15.13.
IR (thin film): 3420.14, 2964.05, 2875.34, 1740.44, 1601.59, 1513.85, 1455.03; **HRMS** (ESI): calculated for $C_{14}H_{21}NO_3$ $[M+H]^+$= 252.1594; found 252.1594.

4.28 *para* isomer. ^{1}H NMR (600 MHz, $CDCl_3$) δ 6.75 (AA'BB', *J* = 9.0 Hz, 2H), 6.59 (AA'BB', *J* = 9.0 Hz, 2H), 3.94 (q, *J* = 7.2 Hz, 2H), 3.86 (brs, 1H), 3.76 (d, *J* = 6.6 Hz, 1H), 3.69 (s, 3H), 2.08 (oct, *J* = 6.6 Hz, 1H), 1.36 (t, *J* = 7.2 Hz, 3H), 1.03 (d, *J* = 6.6 Hz, 3H), 1.01 (d, *J* = 6.6 Hz, 3H). **^{13}C NMR** (151 MHz, $CDCl_3$) δ 174.72, 152.09, 141.52, 115.79, 115.31, 64.10, 63.90, 51.94, 31.73, 19.33, 18.86, 15.15.

IR (thin film): 3365.17, 2964.05, 1733.69, 1514.81, 1233.25; **HRMS** (ESI): calculated for $C_{14}H_{21}NO_3$ $[M+H]^+$= 252.1594; found 252.1592.

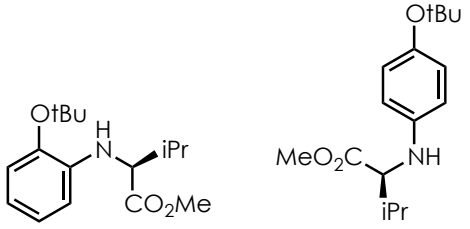

(*S*)-Methyl 2-((2-(*tert*-butoxy)phenyl)amino)-3-methylbutanoate and (*S*)-methyl 2-((4-(*tert*-butoxy)phenyl)amino)-3-methylbutanoate (4.29). The title compound was prepared using Method A with an irradiation time of 4 hours. The title compound was purified by column chromatography on silica gel (5% EtOAc/Hexanes) to give a colorless oil in 82% yield and a mixture of 1:1.3 *ortho* to *para* regioisomers.

4.29 *ortho* isomer. ^{1}H NMR (600 MHz, $CDCl_3$) δ 6.96 (dd, *J* = 7.8, 1.2 Hz, 1H), 6.91 (td, *J* = 7.8, 1.2 Hz, 1H), 6.59 (td, *J* = 7.8, 1.2 Hz, 1H), 6.52 (dd, *J* = 7.8, 1.2 Hz, 1H), 4.84 (brd, *J* = 9.0 Hz, 1H), 3.87 (dd, *J* = 9.0, 6.0 Hz, 1H), 3.69 (s, 3H), 2.16 (broct, *J* = 7.2 Hz, 1H), 1.42 (s, 9H), 1.05 (d, *J* = 7.2 Hz, 3H), 1.02 (d, *J* = 7.2 Hz, 3H). **^{13}C NMR** (151 MHz, $CDCl_3$) δ 174.20, 143.00, 142.01, 123.92, 122.22, 116.67, 110.56, 79.82, 61.79, 51.91, 31.70, 29.20, 19.33, 18.76.

IR (thin film): 3420.14, 2971.77, 2874.38, 1740.44, 1599.66, 1508.06, 1366.32, 1158.04; **HRMS** (ESI): calculated for $C_{16}H_{25}NO_3$ $[M+H]^+$= 280.1907; found 280.1906.

4.29 *para* isomer. ^{1}H NMR (600 MHz, $CDCl_3$) δ 6.81 (AA'BB', *J* = 9.0 Hz, 2H), 6.53 (AA'BB', *J* = 9.0 Hz, 2H), 3.96 (brd, *J* = 9.0 Hz, 1H), 3.79 (dd, *J* = 9.0, 6.6 Hz, 1H), 3.70 (s, 3H), 2.09 (oct, *J* = 6.6 Hz, 1H), 1.27 (s, 9H), 1.04 (d, *J* = 6.6 Hz, 3H), 1.01 (d, *J* = 6.6 Hz,

3H). **^{13}C NMR** (151 MHz, $CDCl_3$) δ 174.59, 147.13, 143.64, 125.58, 114.00, 77.91, 63.36, 51.97, 31.78, 28.81, 19.30, 18.85.

IR (thin film): 3383.50, 2973.70, 2874.38, 1734.66, 1509.03, 1364.39, 1171.54; **HRMS** (ESI): calculated for $C_{16}H_{25}NO_3$ $[M+H]^+$= 280.1907; found 280.1904.

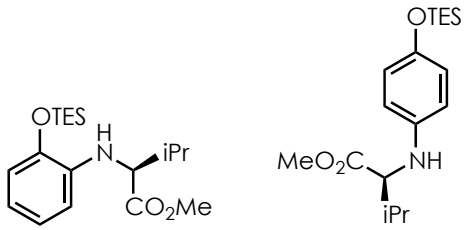

(*S*)-Methyl 3-methyl-2-((2-((triethylsilyl)oxy)phenyl)amino)butanoate and (*S*)-methyl 3-methyl-2-((4-((triethylsilyl)oxy)phenyl)amino)butanoate (4.30). The title compound was prepared using Method A with an irradiation time of 4 hours. The title compound was purified by column chromatography on silica gel (5% EtOAc/Hexanes) to give a colorless oil in 77% yield and a mixture of 1:1.7 *ortho* to *para* regioisomers.

4.30. ^{1}H NMR (600 MHz, $CDCl_3$) δ 6.81 (td, *J* = 7.8, 1.2 Hz, 0.4H), 6.73 (dd, *J* = 7.8, 1.2 Hz, 0.4H), 6.68 (AA'BB', *J* = 9.0 Hz, 2H), 6.56 (td, *J* = 7.8, 1.2 Hz, 0.4H), 6.52 (AA'BB', *J* = 9.0 Hz, 2H), 6.53 – 6.51 (m, 0.4H), 4.69 (brd, *J* = 9.6 Hz, 0.4H), 3.88 – 3.85 (m, 1.4H), 3.75 (d, *J* = 6.6 Hz, 1H), 3.69 (s, 4.2H), 2.16 (broct, *J* = 7.2 Hz, 0.4H), 2.07 (broct, *J* = 6.6 Hz, 1H), 1.06 – 1.00 (m, 12H), 0.97 (t, *J* = 7.8 Hz, 9H), 0.79 (q, *J* = 7.8 Hz, 2.4H), 0.69 (q, *J* = 7.8 Hz, 6H). **^{13}C NMR** (151 MHz, $CDCl_3$) δ 174.71, 174.16, 148.10, 142.92, 141.85, 139.12, 121.94, 120.67, 117.53, 117.10, 115.13, 110.66, 63.86, 62.02, 51.91, 51.90, 31.76, 31.69, 19.32, 19.24, 18.87, 18.76, 6.84, 6.80, 5.35, 5.02.

IR (thin film): 3393.14, 2957.30, 2876.31, 1739.48, 1509.03, 1456.96, 1255.43; **HRMS** (ESI): calculated for $C_{18}H_{31}NO_3Si$ $[M+H]^+$= 338.2146; found 338.2142.

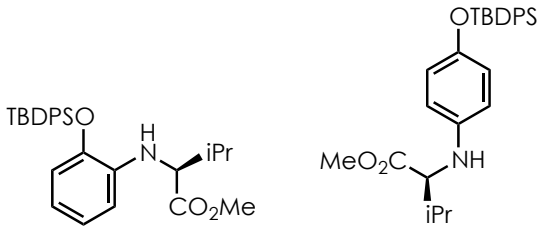

(*S*)-Methyl 2-((2-((*tert*-butyldiphenylsilyl)oxy)phenyl)amino)-3-methylbutanoate and (*S*)-methyl 2-((4-((*tert*-butyldiphenylsilyl)oxy)phenyl)amino)-3-methylbutanoate (4.31). The title compound was prepared using Method A with an irradiation time of 4 hours. The title compound was purified by column chromatography on silica gel (5% EtOAc/Hexanes) to give a colorless oil in 58% yield and a mixture of 1:2.3 *ortho* to *para* regioisomers.

4.31. ^{1}H NMR (600 MHz, $CDCl_3$) δ 7.76 – 7.69 (m, 5.2H), 7.44 – 7.34 (m, 7.8H), 6.74 (td, *J* = 7.8, 1.8 Hz, 0.3H), 6.60 (AA'BB', *J* = 9.0 Hz, 2H), 6.56 (dd, *J* = 7.8, 1.8 Hz, 0.3H), 6.40 (AA'BB', *J* = 9.0 Hz, 2H), 6.34 (dd, *J* = 7.8, 1.8 Hz, 0.3H), 6.27 (td, *J* = 7.8, 1.8 Hz, 0.3H), 5.01 (brd, *J* = 9.6 Hz, 0.3H), 3.99 (dd, *J* = 9.6, 6.0 Hz, 0.3H), 3.78 (brs, 1H), 3.73 (s, 0.9H), 3.68 (d, *J* = 6.6 Hz, 1H), 3.66 (s, 3H), 2.22 (broct, *J* = 6.6 Hz, 0.3H), 2.03 (oct, *J* = 6.6 Hz, 1H), 1.14 (s, 2.7H), 1.10 – 1.06 (m, 1.8H), 1.07 (s, 9H), 1.00 (d, *J* = 6.6 Hz, 3H), 0.97 (d, *J* = 6.6 Hz, 3H). **^{13}C NMR** (151 MHz, $CDCl_3$) δ 174.67, 174.11, 148.33, 142.78, 141.51, 138.66, 135.69, 135.61,135.56, 134.92, 133.46, 130.08, 129.83, 127.96, 127.78, 121.77, 120.27, 117.95, 116.97, 114.99, 110.77, 63.79, 62.11, 51.97, 51.88, 31.71, 26.75, 26.69, 19.60, 19.56, 19.28, 19.26, 18.83, 18.73.

IR (thin film): 3393.14, 3048.91, 2966.20, 2857.99, 1736.58, 1509.03, 1253.50; **HRMS** (ESI): calculated for $C_{28}H_{35}NO_3Si$ $[M+H]^+$= 462.2459; found 462.2456.

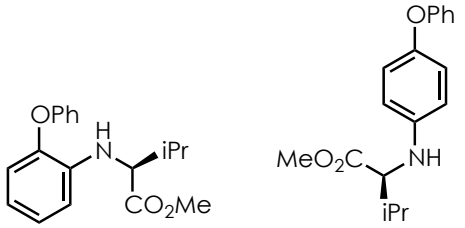

(*S*)-Methyl 3-methyl-2-((2-phenoxyphenyl)amino)butanoate and (*S*)-methyl 3-methyl-2-((4-phenoxyphenyl)amino)butanoate (4.32). The title compound was prepared using Method A with an irradiation time of 4 hours. The title compound was purified by column chromatography on silica gel (5% EtOAc/Hexanes) to give a colorless oil in 84% yield and a mixture of 1:2.2 *ortho* to *para* regioisomers.

4.32. ^{1}H NMR (400 MHz, $CDCl_3$) δ 7.36 – 7.25 (m, 2.5H), 7.12 – 6.99 (m, 3.5H), 6.94 – 6.92 (m, 2H), 6.89 (AA'BB', *J* = 8.8 Hz, 2H), 6.86 – 6.84 (m, 0.5H), 6.68 – 6.66 (m, 1H), 6.63 (AA'BB', *J* = 8.8 Hz, 2H), 4.63 (brd, *J* = 9.6 Hz, 0.5H), 4.04 (brd, *J* = 9.6 Hz, 1H), 3.88 (dd, *J* = 9.6, 6.4 Hz, 0.5H), 3.82 (dd, *J* = 9.6, 6.0 Hz, 1H), 3.73 (s, 3H), 3.68 (s, 1.5H), 2.16 – 2.06 (m, 1.5H), 1.06 (d, *J* = 6.8 Hz, 3H), 1.03 (d, *J* = 6.8 Hz, 3H), 0.96 (t, *J* = 6.8 Hz, 3H). **^{13}C NMR** (151 MHz, $CDCl_3$) δ 174.44, 173.97, 158.97, 157.65, 148.46, 143.98, 143.73, 139.59, 129.77, 129.63, 124.90, 122.96, 122.17, 121.28, 119.60, 117.84, 117.68, 117.36, 114.83, 111.86, 63.25, 62.26, 52.04, 51.99, 31.74, 31.60, 19.30, 19.22, 18.83, 18.81.

IR (thin film): 3393.14, 2963.09, 2874.38, 1737.55, 1608.34, 1589.06, 1509.03, 1488.78, 1231.33; **HRMS** (ESI): calculated for $C_{18}H_{21}NO_3$ $[M+H]^+$= 300.1594; found 300.1592.

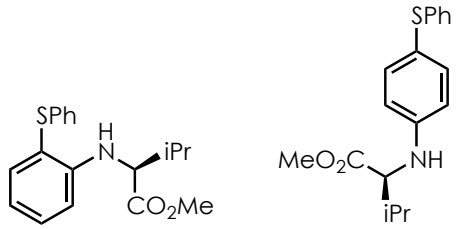

(*S*)-Methyl 3-methyl-2-((2-(phenylthio)phenyl)amino)butanoate and (*S*)-methyl 3-methyl-2-((4-(phenylthio)phenyl)amino)butanoate (4.33). The title compound was prepared using Method B with an irradiation time of 26 hours using 2 lamps. The title compound was purified by column chromatography on silica gel (5% EtOAc/Hexanes) to give a yellow oil in 37% yield by ^{1}H NMR and a mixture of 1:4.4 *ortho* to *para* regioisomers. The product was only partially separated from unreacted diphenyl sulfide.

4.33. ^{1}H NMR (400 MHz, $CDCl_3$) δ 7.51 (dd, *J* = 7.6, 1.2 Hz, 0.1H), 7.32 (AA'BB', *J* = 8.8 Hz, 2H), 7.30 – 7.27 (m, 0.1H), 7.23 – 7.19 (m, 2.2H), 7.13 – 7.07 (m, 3.3H), 6.71 (td, *J* = 7.6, 1.2 Hz, 0.1H), 6.62 (AA'BB', *J* = 8.8 Hz, 2H), 6.58 (brd, *J* = 8.4 Hz, 0.1H), 5.35 (brd, *J* = 8.8 Hz, 0.1H), 4.30 (brd, *J* = 8.4 Hz, 1H), 3.88 (dd, *J* = 8.4, 5.6 Hz, 1H), 3.85 (dd, *J* = 8.8, 6.0 Hz, 0.1H), 3.74 (s, 3H), 3.64 (s, 0.4H), 2.14 (broct, *J* = 6.8 Hz, 1H), 2.05 (broct, *J* = 6.8 Hz, 0.1H), 1.05 (d, *J* = 6.8 Hz, 3H), 1.02 (d, *J* = 6.8 Hz, 3H), 0.85 (d, *J* = 6.8 Hz, 0.4H), 0.84 (d, *J* = 6.8 Hz, 0.4H). **^{13}C NMR** (151 MHz, $CDCl_3$) δ 173.95, 173.55, 148.41, 147.80, 139.82, 137.87, 136.79, 136.30, 131.48, 129.00, 128.91, 127.31, 126.95, 125.64, 125.31, 119.95, 117.67, 114.27, 110.60, 62.17, 61.92, 52.18, 52.02, 31.69, 31.49, 19.19, 19.14, 18.80, 18.45.

IR (thin film): 3390.24, 2963.09, 2932.23, 1735.62, 1596.77, 1506.13, 1477.21, 1320.04, 1203.36, 1180.22, 1154.19; **HRMS** (ESI): calculated for $C_{18}H_{21}NO_2S$ $[M+H]^+$= 316.1366; found 316.1364.

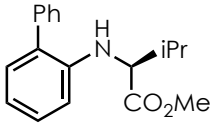

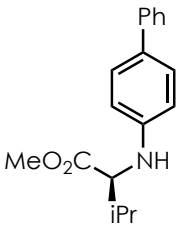

(*S*)-Methyl 2-([1,1'-biphenyl]-2-ylamino)-3-methylbutanoate and (*S*)-methyl 2-([1,1'-biphenyl]-4-ylamino)-3-methylbutanoate (4.34). The title compound was prepared using Method A with an irradiation time of 13 hours. The title compound was purified by column chromatography on silica gel (5% EtOAc/Hexanes) to give a pale yellow solid in 95% yield and a mixture of 1:2.1 *ortho* to *para* regioisomers.

4.34. ^{1}H NMR (400 MHz, $CDCl_3$) δ 7.54 – 7.37 (m, 5.2H), 7.44 (AA'BB', *J* = 8.8 Hz, 2H), 7.29 – 7.24 (m, 1.3H), 7.21 (td, *J* = 7.6, 1.6 Hz, 0.3H), 7.12 (dd, *J* = 7.6, 1.6 Hz, 0.3H), 6.80 (td, *J* = 7.6, 1.6 Hz, 0.3H), 6.71 (AA'BB', *J* = 8.8 Hz, 2H), 6.64 (brd, *J* = 8.0 Hz, 0.3H), 4.40 (brd, *J* = 9.2 Hz, 0.3H), 4.22 (brd, *J* = 9.6 Hz, 1H), 3.94 – 3.87 (m, 1.3H), 3.74 (s, 3H), 3.69 (s, 0.9H), 2.15 (oct, *J* = 6.8 Hz, 1H), 2.02 (oct, *J* = 6.4 Hz, 0.3H), 1.07 (d, *J* = 6.8 Hz, 3H), 1.04 (d, *J* = 6.8 Hz, 3H), 0.94 – 0.92 (m, 1.8H). **^{13}C NMR** (151 MHz, $CDCl_3$) δ 174.26, 174.24, 146.81, 144.15, 141.21, 139.32, 131.27, 130.63, 129.48, 129.01, 128.80, 128.77, 128.50, 128.16, 127.43, 126.48, 126.31, 117.85, 113.84, 110.81, 62.50, 62.31, 52.09, 51.96, 31.73, 31.54, 19.26, 18.86, 18.84.

IR (thin film): 3393.14, 2963.09, 2873.42, 1733.69, 1614.13, 1524.45, 1298.82; **HRMS** (ESI): calculated for $C_{18}H_{21}NO_2$ $[M+H]^+$= 284.1645; found 284.1643.

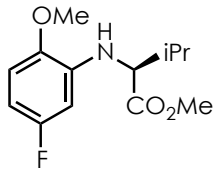

(*S*)-Methyl 2-((5-fluoro-2-methoxyphenyl)amino)-3-methylbutanoate (4.35). The title compound was prepared using Method B with an irradiation time of 18 hours using one lamp. The title compound was purified by column chromatography on silica gel (5% EtOAc/Hexanes) to give a colorless oil in 35% yield as a single regioisomer.

4.35. ^{1}H NMR (600 MHz, $CDCl_3$) δ 6.64 (dd, *J* = 8.4, 4.8 Hz, 1H), 6.32 (td, *J* = 8.4, 3.0 Hz, 1H), 6.25 (dd, *J* = 10.2, 3.0 Hz, 1H), 4.83 (brd, *J* = 9.0 Hz, 1H), 3.83 (s, 3H), 3.78 (dd, *J* = 9.0, 6.6 Hz, 1H), 3.72 (s, 3H), 2.16 (oct, *J* = 6.6 Hz, 1H), 1.06 (d, *J* = 6.6 Hz, 3H), 1.01 (d, *J* = 6.6 Hz, 3H). **^{13}C NMR** (151 MHz, $CDCl_3$) δ 173.88, 158.20 (d, *J* = 235.6 Hz), 143.24 (d, *J* = 1.5 Hz), 138.46 (d, *J* = 10.6 Hz), 110.02 (d, *J* = 9.1 Hz), 101.81 (d, *J* = 22.7 Hz), 98.04 (d, *J* = 28.7 Hz), 62.07, 56.15, 52.10, 31.62, 19.25, 18.89. **^{19}F NMR** (376 MHz, $CDCl_3$) δ -122.03.

IR (thin film): 3420.14, 2964.05, 2837.74, 1739.48, 1620.88, 1522.52, 1456.96, 1217.83; **HRMS** (ESI): calculated for $C_{13}H_{18}FNO_3$ $[M+H]^+$= 256.1343; found 256.1342.

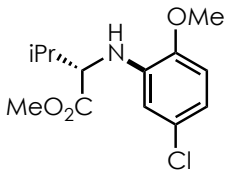

(*S*)-Methyl 2-((5-chloro-2-methoxyphenyl)amino)-3-methylbutanoate (4.36). The title compound was prepared using Method B with an irradiation time of 24 hours. The title compound was purified by column chromatography on silica gel (10% to 30% EtOAc/Hexanes) to give **4.36** in 75% yield and a mixture of 20:1:1 C2:C3:C1 adducts.

4.36. ^{1}H NMR (600 MHz, $CDCl_3$) δ 7.15 (d, *J* = 8.7 Hz, 0.06H, ipso), 7.11 (d, *J* = 8.7 Hz, 0.06H, ipso), 6.69 – 6.58 (m, 2H), 6.54 (d, *J* = 2.2 Hz, 0.07H, meta), 6.47 (d, *J* = 2.3 Hz, 1H), 6.21 (dd, *J* = 8.7, 2.8 Hz, 0.06H), 6.15 (d, *J* = 2.7 Hz, 0.06H), 4.79 (d, *J* = 9.4 Hz, 1H), 3.84 (s, 3H), 3.81 (dd, *J* = 9.3, 6.0 Hz, 1H), 3.76 – 3.69 (m, 3H), 2.16 (dq, *J* = 13.4, 6.7 Hz, 1H), 1.05 (d, *J* = 6.9 Hz, 3H), 1.01 (d, *J* = 6.7 Hz, 3H). **^{13}C NMR** (151 MHz, $CDCl_3$) δ 173.83, 159.59, 145.71, 138.28, 129.25, 126.31, 116.39, 114.73, 110.40, 110.08, 102.64, 98.53,

62.65, 62.21, 61.89, 55.86, 55.47, 52.16, 52.08, 31.61, 31.56, 19.20, 19.19, 19.16, 18.82, 18.79, 18.77.

IR (thin film): 3420.14, 2963.09, 2875.34, 1739.48, 1599.66, 1518.67, 1219.76; **HRMS** (ESI): calculated for $C_{13}H_{18}ClNO_3$ $[M+H]^+$= 272.104794; found 272.10523.

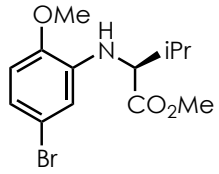

(*S*)-Methyl 2-((5-bromo-2-methoxyphenyl)amino)-3-methylbutanoate (4.37). The title compound was prepared using Method B with an irradiation time of 24 hours using 2 lamps and trifluorotoluene instead of DCE as the solvent. The title compound was purified by column chromatography on silica gel (5% EtOAc/Hexanes) to give a colorless oil in 57% yield and a mixture of 9.1:1 C2:C3 regioisomers. The product was isolated with 6% of (*S*)-methyl 2-((4-bromophenyl)amino)-3-methylbutanoate. The yield was calculated taking contamination into account.

4.37. ^{1}H NMR (400 MHz, $CDCl_3$) δ 6.76 (dd, *J* = 8.8, 2.4 Hz, 1H), 6.61 – 6.59 (m, 2H), 4.78 (brd, *J* = 9.6 Hz, 1H), 3.84 (s, 3H), 3.81 (dd, *J* = 9.6, 6.0 Hz, 1H), 3.73 (s, 3H), 2.16 (broct, *J* = 6.8 Hz, 1H), 1.05 (d, *J* = 6.8 Hz, 3H), 1.01 (d, *J* = 6.8 Hz, 3H). **^{13}C NMR** (151 MHz, $CDCl_3$) δ 173.85, 146.21, 138.62, 119.47, 113.81, 112.83, 110.96, 61.88, 55.84, 52.12, 31.65, 19.23, 18.84.

IR (thin film): 3420.14, 2942.13, 2874.38, 1739.48, 1597.73, 1515.77; **HRMS** (ESI): calculated for $C_{13}H_{18}{}^{81}BrNO_3$ $[M+H]^+$= 318.0523; found 318.0520.

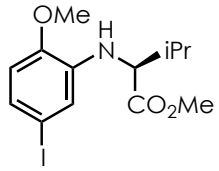

(*S*)-Methyl 2-((5-iodo-2-methoxyphenyl)amino)-3-methylbutanoate (4.38). The title compound was prepared using Method B with an irradiation time of 19 hours using 2 lamps and trifluorotoluene instead of DCE as the solvent. The title compound was purified by column chromatography on silica gel (5% EtOAc/Hexanes) to give a colorless oil in 33% yield and a mixture of 6.7:1 C2:C3 regioisomers. The product was isolated with 7% of (*S*)-methyl 2-((4-iodophenyl)amino)-3-methylbutanoate. The yield was calculated taking contamination into account.

4.38. ^{1}H NMR (400 MHz, $CDCl_3$) δ 6.96 (dd, *J* = 8.4, 2.0 Hz, 1H), 6.76 (d, *J* = 2.0 Hz, 1H), 6.49 (d, *J* = 8.4 Hz, 1H), 4.73 (brd, *J* = 9.2 Hz, 1H), 3.83 (s, 3H), 3.80 (dd, *J* = 9.2, 6.0 Hz, 1H), 3.73 (s, 3H), 2.15 (broct, *J* = 6.8 Hz, 1H), 1.05 (d, *J* = 6.8 Hz, 3H), 1.01 (d, *J* = 6.8 Hz, 3H). **^{13}C NMR** (151 MHz, $CDCl_3$) δ 173.89, 147.03, 138.85, 125.91, 118.49, 111.63, 83.95, 61.85, 55.73, 52.10, 31.66, 19.23, 18.84.

IR (thin film): 3420.14, 2962.13, 2836.77, 1738.51, 1592.91, 1508.06, 1456.96; **HRMS** (ESI): calculated for $C_{13}H_{18}INO_3$ $[M+H]^+$= 364.0404; found 364.0401.

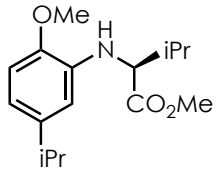

(*S*)-Methyl 2-((5-isopropyl-2-methoxyphenyl)amino)-3-methylbutanoate (4.39). The title compound was prepared using Method B with an irradiation time of 16 hours using one

lamp. The title compound was purified by column chromatography on silica gel (5% EtOAc/Hexanes) to give a pale yellow oil in 43% yield and >10:1 regioselectivity.

4.39. ^{1}H NMR (400 MHz, $CDCl_3$) δ 6.69 (d, *J* = 8.4 Hz, 1H), 6.53 (dd, *J* = 8.4, 2.4 Hz, 1H), 6.42 (d, *J* = 2.4 Hz, 1H), 4.68 (brd, *J* = 9.2 Hz, 1H), 3.86 (dd, *J* = 9.2, 6.4 Hz, 1H), 3.83 (s, 3H), 3.70 (s, 3H), 2.78 (sept, *J* = 6.8 Hz, 1H), 2.14 (broct, *J* = 6.8 Hz, 1H), 1.19 (d, *J* = 6.8 Hz, 6H), 1.08 (d, *J* = 6.8 Hz, 3H), 1.02 (d, *J* = 6.8 Hz, 3H). **^{13}C NMR** (151 MHz, $CDCl_3$) δ 174.55, 145.37, 141.84, 137.00, 114.61, 109.68, 108.87, 62.42, 55.76, 51.91, 33.90, 31.75, 24.47, 24.28, 19.34, 19.14.

IR (thin film): 3421.10, 2959.23, 2872.45, 1741.41, 1598.70, 1523.49, 1463.71, 1429.96, 1246.75, 1225.54; **LRMS** (EI): calculated for $C_{16}H_{25}NO_3$ $[M]^+$= 279.2; found 279.2.

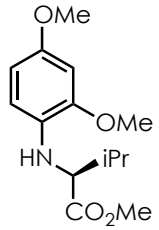

(*S*)-Methyl 2-((2,4-dimethoxyphenyl)amino)-3-methylbutanoate (4.40). The title compound was prepared using Method B with an irradiation time of 16 hours using 2 lamps. The title compound was purified by column chromatography on silica gel (10% EtOAc/Hexanes) to give a yellow oil in 49% yield and a mixture of 10.4:1 C4:C2 regioisomers.

4.40. ^{1}H NMR (600 MHz, $CDCl_3$) δ 6.46 – 6.44 (m, 2H), 6.35 (dd, *J* = 8.4, 2.4 Hz, 1H), 4.40 (brs, 1H), 3.84 (s, 3H), 3.78 (brd, *J* = 6.6 Hz, 1H), 3.74 (s, 3H), 3.69 (s, 3H), 2.12 (oct, *J* = 6.6 Hz, 1H), 1.06 (d, *J* = 6.6 Hz, 3H), 1.02 (d, *J* = 6.6 Hz, 3H). **^{13}C NMR** (151 MHz, $CDCl_3$)

δ 174.69, 152.42, 148.35, 131.53, 110.81, 103.70, 99.46, 63.16, 55.85, 55.71, 51.90, 31.69, 19.32, 19.07.

IR (thin film): 3393.14, 2960.20, 2833.88, 1735.62, 1519.63, 1456.96, 1206.26; **HRMS** (ESI): calculated for $C_{14}H_{21}NO_4$ $[M+H]^+$= 268.1543; found 268.1541.

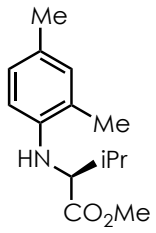

(*S*)-Methyl 2-((2,4-dimethylphenyl)amino)-3-methylbutanoate (4.41). The title compound was prepared using Method B with an irradiation time of 18 hours using 2 lamps with 10 equivalents of *m*-xylene. The title compound was purified by column chromatography on silica gel (5% EtOAc/Hexanes) to give a pale yellow oil in 66% yield by ^{1}H NMR and a mixture of 10.1:1 C4:C5 regioisomers. The product was contaminated with an inseparable impurity.

4.41. ^{1}H NMR (600 MHz, $CDCl_3$) δ 6.89 – 6.88 (m, 2H), 6.47 (d, *J* = 8.4 Hz, 1H), 3.90 – 3.85 (m, 2H), 3.70 (s, 3H), 2.22 (s, 3H), 2.19 (s, 3H), 1.06 (oct, *J* = 7.2 Hz, 1H), 1.07 (d, *J* = 7.2 Hz, 3H), 1.02 (d, *J* = 7.2 Hz, 3H). **^{13}C NMR** (151 MHz, $CDCl_3$) δ 174.71, 143.07, 131.37, 127.45, 127.09, 123.10, 110.81, 62.75, 51.97, 31.77, 20.48, 19.26, 18.96, 17.60.

IR (thin film): 3395.07, 2963.09, 2928.38, 1737.55, 1517.70, 1464.67; **HRMS** (ESI): calculated for $C_{14}H_{21}NO_2$ $[M+H]^+$= 236.1645; found 236.1647.

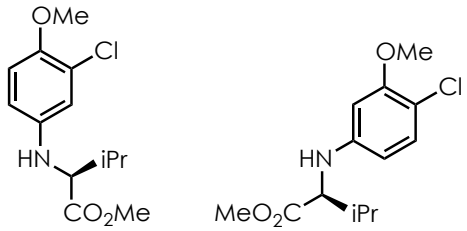

(*S*)-Methyl 2-((3-chloro-4-methoxyphenyl)amino)-3-methylbutanoate and (*S*)-methyl 2-((4-chloro-3-methoxyphenyl)amino)-3-methylbutanoate (4.42). The title compound was prepared using Method B with an irradiation time of 21 hours using 2 lamps. The title compound was purified by column chromatography on silica gel (5% to 10% EtOAc/Hexanes) to give a colorless oil in 63% yield and a mixture of 3.0:1 C4:C5 regioisomers.

4.42. ^{1}H NMR (600 MHz, $CDCl_3$) δ 7.11 (d, *J* = 8.4 Hz, 0.2H), 6.78 (d, *J* = 8.4 Hz, 1H), 6.70 (d, *J* = 3.0 Hz, 1H), 6.51 (dd, *J* = 8.4, 3.0 Hz, 1H), 6.23 (d, *J* = 3.0 Hz, 0.2H), 6.14 (dd, *J* = 8.4, 3.0 Hz, 0.2H), 4.15 (brd, *J* = 9.6 Hz, 0.2H), 3.90 (brd, *J* = 10.2 Hz, 1H), 3.85 (s, 0.6H), 3.83 – 3.80 (m, 0.2H), 3.81 (s, 3H), 3.74 (dd, *J* = 10.2, 6.0 Hz, 1H), 3.72 (s, 0.6H), 3.71 (s, 3H), 2.14 – 2.04 (m, 1.2H), 1.05 – 1.00 (m, 7.2H). **^{13}C NMR** (151 MHz, $CDCl_3$) δ 174.30, 174.10, 155.65, 148.08, 147.47, 142.21, 130.58, 123.43, 116.24, 114.06, 113.03, 111.38, 105.78, 98.65, 63.44, 62.71, 57.00, 56.03, 52.14, 52.08, 31.69, 31.67, 19.29, 19.26, 18.84, 18.75.

IR (thin film): 3383.50, 2963.09, 2836.77, 1732.73, 1507.16, 1456.96, 1228.43; **HRMS** (ESI): calculated for $C_{13}H_{18}ClNO_3$ $[M+H]^+$= 272.1048; found 272.1046.

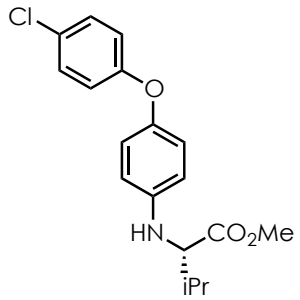

(*S*)-Methyl 2-((4-(4-chlorophenoxy)phenyl)amino)-3-methylbutanoate (4.43). The title compound was prepared using Method A with an irradiation time of 4 hours. The title compound was purified by column chromatography on silica gel (10% to 30% EtOAc/Hexanes) to give **43** in 78% yield and a mixture of 1:2.3 *ortho* to *para* regioisomers.

4.43. ^{1}H NMR (600 MHz, $CDCl_3$) δ 7.33 – 7.30 (m, 0.3H), 7.28 – 7.24 (m, 0.8H, overlapping with residual $CHCl_3$), 7.22 (d, *J* = 9.0 Hz, 1.6H), 7.18 (dd, *J* = 8.4, 1.5 Hz, 0.2H), 7.13 – 7.06 (m, 0.2H), 7.04 – 7.01 (m, 0.2H), 7.00 – 6.98 (m, 0.5H), 6.94 – 6.90 (m, 0.6H), 6.85 (tt, *J* = 9.6, 2.3 Hz, 3.2H), 6.76 – 6.72 (m, 0.4H), 6.69 – 6.65 (m, 0.4H), 6.63 – 6.58 (m, 2H), 4.07 (d, *J* = 9.7 Hz, 1H), 3.87 (dd, *J* = 9.5, 6.1 Hz, 0.3H), 3.83 – 3.78 (m, 1H), 3.78 – 3.71 (m, 3H), 3.69 (d, *J* = 1.1 Hz, 0.8H), 2.11 (tdd, *J* = 9.3, 7.5, 5.1 Hz, 1.2H), 1.08 – 1.00 (m, 6H), 0.95 (td, *J* = 7.2, 5.1 Hz, 2H). **^{13}C NMR** (151 MHz, $CDCl_3$) δ 174.40, 173.94, 173.47, 157.68, 156.35, 148.10, 144.25, 143.35, 139.60, 129.89, 129.71, 129.63, 129.61, 129.54, 127.04, 125.36, 123.34, 121.28, 121.26, 120.23, 119.75, 118.95, 118.54, 117.86, 117.82, 117.36, 117.13, 116.76, 114.82, 112.06, 111.65, 63.15, 62.15, 61.90, 52.15, 52.08, 52.04, 31.73, 31.60, 31.55, 19.30, 19.22, 19.17, 18.82, 18.79, 18.64.

IR (thin film): 3393.14, 2963.09, 2930.31, 1733.69, 1508.06, 1233.25; **HRMS** (ESI): calculated for $C_{18}H_{21}ClNO_3$ $[M+H]^+$= 334.12099; found 334.12099.

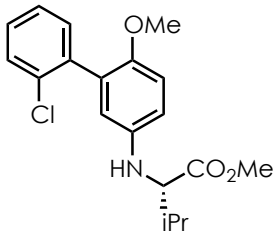

(*S*)-Methyl 2-((2'-chloro-6-methoxy-[1,1'-biphenyl]-3-yl)amino)-3-methylbutanoate (4.44). The title compound was prepared using Method A with an irradiation time of 4 hours. The title compound was purified by column chromatography on silica gel (10% to 30% EtOAc/Hexanes) to give **4.44** in 60% yield and a mixture of 5:1 *para* to *ortho* regioisomers.

4.44. ^{1}H NMR (600 MHz, $CDCl_3$) δ 7.42 (ddd, *J* = 7.3, 3.9, 2.0 Hz, 1.25H), 7.30 – 7.23 (m, 2H), 7.23 – 7.19 (m, 0.25H), 6.97 (d, *J* = 7.9 Hz, 0.25H), 6.82 (dd, *J* = 8.8, 3.6 Hz, 1H), a6.64 (dt, *J* = 8.9, 3.3 Hz, 1H), 6.52 (t, *J* = 3.3 Hz, 1H), 6.27 – 6.22 (m, 0.25H), 3.93 – 3.88 (m, 1.25H), 3.81 – 3.74 (m, 1.25H), 3.73 (d, *J* = 5.7 Hz, 1.5H), 3.68 (dd, *J* = 9.1, 3.6 Hz, 6H), 2.13 (d, *J* = 6.5 Hz, 0.25H), 2.09 – 2.04 (m, 1H), 1.13 (dd, *J* = 7.0, 4.8 Hz, 1H), 1.06 (d, *J* = 6.8 Hz, 1H), 1.01 (ddq, *J* = 13.2, 6.5, 3.4, 2.8 Hz, 6H). **^{13}C NMR** (151 MHz, $CDCl_3$) δ 150.03, 148.69, 141.22, 137.93, 133.90, 132.29, 131.86, 131.73, 129.55, 129.43, 129.39, 128.59, 128.11, 126.49, 126.44, 117.45, 114.48, 112.82, 63.72, 62.49, 56.50, 55.57, 52.51, 52.13, 51.98, 34.33, 31.82, 31.77, 19.33, 19.15, 18.88, 18.85, 17.84.

IR (thin film): 3393.14, 2961.16, 287342, 1732.73, 1507.10, 1262.18, 1235.18; **HRMS** (ESI): calculated for $C_{19}H_{23}ClNO_3$ $[M+H]^+$= 348.136094; found 348.13630.

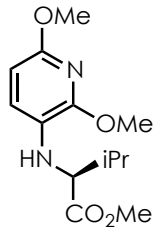

(*S*)-Methyl 2-((2,6-dimethoxypyridin-3-yl)amino)-3-methylbutanoate (4.45). The title compound was prepared using Method B with an irradiation time of 16 hours using 2 lamps. The title compound was purified by column chromatography on silica gel (5% to 10% EtOAc/Hexanes) to give a pale yellow oil in 60% yield as a single regioisomer.

4.45. ^{1}H NMR (600 MHz, $CDCl_3$) δ 6.77 (d, *J* = 8.4 Hz, 1H), 6.16 (d, *J* = 8.4 Hz, 1H), 4.19 (brs, 1H), 3.97 (s, 3H), 3.83 (s, 3H), 3.73 (brd, *J* = 6.6 Hz, 1H), 3.69 (s, 3H), 2.11 (oct, *J* = 6.6 Hz, 1H), 1.06 (d, *J* = 6.6 Hz, 3H), 1.01 (d, *J* = 6.6 Hz, 3H). **^{13}C NMR** (151 MHz, $CDCl_3$) δ 174.38, 154.77, 151.09, 125.56, 121.21, 98.77, 63.24, 53.99, 53.57, 51.99, 31.65, 19.32, 18.98.

IR (thin film): 3393.14, 2962.13, 2900.41, 1739.48, 1593.88, 1489.74, 1291.11, 1395.25; **HRMS** (ESI): calculated for $C_{13}H_{20}N_2O_4$ $[M+H]^+$= 269.1496; found 269.1494.

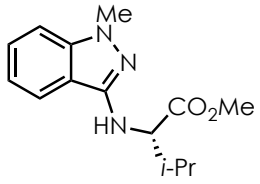

(*S*)-Methyl 3-methyl-2-((1-methyl-1*H*-indazol-3-yl)amino)butanoate (4.46). The title compound was prepared using Method B with an irradiation time of 18 hours. The title compound was purified by column chromatography on neutralized silica gel (20% EtOAc/Hexanes) to give a yellow oil in 64% yield as a single regioisomer.

4.46. ^{1}H NMR (600 MHz, $CDCl_3$) δ 7.65 – 7.50 (d, *J* = 8.6 Hz, 1H), 7.32 (ddd, *J* = 8.2, 6.9, 1.0 Hz, 1H), 7.17 (dt, *J* = 8.5, 0.9 Hz, 1H), 6.99 (d, *J* = 1.0 Hz, 1H), 4.55 – 4.24 (m, 2H), 3.82 (s, 3H), 3.73 (s, 3H), 2.23 (d, *J* = 5.2 Hz, 1H), 1.07 (dd, *J* = 6.8, 3.1 Hz, 6H). **^{13}C NMR**

(151 MHz, $CDCl_3$) δ 174.79, 148.30, 141.72, 126.92, 119.43, 118.15, 114.36, 108.57, 61.86, 51.96, 35.01, 31.61, 19.30, 18.53.

HRMS (ESI): calculated for $C_{14}H_{18}N_3O_2$ $[M+H]^+$= 261.32; found 261.30.

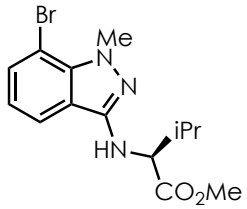

(*S*)-Methyl 2-((7-bromo-1-methyl-1*H*-indazol-3-yl)amino)-3-methylbutanoate (4.47). The title compound was prepared using Method B with an irradiation time of 18 hours using 2 lamps and trifluorotoluene instead of DCE as the solvent. The title compound was purified by column chromatography on neutralized silica gel (20% EtOAc/Hexanes) to give a yellow oil in 66% yield as a single regioisomer.

4.47. ^{1}H NMR (600 MHz, $CDCl_3$) δ 7.50 (dd, *J* = 7.8, 1.2 Hz, 1H), 7.47 (dd, *J* = 7.8, 1.2 Hz, 1H), 6.83 (t, *J* = 7.8 Hz, 1H), 4.41 – 4.37 (m, 2H), 4.16 (s, 3H), 3.74 (s, 3H), 2.25 – 2.20 (m, 1H), 1.06 (d, *J* = 7.2 Hz, 6H). **^{13}C NMR** (151 MHz, $CDCl_3$) δ 174.70, 147.77, 138.83, 131.55, 119.35, 118.76, 117.14, 102.69, 61.66, 52.07, 38.07, 31.58, 19.34, 18.49.

IR (thin film): 3354.57, 2963.09, 2874.38, 1736.80, 1541.81, 1435.74, 1206.26; **HRMS** (ESI): calculated for $C_{14}H_{18}{}^{81}BrN_3O_2$ $[M+H]^+$= 342.0635; found 342.0636.

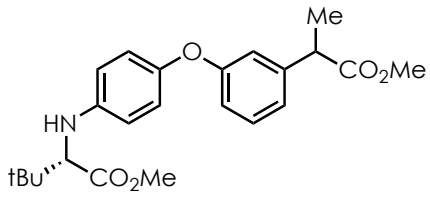

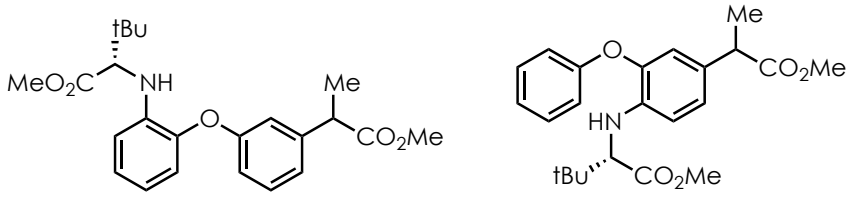

(2*S*)-Methyl 2-((4-(3-(1-methoxy-1-oxopropan-2-yl)phenoxy)phenyl)amino)-3,3-dimethylbutanoate, (2*S*)-methyl 2-((2-(3-(1-methoxy-1-oxopropan-2-yl)phenoxy)phenyl)amino)-3,3-dimethylbutanoate and (2*S*)-methyl 2-((4-(1-methoxy-1-oxopropan-2-yl)-2-phenoxyphenyl)amino)-3,3-dimethylbutanoate (4.48). The title compound was prepared using Method B with an irradiation time of 17 hours using 2 lamps. The title compound was purified by column chromatography on silica gel (10% EtOAc/Hexanes) to give a pale yellow oil in 73% yield and a mixture of 1:1:1 C4:C2:C8 regioisomers. Two additional regioisomers were observed in trace amounts. The C2 and C8 regioisomers were inseparable by chromatography and were therefore further characterized by reduction to the corresponding diols **SI8** and **SI9** (see below).

4.48 C4 isomer. ^{1}H NMR (600 MHz, $CDCl_3$) δ 7.20 (t, *J* = 7.8 Hz, 1H), 6.94 (brd, *J* = 7.2 Hz, 1H), 6.90 – 6.89 (m, 1H), 6.88 (AA'BB', *J* = 9.0 Hz, 2H), 6.77 (ddd, *J* = 7.8, 2.4, 1.2 Hz, 1H), 6.64 (AA'BB', *J* = 9.0 Hz, 2H), 4.09 (brs, 1H), 3.75 (brs, 1H), 3.70 (s, 3H), 3.67 – 3.65 (m, 4H), 1.46 (d, *J* = 7.2 Hz, 3H), 1.07 (s, 9H). **^{13}C NMR** (151 MHz, $CDCl_3$) δ 174.90, 174.19, 159.10, 148.35, 144.28, 142.35, 129.75, 121.25, 121.22, 116.77, 115.77, 115.12, 66.36, 52.24, 51.74, 45.42, 34.55, 26.88, 18.65.

IR (thin film): 3391.21, 2954.41, 1735.62, 1509.03, 1486.85, 1238.08, 1213.97, 1161.90; **HRMS** (ESI): calculated for $C_{23}H_{29}NO_5$ $[M+H]^+$= 400.2118; found 400.2124.

4.48 C2 and C8 isomers. **^{1}H NMR** (600 MHz, $CDCl_3$) δ 7.32 – 7.30 (m, 1.7H), 7.25 – 7.23 (m, 0.7H), 7.08 – 7.05 (m, 0.7H), 7.02 – 6.97 (m, 4H), 6.95 – 6.92 (m, 1.7H), 6.86 – 6.84 (m, 1.7H), 6.83 – 6.82 (m, 0.7H), 6.69 – 6.65 (m, 1.7H), 6.63 – 6.61 (m, 0.7H), 4.66 (d, *J* = 10.2 Hz, 1H), 4.62 (d, *J* = 10.2 Hz, 0.7H), 3.80 (d, *J* = 10.2 Hz, 1H), 3.77 (d, *J* = 10.2 Hz, 0.7H), 3.70 – 3.68 (m, 1H), 3.66 – 3.65 (m, 8.1H), 3.62 (s, 2.1H), 3.55 (q, *J* = 7.2 Hz, 0.7H), 1.48 (d, *J* = 7.2 Hz, 3H), 1.40 (d, *J* = 7.2 Hz, 2.1H), 0.97 (s, 9H), 0.96 (s, 6.3H). **^{13}C NMR** (151 MHz, $CDCl_3$) δ 175.38, 175.37, 174.84, 173.60, 157.79, 157.57, 143.58, 143.38, 142.54, 139.71, 138.84, 129.92, 129.78, 129.66, 125.05, 123.88, 122.93, 122.02, 121.98, 119.70, 119.20, 117.65, 117.51, 117.44, 117.17, 116.29, 111.83, 111.72, 65.02, 65.00, 52.24, 52.11, 51.71, 51.70, 45.42, 44.57, 34.51, 34.49, 26.76, 26.74, 18.71, 18.69.

IR (thin film): 3421.10, 2953.45, 1737.55, 1608.34, 1584.24, 1518.67, 1488.78, 1434.78, 1330.64, 1253.50, 1220.72, 1161.90; **HRMS** (ESI): calculated for $C_{23}H_{29}NO_5$ $[M+H]^+$= 400.2118; found 400.2121.

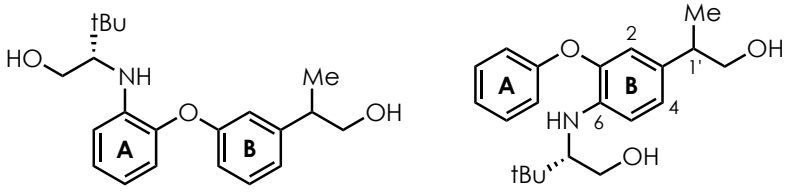

(2*S*)-2-((2-(3-(1-Hydroxypropan-2-yl)phenoxy)phenyl)amino)-3,3-dimethylbutan-1-ol and (2*S*)-2-((4-(1-hydroxypropan-2-yl)-2-phenoxyphenyl)amino)-3,3-dimethylbutan-1-ol (SI8 and SI9). To a solution of the C2 and C8 isomers of **4.48** (19 mg, 0.05 mmol) in diethyl ether (1 mL) at room temperature was added lithium aluminum hydride (4 mg, 0.1 mmol). After 1 hour, the reaction was quenched with water (0.1 mL) then sodium hydroxide (0.05 mL of a 2 M aqueous solution), diethyl ether (3 mL) and $MgSO_4$ were added sequentially. The mixture was filtered through a pad of Celite and the filtrate was concentrated under

reduced pressure. The title compounds were separated by column chromatography on silica gel (20% to 30% EtOAc/Hexanes), allowing the sites of amination to be determined using 2D NMR spectroscopy.

TOCSY of **SI8** shows functionalization of the A ring, with multiplicities consistent with *ortho* substitution. TOCSY of **SI9** shows functionalization of the B ring, with multiplicities consistent with either C4 or C6 substitution. Based on HMBC for **SI9**, a correlation exists between C1' (41.62 ppm) and both H2 (6.76 ppm) and H4 (6.92 ppm), therefore amination occurred at C6.

SI8. **^{1}H NMR** (600 MHz, $CDCl_3$) δ 7.29 – 7.26 (m, 1H), 7.03 (td, *J* = 7.8, 1.8 Hz, 1H), 6.96 (d, *J* = 7.2 Hz, 1H), 6.91 – 6.85 (m, 4H), 6.65 (td, *J* = 7.8, 1.8 Hz, 1H), 4.10 (brs, 1H), 3.80 (dd, *J* = 10.8, 2.4 Hz, 1H), 3.69 – 3.65 (m, 2H), 3.41 – 3.34 (m, 2H), 2.96 – 2.88 (m, 1H), 1.94 (brs, 1H), 1.24 (dd, *J* = 7.2, 5.4 Hz, 3H), 0.88 (s, 9H). **^{13}C NMR** (151 MHz, $CDCl_3$) δ 157.95, 146.22, 142.89, 141.47, 130.11, 125.26, 122.01, 120.04, 117.29, 116.24, 115.56, 113.07, 68.62, 64.27, 62.39, 42.55, 34.99, 26.99, 17.72.
IR (thin film): 3413.39, 2958.27, 2924.52, 2871.49, 1718.26, 1606.41, 1579.41, 1517.70, 1485.88, 1440.56, 1333.53, 1249.65, 1189.86; **HRMS** (ESI): calculated for $C_{21}H_{29}NO_3$ $[M+H]^+$= 344.2220; found 344.2232.

SI9. **^{1}H NMR** (600 MHz, $CDCl_3$) δ 7.34 – 7.31 (m, 2H), 7.09 – 7.07 (m, 1H), 6.99 – 6.98 (m, 2H), 6.91 (dd, *J* = 8.4, 1.8 Hz, 1H), 6.87 (d, *J* = 8.4 Hz, 1H), 6.76 (t, *J* = 1.8 Hz, 1H), 4.06 (brs, 1H), 3.82 (dd, *J* = 10.8, 3.6 Hz, 1H), 3.63 – 3.57 (m, 2H), 3.40 (dd, *J* = 10.8, 9.0 Hz, 1H), 3.33 (dd, *J* = 9.0, 3.6 Hz, 1H), 2.83 – 2.78 (m, 1H), 1.98 (brs, 1H), 1.19 (dd, *J* = 7.2, 2.4 Hz, 3H), 0.87 (s, 9H). **^{13}C NMR** (151 MHz, $CDCl_3$) δ 157.57, 142.93, 140.26, 132.47,

130.00, 124.08, 123.07, 118.94, 117.23, 113.09, 68.93, 64.49, 62.45, 41.62, 34.94, 26.98, 17.74.

IR (thin film): 3391.21, 2959.23, 2924.52, 2854.13, 1716.34, 1540.85, 1520.60, 1507.10, 1488.78, 1456.96, 1261.22, 1218.79; **HRMS** (ESI): calculated for $C_{21}H_{29}NO_3$ $[M+H]^+$= 344.2220; found 344.2231.

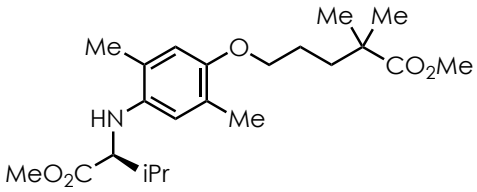

(*S*)-Methyl 5-(4-((1-methoxy-3-methyl-1-oxobutan-2-yl)amino)-2,5-dimethylphenoxy)-2,2-dimethylpentanoate (4.49). The title compound was prepared using Method B with an irradiation time of 19 hours using 2 lamps and 5 equivalents of valine methyl ester hydrochloride salt. The title compound was purified by column chromatography on silica gel (5% to 10% EtOAc/Hexanes) to give a colorless oil in 32% yield as a single regioisomer.

4.49. ^{1}H NMR (600 MHz, $CDCl_3$) δ 6.57 (s, 1H), 6.39 (s, 1H), 3.84 – 3.80 (m, 3H), 3.69 (s, 3H), 3.66 (s, 3H), 2.18 (s, 3H), 2.15 (s, 3H), 2.10 (oct, *J* = 6.6 Hz, 1H), 1.69 – 1.66 (m, 4H), 1.20 (s, 6H), 1.06 (d, *J* = 6.6 Hz, 3H), 1.02 (d, *J* = 6.6 Hz, 3H). **^{13}C NMR** (151 MHz, $CDCl_3$) δ 178.53, 174.98, 149.75, 139.12, 125.30, 121.52, 115.46, 114.78, 69.30, 63.62, 51.92, 51.89, 42.24, 37.28, 31.89, 25.51, 25.33, 25.32, 19.33, 18.96, 17.60, 16.26.

IR (thin film): 3394.1, 2955.38, 2872.45, 1732.73, 1519.63, 1456.96, 1212.04; **HRMS** (ESI): calculated for $C_{22}H_{35}NO_5$ $[M+H]^+$= 394.2588; found 394.2582.

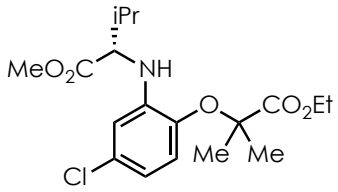

(*S*)-Methyl 2-((5-chloro-2-((1-ethoxy-2-methyl-1-oxopropan-2-yl)oxy)phenyl)amino)-3-methylbutanoate (4.50). The title compound was prepared using Method B with an irradiation time of 24 hours using 2 lamps. The title compound was purified by column chromatography on silica gel (10% EtOAc/Hexanes) to give a colorless oil in 66% yield by ^{1}H NMR and a mixture of 8.7:1 C2:C3 regioisomers. The product was contaminated with an inseparable impurity.

4.50. ^{1}H NMR (600 MHz, $CDCl_3$) δ 6.69 (d, *J* = 8.4 Hz, 1H), 6.51 (dd, *J* = 8.4, 2.4 Hz, 1H), 6.47 (d, *J* = 2.4 Hz, 1H), 5.23 (brd, *J* = 9.0 Hz, 1H), 4.27 (q, *J* = 7.2 Hz, 2H), 3.79 (dd, *J* = 9.0, 6.6 Hz, 1H), 3.71 (s, 3H), 2.18 (oct, *J* = 6.6 Hz, 1H), 1.57 (s, 3H), 1.56 (s, 3H), 1.30 (t, *J* = 7.2 Hz, 3H), 1.05 (d, *J* = 6.6 Hz, 3H), 1.01 (d, *J* = 6.6 Hz, 3H). **^{13}C NMR** (151 MHz, $CDCl_3$) δ 174.54, 173.72, 142.21, 140.80, 129.22, 120.43, 116.11, 110.75, 80.90, 61.80, 61.78, 52.06, 31.59, 25.31, 24.94, 19.29, 18.68, 14.28.

IR (thin film): 3365.17, 2965.98, 2875.34, 1736.58, 1597.73, 1516.74, 1420.32; **HRMS** (ESI): calculated for $C_{18}H_{26}ClNO_5$ $[M+H]^+$= 372.1572; found 372.1567.

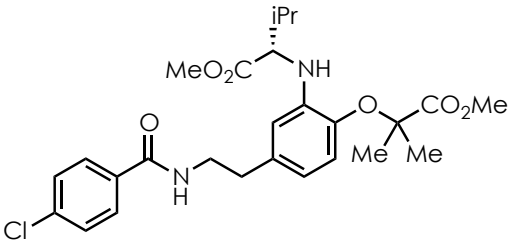

(*S*)-Methyl 2-((5-(2-(4-chlorobenzamido)ethyl)-2-((1-methoxy-2-methyl-1-oxopropan-2-yl)oxy)phenyl)amino)-3-methylbutanoate (4.51). The title compound was prepared using Method B with an irradiation time of 15 hours using 2 lamps. The title compound was purified by column chromatography on silica gel (30% EtOAc/Hexanes) to give a colorless oil in 36% yield by ^{1}H NMR and >10:1 regioselectivity. The product was contaminated with an inseparable impurity.

4.51. ^{1}H NMR (600 MHz, $CDCl_3$) δ 7.61 (AA'BB', *J* = 8.4 Hz, 2H), 7.37 (AA'BB', *J* = 8.4 Hz, 2H), 6.70 (d, *J* = 8.4 Hz, 1H), 6.41 (dd, *J* = 8.4, 1.8 Hz, 1H), 6.37 (d, *J* = 1.8 Hz, 1H), 6.05 (brt, *J* = 5.4 Hz, 1H), 5.13 (brd, *J* = 9.0 Hz, 1H), 3.83 – 3.79 (m, 1H), 3.82 (s, 3H), 3.67 – 3.63 (m, 2H), 3.65 (s, 3H), 2.79 (t, *J* = 7.2 Hz, 2H), 2.15 (oct, *J* = 6.6 Hz, 1H), 1.58 (s, 3H), 1,57 (s, 3H), 1.04 (d, *J* = 6.6 Hz, 3H), 1.00 (d, *J* = 6.6 Hz, 3H). **^{13}C NMR** (151 MHz, $CDCl_3$) δ 175.25, 174.09, 166.40, 141.28, 140.92, 137.69, 134.39, 133.12, 128.92, 128.40, 119.70, 116.82, 111.19, 80.59, 62.01, 52.81, 51.95, 41.16, 35.44, 31.65, 25.39, 25.00, 19.33, 18.76. **IR** (thin film): 3336.25, 2959.23, 2874.38, 1734.66, 1651.73, 1595.81, 1521.56, 1289.18; **HRMS** (ESI): calculated for $C_{26}H_{33}ClN_2O_6$ $[M+H]^+$= 505.2100; found 505.2097.

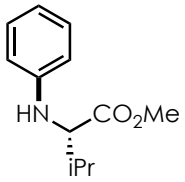

(*S*)-Methyl 3-methyl-2-(phenylamino)butanoate (4.52). The title compound was prepared using Method B with an irradiation time of 15 hours using 0.4 mL : 0.4 mL : 0.2 mL of DCE : benzene : pH 8 Buffer. The title compound was purified by column chromatography on

silica gel (10% to 30% EtOAc/Hexanes) to give **4.52** in 40% yield. The spectral data were in agreement with literature values.[19]

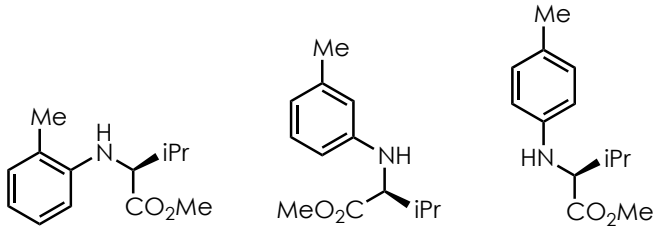

(*S*)-Methyl 3-methyl-2-(*o*-tolylamino)butanoate, (*S*)-methyl 3-methyl-2-(*m*-tolylamino)butanoate and (*S*)-methyl 3-methyl-2-(*p*-tolylamino)butanoate (4.53). The title compound was prepared using Method B with an irradiation time of 15 hours using 0.4 mL : 0.4 mL : 0.2 mL of DCE : toluene : pH 8 Buffer. The title compound was purified by column chromatography on silica gel (5% EtOAc/Hexanes) to give a colorless oil in 50% yield and a mixture of 1.2:1:2.1 *ortho* to *meta* to *para* regioisomers. The *para* isomer has previously been reported; spectral data were in agreement with literature values.[20]

4.53. ^{1}H NMR (600 MHz, $CDCl_3$) δ 7.10 – 7.04 (m, 1.5H), 6.98 (AA'BB', *J* = 8.4 Hz, 2H), 6.68 (td, *J* = 7.2, 1.2 Hz, 0.5H), 6.56 – 6.54 (m, 1H), 6.55 (AA'BB', *J* = 8.4 Hz, 2H), 6.47 – 6.46 (m, 0.5H), 6.44 (dd, *J* = 7.8, 2.4 Hz, 0.5H), 4.06 (brd, *J* = 9.6 Hz, 0.5H), 4.03 (brd, *J* = 9.6 Hz, 0.5H), 3.98 (brd, *J* = 9.6 Hz, 1H), 3.91 (dd, *J* = 9.6, 6.0 Hz, 0.5H), 3.86 (dd, *J* = 9.6, 6.0 Hz, 0.5H), 3.83 (dd, *J* = 9.6, 6.0 Hz, 1H), 3.72 (s, 1.5H), 3.71 (s, 1.5H), 3.70 (s, 3H), 2.27 (s, 1.5H), 2.23 (s, 3H), 2.22 (s, 1.5H), 2.19 – 2.05 (m, 2H), 1.08 – 1.00 (m, 12H). **^{13}C NMR** (151 MHz, $CDCl_3$) δ 174.55, 174.52, 174.44, 147.43, 145.35, 145.14, 139.26, 130.49, 129.94, 129.33, 127.64, 127.24, 122.89, 119.31, 117.85, 114.54, 113.86, 110.61, 110.47, 62.97, 62.51, 62.39, 52.04, 52.01, 51.97, 31.77, 31.73, 31.70, 21.75, 20.54, 19.27, 19.26, 19.23, 18.96, 18.86, 18.84, 17.65.

IR (thin film): 3393.14, 2963.09, 2873.42, 1734.66, 1616.06, 1520.60, 1304.61; **HRMS** (ESI): calculated for $C_{13}H_{19}NO_2$ $[M+H]^+$= 222.1489; found 222.1488.

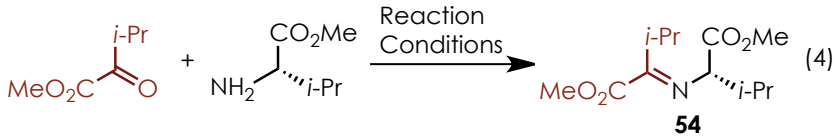

(4)

Methyl 2-((1-methoxy-3-methyl-1-oxobutan-2-yl)imino)-3-methylbutanoate (4.54). It was noted that a significant byproduct in some reactions was imine **4.54**, derived from oxidation and hydrolysis of the starting amine followed by condensation with a second equivalent of amine (equation 4). This observation is consistent with the presence of amine cation radicals under the reaction conditions.

GC-MS: retention time 5.07 min, LRMS (EI) calculated for $C_{12}H_{21}NO_4$ $[M]^+$= 243.1; found 243.1. **4.54** was only observed through GCMS; stability issues precluded isolation.

Redox Potentials.

Oxidation potentials for isopropylamine, [21] glycine ethyl ester, [22] *tert*-butylamine,[23] and propylamine[21] were previously reported. Anisole, TBS phenol, 2,6-dimethoxy pyridine, and biphenyl were previously reported by our lab.[2]

All the other substrate redox potentials in the table were determined using CV with the following method. Electrochemical potentials were obtained with a standard set of conditions to maintain internal consistency. Cyclic voltammograms were collected with a Pine WaveNow Potentiostat. Samples were prepared with 0.05 mmol of substrate in 5 mL of 0.1 M tetra-n-butylammonium hexafluorophosphate in dry, degassed acetonitrile. Measurements employed a glassy carbon working electrode, platinum wire counter electrode, 3.5 M NaCl silver-silver chloride reference electrode, and a scan rate of 100 mV/s. Reductions were measured by scanning potentials in the negative direction and oxidations in the positive direction; the glassy carbon electrode was polished between each scan. Data was analyzed using MATLAB by subtracting a background current prior to identifying the maximum current (Cp) and determining the potential (Ep/2) at half this value (Cp/2). The obtained value was referenced to Ag|AgCl and converted to SCE by subtracting 0.03 V.

Oxidation Potentials of Amines and Arenes

Arene	Oxidation Potential (V vs. SCE in MeCN)
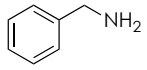	+1.81V
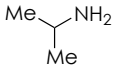	+1.40V
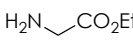	+1.60V
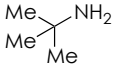	+1.44V
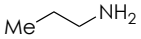	+1.35V
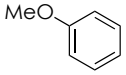	+1.87V
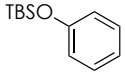	+1.89V
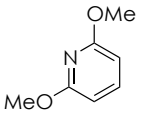	+1.59V
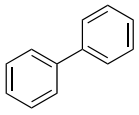	+1.96V
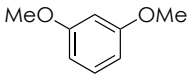	+1.56V
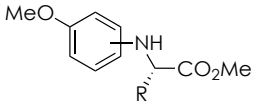	+0.74
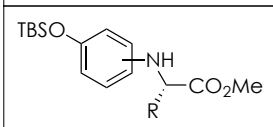	+0.75

Stern-Volmer Quenching Studies

Emission lifetime measurements were taken at ambient temperature using a Edinburgh FLS920 spectrometer and fit to single exponential decay according to a modification of the method previously described by our laboratory.[24] Measurements were made by the time-correlated single photon counting (TCSPC) capability of the instrument with pulsed excitation light (444.2 nm, typical pulse width = 95 ps) generated by a Edinburgh EPL-445 ps pulsed laser diode operating at a repetition rate of 5 MHz. The maximum emission channel count rate was less than 5% of the laser channel count rate, and each data set collected greater than 10000 counts on the maximum channel. The lifetime of fluorescence was determined by reconvolution fit with the instrument response function using the Edinburgh FS900 software. In all cases, after reconvolution, fluorescence decay was satisfactorily fit with a monoexponential function of the form:

$$\boldsymbol{I_t = I_0 e^{-t/\tau}}$$

where *I* is the intensity (counts), and t is the mean lifetime of fluorescence.

Stern-Volmer analysis on the quenching of fluorescence lifetime was carried out in DCE with detection at 500 nm (15 nm bandwidth), where the concentration of acridinium was 1.6 $\times$ 10^{-5} M. The quenching constant was determined with quencher concentrations in the range of 0 M to 2.0 $\times$ 10^{-2} M. Bimolecular quenching constants, k_q, were determined from the corresponding Stern-Volmer constant.[25] Quenching constants were determined for both **Me_2-Mes-Acr+** and ***t*-Bu_2-Mes-Acr+** with a representative arene and amine, and were derived from duplicate experiments. Comparison of UV-Vis absorption spectra taken before and after

lifetime quenching studies verified that the acridinium was unchanged. UV-Vis spectra were taken on a Hewlett-Packard 8453 Chemstation spectrophotometer.

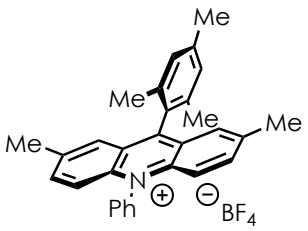

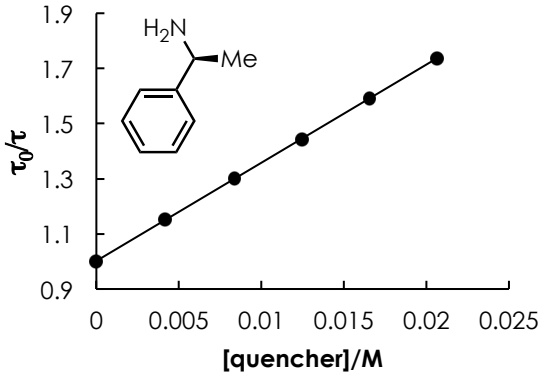

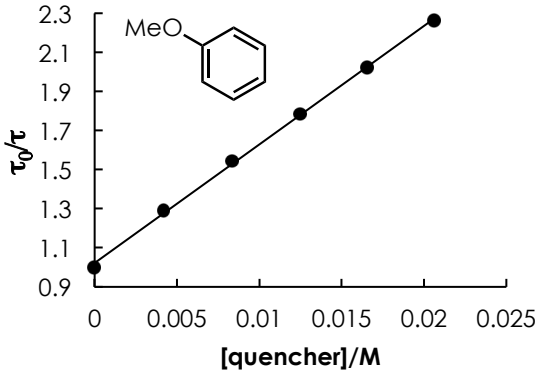

$k_q = 2.79 \times 10^9\ M^{-1}\ s^{-1}$

$k_q = 4.75 \times 10^9\ M^{-1}\ s^{-1}$

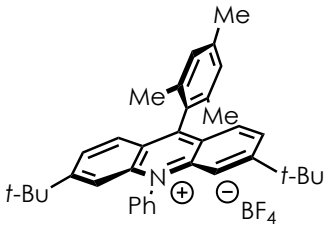

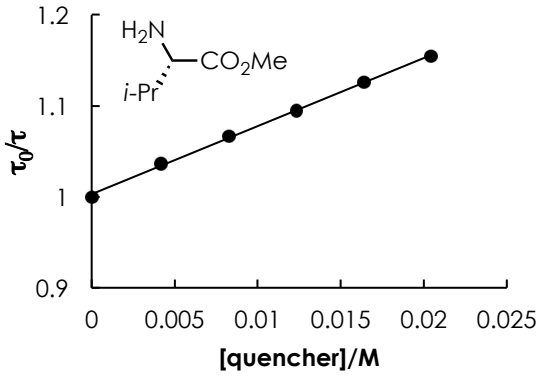

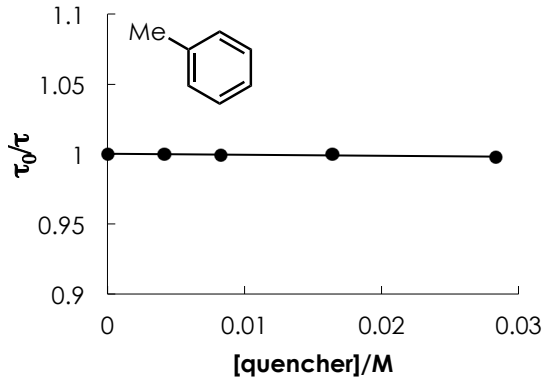

$$k_q = 5.54 \times 10^8\ M^{-1}\ s^{-1}$$

Figure S1. Stern-Volmer Quenching Studies

Since the amine is usually present in 3 equivalents, the corrected quenching rates are **8.4 x 10^8 s^{-1}** for (*S*)-a-methylbenzylamine and **1.7 x 10^8 s^{-1}** for valine methyl ester, compared to **4.75 x 10^8 s^{-1}** for anisole.

Hydrogen Peroxide Detection Experiments

Previously, an aerobic mechanism disclosed by Fukuzumi[26] for benzylic oxidation indicated that oxygen was able to turn over the catalyst, generating hydrogen peroxide *in situ*. Fukuzumi demonstrated the formation of hydrogen peroxide in their reaction by running the reaction and then using ^{1}H NMR, detected a peak for hydrogen peroxide. H_2O_2: ^{1}H NMR (CD_3CN): δ 8.67 (s, 2H) and ^{1}H NMR (CD_2Cl_2): δ 7.55 (s, 2H).[27]

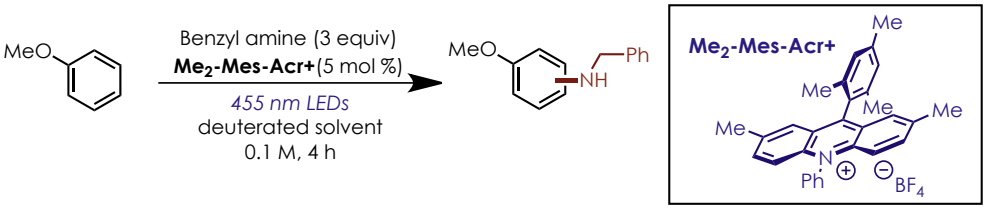

A similar approach was taken for this reaction, in which a ^{1}H NMR was taken before and after irradiation. The reaction was run in both CD_3CN and CD_2Cl_2 in a 1-dram vial and transferred for acquiring NMR data. When using CD_3CN, 10% yield of hydrogen peroxide was observed, and when using CD_2Cl_2, 21% yield of hydrogen peroxide was observed.

Quantum Yield Determination

A vial was charged with acridinium catalyst (2.5 mg, 5 mol %) and dissolved in DCE (1 mL). Anisole (0.1 mmol, 1 equiv) and benzyl amine (0.3 mmol, 3 equiv) were added via syringe. The reaction vial was sparged with oxygen for 3 minutes and then irradiated 10 cm from a single Par38 Royal Blue Aquarium LED lamp (Model #6851) fabricated with high-power Cree LEDs as purchased from Ecoxotic (www.ecoxotic.com). The sample was irradiated for 30 minutes (1800 seconds). The reaction was concentrated and yield was determined by ^{1}H NMR based on an HMDSO internal standard. The quantum yield was determined using the following equation where f is essentially 1 (f > 0.999) due to absorption of all incident light.[28]

$$\Phi = \frac{mole\ of\ product}{flux * t * f}$$

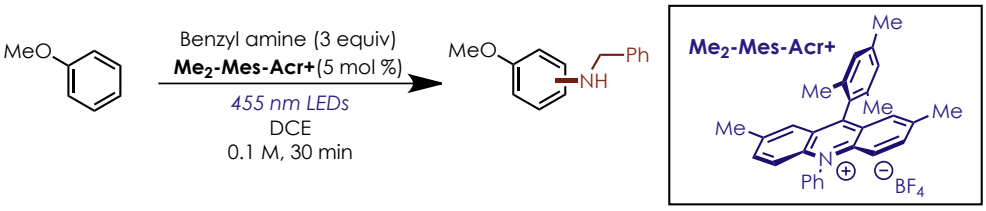

The yield was determined to be 23% (0.0023 mmol) of both regioisomers after 30 minutes (1800 sec) of irradiation. Flux was previously disclosed in our lab using the same light

system and instrumentation. It was reported that flux of the Cree LED set up was 6.43 x 10^{-7} mol photon s^{-1}.[24]

$$\Phi = \frac{2.3x10^{-5}\ mol}{6.43x10^{-7} mol\ photon\ s^{-1} * 1800\ s * 1} = 0.02 = 2\%$$

Fukuzumi previously reported quantum yields for several arenes involved in his aryl bromination chemistry. The quantum yield percentages ranged from 0.01 to 4.8%.

REFERENCES

(1) Wilger, D. J.; Grandjean, J.-M. M.; Lammert, T. R.; Nicewicz, D. A. *Nat. Chem.* **2014**, *6*, 720–726.

(2) Romero, N. A.; Margrey, K. A.; Tay, N. E.; Nicewicz, D. A. *Science* **2015**, *349*, 1326–1330.

(3) Baker, M. S.; Phillips, S. T. *J. Am. Chem. Soc.* **2011**, *133*, 5170–5173.

(4) Bartoli, G.; Bosco, M.; Locatelli, M.; Marcantoni, E.; Melchiorre, P.; Sambri, L. *Org. Lett.* **2005**, *7*, 427–430.

(5) Hudrlik, P. F.; Minus, D. K. *J. Organomet. Chem.* **1996**, *521*, 157–162.

(6) McManus, J. B.; Nicewicz, D. A. *J. Am. Chem. Soc.* **2017**.

(7) Wahba, A. E.; Hamann, M. T. *J. Org. Chem.* **2012**, *77*, 4578–4585.

(8) Kolesnikov, P. N.; Yagafarov, N. Z.; Usanov, D. L.; Maleev, V. I.; Chusov, D. *Org. Lett.* **2015**, *17*, 173–175.

(9) Nacario, R.; Kotakonda, S.; Fouchard, D. M. D.; Tillekeratne, L. M. V.; Hudson, R. A. *Org. Lett.* **2005**, *7*, 471–474.

(10) Saidi, O.; Blacker, A. Joh.; Farah, M.; Marsden, S.; Williams, J. ?J. *Angew. Chem. Int. Ed.* **2009**, *48*, 7375–7378.

(11) Kita, Y.; Sakaguchi, H.; Hoshimoto, Y.; Nakauchi, D.; Nakahara, Y.; Carpentier, J.-F.; Ogoshi, S.; Mashima, K. *Chem. - Eur. J.* **2015**, *21*, 14571–14578.

(12) Zhou, W.; Fan, M.; Yin, J.; Jiang, Y.; Ma, D. *J. Am. Chem. Soc.* **2015**, *137*, 11942–11945.

(13) Yang, P.; Lim, L. H.; Chuanprasit, P.; Hirao, H.; Zhou, J. S. *Angew. Chem. Int. Ed.* **2016**, *55*, 12083–12087.

(14) Perkowski, A. J.; Cruz, C. L.; Nicewicz, D. A. *J. Am. Chem. Soc.* **2015**, *137*, 15684–15687.

(15) Sun, Q.; Wang, Y.; Yuan, D.; Yao, Y.; Shen, Q. *Dalton Trans* **2015**, *44*, 20352–20360.

(16) Fisher, D. J.; Shaum, J. B.; Mills, C. L.; Read de Alaniz, J. *Org. Lett.* **2016**, *18*, 5074–5077.

(17) Barker, T. J.; Jarvo, E. R. *Angew. Chem. Int. Ed.* **2011**, *50*, 8325–8328.

(18) Gage, J. R.; Wagner, J. M. *J. Org. Chem.* **1995**, *60*, 2613–2614.

(19) Sharma, K. K.; Sharma, S.; Kudwal, A.; Jain, R. *Org Biomol Chem* **2015**, *13*, 4637–4641.

(20) Gan, J.; Ma, D. *Org. Lett.* **2009**, *11*, 2788–2790.

(21) Cruz, H.; Bourdelande, J. L.; Gallardo, I.; Guirado, G. *J. Phys. Chem. A* **2015**, *119*, 620–633.

(22) Marquet, J.; Cantos, A.; Moreno-Mañas, M.; Caýon, E.; Gallardo, I. *Tetrahedron* **1992**, *48*, 1333–1342.

(23) Adenier, A.; Chehimi, M. M.; Gallardo, I.; Pinson, J.; Vilà, N. *Langmuir* **2004**, *20*, 8243–8253.

(24) Romero, N. A.; Nicewicz, D. A. *J. Am. Chem. Soc.* **2014**, *136*, 17024–17035.

(25) Lakowicz, J. R. Principles of Fluorescence Spectroscopy; 3rd ed.; Springer: New York, 2006.

(26) K. Ohkubo, K. Mizushima, S. Fukuzumi, *Res. Chem. Intermed.* **2013**, *39*, 205–220.

(27) DiPasquale, A. G.; Mayer, J. M. *J. Am. Chem. Soc.* **2008**, *130*, 1812–1813.

(28) Cismesia, M. A.; Yoon, T. P. *Chem Sci* **2015**, *6*, 5426–5434.

NMR Spectra for New Compounds

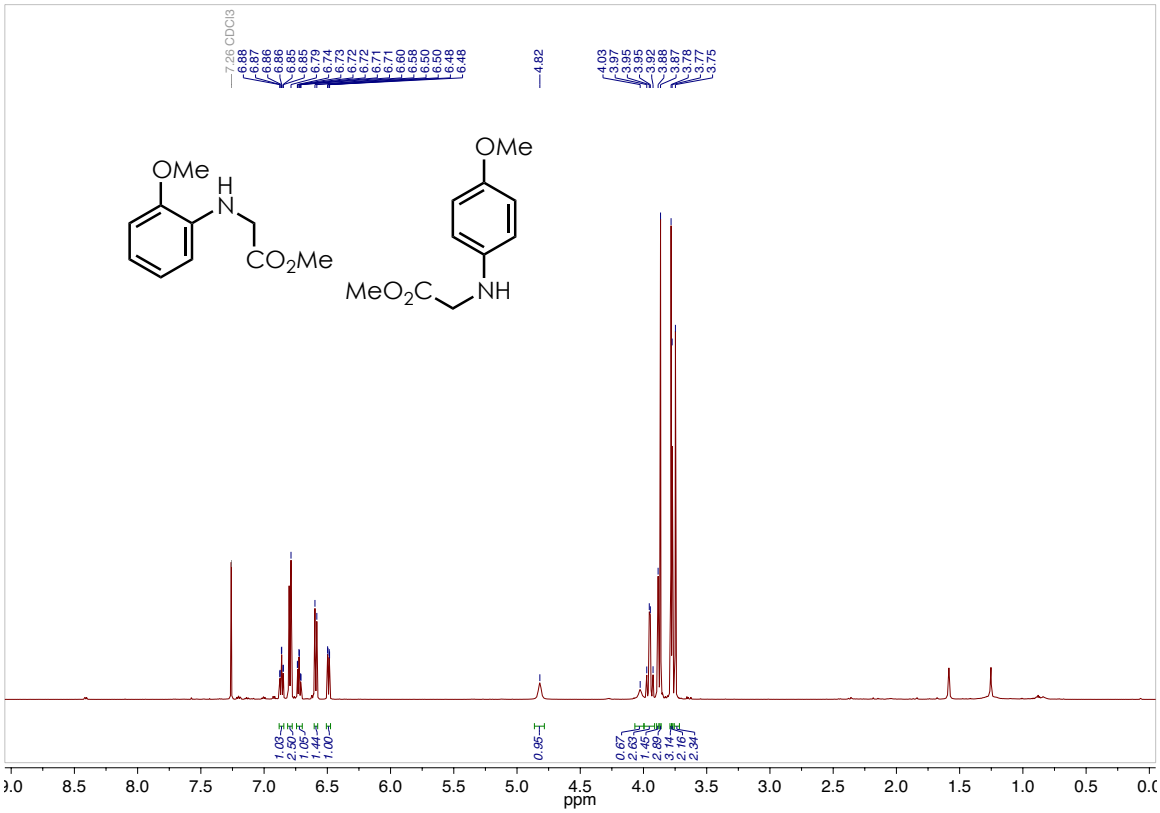

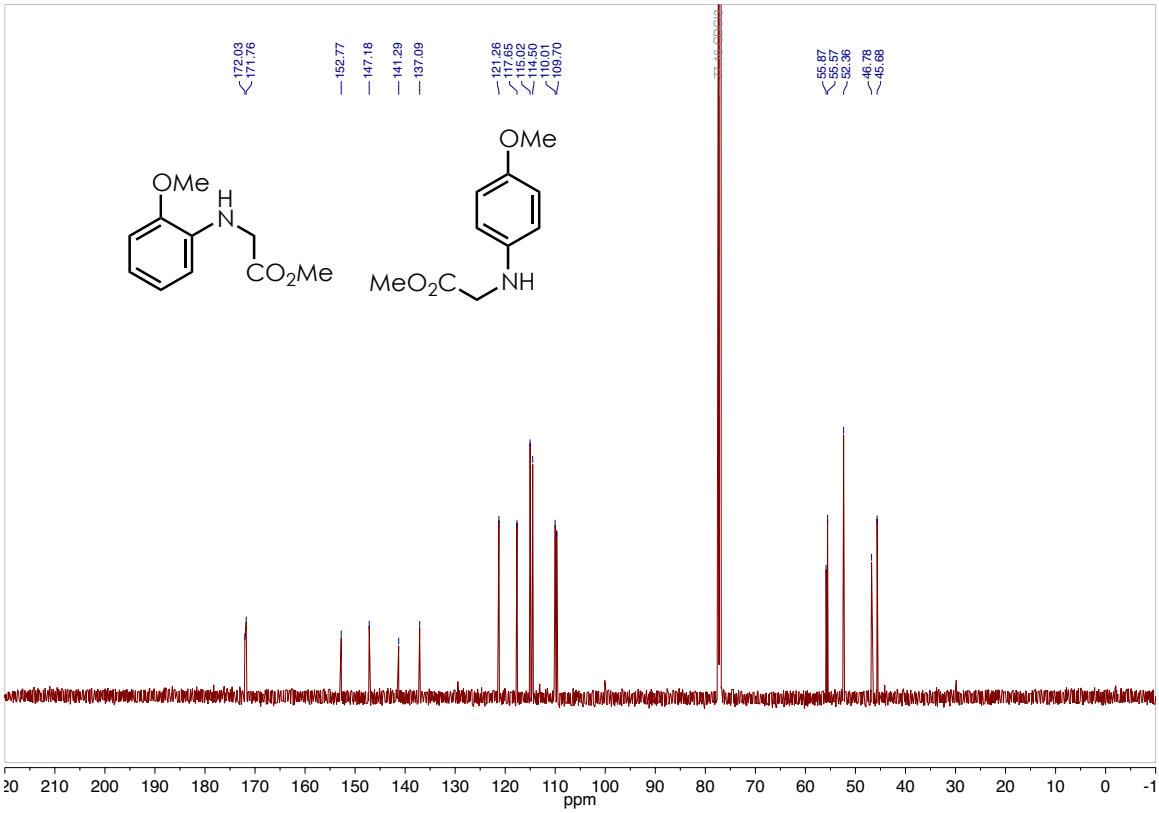

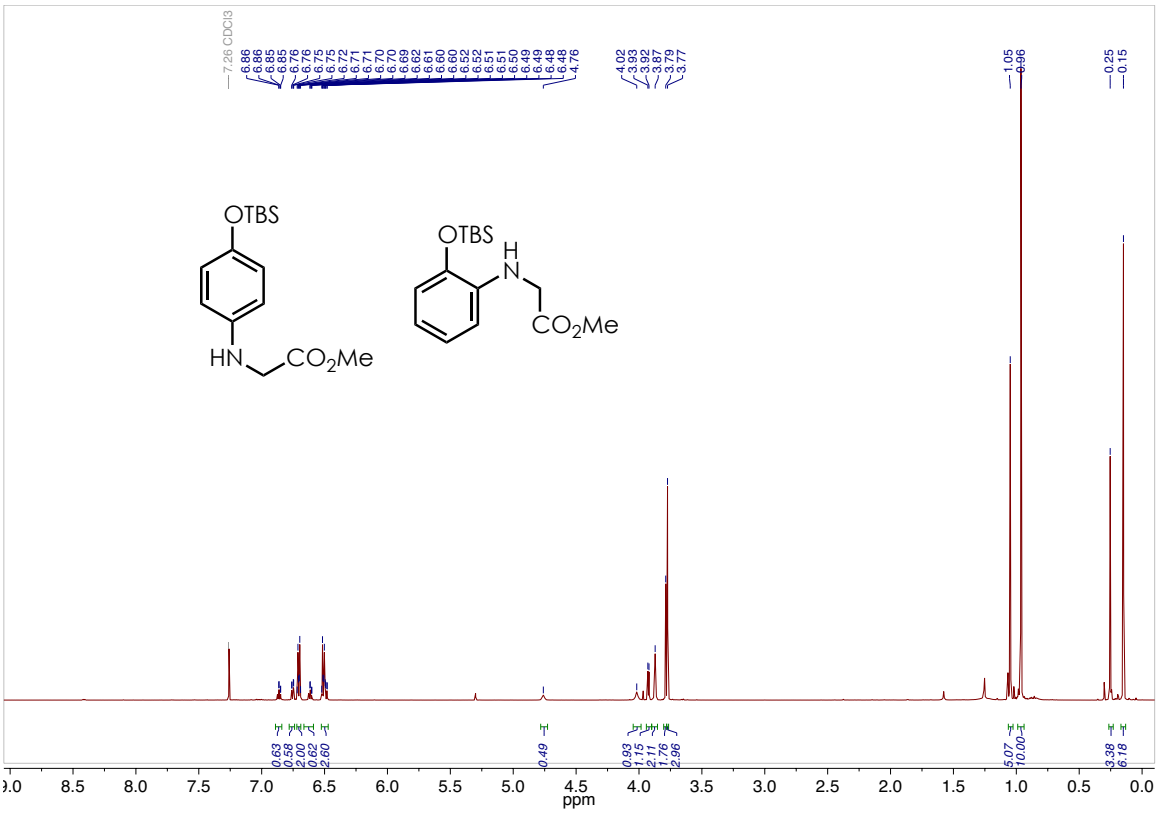
OTBS
HN
CO2Me
OTBS
H
N
CO2Me
ppm

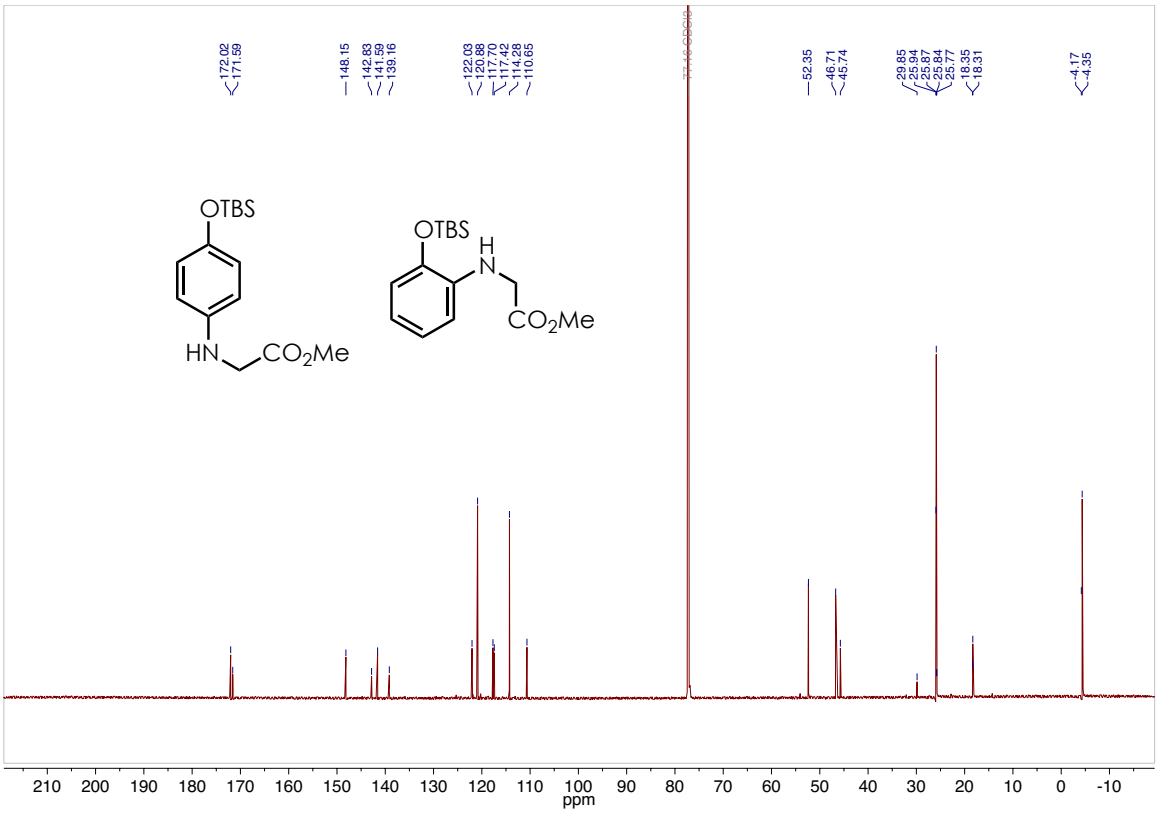
OTBS
HN
CO2Me
OTBS
H
N
CO2Me
ppm

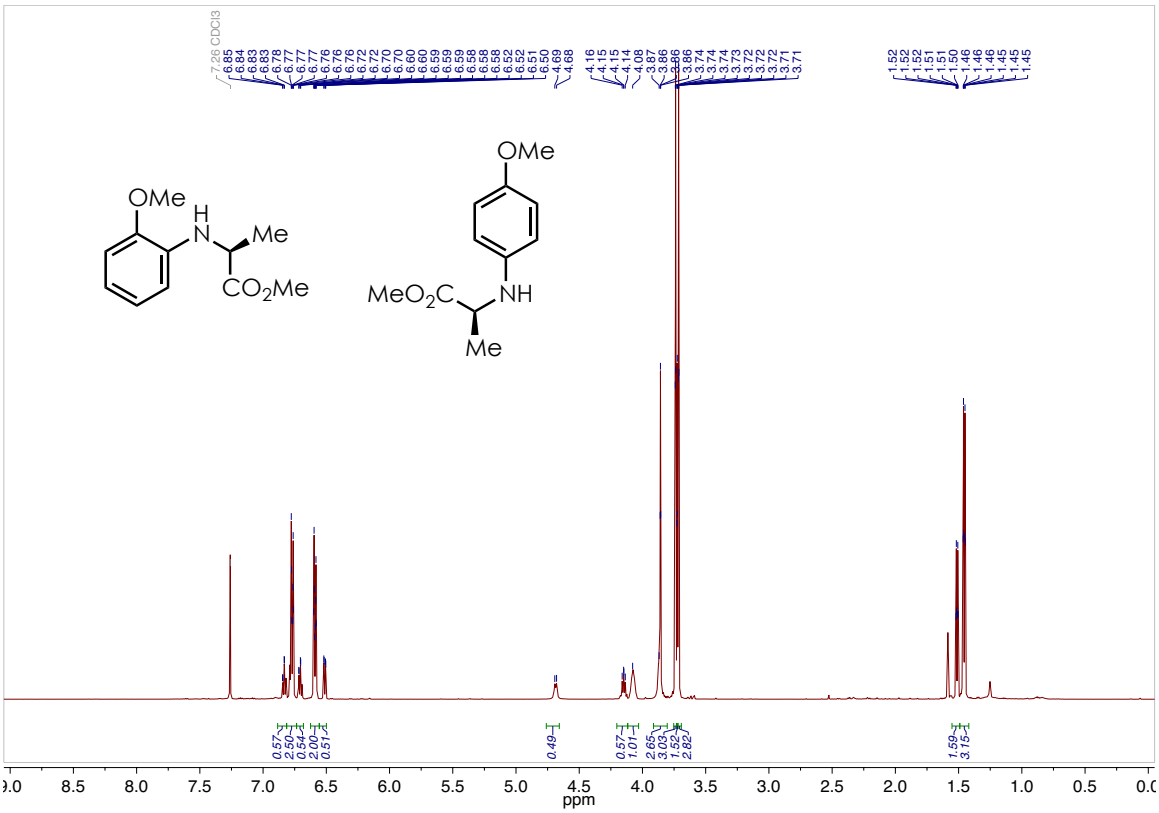

kamv227A_frac_2C

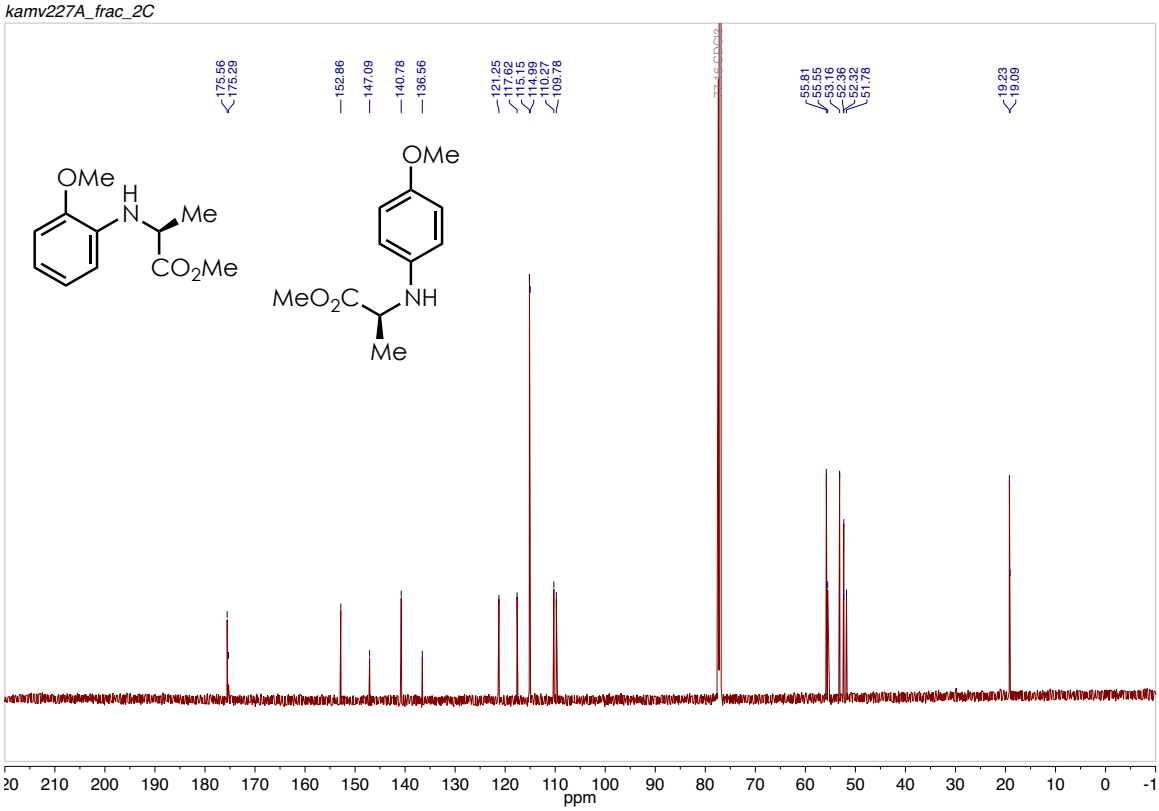

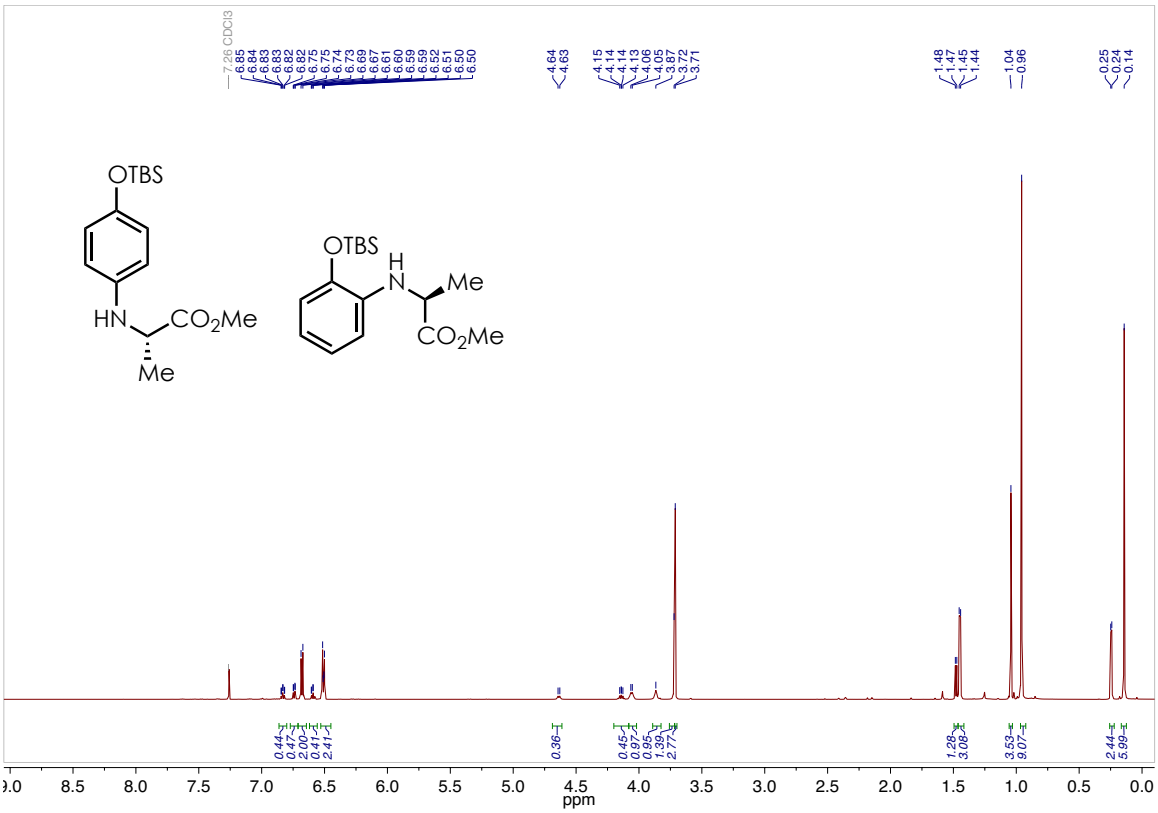
OTBS
HN
CO2Me
Me
OTBS
H
N
Me
CO2Me
ppm

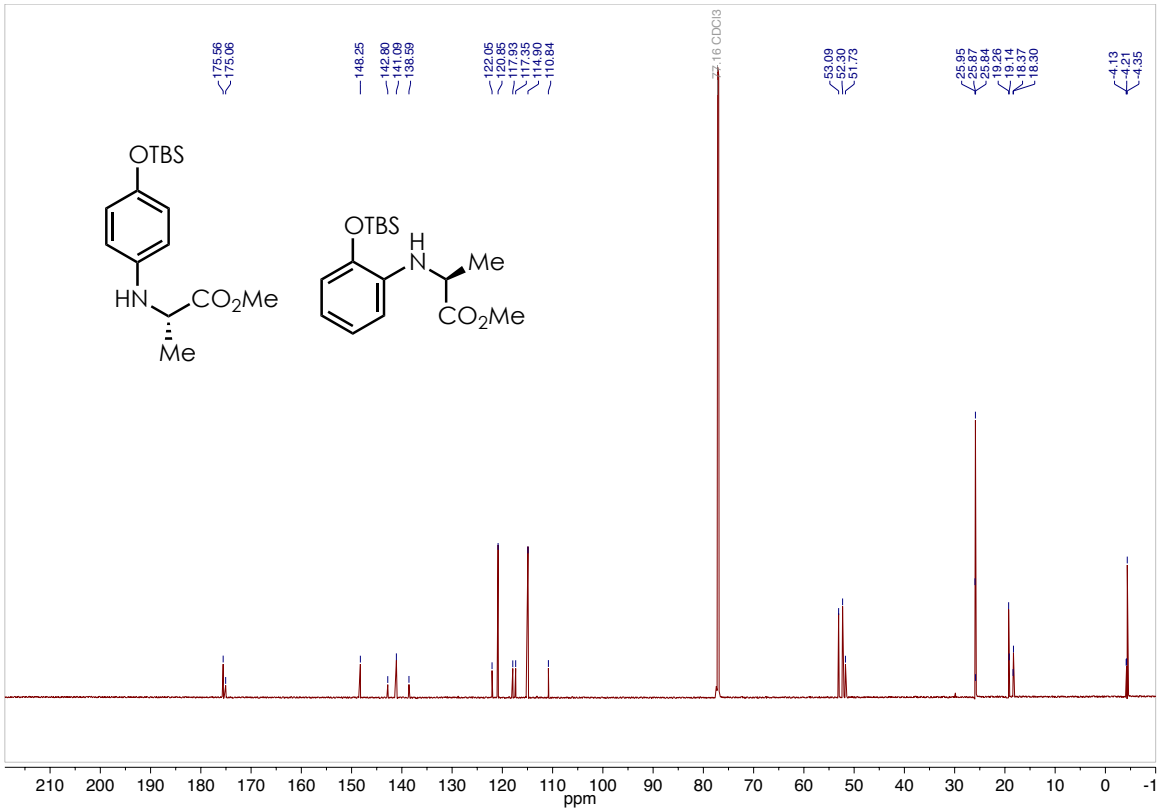
OTBS
HN
CO2Me
Me
OTBS
H
N
Me
CO2Me
ppm

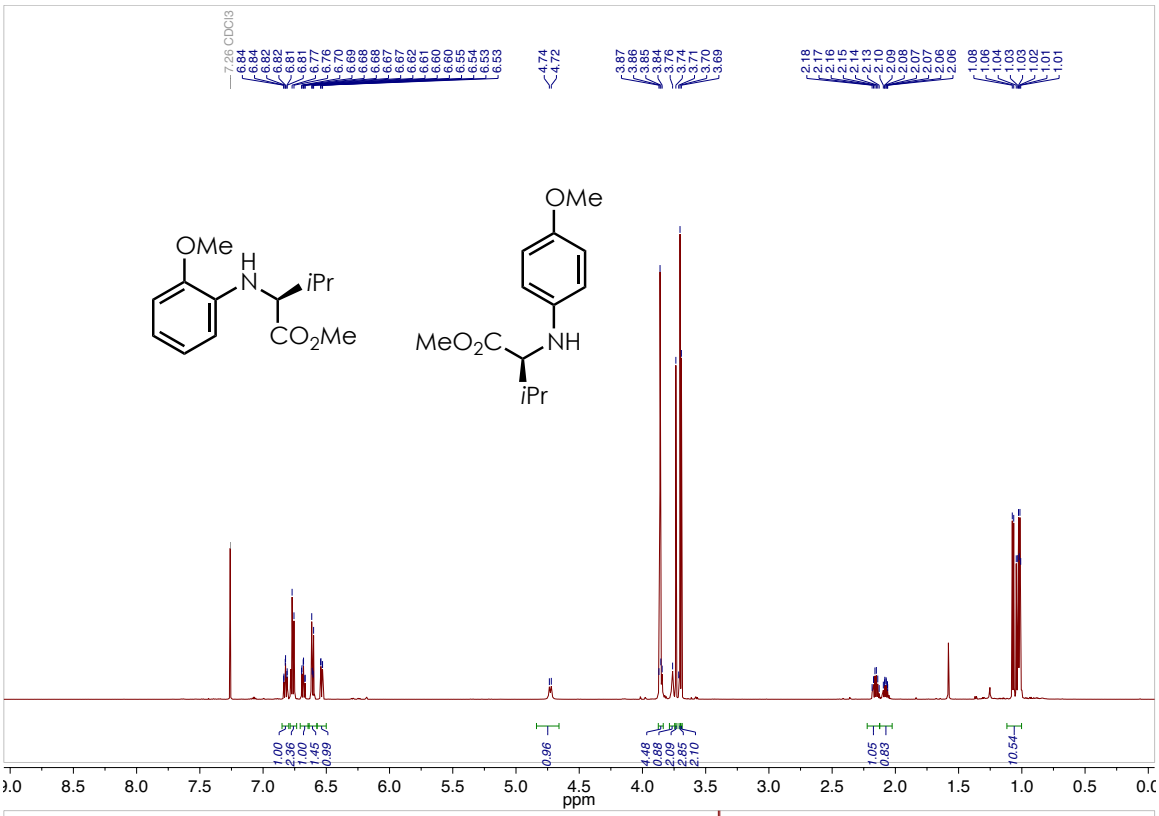
OMe
H
N
iPr
CO2Me
OMe
MeO2C
NH
iPr
ppm

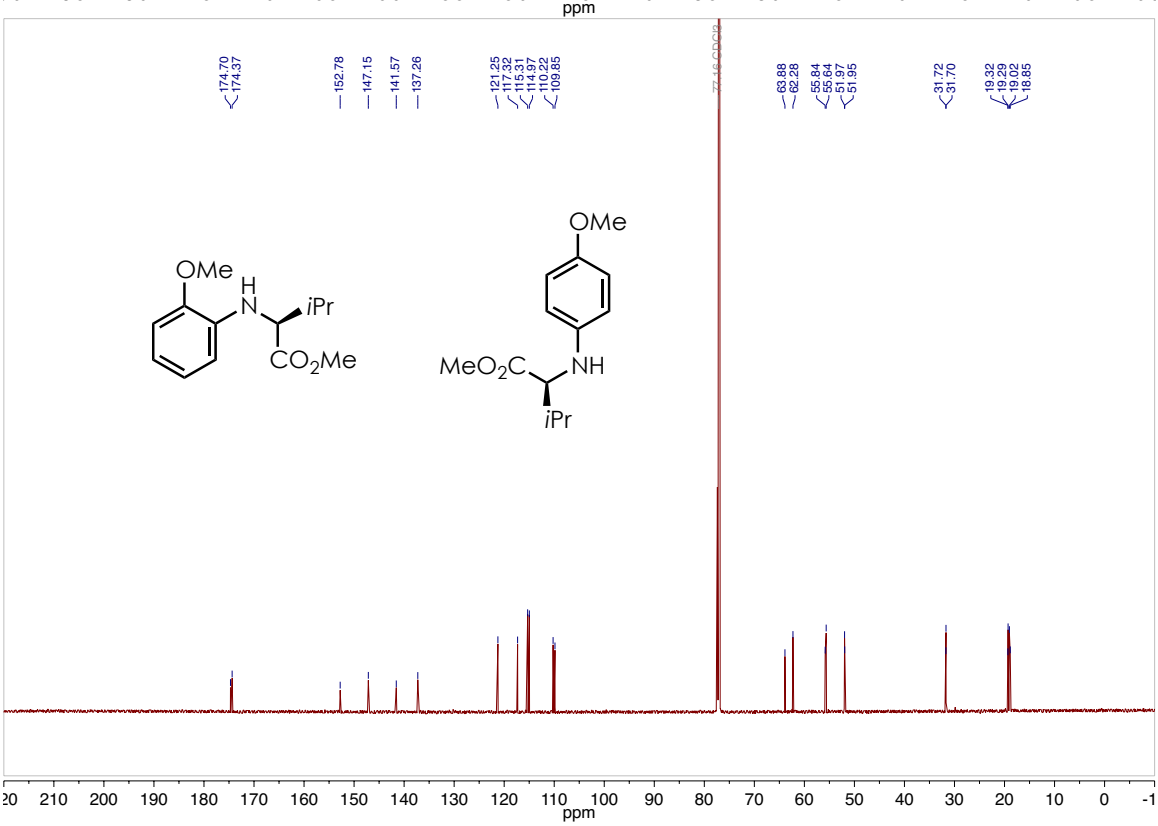
OMe
H
N
iPr
CO2Me
OMe
MeO2C
NH
iPr
ppm

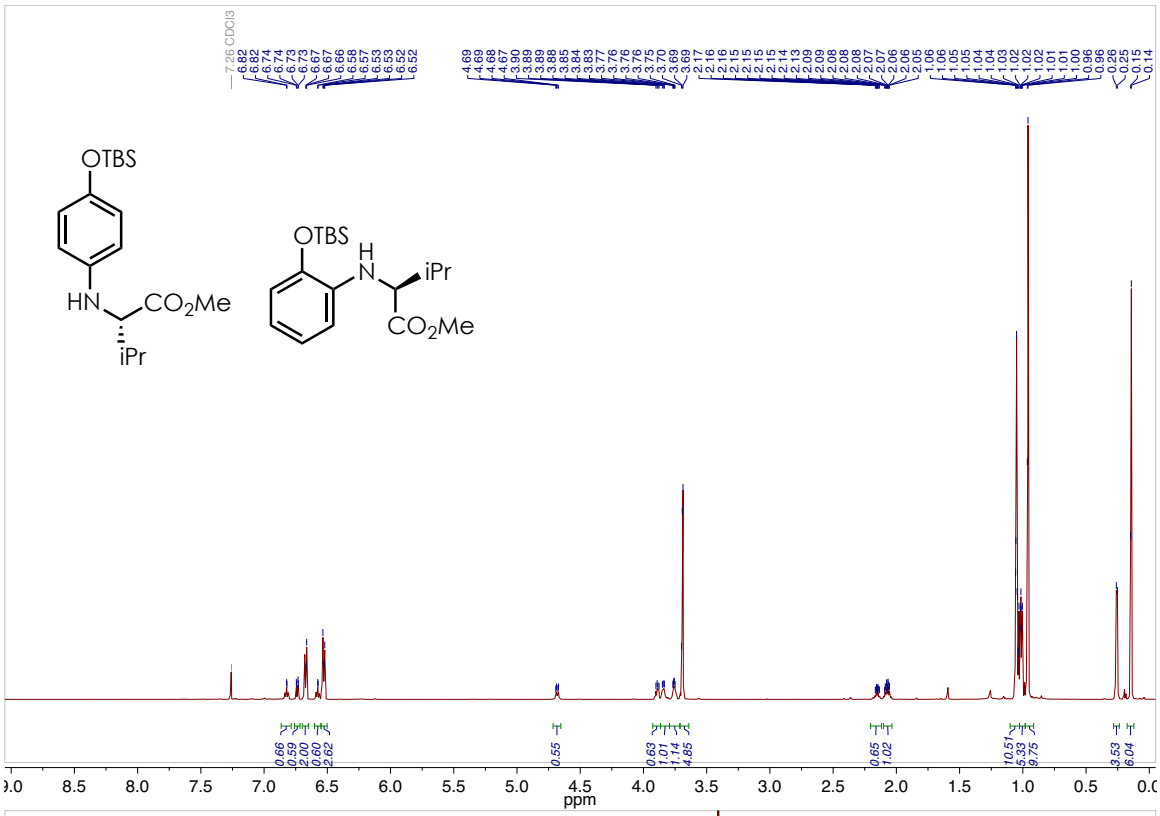
OTBS
HN
CO2Me
iPr
OTBS
H
N
iPr
CO2Me
ppm

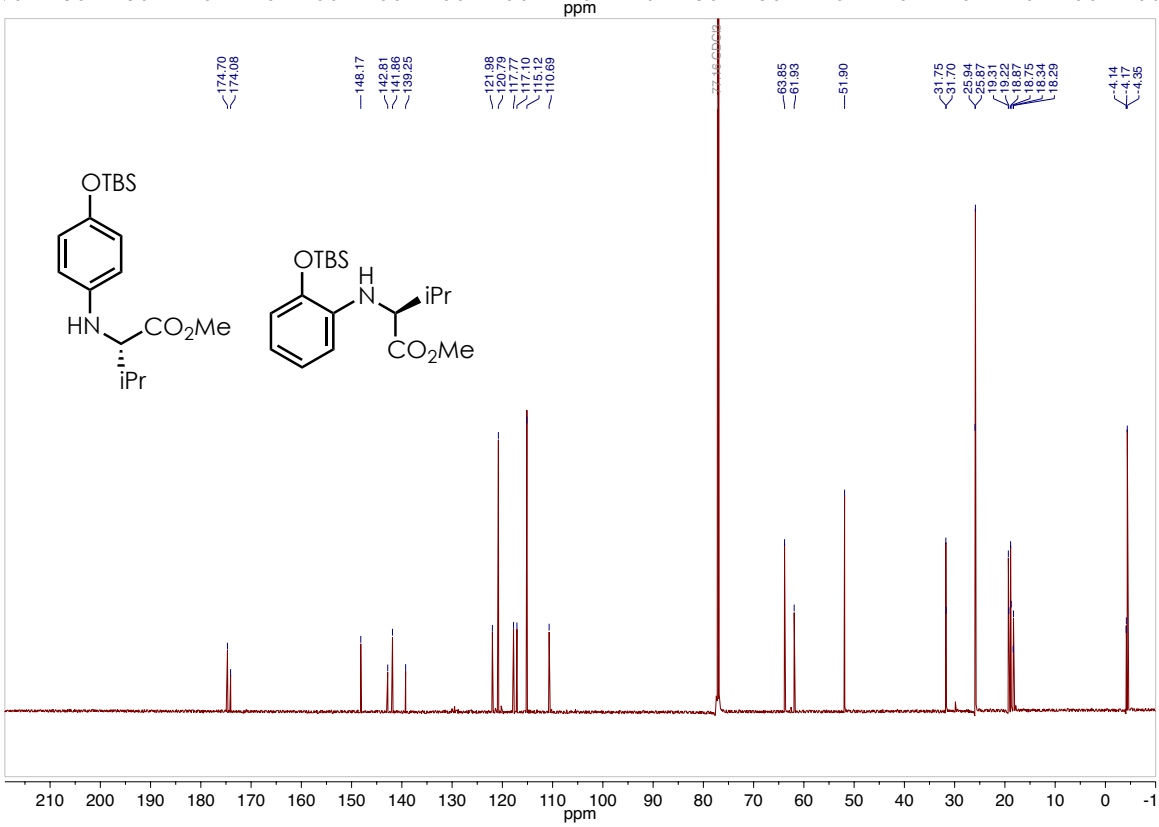
OTBS
HN
CO2Me
iPr
OTBS
H
N
iPr
CO2Me
ppm

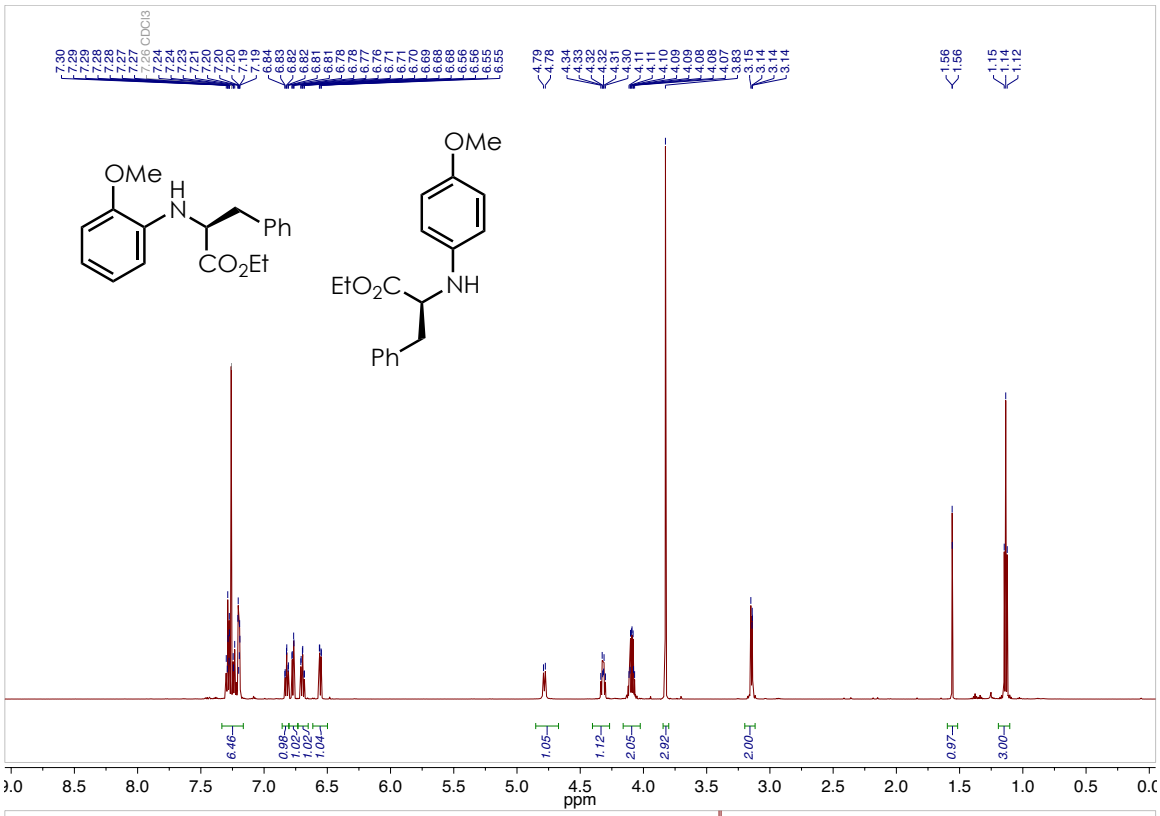
OMe
H
N
Ph
CO2Et
OMe
EtO2C
NH
Ph
ppm

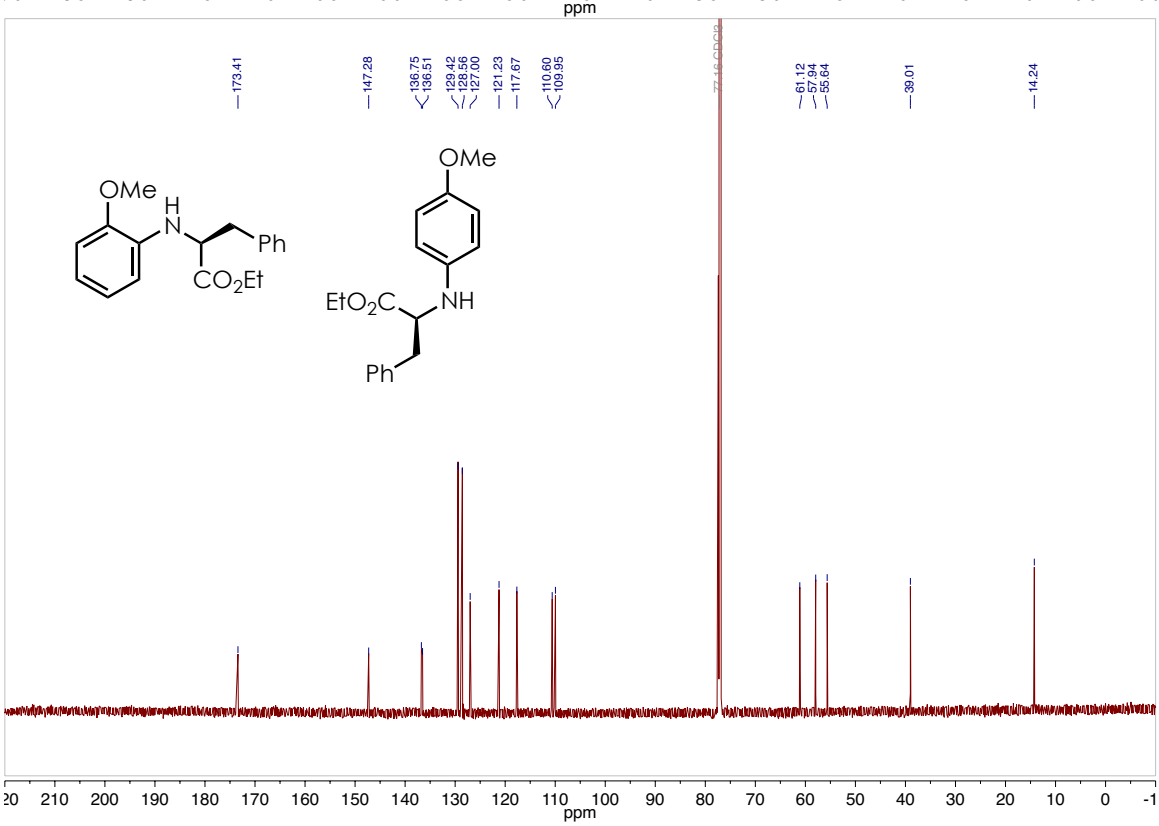
OMe
H
N
Ph
CO2Et
OMe
EtO2C
NH
Ph
ppm

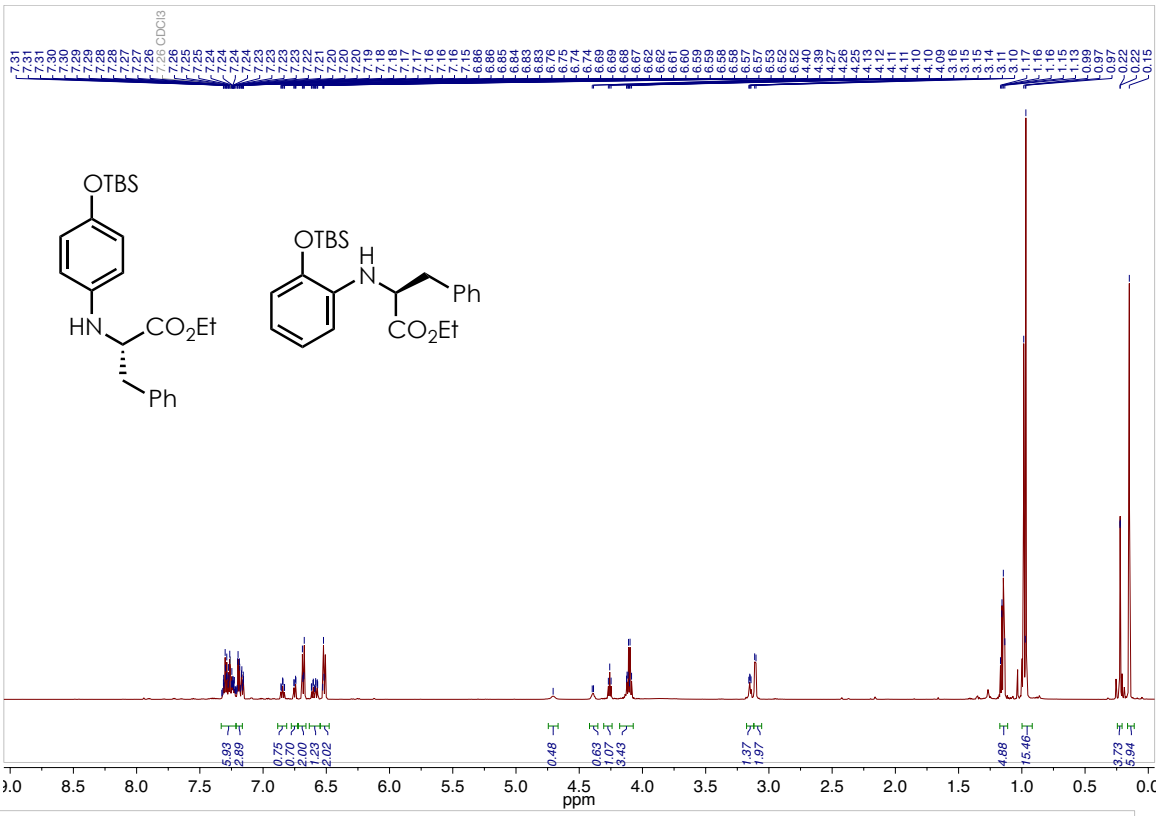
OTBS
HN
CO2Et
Ph
OTBS
H
N
Ph
CO2Et
ppm

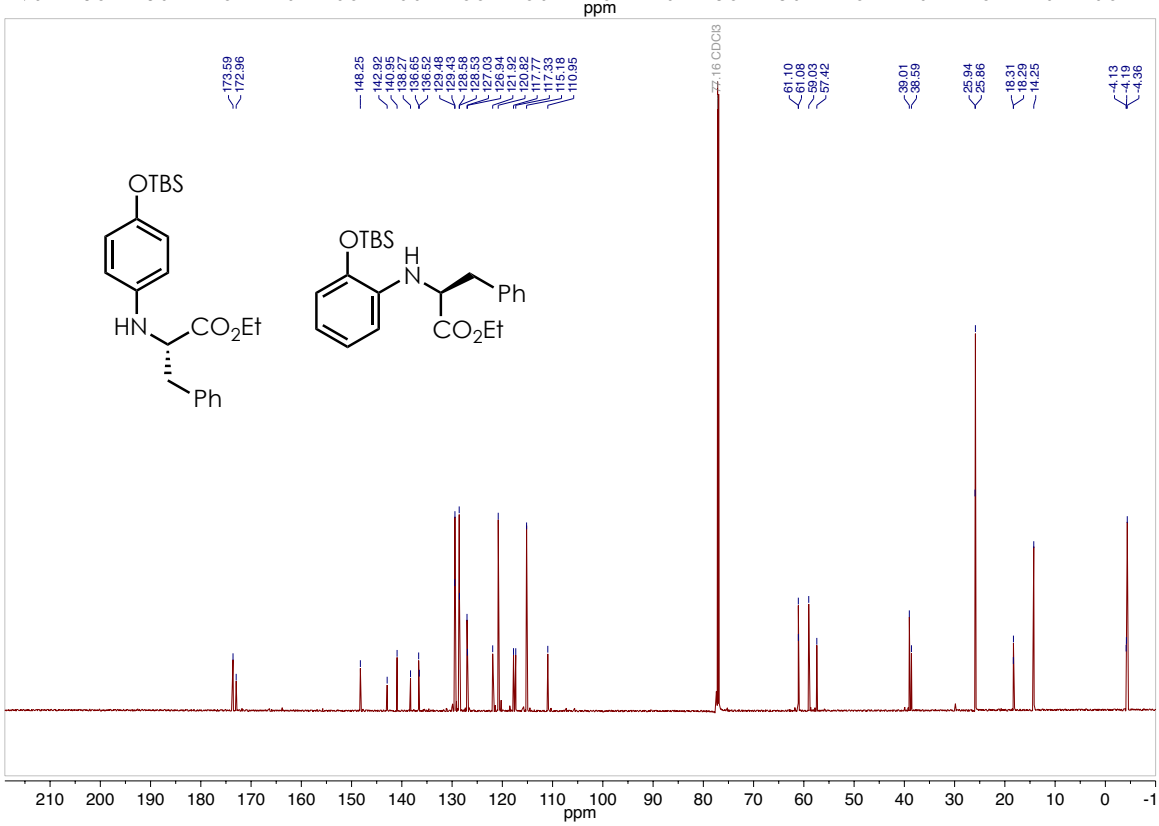
OTBS
HN
CO2Et
Ph
OTBS
H
N
Ph
CO2Et
ppm

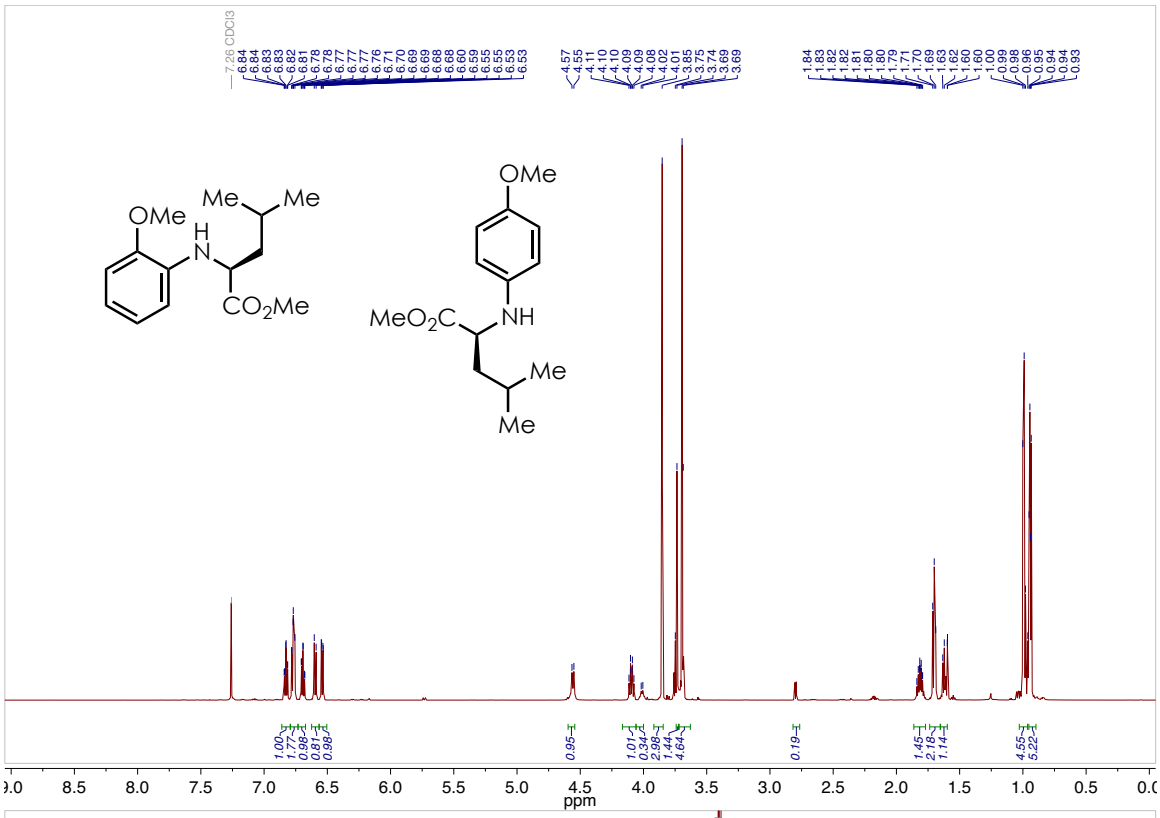
OMe
Me
Me
H
N
CO2Me
MeO2C
NH
Me
Me
ppm

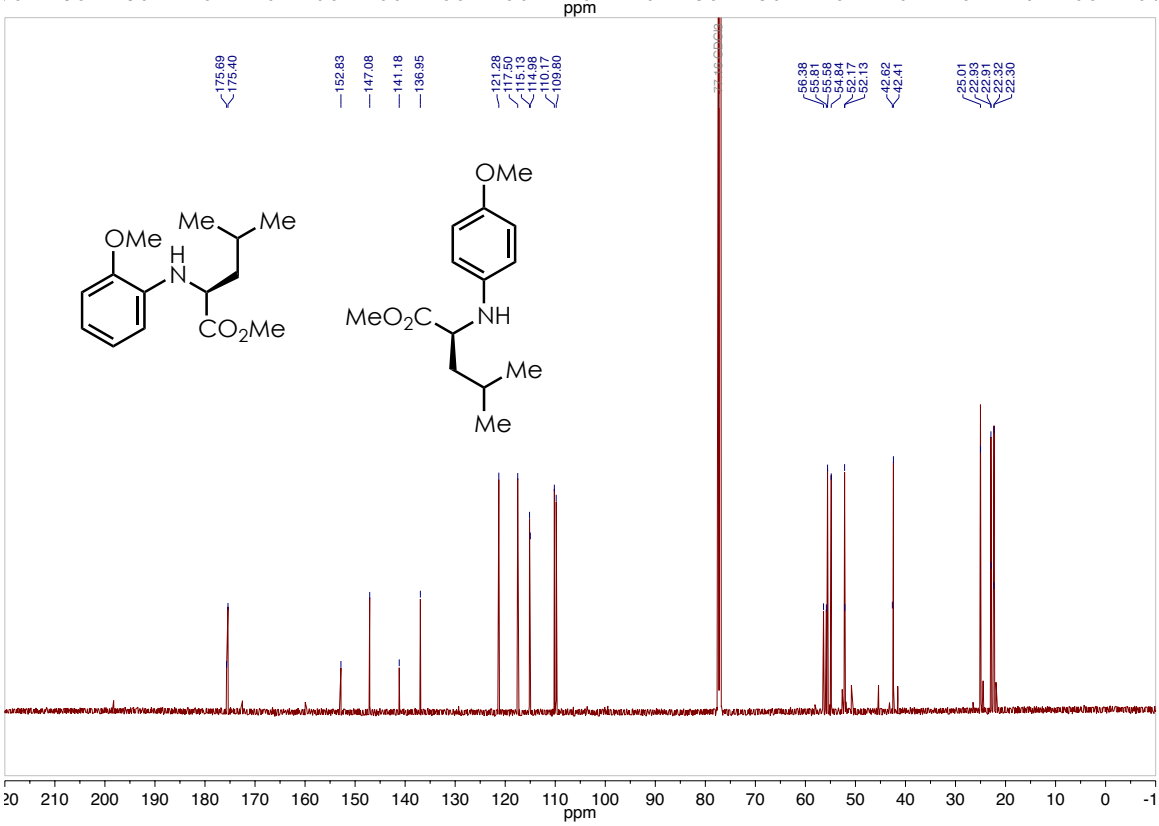
OMe
Me
Me
H
N
CO2Me
MeO2C
NH
Me
Me
ppm

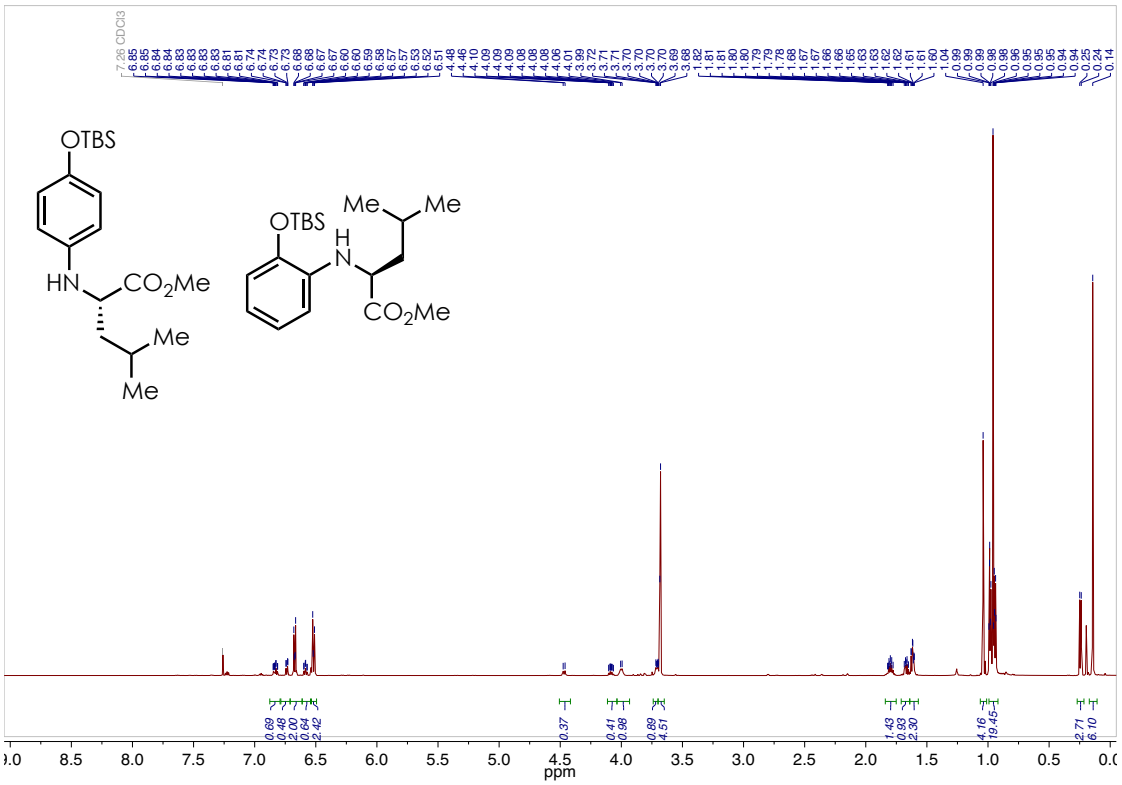
OTBS
HN
CO2Me
Me
Me
OTBS
Me
Me
H
N
CO2Me
ppm

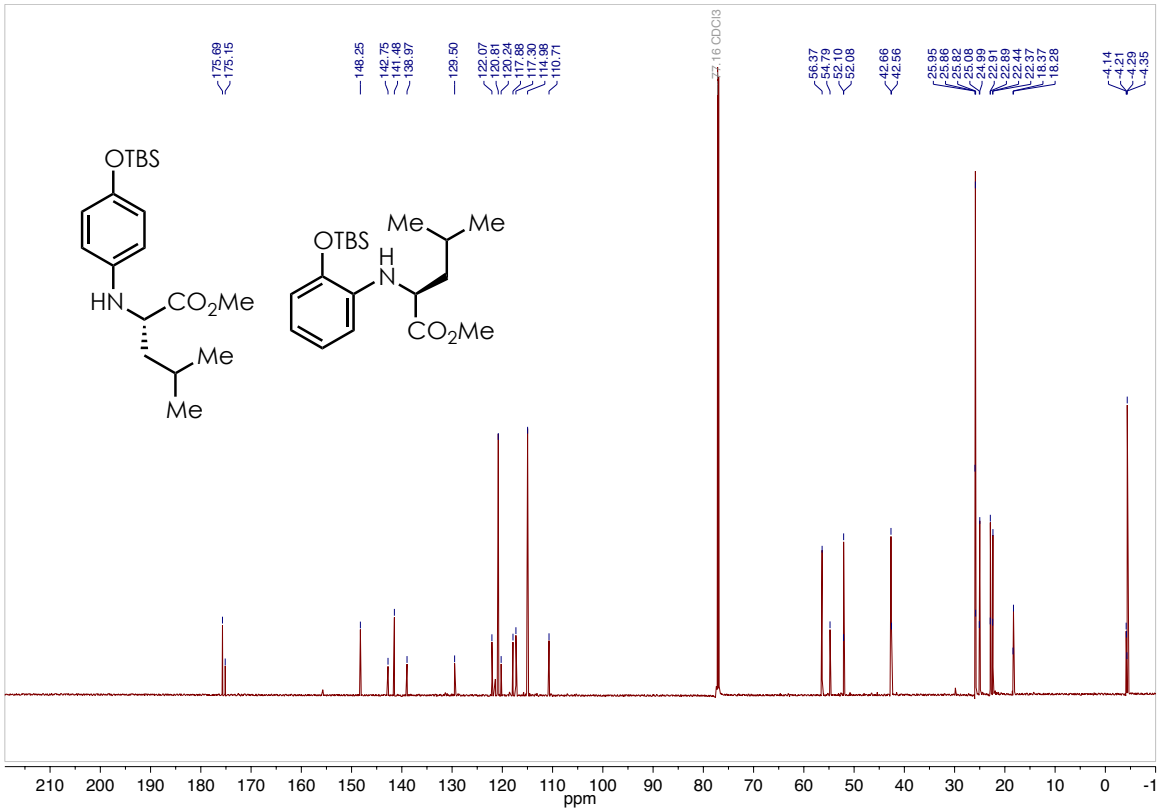
OTBS
HN
CO2Me
Me
Me
OTBS
Me
Me
H
N
CO2Me
ppm

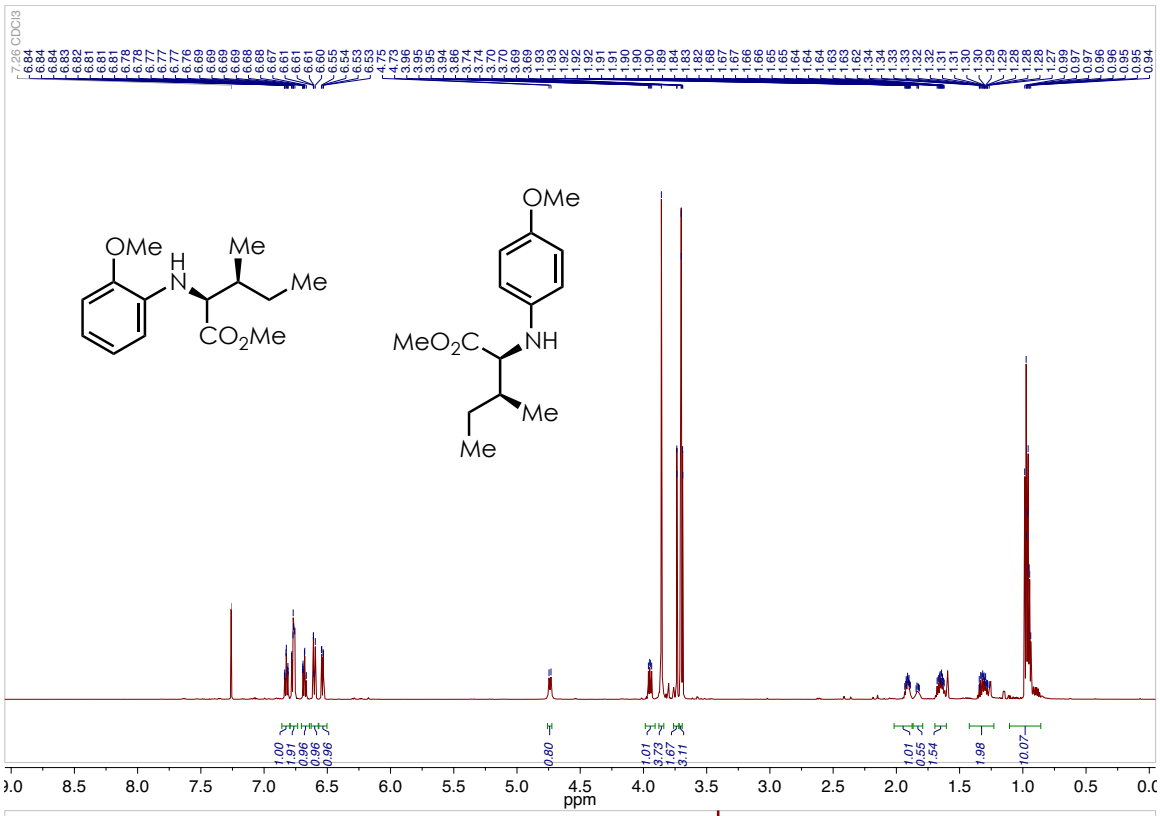
OMe
H
N
Me
Me
CO2Me
OMe
MeO2C
NH
Me
Me
ppm

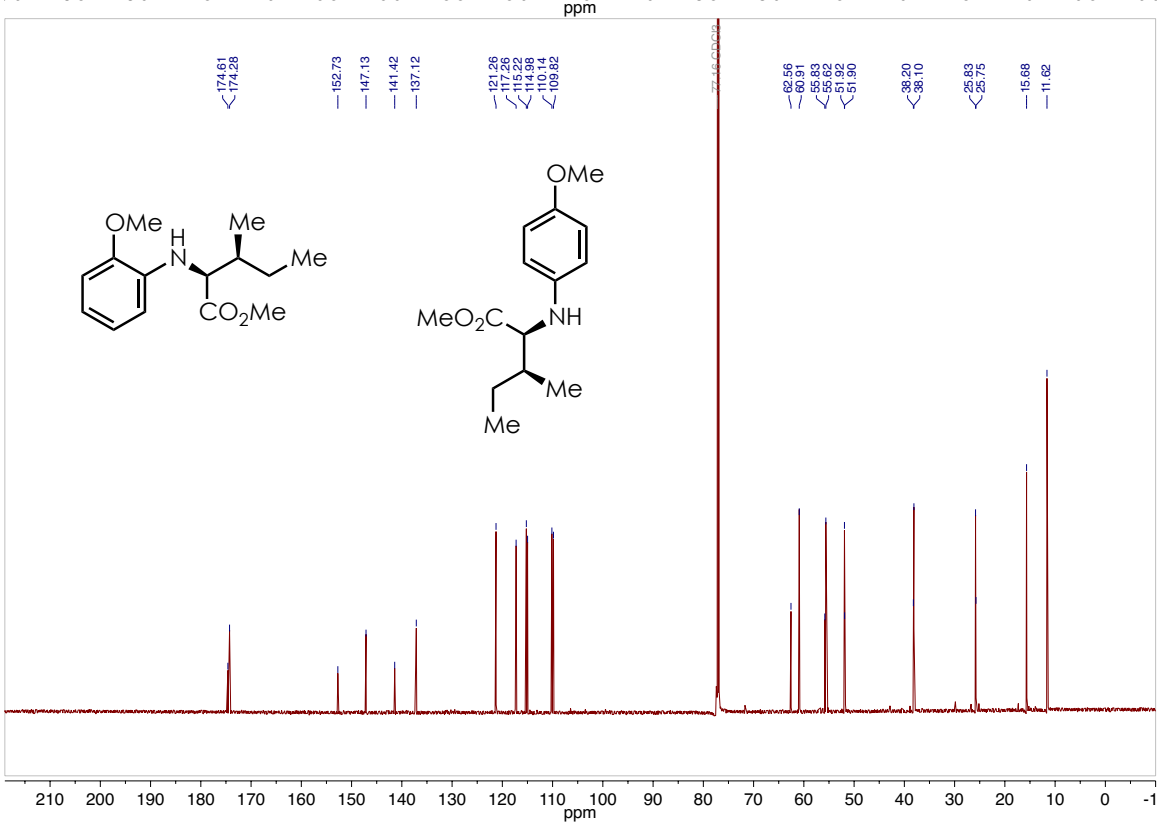
OMe
H
N
Me
Me
CO2Me
OMe
MeO2C
NH
Me
Me
ppm

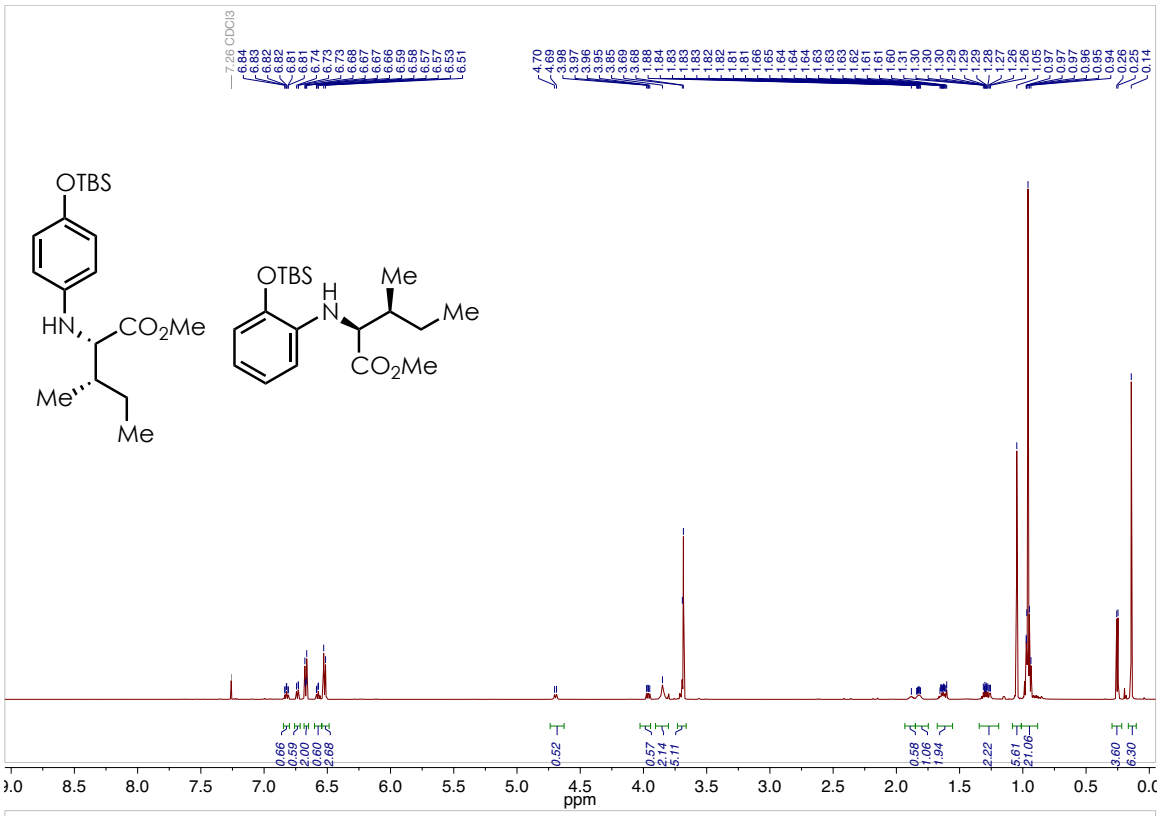
OTBS
HN
CO2Me
Me
Me
OTBS
H
N
Me
Me
CO2Me
ppm

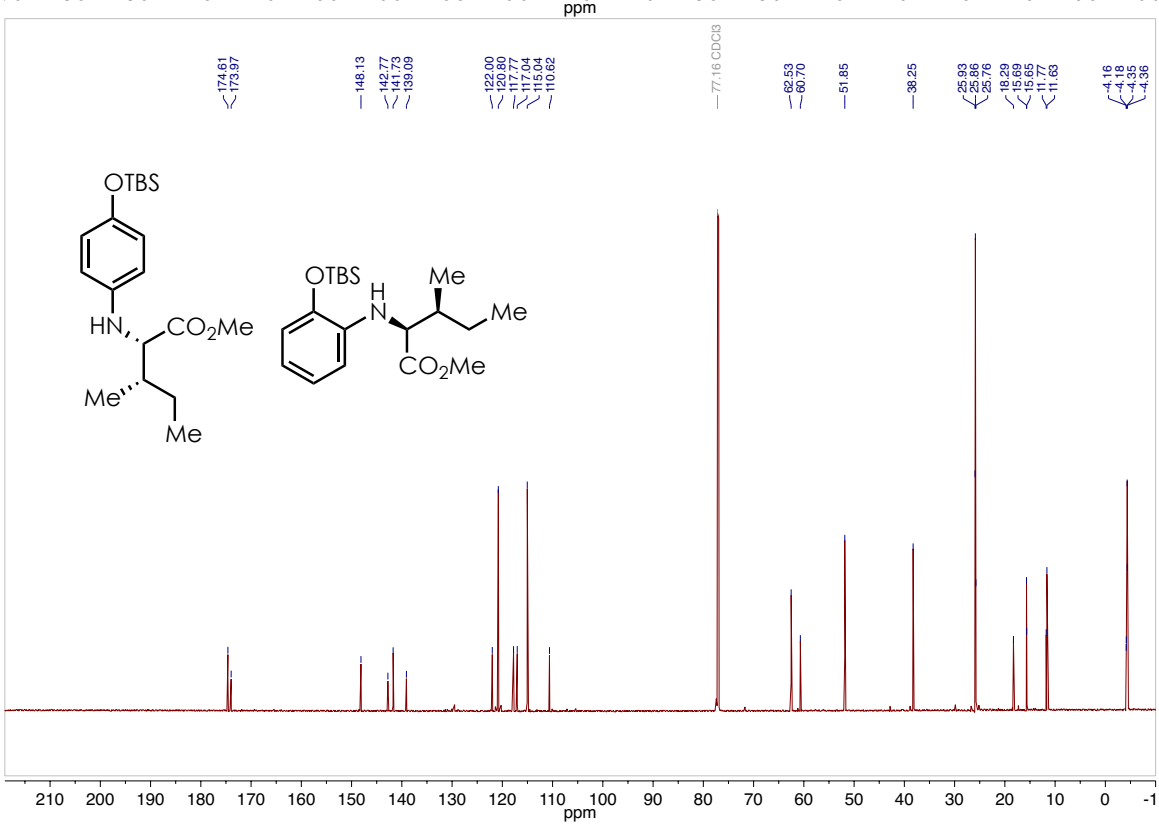
OTBS
HN
CO2Me
Me
Me
OTBS
H
N
Me
Me
CO2Me
ppm

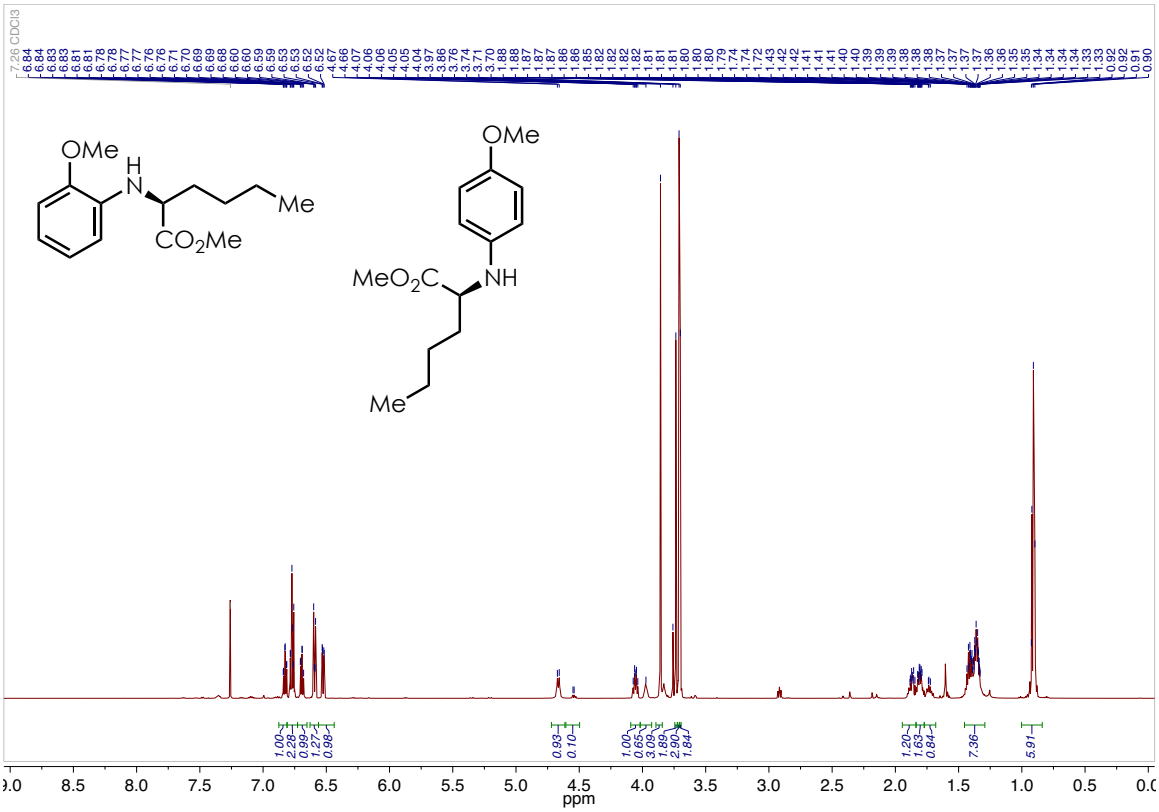
OMe
H
N
Me
CO2Me
OMe
MeO2C
NH
Me
ppm

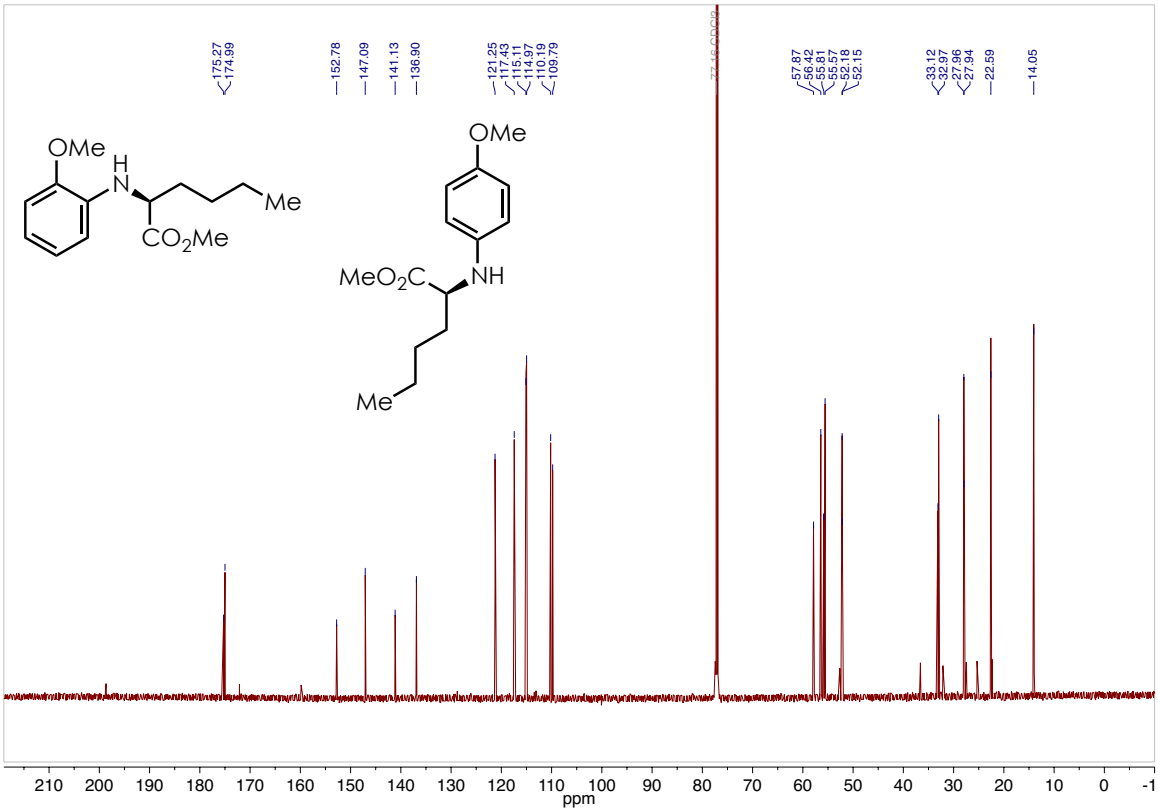
OMe
H
N
Me
CO2Me
OMe
MeO2C
NH
Me
ppm

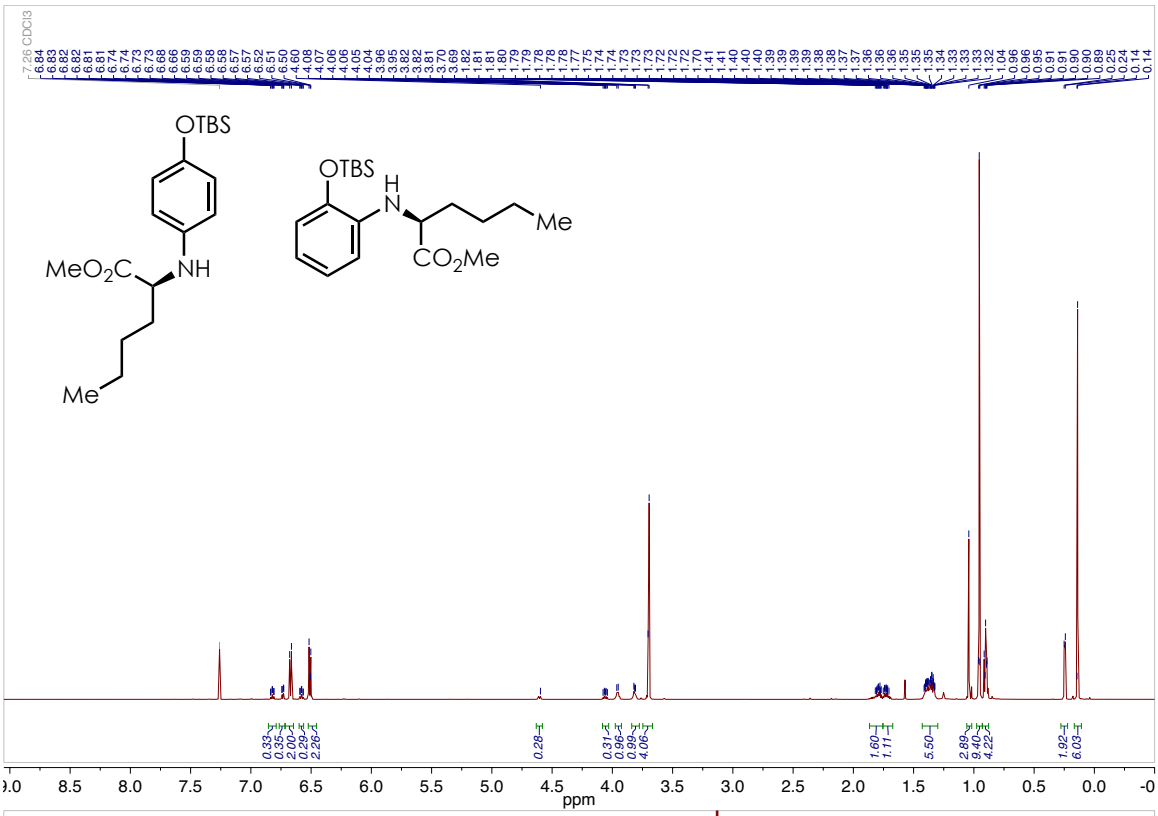
OTBS
MeO2C
NH
Me
OTBS
H
N
Me
CO2Me
ppm

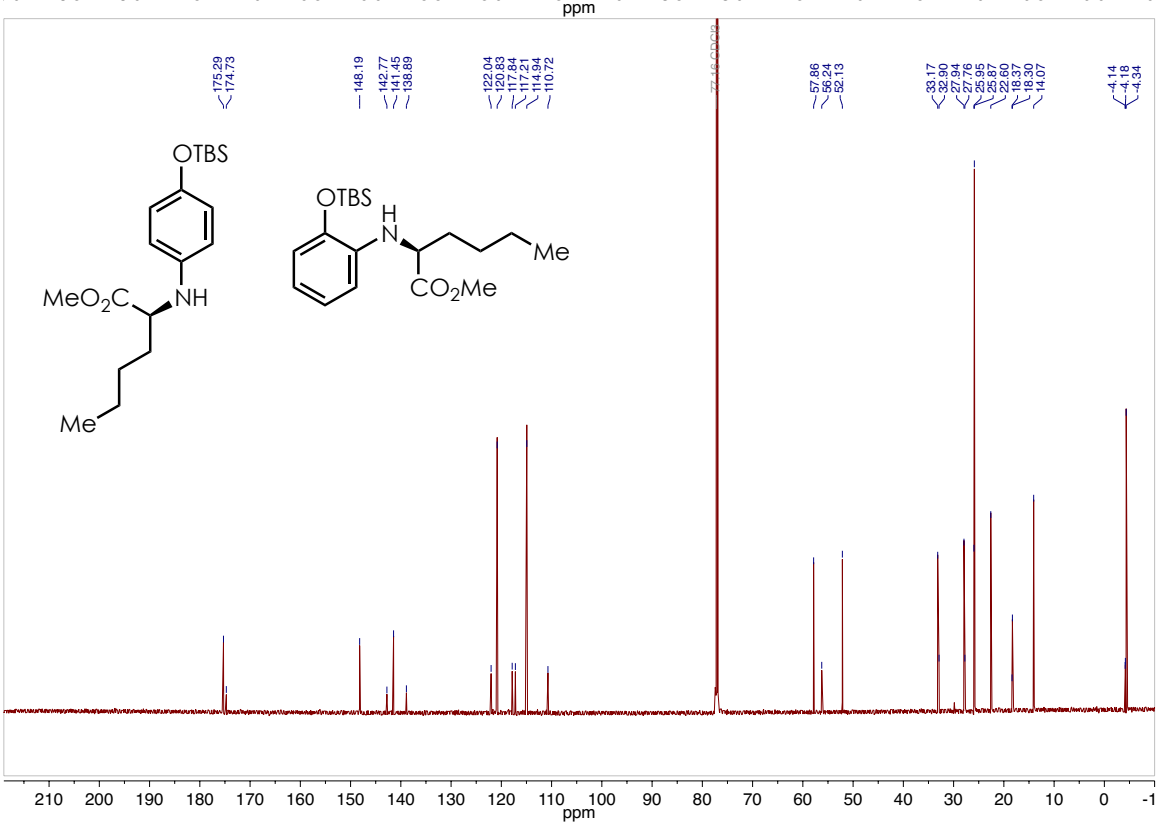
OTBS
MeO2C
NH
Me
OTBS
H
N
Me
CO2Me
ppm

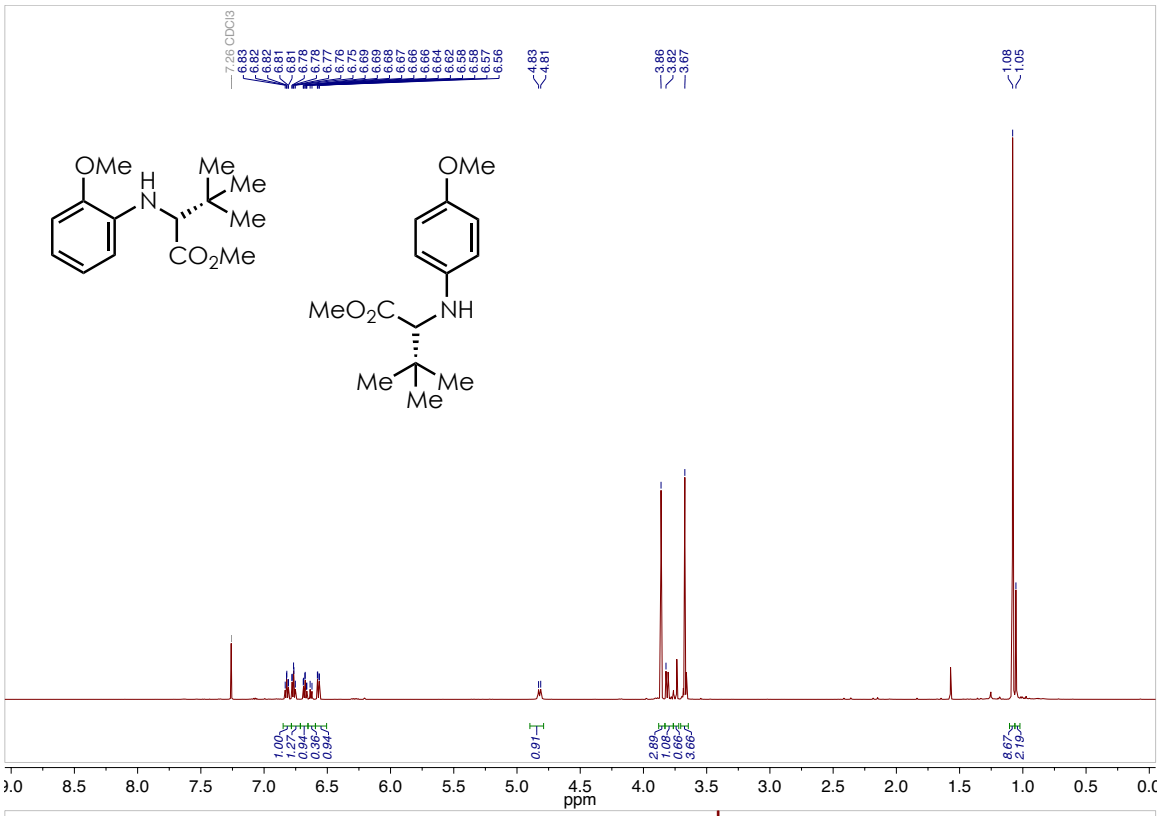
7.26 CDCl3
6.83
6.82
6.82
6.81
6.81
6.78
6.78
6.77
6.76
6.75
6.69
6.68
6.67
6.66
6.66
6.64
6.62
6.58
6.58
6.57
6.56
4.83
4.81
3.86
3.82
3.67
1.08
1.05
OMe
H
N
Me
Me
Me
CO2Me
OMe
MeO2C
NH
Me
Me
Me
1.00
1.27
0.94
0.36
0.94
0.91
2.89
1.08
0.66
3.66
8.67
2.19
ppm

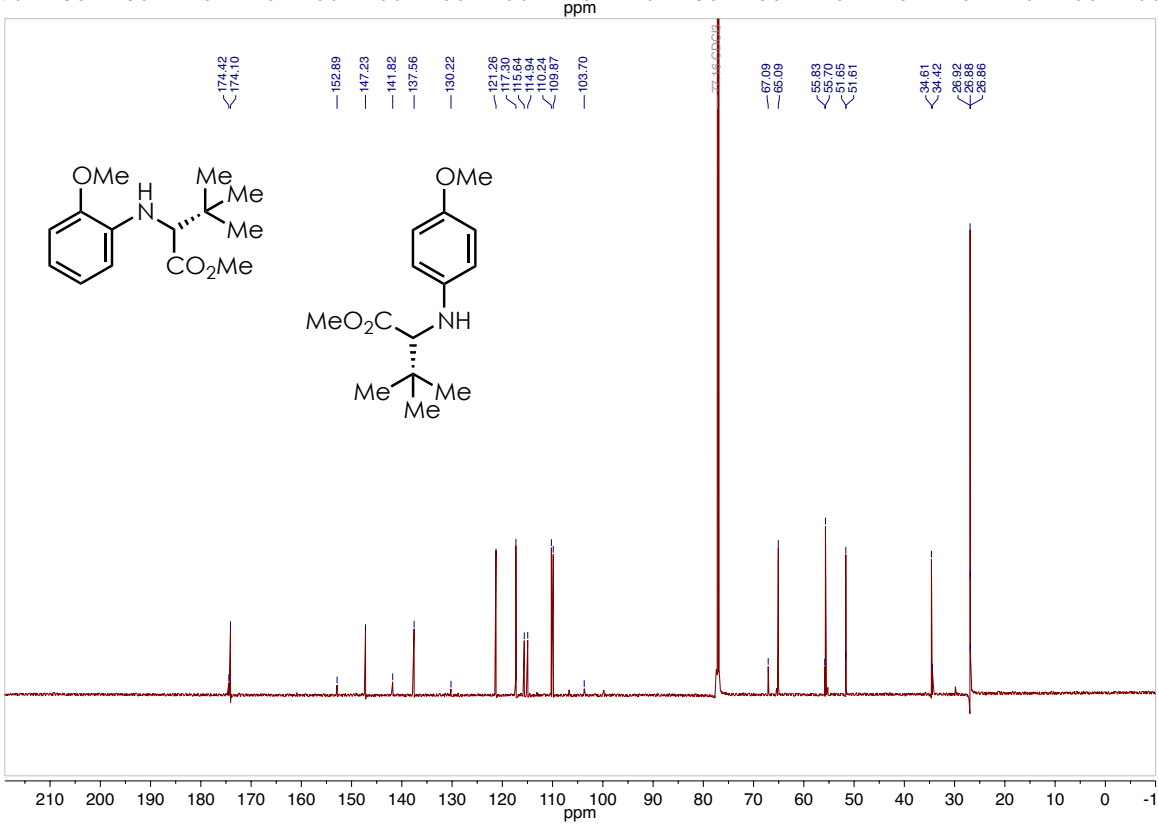
174.42
174.10
152.89
147.23
141.82
137.56
130.22
121.26
117.30
115.64
114.94
110.24
109.87
103.70
77.16 CDCl3
67.09
65.09
55.83
55.70
51.65
51.61
34.61
34.42
26.92
26.88
26.86
OMe
H
N
Me
Me
Me
CO2Me
OMe
MeO2C
NH
Me
Me
Me
ppm

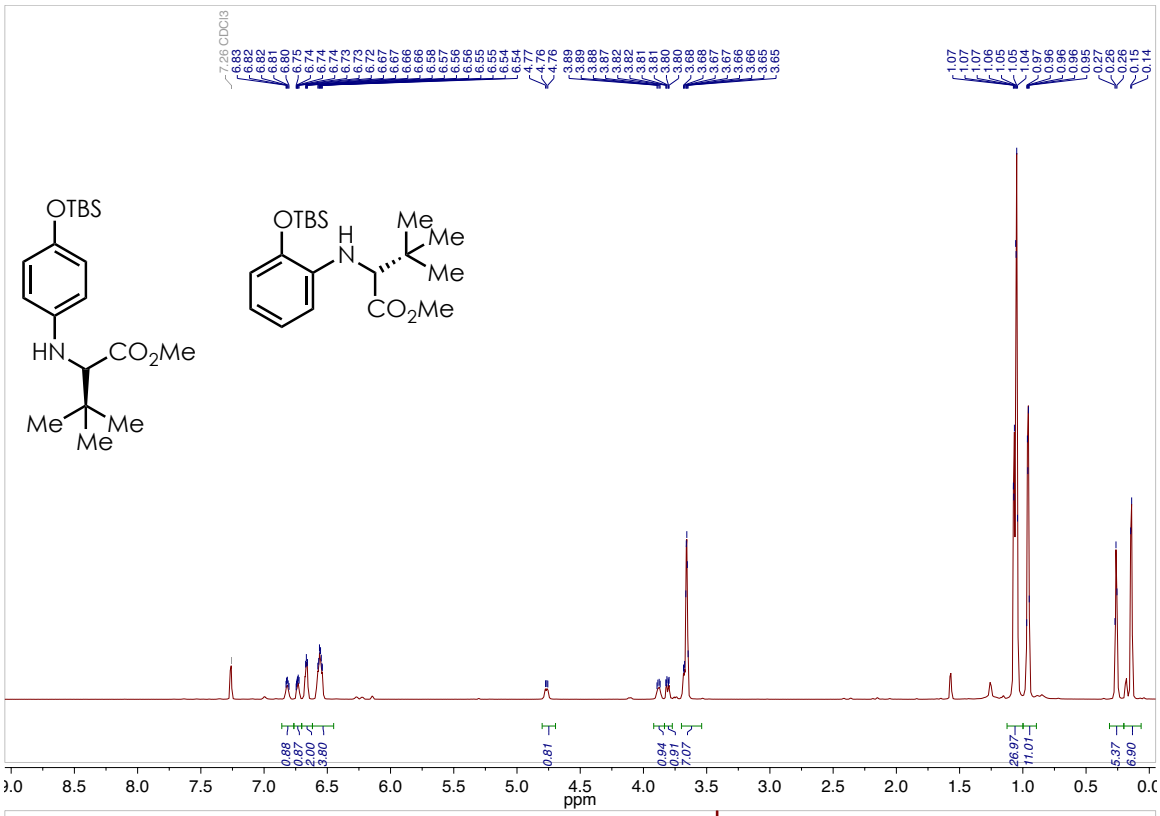
OTBS
HN
CO2Me
Me
Me
Me
OTBS
H
N
Me
Me
Me
CO2Me
ppm

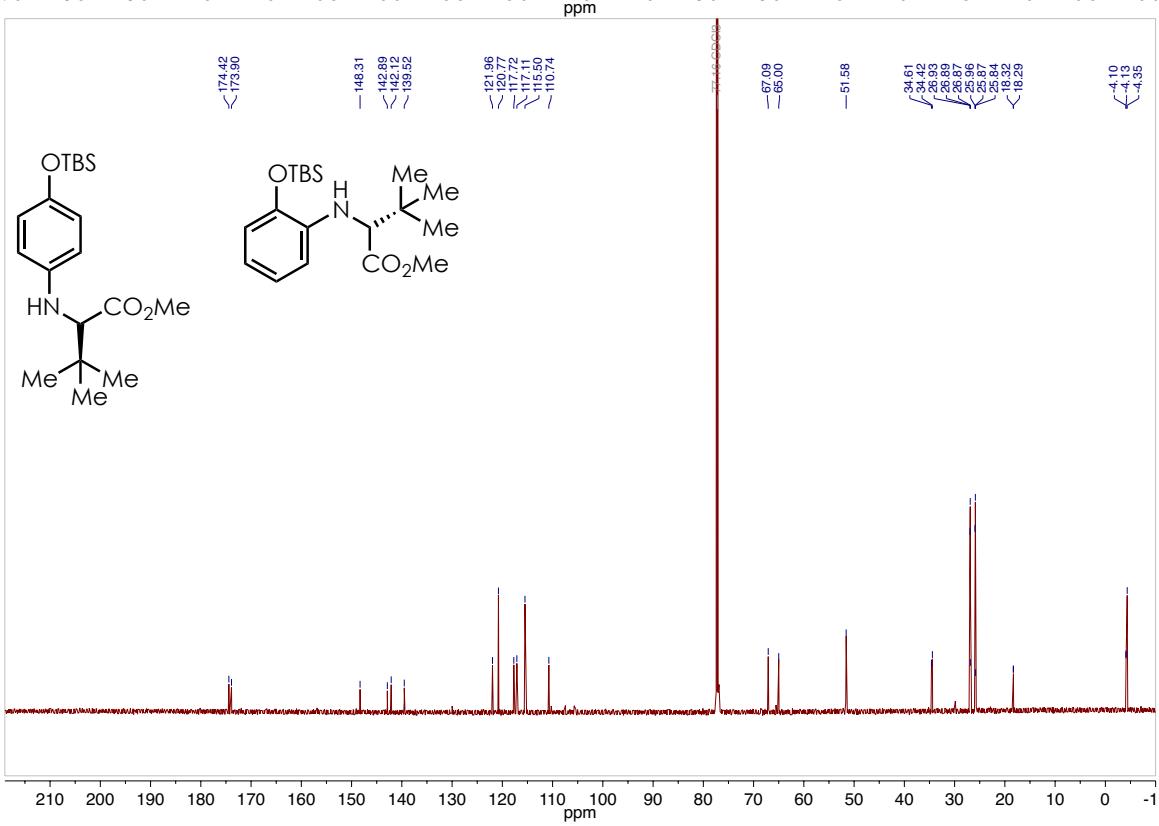
OTBS
HN
CO2Me
Me
Me
Me
OTBS
H
N
Me
Me
Me
CO2Me
ppm

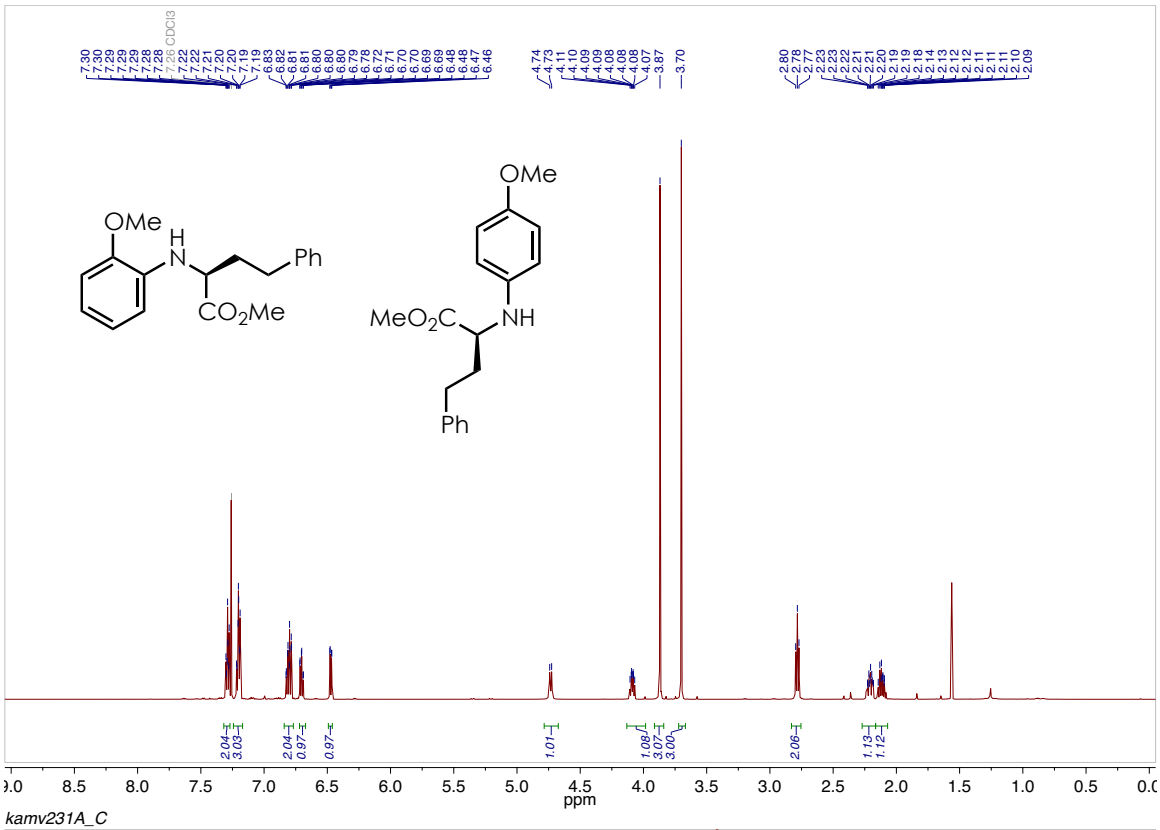
OMe
H
N
Ph
CO2Me
OMe
MeO2C
NH
Ph
ppm

kamv231A_C

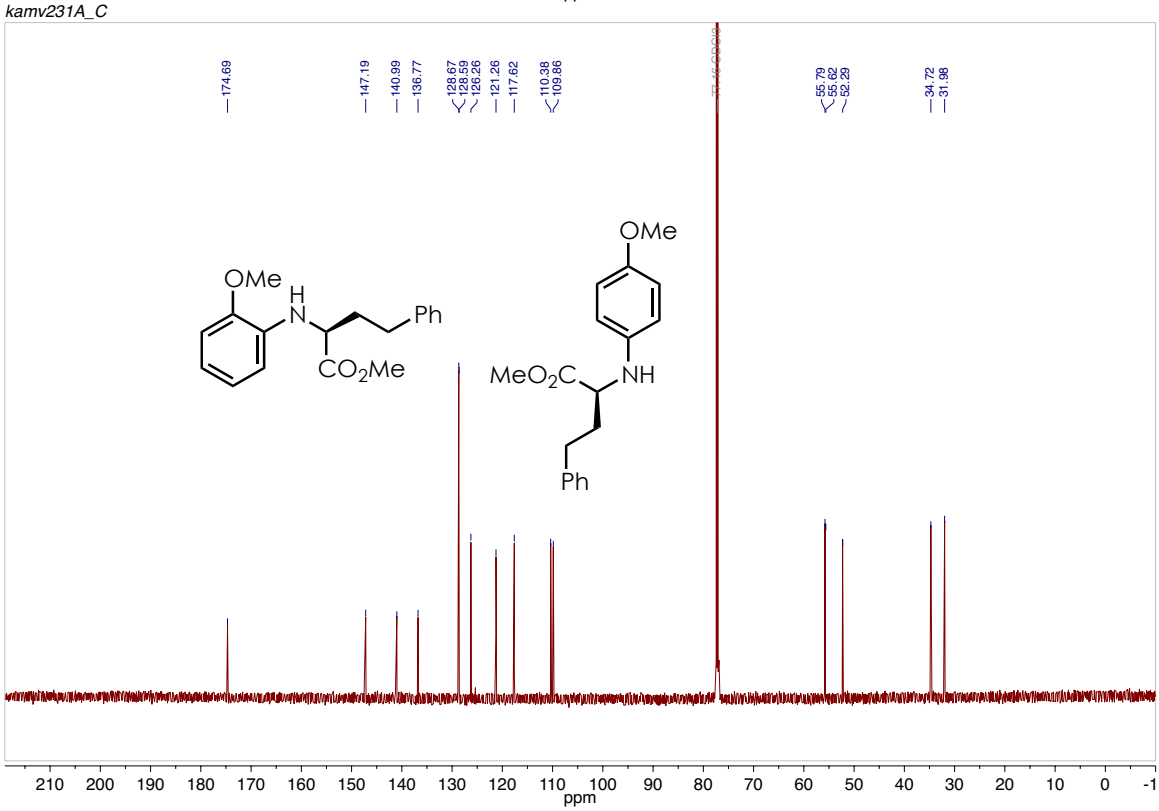
OMe
H
N
Ph
CO2Me
OMe
MeO2C
NH
Ph
ppm

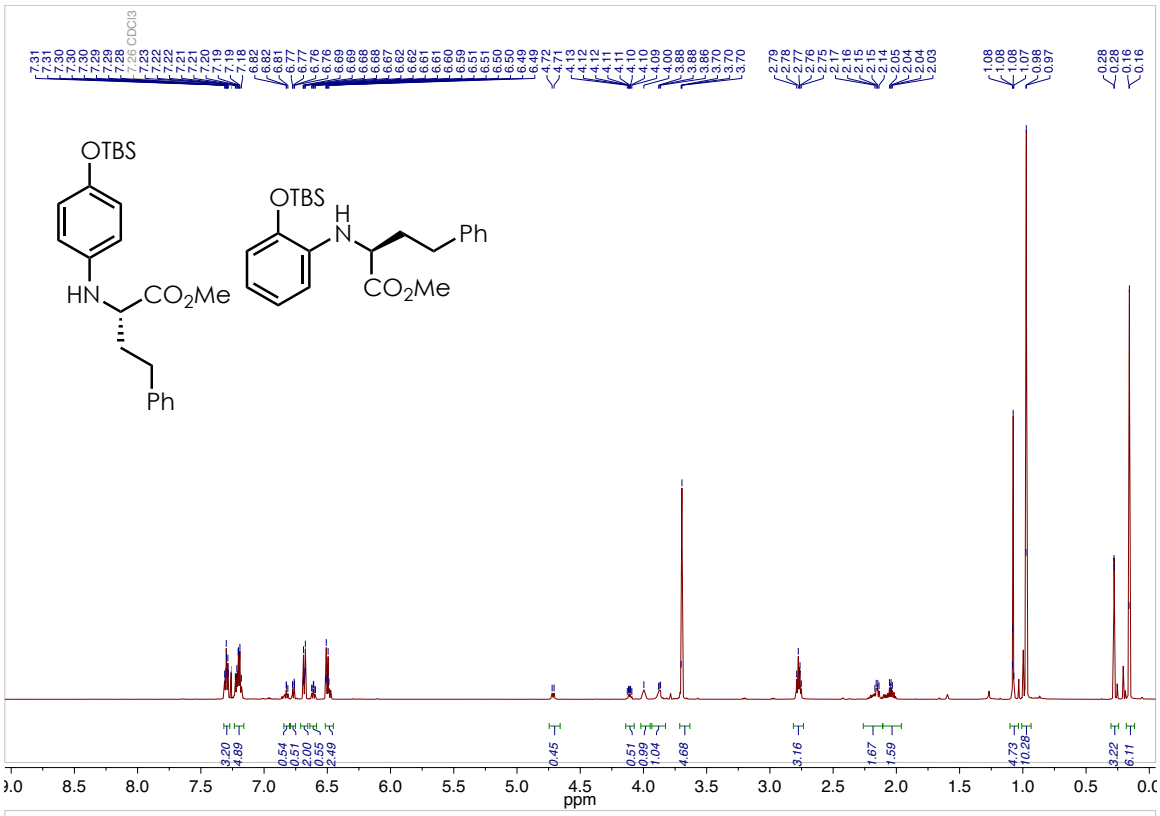
OTBS
HN
CO2Me
Ph
OTBS
H
N
Ph
CO2Me
ppm

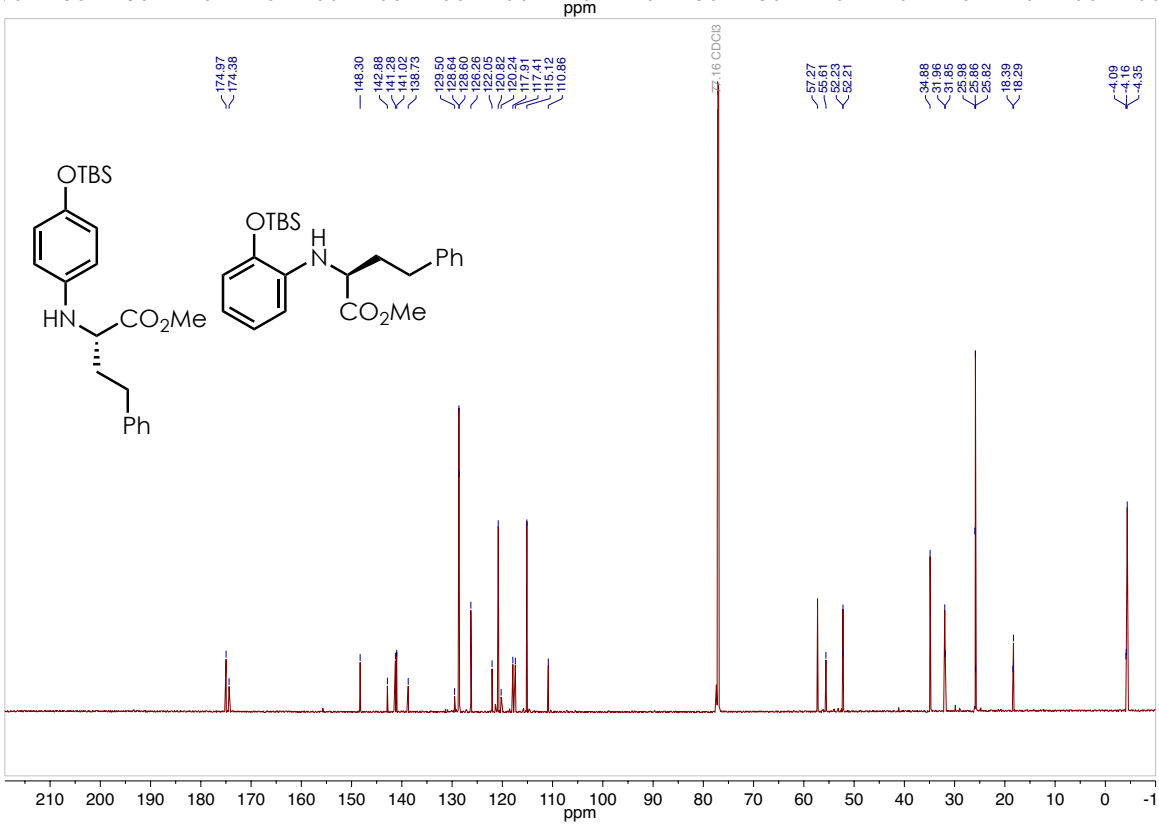
OTBS
HN
CO2Me
Ph
OTBS
H
N
Ph
CO2Me
ppm

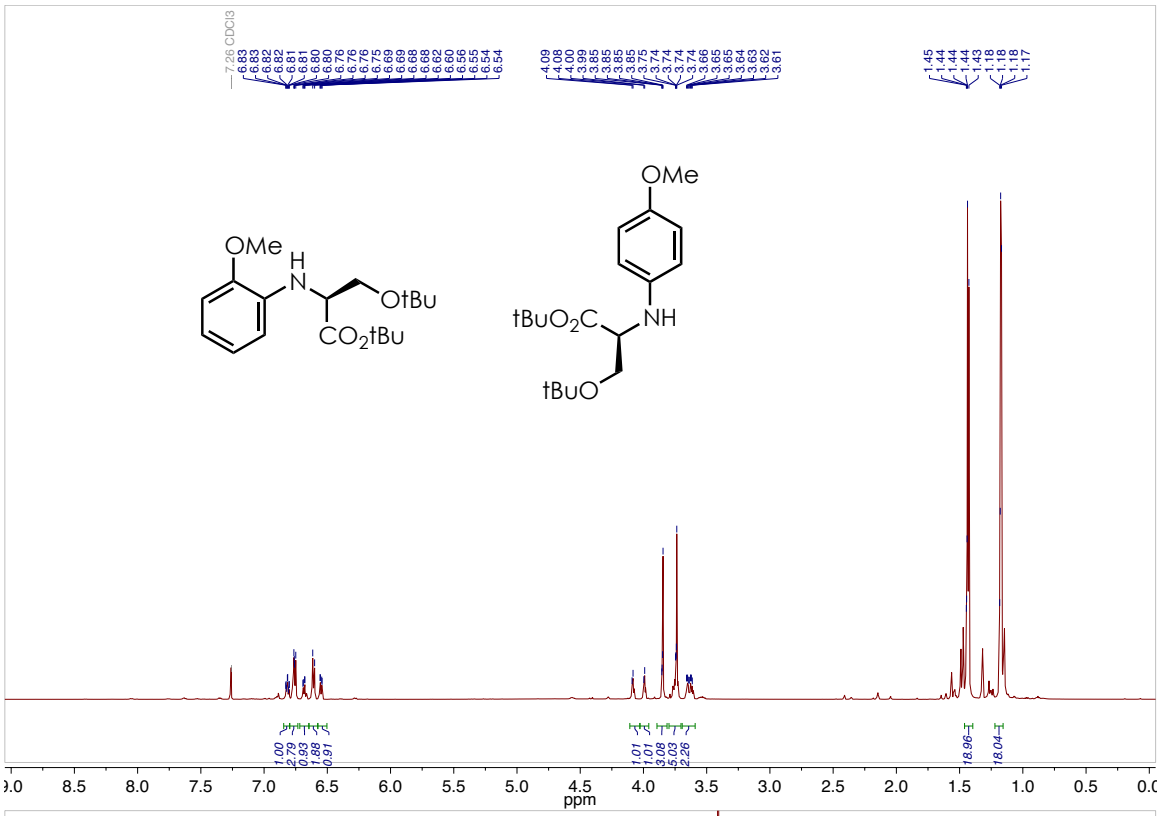
OMe
H
N
OtBu
CO2tBu
OMe
tBuO2C
NH
tBuO
ppm

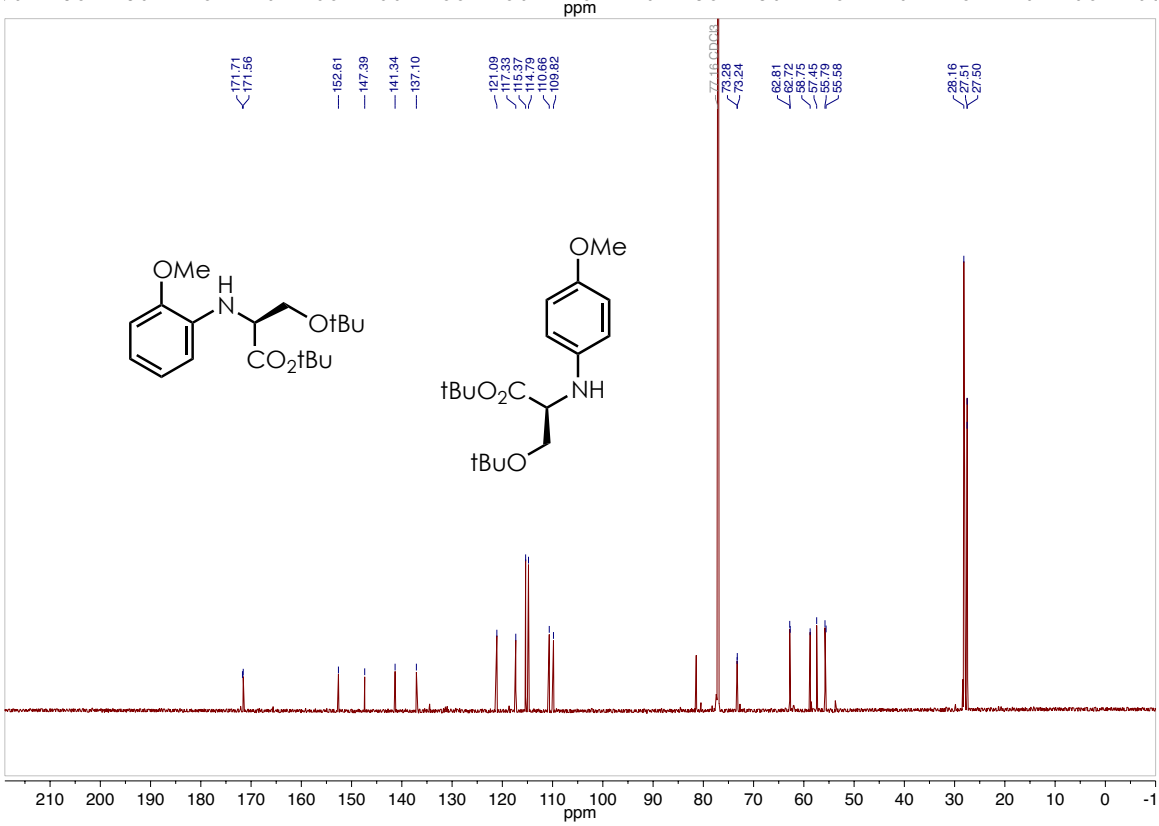
OMe
H
N
OtBu
CO2tBu
OMe
tBuO2C
NH
tBuO
ppm

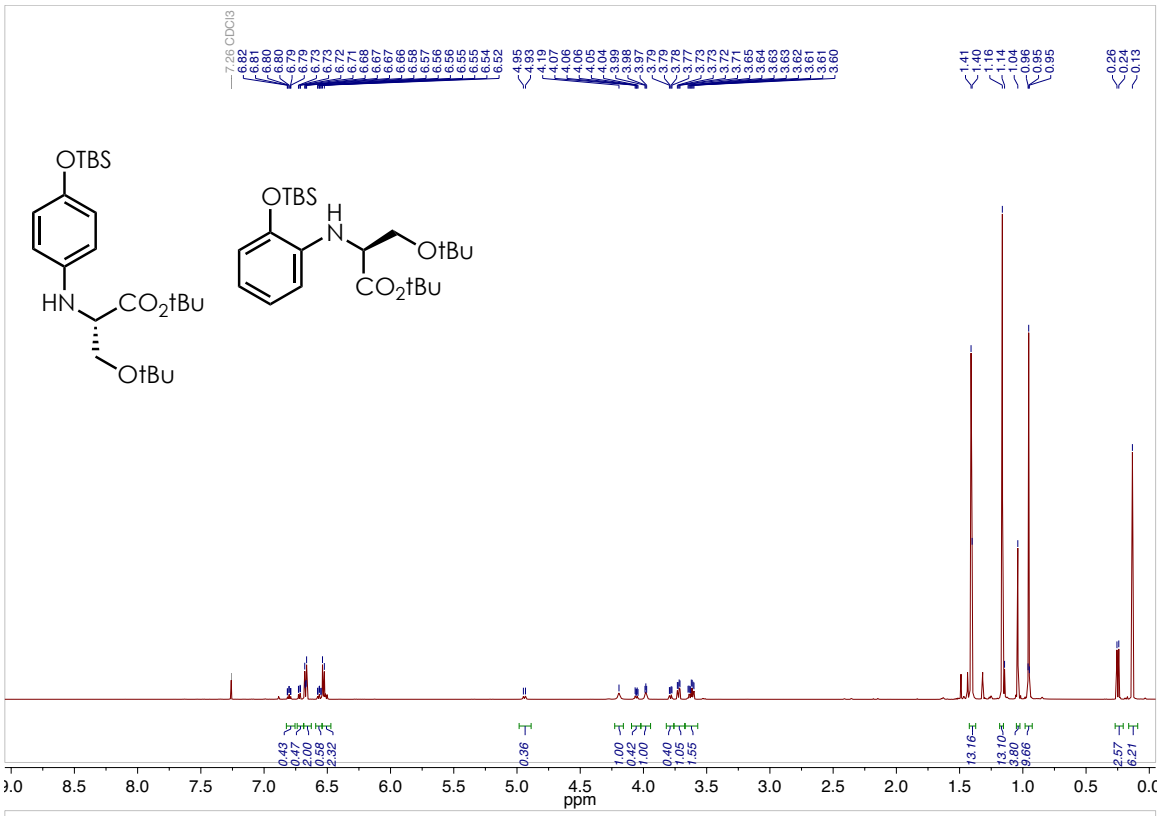
OTBS
HN
CO2tBu
OtBu
OTBS
H
N
OtBu
CO2tBu
ppm

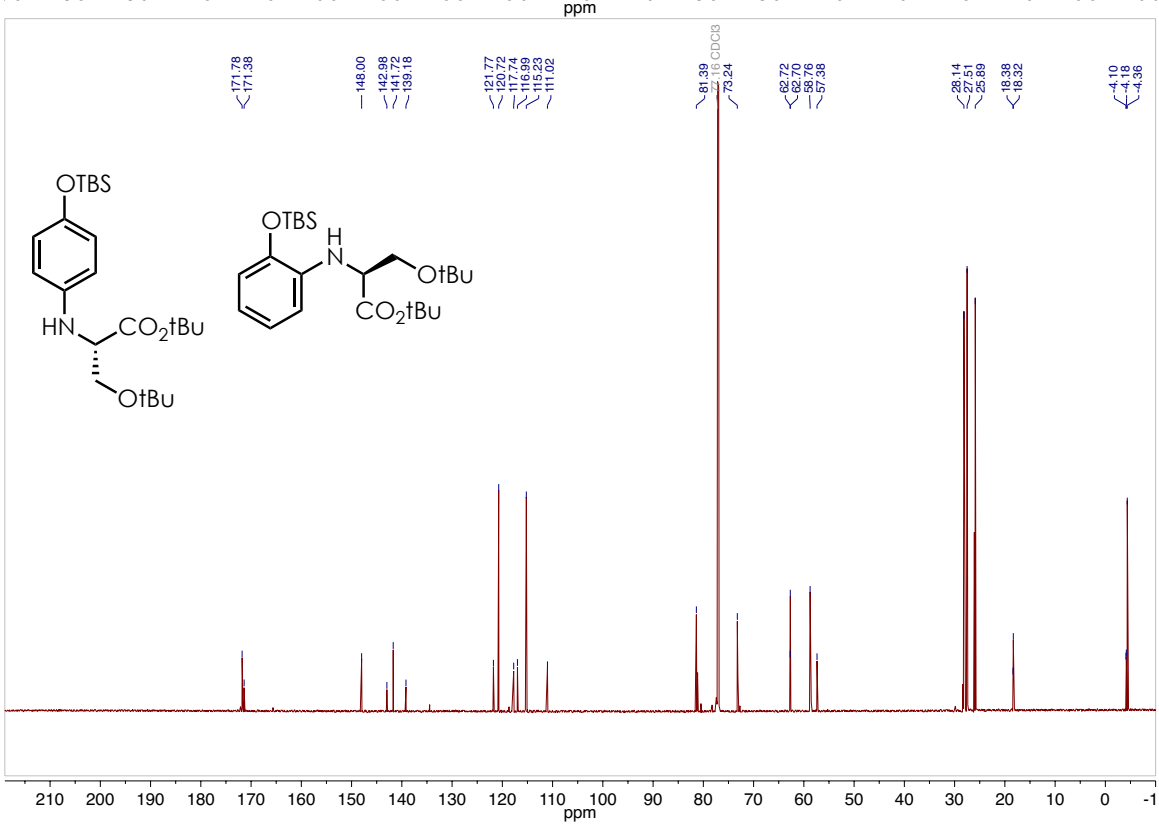
OTBS
HN
CO2tBu
OtBu
OTBS
H
N
OtBu
CO2tBu
ppm

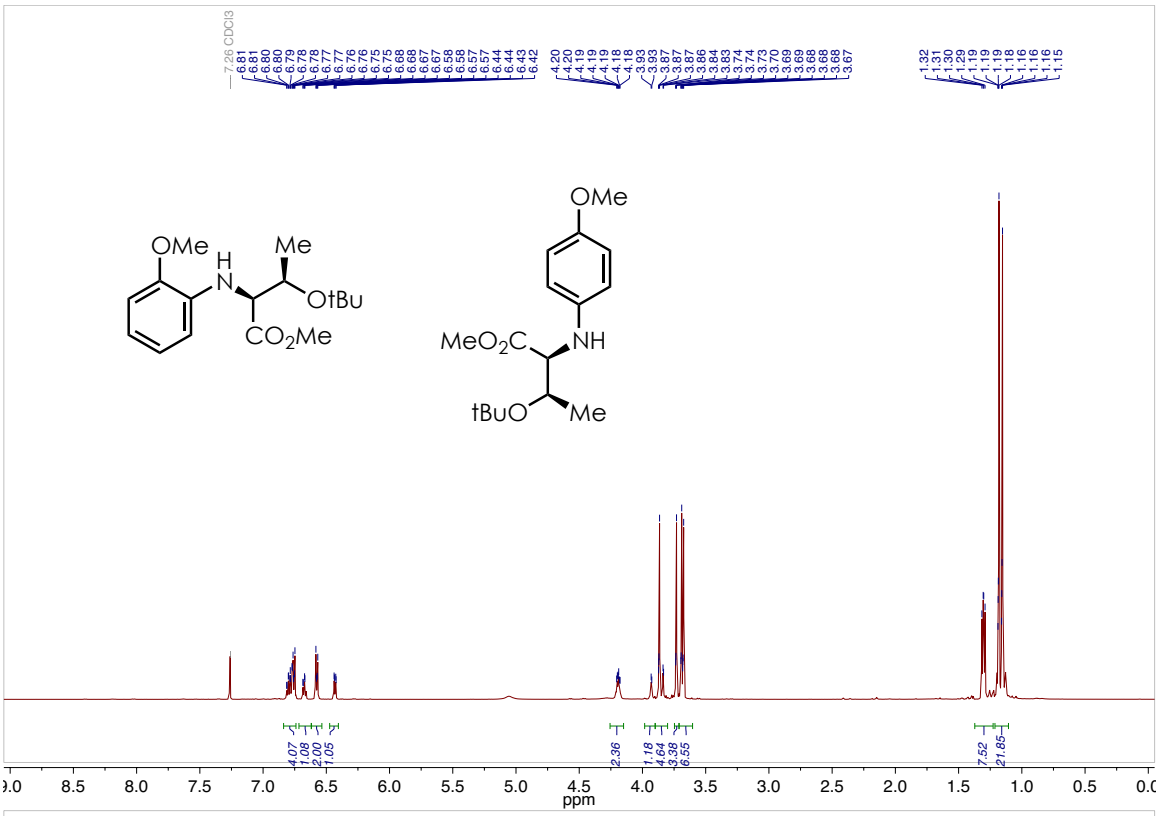
OMe
H
N
Me
OtBu
CO2Me
MeO2C
NH
tBuO
Me
ppm

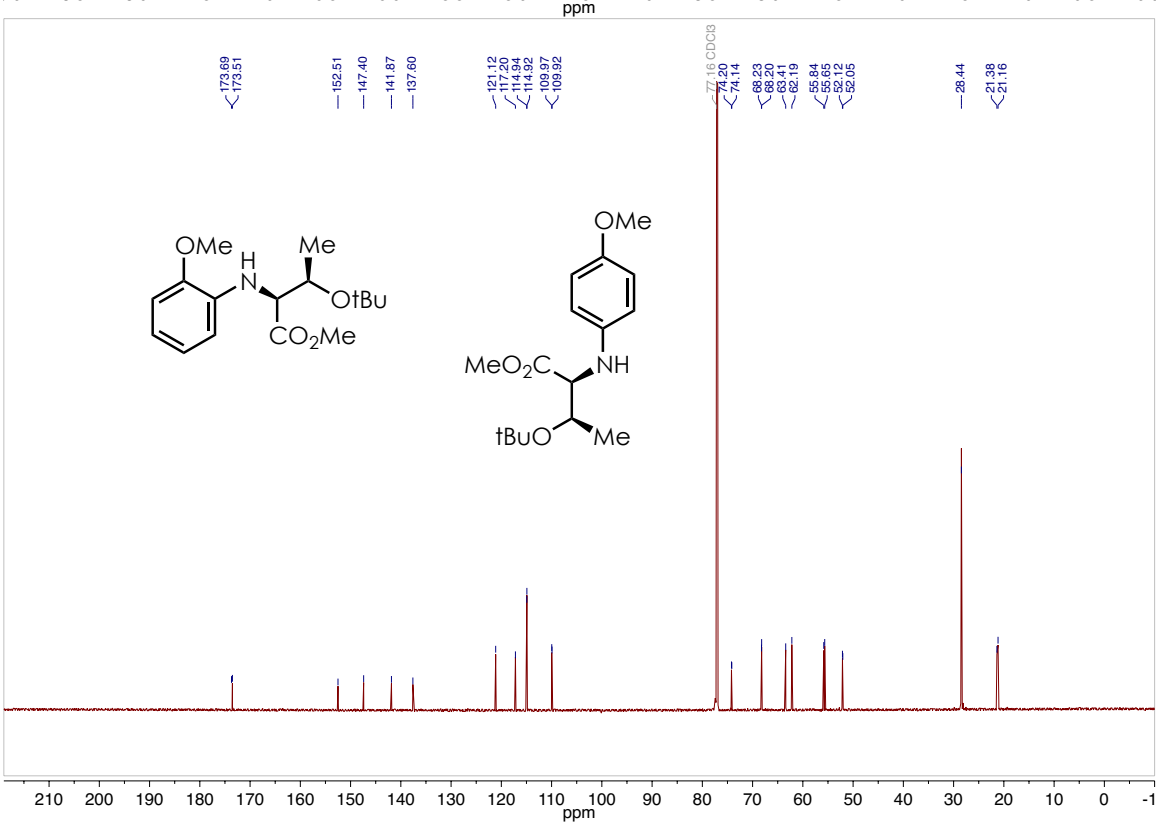
OMe
H
N
Me
OtBu
CO2Me
MeO2C
NH
tBuO
Me
ppm

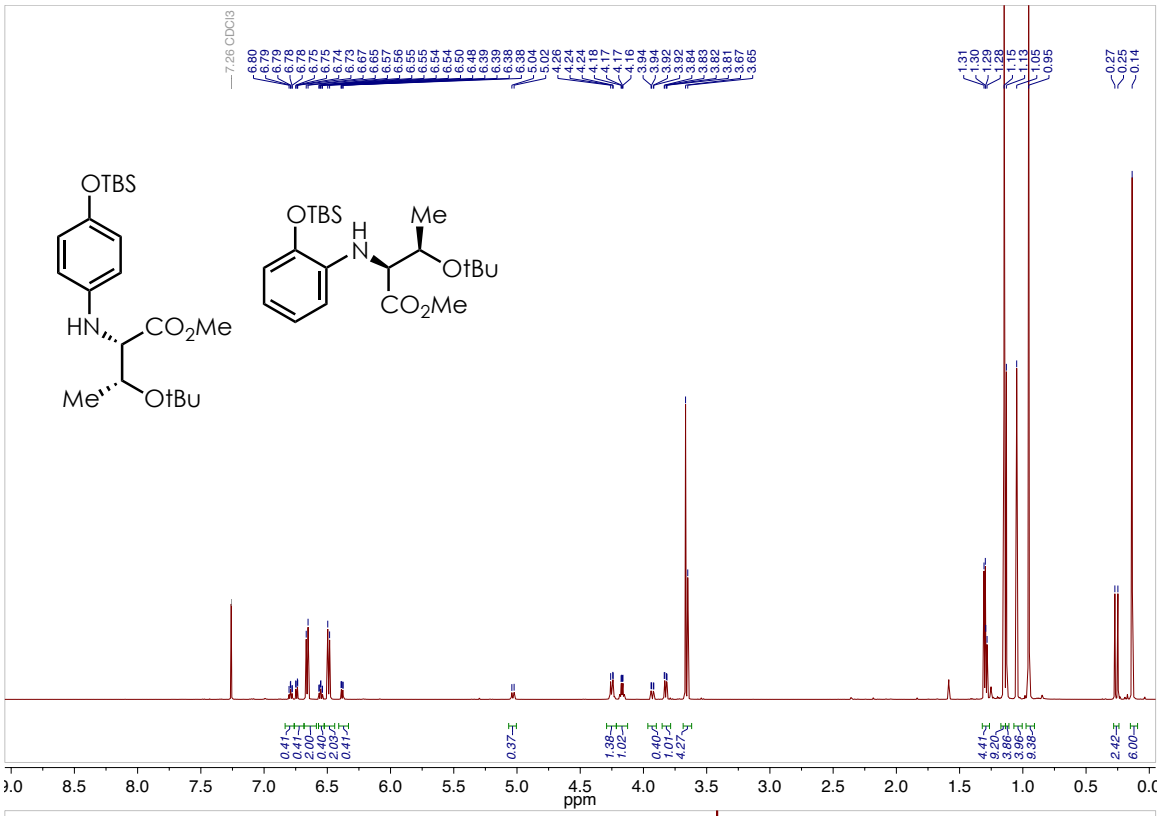
OTBS
HN
CO2Me
Me
OtBu
OTBS
H
N
Me
OtBu
CO2Me
ppm

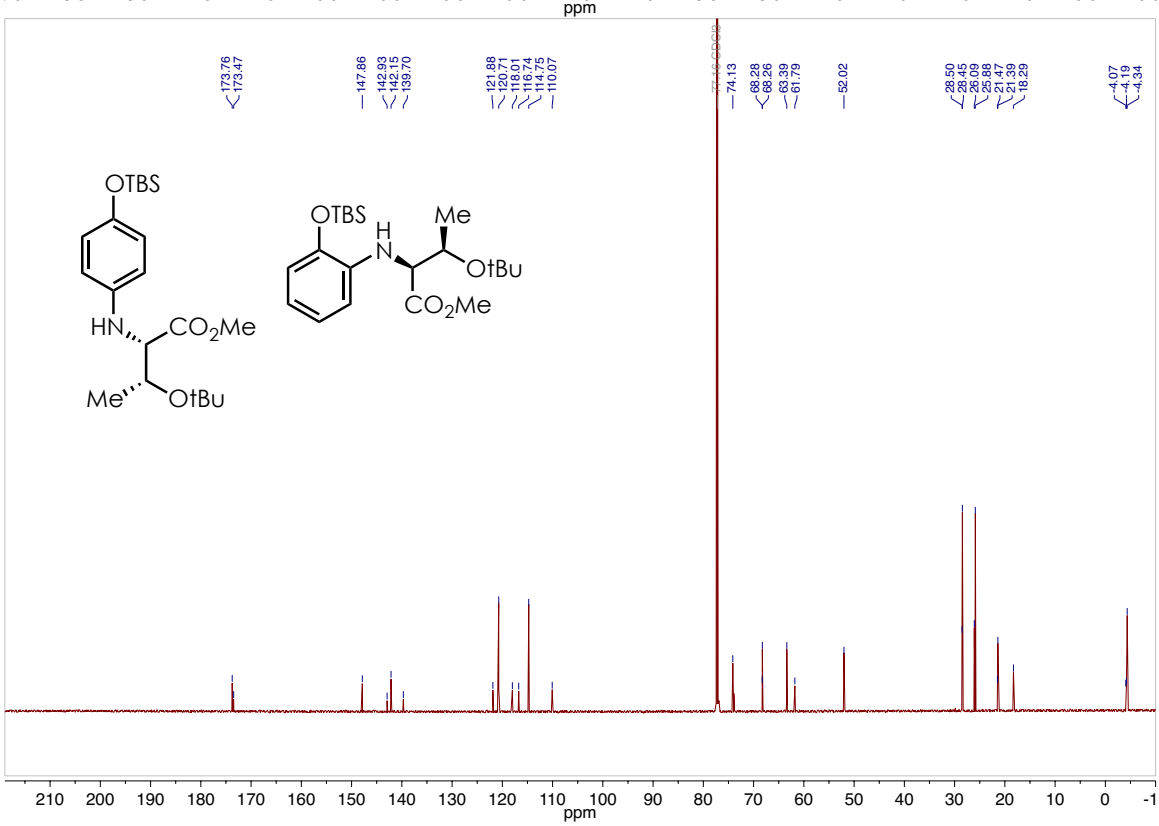
OTBS
HN
CO2Me
Me
OtBu
OTBS
H
N
Me
OtBu
CO2Me
ppm

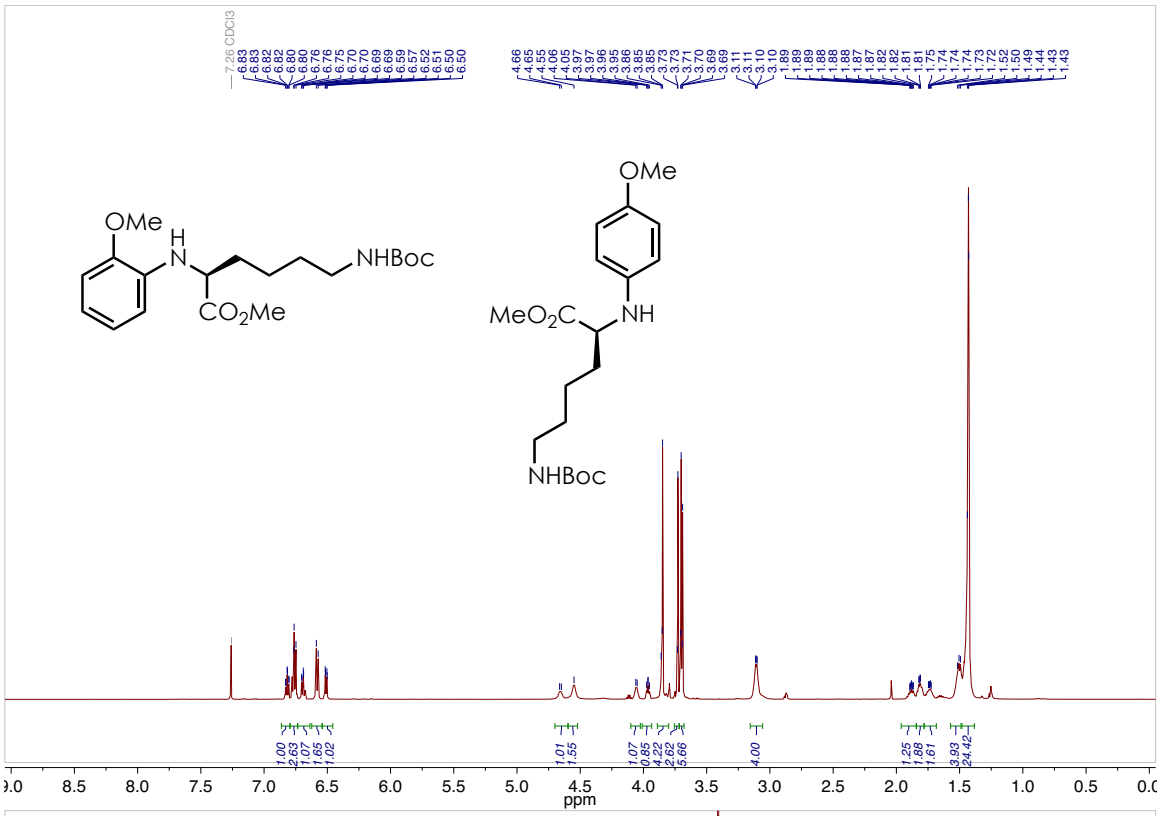
OMe
H
N
NHBoc
CO2Me
MeO2C
NH
NHBoc
ppm

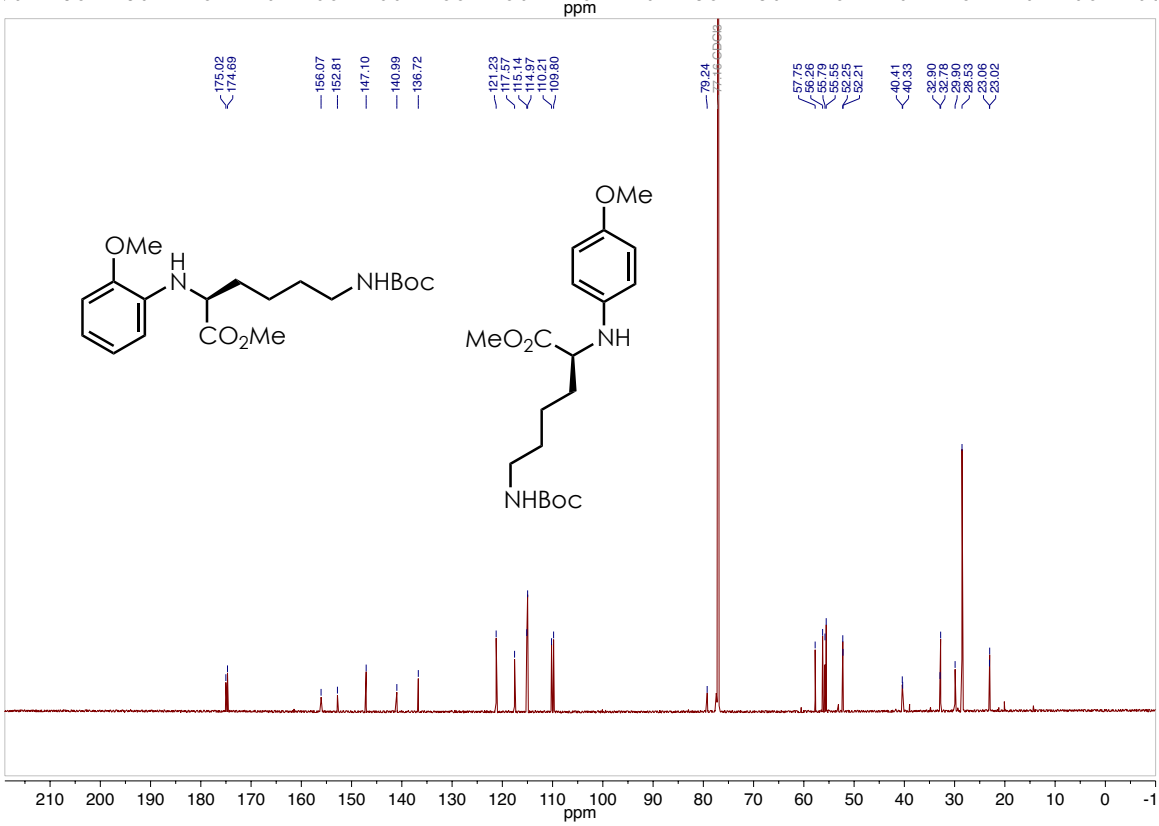
OMe
H
N
NHBoc
CO2Me
MeO2C
NH
NHBoc
ppm

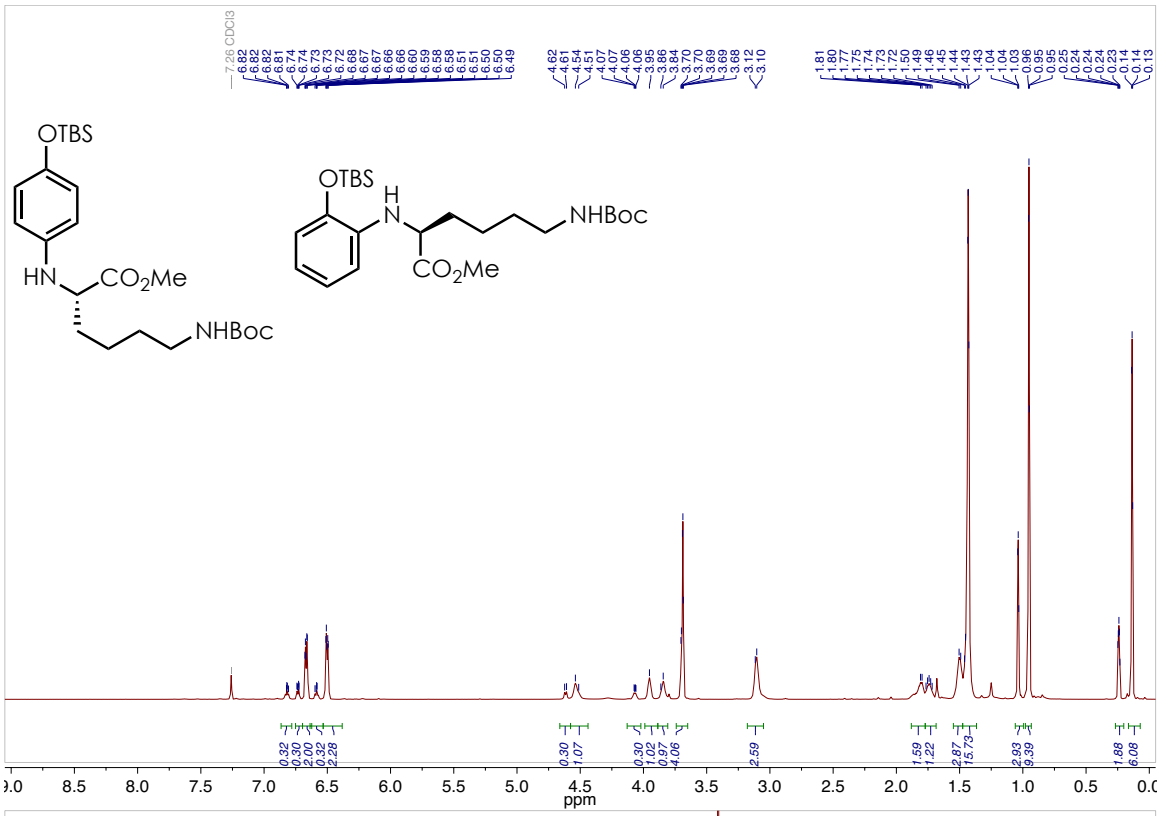
OTBS
HN
CO2Me
NHBoc
OTBS
H
N
NHBoc
CO2Me
ppm

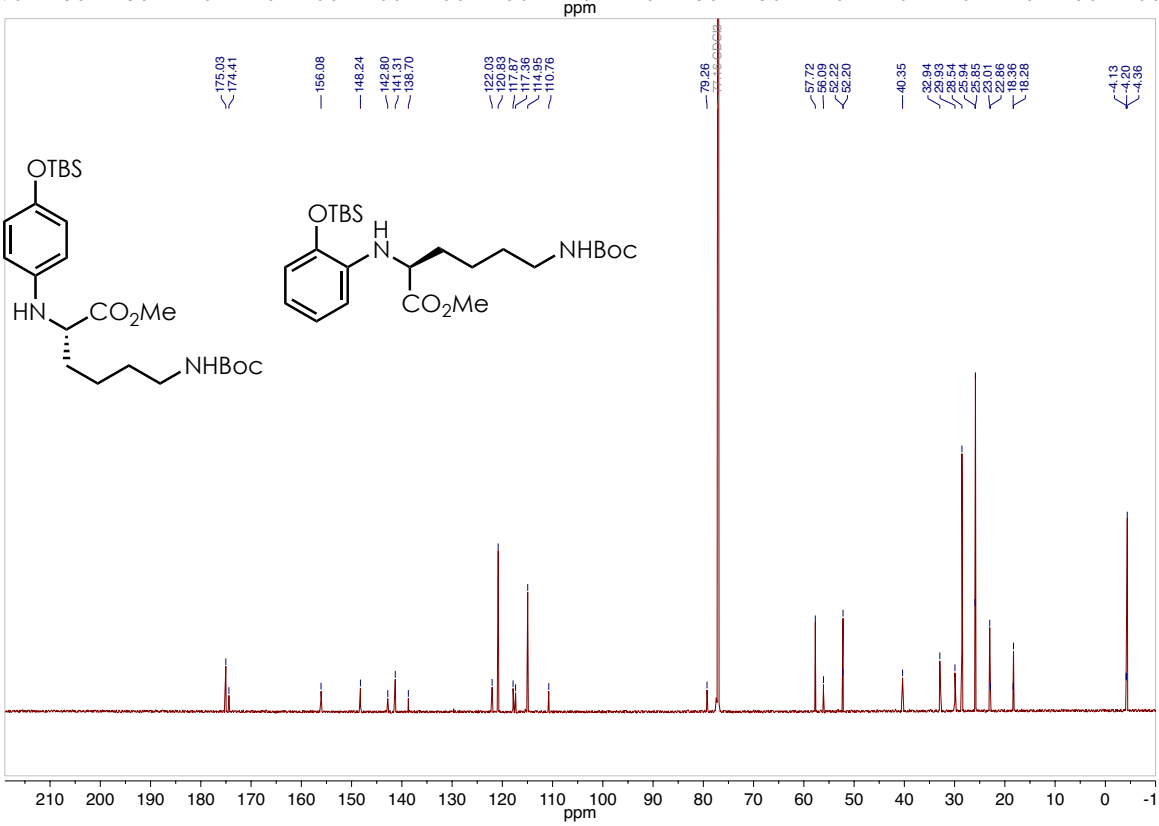
OTBS
HN
CO2Me
NHBoc
OTBS
H
N
NHBoc
CO2Me
ppm

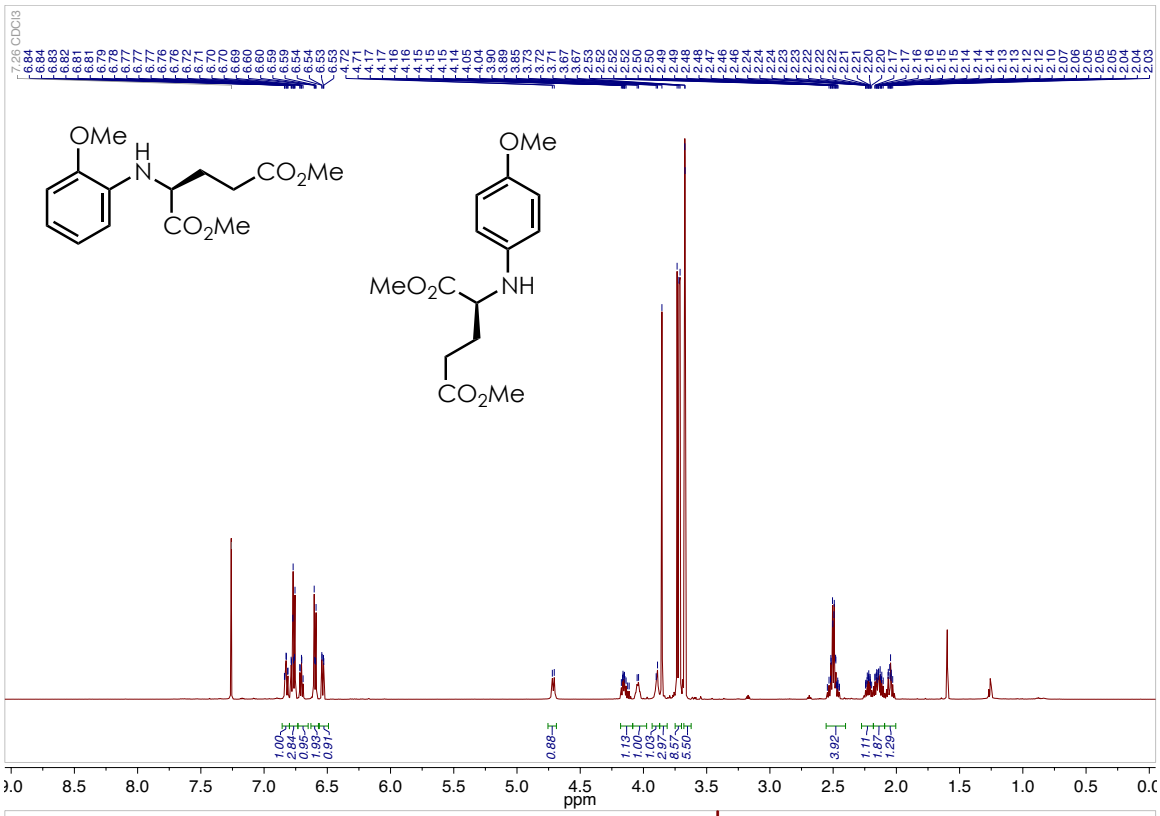
OMe
H
N
CO2Me
CO2Me
OMe
MeO2C
NH
CO2Me
ppm

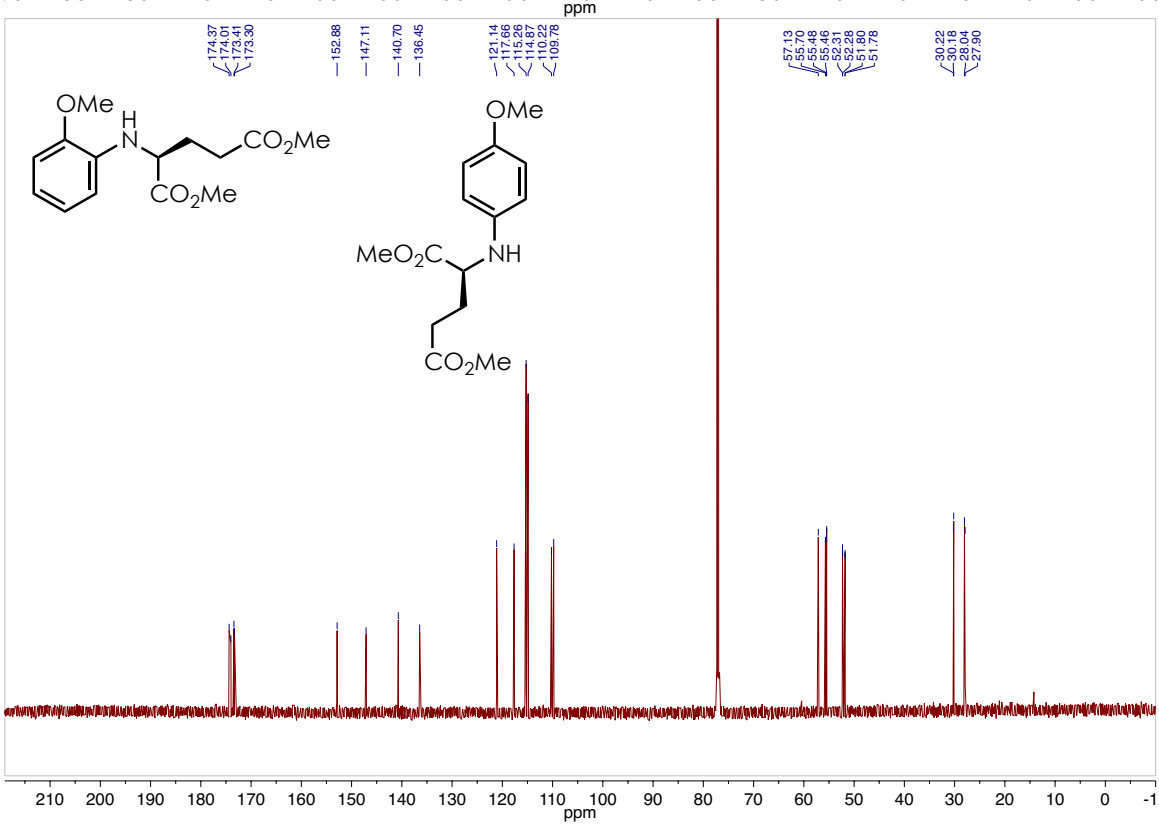
OMe
H
N
CO2Me
CO2Me
OMe
MeO2C
NH
CO2Me
ppm

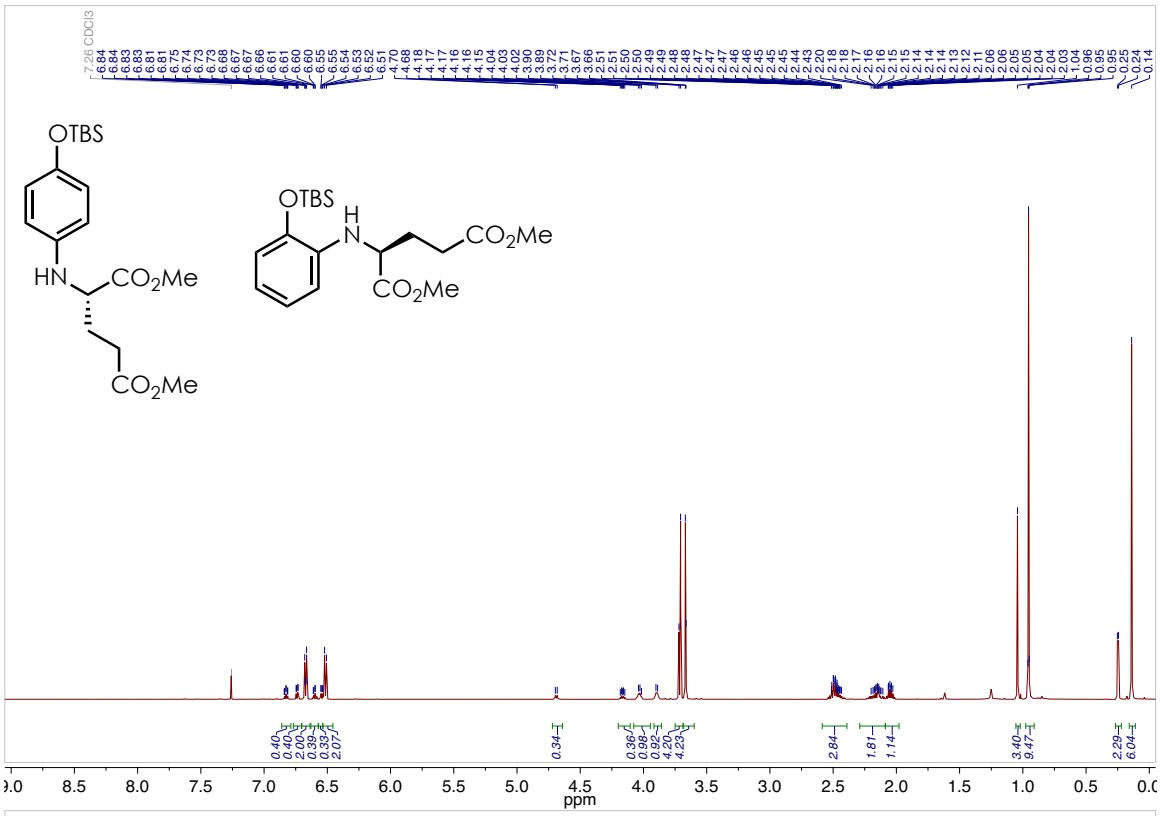
OTBS
HN
CO2Me
CO2Me
OTBS
H
N
CO2Me
CO2Me
ppm

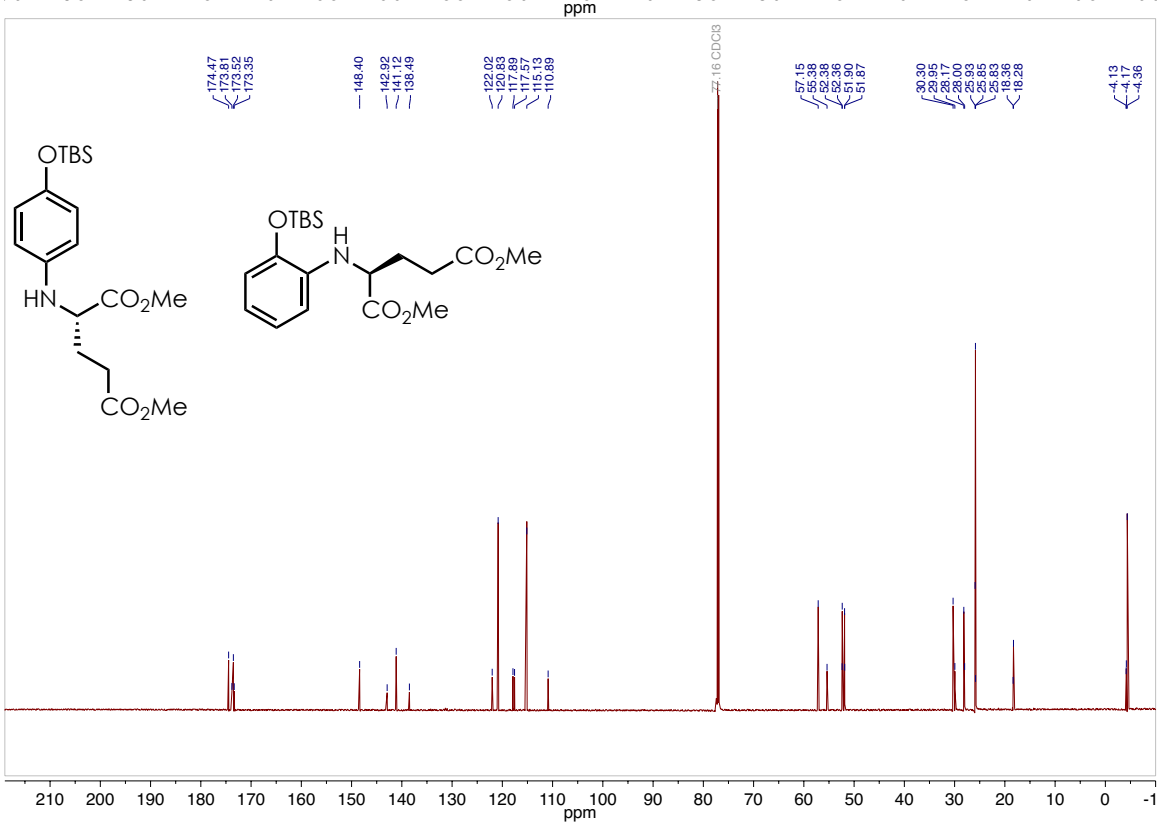
OTBS
HN
CO2Me
CO2Me
OTBS
H
N
CO2Me
CO2Me
ppm

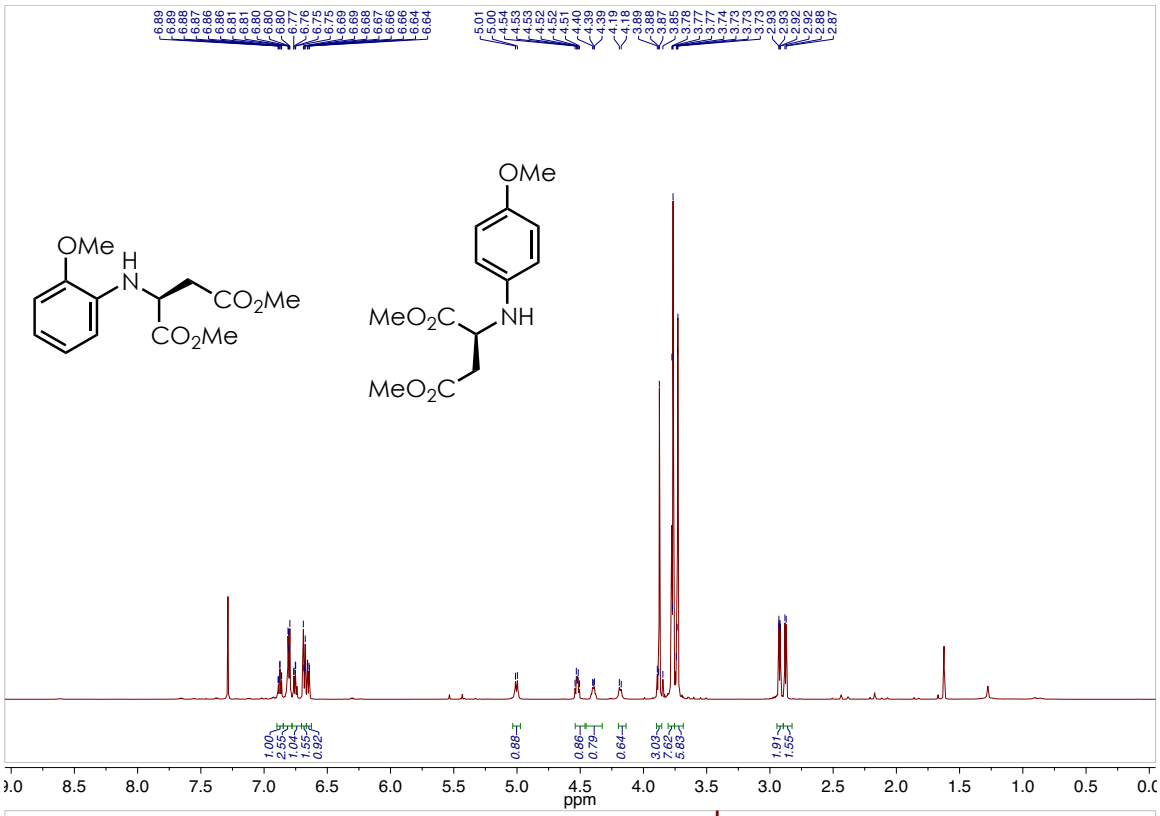
OMe
H
N
CO2Me
CO2Me
OMe
MeO2C
NH
MeO2C
ppm

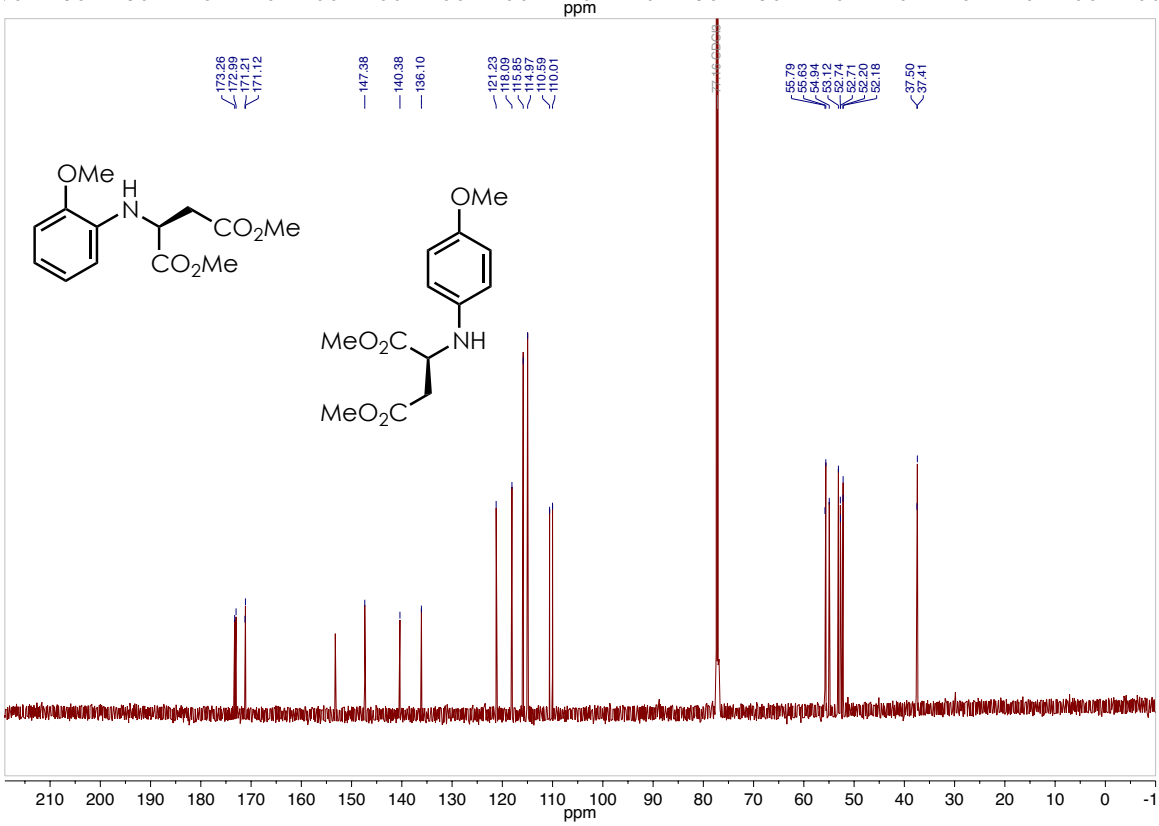
OMe
H
N
CO2Me
CO2Me
OMe
MeO2C
NH
MeO2C
ppm

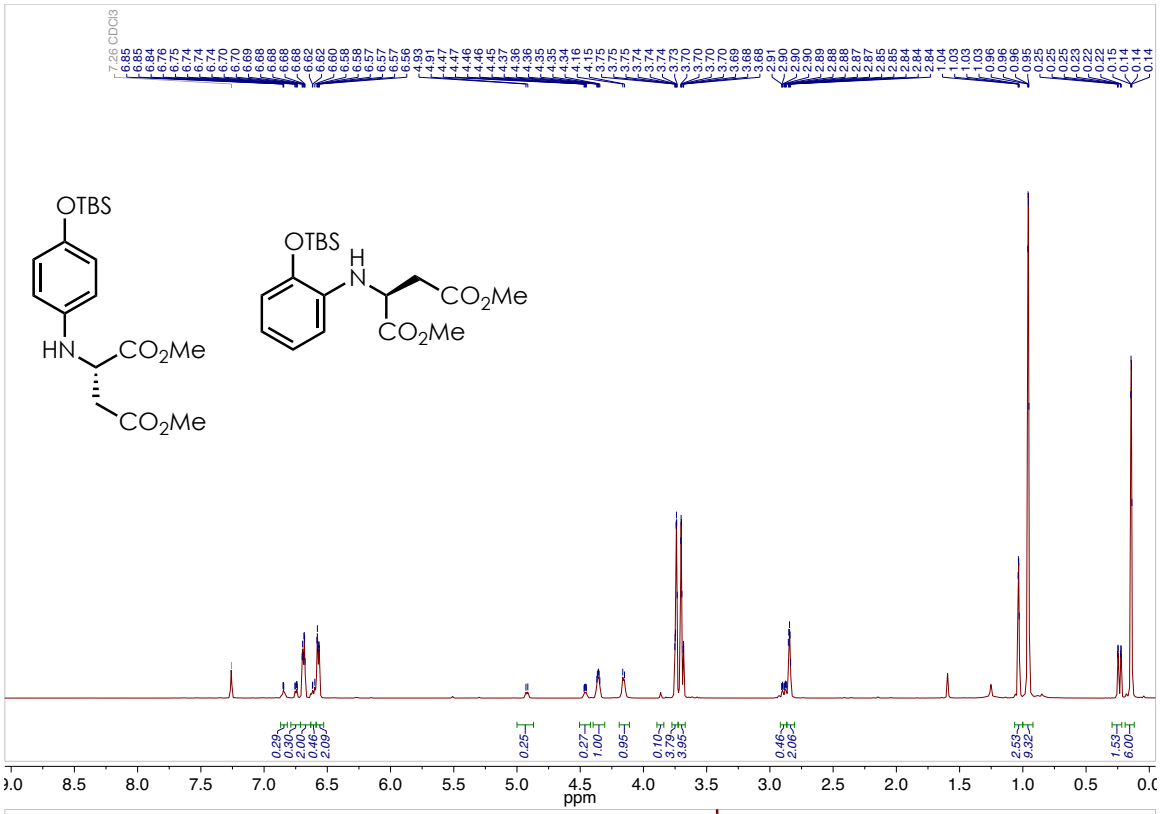
OTBS
HN
CO2Me
CO2Me
OTBS
H
N
CO2Me
CO2Me
ppm

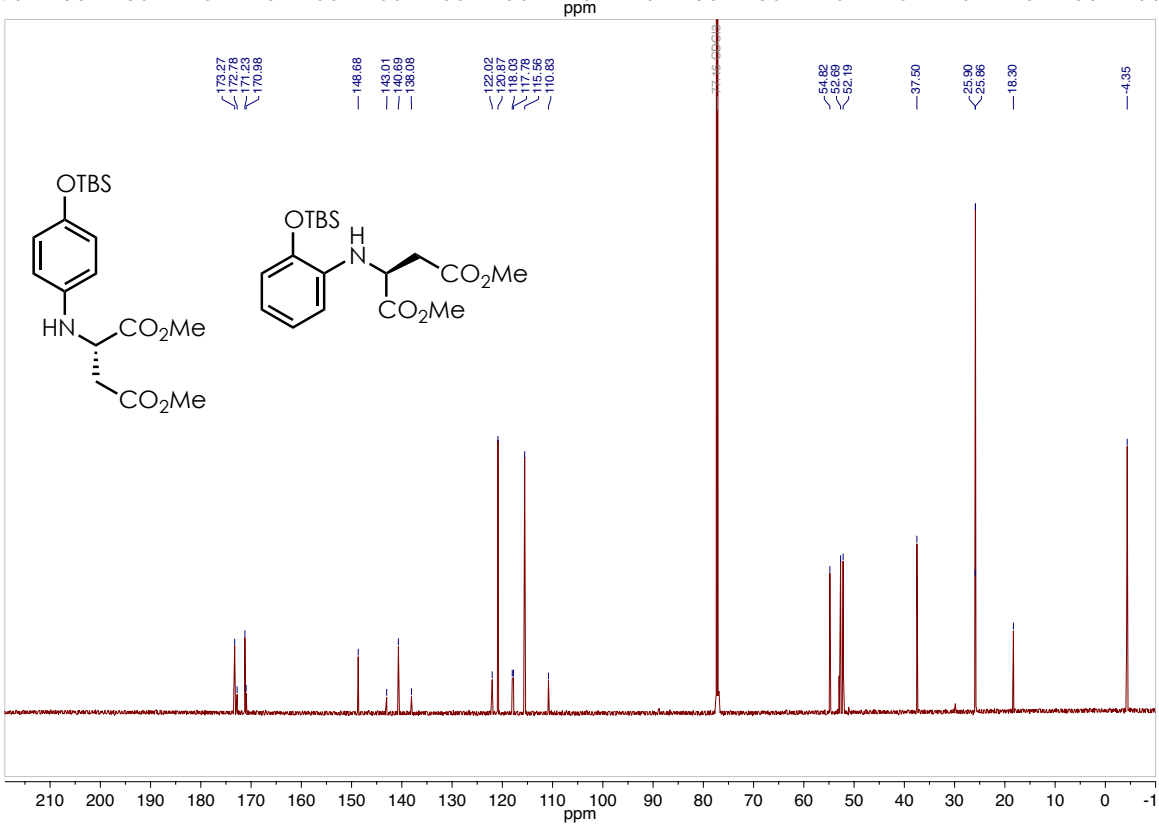
OTBS
HN
CO2Me
CO2Me
OTBS
H
N
CO2Me
CO2Me
ppm

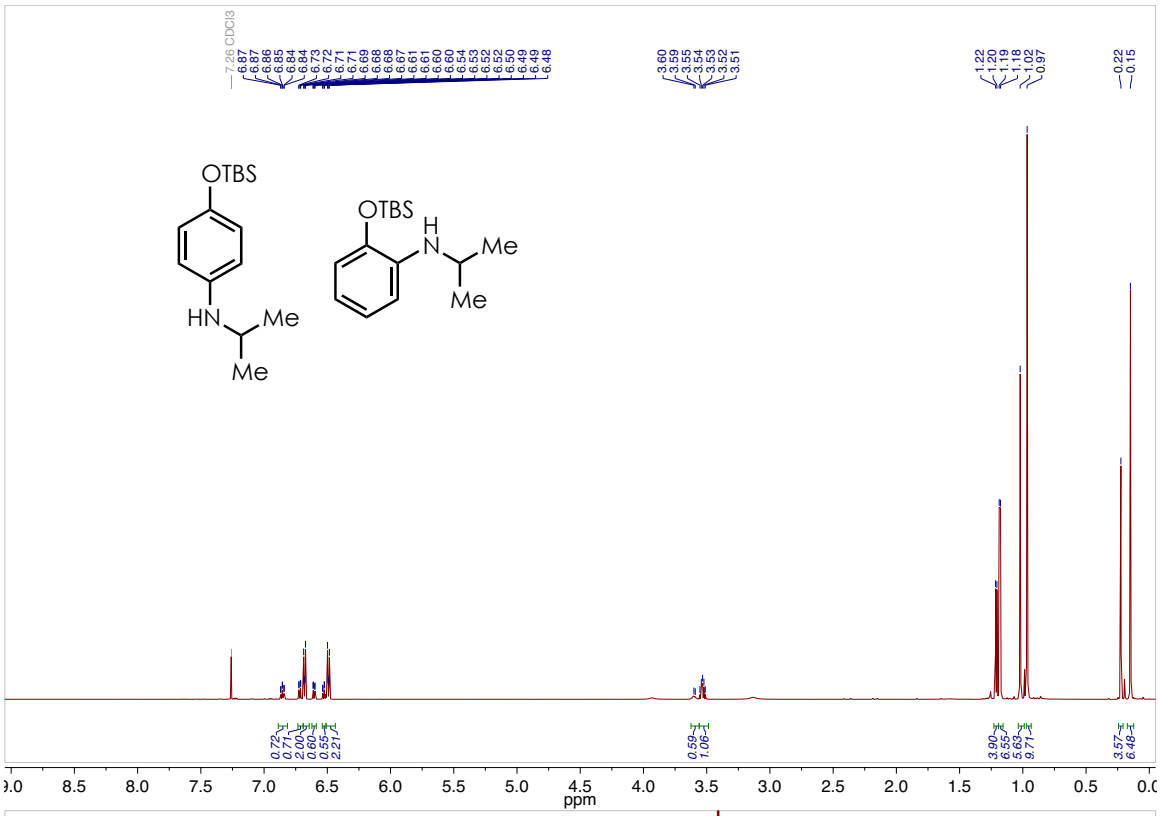
OTBS
HN
Me
Me
OTBS
H
N
Me
Me
ppm

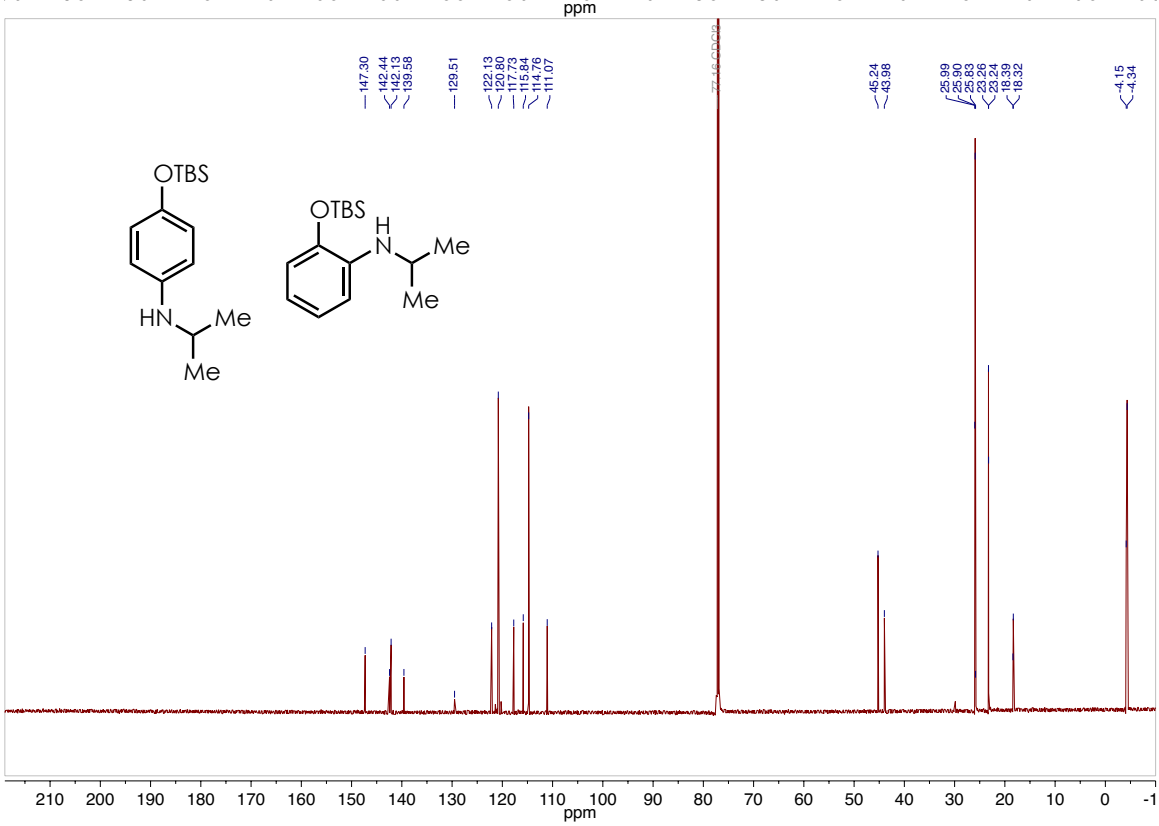
OTBS
HN
Me
Me
OTBS
H
N
Me
Me
ppm

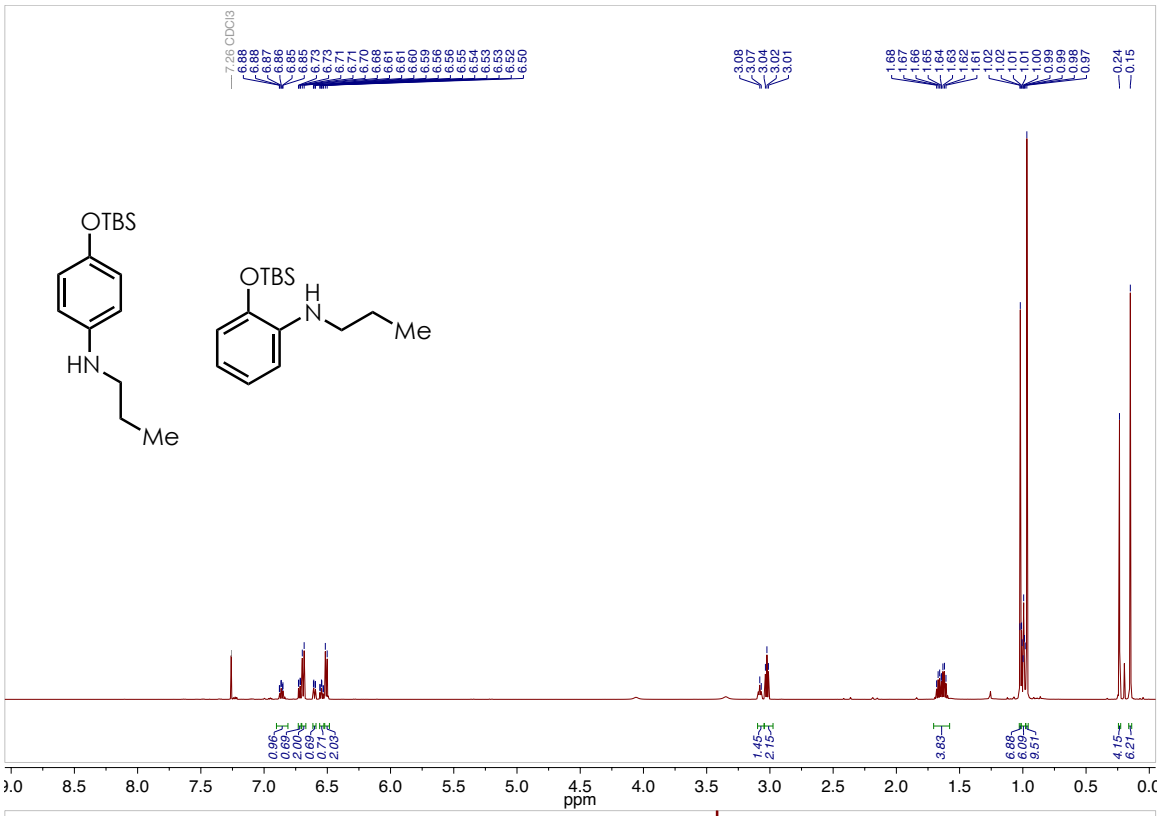
OTBS
HN
Me
OTBS
H
N
Me
ppm

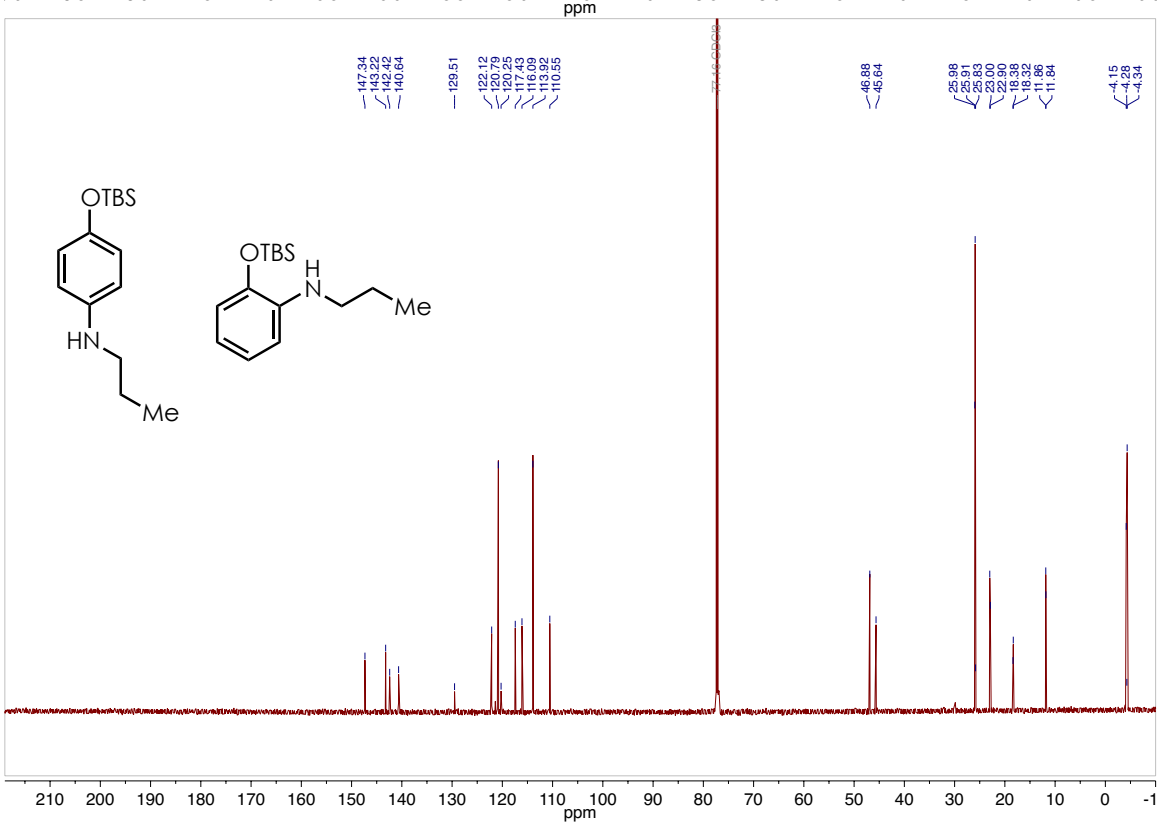
OTBS
HN
Me
OTBS
H
N
Me
ppm

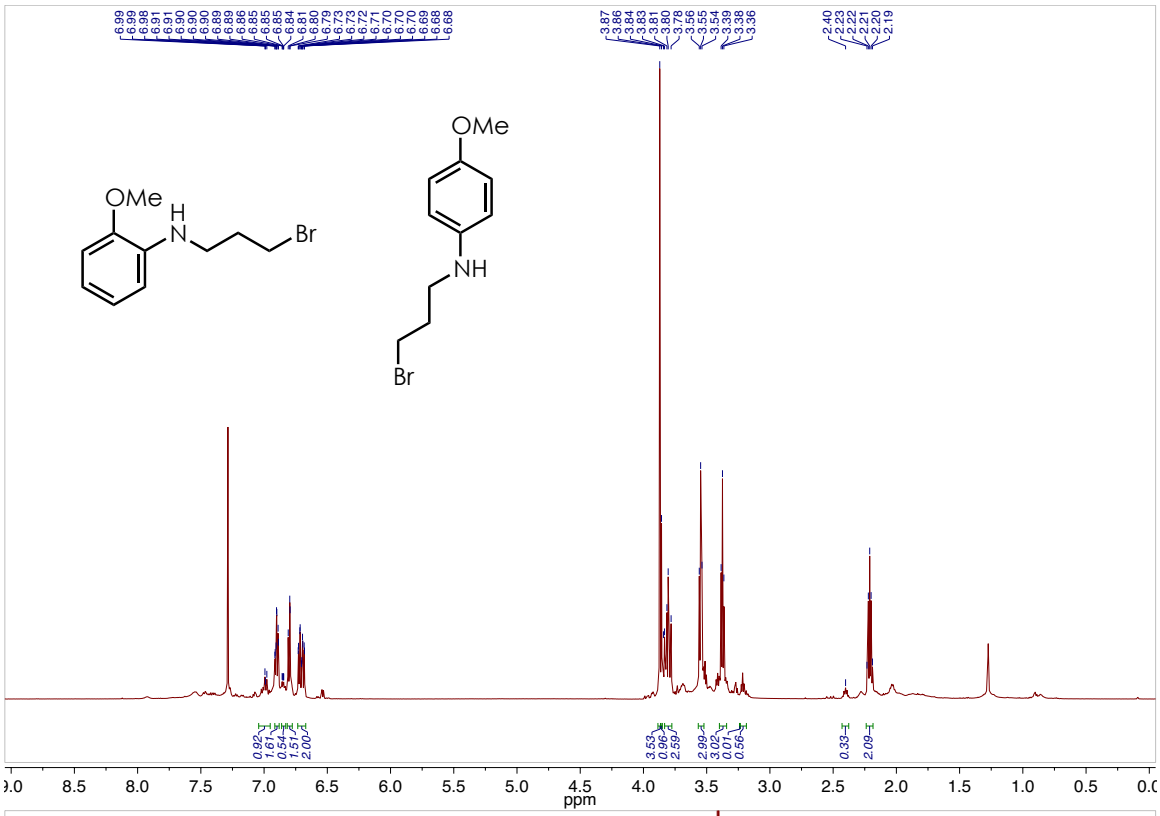
OMe
H
N
Br
OMe
NH
Br
ppm

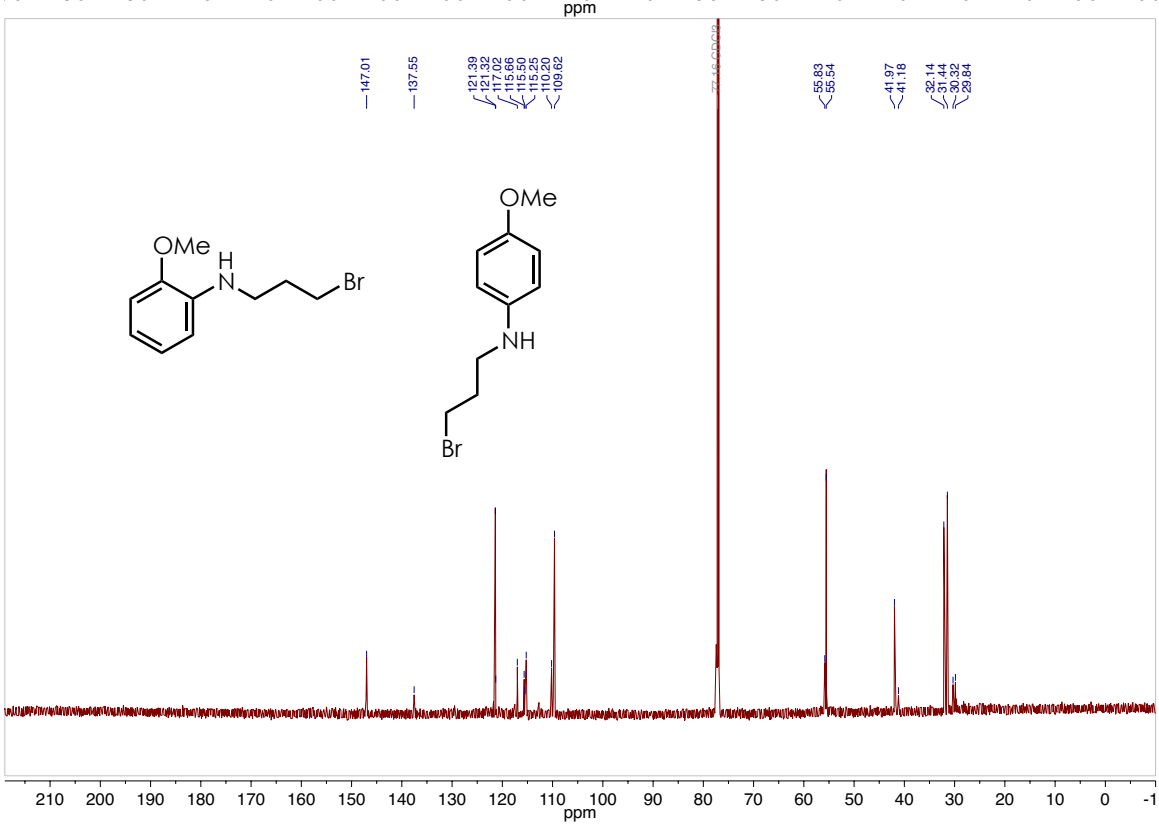
OMe
H
N
Br
OMe
NH
Br
ppm

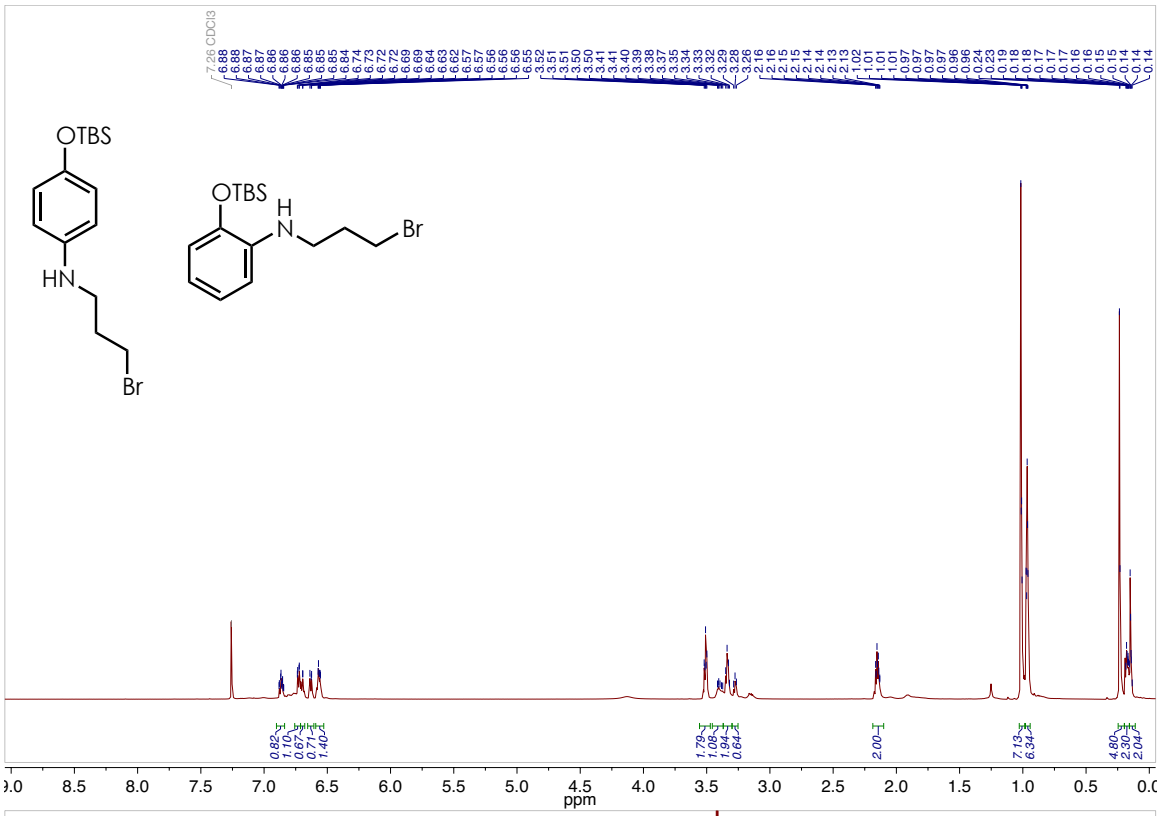
OTBS
HN
Br
OTBS
H
N
Br
ppm

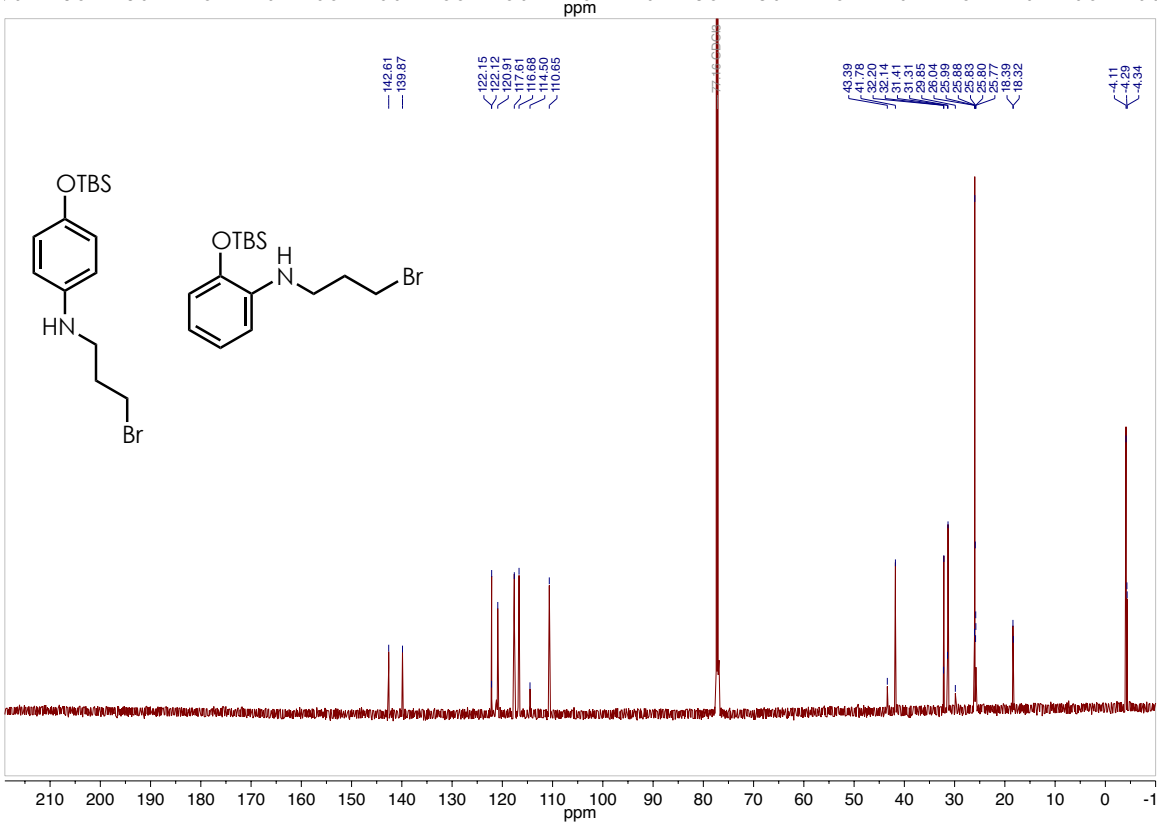
OTBS
HN
Br
OTBS
H
N
Br
ppm

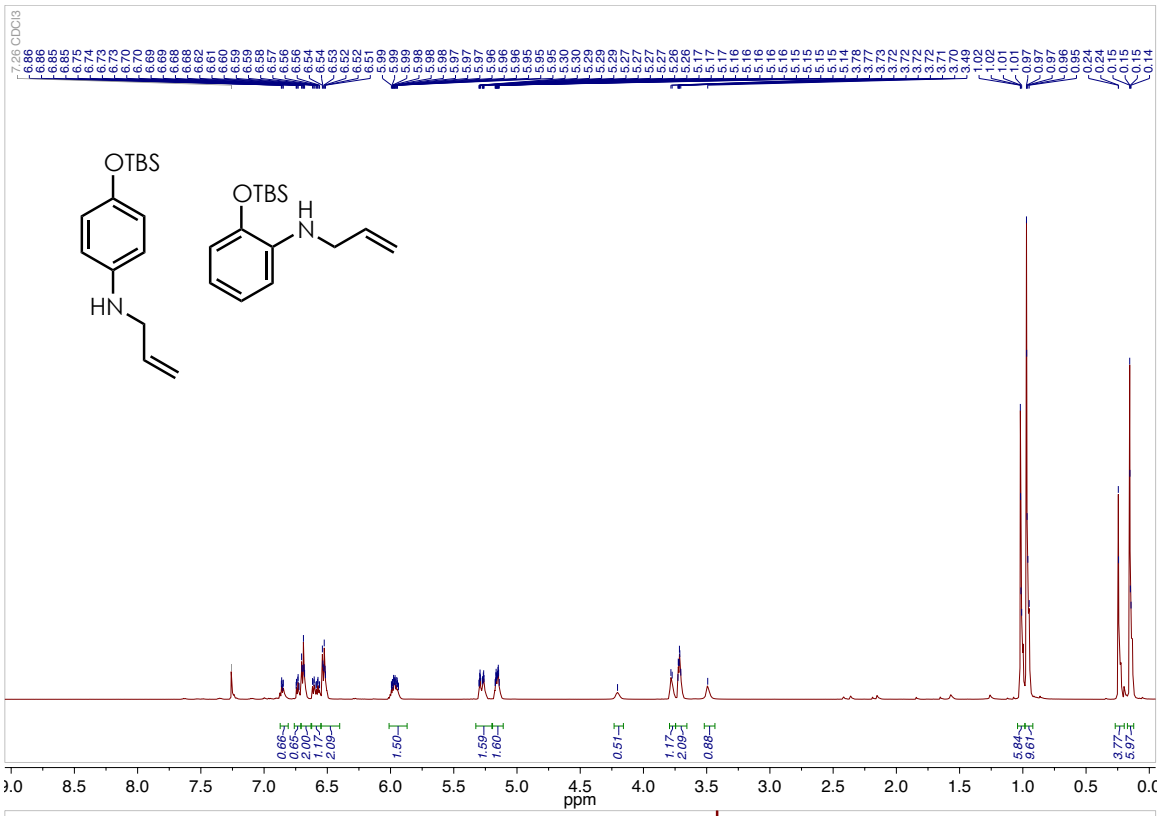
OTBS
HN
OTBS
H
N
ppm

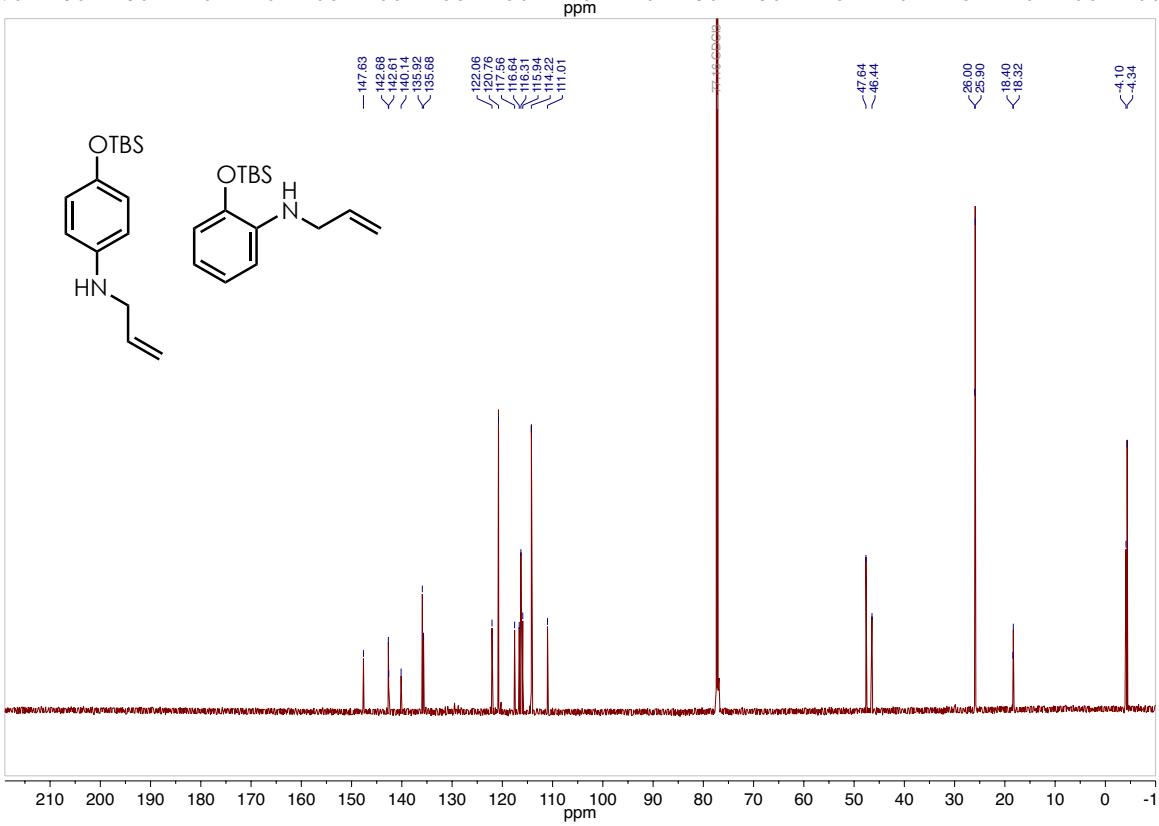
OTBS
HN
OTBS
H
N
ppm

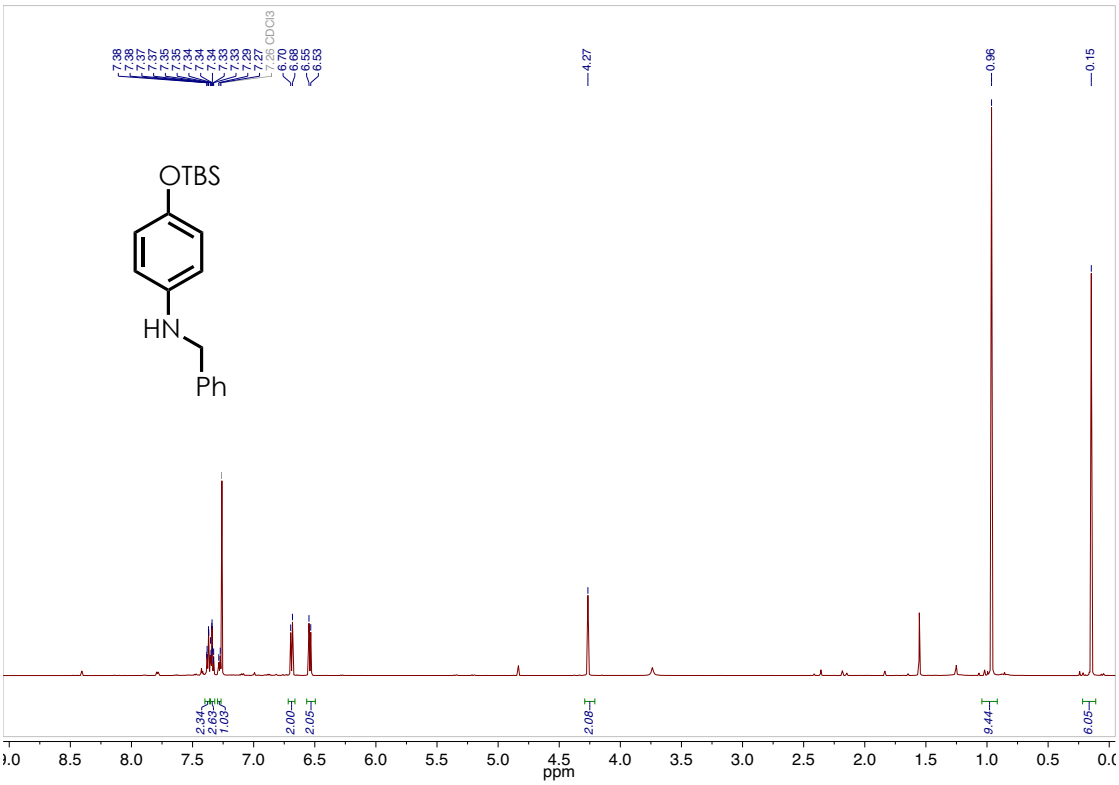
OTBS
HN
Ph
7.38
7.38
7.37
7.37
7.35
7.35
7.34
7.34
7.34
7.33
7.33
7.29
7.27
CDCl3
6.70
6.68
6.55
6.53
4.27
0.96
0.15
2.34
2.63
1.03
2.00
2.05
2.08
9.44
6.05
ppm

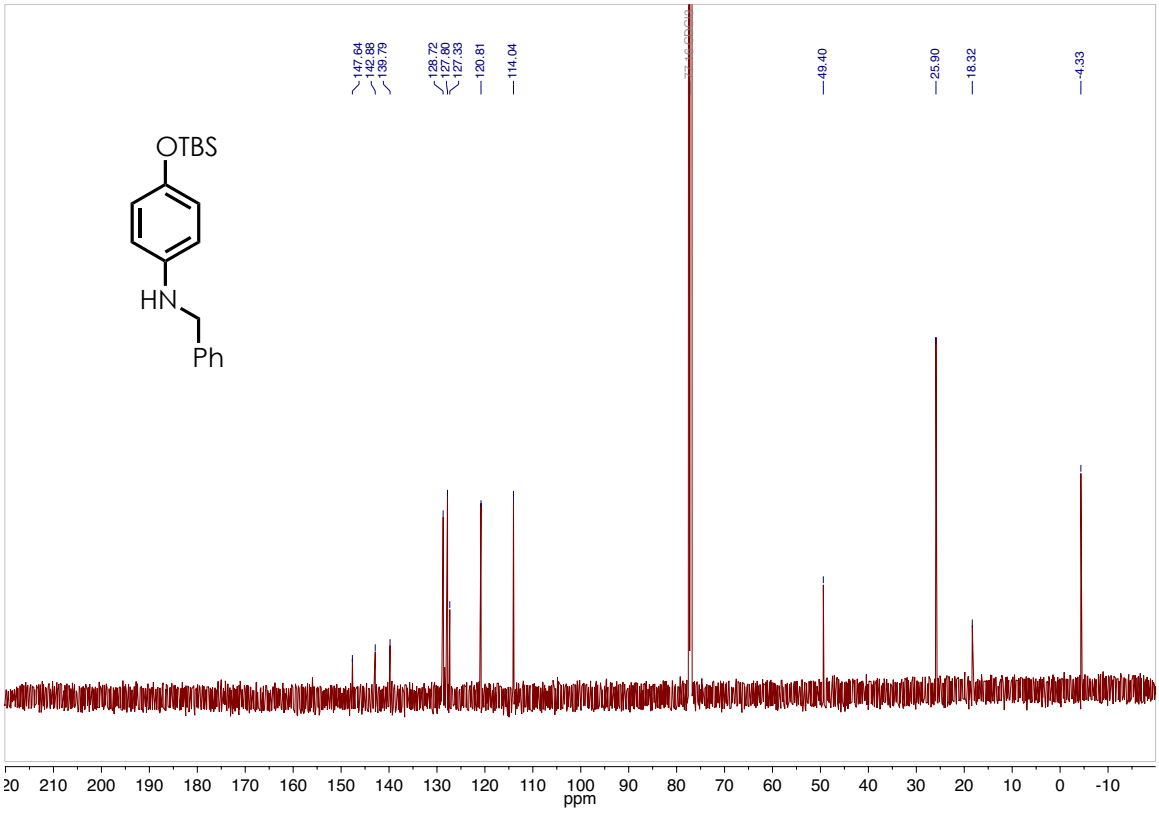
OTBS
HN
Ph
147.64
142.88
139.79
128.72
127.86
127.33
120.81
114.04
77.16
49.40
25.90
18.32
-4.33
ppm

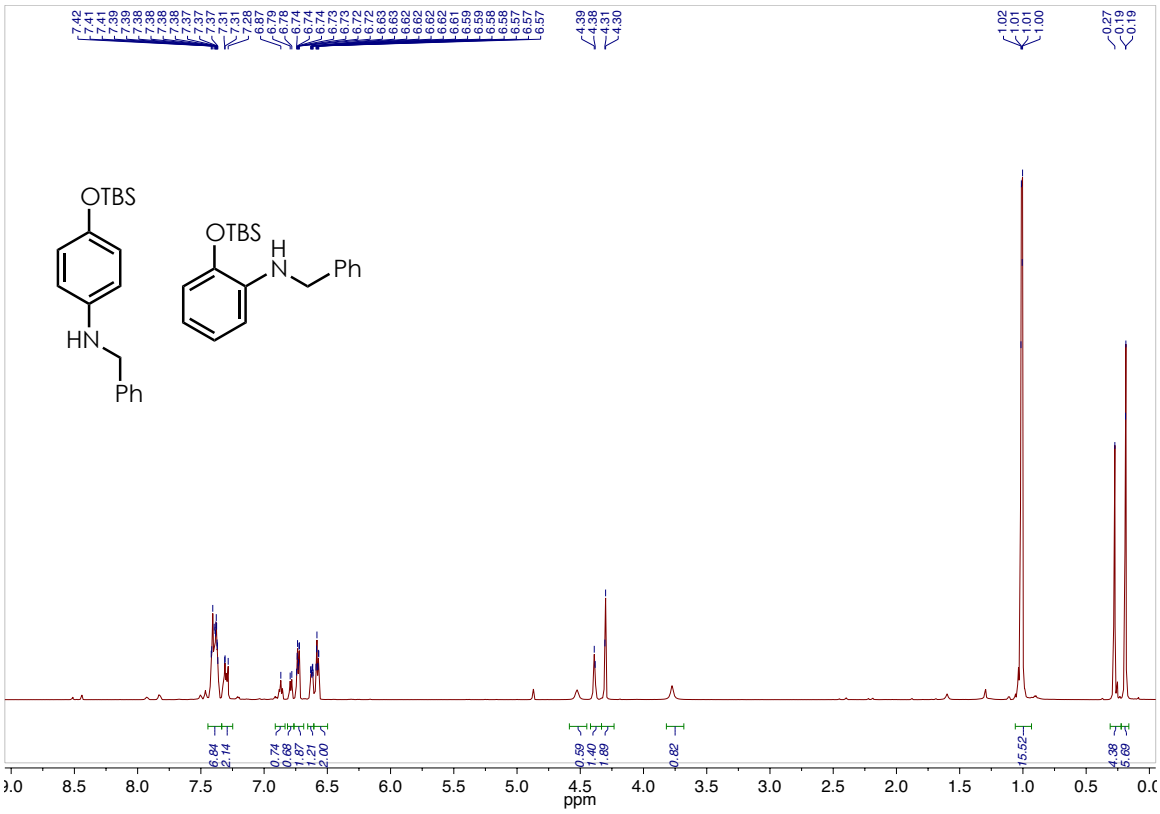
OTBS
HN
Ph
OTBS
H
N
Ph
ppm

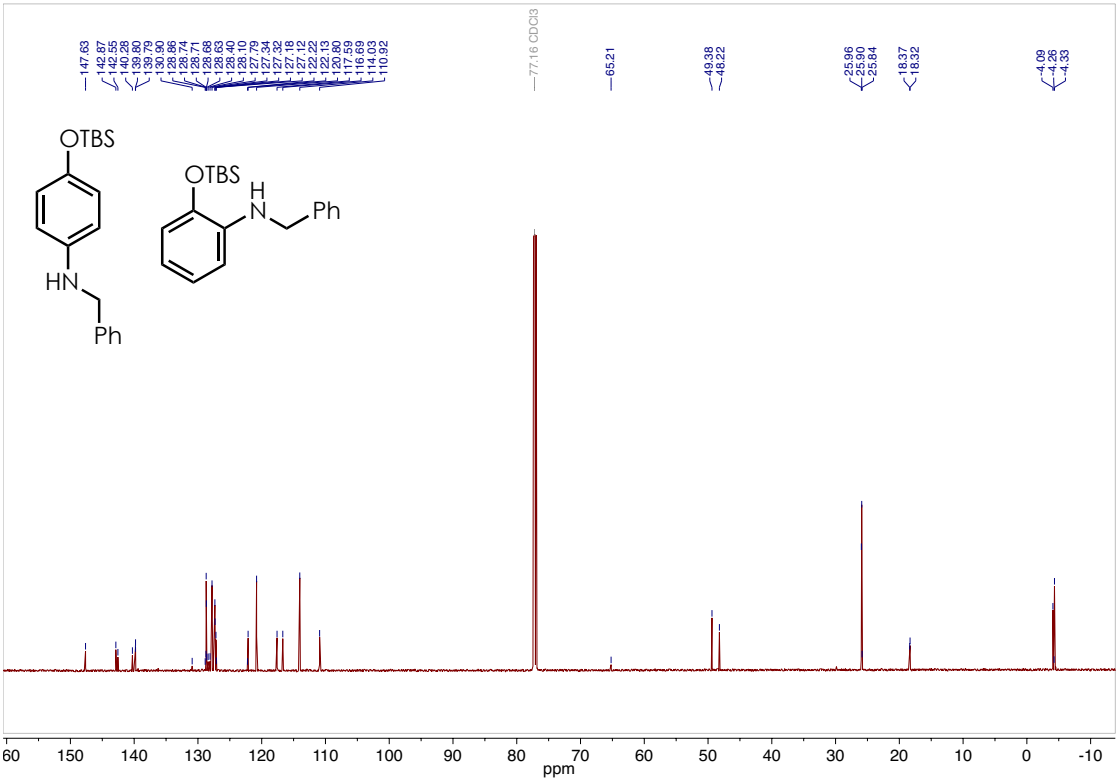
OTBS
HN
Ph
OTBS
H
N
Ph
ppm

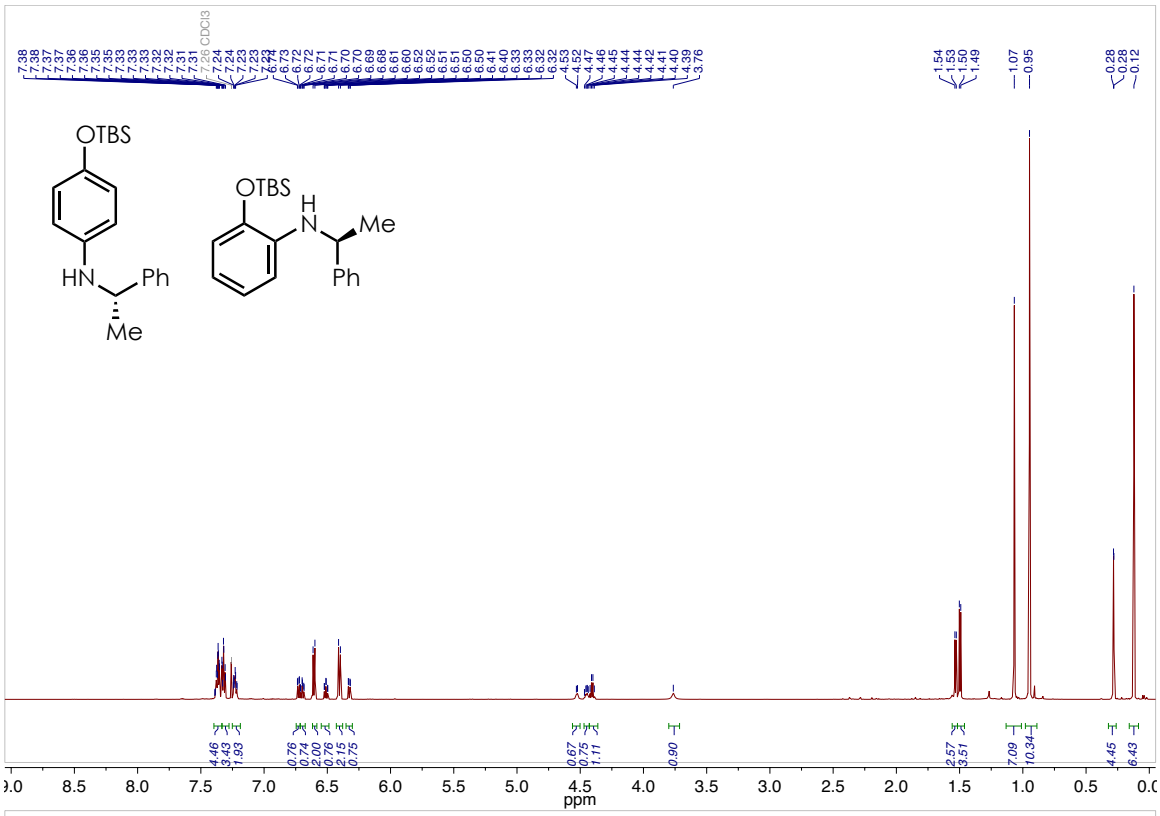
OTBS
HN
Ph
Me
OTBS
H
N
Me
Ph
ppm

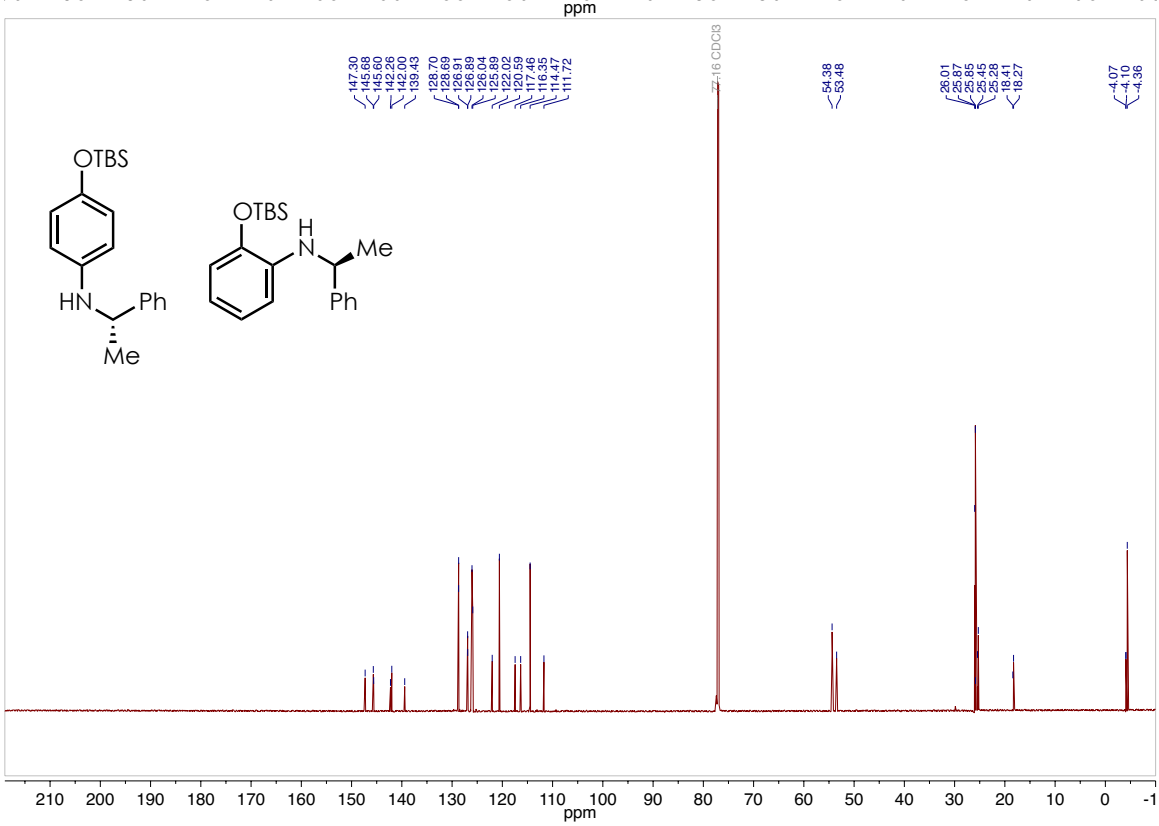
OTBS
HN
Ph
Me
OTBS
H
N
Me
Ph
ppm

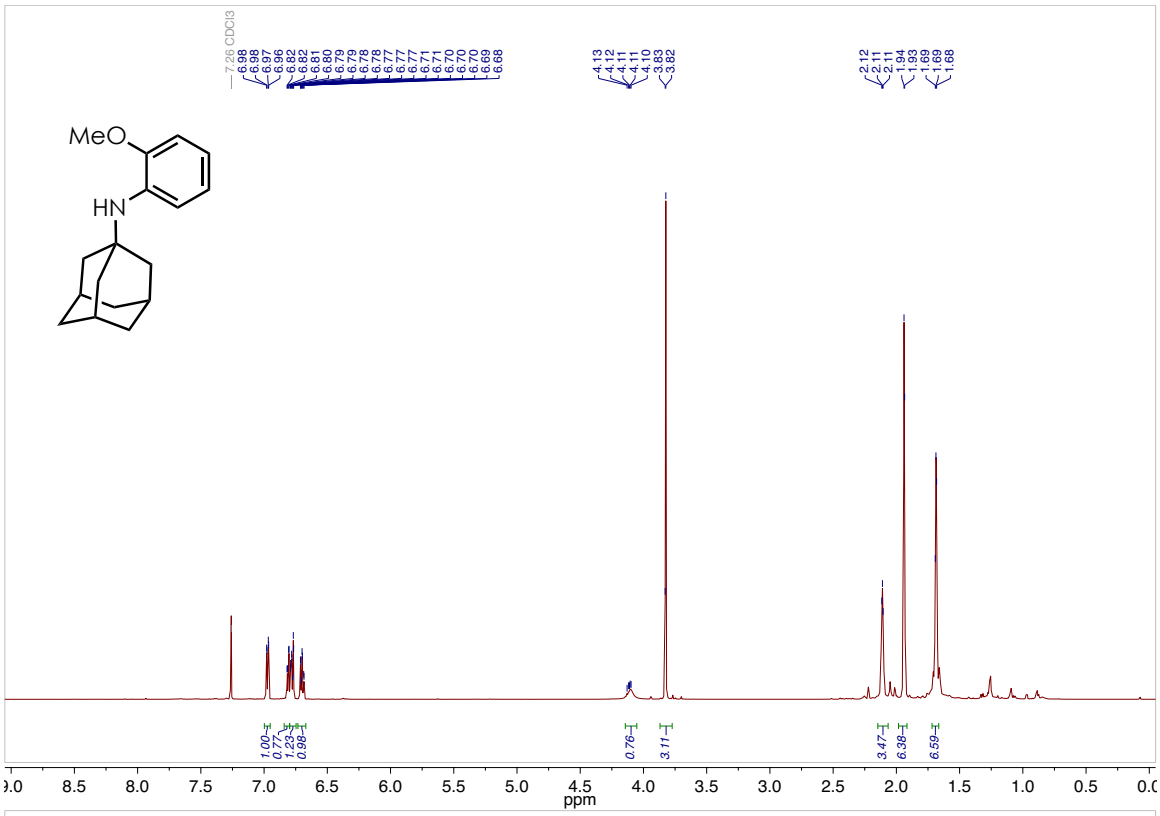
7.26 CDCl3
6.98
6.98
6.97
6.96
6.82
6.82
6.81
6.80
6.79
6.79
6.78
6.78
6.77
6.77
6.71
6.70
6.70
6.69
6.68
4.13
4.12
4.11
4.11
4.10
3.83
3.82
2.12
2.11
2.11
1.94
1.93
1.69
1.69
1.68
MeO
HN
1.00
0.77
1.23
0.98
0.76
3.11
3.47
6.38
6.59
ppm

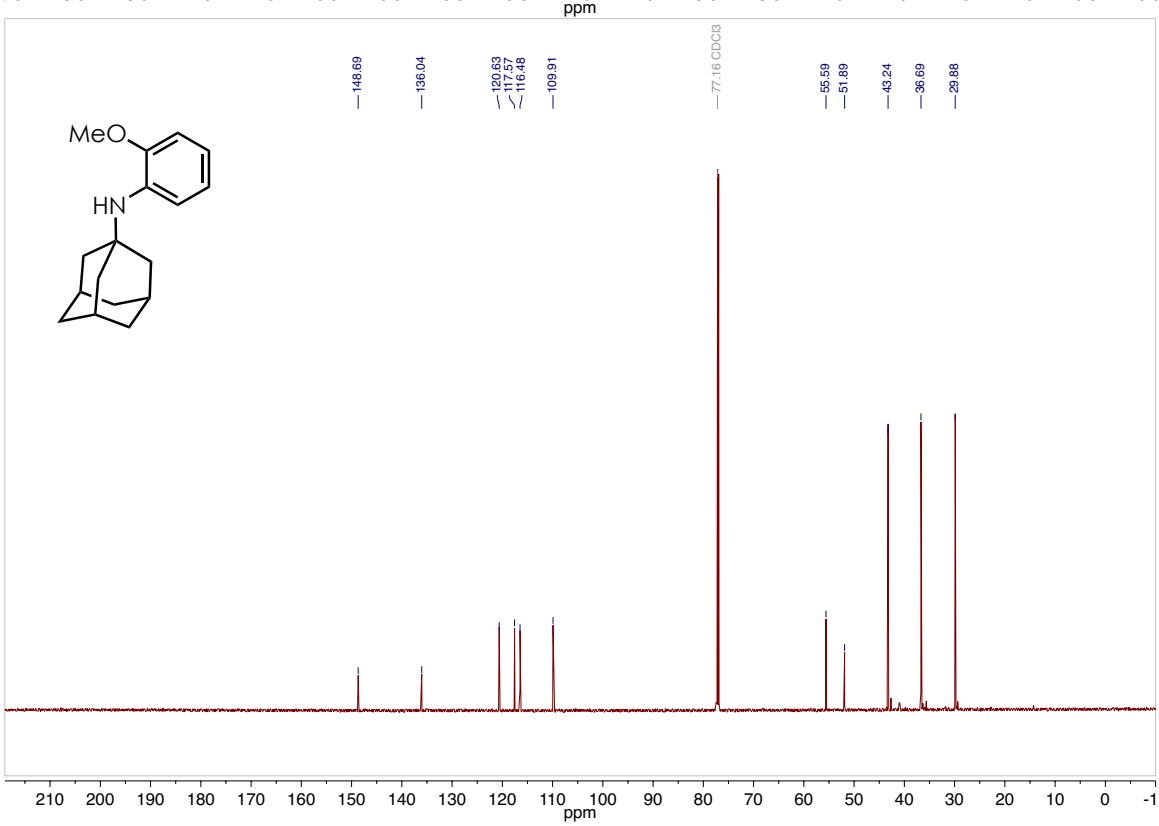
148.69
136.04
120.63
117.57
116.48
109.91
77.16 CDCl3
55.59
51.89
43.24
36.69
29.88
MeO
HN
ppm

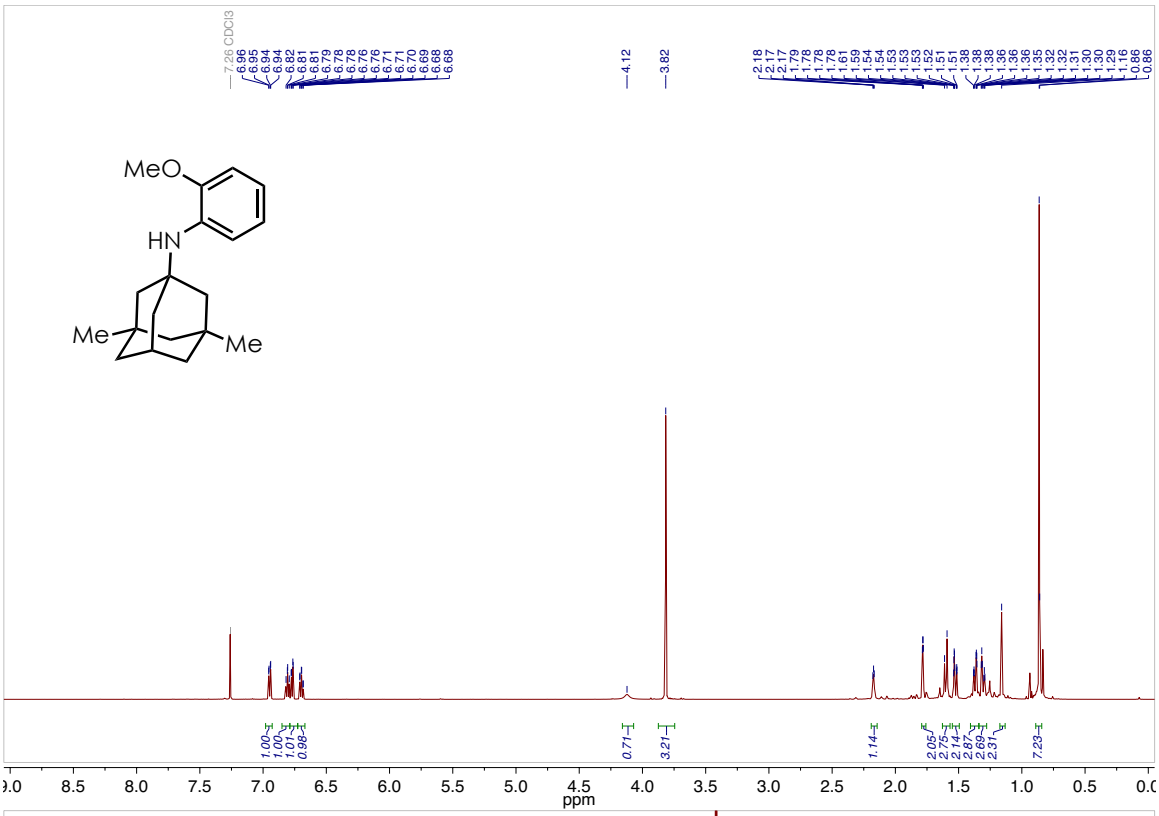
MeO
HN
Me
Me
ppm

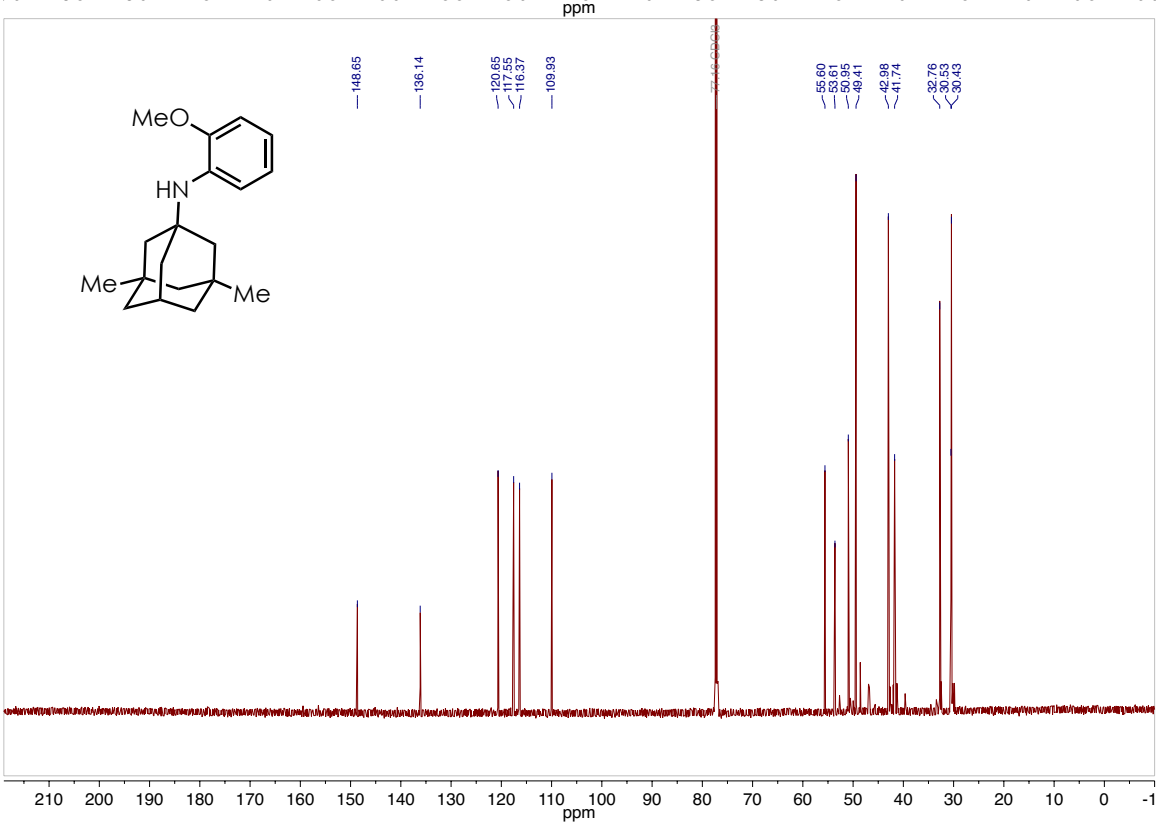
MeO
HN
Me
Me
ppm

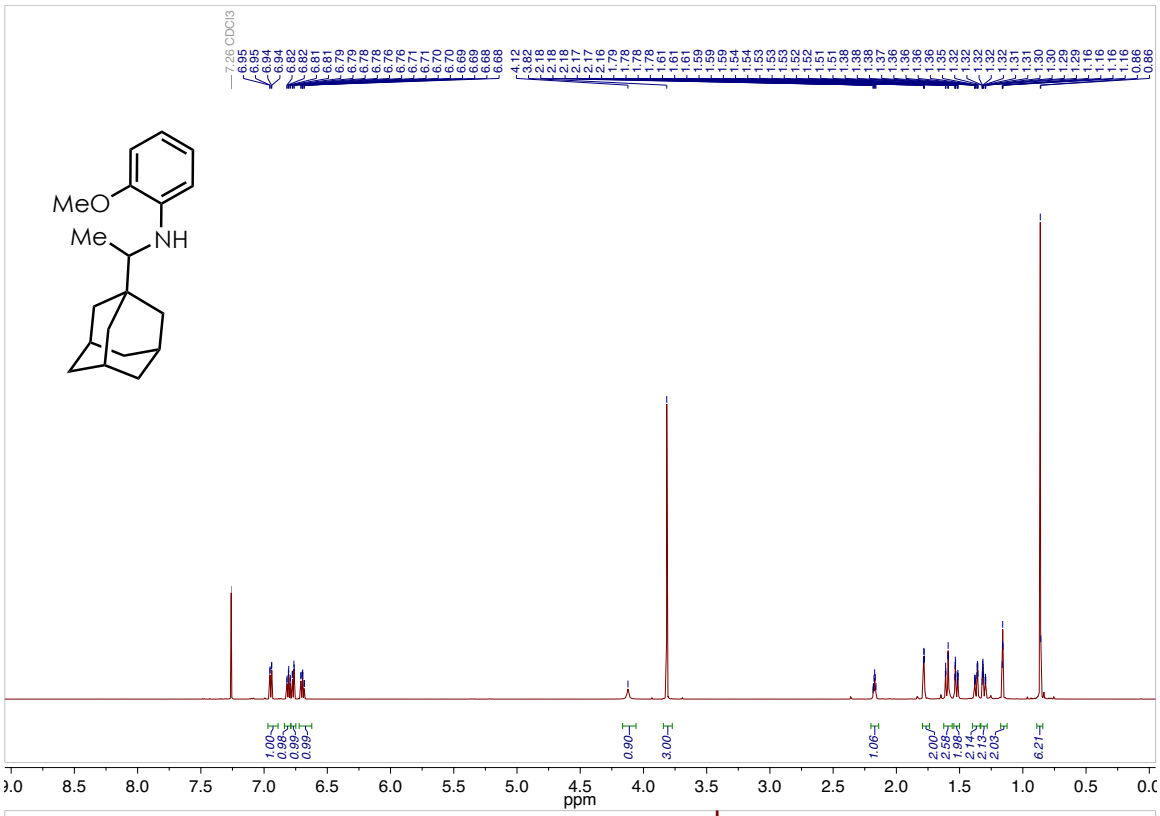
MeO
Me
NH
ppm

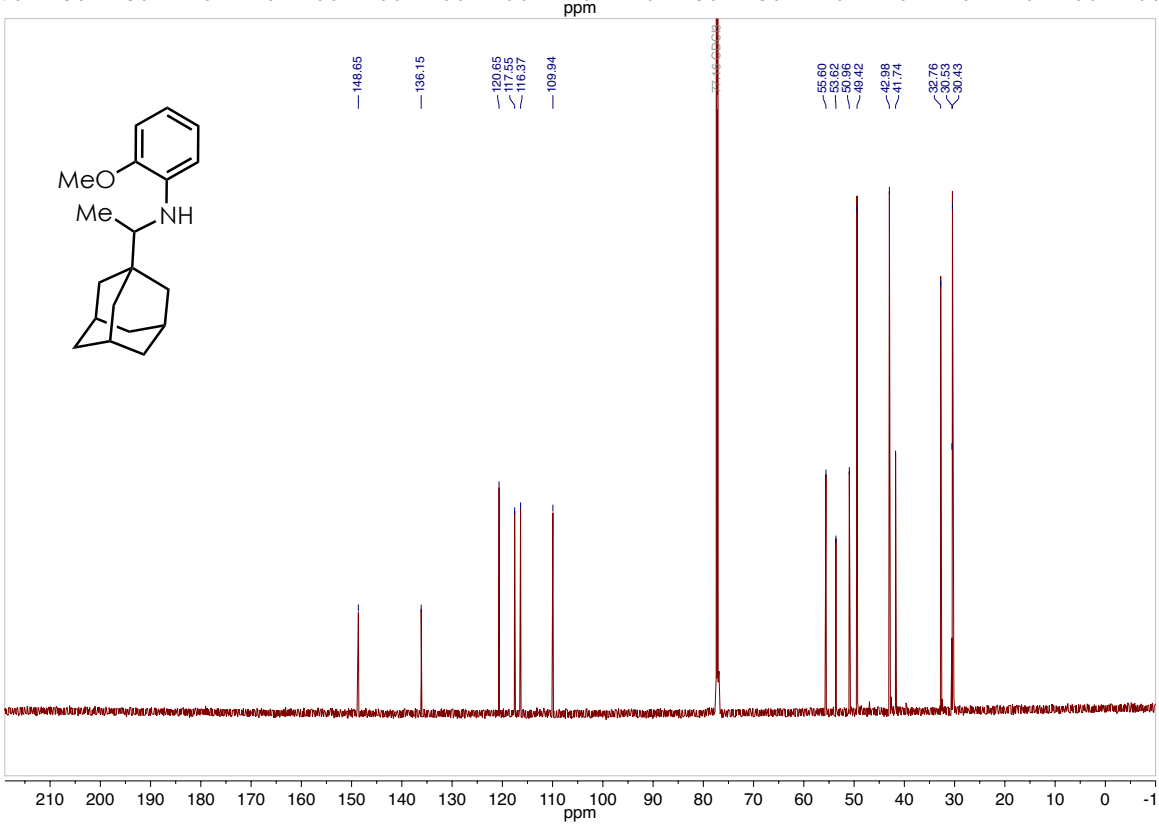
MeO
Me
NH
148.65
136.15
120.65
117.55
116.37
109.94
55.60
53.62
50.96
49.42
42.98
41.74
32.76
30.53
30.43
ppm

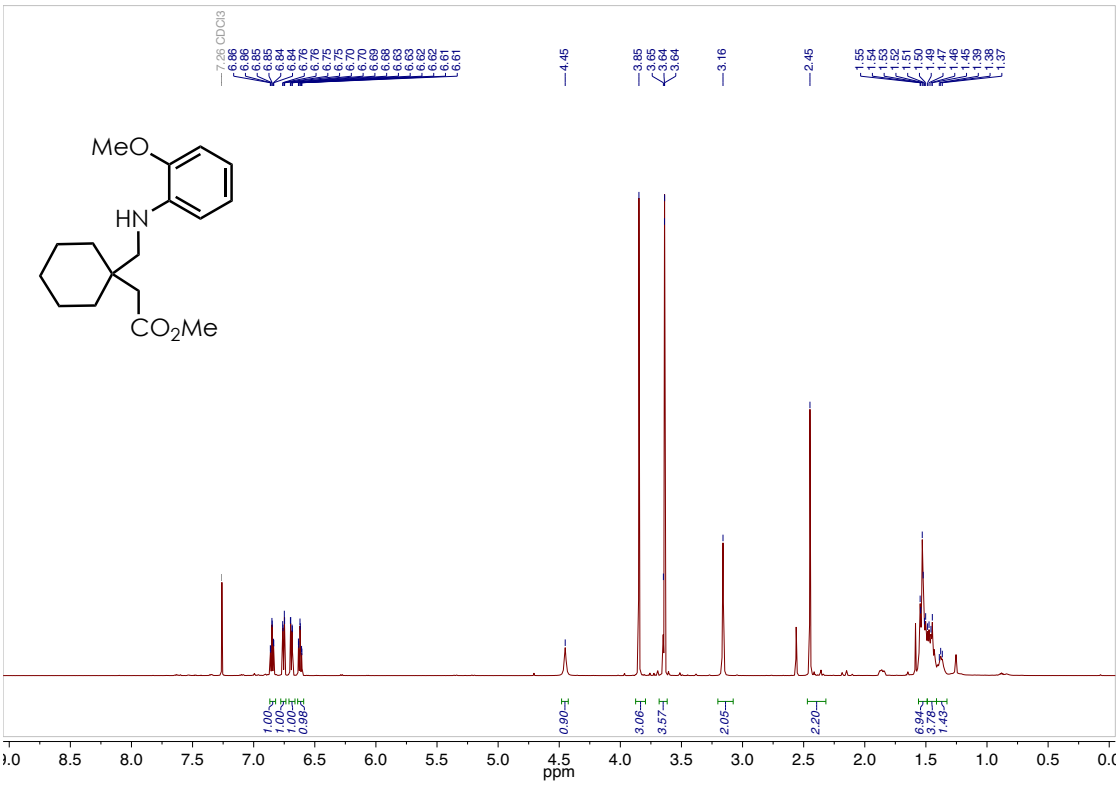
MeO
HN
CO2Me
ppm

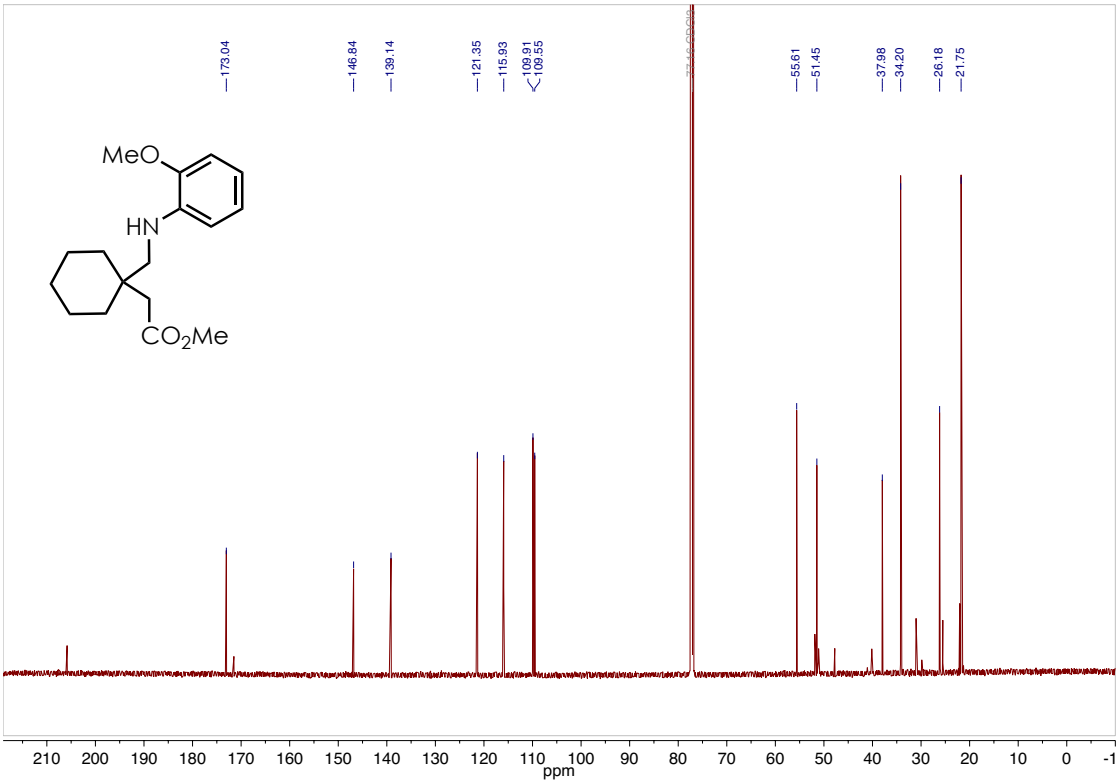
MeO
HN
CO2Me
ppm

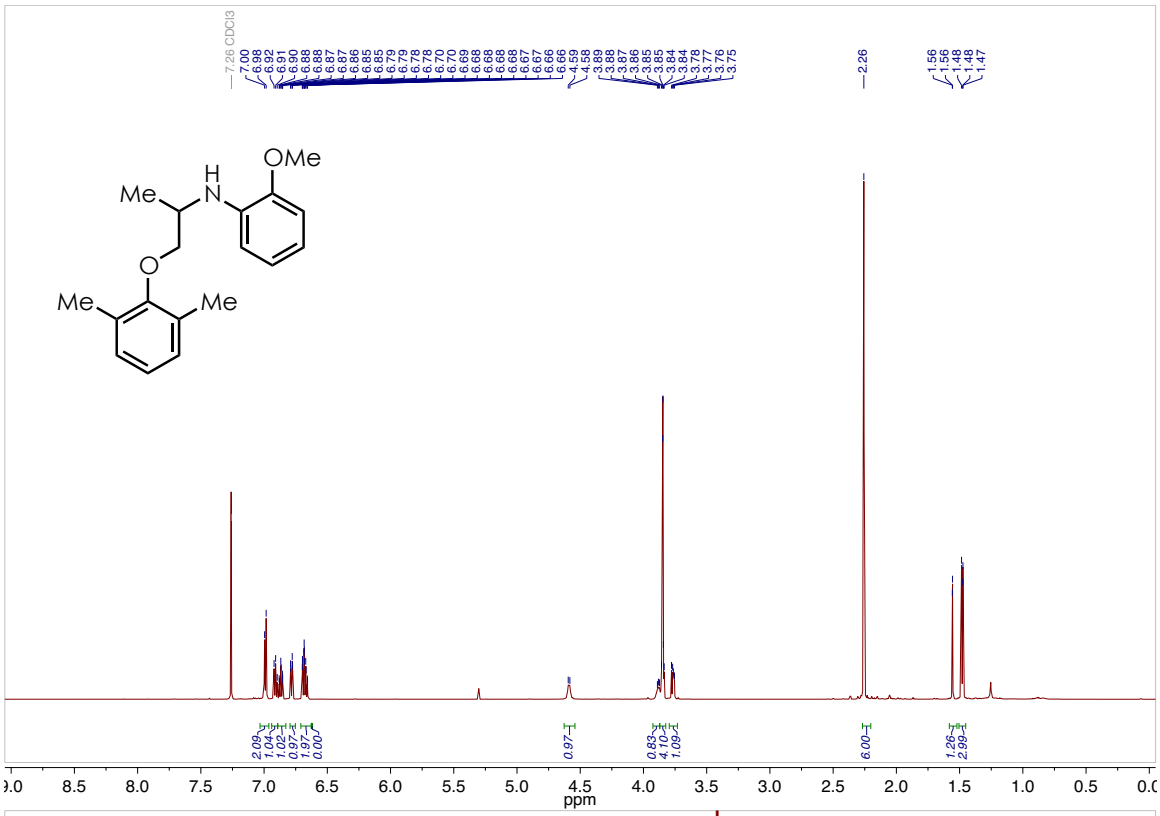
7.26 CDCl3
7.00
6.98
6.92
6.91
6.90
6.88
6.88
6.87
6.87
6.86
6.85
6.85
6.79
6.79
6.78
6.78
6.70
6.70
6.69
6.68
6.68
6.68
6.68
6.67
6.67
6.66
6.66
4.59
4.58
3.89
3.88
3.87
3.86
3.85
3.85
3.84
3.84
3.78
3.77
3.76
3.75
2.26
1.56
1.56
1.48
1.48
1.47
OMe
H
N
Me
O
Me
Me
2.09
1.04
1.02
1.07
1.97
0.00
0.97
0.83
4.10
1.09
6.00
1.26
2.99
ppm

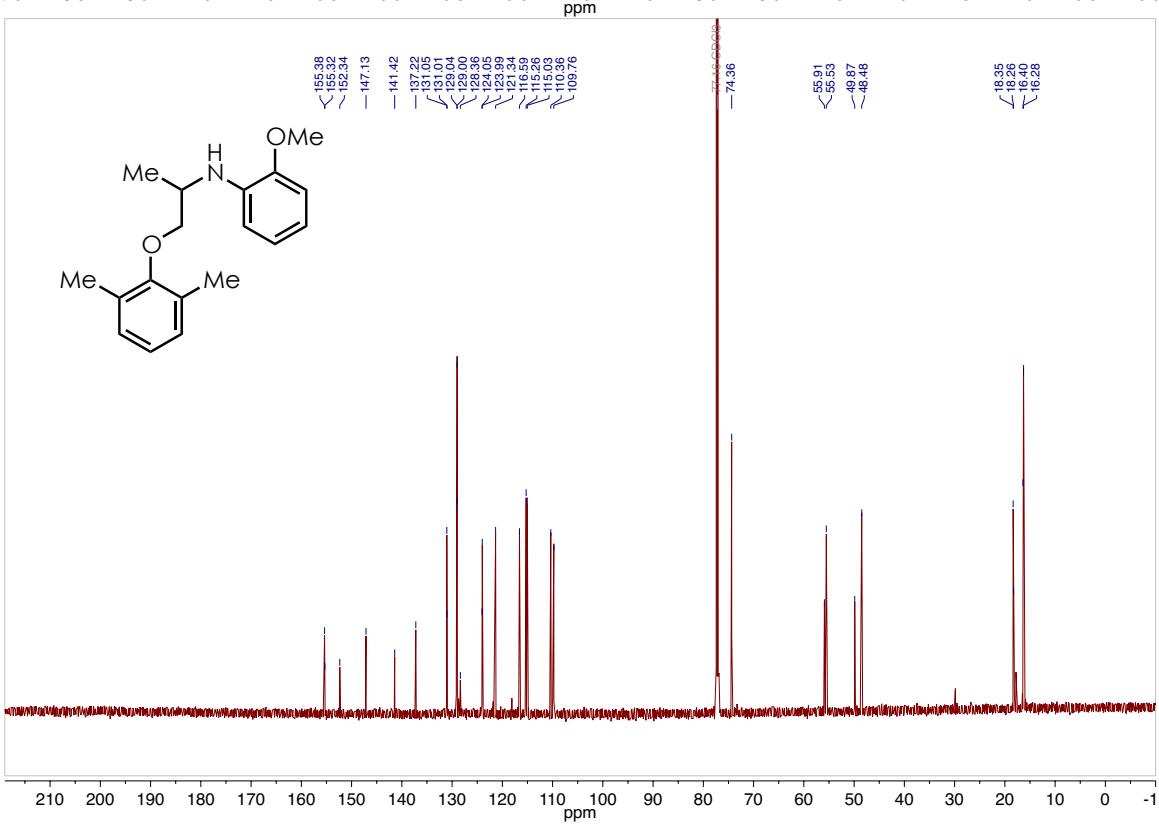
155.38
155.32
152.34
147.13
141.42
137.22
131.05
131.01
129.04
129.00
128.36
124.05
123.99
121.34
116.59
115.26
115.03
110.06
109.76
77.48 CDCl3
74.36
55.91
55.53
49.87
49.48
18.35
18.26
16.40
16.28
OMe
H
N
Me
O
Me
Me
ppm

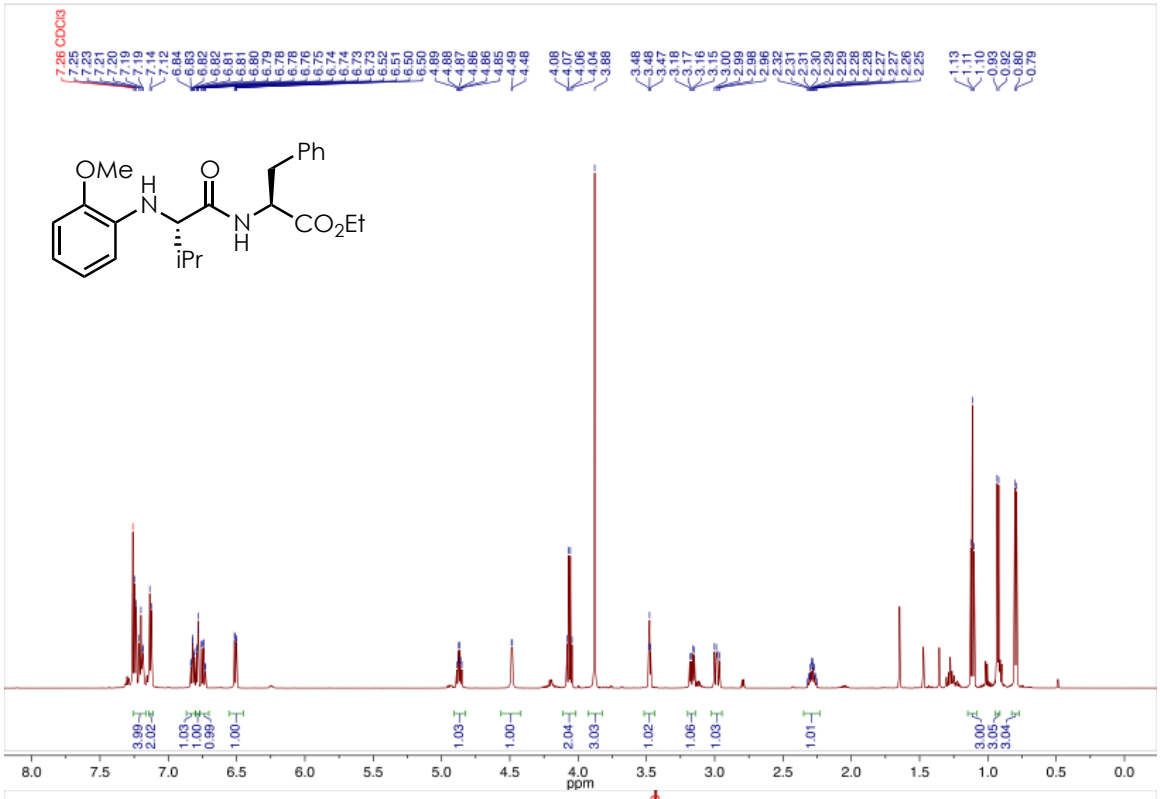
OMe
H
N
O
N
H
Ph
CO2Et
iPr

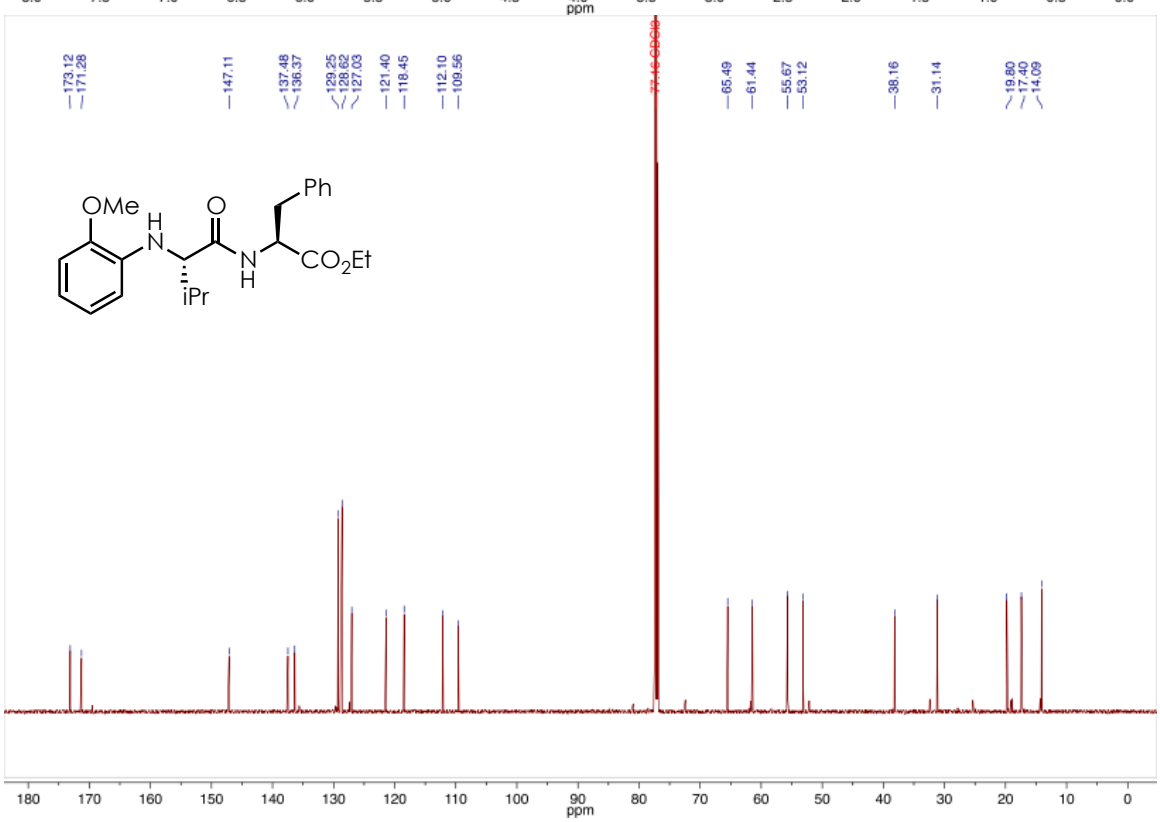
OMe
H
N
O
N
H
Ph
CO2Et
iPr

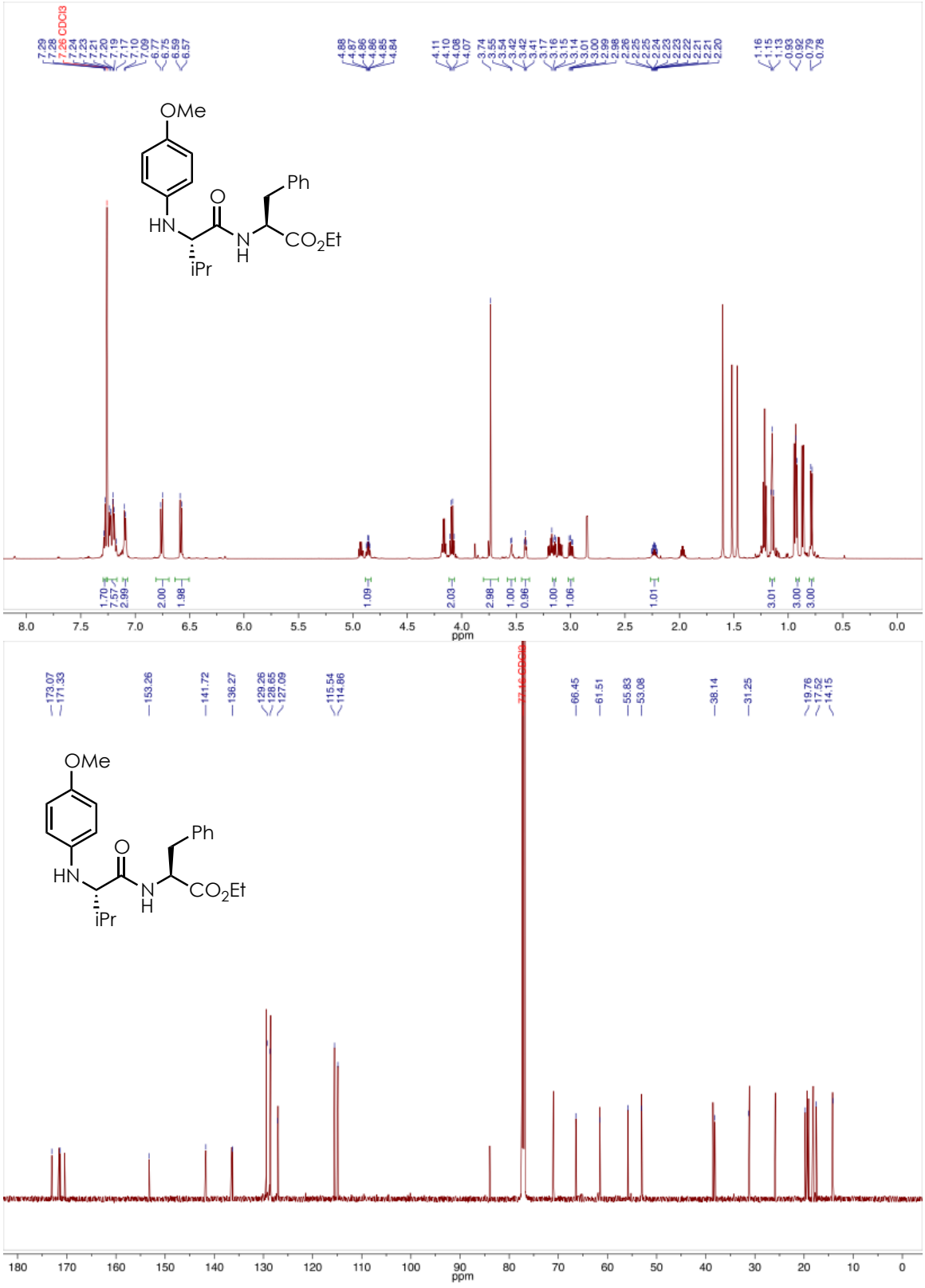
OMe
Ph
HN
O
N
H
CO2Et
iPr
ppm

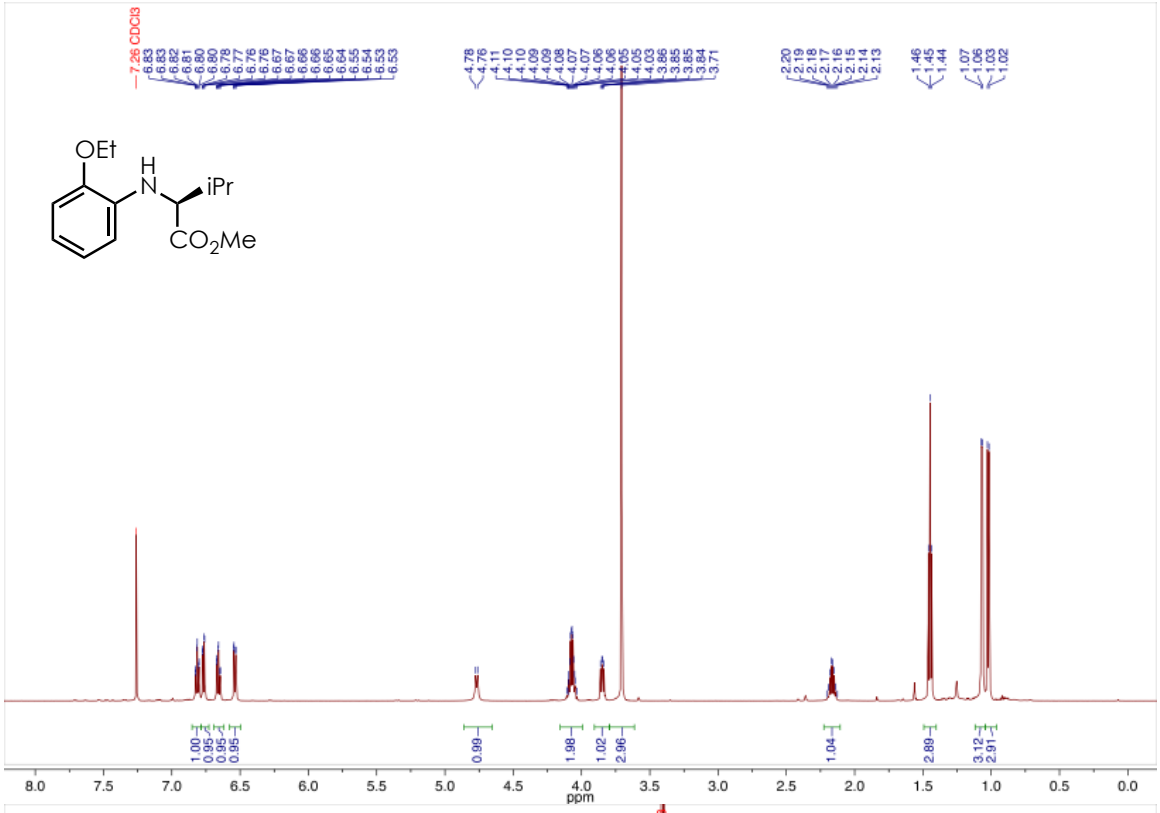
7.26 CDCl3
6.83
6.82
6.81
6.80
6.78
6.77
6.76
6.67
6.66
6.65
6.64
6.55
6.54
6.53
4.78
4.76
4.11
4.10
4.09
4.08
4.07
4.06
4.05
4.03
3.86
3.85
3.84
3.71
2.20
2.19
2.18
2.17
2.16
2.15
2.14
2.13
1.46
1.45
1.44
1.07
1.06
1.03
1.02
OEt
H
N
iPr
CO2Me
1.00
0.95
0.95
0.95
0.99
1.98
1.02
2.96
1.04
2.89
3.12
2.91
ppm

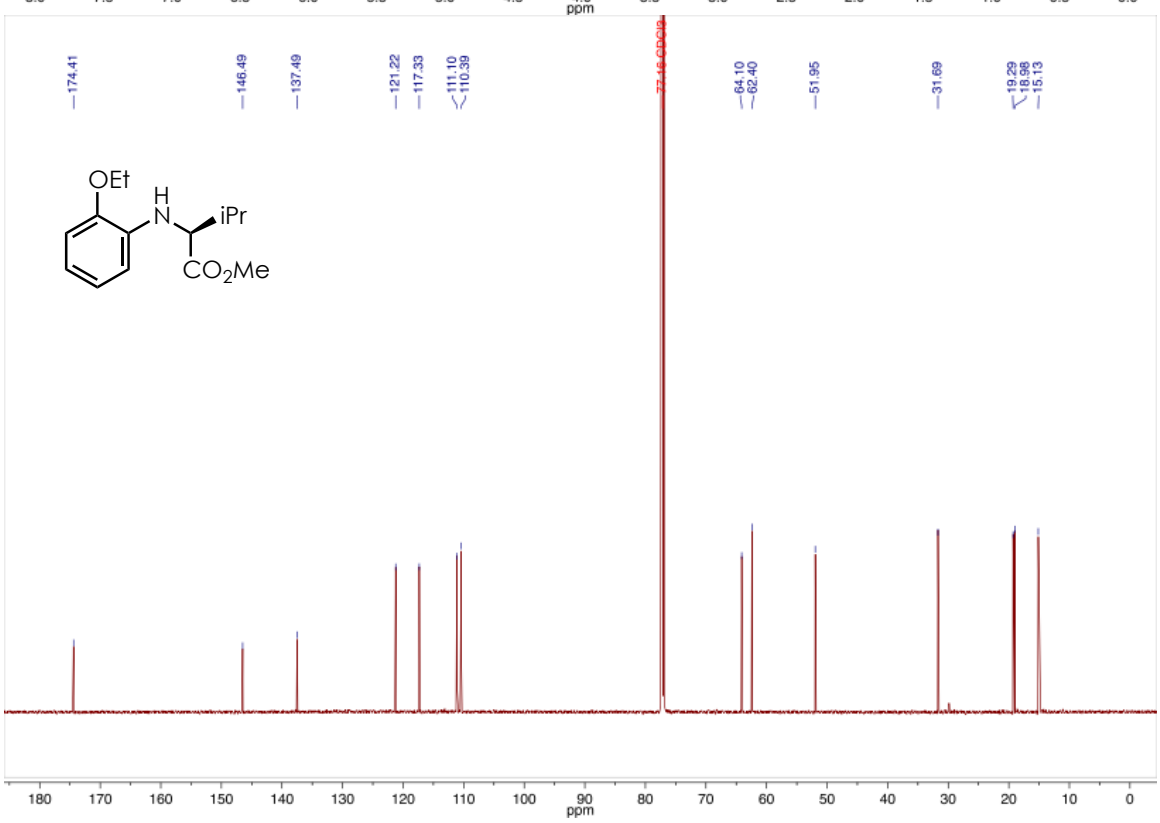
174.41
146.49
137.49
121.22
117.33
111.10
110.39
77.16 CDCl3
64.10
62.40
51.95
31.69
19.29
18.98
15.13
OEt
H
N
iPr
CO2Me
ppm

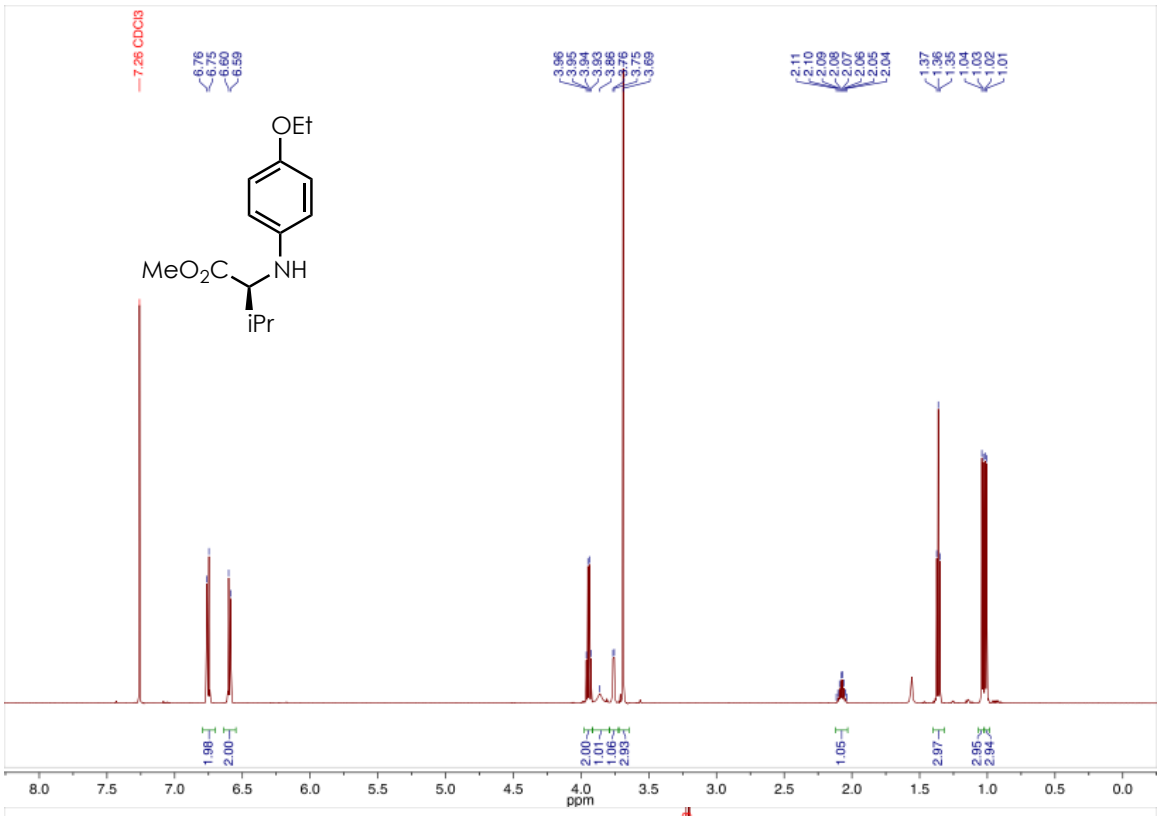
7.26 CDCl3
6.76
6.75
6.60
6.59
3.96
3.95
3.94
3.93
3.86
3.76
3.75
3.69
2.11
2.10
2.09
2.08
2.07
2.06
2.05
2.04
1.37
1.36
1.35
1.04
1.03
1.02
1.01
OEt
MeO2C
NH
iPr
1.98
2.00
2.00
1.01
1.06
2.93
1.05
2.97
2.95
2.94
ppm

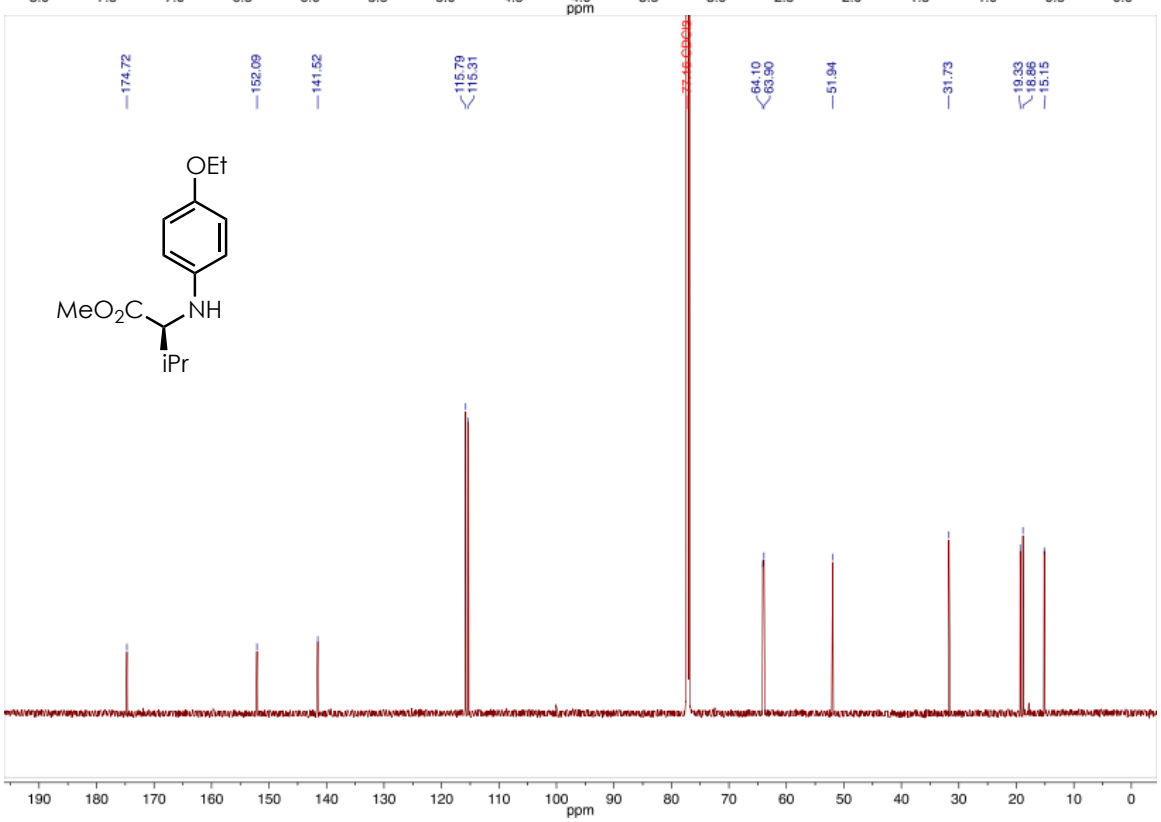
174.72
152.09
141.52
115.79
115.31
77.46 CDCl3
64.10
63.90
51.94
31.73
19.33
18.86
15.15
OEt
MeO2C
NH
iPr
ppm

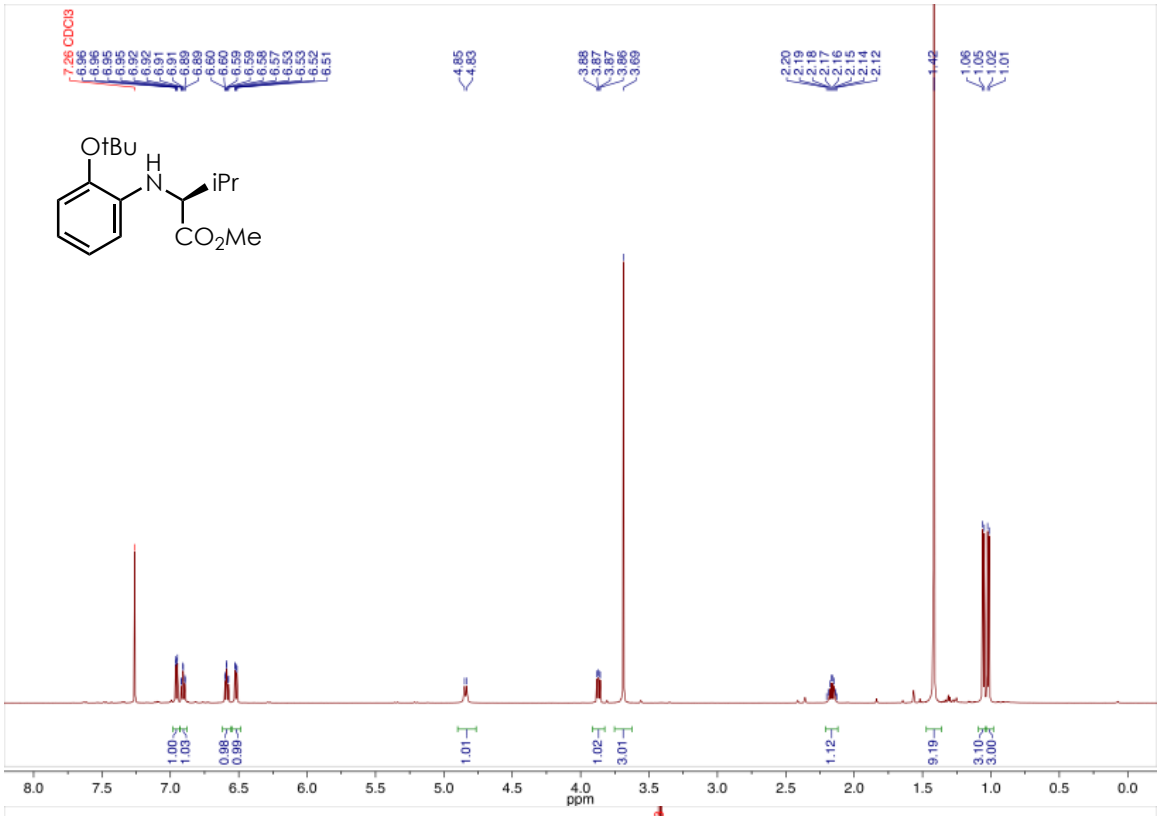
OtBu
H
N
iPr
CO2Me
7.26 CDCl3
6.96
6.95
6.92
6.91
6.89
6.60
6.59
6.58
6.57
6.53
6.52
6.51
4.85
4.83
3.88
3.87
3.86
3.69
2.20
2.19
2.18
2.17
2.16
2.15
2.14
2.12
1.42
1.06
1.05
1.02
1.01
1.00
1.03
0.98
0.99
1.01
1.02
3.01
1.12
9.19
3.10
3.00
ppm

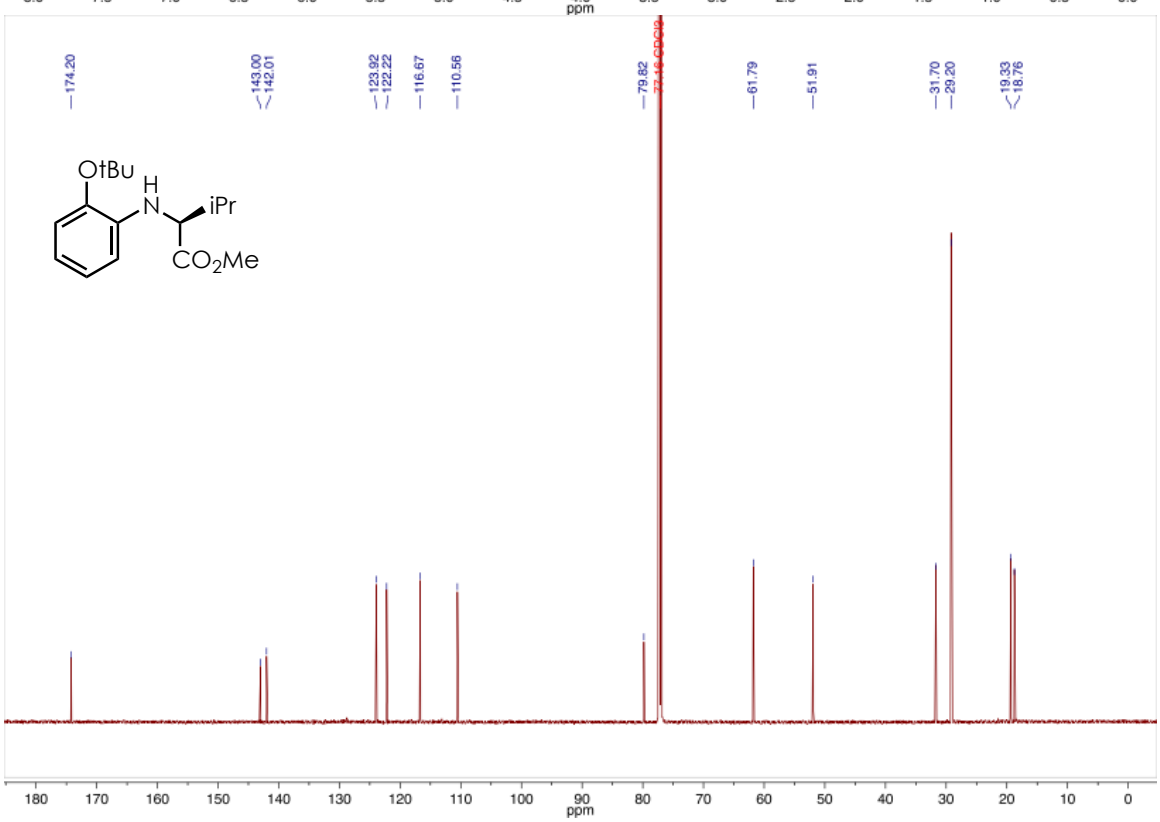
OtBu
H
N
iPr
CO2Me
174.20
143.00
142.01
123.92
122.22
116.67
110.56
79.82
77.16 CDCl3
61.79
51.91
31.70
29.20
19.33
18.76
ppm

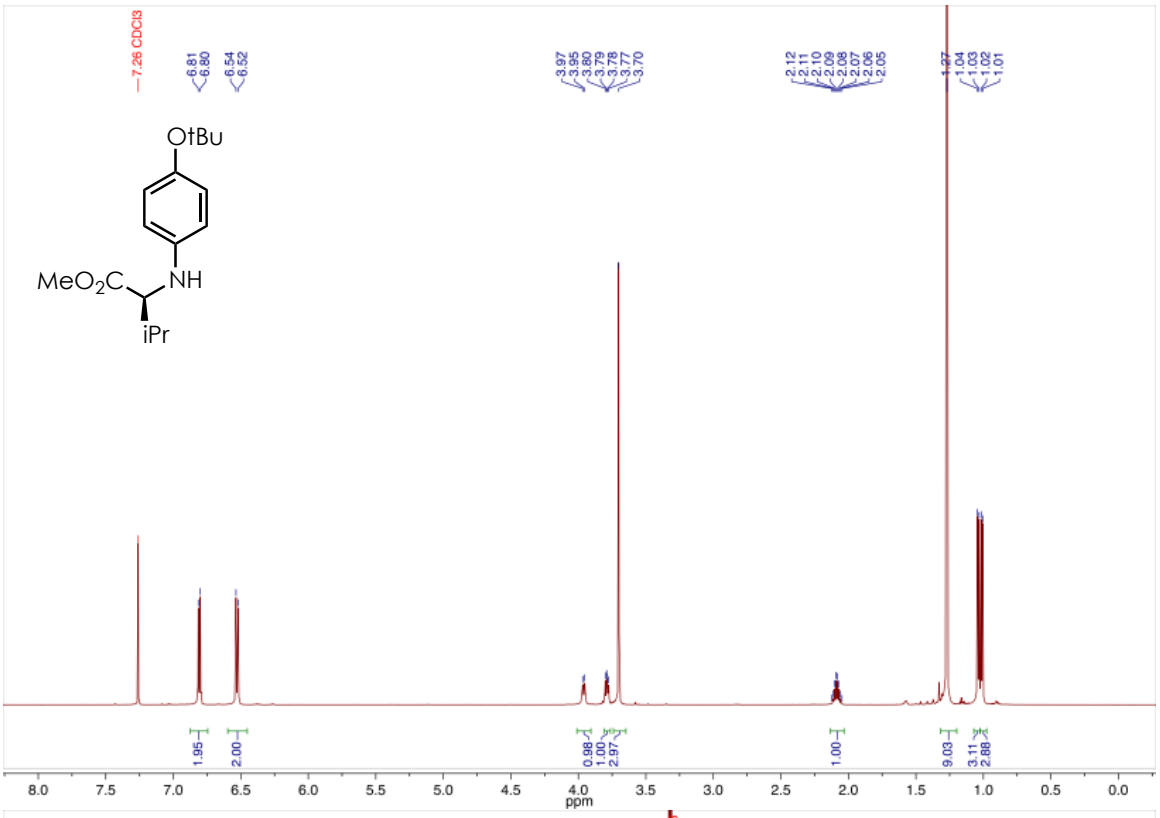
7.26 CDCl3
6.81
6.80
6.54
6.52
3.97
3.95
3.90
3.79
3.78
3.77
3.70
2.12
2.11
2.10
2.09
2.08
2.07
2.06
2.05
1.97
1.04
1.03
1.02
1.01
OtBu
MeO2C
NH
iPr
1.95
2.00
0.98
1.00
2.97
1.00
9.03
3.11
2.88
8.0
7.5
7.0
6.5
6.0
5.5
5.0
4.5
4.0
3.5
3.0
2.5
2.0
1.5
1.0
0.5
0.0
ppm

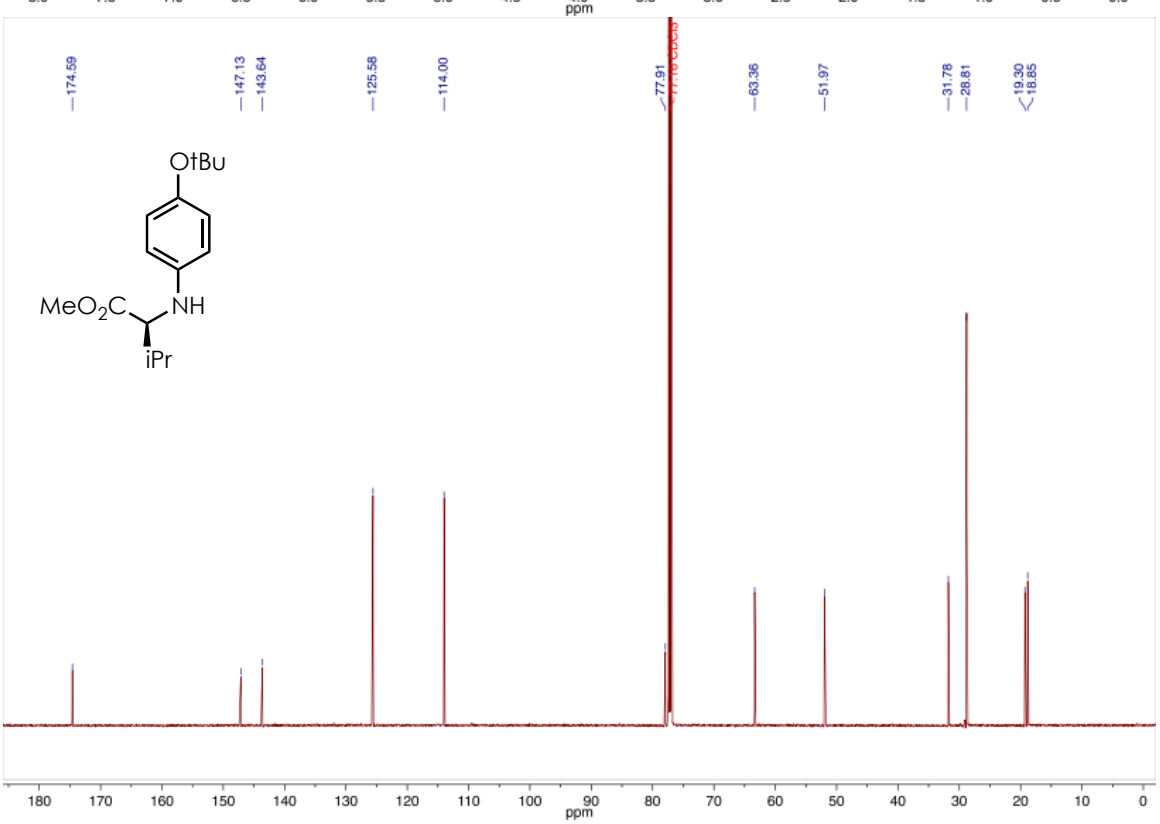
174.59
147.13
143.64
125.58
114.00
77.91
77.16 CDCl3
63.36
51.97
31.78
28.81
19.30
18.85
OtBu
MeO2C
NH
iPr
180
170
160
150
140
130
120
110
100
90
80
70
60
50
40
30
20
10
0
ppm

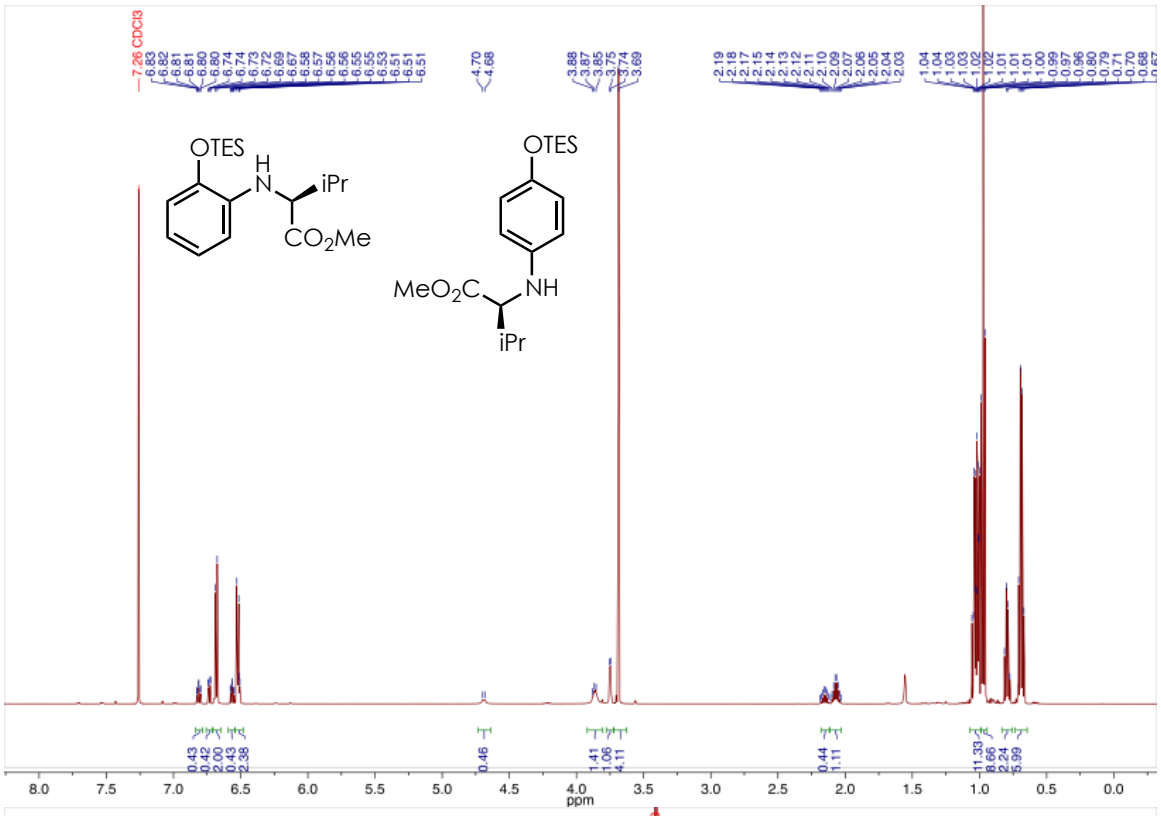
OTES
H
N
iPr
CO2Me
OTES
MeO2C
NH
iPr

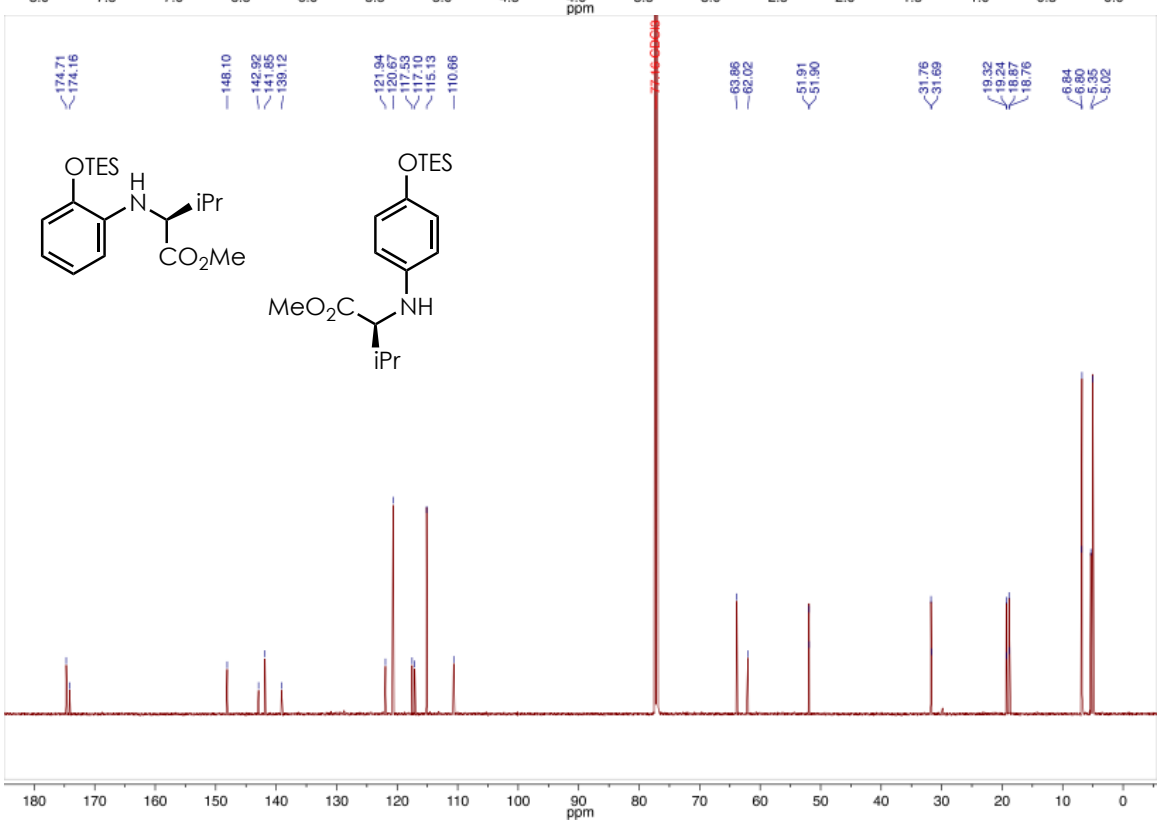
OTES
H
N
iPr
CO2Me
OTES
MeO2C
NH
iPr

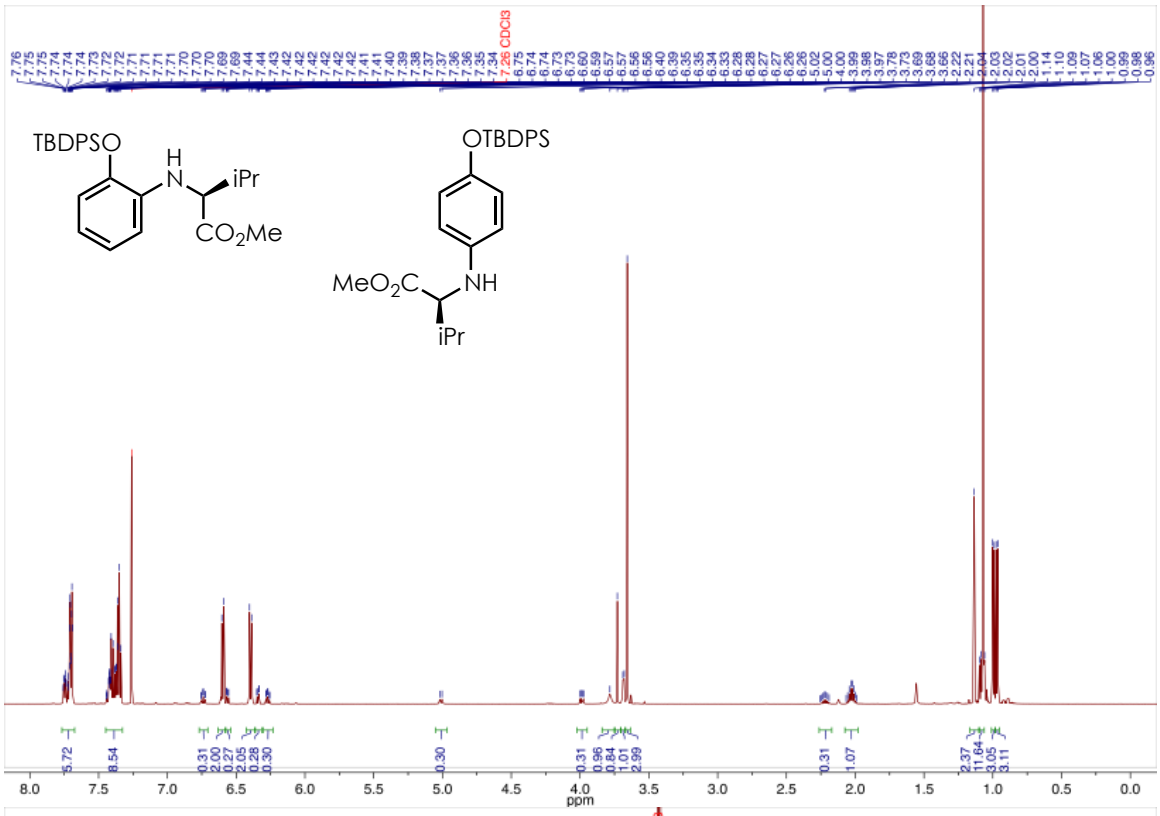
TBDPSO
H
N
iPr
CO2Me
OTBDPS
MeO2C
NH
iPr
ppm

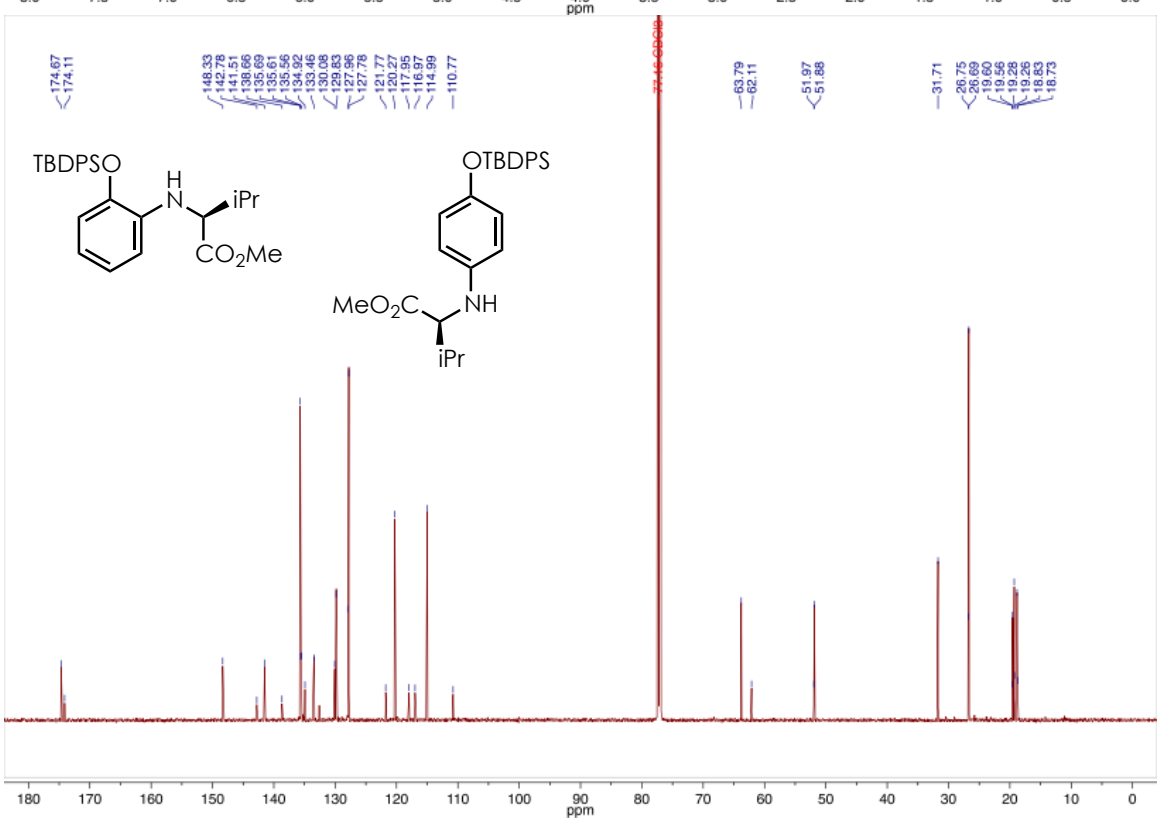
TBDPSO
H
N
iPr
CO2Me
OTBDPS
MeO2C
NH
iPr
ppm

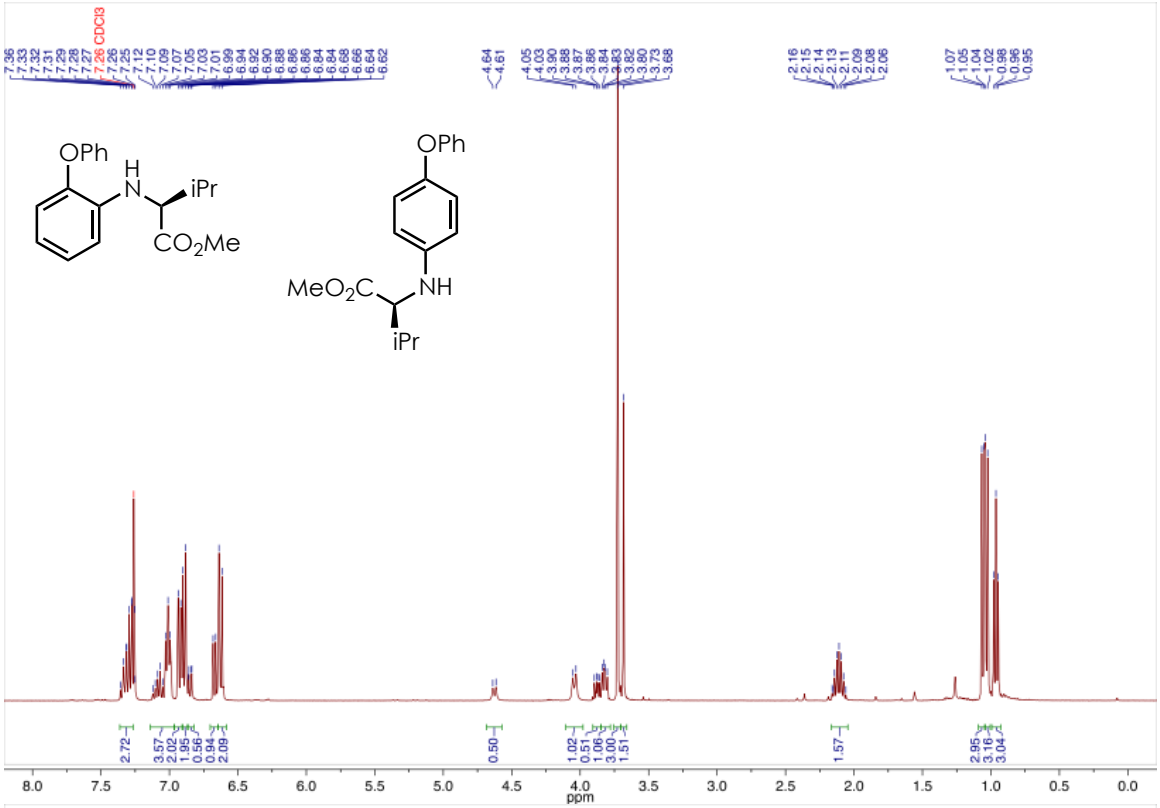
OPh
H
N
iPr
CO2Me
OPh
MeO2C
NH
iPr
ppm

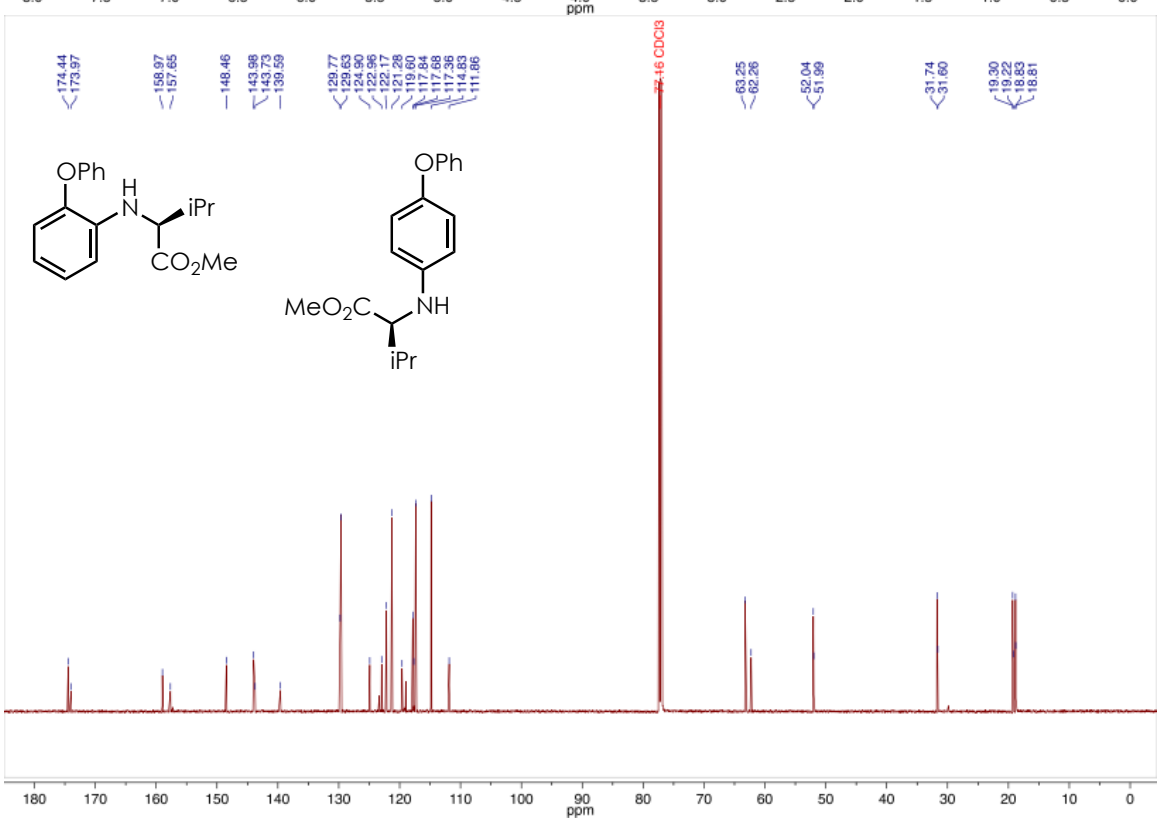
OPh
H
N
iPr
CO2Me
OPh
MeO2C
NH
iPr
77.16 CDCl3
ppm

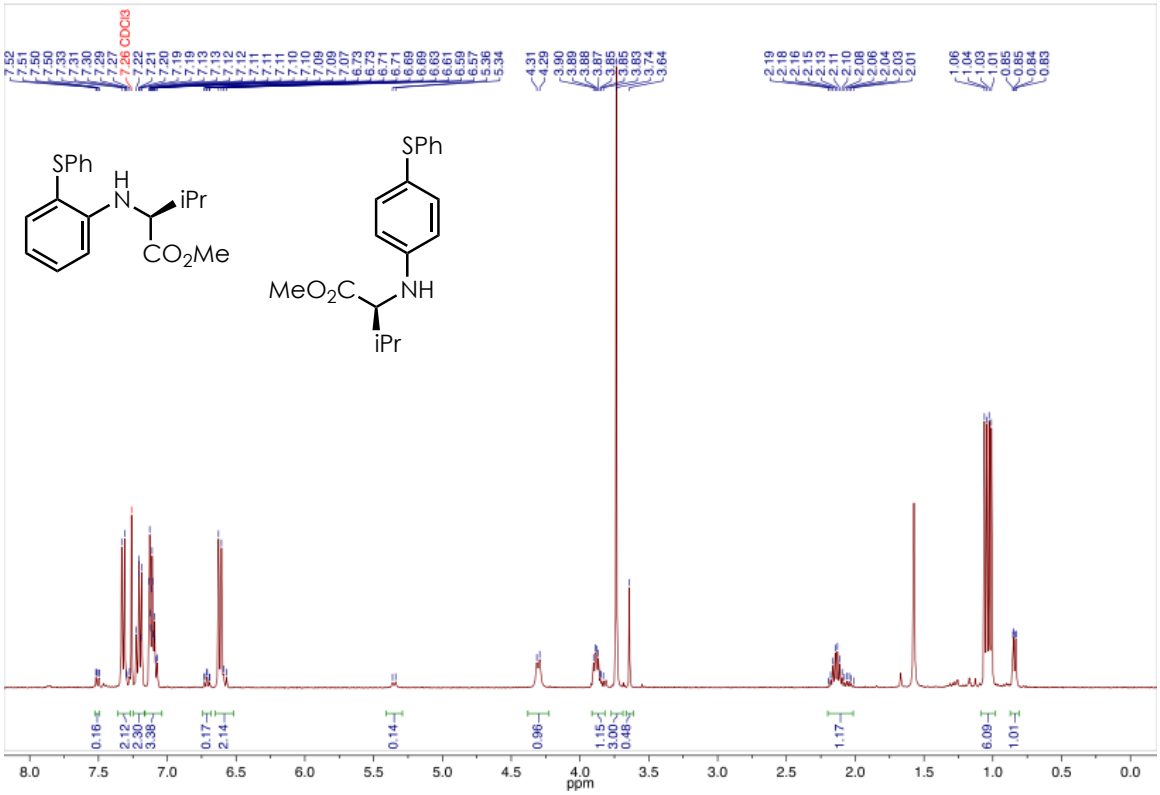
SPh
H
N
iPr
CO2Me
SPh
MeO2C
NH
iPr
ppm

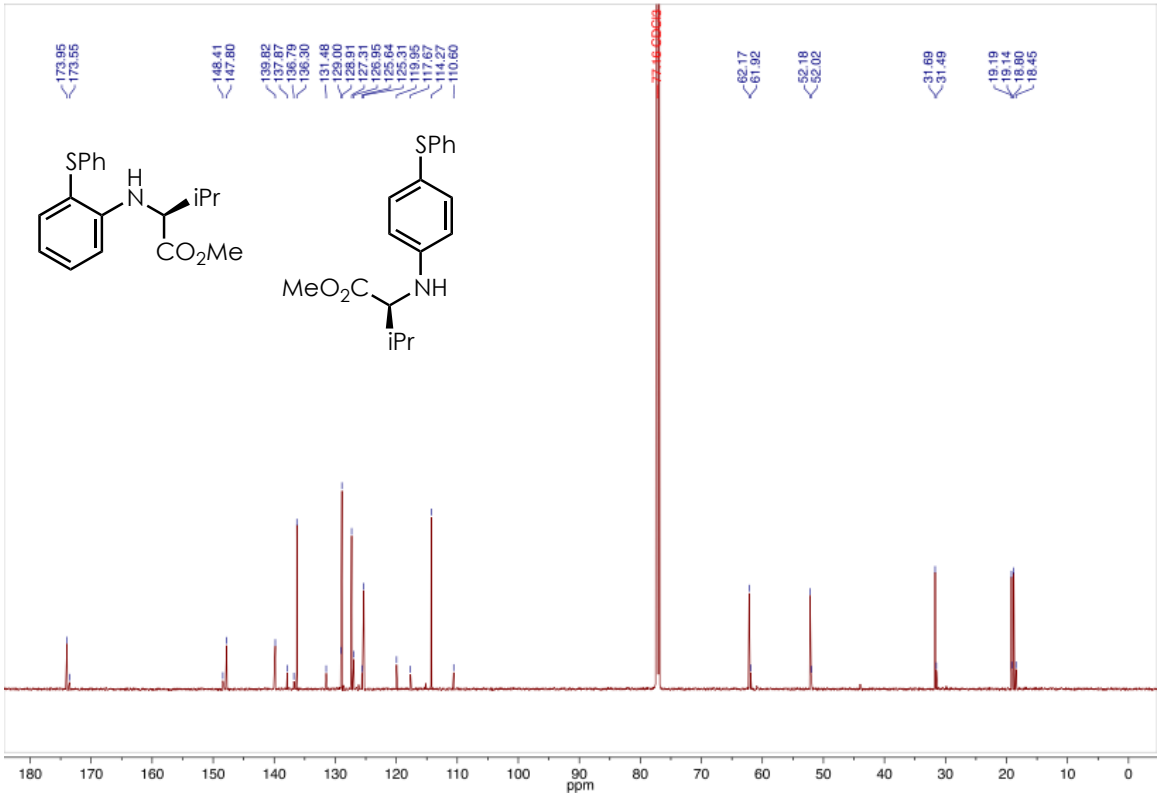
SPh
H
N
iPr
CO2Me
SPh
MeO2C
NH
iPr
ppm

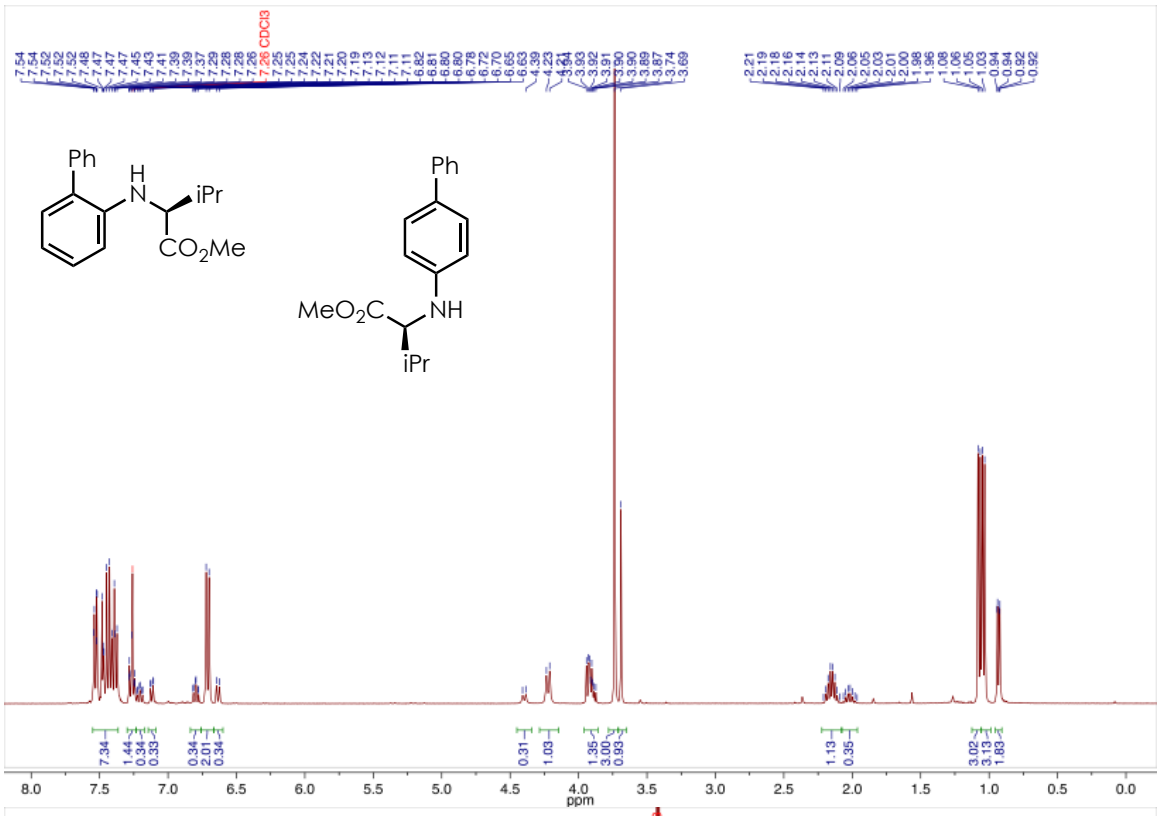
Ph
H
N
iPr
CO2Me
Ph
MeO2C
NH
iPr
ppm

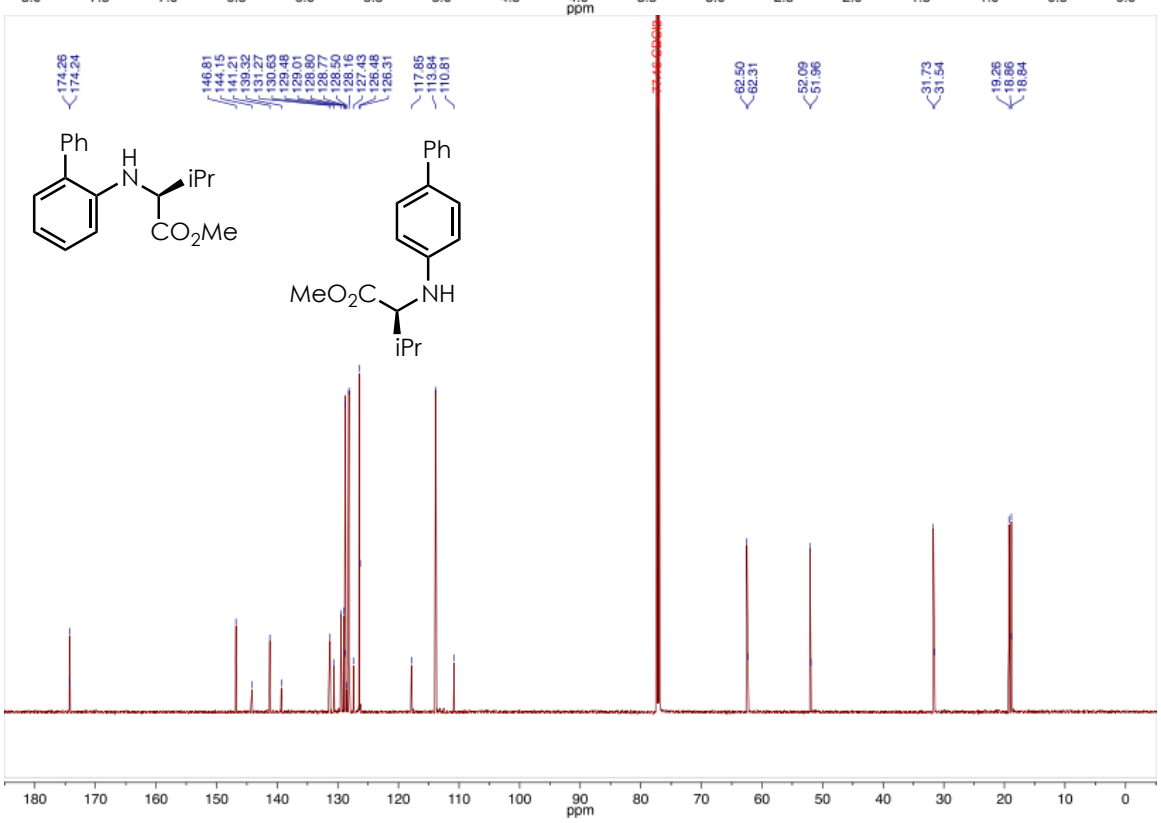
Ph
H
N
iPr
CO2Me
Ph
MeO2C
NH
iPr
ppm

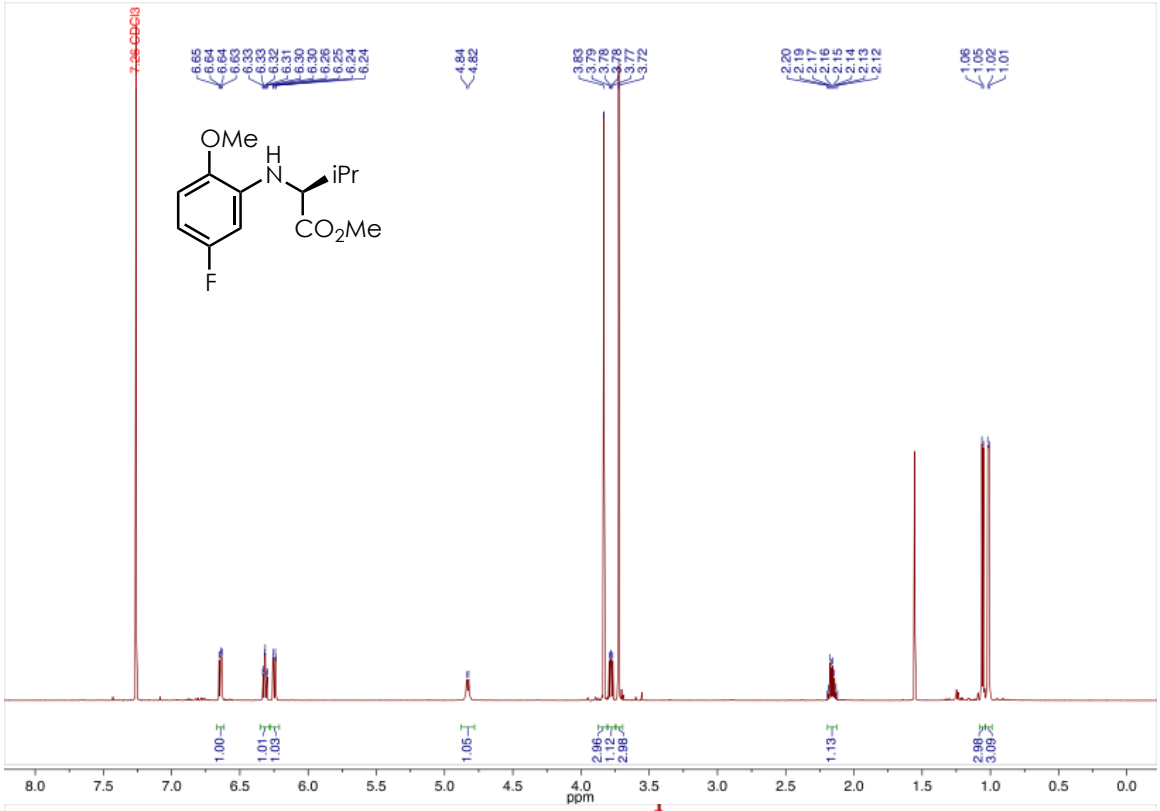
OMe
H
N
iPr
CO2Me
F

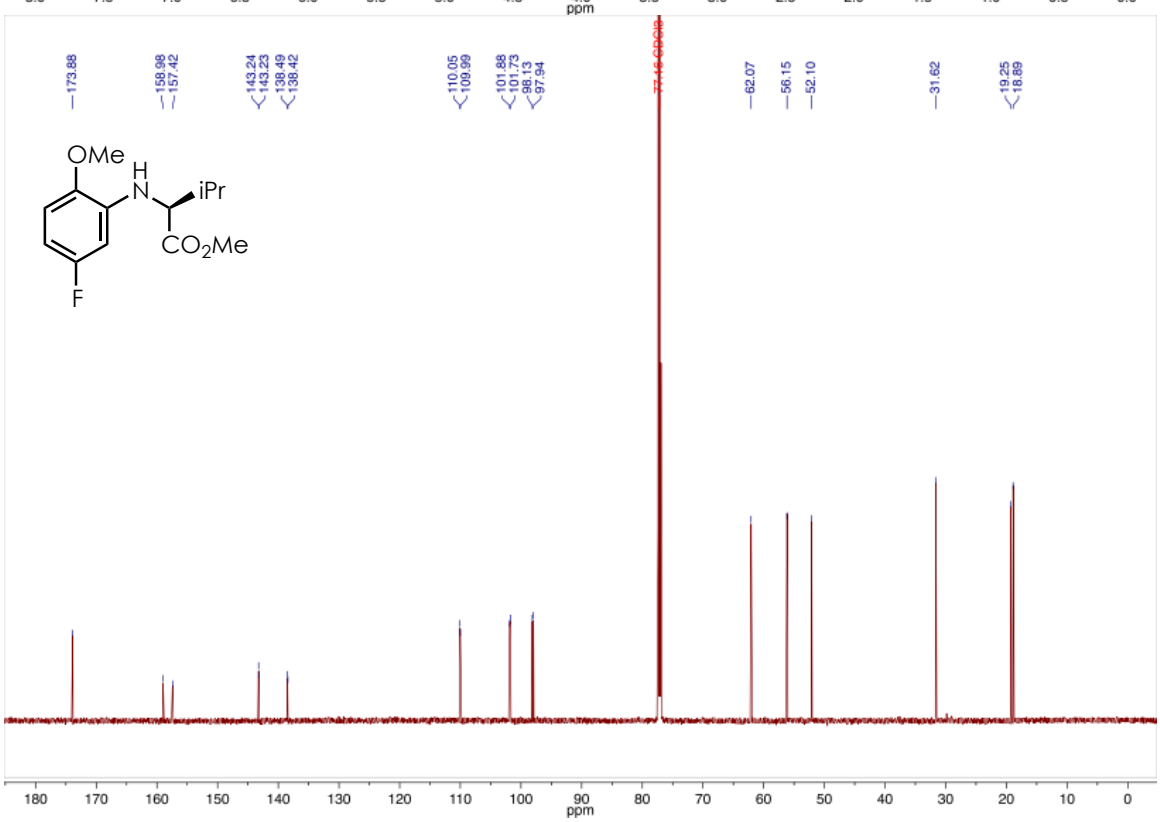
OMe
H
N
iPr
CO2Me
F

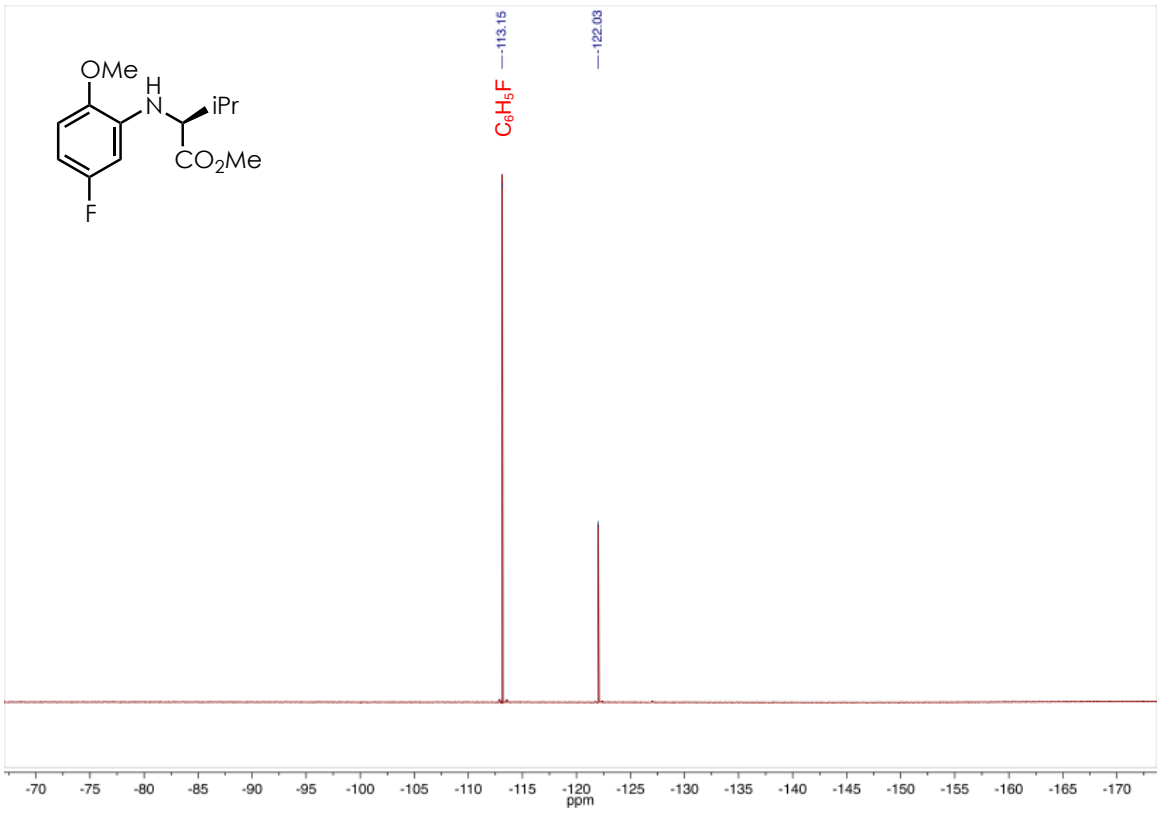
OMe
H
N
iPr
CO2Me
F
C6H5F
-113.15
-122.03
-70 -75 -80 -85 -90 -95 -100 -105 -110 -115 -120 -125 -130 -135 -140 -145 -150 -155 -160 -165 -170
ppm

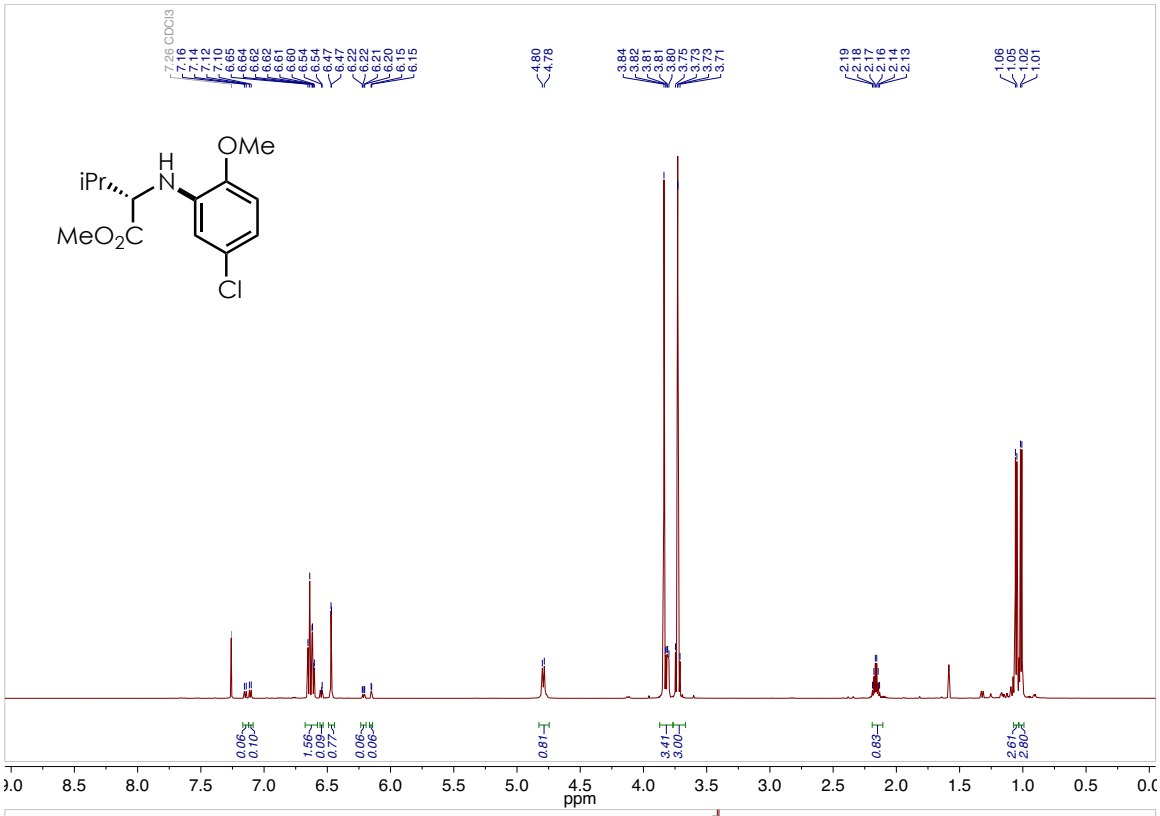
7.26 CDCl3
7.16
7.14
7.12
7.10
6.65
6.64
6.62
6.61
6.60
6.54
6.54
6.47
6.47
6.22
6.21
6.20
6.15
6.15
4.80
4.78
3.84
3.82
3.81
3.81
3.80
3.75
3.73
3.73
3.71
2.19
2.18
2.17
2.16
2.14
2.13
1.06
1.05
1.02
1.01
OMe
H
N
iPr
MeO2C
Cl
0.06
0.10
1.56
0.09
0.77
0.06
0.06
0.81
3.41
3.00
0.83
2.61
2.80
ppm

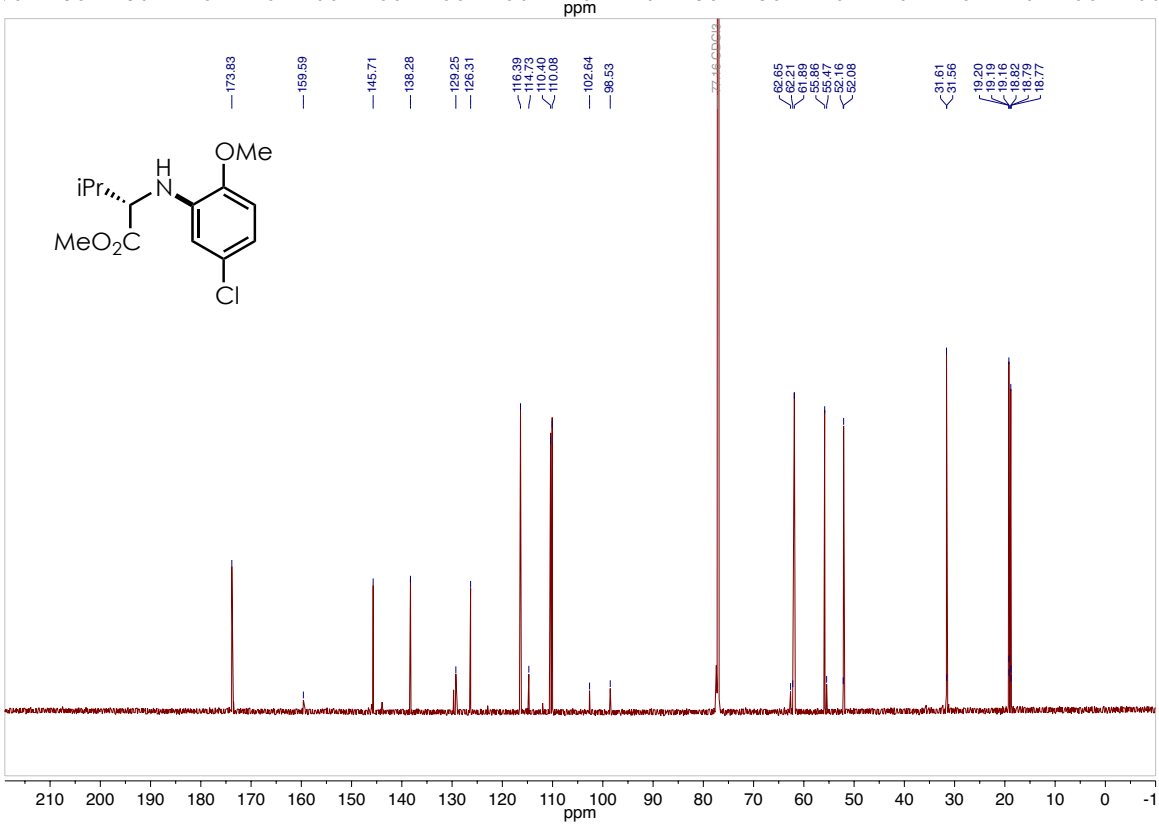
173.83
159.59
145.71
138.28
129.25
126.31
116.39
114.73
110.40
110.08
102.64
98.53
77.16 CDCl3
62.65
62.21
61.89
55.86
55.47
52.16
52.08
31.61
31.56
19.20
19.19
19.16
18.82
18.79
18.77
OMe
H
N
iPr
MeO2C
Cl
ppm

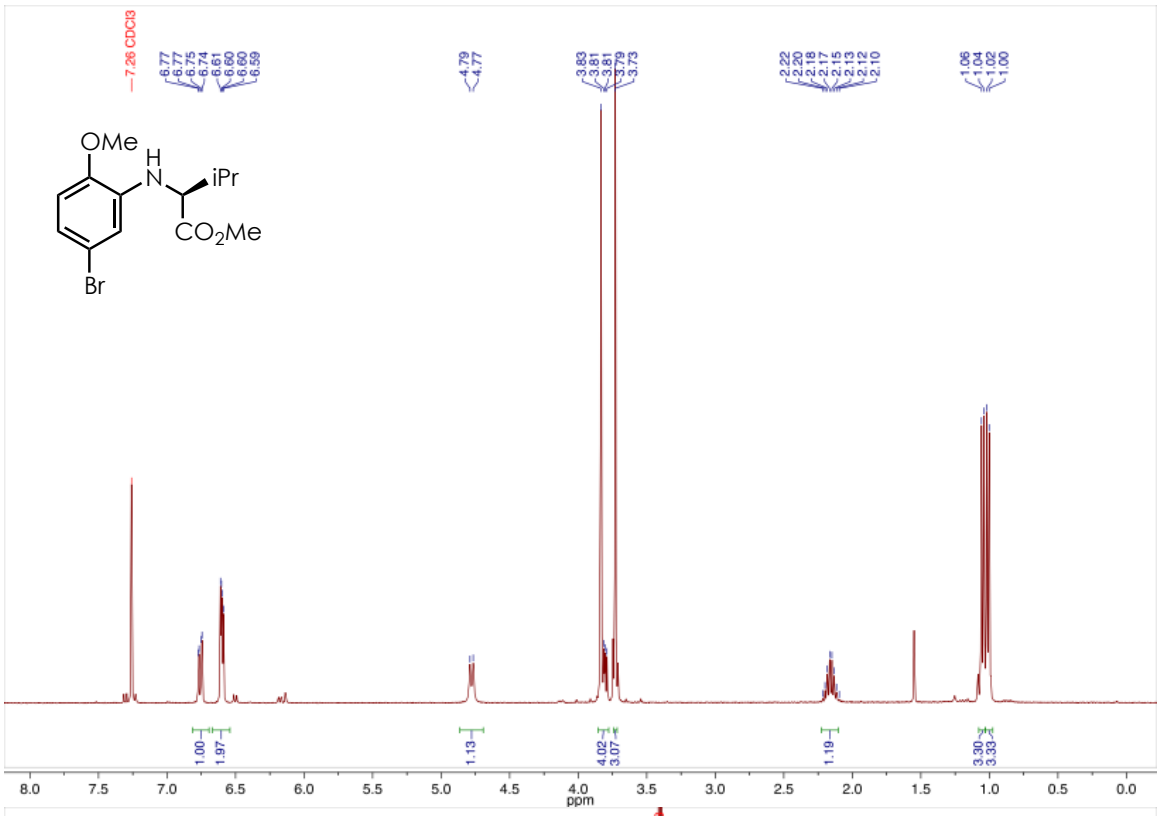
7.26 CDCl3
6.77
6.77
6.75
6.74
6.61
6.60
6.60
6.59
4.79
4.77
3.83
3.81
3.81
3.79
3.73
2.22
2.20
2.18
2.17
2.15
2.13
2.12
2.10
1.06
1.04
1.02
1.00
OMe
H
N
iPr
CO2Me
Br
1.00
1.97
1.13
4.02
3.07
1.19
3.30
3.33
ppm

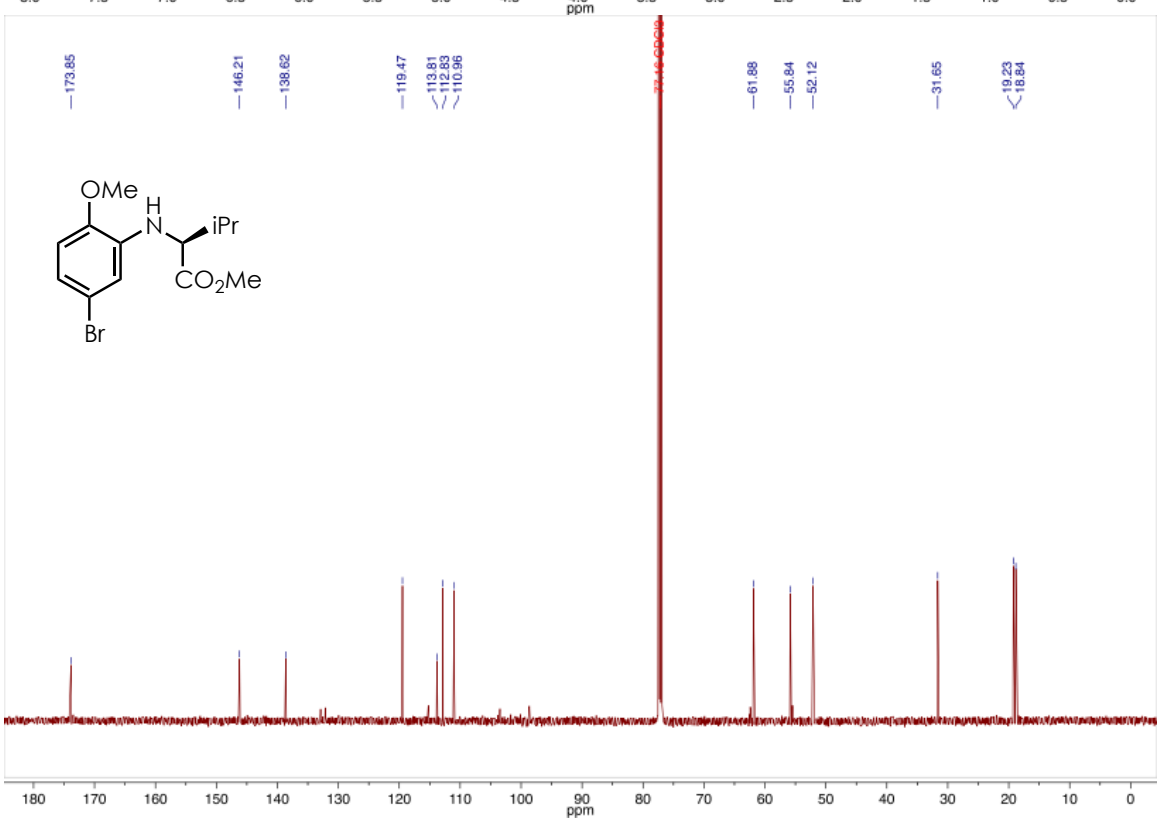
173.85
146.21
138.62
119.47
113.81
112.83
110.96
77.16 CDCl3
61.88
55.84
52.12
31.65
19.23
18.84
OMe
H
N
iPr
CO2Me
Br
ppm

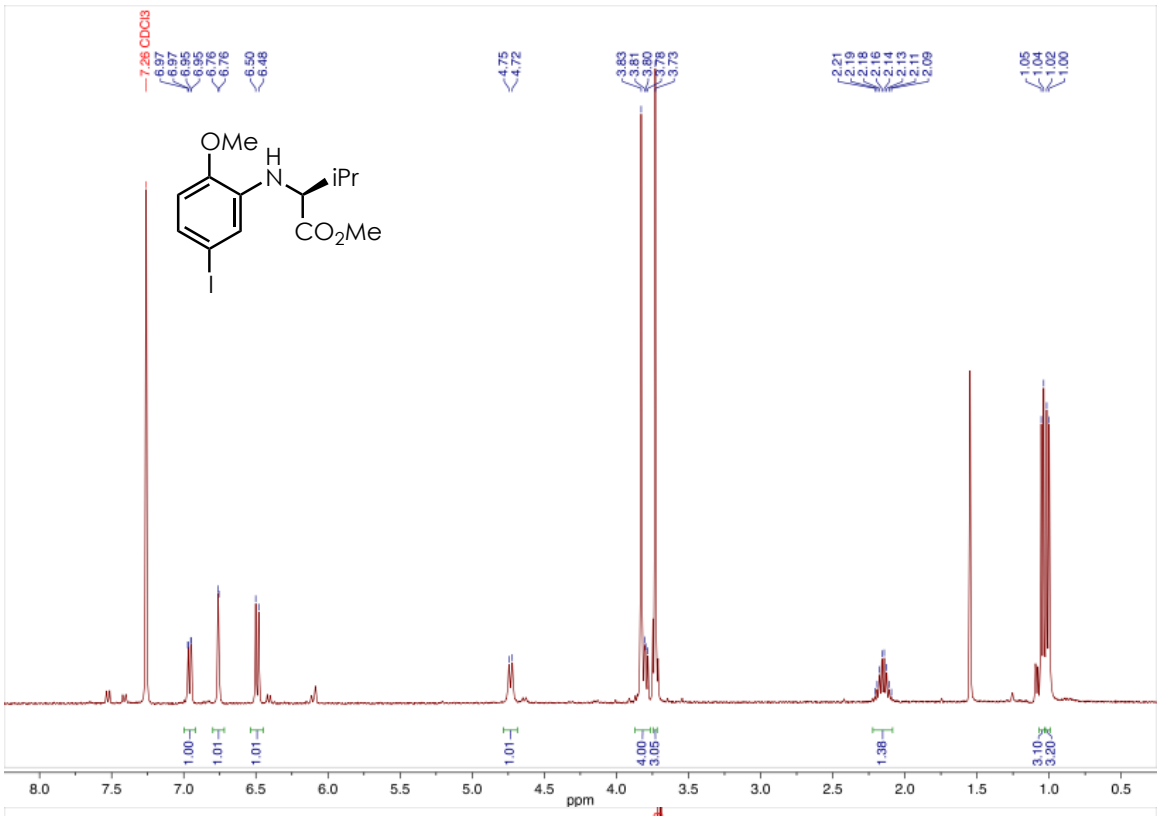
7.26 CDCl3
6.97
6.97
6.95
6.95
6.76
6.76
6.50
6.48
4.75
4.72
3.83
3.81
3.80
3.78
3.73
2.21
2.19
2.18
2.16
2.14
2.13
2.11
2.09
1.05
1.04
1.02
1.00
OMe
H
N
iPr
CO2Me
I
1.00
1.01
1.01
1.01
4.00
3.05
1.38
3.10
3.20
ppm

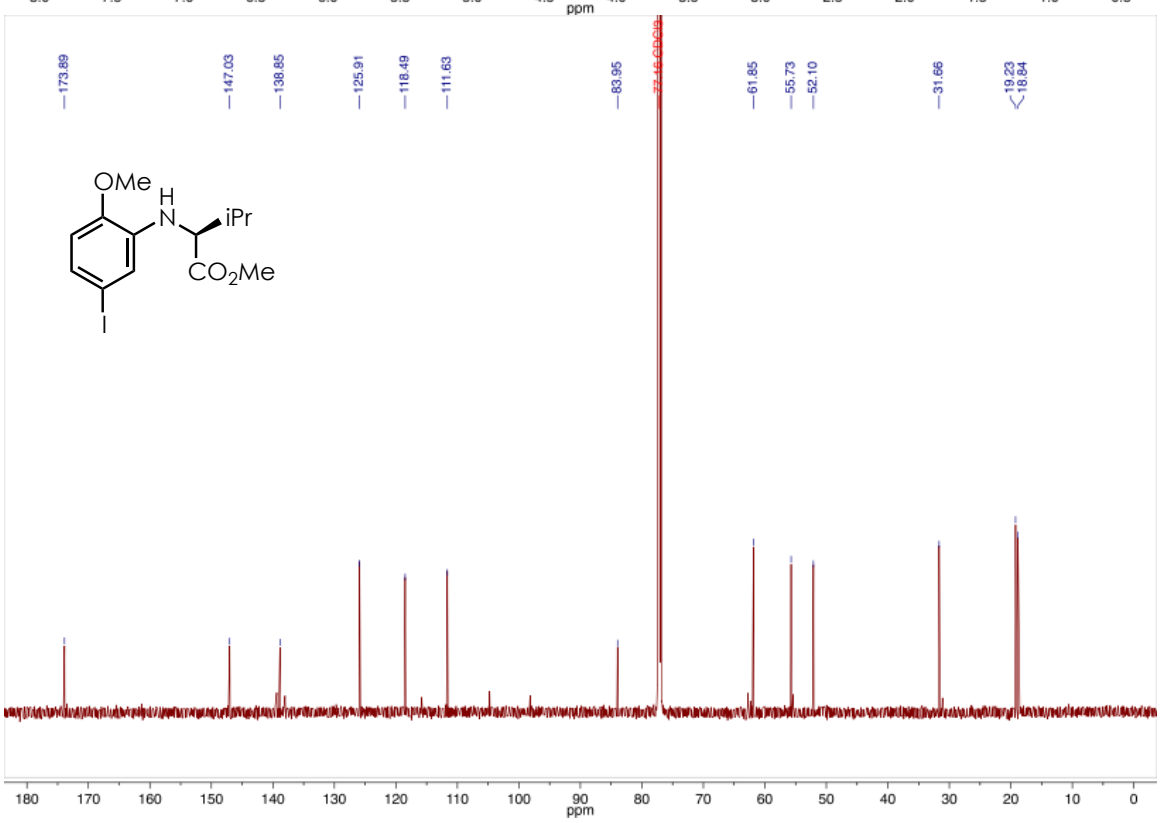
173.89
147.03
138.85
125.91
118.49
111.63
83.95
77.16 CDCl3
61.85
55.73
52.10
31.66
19.23
18.84
OMe
H
N
iPr
CO2Me
I
ppm

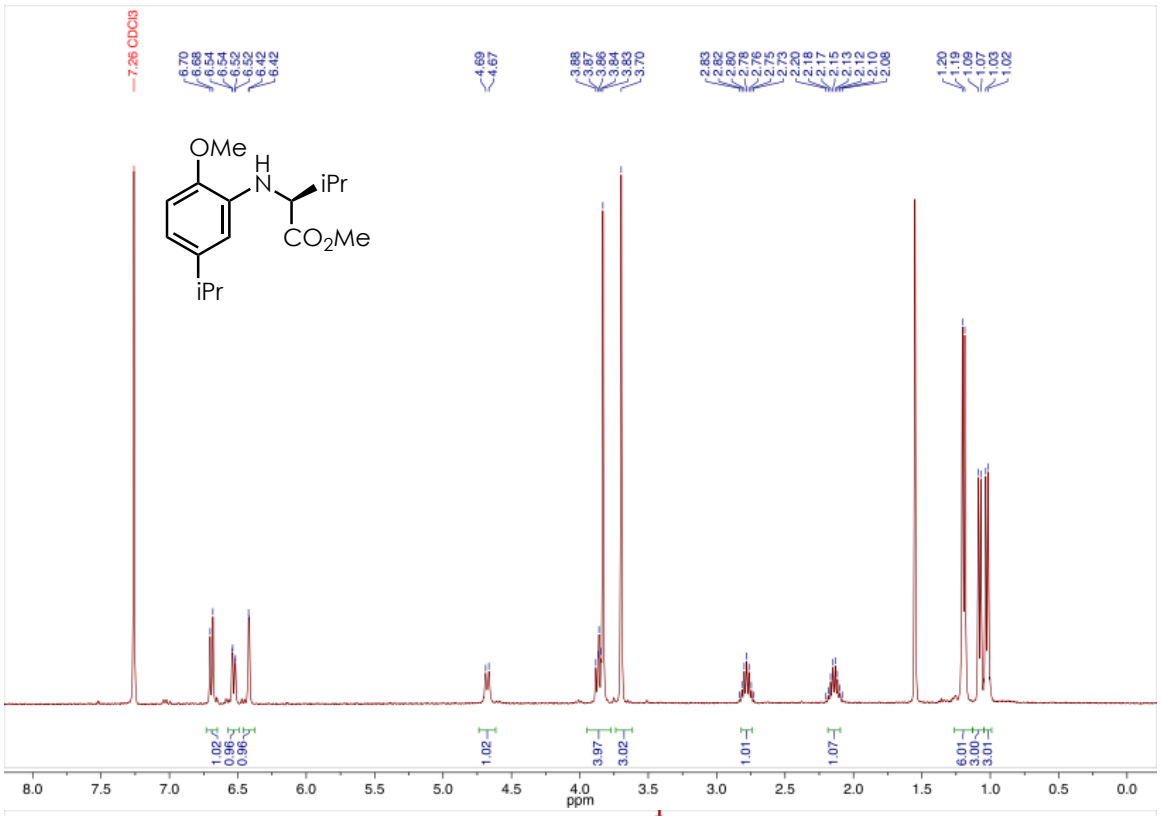
7.26 CDCl3
6.70
6.68
6.54
6.54
6.52
6.52
6.42
6.42
4.69
4.67
3.88
3.87
3.86
3.84
3.83
3.70
2.83
2.82
2.80
2.78
2.76
2.75
2.73
2.20
2.18
2.17
2.15
2.13
2.12
2.10
2.08
1.20
1.19
1.09
1.07
1.03
1.02
OMe
H
N
iPr
CO2Me
iPr
1.02
0.96
0.96
1.02
3.97
3.02
1.01
1.07
6.01
3.00
3.01
8.0
7.5
7.0
6.5
6.0
5.5
5.0
4.5
4.0
3.5
3.0
2.5
2.0
1.5
1.0
0.5
0.0
ppm

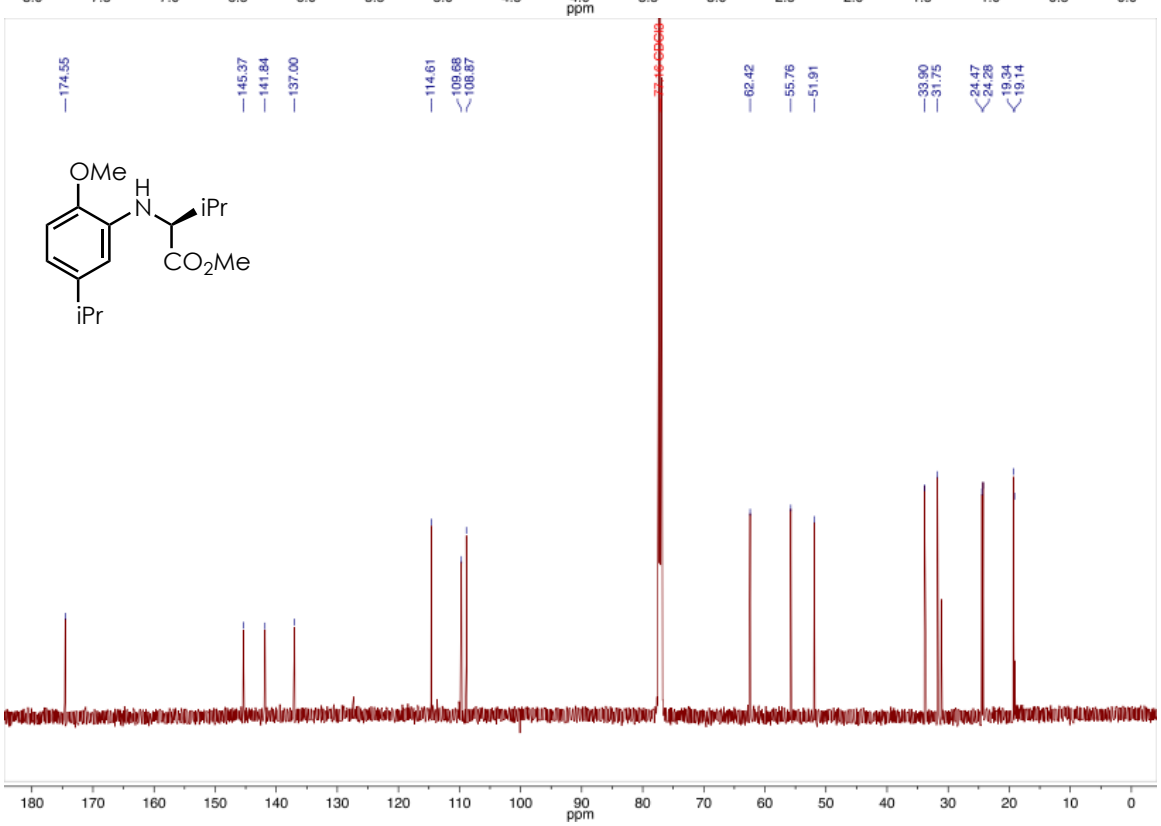
174.55
145.37
141.84
137.00
114.61
109.68
108.87
77.16 CDCl3
62.42
55.76
51.91
33.90
31.75
24.47
24.28
19.34
19.14
OMe
H
N
iPr
CO2Me
iPr
180
170
160
150
140
130
120
110
100
90
80
70
60
50
40
30
20
10
0
ppm

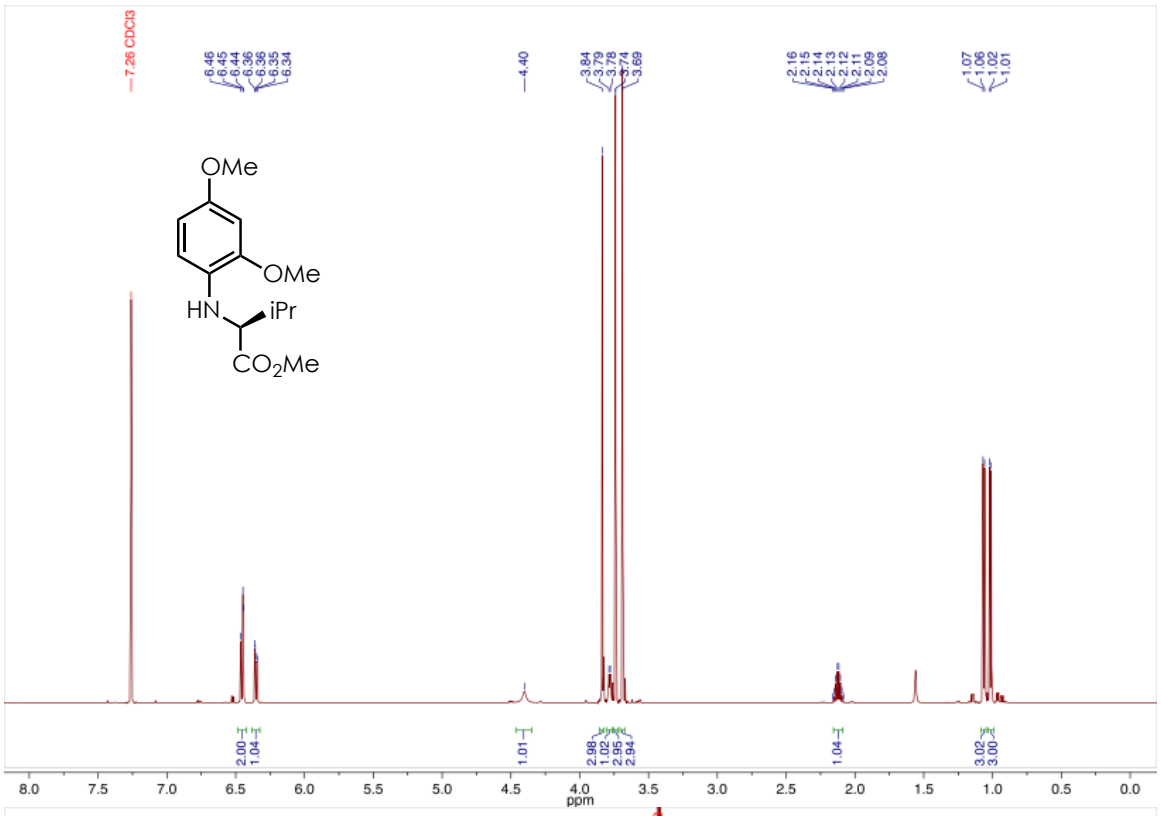
7.26 CDCl3
6.46
6.45
6.44
6.36
6.36
6.35
6.34
4.40
3.84
3.79
3.78
3.74
3.69
2.16
2.15
2.14
2.13
2.12
2.11
2.09
2.08
1.07
1.06
1.02
1.01
OMe
OMe
HN
iPr
CO2Me
2.00
1.04
1.01
2.98
1.02
2.95
2.94
1.04
3.02
3.00
ppm

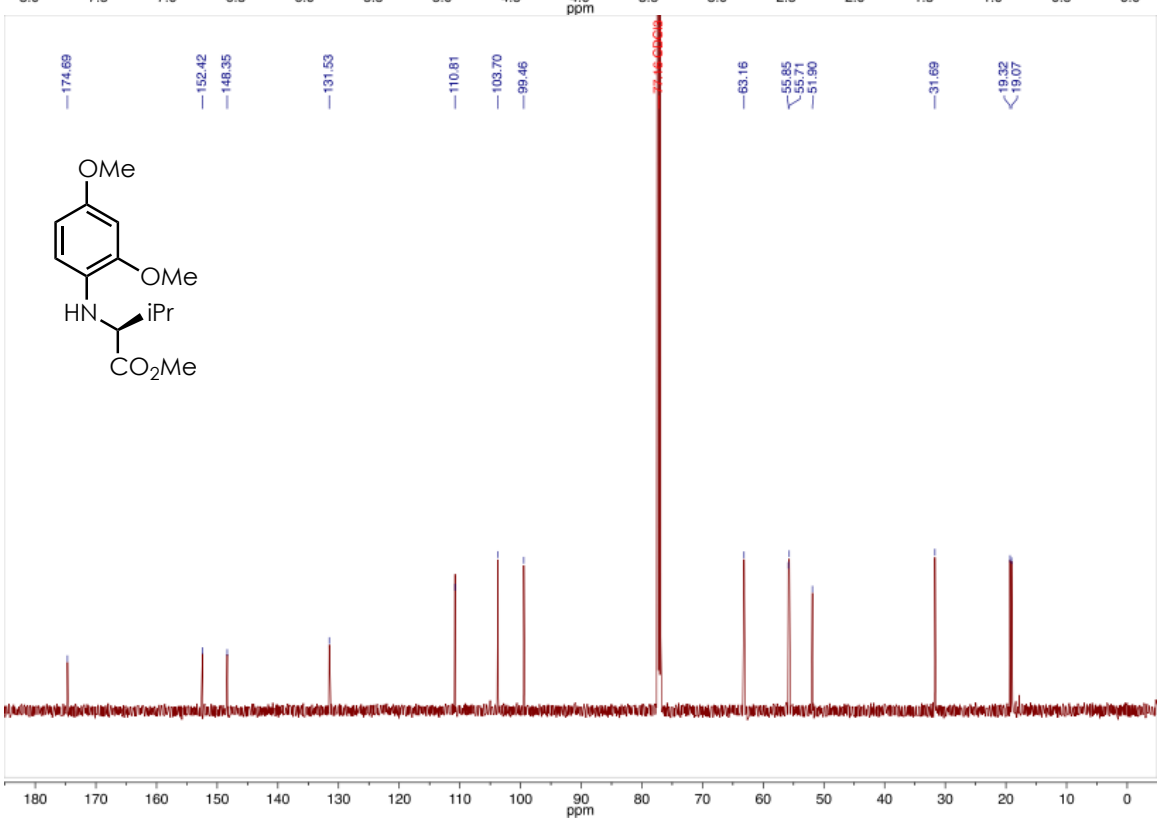
174.69
152.42
148.35
131.53
110.81
103.70
99.46
77.16 CDCl3
63.16
55.85
55.71
51.90
31.69
19.32
19.07
OMe
OMe
HN
iPr
CO2Me
ppm

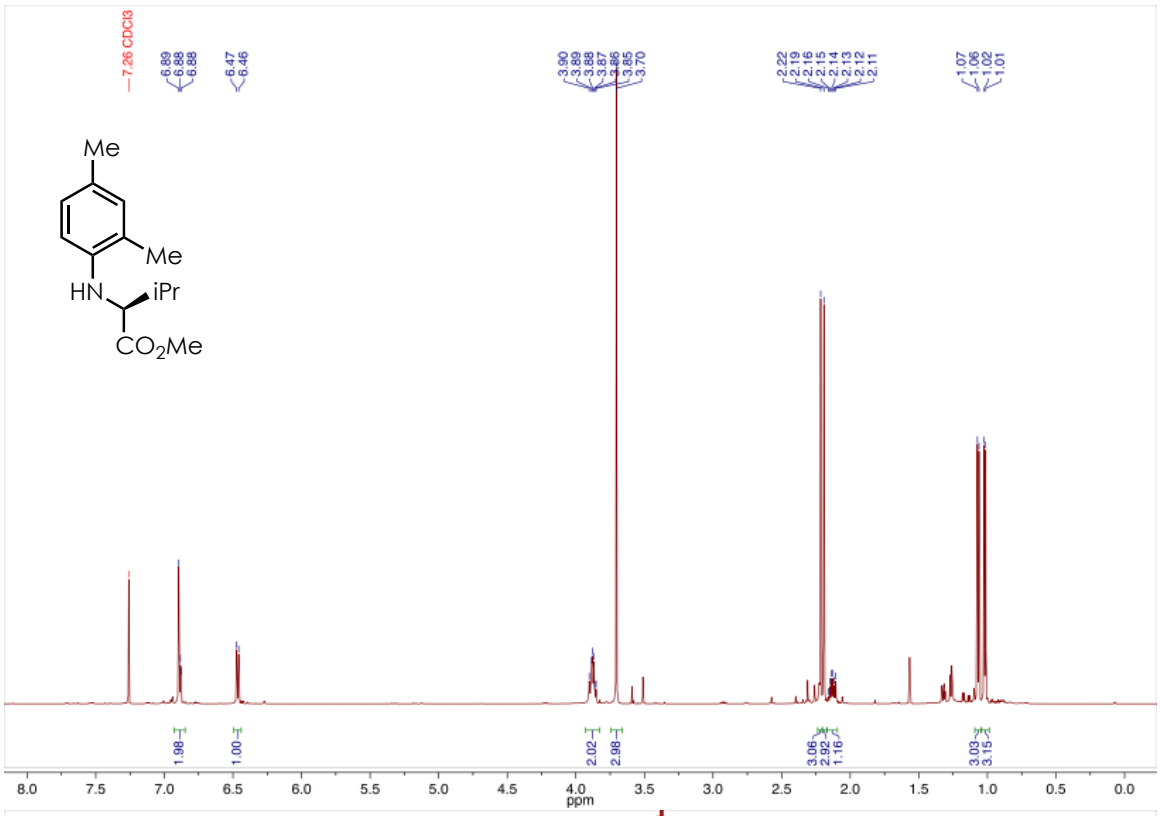
7.26 CDCl3
6.89
6.88
6.88
6.47
6.46
3.90
3.89
3.88
3.87
3.86
3.85
3.70
2.22
2.19
2.16
2.15
2.14
2.13
2.12
2.11
1.07
1.06
1.02
1.01
Me
Me
HN
iPr
CO2Me
1.98
1.00
2.02
2.98
3.06
2.92
1.16
3.03
3.15
8.0
7.5
7.0
6.5
6.0
5.5
5.0
4.5
4.0
3.5
3.0
2.5
2.0
1.5
1.0
0.5
0.0
ppm

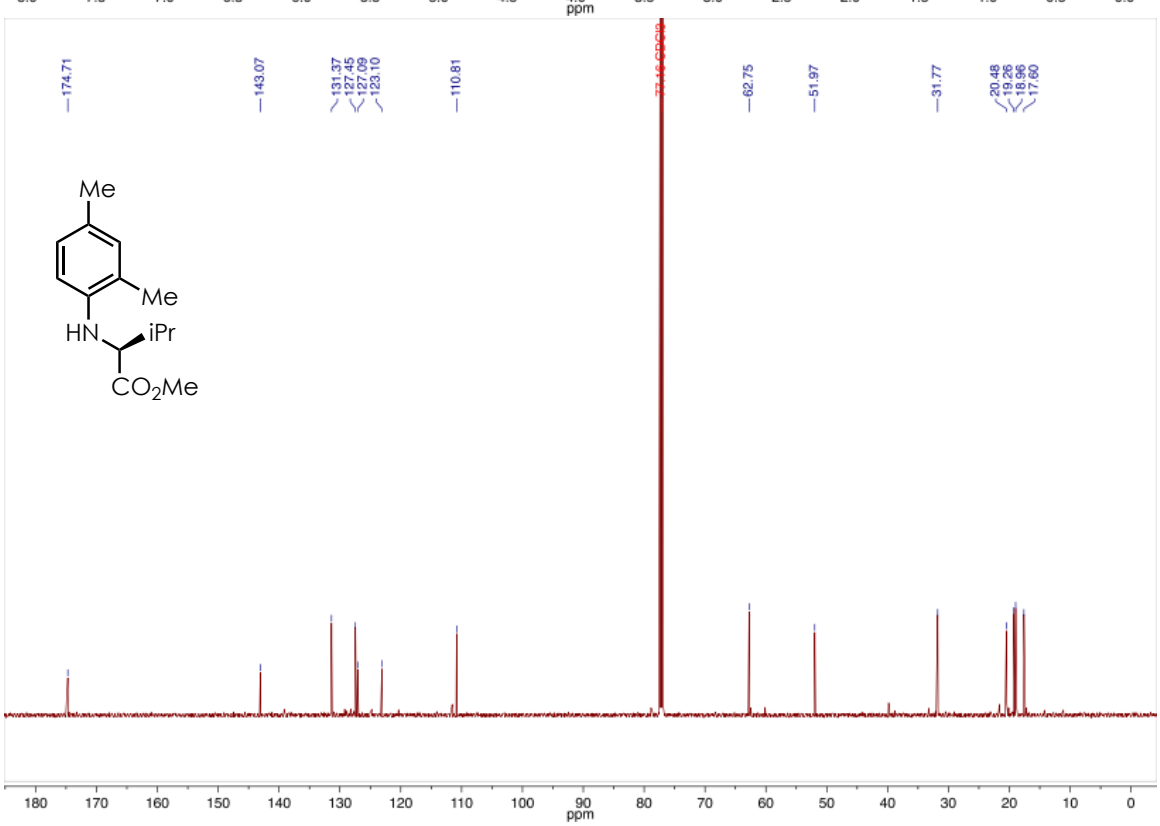
174.71
143.07
131.37
127.45
127.09
123.10
110.81
77.16 CDCl3
62.75
51.97
31.77
20.48
19.26
18.96
17.60
Me
Me
HN
iPr
CO2Me
180
170
160
150
140
130
120
110
100
90
80
70
60
50
40
30
20
10
0
ppm

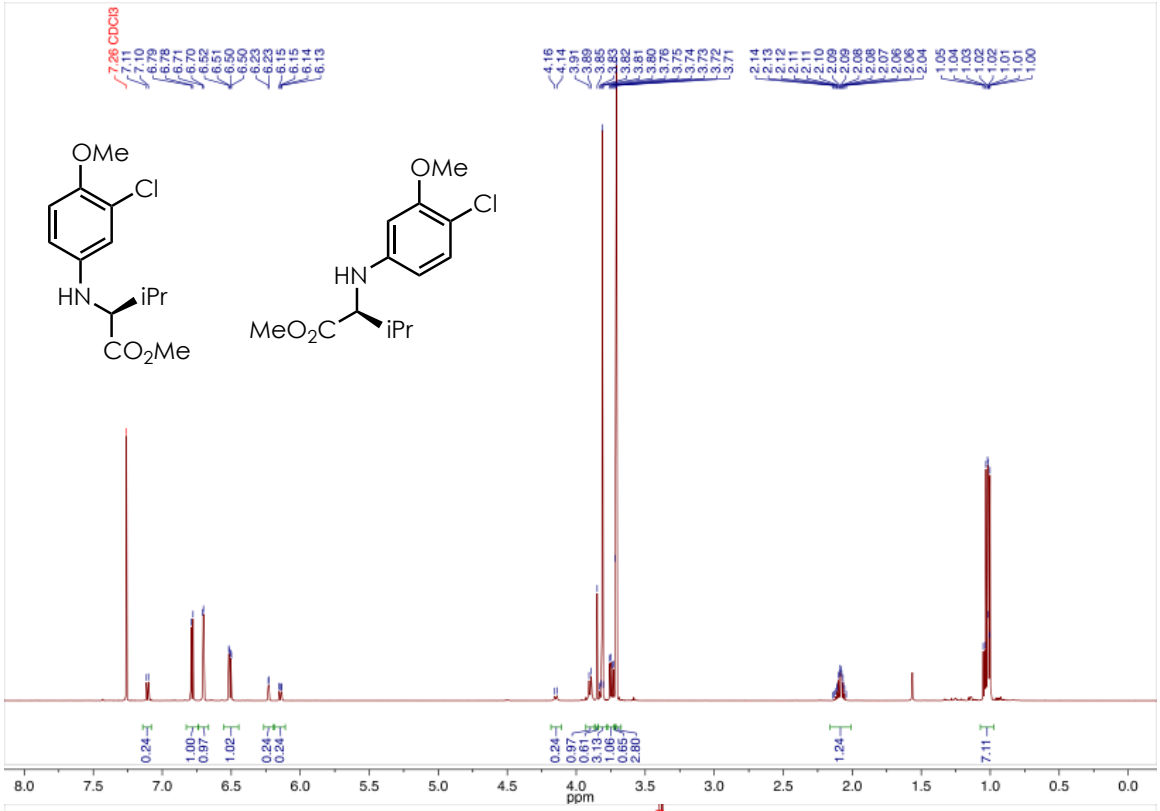
OMe
Cl
HN
iPr
CO2Me
MeO2C
ppm

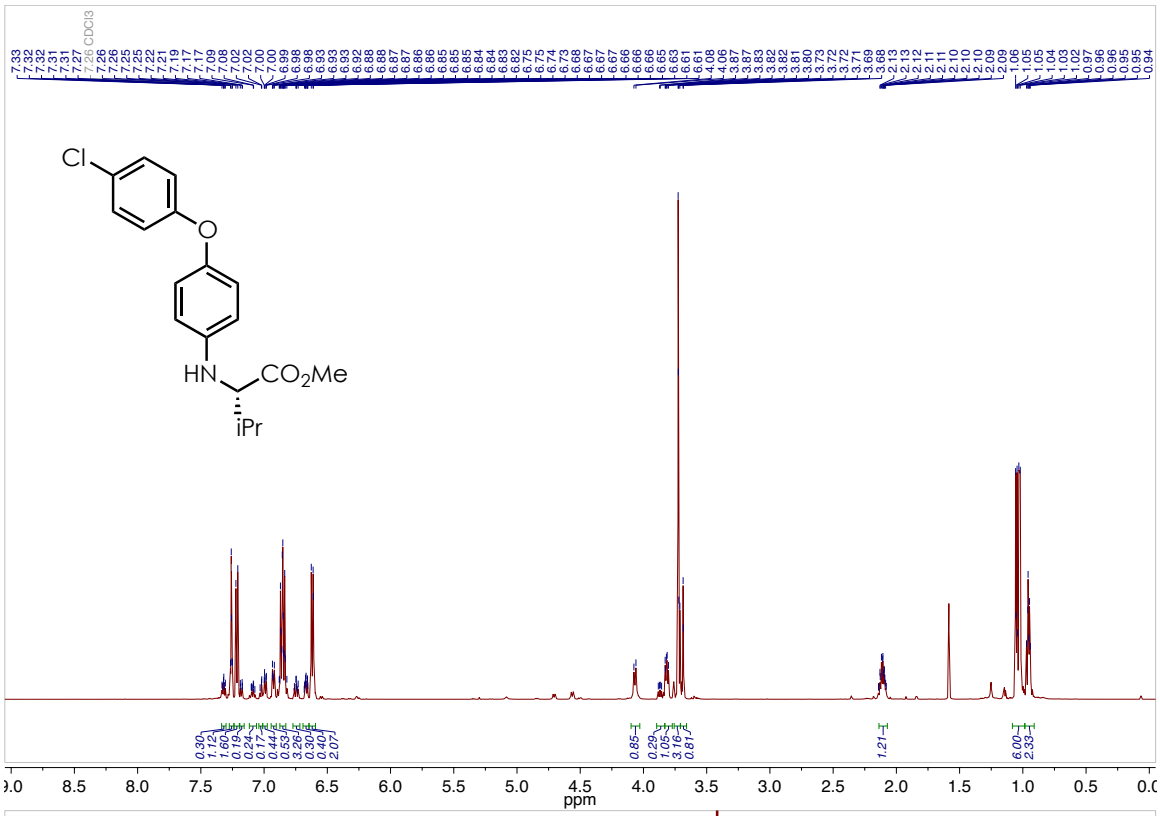
Cl
O
HN
CO2Me
iPr
ppm

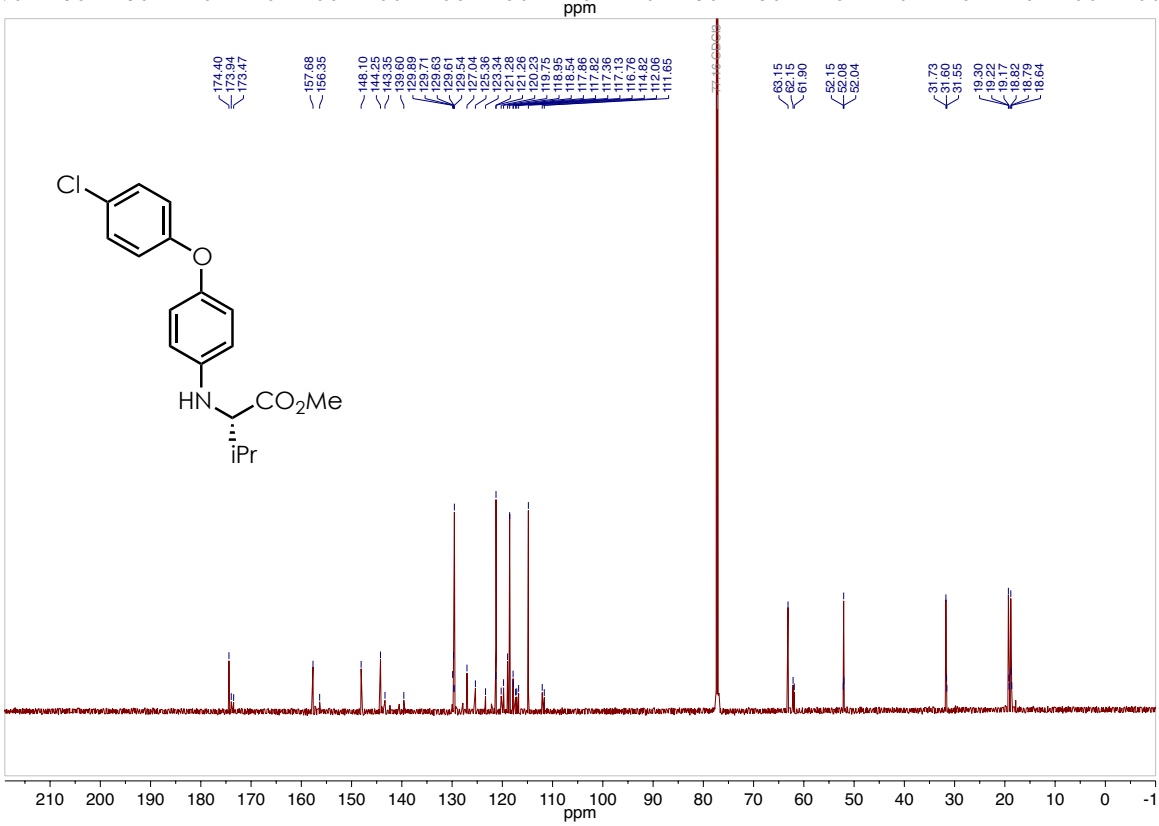
Cl
O
HN
CO2Me
iPr
ppm

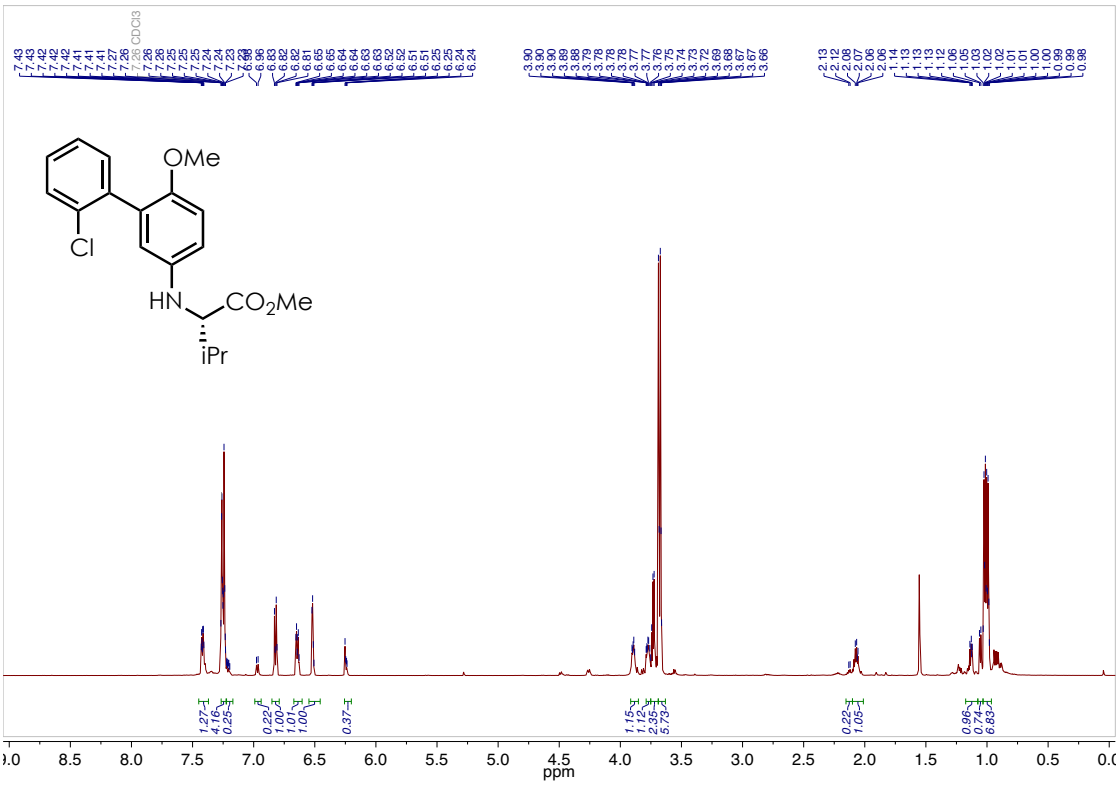
OMe
Cl
HN
CO2Me
iPr
ppm

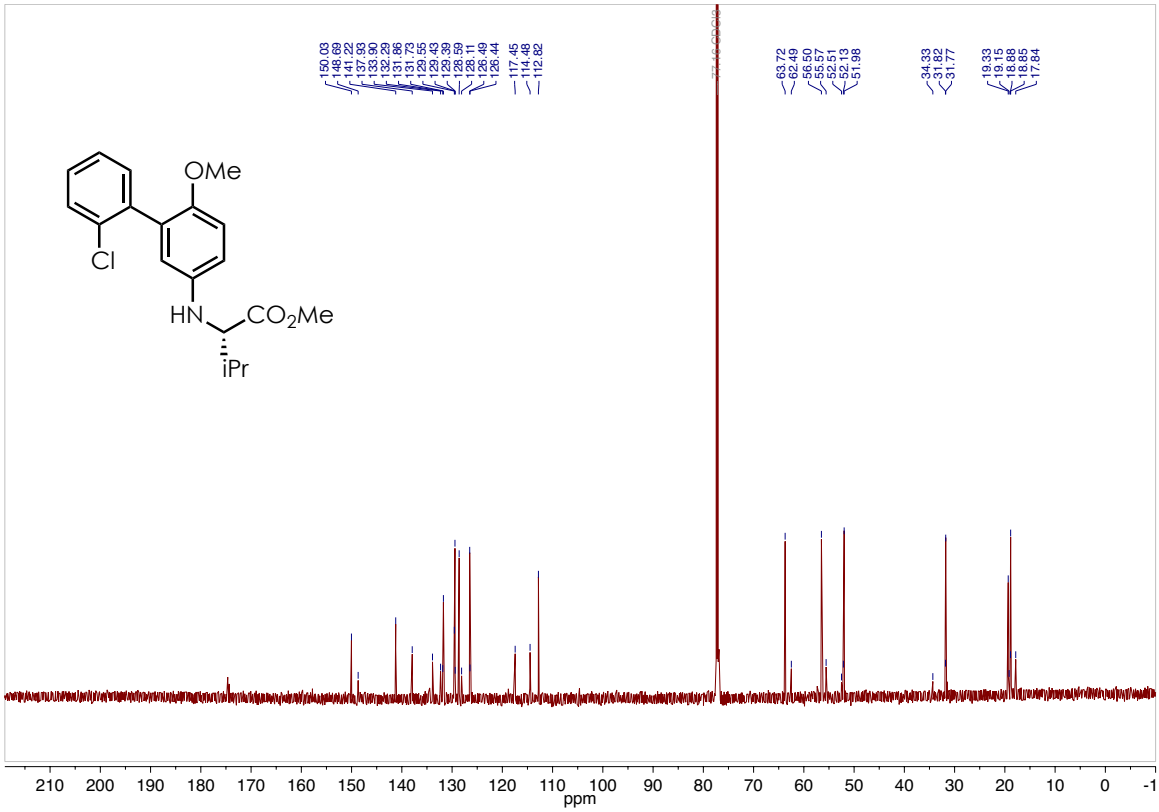
OMe
Cl
HN
CO2Me
iPr
ppm

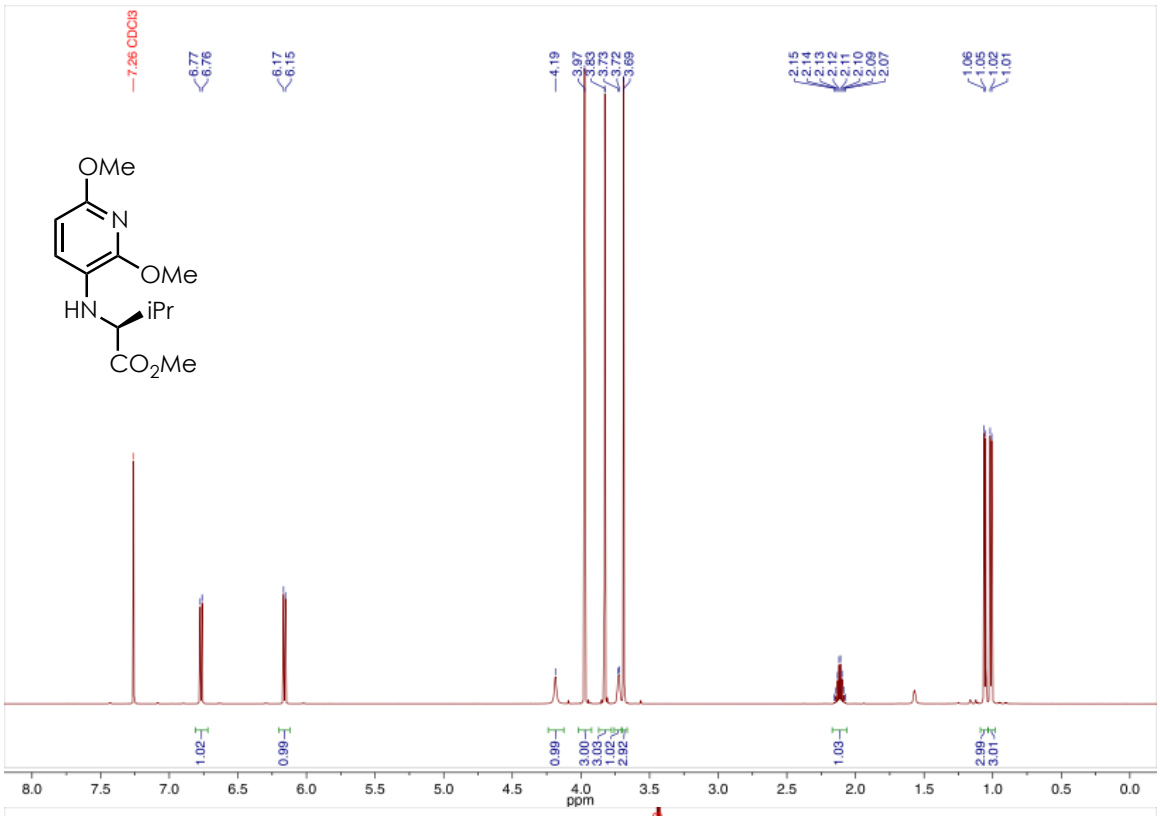
7.26 CDCl3
6.77
6.76
6.17
6.15
4.19
3.97
3.83
3.73
3.72
3.69
2.15
2.14
2.13
2.12
2.11
2.10
2.09
2.07
1.06
1.05
1.02
1.01
OMe
N
OMe
HN
iPr
CO2Me
1.02
0.99
0.99
3.00
3.03
1.02
2.92
1.03
2.99
3.01
8.0
7.5
7.0
6.5
6.0
5.5
5.0
4.5
4.0
3.5
3.0
2.5
2.0
1.5
1.0
0.5
0.0
ppm

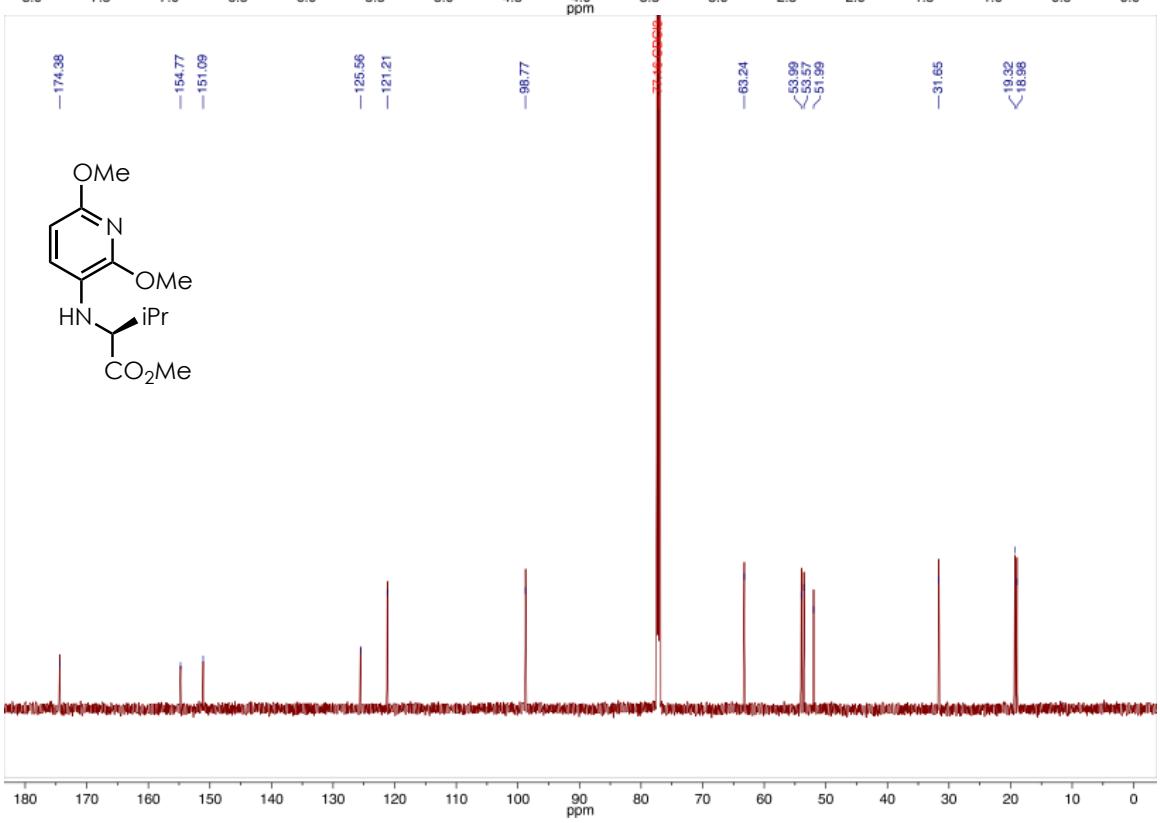
174.38
154.77
151.09
125.56
121.21
98.77
77.16 CDCl3
63.24
53.99
53.57
51.99
31.65
19.32
18.98
OMe
N
OMe
HN
iPr
CO2Me
180
170
160
150
140
130
120
110
100
90
80
70
60
50
40
30
20
10
0
ppm

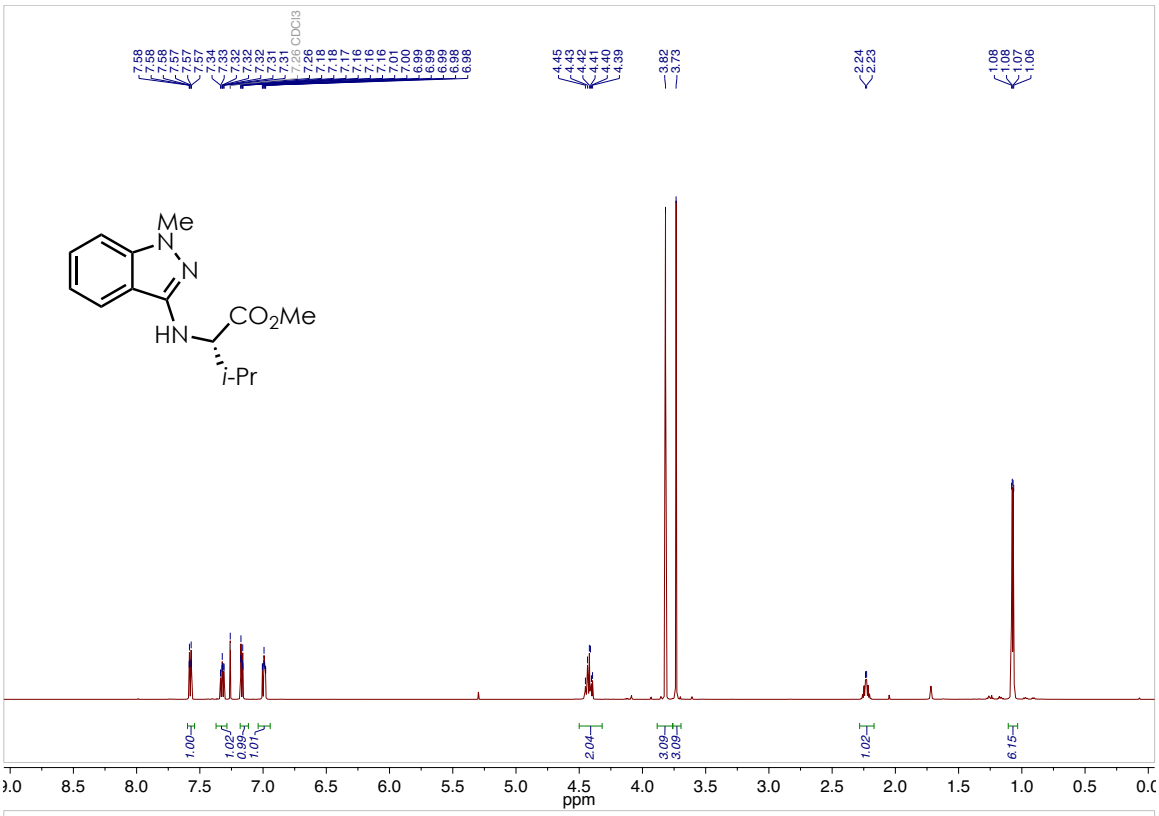
7.58
7.58
7.58
7.57
7.57
7.34
7.33
7.32
7.32
7.32
7.31
7.31
7.26 CDCl3
7.18
7.17
7.16
7.16
7.16
7.01
7.00
6.99
6.99
6.98
6.98
4.45
4.43
4.42
4.41
4.40
4.39
3.82
3.73
2.24
2.23
1.08
1.08
1.07
1.06
Me
N
N
HN
CO2Me
i-Pr
1.00
1.02
0.99
1.01
2.04
3.09
3.09
1.02
6.15
ppm

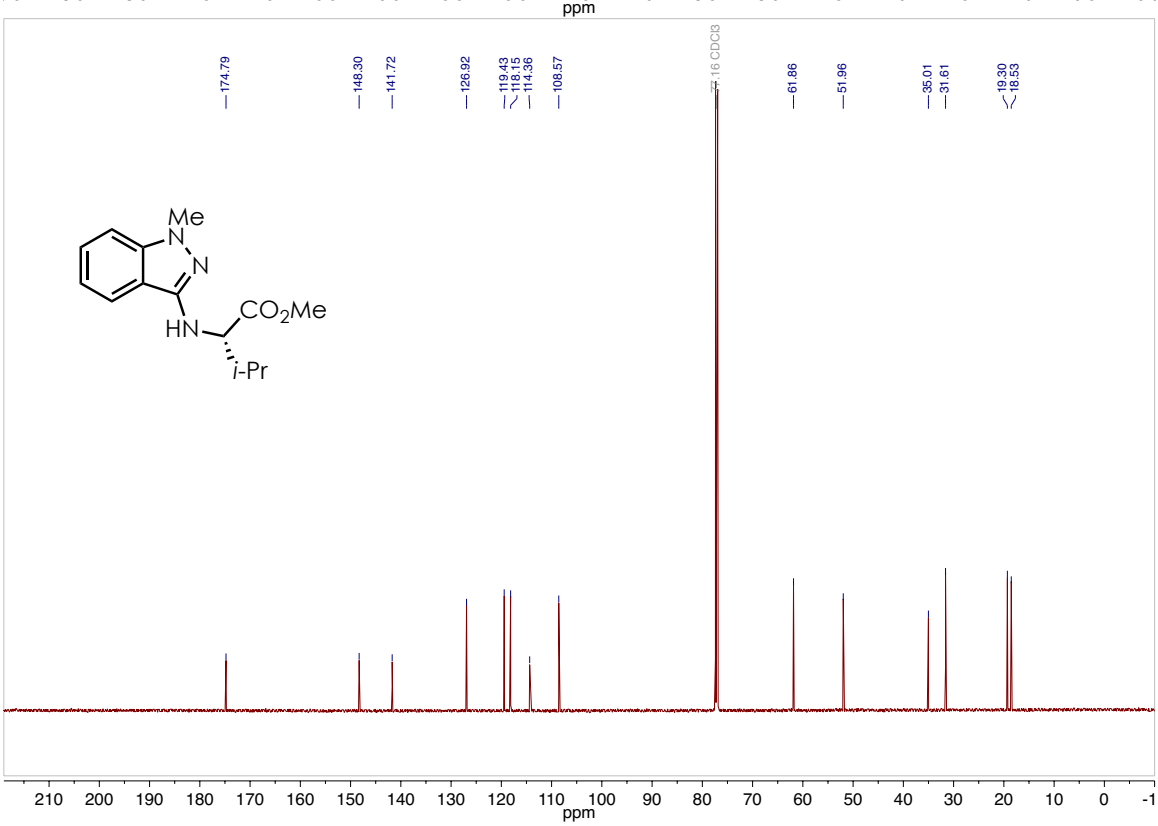
174.79
148.30
141.72
126.92
119.43
118.15
114.36
108.57
77.16 CDCl3
61.86
51.96
35.01
31.61
19.30
18.53
Me
N
N
HN
CO2Me
i-Pr
ppm

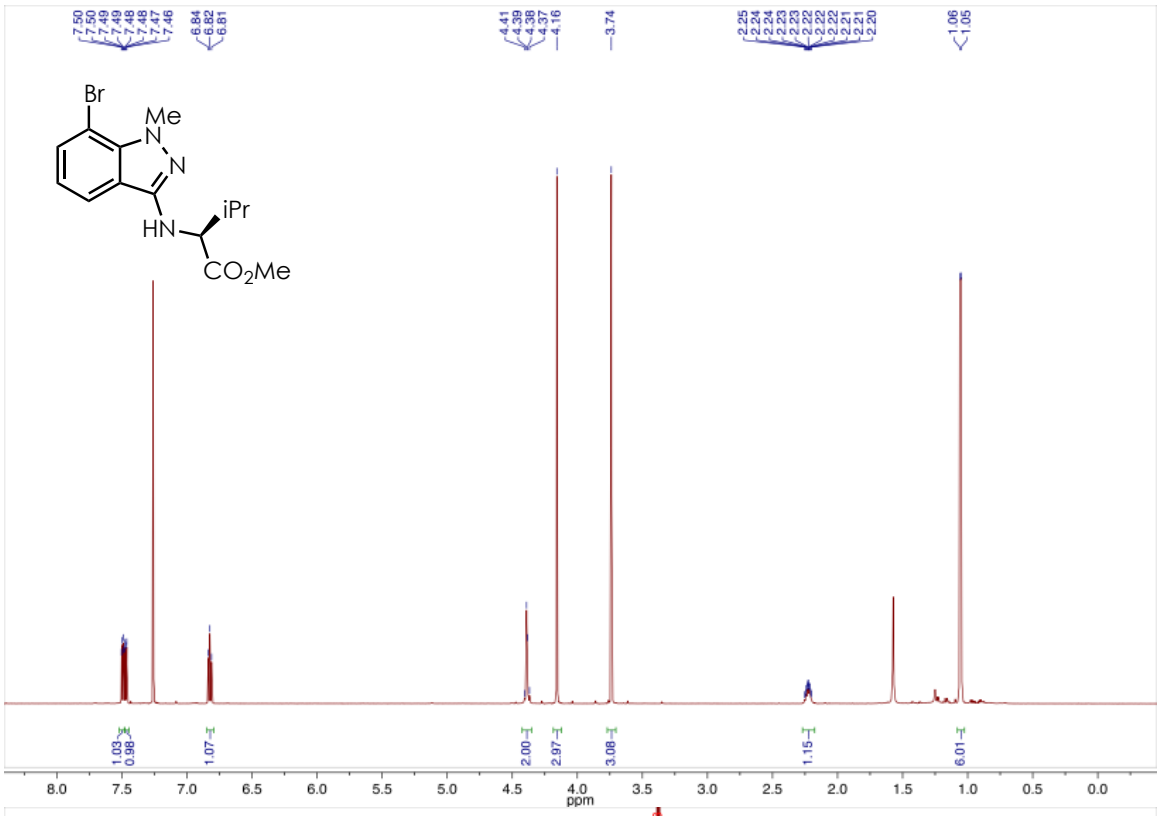
Br
Me
N
N
HN
iPr
CO2Me
7.50
7.50
7.49
7.49
7.48
7.48
7.47
7.46
6.84
6.82
6.81
4.41
4.39
4.38
4.37
4.16
3.74
2.25
2.24
2.24
2.23
2.23
2.22
2.22
2.22
2.21
2.21
2.20
1.06
1.05
1.03
0.98
1.07
2.00
2.97
3.08
1.15
6.01
8.0
7.5
7.0
6.5
6.0
5.5
5.0
4.5
4.0
3.5
3.0
2.5
2.0
1.5
1.0
0.5
0.0
ppm

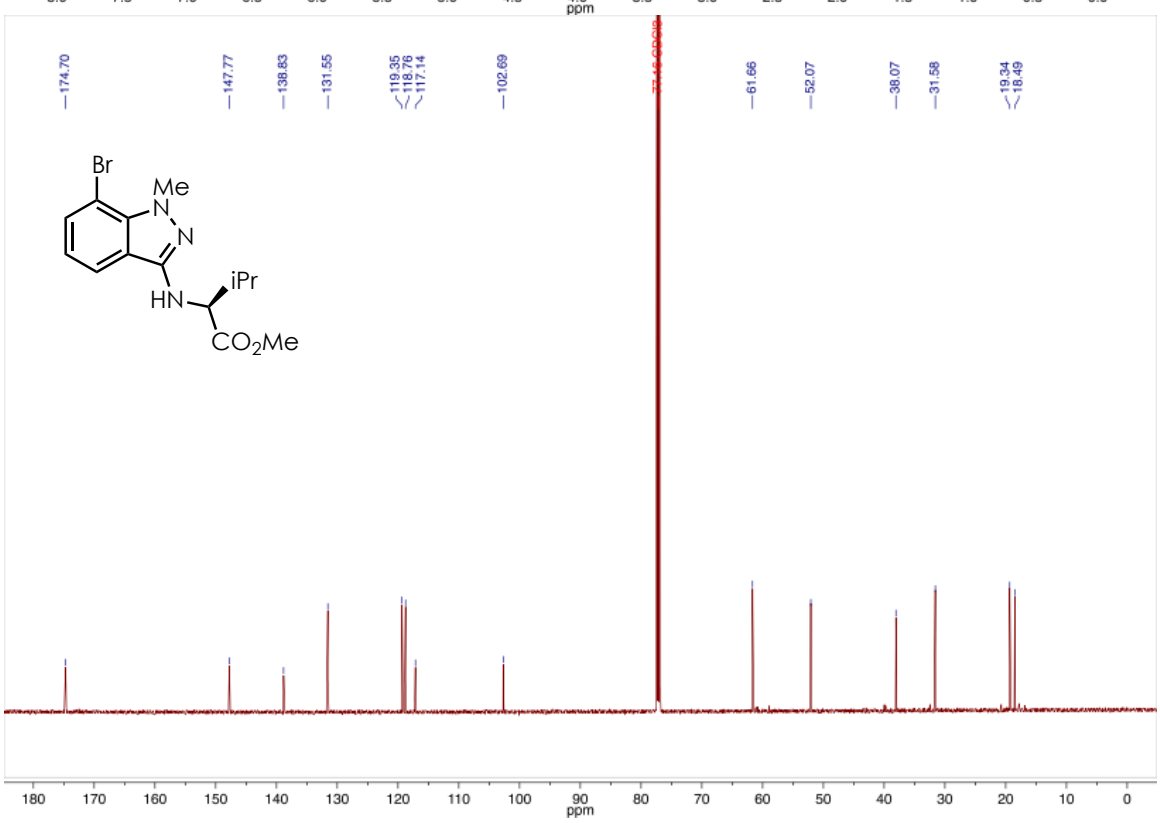
Br
Me
N
N
HN
iPr
CO2Me
174.70
147.77
138.83
131.55
119.35
118.76
117.14
102.69
77.16 CDCl3
61.66
52.07
38.07
31.58
19.34
18.49
180
170
160
150
140
130
120
110
100
90
80
70
60
50
40
30
20
10
0
ppm

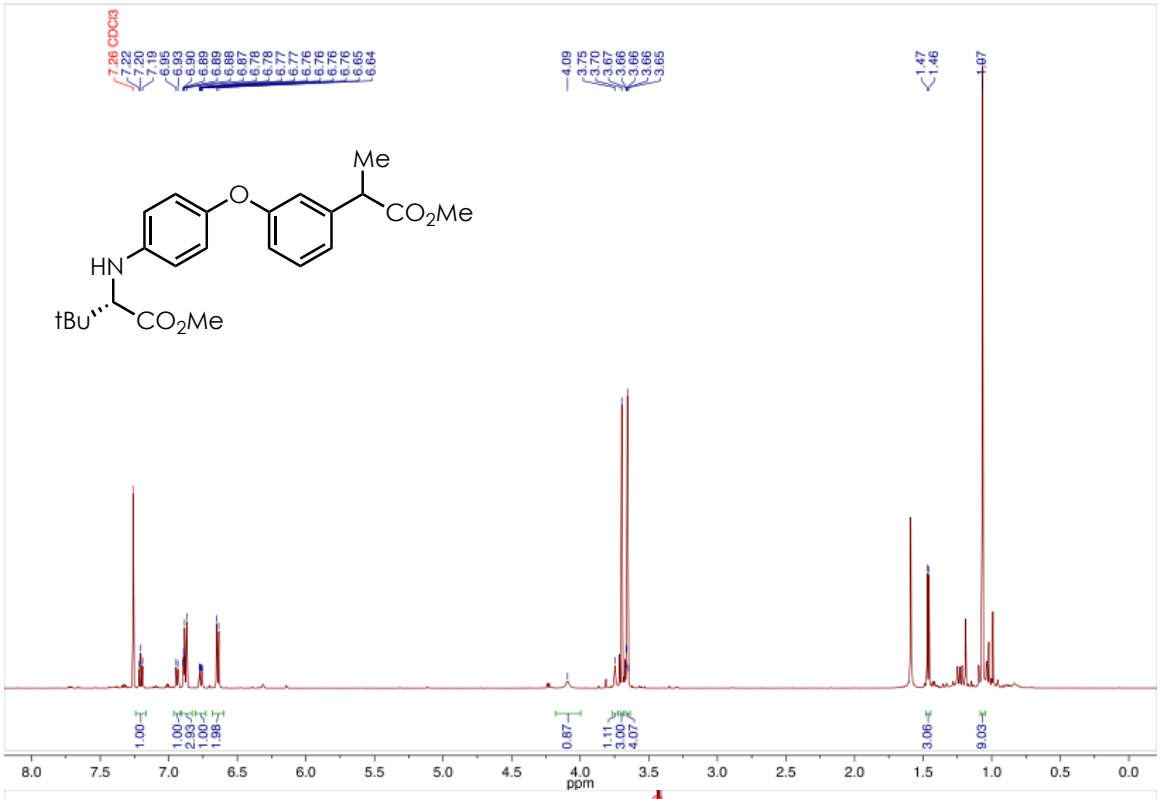
Me
CO2Me
O
HN
tBu
CO2Me

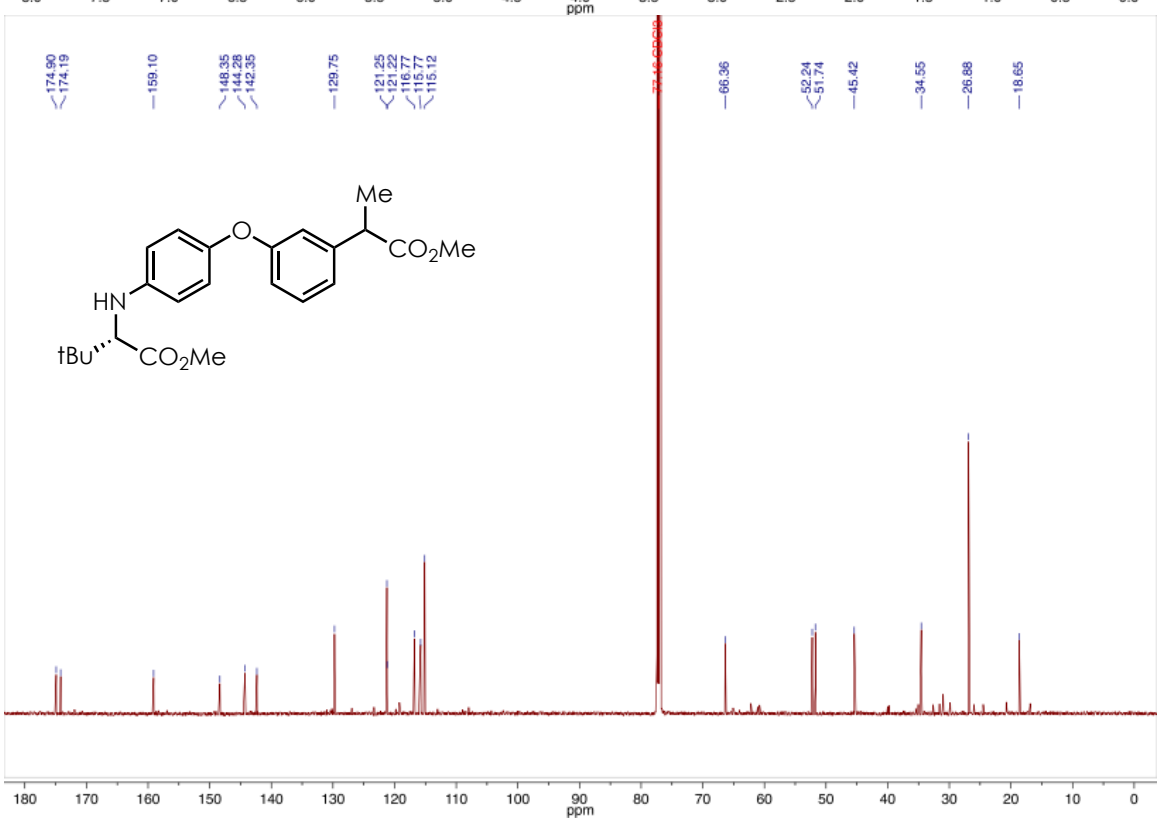
Me
CO2Me
O
HN
tBu
CO2Me

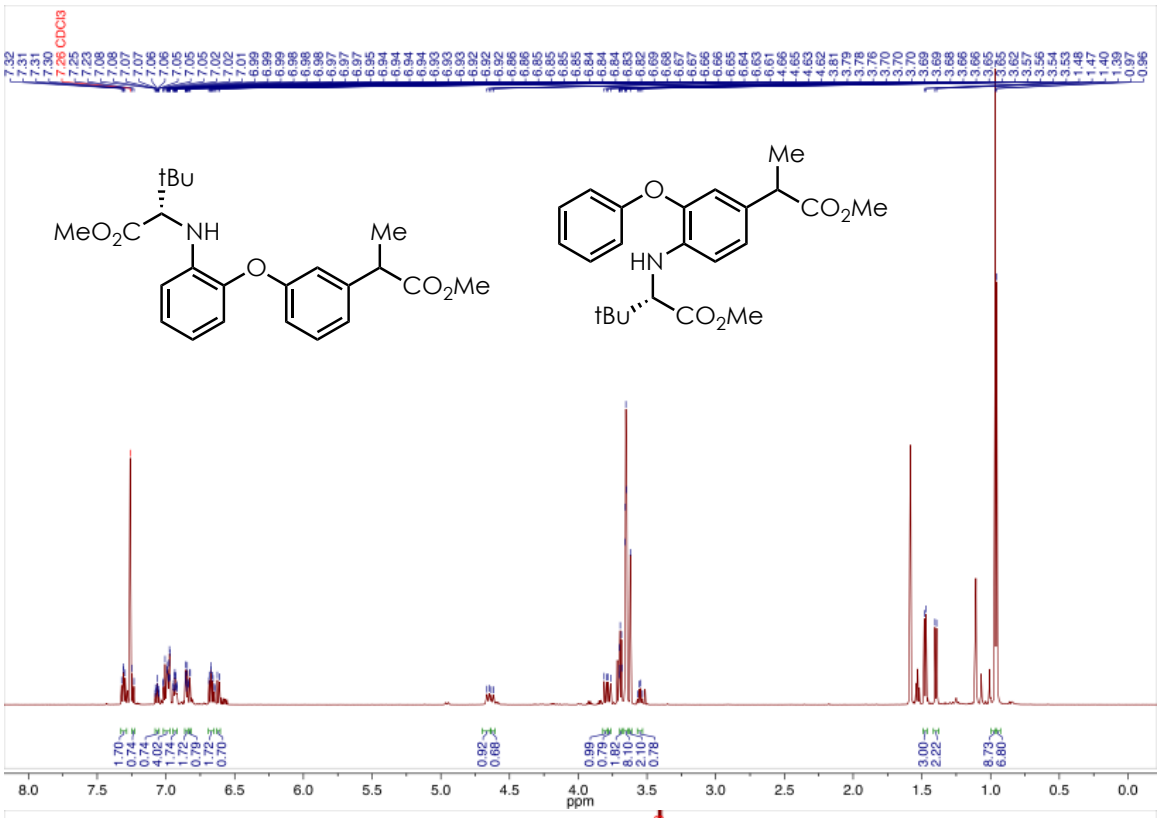
tBu
MeO2C
NH
Me
O
CO2Me
Me
O
CO2Me
HN
tBu
CO2Me
ppm

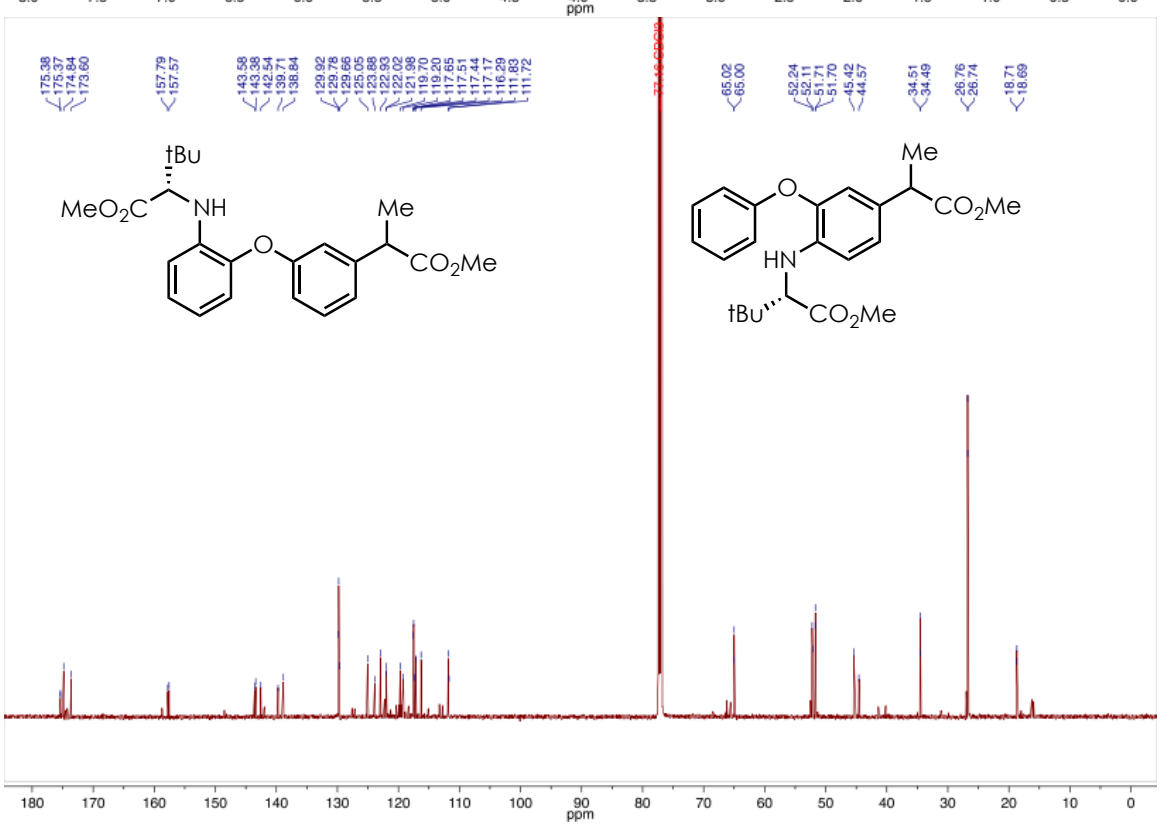
tBu
MeO2C
NH
Me
O
CO2Me
Me
O
CO2Me
HN
tBu
CO2Me
ppm

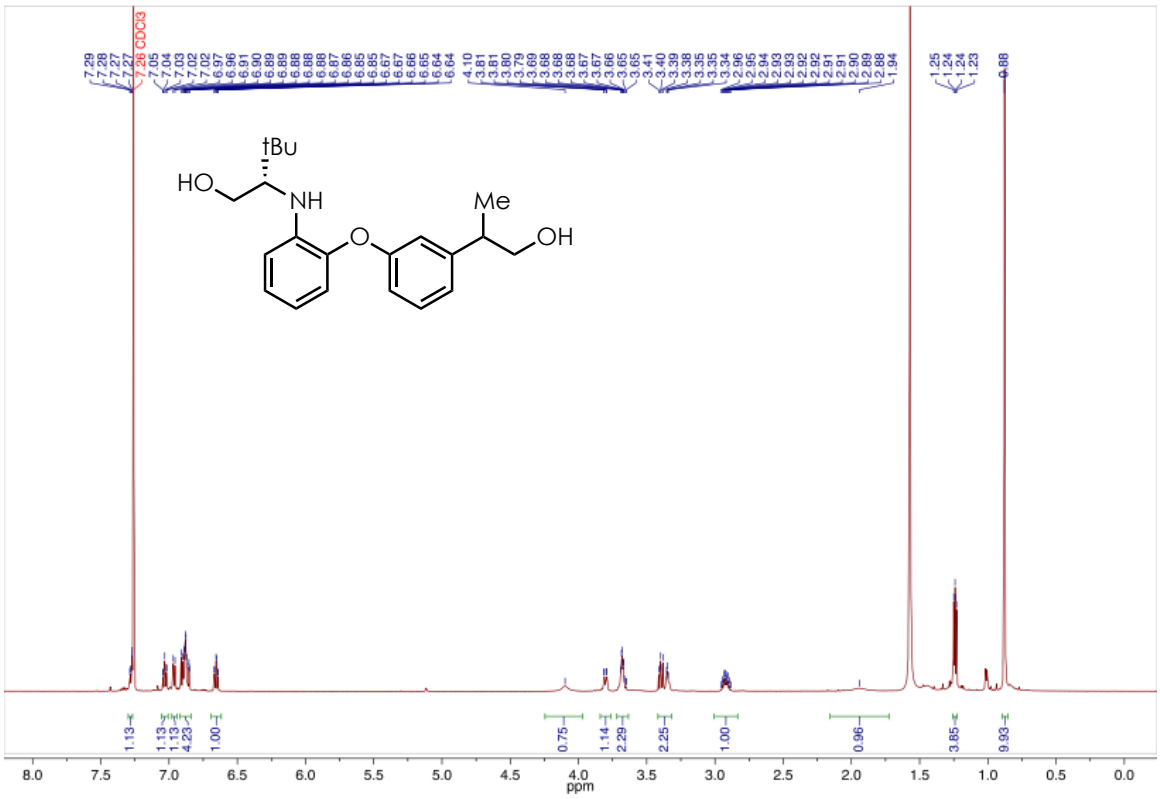
tBu
HO
NH
Me
O
OH
ppm

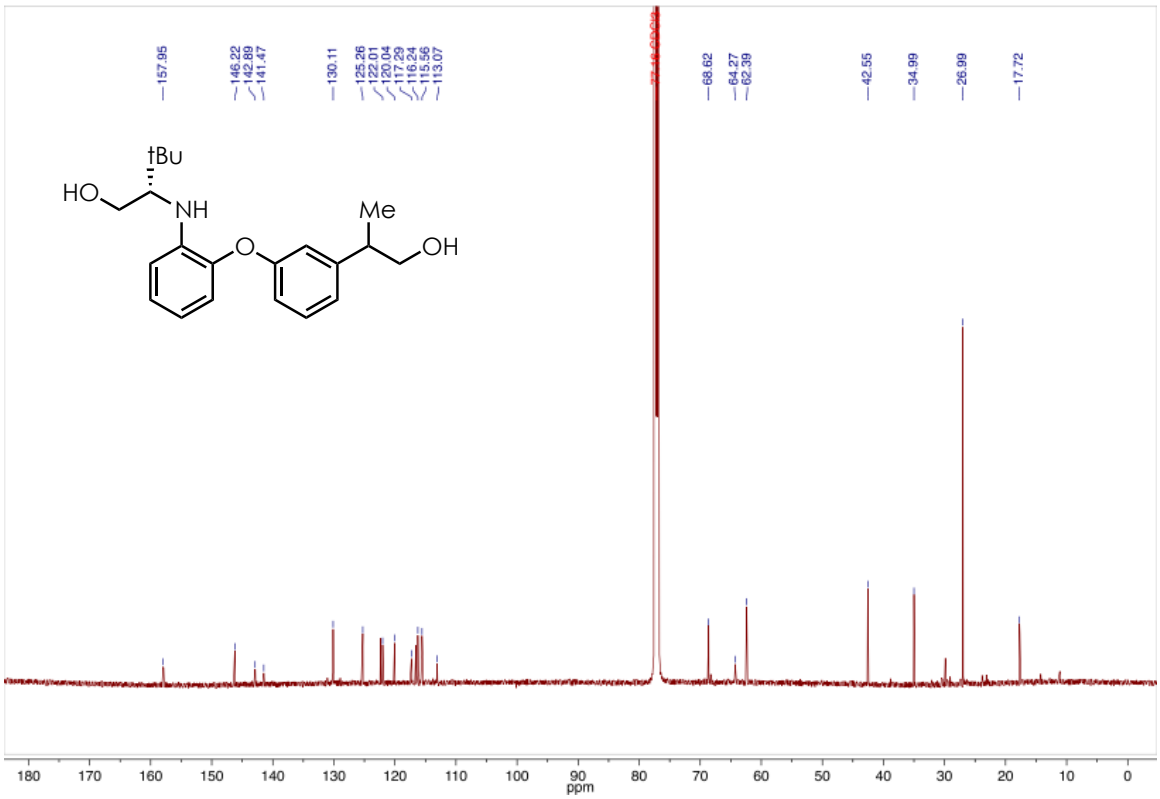
tBu
HO
NH
Me
O
OH
ppm

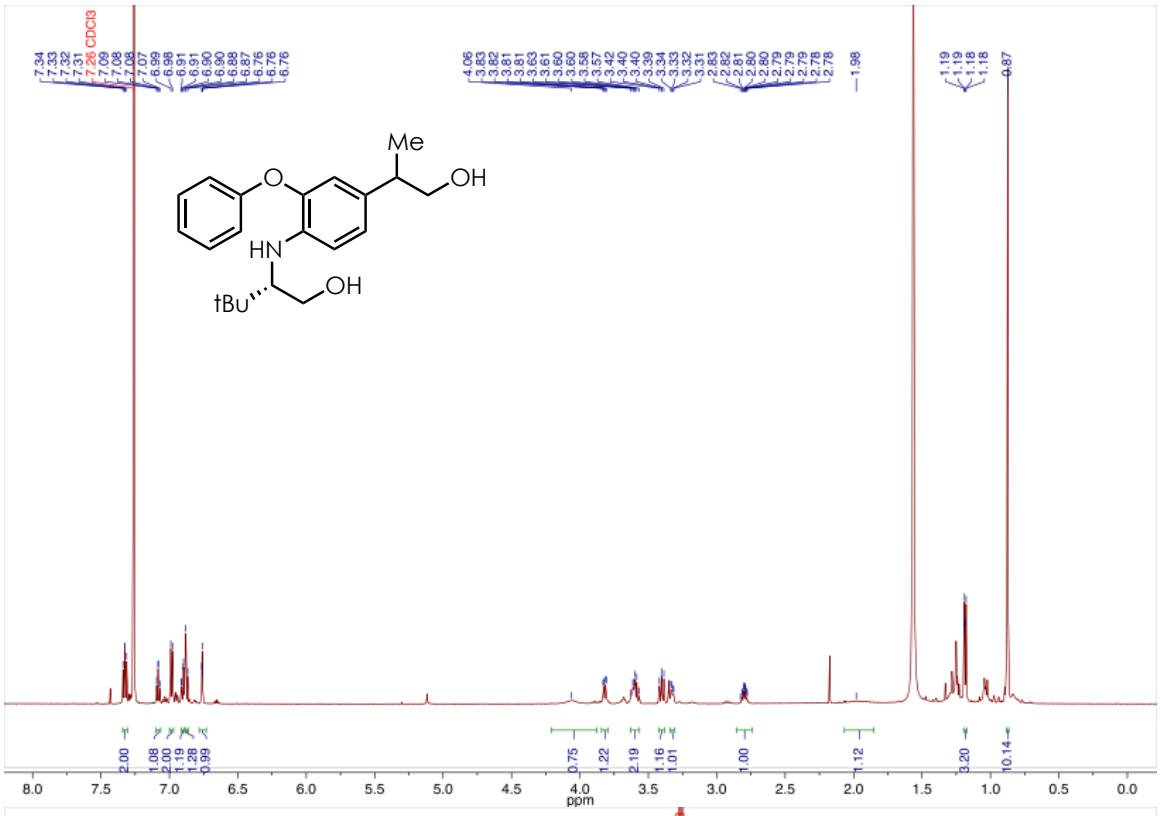
Me
OH
O
HN
OH
tBu

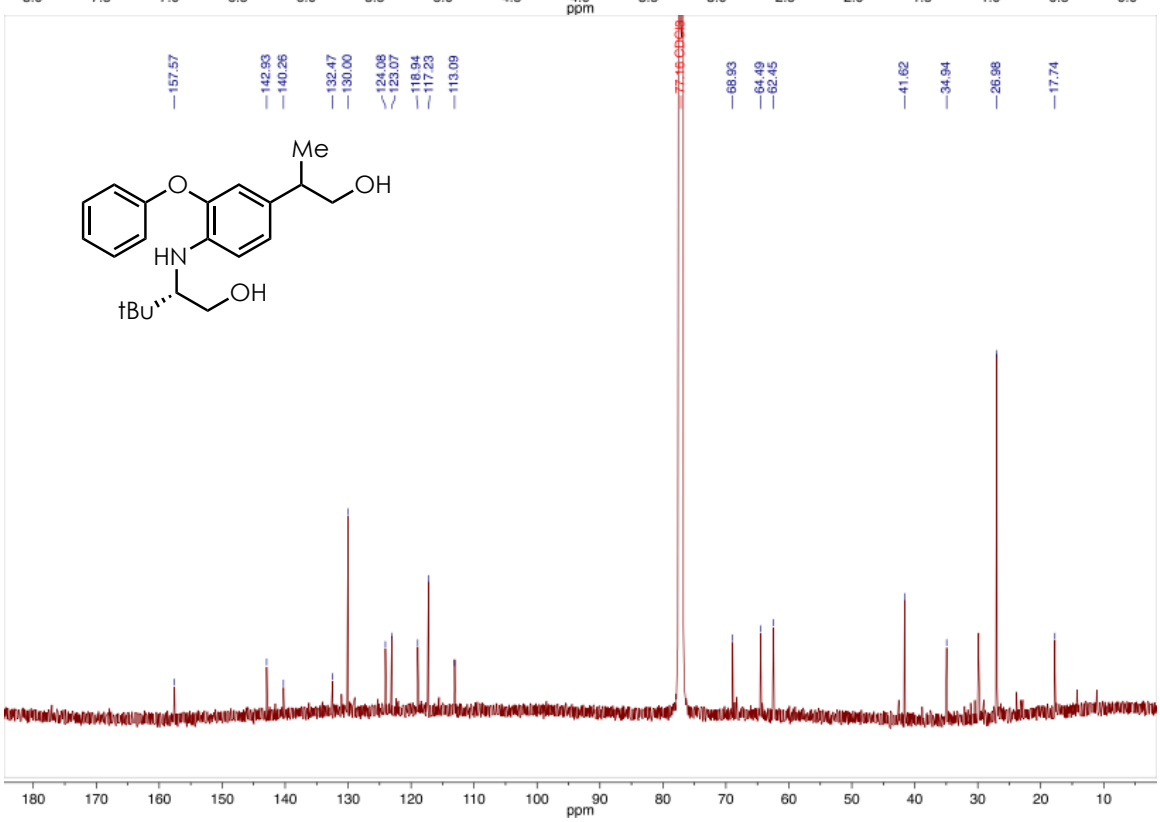
Me
OH
O
HN
OH
tBu

HSQC

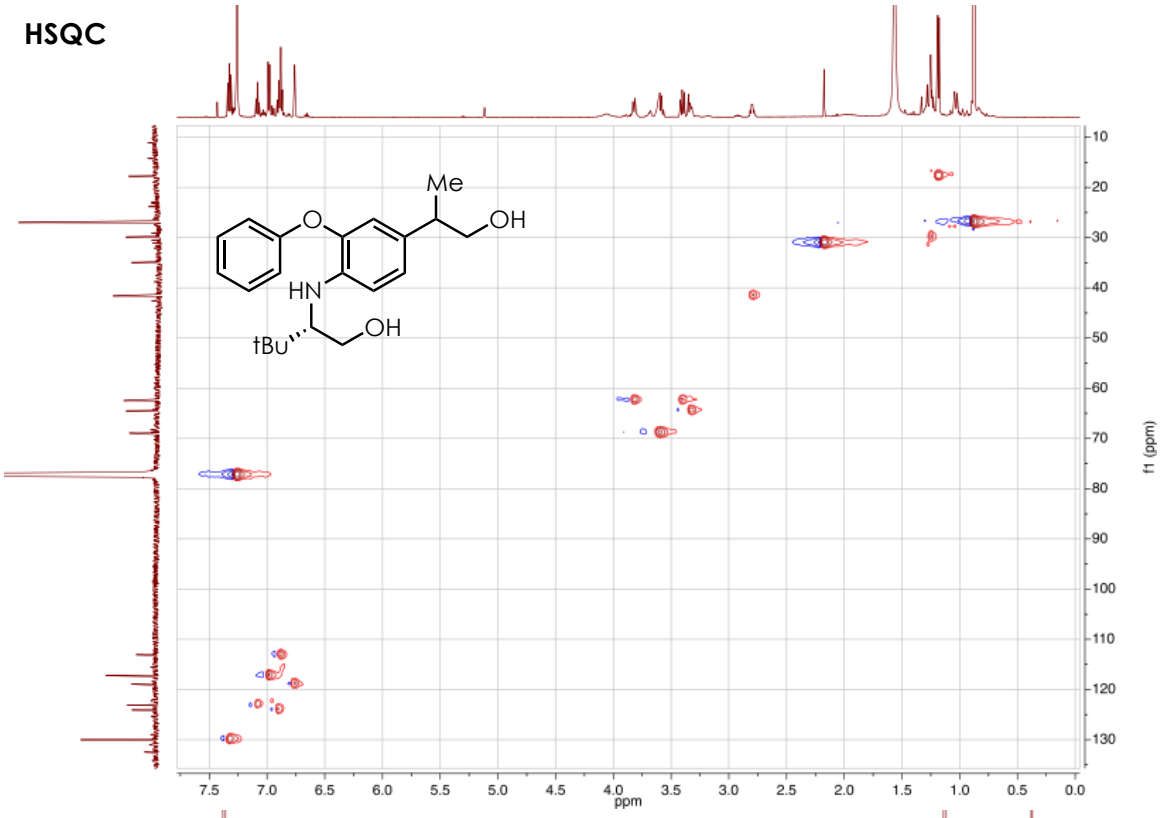

HMBC

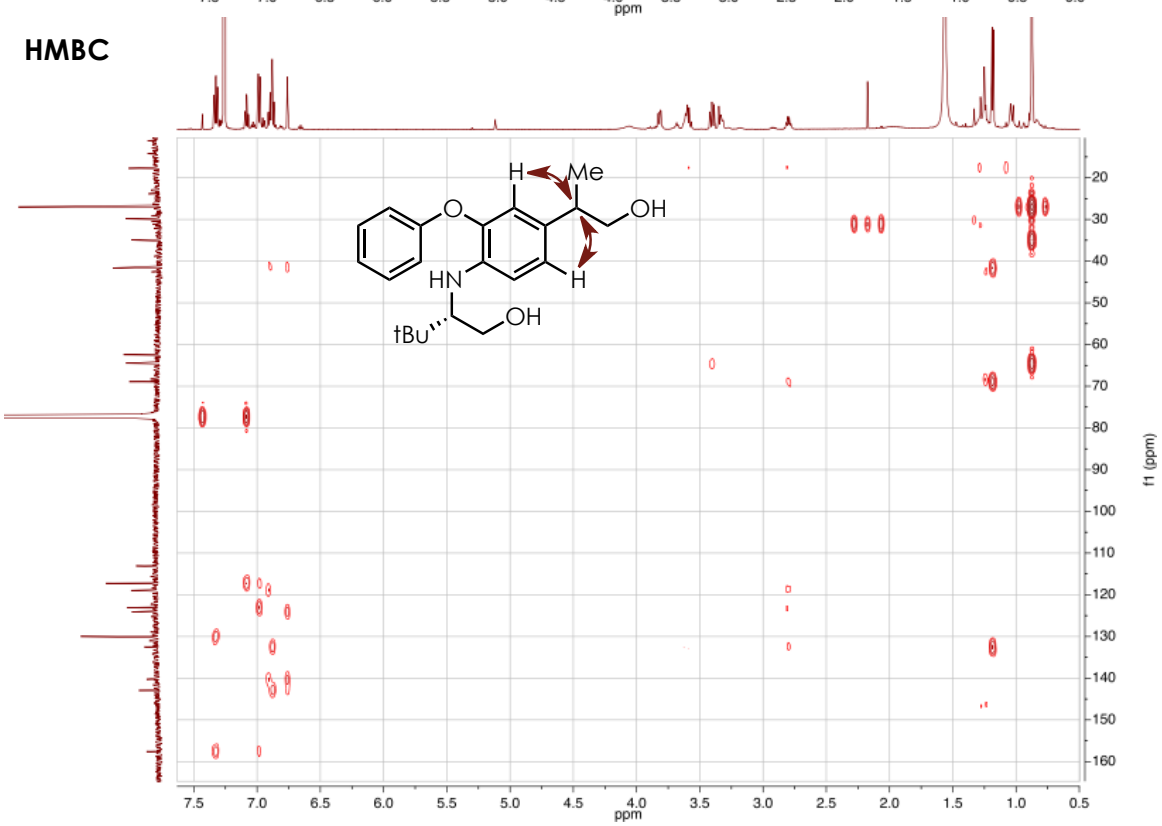

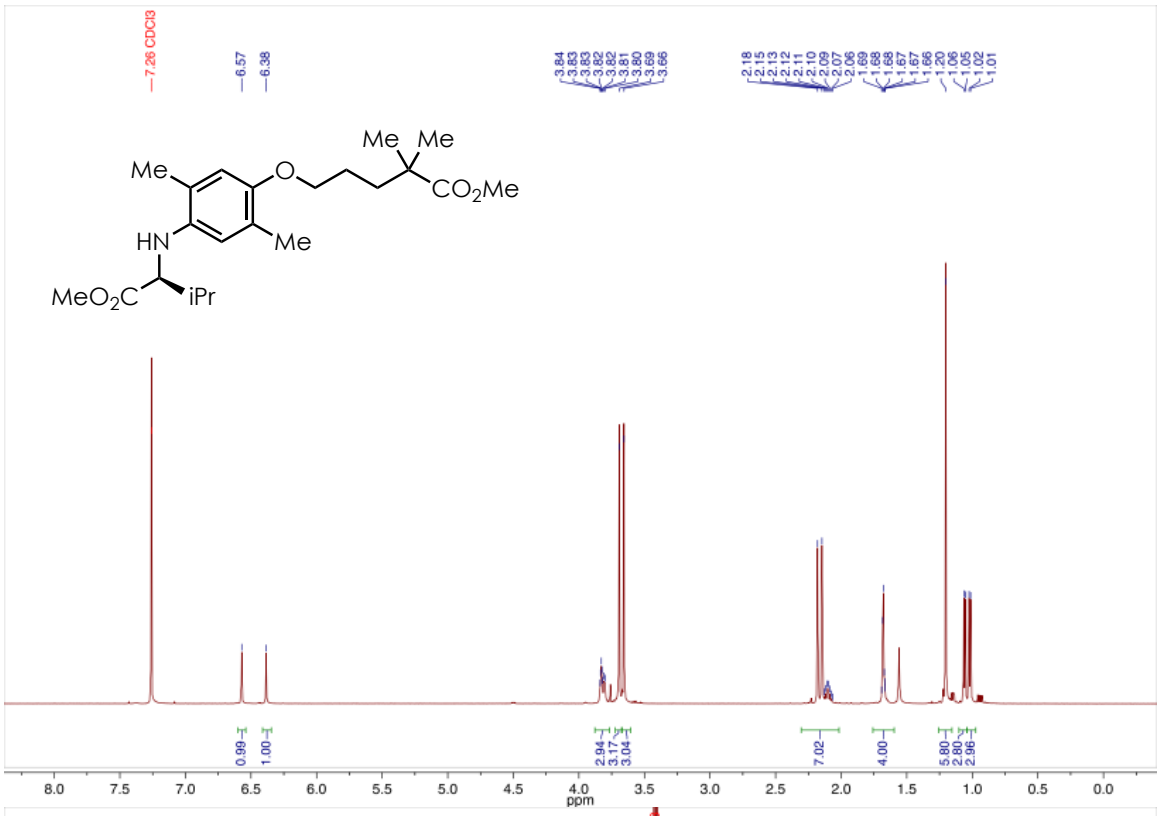
7.26 CDCl3
6.57
6.38
3.84
3.83
3.83
3.82
3.82
3.81
3.80
3.69
3.66
2.18
2.15
2.13
2.12
2.11
2.10
2.09
2.07
2.06
1.69
1.68
1.68
1.67
1.67
1.66
1.20
1.06
1.05
1.02
1.01
Me
Me
Me
O
CO2Me
HN
Me
MeO2C
iPr
0.99
1.00
2.94
3.17
3.04
7.02
4.00
5.80
2.80
2.96
8.0
7.5
7.0
6.5
6.0
5.5
5.0
4.5
4.0
3.5
3.0
2.5
2.0
1.5
1.0
0.5
0.0
ppm

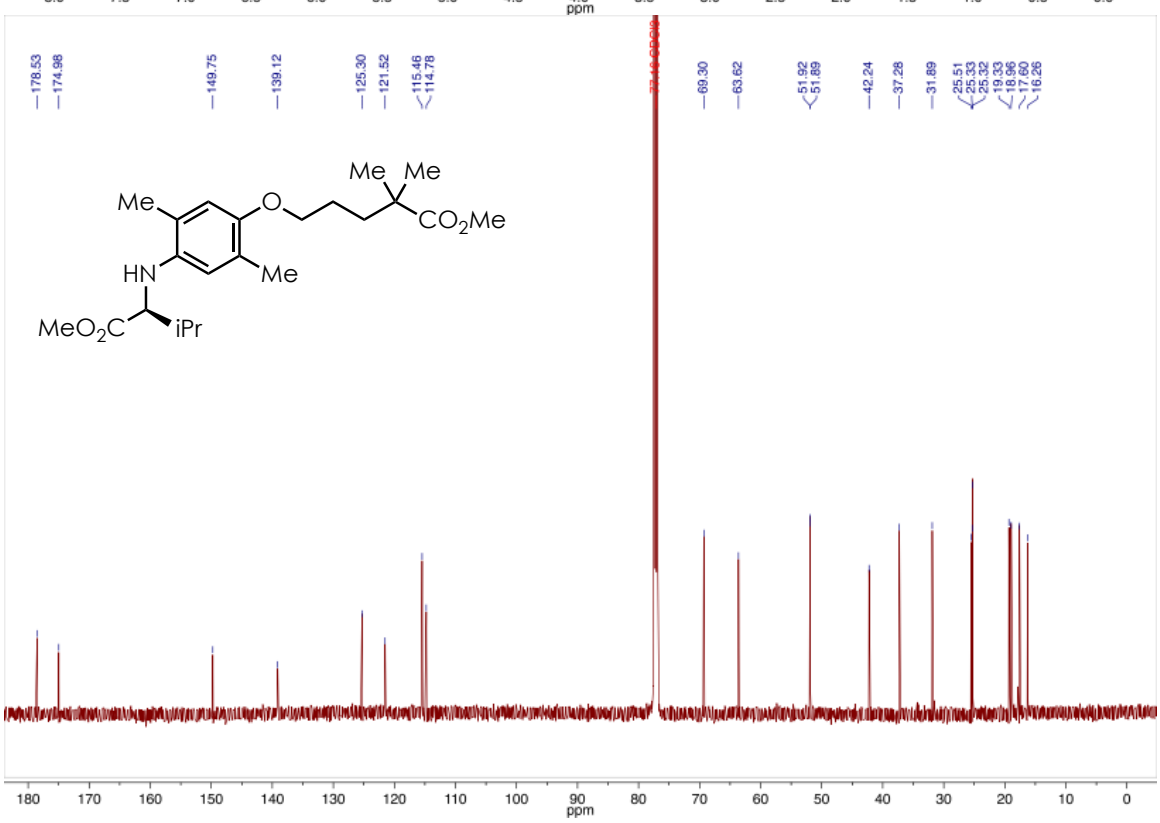
178.53
174.98
149.75
139.12
125.30
121.52
115.46
114.78
77.16 CDCl3
69.30
63.62
51.92
51.89
42.24
37.28
31.89
25.51
25.33
25.32
19.33
18.96
17.60
16.26
Me
Me
Me
O
CO2Me
HN
Me
MeO2C
iPr
180
170
160
150
140
130
120
110
100
90
80
70
60
50
40
30
20
10
0
ppm

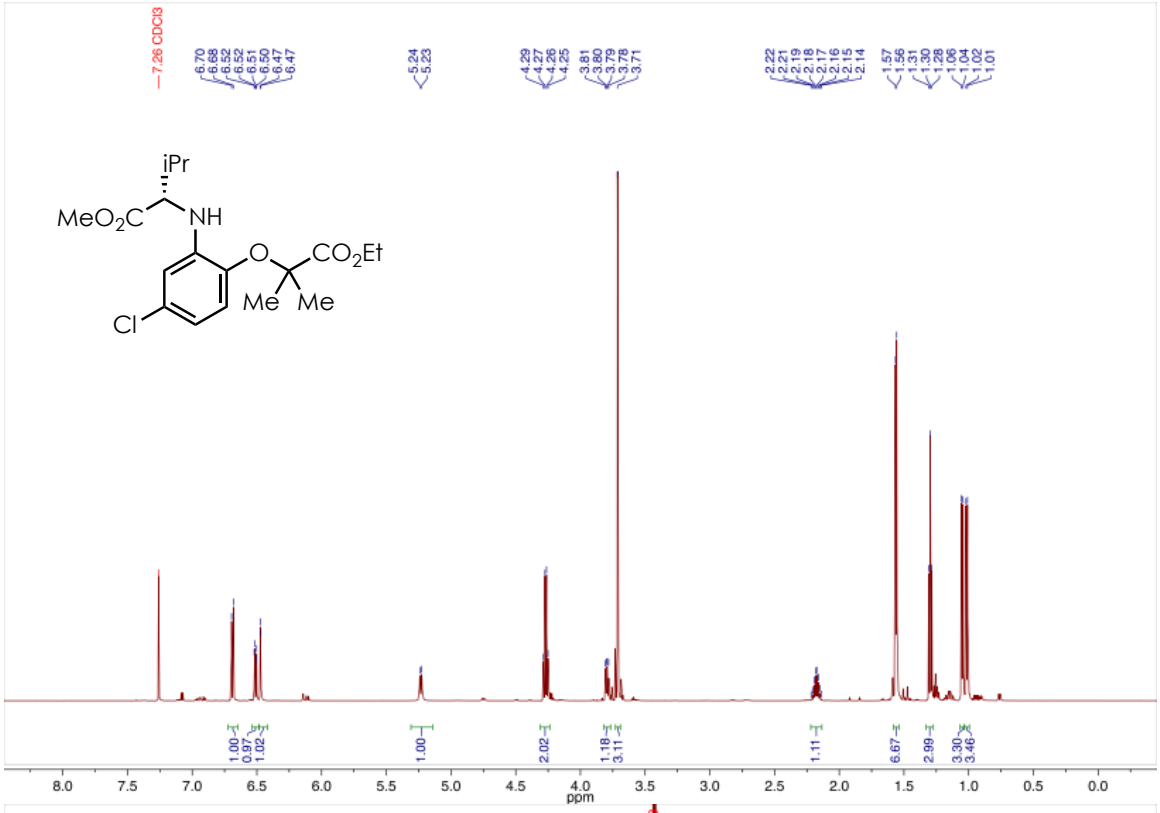
7.26 CDCl3
6.70
6.68
6.52
6.52
6.51
6.50
6.47
6.47
5.24
5.23
4.29
4.27
4.26
4.25
3.81
3.80
3.79
3.78
3.71
2.22
2.21
2.19
2.18
2.17
2.16
2.15
2.14
1.57
1.56
1.31
1.30
1.28
1.06
1.04
1.02
1.01
iPr
MeO2C
NH
O
CO2Et
Me
Me
Cl
1.00
0.97
1.02
1.00
2.02
1.18
3.11
1.11
6.67
2.99
3.30
3.46
8.0
7.5
7.0
6.5
6.0
5.5
5.0
4.5
4.0
3.5
3.0
2.5
2.0
1.5
1.0
0.5
0.0
ppm

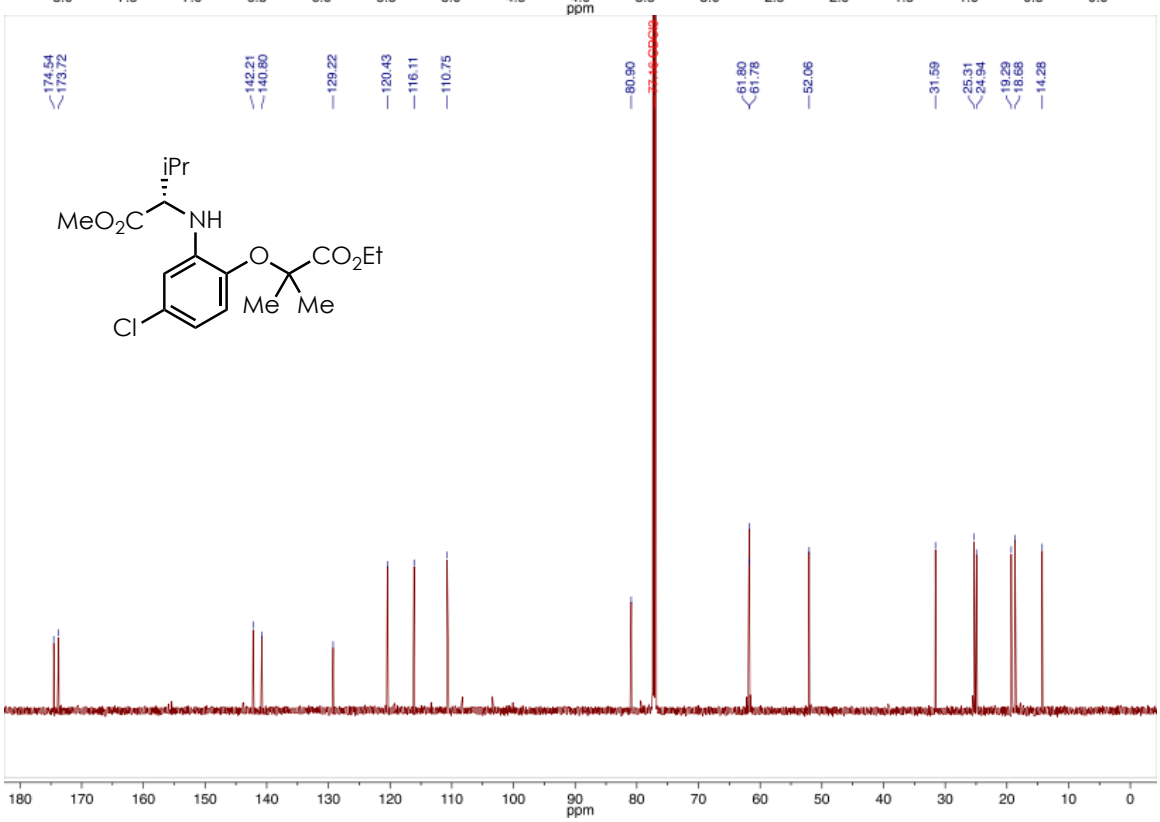
174.54
173.72
142.21
140.80
129.22
120.43
116.11
110.75
80.90
77.16 CDCl3
61.80
61.78
52.06
31.59
25.31
24.94
19.29
18.68
14.28
iPr
MeO2C
NH
O
CO2Et
Me
Me
Cl
180
170
160
150
140
130
120
110
100
90
80
70
60
50
40
30
20
10
0
ppm

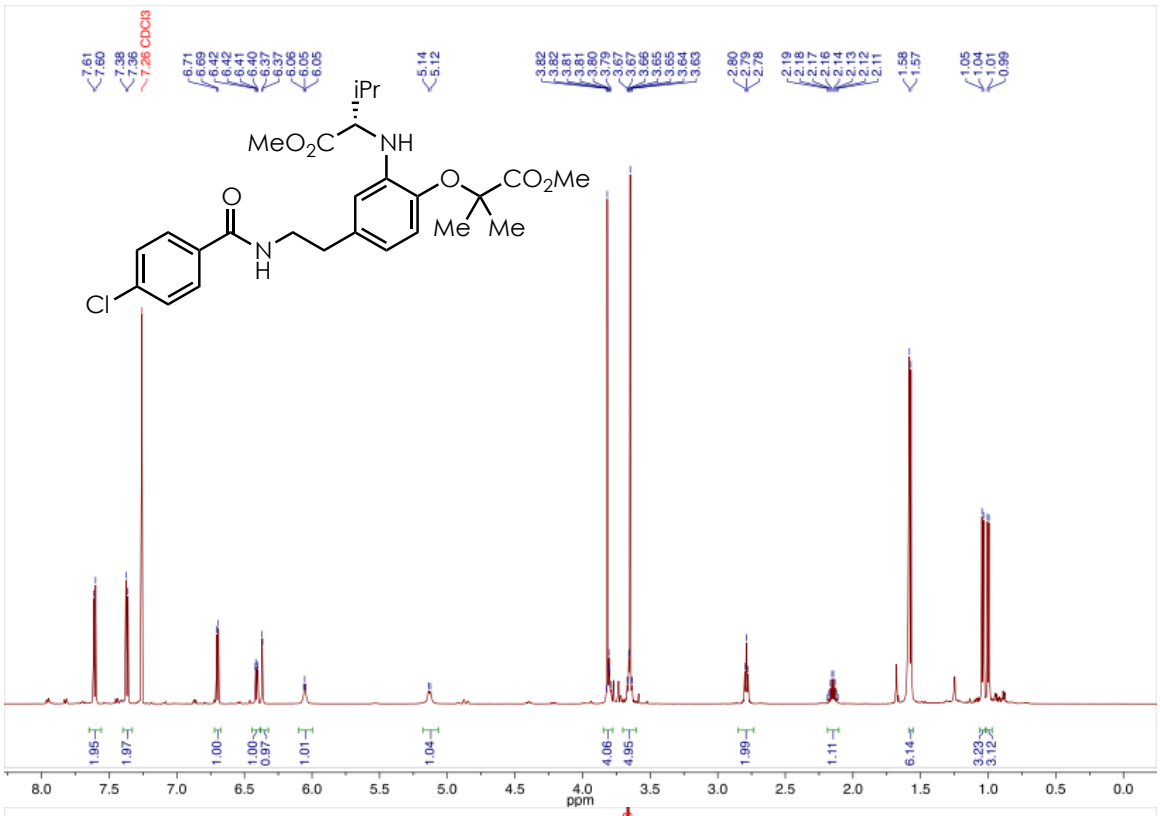
iPr
MeO2C
NH
O
CO2Me
Me
Me
O
N
H
Cl

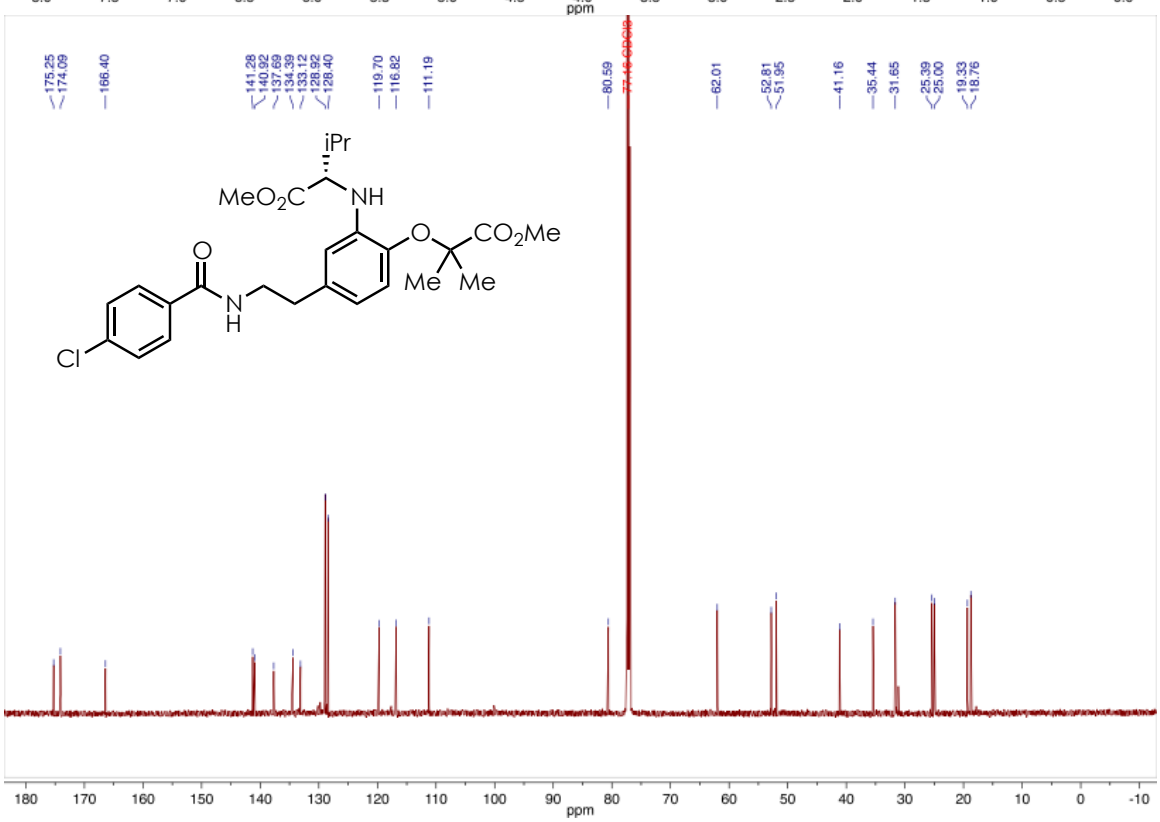
iPr
MeO2C
NH
O
CO2Me
Me
Me
O
N
H
Cl

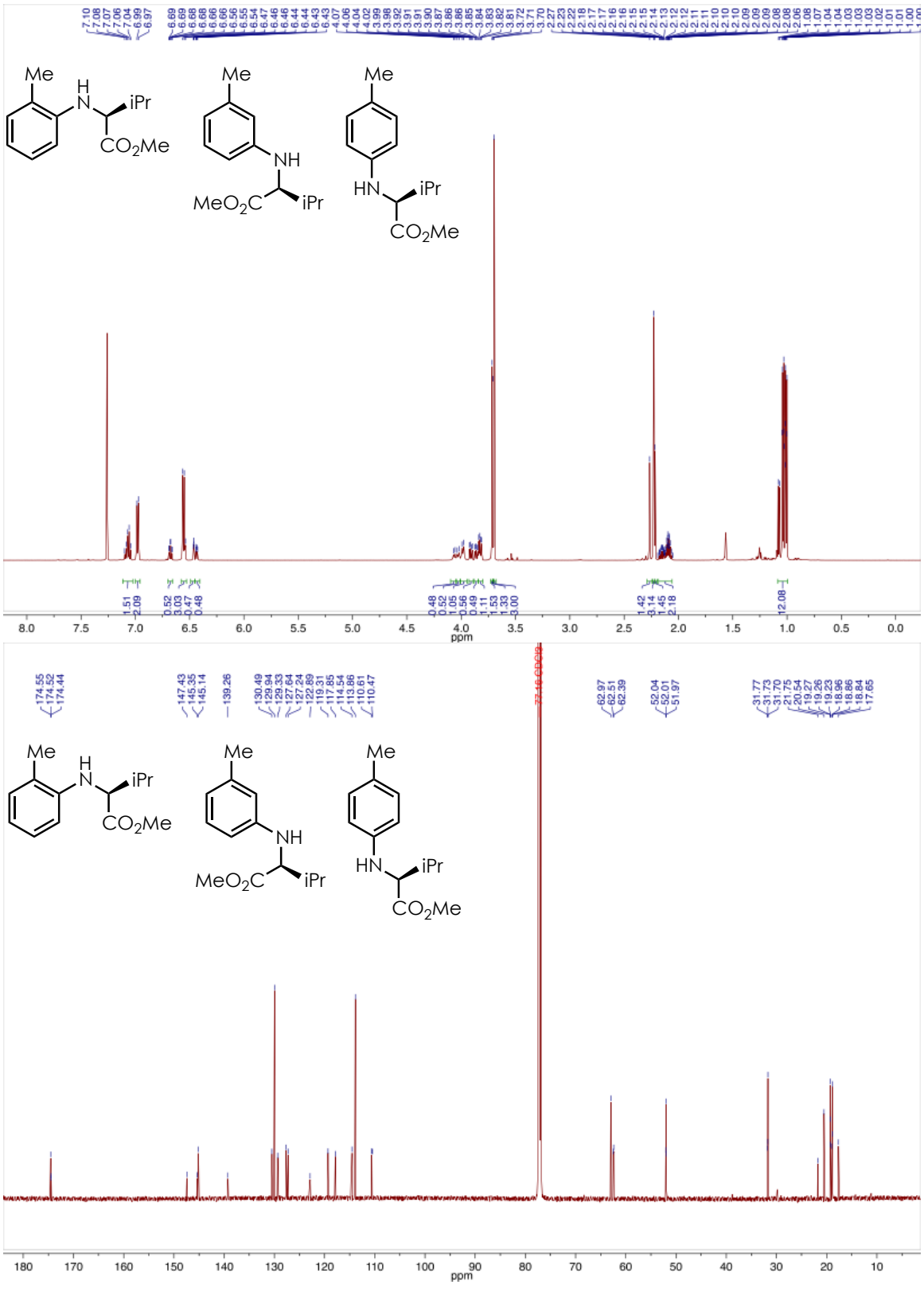
Me
H
N
iPr
CO2Me
Me
NH
MeO2C
iPr
Me
HN
iPr
CO2Me
ppm
ppm

APPENDIX D: SUPPORTING INFORMATION FOR CHAPTER 5

General Methods and Materials

Proton and carbon magnetic resonance spectra (^{1}H NMR and ^{13}C NMR) were recorded on a Bruker model DRX 400 or a Bruker Avance III 600 CryoProbe(^{1}H NMR at 400 MHz and 600 MHz and ^{13}C NMR at 100 and 151 MHz) spectrometer. Chemical shifts for protons are reported in parts per million downfield from tetramethylsilane and are referenced to residual protium in the solvent (^{1}H NMR: $CHCl_3$ at 7.26 ppm). Chemical shifts for carbons are reported in parts per million downfield from tetramethylsilane and are referenced to the carbon resonances of the solvent peak (^{13}C NMR: $CDCl_3$ at 77.16 ppm). Chemical shifts for fluorines are referenced to fluorobenzene as an internal standard (^{19}F NMR: C_6H_5F at –113.15 ppm). ^{1}H NMR data are reported as follows: chemical shift, multiplicity (s = singlet, d = doublet, t = triplet, q = quartet, sept = septet, oct = octet, dd = doublet of doublets, ddt = doublet of doublet of triplets, ddd = doublet of doublet of doublets, dddd = doublet of doublet of doublet of doublets, m = multiplet, and prefixed br = broad), coupling constants (Hz), and integration.

High resolution mass spectra (HRMS) were obtained using a Thermo LTqFT mass spectrometer with electrospray ionization or atmospheric pressure chemical ionization in positive mode. Gas chromatography (GC) was performed on an Agilent 6850 series instrument equipped with a split-mode capillary injection system and Agilent 5973 network mass spec detector (MSD). Thin layer chromatography (TLC) was performed on SiliaPlate 250 μm thick silica gel plates provided by Silicycle. Visualization was accomplished with short wave UV light (254 nm), cerium ammonium molybdate, *p*-anisaldehyde, or potassium permanganate solution followed by heating. Flash chromatography was performed using

SiliaFlash P60 silica gel (40-63 μm) purchased from Silicycle. Irradiation of photochemical reactions was carried out using a PAR38 blue aquarium LED lamp (Model #6851) fabricated with high-power Cree LEDs as purchased from Ecoxotic (www.ecoxotic.com) or Kessil KSH150B Blue 36W LED Grow Lights with standard borosilicate glass vials purchased from Fischer Scientific. For all photolyses, reactions were stirred using a PTFE coated magnetic stir bar on a magnetic stir plate. Yield refers to isolated yield of analytically pure material unless otherwise noted. NMR yields were determined using hexamethyldisiloxane as an internal standard. Tetrahydrofuran, diethyl ether, and dichloromethane were dried by passage through a column of neutral alumina under nitrogen prior to use. All other reagents were obtained from commercial sources and used without further purification unless otherwise noted.

Preparation of Photocatalysts and Reagents

4-Acetamidobenzenesulfonyl azide, *N*-fluorobenzenesulfonimide, diethyl bromomalonate, and *N*-Chlorosuccinimide were used as purchased. Methyl acrylate and methyl vinyl ketone were purchased from commercial sources, deoxygenated via multiple freeze-pump-thaw cycles, purified by vacuum transfer, and stored at –35 ºC under in an argon-filled glovebox prior to use.

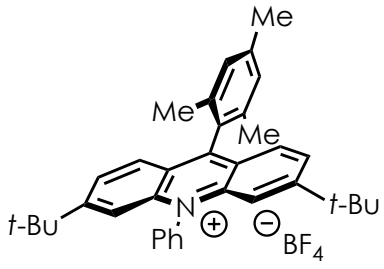

9-Mesityl-3,6-di-*tert*-butyl-10-phenylacridinium tetrafluoroborate (*t*-Bu_2-Mes-Acr+) (A) was prepared as previously reported by the Nicewicz lab. The spectral data matched the values reported in the literature.[1]

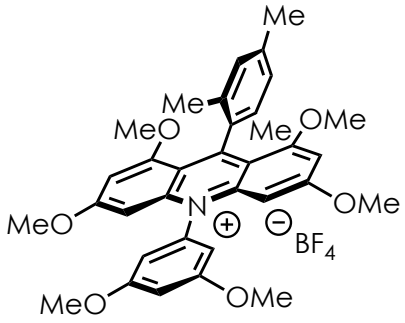

10-(3,5-Dimethoxyphenyl)-9-mesityl-1,3,6,8-tetramethoxyacridin-10-ium tetrafluoroborate (OMe_6-Mes-Acr+) (B) was prepared as previously reported by our lab. The spectral data matched the values reported in the literature.[2]

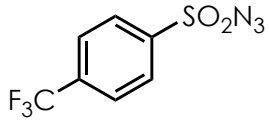

4-(Trifluoromethyl)benzenesulfonyl azide (5.3) was prepared as previously reported. The spectral data matched the values reported in the literature.[3]

Preparation of Substrates

Cyclohexane, cycloheptane, cyclooctane, *trans*-decalin, adamantane, *n*-propylbenzene, *t*-butyl cyclohexane, isopropylbenzene, 3,7-dimethyl-1-octanol, 2-(1-adamantyl)-4-bromoanisole, and 5-α-cholestan-3-one were used as purchased.

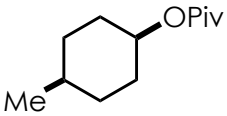

***Cis*-4-methylcyclohexyl pivalate** was prepared according to a published procedure; spectral data were in agreement with literature values.[4]

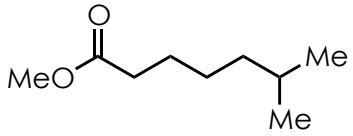

Methyl 6-methylheptanoate was prepared according to a published procedure; spectral data were in agreement with literature values.[5]

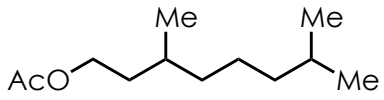

3,7-Dimethyloctyl acetate was prepared according to a published procedure; spectral data were in agreement with literature values.[6]

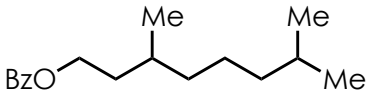

3,7-Dimethyloctyl benzoate was prepared according to a published procedure; spectral data were in agreement with literature values.[7]

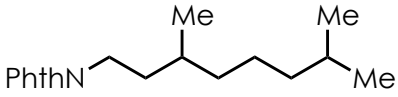

2-(3,7-Dimethyloctyl)isoindoline-1,3-dione was prepared according to a published procedure; spectral data were in agreement with literature values.[8]

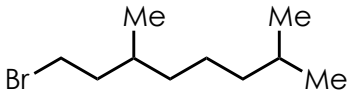

1-Bromo-3,7-dimethyloctane was prepared according to a published procedure; spectral data were in agreement with literature values.[6]

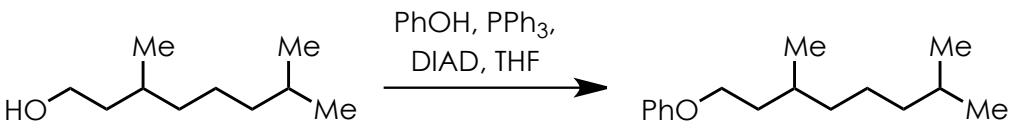

((3,7-Dimethyloctyl)oxy)benzene: To a solution of phenol (1 g, 10.6 mmol) and triphenylphosphine (6.1 g, 23.4 mmol) in THF (100 mL) at 0 ºC was added 3,7-

dimethyloctanol (4.47 mL, 23.4 mmol) followed by DIAD (4.6 mL, 23.4 mmol). The solution was warmed to rt overnight, the concentrated *in vacuo*. The residue was triturated with hexanes, and the solution was concentrated *in vacuo* and purified by flash column chromatography (0 – 5% EtOAc in hexanes) affording the product as a colorless liquid (990 mg, 40% yield). Spectral data were in agreement with literature values.[9]

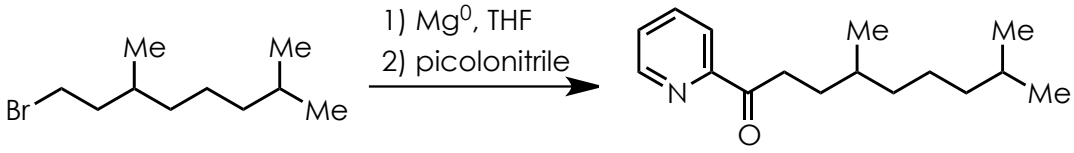

4,8-Dimethyl-1-(pyridin-2-yl)nonan-1-one: To a suspension of magnesium (100 mg, 4.1 mmol) and an iodine crystal in THF (2 mL) was added 1-bromo-3,7-dimethyloctane (995 mg, 4.5 mmol) in THF (7 mL) dropwise. Gentle heating to facilitate initiation was accomplished with a heat gun. Subsequently, picolonitrile (395 mL, 4.1 mmol) was added at room temperature and stirred overnight. The reaction was quenched with 1M HCl, stirred for 3 hours, and then quenched with aqueous $NaHCO_3$. The solution was extracted three times with EtOAc, and the combined organic layers were washed with brine, dried with $MgSO_4$, and concentrated *in vacuo*. The resultant oil was purified by flash column chromatography (10–20% EtOAc/Hex) affording the product in a 17% yield (170 mg):

^{1}H NMR (600 MHz, $CDCl_3$) δ 8.63 (d, J = 5.0 Hz, 1H), 7.98 (d, J = 7.8 Hz, 1H), 7.83 – 7.66 (m, 1H), 7.40 (dd, J = 7.6, 4.8 Hz, 1H), 3.24 – 3.05 (m, 2H), 1.84 – 1.70 (m, 1H), 1.48 (ddt, J = 19.7, 13.4, 6.5 Hz, 3H), 1.33 – 1.16 (m, 2H), 1.10 (h, J = 6.7, 5.4 Hz, 4H), 0.88 (d, J = 6.3 Hz, 3H) 0.81 (d, J = 6.7 Hz, 6H).

^{13}C NMR (151 MHz, $CDCl_3$) δ 202.45, 153.65, 148.94, 136.86, 126.97, 121.78, 39.36, 37.14, 35.48, 32.69, 31.03, 28.03, 24.81, 22.78, 22.68, 19.66.

HRMS (ESI): calculated for $C_{16}H_{26}NO$ $[M+H]^+$= 248.2009; found 248.2010.

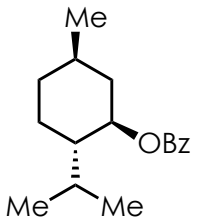

(1*R*,2*S*,5*R*)-2-Isopropyl-5-methylcyclohexyl benzoate was prepared according to a published procedure; spectral data were in agreement with literature values.[10]

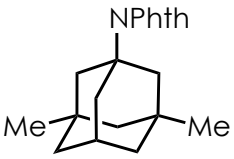

2-(3,5-Dimethyladamantan-1-yl)isoindoline-1,3-dione was prepared according to a published procedure; spectral data were in agreement with literature values.[11]

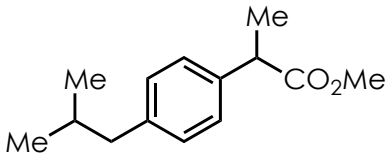

Methyl 2-(4-isobutylphenyl)propanoate was prepared according to a published procedure; spectral data were in agreement with literature values.[12]

Products of Aliphatic C–H Functionalization

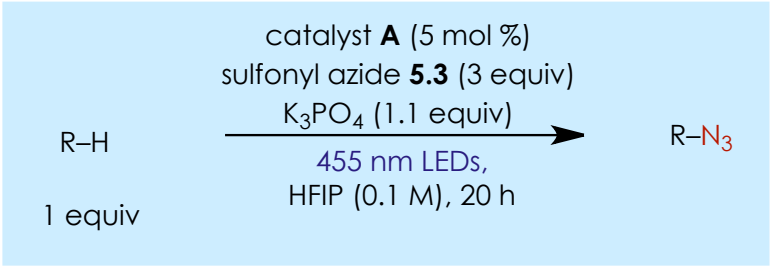

General Procedure A (Azidation): In an argon-filled glovebox, a 1 dram vial with a Teflon-coated magnetic stir bar was charged with ***t*Bu$_2$-Mes-Acr$^+$ A** (0.05 equiv), 4-(trifluoromethyl)benzenesulfonyl azide (3 equiv), K_3PO_4 (1.1 equiv), and the alkane substrate (1 equiv). Hexafluoroisopropanol (HFIP) was added (0.1 M wrt alkane), and the vial was

sealed with a Teflon-lined septum screw cap. The vial was positioned on a stir plate approximately 2 – 3 cm from a Par38 LED lamp supplying blue light (λ = 440-460 nm). After irradiation for 20 hours, the reaction mixture was passed over a short plug of silica and concentrated *in vacuo*. The residue was analyzed by ^{1}H NMR or purified by column chromatography on silica gel with the eluent noted for each substrate.

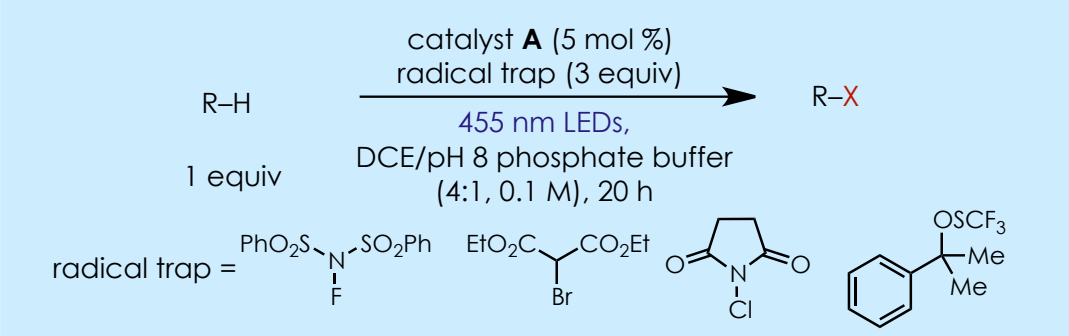

General Procedure B (Halogenation and Trifluoromethylthiolation): In an argon-filled glovebox, a 1 dram vial with a Teflon-coated magnetic stir bar was charged with *t*Bu$_2$-Mes-Acr$^+$ **A** (0.05 equiv), radical trap (3 equiv), and the alkane substrate (1 equiv). 1,2-Dichloroethane (DCE) was added (0.125 M wrt alkane), and the vial was sealed with a Teflon-lined septum screw cap. Upon removal from the glovebox, 4 M pH 8 phosphate buffer was added (0.25 * amount of DCE added such that total solvent amount is 0.1 M wrt alkane). The vial was positioned on a stir plate approximately 2 – 3 cm from a Par38 LED lamp supplying blue light (λ = 440-460 nm). After irradiation for 4 – 20 hours, the reaction mixture was passed over a short plug of silica and concentrated *in vacuo*. The residue was analyzed by ^{1}H NMR or purified by column chromatography on silica gel with the eluent noted for each substrate.

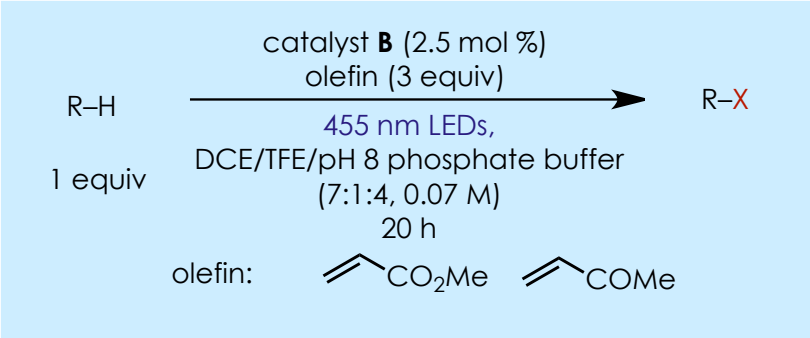

General Procedure C (Alkylation): In an argon-filled glovebox, a 1 dram vial with a Teflon-coated magnetic stir bar was charged with OMe_6-Mes-Acr^+ **B** (0.0025 equiv), olefin (3 equiv), and the alkane substrate (1 equiv). A mixture of DCE and 2,2,2-trifluoroethanol (TFE) was added (7:1, 0.125 M wrt alkane), and the vial was sealed with a Teflon-lined septum screw cap. Upon removal from the glovebox, 4 M pH 8 phosphate buffer was added (0.5 * amount of organic solvent mixture added such that total solvent amount is 0.07 M wrt alkane). For methyl acrylate as the olefin, the vial was positioned on a stir plate approximately 2 – 3 cm from a Par38 LED lamp supplying blue light (λ = 440-460 nm). For methyl vinyl ketone as the olefin, the vial was positioned on a stir plate approximately 2 cm from two Kessil KSH150B Blue 36W LED Grow Lights supplying blue light. After irradiation for 20 hours, the reaction mixture was passed over a short plug of silica and concentrated *in vacuo*. The residue was analyzed by ^{1}H NMR or purified by column chromatography on silica gel with the eluent noted for each substrate.

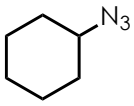

Azidocyclohexane (5.4): Prepared according to General Procedure A (0.1 mmol scale) using cyclohexane, giving 58% yield by ^{1}H NMR. The spectra matched literature values.[13]

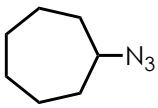

Azidocycloheptane (5.5): Prepared according to General Procedure A (0.1 mmol scale) using cycloheptane, giving 57% yield by ^{1}H NMR. The spectra matched literature values.[14]

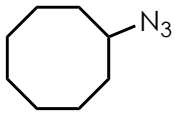

Azidocyclooctane (5.6): Prepared according to General Procedure A (0.1 mmol scale) using cyclooctane, giving 70% yield by ^{1}H NMR. The spectra matched literature values.[6]

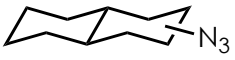

(2*R*,4a*R*,8a*R*)-2-Azidodecahydronaphthalene (5.7): Prepared according to General Procedure A (0.1 mmol scale) using *trans*-decalin, giving 57% yield by ^{1}H NMR and a 1.4:1 ratio of C3:C2. The spectra matched literature values.[13]

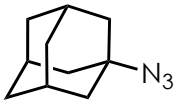

1-Azidoadamantane (5.8): Prepared according to General Procedure A (0.1 mmol scale) using adamantane, giving 75% yield by ^{1}H NMR. The spectra matched literature values.[13]

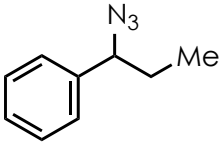

(1-Azidopropyl)benzene (5.9): Prepared according to General Procedure A (0.1 mmol scale) using *n*-propylbenzene, giving 46% yield by ^{1}H NMR. The spectra matched literature values.[13]

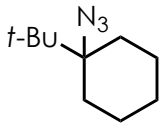

1-Azido-1-(*tert*-butyl)cyclohexane (5.10): Prepared according to General Procedure A (0.1 mmol scale) using *tert*-butylcyclohexane, giving 51% yield by ^{1}H NMR. The spectra matched literature values.[6]

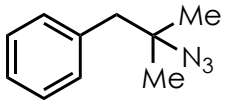

(2-Azido-2-methylpropyl)benzene (5.11). Prepared according to General Procedure A (0.1 mmol scale) using isopropylbenzene, giving 46% combined yield by ^{1}H NMR (1.3:1 site selectivity favoring the tertiary product). The spectra matched literature values.[15]

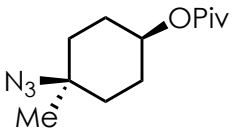

(1*s*,4*s*)-4-Azido-4-methylcyclohexyl pivalate (5.12): Prepared according to General Procedure A (0.1 mmol scale) using *cis*-4-methylcyclohexyl pivalate. ^{1}H NMR analysis of the crude reaction indicated a dr of 1.4:1 with a total NMR yield of 45%. The residue was purified by column chromatography on silica gel (0 to 10% Et_2O/Hexanes) to afford **5.12** (6.3 mg, 24% yield). Characterization data reported for a single isolated diastereomer:

^{1}H NMR (600 MHz, $CDCl_3$) δ 4.68 (tt, J = 9.8, 4.2 Hz, 1H), 1.85 – 1.71 (m, 4H), 1.68 (m, 2H), 1.52 – 1.43 (m, 2H), 1.32 (s, 3H), 1.19 (s, 9H).

^{13}C NMR (151 MHz, $CDCl_3$) δ 178.21, 71.02, 60.54, 38.86, 34.28, 27.35, 27.29, 27.23.

HRMS (APCI): calculated for $C_{12}H_{21}N_3O_2Na$ $[M+Na]^+$= 262.1526; found 262.1436.

IR (film) cm^{-1} 2921.63, 2850.27, 2100.10, 1716.34, 1698.02, 1507.10, 1296.92.

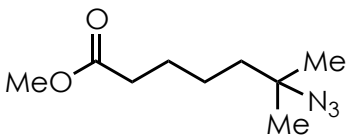

Methyl 6-azido-6-methylheptanoate (5.13): Prepared according to General Procedure A (0.1 mmol scale) using methyl 6-methylheptanoate. The crude residue was purified by column chromatography on silica gel (0 to 10% Et_2O/Hexanes) to afford **5.13** (14.2 mg, 71% yield):

^{1}H NMR (600 MHz, $CDCl_3$) δ 3.74 – 3.63 (m, 3H), 2.36 – 2.28 (m, 2H), 1.66 – 1.59 (m, 2H), 1.52 – 1.44 (m, 2H), 1.38 (dd, *J* = 7.4, 4.1 Hz, 2H), 1.24 (dd, *J* = 4.2, 2.4 Hz, 6H).

^{13}C NMR (151 MHz, $CDCl_3$) δ 174.07, 61.59, 51.64, 41.21, 34.04, 26.09, 25.26, 23.94.

HRMS (ESI): calculated for $C_9H_{17}N_3O_2Na$ $[M+Na]^+$= 222.1213; found 222.1218.

IR (film) cm^{-1} 2949.59, 2869.56, 2096.24, 1740.44, 1463.71, 1370.18, 1252.54.

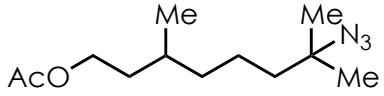

7-Azido-3,7-dimethyloctyl acetate (5.14): Prepared according to General Procedure A (0.1 mmol scale) using 3,7-dimethyloctyl acetate. The crude residue was purified by column chromatography on silica gel (0 to 10% Et_2O/Hexanes) to give **5.14** in 73% yield and a 4:1 ratio of 3˚ isomers. The spectra matched literature values.[6]

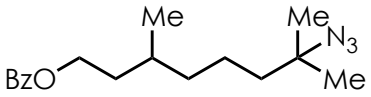

7-Azido-3,7-dimethyloctyl benzoate (5.15): Prepared according to General Procedure A (0.1 mmol scale) using 3,7-dimethyloctyl benzoate. The crude residue was purified by column chromatography on silica gel (0 to 10% Et_2O/Hexanes) to afford **5.15** (27.7 mg, 91% yield, 3:1 ratio of 3˚ isomers). Characterization data reported for major isomer:

^{1}H NMR (600 MHz, $CDCl_3$) δ 8.06 – 8.02 (m, 2H), 7.60 – 7.53 (m, 1H), 7.45 (d, *J* = 7.8 Hz, 2H), 4.40 – 4.32 (m, 2H), 1.85 – 1.78 (m, 1H) 1.70 – 1.63 (m, 1H), 1.62 – 1.57 (m, 1H), 1.49 – 1.30 (m, 5H), 1.25 (s, 6H), 1.23 – 1.15 (m, 1H), 1.00 – 0.97 (m, 3H).

^{13}C NMR (151 MHz, $CDCl_3$) δ 166.81, 132.97, 130.63, 129.67, 128.48, 63.57, 61.79, 41.81, 37.27, 35.69, 30.08, 26.17, 26.14, 21.73, 19.66.

HRMS (ESI): calculated for $C_{17}H_{25}N_3O_2Na$ $[M+H]^+$= 326.1839; found 326.1840.

IR (film) cm^{-1} 2959.23, 2131.92, 2098.17, 1719.23, 1406.82, 1275.68, 1176.36.

The reaction was also performed on 1 mmol scale in a scintillation vial with irradiation from 1 Ecoxotic lamp for 2 days and purified to afford **5.15** (182 mg, 60% yield). The decrease in yield is likely due to reduced light penetration through the thicker-walled scintillation vial.

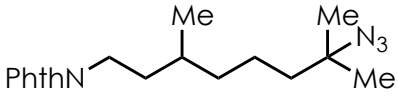

2-(7-Azido-3,7-dimethyloctyl)isoindoline-1,3-dione (5.16): Prepared according to General Procedure A (0.1 mmol scale) using 2-(3,7-dimethyloctyl)isoindoline-1,3-dione. The crude residue was purified by column chromatography on silica gel (0 to 10% Et_2O/Hexanes) to afford **5.16** (24.7 mg, 72% yield, 3:1 ratio of 3˚ isomers). Characterization data reported for major isomer:

^{1}H NMR (600 MHz, $CDCl_3$) δ 7.83 (dd, *J* = 5.4, 3.0 Hz, 2H), 7.70 (dd, *J* = 5.4, 3.1 Hz, 2H), 3.70 (dq, *J* = 7.5, 2.9 Hz, 2H), 1.73 – 1.67 (m, 1H), 1.58 – 1.42 (m, 4H), 1.41 – 1.28 (m, 3H), 1.24 (s, 6H), 1.21 – 1.13 (m, 1H), 0.98 (d, *J* = 5.9 Hz, 3H).

^{13}C NMR (151 MHz, $CDCl_3$) δ 168.53, 133.97, 132.35, 123.28, 61.80, 41.67, 37.07, 36.38, 35.61, 30.73, 26.13, 26.10, 21.63, 19.43.

HRMS (ESI): calculated for $C_{18}H_{24}N_4O_2Na$ $[M+Na]^+$= 351.1792; found 351.1797.

IR (film) cm^{-1} 2955.38, 2870.52, 2098.17, 1772.26, 1715.37, 1321.14, 1266.04.

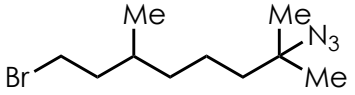

7-Azido-1-bromo-3,7-dimethyloctane (5.17): Prepared according to General Procedure A (0.1 mmol scale) using 1-bromo-3,7-dimethyloctane. The crude residue was purified by column chromatography on silica gel (0 to 10% Et_2O/Hexanes) to afford **5.17** in 67% yield and a 3:1 ratio of 3˚ isomers. The spectra matched literature values.[6]

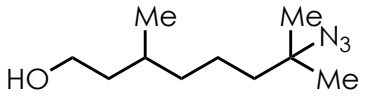

7-Azido-3,7-dimethyloctan-1-ol (5.18): Prepared according to General Procedure A (0.1 mmol scale) using 3,7-dimethyl-1-octanol to afford **5.18** in 63% yield and a 2.7:1 ratio of 3˚ isomers. The spectra matched literature values.[6]

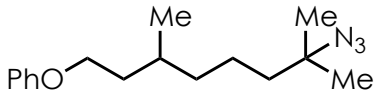

((7-Azido-3,7-dimethyloctyl)oxy)benzene (5.19): Prepared according to General Procedure A (0.1 mmol scale) using ((3,7-dimethyloctyl)oxy)benzene. The crude residue was purified by column chromatography on silica gel (0 to 10% Et_2O/Hexanes) to afford **5.19** (8.6 mg, 31% yield by ^{1}H NMR, 2.1:1 ratio of 3˚ isomers). The product was characterized as an inseparable mixture from an impurity:

^{1}H NMR (600 MHz, $CDCl_3$) δ 7.30 – 7.26 (m, 2H), 6.95 – 6.91 (m, 1H), 6.91 – 6.87 (m, 2H), 4.04 – 3.95 (m, 2H), 2.05 – 1.94 (m, 1H), 1.83 (dtd, *J* = 13.8, 7.0, 5.3 Hz, 1H), 1.74 – 1.65 (m, 1H), 1.64 – 1.55 (m, 2H), 1.50 – 1.43 (m, 2H), 1.39 – 1.32 (m, 3H), 1.29 – 1.23 (m, 6H), 1.00 – 0.94 (m, 3H).

^{13}C NMR (151 MHz, $CDCl_3$) δ 129.56, 128.86, 120.64, 114.64, 66.17, 61.84, 41.82, 37.38, 36.33, 29.92, 26.19, 22.72, 21.75, 19.71.

HRMS (ESI): calculated for $C_{16}H_{25}N_3ONa$ $[M+Na]^+$= 298.1890; found 298.1896.

IR (film) cm^{-1} 2929.34, 2870.52, 2098.17, 1558.20, 1540.85, 1520.60, 1244.83.

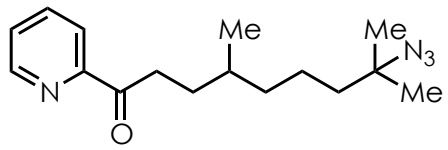

8-Azido-4,8-dimethyl-1-(pyridin-2-yl)nonan-1-one (5.20): Prepared according to General Procedure A (0.1 mmol scale) using 4,8-dimethyl-1-(pyridin-2-yl)nonan-1-one. The crude residue was purified by column chromatography on silica gel (0 to 10% Et_2O/Hexanes) to afford **5.20** (11.2 mg, 39% yield, 3:1 ratio of 3˚ isomers):

^{1}H NMR (600 MHz, $CDCl_3$) δ 8.68 (ddd, *J* = 4.8, 1.7, 0.9 Hz, 1H), 8.04 (dt, *J* = 7.9, 1.1 Hz, 1H), 7.83 (td, *J* = 7.7, 1.7 Hz, 1H), 7.50 – 7.43 (m, 1H), 3.25 – 3.18 (m, 2H), 1.83 – 1.75 (m, 1H), 1.58 – 1.51 (m, 3H), 1.50 – 1.43 (m, 2H), 1.43 – 1.31 (m, 2H), 1.25 (s, 6H), 1.21 – 1.17 (m, 1H), 0.95 (d, *J* = 6.4 Hz, 3H).

^{13}C NMR (151 MHz, $CDCl_3$) δ 202.52, 153.69, 149.06, 137.01, 127.14, 121.93, 61.87, 41.86, 37.18, 35.53, 32.67, 31.03, 26.17, 26.14, 21.84, 19.66.

HRMS (ESI): calculated for $C_{16}H_{24}N_4ONa$ $[M+Na]^+$ = 311.1843; found 311.1852.

IR (film) cm^{-1} 2933.20, 2869.56, 2097.21, 1698.02, 1540.85, 1520.60,1321.00, 1267.69.

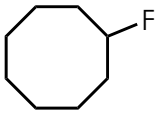

Fluorocyclooctane. Prepared according to General Procedure B (0.1 mmol scale) using cyclooctane as the substrate and NFSI as the radical trap with 4 hours of irradiation, affording 64% yield by ^{19}F NMR. The spectra matched literature values.[16]

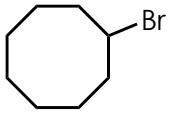

Bromocyclooctane. Prepared according to General Procedure B (0.1 mmol scale) using cyclooctane as the substrate and diethyl bromomalonate as the radical trap with 20 hours of irradiation, affording 60% yield by ^{1}H NMR. The spectra matched literature values.[17]

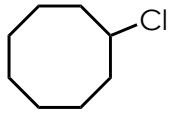

Chlorocyclooctane. Prepared according to General Procedure B (0.1 mmol scale) using cyclooctane as the substrate and NCS as the radical trap with 20 hours of irradiation, affording 32% yield by ^{1}H NMR. The spectra matched literature values.[18]

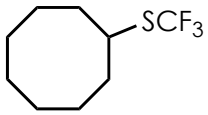

Cyclooctyl(trifluoromethyl)sulfane. Prepared according to General Procedure B (0.1 mmol scale) using cyclooctane as the substrate and ((2-phenylpropan-2-yl)oxy)(trifluoromethyl)sulfane[19] as the radical trap with 4 hours of irradiation. The title compound cyclooctyl(trifluoromethyl)sulfane was afforded in 30% yield by ^{1}H NMR. The spectra matched literature values.[20]

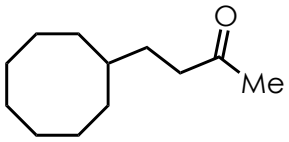

4-Cyclooctylbutan-2-one. Prepared according to General Procedure C using cyclooctane as the substrate and methyl vinyl ketone as the alkene. The title compound was afforded in 76% yield by ^{1}H NMR. The title compound was purified by column chromatography on silica gel to afford 4-cyclooctylbutan-2-one (13.8 mg, 74% yield):

^{1}H NMR (600 MHz, $CDCl_3$) δ 2.45 – 2.38 (m, 2H), 2.14 (s, 3H), 1.69 – 1.61 (m, 2H), 1.60 – 1.54 (m, 5H), 1.52 – 1.38 (m, 8H), 1.26 (dtd, J = 14.0, 8.6, 2.8 Hz, 2H).

^{13}C NMR (151 MHz, $CDCl_3$) δ 209.79, 42.17, 37.06, 32.31, 32.08, 30.02, 27.38, 26.42, 25.57.

HRMS (ESI): calculated for $C_{12}H_{22}ONa$ $[M+Na]^+$= 205.1563; found 205.1563.

IR (film) cm^{-1} 2923.56, 2854.13, 1717.30, 1455.99, 1361.50.

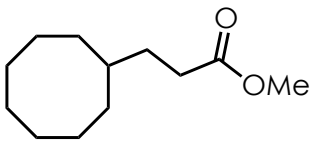

Methyl 3-cyclooctylpropanoate: Prepared according to General Procedure C using cyclooctane as the substrate and methyl acrylate as the alkene. The residue was purified by column chromatography on silica gel to give methyl 3-cyclooctylpropanoate in 43% yield. The spectra matched literature values:[21]

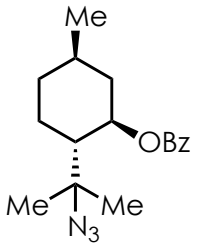

(1*R*,2*S*,5*R*)-2-(2-Azidopropan-2-yl)-5-methylcyclohexyl benzoate (5.22): Prepared according to General Procedure A (0.1 mmol scale) using (1*R*,2*S*,5*R*)-2-isopropyl-5-methylcyclohexyl benzoate. The crude residue was purified by column chromatography on silica gel (0 to 10% Et_2O/Hexanes) to afford **5.22** (16.3 mg, 54% yield):

^{1}H NMR (600 MHz, $CDCl_3$) δ 8.07 (d, *J* = 7.8 Hz, 2H), 7.61 – 7.51 (m, 1H), 7.50 – 7.39 (m, 2H), 5.10 (td, *J* = 11.5, 10.9, 4.4 Hz, 1H), 2.10 (d, *J* = 12.3 Hz, 1H), 2.07 – 1.99 (m, 1H), 1.85 (td, *J* = 11.6, 10.9, 3.6 Hz, 1H), 1.78 – 1.70 (m, 1H), 1.66 – 1.52 (m, 1H), 1.29 (d, *J* = 4.9 Hz, 6H), 1.24 – 1.10 (m, 2H), 1.02 – 0.95 (m, 1H), 0.93 (dd, *J* = 6.6, 2.0 Hz, 3H).

^{13}C NMR (151 MHz, $CDCl_3$) δ 165.84, 133.05, 130.77, 129.77, 128.53, 74.01, 63.74, 49.31, 41.48, 34.24, 31.38, 26.70, 25.32, 24.64, 21.86.

HRMS (ESI): calculated for $C_{17}H_{23}N_3O_2Na$ $[M+Na]^+$= 324.1683; found 324.1678.

IR (film) cm^{-1} 2958.27, 2872.45, 2131.92, 2102.03, 1715.37, 1322.93, 1276.65.

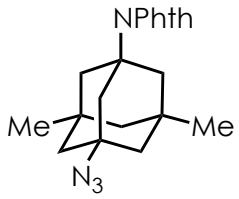

2-(3-Azido-5,7-dimethyladamantan-1-yl)isoindoline-1,3-dione (5.23): Prepared according to General Procedure A (0.1 mmol scale) using 2-(3,5-dimethyladamantan-1-yl)isoindoline-1,3-dione. The crude residue was purified by column chromatography on silica gel (0 to 10% Et_2O/Hexanes) to afford **5.23** (19.3 mg, 55% yield):

^{1}H NMR (600 MHz, $CDCl_3$) δ 7.76 (dd, *J* = 5.4, 3.0 Hz, 2H), 7.68 (dd, *J* = 5.5, 3.0 Hz, 2H), 2.45 (s, 2H), 2.14 (s, 4H), 1.61 – 1.54 (m, 2H), 1.44 (d, *J* = 11.9 Hz, 2H), 1.26 (dt, *J* = 12.7, 2.3 Hz, 1H), 1.20 – 1.10 (m, 1H), 0.99 (s, 6H).

^{13}C NMR (151 MHz, $CDCl_3$) δ 169.60, 134.04, 131.87, 122.86, 61.90, 60.79, 49.20, 46.57, 44.99, 42.78, 34.02, 29.55.

HRMS (ESI): calculated for $C_{20}H_{23}N_4O_2$ $[M+H]^+$= 351.1833; found 351.1816.

IR (film) cm^{-1} 2900.55, 2862.81, 2090.46, 1706.69, 1540.85, 1316.18, 1247.72.

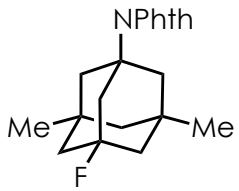

2-(3-Fluoro-5,7-dimethyladamantan-1-yl)isoindoline-1,3-dione (5.24). Prepared according to General Procedure B (0.1 mmol scale) using 2-(3,5-dimethyladamantan-1-yl)isoindoline-1,3-dione as the substrate and NFSI as the radical trap with 4 hours of irradiation. The residue was purified by column chromatography on silica gel to afford **5.24** (28.2 mg, 86% yield). Minor amounts of secondary fluorination product are also present:

^{1}H NMR (600 MHz, $CDCl_3$) δ 7.76 (dd, *J* = 5.4, 3.1 Hz, 2H), 7.68 (dd, *J* = 5.5, 3.0 Hz, 2H), 2.60 – 2.57 (m, 2H), 2.18 – 2.13 (m, 2H), 2.08 (ddd, *J* = 12.4, 2.4, 1.2 Hz, 2H), 1.70 – 1.64 (m, 2H), 1.58 – 1.53 (m, 2H), 1.23 (ddt, *J* = 12.8, 4.1, 2.2 Hz, 1H), 1.16 (dt, *J* = 12.7, 2.3 Hz, 1H), 1.01 (s, 6H).

^{13}C NMR (151 MHz, $CDCl_3$) δ 169.57, 134.03, 131.84, 122.86, 93.50 (d, *J* = 183.7 Hz), 62.51 (d, *J* = 12.1 Hz), 49.18 (d, *J* = 1.5 Hz), 47.73 (d, *J* = 16.6 Hz), 45.01 (d, *J* = 1.5 Hz), 43.95 (d, *J* = 21.1 Hz), 34.91 (d, *J* = 10.6 Hz), 29.34.

^{19}F NMR (400 MHz, $CDCl_3$) δ –135.68.

HRMS (ESI): calculated for $C_{20}H_{22}FNO_2$ $[M+H]^+$= 328.1707; found 328.1720.

IR (film) cm^{-1} 2925.48, 2906.20, 1771.30, 1707.66, 1456.96, 1316.18, 717.39.

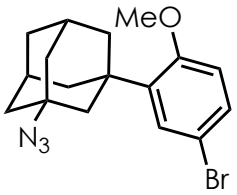

1-Azido-3-(5-bromo-2-methoxyphenyl)adamantane (5.25): Prepared according to General Procedure A (0.1 mmol scale) using 2-(1-adamantyl)-4-bromoanisole. The crude residue was purified by column chromatography on silica gel (0 to 10% Et_2O/Hexanes) to give **5.25** in 40% yield by ^{1}H NMR due to the product being inseparable from an impurity:

^{1}H NMR (600 MHz, $CDCl_3$) δ 7.34 – 7.31 (m, 1H), 7.28 (s, 1H), 6.77 (d, *J* = 8.7 Hz, 1H), 3.84 (d, *J* = 3.8 Hz, 3H), 2.34 (dq, *J* = 6.5, 3.2 Hz, 2H), 2.14 (d, *J* = 5.9 Hz, 2H), 2.07 (dt, *J* = 12.9, 2.8 Hz, 2H), 1.97 (q, *J* = 14.5, 12.6 Hz, 2H), 1.86 (d, *J* = 3.3 Hz, 3H), 1.76 – 1.65 (m, 2H).

^{13}C NMR (151 MHz, $CDCl_3$) δ 157.75, 138.48, 130.07, 129.73, 113.49, 112.42, 59.92, 55.61, 55.40, 44.02, 43.89, 41.00, 39.72, 39.69, 39.11, 35.48, 30.31.

HRMS (APCI): calculated for $C_{17}H_{20}N_3OBrNa$ $[M+Na]^+$= 384.0682; found 384.0738.

IR (film) cm^{-1} 2912.95, 2865.06, 2089.49, 1558.20, 1496.49, 1234.22.

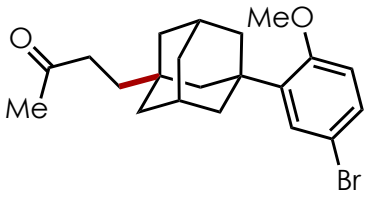

4-((1*r*,3*s*,5*R*,7*S*)-3-(5-bromo-2-methoxyphenyl)adamantan-1-yl)butan-2-one (5.26). Prepared according to General Procedure C using 2-(1-adamantyl)-4-bromoanisole as the substrate and methyl vinyl ketone as the alkene. The residue was purified by column chromatography on silica gel to afford **5.26** (17.6 mg, 45% yield):

^{1}H NMR (600 MHz, $CDCl_3$) δ 7.27 – 7.24 (m, 2H), 6.73 (d, *J* = 9.3 Hz, 1H), 3.80 (s, 3H), 2.44 – 2.37 (m, 2H), 2.15 (s, 3H), 2.14 – 2.11 (m, 2H), 1.98 – 1.94 (m, 3H), 1.85 – 1.68 (m, 4H), 1.65 – 1.57 (m, 2H), 1.47 (d, *J* = 2.7 Hz, 3H), 1.46 – 1.41 (m, 2H).

^{13}C NMR (151 MHz, $CDCl_3$) δ 209.98, 157.96, 140.29, 129.81, 129.58, 113.49, 113.39, 55.36, 44.98, 41.59, 39.97, 38.02, 37.81, 37.66, 36.51, 32.84, 30.08, 29.38.

HRMS (ESI): calculated for $C_{21}H_{27}BrO_2Na$ $[M+Na]^+$ = 413.1087; found 413.1082.

IR (film) cm^{-1} 2904.27, 2848.35, 1716.34, 1520.61, 1473.35, 1234.22, 1027.87.

The reaction was also performed on 1 mmol scale in a scintillation vial with irradiation from 2 Kessil lamps for 2 days and purified to afford **4.26** (152 mg, 39% yield).

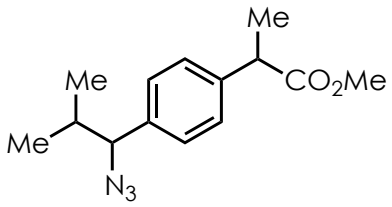

Methyl 2-(4-(2-azido-2-methylpropyl)phenyl)propanoate (5.27): Prepared according to General Procedure A (0.1 mmol scale) using methyl 2-(4-isobutylphenyl)propanoate. ^{1}H NMR analysis of the crude reaction mixture revealed a 1.1:1 ratio of benzylic to tertiary azide isomers. The residue was purified by column chromatography on silica gel (0 to 10% Et_2O/Hexanes) to afford **5.27** (14.8 mg, 57% yield). Characterization data are reported for the previously unreported tertiary isomer; both benzylic azide diastereomers are also present as impurities in the product:[13]

^{1}H NMR (600 MHz, $CDCl_3$) δ 7.30 (d, J = 8.1 Hz, 1H), 7.25 – 7.20 (m, 2H), 7.16 (d, J = 8.1 Hz, 1H), 3.72 (m, 1H), 3.66 (s, 3H), 2.74 (s, 2H), 1.50 (dd, J = 7.2, 5.5 Hz, 3H), 1.26 (s, 6H).

^{13}C NMR (151 MHz, $CDCl_3$) δ 175.17, 139.10, 135.81, 130.87, 127.34, 61.96, 52.17, 47.22, 45.19, 26.06, 18.73.

IR (film) cm^{-1} 2958.27, 2936.09, 2099.14, 1739.48, 1456.96, 1210.11.

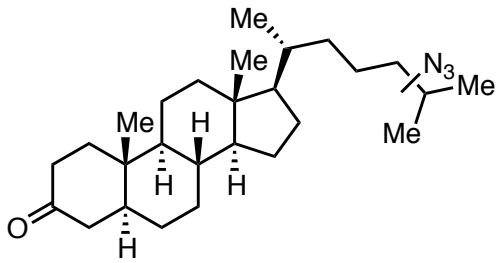

(5*S*,8*R*,9*S*,10*S*,13*R*,14*S*,17*R*)-17-((*R*)-6-Azido-6-methylheptan-2-yl)-10,13-dimethyltetradecahydro-1*H*-cyclopenta[*a*]phenanthren-3(2*H*)-one (5.28):

Prepared according to General Procedure A (0.1 mmol scale) using 5-α-cholestan-3-one. The crude residue was purified by column chromatography on silica gel (0 to 10% Et_2O/Hexanes) to afford **5.28** (13.8 mg, 37% yield), favoring functionalization at the C25 and C17 tertiary positions (approximately 1:1). The ^{13}C spectrum is complicated due to the presence of minor secondary azidation products:

^{1}H NMR (600 MHz, $CDCl_3$) δ 2.41 – 2.34 (m, 1H), 2.32 – 2.23 (m, 2H), 2.11 – 2.05 (m, 1H), 2.04 – 1.95 (m, 2H), 1.86 – 1.60 (m, 3H), 1.60 – 1.46 (m, 5H), 1.46 – 1.29 (m, 8H), 1.28 – 1.19 (m, 1H), 1.25 (s, 3H), 1.19 – 1.04 (m, 4H), 1.04 – 0.98 (m, 1H), 1.01 (d, J = 1.4 Hz, 3H), 0.97 – 0.85 (m, 7.5H), 0.85 – 0.77 (m, 1H), 0.77 – 0.71 (m, 1H), 0.68 (s, 1.5H).

^{13}C NMR (151 MHz, $CDCl_3$) δ 212.34, 212.31, 80.95, 61.93, 56.44, 56.42, 56.33, 53.97, 53.95, 46.86, 44.89, 44.86, 44.80, 42.78, 42.75, 42.07, 42.02, 40.07, 40.05, 39.66, 38.72, 38.36, 38.33, 38.28, 36.30, 35.94, 35.85, 35.80, 35.74, 35.56, 31.89, 31.87, 31.82, 29.14, 29.13, 29.01, 28.39, 28.17, 28.13, 26.23, 26.16, 25.75, 24.39, 24.37, 23.99, 22.97, 22.92, 22.71, 22.65, 21.60, 21.36, 20.91, 18.82, 18.75, 14.80, 14.75, 12.23, 11.63, 11.59.

HRMS (ESI): calculated for $C_{27}H_{45}N_3ONa$ $[M+Na]^+$= 450.3455; found 450.3469.

IR (film) cm^{-1} 2932.23, 2866.62, 2098.17, 1715.37, 1455.99, 1267.97.

The singlet at δ 0.68 ppm corresponds to the methyl at C13, and this signal is underintegrated (1.5H instead of 3H), indicating that the methyl has been shifted for one of the azidation products. Since there is only trace secondary azidation, the methyl at C13 cannot be shifted from azidation at C12 and instead arises from tertiary azidation at C17. Additionally, the isopropyl methyl signals that lie between 0.85 and 0.90 ppm are underintegrated and there is a new signal at 1.25 ppm corresponding to azidation of the isopropyl group at C25. This

signal integrates to 3H instead of 6H, however, indicating that it is only from one of the two products.

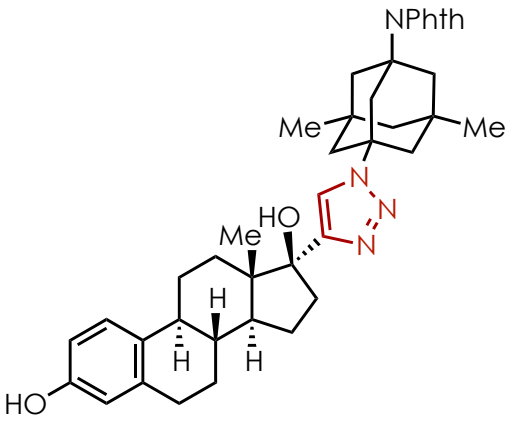

2-((1*S*,3*s*,5*R*,7*S*)-3-(4-((8*R*,9*S*,13*S*,14*S*,17*S*)-3,17-dihydroxy-13-methyl-7,8,9,11,12,13,14,15,16,17-decahydro-6*H*-cyclopenta[*a*]phenanthren-17-yl)-1*H*-1,2,3-triazol-1-yl)-5,7-dimethyladamantan-1-yl)isoindoline-1,3-dione (5.29). In a 1-dram vial in the glovebox, copper (II) sulfate (1 mg, 0.006 mmol) and sodium ascorbate (13 mg, 0.066 mmol) were dissolved in degassed DMF/H_2O (0.19/0.01 mL). The solution was stirred for 30 min, after which memantine azide **5.29** (23 mg, 0.066 mmol) and ethynylestradiol (39 mg, 0.13 mmol) in DMF (0.4 mL) were added. The vial was sealed with a PTFE-lined screw cap and Teflon tape and stirred outside the glovebox for 48 h at room temperature. The reaction mixture was concentrated and purified by flash column chromatography on silica gel (0 – 5% MeOH/DCM) to give **5.29** in 61% yield.

5.29. ^{1}H NMR (600 MHz, $CDCl_3$) δ 7.76 (dd, *J* = 5.4, 3.0 Hz, 2H), 7.69 (dd, *J* = 5.5, 3.0 Hz, 2H), 7.51 (s, 1H), 7.05 (d, *J* = 8.4 Hz, 1H), 6.58 (dd, *J* = 8.4, 2.7 Hz, 1H), 6.55 (d, *J* = 2.6 Hz, 1H), 5.04 (br s, 1H), 2.88 (d, *J* = 3.2 Hz, 2H), 2.78 (tdd, *J* = 14.6, 8.8, 5.2 Hz, 2H), 2.71 (s, 1H), 2.42 (d, *J* = 10.2 Hz, 1H), 2.37 – 2.32 (m, 2H), 2.23 (d, *J* = 12.3 Hz, 2H), 2.12 (td, *J* = 14.3, 13.4, 7.3 Hz, 2H), 2.08 – 2.03 (m, 2H), 1.98 – 1.88 (m, 5H), 1.65 – 1.51 (m, 4H), 1.47

(qd, J = 11.0, 2.6 Hz, 1H), 1.43 – 1.36 (m, 2H), 1.36 – 1.31 (m, 2H), 1.07 (d, J = 1.4 Hz, 6H), 1.04 (s, 3H). **^{13}C NMR** (151 MHz, $CDCl_3$) δ 169.62, 153.52, 152.98, 138.37, 134.16, 132.74, 131.79, 126.56, 122.94, 117.78, 115.39, 112.79, 61.88, 61.73, 49.19, 48.62, 47.94, 47.44, 45.05, 44.00, 43.39, 39.61, 38.19, 33.92, 33.14, 29.84, 29.60, 27.39, 26.39, 23.61, 14.43.

HRMS (APCI): calculated for $C_{40}H_{47}N_4O_4$ $[M+H]^+$= 647.3592; found 647.3605.

Robustness Screen

Below are the results from a robustness screen surveying several different additives containing useful functionality or pharmaceutically relevant heterocycles. Yields of the cyclooctane azidation product **5.6** are given below each additive.

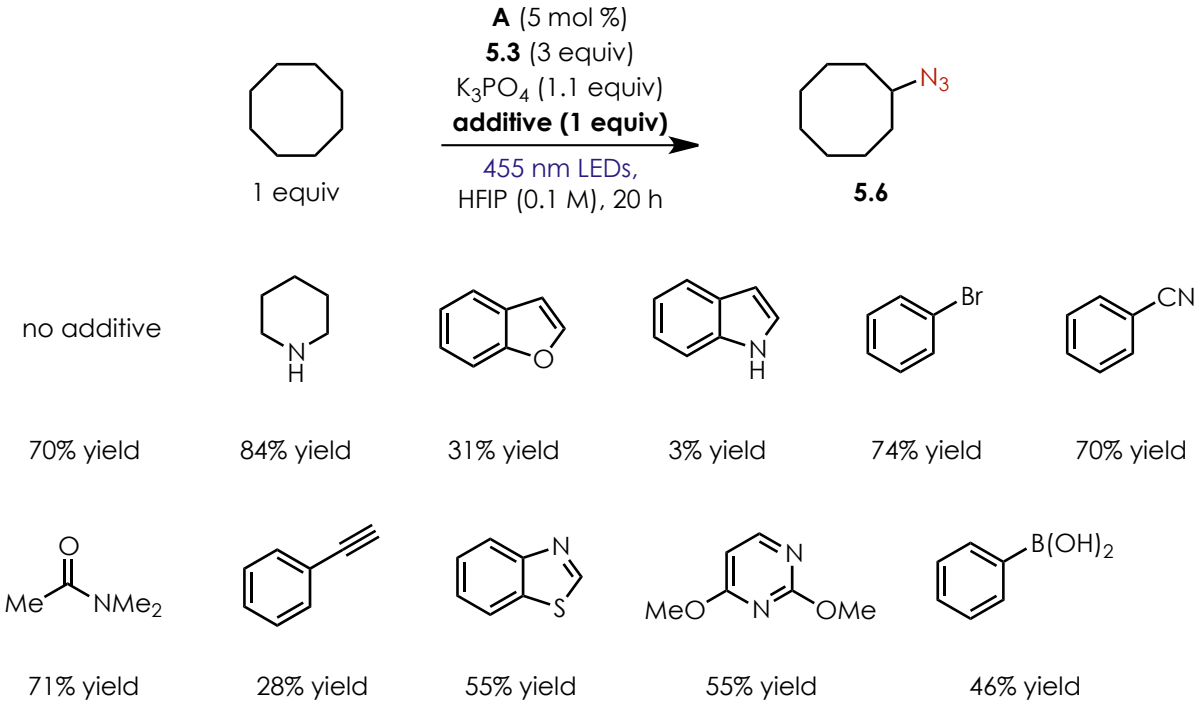

Mechanistic Studies

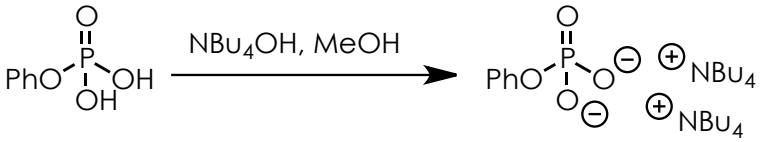

Di(tetrabutylammonium) phenyl phosphate (5.30): To a solution of phenyl dihydrogen phosphate[22] (1.22 g, 7 mmol) in methanol (7 mL) was added tetrabutylammonium hydroxide in methanol (1M, 14 mL, 14 mmol). The solution was stirred overnight and then concentrated *in vacuo*. The resultant oil was dried via high vacuum for one week to afford **5.30** as an amorphous solid. The compound is extremely hygroscopic and unstable outside of an inert atmosphere:[23]

^{1}H NMR (600 MHz, $CDCl_3$) δ 7.19 – 7.10 (m, 2H), 7.06 (t, J = 7.8 Hz, 1H), 6.97 (d, J = 8.0 Hz, 1H), 3.31 – 3.25 (m, 16H), 1.63 – 1.55 (m, 16H), 1.39 (q, J = 7.4 Hz, 16H), 0.94 (t, J = 7.3 Hz, 24H).

^{13}C NMR (151 MHz, $CDCl_3$) δ 129.12, 128.85, 118.14, 116.11, 58.96, 24.20, 19.82, 13.79.

As determined by cyclic voltammetry, the oxidation potential of **5.30** was $E_{p/2}$ = + 0.87 V vs SCE in MeCN. Phosphate esters including **5.30** are known to be unstable for prolonged periods in MeCN.[23]

Stern-Volmer Quenching:

Emission lifetime measurements were taken at ambient temperature using a Edinburgh FLS920 spectrometer and fit to single exponential decay according to a modification of the method previously described by our laboratory.[24] Measurements were made by the time-correlated single photon counting (TCSPC) capability of the instrument with pulsed excitation light (444.2 nm, typical pulse width = 95 ps) generated by a Edinburgh EPL-445 ps pulsed laser diode operating at a repetition rate of 5 MHz. The maximum emission channel count rate was less than 5% of the laser channel count rate, and each data set collected greater than 10000 counts on the maximum channel. The lifetime of fluorescence was determined by reconvolution fit with the instrument response function using the

Edinburgh FS900 software. In all cases, after reconvolution, fluorescence decay was satisfactorily fit with a monoexponential function of the form:

$$\boldsymbol{I_t = I_0 e^{-t/\tau}}$$

where I is the intensity (counts), and t is the mean lifetime of fluorescence.

Stern-Volmer analysis on the quenching of fluorescence lifetime was carried out in DCE or HFIP with detection at 500 nm (15 nm bandwidth), where the concentration of acridinium was 1.6×10^{-5} M. The quenching constant was determined with quencher concentrations in the range of 0 M to 2.0×10^{-2} M. Bimolecular quenching constants, k_q, were determined from the corresponding Stern-Volmer constant.[25] Quenching constants were determined for ***t*-Bu$_2$-Mes-Acr+** with sulfonyl azide **53,** sodium 1,1,1,3,3,3-hexafluoroisopropoxide, and dibasic phosphate **5.30**. Comparison of UV-Vis absorption spectra taken before and after lifetime quenching studies verified that the acridinium was unchanged. UV-Vis spectra were taken on a Hewlett-Packard 8453 Chemstation spectrophotometer.

REFERENCES

(1) Romero, N. A.; Margrey, K. A.; Tay, N. E.; Nicewicz, D. A. *Science* **2015**, *349*, 1326–1330.

(2) Joshi-Pangu, A.; Lévesque, F.; Roth, H. G.; Oliver, S. F.; Campeau, L.-C.; Nicewicz, D.; DiRocco, D. A. *J. Org. Chem.* **2016**, *81*, 7244–7249.

(3) Chuprakov, S.; Malik, J. A.; Zibinsky, M.; Fokin, V. V. *J. Am. Chem. Soc.* **2011**, *133*, 10352–10355.

(4) Shen, D.; Miao, C.; Wang, S.; Xia, C.; Sun, W. *Org. Lett.* **2014**, *16*, 1108–1111.

(5) Dickschat, J. S.; Bruns, H.; Riclea, R. *Beilstein J. Org. Chem.* **2011**, *7*, 1697–1712.

(6) Sharma, A.; Hartwig, J. F. *Nature* **2015**, *517*, 600–604.

(7) Fung, Y.-S.; Yan, S.-C.; Wong, M.-K. *Org. Biomol. Chem.* **2012**, *10*, 3122.

(8) Mukherjee, S.; Maji, B.; Tlahuext-Aca, A.; Glorius, F. *J. Am. Chem. Soc.* **2016**, *138*, 16200–16203.

(9) Skattebøl, L.; Stenstrøm, Y.; Syvertsen, C. *J. Agric. Food Chem.* **2004**, *52*, 6944–6949.

(10) Dander, J. E.; Weires, N. A.; Garg, N. K. *Org. Lett.* **2016**, *18*, 3934–3936.

(11) Schmidt, V. A.; Quinn, R. K.; Brusoe, A. T.; Alexanian, E. J. *J. Am. Chem. Soc.* **2014**, *136*, 14389–14392.

(12) Bogdan, A. R.; Poe, S. L.; Kubis, D. C.; Broadwater, S. J.; McQuade, D. T. *Angew. Chem. Int. Ed.* **2009**, *48*, 8547–8550.

(13) Huang, X.; Bergsten, T. M.; Groves, J. T. *J. Am. Chem. Soc.* **2015**, *137*, 5300–5303.

(14) Klich, K.; Pyta, K.; Kubicka, M. M.; Ruszkowski, P.; Celewicz, L.; Gajecka, M.; Przybylski, P. *J. Med. Chem.* **2016**, *59*, 7963–7973.

(15) Dryzhakov, M.; Hellal, M.; Wolf, E.; Falk, F. C.; Moran, J. *J. Am. Chem. Soc.* **2015**, *137*, 9555–9558.

(16) L'Heureux, A.; Beaulieu, F.; Bennett, C.; Bill, D. R.; Clayton, S.; LaFlamme, F.; Mirmehrabi, M.; Tadayon, S.; Tovell, D.; Couturier, M. *J. Org. Chem.* **2010**, *75*, 3401–3411.

(17) Manabe, Y.; Kitawaki, Y.; Nagasaki, M.; Fukase, K.; Matsubara, H.; Hino, Y.; Fukuyama, T.; Ryu, I. *Chem. - Eur. J.* **2014**, *20*, 12750–12753.

(18) Combe, S. H.; Hosseini, A.; Parra, A.; Schreiner, P. R. *J. Org. Chem.* **2017**, *82*, 2407–2413.

(19) Shao, X.; Xu, C.; Lu, L.; Shen, Q. *Acc. Chem. Res.* **2015**, *48*, 1227–1236.

(20) Wu, H.; Xiao, Z.; Wu, J.; Guo, Y.; Xiao, J.-C.; Liu, C.; Chen, Q.-Y. *Angew. Chem. Int. Ed.* **2015**, *54*, 4070–4074.

(21) van Bruggen, E.; Boelens, H.; Rijkens, F. *Recl. Trav. Chim. Pays-Bas* **2010**, *86*, 958–960.

(22) Cohen, A.; Bergel Franz; Frank Atherton Ratcliffe; Alexander Todd Robertus; Harry Openshaw Tacon; John Wynne Haworth. US2490573 (A).

(23) Friedman, J. M.; Freeman, S.; Knowles, J. R. *J. Am. Chem. Soc.* **1988**, *110*, 1268–1275.

(24) Romero, N. A.; Nicewicz, D. A. *J. Am. Chem. Soc.* **2014**, *136*, 17024–17035.

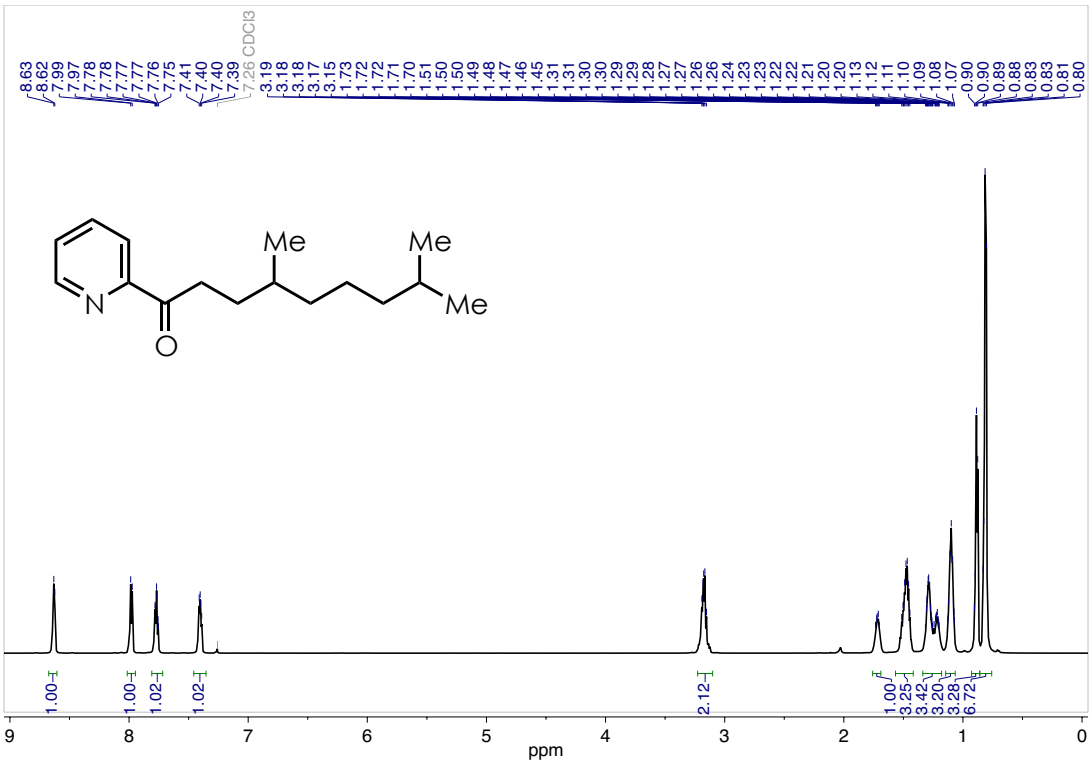
8.63
8.62
7.99
7.97
7.78
7.78
7.77
7.77
7.76
7.75
7.41
7.40
7.40
7.39
7.26 CDCl3
3.19
3.18
3.18
3.17
3.15
1.73
1.72
1.72
1.71
1.70
1.51
1.50
1.50
1.49
1.48
1.47
1.46
1.45
1.31
1.31
1.30
1.30
1.29
1.29
1.28
1.27
1.27
1.26
1.26
1.24
1.23
1.23
1.22
1.22
1.21
1.20
1.20
1.13
1.12
1.11
1.10
1.09
1.08
1.07
0.90
0.90
0.89
0.88
0.83
0.83
0.81
0.80
Me
Me
Me
N
O
1.00
1.00
1.02
1.02
2.12
1.00
3.25
3.42
3.20
3.28
6.72
9
8
7
6
5
4
3
2
1
0
ppm

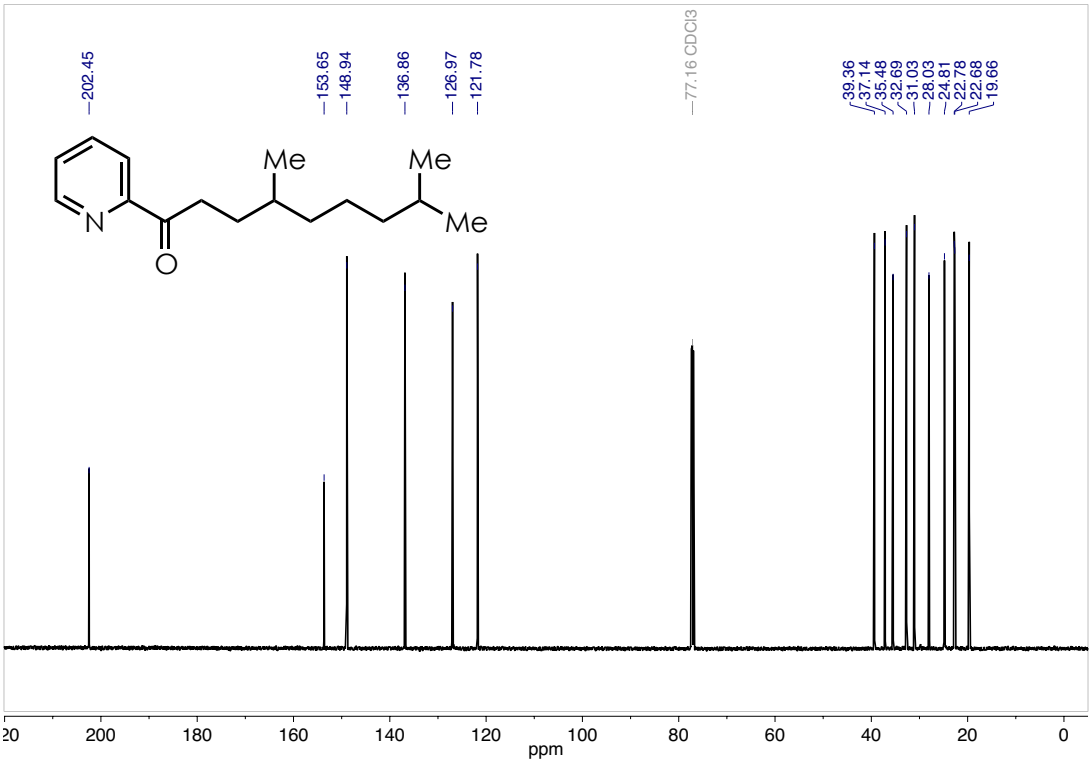
202.45
153.65
148.94
136.86
126.97
121.78
77.16 CDCl3
39.36
37.14
35.48
32.69
31.03
28.03
24.81
22.78
22.68
19.66
Me
Me
Me
N
O
220
200
180
160
140
120
100
80
60
40
20
0
ppm

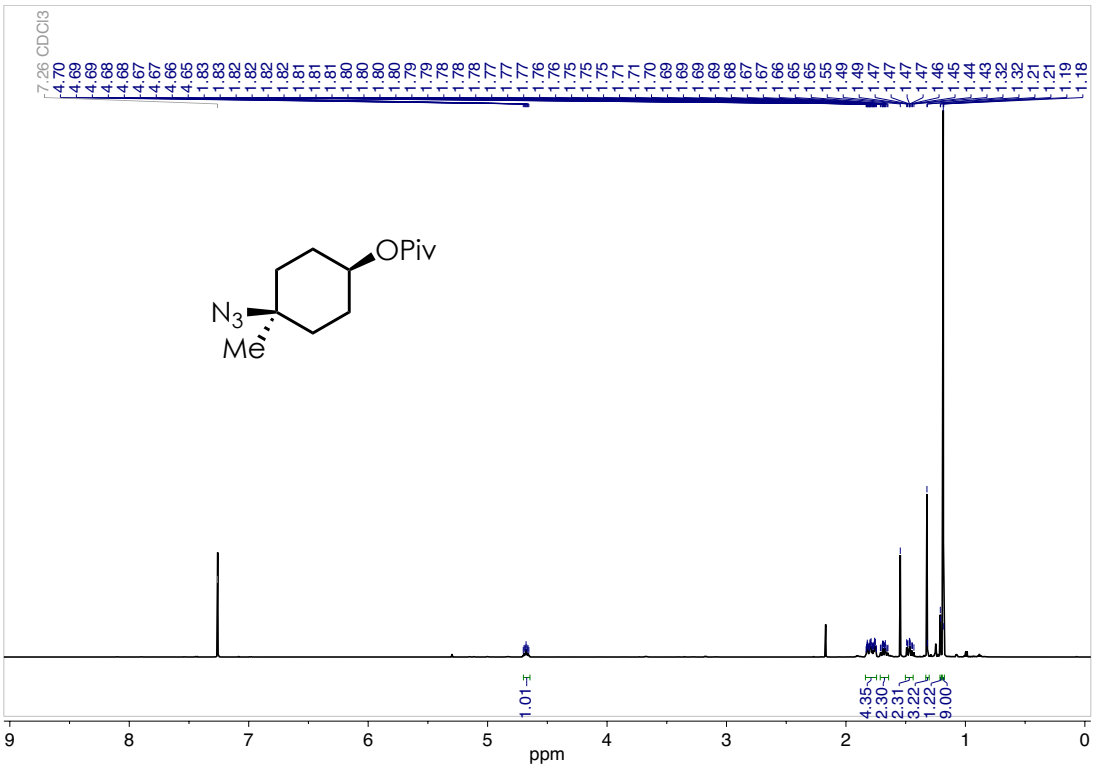
7.26 CDCl3
4.70
4.69
4.69
4.68
4.68
4.67
4.67
4.66
4.65
1.83
1.83
1.82
1.82
1.82
1.82
1.81
1.81
1.81
1.80
1.80
1.80
1.80
1.79
1.79
1.78
1.78
1.78
1.77
1.77
1.77
1.76
1.76
1.75
1.75
1.75
1.71
1.71
1.70
1.69
1.69
1.69
1.69
1.68
1.67
1.67
1.66
1.65
1.65
1.55
1.49
1.49
1.47
1.47
1.47
1.47
1.46
1.45
1.44
1.43
1.32
1.21
1.21
1.19
1.18
OPiv
N3
Me
1.01
4.35
2.30
2.31
3.22
1.22
9.00
9
8
7
6
5
4
3
2
1
0
ppm

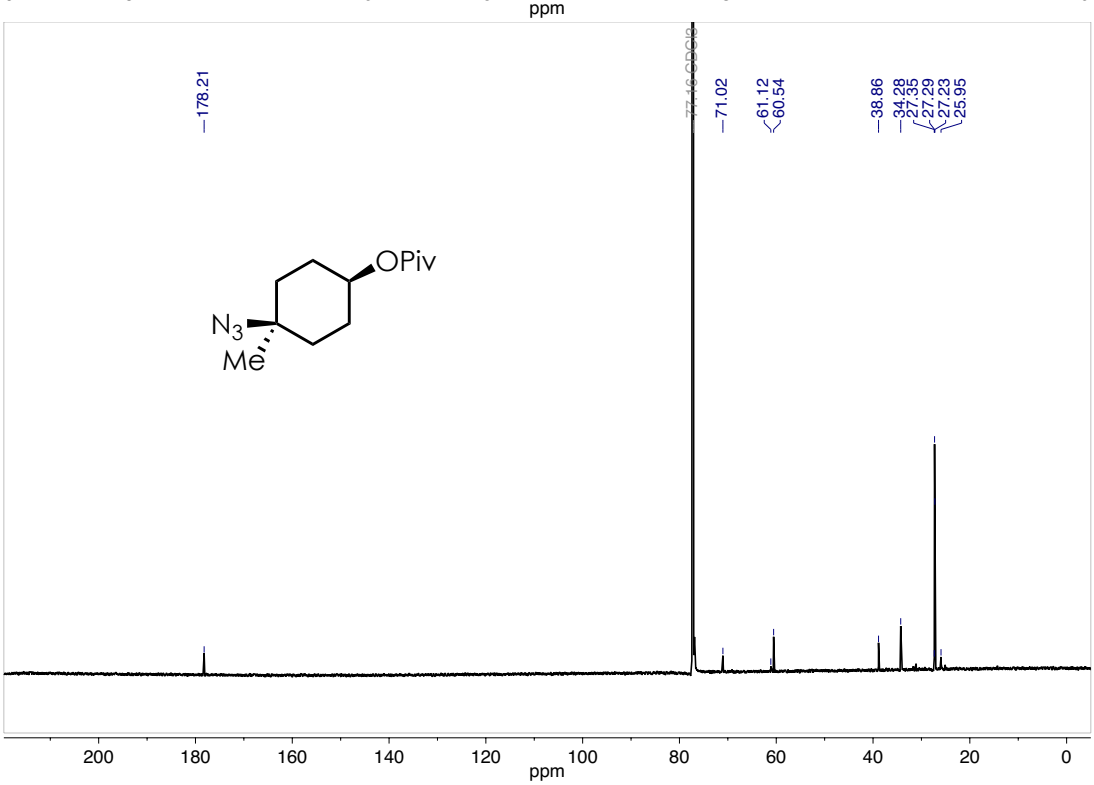
178.21
77.48 CDCl3
71.02
61.12
60.54
38.86
34.28
27.35
27.29
27.23
25.95
OPiv
N3
Me
200
180
160
140
120
100
80
60
40
20
0
ppm

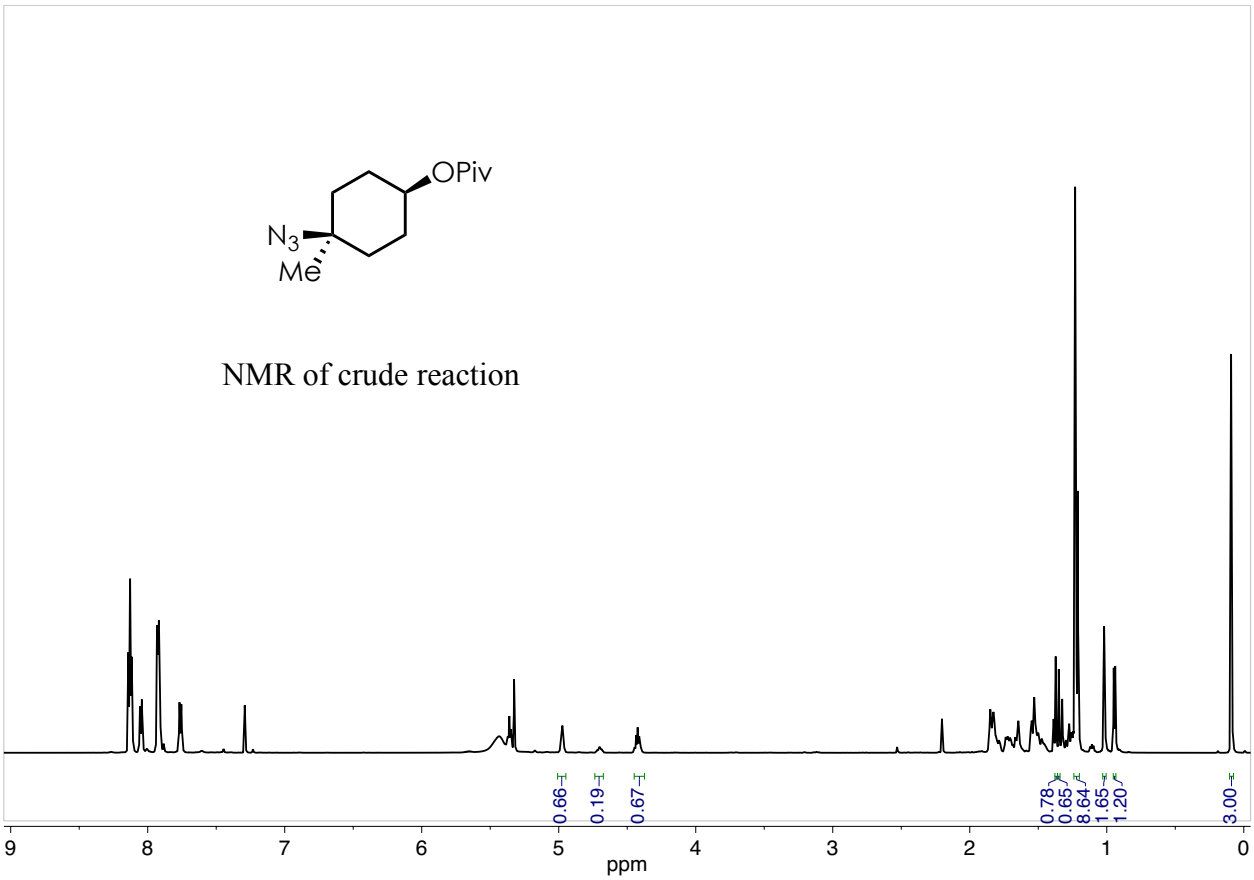

The methyl doublet below 1.0 ppm indicates 40% remaining starting material. The peaks at 5.0 ppm and 4.7 ppm correspond to both diastereomers of product, but the starting material also has a peak at 5.0 ppm. Subtraction of 40% from the peak at 5.0 ppm gives 26% yield of one diastereomer and 19% yield of the other, for a combined NMR yield of 45% and a dr 1.4:1.

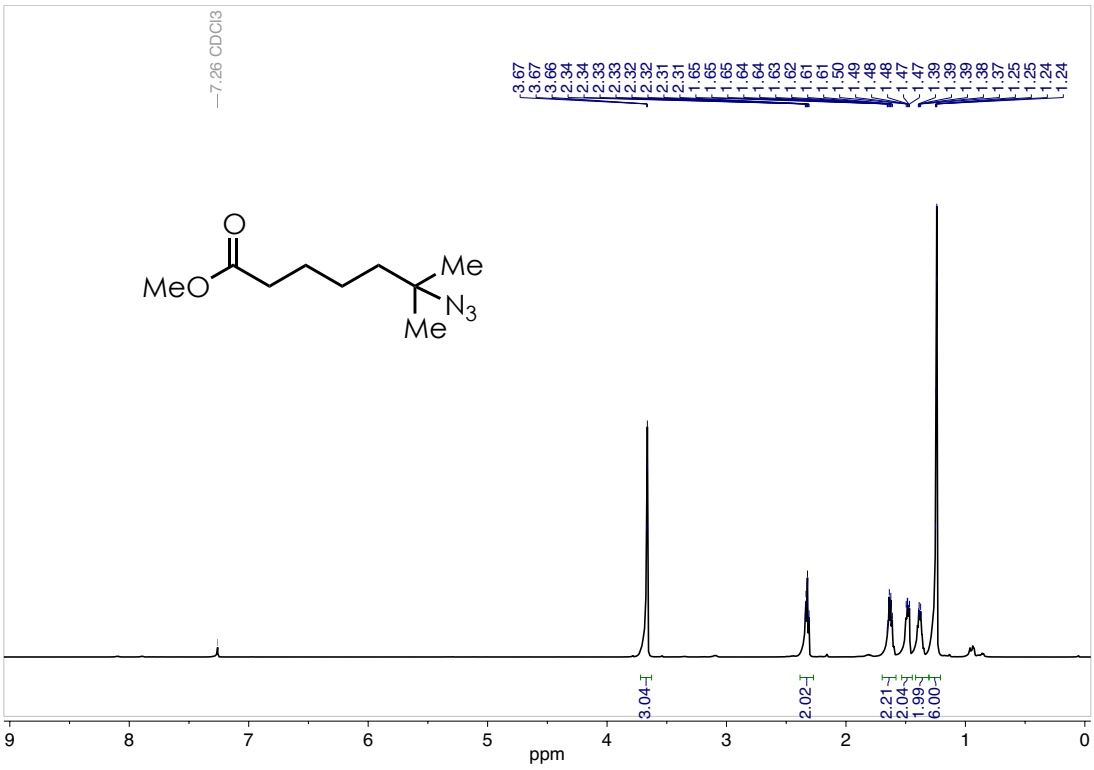
7.26 CDCl3
3.67
3.67
3.66
2.34
2.34
2.33
2.33
2.32
2.32
2.31
2.31
1.65
1.65
1.64
1.64
1.63
1.62
1.61
1.61
1.50
1.49
1.48
1.48
1.47
1.47
1.39
1.39
1.39
1.38
1.37
1.25
1.25
1.24
1.24
MeO
Me
N3
Me
3.04
2.02
2.21
2.04
1.99
6.00
9
8
7
6
5
4
3
2
1
0
ppm

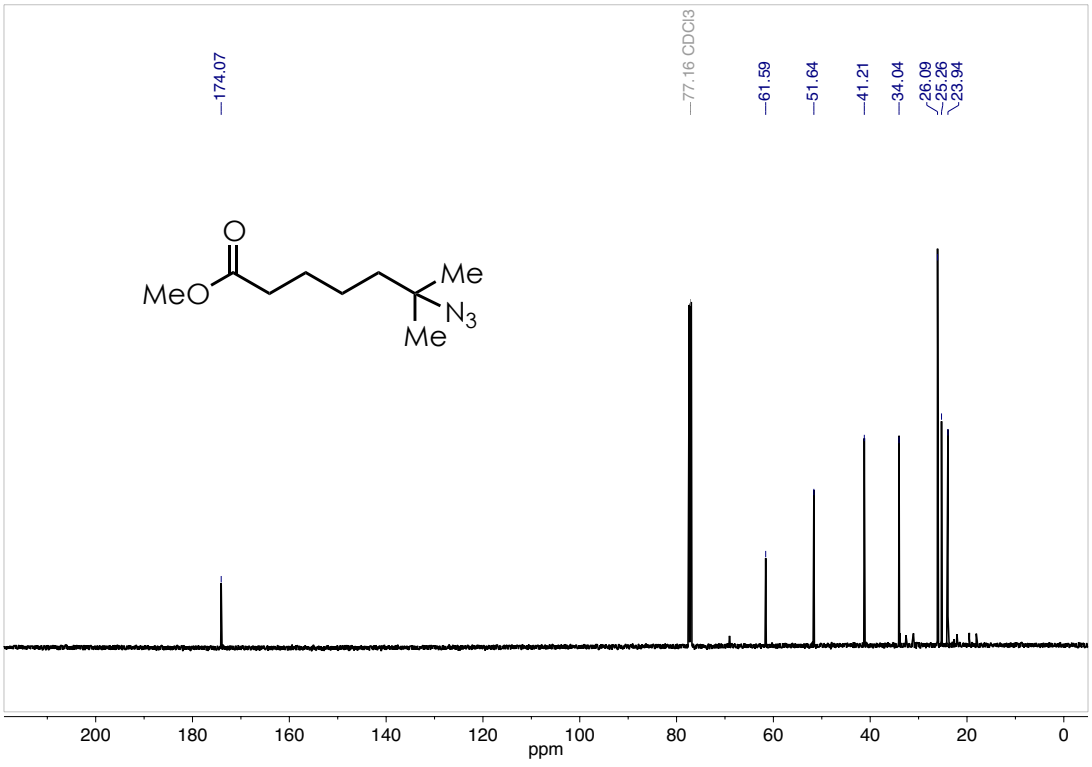
174.07
77.16 CDCl3
61.59
51.64
41.21
34.04
26.09
25.26
23.94
MeO
Me
N3
Me
200
180
160
140
120
100
80
60
40
20
0
ppm

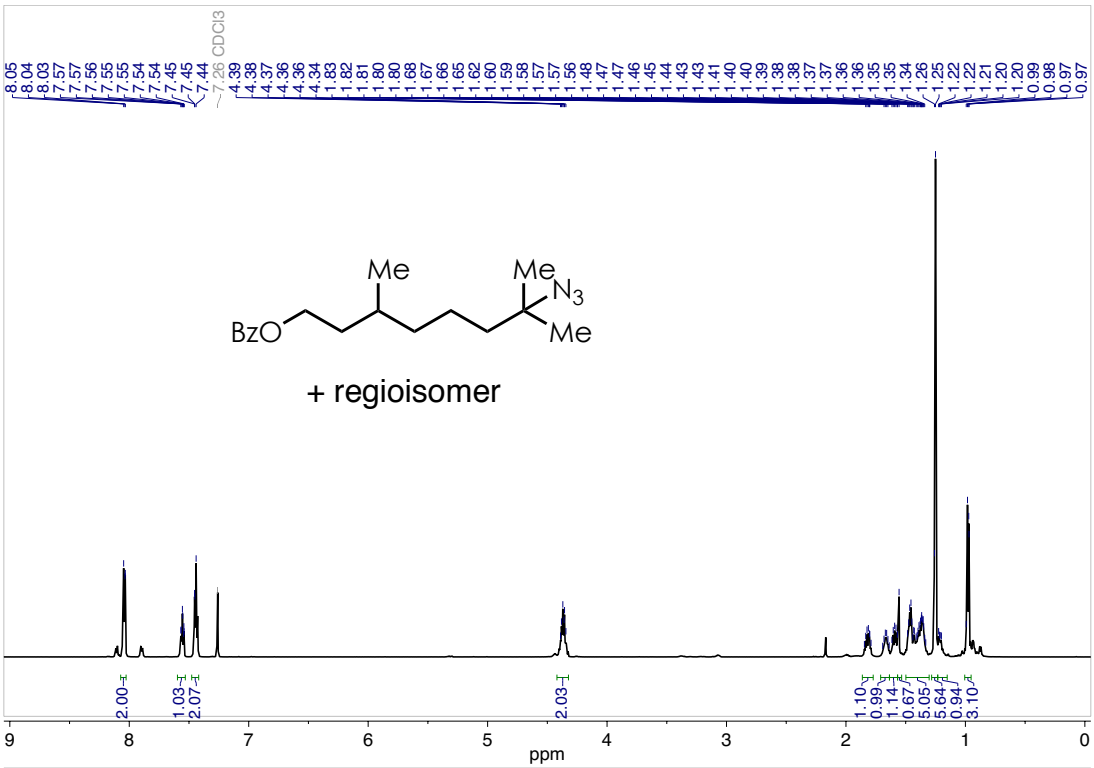
8.05
8.04
8.03
7.57
7.57
7.56
7.55
7.55
7.54
7.54
7.45
7.45
7.44
7.26 CDCl3
4.39
4.38
4.37
4.36
4.36
4.34
1.83
1.82
1.81
1.80
1.80
1.68
1.67
1.66
1.65
1.62
1.60
1.59
1.58
1.57
1.57
1.56
1.48
1.47
1.47
1.46
1.45
1.44
1.43
1.43
1.41
1.40
1.40
1.39
1.38
1.38
1.37
1.37
1.36
1.36
1.35
1.35
1.34
1.26
1.25
1.22
1.22
1.21
1.20
1.20
0.99
0.98
0.97
0.97
Me
Me
N3
Me
BzO
+ regioisomer
2.00
1.03
2.07
2.03
1.10
0.99
1.14
0.67
5.05
5.64
0.94
3.10
9
8
7
6
5
4
3
2
1
0
ppm

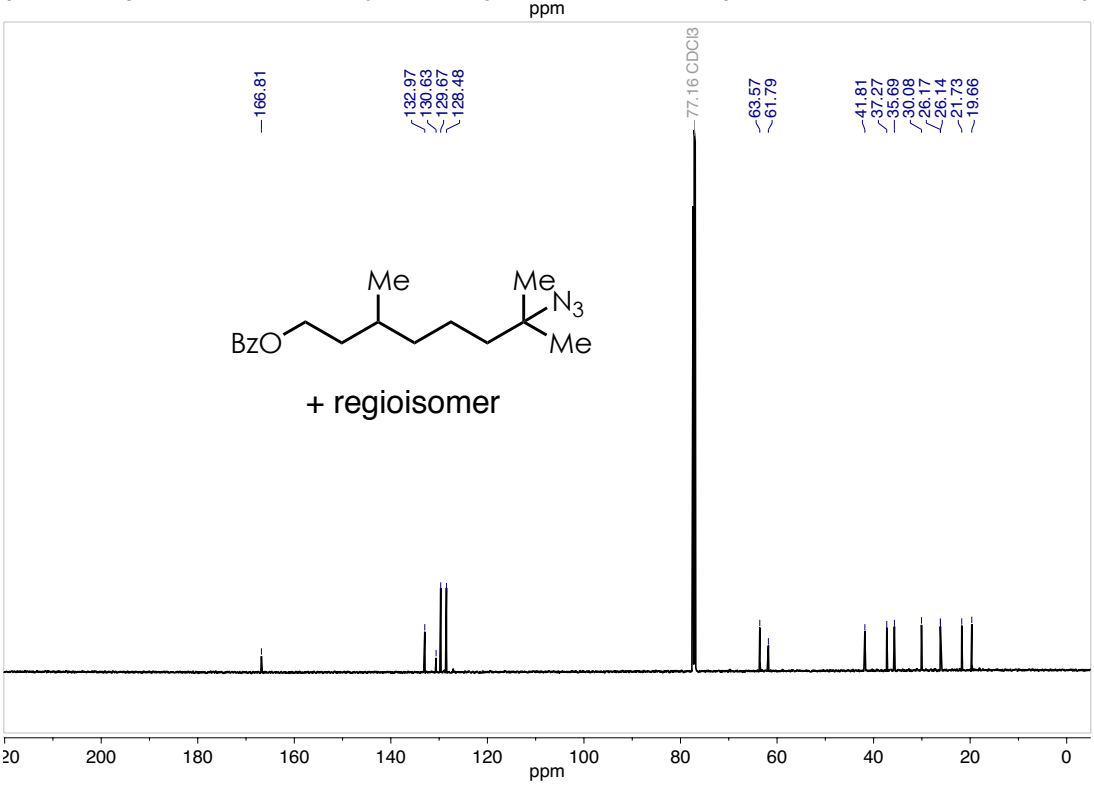
166.81
132.97
130.63
129.67
128.48
77.16 CDCl3
63.57
61.79
41.81
37.27
35.69
30.08
26.17
26.14
21.73
19.66
Me
Me
N3
Me
BzO
+ regioisomer
200
180
160
140
120
100
80
60
40
20
0
ppm

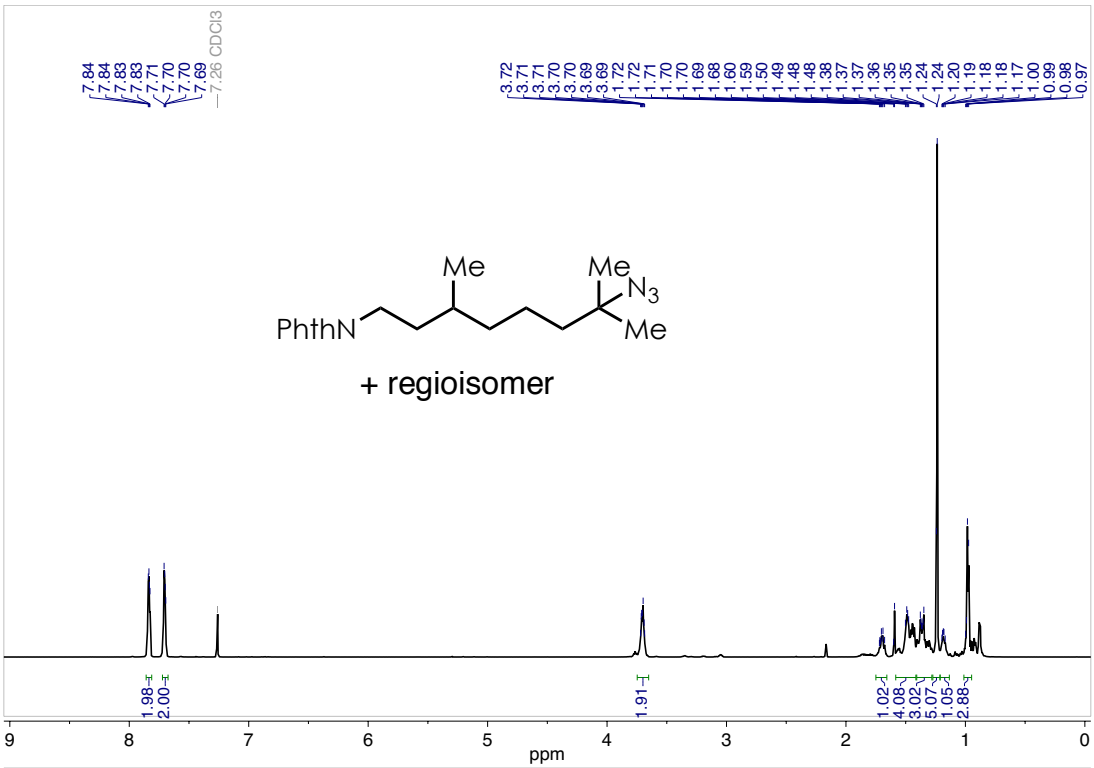
7.84
7.84
7.83
7.83
7.71
7.70
7.70
7.69
7.26 CDCl3
3.72
3.71
3.71
3.70
3.70
3.69
3.69
1.72
1.71
1.70
1.70
1.69
1.68
1.60
1.59
1.50
1.49
1.48
1.48
1.38
1.37
1.37
1.36
1.35
1.35
1.24
1.24
1.20
1.19
1.18
1.18
1.17
1.00
0.99
0.98
0.97
Me
Me
N3
PhthN
Me
+ regioisomer
1.98
2.00
1.91
1.02
4.08
3.02
5.07
1.05
2.88
9
8
7
6
5
4
3
2
1
0
ppm

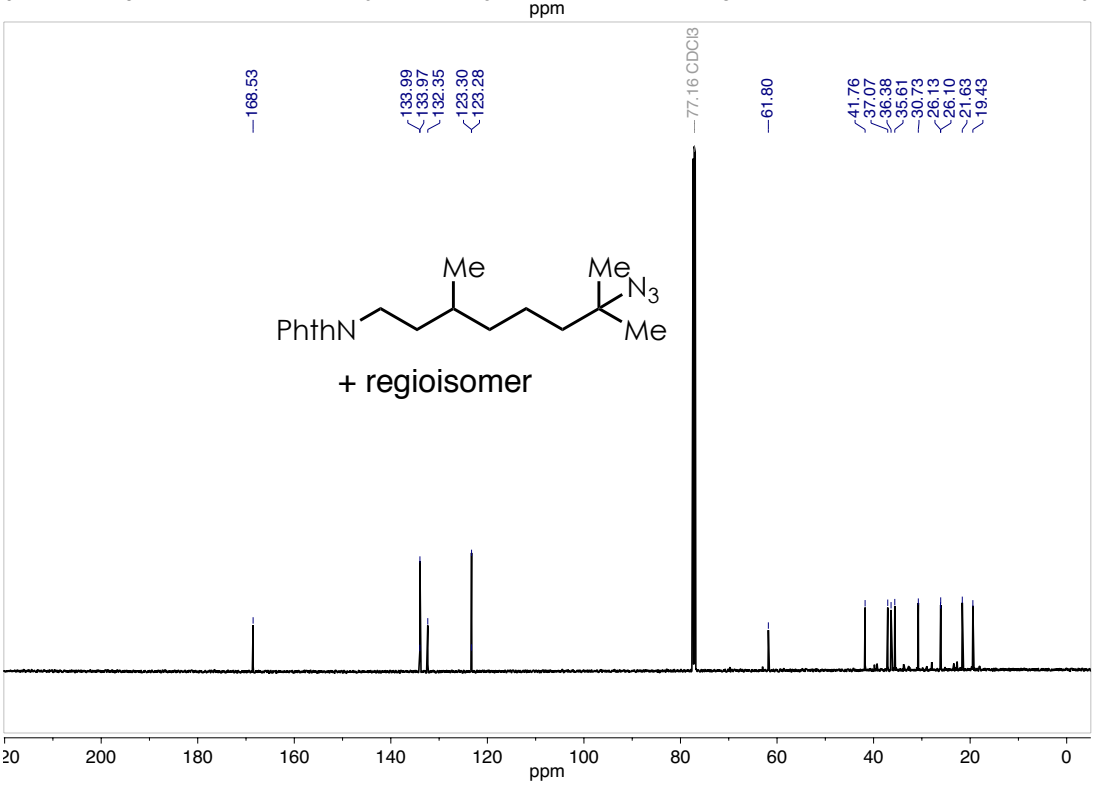
168.53
133.99
133.97
132.35
123.30
123.28
77.16 CDCl3
61.80
41.76
37.07
36.38
35.61
30.73
26.13
26.10
21.63
19.43
Me
Me
N3
PhthN
Me
+ regioisomer
200
180
160
140
120
100
80
60
40
20
0
ppm

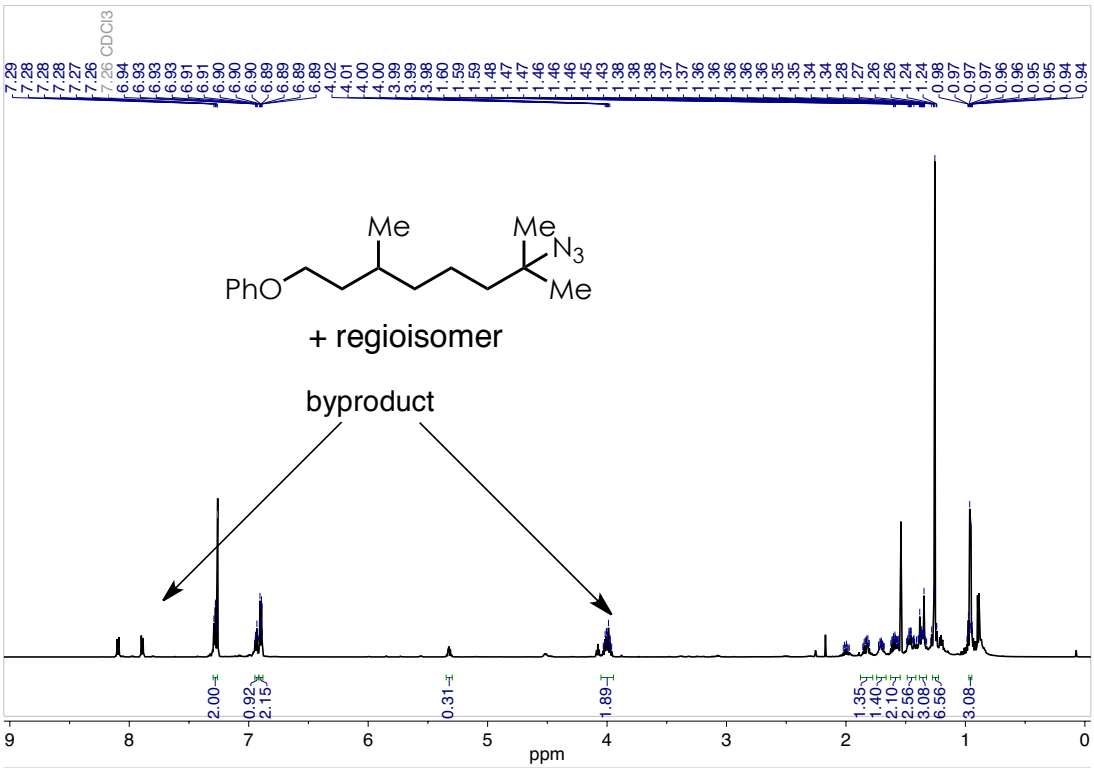
7.29
7.28
7.28
7.28
7.27
7.26
7.26 CDCl3
6.94
6.93
6.93
6.93
6.91
6.91
6.90
6.90
6.90
6.89
6.89
6.89
4.02
4.01
4.00
4.00
3.99
3.99
3.98
1.60
1.59
1.59
1.48
1.47
1.47
1.46
1.46
1.46
1.45
1.43
1.38
1.38
1.38
1.37
1.37
1.36
1.36
1.36
1.36
1.36
1.35
1.35
1.34
1.34
1.28
1.27
1.26
1.26
1.24
1.24
0.98
0.97
0.97
0.97
0.96
0.96
0.95
0.94
0.94
Me
Me
N3
PhO
Me
+ regioisomer
byproduct
2.00
0.92
2.15
0.31
1.89
1.35
1.40
2.10
2.56
3.08
6.56
3.08
9
8
7
6
5
4
3
2
1
0
ppm

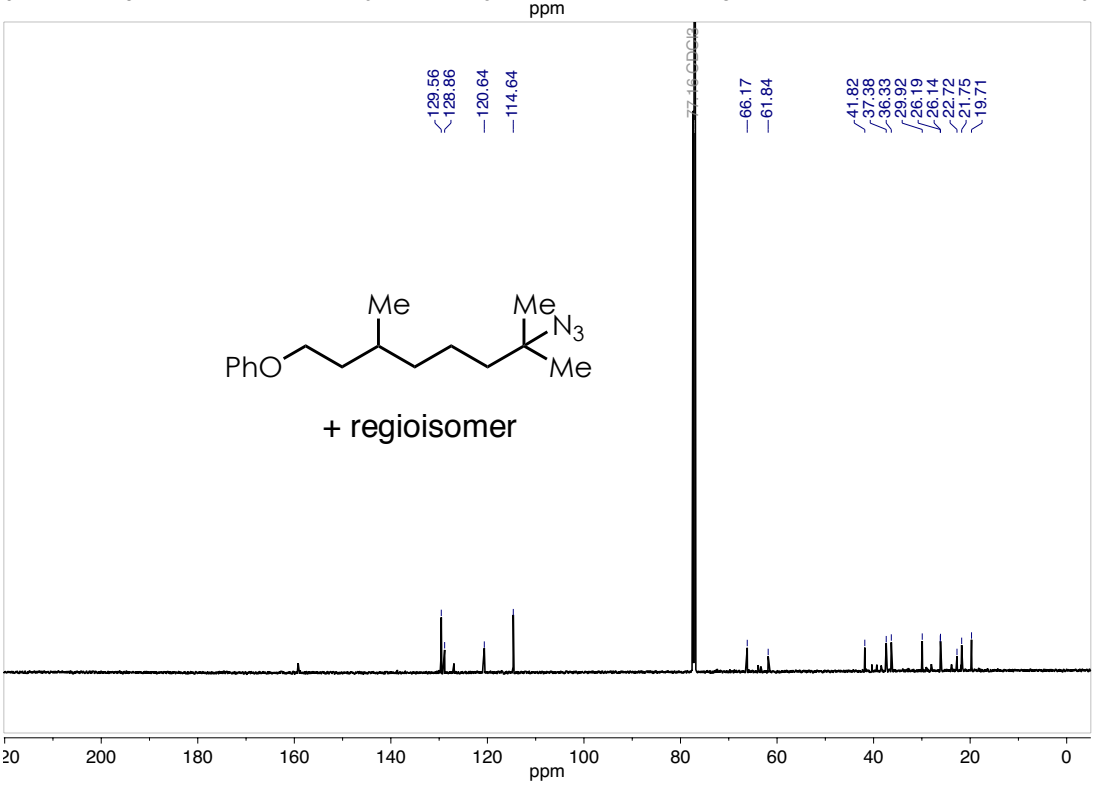
129.56
128.86
120.64
114.64
77.16 CDCl3
66.17
61.84
41.82
37.38
36.33
29.92
26.19
26.14
22.72
21.75
19.71
Me
Me
N3
PhO
Me
+ regioisomer
200
180
160
140
120
100
80
60
40
20
0
ppm

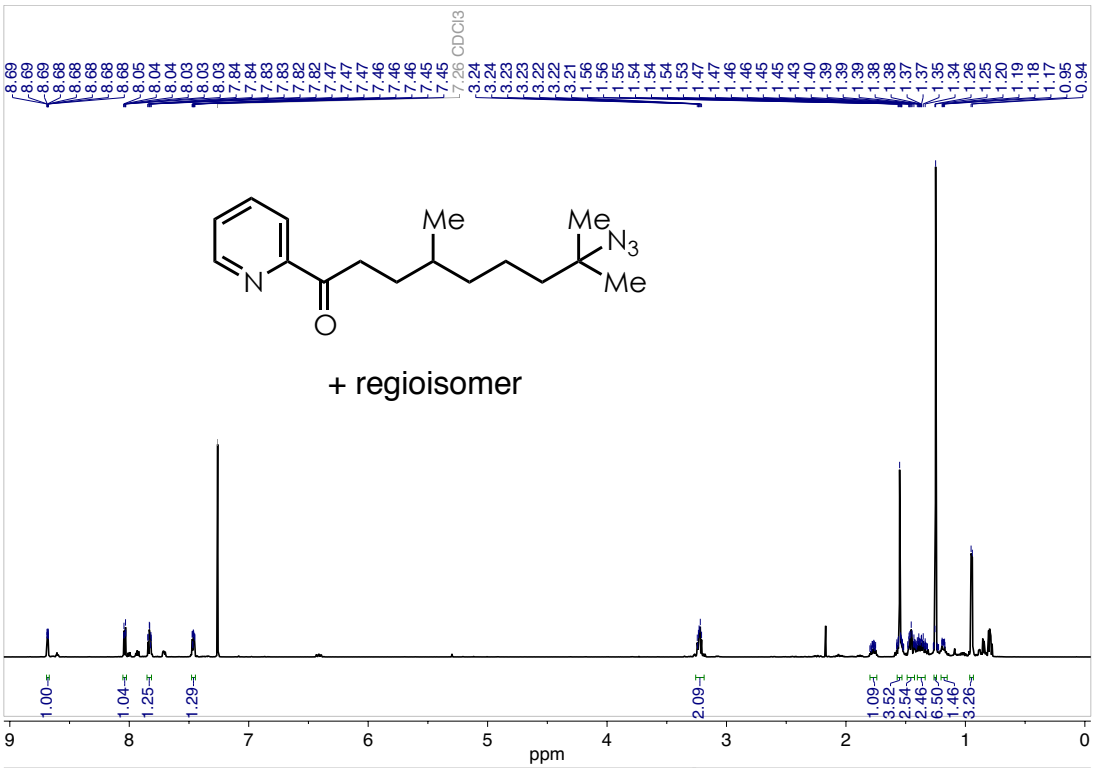
Me
Me
N3
Me
N
O
+ regioisomer
ppm

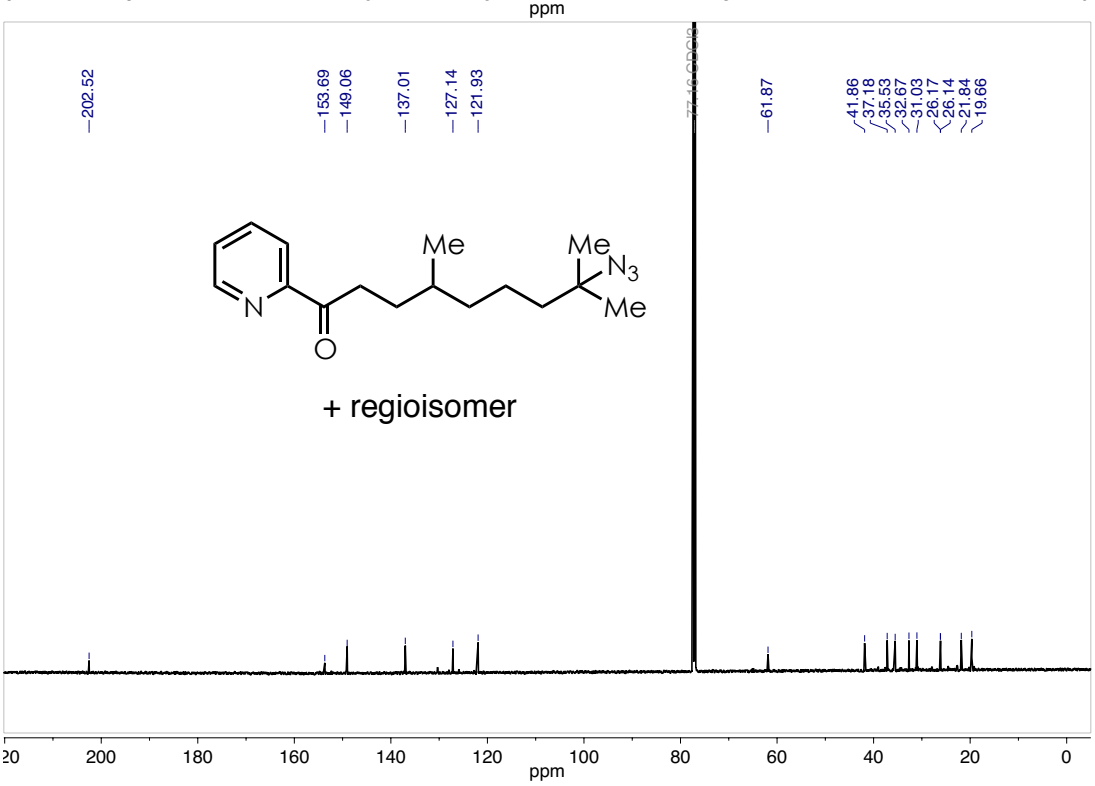
Me
Me
N3
Me
N
O
+ regioisomer
ppm

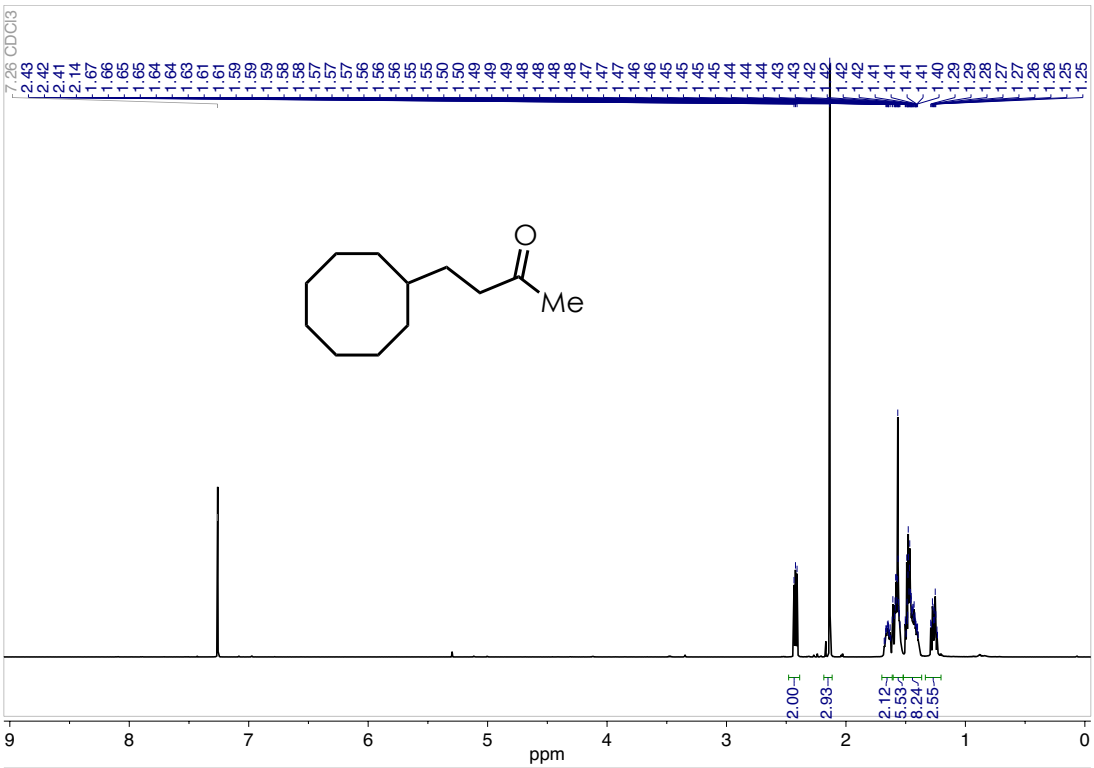
7.26 CDCl3
2.43
2.42
2.41
2.14
1.67
1.66
1.65
1.65
1.64
1.64
1.63
1.61
1.61
1.59
1.59
1.59
1.58
1.58
1.57
1.57
1.57
1.56
1.56
1.56
1.55
1.55
1.50
1.50
1.49
1.49
1.49
1.48
1.48
1.48
1.48
1.47
1.47
1.47
1.46
1.46
1.45
1.45
1.45
1.44
1.44
1.44
1.43
1.43
1.42
1.42
1.42
1.42
1.41
1.41
1.41
1.41
1.40
1.29
1.29
1.28
1.27
1.27
1.26
1.26
1.25
1.25
O
Me
2.00
2.93
2.12
5.53
8.24
2.55
9
8
7
6
5
4
3
2
1
0
ppm

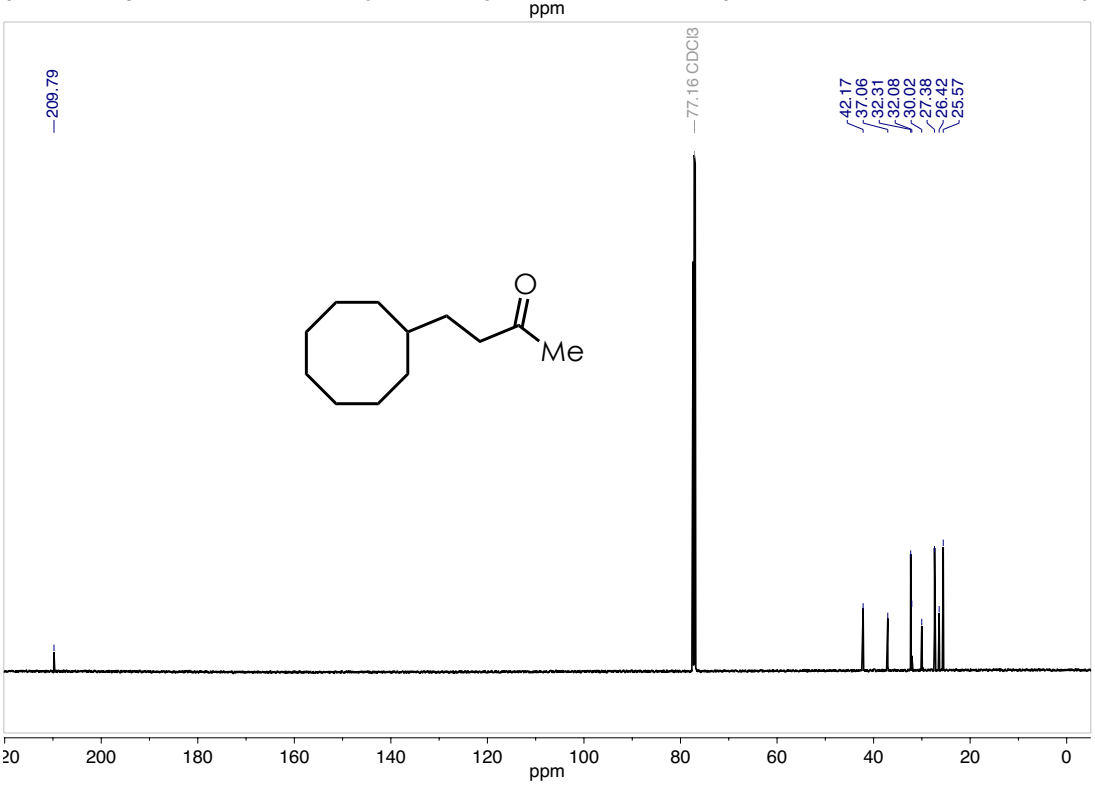
209.79
77.16 CDCl3
42.17
37.06
32.31
32.08
30.02
27.38
26.42
25.57
O
Me
220
200
180
160
140
120
100
80
60
40
20
0
ppm

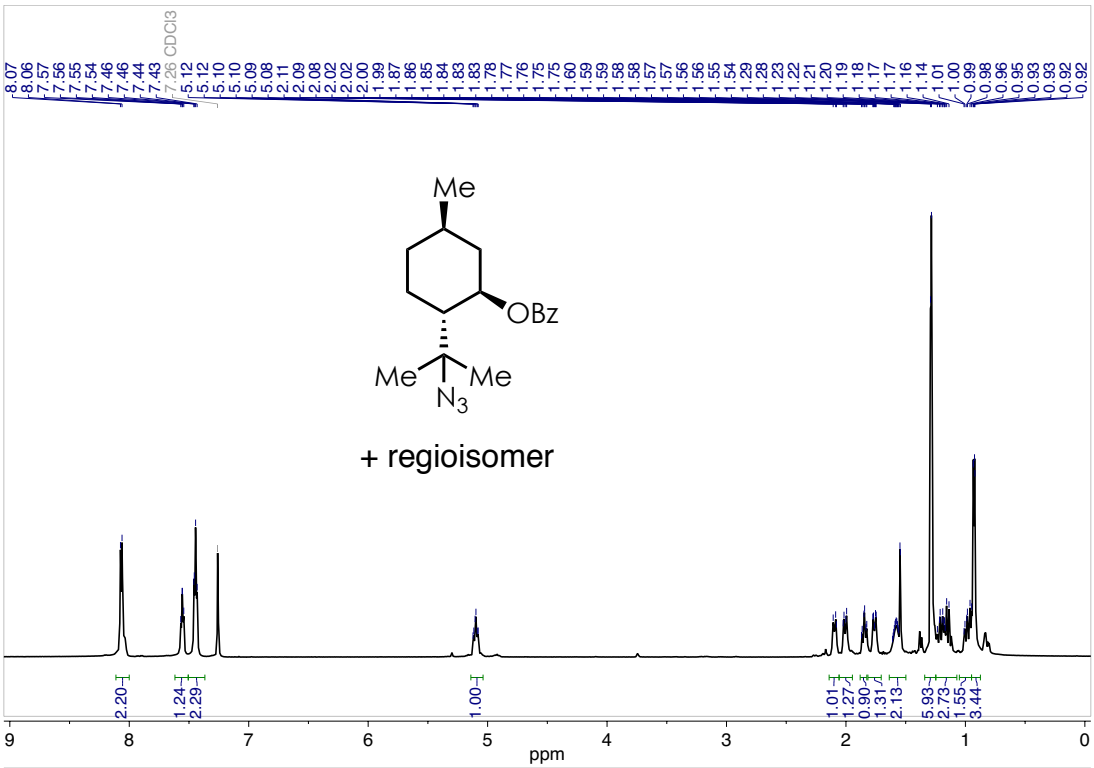
Me
OBz
Me
Me
N3
+ regioisomer
ppm

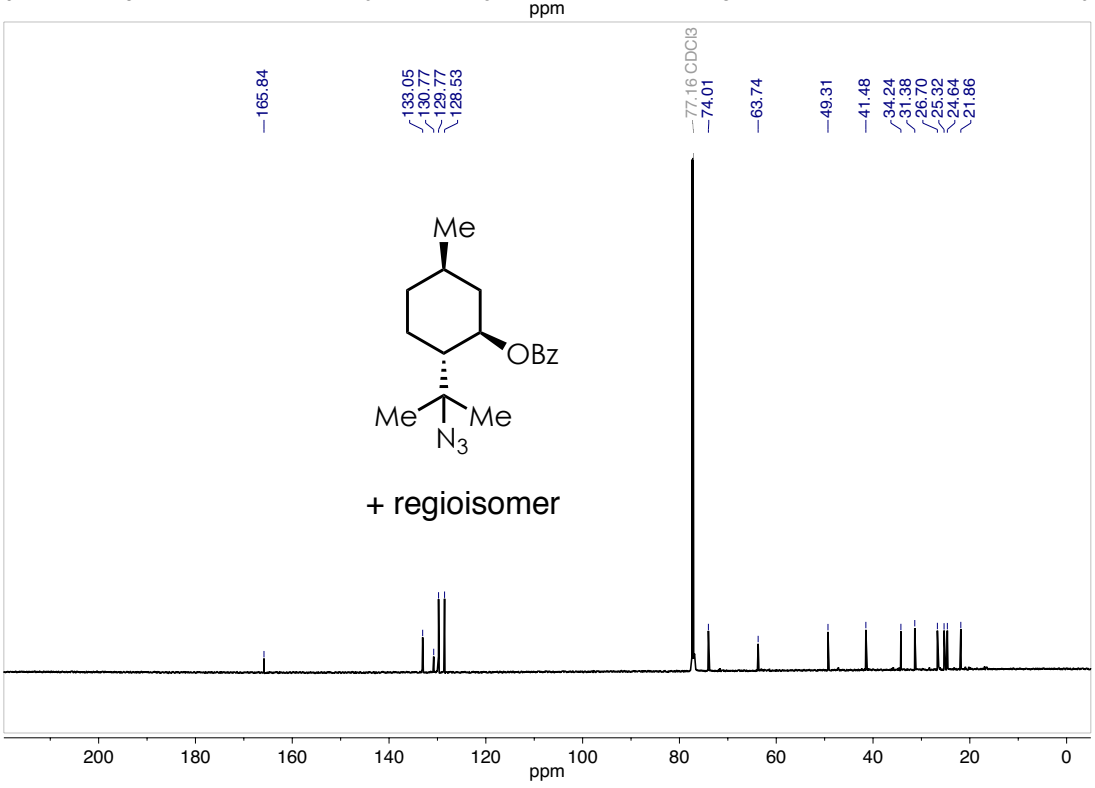
Me
OBz
Me
Me
N3
+ regioisomer
ppm

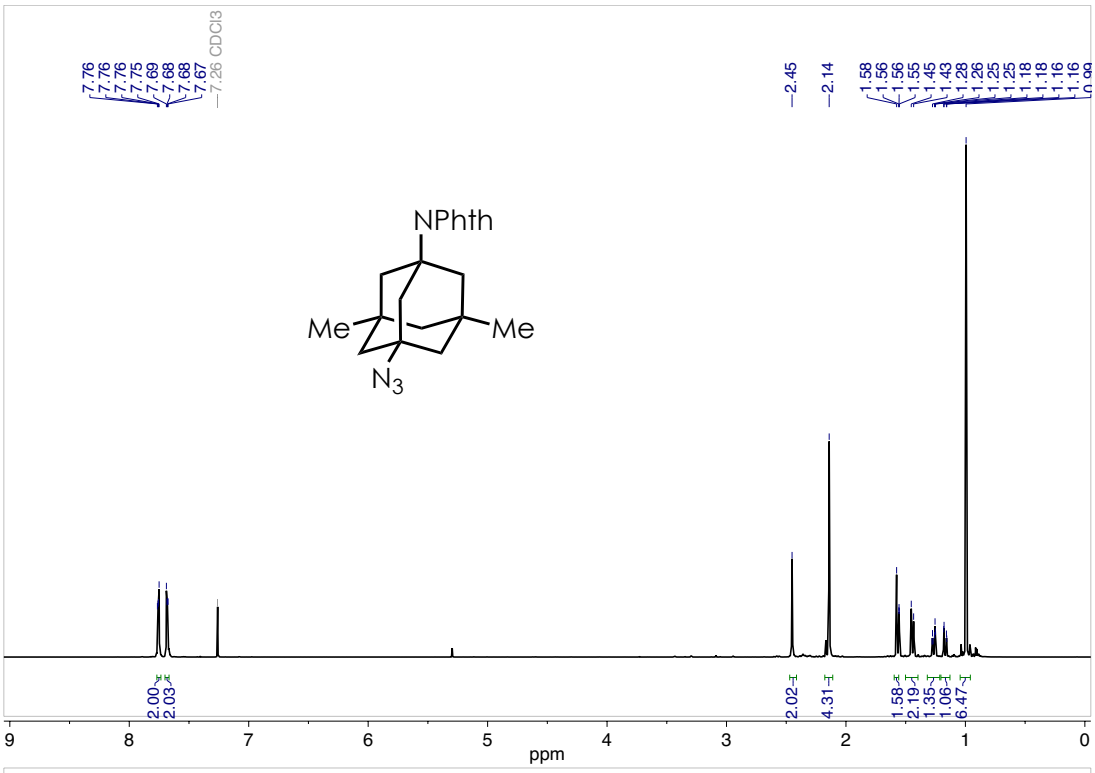
7.76
7.76
7.76
7.75
7.69
7.68
7.68
7.67
7.26 CDCl3
2.45
2.14
1.58
1.56
1.56
1.55
1.45
1.43
1.28
1.26
1.25
1.25
1.18
1.18
1.16
1.16
NPhth
Me
Me
N3
2.00
2.03
2.02
4.31
1.58
2.19
1.35
1.06
6.47
9
8
7
6
5
4
3
2
1
0
ppm

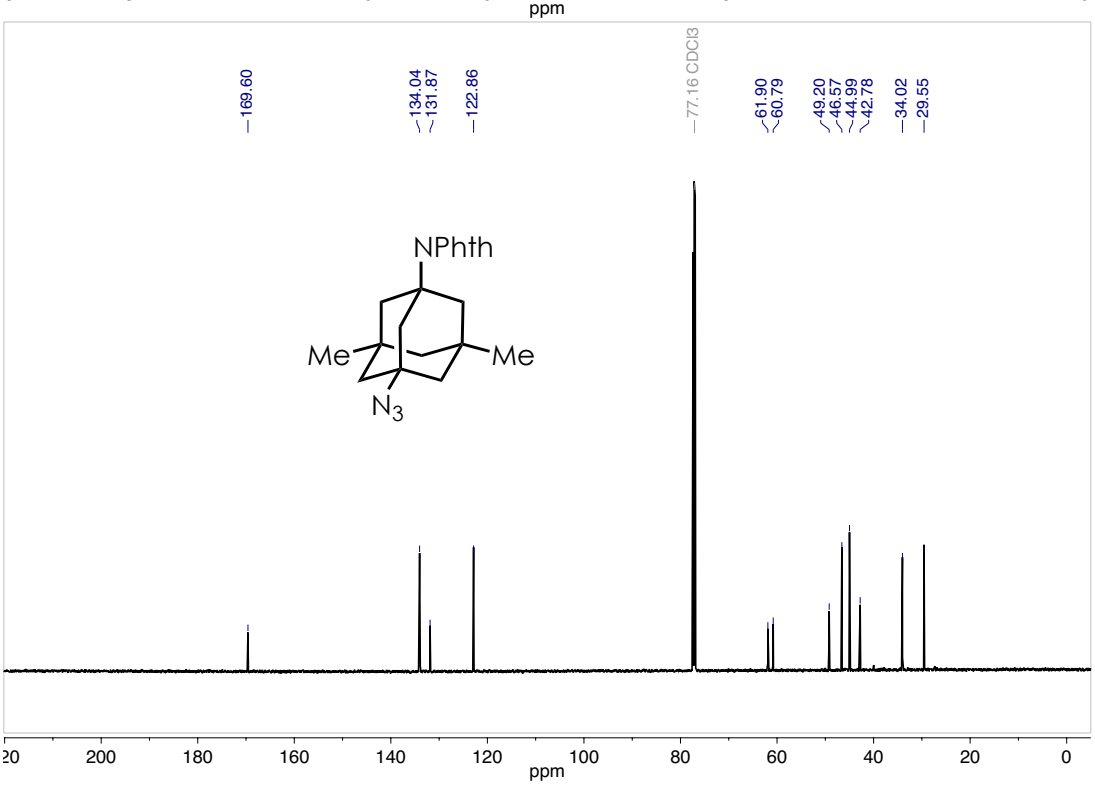
169.60
134.04
131.87
122.86
77.16 CDCl3
61.90
60.79
49.20
46.57
44.99
42.78
34.02
29.55
NPhth
Me
Me
N3
220
200
180
160
140
120
100
80
60
40
20
0
ppm

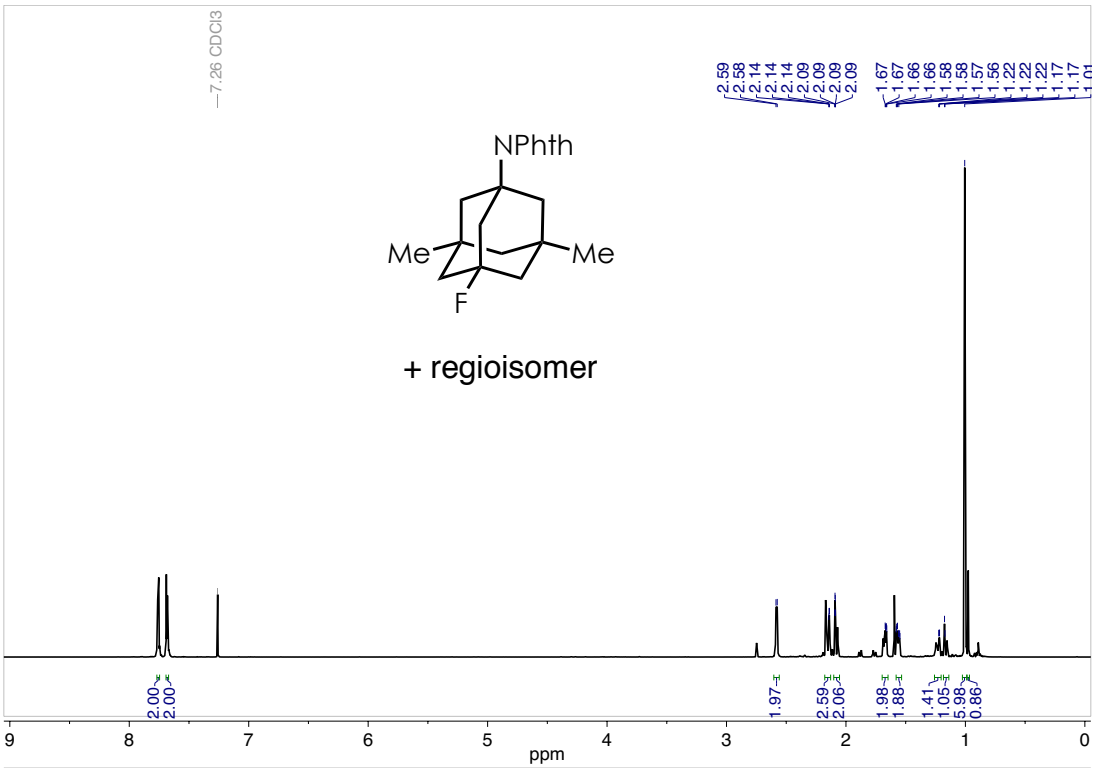
7.26 CDCl3
2.59
2.58
2.14
2.14
2.09
2.09
2.09
1.67
1.67
1.66
1.66
1.58
1.58
1.57
1.56
1.22
1.22
1.17
NPhth
Me
Me
F
+ regioisomer
2.00
2.00
1.97
2.59
2.06
1.98
1.88
1.41
1.05
5.98
0.86
9
8
7
6
5
4
3
2
1
0
ppm

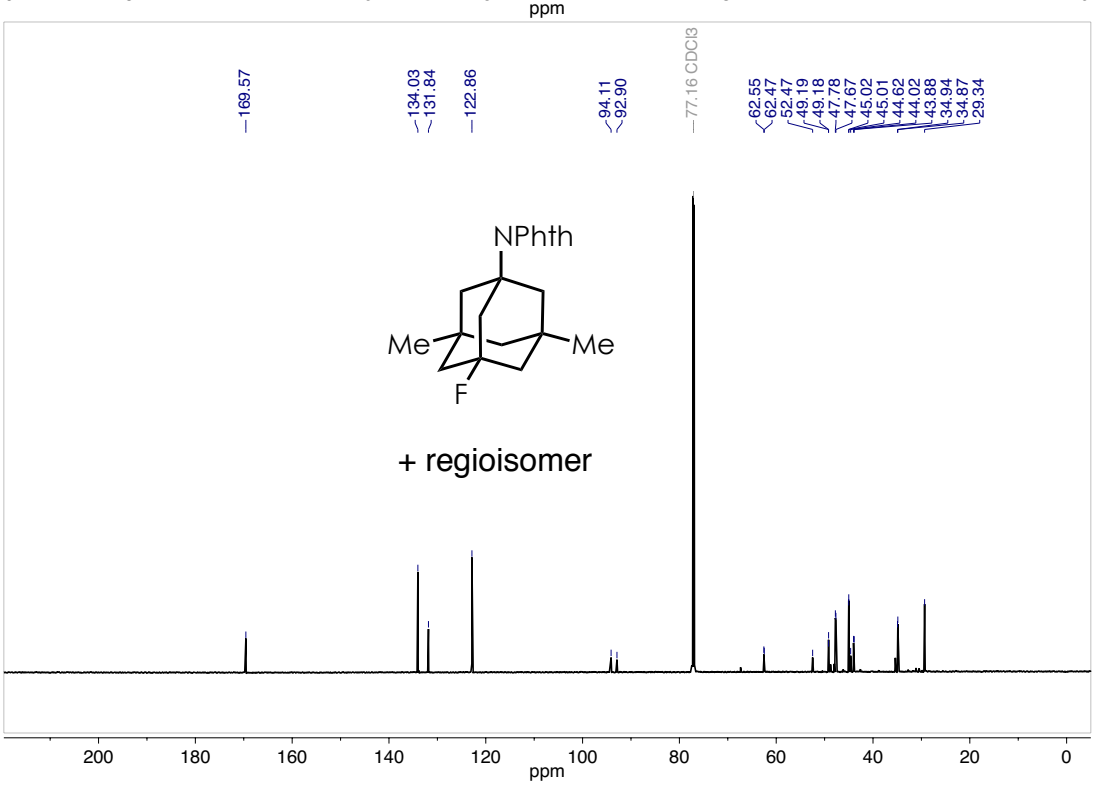
169.57
134.03
131.84
122.86
94.11
92.90
77.16 CDCl3
62.55
62.47
52.47
49.19
49.18
47.78
47.67
45.01
44.62
44.02
43.88
34.94
34.87
29.34
NPhth
Me
Me
F
+ regioisomer
200
180
160
140
120
100
80
60
40
20
0
ppm

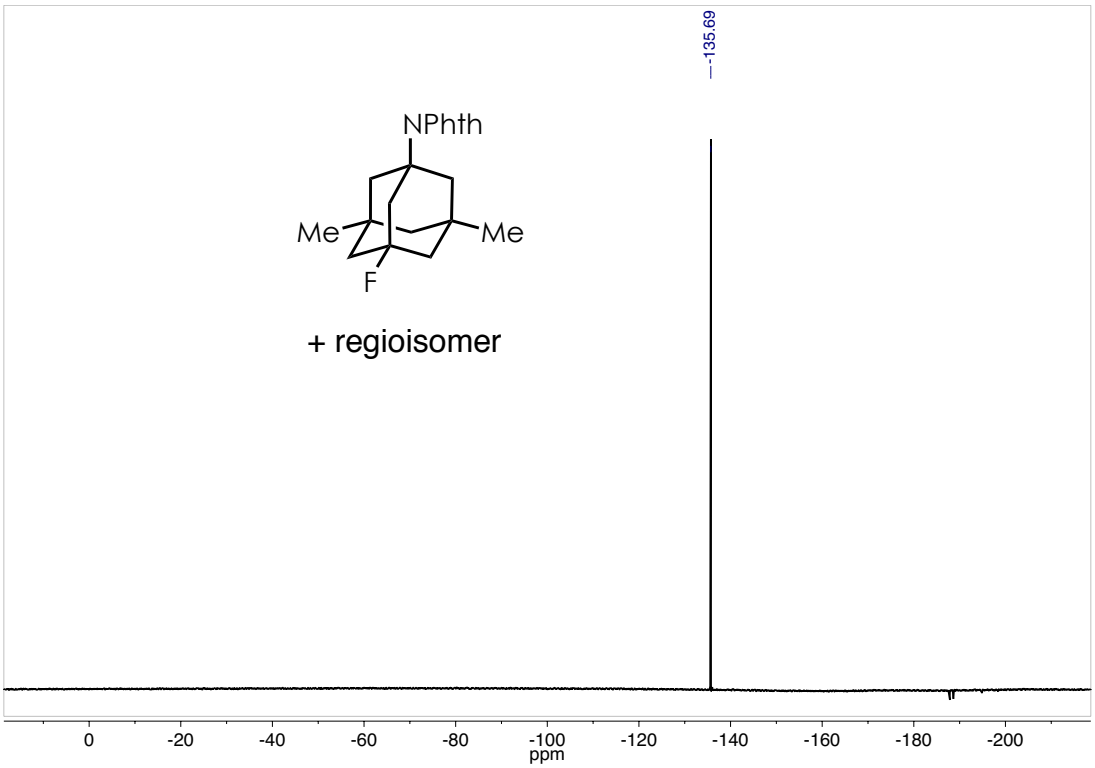
-135.69
NPhth
Me
Me
F
+ regioisomer
0
-20
-40
-60
-80
-100
-120
-140
-160
-180
-200
ppm

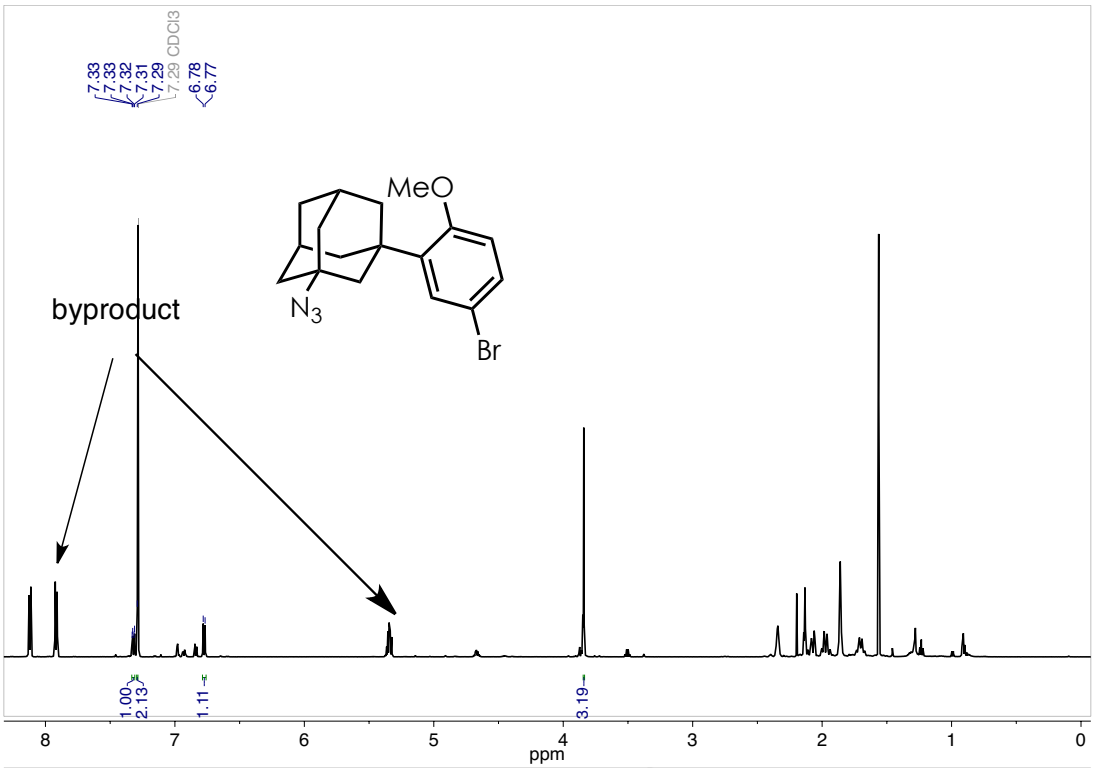
7.33
7.33
7.32
7.31
7.29
7.29 CDCl3
6.78
6.77
MeO
N3
Br
byproduct
1.00
2.13
1.11
3.19
8
7
6
5
4
3
2
1
0
ppm

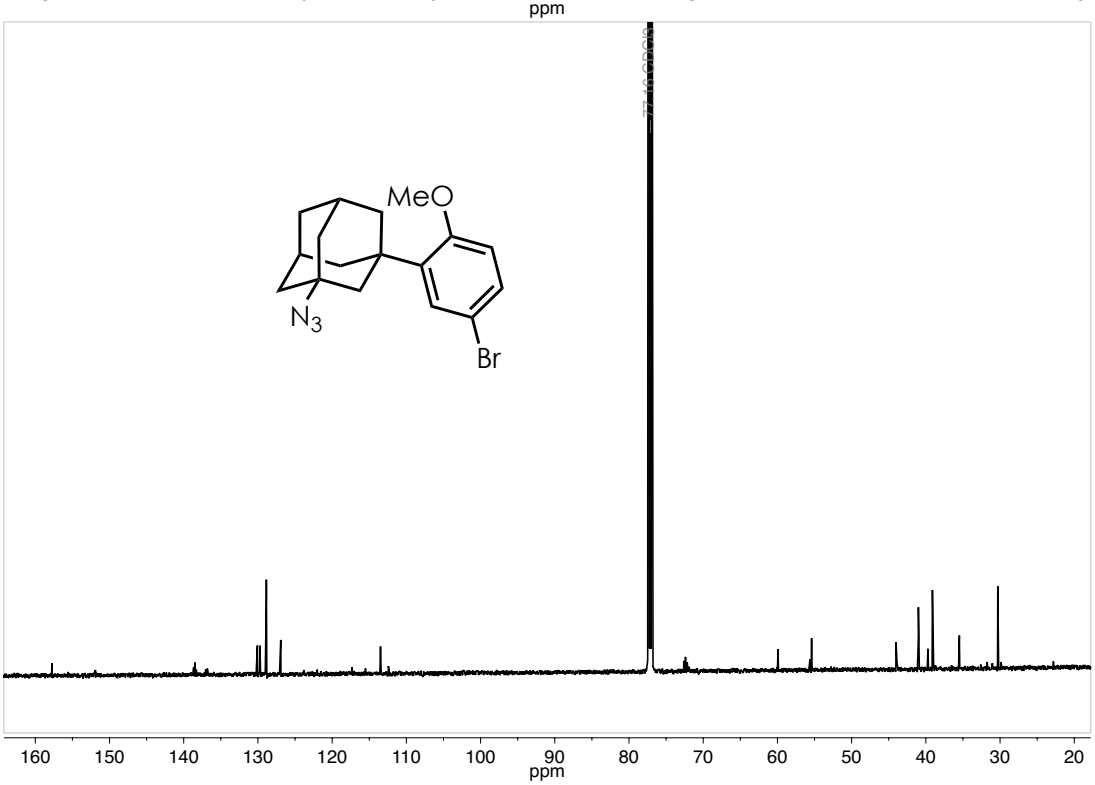
MeO
N3
Br
160
150
140
130
120
110
100
90
80
70
60
50
40
30
20
ppm

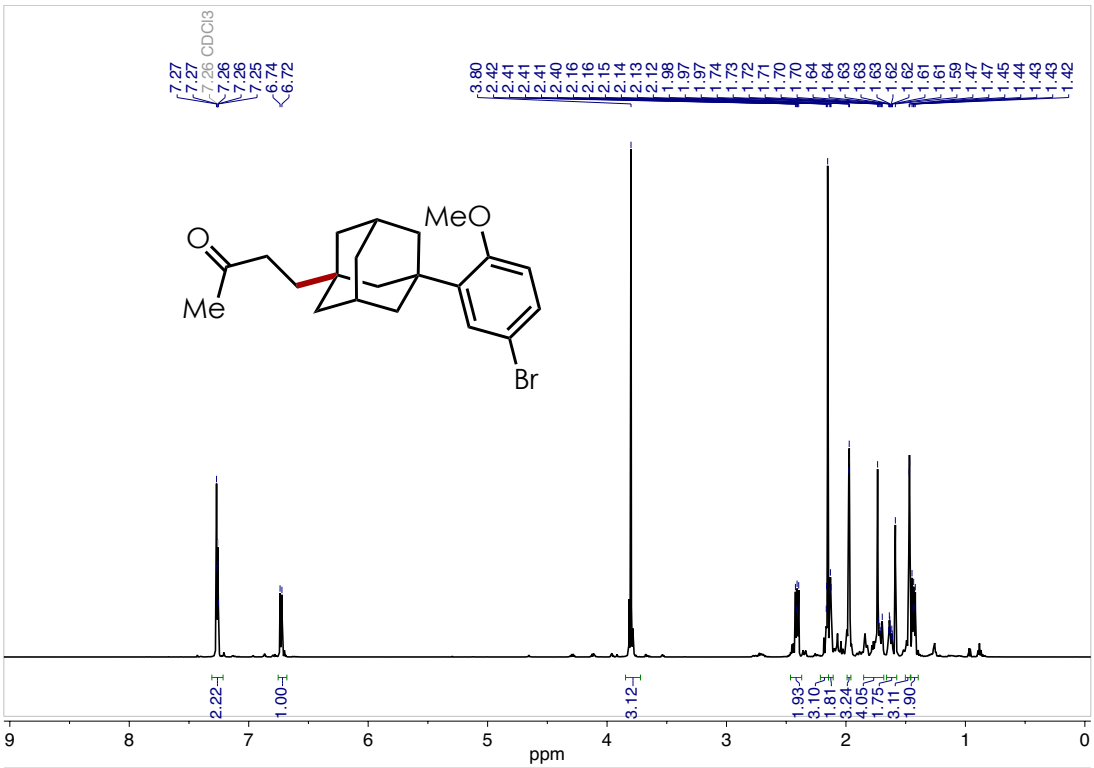
7.27
7.27
7.26 CDCl3
7.26
7.25
6.74
6.72
3.80
2.42
2.41
2.41
2.41
2.40
2.16
2.16
2.15
2.14
2.13
2.12
1.98
1.97
1.97
1.74
1.73
1.72
1.71
1.70
1.70
1.64
1.64
1.63
1.63
1.63
1.62
1.62
1.61
1.61
1.59
1.47
1.45
1.44
1.43
1.42
MeO
O
Me
Br
2.22
1.00
3.12
1.93
3.10
1.81
3.24
4.05
1.75
3.11
1.90
9
8
7
6
5
4
3
2
1
0
ppm

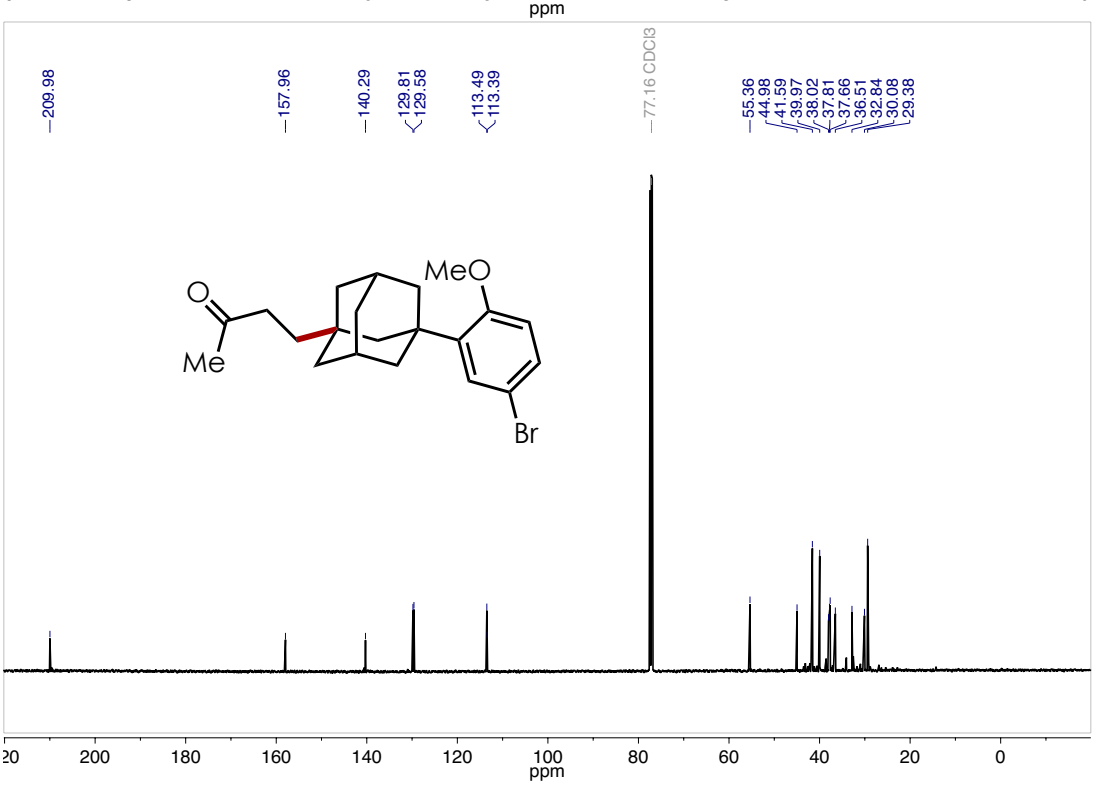
209.98
157.96
140.29
129.81
129.58
113.49
113.39
77.16 CDCl3
55.36
44.98
41.59
39.97
38.02
37.81
37.66
36.51
32.84
30.08
29.38
MeO
O
Me
Br
200
180
160
140
120
100
80
60
40
20
0
ppm

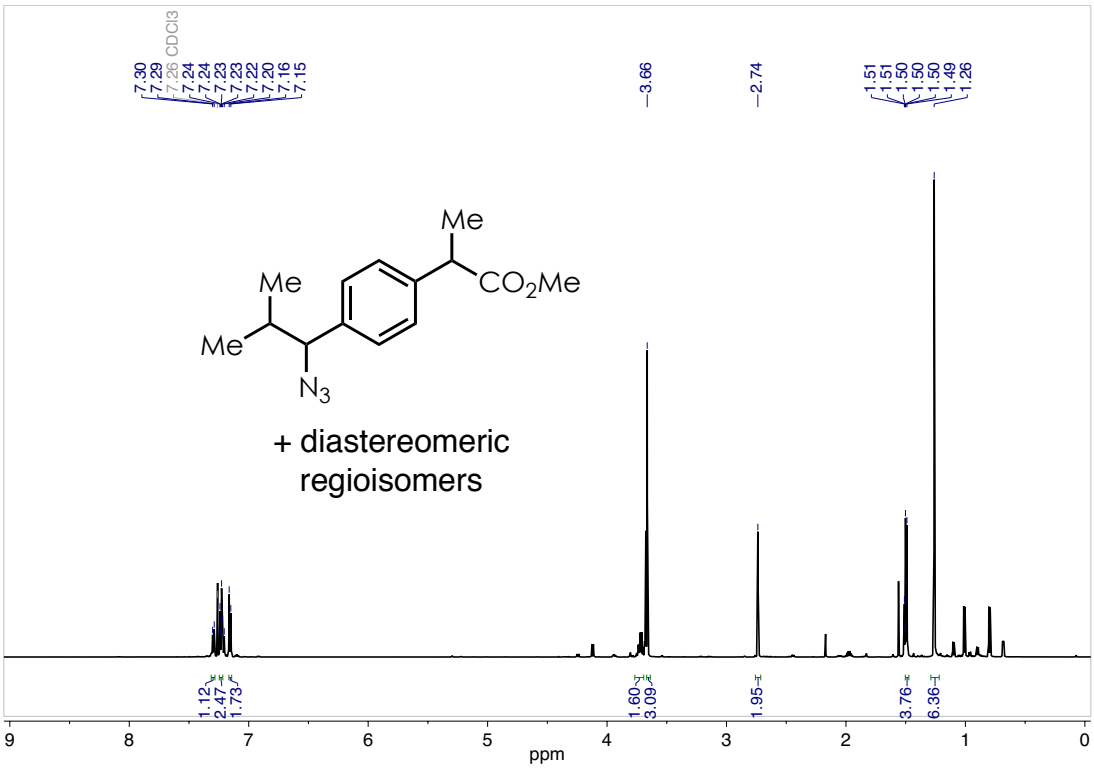
7.30
7.29
7.26 CDCl3
7.24
7.24
7.23
7.23
7.22
7.20
7.16
7.15
3.66
2.74
1.51
1.51
1.50
1.50
1.50
1.49
1.26
Me
Me
Me
CO2Me
N3
+ diastereomeric
regioisomers
1.12
2.47
1.73
1.60
3.09
1.95
3.76
6.36
9
8
7
6
5
4
3
2
1
0
ppm

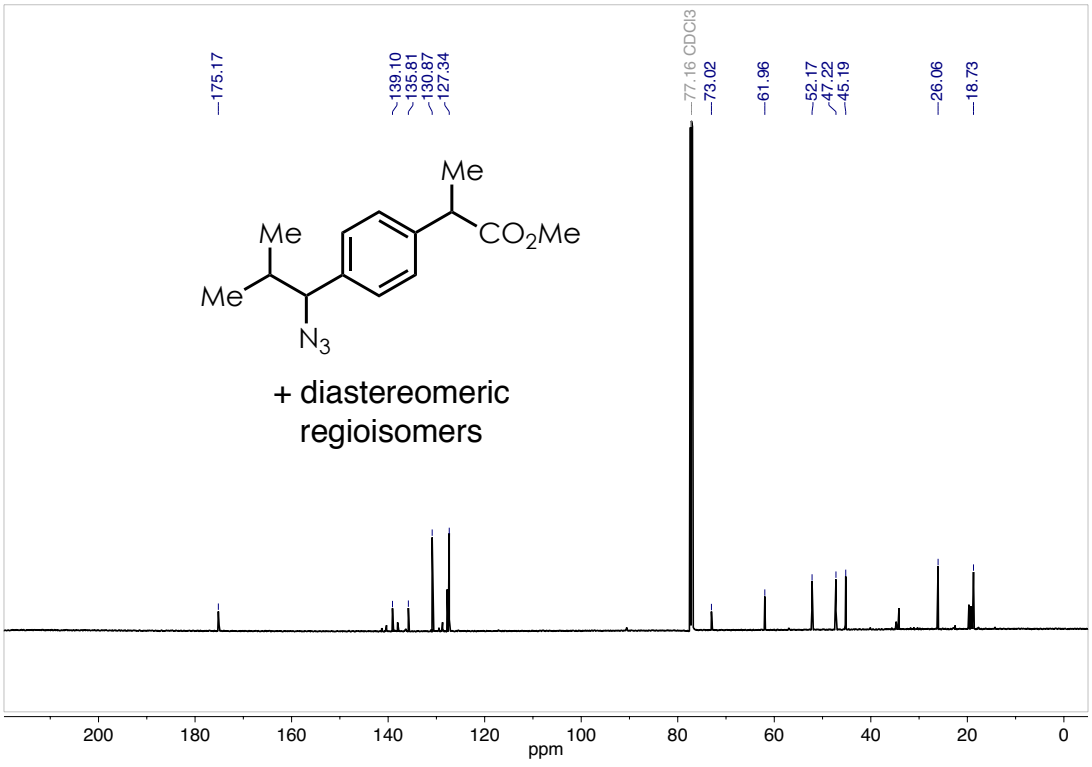
175.17
139.10
135.81
130.87
127.34
77.16 CDCl3
73.02
61.96
52.17
47.22
45.19
26.06
18.73
Me
Me
Me
CO2Me
N3
+ diastereomeric
regioisomers
200
180
160
140
120
100
80
60
40
20
0
ppm

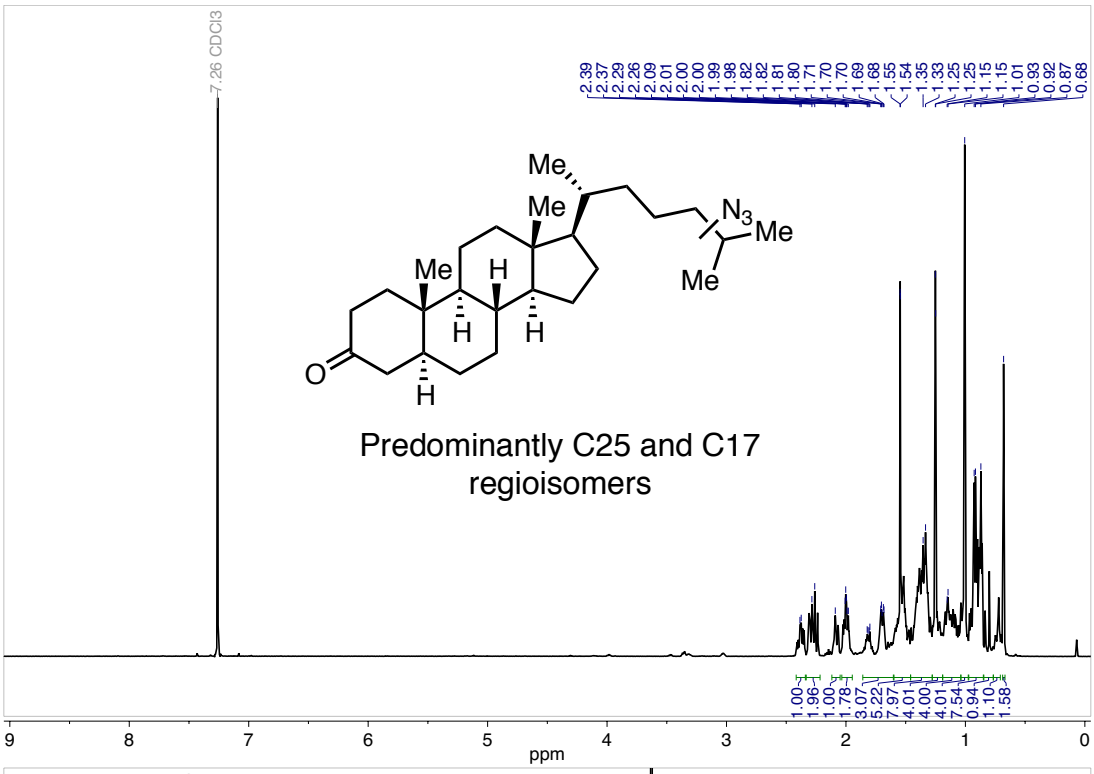
7.26 CDCl3
Me
Me
N3
Me
Me
Me
H
H
H
H
O
Predominantly C25 and C17
regioisomers
ppm

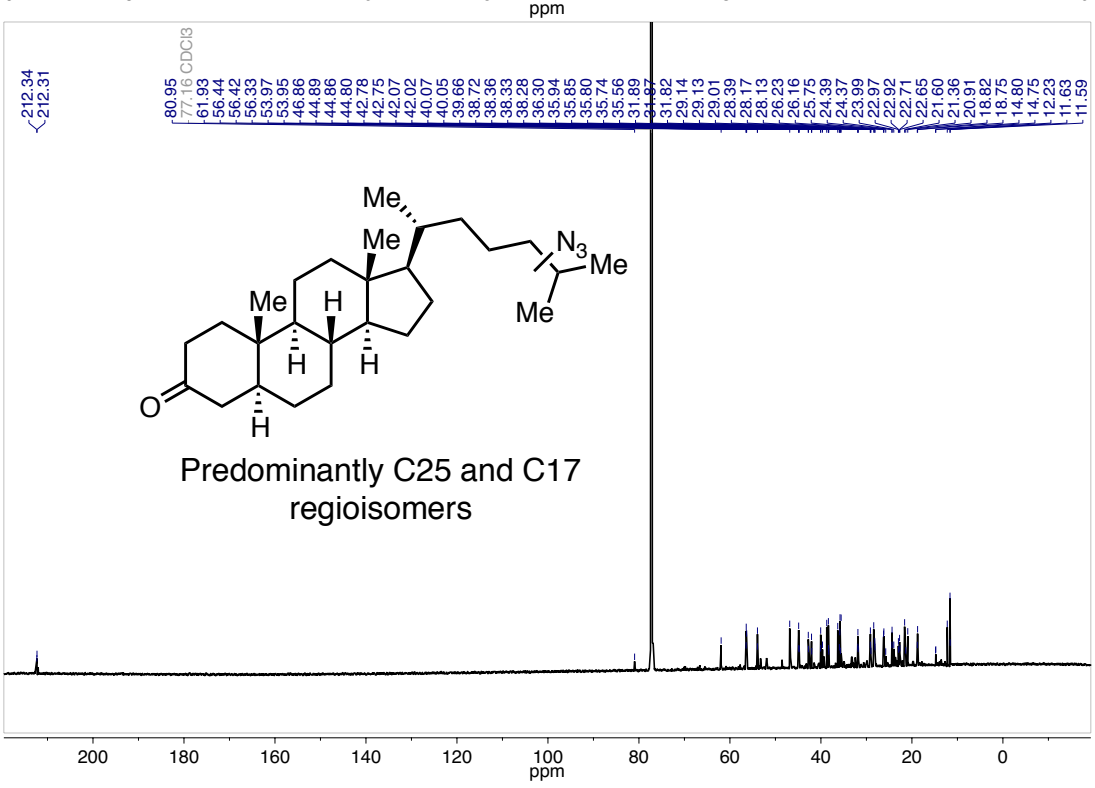
77.16 CDCl3
Me
Me
N3
Me
Me
Me
H
H
H
H
O
Predominantly C25 and C17
regioisomers
ppm

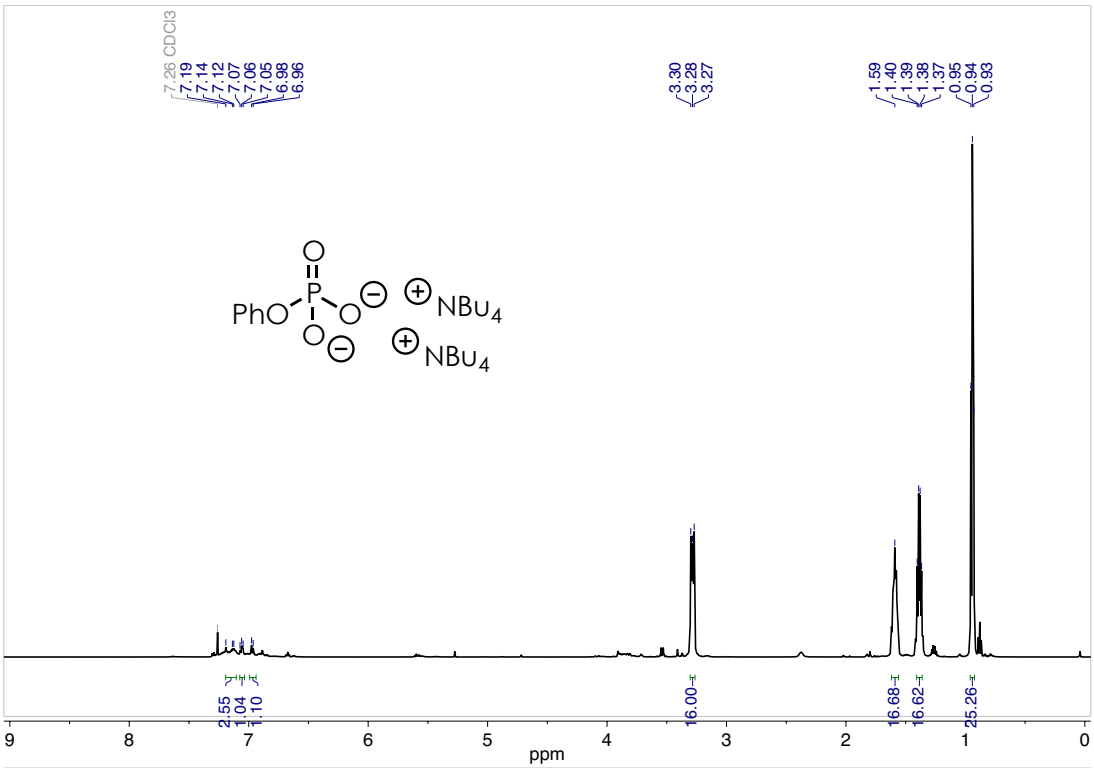
7.26 CDCl3
7.19
7.14
7.12
7.07
7.06
7.05
6.98
6.96
3.30
3.28
3.27
1.59
1.40
1.39
1.38
1.37
0.95
0.94
0.93
PhO
NBu4
NBu4
2.55
1.04
1.10
16.00
16.68
16.62
25.26
9
8
7
6
5
4
3
2
1
0
ppm

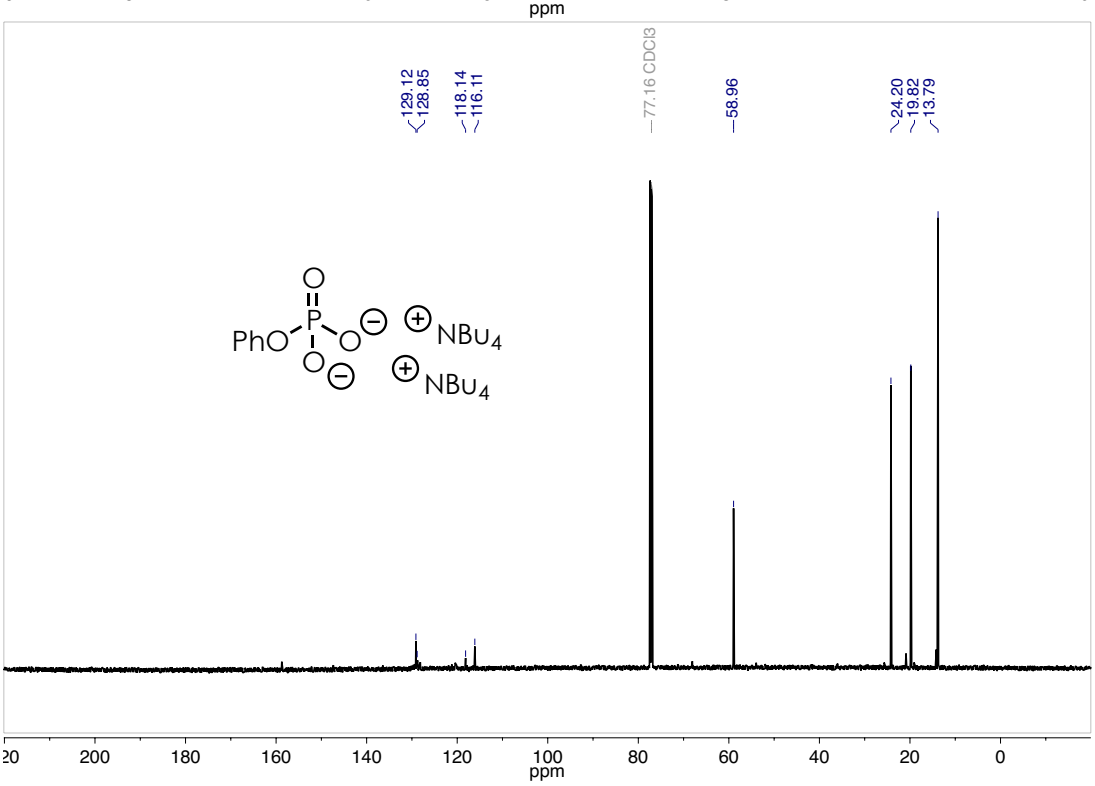
129.12
128.85
118.14
116.11
77.16 CDCl3
58.96
24.20
19.82
13.79
PhO
NBu4
NBu4
200
180
160
140
120
100
80
60
40
20
0
ppm